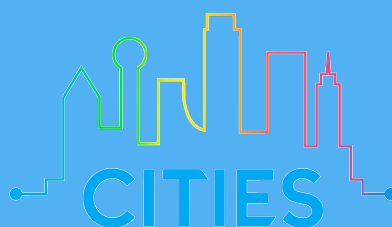





VI Ibero-American Congress of Smart Cities ICSC-CITIES 2023

Ciudad de México and Cuernavaca, México
November 13th to 17th

Pedro Moreno-Bernal
Ponciano Escamilla-Ambrosio
Luis Hernández-Callejo
Sergio Nesmachnow
Diego Rossit
Carlos Torres-Aguilar (Eds.)




Editors


Pedro Moreno-Bernal 
Universidad Autónoma del Estado de Morelos (UAEM), Morelos, México

Ponciano Escamilla-Ambrosio 
Centro de Investigación en Computación, Instituto Politécnico Nacional
(CIC-IPN), Ciudad de México, México

Luis Hernández-Callejo 
Universidad de Valladolid (UVa), Soria, España

Sergio Nesmachnow 
Universidad de la República (UDELAR), Montevideo, Uruguay

Diego Rossit 
Universidad Nacional del Sur (UNS-CONICET), Bahía Blanca, Argentina

Carlos Torres-Aguilar 
Universidad Juárez Autónoma de Tabasco (UJAT), Tabasco, México

Elaborated by the Organizing Committee of the VI Ibero-American Congress of Smart Cities (ICSC-CITIES 2023).

Disclaimer: The information in this book is true and complete to the best of the editor's knowledge. All recommendations are made without a guarantee on the part of the editors. The editors disclaim any liability in connection with the use of this information.

How to cite this book: Moreno-Bernal, P., Escamilla-Ambrosio, P., Hernández-Callejo, L., Nesmachnow, S., Rossit, D. and Torres-Aguilar, C. (Eds). (2023). VI Ibero-American Congress of Smart Cities. CITIES.

Cover: Carlos Torres-Aguilar

ISBN: 978-607-99960-1-7



This work is licensed under a Creative Commons Attribution 4.0 International License.

Preface

The Ibero-American Congress of Smart Cities (ICSC-CITIES), a forum for Smart Cities discussion, presents this book of articles from its sixth conference, held in presential and virtual mode format in Ciudad de México and Cuernavaca, México, from November 13-17, 2023.

A Smart City is a framework composed mainly of Internet of Things systems and Information and Communication Technologies integrated to develop, implement, and promote sustainable development practices and face the challenges of urbanization. ICSC-CITIES aims to create synergies among different research groups to promote the development of Smart Cities and contribute to their knowledge and integration in different scenarios.

The conference has been held yearly since 2018. The first and the second editions, i.e., 2018 and 2019, were celebrated in Soria, Spain. The third edition was celebrated virtually but hosted by the Costa Rica Institute of Technology. The fourth edition was hosted by Instituto Politécnico Nacional de México, celebrated in presential and virtual mode in Cancún, México. The fifth edition was hosted by Universidad de Cuenca and celebrated in presential and virtual mode in Cuenca, Ecuador.

The VI Ibero-American Congress of Smart Cities (ICSC-CITIES 2023) was held in a hybrid way (face-to-face and virtual) from November 13th to 17th, 2023, in Ciudad de México and Cuernavaca, hosted and sponsored by the Centro de Investigación en Computación of the IPN and Universidad Autónoma del Estado de Morelos, México. Seventy-five technical presentations were given by researchers from 26 different countries during the ICSC-CITIES 2023. Eleven papers were included as posters. Papers were divided into eleven tracks, i.e., Artificial Intelligence for Smart Cities, Energy, Energy Efficiency and Sustainability, Smart grid, Governance and Citizenship, Smart Economy, Development and Education, Smart Environment, Smart Industry, Smart Mobility, Smart Public Services and Urban Informatics, Big Data, Analytics for Smart Cities & Other developments for Smart Cities; those contributions were selected from a pool of 94 submitted papers, yielding an acceptance rate of 91.4%.

ICSC-CITIES 2023 was enriched by three-featured panel discussions focusing on specific aspects of Smart Cities. The first panel explored how new technologies foster the development of new smart cities. The second panel discussed the digitalization of public transportation and its benefits. The final panel examined smart cities from a gender perspective.

The editors

Organization

General Chairs

Sergio Nesmachnow, Universidad de la República, Uruguay

Luis Hernández Callejo, Universidad de Valladolid, Spain

Pedro Moreno Bernal, Universidad Autónoma del Estado de Morelos, México

Ponciano Jorge Escamilla Ambrosio, Instituto Politécnico Nacional, México

Organizing Committee

Luis Hernández Callejo, Universidad de Valladolid, Spain, Spain

Sergio Nesmachnow, Universidad de la República, Uruguay

Pedro Moreno Bernal, Universidad Autónoma del Estado de Morelos, México

Diego Rossit, Universidad Nacional del Sur, Argentina

Carlos Enrique Torres Aguilar, Universidad Juárez Autónoma de Tabasco, México

Rodrigo Porteiro, UTE, Uruguay

Submission and Conference Management Chair

Santiago Iturriaga, Universidad de la República, Uruguay

Local Organization Chairs

Ponciano Jorge Escamilla Ambrosio, Instituto Politécnico Nacional, México

Pedro Moreno Bernal, Universidad Autónoma del Estado de Morelos, México

Program Committee

Abdelkarim Bouras, Annaba University, Algeria

Abigail Parra, Universidad Autónoma del Estado de Morelos, México

Adrian Toncovich, Universidad Nacional del Sur, Argentina

Adriana Correa-Guimaraes, Universidad de Valladolid, España

Alberto López Casillas, Diputación de Ávila, España

Alberto Redondo, Universidad de Valladolid, España

Alejandro Valencia-Arias, Universidad Señor de Sipán, Perú

Alessandra Bussador, Universidade Federal da Integração Latino-Americana, Brasil

Alex Adiels Cano Heredia, Universidad de Quintana Roo, México

Alexander Vallejo Díaz, Instituto Tecnológico de Santo Domingo, República Dominicana

Alicia Martinez, Centro Nacional de Investigación y Desarrollo Tecnológico, México

Ana Carolina Olivera, Universidad Nacional de Cuyo-CONICET, Argentina
Ana Ruiz, Universidad San Jorge, España
Ana Lilia Sánchez Brito, Centro Nacional de Investigación y Desarrollo Tecnológico, México
Andrei Tchernykh, CICESE Research Center, México
Andrés Adolfo Navarro Newball, Pontificia Universidad Javeriana, Cali, Colombia
Andres Felipe Fuentes Vasquez, Pontificia Universidad Javeriana, Colombia
Ángel Hernández Jiménez, CEDER-CIEMAT, España
Ángel Zorita Lamadrid, Universidad de Valladolid, España
Angela Ferreira, Polytechnic Institute of Bragança, Portugal
João Coelho, Polytechnic Institute of Bragança, Portugal
Yahia Amoura, Polytechnic Institute of Bragança, Portugal
Antonella Cavallin, Universidad Nacional del Sur, Argentina
Antonio Mauttone, Universidad de la República, Uruguay
Antonio Muñoz, University of Malaga, España
Araceli Ávila Hernández, Instituto Tecnológico Superior de Perote, México
Armando Huicochea, Universidad Autónoma del Estado de Morelos, México
Beatriz Martinez, Universidad Autónoma del Estado de Morelos, México
Begoña González Landin, Universidad de Las Palmas de Gran Canaria, España
Belén Carro, Universidad de Valladolid, España
Benjamín Álvarez Alor, Centro Nacional de Investigación y Desarrollo Tecnológico, México
Bernardo Pulido-Gaytan, CICESE Research Center, México
Carlos Barroso-Moreno, Universidad Europea de Madrid, España
Carlos Enrique Torres Aguilar, Universidad Juárez Autónoma de Tabasco, México
Carlos Meza Benavides, Anhalt University of Applied Sciences, Alemania
Carlos Miguel Jiménez-Xaman, Universidad Autónoma de San Luis Potosí, México
César Varela, Centro Nacional de Investigación y Desarrollo Tecnológico, México
Christian Cintrano, Universidad de Málaga, España
Claudio Paz, Universidad Tecnológica Nacional, Argentina
Claudio Risso, Universidad de la República, Uruguay
Cristina Sáez Blázquez, Universidad de Salamanca, España
Daniel H. Stolfi, University of Luxembourg, Luxemburgo

Daniel Morinigo-Sotelo, Universidad de Valladolid, España
Daniel Rossit, Universidad Nacional del Sur-CONICET, Argentina
David Balladares de la Cruz, Universidad Juárez Autónoma de Tabasco, México
David Peña Morales, Universidad de Cádiz, España
Deyslen Mariano, Instituto Tecnológico de Santo Domingo, República Dominicana
Diego Alberto Godoy, Universidad Gastón Dachary, Argentina
Diego Arcos-Aviles, Universidad de las Fuerzas Armadas, Ecuador
Diego Rossit, Universidad Nacional del Sur-CONICET, Argentina
Edgar Vazquez Beltran, Universidad de Sonora, México
Edgar Vicente Macias Melo, Universidad Juárez Autónoma de Tabasco, México
Edith Gabriela Manchego Huaquipaco, Universidad Nacional de San Agustín de Arequipa, Perú
Eduardo Fernández, Universidad de la República, Uruguay
Emmanuel Millan, Universidad Nacional de Cuyo, Argentina
Enrique González, Universidad de Salamanca, España
Erick Iván Téllez Velázquez, Instituto Tecnológico Superior de Perote-TecNM, México
Erika Martinez Sanchez, Universidad Autónoma de Coahuila, México
Esteban Mocskos, Universidad de Buenos Aires, Argentina
Evandro Melo, Universidade Federal de Viçosa, Brasil
Fabian Castillo Peña, Universidad Libre Seccional Cali, Colombia
Federico Alonso Pecina, Universidad Autónoma del Estado de Morelos, México
Francisco Garrido-Valenzuela, Technology University of Delft, Países Bajos
Francisco Valbuena, Universidad de Valladolid, España
Gilberto Martinez, Centro de Investigación en Computación-Instituto Politécnico Nacional, México
Gina Paola Maestre Gongora, Universidad Cooperativa de Colombia, Colombia
Gustavo Medina Angel, Universidad Autónoma del Estado de Morelos, México
Héctor Chicchiarini, Universidad Nacional del Sur-CONICET, Argentina
Hector Felipe Mateo Romero, Universidad de Valladolid, España
Héctor Sotelo, Universidad Autónoma del Estado de Morelos, México
Heidi Paola Díaz Hernández, Universidad Juárez Autónoma de Tabasco, México
Hortensia Amaris, Universidad Carlos III de Madrid, España
Hugo Saldarriaga, Universidad Autónoma del Estado de Morelos, México
Ignacio de Godos, Universidad de Valladolid, España
Ignacio Turias, Universidad de Cádiz, España

Irene Lebrusán, Harvard University, EEUU
Irving Osiris Hernández López, Universidad de Sonora, México
Isidro Hernández, Instituto Tecnológico de Nuevo León, México
Ivonne Yazmín Arce García, Universidad Autónoma del Estado de Morelos,
México
Jaime Lloret, Universitat Politècnica de València, España
Jamal Toutouh, Universidad de Málaga, España
Javier Rocher Morant, Universitat Politècnica de València, España
Javier Uriarte Flores, Universidad de Sonora, México
Jesús Armando Aguilar, Universidad Autónoma de Baja California, México
Jesús Del Carmen Peralta Abarca, Universidad Autónoma del Estado de Morelos,
México
Jesús Vegas, Universidad de Valladolid, España
João Coelho, Polytechnic Institute of Bragança, Portugal
Jonathan Muraña, Universidad de la República, Uruguay
Jorge Arturo Del Ángel Ramos, Universidad Veracruzana, México
Jorge De La Cruz, Aalborg University, Dinamarca
Jorge López-Rebollo, Universidad de Salamanca, España
Jorge Mario Cortés-Mendoza, Universidad Politécnica de Amozoc, México
Jorge Luis Cerino Isidro, Universidad Juárez Autónoma de Tabasco, México
José Alberto Hernández, Universidad Autónoma del Estado de Morelos, México
José Ángel Morell Martínez, Universidad de Málaga, España
Jose Ignacio Morales Aragonés, Universidad de Valladolid, España
José Ramón Aira, Universidad Politécnica de Madrid, España
Jose Alfredo Jimenez Alvarez, Instituto Tecnológico Superior de Perote, México
Juan Carlos Martínez Serra, Universidad UTE, Ecuador
Juan Chavat, Universidad de la República, Uruguay
Juan Espinoza, Universidad de Cuenca, Ecuador
Juan Manuel Ramírez Alcaraz, Universidad de Colima, México
Juan Moises Mauricio Villanueva, Universidade Federal da Paraíba, Brasil
Juan Paul Ayala Taco, Universidad de las Fuerzas Armadas, Ecuador
Juan Pavón, Universidad Complutense de Madrid, España
Juan R. Coca, Universidad de Valladolid, España
Karla María Aguilar Castro, Universidad Juárez Autónoma de Tabasco, México
Leonardo Cardinale, Instituto Tecnológico de Costa Rica, Costa Rica
Lilian Johanna Obregón, Universidad de Valladolid, España
Lorena Parra, Universitat Politècnica de València, España

Lucas Mohimont, Université de Reims, Francia
Lucas Spierenburg, Technology University of Delft, Países Bajos
Luis Enrique Ángeles Montero, Universidad Juárez Autónoma de Tabasco,
México
Luis G. Montané Jiménez, Universidad Veracruzana, México
Luis Hernández Callejo, Universidad de Valladolid, España
Luis Manuel Navas Gracia, Universidad de Valladolid, España
Luis Marrone, Universidad Nacional de La Plata, Argentina
Luis Omar James Boza, Universidad Veracruzana, México
Luis Tobon, Pontificia Universidad Javeriana Cali, Colombia
Manuel Gonzalez, Universidad de Valladolid, España
Marcin Sredynski, E-Bus Competence Center, Luxemburgo
María Clara Tarifa, Universidad Nacional de Río Negro-CONICET, Argentina
Maria Teresa Cepero, Universidad Veracruzana, México
Mariana Coccola, Universidad Tecnológica Nacional-CONICET, Argentina
Mariano Frutos, Universidad Nacional del Sur-CONICET, Argentina
Mario Andrés Paredes Valverde, ITS de Teziutlán-TecNM, México
Mario Carbono de la Rosa, Universidad Nacional Autónoma de México, México
Mario Hernandez Dominguez, sev, México
Mario Limon, Universidad Autónoma del Estado de Morelos, México
Máximo Méndez Babey, Universidad de Las Palmas de Gran Canaria, España
Miguel Angel Che Pan, Instituto Tecnológico Superior de Perote, México
Miguel Ángel Juárez Merino, Universidad Nacional Autónoma de México,
México
Miguel Aybar, Instituto Tecnológico de Santo Domingo, República Dominicana
Miguel Davila, Universidad Politécnica Salesiana del Ecuador, Ecuador
Miguel Quimbayo, University of Tolima, Colombia
Miguel-Ángel Muñoz-García, Universidad Politécnica de Madrid, España
Monica Alonso, University Carlos III de Madrid, España
Mónica Montoya Giraldo, CIDET, Colombia
Muhyettin Sirer, DEMIR Enerji, Turquía
Nestor Rocchetti, Universidad de la República, Uruguay
Noelia Uribe-Perez, Tecnalia Research & Innovation, España
Olalla García Pérez, Universidad Europea de Madrid, España
Oscar Duque-Perez, Universidad de Valladolid, España
Oscar Izquierdo, CEDER-CIEMAT, España
Oscar May Tzuc, Universidad Autónoma de Campeche, México

Outmane Oubram, Universidad Autónoma del Estado de Morelos, México
Pablo Daniel Godoy, Universidad Nacional de Cuyo, Argentina
Pablo Vidal, Universidad Nacional de Cuyo-CONICET, Argentina
Paula de Andrés Anaya, Escuela Politécnica Superior de Ávila, España
Paula Guerra, Kennesaw State University, EEUU
Paula Peña-Carro, CEDER-CIEMAT, España
Pedro Moreno Bernal, Universidad Autónoma del Estado de Morelos, México
Pedro Piñeyro, Universidad de la República, Uruguay
Ponciano Jorge Escamilla-Ambrosio, Centro de Investigación en
Computación-Instituto Politécnico Nacional, México
Rafael Rosa, Universidad de la República, Uruguay
Ramiro Martins, Polytechnic Institute of Bragança, Portugal
Rasikh Tariq, Tecnológico de Monterrey, México
Raúl Alberto López Meraz, Universidad Veracruzana, México
Renato Andara, Universidad Nacional Experimental Politécnica Antonio José de
Sucre, Venezuela
Renzo Massobrio, Universidad de la República, Uruguay
Ricardo Beltran-Chacon, Centro de Investigación en Materiales Avanzados,
México
Roberto Flores, Universidad Autónoma del Estado de Morelos, México
Roberto Villafáfila, Universitat Politècnica de Catalunya, España
Rodrigo Alonso-Suárez, Universidad de la República, Uruguay
Rodrigo Porteiro, Universidad de la República, Uruguay
Rogelio Vargas Lopez, Universidad Autónoma de Guadalajara, México
Roger Castillo Palomera, Universidad Juárez Autónoma de Tabasco, México
Rui Pedro Lopes, Polytechnic Institute of Bragança, Portugal
Ryszard Edward Rozga Luter, Universidad Autónoma Metropolitana Unidad
Lerma, México
Samanta López Salazar, Centro Nacional de Investigación y Desarrollo
Tecnológico, México
Santiago Iturriaga, Universidad de la República, Uruguay
Sara Gallardo-Saavedra, Universidad de Valladolid, España
Sebastian Montes de Oca, Universidad de la República, Uruguay
Sergio Nesmachnow, Universidad de la República, Uruguay
Silvia Soutullo, CEDER-CIEMAT, España
Susana del Pozo, Universidad de Salamanca, España
Teodoro Calonge, Universidad de Valladolid, España

Thania Guadalupe Lima Tellez, Universidad de Sonora, México

Valentín Cardeñoso-Payo, Universidad de Valladolid, España

Verônica de Menezes Nascimento Nagata, Universidade do Estado do Pará,
Brasil

Veronica Gonzalez, Universidad Autónoma del Estado de Morelos, México

Vicente Canals, Universidad de las Islas Baleares, España

Vicente Leite, Polytechnic Institute of Bragança, Portugal

Víctor Alonso Gómez, Universidad de Valladolid, España

Zakaryaa Zarhri, Universidad Autónoma del Estado de Morelos, México

Program

ICSC-CITIES 2023 coincided in more than ten countries throughout Latin America, Spain, and Portugal. The event was scheduled for a suitable period of the day to facilitate the attendance of students, researchers, and professionals from different countries. The conference program is shown below at the local time of the hosting institution (UTC-6).

Centro de Investigación en Computación - Instituto Politécnico Nacional			
Monday, November 13 (UTC -6)			
Hour (UTC -6)	Speaker(s)	Activity/Paper/Panel name	Session
8:00 - 8:30	Francisco Gutiérrez Galicia, Director de Posgrado del IPN Vianey Urdapilleta Inchaurregui, Jefa de la División de Apoyo a la Investigación, en representación de la Dirección de Investigación. Eusebio Ricárdez Vázquez, Subdirector Académico del CIC Felipe de Jesús Bonilla Sánchez, Director de la Facultad de Contaduría, Administración e Informática, UAEM Luis Hernández Callejo, Universidad de Valladolid (España) Ponciano Jorge Escamilla Ambrosio CIC-IPN	Opening. Chair Santiago Reyes	
8:30 - 10:00	1. Pamela Márquez Morales (Google Cloud México) 2. Vanessa Hernández Mateos (AWS) 3. Huibert Aalbers (IBM) 4. Juan Humberto Sossa Azuela (CIC-IPN)	Panel: ¿Cómo las nuevas tecnologías potencian la creación de ciudades inteligentes? Chair: Juan Humberto Sossa Azuela	
10:00 - 10:20	Coffee break		
10:20 - 10:40	Héctor Mateo, Mario Carbonó, Luis Hernández, Valentin Cardenoso, Miguel Gonzalez, Victor Alonso, Sara Gallardo	Enhancing Solar Cell Classification using Mamdani Fuzzy Logic over Electroluminescence Images: A Comparative Analysis with Machine Learning Methods	

10:40 - 11:00	Hector Mateo, Mario Carbono, Luis Hernández, Miguel González, Valentín Cardeñoso, Víctor Alonso, Oscar Martínez, Sara Gallardo	Estimation of the performance of Photovoltaic Cells by means of an Adaptative Neural Fuzzy Inference model	Artificial Intelligence for Smart Cities Chair: Gilberto Martínez
11:00 - 11:20	Sergio Nesmachnow, Claudio Riso	Forecasting solar photovoltaic power generation: a real-world case study in Uruguay	
11:20 - 11:40	José Hernández, Yessica Calderon, Gustavo Medina, Pedro Moreno, Felipe Bonilla	A new sentiment Analysis methodology for analyzing football game matches utilizing social networks, Artificial Intelligence	
11:40 - 12:00	Alfonso Valenzuela, Guillermo Romero	AI & real estate markets	
12:00 - 12:20	Alejandro Hernandez, Elsa Rubio, Rogelio Álvarez	Intelligent urban cycling assistance based on simplified machine learning	
12:20 - 12:40	Coffee break		
12:40 - 13:00	Halleluyah Kupolati	A PV-Tied Multi-Port Converter	Energy Chair: Víctor Alonso
13:00 - 13:20	Samuel Borroy, Gregorio Fernández, Miguel Sota, Andrés Llombart, Matteo Salani, Marco Derboni, Vincenzo Giuffrida, Angel Zorita, Víctor Alonso, Luis Hernández Callejo	Assessing the Impact of Increasing Electric Vehicle Penetration on Distribution Networks within Sustainable Local Energy Community Frameworks	
13:20 - 13:40	Edwin Garabitos, Alexander Vallejo, Carlos Pereyra	Methodology for the dimensioning of PV systems for self-consumption without surpluses through the specific yield	
13:40 - 14:00	Muhyettin Sirer, Beril Alpagut, Miguel García, José Hernández, Ana Mera, Eduardo Miera	Definition of an evaluation framework to assess the performance, impacts of Positive, Clean Energy Districts (PCEDs) in cities	
14:00 - 14:20	Ángel Germán, Ángel Sánchez, Víctor Peralta, Deyslen Mariano, Eduardo De León, Miguel Aybar	Small Signal Stability Study in Power System with Low Penetration of Renewable Sources	
14:20 - 14:40	Jacinto Vidal, Pere Bibiloni, Iván Alonso, Víctor Martínez, Vicente Canals	Escenario de generación fotovoltaica de la isla de Mallorca para el periodo 2022-2035	
14:40 - 15:00	Alberto Redondo, Luis Hernández, Víctor Alonso, Héctor Mateo, Jose Morales, Sara Gallardo, Víctor Ngungu, Mario Carbono	Novel Passive Luminescence Technique for Photovoltaic Module Characterization: Proof of Concept	

Tuesday, November 14 (UTC -6)			
8:00 - 8:20	Raúl López, Ce Méndez, Yanitzia Reyes, Luis Jamed	Identification of the solar resource in Mexico City applying multivariate analysis	Energy Efficiency, Sustainability Chair: Andrei Tchernykh
8:20 - 8:40	José Morales, Víctor Ndeti, Víctor Alonso, Alberto Redondo, Luis Hernández Callejo, Sara Gallardo, Mario De la Rosa, Héctor Mateo	Integración de Trazador I-V de bajo costo con Sistema de comunicación PLC por lazo resonante en sistemas fotovoltaicos	
8:40 - 9:00	Oscar Izquierdo, Alfonso Madrazo, Ángel Hernández, Paula Peña, Alberto Redondo, Ángel Zorita	Comparative study of the annual production of a floating vs. ground-mounted pilot PV system	
9:00 - 9:20	Samanta López, Efraín Simá, Ruitong Yang, Dong Li, Miguel Chagolla	Numerical study on dynamic thermal characteristics, potential for reducing energy consumption, CO ₂ emissions of multi-glazed windows in developing cities of Mexico	
9:20 - 9:40	Samanta López, Tania Lima-Téllez, Ruitong Yang, Efraín Simá, Irving Hernández, Dong Li	Dynamic and thermal analysis of different strategies to reduce the thermal load of roofs in a tropical climate	
9:40 - 10:20	Coffee break		
10:20 - 12:00	<ol style="list-style-type: none"> 1. Lucía Taboada (ITDP) 2. Oswaldo Sanchez (Director General de la empresa Vinden) 3. Alvaro Madrigal Montes de Oca (Director General de Coordinación de Organismos Públicos y Proyectos Estratégicos) 4. Sergio Nesmachnow (Universidad de la República Uruguay) 	<p>Panel: Digitalización del Transporte Público y sus beneficios.</p> <p>Chair: Sergio Nesmachnow</p>	
12:00 - 12:20	Coffee break		
12:20 - 12:40	Roberto Flores, Nadia Lara	Aplicación de la economía circular para una industria química sustentable	
12:40 - 13:00	Silvina Hipogrosso, Sergio Nesmachnow	Lessons learned from a sustainable mobility analysis in Montevideo, Uruguay	

13:00 - 13:20	Jorge Del Ángel, Ángel Cervantes, Mariel Morales	Aprovechamiento del vapor geotérmico para activar la refrigeración por absorción (ARS) en aplicaciones aledañas a las centrales geotérmicas	Energy Efficiency, Sustainability Chair: Luis Navas
13:20 - 13:40	Margarita Tecpoyotl, Pedro Vargas, Alan Estrada, Ramón Cabello, Volodymyr Grimalsky	Grippers Developed for Intelligent Manufacture Based on a Bioinspired Microgripper	
13:40 - 14:00	Carlos Jiménez, Alfredo Aranda, Moisés Montiel, Martín Rodríguez, Pedro Cruz	Passive solar system: evaluation of the thermal effects of a solar chimney in a room	
14:00 - 14:20	Carlos Torres, Pedro Moreno, Sergio Nesmachnow, Edgar Macias, Karla Aguilar, Luis Hernández, Jesús Arce	Annual evaluation of a single air-channel solar chimney with phase change material under hot-humid climatic conditions of Mexico	
14:20 - 14:40	Oscar Izquierdo, Luis Alvira, Angel Hernández, Paula Peña	Energy management in the CEDER-CIEMAT microgrid based on the time response of the distributed energy storage systems	
14:40 - 15:00	Jorge López, Xavier Cárdenas, Juan Parra, Kevin Narváez, Julver Pino	Catalogue for the construction of sustainable housing from compressed earth blocks	
15:00 - 15:20	Jorge Cerino, Edgar Macias, Karla Aguilar, Oscar May, Carlos Torres, Juan Serrano	Effect of interior and exterior roof coating on heat gain inside a house	
Wednesday, November 15 (UTC -6)			
8:00 - 8:20	Marina Codina, José Forero, Roberto Villafáfila, Sara Barja, Francisco Díaz	Provision of short-term flexibility service from prosumer's facilities	Energy Efficiency, Sustainability Chair: José Morales
8:20 - 8:40	Ofir Alvarez, Mayra Bello, Nancy Ortega, Javier Delgado, David Juárez, José Hernández, Arianna Parrales	Exergoeconomics in Energy Systems: Evaluating technological, economic costs of an AHT	
8:40 - 9:00	Alexander Vallejo, Héctor Morban, Naomy Domínguez, Marino Cabrera, Edwin Garabitos, Idalberto Herrera, José Rickson, Carlos Mariñez, Juan Castellanos, Elvin Jiménez	Urban wind energy potential in the southern region of the Dominican Republic	
9:00 - 9:20	Daniel Alfonso, Vasile Gabriel Amitroae, Santiago Pindado	Estudio práctico de ahorro energético mediante iluminación adaptativa de plataformas aeroportuarias en el Aeropuerto Adolfo Suárez Madrid-Barajas	

9:20 - 9:40	Leonardo Cardinale, Luis Murillo, Efen Jimenez, José Sequeira	Detection of suboptimal conditions in photovoltaic systems integrating data from several domains	
9:40 - 10:00	Oscar Izquierdo, Paula Peña, Ángel Hernández	Integration of Energy Storage, Management Technologies for Optimization of Renewable Energy Operation: CEDER-CIEMAT Demonstration	
10:00 - 10:20	Coffee break		
10:20 - 12:00	<ol style="list-style-type: none"> 1. Ana Villarreal (ITDP-México) 2. Genoveva Vargas Solar (CNRS-Francia) 3. Rosa de Guadalupe González Huerta (ESIQIE-IPN) 4. Marcela Quiroz Castellanos (Univ. Veracruzana) 5. Elsa Rubio Espino (CIC-IPN) 	<p>Panel: Ciudades Inteligentes con perspectiva de género. Chair: Elsa Rubio Espino</p>	
12:00 - 12:20	Coffee break		
12:20 - 12:40	Oscar Izquierdo, Aurora Arroyo, Ángel Hernández, Paula Peña, Angel Zorita, Luis Hernández	Methodology for managing the recharging of EV batteries in a smart microgrid using surplus renewable generation	Smart grid Chair: Rodrigo Porteiro
12:40 - 13:00	Oscar Izquierdo, Paula Peña, Ángel Hernández	The hybrid AC/DC microgrid of CE.D.E.R.-CIEMAT	
13:00 - 13:20	Mahshid Javidsharifi, Najmeh Bazmohammadi, Hamoun Pourroshanfekr Arabani, Juan. Vasquez and Josep. Guerrero	Evaluation of Microgrid Energy Management System in Normal and Abnormal Operation Conditions	
13:20 - 13:40	Yan Pérez, Jack Camacho, Gualberto Magallanes, Deyslen Mariano, Armando Taveras, Giuseppe Sbriz, Miguel Aybar	Implementation of Agrivoltaic Systems under Operating Photovoltaic Park Conditions	
13:40 - 14:00	Miguel Davila, Luis Gonzalez, Luis Hernández Callejo, Oscar Duque-Perez, Ángel L Zorita Lamadrid and Juan Espinoza	Benefits of multiple Electric vehicle aggregators in mountainous areas with high variability of photovoltaic resources	
14:00 - 14:20	Andrei Tchernykh, Mikhail Babenko, Ekaterina Bezuglova, Sergio Nesmachnow, Alexander Drozdov	Securing Smart-city IoT Devices: Challenges, Regulations, Solutions	

14:20 - 15:15	Miguel Ángel Juárez	Ciudadanía digital: hacia la innovación en la administración pública moderna	Posters Chair: Alberto Redondo
	Carlos Barroso, Hortensia Amaris, Monica Alonso, Enrique Puertas	Gestión de baterías de vehículos eléctricos mediante business intelligence y aprendizaje por refuerzo	
	Mario Ibarra, Jonathan Cruz, Jesús Yaljá Montiel, Herón Molina, José Luis López	Prototipo de arreglo tensor sistólico para evaluación de redes neuronales convolucionales	
	Francisco Becerra, José Vera, Luis Cisneros, Zakaryaa Zarhri	Mapping Evolution in Solar Panel Research: A Bibliometric Analysis of Research Results during 1992-2023	
	Pedro Flores, Luis Cisneros, Zakaryaa Zarhri, Mario Limon	Research in Electromechanical Efficiency: A Bibliometrics Analysis of the Last 82 Years (1941 to 2023)	
	Luis Lira, Zakaryaa Zarhri, Luis Cisneros, Mario Limon	Bibliometric Analysis of Contemporary Research on Charge Transfers between Medium Voltage Power Distribution Circuit	
	Eduardo Barreiro, Zakaryaa Zarhri, Roy Lopez, Mario Limón	Bibliometric research for design, build a Potentiostat with WiFi connectivity to electrochemical characterization of metal surfaces.	
	Juan Rodríguez, Domingo Martin, Javier Maroto, Alfredo Marín, Ana García, Jorge Costafreda	CanarIoT: Monitoring of environmental variables such as CO ₂ , at the service of university resilience in a pandemic, through IoT solutions	
	Luis Ruiz, Luis Cisneros, Zakaryaa Zarhri	Global bibliometric analysis of railway, train research: focus on Latin America, Mexico	
	David Flores, Zakaryaa Zarhri, Jose Vera, Mario Limon	Bibliometric study: feasibility of RFID technology. IoT systems for their integration in mexican educational institutions	
Juan Peralta, Zakaryaa Zarhri, Guadalupe Velásquez, Mario Limon	Economic feasibility analysis of the implementation of solar panels in educational institutions in the State of Morelos. A bibliometric analysis		

Universidad Autónoma del Estado de Morelos			
Thursday, November 16 (UTC -6)			
9:00 - 9:20	Gustavo Urquiza - Rector UAEM		Bienvenida sede UAEM
	Felipe Bonilla - Director de la Facultad de Contaduría, Administración e Informática		
	Angélica Galindo - Encargada de la Dirección de la Facultad de Ciencias Químicas e Ingeniería		
	Luis Hernández - Universidad de Valladolid		
	Ponciano Escamilla - CIC-IPN		
9:20 - 9:40	Montse Delpino	VISUALIZING CITIZENS' PERCEPTIONS. Subjective indicators for the assessment of urban environments based on digital platforms.	Governance, Citizenship
9:40 - 10:00	Carlos Grande, Luis Navas, Misael Martínez	Características institucionales que impulsan la movilidad urbana socialmente sostenible, aportes desde del Triángulo Norte Centroamericano	Chair: Leticia Neria
10:00 - 10:20	Coffee break		
10:20 - 10:40	Raúl Maján, Lidia Sanz, Susana Gómez, Lilian Johanna	Third sector agents, the University of Valladolid as one of the driving forces of the urban agenda in the city of Soria, Spain.	Smart Economy, Development, Education Chair: Pedro Moreno
10:40 - 11:00	Ana Lozano, Diego Revilla, Sonia Ortega, Judith Quintano	El valor de la Educación para la Ciudadanía Mundial en el marco de Agenda 2030 y la construcción de ciudades inteligentes y sostenibles: La iniciativa Soria 2030	
11:00 - 11:20	Luis Andrade, César Castrejón, Jordi González, Jesús Montiel, José López	Linear Predictive Coding vs. Kalman Filter for Urban Finance Prediction in Smart Cities with S&P/BMV IPC	
11:20 - 11:40	Juan Rodríguez, Alfredo Marín, Domingo Martín, Javier Maroto, Fernando Barrio, Luis Fernández	3D printing as an enabler of innovation in universities. Tellus UPM Ecosystem Case	
11:40 - 12:00	Luisa Lozano, Luis Navas, Isabel Lozano, Adriana Correa	Structural challenges, solutions to improve indoor agriculture	Smart Environment

12:00 - 12:20	Ouiam Boukharta, Iona Huang, Laura Vickers, Luis Navas, Leticia Chico	Benefits of non-commercial Urban Agriculture practices – a Systematic Review	Chair: Alberto Hernández
12:20 - 12:40	Jesús Aboytes, Eric Ibarra, Marco Ramírez, Gina Gallegos, Ponciano Escamilla	Innovative Compression plus Confusion Scheme for Digital Images used in Smart Cities	
12:40 - 13:00	Coffee break		
13:00 - 13:20	Pablo Guerrero, Belem Hernández, José Guerrero, Victor Pacheco, Rosa Álvarez, Felipe Bonilla	Harnessing Computer Science to Drive Sustainable Supply Chains Facing Resilience Organizational Complexity	Smart Industry Chair: Diego Rossit
13:20 - 13:40	Diego Rossit, Daniel Rossit, Sergio Nesmachnow	Smart industry strategies for shop-floor production planning problems to support mass customization	
13:40 - 14:00	Carmen Peralta, Pedro Moreno, Beatriz Martínez, Juana Enríquez, Felipe Bonilla	Optimizing the Rework Area in an Automotive Parts Supplier Company by digital tools: A Foundation for Smart Industry Transformation	
14:00 - 14:20	Arismendy Del Orbe, José Durán, Deyslen Hernández, Elvin Jiménez, Giuseppe Sbriz, Miguel Aybar	Analysis of the incorporation of battery electric scooters, trucks in an underground mining company in the Dominican Republic	Smart Mobility Chair: Ponciano Escamilla
14:20 - 14:40	Alexander Vallejo, Elvin Jiménez	Analysis of optimization of the charge of electric vehicles in a subsidized market based on the tariff of the time of use of electricity. Dominican Republic case study	
14:40 - 15:00	Ernesto De La Cruz, Alicia Martínez, Hugo Estrada, Odette Pliego	Methodology to obtain traffic data, road incidents through maps applications	
15:00 - 15:20	Julio Carmona, Raúl López, Tochtli Méndez, Miguel Maldonado	Development of a single-phase speed regulating inverter using pulse width modulation	
Friday, November 17 (UTC -6)			
8:00 - 8:20	Pablo Llagueiro, Rodrigo Porteiro, Sergio Nesmachnow	Characterization of household electricity consumption in Uruguay	Smart Public Services
8:20 - 8:40	Adriana Cervantes, Ulises León, María Nicho	Síntesis novedosa de alginato de sodio, celulosa y nanocelulosa para	Chair: Diego Rossit

		la valorización de la biomasa de sargazo	
8:40 - 9:00	Víctor Padrón, José Esteban, Esther Pizarro, Juan López, Esther Delgado, Alberto Bellido, Rafael Muñoz, Olalla García, Patricio Martínez, Ignacio Loscertales, Silvia Álvarez, Mariana Arteaga	The design of HERMÓPOLIS. An architectonic, artistic, technological, entertainment, health, social Smart Cities platform oriented to improve the quality of life of the elder people	
9:00 - 9:20	Diego Rossit, Sergio Nesmachnow, Antonella Cavallin	Municipal Solid waste management systems: application of SWOT methodology to analyze an Argentinean case study	
9:20 - 9:40	Olegs Cernisevs, Sergejs Popovs	Smart city Green fintech: impact of the EU policies on Sustainable Urban Development, Financial innovations	
9:40 - 10:00	Gustavo Medina, Gennadiy Burlak, Felipe Bonilla	Levels of plasmon-polariton oscillations produced by Cherenkov radiation on a CNT system for different nanotube saturations	
10:00 - 10:20	Coffee break		
10:20 - 10:40	Diego Godoy, César Gallardo, Ricardo Selva, Nicolas Ibarra, Carlos Kornuta, Enrique Albornoz	Detection of personal protection elements in a recycling plant using convolutional neural networks	Smart Public Services Chair: Rodrigo Porteiro
10:40 - 11:00	Victor Ortega, Eugenio Tamura	Aquality: A Scalable IoT-enabled Drinking Water Quality Monitoring System	
11:00 - 11:20	Diego Rossit, Begoña González, Mariano Frutos, Máximo Méndez	An allocation-routing problem in waste management planning: exact, heuristic resolution approaches	
11:20 - 11:40	Jorge Mírez	Modelamiento y simulación de disponibilidad de agua dulce en entornos urbanos a partir de humedad atmosférica	
11:40 - 12:00	Ivonne Arce, Pedro Moreno, Víctor Pacheco, Maria Torres, Sergio Nesmachnow, Viridiana León	Simulated Annealing metaheuristic approach for municipal solid waste collecting route problem in the Historical Center of a Mexican city	
12:00 - 12:20	Coffee break		

12:20 - 12:40	Galileo Tinoco, Jorge El Mariachet, Roberto Tapia, Gustavo Branco, José Matas, Wael Al Hanaineh	Proposal for clean urban on-boat transportation with photovoltaic and biomass hybridity in the Patzcuaro Lake of Michoacán (Mexico)	Urban Informatics, Big Data, Analytics for Smart Cities & Other developments for Smart Cities Chair: Carlos Torres
12:40 - 13:00	Eduardo Bennesch, Diego Godoy, Karina Eckert	GeoLocation accuracy measurement of free to use available GIS API's	
13:00 - 13:20	Diego Godoy, Lucas Martín, Luna Blanco	Posadas SDI: Transparent Integration with KoboToolBox using Foreign Data Wrappers	
13:20 - 13:40	Diana Romero, Ricardo Alcaraz, Ponciano Escamilla	Framework for Upscaling Missing Data in Electricity Consumption Datasets Using Generative Adversarial Networks	
13:40 - 14:00	Christopher Almachi, Rolando Armas, Erick Cuenca	Visual Analytic of Traffic Simulation Data: A review	
14:00 - 14:20	Marco Moreno, Magdalena Saldaña, Juan Venegas	Leveraging User-Generated Content to Improve Urban Traffic Management in the context of Smart Cities	
14:20 - 14:40	Juan Martínez	Centros Históricos en el contexto de las Ciudades Inteligentes y Sostenibles	
14:40 - 15:00	Felipe Bonilla	Awards for the best works. Closure.	
	Angélica Galindo		
	Luis Hernández		

Contents

Artificial Intelligence for Smart Cities

Forecasting solar photovoltaic power generation: a real-world case study in Uruguay 1
Sergio Nesmachnow and Claudio Risso

AI & real estate markets 16
Alfonso Valenzuela Aguilera and Guillermo Romero Tecua

Energy

A PV-Tied Multi-Port Converter 31
Hallehuyah Kupolati

Assessing the Impact of Increasing Electric Vehicle Penetration on Distribution Networks within Sustainable Local Energy Community Frameworks 49
Samuel Borroy, Gregorio Fernández, Miguel Sota, Andres Llombart, Matteo Salani, Marco Derboni, Vincenzo Giuffrida, Angel Luis Zorita Lamadrid, Víctor Alonso Gómez and Luis Hernández-Callejo

Methodology for the dimensioning of PV systems for self-consumption without surpluses through the specific yield 64
Edwin Garabitos Lara, Alexander Vallejo Díaz and Carlos Napoleón Pereyra Mariñez

Definition of an evaluation framework to assess the performance and impacts of Positive and Clean Energy Districts (PCEDs) in cities 81
Muhyettin Siner, Beril Alpagut, Miguel Á. García-Fuentes, José L. Hernández, Ana Mera and Eduardo Miera

Small Signal Stability Study in Power Systems with Low Penetration of Renewable Sources 96
Angel-Dagoberto Germán-Encarnación, Angel-José Sánchez-Sánchez, Víctor Ernesto Peralta Maxwell, Deyslen Mariano-Hernández, Eduardo De León-Concepción and Miguel Aybar-Mejía

Escenario de generación fotovoltaica de la isla de Mallorca para el periodo 2022-2035 110
Jacinto Vidal-Noguera, Pere Antoni Bibiloni-Mulet, Iván Alonso de Miguel, Víctor Martínez-Moll, Andreu Mojà-Pol and Vicente José Canals Guinand

Electronic device for passive luminescence imaging acquisition: Proof of concept 123
Alberto Redondo Plaza, José Ignacio Morales Aragonés, Víctor Alonso Gómez, Ángel L. Zorita Lamadrid, Sara Gallardo Saavedra, Héctor Felipe Mateo Romero, Mario Eduardo Carbono dela Rosa, Victor Ndeti Ngungu, Laura Gabriela Rojas Delgado and Luis Hernández Callejo

Levels of plasmon-polariton oscillations produced by Cherenkov radiation on a CNT system for different nanotube saturations	137
<i>Gustavo Medina Angel, Gennadiy Burlak and Felipe Bonilla-Sánchez</i>	
Energy Efficiency and Sustainability	
Identification of the solar resource in Mexico City applying multivariate analysis	150
<i>López-Meraz R. A., Méndez-Ramírez C., Reyes-Cárcamo Y. and Jamed-Boza L. O.</i>	
Optimización de dispositivo para trazado I-V en línea de módulos solares individuales y comunicaciones PLC	163
<i>José Ignacio Morales Aragonés, Víctor Ndeti Ngungu, Víctor Alonso Gómez, Alberto Redondo Plaza, Luis Hernández Callejo, Sara Gallardo Saavedra, Mario Eduardo Carbonó Dela Rosa and Héctor Felipe Mateo Romero</i>	
Comparative study of the annual production of a floating vs. ground-mounted pilot PV system	178
<i>Oscar Izquierdo Monge, Alfonso Madrazo Alonso-Majagranzas, Paula Peña Carro, Alberto Redondo Plaza, Ángel Hernández Jiménez and Ángel Zorita Lamadrid</i>	
Numerical study on dynamic thermal characteristics, potential for reducing energy consumption, CO ₂ emissions of multi-glazed windows in developing cities of Mexico	193
<i>Samanta López Salazar, E. Simá, Ruitong Yang, Dong Li and M.A. Chagolla-Aranda</i>	
Comparative assessment of roofing strategies for thermal load reduction, energy efficiency, and CO ₂ emission mitigation in a tropical climate	208
<i>Samanta López Salazar, T. Lima-Téllez, Ruitong Yang, E. Simá, I. Hernández-López and Dong Li</i>	
Aplicación de la economía circular para una industria química sustentable	223
<i>Roberto Flores and Nadia Lara</i>	
Lessons learned from a sustainable mobility analysis in Montevideo, Uruguay	236
<i>Sergio Nesmachnow and Silvina Hipogrosso</i>	
Aprovechamiento del vapor geotérmico para activar la refrigeración por absorción (ARS) en aplicaciones aledañas a las centrales geotérmicas	250
<i>A. Uriel Cervantes C., Jorge A. Del Angel R., Omar Montiel P., Mariel Morales M. and Luz M. Hernández A.</i>	
Grippers Developed for Intelligent Manufacture Based on a Bioinspired Microgripper	264
<i>M. Tecpoyotl-Torres, P. Vargas-Chable, A.J. Estrada-Cabrera, R. Cabello-Ruiz and V. Grimalsky</i>	
Passive solar system: evaluation of the thermal effects of a solar chimney in a room	280
<i>C. Jiménez-Xaman, Alfredo Aranda-Arizmendi, Moisés Montiel-González, Martín Rodríguez-Vázquez and Pedro Cruz-Alcantar</i>	

Annual evaluation of a single air-channel solar chimney with phase change material under hot-humid climatic conditions of Mexico	295
<i>Carlos E. Torres-Aguilar, Pedro Moreno-Bernal, Sergio Nesmachnow, Edgar V. Macias-Melo, Karla M. Aguilar-Castro, Luis Hernández-Callejo and Jesús Arce</i>	
Energy management in the CEDER-CIEMAT microgrid based on the time response of the distributed energy storage systems	311
<i>Luis Alvira Ballano, Oscar Izquierdo-Monge, Angel Hernandez Jimenez and Paula Peña Carro</i>	
Catalogue for the construction of sustainable housing from compressed earth blocks	326
<i>Jorge López-Rebollo, Xavier Cárdenas-Haro, Juan Parra-Vargas, Kevin Narváez-Berrezueta and Julver Pino</i>	
Effect of interior and exterior roof coating on heat gain inside a house	341
<i>J. L. Cerino-Isidro, E. V. Macias-Melo, K.M. Aguilar-Castro, O. May Tzuc, C.E. Torres-Aguilar and J. Serrano-Arellano</i>	
Provision of short-term flexibility service from prosumer's facilities	356
<i>Marina Codina Escolar, José Fernando Forero-Quintero, Roberto Villafáfila Robles, Francisco Díaz Gonzalez and Sara Barja-Martinez</i>	
Exergoeconomics in Energy Systems: Evaluating technological and economic costs of an AHT	370
<i>Lailani Alvarez, Mayra Harumi Bello Guadarrama, N.I. Ortega-Mojica, J. Delgado-Gonzaga, D. Juárez-Romero, J.A. Hernández and A. Parrales</i>	
Urban wind energy potential in the southern region of the Dominican Republic	385
<i>Alexander Vallejo, Héctor Morban, Naomy Domínguez, Marino Cabrera, Edwin Garabitos, Idalberto Herrera, José Andrickson, Carlos Pereyra, Juan Castellanos, Elvin Jiménez and Cándida Casilla</i>	
Estudio práctico de ahorro energético mediante iluminación adaptativa de plataformas aeroportuarias en el Aeropuerto Adolfo Suárez Madrid-Barajas	401
<i>Daniel Alfonso-Corcuera, Vasile Gabriel Amitroae and Santiago Pindado</i>	
Integration of Energy Storage and Management Technologies for Optimization of Renewable Energy Operation: CEDER-CIEMAT Demonstration	416
<i>Paula Peña-Carro, Oscar Izquierdo-Monge and Angel Hernandez-Jimenez</i>	

Smart grid

Methodology for managing the recharging of EV batteries in a smart microgrid using surplus renewable generation	431
<i>Oscar Izquierdo-Monge, Aurora Arroyo Garcia, Paula Peña-Carro, Ángel Hernández Jiménez, Ángel Zorita Lamadrid and Luis Hernández-Callejo</i>	
The hybrid AC/DC microgrid of CEDER-CIEMAT	446
<i>Paula Peña-Carro, Ángel Hernandez-Jimenez and Oscar Izquierdo-Monge</i>	
Evaluation of Microgrid Energy Management System in Normal and Abnormal Operation Conditions	460
<i>Mahshid Javidsharifi, Najmeh Bazmohammadi, Hamoun Pourroshanfekr Arabani, Juan. C. Vasquez and Josep. M. Guerrero</i>	
Implementation of Agrivoltaic Systems under Operating Photovoltaic Park Conditions	475
<i>Yan Carlos Pérez Mejía, Jack Wesly Camacho, Gualberto Magallanes-Galla, Deyslen Mariano, Armando J. Taveras Cruz, Giuseppe Sbriz-Zeitun and Miguel Aybar Mejía</i>	
Benefits of multiple Electric vehicle aggregators in mountainous areas with high variability of photovoltaic resources	490
<i>Miguel Davila-Sacoto, L.G. González, Luis Hernández-Callejo, Óscar Duque-Perez, Ángel L. Zorita-Lamadrid and J.L. Espinoza</i>	
Securing Smart-city IoT Devices: Challenges, Regulations, and Solutions	503
<i>Andrei Tchernykh, Mikhail Babenko, Ekaterina Bezuglova, Sergio Nesmachnow and Alexander Yu. Drozdov</i>	

Governance and Citizenship

Visualizing Citizens' perceptions. Subjective indicators for the assessment of urban environments based on digital platforms	518
<i>Montse Delpino-Chamy</i>	
Características institucionales que impulsan la movilidad urbana socialmente sostenible: Aportes del Triángulo Norte Centroamericano	533
<i>Carlos Ernesto Grande, Luis Manuel Navas and Misael Martínez</i>	

Smart Economy, Development and Education

Third sector actors and the University of Valladolid as one of the drivers of the urban agenda in the city of Soria, Spain 548

*Raúl Maján-Navalón, Lidia Sanz-Molina, Susana Gómez-Redondo
and Lilian Johanna-Obregón*

El valor de la Educación para la Ciudadanía Mundial en el marco de Agenda 2030 y la construcción de ciudades inteligentes y sostenibles: La iniciativa Soria 2030 562

*Ana Isabel Lozano Sobrino, Sonia Ortega Gaité, Judith Quintano Nieto
and Diego Miguel-Revilla*

Smart Environment

Structural challenges and solutions to improve indoor agriculture 572

*Luisa F. Lozano-Castellanos, Luis M. Navas-Gracia, Isabel C. Lozano-Castellanos
and Adriana Correa-Guimaraes*

Benefits of non-commercial Urban Agricultural practices – a Systematic Review 584

O.F. Boukharta, L. Chico-Santamarta, I.Y. Huang, L. Vickers and L.M. Navas-Gracia

Smart Mobility

Analysis of the incorporation of battery electric scooters and trucks in an underground mining company in the Dominican Republic 599

*Arismendy José Del Orbe, José Gabriel Durán García, Deyslen Mariano-Hernández,
Elvin Arnaldo Jiménez Matos, Giuseppe Sbriz-Zeitun and Miguel Aybar-Mejía*

Electric vehicles charging schedule optimization based on time-of-use tariff. Case study of the Dominican Republic 613

Alexander Vallejo Díaz and Elvin Arnaldo Jiménez Matos

Development of a single-phase speed regulating inverter using pulse width modulation 628

*Carmona-Valdés J.C., López-Meraz R.A., Méndez-Ramírez C.T.
and Maldonado-Martínez M.*

Smart Public Services

Síntesis novedosa de alginato de sodio, celulosa y nanocelulosa para la valorización de la biomasa de sargazo 641

*Adriana Cervantes, U. León-Silva, M.E. Nicho, J. Jesús Escobedo-Alatorre
and Carlos F. Castro-Guerrero*

The design of HERMÓPOLIS. An architectonic, artistic, technological, entertainment, health and social Smart Cities platform oriented to improve the quality of life of the elder people 653

*Víctor Manuel Padrón Nápoles, José Luis Esteban Penelas, Esther Pizarro Juanas,
Juan Diego López Arquillo, Esther Delgado Pérez, Alberto Bellido, Rafael Muñoz Gil,
Olalla García Pérez, Patricio Martínez García, Ignacio Loscertales,
Silvia Álvarez Menéndez and Mariana Bernice Arteaga Orozco*

Municipal Solid waste management systems: application of SWOT methodology to analyze an Argentinean case study 668

Diego Rossit, Sergio Nesmachnow and Antonella Cavallin

Smart city Green fintech: impact of the EU policies on Sustainable Urban Development and Financial innovations 681

Olegs Cernisevs and Sergejs Popovs

Freshwater availability in urban environments from atmospheric humidity 699

Jorge Mírez

Urban Informatics, Big Data, Analytics for Smart Cities & Other developments for Smart Cities

Proposal for clean Urban on-boat transportation with photovoltaic and biomass hybridity in the Patzcuaro Lake of Michoacán (Mexico) 707

*Galileo Cristian Tinoco Santillán, Jorge El Mariachet Carreño,
Roberto Tapia Sanchez, Gustavo C. Branco, José Matas Alcalá and Wael Al Hanaineh*

GeoLocation accuracy measurement of free-to-use available GIS API's 717

Eduardo Hugo Bennesch, Diego Alberto Godoy and Karina Eckert

Posadas SDI: Transparent Integration with KoboToolBox using Foreign Data Wrappers 726

Diego Alberto Godoy, Lucas Martín Jardín and Luna Blanco

Leveraging User-Generated Content to Improve Urban Traffic Management in the context of Smart Cities 737

Marco Moreno-Ibarra, Magdalena Saldaña-Perez and Juan Carlos Venegas Segura

Centros Históricos en el contexto de las Ciudades Inteligentes y Sostenibles 744

Juan Carlos Martínez Serra

Posters

Ciudadanía digital: hacia la innovación en la administración pública moderna	762
<i>Miguel Ángel Juárez</i>	
Gestión de baterías de vehículos eléctricos mediante business intelligence y aprendizaje por refuerzo	763
<i>Carlos Barroso, Hortensia Amaris, Monica Alonso and Enrique Puertas</i>	
Prototipo de arreglo tensor sistólico para evaluación de redes neuronales convolucionales	764
<i>Mario Ibarra, Jonathan Cruz, Jesús Yaljá Montiel, Herón Molina and José Luis López</i>	
Mapping Evolution in Solar Panel Research: A Bibliometric Analysis of Research Results during 1992-2023	765
<i>Francisco Becerra, José Vera, Luis Cisneros and Zakaryaa Zarhri</i>	
Research in Electromechanical Efficiency: A Bibliometrics Analysis of the Last 82 Years (1941 to 2023)	766
<i>Pedro Flores, Luis Cisneros, Zakaryaa Zarhri and Mario Limon</i>	
Bibliometric Analysis of Contemporary Research on Charge Transfers between Medium Voltage Power Distribution Circuit	767
<i>Luis Lira, Zakaryaa Zarhri, Luis Cisneros and Mario Limon</i>	
Bibliometric research for design, build a Potentiostat with WiFi connectivity to electrochemical characterization of metal surfaces	768
<i>Eduardo Barreiro, Zakaryaa Zarhri, Roy Lopez and Mario Limón</i>	
CanarIoT: Monitoring of environmental variables such as CO ₂ , at the service of university resilience in a pandemic, through IoT solutions	769
<i>Juan Rodríguez, Domingo Martin, Javier Maroto, Alfredo Marín, Ana García and Jorge Costafreda</i>	
Global bibliometric analysis of railway, train research: focus on Latin America, Mexico	770
<i>Luis Ruiz, Luis Cisneros and Zakaryaa Zarhri</i>	
Bibliometric study: feasibility of RFID technology. IoT systems for their integration in Mexican educational institutions	771
<i>David Flores, Zakaryaa Zarhri, Jose Vera and Mario Limon</i>	
Economic feasibility analysis of the implementation of solar panels in educational institutions in the State of Morelos. A bibliometric analysis	772
<i>Juan Peralta, Zakaryaa Zarhri, Guadalupe Velásquez and Mario Limon</i>	

Articles selected for publication in Volume 1938 of the Communications in Computer and Information Science series by Springer-Nature with DOI:
<https://doi.org/10.1007/978-3-031-52517-9>

Enhancing Solar Cell Classification using Mamdani Fuzzy Logic over Electroluminescence Images: A Comparative Analysis with Machine Learning Methods

Héctor Felipe Mateo Romero, Mario Eduardo Carbonó Dela Rosa, Luis Hernández Callejo, Valentin Cardeñoso Payo, Miguel Angel Gonzalez Rebollo, Victor Alonso Gomez and Sara Gallardo Saavedra

Harnessing Computer Science to Drive Sustainable Supply Chains Facing Resilience Organizational Complexity

Pablo Guerrero, Belem Hernández, José Guerrero, Victor Pacheco, Rosa Álvarez and Felipe Bonilla-Sanchez

Estimation of the performance of Photovoltaic Cells by means of an Adaptive Neural Fuzzy Inference model

Hector Felipe Mateo Romero, Mario Carbono de la Rosa, Luis Hernández Callejo, Miguel Angel González, Valentin Cardeñoso-Payo, Víctor Alonso Gómez, Oscar Martinez Sacristan and Sara Gallardo-Saavedra

Smart industry strategies for shop-floor production planning problems to support mass customization

Diego Rossit, Daniel Rossit and Sergio Nesmachnow

Optimizing the Rework Area in an Automotive Parts Supplier Company by digital tools: A Foundation for Smart Industry Transformation

Jesús Del Carmen Peralta-Abarca, Pedro Moreno-Bernal, Beatriz Martínez-Bahena, Juana Enríquez-Urbano and Felipe Bonilla-Sánchez

Framework for Upscaling Missing Data in Electricity Consumption Datasets Using Generative Adversarial Networks

Diana Romero, Ricardo Alcaraz-Fraga and Ponciano Jorge Escamilla-Ambrosio

Methodology to obtain traffic data and road incidents through maps applications

Ernesto De La Cruz Nicolás, Alicia Martínez Rebollo, Hugo Estrada Esquivel and Odette Alejandra Pliego Martínez

Detection of personal protection elements in a recycling plant using convolutional neural networks

Diego Alberto Godoy, Cesar Gallardo, Ricardo Selva, Nicolas Ibarra, Carlos Kornuta and Enrique Marcelo Albornoz

Aquality: A Scalable IoT-enabled Drinking Water Quality Monitoring System

Victor M. Ortega Pabon and Eugenio Tamura

[A new sentiment Analysis methodology for analyzing football game matches utilizing social networks and Artificial Intelligence](#)

José Alberto Hernández, Yessica Calderon-Segura, Gustavo Medina-Angel, Pedro Moreno-Bernal, Felipe Bonilla-Sanchez, Jesús del Carmen Peralta-Abarca and Gennadiy Burlak

[Detection of suboptimal conditions in photovoltaic systems integrating data from several domains](#)

Leonardo Cardinale-Villalobos, Luis D. Murillo-Soto, Efrén Jiménez-Delgado and Jose A. Sequeira

[Characterization of household electricity consumption in Uruguay](#)

Pablo Llagueiro, Rodrigo Porteiro and Sergio Nesmachnow

[An allocation-routing problem in waste management planning: exact and heuristic resolution approaches](#)

Diego Rossit, Begoña González Landín, Mariano Frutos and Máximo Méndez Babey

[Simulated Annealing metaheuristic approach for municipal solid waste collecting route problem in the Historical Center of a Mexican city](#)

Ivonne Arce-García, Pedro Moreno-Bernal, Víctor Pacheco-Valencia, María del Carmen Torres-Salazar, Sergio Nesmachnow and Viridiana A. León-Hernández

[3D printing as an enabler of innovation in universities: Tellus UPM Ecosystem Case](#)

Juan Antonio Rodríguez Rama, Alfredo Marín Lázaro, Domingo Alfonso Martín Sánchez, Javier Maroto Lorenzo, Fernando Barrio Parra and Juis J. Fernández Gutiérrez del Álamo

[Visual Analytic of Traffic Simulation Data: A review](#)

Christopher Almachi, Rolando Armas and Erick Cuenca

[Innovative Compression plus Confusion Scheme for Digital Images used in Smart Cities](#)

Jesús Agustín Aboytes-González, Eric Ibarra-Olivares, Marco Tulio Ramírez-Torres, Gina Gallegos-García and Ponciano Jorge Escamilla-Ambrosio

[Intelligent urban cycling assistance based on simplified machine learning](#)

Alejandro Hernández Herrera, Elsa Rubio Espino and Rogelio Álvarez Vargas

[Linear Predictive Coding vs. Kalman Filter for Urban Finance Prediction in Smart Cities with S&P/BMV IPC](#)

Luis Enrique Andrade-Gorjoux, Cesar Castrejón-Peralta, Jordi Fabián González-Contreras, Jesús Yaljá Montiel-Pérez and José Luis López-Bonilla

Artificial Intelligence for Smart Cities

Forecasting solar photovoltaic power generation: a real-world case study in Uruguay

Sergio Nesmachnow ^[0000–0002–8146–4012]
and Claudio Riso ^[0000–0000–0000–0000]

Facultad de Ingeniería
Universidad de la República, Uruguay
sergion@fing.edu.uy, crisso@fing.edu.uy

Abstract. This article presents the application of Artificial Neural Networks to forecast renewable (solar photovoltaic) power generation in Uruguay. Accurate prediction of the power output is crucial for designing a reliable photovoltaic power generation system. Predictions allows applying effective planning, management, and distribution strategies of the generated power, improving the performance and efficiency of the system. The study considers real data of solar photovoltaic power generation in Uruguay between 2018 and 2022. A Long Short Term Memory artificial neural network is applied for forecasting. The main results indicate that the proposed approach is effective for forecasting, accounting for average values of root mean square error of 0.14. The generated forecasts are useful to be applied in planning and scheduling to improve the quality of service.

Keywords: renewable energy, forecasting, Artificial Neural Networks, real-wold case study

1 Introduction

Renewable energy sources, such as wind and solar power, have become increasingly important as a means of reducing greenhouse gas emissions and mitigating climate change. However, the variability and intermittency of renewable energy sources pose significant challenges for their integration into the electricity grid. Accurate and reliable predictions of renewable energy generation are essential to provide useful methods for the effective integration into smart grid operation mechanisms. In turn, the predictions are key for optimizing energy management and ensuring the stability and reliability of the electric grid.

* Corresponding author: Sergio Nesmachnow, sergion@fing.edu.uy

This research was developed within a joint project with the Uruguayan electricity company, UTE

2 Sergio Nesmachnow and Claudio Risso

In recent years, significant progress has been made in the development of forecasting models for renewable energy generation. The proposed models use several different data sources, including historical energy production data, weather forecasts, and other relevant information. Computational intelligence and machine learning algorithms are applied to predict the output of renewable energy sources with high accuracy. The benefits of accurate predictions of renewable energy generation are significant, including improved grid reliability, reduced energy costs, and increased renewable energy integration. In particular, accurate prediction of the power output is essential in the design of a reliable photovoltaic power generation system. This capability enables effective planning, management, and distribution of the generated power, ensuring optimal performance and efficiency of the system.

In this line of work, this article presents the application of computational intelligence models, namely artificial neural networks to forecast renewable (solar photovoltaic) power generation in Uruguay, developed in a joint research project between UTE and Universidad de la República. The study considers several data sources accounting for real data in the 2018–2022 period. Uruguay has made significant progress in recent years in transitioning its electricity grid towards renewable energy sources, with wind and solar power accounting for over 60% of the electricity generation in the country, and over 85% of share (sixth in the World, according to the Latin American Energy Organization, www.olade.org, June 2023). Proper forecasting tools for renewable energy generation allow developing and optimizing operation schemes to guarantee a proper reliability and quality of service, under the smart grid paradigm [1].

A Long Short Term Memory artificial neural network is applied for forecasting. The experimental evaluation of the proposed computational intelligence method indicates that the approach is effective for forecasting. The main results showed an average value of the Root Mean Square Error (RMSE) metric of 0.14. The generated forecasts are useful inputs to be used in stochastic optimization models for planning and scheduling to improve the quality of service of the electric grid.

The article is organized as follows. Section 2 describes the problem of forecasting renewable energy generation and reviews related works, with especial focus on the considered case study in Uruguay. Section 3 describes the proposed approach and the details of the developed artificial neural network implementation. Section 4 presents the experimental evaluation of the proposed approach for solar photovoltaic power generation forecasting and discusses the obtained results. Finally, Section 5 presents the conclusions of the research and formulates the main lines for future work.

2 Problem definition and literature review

This section describes the addressed forecasting problem and reviews relevant related works.

2.1 Problem description

The proposed problem is forecasting the time series of solar photovoltaic power generation in Uruguay, using real data provided by the National electricity utility UTE (Administración Nacional de Usinas y Trasmisiones Eléctricas).

The forecast must be computed for each hour within a horizon of three days (72 hours), to be properly applied in the process of determining the optimal scheduling and allocation of available electricity generation resources to meet the demand for electricity in a power system. The scheduling/control problem involves making decisions on which power plants to operate, how much power each plant should generate, and when to dispatch the generated electricity to meet the load requirements. This is a crucial problem to guarantee a reliable and efficient operation of the power system while minimizing costs, improving grid reliability, and also increasing renewable energy integration.

The multi-hours forecasting problem is a significantly harder problem than the short-term photovoltaic power generation forecasting problem (e.g., considering a forecasting horizon of only one or a few hours), which has been previously solved in several related works. The forecasting tool must predict a sequence of multiple values of the time series of solar photovoltaic power generation in Uruguay. The available information to perform the predictions is the time series of past solar photovoltaic power generation observations, and estimations provided by the Spanish global service provider Meteologica (www.meteologica.com/, accessed on September 2023), computed based on numerical weather prediction models.

According to the considered forecasting horizon, the problem falls within the long-term forecast category [2]. Although some authors have considered long-term forecasting problems ranging from one month to one year, to take advantage of seasonal variations and specific climate and/or generation patterns, the most usual categorizations include forecasts in an horizon of more than 24 hours as long-term [19]. The multi-hour forecasting problem is more challenging than the short-term (up to six hours) and medium-term (six hours to a day) forecasting problems. When using an extended forecasting horizon, because the prediction error tends to increase for forecasts made further into the future. In other words, the accuracy of the forecast decreases as the time horizon extends, making it more difficult to accurately predict electricity demand or other relevant factors for later hours in the forecast period.

2.2 Related work

Several articles have studied the problem and demonstrated the importance of renewable energy forecasting for energy management.

A recent article by Iheanetu [8] has reviewed several approaches applying artificial neural networks, metaheuristics, fuzzy logic, and hybrid models. Most of the reviewed articles focused on short-term solar power forecasting.

Ding et al. [5] applied artificial neural networks and a similarity method to forecast the power generated by a photovoltaic system one day ahead. The minimum Mean Absolute Percentage Error (MAPE) values obtained were 10.1% on sunny days and 18.9% on rainy days. Zhu et al. [27] applied an hybrid method combining artificial neural networks and wavelet decomposition for solar photovoltaic power generation. RMSE values ranged from 7.2% (for clear days) to 16-19% (cloudy and rainy days).

El hendouzi et al. [6] applied artificial neural networks for very short-term solar power forecasting for small photovoltaic installations. RMSE values between 8% and 11% were reported for the small case studies using a nonlinear autoregressive exogenous neural network model.

Zhang et al. [26] studied artificial neural networks models for predicting the short-term power generation of a photovoltaic panel. The comparative analysis for a single case study computed accurate RMSE values. Yang et al. [24] combined weather data and machine learning one-day ahead forecasting of photovoltaic power. The hybrid model had a mean error of 4%, improving over standard models.

Pedro and Coimbra [15] combined artificial neural networks and metaheuristics [11], computing accurate results for a photovoltaic power plant in California, USA. Wang et al. [23] combined wavelets, artificial neural networks, and regression and computed accurate results for photovoltaic farms: MAPE below 5% for one-hour-ahead forecasting and average RMSE from 6.75 to 22.26. Zang et al. [25] applied deep artificial neural networks and a feature maps method using several data sources. The approach computed RMSE between 2.0% and 7% for a a single photovoltaic array. Luo et al. [9] applied a Long Short Term Memory artificial neural network for day-ahead forecasting of photovoltaic generation, obtaining accurate R^2 values, from 0.84 and 0.93.

Some studies have addressed the problem of forecasting photovoltaic generation in Uruguay. Theocharides et al. [22] applied artificial neural networks for one-hour forecasting of photovoltaic generation for a power plant in Salto (in the North of Uruguay). Normalized RMSE between 7.6% and 14.2% for up to one hour ahead. Fraccanabbia et al. [7] applied meta learning techniques for a photovoltaic plant in Artigas (also in the North of Uruguay), obtaining accurate values of MAPE, R^2 , and RMSE, for a small data sample.

The obtained forecasts are useful for relevant problems concerning stochastic renewable energy optimization [20], and for the planning of renewable energy utilization in households [12,4,18], medium-large consumers [14,16,21], industrial facilities [17], and datacenters [10].

3 Forecasting solar photovoltaic power generation with neural networks

This section reports the development of predictors for solar photovoltaic power generation applying neural networks.

3.1 Description of the approach applying neural networks

Predictors based on neural networks were implemented, following the approach of modeling the generation time series with an architecture based on Long Short Term Memory. The general approach was instantiated for the prediction of wind generation and solar generation, with minor changes in its implementation.

The predictive approach developed applies a multi-step strategy, in accordance with the objectives of the proposed research. The horizon considered for the definition of the multi-step prediction is 72 hours, according to the objectives set for the planning problem.

Several strategies have been proposed in the related literature to deal with multistep ahead forecasting [3]. The most used approaches are recursive and direct forecasting. On the one hand, the recursive approach employs the first predicted value as input for the subsequent step, resulting in error accumulation. On the other hand, two different implementations have been applied for the direct approach: creating separate models for each forecasting step or constructing a model capable of accepting multiple inputs and generating multiple prediction outputs. The latter approach, known as the sequence-to-sequence method, requires less computational time. The proposed model for development of predictors for solar photovoltaic power generation applying neural networks follows the direct approach, using multiple inputs and generating multiple outputs.

The predictive approach follows a multivariate scheme, to consider as inputs to the learning process the time series of solar photovoltaic power generation within a configurable period in the past. In addition, the available set of estimations at the time of making the prediction is considered as covariate during the learning process. The input data is processed and formatted specifically to suit the developed neural network architectures and the applied training model.

3.2 Model and architecture of the proposed neural network

The applied neural network uses a Long Short Term Memory model, considering its suitability and accuracy for time series forecasting. The explored architectures were similar to the ones applied in the literature for related problems [2,9,19]. A Sequential model is applied, which is structured as a plain stack of layers. In this model, each layer is designed to have precisely one input tensor and one output tensor. The input layer is a tensor of dimensions $1 \times \text{HOURS} \times 2$ with the past observations in the previous HOURS horas. The first hidden layer is the Long Short Term Memory layer. Different configurations were studied and the best results were computed using a Long Short Term Memory layer with

6 Sergio Nesmachnow and Claudio Risso

200 cells. Then, an additional layers is used, consisting of a Dense layer with 100 densely connected neurons (dimension 200×100). Every neuron in the dense layer takes the input from all the other neurons of the previous layer. The output layer is a Dense layer with 72 neurons (dimension 100×72) to represent the solar photovoltaic power forecast for each one of the 72 hours in the forecasting horizon.

The proposed Long Short Term Memory was implemented in Keras. Listing 1 presents the architecture of the applied Long Short Term Memory neural network, in the format reported by the Keras `model.summary()` function.

Layer (type)	Output Shape	Param #
lstm (LSTM)	(None, 200)	41200
dense (Dense)	(None, 100)	5050
dense_1 (Dense)	(None, 100)	2550
dense_2 (Dense)	(None, 72)	3672

Listing 1.1: Definition of the applied Long Short Term Memory neural network

3.3 Training and validation approach of the proposed neural network

The training of the model uses a sliding window scheme to increase the dimension of the training dataset. The sliding windows scheme for augmentation is necessary, since the usual approach of partitioning the available dataset into 80% for training and 20% for validation would result in a very small dataset of 24-hours (disjoint) training blocks. The sliding window scheme allows significantly increasing the number of training blocks from the original blocks available in the input file. The criterion used in the optimization applied to train the neural network is the minimization of the RMSE in each period to be predicted. The RMSE is used as the loss function of the neural network since it provides a robust estimator of the prediction quality in the training dataset and is preferable to an absolute metric, such as Mean Absolute Error (MAE), since that RMSE penalizes forecast errors more heavily.

For the evaluation of the predictor based on neural networks, a walk-forward procedure is applied. The procedure assumes that the data for the period predicted in the previous step is available to make the prediction in the next period. The number of previous observations used for the prediction is a parameter in

the evaluation routine (`evaluate_model()`). In the evaluation of the errors in the validation dataset, the global RMSE value and the RMSE value are calculated for each hour that is predicted, with the objective of determining the quality of the prediction as the time horizon is extended. The optimizer used in the training was the Adam implementation of the Stochastic Gradient Descent (SGD) algorithm. The batch training scheme was used, with a batch size of 24 training blocks propagated through the neural network.

4 Training and forecasting results

This section reports and analyzes the obtained results for the solar photovoltaic power generation forecasting problem.

4.1 Development and execution platform

The applied Long Short Term Memory neural network model was developed in Python, using the libraries Tensorflow and Keras. The executions were carried out in the high-performance computing infrastructure of the National Supercomputing Center (Cluster-UY) [13].

For the training of the neural network, the parallel implementation provided by Tensorflow was used, executed on Tesla P100 graphic processing units (12 GB RAM), available in standard Cluster-UY nodes (HPE DL380 Gen10 servers with Intel Xeon-Gold 6138 at 2.00GHz).

4.2 Data sources

The considered data source is solar photovoltaic power generation data gathered by the Supervisory Control And Data Acquisition (SCADA) of UTE. The SCADA collects data for the global national demand, wind power generation, and solar photovoltaic power generation. Solar photovoltaic power represents 14% of the non-controllable renewable power generation park in the country, accounting for 242 MW. Measures are collected every one hour.

The complete historical data of solar photovoltaic power generation is used, from January 1st, 2018 to August 28th, 2022. The available dataset includes the following fields: TimeStamp, Date, Year, Month, Day, Hour, Delivered Power [MWh], Curtails [MWh], Total Power [MWh], Equivalent Plant [MW], and Plant Load Factor. Total power is the potential solar photovoltaic power generation of the installed infrastructure. This value can be larger than the one needed to meet the electricity demand. Delivered power correspond to the actual power that entered to the distribution network after planning and dispatching, which applies reductions to the generation sources in case the generation is over the demand. The difference between total and delivered is the curtail for each timestamp. Equivalent Plant, or simply Plant, is the total installed capacity for solar photovoltaic power generation. The Plant Load Factor field is the normalized value of the Total Power field, considering the total installed capacity.

8 Sergio Nesmachnow and Claudio Risso

Data were obtained from the raw SCADA logs. A substantial data cleansing process was needed to impute, complete and correct omitted or erroneous values. Listing 2 presents sample records of the training dataset, after cleansing and preprocessing.

TimeStamp	Date[D/M/Y]	Hour	Delivered	Curtailed	Total	Power	Plant	Plant	Load	Factor
8769	01/01/2018	800	59	0	59	239			0.246862	
8770	01/01/2018	900	63	0	63	239			0.263598	
8771	01/01/2018	1000	57	0	57	239			0.238494	
8772	01/01/2018	1100	45	0	45	239			0.188285	
8773	01/01/2018	1200	67	0	67	239			0.280335	
8774	01/01/2018	1300	56	2	58	239			0.242678	
8775	01/01/2018	1400	45	4	49	239			0.205021	

Listing 1.2: Sample records of the training dataset

Fig. 1 presents samples of the available historical data of solar photovoltaic power generation (Plant Load Factor values) from UTE.

4.3 Training results

The training was carried out with the values of the Plant Load Factor field, which are normalized in the interval $[0,1]$ and therefore are more robust to avoid training pathologies due to values much higher than the average. Training with the Plant Load Factor values avoids including an input normalization layer in the applied Long Short Term Memory neural network. Also, using the Plant Load Factor values gives greater extensibility to the designed predictors in case the total amount of energy delivered by the installed solar farms changes in the near future.

From the considered solar photovoltaic power generation data, the sliding window scheme allowed obtaining 40752 training blocks from the 566 original blocks available in the input file.

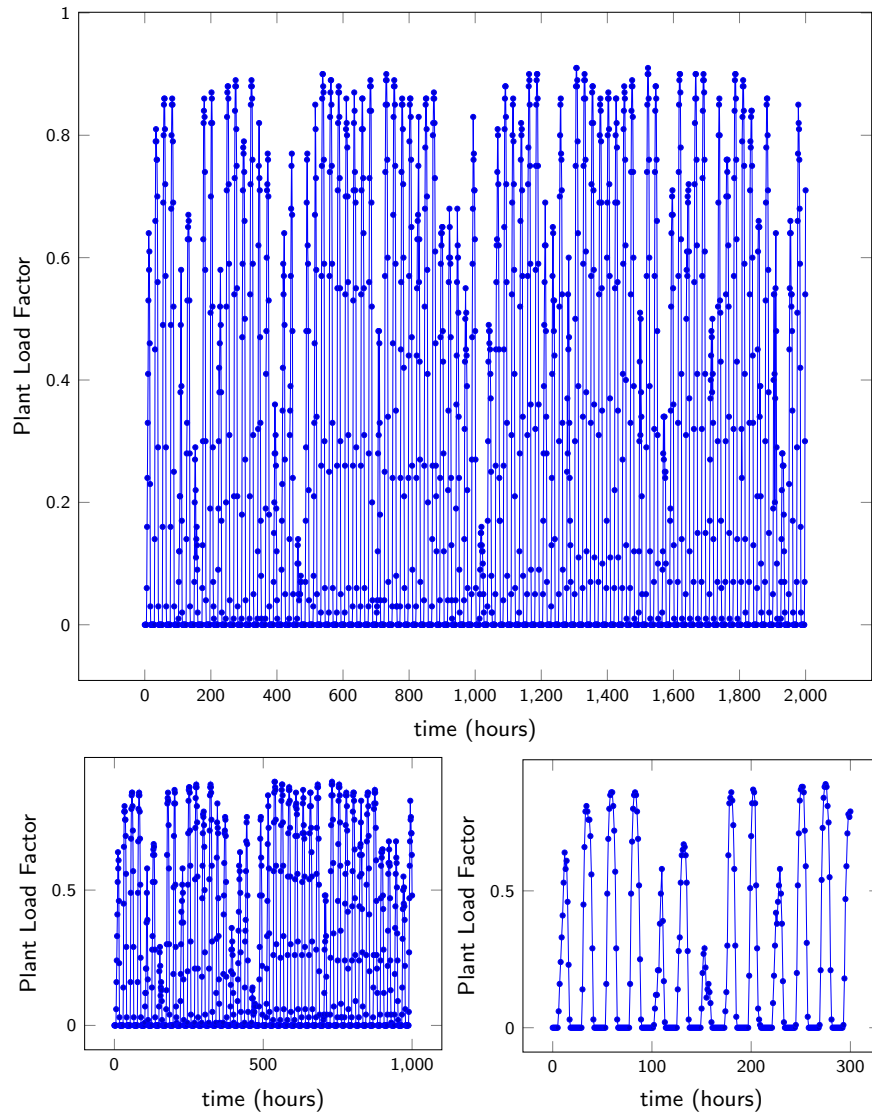


Fig. 1: Samples of solar photovoltaic power generation data from UTE (Plant Load Factor values)

10 Sergio Nesmachnow and Claudio Risso

The training was carried out for 100 epochs, although the applied Long Short Term Memory neural network was already able to reach very robust results of mean square error for each period that is predicted after 40 epochs. These results imply an appropriate precision for the predictions made on the validation set. The training process required about 10 minutes of execution time on a standard Cluster-UY node with a Tesla P100 GPU.

Fig. 2 presents a representative graph of the evolution of the loss function (RMSE) of the Long Short Term Memory neural network in the training experiments on the solar generation data set.

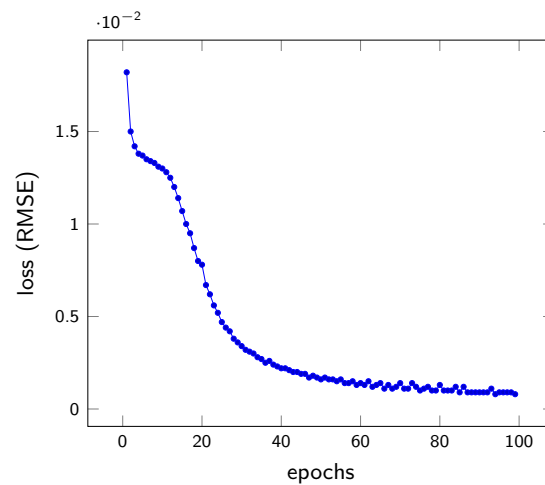


Fig. 2: Evolution of the values of the loss function (RMSE) during the training of the Long Short Term Memory neural network for the solar generation dataset

Fig. 3 presents a representative graphics of the root mean square error values for each hour of the prediction in the validation experiments, on the solar generation data set.

The validation set yielded mean square error values ranging from 0.05 (for the first predicted hour of generation) to 0.26 (corresponding to the hour with the highest generation peak). The average RMSE value was approximately 0.14. The training set exhibited an error of approximately 0.027.

For an objective assessment of the results obtained, the difference between the real values of solar generation and the predictions made by the Long Short Term Memory neural network was analyzed. Table 1 reports the averages of the differences between the prediction and the actual value for each hour in the validation experiments. Table 2 reports the medians of the differences between the prediction and the actual value for each hour in the validation experiments.

Forecasting solar photovoltaic power generation in Uruguay 11

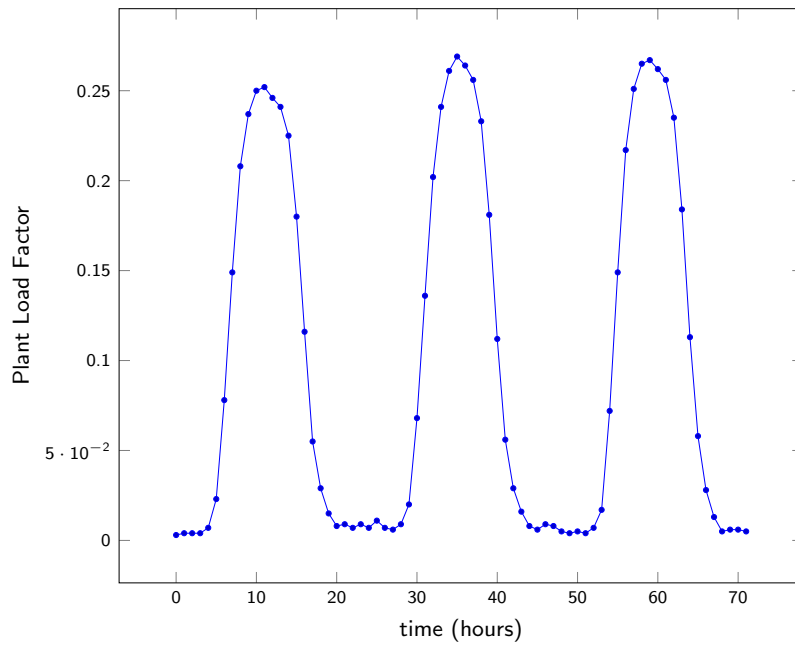


Fig. 3: RMSE for each hour of the prediction in the validation experiments of the Long Short Term Memory neural network for the solar generation data set

H	$\overline{\Delta_S}$	H	$\overline{\Delta_S}$	H	$\overline{\Delta_S}$	H	$\overline{\Delta_S}$	H	$\overline{\Delta_S}$	H	$\overline{\Delta_S}$
1	0.00616	2	0.00689	3	0.00183	4	-0.00477	5	-0.00482	6	-0.00151
7	0.00844	8	0.00275	9	-0.00477	10	-0.01969	11	-0.02954	12	-0.04132
13	-0.03873	14	-0.03780	15	-0.04405	16	-0.01915	17	-0.00863	18	-0.00466
19	-0.00221	20	-0.00106	21	-0.00644	22	0.00676	23	0.00103	24	0.01027
25	0.00398	26	0.00285	27	-0.00015	28	-0.00425	29	0.00452	30	-0.00104
31	0.01188	32	0.01526	33	0.00491	34	-0.00162	35	-0.00767	36	-0.00924
37	0.02920	38	0.05956	39	0.04902	40	0.05282	41	0.01769	42	0.00195
43	-0.00649	44	-0.00115	45	-0.00378	46	0.00102	47	-0.00228	48	0.00053
49	0.00763	50	0.01180	51	0.00833	52	0.00199	53	0.00314	54	-0.00332
55	0.00516	56	0.03111	57	0.03184	58	0.01861	59	0.02606	60	0.03750
61	0.03272	62	0.03050	63	0.04762	64	0.03253	65	0.01874	66	0.00412
67	-0.00311	68	-0.00107	69	-0.00288	70	0.00730	71	0.00312	72	0.00446

Table 1: Average values of the difference between the prediction and the actual value of solar generation ($\overline{\Delta_S}$) for each hour (H) in the validation experiments

12 Sergio Nesmachnow and Claudio Risso

H	$\tilde{\Delta}_S$	H	$\tilde{\Delta}_S$	H	$\tilde{\Delta}_S$	H	$\tilde{\Delta}_S$	H	$\tilde{\Delta}_S$	H	$\tilde{\Delta}_S$
1	0.00629	2	0.00715	3	0.00147	4	-0.00387	5	-0.00417	6	0.00103
7	-0.01097	8	-0.00325	9	0.00396	10	0.01182	11	0.00556	12	0.00499
13	0.01516	14	0.01135	15	-0.00325	16	0.00573	17	-0.00350	18	0.00178
19	-0.00152	20	-0.00151	21	-0.00621	22	0.00745	23	0.00126	24	0.00979
25	0.00442	26	0.00318	27	0.00008	28	-0.00451	29	0.00395	30	0.00156
31	0.00798	32	0.02799	33	0.03186	34	0.03111	35	0.03976	36	0.03760
37	0.06547	38	0.09630	39	0.07014	40	0.07147	41	0.01738	42	0.00111
43	-0.00616	44	-0.00096	45	-0.00295	46	0.00211	47	-0.00259	48	0.00085
49	0.00810	50	0.01156	51	0.00851	52	0.00209	53	0.00287	54	-0.00378
55	0.00393	56	0.02721	57	0.05249	58	0.04798	59	0.06832	60	0.08548
61	0.07316	62	0.06235	63	0.07162	64	0.05653	65	0.02387	66	0.00379
67	-0.00304	68	-0.00201	69	-0.00253	70	0.00680	71	0.00286	72	0.00471

Table 2: Median of the differences between the prediction and the real value of solar generation ($\tilde{\Delta}_S$) for each hour in the validation experiments

Boxplots in Fig. 4 summarize the information of the distributions of results (difference between real value of solar photovoltaic generation and the forecasted value) in the validation experiments (results reported for 381 predictions made, one for each hour).

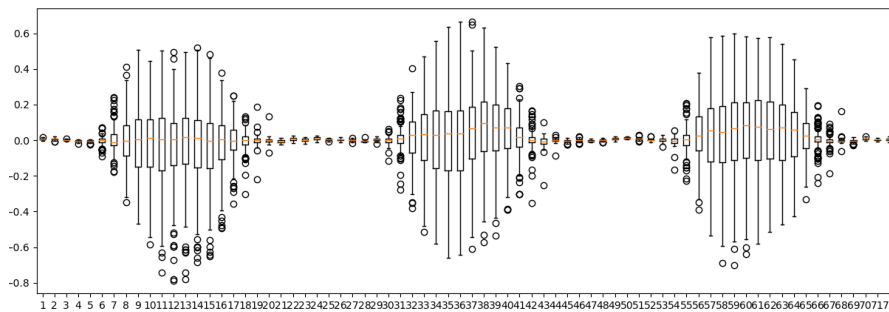


Fig. 4: Boxplots summarizing the information of the distributions of the differences between the real value and the Long Short Term Memory prediction for each hour, in the validation experiments for the photovoltaic solar power generation dataset

Fig. 5 presents a representative example of solar generation predictions obtained using the Long Short Term Memory neural network. The figure shows a very good predictive quality of the Long Short Term Memory neural network, which is capable of accurately modeling the dynamics of the time series, with very minor deviations from the real values of wind generation.

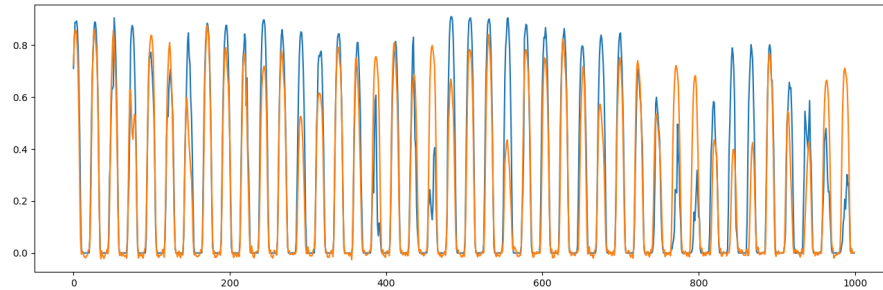


Fig. 5: Example of forecasts (orange curve) and actual values (blue curve) in the validation experiments for the photovoltaic solar power generation dataset

The forecasted results are useful for creating scenarios in a short-term renewable energy bands model, to be used for stochastic optimization planning and scheduling [20]. For the use in the energy band model, solar generation predictions were reported in blocks of 72 predictions (for the next 72 hours in the future), made every 24 hours. The errors of the predictions made every 24 hours followed the trend of the previously reported general errors, with mean values of RMSE in the order of 0.14 in the validation set and 0.027 in the training set.

5 Conclusions and future work

This article presented an approach applying a Long Short Term Memory neural network for forecasting solar photovoltaic power generation. A specific case study was analyzed for the total solar photovoltaic power generation in Uruguay, using real data from 2018 to 2022. This is a relevant problem in Uruguay to contribute in the development of smart operation techniques for the electricity grid.

Results computed in the experimental evaluation showed that the Long Short Term Memory approach is effective for solar photovoltaic power generation forecasting. Accurate results were computed, with an average RMSE value of 0.14 for the forecast of up to 72 hours in the future. The obtained results are valuable to be applied in stochastic optimization models for planning and scheduling of the electric grid.

The main lines for future work include expanding the analysis considering other artificial neural network architectures and expanding the analysis to evaluate the forecasting capabilities of the proposed approach for other renewable energy sources.

14 Sergio Nesmachnow and Claudio Risso

References

1. Aguiar, J., Pérez, M.: An insight of deep learning based demand forecasting in smart grids. *Sensors* **23**(3), 1467 (2023). <https://doi.org/10.3390/s23031467>
2. Ahmed, R., Sreeram, V., Mishra, Y., Arif, M.: A review and evaluation of the state-of-the-art in PV solar power forecasting: Techniques and optimization. *Renewable and Sustainable Energy Reviews* **124**, 109792 (2020). <https://doi.org/10.1016/j.rser.2020.109792>
3. Alkhatay, G., Mehmood, R.: A review and taxonomy of wind and solar energy forecasting methods based on deep learning. *Energy and AI* **4**, 100060 (2021). <https://doi.org/10.1016/j.egyai.2021.100060>
4. Chavat, J., Nesmachnow, S., Graneri, J., Alvez, G.: ECD-UY, detailed household electricity consumption dataset of uruguay. *Scientific Data* **9**(1) (2022). <https://doi.org/10.1038/s41597-022-01122-x>
5. Ding, M., Wang, L., Bi, R.: An ANN-based approach for forecasting the power output of photovoltaic system. *Procedia Environmental Sciences* **11**, 1308–1315 (2011). <https://doi.org/10.1016/j.proenv.2011.12.196>
6. El hendouzi, A., Bourouhou, A., Ansari, O.: The importance of distance between photovoltaic power stations for clear accuracy of short-term photovoltaic power forecasting. *Journal of Electrical and Computer Engineering* **2020**, 1–14 (2020). <https://doi.org/10.1155/2020/9586707>
7. Fraccanabbia, N., Gomes, R., Dal Molin, M., Rodrigues, S., dos Santos, L., Cocco, V.: Solar power forecasting based on ensemble learning methods. In: *International Joint Conference on Neural Networks*. IEEE (2020). <https://doi.org/10.1109/ijcnn48605.2020.9206777>
8. Iheanetu, K.: Solar photovoltaic power forecasting: A review. *Sustainability* **14**(24), 17005 (2022). <https://doi.org/10.3390/su142417005>
9. Luo, X., Zhang, D., Zhu, X.: Deep learning based forecasting of photovoltaic power generation by incorporating domain knowledge. *Energy* **225**, 120240 (2021). <https://doi.org/10.1016/j.energy.2021.120240>
10. Muraña, J., Nesmachnow, S.: Simulation and evaluation of multicriteria planning heuristics for demand response in datacenters. *Simulation* **99**(3), 291–310 (2021). <https://doi.org/10.1177/00375497211020083>
11. Nesmachnow, S.: An overview of metaheuristics: accurate and efficient methods for optimisation. *International Journal of Metaheuristics*, **3**(4), 320–347 (2014). <https://doi.org/10.1504/IJMHEUR.2014.068914>
12. Nesmachnow, S., Colacurcio, G., Rossit, D.G., Toutouh, J., Luna, F.: Optimizing household energy planning in smart cities: A multiobjective approach. *Revista Facultad de Ingeniería Universidad de Antioquia* (101) (2021). <https://doi.org/10.17533/udea.redin.20200587>
13. Nesmachnow, S., Iturriaga, S.: Cluster-UY: Collaborative Scientific High Performance Computing in Uruguay. In: *Torres, M., Klapp, J. (eds.) Supercomputing, Communications in Computer and Information Science*, vol. 1151, pp. 188–202. Springer (2019). https://doi.org/10.1007/978-3-030-38043-4_16
14. Nesmachnow, S., Rossit, D.G., Toutouh, J., Luna, F.: An explicit evolutionary approach for multiobjective energy consumption planning considering user preferences in smart homes. *International Journal of Industrial Engineering Computations* **12**(4), 365–380 (2021). <https://doi.org/10.5267/j.ijiec.2021.5.005>
15. Pedro, H., Coimbra, C.: Assessment of forecasting techniques for solar power production with no exogenous inputs. *Solar Energy* **86**(7), 2017–2028 (2012). <https://doi.org/10.1016/j.solener.2012.04.004>

16. Porteiro, R., Chavat, J., Nesmachnow, S.: A thermal discomfort index for demand response control in residential water heaters. *Applied Sciences* **11**(21), 10048 (2021). <https://doi.org/10.3390/app112110048>
17. Porteiro, R., Hernández-Callejo, L., Nesmachnow, S.: Electricity demand forecasting in industrial and residential facilities using ensemble machine learning. *Revista Facultad de Ingeniería Universidad de Antioquia* (102), 9–25 (2020). <https://doi.org/10.17533/udea.redin.20200584>
18. Porteiro, R., Nesmachnow, S., Moreno-Bernal, P., Torres-Aguilar, C.E.: Computational intelligence for residential electricity consumption assessment: Detecting air conditioner use in households. *Sustainable Energy Technologies and Assessments* **58**, 103319 (2023). <https://doi.org/10.1016/j.seta.2023.103319>
19. Ren, Y., Suganthan, P., Srikanth, N.: Ensemble methods for wind and solar power forecasting—a state-of-the-art review. *Renewable and Sustainable Energy Reviews* **50**, 82–91 (2015). <https://doi.org/10.1016/j.rser.2015.04.081>
20. Risso, C., Guerberoff, G.: A learning-based methodology to optimally fit short-term wind-energy bands. *Applied Sciences* **11**(11), 5137 (2021). <https://doi.org/10.3390/app11115137>
21. Rossit, D.G., Nesmachnow, S., Toutouh, J., Luna, F., and: Scheduling deferrable electric appliances in smart homes: a bi-objective stochastic optimization approach. *Mathematical Biosciences and Engineering* **19**(1), 34–65 (2022). <https://doi.org/10.3934/mbe.2022002>
22. Theocharides, S., Alonso, R., Giacosa, G., Makrides, G., Theristis, M., Georghiou, G.: Intra-hour forecasting for a 50 MW photovoltaic system in uruguay: Baseline approach. In: *IEEE 46th Photovoltaic Specialists Conference*. IEEE (2019). <https://doi.org/10.1109/pvsc40753.2019.8980756>
23. Wang, H., Yi, H., Peng, J., Wang, G., Liu, Y., Jiang, H., Liu, W.: Deterministic and probabilistic forecasting of photovoltaic power based on deep convolutional neural network. *Energy Conversion and Management* **153**, 409–422 (2017). <https://doi.org/10.1016/j.enconman.2017.10.008>
24. Yang, H.T., Huang, C.M., Huang, Y.C., Pai, Y.S.: A weather-based hybrid method for 1-day ahead hourly forecasting of PV power output. *IEEE Transactions on Sustainable Energy* **5**(3), 917–926 (2014). <https://doi.org/10.1109/tste.2014.2313600>
25. Zang, H., Cheng, L., Ding, T., Cheung, K.W., Wei, Z., Sun, G.: Day-ahead photovoltaic power forecasting approach based on deep convolutional neural networks and meta learning. *International Journal of Electrical Power & Energy Systems* **118**, 105790 (2020). <https://doi.org/10.1016/j.ijepes.2019.105790>
26. Zhang, J., Verschae, R., Nobuhara, S., Lalonde, J.F.: Deep photovoltaic nowcasting. *Solar Energy* **176**, 267–276 (2018). <https://doi.org/10.1016/j.solener.2018.10.024>
27. Zhu, H., Li, X., Sun, Q., Nie, L., Yao, J., Zhao, G.: A power prediction method for photovoltaic power plant based on wavelet decomposition and artificial neural networks. *Energies* **9**(1), 11 (2015). <https://doi.org/10.3390/en9010011>

AI & real estate markets

Alfonso Valenzuela Aguilera¹ and Guillermo Romero Tecua²

^{1,2} Universidad Autónoma del Estado de Morelos, MEXICO
aval@uaem.mx

Abstract. Smart cities often prioritize technological efficiency over values like transparency, solidarity, and community, raising concerns about the digital divide and the erosion of democracy through automated manipulation of public opinion. It's crucial to emphasize that smart cities should empower individuals to retain control over the technologies shaping their urban environments. The current trend of integrating technology into urban landscapes without thorough consideration of its purpose and impact on residents' well-being is concerning. Hidden agendas, such as increased surveillance and capital dominance, are often obscured by the allure of smart cities. While artificial intelligence offers transformative potential, its deployment in smart cities driven by economic interests can overlook the well-being of the population, favoring economic gains over environmental, distributional, and social concerns. Moreover, AI's autonomy in public management may raise issues in handling complex public decision-making. The core challenge is balancing automation with human oversight for sound public policy. Just as smart cities emphasize technology, the real estate sector is undergoing a transformation, underscoring the significant influence of our technological path.

Keywords: Digital Transformation, Smart cities, Technology.

1.1 A new urban realm

Smart cities often overlook elements valued by their citizens in daily life, such as transparency, solidarity, and a sense of community. This raises questions about the digital divide, persistent inequalities, and the future of democracy in the face of automated manipulation of public opinion. It is crucial to consider the importance of individuals retaining control over tools to ensure harmonious coexistence in complex urban environments, where technology itself is not the focal point, but rather the possibilities for connection it offers to citizens.

According to Ivan Illich¹ (1972), technological development can become an imperative when adopted uncritically and at any cost, regardless of a society's defined priorities. Technology shifts from being a tool that facilitates everyday activities to an imposition or obligation society must adopt, irrespective of whether it genuinely meets the needs or priorities of a community. Such is the case of facial recognition CCTV camera systems, which are defended as public safety measures but intrude upon citizens' privacy. Illich emphasizes the importance of "conviviality," where peo-

2

ple collaborate and cooperate in a decentralized manner through active and supportive participation in decision-making that affects the overall well-being of the population.

Similarly, Jean Robert² (1998) notes that new technologies create their own rationality that extends beyond the inventions themselves. This rationality shapes how we think and understand the world, defining what is considered ideal, desirable, or acceptable. It also alters our identity, privacy perceptions, living standards, beauty ideals, and comfort preferences, influencing our decisions and preferences.

In this context, the digitization of daily life can lead to labor, social, and academic rationalities, with implications for urban spaces and infrastructure needs. However, equitable and rational solutions may not always be provided, potentially leading to excessive dependence on technology and loss of control over certain aspects of daily life without effective digital access.

Given this preamble, we question the current trend of imbuing cities with intelligence by implementing technologies without thorough discussions on their purpose and, most importantly, their potential impact on residents' well-being. In the pursuit of not falling behind in the technological race, hidden strategies that reshape urban spaces, such as surveillance or the dominance of capital over the real estate market, are reinforced.

Thus far, smart cities are presented as those integrating digital technologies into the management of networks, services, and infrastructure to operate more efficiently. However, this transformation could reduce citizens to mere service users or providers—voluntary or involuntary—of information for businesses, public agencies, and production chains. Perhaps the most concerning aspect is the ability to identify our preferences and dislikes, opening the possibility of programmed manipulation of public opinion on matters of common interest, such as in the case of the *Facebook–Cambridge Analytica* data scandal during Donald Trump's 2016 presidential campaign.

Artificial Intelligence (AI) is revolutionizing many industries by enhancing, augmenting, or complementing human intelligence through efficient and highly precise processes. Presently, digital capabilities enable learning from experience, recognizing patterns, and adapting to changes in the environment using decision-making mechanisms closely aligned with human reasoning.

In the early days of AI, the initial models sought to emulate the functioning of a neuron through simplified input and output procedures, while in subsequent decades, they became more complex by incorporating learning functions³ (McCulloch and Pitts, 1943). In parallel, Alan Turing⁴ worked on a model that imitated human intelligence and introduced a test for validation (1950). This went beyond a machine's ability to follow encoded instructions and execute them efficiently, responding to external stimuli but within a predetermined framework that determined possible responses (e.g., a chess game).

Currently, the idea of introducing intelligent metropolitan systems, or even in newly created city sectors with the aim of automating most of their services and functions, has become a significant economic and real estate attraction for countries in various regions of the world, with an emphasis on mainland China, the European Union, and the Pacific Rim. However, despite the fact that the smart city model is not entirely

2

defined, major construction and real estate companies view digital transformation of space as a highly profitable investment. Yet, the direct benefits for the population remain somewhat unclear, as some authors assert that "[...] the smart city belongs, in part, to the imagination."⁵ (Picon, 2018, 270).

These digital imaginaries converge in the narrative of modernity, suggesting that technology appears to steer economies toward employment, prosperity, and development, even though each city determines the necessary variants for its particular conditions. The smart urban agenda, also driven by development banks, includes the installation of sensors, cameras, readers, and other data generators that serve as the raw material for systems functioning through data processing. In a medical metaphor, cities would be in a position to control their metabolism through sensors that determine urban system flows, energy consumption, mobility, or waste disposal using cutting-edge technologies, ensuring maximum efficiency and subsequent sustainability of natural and built environments.

However, the digital economy, with its inherent technological optimism, brings a political and operational agenda to promote the benefits of smart cities without necessarily making these benefits evident. As mentioned in the first chapter, technology, science, and progress have been used as tools to justify existing power relations, prioritize the use of public funds, and drive technological and real estate projects that would otherwise be difficult to sustain or justify. Therefore, economic interests often prevail over environmental, distributional, and social concerns. Furthermore, the increasing autonomy resulting from the automation of public management could result in decision-making through artificial intelligence algorithms in complex areas such as urban planning, public policies, and city governance.

The optimization of functions, infrastructure, and services through automation is not the core issue; rather, the concern lies in the possibility that intelligent systems do not depend on human supervision to decide on the best way to resolve issues that may arise at any given moment. Due to its nature, AI may not encompass the complexities inherent in social participation in public decision-making, which are crucial for determining the best strategies for public policy.

While rational decision-making is attractive in principle, the long-term perspective is challenging to establish based on current information, as it involves a degree of uncertainty. Additionally, ethical dimensions continue to manifest, and consensus on underlying moral values will need to be reconciled. The perspective presented by AI is not entirely clear, as new technologies may lead to unprecedented urban scenarios that could approach a future without considering the imprint of the past, while the environment may become responsive to external stimuli through sensors, where devices communicate, exchange information, and decide on the processes to be initiated.

In this same vein, it is common to hear that we are facing technologies classified as "disruptive"⁶ (Greenfield, 2018: 8), in the sense that they alter life as we knew it. However, it is paradoxical that this apparent transgressiveness does not fundamentally alter the power structures, imbalances, and inequities of the socio-economic and political system, keeping the structures of productive systems intact. Throughout the history of technology and its implementation, the aura of progress continues to amaze us, not only leading us to accept new lifestyles but also demanding that we be considered

4

part of that global narrative. Therefore, on the path to automation, it will be necessary to qualify autonomy as a destination, ensuring that the moral, civic, and ethical values underlying intelligent proposals are shared among citizens, allowing them to move from being mere recipients of optimized decisions by digital systems to being active participants in public decision-making.

1.2 Artificial Intelligence and Its Impact on Urban Economy

What would the new data-driven economy look like? According to Pentland⁷ (2021: 7), there are certain controversial issues such as data ownership, control of the means of production, renegotiation of property rights, and handling of personal information. The latter is crucial to ensure people's privacy, transparency, and the reliability of algorithms, as well as the fairness of the principles and methods used in machine learning. Additionally, the proposal to transform cities into smart devices carries the drawback of segregating those that cannot make the transition. In other words, on a city-wide scale, there will be groups or individuals who do not have the ability to harness available data—or lack the skills or tools to do so—creating a new dependence on those who can interpret them, thus becoming users/customers of the new services.

Pentland and colleagues⁸ (2021) advocate for a better redistribution of this new data capital and even highlight the greater resilience capabilities of distributed network systems, which do not rely on a central core and are, therefore, more adaptable to changes, crises, and disasters. So, "[...] this shift from centralized systems to networks of local systems is driven not only by the recognition that current systems are fragile and inadequately expeditious but also by issues of inclusion, transparency, cost, and security"⁹ (2021: 6). In this way, decentralized systems allow for greater distribution of functions—now entirely digital—across blockchains or distributed ledgers.

Blockchain technology is based on a radically innovative concept: creating a decentralized and shared digital ledger that is updated in real-time and cannot be altered once information is entered into the database, keeping records of every transaction, making it highly secure. This decentralized management is the antithesis of central banks, where a single entity validates transactions and acts as an intermediary, whereas blockchain is validated by a large number of nodes that eliminate intermediaries. Another alternative is data exchanges, which are "[...] platforms that store data from various sources and allow third parties to run algorithms on this data. As a result, third parties can generate insights with new data sources. Thus, data sharing gives rise to the concept of shared data, which is the natural next step after handling Big Data"¹⁰ (Pentland: 2021: 36).

Behavioral economics, psychobiology, and neuroscience identify that everyday decision-making does not necessarily respond to a rational process of choice but rather to the calculation of probabilities and the consequent identification of patterns in fractions of a second. Thus, what was once recognized as "human intuition" can be equated with this pattern recognition that artificial intelligence can perform exceptionally¹¹ (Harari, 2018: 71, Bubeck et al., 2023: 34). The algorithmic capabilities of artificial

4

intelligence have a wide range of actions that allow for an understanding of human behavior to previously unthinkable levels. However, there are concerns that worry people when creating a new, irrelevant or "useless" class that may not find a place in the new information economy. Furthermore, Harari argues that it would be even more concerning if humans ceded their authority to algorithms for decisions related to the common good, which could open the possibility of digital dictatorships¹² (2018: 130).

Another characteristic of new technologies—and particularly artificial intelligence—is that they have the ability to delocalize mechanisms that create personal connections among citizens through "high-intensity and short-duration" movements, where "[...] de-citizenization becomes radical" as circumstantial affinities emerge around a particular issue¹³ (García Canclini, 2019: 10). In the face of data monopolization and control, citizens are beginning to seek modes of expression and intervention in decisions that impact their living conditions but are not finding cohesion mechanisms that withstand the test of time.

What is clear is that we are facing a substantial change in the social structures of the economy, where the future seems to be free from hierarchies but is actually dominated by multinational corporations that control and manage the use of public information while receiving most of the benefits. Furthermore, in the information economy, it is not the market that resolves the contradictions of the system, but rather the free flow of data that repositions imbalances within the system. Additionally, the information circulating in networks may have never been private, as there are no clear limitations on its use once the operating conditions are accepted. This is a delicate matter as it exposes people's personal information to leaks or can be used to discredit, extort, or threaten a presumed involved party. Therefore, given the ability of algorithms to detect patterns, predict behaviors, and determine a person's eligibility for a service, clear and effective regulatory frameworks are required.

In this regard, one of the foundational arguments of smart cities is the possibility of collecting and using data from sensors, social networks, applications, or official records, allowing for extensive use due to its open, public, and transparent nature. However, even if this objective could be achieved without affecting the interests of the parties involved, a fundamental element is missing, which is the algorithms. These algorithms have the ability to transform massively stored data (Big Data) into useful information for use in service provision, prospective plans, or the detection of possible population needs, leaving more questionable uses such as the manipulation of public opinion or the misuse of personal information pending.

It is through systematic data collection that it has been possible to prefigure current or historical processes, identify useful patterns for projecting the future, and even visualize emerging trends that may be decisive within a particular time frame. To create this scenario, it is essential to have access to high-capacity processing centers (including cloud computing) and physical data transmission networks through broadband systems that allow the efficient, fast, and secure transmission of large volumes of information in real-time. It should be clear that the perspective of continuous process optimization through the automation of functions is very attractive in terms of production, as it involves minimizing human errors, although we should always be

6

aware of the limitations of artificial intelligence in terms of contextual perspective, common sense, and human rationality.

Therefore, one of the fundamental aspects that should be included in AI-integrated criteria is that within the processes of planning, monitoring, and decision-making in the political sphere, it will be necessary to prioritize the needs and interests of citizens over criteria of efficiency, economy, and operability. In other words, decisions in terms of policy and public management based on these technologies should prioritize access, participation, and inclusion of the inhabitants in deciding the present and future of cities. This is why questions about these technologies have focused on the risk of automating public decisions through algorithms, which could potentially disempower citizens¹⁴ (García Canclini, 2020: 221).

Digital technologies are changing the way we use physical space, whether it's residential, educational, or work-related. This has led to new interactions and economic configurations different from those prevalent during the last century, generating new business models, value chains, and forms of financing. Regarding this last point, it is important to highlight that capital flows have accelerated as never before in history through financialization, money laundering, and cryptocurrencies. Real estate developers can thus have the necessary liquidity to build projects quickly, which has implications for the real estate market, urban management, and the quality of life of city residents. Therefore, even as urban areas reaffirm themselves as potential markets for new technologies, they become agents of innovation with great potential for value creation, turning into scenarios of disputes among the new protagonists of the economy (such as *Uber*, *Glovo*, *Rapi*, and *Airbnb*). These dynamics give rise to major challenges for public administration, such as ensuring the expansion, efficiency, and maintenance of the services and infrastructure required for new production models.

1.3 Challenges of Artificial Intelligence

The potential of Artificial Intelligence (AI) in everyday life spans various spheres, including public administration and urban management. In these areas, derivative technologies are used for prospective analysis, designing mobility systems, or innovations in education, security, health, and finance, among many other fields. All of this leads us to ethical considerations regarding the degree of algorithmic intervention in areas of public interest. In this sense, AI feeds on information available in digital media, which can inherently imply cognitive biases in that data or simply reflect the priorities that major media outlets want to emphasize based on corporate or ideological interests.

There are already operational technologies used in the United States to calculate an individual's likelihood of reoffending, known as the COMPAS2 system for justice administration and criminal process monitoring. This system is used to support judicial decision-making by indicating the risk of reoffending on a risk scale, based on personal and historical data from the penal system. However, when reviewing the results of the application of this system, significant biases were detected, such as the over-surveillance of certain racial and socioeconomic groups. Furthermore, the predictions were not infallible, resulting in unjust sentences or the denial of parole for

6

some offenders. Nevertheless, some aspects of algorithmic surveillance have the ability to predict where future crimes will occur, their timing, the type of crime, as well as likely offenders (somewhat reminiscent of the movie "Minority Report").

While it is argued that AI has transformative potential for cities and everyday life in general, questions arise about whether its effects will ultimately be disruptive or revolutionary. Additionally, there are persistent questions about who benefits from these technologies: the government, corporations, or citizens? In the case of a combination of these, who should control the information that is of public interest? And, even more importantly, on what values are the systems or algorithms designed, and who should define them? Immediate scenarios involve imminent risks related to the handling of personal information by major technology corporations and their subsidiaries. In future scenarios, decisions are delegated to algorithm-based systems, which determine optimal solutions under a linear and one-directional logic that responds to narratives propagated by digital media, leaving behind the contextualization of decisions and the multidimensionality of the exercise of public policies.

Another point of contention regarding AI is the very essence of knowledge, where it is argued that the mechanisms or algorithms operating in a system lack intentionality, common sense, or a genuine understanding of the meaning of an action in a given context. The transhumanist vision, advocating for incorporating devices into the human body to enhance its capabilities, insists on the dignity and value of human nature. Indeed, AI allows for calculating the best conditions to optimize processes, but it still falls short of comprehending more complex issues or incorporating the various dimensions that make up human beings. The discussion can take us beyond the dilemma between algorithmic mechanics and human rationality to explore the fields of posthumanism, which questions the assumed centrality of our species in relation to other non-human manifestations. It anticipates a world where coexistence with artificial entities is part of our daily lives and forces us to recognize this shared existence¹⁵ (Haraway, D., 1991).

It is essential to highlight that AI has an indispensable material component within urban planning. Even though these systems are perceived in the social imagination as a series of virtual mechanisms that transcend time and space, the reality is that they require urban infrastructure and physical installations to enable the interconnection of networks and data storage. Therefore, to place the potential of AI in a broader context, cities need to budget for the costs of facilities, data processing and storage, and the energy consumption of the system as a whole, all before prioritizing it in development policies.

Historically, technological revolutions have represented a radical shift in production paradigms and economic development, from the industrial revolution to the present day. However, these innovations have not necessarily translated into an improvement in the quality of life for residents. Access to knowledge, information, and the benefits derived from these advances depend on an individual's position in the corresponding socioeconomic structure. These paradigms need to enter the public arena to be structured, regulated, and audited by governmental and citizen bodies as part of the mechanisms and public policies that shape our social coexistence.

8

Therefore, the identification of patterns (or structures) is of great use in understanding the processes taking place in the territory, such as using urban mobility flows to define transportation routes or anticipate the expansion of infrastructure and public services to certain parts of the city, modeling risk scenarios for natural disasters, or forecasting crime incidence in certain areas of the city through territorial projections. Identifying patterns from data allows AI to generate interpretation models that serve analysts in exploring different explanations for phenomena of public interest.

While these patterns are derived from statistical data analysis, the result may not necessarily make sense in a given context. Therefore, AI requires constant feedback on the relevance of its analyses, allowing it to improve or learn from experience and propose better alternatives within a more solidly defined and structured framework. Thus, human intervention remains a key element for the better functioning of algorithms, involving data selection, framing problems, and supervising the set of processes involved. Furthermore, the information derived from such analyses must be understood, placed in context, and assessed for its relevance. All of this still depends on individuals who can make sense of the information derived from data. In this way, it is possible to determine whether correlations between variables imply causality, depend on a third variable, result from a combination of variables, or are due to specific circumstances that are not necessarily the product of an interaction.

There is a relative consensus that certain uses of AI are closely tied to a moral and ethical assessment that is central to evaluating applications that can lead to political manipulation, sentencing validation based on offender recidivism probabilities, mortgage credit allocation based on applicant assessment, or the use of unmanned devices to identify and eliminate war targets without the intervention of a human mediator. Therefore, even in cases where decisions are made by a person based on AI-derived recommendations, the discussion about the so-called algorithmic black box cannot be disregarded. These are those undefined intermediate layers or processes from which recommendations are ultimately issued. Furthermore, AI can feed on the assumed rationality used by the general population, which does not necessarily stem from a causal chain but largely depends on emotional framing and the selection of concurrent explanations¹⁶ (Dignum et al., 2018; Ariely, 2010), which in some cases can result in biased explanations of reality.

In summary, it is possible to argue that there are significant implications arising from the normalization of algorithm-based public decisions, including the potential to deepen inequities, replicate discrimination, increase socio-economic exclusion, or contribute to reducing transparency mechanisms in public decision-making¹⁷ (Villani, 2018). Therefore, the way algorithms are used in the decision-making of public interest must be understandable to the general public, adapting explanations to different levels of comprehension and expertise within the population¹⁸ (European Commission AI HLEG, 2019: 18). Thus, citizen participation in establishing criteria, values, and priorities becomes essential for AI to gain legitimacy among people. Instead of technology corporations setting parameters, values, and limits for their own applications, there should be public bodies evaluating and determining the scope and constraints that new technologies must adhere to, prioritizing the safety, privacy, and well-being of the general population.

8

1.4 Smart Cities, Rationality, and Equity

The rationality underlying smart cities assumes that urban problems can be solved with technological solutions, treating the city as a machine whose processes can be improved by interconnecting them, resulting in more efficient, productive, and sustainable functioning. This model also posits that urban life is measurable, manageable, and predictable through algorithms that use data produced or collected by devices, sensors, or administrative mechanisms. The underlying premise is that efficiency brings improvements in the quality of life, enabling the rational and potentially equitable management and use of resources. However, there is no evidence that the latter is true since technology does not necessarily alter the socio-economic structure—rather, it often consolidates it—by making existing processes and mechanisms more efficient within an economy focused on the production and distribution of goods and services.

This has led to increasing criticism of the possibility of applying technological integration models without first considering the specificities, lifestyles, and values of the resident population. Moreover, it is evident that the benefits of the smart city are distributed unevenly among the population, with advantages concentrated in certain areas of the city inhabited by more privileged sectors. This replicates traditional mechanisms of social segregation and territorial fragmentation and where the advantages of a technified, digital, and connected city are concentrated. Beyond the corporate vision of the benefits of creating a conducive environment for innovation and technological development, it is necessary to define the desired city model, assessing the implications of implementing the inherent rationality and the socio-political implications of the strategies to be used.

The integration of AI in urban management could radically change how cities are governed by transforming mechanisms of citizen participation and the provision of public services. If we consider that urban planning is based on the assumption that it is possible to identify patterns that allow anticipation of the trend development of a particular place through analysis and diagnosis of reality, then it would seem reasonable to establish a plan or critical path that allows achieving specific objectives within a set timeframe, validating the use of certain instruments that would facilitate this process and provide greater precision, efficiency, and economy.

However, the term "smart city" conceals a particular political direction and an implicit justification of the type of technological networks being promoted within its ambiguity. This model has roots in the business city, innovation hubs, and technopolises, which historically have proposed converting specific city sectors into the global economy¹⁹. Furthermore, there is a technological aura around urban promotion when designating a particular city as the smartest in the region, with the hope of attracting investments and human capital to these centers of technological innovation and global connectivity.

Thus, the smart city model functions as a promise of control over a chaotic, unpredictable, and disorderly world, where public administration and service management are transformed into optimized mechanisms that, with the integration of artificial intelligence, could become entirely automated. Drawing from technological rationali-

10

ty, where system flaws are detected and subsequently fixed, urban life would be reduced to a series of quantifiable, measurable exchanges that can be compared and improved in terms of objective performance. While cities can be considered integral parts of productive systems, the digital environment now envelops the private and social lives of people, expanding the sphere of work through social networks and even entertainment media.

As a result, process optimization becomes a central goal, and the use of intelligent technologies enables the reduction of costs and increased efficiency. The entrepreneurial mindset contrasts with the political environment, which must be attentive to the electorate through citizen participation in city management. Under this logic, cities function as machines, and their greatest attribute would be their performance, meaning their responsiveness to everyday issues such as security, services, or economic growth, now based on real-time data. However, cities exhibit contrasting spaces, segregation, and inequalities—especially in peripheral countries—where greater information about water leaks, lack of public lighting, potholes in the streets, or signs of conflict between rival criminal groups may not necessarily have a decisive effect on addressing these issues. In this regard, we cannot underestimate the fact that in Latin American cities, half of the population operates in the formal economy, where invisibility is an essential characteristic of survival strategies. Additionally, it is essential to note that the data recorded by various sensors and devices do not have an explicit strategy for how to respond to fluctuations in certain indicators, or whether decision-making based on such considerations would ultimately improve the quality of life for citizens.

In recent decades, cities seek to position themselves as innovation hubs to lead new industries and thereby attract highly specialized human capital—the so-called creative class that forms internal markets for new products—as well as to serve as laboratories for testing new systems, technologies, and devices. However, the presumed access to open data platforms about the conditions in which city activities unfold does not automatically generate greater citizen participation. Additionally, interaction on social networks does not seem to necessarily strengthen social commitment, even though constructing networks of trust through strengthening citizen bonds is a desirable goal. Therefore, the mere expectation that smart cities will empower the population and lead to better resource redistribution does not appear to be among the priorities of promoters of smart cities, who generally seek to maximize their profits and benefit certain segments of society.

Smart cities operate with models similar to creative districts, where the concentration of experts in the entertainment, advertising, and design industries generates the necessary synergy to create an innovative environment, often supported by metropolitan or even federal governments. In this sense, these cities aim to generate similar dynamics but focused on harnessing information technologies, communications, and data management. Among the significant attractions associated with fostering innovation—whether through creative or technological smart cities—is their potential to create value chains, new companies, or highly profitable industrial complexes that allow them to position themselves within the global economy by attracting capital, companies, and talent from different parts of the world.

10

Cities then become command centers that manage infrastructure, facilitate the establishment of businesses, and offer low-cost land through zoning plans, regulations, and various incentives associated with territorial promotion. However, new projects often lack a sufficient, specialized population to justify the construction of extensive infrastructure systems and metropolitan facilities, as seen in the case of Songdo, South Korea. In contrast, when the intention is to reconvert an existing city by introducing technological systems, sensors, infrastructures, and services, this action is referred to as an upgrade, refurbishment, or retrofitting.

In these cases, urban transformations can be partial or focused on a particular aspect (transportation, waste collection, etc.). There is, however, a risk that the proposed changes may not be compatible with existing analog management or that their potential may be limited if the devices are not connected to other systems (e.g., autonomous vehicles and synchronized traffic lights). Another recent critique concerns bundled solutions, such as software suites or a set of solutions that manage various infrastructures and services. Consequently, the digital agenda becomes a critical path for many politicians who use the installation and coverage of one or more systems as a symbol of progress with the intention of achieving a benchmark that guarantees that the intervention falls within international reference standards. Furthermore, the efficiency in infrastructure and service management can be expected to lead to cost reduction, energy consumption reduction, or service operation time reduction, which has a media impact that results in increased political capital.

Therefore, the installation of intelligent systems in cities is generally oriented towards resolving technical issues to improve infrastructure or service management, rather than addressing structural conditions of inequity or redistributing access to goods and services. In this sense, the dissemination of such systems is more agile and fluid in a homogeneous environment than in one with significant differences that need to be leveled or standardized in advance. Regarding this, some planners like Carlo Ratti²⁰ (2018) emphasize the importance of sociability over efficiency, where citizens would be data producers as well as users (defined with the neologism "producers"). In this context, the author proposes creative interventions that seek to integrate art, new media, video art, etc., to involve citizens in various interactive experiences in streets and public spaces, all aimed at enriching urban experiences through participation initiatives using open data (e.g., hackathons, collaborations, etc.), or so-called open-source urbanism (crowdmapping) (Sassen, 2013). This raises the question of how these new technologies will structure urban space and life.

Initially, the incorporation of intelligent systems in cities would serve to make the processes of control and service management administered by city governments more efficient. Then, it would be necessary to assess the ability to provide feedback to big data systems, sensors, and information from these systems for the analysis and detection of processes and patterns that allow the generation of new urban and territorial models. However, the discussion about the potential of these technologies to trigger urban transformations, improve the quality of life of the population as a whole, and integrate participation mechanisms to define and prioritize systems for development, monitoring, and the permitted use of such information resurfaces.

12

Beyond the promises that digital technologies have the capacity to make cities "more sustainable, prosperous, and inclusive" (CityNext [2]), the reality is that the primary beneficiaries of the introduction of these systems are companies and corporations that benefit commercially and operationally from these large-scale infrastructures. In this sense, the image of a blanket covering the city with sensors and monitoring systems that connect all inhabitants and record the data they generate primarily benefits governments at various levels—given their potential to control citizens' behavior—and also provides companies with the opportunity to use the data as inputs to improve their marketing, detect preferences, streamline production systems, monitor their energy efficiency, carbon production, or measure their market share.

1.5 Conclusions: The Digitalization of Daily Life

From a technological standpoint, digital systems would favor greater citizen participation in government decisions, integrating their priorities and viewpoints into plans and programs—possibly even allowing anonymous collaboration. This could lead to more equitable access to public goods and services. In this regard, it is important to remember the long journey undertaken by urban planners in the struggle to create effective participation mechanisms for citizens (Friedman, Arnstein, Forester, etc.). However, beyond the mechanisms or instruments for capturing citizen opinions, there are political-economic structures that either encourage or inhibit the implementation of plans and programs based on the existing power configuration at any given moment.

Historically, it is social pressure and political action that advance the causes of specific groups, such as the right to the city and other social struggles, rather than the result of the incorporation of digital technologies into public administration. Nevertheless, it is also necessary to acknowledge that making open data available for public use at the federal, state, or metropolitan levels has great potential for academia and social organizations. Official information of this kind allows for timely analysis that would otherwise be costly and challenging to obtain. Initiatives like these are being promoted by the World Bank and the Inter-American Development Bank through toolboxes offered to public administrators, assuming that open data promotes collaboration and innovation, ultimately leading to the economic growth of the involved social actors.

We have discussed the overemphasis on information access as an end in itself and instead consider how citizens can use that information to be of greater relevance. It's essential to establish the necessary considerations to address privacy issues. We can conclude that data is not actually neutral; it is constructed and contextualized under an instrumental rationality²¹ (Kitchin et al, 2015). As a result, data reflects power relations and the values they represent. Therefore, the fact that a city has a high standard in certain indicators does not necessarily indicate a higher quality of life for its citizens. Thus, the use of data should be linked to specific objectives to justify the recording of structured information that can identify patterns or systems important for daily life.

12

On the other hand, data capture itself does not ensure democratic decision-making or the creation of fair, participatory, or sustainable cities. Instead, it introduces an informational dimension to governance relationships without necessarily changing power balances, hierarchies, resource allocation, or the willingness to use such information to address social, economic, or territorial disparities. This leads to a process of individualizing needs, neglecting the sense of community or the capacities of residents as producers of the city in a Lefebvrian sense. There are collectives with specific needs that go beyond possible access to the cloud of generated information. This is why the right to the city resurfaces in its digital dimension, focusing on how these processes and tools affect the lives of residents, rather than idealizing the means and infrastructure for decision-making.

Since the technological vision of the city is based on the efficiency of mechanisms and tools to manage the infrastructures and services that support productive processes, it is not surprising that citizen participation is not included as a fundamental component of these mechanisms. Citizens often participate only in the initial stages of urban processes and, in most cases, do not have enough influence in significant decisions that define priorities, instruments, and funding. In other words, while large corporations encourage participation as a mechanism to gauge public preferences, this does not necessarily mean that people have control over decisions.

Perhaps the most delicate issue is the potential for artificial intelligence to reproduce discrimination, segregation, and inequities through the biases and values behind algorithm design. This results in the automation of such biases on a large scale without facing direct challenges²² (Eubanks, 2018; Umoja, 2018). This is why, in the context of smart cities, there is an insistence on the need for "smart" citizens who can counterbalance corporate dominance and associated political forces. In this way, these citizens can revalue the role of communities, civil organizations, and non-governmental entities in defining urban plans, their goals, and priorities. Furthermore, the use of open and public data would allow the social sector to question resource allocation, public expenditure distribution, and the institutionalization of disadvantages against certain social sectors to redirect spending more equitably.

Using information to advance social causes requires top-level analysts who can help visualize information, compare it, and offer alternatives to influence public policies. In this way, the specific needs and requirements of vulnerable or disadvantaged sectors of society can be integrated. Even though there are initiatives to promote digital literacy, providing residents with training and support to develop their tools, we believe that the participation of academia is necessary and timely. Academia has the laboratories, personnel, and necessary equipment to undertake projects with significant social impact. This is why the discussion about the centralization of decision-making power—and with it, citizen control—is unavoidable if the intention is to move beyond a neoliberal model of capital concentration that currently operates through high-tech interfaces. Avoiding the reproduction of hierarchical and vertical schemes in the exercise of power is crucial.

Therefore, we argue that technology can serve as an instrument that goes beyond corporate interests and, ideally, serves as a social equalizer by addressing inequities through explicit, measurable mechanisms that promote social justice. The city, as an

interconnected network where production and distribution are balanced, is an ideal image that can depart from the hierarchical reality of power struggles, where interests are well-defined and sometimes incompatible with certain groups. However, it will be necessary to demonstrate the need for these processes to be centered on residents, fostering plurality, the complexity of urban life, and community identities. Therefore, the information revolution based on data will depend on how data is used, meaning how it serves the development of its residents, prioritizing equity, accessibility, and inclusion.

References

- ¹ Illich, Ivan (1972). *Rebirth of Epimethean Man*, en *Deschooling Society*, p. 151-167. Nueva York: Harper & Row. Society, p. 151-167. Nueva York: Harper & Row.
- ² Robert, Jean (1998). *Una visión filosófica de la tecnología*. 3er Cuaderno de Humanidades. Cuernavaca: Universidad La Salle.
- ³ McCulloch and Pitts, 1943] W. S. McCulloch and W. Pitts. A Logical Calculus of the Ideas Immanent in Nervous Activity. *Bulletin of Mathematical Biophysics*, 5: 115–133, 1943.
- ⁴ Turing, A. (1950). Computing machinery and intelligence. *Mind* 236, 433–460. doi: 10.1093/mind/LIX.236.433.
- ⁵ Picon, A. (2018). Urban infrastructure, imagination and politics: from the networked metropolis to the smart city. *Int. J. Urban Region. Res.* 42, 263–275. doi: 10.1111/1468-2427.12527
- ⁶ Greenfield, A. (2018). *Radical Technologies: The Design of Everyday Life*. London: Verso Books.
- ⁷ Pentland, A., Lipton, A., & Hardjono, T. (2021). *Building the New Economy: Data as Capital*. Amsterdam: Amsterdam University Press.
- ⁸ Ibid.
- ⁹ Ibidem.
- ¹⁰ Ibid. P.36.
- ¹¹ Harari, Yurval. N. (2018). 21 lecciones para el siglo XXI. Ciudad de México: Debate. Bubeck, S., Chandrasekaran, V., Eldan, R., Gehrke, J., Horvitz, E., Kamar, E., & Zhang, Y. (2023). Sparks of artificial general intelligence: Early experiments with gpt-4. arXiv preprint arXiv:2303.12712.
- ¹² Harari, Yurval. N. (2018). P.130.
- ¹³ García-Canclini, Nestor (2019). *Ciudadanos reemplazados por algoritmos*. Bielefeld, Alemania: Bielefeld University Press.
- ¹⁴ Ibid. P. 221
- ¹⁵ Haraway, D. (1991), “A Cyborg Manifesto: Science, Technology, and Socialist-Feminism in the Late Twentieth Century”, in *Simians, Cyborgs and Women: The Reinvention of Nature*, Routledge, New York, pp.149-181.
- ¹⁶ Dignum, V. Ethics in artificial intelligence: introduction to the special issue. *Ethics Inf Technol* 20, 1–3 (2018). <https://doi.org/10.1007/s10676-018-9450-z>; Ariely, Dan. (2010). *Predictably irrational : the hidden forces that shape our decisions*. New York :Harper Perennial.
- ¹⁷ Villani, C., Bonnet, Y., & Rondepierre, B. (2018). *For a meaningful artificial intelligence: Towards a French and European strategy*. Conseil national du numérique.
- ¹⁸ European Commission, Directorate-General for Communications Networks, Content and Technology, *Ethics guidelines for trustworthy AI*, Publications Office (2019), <https://data.europa.eu/doi/10.2759/346720>. P.18.
- ¹⁹ Castells, Manuel and Hall , Peter (1994). *Technologies of the World*, London: Routledge.

-
- ²⁰ Ratti, Carlo & Claudel, Matthew *The City of Tomorrow: Sensors, Networks, Hackers, and the Future of Urban Life* (The Future Series). Cambridge, MA: MIT Press.
- ²¹ Kitchin, Rob & Lauriault, Tracey & McArdle, Gavin. (2015). Knowing and governing cities through urban indicators, city benchmarking and real-time dashboards. *Regional Studies, Regional Science*. 2. 6-28. 10.1080/21681376.2014.983149.
- ²² Eubanks, V. (2018) *Automating Inequality: How High-Tech Tools Profile, Police and Punish the Poor*. New York: St. Martin's Press; Umoya, Safiya (2018). *Algorithms of Oppression. How Search Engines Reinforce Racism*. New York: NYU Press.

Energy

A PV-Tied Multi-Port Converter

Halleluyah Kupolati¹[0000-0002-3018-9620]

University of Pretoria, Hatfield, Pretoria, 0002, South Africa u15078486@tuks.co.za

Abstract. The aim of this work is to outline the design and implementation of a multi port converter based on the conventional single switch non-isolated buck converter. Compactness in the design of power electronics converters is required for the optimization of the physical size and weight. Additionally, there could be a potential reduction in the production cost of such a system. In the event of the requirement of multiple output voltage or current levels that are amplitude modulated, the number of magnetic components needed will be directly proportional to the number of channels required. The converter proposed in this case makes an attempt to reduce the size by utilizing multiple inductors on a single ferrite core. The mutual inductance experienced by each inductor changes the mathematical model of this converter from the conventional buck converter. This work outlines the mathematical model of this converter in addition to the modification of the conventional MPPT algorithm for use with three switching elements. The results show a maximum deviation of 28% from the practical and analytical system. The model accuracy was shown to increase as the duty cycles of all three switching elements were increase and similar to each other. At a similar duty across all three converters, there was a deviation of 5% between the practical and analytical system. The three channels were shown to be capable of independent channel control (ICC). The three MPPT algorithms utilized were the Incremental Conductance(IC), Perturb and Observe(PO), and Fractional Open Circuit Voltage(FOCV) algorithms. The modification of the PO algorithms was shown to limit the output current of the converter. Although such a system plays a crucial role in MCLEDD applications, it could be utilized in other applications as well such as battery charging.

Keywords: ICC (Independent Channel Control) · MPPT (Maximum Power Point Tracking) · MCLEDD (Multi Channel LED Drivers).

1 Multi Channel LED drivers

The use of artificial lighting has been found to have positive effects on plant growth. As a result, the use of these light sources have found use in industrial greenhouses and indoor growth warehouse units. LED driver in these applications often exhibits features, such as heat, overcurrent, overvoltage protection, as well as light intensity stability and control by way of current control. Both AC-DC, and DC-DC variety of LED drivers are efficacious for this application, [1]. The

2 H. Kupolati et al.

types can be classified as follows: Regarding the element controlled on the output, and Regarding the nature of its source. The drivers could be constant voltage or constant current controlled. In terms of the source, horticultural LED drivers could either be offline or online LED drivers. Offline LED drivers are powered from AC sources, i.e. an inverter or the grid. Disadvantages of which are increased design complexity, and a subsequent increase in cost. Online LED drivers are powered from DC sources, i.e. batteries and solar panel arrays. Advantages of which are a decreased design complexity and subsequent reduction in cost. In either type of LED driver, its efficiency is an important aspect of its operation due to the cost implication.

Sunlight, although presenting an effective source of energy for plants, also exhibit spectral qualities that affect the growth of certain types of plants negatively, such as the presence of UV lights on the spectrum, [2]. In the use of artificial lighting for plant growth, the nature of the light is often modified to spectrally emulate sunlight without or with a significantly diminished UV portion for some plants. This leads to the importance of color mixing in these applications. Color mixing requires a multiple colored LED array. Multiple colored LED arrays require MCLED drivers due to the variety of IV characteristic curves for LEDs of different colours.

The following methods of realizing an MCLED driver are classified according to their level of independent channel control. The use of linear current regulators by means of high side or low side MOSFETs presents the least complex circuitry for the realization of an MCLED driver. Additionally, it exhibits a full degree of ICC, due to the lack of presence of energy storage elements such as inductors, which could induce cross-conduction. However, this method exhibits certain disadvantages such as switching frequency limitations and possible inducing of Electro-Magnetic Interference(EMI) caused by hard switching.

In applications that require adjustable peak current levels, a voltage pre-regulator is utilized that precedes the linear current regulator stage. The regulator could take on the form of several Switch Mode Converter(SMC) topologies. Similar to first method mentioned, it exhibits a full degree of ICC.

Single Inductor Multiple Output(SIMO) converters exhibit an ability to reduce the component count significantly. They have been found to operate both continuous conduction mode(CCM) and discontinuous conduction mode(DCM). During CCM operation of the inductor, these converters exhibit a limited level of ICC due to cross conduction that occurs. During DCM, they exhibit a higher level of ICC, as a result of the limited amounts of cross conduction, i.e. the inductor is fully discharged before activation of the next channel.

Multi output converters are used for the purpose of current sharing in MCLED applications. Due to the lack of presence of MOSFET switching devices on the secondary side, they is a lack of ICC. The DCC functionality exhibited by this MCLED driver topology depends on the transformer ratio across the 3 channels. This work aims to accomplish ICC using an MCLED driver with triple coupled inductor with the objective of reducing the physical size and weight of the converter. The report is structured as follows: The converters using the least amount

of components are described in the next section. Subsequently, The design and implementation of the converter including the MPPT modifications is outlined. The next section deals with the experimental procedure. Lastly, the results of the converter and MPPT modifications are outlined and discussed followed by the conclusion and acknowledgements.

2 Topologies associated with PV arrays and MCLEDD interfaces

In essence, the circuit system that will present the best balance between circuit complexity and system efficiency is the use of switch mode converters. Although low rms current MCLED drivers can be realized with the use of linear voltage regulators, the most efficient way is with the use of DC-DC converters. A category of converters observed to have a minimal amount of components are non-isolated single capacitor based converters. They are typified by the requirement of at least a single capacitor in their circuitry. Notable examples of these are the buck, boost, and buck-boost converter topologies, [3], [4], [5]. Transformers are absent, indicating that they are non-isolated. In the case of the buck converter, the output current is higher than the input current whilst the boost converter exhibits an input current which is higher than the output current. This indicates boost converter importance in applications of high voltage LED arrays. The buck-boost varieties that require an output current that needs to higher or lower than the input current at any given point in time. The buck-boost topology is most important in systems with unstable inputs. A notable disadvantage of the buck-boost converter topology presented in the figure is such that the output polarity is inverted to the input. In the case of a minimum number of components, the above mentioned topologies present the best options. Therefore, the buck converter is amalgamated and modified for the proposed converter.

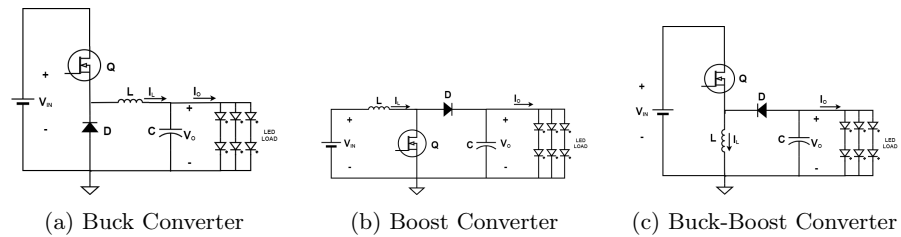


Fig. 1: Schematic for low component count DC-DC Converters

4 H. Kupolati et al.

3 Solar PV Interfacing Algorithms, The Types

There are several different types of Maximum Power Point Tracking (MPPT) algorithms that can be used in solar charge controllers and other renewable energy systems, including:

3.1 Perturb and Observe (PO) Algorithm

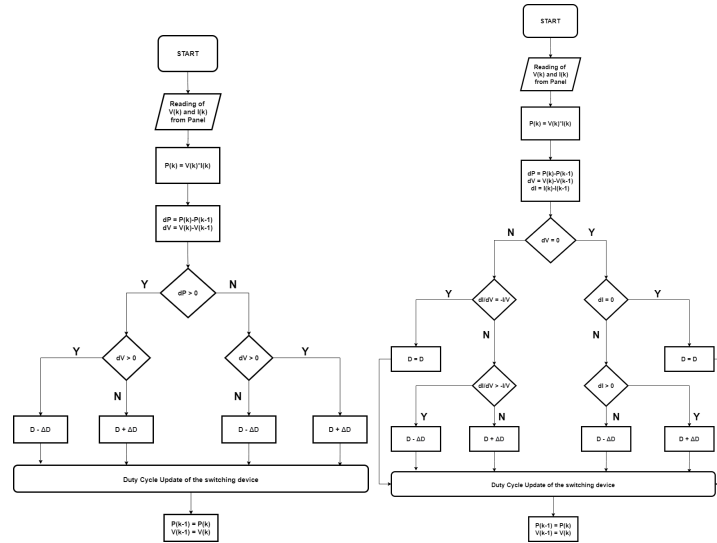
This is one of the most commonly used MPPT algorithms, which perturbs the operating point of the PV array and observes the resulting change in the output power. It adjusts the operating point in the direction that increases the power output. PO have been found to be easily implemented, [6], but they suffer from oscillations around the maximum power point. The implementation flow diagram of this algorithm is given IN figure 2a.

3.2 Incremental Conductance (IC) Algorithm

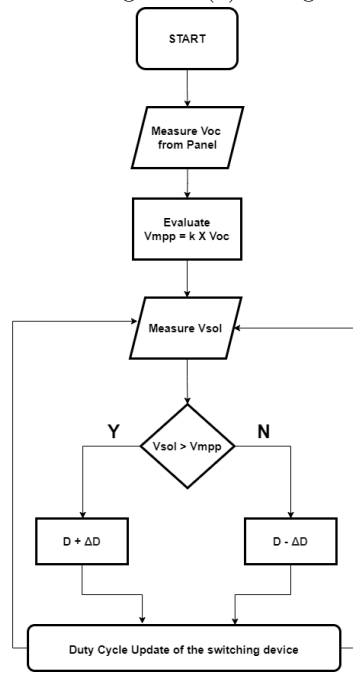
This algorithm uses the incremental conductance of the PV array to determine the operating point that maximizes the power output. It calculates the derivative of the power with respect to the voltage and adjusts the operating point to match the maximum power point, [7]. This algorithm is more complex than PO, but it can track the maximum power point more accurately and with less oscillations. The flow diagram can be found in figure 2b.

3.3 Fractional Open Circuit Voltage (FOCV) Algorithm

This algorithm calculates the open circuit voltage of the PV array and uses a fractional value of this voltage to determine the operating point that maximizes the power output. FOCV is simple to implement, but it may not be as accurate as other MPPT algorithms, [8]. Additionally, there is a requirement for open circuit voltage measurement from time to time. The flow diagram is given in figure 2c.



(a) P&O Algorithm flow diagram (b) IC Algorithm flow diagram



(c) FOCV Algorithm flow diagram

Fig. 2: Conventional MPPT Algorithms

6 H. Kupolati et al.

4 Design and Implementation

This section chronicles the design of the multi port converter. The design includes the passive component calculations and active component sizing. The image below shows the schematic of the proposed system.

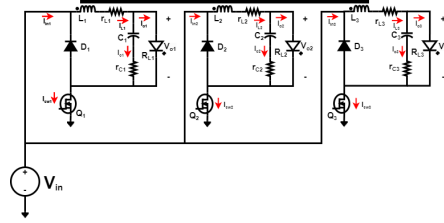


Fig. 3: The proposed converter.

In Figure 3, the proposed converter is shown, the inductors utilized are wound on the same core. This is an indication that they are coupled.

The modification of the conventional MPPT algorithm is required as the system deals with supplying power to three channels.

4.1 Open Loop System Design

The converter designed with the following requirements:

$$\begin{aligned}
 V_{in} &= (24 - 28) V; V_{out1} = (10.2 - 20.8) V, V_{out2} = (10.8 - 21.3) V, V_{out3} = (11.4 - 21.5) V \\
 \Delta V_{o1,pk-pk} &= 0.02V_{out1}, \Delta V_{o2,pk-pk} = 0.02V_{out2}, \Delta V_{o3,pk-pk} = 0.02V_{out3} \\
 \Delta I_{L1,pk-pk} &= 0.1I_{L1}, \Delta I_{L2,pk-pk} = 0.1I_{L2}, \Delta I_{L3,pk-pk} = 0.1I_{L3} \\
 V_{ce,sat1}, V_{ce,sat2}, V_{ce,sat3} &= 0.075V; V_{fwd1}, V_{fwd2}, V_{fwd3} = 0.9V \\
 r_{L1}, r_{L2}, r_{L3} &= 100m\Omega; resr1, resr2, resr3 = 3m\Omega \\
 I_{out1} &= (0.325 - 2.28) A; I_{out2} = (0.51 - 2.34) A; I_{out3} = (0.49 - 2.48) A
 \end{aligned} \tag{1}$$

The voltage range of 21V to 28.0V represents nominal maximum power point voltages for 120W and 215W panels respectively.

$$\begin{aligned}
 \delta_1 &= \frac{(V_{fwd1} + i_{L1}r_{L1} + V_{out1})}{V_{in} + V_{fwd1} - V_{ce,sat1}} \\
 \delta_2 &= \frac{(V_{fwd2} + i_{L2}r_{L2} + V_{out2})}{V_{in} + V_{fwd2} - V_{ce,sat2}} \\
 \delta_3 &= \frac{(V_{fwd3} + i_{L3}r_{L3} + V_{out3})}{V_{in} + V_{fwd3} - V_{ce,sat3}}
 \end{aligned} \tag{2}$$

The converter operation is split into three types. Type 1 depicts a scenario when all duty cycles are different. Type 2 depicts a scenario when two channels

have the same duty cycle, but the third is different. Type 3 depicts a scenario when all duty cycles are equal. Hence, inductor values are calculated for each conduction zone, the maximum of which is the optimal value for the inductor.

The component calculations are modified as a result of the use of a triple coupled inductor.

The ripple current for the inductor of port 1 is obtained as:

$$\Delta I_{L1,pk-pk} = \frac{V_{L1}(M_{23}^2 - L_2L_3) + V_{L2}(L_3M_{12} - M_{12}M_{23}) + V_{L3}(L_2M_{12} - M_{12}M_{23})}{L_3M_{12}^2 - 2M_{12}M_{13}M_{23} + L_2M_{13}^2 + L_1M_{23}^2 - L_1L_2L_3} \times dt \quad (3)$$

The ripple current for the inductor of port 2 is obtained as:

$$\Delta I_{L2,pk-pk} = \frac{V_{L1}(L_3M_{12} - M_{13}M_{23}) + V_{L2}(M_{13}^2 - L_1L_3) + V_{L3}(L_1M_{23} - M_{12}M_{13})}{L_3M_{12}^2 - 2M_{12}M_{13}M_{23} + L_2M_{13}^2 + L_1M_{23}^2 - L_1L_2L_3} \times dt \quad (4)$$

The ripple current for the inductor of port 3 is obtained as:

$$\Delta I_{L3,pk-pk} = \frac{V_{L1}(L_2M_{13} - M_{12}M_{23}) + V_{L2}(L_1M_{23} - M_{12}M_{13}) + V_{L3}(M_{12}^2 - L_1L_2)}{L_3M_{12}^2 - 2M_{12}M_{13}M_{23} + L_2M_{13}^2 + L_1M_{23}^2 - L_1L_2L_3} \times dt \quad (5)$$

dt is determined by the time intervals.

According to the equation of the inductor ripple, the number of unknowns make the calculation a time consuming iterative process. In the quest to reduce the calculation time. Some assumptions are made. The major assumption made is that the individual inductor of each port are equal, in addition to the mutual inductance values being equal. Hence the following applies:

$$\begin{aligned} L_1 &= L_2 = L_3 = L \\ M_{12} &= M_{13} = M_{23} = M \end{aligned} \quad (6)$$

The relationship between the mutual inductance and individual inductance is as follows:

$$M = 0.75 \times L \quad (7)$$

The relationship described above is based on the observation on a radial winding pattern.

Table 1 represents the duty cycle for all the types:

Table 1: Duty Cycle Values for all Types

	δ_1	δ_2	δ_3
Type 1	0.3	0.5	0.7
Type 2	0.3	0.5	0.5
Type 3	0.6	0.6	0.6

$$C \geq \frac{\Delta Q}{\Delta V_{o,pk-pk}} \quad (8)$$

8 H. Kupolati et al.

It should be noted that a tradeoff was made between the inductance values and the space available for the purpose of achieving a reduction in weight. The inductance values in table 2 is obtained using a 10% ripple.

Table 2: Minimum Inductance Values

	$L_1(uH)$	$L_2(uH)$	$L_3(uH)$
Type 1	3485	2142	505.5
Type 2	2695	670	662
Type 3	226	181.1	183

The chosen ferrite core is the 77439A7 core. The core was found to have a maximum capacity of 43 turns on three sides. This produced a maximum inductance of $226\mu H$. Hence, the inductance of mutual inductance obtained is as follows:

$$\begin{aligned} L_1 &= 202\mu H, L_2 = 204.5\mu H, L_3 = 194.9\mu H \\ M_{12} &= 152.3\mu H, M_{13} = 154.1\mu H, M_{23} = 152.1\mu H \end{aligned} \quad (9)$$

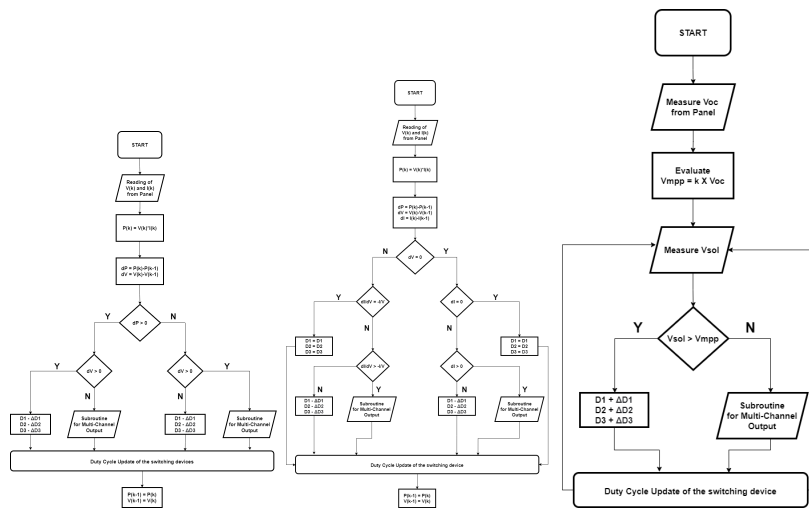
Taking into account the values above. Equation (3), (4), (5) are used to obtain the inductor current ripples for all conduction zones. Table 3 shows the minimum capacitance values required to match with the designed inductors.

Table 3: Minimum Capacitance Values

	$C_1(uF)$	$C_2(uF)$	$C_3(uF)$
Type 1	1.22	1.24	0.793
Type 2	1.783	0.613	0.791
Type 3	0.195	0.186	0.220

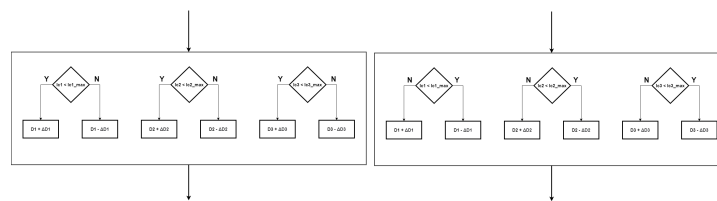
4.2 MPPT System

This section illustrates the modified flow diagram of the PO, IC, and FOCV algorithms. The modified flow diagrams for the PO, IC, and FOCV can be found in figure 4a, 4b, and 4c respectively. The subroutine for both the IC and PO method takes into account each channel of the converter. The flow diagram of which is shown in Figure 5a. The subroutine for both the FOCV method takes into account each channel of the converter. The flow diagram of which is shown in Figure 5b.



(a) P&O Algorithm flow diagram (b) IC Algorithm flow diagram (c) FOCV Algorithm flow diagram

Fig. 4: The Modified MPPT Algorithm Flow Diagrams



(a) PO and IC subroutine. (b) FOCV subroutine.

Fig. 5: The Subroutines

10 H. Kupolati et al.

5 Experimental Procedure

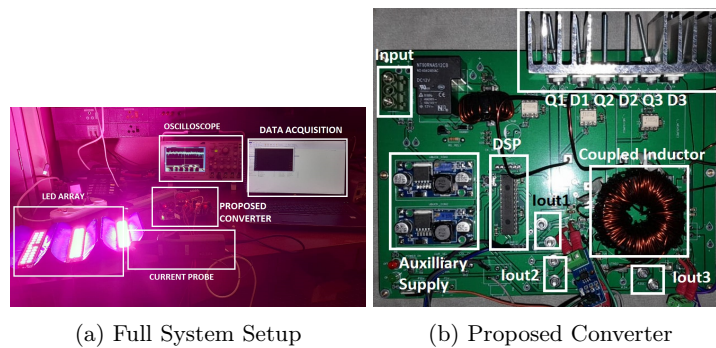
This section highlights the experimental procedure and apparatus used for both systems.

5.1 Fixed Input Voltage System

The experimental apparatus for this are as follows:

- A tektronix oscilloscope
- A 300kHz current probe
- The proposed multiport converter
- 150W Multi channel LED Array Load
- Data Acquisition

Figure 6a shows the full experimental setup for a fixed voltage input. Figure 6b shows the parts of the proposed converter consisting of the controller, MOSFETs, diodes and coupled inductor.



(a) Full System Setup

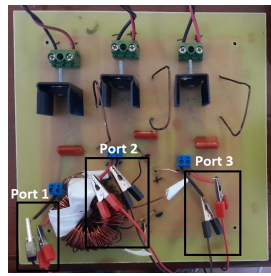
(b) Proposed Converter

Fig. 6: Fixed Input Voltage System Setup

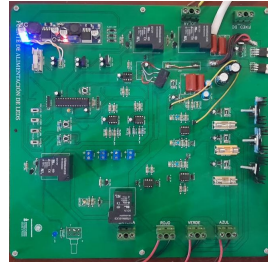
5.2 MPPT System

The system has the current sensors on the input of the converter. The experimental apparatus for this are as follows:

- A data acquisition system
- 120W solar panel
- The proposed multiport converter



(a) Coupled Inductor and System Output



(b) Controller Board



(c) 120W Solar Panel

Fig. 7: System Setup for Solar PV Input

Table 4: Solar Panel Characteristics

Parameters	Values
Rated Maximum Power (P_{mp})	120W
Voltage at Pmax (V_{mp})	21.024V
Current at Pmax (I_{mp})	5.71A
Open-Circuit Voltage (V_{oc})	24.696V
Short-Circuit Current (I_{sc})	6.03A

6 Results and Discussion

In this section, the results for both the open loop system and MPPT system are outlined and discussed.

6.1 Open Loop Results

Figure 8 shows the inductor currents comparison observed for the type 1 system.

12 H. Kupolati et al.

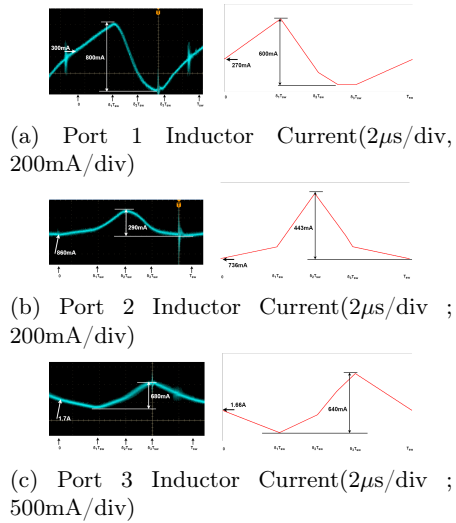


Fig. 8: Type 1 Inductor current waveforms

Figure 9 shows the inductor currents comparison observed for the type 2 system.

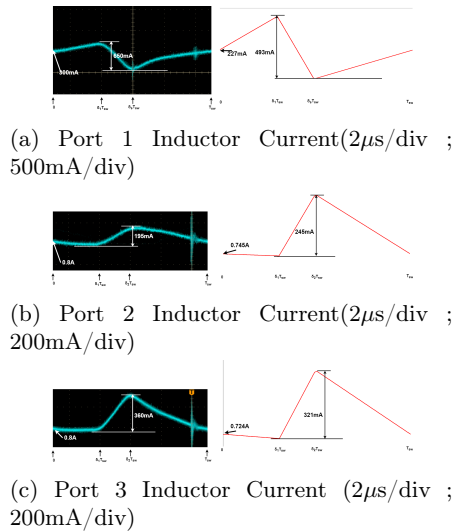


Fig. 9: Type 2 Inductor current waveforms

Figure 11 shows the inductor currents comparison observed for the type 3 system.

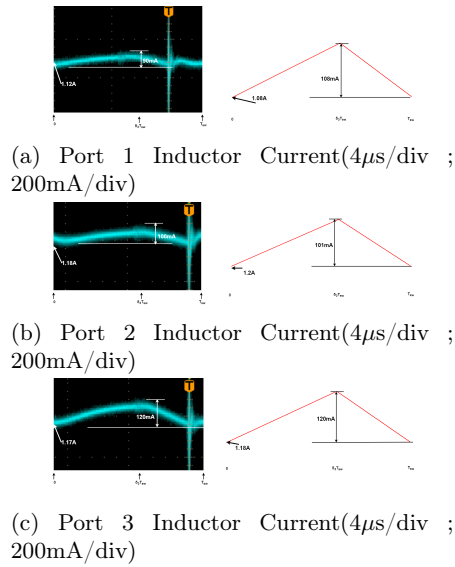


Fig. 10: Type 3 Inductor current waveforms

Table 5: Table Summarizing the inductor current ripple values for the type 1 system

	Analytical(mA)	Simulated(mA)	Experimental(mA)
Channel 1	623.9	600	800
Channel 2	395.8	443	290
Channel 3	668.3	640	680

Table 6: Table Summarizing the inductor current ripple values for the type 2 system

	Analytical(mA)	Simulated(mA)	Experimental(mA)
Channel 1	516.3	493	650
Channel 2	255	245	195
Channel 3	334	321	360

14 H. Kupolati et al.

Table 7: Table Summarizing the inductor current ripple values for the type 3 system

	Analytical(mA)	Simulated(mA)	Experimental(mA)
Channel 1	112.32	108	90
Channel 2	107.3	101	100
Channel 3	126.8	120	120

6.2 Discussion of the Open Loop Results

This section focuses on the model accuracy with regards to inductor current ripple. In this system, the inductor current ripple represents a key performance index for the system. Although, the method proposed aims to reduce the space required, the disadvantage observed has been an increase in the current ripple. According to table 5, 6, and 7. The general trend is that as the duty cycle increases the percentage difference between the analytical ripple and the experimental ripple is reduced. Hence, model accuracy increases with an increase in the duty cycle. Additionally, the closer the duty cycles of all three channels, the better the model approximates the experimental system. According to row 2 of table 5, the highest difference between the analytical and experimental system is the port 1 of the type 1 system. It should be noted that the inductor current becomes negative in the experimental system for a brief period of time.

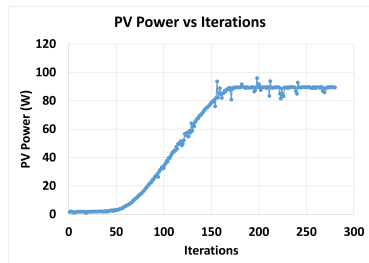
6.3 Solar MPPT Systems

This section illustrates the power limiting feature in addition to the speed at which MPPT is achieved using the algorithms PO, IC, and FOCV. The update time for the MPPT was chosen to be 15ms. The duty cycle is increased or decreased by 0.5%. The objective is to illustrate a performance comparison between the different types of algorithms with regards to their interaction with three different ports. Additionally, this section aims to evaluate the effectiveness of the modification at different current levels.

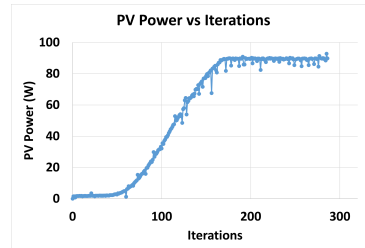
Perturb and observe algorithm outcome Figure 11a shows the curve of the PV power vs the number of iterations. It indicates that the number of iterations to extract maximum power from the panel is 172 iterations. The maximum power output is 89W.

Incremental conductance algorithm outcome Figure 11b shows the curve of the PV power vs the number of iterations. It indicates that the number of iterations to extract maximum power from the panel is 169 iterations. The maximum power output is 89W. This aligns with the characteristics of the IC algorithm which entails lesser amounts of oscillation around the maximum power point in comparison to the PO algorithm.

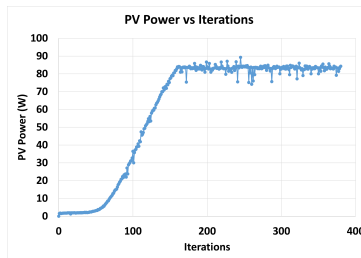
Fractional Open Circuit Voltage Algorithm Outcome Figure 11c shows the curve of the PV power vs the number of iterations. It indicates that the number of iterations to extract maximum power from the panel is 160 iterations. The maximum power output is 84W. The PV power is lower in this instant due to the assumption of the V_{mp} of the panel. The input power sensing circuitry is less complex than that of the IC, and PO algorithms. However, there is a 5.95% reduction in the power extracted from the solar panel.



(a) Input power vs Iterations for the PO algorithm



(b) Input power vs Iterations for the IC algorithm



(c) Input power vs Iterations for the FOCV algorithm

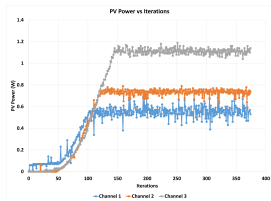
Fig. 11: Input Power vs Iterations

16 H. Kupolati et al.

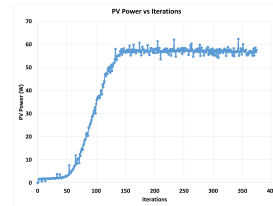
6.4 Current Limited Output

The maximum input current was 1.85A. Hence the values specified are fractions of this particular value, i.e. A value of 0.1, indicates an actual current of 0.185A(0.1*1.85). Six scenarios of current outputs are obtained whereby, each channel has the maximum current flowing through it at any particular point in time. The experimental IV plot of each channel is obtained as follows:

Figure 12 shows the average input current readings for a setpoint of $I_{set1} = 0.3A$, $I_{set2} = 0.4A$, and $I_{set3} = 0.6A$.

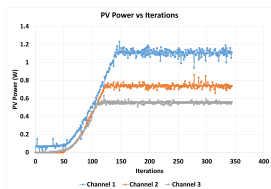


(a) Channel Currents vs Iterations

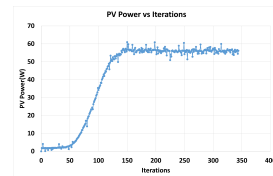


(b) PV Power vs Iterations

Fig. 12: Current and Power curves at Array 1 = 0.3; Array 2 = 0.4; Array 3 = 0.6



(a) Channel Currents vs Iterations



(b) PV Power vs Iterations

Fig. 13: Current and Power curves at Array 1 = 0.6; Array 1 = 0.4; Array 1 = 0.3



Fig. 14: Current and Power curves at Array 1 = 0.3; Array 1 = 0.6; Array 1 = 0.4

6.5 Discussion of the MPPT Results

According to figures 11a, 11b, 11c, the modification of the conventional MPPT algorithm for 3 switching elements extracts the maximum power from the solar panel. The results of the current limiting feature is an indication of the functionality of the algorithm modification. Figure 12, 13, 14 shows the different scenarios of readings to account for each port having a highest current output.

7 Conclusion

This work had two major objectives which are as follows: The first was to present a mathematical model for a multi port converter adapted from a buck converter that utilized a triple coupled inductor. The second was to modify the conventional MPPT algorithms to be used with three switching elements. The ultimate goal being to reduce the required physical size and weight of the system. The conventional algorithms were researched and outlined as well as the conventional converters that utilized the least amount of components. The results indicated a maximum difference between the analytical and experimental model of 28% with regards to the inductor current ripple. The FOCV Algorithm exhibited the fastest tracking speed in comparison to the IC and PO Algorithms. The current limiting functionality of the modified algorithm was tested using 3 different scenarios. This showed a current limiting functionality in scenarios of ports having the same output currents and differing current levels on each port.

Future recommendations are to do with studying the effects of winding patterns on the coupling coefficient. It should be noted that a lower mutual inductance resulted in lower cross conductance, thereby, maximizing the effectiveness of the reduction in space required for the system. More complex MPPT algorithms should be modified and performance evaluated for multi port functionalities. Additionally, other types of active loads should be considered for use with the proposed converter.

Acknowledgements Thanks to the Electrical, Electronics, and Computer Engineering (EECE) Department of the University of Pretoria, South Africa for

18 H. Kupolati et al.

the provision of lab equipment used to evaluate the system. Special thanks to the Escuela de Ingeniería de la Industria Forestal, Agronómica y de la Bioenergía (EIFAB) in the Campus Universitario Duques de Soria, Spain for the laying the foundations on which this work was built. A special acknowledgement to ICSC-CITIES 2023 for the opportunity to share this work.

References

- [1] D. G. Lamar, “Latest developments in LED drivers,” *Electronics*, vol. 9, no. 4, p. 619, Apr. 2020. DOI: 10.3390/electronics9040619. [Online]. Available: <https://doi.org/10.3390/electronics9040619>.
- [2] A. Yadav, D. Singh, M. Lingwan, P. Yadukrishnan, S. K. Masakapalli, and S. Datta, “Light signaling and UV-b-mediated plant growth regulation,” *Journal of Integrative Plant Biology*, vol. 62, no. 9, pp. 1270–1292, May 2020. DOI: 10.1111/jipb.12932. [Online]. Available: <https://doi.org/10.1111/jipb.12932>.
- [3] F. Loose *et al.*, “Efficient hybrid buck converter for visible light communication in LED drivers,” *IEEE Transactions on Industrial Electronics*, vol. 69, no. 2, pp. 1877–1887, Feb. 2022. DOI: 10.1109/tie.2021.3060651. [Online]. Available: <https://doi.org/10.1109/tie.2021.3060651>.
- [4] P.-J. Liu and Y.-C. Hsu, “Boost converter with adaptive reference tracking control for dimmable white LED drivers,” *Microelectronics Journal*, vol. 46, no. 6, pp. 513–518, Jun. 2015. DOI: 10.1016/j.mejo.2015.03.022. [Online]. Available: <https://doi.org/10.1016/j.mejo.2015.03.022>.
- [5] K. Eguchi, K. Kuwahara, and T. Ishibashi, “Analysis of an LED lighting circuit using a hybrid buck–boost converter with high gain,” *Energy Reports*, vol. 6, pp. 250–256, Feb. 2020. DOI: 10.1016/j.egy.2019.11.070. [Online]. Available: <https://doi.org/10.1016/j.egy.2019.11.070>.
- [6] R. Lopez-Erauskin, A. Gonzalez, G. Petrone, G. Spagnuolo, and J. Gyselinck, “Multi-variable perturb and observe algorithm for grid-tied PV systems with joint central and distributed MPPT configuration,” *IEEE Transactions on Sustainable Energy*, vol. 12, no. 1, pp. 360–367, Jan. 2021. DOI: 10.1109/tste.2020.2996089. [Online]. Available: <https://doi.org/10.1109/tste.2020.2996089>.
- [7] M. A. B. Siddique, A. Asad, R. M. Asif, A. U. Rehman, M. T. Sadiq, and I. Ullah, “Implementation of incremental conductance MPPT algorithm with integral regulator by using boost converter in grid-connected PV array,” *IETE Journal of Research*, pp. 1–14, May 2021. DOI: 10.1080/03772063.2021.1920481. [Online]. Available: <https://doi.org/10.1080/03772063.2021.1920481>.
- [8] A. Nadeem, H. A. Sher, and A. F. Murtaza, “Online fractional open-circuit voltage maximum output power algorithm for photovoltaic modules,” *IET Renewable Power Generation*, vol. 14, no. 2, pp. 188–198, Jan. 2020. DOI: 10.1049/iet-rpg.2019.0171. [Online]. Available: <https://doi.org/10.1049/iet-rpg.2019.0171>.

Assessing the Impact of Increasing Electric Vehicle Penetration on Distribution Networks within Sustainable Local Energy Community Frameworks

Samuel Borroy¹[0000-0002-2412-576X], Gregorio Fernández¹[0000-0003-0751-1658], Miguel Sota¹[0000-0001-7006-9888], Andres Llombart¹[0000-0001-6350-4474], Matteo Salani²[0000-0003-2809-4347], Marco Derboni²[0000-0003-4590-3628], Vincenzo Giuffrida²[0009-0009-4627-7391], Angel Luis Zorita Lamadrid³[0000-0001-7593-691X], Victor Alonso Gómez⁴[0000-0001-5107-4892] and Luis Hernandez-Callejo⁵[0000-0002-8822-2948]

¹ Fundacion CIRCE, Parque Empresarial Dinamiza, Avenida Ranillas 3-D, 1st Floor, 50018 Zaragoza, Spain

² IDSIA Dalle Molle Institute for Artificial Intelligence, USI-SUPSI, via La Santa 1, 6962 Lugano, Switzerland

³ Departamento de Ingeniería Eléctrica, Universidad de Valladolid, 47002 Valladolid, Spain

⁴ Departamento de Física Aplicada, Universidad de Valladolid, 47002 Valladolid, Spain

⁵ ADIRE-ITAP, Departamento Ingeniería Agrícola y Forestal, Universidad de Valladolid, Campus Duques de Soria, 42004 Soria, Spain

sborroy@fcirce.es

Abstract. This paper presents a detailed investigation into the impacts of increasing Electric Vehicle (EV) penetration on low voltage distribution networks which integrate local energy communities with photovoltaic-based self-consumption. A benchmark system, inspired by the IEEE European Low Voltage Test Feeder and representing urban environments, is analyzed under various scenarios. While keeping photovoltaic penetration constant, the study varies EV penetration levels to isolate and understand the effects of EV adoption on the grid. To evaluate potential strategies for mitigating negative impacts, the study compares two different charging strategies: unmanaged charging and economic charging management strategy. The assessment, based on power flow simulations focusing on key indicators, show that increased EV penetration can lead to voltage alterations, overloads, and technical losses, but economic charging management significantly mitigates these impacts, reducing voltage and load violations and decreasing technical losses. The paper sets the stage for future investigations into advanced strategies for sustainable grid management, including the integration of EVs within sustainable local energy communities.

Keywords: Electric Vehicle, Sustainability, Energy Transition, Voltage levels, Overloads, Technical losses, Local Energy Communities.

2

1 Introduction

Electricity systems and processes, including generation, transmission, distribution and consumption, will play a pivotal role at the core of the energy transition, which aims to alleviate dependence on fossil fuels and mitigate the effects of climate change. International initiatives such as the European Green Deal [1] and The United States Federal Green New Deal (GND) [2] promote policy proposals incentivizing scenarios which allow the feasibility of the mentioned transition.

In line with such scenarios, the International Energy Agency (IEA) forecasts a relevant rise in electricity demand for next years [3], which is consistent with the great potential of electrification to mitigate emissions and decarbonise energy supply chains. Particularly, the segment whose electrification is expected to represent the higher impact on CO₂ emission reductions is the road transport sector, specifically within the light-duty vehicle section. In this sense, considering IEA's Net Zero Scenario, electrification accounts for about 7% of all mitigated emissions between 2020 and 2030, being electric vehicles (hereinafter EV) responsible for the majority of these reductions [4].

Trends and projections in EV sales are fully consistent with the relevant role of mobility in the electrification scenarios. In 2022 electric car markets experienced significant growth, being electric a total of 14% of all new cars sold, up from around 9% in 2021 and less than 5% in 2020. In 2023 sales keep the rising trend, with figures for the first quarter about 25% higher than in the same period last year. Moreover, IEA forecasts that global EV sales increase around fourfold from 2022 to 2030 [5].

Along with the electrification, the integration of renewable energies represents a cornerstone for achieving the objectives of energy transition. Large plants are growing, but particularly, sustainable self-consumption is expected to experience relevant increases, with perspectives for renewable energies to reach about 40% of building electricity use supply by 2030 [6]. Specific advanced configurations of self-consumption and distributed energy resources (DER) are represented by Local Energy Communities (LEC), which are in development phase both in regulatory aspects and in potential technology capabilities such as energy efficiency services or consumptions aggregation [7].

Electricity networks are core elements with a backbone role to make feasible the guarantee of supply in the promising scenarios presented, facing the challenge of feeding growing electricity demands and integrating new generation based on non-manageable primary resources. Specially for medium (MV) and low voltage (LV) distribution networks, the challenge becomes notably arduous since such proliferation of distributed renewable generation sources introduces profoundly different conditions compared to their original design. Regarding electric mobility penetration, the distribution networks need to address the issue of managing massive EV charging, due to the overall increase in energy consumption and peak demand, which consequently leads to a higher probability of grid congestions and larger distribution energy losses. Furthermore, voltage deviations and phase unbalances can increase, resulting in adverse impacts on grid stability [8], [9], [10].

Fortunately, not only challenges, but also means and instruments for achieving sustainable transition objectives appear with the increased penetration of DER and new electric demands, provided that Smart Grids concepts and technologies are considered

for their deployment. Technologies for DER integration and advanced transmission and distribution assets operation, contribute to pave the way towards energy transition and sustainability [11], [12], [13]. Moreover, potential negative effects of EV rising can be solved by applying demand management to adapt the charging process, according to the grid status, local energy demand and renewable sources availability. Solutions for coordinating the management and control of dispersed resources and loads (including aggregation and LEC) provide flexibility to the system, which is critical to cope with the variability of the primary resource associated with renewable generation [14]. The synergies of renewable generation and electrification, particularly those demands with manageability perspectives (such as evolving electric vehicle technology) which allow mitigating primary sources variability, provide valuable tools to foster the transition, as it is analyzed in Smart Grids research lines which frame the presented work.

With the objective of quantifying the effects of embedded connection of renewable generation sources and self-consumption installations in distribution networks, in [15] the authors explored the technical impacts that the irruption and proliferation of renewable-based LEC can have on electrical distribution systems, which was the novelty exposed. The results obtained shown that the enhancement observed in the scenarios which consider LEC integration is remarkable, improving voltage, load, and losses indicators. In addition, the work concluded that further analyses should be performed considering more complex structures, integrating additional elements aligned with Smart Grids paradigm, such as storage systems or electric vehicles. The work presented in this paper, maintaining the framework of the integration of solar photovoltaic (PV)-based LEC, expands the research line analyzing the role of EV in sustainable scenarios examining the impact on network operation-oriented key performance indicators (KPIs) of different levels of EV penetration comparing different management strategies for charging processes.

This paper is organized as follows: Section 2 describes the general methodology followed in the work, section 3 presents the results obtained and section 4 summarizes the main conclusions of the study and introduces further working lines.

2 Methodology

The technical impacts of EV penetration in sustainable distribution networks are evaluated through the analysis and comparison of scenarios based on different penetration levels of EV and charging strategies, which are implemented in a representative European system, representing urban distribution networks including a specific rate of PV-based LEC.

The quantification of impacts is based on voltage and load levels since they are power systems operational variables representative of the status of the system. Moreover, these variables are directly impacted by variations in electric demand and DER penetration.

Considering such framework, following subsections present details of indicators, simulation methods, benchmark network and scenarios.

4

2.1 Impact assessment indicators

The different scenarios are assessed in terms of load and voltage levels in LV benchmark distribution networks. Particularly, the indicators are based on the number of occurrences of healthy limits violations, considering one-month extension analysis with a resolution of one minute, as detailed in subsection 2.2:

- Voltage levels KPI: number of occurrences of node voltage level above or below healthy operational range
- Load levels KPI: number of occurrences of line section load level above healthy operational range (i.e., overloads)

Two levels of range violations severity are considered to quantify the occurrences of voltage/load events. Table 1 summarizes the criteria defined, which follows a “traffic light” approach.

(Note: for each variable it is counted as an occurrence every instance that an element falls in the defined limits considering the whole analyzed period).

Table 1. Voltage and loads limits criteria. Limits relative to nominal values.

“Traffic light”	Severity	Variable	Urban network
Green	NA (Healthy)	Voltage (V)	$95\% < V < 105\%$
		Load level (L)	$L < 90\%$
Yellow	Medium	Voltage (V)	$93\% < V < 95\%$ or $107\% > V > 105\%$
		Load level (L)	$100\% > L > 90\%$
Red	High	Voltage (V)	$V < 93\%$ or $V > 107\%$
		Load level (L)	$L > 100\%$

Additionally, given their relevance in efficiency and sustainability, technical losses are calculated for each scenario, being as well relevant KPIs for the assessment. For the sake of consistency, the same period considered for voltage and loads KPIs has been analyzed (future works will explore extending the analysis to a one-year period).

2.2 Simulation methods

Power flow simulations are performed in order to obtain results that feed the calculation process of the indicators presented above. Based on the network model and scenarios implemented, simulations allow the study of the evolution of load and generation profiles along the analyzed period, and the subsequent effect on the state variables selected. The software platform selected to conduct such analyses is PowerFactory DIGSILENT [16] in which the network and the case studies explained in 2.3 have been modelled.

Taking advantage of the capabilities of the simulation platform, a Python-based tool has been developed with the goal of generating a comprehensive database of occurrences of limit violations following criteria described in 2.1. This tool, applied for each scenario, automatically executes power flow simulations every minute considering the evolution of load and generation profiles along a whole month.

After each simulation, the tool automatically records and captures voltage and load events considering the ranges specified in Table 1, storing the information in a structured database. This approach allows for an extensive analysis of network performance with respect to the predefined KPIs.

2.3 Case studies

A representative benchmark system has been defined based on anonymized real data of European DSOs. For the sake of confidentiality and generality of the results, and taking into account its typology, it is named in this work as Urban network. This system follows, with the particularities defined by the corresponding DSO, general criteria represented by *IEEE European Low Voltage Test Feeder*, included in the resources provided in [17].

The benchmark system and the charging profiles for EV integrated in the network, as well as the scenarios defined for the analysis, are described in this section.

2.3.1 Benchmark system

Urban network

Based on network topology obtained from a real urban European network and data of lines, transformers, generators and loads, provided by a European DSO, this benchmark network is built and modelled in the simulation platform. The Urban network comprises a radial LV system connected to a 20/0.4 kV secondary substation and feeds a total of 193 supply points, whose load profiles have been modelled anonymizing data based on real information from DSO. Two of these supply points initially included self-consumption PV units. In order to establish a base case with a more relevant self-consumption rate, additional PV units have been modelled and randomly assigned to supply nodes until 20% of users integrate PV units. Nominal power of each PV unit is defined according to the maximum demand connected at each point (it is assigned randomly from 50% to 75% of such value), while for modelling hourly solar generation profiles generic public data have been considered [18, 19, 20].

EV consumption is incorporated into this model, according to penetration levels specified in 2.3.2, and considering the charging profiles and charging management strategies described in 2.4.

Fig. 1 shows the one-line diagram of Urban benchmark network, including the representation of customers (represented as arrows) and PV units (highlighted).

6

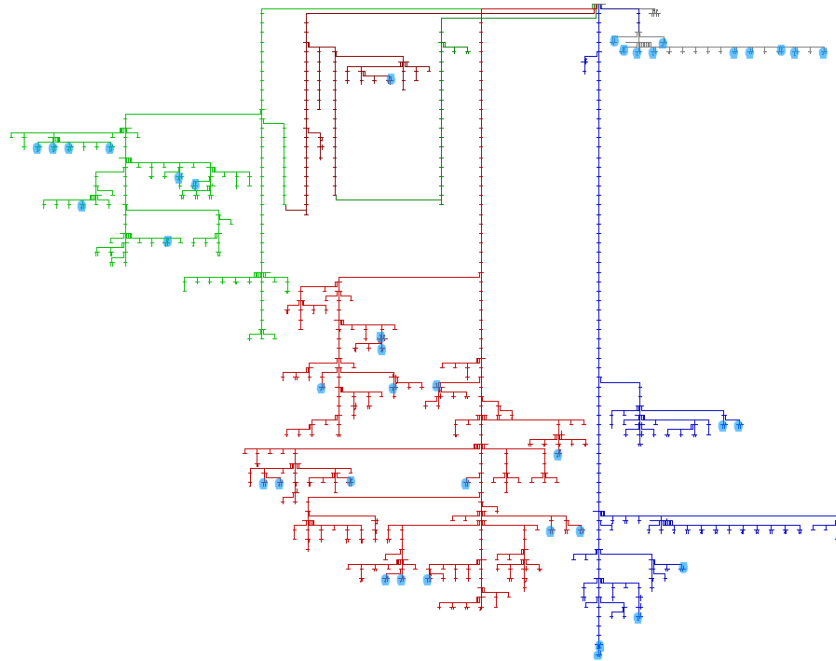


Fig. 1. One-line diagram of Urban Network.

2.3.2 Scenarios

The scenarios defined to compare the results of the indicators described are based on different penetration levels of EV and charging strategies, being each scenario evaluated for the benchmark system described above. Table 2 summarizes the set of scenarios analyzed for the benchmark system.

A key factor for the classification of scenarios is the EV charging strategies, which are detailed in section 2.4. Additionally, as it can be observed, PV penetration remains stable along the scenarios (considering already a penetration in the base case), while EV penetration grows for each scenario. The objective of such definition of scenarios is to yield insights specifically associated with the evolution of electric mobility, which complements prior studies focused on PV penetration, such as those elaborated in [15], and thus helps shaping further studies related to complete energy transition scenarios.

Table 2. Scenarios definition for Urban benchmark system.

Charging Strategy	Scenario	PV&EV penetration level	
		PV (% of consumers)	EV (% of consumers)
Unmanaged charging	Base case	20%	0%
	Scenario 1	20%	20%
	Scenario 2	20%	40%
	Scenario 3	20%	60%
Economic charging management	Base case	20%	0%
	Scenario 1	20%	20%
	Scenario 2	20%	40%
	Scenario 3	20%	60%

2.4 Electric Vehicle charging modeling

EV charging processes play a relevant role in the modeling of the scenarios presented. This section provides an overview of the charging profiles assumed for EVs, along with the two charging strategies considered for the scenarios described.

2.4.1 EV chargers

Two types of EV charging facilities have been considered: domestic chargers and public charging stations. For domestic cases the locations of the charging points have been determined considering the proportion of consumers with EV chargers as defined for each scenario (section 2.3.2). This process follows the same approach as with PV units for initial penetration level; that is, for Scenarios n°1 of Table 2, the sustainable self-consumption configuration of the affected consumers includes both PV units and EV chargers. For the subsequent scenarios, the locations of EV chargers have been determined randomly. Regarding electrical connections, generally single-phase chargers with a power rating of 3.7 kW are considered, characteristic for EV chargers.

Two types of generic charging profiles have been assigned and implemented in the model, according to the existing conventional load profile of each consumer: a domestic profile for consumers who typically charge their vehicles at home overnight, and a commercial profile for those who charge their EV during the workday midday hours.

Concerning public charging points, the benchmark system includes one station connected to the Low Voltage (LV) terminal of the secondary substation transformer. These stations include fast charging points with capacities of 100 kW and moderate charging points rated at 50 kW. To generate load profiles for these stations, a specially designed tool was utilized. This tool operates based on an hourly estimation of the percentage use of each charging point, based on probability distributions, subsequently generating random power profiles on a minute scale.

8

2.4.2 EV charging strategies

Considering the charging points detailed in subsection 2.4.1, two types of charging strategies are implemented and modelled:

Unmanaged charging

This type of charging does not consider any specific strategy for optimizing the charging process; instead, it takes into account the existing conventional load profile of each consumer. Therefore, EVs adapt their charging profiles to align with the consumption patterns of the affected consumers. Thus, steady slow-charging process has been modeled, with average charging duration of 8 hours.

Economic charging management

This strategy has been developed in the framework of the Horizon 2020 project PARITY [21] with details provided in the corresponding deliverables. This subsection presents the main concepts of the methodology.

The primary focus of this strategy is to accommodate most charging requests while minimizing the associated costs. Each charging request, considered in the strategy, is characterized by several critical parameters, including the expected arrival time, the expected unplug time, the initial state of the battery charge, and the minimum desired state of charge at the unplug time. Additionally, each request incorporates static properties of the EV, such as the maximum charging power and the battery capacity.

The charging management strategy operates within a predetermined time horizon, conveniently divided into constant time slots. During each of these slots, the strategy aims to optimize costs associated with power consumption from the grid. Strategic management of these costs across all charging operations enhances the overall economic efficiency of the system.

The mathematical model that informs the charging management strategy optimizes these charging requests and their respective parameters to create a charging schedule that minimizes monetary costs. In this context, the cost function is significantly influenced by the cost of absorbing a constant power from the grid during a specific time slot. This cost consideration plays a pivotal role in the decision-making process of the model, underscoring the inherent cost-effectiveness of the approach.

The strategy respects the specific power constraints of each charging station and the maximum power available for the entire set of stations at each time slot. These power constraints ensure that each charging station operates within its technical capacity. This approach facilitates the servicing of as many charging requests as possible without compromising the stability of the station or the grid.

In essence, the implemented economic charging management strategy presents a balanced approach between economic efficiency and the technical constraints of EV charging stations and the grid. Fig. 2 illustrates an example of charging profiles (unmanaged vs. economic charging management) in which it can be observed that the unmanaged profile requests higher power concentrated in the first part of the available time while the optimized profile distributes it more evenly.

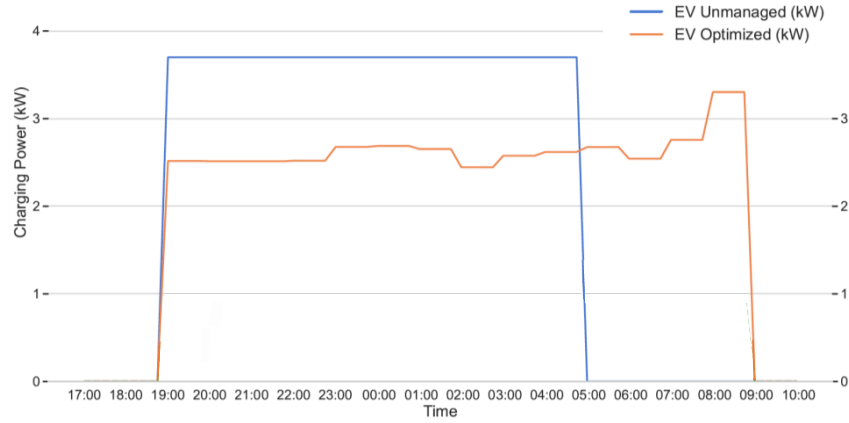


Fig. 2. Example of two charging profiles (unmanaged vs. optimized) of an EV connected in the evening at 19:00.

3 Results

This section summarizes the results of the study performed for each scenario implemented in the benchmark system considering both charging strategies described above (2.4.2). The results are expressed in terms of number of occurrences of variables exceeding the limits defined in Table 1.

3.1 Unmanaged charging

3.1.1 Nodes voltages.

Table 3 provides a summary of voltage violation results for each EV penetration scenario, based on a one-month analysis period. The data show an increase in medium-severity voltage violations as EV penetration rises to 40% and 60%.

Table 3. Node voltage results for urban network-unmanaged charging.

Scenario	Number of voltage violations (one-month analysis)	
	Yellow light: Medium severity 93%<V<95%	Red light: High severity V<93%
base (no EV)	0	0
Sc. 1: 20%PV-20%EV	0	0
Sc. 2: 20%PV-40%EV	873	0
Sc. 3: 20%PV-60%EV	4941	0

10

3.1.2 Overloads

Table 4 presents overload results for urban network in one month. It can be observed that already for a penetration level of 20% a significant number of overload cases, both medium and high severity, occur. As EV penetration rises from 20% to 60%, the number of medium-severity cases initially declines from Scenario 1 to Scenario 2, despite an increase in high-severity cases. This reduction in medium-severity cases could be explained by a shift of some cases escalating to high-severity. In Scenario 3, both medium and high-severity cases see a substantial increase.

Table 4. Overloads results for urban network-unmanaged charging.

Scenario	Number of load violations (one-month analysis)	
	Yellow light: Medium severity	Red light: High severity
	100%>L>90%	L>100%
base (no EV)	0	0
Sc. 1: 20%PV-20%EV	12382	13386
Sc. 2: 20%PV-40%EV	2060	25660
Sc. 3: 20%PV-60%EV	69606	35889

3.1.3 Technical losses

Table 5 shows technical losses results for each EV penetration scenario. Notably, given the low initial consumption of customers in the base case for this benchmark system, as the EV penetration rises, technical losses increase dramatically.

Table 5. Technical losses results for urban network-unmanaged charging.

Scenario	Losses (kWh) one-month	Increase regarding base case (%)
base (no EV)	97	NA
Sc. 1: 20%PV-20%EV	806	731%
Sc. 2: 20%PV-40%EV	1703	1656%
Sc. 3: 20%PV-60%EV	2492	2469%

3.2 Economic charging management

3.2.1 Nodes voltages.

Table 6 provides an overview of the node voltage results for urban network under economic charging management over a one-month analysis period. The results indicate that only the highest level of EV penetration leads to the occurrence of medium-severity voltage violations. No such violations are observed in the base case or the lower EV penetration scenarios. Furthermore, no high-severity voltage violations are detected across all scenarios.

Table 6. Node voltage results for urban network-economic charging management.

Scenario	Number of voltage violations (one-month analysis)	
	Yellow light: Medium severity	Red light: High severity
	93%<V<95%	V<93%
base (no EV)	0	0
Sc. 1: 20%PV-20%EV	0	0
Sc. 2: 20%PV-40%EV	0	0
Sc. 3: 20%PV-60%EV	1440	0

3.2.2 Overloads

Table 7 shows overload results for urban network in one month. It can be observed that as EV penetration grows the number of medium-severity cases rises, although not linearly correlate with EV penetration increase.

Table 7. Overloads results for urban network-economic charging management.

Scenario	Number of load violations (one-month analysis)	
	Yellow light: Medium severity	Red light: High severity
	100%>L>90%	L>100%
base (no EV)	0	0
Sc. 1: 20%PV-20%EV	12066	384
Sc. 2: 20%PV-40%EV	25213	11013
Sc. 3: 20%PV-60%EV	25691	14280

3.2.3 Technical losses

Table 8 provides a one-month summary of technical losses across EV penetration scenarios, showing a substantial increase in losses as EV penetration level rises.

Table 8. Technical losses results for urban network-economic charging management.

Scenario	Losses (kWh) one-month	Increase regarding base case (%)
base (no EV)	97	NA
Sc. 1: 20%PV-20%EV	747	670%
Sc. 2: 20%PV-40%EV	1612	1562%
Sc. 3: 20%PV-60%EV	2425	2400%

3.3 Urban network: comparison of scenarios

This subsection presents a quantitative comparison of node voltages, overloads, and technical losses considering the two EV charging strategies considered.

12

3.3.1 Nodes voltages.

Table 9 presents a comparison of node voltage results, focusing specifically on medium severity voltage violations. The data reveal a significant difference, regarding impact on voltage violations, between the two strategies. At 40% EV penetration, the economic charging management strategy completely eliminates the voltage violations observed under unmanaged charging. Further, at the higher EV penetration of 60%, the economic strategy drastically reduces the number of voltage violations by 71% compared to the unmanaged approach.

Table 9. Node voltage results comparison for urban network (unmanaged charging vs economic charging management).

Scenario	Number of voltage violations (one-month analysis)		
	Yellow light: Medium severity 93%<V<95%		
	Unmanaged	Economic management	Difference (%)
base (no EV)	0	0	NA
Sc. 1: 20%EV	0	0	NA
Sc. 2: 40%EV	873	0	-100%
Sc. 3: 60%EV	4941	1440	-71%

3.3.2 Overloads

Table 10 presents a comparison of overload results in an urban network under both charging strategies.

Table 10. Overloads results comparison for urban network (unmanaged charging vs economic charging management).

Scenario	Number of load violations (one-month analysis)					
	Yellow light: Medium severity 100%>L>90%			Red light: High severity L>100%		
	Unmanaged	Economic management	Diff (%)	Unmanaged	Economic management	Diff (%)
base (no EV)	0	0	NA	0	0	NA
Sc. 1: 20%EV	12382	12066	-3%	13386	384	-97%
Sc. 2: 40%EV	2060	25213	1124%	25660	11013	-57%
Sc. 3: 60%EV	69606	25691	-63%	35889	14280	-60%

As it can be appreciated, in the 20% EV penetration scenario, the economic charging management strategy results in a moderate decrease in medium-severity overloads and a substantial reduction in high-severity overloads. However, at 40% EV penetration, the economic charging management strategy leads to an increase in medium-severity overloads, but a significant reduction in high-severity overloads. The explanation for

this behaviour is that economic optimization adapts the duration and power of charging periods, resulting in more vehicles charging at the same time (although with lower peak consumption than in unmanaged case), thus producing medium congestions instead of high ones, which are reduced.

Finally, at the highest level of EV penetration considered (60%), the economic charging strategy results in substantial reductions in both medium and high-severity overloads compared to the unmanaged approach.

3.3.3 Technical losses

Table 11 shows a comparative summary of technical losses results. It clearly shows that the economic charging management strategy consistently results in fewer technical losses compared to the unmanaged charging strategy, regardless of the level of EV penetration. However, the relative advantage of the economic strategy in reducing losses diminishes as EV penetration increases. Given that the level of PV penetration remains static in these scenarios, there lies a potential research opportunity to explore synergies between increasing levels of EV and PV penetration, with the objective of optimizing the integration of renewable energy sources and mobility electrification, thus advancing sustainability goals.

Table 11. Technical losses results comparison for urban network (unmanaged charging vs economic charging management).

Scenario	Losses (kWh) one-month analysis		
	Unmanaged	Economic management	Difference (%)
base (no EV)	97	97	NA
Sc. 1: 20%PV-20%EV	806	747	-7.3%
Sc. 2: 20%PV-40%EV	1703	1612	-5.3%
Sc. 3: 20%PV-60%EV	2492	2425	-2.7%

4 Conclusion

The study presented in this paper analyzes the impacts of Electric Vehicle (EV) penetration on LV distribution network, represented by a benchmark urban system inspired in IEEE European Low Voltage Test Feeder. The analyses are based on different scenarios considering the integration of Sustainable Local Energy Communities (LEC) in which the level of photovoltaic (PV) penetration remains constant, while EV penetration levels rise, allowing a clearer analysis of the sole effect of increasing EV penetration. This strategy provides insights that can be integrated into further analyses exploring simultaneous evolution of electrification of loads and distributed generation penetration.

One key conclusion drawn from the results is the potential impact increased EV penetration may have, particularly on voltage alterations, overloads, and increased

14

technical losses. Additionally remarkable, the study shows that these challenges could be significantly mitigated through the deployment of charging management strategies.

In terms of voltage, a clear distinction between the two charging strategies emerges as the level of EV penetration increases. For scenarios with higher EV penetration, the economic charging management strategy significantly reduces the occurrence of voltage violations compared to the unmanaged charging strategy.

Regarding load violations it is observed a general trend of increasing overloads with escalating EV penetration in an unmanaged scenario. However, the application of an economic charging management strategy alters this landscape significantly. Despite a rise in medium-severity overloads at 40% EV penetration, high-severity overloads are consistently mitigated across all scenarios. Even at the peak EV penetration of 60%, this strategy succeeds in substantially decreasing both types of overloads.

In addition, as the EV penetration rises, so do the technical losses. However, the strategic economic charging management is able to curb this increase, showcasing a potential for efficient load management, even as EV penetration increases.

These findings provide a foundation for future research. The impacts of different charging management strategies on the lifespan and performance of electrical grid infrastructure represent a research area whose outputs can offer valuable insights for sustainable infrastructure planning and aid in the successful integration of EVs into power systems, including V2G technologies, not considered in the present analysis.

Further research lines will intensify the exploration of the integration of EV infrastructure into sustainable LEC based on the connection of diverse distributed generation from renewable sources. The study of such evolving LEC configuration will provide conclusions on the effects of control and management strategies allowing the maximization of synergies between rising electrification and clean generation technologies while enhancing the impacts on distribution networks variables.

Acknowledgments

This research has received funding from the European Union's Horizon 2020 Framework Programme for Research and Innovation under grant agreement no. 864319, project PARITY.

In addition, this study has been carried out under the collaboration framework signed by CIRCE Technology Center and University of Valladolid.

References

1. European Commission, Directorate-General for Communication, European green deal – Delivering on our targets, Publications Office of the European Union, 2021, <https://data.europa.eu/doi/10.2775/373022>
2. Alaina D. Boyle, Graham Leggat, Larissa Morikawa, Yanni Pappas, Jennie C. Stephens. "Green New Deal proposals: Comparing emerging transformational climate policies at multiple scales". *Energy Research & Social Science*. Volume 81, November 2021, 102259. <https://doi.org/10.1016/j.erss.2021.102259>

3. IEA (2021), "Net Zero by 2050", IEA, Paris <https://www.iea.org/reports/net-zero-by-2050>
4. IEA (2022), "Electrification", IEA, Paris <https://www.iea.org/reports/electrification>, License: CC BY 4.0
5. IEA (2023), "Global EV Outlook 2023", IEA, Paris <https://www.iea.org/reports/global-ev-outlook-2023>, License: CC BY 4.0
6. IEA report (2022): "Solar PV and wind supply about 40% of building electricity use by 2030". <https://www.iea.org/reports/solar-pv-and-wind-supply-about-40-of-building-electricity-use-by-2030>
7. Josh Eichman, Marc Torrecillas Castelló and Cristina Corchero. "Reviewing and Exploring the Qualitative Impacts That Different Market and Regulatory Measures Can Have on Encouraging Energy Communities Based on Their Organizational Structure". *Energies* 2022, 15(6), 2016; <https://doi.org/10.3390/en15062016>
8. Dharmakeerthi, C. H., Mithulananthan, N., & Saha, T. K. (2011, November). Overview of the impacts of plug-in electric vehicles on the power grid. In *2011 IEEE PES Innovative Smart Grid Technologies* (pp. 1-8). IEEE.
9. Yong, J. Y., Ramachandaramurthy, V. K., Tan, K. M., & Mithulananthan, N. (2015). A review on the state-of-the-art technologies of electric vehicle, its impacts and prospects. *Renewable and sustainable energy reviews*, 49, 365-385.
10. Richardson, D. B. (2013). Electric vehicles and the electric grid: A review of modeling approaches, Impacts, and renewable energy integration. *Renewable and Sustainable Energy Reviews*, 19, 247-254.
11. P. Pijarski, P. Kacejko and M.Wancerz. "Voltage Control in MV Network with Distributed Generation—Possibilities of Real Quality Enhancement". *Energies* 2022, 15(6), 2081
12. Prashant, A. Shahzad Siddiqui, Md Sarwar, A. Althobaiti and S. S. M. Ghoneim. "Optimal Location and Sizing of Distributed Generators in Power System Network with Power Quality Enhancement Using Fuzzy Logic Controlled D-STATCOM". *Sustainability* 2022, 14(6), 3305
13. Md Masud Rana, Mohamed Atef, Md Rasel Sarkar, Moslem Uddin and GM Shafiullah. "A Review on Peak Load Shaving in Microgrid—Potential Benefits, Challenges, and Future Trend". *Energies* 2022, 15(6), 2278
14. Gregorio Fernández, Noemi Galán, Daniel Marquina, Diego Martínez, Alberto Sanchez, Pablo López, Hans Bludszuweit and Jorge Rueda. "Photovoltaic Generation Impact Analysis in Low Voltage Distribution Grids". *Energies* 2020, 13(17), 4347
15. Samuel Borroy, Daniel Marquina, Andrés Llombart and Luis Hernández-Callejo. "Effect of sustainable Local Energy Communities on low voltage distribution networks". V Iberoamerican Conference of Smart Cities - ICSC-CITIES 2022, November 28-30.
16. DIgSILENT PowerFactory. <https://www.digsilent.de/en/>
17. The IEEE European Low Voltage Test Feeder. <https://cmte.ieee.org/pes-testfeeders/>
18. Pfenninger, Stefan and Staffell, Iain (2016). Long-term patterns of European PV output using 30 years of validated hourly reanalysis and satellite data. *Energy* 114, pp. 1251-1265. doi: 10.1016/j.energy.2016.08.060
19. Staffell, Iain and Pfenninger, Stefan (2016). Using Bias-Corrected Reanalysis to Simulate Current and Future Wind Power Output. *Energy* 114, pp. 1224-1239. doi: 10.1016/j.energy.2016.08.068
20. <https://www.renewables.ninja/>
21. Horizon 2020 Project PARITY. <https://parity-h2020.eu/>

Methodology for the dimensioning of PV systems for self-consumption without surpluses through the specific yield

Edwin Garabitos Lara^{1,2,*}[0000-0003-2000-8192], Alexander Vallejo Díaz¹[0000-0003-3215-6352]
and Carlos Napoleón Pereyra Mariñez¹[0000-0003-1102-3147]

¹ Facultad de ingeniería, Instituto Especializado de Estudios Superiores Loyola (IEESL), 91000
San Cristóbal, Dominican Republic
egarabitos@ipl.edu.do

² Escuela de Física | Escuela de Matemáticas, Facultad de Ciencias, Universidad Autónoma de
Santo Domingo (UASD), 10103 Santo Domingo, Dominican Republic
egarabitos73@uasd.edu.do

Abstract. The required use of distributed renewable sources have driven the growth of photovoltaic self-consumption. One of the most important parameters for the study and verification of the operation of photovoltaic systems (PVS) is the specific yield (SY). This parameter can be adopted to facilitate the estimation of energy production with the advantage of photovoltaic geographic information systems (PV-GIS). This paper presents a practical methodology for the sizing of PVS for self-consumption without surpluses, with the use of three open-access tools: (1) PVwatts Calculator to obtain the power output, (2) PVGIS to determine the optimal orientation and (3) Google Earth to validate the final orientation of the panels. In addition, a case study was carried out for self-consumption without surpluses in the residential sector of the Dominican Republic. The use of the SY from the PVwatts Calculator, significantly facilitated the integration of the power generation model with the techno-economic model, implemented in an Excel spreadsheet. A monthly energy demand of more than 550 kWh is adequate to implement self-consumption without surpluses, at the residential rate in the Dominican Republic. With a peak power of 1.20 kWp, it is possible to achieve an internal rate of return (IRR) between 10% and 23% for a monthly energy demand between 550 and 786 kWh/month, respectively.

Keywords: Specified yield, self-consumption, PVGIS, PVwatts Calculator.

1 Introduction

The need for energy sources that are less aggressive with the environment and that favor sustainable development, has motivated the implementation of Distributed Renewable Energy Sources (DRES) throughout the world, which contributes to the 7th Sustainable Development Goal [1]. Within the DRES to mitigate the use of fossil energy sources, photovoltaic self-consumption is one of the most effective and fastest growing [2].

2

The procedure or methodology for the sizing of photovoltaic systems (PVS) for self-consumption plays a vital role in its promotion and implementation in a society that increasingly requires clean energy sources. Within these methodologies, the photovoltaic geographic information systems (PV-GIS) have been frequently considered, since they provide data on irradiation, air temperature, optimal angle of inclination of the panels and even the calculation of the power of photovoltaic systems. The ideal would be to obtain information on the solar resource on the site, however this is not possible in the practice of PVS implementation, except for rare exceptions where technological resources and data collection time are available [3]. Some free access software are used for the dimensioning of photovoltaic systems, such as PVGIS [4], NASA [5] and PVwatts Calculator [6]. Although this type of tool is very useful, they do not have the capabilities for economic analysis or particular aspects required depending on the place of implementation [7]. In addition, not even the most capable tools, which include economic analysis and other aspects, cover all the aspects to dimension PVS in any country [8]. For this reason, it is necessary to create clear procedures or methodologies for the efficient use of these tools and their complementation with other tools, the information and conditions of the particular case of application.

One of the most important parameters in the analysis and verification of the PVS operation is the specific yield (SY), which is defined as the quotient between the generated energy (usually annual) and the installed peak power. This parameter depends on the irradiation, the temperature, the performance of the inverter and the performance of the PVS (PR), which is associated with the effect of shadows and other factors. In this context, obtaining the SY from free access software or tools for PVS sizing or even from real systems in operation, could greatly facilitate the estimation of the energy generated and with it the economic analysis in the place of implementation. The SY is often used to verify the correct operation of facilities or to validate energy prediction models [9]. However, there are few studies where it is used as an output variable from a PV-GIS tool towards a techno-economic model.

Guerrero-Lemus et al. [9] developed a theoretical model for the prediction of the SY of photovoltaic plants of different sizes of peak power in the Canary Islands. This model helps to detect anomalous specific yields of plants in operation. The error of the proposed model in comparison with the plants was approximately 3%. This model presents several equations that explicitly consider irradiance and temperature; it is a useful model, but it has the disadvantage of the complexity of the mathematical expressions. Recently, Sahu et al. [10] conducted a study to determine the SY of a bifacial panel and to validate a power prediction model that is useful for different climatic conditions. In this case, the SY for one year of operation was 1,569 kWh/kWp.

Garabitos Lara et al. [8] presented a power generation model for PVS, to determine the profitability of PVS in the residential sector. The model was validated by means of real systems, obtaining errors less than 5%. The main disadvantage of the generation model presented was the complexity of the equation for calculating the energy generated, due to the explicit use of different variables, such as temperature and irradiance. In other works, the equations presented also do not contain the use of the SY for the calculation of the generated energy. Table 1 shows several articles in which equations

are presented for the calculation of the energy generated and that do not include the SY, therefore they use more explicit variables. Table 1 indicates that the explicit variables for each item, and those may be implicitly included in the SY to facilitate calculations.

Table 1. Papers that use equations for energy calculation without making use of specific yield. Nomenclature for this Table: G : solar irradiation, PR : performance ratio, T_a : outdoor air temperature, η_{inv} : inverter efficiency, β : angle of inclination of the panels, and ϕ : azimuth angle.

No.	Refer- ence	Use spe- cific yield?	Explicit variables used that may be contained in the specific yield					
			G	PR	T_a	η_{inv}	β	ϕ
1	[11]	x	✓	✓	x	x	✓	✓
2	[12]	x	✓	x	x	x	x	x
3	[13]	x	✓	✓	✓	x	x	x
4	[14]	x	✓	x	x	x	x	x
5	[15]	x	✓	✓	x	x	x	x
6	[16]	x	✓	✓	x	x	x	x
7	[17]	x	✓	✓	✓	x	x	x
8	[18]	x	✓	✓	x	x	x	x
9	[19]	x	✓	✓	x	x	x	x
10	[20]	x	✓	✓	x	x	x	x
11	[21]	x	✓	✓	x	x	x	x
12	[8]	x	✓	✓	✓	✓	x	x

The growth of PVS for self-consumption has been due the schemes with surpluses, promoted by governments in most countries. The most determining factor in the growth of the distributed photovoltaic systems (DPVS) for a sustainable development, has been the reduction of the capital cost of the PVS during the last decade [22], which has caused the reach of the grid parity of the DPVS compared to the conventional supply from the electricity grid in several countries [23]. Despite the contribution of self-consumption schemes to the decarbonization of electricity networks, it is necessary to consider the external effects of their implementation beyond the benefits of customers. For this reason, it is common for countries where grid parity has been reached to modify or contemplate different modes of self-consumption, in such a way that their growth is sustainable [24]–[27].

Self-consumption without surpluses leaves fewer benefits for customers than self-consumption with surplus, since the PVS turn out to be under-dimensioned to maximize profitability. However, they turn out to be an alternative when it is not possible to implement self-consumption with surpluses, either due to restrictions in the distribution networks or limited capacity to install due to space constraints.

In the literature there are few studies on self-consumption without surpluses. Garabitos Lara et al. [28] presented a techno-economic model for self-consumption without surplus in the Dominican Republic (DR). Although the model was based on a one-minute resolution profile to estimate self-consumed energy, it has the limitation of using the generation profile for one day and that profile was built by interpolating an hourly resolution profile. In addition, the daily demand profile with a resolution of one minute, was built manually since there was no measured data.

4

Arcos-Vargas et al. [29] proposed a techno-economic model to evaluate the profitability of residential photovoltaic systems in different cities in Spain and France, requiring a smart meter in the home to obtain the hourly demand curve and a tool to generate the irradiance curve. In that study, the price of electricity is constant in relation to the energy consumed monthly and the dimensioning of the PVS were based on the maximization of the net present value. Simola et al. [30] proposed a methodology similar to Arcos-Vargas et al. [29], carried out in Finland and case studies from the commercial and residential sector were evaluated. In those works, the SY was not considered either for the calculation of the energy generated.

The importance of PVS study for self-consumption without surpluses lies in being an alternative to self-consumption with surpluses, which, although it does not offer the same economic and environmental benefits, constitutes a way to increase the participation of photovoltaic solar energy through systems more economical and easier to implement, and which also affect less the stability of distribution networks. There are two main contributions of this work. The first is to provide a methodology to size photovoltaic systems, starting from the specific yield, to simplify the calculations and procedures, prior to the economic study. The second is to address the profitability of photovoltaic self-consumption without surpluses in the Dominican Republic, considering an hourly generation profile, both for demand and for photovoltaic generation.

2 Materials and methods

2.1 Demand profile and energy generation

In this study, an annual energy demand profile with hourly resolution is considered. The energy demanded each hour is represented by the Eq. (1), where P_{Dh} is the average power for hour h that corresponds to the set of 0 to 8,760 hours in a year. The energy demand will be grouped by months since the energy billing model is applied monthly.

$$E_{Dh} = P_{Dh}h; \forall h: h \in [0; 8,760h] \quad (1)$$

The generation profile is obtained by Eq. (2), a contribution from this work, where N_p is the number of panels, P_p is the peak power of each panel in kWp, SY_h is the specific yield with hourly resolution in kWh/kWp. It should be noted that SY_h is obtained from a PV-GIS. Eq. (3) shows that SY_h is a variable that depends on the time, the global irradiation level (G_h), the azimuth angle (ϕ), the inclination angle (β) of the panels, the inverter efficiency (η_{inv}), the power peak chosen in the PV-GIS or the PVS in operation (P_{PGISh}) and the performance of the system (PR). The specific yield is obtained by defining it, dividing the energy forecast with hourly resolution by a PV-GIS between the peak power considered (E_{GISh}/P_{PGISh}) or the energy generated and the peak power of a project in operation in the locality. of the study or implementation (E_{prh}/P_{Pprh}).

$$E_{PVh} = N_p \cdot P_p \cdot SY_h \quad (2)$$

$$SY_h = SY_h(G_h, \phi, \beta, PR, \eta_{inv}) = E_{GISh}/P_{PGISh} = E_{prh}/P_{Pprh} \quad (3)$$

The use of Eq. (2) presents two main advantages compared to other generation models. The first advantage is that SY_h implicitly contains the most complex variables, such as outdoor air temperature and irradiance with the optimal orientation or another one specified in the PV-GIS, which facilitates the calculations. The second is that the SY can be obtained both from some freely accessible geographic information systems and from real generation data, although in the latter case one would have to work with parameters set in the installed system or adjust to the conditions. In the place of study, for example, consider the shadows due to nearby objects. The study of shadows is a relevant factor in the performance of the system, however, that issue is beyond the scope of this article.

2.2 Self-consumed energy and demand from the electricity grid

To model self-consumption without surpluses, the annual energy consumed is required, minimally with hourly resolution, as well as the annual energy generated. Based on this information, the self-consumed energy and the energy that is injected into the electrical grid can be determined hourly. The self-consumed monthly energy is obtained with Eq. (4) [8], where $E_{PV Dh}$ is the self-consumed energy in kWh in the hour h and is obtained by Eq. (5), where n is the year and α_p is the annual loss coefficient of the panel efficiency. In Eq (5), $E_{PV h}$ is the energy that the PVS can produce and E_{Dh} are the energy demands, both with hourly resolution.

$$E_{PVDmn} = \left(\sum_{d=1}^{d_m} \sum_{t=1}^{24} E_{PV Dh} \right) \cdot [1 + (1 - n)\alpha_p] \quad (4)$$

$$E_{PV Dh} = \min(E_{PV h}, E_{Dh}) \quad (5)$$

The monthly energy demanded from the grid when implementing the PVS (E_{GDm}) in a non-surplus mode is determined by Eq. (6) [28]. When the energy generated by the PVS is less than the energy demanded, the energy demanded from the grid is the difference between the energy demanded (E_{Dm}) and the self-consumed energy (E_{PVDmn}), and its value is zero when more than what is demanded.

$$E_{GDm} = \begin{cases} E_{Dm} - E_{PVDmn}, & E_{Dm} > E_{PVDmn}; \forall m \\ 0, & E_{Dm} \leq E_{PVDmn}; \forall m \end{cases} \quad (6)$$

2.3 Energy cost function and annual savings

In the Dominican Republic, the residential rate is known as the simple low voltage rate (BTS1) tariff, where the cost function for electrical energy is determined by Eq. (7) [28]:

$$f_E(E_{GDm}) = \begin{cases} c_1 E_{GDm}, & 0 < E_{GDm} \leq E_1 \\ c_1 E_1 + c_2 (E_{GDm} - E_1), & E_1 < E_{GDm} \leq E_2 \\ c_1 E_1 + c_2 (E_2 - E_1) + c_3 (E_{GDm} - E_2), & E_2 < E_{GDm} \leq E_3 \\ c_4 E_{GDm}, & E_3 < E_{GDm} \end{cases} \quad (7)$$

6

Where E_{GDM} is monthly energy demand from the electricity grid in kWh, E_1 is upper limit of the first tranche of energy consumed, which in this case is 200 kWh and is paid at the unit price c_1 in \$/kWh, E_2 is upper limit of the second section of energy consumed, which in this case is 300 kWh and is paid at the unit price c_2 in \$/kWh, E_3 is upper limit of the third tranche of energy consumed, which in this case is 700 kWh and is paid at the unit price c_3 in US\$/kWh, and c_4 is the unit price in US\$/kWh at which all energy is paid when the monthly consumption of 700 kWh is exceeded.

Eq. (8) is adopted to calculate the monthly savings and Eq. (9) is for annual savings in self-consumption without surpluses.

$$A_m = f_E(E_{Dmi}) - f_E(E_{Dmf}) \quad (8)$$

$$A_n = \sum_{n=1}^{12} [f_E(E_{Dm}) - f_E(E_{RDm})] \quad (9)$$

2.4 Costs and economic indicators

The initial investment of the PVS is determined by Eq. (10) [8], where r_{imp} is tax transferred to the client by the company that offers the PVS, C_{PVS} is PVS cost of capital [US\$/kWp], C_p is capital cost of panels [US\$/kWp], C_{sup} is the cost of a photovoltaic panel support [US\$/panel], C_{ae} is the cost for electrical accessories of a photovoltaic panel [US\$/panel], C_{inv} is the inverter cost of capital [US\$/kW], C_{fi} is fixed cost associated with project design and labor [US\$], P_{pL} is PVS power below which the C_{PVS} is not considered constant [kW] and I_0 is initial investment of the PVS [US\$].

$$I_0 = \begin{cases} (1 + r_{imp})[N_p(P_p C_p + C_{sup} + C_{ae}) + P_{inv} C_{inv} + C_{fi}], & P_p < N_p P_p < P_{pL} \\ N_p P_p C_{SFV}, & P_{pL} \leq N_p P_p < P_{pH} \end{cases} \quad (10)$$

The present value (VP) of A_n is obtained by Eq. (11), where N is the life of the project in years and i_r is the real discount rate. The present value of the annual costs of operation and maintenance ($VP_{CO\&M}$) is calculated with Eq. (12), where $f_{O\&M}$ is the fraction that represents the cost of operation and maintenance relative to I_0 . The VP of the replacement of the inverters ($VP_{Cre-inv}$) is calculated with Eq. (13), in this case the inverter is replaced twice, because a lifetime of project is assumed as 25 years and the of inverter is 10 years.

$$VP_{A_n} = \sum_{T=1}^N \frac{A_n}{(1+i_r)^T} \quad (11)$$

$$VP_{CO\&M} = f_{O\&M} I_0 \left[\frac{(1+i_r)^N - 1}{i_r(1+i_r)^N} \right] \quad (12)$$

$$VP_{Cre-inv} = \frac{C_{inv} P_{inv}}{(1+i_r)^{T_{inv}}} + \frac{C_{inv} P_{inv}}{(1+i_r)^{2T_{inv}}} \quad (13)$$

The economic indicators adopted are the IRR, the recovery period and the levelized cost of electricity (LCOE). The IRR is determined from the net present value (NPV) presented in Eq. (14), where VP_{costs} is the VP of the costs and is calculated using Eq. (15). The IRR is the value of the real interest rate that makes the NPV equal to zero. The payback time (PBT) of the investment is determined by Eq. (16).

$$NPV = VP_{A_n} - VP_{costs} \quad (14)$$

$$VP_{costs} = I_0 + VP_{C_{O\&M}} + VP_{C_{re-inv}} \quad (15)$$

$$PBT = I_0 / \left[(VP_{A_n} - VP_{C_{O\&M}} - VP_{C_{re-inv}}) \frac{i_r(1+i_r)^N}{(1+i_r)^N - 1} \right] \quad (16)$$

The self-consumption ratio (SCR) in percentage is determined with Eq. (17), while the self-sufficiency ratio (SSR) in percentage is determined with Eq. (18). In those equations, sub-index 1 refers to energy for the period of the first year, where $E_{PV_{Dm1}}$ is the self-consumed energy, $E_{PV_{m1}}$ the total energy generated and E_{Dm1} the energy demanded, all in kWh.

$$SCR = E_{PV_{Dm1}} / E_{PV_{m1}} \times 100 \quad (17)$$

$$SSR = E_{PV_{Dm1}} / E_{Dm1} \times 100 \quad (18)$$

2.5 Methodology for research and sizing

Fig. 1 shows the methodological approach proposed. First, the specific performance of PVwatts and PVGIS is validated with reference to the specific performance of a real installation. Second, the techno-economic model is applied to a case study, a client in the residential sector of the Dominican Republic. And finally, the client profile is varied to study the behavior of economic indicators with the increase in energy demand.

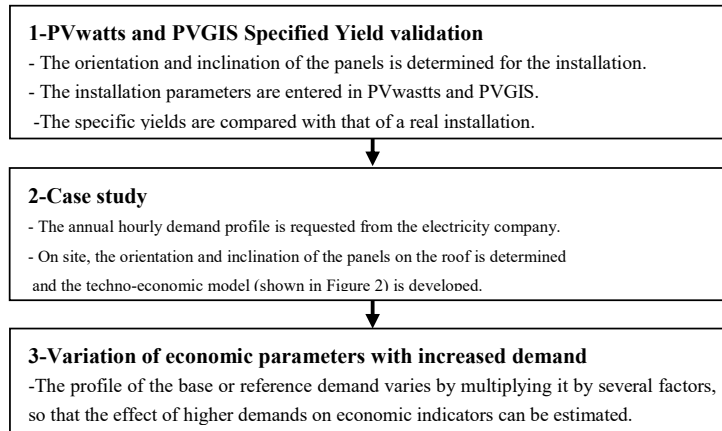


Fig. 1. Research methodological diagram.

Fig. 2 shows the scheme of the techno-economic model and how the PV-GIS is used. In PVGIS [31] it is located at the study site, in order to determine the inclination (β_{op}) and optimal orientation (ϕ_{op}), to produce the greatest annual energy. Then the

8

orientation of the sides of the roof perimeter, where the panels will be installed, is determined with Google Earth. Fig. 3 shows a blue line that indicates the geographic North, with respect to which the orientation of one of the sides of the roof is measured, in this case ϕ_1 is that angle determined by placing an angle protractor on the computer screen in the Google Earth window. On the other hand, the optimal angle (ϕ_{op}) that the panel must have been already known from PVGIS, from which it is determined that the orientation that the panel must have with respect to the left side of the roof perimeter is $\phi_2 = \phi_{op} - \phi_1$. It may also be that the orientation of the sides differs little from the optimal orientation, so the panels can be oriented parallel or perpendicular to the sides, which would be the most practical way to do it, since it makes better use of the space, and it hinders less access to different areas in the roof.

It should be noted that the optimal orientation of the panels may depend on the annual demand profile, mainly in countries where weather conditions produce a significant seasonal variation in demand, as well as in the solar resource. However, in the Caribbean, energy demand does not vary significantly during the 12 months and neither does solar resources. For this reason, in this article the orientation is optimized to produce the greatest amount of annual energy, regardless of the demand profile.

Once the most convenient, optimal or different orientation is confirmed for practical reasons (but without significantly changing energy production in comparison of the optimal case), the most convenient inclination and azimuth angle are entered into the PVwatts Calculator. From the PVwatts Calculator, the SY with hourly resolution is obtained for a period of one year (SY_h), then it is used in Eq. (2) to determine the generated energy and later the self-consumed energy. Finally, this information is integrated into the economic model implemented in an Excel spreadsheet, obtaining the economic indicators as shown in Fig. 2.

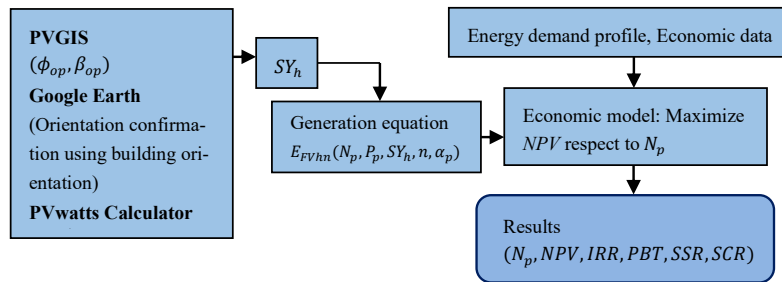


Fig. 2. Use of the PV-GIS tool in the implementation of the techno-economic model.

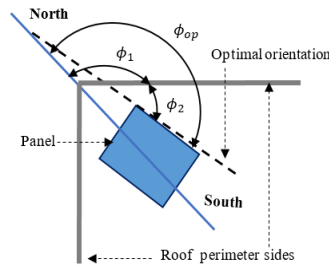


Fig. 3. Use of Google Earth in 2D view to determine the orientation of the panels with reference to one of the sides of the roof.

3 Results and discussion

3.1 Comparison with the specific yield of a real installation

On September 23, 2022, a HUAWEI PVS with 2.2 kWp and batteries storage system were installed at the Loyola Development and Innovation Research Center (CIDIL) in San Cristóbal city, DR. Since then, it has been in operation, and injecting power to the CIDIL circuit, which has a much higher power demand, so that all the energy is self-consumed. The panels of this system are located on the center of the roof, approximately 6 m from the first level, with no visible shadows that reduce performance, neither from nearby objects nor between the panels themselves, as seen in Fig. 4 (A) and (B); the structure that supports 4 panels of 550 Wp, avoids the shadows that could be caused by the wall on the perimeter of the tray and other elements that can be seen. The other parts of the PVS are located on the first level, see Fig. 4 (B). That PVS includes a datalogger that records the energy supplied into the grid, with hourly, daily, and monthly resolutions.



Fig. 4. Front view of CIDIL, where the 2.20 kWp PVS is located, Lat. 18.41° y Long. -70.1° .

Fig. 5 shows the generation profile of the PVS installed in the CIDIL for July 7, 2023. The production for that day was 12.35 kWh and therefore a specific yield of 5.61 kWh/kWp. It should be noted that the inverter yield is 98.2%, and for the reasons mentioned above the effect of shadows and dirt are negligible. In this province of San Cristóbal, there are clouds that significantly reduce irradiation for seconds or minutes, hence the shape of the generation profile is shown in Fig. 5.

10



Fig. 5. Daily generation profile of the PVS in CIDIL, July 7, 2023.

By means of on-site measurements with an angle protractor and the IRR1-Fluke irradiance meter [32], a panel inclination of approximately 15° was determined, as shown in Fig. 6 (A). With the use of Google Earth and an angle protractor placed on the computer screen, it was determined that the orientation of the panels is 145° with reference to geographic north (blue line). In Fig. 6 (B), the yellow line shows the orientation of one of the sides of the building, which coincides with the orientation of the panels. According to PVGIS, the optimal tilt angle and azimuth orientation are approximately 15° and 173° . According to PVGIS, the variation of the SY due to not using the optimal angles is approximately 1.0%, which is not very significant, in addition to the fact that the orientation of the panels in the same orientation of the building facilitates their assembly, as observed in Fig. 4 (A).

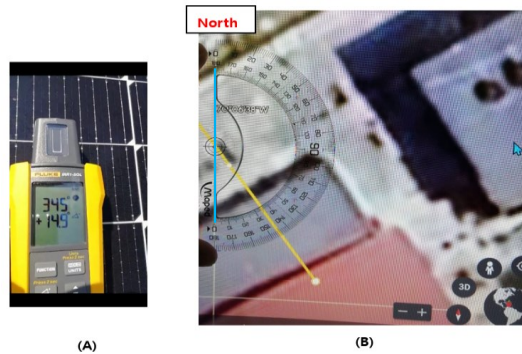


Fig. 6. Determination of the angle of inclination (A) and the orientation of the panels, (B). The orientation angle is determined with Google Earth and a protractor.

Table 2 shows the PVwatts Calculator and PVGIS report, from the data entered, based on the conditions of the CIDIL PVS. In the case of PVGIS, there are two additional loss factors to the PR, and that cannot be modified, these are angle of incidence, temperature and low irradiance, with which the system losses reach 23.96%. For the chosen location, the SY with monthly resolution is determined for the two PV-GIS (PVGIS and PVwatts Calculator) and for the PVS in CIDIL, as shown in Table 3. As in both PV-GIS it was specified a peak power of 1 kW_p, the specific yield is directly

obtained. On the other hand, the SY of the CIDIL PVS is obtained with Eq. (3), only with a monthly resolution, that is, $SY_m = E_{prm}/P_{pprm} = E_{prm}/(2.20 \text{ kWp})$.

Table 2 shows the percentage relative error of each PV-GIS with reference to the specific yield of CIDIL (SY_{CIDIL}). In the case of PVwatts Calculator, all the percentage relative errors are below 8% and the 10-month average is 2.3%. The biggest error with the SY_{CIDIL} is presented by PVGIS. This is mainly since PVGIS contains by default additional losses to the PVS losses, which are presented in Table 1 under the heading “Changes in output due to”.

Table 2. Specifications of inputs and outputs in PVGIS and in PVwatts Calculator.

PVGIS (Source: [31])		PVwatts Calculator (Source: [33])	
<i>Provided inputs</i>		<i>Location and Station Identification</i>	
Latitude / Longitude:	18.410°, -70.100°	Requested Location	Dominican Republic
Horizon	Calculated	Weather Data Source	Lat, Lng: 18.41, -70.1, 14 mi
Database used	PVGIS-ERA5	Latitude	18.41° N
PV technology	Crystalline silicon	Longitude	70.10° W
PV installed	1 kWp	<i>PV System Specifications</i>	
System loss	9.61 %	DC System Size	1 kW
<i>Simulation outputs</i>		Module Type	Premium
Slope angle	15°	Array Type	Fixed (roof mount)
Azimuth angle (south reference)	-35°	System Losses	9.61%
Yearly PV energy production	1575.44 kWh	Array Tilt	15°
Yearly in-plane irradiation	2071.97 kWh/m ²	Array Azimuth	145°(north reference)
Changes in output due to:		DC to AC Size Ratio	1.2
Angle of incidence	-2.65 %	Inverter Efficiency	98.2%
Temperature and low irradiance	-13.59 %	Ground Coverage Ratio	0.4
Total loss	-23.96 %		

Table 3. Specifications in PVGIS and in PVwatts Calculator.

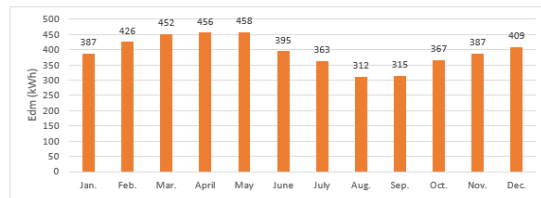
Month-year	Y_{CIDIL} (kWh/kWp)	$Y_{PVwatts}$ (kWh/kWp)	Y_{PVGIS} (kWh/kWp)	Relative error PVwatts	Relative error PVGIS
October-22	132.3	135.5	125.5	2.4%	5.1%
November-22	128.2	128.2	117.5	0.1%	8.3%
December-22	135.2	124.9	122.5	7.6%	9.4%
January-23	131.9	131.0	126.7	0.6%	3.9%
February-23	133.2	135.9	124.9	2.0%	6.2%
March-23	159.1	159.3	146.0	0.1%	8.2%
April-23	155.7	156.0	139.6	0.1%	10.4%
May-23	144.8	147.5	135.6	1.9%	6.3%

12

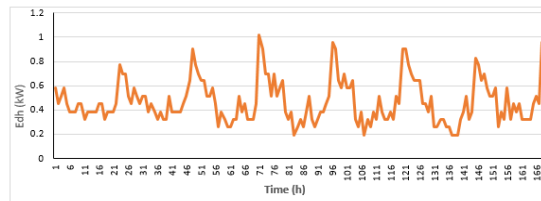
June-23	139.3	134.3	130.2	3.6%	6.6%
July-23	140.9	147.0	138.1	4.3%	2.0%
Average	140.0	140.0	130.6	2.3%	6.6%

3.2 Case study

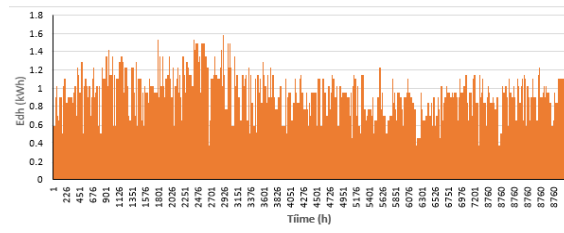
An annual demand profile with hourly resolution is considered, corresponding to a client in the residential rate of the DR, this information was obtained through a request to the distribution company EDESUR [34]. The profile for different periods is shown in Fig.7. It is a customer with an average monthly energy of 394 kWh (4,726 kWh/year). The investment is profitable if $NPV > 0$, $PBT < 9$ years and $IRR > 10\%$. The place of application is in the same town as CIDIL, 1.12 km away in an apartment building. The available area is located on the building's surface, with an effective area of 25.0 m² for the client, the perimeter of the building also has a wall 0.850 m high. Under these conditions, a flat structure with supports must be installed, whose height is greater than this edge, or install a structure on the edges, as seen in Fig. 3 (A). According to PVGIS, the optimal inclination angle is 20°, while the optimal azimuth angle is 173° with reference to north. In Fig. 8 (see the yellow line) it is shown that the building is oriented at 171°, which practically coincides with the optimum angle, so for practical reasons the same orientation of the building is adopted for the azimuth angle. Regarding the angle of inclination, the optimum one proposed by PVGIS is chosen.



(A)



(B)



(C)

Fig. 7. Energy demand of a residential customer. (A) annual demand; (B) weekly demand; (C) annual demand.

Table 4 shows the information entered in PVwatts Calculator [33]. Since the building is far from taller objects, a value of zero shadow loss can be assumed, as well as in the case of dirt. The technical and economic data corresponding to the local market are shown. Table 5 shows the economic indicators for the base demand profile with monthly average energy of 393 kWh/month, see under Ref. case. A negative NPV is observed, a PBT greater than 9 years and an IRR of 5.62% < 10%. The values of the parameters in this table were obtained using equations (10) to (18).

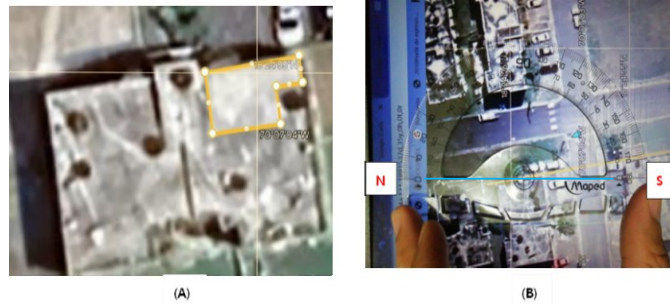


Fig. 8. Place of application. (A) The available area is shown by a perimeter in yellow; (B) The azimuth angle of the orientation of the building with reference to the geographic north, see the yellow line.

Table 4. Technical and economic data for the place of application.

Economic and technical parameters (From the local context)		PV-system Information (from PVwatts Calculator)	
Parameter	Value	Requested Location	Dominican Republic
E_1 (kWh), E_2 (kWh)	200, 300	Weather Data Source	Lat, Lng: 18.41, -70.10, 14 mi
E_3 (kWh)	700	Latitude	18.41° N
c_1 (US\$ / RD\$)	6.05 / 0.107	Longitude	70.10° W
c_2 (US\$ / RD\$)	8.59 / 0.152	<i>PV System Specifications (from PVwatts C.)</i>	
c_3 (US\$ / RD\$)	12.89 / 0.2285	DC System Size	1 kW
c_4 (US\$ / RD\$)	13.09 / 0.2321	Module Type	Premium
T_{imp} / I_r	0.0815/0.0644	Array Type	Fixed (roof mount)
C_{SFV}, C_p (US\$/kWp)	1200, 183.5	System Losses	9.61%
C_{sop}, C_{ae} (US\$/panel)	59.63, 61.93	Array Azimuth	20°
C_{inv} (US\$/kW), C_{fi} (US\$)	298, 1139.2	Array Azimuth	171°(north reference)
P_{pL} (kW), P_{pH} (kW)	3.3, 20	DC to AC Size Ratio	1.2
P_p (kWp), N (years)	0.300, 25	Inverter Efficiency	98.2%
α_p (1/year), T_{inv} (year), $f_{o\&m}$	0.008, 10, 0.01	Ground Coverage Ratio	0.4

Table 5. Results for the base case and the variation of the energy demanded.

Parameters	Ref. case	Results for increments in the demand				
Multiplier (Mu)	1	1.2	1.4	1.6	1.8	2
Edmp (kWh/month)	393.0	471.5	550.1	628.7	707.2	785.8
I ₀ (US\$)	2479.5	2479.5	2479.5	2479.5	2479.5	2479.5
NPV (US\$)	-166.2	396.4	796.4	2360.4	3862.6	4150.0
Pp (kWp)	1.2	1.2	1.2	1.2	1.2	1.2
IRR (%)	6%	8%	10%	16%	22%	23%
PBT (y)	13.15	10.58	9.29	6.29	4.80	4.59
SSR (%)	26.4%	24.9%	23.5%	22.1%	20.7%	19.4%
SCR (%)	60.3%	68.2%	75.0%	80.5%	85.0%	88.4%

To analyze what would happen if the customer demanded a higher consumption, keeping the peak power of the PVS fixed, the base profile is multiplied by the factors 1.2, 1.4, 1.6, 1.8 and 2.0. Table 5 shows that the profitability parameters met for monthly consumption above 550 kWh/month; this result is consistent with the study on self-consumption without surpluses carried out by [28], where an average monthly energy of 579 kWh/month was considered. A determining factor in the profitability of the investment is the higher price of electricity with the higher demand for energy, the price remaining constant above 700 kWh. For monthly consumption between 550 and 786 kWh/month, the IRR was 10 to 23%, respectively, which are attractive rates in the DR context.

It should be noted that Eq. (10), for the initial cost, refers to a PVS with connection to the grid, which has a surplus anti-dumping system, and which requires mounting accessories that are expensive if the PVS is under-dimensioned. An option that could make the investment profitable, for consumption ≤ 394 kWh/month, are the panels with micro inverters. It is a simpler arrangement that does not require so many additional accessories, however its sizing should not exceed the power demand at any [35].

The main advantage of the methodology presented in this work is that through specific yield, open access web tools such as PVwatts and PV-GIS are efficiently used. In addition, commonly used computer tools, such as Excel, are used to implement the model. The SY can not only be obtained from web pages, but from real photovoltaic systems under conditions similar to the case study.

Future studies: The advance of self-consumption has been increasing, which has been mainly due to self-consumption with surpluses. Although this is a modality that provides greater energy production, limitations and regulations have slowed its progress, so the feasibility of more alternatives needs to be studied. In future studies we plan to use the concept of grid parity to analyze a greater number of types of self-consumption for low-voltage customers in the Dominican Republic, thereby contributing to the 7th Sustainable Development Goal.

4 Conclusions

In this work, a methodology was presented for the dimensioning of photovoltaic systems for self-consumption without surpluses, through the specific yield, which facilitates the calculations in comparison with other methodologies that require an explicit consideration of more variables. In addition, this methodology was applied to a case study in Dominican Republic (DR), the main conclusions are presented below:

1. The specific yield of PVwatts Calculator and PVGIS were such that they yielded values with errors of less than 11% compared to the specific yield of a photovoltaic system installed into the CIDIL building, in San Cristóbal city, DR.
2. PVwatts Calculator is a free access and useful tool for integration with economic models, adopting specific yield. Compared to the specific yield of the PVS in the CIDIL building, the average percentage relative error of the PVwatts Calculator was 2.20%.
3. A monthly energy demand ≤ 394 kWh is not adequate to implement self-consumption without surpluses in DR with a standard photovoltaic system.
4. With a peak power of 1.20 kWp it is possible to achieve an IRR of 10%, 16% and 23%, for consumptions greater than 550, 629 and 786 kWh/month, respectively.

Acknowledgments

The authors gratefully acknowledge the financial support by FONDO NACIONAL DE INNOVACIÓN CIENTÍFICO Y TECNOLÓGICO (FONDOCYT), Dominican Republic, grant number **2022-3A9-140**.

References

- [1] M. J. Gamez, "Objetivos y metas de desarrollo sostenible," *Desarrollo Sostenible*. Accessed: Jun. 04, 2023. [Online]. Available: <https://www.un.org/sustainabledevelopment/es/objetivos-de-desarrollo-sostenible/>
- [2] Y. An, T. Chen, L. Shi, C. K. Heng, and J. Fan, "Solar energy potential using GIS-based urban residential environmental data: A case study of Shenzhen, China," *Sustain. Cities Soc.*, vol. 93, p. 104547, Jun. 2023, doi: 10.1016/j.scs.2023.104547.
- [3] D. L. Talavera, F. J. Muñoz-Rodríguez, G. Jimenez-Castillo, and C. Rus-Casas, "A new approach to sizing the photovoltaic generator in self-consumption systems based on cost-competitiveness, maximizing direct self-consumption," *Renew. Energy*, vol. 130, pp. 1021–1035, Jan. 2019, doi: 10.1016/j.renene.2018.06.088.
- [4] PVGIS, "JRC Photovoltaic Geographical Information System (PVGIS) - European Commission." Accessed: Aug. 18, 2022. [Online]. Available: https://re.jrc.ec.europa.eu/pvg_tools/en/
- [5] NASA, "POWER Data Access Viewer." Accessed: Jul. 02, 2021. [Online]. Available: <https://power.larc.nasa.gov/data-access-viewer/>
- [6] "PVWatts Calculator." Accessed: Aug. 22, 2022. [Online]. Available: <https://pvwatts.nrel.gov/pvwatts.php>

16

- [7] W. M. P. U. Wijeratne, R. J. Yang, E. Too, and R. Wakefield, "Design and development of distributed solar PV systems: Do the current tools work?," *Sustain. Cities Soc.*, vol. 45, pp. 553–578, Feb. 2019, doi: 10.1016/j.scs.2018.11.035.
- [8] E. Garabitos Lara, A. Vallejo Díaz, V. S. Ocaña Guevara, and F. Santos García, "Tecno-economic evaluation of residential PV systems under a tiered rate and net metering program in the Dominican Republic," *Energy Sustain. Dev.*, vol. 72, pp. 42–57, Feb. 2023, doi: 10.1016/j.esd.2022.11.007.
- [9] R. Guerrero-Lemus, D. Cañadillas-Ramallo, T. Reindl, and J. M. Valle-Feijóo, "A simple big data methodology and analysis of the specific yield of all PV power plants in a power system over a long time period," *Renew. Sustain. Energy Rev.*, vol. 107, pp. 123–132, Jun. 2019, doi: 10.1016/j.rser.2019.02.033.
- [10] P. K. Sahu, J. N. Roy, and C. Chakraborty, "Performance assessment of a bifacial PV system using a new energy estimation model," *Sol. Energy*, vol. 262, p. 111818, Sep. 2023, doi: 10.1016/j.solener.2023.111818.
- [11] M. Lee, T. Hong, and C. Koo, "An economic impact analysis of state solar incentives for improving financial performance of residential solar photovoltaic systems in the United States," *Renew. Sustain. Energy Rev.*, vol. 58, pp. 590–607, May 2016, doi: 10.1016/j.rser.2015.12.297.
- [12] X. Ruhang, "The restriction research for urban area building integrated grid-connected PV power generation potential," *Energy*, vol. 113, pp. 124–143, Oct. 2016, doi: 10.1016/j.energy.2016.07.035.
- [13] J. Every, L. Li, and D. G. Dorrell, "Leveraging smart meter data for economic optimization of residential photovoltaics under existing tariff structures and incentive schemes," *Appl. Energy*, vol. 201, pp. 158–173, Sep. 2017, doi: 10.1016/j.apenergy.2017.05.021.
- [14] R. AbdelHady, "Modeling and simulation of a micro grid-connected solar PV system," *Water Sci.*, vol. 31, no. 1, pp. 1–10, Apr. 2017, doi: 10.1016/j.wsj.2017.04.001.
- [15] J. Chen, X. Wang, Z. Li, S. Qiu, and J. Wu, "Deploying residential rooftop PV units for office building use: a case study in Shanghai," *Energy Procedia*, vol. 152, pp. 21–26, Oct. 2018, doi: 10.1016/j.egypro.2018.09.053.
- [16] K. Kusakana, "Impact of different South African demand sectors on grid-connected PV systems' optimal energy dispatch under time of use tariff," *Sustain. Energy Technol. Assess.*, vol. 27, pp. 150–158, Jun. 2018, doi: 10.1016/j.seta.2018.04.009.
- [17] C. Liu, W. Xu, A. Li, D. Sun, and H. Huo, "Energy balance evaluation and optimization of photovoltaic systems for zero energy residential buildings in different climate zones of China," *J. Clean. Prod.*, vol. 235, pp. 1202–1215, Oct. 2019, doi: 10.1016/j.jclepro.2019.07.008.
- [18] O. Ellabban and A. Alassi, "Integrated Economic Adoption Model for residential grid-connected photovoltaic systems: An Australian case study," *Energy Rep.*, vol. 5, pp. 310–326, Nov. 2019, doi: 10.1016/j.egypr.2019.02.004.
- [19] M. Zhang and Q. Zhang, "Grid parity analysis of distributed photovoltaic power generation in China," *Energy*, vol. 206, p. 118165, Sep. 2020, doi: 10.1016/j.energy.2020.118165.
- [20] P. Lazzaroni, F. Moretti, and F. Stirano, "Economic potential of PV for Italian residential end-users," *Energy*, vol. 200, p. 117508, Jun. 2020, doi: 10.1016/j.energy.2020.117508.
- [21] G. Jiménez-Castillo, F. J. Muñoz-Rodríguez, C. Rus-Casas, and D. L. Talavera, "A new approach based on economic profitability to sizing the photovoltaic generator in self-consumption systems without storage," *Renew. Energy*, vol. 148, pp. 1017–1033, Apr. 2020, doi: 10.1016/j.renene.2019.10.086.
- [22] IEA-PVPS, "Trends in PV applications 2021," IEA-PVPS. Accessed: Jul. 09, 2022. [Online]. Available: https://iea-pvps.org/trends_reports/trends-in-pv-applications-2021/
- [23] Á. Ordóñez, E. Sánchez, L. Rozas, R. García, and J. Parra-Domínguez, "Net-metering and net-billing in photovoltaic self-consumption: The cases of Ecuador and Spain," *Sustain. Energy Technol. Assess.*, vol. 53, p. 102434, Oct. 2022, doi: 10.1016/j.seta.2022.102434.
- [24] G. A. Barzegkar-Ntovom *et al.*, "Assessing the viability of battery energy storage systems coupled with photovoltaics under a pure self-consumption scheme," *Renew. Energy*, vol. 152, pp. 1302–1309, Jun. 2020, doi: 10.1016/j.renene.2020.01.061.

- [25] M. Castaneda, S. Zapata, and A. Aristizabal, "Assessing the Effect of Incentive Policies on Residential PV Investments in Colombia," *Energies*, vol. 11, no. 10, Art. no. 10, Oct. 2018, doi: 10.3390/en11102614.
- [26] R. Pacudan, "Feed-in tariff vs incentivized self-consumption: Options for residential solar PV policy in Brunei Darussalam," *Renew. Energy*, vol. 122, pp. 362–374, Jul. 2018, doi: 10.1016/j.renene.2018.01.102.
- [27] J. Thakur and B. Chakraborty, "Impact of compensation mechanisms for PV generation on residential consumers and shared net metering model for developing nations: A case study of India," *J. Clean. Prod.*, vol. 218, pp. 696–707, May 2019, doi: 10.1016/j.jclepro.2019.01.286.
- [28] E. Garabitos Lara, "Techno-economic model of nonincentivized self consumption with residential PV systems in the context of Dominican Republic: A case study," *Energy Sustain. Dev.*, vol. 68, pp. 490–500, Jun. 2022, doi: 10.1016/j.esd.2022.05.005.
- [29] A. Arcos-Vargas, J. M. Cansino, and R. Román-Collado, "Economic and environmental analysis of a residential PV system: A profitable contribution to the Paris agreement," *Renew. Sustain. Energy Rev.*, vol. 94, pp. 1024–1035, Oct. 2018, doi: 10.1016/j.rser.2018.06.023.
- [30] A. Simola, A. Kosonen, T. Ahonen, J. Ahola, M. Korhonen, and T. Hannula, "Optimal dimensioning of a solar PV plant with measured electrical load curves in Finland," *Sol. Energy*, vol. 170, pp. 113–123, Aug. 2018, doi: 10.1016/j.solener.2018.05.058.
- [31] European Commission, "JRC Photovoltaic Geographical Information System (PVGIS) - European Commission." Accessed: Aug. 05, 2023. [Online]. Available: https://re.jrc.ec.europa.eu/pvg_tools/en/
- [32] Fluke-IRR1, "Fluke Solar Irradiance Meter." Accessed: Aug. 22, 2023. [Online]. Available: <https://www.fluke.com/en-us/product/electrical-testing/best-solar-energy-industry-tools/flk-irr1-sol>
- [33] NREL, "PVWatts Calculator." Accessed: Aug. 05, 2023. [Online]. Available: <https://pvwatts.nrel.gov/>
- [34] EDESUR, "Edesur Dominicana S.A. | Edesur Dominicana, S.A.," Edesur Dominicana. Accessed: Jun. 22, 2020. [Online]. Available: <http://www.edesur.com.do/>
- [35] Borja - Academia Energía Solar, * *PANELES SOLARES para BALCÓN usando MICROINVERSORES | Autoconsumo Fotovoltaico*, (Jul. 13, 2023). Accessed: Aug. 08, 2023. [Online Video]. Available: <https://www.youtube.com/watch?v=8-goNKE5jJE>

Definition of an evaluation framework to assess the performance and impacts of Positive and Clean Energy Districts (PCEDs) in cities

Muhyettin Sirer¹[0009-0008-7698-7864], Beril Alpogut¹[0000-0002-7285-5388], Miguel Á. García-Fuentes²[0000-0001-6739-599X], José L. Hernández²[0000-0002-7621-2937], Ana Mera³[0000-0001-7291-4440], Eduardo Miera³[0000-0002-6697-0056]

¹ DEMIR Enerji, Halil Sokagi, No: 7, Kosuyolu, Kadikoy, Istanbul, Turkiye

² CARTIF Technology Centre, Parque Tecnológico de Boecillo, 205, 47151 Boecillo, Spain

³ Fundación TECNALIA R&I, Parque Científico y Tecnológico de Bizkaia, 700, Derio, Spain
msirer@demirenerji.com

Abstract. The challenge of EU cities to be decarbonized and become climate neutral by 2050 is currently the main topic within their agendas. In this pathway, establishing mechanisms in order to evaluate adequately the evolution and the impact of every city transformation is key. The EU project NEUTRALPATH, which works towards advancing this climate-neutrality goal in two EU cities (Zaragoza in Spain and Dresden in Germany) through the deployment of Positive and Clean Energy Districts, is developing an evaluation framework in order to ensure that all levels of evaluation are covered through a harmonized and comprehensive mechanism that provides the relevant indicators and calculation procedures. The levels of this framework cover the performance of the district and the specific solutions deployed, and to measure direct (Scope 1), indirect (Scope 2), and induced (Scope 3) emissions. This paper presents the overall framework and such levels, while depicting the main elements that have considered in their definition as the boundaries considered or the relevant indicators.

Keywords: PCED, PED, Climate Neutrality, Evaluation

1 Introduction

In response to the need of cities to address the goals of the European Green Deal and become climate neutral by 2050, the EU Commission launched an initiative aimed at bringing solutions to the main challenges on urban areas which are home to 75% of EU citizens [1]. This initiative, known as the EU Mission on Climate-Neutral and Smart Cities, aims to transform 100 EU cities into climate-neutral and smart cities by 2030 and to act as lighthouses of experimentation and innovation hubs to enable all European cities to follow suit by 2050 [2].

One of the pathways to achieving these goals is through the deployment of Positive and Clean Energy Districts (hereinafter, PCEDs), which are defined as “energy efficient and energy-flexible urban areas or groups of connected buildings which produce net

2

zero greenhouse gas emissions and actively manage an annual local or regional surplus production of renewable energy.” [3].

The cities of Dresden (Germany) and Zaragoza (Spain), which are fully aligned with the Cities Mission challenges, are working in the framework of the NEUTRALPATH project, funded by the EU Commission through the Horizon Europe Program, to deliver two PCEDs and demonstrate how these elements can contribute to the urban transformation as pivotal strategies into their decarbonisation roadmap. Along with Zaragoza and Dresden, the cities of Ghent (Belgium), Istanbul (Turkey) and Vantaa (Finland) are working to support exploiting the knowledge and capacities generated to other cities. All these five cities will do so through the implementation of a Climate Neutral Lab conceived as an innovation and stakeholders’ hub in the city to foster and facilitate participation and co-creation.

Within these objectives, an adequate evaluation framework becomes essential as a pillar to ensure appropriate measurement of the impacts of the actions and analysis of the cities’ emissions towards achieving the goal of becoming climate-neutral. This evaluation framework needs to be comprehensive, transparent and standard, while ensuring the integration of the relevant indicators which allow covering the levels of evaluation that contribute to scale-up the impacts and measure both concrete actions and the complete city boundary.

This paper presents the approach to this evaluation framework which is being developed in the framework of the NEUTRALPATH project. Section 2 describes the levels of evaluation while sections 3, 4, and 5 depict the main elements of these levels, describing their boundaries, sets of indicators or calculation procedures. Finally, section 6 provides the conclusions of the current development of this framework and future steps in its implementation in the cities which are part of the project.

2 Definition of the evaluation framework

The evaluation framework developed at NEUTRALPATH project sets a general methodology for evaluating and assessing the performance and impacts of PCEDs. The aim is to provide a common framework that, beyond specific circumstances, can be applied and used in the evaluation of any PCED implementation. Therefore, all aspects are integrated, including scale and domains, although not all are considered in all cases.

Discussions on a proper definition of PCED are ongoing. Nonetheless a common understanding is the self-sufficiency and the goal of delivering through renewable local energy a positive energy balance at an annual period. This means that geographical boundaries play an important role [4] and hence the evaluation framework must identify the different scale levels and the interaction with the grid. These will be detailed as levels of evaluation in this definition.

But there are other aspects that the proposed evaluation framework is also looking at for delivering a full assessment on the performance and impact of the PCED. In one hand the topics that should be included and that complement the energy field [5]. And in the other hand the measurement of emissions in terms of the three Scopes and the contribution of the PCED to the three of them.

In this sense, the first objective of the Evaluation of Framework is to identify a solid procedure associated to the definition of the PCEDs, defining the project-scale performance evaluation based on not only Energy, but also Environmental, ICT (Information and Communication Technologies), Mobility, Social and Economic indicators.

The second objective is to define a calculation procedure to evaluate the contribution to Scope 1, Scope 2 and Scope 3 emissions at city scale as a basis to monitor the evolution of the cities transition towards climate neutrality. A set of relevant indicators to measure direct, indirect and induced emissions are defined as a result. Scope 3 emissions in cities requires detailed analysis of the urban economy and urban metabolism approach which considers the inward and outward flows of energy, natural resources, waste, water and food.

2.1 Levels of evaluation

The following Figure 1 depicts the assessment levels within the evaluation framework of the NEUTRALPATH project:

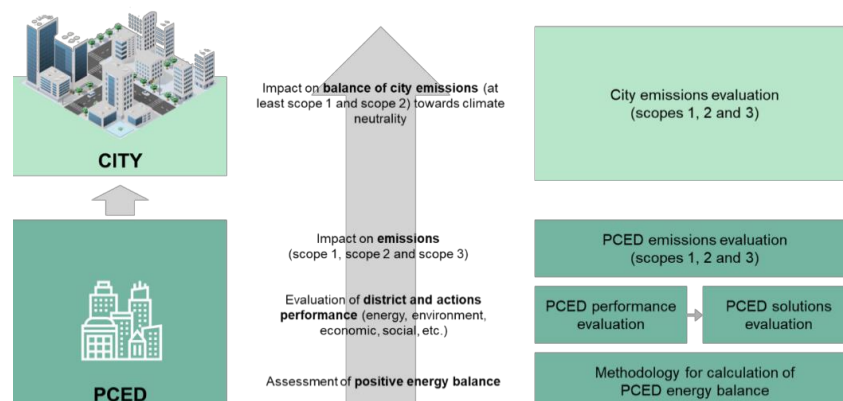


Figure 1. Levels of the evaluation framework

These four levels of the evaluation framework are described as follows:

1. **PCED positive energy balance assessment:** this evaluation level is aimed at assessing the positive energy balance of the buildings of a district (meaning that it produces more energy than it consumes in an annual primary energy balance). The boundaries of this level match with the physical limits of the district and the indicators are those that allow calculating the energy balance during a year of operation.
2. **PCED performance evaluation of district and solutions:**
 - a. **District:** this evaluation level allows the complete assessment of the performance of the district in terms of technical, economic, environmental and social indicators comparing, generally, a baseline situation and a post-retrofit situation. The boundaries of this level match with the physical limits of the district and the indicators generally compare a baseline situation and post-intervention situation.

4

- b. **Solutions:** this evaluation aims to evaluate the performance of the specific actions implemented to achieve the PCED. Thus, the indicators will generally be sub-sets of the previous and the boundaries will be those of the solution under evaluation.
3. **PCED emissions evaluation:** this evaluation level allows assessing the performance of the district in terms of emissions in scope 1 (direct emissions from onsite sources), scope 2 (indirect emissions from energy) and scope 3 (indirect emissions from upstream and downstream supply chain) so that the contribution of the PCED to the climate neutrality can be assessed.
4. **City emissions evaluation:** this evaluation level is fully aligned with the Cities Mission and allows the assessment of the climate neutrality of the city fully covering scopes 1 and 2, and scope 3 as much as possible and following the principles established in this document. The boundaries are those of the city considering the urban economy and urban metabolism.

3 PCED energy balance assessment

The calculation of the energy balance becomes essential in order to ensure that the district is positive in terms of non-renewable primary energy. This balance is calculated as the difference between the energy delivered to the boundary and the energy exported outside that boundary [6].

3.1 Boundaries and methods

The boundaries for the calculation of the energy balance depend on the type of PCED to be considered, which can be geographical, functional or virtual [4, 5, 7]. The geographical boundary covers the buildings, local production of energy (solar thermal, solar photovoltaics, centralized energy systems (including local district heating networks), thermal or electric storage, etc., which are delimited by spatial-physical limits. Other district heating and cooling networks or any type of RES (Renewable Energy Systems) existing outside the spatial boundary and connected to other uses, virtual power plants or storage, or other PCEDs, are considered outside the geographical boundary and, when integrated as part of the energy balance, then a virtual boundary is considered [8, 9].

The method is based on the evaluation of the energy flows required to cover the energy needs of the district in terms of space heating and cooling, domestic hot water, ventilation and humidification, and lighting based on the current provisions of the EPBD [6], while uses as appliances or EV cars are not currently considered but likely to be part of the directive in the future [7]. Then, the energy use is calculated as the energy inputs to the systems that provide the services that cover these energy needs. The energy delivered or exported by the production systems is then calculated in the form of inputs to the boundaries (from the electricity system or from fuels) or outputs outside the boundaries (from RES produced within the district). These flows of energy delivered are then transformed into primary energy through the application of the corresponding national conversion factor.

The following Sankey diagram (Figure 2) reflects this procedure to calculate the energy balance for the boundaries defined, including the relations among the flows.

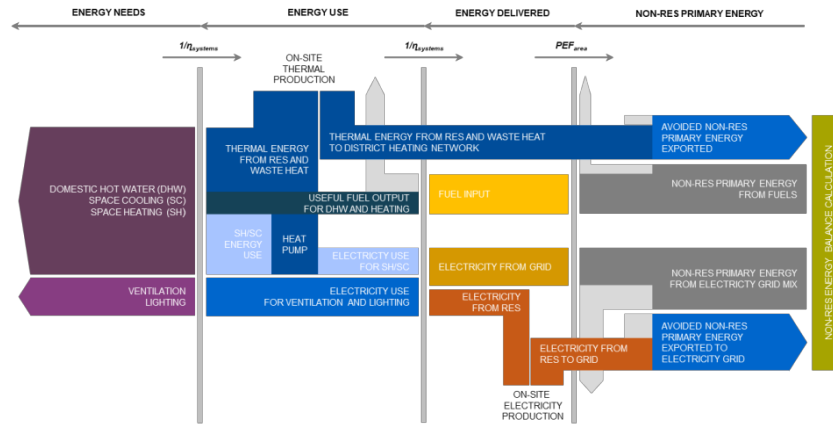


Figure 2. Scheme of the methodology to calculate the positive energy balance.

3.2 Metrics to calculate the positive energy balance

Based on the previous, the main metrics to calculate the energy balance are the following, which are based on the provisions of the EN ISO-52000-1:2007 [10]:

Table 1. Definition of main components of the energy balance calculation.

Concept	Definition
Positive and Clean Energy District	energy-efficient and energy-flexible urban areas or groups of connected buildings which produce net zero green-house gas emissions and actively manage an annual local or regional surplus production of renewable energy. Mobility is excluded from the building energy balance.
Thermal Energy Need	<u>for domestic hot water (DHW):</u> heat to be delivered to the needed amount of domestic hot water to raise its temperature from the cold network temperature to the prefixed delivery temperature at the delivery point, without the losses of the domestic hot water system. <u>for space heating:</u> heat to be delivered to or extracted from a thermally conditioned space to maintain the intended space temperature conditions during a given period of time, without the losses of the heating system.
Electrical Energy Need	electrical energy to be delivered to cover the energy needs for domestic hot water, heating and cooling when an electricity-driven system is used, ventilation, and lighting, without the losses of the system.
Energy Use	<u>for space heating or cooling or DHW:</u> energy input to the heating, cooling or DHW.

6

for ventilation: electrical energy input to a ventilation system for air transport and heat recovery.

for lighting: electrical energy input to a lighting system.

for other services: energy input to appliances providing services not included in the EPB services.

Delivered Energy	energy, expressed per energy carrier, supplied to the technical building (or district) systems through the assessment boundary, to satisfy the uses considered or to produce the exported energy.
Exported Energy	energy, expressed per energy carrier, supplied by the technical building (or district) systems through the assessment boundary.
Non-Renewable Energy	energy taken from a source which is depleted by extraction (e.g., fossil fuels) (note: resource that exists in a finite amount that cannot be replenished on a human time scale).
Primary Energy	energy taken from a source that has not been subjected to any conversion or transformation process. (Note: primary energy includes non-renewable energy and renewable energy. If both are considered, it can be called total primary energy).
<u>Total Energy</u>	<u>energy from both renewable and non-renewable sources.</u>

4 PCED performance evaluation

The procedure for PCED performance evaluation consists of a methodology to evaluate the actions of the project with the identified indicators in following steps:

- Step I: Identification of the application-level indicators in accordance with the PCED actions, setting the objective for monitoring and impact assessment,
- Step II: Definition of the initial (baseline) situation of the PCED and calculation of the indicator values before the planned project (PCED) level interventions,
- Step III: Monitoring the actions/action groups with key performance indicators during the monitoring phase of the project,
- Step IV: Calculation of the indicators at the end of the project applications for final assessments.

The indicators for assessing the project actions serve the evaluation of the interventions in PCED areas. The calculated indicators show the difference that the project actions have made, through a comparison of the baseline conditions without any intervention with the situation after the implementation of the planned actions. The indicators also serve to benchmark projects against each other. The evaluation framework includes evaluation boundaries as well as approaches to assess the impact of the project implementations in specified indicator categories, including energy, environment, information and communication technologies, mobility and economy (quantitative indicators) and social aspects (qualitative indicator).

4.1 Step 1: Selection of Indicators

The indicators can be classified as input, process, output, outcome, and impact indicators as summarized below:

- Input indicators are used to measure the quantity, quality, and timeliness of such resources as materials, financial resources, human resource and policies.
- Process indicators refer to the realization of the planned actions, such as meetings and training courses.
- Output indicators provide details of the outputs of the actions, such as the number of new jobs created or the square meter of the insulated surfaces.
- Outcome indicators refer to the objectives and intermediate results of the project actions, e.g., the rate of reach of the targeted population.
- Impact indicators are related to the states (impacts) of the targets, such as the decreased energy consumption in a Positive and Clean Energy District, following the realization of the interventions.

4.2 Step 2: Calculation of the baseline

The main purpose of the baseline calculations is to analyze the existing situation before the applications take place. In this section general guidelines to analyze the results of the potential actions to be realized at project level are presented.

A boundary of analysis must be defined before the calculations of the baseline conditions. As an example, baseline energy analysis of a building is the calculation of the actual situation, either based on collected or simulated data in advance the planned actions take place, if the target of the planned intervention is to improve the energy efficiency of the building. For new buildings the baseline analyses can be conducted based on existing building regulations or energy performance simulations.

In such analyses, International Performance Measurement and Verification Protocol (IPMVP) [11] or similar methodologies can be directly applicable. IPMVP is a best practice methodology commonly used for measuring, computing, and reporting savings achieved by energy efficiency projects at end user facilities. This protocol describes how to perform an energy assessment, by comparing consumption levels before and after implementation of energy actions.

4.3 Step 3: Monitoring of performance

A monitoring program concentrates on monitoring all the incoming and outgoing energy flows for each building of the district and for the whole district separately. Monitoring must handle all the energy types that flow to building/district at own lines/pipes separately (e.g., electricity from grid or thermal energy from district heating pipes or gas from gas pipes).

The first level of the monitoring is the baseline assessment. Although baseline calculations differ for a new or renovated building, methodologies including IPMVP [11] can be directly applicable. For new buildings, there is no existing data to which against

8

the comparison is made. Therefore, baseline is based on the energy performance of reference buildings without implementing the interventions mentioned in the project plan, including simulations. For renovated buildings, the essential action is to meter all the needed parameters of energy performance before any intervention is realized. In this case, the baseline analysis covers pure metrics calculated from one year, including different seasonal conditions, before applications without weather-related corrections.

For monitoring phases of the qualitative data, it is important at first to identify the requirements that are needed to reach the value for the indicators. All the required data may not be able to be collected from the same data source. Therefore, it is important to identify all the required data sources. In the case of qualitative data, these data sources mean people, i.e., stakeholders that are relevant in the context of the monitored target. Different kinds of stakeholders are classified into different groups. For each group, the minimum and maximum number of stakeholders must be defined. For each stakeholder group, the goals for the data collection must be defined.

4.4 Step 4: Calculation and impact assessment

Final calculation of indicators and impact assessment of the project interventions are performed at the end of the monitoring period of a project, through a standardized evaluation methodology, such as IPMVP. After a suitable time period following the realization of the planned interventions, related key performance indicators are once again measured to define the “post-retrofit” performance period. The baseline and reporting periods are then compared using the following general M&V equation:

$$\text{Savings} = (\text{Baseline period} \pm \text{Adjustments}) - (\text{Reporting period} \pm \text{Adjustments}) \quad (1)$$

The adjustment terms shown in the equation should be computed from identifiable physical facts. Appropriate adjustments shall be made by considering changes in the existing conditions. The adjustments include routine adjustments and non-routine adjustments [11].

Routine adjustments are made on parameters that are expected to change regularly, such as outdoor temperature. These adjustments are usually conducted by using mathematical models that are developed to correlate energy to one or more independent variables, e.g., outdoor temperature or degree-days.

Non-routine adjustments are reflected on static factors which are not usually expected to change, such as the following in energy consumption:

- Square meter of conditioned floor area.
- Components and characteristics of the building envelope, including windows, doors, insulation, air tightness, etc.
- Changes in the type, amount, or use profile of the equipment in the building.
- Indoor environmental conditions, such as temperature and humidity set points, lighting levels, ventilation rate, etc.

4.5 Identification of KPIs for PCED performance evaluation

Key Performance Indicators (KPIs) for PCED performance evaluation can be identified in six categories, including energy, ICT, mobility, environment, social, and economy [12, 13, 14, 15]. The following table is a list of KPIs which could be selected and applied, depending on the project interventions at PCED level, for each category.

Table 2. List of identifiable KPIs for PCED performance evaluation.

Field of action	Indicators
Energy	<ul style="list-style-type: none"> • Thermal Energy Need per sqm of Usable Conditioned Floor Area (CFA) (H&C) • Thermal Energy Need per sqm of Usable CFA (DHW) • Electrical Energy Need per sqm of Usable CFA • Delivered Thermal Energy per sqm of Usable CFA (H&C) • Delivered Thermal Energy per sqm of Usable CFA (DHW) • Delivered Electrical Energy per sqm of Usable CFA • Thermal Energy Use per sqm of Usable CFA (H&C) • Thermal Energy Use per sqm of Usable CFA (DHW) • Primary Thermal Energy Use per sqm of Usable CFA (H&C) • Primary Thermal Energy Use per sqm of Usable CFA (DHW) • Electrical Energy Use per sqm of Usable CFA • Primary Electrical Energy Use per sqm of Usable CFA • Thermal Energy Savings Ratio (H&C) • Thermal Energy Savings Ratio (DHW) • Electrical Energy Savings Ratio • Primary Thermal Energy Produced by RES per sqm of Usable CFA (H&C) • Primary Thermal Energy Produced by RES per sqm of Usable CFA (DHW) • Primary Electrical Energy Produced by RES per sqm of Usable CFA • Storage Thermal Energy Losses • Storage Electrical Energy Losses • Degree of Self-Supplied Primary Thermal Energy by RES (H&C) • Degree of Self-Supplied Primary Thermal Energy by RES (DHW) • Degree of Self-Supplied Primary Electrical Energy by RES • Degree of Primary Thermal Energy Exported • Degree of Primary Electrical Energy Exported
Environment	<ul style="list-style-type: none"> • Greenhouse Gas Emissions After Interventions per 100 Inhabitants • Greenhouse Gas Emissions After Interventions per sqm of Usable CFA • Greenhouse Gas Emissions Reduction
E-mobility	<ul style="list-style-type: none"> • Ratio of Solar Powered EV and V2G Charging Points • Total Installed Solar Power • Ratio of Annual Renewable Energy Delivered by Charging Points
ICT	<ul style="list-style-type: none"> • Improved Energy Performance by ICT Strategies • Quality of Open Data

10

Social	<ul style="list-style-type: none"> • People Reached • Distribution of People Reached by the type of Citizen • Consciousness of Residents • Community Involvement • Number of Community Participation Events and Actions • Percentage of Participants in the Community Events • Degree of Satisfaction • Social Compatibility • Perceived Usefulness • Ease of Use • Perceived Knowledge / Education • Number of Jobs Created
Economy	<ul style="list-style-type: none"> • Total Investment for Electrical Energy Savings per sqm of Usable CFA • Total Investment for Thermal Energy Savings per sqm of Usable CFA • Total Investment for Electrical Energy Generation by RES per sqm of Usable CFA • Total Investment for Thermal Energy Generation by RES per sqm of Usable CFA • Investment to Electrical Energy Savings Ratio • Investment to Thermal Energy Savings Ratio • Investment to Electrical Energy Cost Savings Ratio • Investment to Thermal Energy Cost Savings Ratio • Energy Poverty • Ratio of Investment plus Operational Costs to Reduced CO₂eq Emissions • Return on Investment • Net Present Value

5 PCED emissions evaluation and impacts at city level

The Global Protocol for Community-Scale Greenhouse Gas (GHG) Inventories (GPC) [16] is a standardized framework and set of guidelines designed to help local governments and communities measure, report, and manage greenhouse gas emissions at a local or community level. The GPC was developed to assist cities, municipalities, and regions in assessing their contributions to global climate change and to track progress in reducing their emissions.

To use the GPC, PCEDs and cities must first define a Greenhouse Gas (GHG) inventory boundary. Also referred to as the inventory boundary, it is a fundamental concept in the process of measuring and accounting for greenhouse gas emissions. It defines the scope and extent of the area or activities for which greenhouse gas emissions are being assessed. The inventory boundary is a critical element in establishing the limits of what is included in a GHG inventory and what is excluded.

When preparing a GHG inventory, PCEDs, cities, or regions need to specify what is included and what is excluded from the assessment. The boundary is typically determined based on the objectives of the inventory, factors of the operational control, and the geographical or sectoral focus.

Greenhouse gas (GHG) emissions from city or community activities are typically classified into several main sectors to facilitate the measurement and analysis of emissions. The specific sectors can vary depending on the methodology or framework used, but a common approach is to categorize them into the following sectors:

- **Energy:** This sector includes emissions from the production and consumption of energy within the city, which encompasses electricity generation, heating, cooling, and transportation. It often includes subcategories like stationary energy (emissions from buildings and facilities) and transportation energy (emissions from the transportation sector, including road, rail, air, and marine transport).
- **Buildings:** Emissions from the residential, commercial, and industrial buildings within the city are categorized under this sector. It covers energy use for heating, cooling, lighting, and appliances within buildings.
- **Transportation:** This sector focuses on emissions from the movement of people and goods within the city. It includes emissions from cars, trucks, buses, trains, planes, and ships. Subcategories can include passenger transport and freight transport.
- **Waste:** Emissions related to the management of solid waste, including landfilling, incineration, and recycling, fall under this sector. Methane emissions from decomposing organic waste in landfills are a significant component.
- **Industrial Processes and Product Use:** This sector accounts for emissions from industrial activities, including emissions from chemical reactions, manufacturing processes, and product use within the city.
- **Agriculture and Land Use Change:** While not always included in city-level inventories, this sector encompasses emissions from agricultural activities within the city's boundaries and any land-use changes that release or sequester carbon.
- **Water and Wastewater:** This sector may include emissions from the energy used in water treatment and distribution, as well as wastewater treatment processes. It also accounts for methane emissions from anaerobic processes in wastewater treatment.
- **Fugitive Emissions:** This category deals with emissions that escape into the atmosphere because of leaks and venting of greenhouse gases from infrastructure such as pipelines and natural gas distribution systems.
- **Other:** This category can encompass emissions from other sources that do not neatly fit into the above sectors, such as emissions from refrigerants, chemicals, and other miscellaneous sources.

Activities taking place within a PCED, or city can generate GHG emissions that occur inside the PCED or city boundary as well as outside the city boundary. To distinguish among them, the GPC groups emissions into three categories based on where they occur: scope 1, scope 2 or scope 3 emissions. The scopes framework helps to differentiate emissions occurring physically within the PCED or city (scope 1), from those occurring outside the PCED or city (scope 3) and from the use of electricity, steam, and/or

12

heating/cooling supplied by grids which may or may not cross PCED or city boundaries. Scope 1 emissions may also be termed “territorial” emissions because they occur discreetly within the territory defined by the geographic boundary.

Table 3. Definitions of scopes for PCED and city inventories.

Scope	Definition
Scope 1	GHG emissions from sources located within the PCED or city boundary.
Scope 2	GHG emissions occurring as a consequence of the use of grid-supplied electricity, heat, steam and/or cooling within the city boundary.
Scope 3	All other GHG emissions that occur outside the city boundary as a result of activities taking place within the city boundaries.

Selecting the most appropriate methodologies to calculate greenhouse gas (GHG) emissions for cities or PCEDs involves a thoughtful and systematic approach, including the following steps:

- **Definition of goals and objectives:** Start by clearly defining your objectives for calculating GHG emissions. Are you doing this for baseline assessment, monitoring progress, or setting emissions reduction targets? Understanding your goals will guide your method selection.
- **Identification of data availability:** Assess the availability of data and resources, as this will significantly influence the choice of methodologies. Data availability includes factors like data quality, quantity, and geographic coverage.
- **Consideration of the scope and boundaries:** Determine the scope of your assessment, including what emissions sources and sectors you intend to include. You should also establish the geographic boundaries, such as the entire city, a specific PCED, or a specific economic development zone.
- **Assessment of international standards and guidelines:** Familiarize yourself with internationally recognized standards and guidelines for GHG emissions calculations, such as the Greenhouse Gas Protocol, the Intergovernmental Panel on Climate Change (IPCC) guidelines, and ISO 14064. These provide valuable frameworks for measurement.
- **Tailoring methodologies to the local context:** Adapt the selected methodologies to your specific context. Consider factors like the size of your city or PCED, the sources of emissions (e.g., energy, transportation, industry), and local circumstances.
- **Engaging stakeholders:** Involve relevant stakeholders, including local government agencies, industry representatives, environmental organizations, and academic experts, in the selection process. Their input can provide diverse perspectives and improve the credibility of your calculations.
- **Assessment of available tools and software:** There are various GHG accounting tools and software available that can help streamline the calculation process. Evaluate the suitability of these tools based on your specific requirements and available resources.

- **Consideration of combination of methodologies:** It may be beneficial to use a combination of methodologies to capture all relevant emissions sources and sectors. This can improve the comprehensiveness and accuracy of your GHG inventory.
- **Conducting a pilot study:** Before implementing the chosen methodologies on a larger scale, conduct a pilot study to test the data collection process and methodology. This can help identify any challenges and refine the approach.
- **Ensuring transparency and documentation:** Document your methodology selection and data sources transparently to enhance credibility and enable others to understand and replicate your calculations.
- **Regular review and update:** GHG emissions calculations should be an ongoing process. Periodically review and update your methodologies and data sources to reflect changes in your city or PCED and to track progress toward emission reduction goals.

Due to its size and location, the PCED area functions as a subcomponent of the city. Therefore, as a result of this, the content related to Scopes 1, 2, and 3 contains certain similarities and differences. In PCED areas, emissions from stationary fuels under Scope 1 and emissions from grid-supplied energy under Scope 2 are necessarily included. However, in contrast to city scale emissions, PCED areas may not include agriculture and other land use, industrial processes and production in Scope 1, waste and wastewater in Scope 3, emissions from transportation in Scope 3 and emissions from transmission/distribution. Figure 3 exhibits the sources and boundaries of city GHG emissions, while city and PCED scale emission contents are compared in Figure 4.

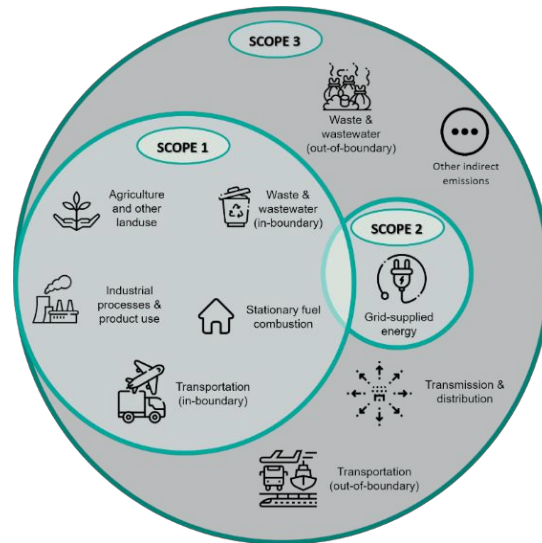


Figure 3. Sources and boundaries of city GHG emissions.

14

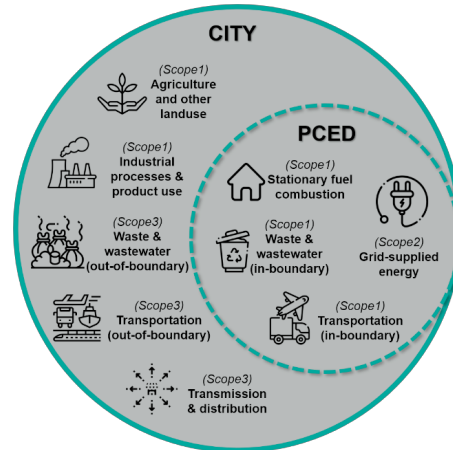


Figure 4. Comparison of city and PCED scale emissions contents.

6 Conclusions

This paper presents a comprehensive and standardized evaluation framework for the evaluation of PCED performance integrating different levels of evaluation and measuring individual solutions as well as the overall impact from PCED to the city boundary. The framework describes a bottom-up approach in four levels: PCED positive energy balance, PCED performance and solutions evaluation, PCED emissions and City emissions covering 6 dimensions: energy, ICT, mobility, environment, social and economy.

The framework provides a methodology including the set of KPIs that are needed for the correct assessment and evaluation at the different levels. Whenever was possible based on standardized metrics such as the ones based on EN ISO 52000-1:2007 so that misinterpretation is avoided which is a common problem. But also provides a full procedure from project level, definition of the baseline situation and monitoring actions to evaluating the impact of the performance.

This is not only a theoretical exercise since it will be tested in two EU cities: Dresden (Germany) and Zaragoza (Spain) with own PCED implementations. The adequacy of the framework to each city will be worked considering the specific features at PCED and City level to show the adaptability of the framework to different realities.

When it comes to evaluating the City level, the framework is ambitious presenting not only Scopes 1 and 2 emissions, but also Scope 3. However, its calculation presents problems derived from the lack of easily accessible data. Therefore, the framework suggests a flexible mapping of these emissions.

Furthermore, when looking to find a correlation between PCED and city levels, the boundaries for each Scope is less clear. The paper presents a possible design of how to consider each level due to their activities. Nevertheless, further research in measuring more easily Scope 3 is needed specially from real case studies as those that will be carried out within the project.

References

1. Clark, G., Moonen, T., Nunley, J. (2018) The Story of Your City: Europe and its Urban Development, 1970 to 2020. Part of the “City, transformed” essay series. European Investment Bank.
2. EU Commission. COM (2021) 609 final. Communication from the Commission to the European Parliament, the Council, the European Economic and Social Committee and the Committee of the Regions on European Missions.
3. Urban Europe: Europe towards Positive Energy Districts (https://jpi-urbaneurope.eu/wp-content/uploads/2020/06/PED-Booklet-Update-Feb-2020_2.pdf).
4. Quijano, A.; Hernández, J.L.; Nouaille, P.; Virtanen, M.; Sánchez-Sarachu, B.; Pardo-Bosch, F.; Knieilng, J. Towards Sustainable and Smart Cities: Replicable and KPI-Driven Evaluation Framework. *Buildings* 2022, *12*, 233. <https://doi.org/10.3390/buildings12020233>.
5. Quijano, A.; Hernández, J.L.; Nouaille, P.; Virtanen, M.; Sánchez-Sarachu, B.; Pardo-Bosch, F.; Knieilng, J. Sustainable Cities: A KPI-Driven Sustainable Evaluation Framework for Smart Cities. *Environ. Sci. Proc.* 2021, *11*, 21. <https://doi.org/10.3390/envirosciproc2021011021>.
6. Energy Performance of Buildings Directive (2010/31/EU).
7. Gabaldón Moreno, A.; Vélez, F.; Alpagut, B.; Hernández, P.; Sanz Montalvillo, C. How to Achieve Positive Energy Districts for Sustainable Cities: A Proposed Calculation Methodology. *Sustainability* 2021, *13*, 710. <https://doi.org/10.3390/su13020710>.
8. Vandevyvere, H. Positive Energy Districts Factsheet, Smart Cities Marketplace, Horizon 2020 Programme. Available at: <https://smart-cities-marketplace.ec.europa.eu/sites/default/files/2021-06/Positive%20Energy%20Districts%20Factsheet.pdf> (last accessed on 12 September 2023).
9. Guidelines for Positive Energy District Design. Making City Project, Horizon 2020 Programme. Available at: <https://makingcity.eu/wp-content/uploads/2020/12/Guidelines-for-PED-DEsign.pdf> (last accessed on 12 September 2023).
10. International Organization for Standardization. ISO 52000-1:2017. Energy performance of buildings — Overarching EPB assessment — Part 1: General framework and procedures. 2017.
11. International Performance Measurement and Verification Protocol (IPMVP).
12. Evaluation Procedure for PED Actions, Making City Project, Horizon 2020 Programme, November 2020.
13. EET-Centric KPIs Definition, with All Evaluation Metrics and Formulas Derived, POCITYF Project, Horizon 2020 Programme, June 2020.
14. Approach and Methodology for Monitoring and Evaluation, CityXChange Project, Horizon 2020 Programme, June 2019.
15. Definition of SPARCS Holistic Impact Assessment Methodology and Key Performance Indicators, SPARCS Project, Horizon 2020 Programme, March 2020.
16. Greenhouse Gas Protocol, Global Protocol for Community-Scale Greenhouse Gas Inventories, An Accounting and Standard for Cities, v.1.1.
17. PAS 2070:2013, Specification for the Assessment of Greenhouse Gas Emissions of a City.

Small Signal Stability Study in Power Systems with Low Penetration of Renewable Sources

Angel-Dagoberto Germán-Encarnación ¹[0009-0004-0423-5699], Angel-José Sánchez-Sánchez ¹[0009-0000-0080-6547], Víctor Ernesto Peralta Maxwell ¹[0009-0009-8519-1494], Deyslen Mariano-Hernández ¹[0000-0002-4255-3450], Eduardo De León-Concepción ¹[0000-0002-0149-5266] and Miguel Aybar-Mejía ¹[0000-0002-4715-3499]

¹ Área de Ingenierías, Instituto Tecnológico de Santo Domingo (INTEC), Dominican Republic
miguel.aybar@intec.edu.do

Abstract. Small signal stability refers to the ability of the system to maintain stable operation against low amplitude oscillations generated by variations in electrical demand or the connection/disconnection of generators. The stability analysis of small signals is a study of great importance in power systems since it allows analysis of the system's behavior in the face of disturbances of small magnitude, such as differences between generation and load blocks and unforeseen disconnection of loads or generators. When these disturbances are too significant, they can trigger situations of instability with severe consequences, such as massive power outages. In order to address this problem, various mathematical methods are employed, including the Prony method and the Fourier transform. The method developed in MATLAB analyzes the oscillations of small signals in a 138 kV substation of the electric grid with low penetration of renewable energies. The mention above will improve the safety and performance of the country's electricity system. The method provides accurate and efficient tools to assess the stability of small signals and takes preventive or corrective measures, ensuring a more reliable and stable electricity supply for Dominican citizens and industries.

Keywords: Frequency stability, Prony's method, renewable energies, maximum damping, small signal.

1 Introduction

Stability has become crucial in an ever-evolving world where technological advances and the complexity of electrical and electronic systems have become increasingly prominent. The ability to predict and understand the behavior of systems in response to small amplitude disturbances has become imperative to ensure their optimal and reliable operation.

Small signal stability analysis emerged as a fundamental discipline in electrical, electronic, and control systems engineering [1]. It focuses on evaluating the dynamic response of a system around its stable operating point, examining the influence of low-magnitude variations and disturbances. This assessment is essential to determine

2

the robustness of the system and its ability to maintain stable performance under various operating conditions.

Small signals have a tendency where, over time, they have been evaluated in the following ways: adopting renewable energy sources such as solar and wind have increased the complexity of small signal analysis [3] due to the intermittent they generate. These sources' intermittency and lower predictability can cause power generation fluctuations, affecting the system's stability.

The study of small signals can be performed through early instability analysis [4], which allows the design and implementation of control strategies that can accommodate the intermittent nature of sources such as solar and wind energy [5].

This paper's objective is to propose a tool for assessing the behavior of the electrical system where intermittent renewable energies are integrated, seeking to determine how renewable energies intervene in the stability of small signals. For this, a mathematical model was designed to perform stability evaluations of the Wavelet transform of small signals in an electrical power system (EPS).

2 Methodology

For the development of this research, the following steps were carried out to analyze and interpret the behavior of small signal oscillations in a power system:

- Critical analysis of small signal stability analysis methods. This step determined the mathematical and engineering tools helpful in performing small signal stability studies in power systems.
- Evaluation of methods to analyze the stability of small signals. This step was designed to select computer tools that would allow mathematical operations, simulations, programming, and any activity related to developing a study of this magnitude.
- Delimitation and design of methods for the development of the program. The types of calculations and procedures to follow to develop the analysis are selected.
- Test scenarios delimitation. The operation data of the electrical power system you want to analyze is compiled, taking from this frequency history under different scenarios, events, or periods.
- Application programming for the analysis of small signal stability. This step is intended to develop the program to allow the interpretation of the small signal stability study. All the necessary procedures will be carried out to obtain the results delimited above.
- Approach validation. In this step, verification of compliance with the previous steps proposed in the methodology is carried out.

3 Analysis of Low Oscillations in a Power System

The small signal stability study is an analysis tool that allows analyzing the behavior of an EPS in the face of small magnitude events that may occur. Small signal oscilla-

tions can be generated by the connection or disconnection of load blocks or generators, opening of transmission lines, or management of the EPS [6].

Small signal oscillations are usually classified into signal oscillation modes [7]. These modes indicate the type of oscillation that occurs in the system and the behavior that occurs in it, as well as serve as an indicator for the criticality of the oscillations [8]. Table 1 shows the classification of EPS oscillation modes, their frequency ranges, the location where these oscillations typically occur, and some of their most critical effects.

Table 1. Summary of oscillation modes.

Ref.	Mode	Minimum Frequency (Hz)	Maximum Frequency (Hz)	Occurrence Place	Effects
[9]	Interarea	0.1	0.8	Between areas	Active and reactive power oscillations
[10]	Local	0.8	1.8	Power plant	Frequency oscillation
[12]	Control	2	3	Control equipment	Insertion of poles in the stability diagram.
[14]	Torsional	4	> 4	Mechanical systems	Vibrations in the axes of the machines.

- Interarea mode is the oscillation mode that appears in interconnected or large-scale EPSs where transmission lines connect two or more large regions. These oscillations are the product of weak links and can affect the operation of all generators in the grid [9].
- Local mode is the oscillation mode produced by a generator or a power plant that is interconnected to a large EPS. In this mode, the oscillations of the generator interact with the network, affecting this behavior. They can be oscillations generated in specific generating units connected to the grid or between generators of the same plant or nearby plants [10] [11].
- In control mode, these oscillation patterns originate due to drawbacks in the management mechanisms of power plants. They are associated with the control circuits of power systems, such as voltage regulators, frequency regulators, excitation devices, and other management components used to ensure the stability of the electrical system against disturbances. They are also called internal plant modes since they usually occur when one plant oscillates concerning another [12].
- Torsional modes are those oscillations generated by the mechanical systems of the generating plants. They manifest as mechanical oscillations in the electrical system, especially in the rotating parts of generators, such as the rotor and shaft. They are related to the tendency of the constituent parts of the turbine to oscillate with

4

each other and concerning the electrical network to which the generator is connected [13] [14].

The stability of a small signal in a topic can be treated from different edges depending on the system's data with which it is counted and the disposition of the different methods that can be used to perform the analysis. The EPS can be analyzed through the system's frequency, on an extract of the EPS modeling the necessary machines and other methods that allow the study of this topic. Regarding evaluation methods, EPS can be evaluated using mathematical models such as the Prony method, the Fourier transform, eigenvalue decomposition, modal analysis, and other methods. This study uses the Fourier transform and the Prony method to interpret the data [15].

The Prony method is a signal analysis method used in post-event stability studies which allows us to determine the oscillations of the signal, the damping of these, and the components of the oscillation frequencies [16].

The Fourier transform is a mathematical tool that decomposes a function or signal into its frequency components. The Fourier transform converts a function or signal from the time domain to the frequency domain, which makes it possible to analyze and understand the different frequency components present in the signal. By applying the Fourier transform to a signal, a frequency spectrum shows the amplitude and phase of each frequency component present in the original signal [17] [18].

The wavelet transform is a mathematical equation used for signal analysis of different applications in engineering. It deals with the decomposition of a signal into several components called wavelets, which are functions located in the time and frequency domain. Applying this transform generates a representation of high-frequency and low-frequency information [19] [20].

3.1 Methods Delimitation

To better understand this evaluation, it is essential to consider the specific study scenario in which this analysis will occur. The above-mentioned helps in defining the appropriate methods for analyzing minor disturbances.

The frequency spectrum is a graphical or conceptual representation of the different frequency components present in a signal. When a frequency analysis is performed using techniques such as the Fourier transform, information is obtained about the amplitudes and phases of the various frequency components that make up the original signal. This information is represented in the frequency spectrum [21] [22].

Related to stability, poles and zeros is a method of graphing the stability of a system [23]. Both poles and zeros are essential points in the complex plane and provide information about the system's stability. The stability of a system is affected by the location of the poles in the complex plane. If the poles have negative real parts, the system is considered stable. However, if a pole is presented in the imaginary part of the graph, it tends to become unstable and exhibit oscillatory or divergent behaviors [24].

The own values are the solutions of the equation characteristic of a linear system, also known as the eigenvalue equation. The eigenvalues are the elements necessary to

calculate the natural frequency of a system, as well as the modes of response of the SEP to the disturbances that occur in them. Each eigenvalue is composed of a real part and an imaginary part, corresponding to the frequency and damping of the associated response mode. The real part of the eigenvalue determines the natural frequency of the mode, while the imaginary part indicates the damping rate of the mode [25] [26] [27] [28].

3.2 Scenarios

The Dominican electrical power system is considered to have low renewable penetration since less than 10% of the total renewable energy generated in the country [29]. For this study, the operation of the electrical system of the Dominican Republic will be taken as a reference, specifically in the Hainamosa substation of this system. This system has a voltage level of 138 kV, and within the substation installation, frequency meter equipment allows frequency oscillations to be measured in this location. It has 12 connection fields within the substation, which makes it optimal for this analysis because it is in contact with many other substations and can generate oscillations between them. Fig. 1 shows the interconnection between the different substations located in the areas surrounding Hainamosa.

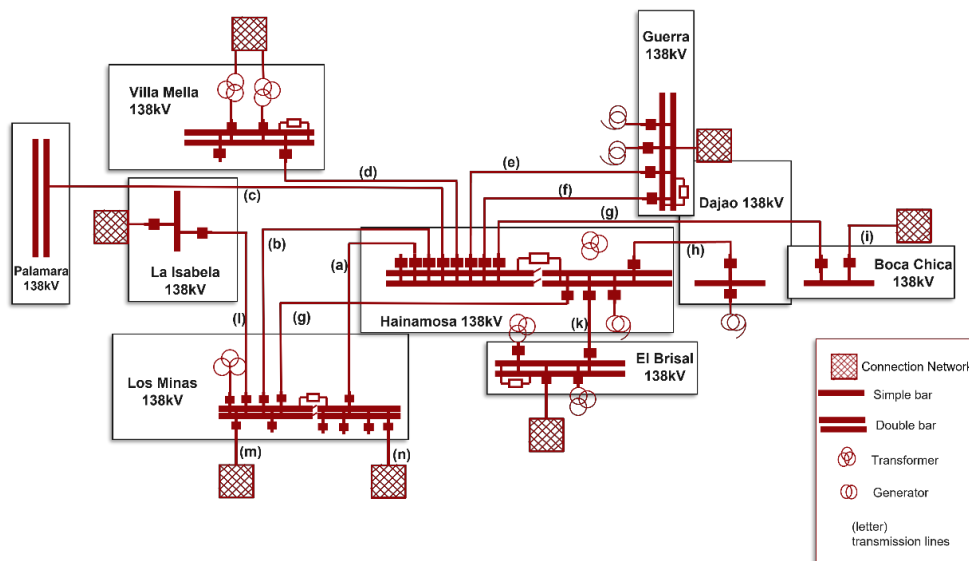


Fig. 1. Connection diagram of the 138kV substations of the national electrical system.

The behavior of the frequency oscillations of the Dominican electrical system was evaluated by taking the 138 kV Hainamosa substation as a reference point to analyze

6

the fire of renewable energy sources in the oscillations of small signals of the network.

For the proposed study, several frequency databases are grouped into two-hour blocks of information by period. The mentioned above allowed it to perform many test simulations to verify if there is an instability of small signals. The scenarios occur between 11:00 and 16:00 because these are the times when renewable energy sources have a more significant presence within the energy matrix of the Dominican Republic.

Within it, three scenarios were evaluated in which different frequency values given on the day and time were evaluated, as described below.

- Scenario 1
In this scenario, the frequency spectrum of the electrical system was taken under the operating conditions at the time and time. From this period, 150 seconds of sample were taken for this first scenario. At a time when there is a significant participation of renewable sources in the electrical grid for this period
Hours: 09:00 A.M. – 11:00 A.M. Location: Hainamosa Substation 138 kV.
Date: 09/05/2023
- Scenario 2
Hours: 02:00 P.M. – 04:00 P.M. Location: Hainamosa Substation 138 kV.
Date: 09/05/2023
- Scenario 3
In this scenario, their damping is very low since it is not possible to maintain the system frequency at a constant point.
Hours: 02:00 P.M. – 04:00 P.M. Location: Hainamosa Substation 138 kV.
Date: 09/04/2023
- Scenario 4
In this scenario, a sample of 200 seconds of system frequency was taken, extracted from the first extract of sampled frequencies (continuation of scenario #1).
- Scenario 5
For this scenario, a period of 150 seconds included in a schedule was taken.
Hours: 02:00 P.M. – 04:00 P.M. Location: Hainamosa Substation 138 kV.
Date: 09/04/2023
- Scenario 6
For this scenario, it proceeded to simulate a small signal oscillation in the grid. For this, the Excel calculation tool was used to generate random values that can generate small signal oscillations.
- Scenario 7 and 8
For this scenario, the Peru electric system was evaluated, which will be analyzed on a typical operating day.

3.3 Method Development

A method was proposed that would allow stability analysis of a small EPS signal under the presence of renewable energy sources in the network.

For this, a mathematical analysis program developed in MATLAB was used, in which the mathematical tools that this program has to perform power system analysis and complex mathematical calculations were used. The use of this program was determined due to the wide variety of mathematical models available and the easy implementation of these.

The development of the program was carried out through a flowchart (see Fig. 2), which explains how the program evaluates the frequency data to determine if there is a small signal.

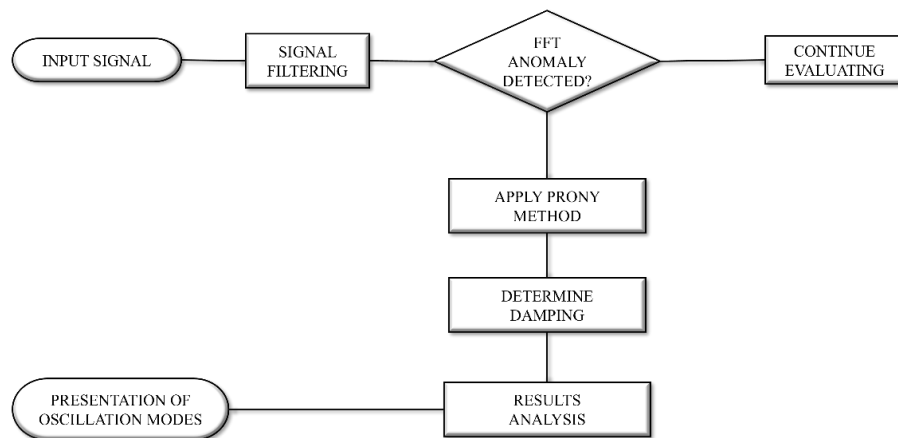


Fig. 2. Small signal stability analysis methodology.

The proposed program was evaluated to determine the reliability of its results. For this, comparisons were made between the results and the procedures carried out by other sources of consultation.

4 Results

The damping results presented are expressed positively for those damping applied to stable oscillation modes in the system while negatively when these dampings were applied to an unstable mode. The mentioned above is to facilitate the understanding of these results. Eight scenarios of small signal oscillations are presented, corresponding to frequency periods of hours at different system operation times.

The systems evaluated are the Dominican Republic's electrical system and the Peru's electrical system. Table 2 summarizes the energy matrix of these systems based on renewable and conventional energy sources.

8

Table 2. General characteristics of energy matrix by country.

Installed Capacity	Peru (MW)	Dominican Republic (MW)
Renewable Energy Sources	6,280	1,445.98
Conventional Energy Sources	9,062	3,629.40
Total	15,342	5,075.38

Scenario 1

The results obtained in this first scenario are presented in Table 3, in which we can see the predominance of oscillation modes due to the operation of the electrical system, which corresponds to oscillation modes at frequencies less than 0.08 Hz. In addition, 257 inter-area oscillation modes were presented at simulation time, as well as 37 local oscillation modes. These final oscillation modes in the grid quickly dampened when the system applied this transform.

Table 3. Scenario 1 Results.

Oscillation Modes	Quantity
System Operation	439
Interarea	257
Local	37

Scenario 2

In this scenario, 248 interarea oscillation modes were obtained in the system, and only 39 local oscillation modes, as shown in Table 4. For this test, oscillations with a maximum frequency of 1.12 Hz were obtained.

Table 4. Scenario 2 Results.

Oscillation Modes	Quantity
System Operation	323
Interarea	248
Local	37

Scenario 3

Table 5 presents the results produced by the program when evaluating the frequency oscillations of this scenario. In this, no small signal oscillations were obtained that generated instability in the system; however, prolonged stable oscillations occurred, such as oscillations, due to the modes of operation of the system.

Table 5. Scenario 3 Results.

Oscillation Modes	Quantity
System Operation	316
Interarea	259
Local	38

Scenario 4

In this scenario, an unstable system was simulated, so in the results presented in Table 6, The presence of an unstable oscillation mode in the network can be appreciated, which is enough to qualify this scenario as unstable. This unstable oscillation mode was presented in the system on the right side of the stability plane.

Table 6. Scenario 4 Results.

Oscillation Modes	Quantity
System Operation	732
Interarea	425
Local	67

Scenario 5

Frequency data were analyzed from 2:00 P.M. to 4:00 P.M. (see Table 7). 20% of local and interarea oscillation modes were detected compared to other modes. No small signal oscillations were detected in the system.

Table 7. Scenario 5 Results.

Oscillation Modes	Quantity
System Operation	974
Interarea	217
Local	32

Scenario 6

A random scenario was created to assess system instability (see Table 8). An unstable oscillation mode with negative damping was identified.

10

Table 8. Scenario 6 Results.

Mode	Frequency (Hz)	Deadening	Damping (%)
Mode 1	0.0321	0.121553	12.1553
Mode 2	0.0321	0.121553	12.1553
Mode 3	0.1333	0.407751	40.7751
Mode 4	0.0114	0.069258	6.9258
Mode 5	0.0022	-1	-100

Scenario 7

Frequency data from Peru's electricity system were analyzed (see Table 9). Nine local oscillation modes, 70 interarea oscillation modes, and 115 oscillation modes corresponding to the system's operation were detected. Most modes had a good level of damping, above 15%. In this scenario of the Peruvian system, no modes of unstable oscillation were detected.

Table 9. Scenario 7 Results.

Oscillation Modes	Quantity
System Operation	115
Interarea	70
Local	9

Scenario 8

Frequency data from Peru's electricity system were analyzed (see Table 10). Instability was detected in the system with an oscillation mode in the right half-plane. The maximum frequency was 1.49 Hz, and the minimum was 0.02 Hz. The damping in the system was stable. In this scenario, a small signal instability event occurred. However, it was a transient event, as the damping of this was quite good.

Table 10. Scenario 8 Results.

Oscillation Modes	Quantity
System Operation	30
Interarea	26
Local	1

5 Conclusion

The development of this project sought to verify the close relationship between the stability of small signals and the integration of renewable energy sources in a power system with a low proportion of these generation technologies in the matrix. However, the results obtained revealed a different scenario than expected.

It was possible to demonstrate that analyzing the stability of small signals in a power system with reduced penetration of renewable sources is a viable method to examine the system's behavior when these unconventional sources are in operation. Various tests were conducted using the available historical frequency data, and the results were favorable for the study. It was concluded that the low penetration of renewable sources in an electrical system does not generate worrisome small signal oscillations since the oscillation modes generated tend to be damped naturally and effectively by the power system.

It was determined that the electrical system damps small signal oscillations due to the low participation of renewable sources in the energy matrix. Conventional generators can absorb such oscillations in a small signal disturbance and safely maintain system stability.

Frequency analysis showed that the variability or intermittency of renewable energy sources in the case study does not cause significant variability in system frequency, which could lead to poorly damped or undamped oscillation. Therefore, it is unlikely that failures or blackouts will occur in the network due to these oscillations in this studied system. The abovementioned contrasts with the events that have occurred in recent years in the Dominican Republic's electrical system, where only one blackout has been recorded in a transmission line, demonstrating the system's ability to absorb small signal disturbances largely.

On the other hand, the Peruvian electricity system did present scenarios of small signal instability in it. However, Peru's electrical system can dampen these small signal oscillations; this was demonstrated in the scenarios evaluated in which most of the oscillations were damped stably. Therefore, it was determined that an electrical system could generate oscillations due to small signal instability by renewable sources as long as the installed capacity of this system is high, and the variations of this are considerably severe.

6 Acknowledgment

The authors acknowledge the support provided by the Thematic Network 723RT0150 "Red para la integración a gran escala de energías renovables en sistemas eléctricos (RIBIERSE-CYTED)" financed by the call for Thematic Networks of the CYTED (Ibero-American Program of Science and Technology for Development) for 2022.

12

References

1. A. Sajadi, S. Zhao, K. Clark, and K. A. Loparo, "Small-Signal Stability Analysis of Large-Scale Power Systems in Response to Variability of Offshore Wind Power Plants," *IEEE Syst J*, vol. 13, no. 3, pp. 3070–3079, Sep. 2019, doi: 10.1109/JSYST.2018.2885302.
2. A. U. Rahman, I. Syed, and M. Ullah, "Small-Signal Stability Criteria in AC Distribution Systems—A Review," *Electronics* 2019, Vol. 8, Page 216, vol. 8, no. 2, p. 216, Feb. 2019, doi: 10.3390/ELECTRONICS8020216.
3. M. B. Dastas and H. Song, "Renewable Energy Generation Assessment in Terms of Small-Signal Stability," *Sustainability* 2019, Vol. 11, Page 7079, Vol. 11, No. 24, p. 7079, Dec. 2019, Doi: 10.3390/SU11247079.
4. C. Canizares et al., "Benchmark Models for the Analysis and Control of Small-Signal Oscillatory Dynamics in Power Systems," *IEEE Transactions on Power Systems*, Vol. 32, no. 1, pp. 715–722, Jan. 2017, doi: 10.1109/TPWRS.2016.2561263.
5. A. Musengimana, H. Li, X. Zheng, and Y. Yu, "Small-Signal Model and Stability Control for Grid-Connected PV Inverter to a Weak Grid," *Energies* 2021, Vol. 14, Page 3907, vol. 14, no. 13, p. 3907, Jun. 2021, doi: 10.3390/EN14133907.
6. M. S. Soria C. and A. F. Tovar A., "Small signal stability evaluation by probabilistic modal analysis based on simulation and signal approaches.," 2019, Accessed: Jun. 28, 2023. [Online]. Available: <https://bibdigital.epn.edu.ec/handle/15000/24062>
7. Y. Li, L. Fu, Q. Li, W. Wang, Y. Jia, and Z. Y. Dong, "Small-signal modelling and stability analysis of grid-following and grid-forming inverters dominated power system," *Global Energy Interconnection*, vol. 6, no. 3, pp. 363–374, Jun. 2023, doi: 10.1016/J.GLOEI.2023.06.010.
8. R. I. Zúñiga Gajardo, "Technical Analysis of Regional Interconnections from a Stability Perspective," 2021, Accessed: Jun. 28, 2023. [Online]. Available: <https://repositorio.uchile.cl/handle/2250/182465>
9. M. A. Carreño Galeano, "Small signal stability of a power system with VSCs of grid-following and grid-forming types considering the VSM, droop control and VOC algorithms," 2022, Accessed: Apr. 08, 2023. [Online]. Available: <https://repositorio.uniandes.edu.co/handle/1992/58724>
10. P.M. Maykop, R. D. Yandry, and G. H. Ernesto, "Transient stability of small oscillations in electrical power systems. Devices used to improve it.," *CIPEL*, May 2018, Accessed: Mar. 19, 2023. [Online]. Available: https://www.researchgate.net/publication/331357789_Estabilidad_transitoria_de_pequeñas_oscilaciones_en_los_sistemas_eléctricos_de_potencia_Dispositivos_usados_para_mejorarla
11. R. E. Cubillo, "Determination of Oscillatory Modes Present in the Ecuadorian Electrical System through Statistical Techniques," *Technical Journal "Energy"*, vol. 13, no. 1, pp. 139-145 pp., Jan. 2017, doi: 10.37116/revistaenergia.v13.n1.2017.16.
12. D. J. Siles Granados, "Design and Adjustment of a Discrete Time Power System Stabilizer from Time-Domain Signals," University of Costa Rica, San Jose, Costa Rica, 2020, Accessed: Apr. 28, 2023. [Online]. Available: <https://www.kerwa.ucr.ac.cr/handle/10669/81867>
13. IEEE 421.5-1992 IEEE Recommended Practice for Excitation System Models for Power System Stability Studies. IEEE, 1992. Accessed: Mar. 19, 2023. [Online]. Available: <https://ieeexplore.ieee.org/document/182869>
14. E. F. Guanochanga Collaguazo and M. G. Ocaña Frutos, "Location of a sliding mode control and PSS's with the aim of damping electromechanical oscillations using the residue

- and fuzzy method," Jan. 2018, Accessed: Apr. 08, 2023. [Online]. Available: <https://bibdigital.epn.edu.ec/handle/15000/19083>
15. D. S. Zambrano Chicaiza and Espol, "Study of stability and reliability before the integration of distributed generation in the distribution network UN Milagro," 2022, Accessed: Jun. 28, 2023. [Online]. Available: <https://www.dspace.espol.edu.ec/handle/123456789/57026>
 16. S. Ando, "Frequency-Domain Prony Method for Autoregressive Model Identification and Sinusoidal Parameter Estimation," *IEEE Transactions on Signal Processing*, Vol. 68, pp. 3461–3470, 2020, doi: 10.1109/TSP.2020.2998929.
 17. C. A. Juárez and D. G. Colomé, "Estimation en línea de modos interarea using the Discrete Wavelet Transform and the Prony Analysis," *Proceedings of the 2018 IEEE 38th Central America and Panama Convention, CONCAPAN 2018*, Dec. 2018, doi: 10.1109/CONCAPAN.2018.8596557.
 18. F. J. Villalobos-Piña and R. Alvarez-Salas, "Robust algorithm for the diagnosis of electrical faults in the three-phase induction motor based on spectral tools and ondeletas.," *Ibero-American Journal of Automation and Industrial Informatics RIAI*, vol. 12, no. 3, pp. 292–303, Jul. 2015, doi: 10.1016/J.RIAI.2015.04.003.
 19. J. López Espejel, M. S. Yahaya Alassan, E. M. Chouham, W. Dahhane, and E. H. Ettifouri, "A comprehensive review of State-of-The-Art methods for Java code generation from Natural Language Text," *Natural Language Processing Journal*, vol. 3, p. 100013, Jun. 2023, doi: 10.1016/J.NLP.2023.100013.
 20. I. Abdulrahman, "Matlab-based programs for power system dynamic analysis," *IEEE Open Access Journal of Power and Energy*, Vol. 7, No. 1, pp. 59–69, 2020, DOI: 10.1109/OAJPE.2019.2954205.
 21. F. Zonzini, M. Mohammadgholiha, and L. De Marchi, "A Combination of Chirp Spread Spectrum and Frequency Hopping for Guided Waves-based Digital Data Communication with Frequency Steerable Acoustic Transducers," *IEEE International Ultrasonics Symposium, IUS*, vol. 2022-October, 2022, doi: 10.1109/IUS54386.2022.9958662.
 22. J. Lin, L. Ma, and Y. Yao, "A Fourier Domain Training Framework for Convolutional Neural Networks Based on the Fourier Domain Pyramid Pooling Method and Fourier Domain Exponential Linear Unit," *IEEE Access*, Vol. 7, pp. 116612–116631, 2019, doi: 10.1109/ACCESS.2019.2936591.
 23. O. V. Prokhorova and S. P. Orlov, "Parametric optimization of control systems by the Etlon Control System assign using the root locus method or the poles and zeros location," *Proceedings of 2017 IEEE 2nd International Conference on Control in Technical Systems, CTS 2017*, pp. 16–19, Nov. 2017, doi: 10.1109/CTSUS.2017.8109476.
 24. Y. Su, C. Zeng, D. Kang, X. Wang, and H. Wang, "Analytic study on the poles and zeros for mechanical plants," *2017 3rd IEEE International Conference on Computer and Communications, ICC 2017*, vol. 2018-January, pp. 2940–2944, Mar. 2018, doi: 10.1109/COMPCOMM.2017.8323070.
 25. Z. L. Wang, X. O. Song, and X. R. Wang, "Spectrum sensing detection algorithm based on eigenvalue variance," *Proceedings of 2019 IEEE 8th Joint International Information Technology and Artificial Intelligence Conference, ITAIC 2019*, pp. 1656–1659, May 2019, doi: 10.1109/ITAIC.2019.8785807.
 26. P. Jorkowski and R. Schuhmann, "Mode tracking for parametrized eigenvalue problems in computational electromagnetics," *2018 International Applied Computational Electromagnetics Society Symposium in Denver, ACES-Denver 2018*, May 2018, doi: 10.23919/ROPACES.2018.8364147.

14

27. C. Li, G. Li, C. Wang, and Z. Du, "Eigenvalue Sensitivity and Eigenvalue Tracing of Power Systems with Inclusion of Time Delays," *IEEE Transactions on Power Systems*, Vol. 33, No. 4, pp. 3711–3719, Jul. 2018, doi: 10.1109/TPWRS.2017.2787713.
28. X. Cun, X. Chen, G. Geng, and Q. Jiang, "Online Tracking of Small-Signal Stability Rightmost Eigenvalue Based on Reference Point," *IEEE Access*, 2023, doi: 10.1109/ACCESS.2023.3267802.
29. International Renewable Energy Agency (2017) *Perspectivas de Energías Renovables: República Dominicana, REmap 2030*. Abu Dhabi

Escenario de generación fotovoltaica de la isla de Mallorca para el periodo 2022-2035

Jacinto Vidal-Noguera, Pere Antoni Bibiloni-Mulet, Iván Alonso de Miguel, Víctor Martínez-Moll, Andreu Moià-Pol y Vicente José Canals Guinand

Universidad de las Islas Baleares, Departamento de Ingeniería Industrial y Construcción,
Palma, Ctra. Valldemossa km 7.5, Campus UIB, Islas Baleares ES07122, España
jacinto.vidal@uib.cat

Abstract. El cambio y la crisis climática asociada, impulsados principalmente por las emisiones de gases de efecto invernadero (GEI) de origen humano, representan un desafío global innegable. Este estudio presenta una herramienta de simulación numérica desarrollada en Python para estimar la generación de energía renovable, con un enfoque particular en la generación fotovoltaica. La herramienta utiliza datos de entrada, condiciones de contorno, datos de instalaciones fotovoltaicas y mapas de potencial fotovoltaico para generar instalaciones aleatorias con la finalidad de simular la generación de un escenario de despliegue renovable. El estudio se centra en un caso práctico en Mallorca, España, y proyecta el crecimiento de la generación fotovoltaica en la isla. Los resultados indican un crecimiento constante y la posibilidad de excedentes a partir del 2028, pero analizándolo de forma mensual no aparecerán hasta el 2029. Si se analiza de forma horaria, se puede ver que a partir del 2030 en los meses de menos generación y en el rango de -3σ existirán excedentes permitiendo llegar a la conclusión de cuál es el límite de potencia instalada fotovoltaica sin complementarlo con otras tecnologías. Además, se diagnostican posibles problemáticas como la gestión de la red eléctrica y la importancia de la gestión de los excedentes. Determinando la necesidad de estrategias efectivas de gestión de excedentes y la complementación con tecnologías, como la acumulación, para lograr una transición exitosa. Llegando a la conclusión de que esta herramienta permite ayudar a la planificación de políticas energéticas sostenibles y la toma de decisiones tanto a corto como a largo plazo.

Keywords: Fotovoltaica, Simulación dinámica, energías renovables, diagnóstico.

1 Introduction

El calentamiento global y el consecuente Cambio Climático (CC) son ambos producidos en su mayor parte por la actividad humana, la principal fuente de emisiones de Gases de Efecto Invernadero (GEI)[1], [2]. La extracción, el transporte, la conversión y, en particular, la combustión de los combustibles fósiles tiene varios impactos negativos en el medio ambiente e influyen directamente en la economía y las sociedades

2

alrededor del mundo. La crisis climática se ha convertido en un hecho global innegable, como lo pone de manifiesto el aumento de la frecuencia de las olas de calor y los incendios forestales y el derretimiento de glaciares y polos. El objetivo de mitigación del cambio climático más ambicioso se estableció en el Acuerdo de París de 2015[3], en el que las Naciones Unidas acordaron los objetivos para mantener un aumento de la temperatura media mundial muy por debajo de los 2°C por encima de los niveles preindustriales.

La integración de las fuentes de energía renovables (RES) en el sistema eléctrico se ha convertido en un tema relevante en Europa, ya que se considera una de las soluciones para disminuir las emisiones de gases de efecto invernadero (GEI) y aumentar la seguridad energética [4]. Resulta de gran importancia realizar un análisis sobre la futura producción de energía de las RES. Primeramente, por tener una previsión de la cantidad de energía generada en un futuro y poder estimar si se cumplen los objetivos de gobierno. En segundo lugar, para poder estimar como se integrarán estas tecnologías en el Mix Energético y como pueden afectar el incremento de estas. Finalmente, poder prever el uso de tecnologías necesarias a lo largo del tiempo para poder realizar la descarbonización del sistema energético.

En este artículo, se aborda el funcionamiento de una herramienta de simulación numérica diseñada específicamente para estimar la generación de Energías Renovables (RES) en un determinado territorio. Esta herramienta se ha desarrollado con la capacidad de analizar diversos escenarios de despliegue de RES en una región dada, habiéndose enfocado en la generación fotovoltaica en su primera versión. Los datos obtenidos mediante esta herramienta están destinados a servir de base para el desarrollo de estudios de despliegue de RES en cualquier ubicación, utilizando un conjunto de datos de entrada predefinidos. La herramienta numérica se ha desarrollado mediante el lenguaje de programación Python.

Adicionalmente, la herramienta propuesta incorpora como motor de simulación de la generación fotovoltaica PVGIS Online Tool [5] en base a la información del territorio y de las instalaciones. Como datos de entrada la herramienta admite ficheros de información geográfica (GIS) para introducir la delimitación del territorio a analizar, patrones de crecimiento de las energías renovables, así como información relativa a zonas priorización de para el despliegue de renovables.

Una vez que los datos aportados son procesados, se obtiene información detallada sobre la generación de Energías Renovables a nivel horario, mensual y anual en el territorio específico en consideración. Esto permite evaluar diversos escenarios de generación, cuantificar la producción de energía dentro del territorio, identificar posibles desafíos y realizar proyecciones acerca de la producción de RES en el futuro. Todo ello, considerando tanto la ubicación de las instalaciones como el área que ocupan y su potencial crecimiento.

El presente trabajo está organizado en tres secciones, además de la Introducción. En primer lugar, se detalla la metodología propuesta para recopilar, simular y analizar los resultados. La sección posterior se enfoca en un caso de estudio con la presentación de datos. Finalmente, en la última sección se ofrecen las conclusiones del trabajo.

2 Metodología

La metodología sobre la que se fundamenta el desarrollo de la herramienta numérica se basa en disponer de un conjunto de datos de entrada, obtenidos de fuentes abiertas. Primeramente, deben recopilarse los datos históricos de la generación horaria renovable de al menos los últimos 10 años, desglosados por tecnologías, que seguidamente son filtrados y acondicionados. Cabe mencionar que este trabajo se ha centrado en los datos de generación fotovoltaica. A continuación, debe introducirse un conjunto de patrones mediante el cual modelar el despliegue de las diferentes fuentes renovables en un determinado territorio. Estos patrones pueden obtenerse según la tendencia histórica del despliegue de las diferentes fuentes renovables en una determinada región, con sus correspondientes patrones de despliegue (distribución de instalaciones por potencia pico instalada, etc.), o por el contrario se pueden corresponder con los objetivos de crecimiento propuestos por las diferentes administraciones. De acuerdo con estos patrones de despliegue, la herramienta numérica despliega de manera aleatoria instalaciones/plantas RES (virtuales) en diferentes ubicaciones del territorio, reproduciendo los patrones anuales de despliegue previamente establecidos. Seguidamente la herramienta se encargará para cada planta virtual desplegada de estimar su generación horaria, en función de su ubicación y características de la instalación previamente fijadas, para un periodo de 10 años. Estos datos de generación se obtienen en base a series históricas de radiación “PVGIS-SARAH2” para 10 años diferentes. Los datos de generación obtenidos de cada una de las plantas se tratan conjuntamente para evaluar los datos de generación globales. Finalmente, la herramienta procesa los datos de generación para graficar los diferentes resultados obtenidos. En los siguientes subapartados se detalla el funcionamiento de los diferentes bloques de la metodología propuesta, **Fig. 1**.

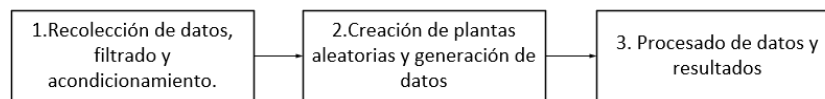


Fig. 1. Esquema de resolución de la metodología propuesta.

2.1 Recopilación de datos, filtrado y acondicionamiento

Este primer bloque se encarga de la recopilación, filtrado y acondicionamiento de todos los datos de entrada que describen de manera precisa el territorio que se pretende modelar, de modo que se ajusten de manera adecuada al sistema en cuestión. A continuación, se detalla el conjunto de parámetros de entrada:

4

- **Tendencias del despliegue de fuentes renovables.** Con el objetivo de representar el desarrollo de las energías renovables a lo largo de los años, se requiere de unas tablas con los datos del número de instalaciones/plantas de RES delegadas por tecnologías y año, así como, un diagrama de frecuencia de las potencias de RES instaladas por tecnología. Estos datos pueden ser obtenidos de fuentes históricas o generados sintéticamente.

A partir de los datos anteriores, la herramienta ajusta un conjunto de funciones de probabilidad. El proceso empleado para crear estas funciones de probabilidad se basa en una función de kernel normalizada (KDE) [6].

$$\hat{f}(x) = \frac{1}{n \cdot h} \sum_{i=1}^N k\left(\frac{x-x_i}{h}\right) \quad (1)$$

Donde en la expresión (1):

- **h**, es el ancho de banda
- **n** es el número de observaciones
- **k()** la función de kernel por defecto es una gaussiana, que resigue la expresión (2) [7]:

$$f(x) = \frac{1}{\sigma\sqrt{2\pi}} e^{-\frac{x^2}{2}}, x \in (-\infty, \infty) \quad (2)$$

- **Información geográfica del territorio.**

Para la definición del contorno geográfico o territorio a analizar se hace uso de archivos georreferenciados en formato GeoTIFF. Estos archivos permiten la representación y almacenamiento de datos geoespaciales. Los ficheros con los contornos a analizar pueden incluir o no información acerca de las zonas de aptitud relativa al despliegue de RES, según sea la disponibilidad de esta. Al importar un fichero GeoTIFF, se realiza la discretización píxel a píxel, creándose una matriz en la que cada celda tiene asignada una localización geográfica (coordenadas de latitud y longitud). El proceso descrito anteriormente se presenta de forma gráfica en la **Fig. 2**.

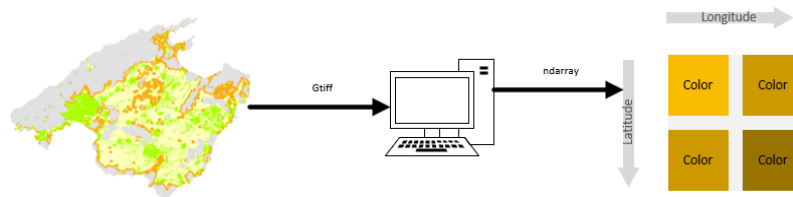


Fig. 2. Conversión de un fichero GeoTIFF en una matriz de datos.

- **Obtención de la base de datos de generación RES con la API de PVGIS.**

Una vez, definido el contorno del territorio sobre el que se pretende analizar el potencial despliegue de RES, se obtiene, para el conjunto de coordenadas englobadas en dicho contorno la generación horaria de una planta de 1 kW_p (referencia) para un periodo de 10 años. una base de datos de generación fotovoltaica para todas localizaciones del territorio. Para ello, se ha hecho uso de la API de PVGIS descargándose los datos históricos horarios correspondientes a cada localización geográfica. El procedimiento seguido se presenta de forma resumida en la **Fig. 3**

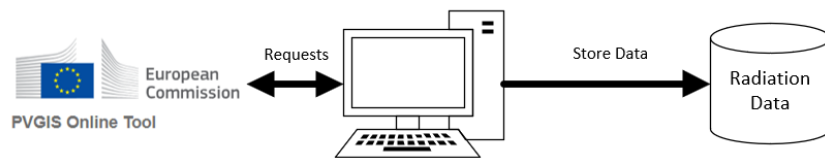


Fig. 3. Procedimiento de solicitud en la herramienta PVGIS online Tool.

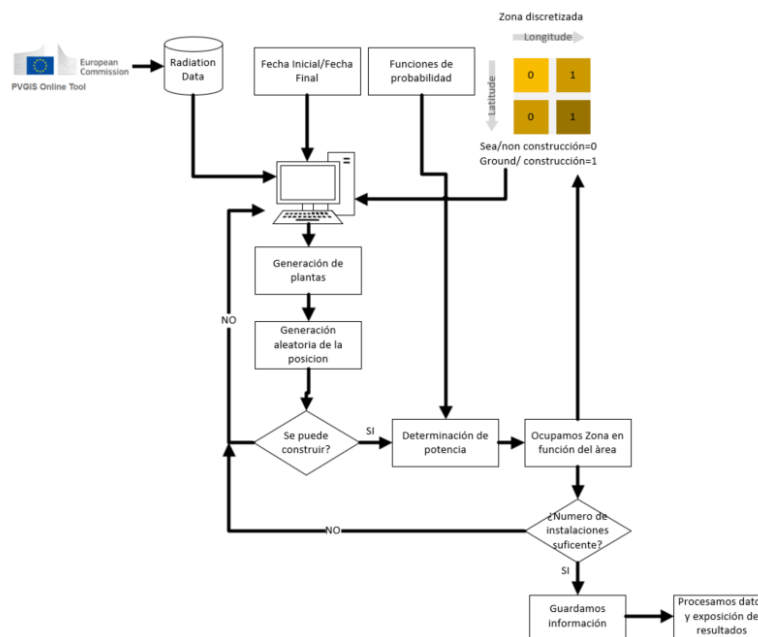


Fig. 4. Esquema reseguído por la herramienta realizada.

6

2.2 Escenarios de la generación de RES y presentación de los resultados

Una vez se han introducido el conjunto de datos presentados anteriormente, la herramienta numérica procede a la evaluación del escenario de despliegue de RES para un periodo (Fecha inicial / fecha final) a elegir por el usuario. El procedimiento seguido para la obtención de cada uno de estos escenarios, en base a los patrones de despliegue preestablecidos, se presenta en la Fig. 4.

El procedimiento desarrollado consiste en generar un conjunto de localizaciones aleatorias donde se ubicarán las potenciales plantas/instalaciones de RES, tantas como para año establezca el patrón de despliegue prefijado. Seguidamente, en base a los patrones de aptitud solar, si estos se han definido, se debe evaluar en función de su ubicación si la planta o instalación es viable o no. En el supuesto que esta no fuere viable, se repite el procedimiento anterior para para una nueva ubicación. En caso de que la ubicación de la planta fuere apta, se determina aleatoriamente una potencia instalada para ésta, según el patrón de distribución de potencias establecido, y mediante una relación potencia/área se evaluará el área que esta potencialmente ocupará. El área ocupada por la planta se indica en la matriz geolocalizada, a fin de que ninguna otra planta pueda desplegarse en la misma ubicación. Una vez se hayan generado el conjunto de instalaciones para el periodo a analizar, se procede a tratar el conjunto de datos de la generación horaria para el periodo a analizar.

Num.Plant	Nominal Power[kW]
1.0	1000.0
2.0	2277.0
3.0	1485.0
4.0	2500.0
5.0	1383.0
6.0	2673.0
7.0	1600.0
8.0	2970.0
9.0	990.0
10.0	1200.0
11.0	2178.0
12.0	1980.0
13.0	2970.0
14.0	2277.0
15.0	1200.0
16.0	2000.0
17.0	2100.0
18.0	2178.0
19.0	2772.0
20.0	2297.7
21.0	1500.0

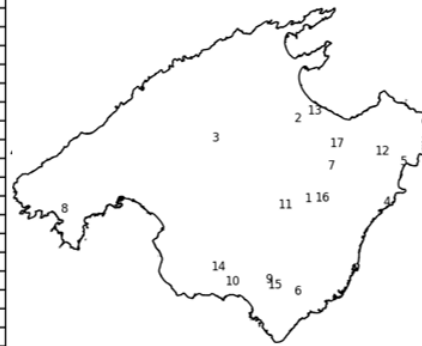


Fig. 5. Ubicación y potencia instalada de las grandes plantas fotovoltaicas en la isla de Mallorca, España.

3 Caso Práctico

Para evaluar la eficacia de la herramienta numérica desarrollada, se ha decidido aplicarla en un escenario real, específicamente a la isla Mallorca, España. Es necesario mencionar que en la isla de Mallorca no hay un gran potencial eólico, salvo en zonas protegidas, no existiendo ningún parque eólico en la isla. Por su parte, el despliegue de

aerogeneradores de menor potencia es totalmente residual. A raíz de tal circunstancia las diferentes administraciones regionales han optado por la energía fotovoltaica como fuente principal de RES para la descarbonización de la isla. Esto explica que en este trabajo se haya decidido prescindir de la generación eólica, centrándose únicamente en la generación fotovoltaica.

A fin de plantear un escenario de despliegue potencial de la generación renovable en esta región, se ha optado por modelar las tendencias históricas (número y potencias instaladas) del despliegue de las diferentes soluciones fotovoltaicas (autoconsumo y grandes parques) [10] en dicho territorio, con el fin de evaluar si los objetivos regionales de despliegue de generación renovable en los horizontes de 2030 y 2035 son alcanzables.

Para ello, como punto de partida se ha tomado el parque de generación eléctrica fotovoltaica preexistente, así como el conjunto de las instalaciones de autoconsumo identificadas por las autoridades regionales. En la actualidad, en este territorio se encuentran en funcionamiento un total de 21 grandes plantas fotovoltaicas ($P > 100\text{kW}$) con una potencia instalada combinada de 62MW_e , como se muestra en la **Fig. 5**. Cabe señalar que la administración regional distingue entre las instalaciones fotovoltaicas con potencia instalada superior a los 100kW [8] y las instalaciones de autoconsumo fotovoltaico. A finales de 2022, en Mallorca se contabilizaron unas 7,900 instalaciones de autoconsumo fotovoltaico con una potencia instalada de 67.98 MW [9].

Como ejemplo del procedimiento seguido, para establecer las tendencias actuales de despliegue del autoconsumo fotovoltaico se ha procedido a ajustar una función cuadrática a la evolución histórica del número de instalaciones de autoconsumo fotovoltaico exhibiendo un coeficiente de correlación de 0.996, como se muestra en la **Fig. 6**. Esta función se ha usado para establecer el número de instalaciones de autoconsumo fotovoltaico que se espera que se desplieguen en la isla, en el periodo comprendido entre los años 2023 y 2035.

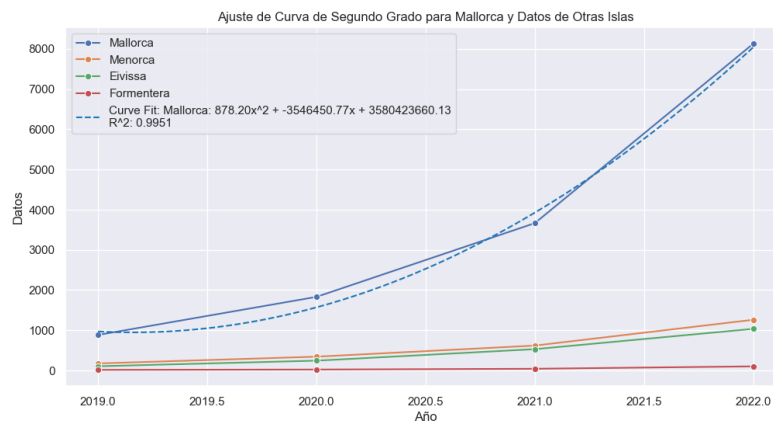


Fig. 6. Histórico de autoconsumos en la Islas Baleares.

8

Una vez introducidos los datos iniciales relativos al escenario de despliegue y a los datos históricos de generación fotovoltaica en la isla de Mallorca, la herramienta numérica se ha encargado de generar aleatoriamente el conjunto necesario de instalaciones de generación fotovoltaica (parques y autoconsumos) para replicar la tendencia actual de despliegue, en el periodo comprendido entre los años 2023 y 2034 (2035). Todo ello, en base al mapa de aptitud fotovoltaica georreferenciado publicado por el gobierno regional [8], **Fig. 7**. Finalmente, mediante este mapa se delimita el territorio a analizar y se fijan las zonas de exclusión, de baja, media y alta aptitud fotovoltaica que sirve de base para establecer la ocupación de las plantas/instalaciones fotovoltaicas.

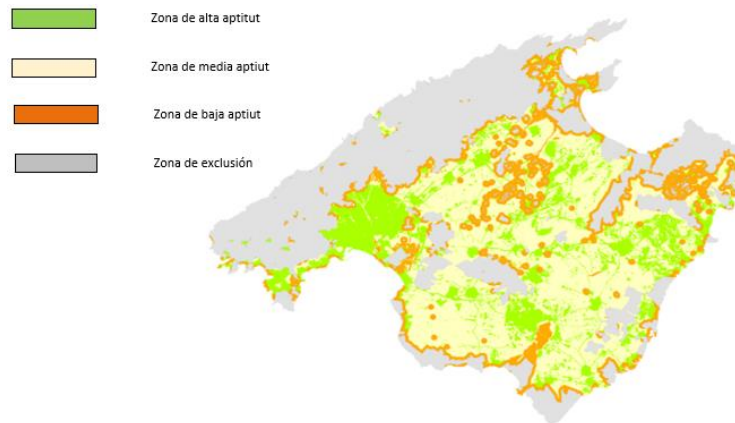


Fig. 7. Mapa de aptitud fotovoltaica de Mallorca publicado por el Gobierno autonómico de las Islas Baleares (GOIB) [8].

4 Análisis y discusión de los resultados

En esta sección se presentan los resultados obtenidos con la herramienta numérica para el escenario de generación renovable presentado en la sección anterior. El análisis de los resultados se ha realizado para diferentes horizontes. De esta manera se han abordado la evaluación anual, las generaciones mensuales y las curvas de generación diarias.

4.1 Análisis de los resultados de generación anual

Los resultados de la generación acumulada anual permiten proyectar la capacidad de generación fotovoltaica en la isla de Mallorca para el periodo comprendido entre el año 2025 y el año 2030, en base a las tendencias históricas de despliegue de instalaciones fotovoltaicas.

Referente a la potencia instalada, según los resultados aportados por la herramienta, para el año 2025 se espera que la capacidad instalada alcance los 318 MW_e, de los cuales cerca de 60 MW_e corresponderían a grandes parques y 258 MW_e a instalaciones de autoconsumo fotovoltaico. Asimismo, para el año 2030 la potencia instalada en Mallorca se vería incrementada, alcanzando un total de 850 MW. Este fuerte aumento del autoconsumo fotovoltaico sigue la tendencia observada en los últimos años y refleja un crecimiento continuo en la infraestructura de generación eléctrica en la región que de seguir con la actual tendencia alcanzaría los 25 GW_e instalados a principios del año 2035.

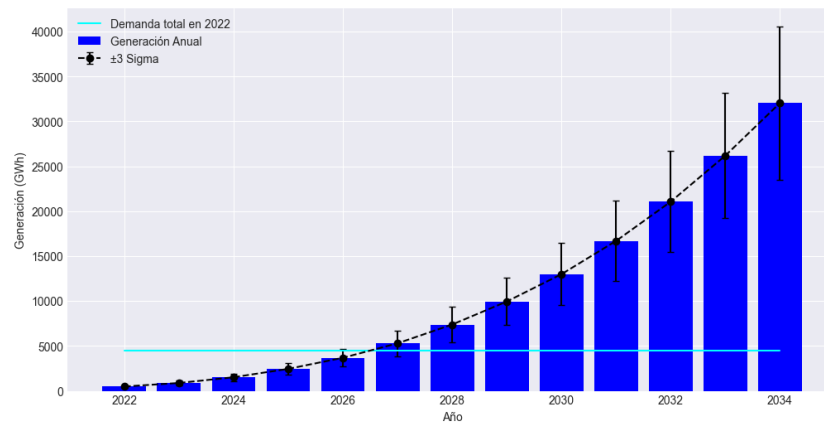


Fig. 8. Generación fotovoltaica anual para la isla de Mallorca, en base al escenario propuesto.

La generación eléctrica agregada del conjunto de las plantas simuladas se presenta en la **Fig. 8**. En dicha figura se ha incluido la variabilidad en la generación ($\pm 3\sigma$) anual obtenida del conjunto de las 10 simulaciones anuales realizadas para diferentes datos históricos de radicación. A su vez, en la figura **Fig. 8** se ha incorporado mediante una línea azul claro la demanda eléctrica anual de la isla de Mallorca del año 2022, con el propósito de establecer una referencia del año a partir del cual se podrían comenzar a registrar excedentes de energía netos en el sistema eléctrico. En base a los resultados obtenidos en este escenario, los excedentes energéticos podrían empezar a manifestarse a partir del año 2026. Pero no sería hasta el año 2028, cuando claramente el intervalo -3σ la generación fotovoltaica anual se situará claramente por encima de la demanda.

4.2 Análisis de los resultados de generación mensual

Si bien pueden darse excedentes a nivel anual a partir del año 2026, la producción fotovoltaica varía inexorablemente a lo largo de los meses del año en función de la variación de las horas solares. Por ello, es necesario un análisis detallado de la generación fotovoltaica agregada mensualmente para determinar los periodos anuales en los que se dispondría de excedentes netos de generación y cuantificar estos. En la **Fig. 9** se

10

presentan los resultados obtenidos de la generación mensual media para diferentes años frente a la demanda mensual del año 2022, usada como referencia. Concretamente, los resultados obtenidos muestran cómo la generación mensual media no sería superior a la demanda del año 2022 a lo largo de todos los meses hasta, al menos, el año 2029. Además, los resultados muestran como a partir de 2031 podría haber considerables excedentes a lo largo de todos los meses del año.

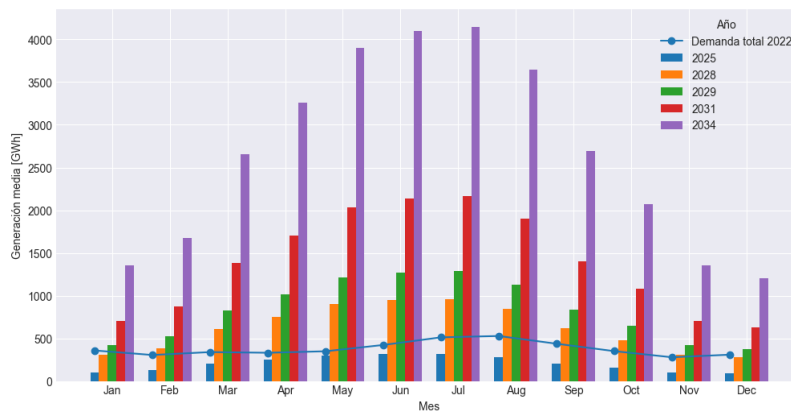


Fig. 9. Generación fotovoltaica mensual media para la isla de Mallorca, en base al escenario propuesto.

4.3 Análisis de los resultados de generación diaria

A continuación, se procede a analizar la generación fotovoltaica horaria en el periodo de menor radiación solar anual, mes de enero, para los años 2025 (Fig. 10) y 2030 (Fig. 11) con respecto a la demanda eléctrica horaria del año 2022.

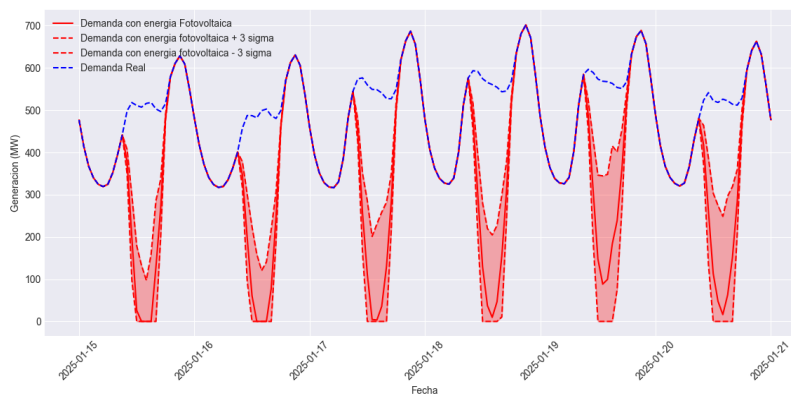


Fig. 10. Generación fotovoltaica diaria para la isla de Mallorca, enero del año 2025.

Los resultados presentados en la **Fig. 10** muestran como en las horas centrales del mes de enero de 2025, el periodo con menor número de horas solares, podrían darse excedentes netos de generación. Esto implica a su vez que, durante los meses centrales del año (junio y julio) los excedentes serían claramente notables. Esto conllevaría a la aparición de problemas severos en la gestión de las redes de distribución eléctrica para administrar los excedentes de la generación fotovoltaica. Por su parte, los resultados presentados en la **Fig. 11** muestran como en las horas centrales del mes de enero de 2030 existirían excedentes netos de generación fotovoltaica prácticamente en todas las horas solares del día.

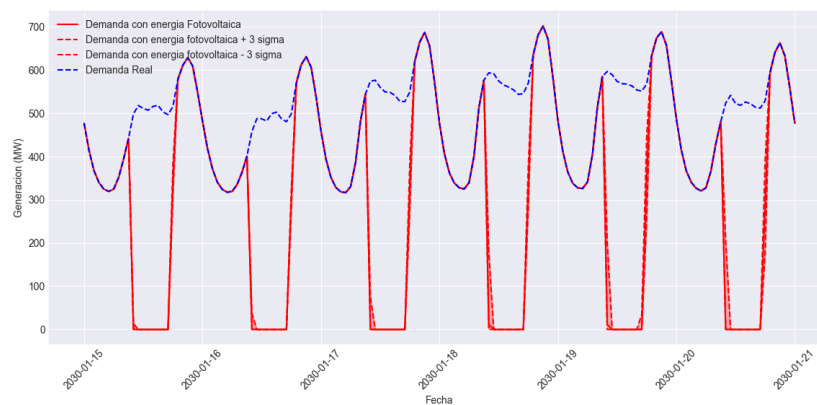


Fig. 11. Generación fotovoltaica diaria para la isla de Mallorca, año 2030.

4.4 Discusión de los resultados

Los resultados obtenidos muestran como los excedentes de generación fotovoltaica pueden representar un desafío significativo para la red eléctrica de la isla de Mallorca, en un horizonte relativamente cercano como es el año 2025. Estos resultados muestran la necesidad de abordar de manera satisfactoria tanto una gestión de estos excedentes como la expansión de la capacidad de la red, especialmente para poder evacuar la generación en las horas de mayor producción solar. Sin una correcta gestión de los excedentes, instalar más potencia renovable carecerá de sentido en pocos años dado que la nueva potencia renovable instalada no se traducirá en energía aprovechable para cubrir la demanda.

Para solventar este problema deberán desarrollarse, entre otros, nuevas estrategias de gestión del binomio generación-demanda consumo y el despliegue masivo de sistemas de acumulación de energía, como pueden ser los sistemas de baterías eléctricas (Li-FePO4...) y la producción de hidrogeno verde, por citar algunos. Se requerirá coordinación entre las diferentes administraciones públicas (Consellerias, Consejos Insulares,

12

Ayuntamientos, empresas públicas,) y las principales empresas para que haya una correcta gestión de la demanda y aprovechar al máximo la generación renovable.

Por las mencionadas razones, siempre que el problema de la gestión de excedentes no se haya solventado, la operación del sistema eléctrico únicamente en base a la generación fotovoltaica no es viable. En este escenario, la generación mediante esta tecnología deberá coexistir con otras tecnologías de respaldo, como pueden ser: los ciclos combinados, plantas de cogeneración, plantas de RSU, sistemas de acumulación distribuidos (realizando funciones de agregadores de la demanda), sistemas de bombeo y desalinización [11], etc.

5 Conclusiones

En este trabajo se ha presentado una herramienta numérica con la capacidad de estimar la generación fotovoltaica en un territorio en un conjunto de escenarios de despliegue de renovables. A su vez, la herramienta permite visualizar la evolución de la generación y comprender su crecimiento para un periodo dado. Más allá de esto, la herramienta puede ser utilizada para explorar diferentes escenarios y diagnosticar posibles problemáticas futuras, así como para cuantificar el impacto del despliegue de las RES en el mix energético. Este enfoque puede ser útil para desarrollar un plan estratégico de la expansión de la energía renovable y proporcionar una amplia gama de alternativas para modelar sistemas energéticos, proporcionando asesoramiento para técnicos y legisladores al formular políticas y tomar decisiones en el ámbito del cambio estructural de los sistemas energéticos, con el objetivo de alcanzar los objetivos de transición energética y descarbonización.

Finalmente, la herramienta se ha aplicado en el contexto de la isla de Mallorca con el propósito de evaluar la capacidad de generación de energía renovable (fotovoltaica) y su proyección futura. Los resultados obtenidos indican que en el caso de que la generación fotovoltaica siga con su actual tendencia de crecimiento, ésta superará la demanda eléctrica de referencia en el año 2028 (con un intervalo de 6σ). A su vez, la generación fotovoltaica en los meses invernales no cubrirá la demanda hasta el año 2029. Mientras que para el año 2025 los resultados muestran la existencia de excedentes de generación sólo durante las horas centrales del día, para el año 2030 los resultados muestran la existencia de excedentes incluso en el escenario más desfavorable (-3σ) durante los meses invernales. Este posible aumento en la generación fotovoltaica planteará desafíos muy serios en lo que a la gestión de la red eléctrica se refiere, hasta el punto de que instalar nueva potencia renovable no se traducirá en energía aprovechable para cubrir la demanda. Para afrontar este problema, deberán implementarse nuevas estrategias efectivas de gestión del binomio generación-demanda, incluyendo el despliegue masivo de sistemas de almacenamiento para aportar mayor flexibilidad al sistema eléctrico.

References

- [1] T. N. Veziroğlu and S. Şahin, “21st Century’s energy: Hydrogen energy system,” *Energy Convers Manag*, vol. 49, no. 7, pp. 1820–1831, 2008, doi: 10.1016/j.enconman.2007.08.015.
- [2] R. S. J. Tol, “The Economic Effects of Climate Change,” *Economic Perspectives*, vol. 23, no. 2, pp. 29–51, 2009.
- [3] C. A. Horowitz, “Paris Agreement,” *International Legal Materials*, vol. 55, no. 4, 2016, vol. 740, pp. 740–755, 2016, doi: 10.1017/s0020782900004253.
- [4] E. Union, “Directive 2009/28/EC of the european parliament and of the council of 23 April 2009 on the promotion of the use of energy from renewable sources and amending and subsequently repealing Directives 2001/77/EC and 2003/30/EC,” *Official Journal of the European Union*, pp. 16–62, 2009.
- [5] T. Huld, R. Müller, and A. Gambardella, “A new solar radiation database for estimating PV performance in Europe and Africa,” *Solar Energy*, vol. 86, no. 6, pp. 1803–1815, 2012, doi: 10.1016/j.solener.2012.03.006.
- [6] G. R. Terrell and D. W. Scott, “Variable Kernel Density Estimation,” 1992.
- [7] L. R. Ojeda, “Construcción de kernels y funciones de densidad de probabilidad.”
- [8] IDEIB, “Visor Ideib.” Accessed: Jan. 12, 2023. [Online]. Available: <https://ideib.caib.es/visor/>
- [9] “Presentació trimestral de dades de la transició energètica a les Illes Balears,” 2022.
- [10] GOIB, “Presentació trimestral de dades de la transició energètica a les Illes Balears,” 2022.
- [11] A. Moià-Pol, V. Canals, Víctor Martínez-Moll, Strategies for Electricity with Zero Carbon Emissions at 2050 using the water Management at Mallorca-Menorca Electric system. April 2017. Environmental Science Renewable energy & power quality journal

Electronic device for passive luminescence imaging acquisition: Proof of concept

Alberto Redondo Plaza¹ [0000-0002-2109-5614], José Ignacio Morales Aragón² [0000-0002-9163-9357], Víctor Alonso Gómez² [0000-0001-5107-4892], Ángel L. Zorita Lamadrid³ [0000-0001-7593-691X], Sara Gallardo Saavedra¹ [0000-0002-2834-5591], Héctor Felipe Mateo Romero⁴ [0000-0002-5569-3532], Mario Eduardo Carbone de la Rosa⁵ [0000-0002-6741-6145], Victor Ndeti Ngun-gu⁶ [0009-0001-5933-8482], Laura Gabriela Rojas Delgado¹ and Luis Hernández Callejo¹ [0000-0002-8822-2948]

¹ Departamento en Ingeniería Agrícola y Forestal, Universidad de Valladolid, Spain

² Departamento de Física Aplicada, Universidad de Valladolid, Spain

³ Departamento de Ingeniería Eléctrica, Universidad de Valladolid, Spain

⁴ Departamento de Física de la Materia Condensada, Universidad de Valladolid, Spain

⁵ Instituto de Geofísica, Universidad Nacional Autónoma de México, Mexico

⁶ Department of Electrical, Electronic & Computer Engineering, University of Pretoria, South Africa

albertogregorio.redondo@uva.es

joseignacio.morales@uva.es

victor.alonso.gomez@uva.es

zorita@uva.es

sara.gallardo.uva.es

hectorfelipe.mateo@uva.es

mecr@ier.unam.mx

lauragrojasd@gmail.com

u15292747@tuks.co.za

luis.hernandez.callejo@uva.es

Abstract: Photovoltaic power is an emerging technology that has experienced significant growth in recent years and presents immense potential in urban areas. Photovoltaic power plants require maintenance tasks that involve the inspection of photovoltaic modules using various techniques. Luminescence techniques allow the acquisition of images that capture the signals generated by the structures of solar cells, providing valuable information about the module's performance and potential faults. This article presents the validation of an electronic device designed to enhance and improve conventional techniques. Firstly, it enables the acquisition of luminescence images in high-irradiance environments through a lock-in technique. Additionally, the device, connected to the photovoltaic module within a string, allows for polarity shifts, enhancing current injection in the module and generating pulsed electroluminescence signals. Furthermore, the device can short-circuit or open-circuit the module, resulting in pulsed photoluminescence signals. This device has undergone validation through simulations and has been successfully constructed and tested in a real photovoltaic plant. Its unique selling point lies in its ability to operate without

2

the need for a separate power supply for current injection and its capability to acquire images while the power plant is in operation.

Keywords: Renewable energy; solar energy; photovoltaic; inspection techniques; luminescence; electroluminescence; photoluminescence

1 Introduction

Around 55% of the world's population lives in urban areas, and it is estimated that by 2050, 66% of the population will live in urban areas [1]. This gives rise to several challenges related to energy supply in cities. The cities of the future, smart cities, will have significant electricity requirements while aiming for sustainable growth and development [2]. Many cities are pursuing the implementation of strategies to transform themselves into sustainable environments from an energy perspective, aiming to achieve carbon neutrality. Over 700 cities around the world have implemented strategies to reduce their emissions levels and achieve a net-zero emissions scenario [3]. Moreover, smart cities imply an increase in electricity demand due to the deployment of electric cars, the implementation of electrolyzers, and the use of heat pumps.

With limited space, integrating renewable energy for electricity generation is a challenge. Photovoltaic technology presents significant potential for integration on the roofs and facades of buildings in urban environments. In fact, urban integrated photovoltaic systems have the ability to meet between 14.2% and 66% of a city's total electrical needs [4,5]. The cost of photovoltaic installations has been reduced by more than 60% since 2010 [6], leading to a substantial growth in total capacity. Therefore, it is expected that approximately 100 million households rely on rooftop solar PV by 2030 [7]. Finally, the integration of photovoltaic into urban environments brings other advantages such as not requiring land, reducing grid losses, and alleviating congestion issues in the distribution grid.

Among photovoltaic facilities, the operation and maintenance play a key role in maximizing energy yield, extending the useful life of the power plant, and minimizing the cost of energy [8]. Throughout the lifespan of a photovoltaic power plant, several maintenance tasks can be carried out, where inspection techniques play a crucial role. These techniques enable the characterization of photovoltaic modules and the detection of faults. Fault detection and characterization are essential in determining the degradation of the photovoltaic module, serving as a tool to support decision-making, such as module replacement. Furthermore, they allow determining if the degradation rate is lower than the manufacturer's guaranteed rate.

Visual inspection, current-voltage curve measurements, thermographic inspections, luminescence imaging, and the ultraviolet fluorescence method are some of the most widely used techniques for detecting faults in photovoltaic cells and modules [9,10]. Specifically, the luminescence technique is an imaging method based on capturing the electromagnetic emission generated by the crystalline silicon structures that constitute the solar cells. It should be noted that currently, approximately 95% of the manufactured modules are based on silicon technology [11]. The luminescence emission exhibits a peak wavelength at 1150 nm and can be captured primarily using silicon or

gallium arsenide (InGaAs) sensors [12]. Silicon sensors are inexpensive and offer high resolution. In contrast, InGaAs sensors are more expensive and have lower resolution. However, unlike silicon sensors, InGaAs sensors have a sensitivity that perfectly matches the luminescence wavelength, enabling faster acquisition.

Luminescence emission can be generated in two ways: through current injection, known as electroluminescence (EL), or through optical excitation using appropriate light, known as photoluminescence (PL). Although both EL imaging and PL imaging provide similar information, EL imaging provides more insight into the electrical performance of photovoltaic devices, while PL imaging offers more information about the quality of the silicon structure [13]. Consequently, the simultaneous acquisition of PL and EL images enables a complementary characterization of photovoltaic devices. Moreover, EL and PL imaging offer the ability to detect failures that do not affect the electrical or thermal performance of photovoltaic devices. These failures cannot be detected by other techniques such as current-voltage curve measurements or thermographic inspection.

However, EL and PL techniques have some drawbacks that limit their use in outdoor photovoltaic power plants. The main disadvantage is that the intensity of the luminescence signal is much lower than that of sunlight, which hinders the acquisition of imaging in high irradiance levels. Therefore, the conventional technique consists of injecting current into the modules during the night to achieve the electroluminescence effect in a dark environment. This requires the use of a power supply, which can be considered an additional disadvantage. The process of acquiring images during the night and the requirement of using a power supply has led to operational problems that limit the effectiveness of the technique. As a result, several approaches have been developed to address these issues.

First, a comprehensive characterization of photovoltaic modules can be achieved using a truck equipped with various measuring devices [14,15]. This includes a EL characterization conducted inside the truck, which provides a dark environment to avoid sunlight noise and enables measurements during the day. However, this solution requires the disassembly of the modules, which increases the acquisition time and the risk of module damage.

Another solution that addresses the disadvantage of requiring a power supply to achieve EL emission is the use of bidirectional inverters [16]. A bidirectional inverter is a power electronic device that can function as a conventional photovoltaic inverter, converting direct current into alternating current to inject it into the grid. Additionally, it can convert alternating current into direct current to inject it into the photovoltaic array, facilitating the EL effect.

In recent years, an advanced technique has been developed to enable luminescence imaging in high irradiance environments [17–23]. This technique is known as lock-in and involves capturing pairs of images. One image in the pair has a high luminescence emission, while the second image has a null luminescence emission. By subtracting these two images and repeating the process, it becomes possible to eliminate the noise generated by sunlight. This iterative process results in a high-quality luminescence picture that can be compared with conventional images.

4

This technique relies on generating a pulsed luminescence signal in the photovoltaic module. To achieve this, an electronic device is connected between the photovoltaic module and a power supply [17]. This device can switch the current injection state and is synchronized with an InGaAs camera to acquire the necessary EL paired images. Furthermore, this device facilitates the acquisition of PL images using sunlight as an excitation source. It has the capability to alternate the module's state between open circuit and short circuit. In the open circuit state, the PL emission is high, while in the short circuit state, the PL emission is null. By switching between these states, a pulsed PL emission is generated, enabling the acquisition of PL images.

This technique still requires the disconnection of the photovoltaic modules to attach the electronic device for generating the luminescence pulsed signal. However, there are other techniques that can solve this problem. Firstly, it is possible to use a control cell approach to achieve a pulsed PL signal [18]. By shading a control cell, all the solar cells in that substring will operate in open circuit state where the PL emission is high. When the control cell is not shaded, the photovoltaic cells operate at the maximum power point, resulting in almost null PL emission. Shading one solar cell would mean sacrificing 1/3 of the power output of the photovoltaic module. While this may not be an issue for facilities which use a central or string inverter, it can be problematic for microinverters. In the case of microinverters, due to the high percentage of power loss, the maximum power point algorithm takes around 6 seconds to reach the maximum power point from open circuit condition. Since multiple pairs of images are required to achieve good quality, the acquisition time becomes significantly longer, and issues related to changing weather conditions may arise. Therefore, a batch measurement approach has been proposed [20]. In this technique, the module's state is switched only once, from the maximum power point to open circuit. The final PL images are generated by taking the difference between the average of all maximum power point images and the average of all open circuit images. Additionally, this technique can be adapted to increase throughput by controlling one cell per substring in five modules of a large photovoltaic string [19]. Shading all the cells enhances the operation of the entire string at a higher voltage close to the open circuit state, resulting in high PL emission.

Indeed, the modulation of the PL signal using sunlight as an excitation source can also be achieved using the photovoltaic inverter [21,22]. The modulation is achieved by the inverter switching the state of the photovoltaic array between the maximum power point and open circuit conditions. However, it's important to note that the inverter typically requires around 6 seconds to reach the maximum power point from open circuit conditions. Therefore, a batch measurement approach is always required when using this method.

Another approach involves harnessing the energy generated by the solar module, storing it, and then injecting it back into the module to induce the EL effect [23]. An electronic device is used to store the energy in a capacitor and subsequently boost the voltage to inject current into the photovoltaic device. This method enables the creation of a pulsed EL signal, facilitating the implementation of a lock-in technique for EL imaging acquisition.

It's worth noting that many techniques utilize optical filters to reduce sunlight noise, thereby minimizing the number of image pairs required. In fact, optical filters can be used to capture PL pictures using sunlight as an excitation source at a constant operating point [24]. A primary filter allows PL transmission, facilitating the capture of images with a strong PL signal. On the other hand, a secondary filter blocks PL transmission, resulting in images with a low PL signal. By subtracting these two images and repeating the process, good-quality PL pictures can be acquired.

The present paper introduces a novel approach for the outdoor daylight acquisition of EL and PL images. This approach is based on an electronic device that is connected to the solar module in a photovoltaic string. The device can switch the polarity of the module in order to inject the current generated by the rest of the modules into the tested photovoltaic module. Moreover, the device can bypass the module and switch its operation point between open circuit and short circuit. This allows for the modulation of both EL and PL signals for the integration of a lock-in technique and the simultaneous acquisition of PL and EL images in a photovoltaic string under operation. The second section describes the materials and methodology, including the initial simulation of the electronic board followed by its construction. The third section presents both the simulation results and the electronic board's performance in a real power plant. Finally, the fourth section includes conclusions and outlines future work.

2 Materials and methods

The topology of the electronic device presented in this work has been designed and optimized using LTspice [25], a simulation software for analog electronic circuits. This software facilitated the simulation and validation of the device's topology. Subsequently, a prototype electronic board was manufactured to test the device in a photovoltaic plant.

2.1 Simulation process

The simulation process encompasses the modeling of a photovoltaic module string, along with the modeling of various electronic components that constitute the electronic device.

Simulation of the photovoltaic string

The simulation of the photovoltaic modules comprising the string has been performed using the one diode model [26]. The one diode model is utilized to simulate the electrical behavior of a photovoltaic device, incorporating a current source, a diode, and two resistances: series resistance (R_S) and shunt resistance (R_{SH}). The circuit configuration and the equation of the model are depicted in Fig. 1. The one diode model is governed by five parameters. It is important to note that the thermal voltage (V_T) is influenced by the operating temperature and two constants: the charge of an electron and the Boltzmann constant.

6

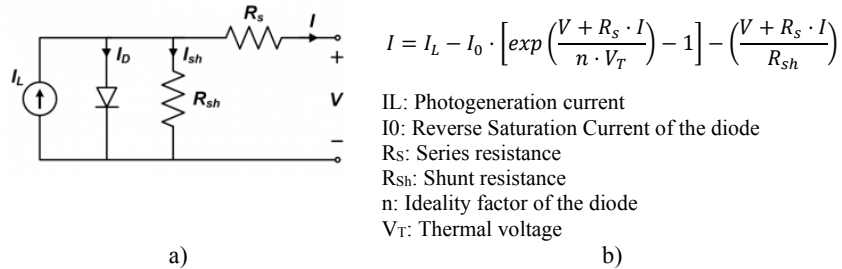


Fig. 1. One diode model circuit (a) and one diode model equation and parameters (b).

The luminescence emission can be interpreted as the current through the diode of the model (I_D), and it exponentially depends on the operational voltage of the circuit (V). Fig. 2 displays a typical current-voltage curve and the corresponding luminescence signal as a function of the operational voltage. As mentioned in the introduction, the luminescence emission is null in short circuit (SC) state and almost null at the maximum power point (MPP). The PL emission is found in the first quadrant of the curve, reaching its maximum at the open circuit (OC) point. Operating at a higher voltage than the open circuit voltage allows for working in the fourth quadrant, which leads to current injection (CI) and the EL effect, resulting in higher luminescence emission.

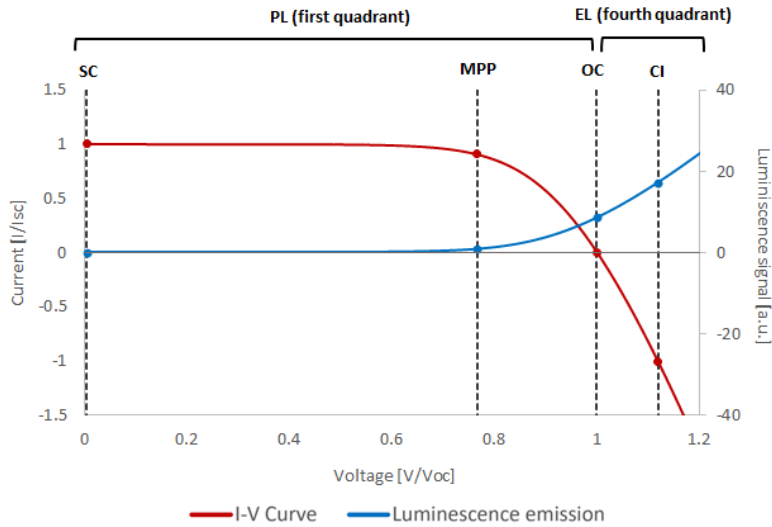


Fig. 2. Current-Voltage Curve and Luminescence emission at short circuit (SC), maximum power point (MPP), open circuit (OC) and current injection (CI).

During the simulation process, twelve one-diode models were connected in series to simulate a string. The characteristics of the one-diode model used to simulate the behavior of the photovoltaic modules are presented in Table 1. Note that the behavior of the inverter has not been simulated since the complexity of emulate the performance of the maximum power point tracking system. Therefore, the string has been simulated working in a constant voltage that corresponds with the maximum power point of the twelve modules string.

$V_{OC}(STC)$	45.6 V	Temperature	25 °C
$I_{SC}(STC)$	8.60 A	Irradiance	1,000 W/m ²
$\alpha(I_{SC})$	0.05 %	N° solar cells	72
$\beta(V_{OC})$	-0.34%	Ideality factor	1.8
R_S	0.36 Ω	R_{Sh}	72,000 Ω

Table 1. Parameters and weather condition for simulating a photovoltaic module.

Simulation of the electronic device

The topology of the electronic device is shown in Fig. 3. As can be seen, the device should be connected to the solar module that is intended to be measured. The power circuit consists of two diodes and three N-channel IGBTs (Insulated-Gate Bipolar Transistors). The performance of the IGBT has been simulated through an equivalent circuit, which is formed by one N-channel MOSFET (Metal-Oxide-Semiconductor Field-Effect Transistor) and one PNP transistor [27]. The IGBTs function as switches, and their proper control enables the change of the state of the tested module. The truth table shown in Fig. 3 displays the IGBTs that must be in conduction in order to open circuit the module, short circuit the module, achieve normal performance in maximum power point, and inject current into the module. The control of these states allows the generation of the required pulsed EL and PL signals for lock-in image acquisition.

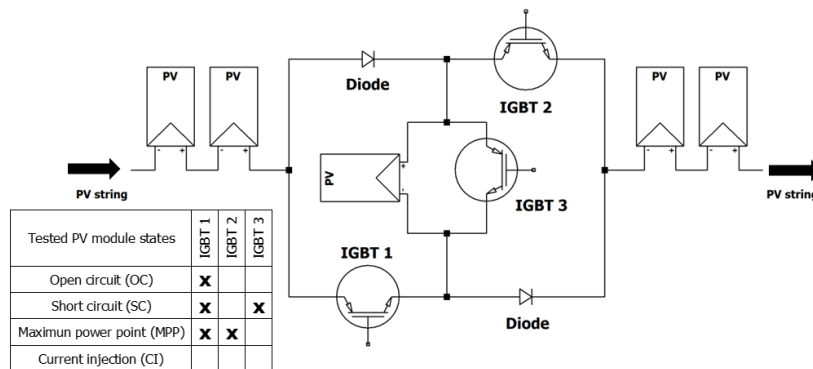


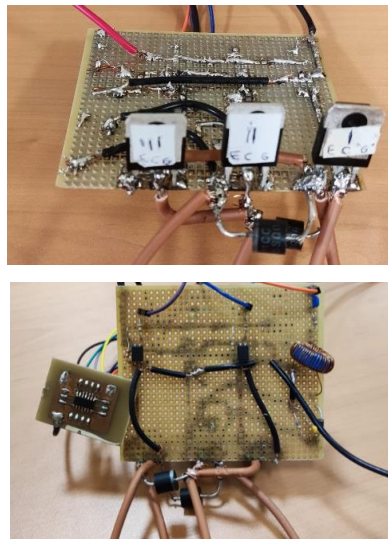
Fig. 3. Topology of the simulated electronic device.

8

2.2 Prototype implementation

An electronic board has been constructed to validate the proposed concept under real conditions within a photovoltaic power plant. Fig. 4 displays the final implemented electronic prototype along with the components used and their references.

The design of the control system presents some challenges because the emitters of the different IGBTs are located in different nodes. Consequently, IGBT 1 and IGBT 2 are controlled using optocouplers and an external 12 V supply, while IGBT 3, situated with its emitter in a separate node, is directly controlled by the microcontroller through an isolation transformer, ensuring sufficient voltage between the gate and the emitter. The microcontroller has been programmed to receive four commands via its serial port, with each command corresponding to one of the four states mentioned earlier. The electronic board has undergone testing in a real photovoltaic power plant comprising 10 modules (V_{OC} : 40V and I_{SC} : 5A) connected in series. These solar modules form a string that connects to a solar inverter.



Power circuit	
×3	IGBT (FGA25N120)
×2	Diode (15SQ045)
Control circuit	
×1	Microcontroller (PIC 16F1615)
×2	Optocoupler (SFH610-2)
×1	Diode (1N4936-T)
×2	Capacitors (0.1 uF, 10 uF)
×6	Resistors (150, 470, 4.7k, 46k Ω)
×1	Toroidal core

Fig. 4. Electronic circuit board and components summary.

3 Results and discussion

3.1 Simulation validation

The electronic device has been simulated using three voltage pulsed signals to control the three IGBTs of the device. The simulation process demonstrates that its topology

allows for an alternation between the states required for EL and PL acquisition using a lock-in technique.

On the one hand, Fig. 5 displays the current flowing through the tested module in a configuration for lock-in EL imaging acquisition. It is evident how the current cyclically changes between the current at the maximum power point (during normal operation with almost no luminescence signal) and a negative current that enables current injection and EL effect. Regarding the behaviour of the photovoltaic string, it is important to note that there is a voltage drop that is inversely proportional to the number of modules in the string. Additionally, a slight decrease in the string current is observed due to the modification of the string's IV curve. This simulation indicates that the device allows for the integration of an EL lock-in technique under operational conditions.

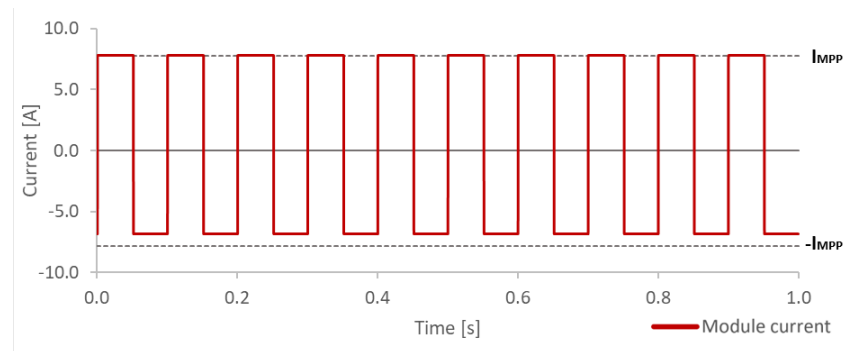


Fig. 5. Simulated modulation between current injection and normal module operation for EL pulsed signal.

On the other hand, Fig. 6 illustrates the voltage profile of the tested module in a configuration designed for PL lock-in imaging acquisition. The graph shows the voltage transition between the open circuit voltage, where the PL emission is high, and the short circuit state with zero voltage, where the PL emission is null. During the measurement process, the behavior of the photovoltaic string remains unaltered as the device allows for bypassing the tested solar module. This simulation demonstrates that the device enables the integration of a PL lock-in technique under operational conditions.

10

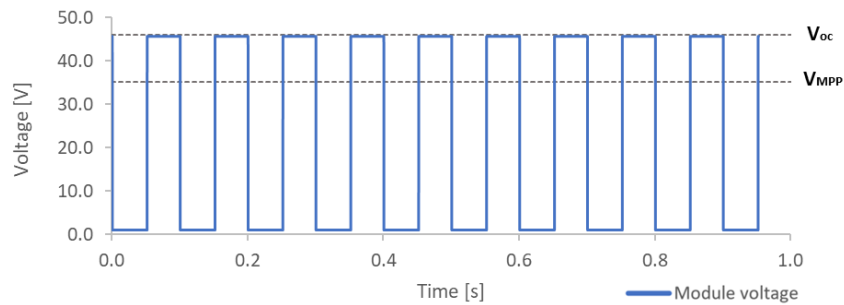


Fig. 6. Simulated modulation between open circuit module and short circuit module for PL pulsed signal.

3.2 Prototype testing

As previously mentioned, the developed electronic board has been tested in a real photovoltaic facility. As can be seen in Fig. 7 and Fig. 8, real electrical measurements in the tested solar module show that the electronic board is capable of generating modulation between current injection and normal operation, as well as modulation between open circuit and short circuit, respectively. This results in a pulsed signal for both PL and EL, which can be used for high-irradiance luminescence imaging acquisition.

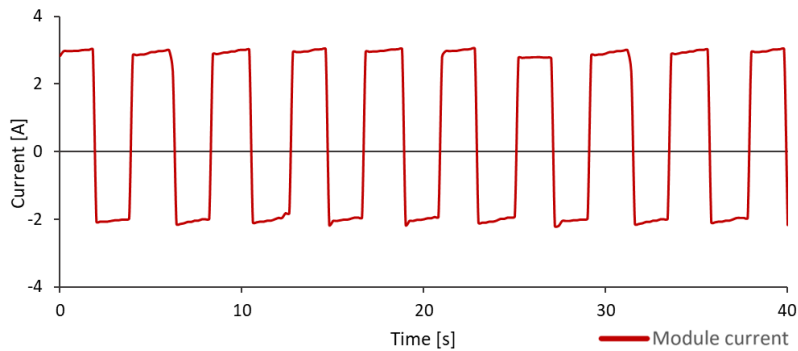


Fig. 7. Modulation between current injection and normal module operation in a real photovoltaic module.

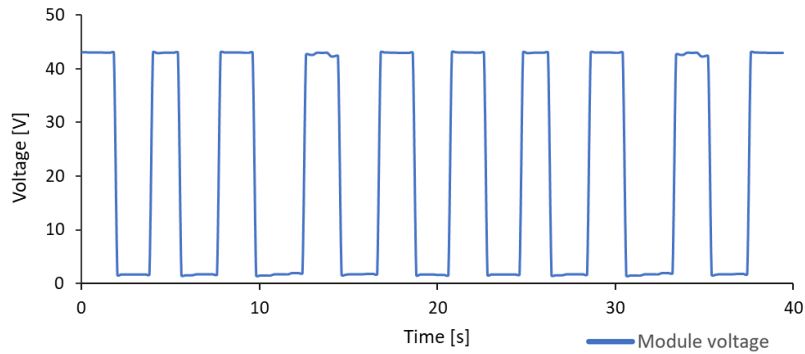


Fig. 8. Modulation between open circuit module and short circuit in a real photovoltaic module.

Note that the modulation was generated while the solar string was connected to the solar inverter. Therefore, the modulation does not interrupt the energy generation in the string, which is highly desirable when performing any kind of inspection technique in a photovoltaic plant.

During the modulation between normal operation and current injection, a voltage drop has been observed in the string, as previously shown in simulations. This voltage drop is inversely proportional to the number of modules that make up the string. Therefore, in conventional photovoltaic strings with more than 8 to 10 modules, the voltage drop is low, which allows the maximum power point system to continue working and consequently enables power generation during the modulation. On the other hand, the voltage remains constant during the modulation between open circuit and short circuit since the tested module is bypassed. Therefore, this modulation does not interrupt the current generation, as the previous case.

4 Conclusions and future work

This work presents the validation of a novel electronic board designed for luminescence imaging acquisition under high-irradiance conditions. The device is capable of generating a pulsed EL or PL signal, which is essential for high-irradiance acquisition using a lock-in technique. Initially, the electronic board's performance was successfully validated through simulations. Subsequently, the construction of the electronic device enabled its validation in a real-world environment within a photovoltaic plant, yielding results consistent with the earlier simulations.

The electronic device is capable of operating while the photovoltaic string is connected. Therefore, this technique could help alleviate two of the main drawbacks of conventional daylight luminescence techniques. First, a separate power supply is not needed since the power for the EL effect is generated by the string itself. Second, the technique does not require the disconnection of the solar string, making it less invasive. It's also worth mentioning that the device allows for the acquisition of both EL

12

and PL images, providing complementary information about the solar module's performance and potential faults.

Future work involves the development of an informatics program that enhances the coordination between the designed electronic board and an InGaAs camera to obtain EL and PL images. The informatic program will also be capable of processing the images through consecutive subtractions and additions to remove the background signal. Other secondary future tasks will include designing a system to power the board directly from the solar module and reducing the switching time of the IGBT to minimize acquisition time.

Funding

This work has been funded by the Spanish Ministry of Education through the National Program FPU (grant number FPU21/04288).

Acknowledgments

This study was supported by the Universidad de Valladolid with ERASMUS+ KA-107. We also appreciate the help of other members of our departments.

References

1. United Nations *Department of Economic and Social Affairs*; 2018;
2. Lai, C.S.; Jia, Y.; Dong, Z.; Wang, D.; Tao, Y.; Lai, Q.H.; Wong, R.T.K.; Zobia, A.F.; Wu, R.; Lai, L.L. A Review of Technical Standards for Smart Cities. *Clean Technologies* **2020**, *2*, 290–310, doi:10.3390/cleantechnol2030019.
3. Thellufsen, J.Z.; Lund, H.; Sorknæs, P.; Østergaard, P.A.; Chang, M.; Drysdale, D.; Nielsen, S.; Djørup, S.R.; Sperling, K. Smart Energy Cities in a 100% Renewable Energy Context. *Renewable and Sustainable Energy Reviews* **2020**, *129*, 109922, doi:10.1016/j.rser.2020.109922.
4. Gassar, A.A.A.; Cha, S.H. Review of Geographic Information Systems-Based Rooftop Solar Photovoltaic Potential Estimation Approaches at Urban Scales. *Appl Energy* **2021**, *291*, 116817, doi:10.1016/j.apenergy.2021.116817.
5. Kammen, D.M.; Sunter, D.A. City-Integrated Renewable Energy for Urban Sustainability. *Science (1979)* **2016**, *352*, 922–928, doi:10.1126/science.aad9302.
6. Feldman, D.; Ramasamy, V.; Fu, R.; Ramdas, A.; Desai, J.; Margolis, R. *U.S. Solar Photovoltaic System and Energy Storage Cost Benchmark: Q1 2020*; 2021;
7. IEA *Technology and Innovation Pathways for Zero-Carbon-Ready Buildings by 2030*; Paris, 2022;

8. Hernández-Callejo, L.; Gallardo-Saavedra, S.; Alonso-Gómez, V. A Review of Photovoltaic Systems: Design, Operation and Maintenance. *Solar Energy* **2019**, *188*, 426–440, doi:10.1016/j.solener.2019.06.017.
9. Hong, Y.-Y.; Pula, R.A. Methods of Photovoltaic Fault Detection and Classification: A Review. *Energy Reports* **2022**, *8*, 5898–5929, doi:10.1016/j.egyr.2022.04.043.
10. Waqar Akram, M.; Li, G.; Jin, Y.; Chen, X. Failures of Photovoltaic Modules and Their Detection: A Review. *Appl Energy* **2022**, *313*, 118822, doi:10.1016/j.apenergy.2022.118822.
11. Fraunhofer Institute for Solar Energy Systems, I. with support of P.P.G. *Photovoltaics Report*; 2023;
12. Ulrike Jahn, M.H.; Marc Köntges; David Parlevliet; Marco Pagg; Ioannis Tsanakas; Joshua S. Stein; Karl A. Berger; Samuli Ranta; Roger H. French; Mauricio Richter; et al. *Review on Infrared and Electroluminescence Imaging for PV Field Applications*; 2018;
13. Høiaas, I.; Grujic, K.; Imenes, A.G.; Burud, I.; Olsen, E.; Belbachir, N. Inspection and Condition Monitoring of Large-Scale Photovoltaic Power Plants: A Review of Imaging Technologies. *Renewable and Sustainable Energy Reviews* **2022**, *161*, 112353, doi:10.1016/j.rser.2022.112353.
14. Coello, J.; Pérez, L.; Domínguez, F.; Navarrete, M. On-Site Quality Control of Photovoltaic Modules with the PV MOBILE LAB. In Proceedings of the Energy Procedia: 2013 ISES Solar World Congress; Elsevier, January 1 2014; Vol. 57, pp. 89–98.
15. Navarrete, M.; Pérez, L.; Domínguez, F.; Castillo, G.; Gómez, R.; Martínez, M.; Coello, J.; Parra, V. On-Site Inspection of PV Modules Using an Internationally Accredited PV Mobile Lab: A Three-Years Experience Operating Worldwide. In Proceedings of the 31st European Photovoltaic Solar Energy Conference and Exhibition; 2015; pp. 1989–1991.
16. Ballestín-Fuertes, J.; Muñoz-Cruzado-Alba, J.; Sanz-Osorio, J.F.; Hernández-Callejo, L.; Alonso-Gómez, V.; Morales-Aragones, J.I.; Gallardo-Saavedra, S.; Martínez-Sacristan, O.; Moretón-Fernández, Á. Novel Utility-Scale Photovoltaic Plant Electroluminescence Maintenance Technique by Means of Bi-directional Power Inverter Controller. *Applied Sciences* **2020**, *10*, 3084, doi:10.3390/app10093084.
17. Guada, M.; Moretón, Á.; Rodríguez-Conde, S.; Sánchez, L.A.; Martínez, M.; González, M.Á.; Jiménez, J.; Pérez, L.; Parra, V.; Martínez, O. Daylight Luminescence System for Silicon Solar Panels Based on a Bias Switching Method. *Energy Sci Eng* **2020**, *8*, 3839–3853, doi:10.1002/ese3.781.
18. Bhoopathy, R.; Kunz, O.; Juhl, M.; Trupke, T.; Hameiri, Z. Outdoor Photoluminescence Imaging of Photovoltaic Modules with Sunlight Excitation. *Progress in Photovoltaics: Research and Applications* **2018**, *26*, 69–73, doi:10.1002/pip.2946.
19. Kunz, O.; Rey, G.; Juhl, M.K.; Trupke, T. High Throughput Outdoor Photoluminescence Imaging via PV String Modulation. In Proceedings of the 2021

14

- IEEE 48th Photovoltaic Specialists Conference (PVSC); IEEE, June 20 2021; pp. 0346–0350.
20. Bhoopathy, R.; Kunz, O.; Juhl, M.; Trupke, T.; Hameiri, Z. Outdoor Photoluminescence Imaging of Solar Panels by Contactless Switching: Technical Considerations and Applications. *Progress in Photovoltaics: Research and Applications* **2020**, *28*, 217–228, doi:10.1002/PIP.3216.
 21. Koester, L.; Astigarraga, A.; Lindig, S.; Moser, D. Development of Daylight Photoluminescence Technique for Photovoltaic Modules and Investigation of Temperature Dependency. In Proceedings of the 37th European Photovoltaic Solar Energy Conference and Exhibition (EU PVSEC); 2020; pp. 908–913.
 22. Vuković, M.; Høiaas, I.E.; Jakovljević, M.; Flø, A.S.; Olsen, E.; Burud, I. Outdoor Photoluminescence and Electroluminescence Imaging of Photovoltaic Silicon Modules in a String. In Proceedings of the 11TH INTERNATIONAL CONFERENCE ON CRYSTALLINE SILICON PHOTOVOLTAICS (SILICONPV 2021); 2022; p. 030012.
 23. Kropp, T.; Berner, M.; Stoicescu, L.; Werner, J.H. Self-Sourced Daylight Electroluminescence From Photovoltaic Modules. *IEEE J Photovolt* **2017**, *7*, 1184–1189, doi:10.1109/JPHOTOV.2017.2714188.
 24. Kunz, O.; Rey, G.; Bhoopathy, R.; Hameiri, Z.; Trupke, T. Outdoor PL Imaging of Crystalline Silicon Modules at Constant Operating Point. In Proceedings of the 2020 47th IEEE Photovoltaic Specialists Conference (PVSC); IEEE, June 14 2020; pp. 2140–2143.
 25. Analog Devices LTspice Available online: <https://www.analog.com/en/design-center/design-tools-and-calculators/ltspice-simulator.html> (accessed on 10 July 2023).
 26. Cotfas, D.T.; Cotfas, P.A.; Kaplanis, S. Methods to Determine the Dc Parameters of Solar Cells: A Critical Review. *Renewable and Sustainable Energy Reviews* **2013**, *28*, 588–596, doi:10.1016/J.RSER.2013.08.017.
 27. Mihalic, F.; Jezernik, K.; Krischan, K.; Rentmeister, M. IGBT SPICE Model. *IEEE Transactions on Industrial Electronics* **1995**, *42*, 98–105, doi:10.1109/41.345852.

Levels of plasmon-polariton oscillations produced by Cherenkov radiation on a CNT system for different nanotube saturations.

Gustavo Medina-Ángel^{1,2}[0000-0002-0279-3492], Gennadiy Burlak¹[0000-0003-4829-8435], and Felipe Bonilla-Sánchez²[0009-0001-8674-8209]

¹ Centro de Investigación en Ingeniería y Ciencias Aplicadas, Universidad Autónoma del Estado de Morelos, Av. Universidad 1001, Cuernavaca, Morelos 62209, México

² Facultad de Contaduría, Administración e Informática, Universidad Autónoma del Estado de Morelos, Av. Universidad 1001, Cuernavaca, Morelos 62209, México
gustavo.isc@hotmail.com

Abstract. The levels of Plasmon-Polariton (PP) produced by a charge (Cherenkov Radiation) on a 3D nanostructure of carbon nanotubes (CNT) with variable morphology in sizes were studied. Different saturations of nanotubes in the system ranging from 100 to 1000 CNTS, and which are resonating at a plasma frequency ω_p were considered. The FDTD method in the numerical calculations was applied to study the resulting PP that occurs in the CNT array affected by Cherenkov radiation, and a peak of best energetic coupling between the charge and the resonant nanotube system was found when there is a moderate saturation of approximately 300 nanotubes; at this point, a greater dispersion of the PP oscillations can be detected with a better coupling between the charge and the carbon nanotube system.

Keywords: Plasmon-Polariton · Cherenkov Radiation · Carbon nanotubes.

1 Introduction

CNTs have extraordinary properties for electrical conduction as well as electromagnetic properties that can be combined and taken advantage of with modern technology. CNTs can generate an electromagnetic field reacting to certain phenomena when they are made to resonate at a certain frequency. This is the case when a particle passes through an array of resonant nanostructure, where the charge traveling at constant velocity releases energy that is absorbed by the group of carbon nanotubes, producing an electromagnetic field within its structure that liberates surface plasmons-polaritons, generating an energy field on the main path through which the charge passes.[1, 2]. Surface plasmons are known for their high levels of oscillation (optical frequencies) and are the result of the optical properties of conducting metals since light is reflected when its frequency is lower than the plasma frequency. Plasmons are quanta of plasma oscillation[3] and can interact with a photon creating plasma polaritons.

2 G. Medina-Ángel et al.

The plasmon energy (E_p) can be estimated by the free electron model of the equation: $E_p = \hbar \frac{ne^2}{m\epsilon_0}^{\frac{1}{2}}$, where n is the number of conduction electrons, e is the elementary charge of the electron, m is the mass of the electron, ϵ_0 is the permittivity of free space, and \hbar is Planck's constant.

Coupled surface plasmon polaritons (SPP) have shown to provide effective transfer of excitation energy from donor molecules to acceptor molecules on opposite sides of metal films and dielectric nanostructures such as CNT[4, 5].

The evolution of the nanotechnology industry, has enabled us advantage of the optical frequencies of surface plasmons. Plasmons are widely used as means of transmitting information in optical communications and in microprocessors since they can reach frequencies at Terahertz (THz) levels[6]. Plasmon-polariton oscillations can be used in solar cells and panels where the absorbed radiation is transferred to the charge-generating layers through surface plasmon polaritons (SSP)[7][8]. The formation of SPP finds application in nanophotonic devices for optical computing due to the unique plasmonic properties of graphene (the base material of CNTs). This may be applicable for high-speed data switching in microprocessors and random access memories (RAM), as well as for optical interconnection in VLSI (Very-large-scale integration) design technology [9] and in sensor hybrids with vertical coupler composed of short-range surface plasmon waveguides (SRSP) [10], while other low-frequency SPP called SPoof (SSPP) can be applied to coupler systems, frequency dividers, antennas [11, 6, 12, 13] and in filters for noise reduction in modern systems[14], in addition to in various functional pieces of transmission lines (TL)[13]. PPs are also applicable to optical biosensors that use long-range surface plasmon-polariton waveguides for protein detection, cell detection, disease diagnosis, and small molecule detection[15]. This paper is organized as follows: In Section 2, we describe the system and the components that make it up. In Section 3, we address the hybrid system numerically. In Section 4, we present our results. In section 5 we discuss our research and in the last section, we present our conclusions.

2 Plasma-generating conductive nanotubes coupled to a rapid charge (Cherenkov radiation)

Cherenkov radiation occurs when a charged particle in a dielectric medium exceeds the phase speed of light in that medium, reaching its maximum velocity in a vacuum[16]. Cherenkov radiation has a conical shape[17] when the particle passes over the dielectric medium, very similar to the waves generated by the bow of a ship when traveling over the sea. Cherenkov radiation is produced in nuclear reactors, generally visible as a bluish hue[18]. The typical formula for Cherenkov radiation is given by:

$$\frac{d^2E}{dx d\omega} = \frac{q^2}{4\pi} \omega \left(1 - \frac{c^2}{v^2 n^2(\omega)} \right), \quad (1)$$

Levels of PP produced by Cherenkov radiation on different CNT saturations 3

Here $n(\omega)$ is the refractive index of the material in which the particle charge moves with constant velocity v , ω is the frequency emitted by the particle radiation, q is the charge that passes through the dielectric medium and c is the speed of light. To analyze the energy emitted by an object we use the theory

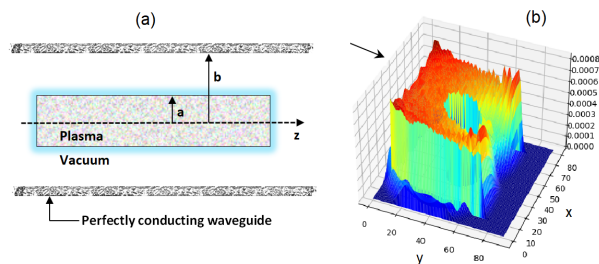


Fig. 1. (Color online), (a) Partial scheme of the demagnetized cylinder of radius b , which produces a plasma column of radius a , the arrow vertical to the plasma represents the orientation of the plasma parallel to the Z axis. (b) Simulation of a nanotube irradiated by the Cherenkov particle, we can observe the internal cavity of the nanotube and around the dispersed plasma of PP that propagates in the XY directions and along the nanotubular cavity.

of dispersive conductivity in cylinders [19][20]. In an analytical approach, the conductivity in nanotubes is represented by the conductivity in a conducting cylinder (nanotube), having a Drude dielectric permittivity $\varepsilon(\omega)$ as shown in the following equation.

$$\varepsilon(\omega) = \varepsilon_h - \frac{\omega_p^2}{\omega^2 + i\gamma\omega}, \tag{2}$$

Where ω_p is the plasma frequency ($\omega_p^2 = e^2 N_e / \varepsilon_0 m_e$), $\varepsilon_h = 1$ for cases $\varepsilon_h > 1$, where ε_0 is the permittivity in vacuum, γ_e the electron energy loss fluxes, N_e the electron density and m_e, e the electron mass, This relation can be observed in figure 1(a) where we consider a magnetized plasma column of radius a , in a conductive nanotube of radius b inside a substance with dielectric constant, the arrow z , represents the parallel orientation of the CNT plasma where the nanotube walls serve as waveguide and allow energy distribution. We generate the simulation for such a case on a resonant nanotube and the Cherenkov particle that transfers energy [21] to the nanotube in which a resulting electromagnetic field is generated, we observed the cavity of the nanotube and the field around it generates dispersing energy, we can see this figure 1(b), the direction of the charge in this picture is indicated by the arrow \perp to the CNT, where the field of PP is generated as a result of the effect of Cherenkov radiation on an independent nanotube with dispersion, in this case, the structure of the CNT is not shown, only the field that is produced around it.

4 G. Medina-Ángel et al.

3 Numerical simulation

We use the FDTD method, finite difference function in the time domain[22, 23], given that the hybrid system (charge + nanotubes) that we address in this article is a dynamic system that is calculated based on the electric and magnetic field, the FDTD method is appropriate to generate numerical results that are based on the calculation of the Electromagnetic Field (EMF), since it allows the calculation to be partitioned into finite systems that are backed up in memory and that are subsequently integrated for the next calculation until the complete EMF is generated. The result is a simulation with real-time values established in the parameters of the hybrid system.

In the nanotechnology industry, there are two possible variations in the creation of nanostructures, taking this approach we analyze two nanotube manufacturing situations; a) periodic nanotubes with structure without deviations in measurements in an ideal simulation situation[24] and b) nanotubes with random asymmetry in thickness and length [25], both single-walled CNTs. Since structure is based on hexagonal bonds, CNTs have a low permittivity for the passage of electrons over their structure[26], which is why it was decided to consider single-walled nanotubes (SWCNT, see figure 2(a)) to form a system where we embed a series of periodic and random nanotubes, as shown in figure 2(b,c). In the first case we observe a structure for nanotubes with a periodic structure of CNTs where typical measurements in nanometers are considered, for the radius of the CNT $R=140$ nm and a length of $h = 6l = 3 \times 10^3$ nm, where $l = 500$ nm, we can appreciate a fragment of the periodic structure based on periodic CNTs. The charge (indicated by the arrow Q) with constant velocity moves above the nanotubes and parallel to the X axis of the nanostructure, the nanostructure is formed by 6×10 SWCNTs while the permittivity with a dielectric constant is $\epsilon_h = 2$. In figure 2(c), we observe the same situation as in figure 2(b), but with variable radius and length in each CNT. In regarding nanotube thickness there are nanotubes with radii ranging from 0 (where vacant spaces are considered, in the absence of nanotubes[25], very frequently found in systems with defective where nanotubes are not successfully created) to $R=140$, while the length of the nanotube ranges from a minimum of 1 nm up to a maximum value of $h = 6l = 3 \times 10^3$ nm, as long as $R > 0$.

In the images in figures 3(a) and 3(b), we can see the effect produced by the charge and the resonant system where the electron releases up part of its energy to the resonant nanotubes, which produce an electromagnetic field of plasmons and surface polaritons, the first case for periodic nanotubes and the second case for nanotubes of random size. This image shows the effect generated once the charge passes over the nanotubes starting from a time $t = 0$ until the charge touches the terminal of the simulation grid. The surface plasmon-polariton formed by the cone-shaped CNTs is observed for both cases, the charge velocity is $v = 0.98$ and with an oscillation frequency of $\omega_p = 2.1 \times 10^{15} s^{-1}$ for both cases. The arrows indicate the entry and exit of the charge that follows a path along the x direction. In the case of the periodic structure, there is field generation with small similar peaks that protrude over the path through which

Levels of PP produced by Cherenkov radiation on different CNT saturations 5

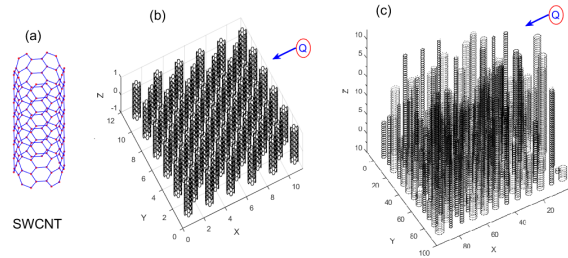


Fig. 2. (Color online), (a) basic morphology of a single-walled carbon nanotube SWCNT, basic symmetry used to consider a demagnetized plasma column (see figure 1(a)), (b) CNT system with periodic nanotubes, where Q is the fast charge that passes over the nanostructure generating the Cherenkov radiation. In (c) we have the same situation as in (b), but with nanotubes of variable symmetry in their radii and lengths.

the charge passes, forming the typical cone of Cherenkov radiation on the CNT material. For the second case, we see the same phenomenon but the energy peaks tend to grow and decrease according to the random morphology of the nanotubes in the system. For both cases, a very different field generation is observed. In the periodic case there is a field with a more conical shape in its wave front, while on the second case, we can observe a wavefront with a more circular shape. These variations lead us to study both cases in order to measure the energy recorded for each of them; and with better coupling for each system. Therefore, we endeavored to the task of carrying out a set of tests considering both cases. The importance of the interaction of the charge as well as the resonant structure involves studying dynamic parameters such as the charge velocity and the plasma frequency ω_p to which the nanotubes are exposed, making this phenomenon a non-trivial case.

4 Results

Several tests were carried out where the charge (Cherenkov Radiation) passes over the resonant structure with 1000 CNTs for both cases. First, we perform the relevant tests for the periodic case and subsequently for the random case. For simulation purposes, we established four charging velocities close to the speed of light. For the resonant structure, we study a wide range of frequencies $[\omega_p = 2 \times 10^8 - 4 \times 10^{16}]s^{-1}$.

In figure 4(a) we observe the previously mentioned interval for the case of the periodic structure. We observe 4 lines in the shape of W with a well defined double-well, the velocities at which the charge travels are represented for $v_1 = 0.81$, $v_2 = 0.87$, $v_3 = 0.92$ and $v_4 = 0.98$. We can observe that in this case as the velocity increases, the energy field for the studied frequency range also increases,

6 G. Medina-Ángel et al.

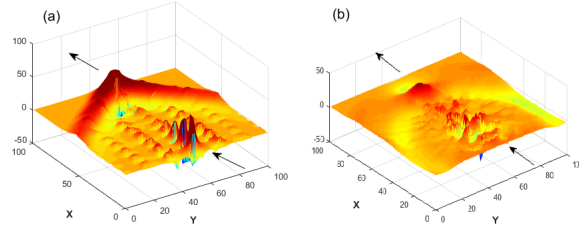


Fig. 3. (Color online), (a), shows the simulation of Cherenkov radiation as the charge passes with a velocity of $v = 0.98$ above the nanostructure (see Fig.2(a)) that is resonating at a plasma frequency $\omega_p = 2.1 \times 10^{15} s^{-1}$ with periodic CNTs, the cone-shaped surface polariton plasmon field is observed, typical morphology of Cherenkov radiation, the arrows indicate the entry and exit of the charge. In (b) we observe the same situation as in case (a), but with nanotubes of random symmetry (as in the structure 2(b)). For both cases a different PP field is observed.

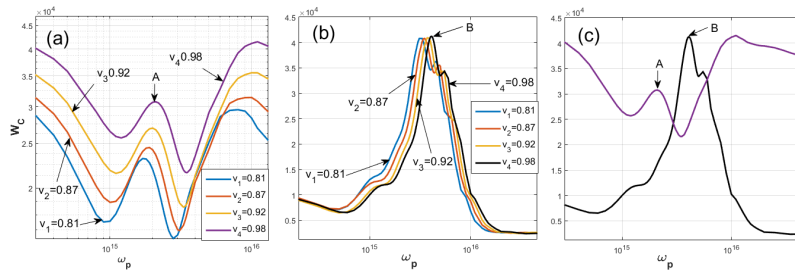


Fig. 4. (Color online), (a), a frequency range is observed applied to the nanostructure of periodic CNTs that comprises; $[\omega_p = 2 \times 10^8 - 4 \times 10^{16}] s^{-1}$, each line represents a velocity ranging from $v_1 = 0.81$, $v_2 = 0.87$, $v_3 = 0.92$ and $v_4 = 0.98$, We observe that there is a better energy dispersion (arbitrary units) of PP when there is a velocity of $v_4 = 0.98$ with a frequency of $\omega_p = 2.1 \times 10^{15} s^{-1}$ indicated by the arrow **A**. For figure (b), the same test is repeated but with CNTs of random morphology, in this case, a better coupling between charge and nanotubes is achieved when $v_4 = 0.98$, but with an oscillation frequency of $\omega_p = 4.1 \times 10^{15} s^{-1}$ indicated with the arrow **B**. In image (c) a comparison of the two maximum peaks A and B is observed, for periodic and randomly nanotubes respectively.

each curve W has a maximum energy peak W_c (arbitrary units) but the peak with the best energy dispersion of PP is that of $v_4 = 0.98$, where we observe a maximum energy dispersion peak W_c indicated with arrow **A** which is approximately in the middle of the frequency range studied applying the nanostructure, this point has a plasma frequency of $\omega_p = 2.1 \times 10^{15} s^{-1}$, considered as the best-coupled frequency between the charge and the resonant nanotube system. However, as we mentioned before, periodic systems are not always identical, since the random factor is always present both in nature and in systems of artificial

Levels of PP produced by Cherenkov radiation on different CNT saturations 7

construction, where there is always a error deviation σ in their manufacturing and; moreover even more when it refers to nanometric systems, where nanocomposites are difficult to control, resulting in a second study that contemplates the errors of variable thickness and length in the manufacture of nanotubes, considered in our tests. The results of this variable morphology characteristic are shown in figure 4(b), where we observe the same parameters of the image 4(a), also considering the same charge velocities and the same plasma frequency range. On the other hand, we observe that for this second case, there is a well-defined increase mountain shape, where at the beginning a decreased energy generation is marked. But, as the frequency interval raises the energy level of PP also tends to increase, reaching a maximum peak indicated by the arrow **B** with plasma frequency $\omega_p = 4.1 \times 10^{15} s^{-1}$ and subsequently, there is a decrease in energy until reaching a minimum that ends in the final interval of the studied frequency range. Both cases demonstrated to generate a considerable amount of

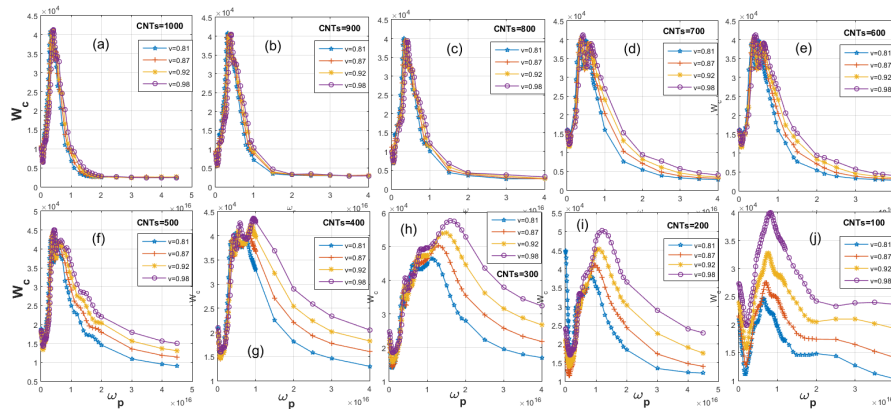


Fig. 5. (Color online), (a-j) They show the PP dispersion levels for different saturations of CNTs with variable morphology, for the case (a) CNTs=1000, (b) CNTs=900, (c) CNTs=800, ... (j) CNTs=100. The frequency range studied and the charge velocities are the same for all cases; $[\omega_p = 2 \times 10^8 - 4 \times 10^{16}] s^{-1}$, with $v_1 = 0.81$, $v_2 = 0.87$, $v_3 = 0.92$ and $v_4 = 0.98$.

energy in the form of plasmon-polaritons, however, by making a comparison of the maximum frequency points reached for each case, it can be observed in figure 4(c) that there is a higher dispersion of plasmons-polaritons when the structure follows a random behavior in the measures of thickness and length of nanotubes. This leads us to pay priority attention to the type of nanostructure with variable morphology in CNTs.

Our next task is to vary the CNT saturation parameter within the resonant matrix, for this, we generate several scenarios by changing the number of CNTs that are established in the structure. The charging velocities and frequency range

8 G. Medina-Ángel et al.

remain the same: $[\omega_p = 2 \times 10^8 - 4 \times 10^{16}]s^{-1}$ and $v = 0.81 - 0.98$. Nevertheless, the saturation number differs with increments of 100 up to a maximum saturation level of 1000 nanotubes for our case study.

In figure 5(a-j) we observe the energy behavior pattern in random nanotubes for the different saturations corresponding to (a) with 1000 nanotubes, (b) with 900 nanotubes, (c) with 800 nanotubes, (d) with 700 nanotubes, (e) with 600 nanotubes, (f) with 500 nanotubes, (g) with 400 nanotubes, (h) with 300 nanotubes, (i) with 200 nanotubes and (j) with 100 nanotubes. We observe an almost uniform energy broadening behavior for the interval of the frequency ordinate ω_p . The lower the CNTs saturation, the greater the energy magnification, except for the saturation levels 100 and 200 in figure 5(i,j). And the higher the concentration of nanotubes in the system, the more defined the energy peak is and there is a more narrow energy field over ω_p .

This series of data reveals an important region of behavior for the energy levels that exist when we vary the population of CNTs on the nanotubular matrix, this induces to compare and analyze each of the energy peaks for the values in a single graph, where we obtain the peak with the greatest energy dispersion of each of the graphs in figure 5(a-j), and we group them in a single schema to be able to observe the maximum energy levels for each case as illustrated in figure 6. In figure 6 we observe a minimum dispersion of PP with a population of 1000

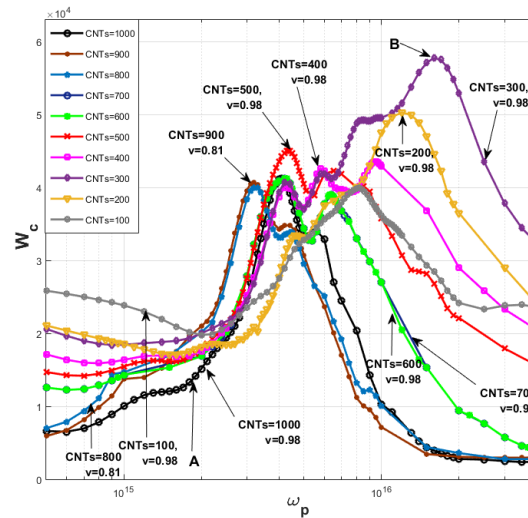


Fig. 6. (Color online). The grouping of the maximum energy levels in the figure 5 is observed for each case (a-j), where we can observe that of all of them there is an energy peak that stands out when the charge velocity is $v = 0.98$ with a saturation of 300 CNTs at a better-coupled frequency point of $\omega_p = 1.6 \times 10^{16} s^{-1}$ (See arrow B).

Levels of PP produced by Cherenkov radiation on different CNT saturations 9

nanotubes (See arrow A) where there is an growing trend that indicates that; the greater the number of CNTs the dispersed energy W_c is minor, compared to a system with few nanotubes but a higher frequency and with a moderate saturation of 300 CNTs, a high energy level (see arrow B) can be reached with a great collective of plasmon-polariton oscillations, compared to the other cases of nanotubes saturation. The mountain shape energy peak in figure 6 comprises a maximum level of PP with the parameters $\omega_p=1.6 \times 10^{16} s^{-1}$, with a saturation of 300 CNTs and with a charge velocity of $v=0.98$. As it can be discerned, this research provides a more accurate level of the saturation parameter (nanotube population) compared to previous research [2,27,28]. While others defined a fixed of number of CNTs, here the saturation parameter was varied and the number of essential CNTs to generate the greatest number of possible PP (when they are affected by a radiant charge) was identified.

5 Discussion

The importance of energy consumption and communication systems using cheap meta-materials such as graphene is increasingly sought after and relevant due to its low manufacturing costs, such is the case of CNT (carbon nanotubes) that has a low permittivity to the passage of electrons (graphene rolled forming a single-walled nanotube SWCNT) and that exposed to plasma frequencies in interaction with high velocities charges can generate clean energy and environmentally friendly[29] in the form of plasmons and polaritons. This issue becomes relevant since the generation of plasmon and polariton oscillations has major impact on the construction of microchips, sensors, and signal filters, as well as the simultaneous transfer of different signals at variable wave amplitudes[6]. The outcome of this research may be applicable to certain disciplines such as spectroscopy, instrumentation and calibration systems, and in radiation emitting polarized particle accelerators as well[30]. This article studies the best couplings of a charge and an array of nanotubes arranged in a resonant matrix that interacts with the charge passing over the nanotubes energizing the nanotubes to create a surface plasma field within the system.

The best couplings where more plasma is generated are derived from a series of simulated tests; firstly by varying the number of nanotubes (population) that are integrated into the structure, and secondly by varying the velocity of the charge at high velocities in order to achieve Cherenkov radiation. In a more approximate ideal case of experimentation, random measurements can be contemplated on the nanotubes considered as systems defective, where our numerical simulations can have a highly significant impact. The mountain-shaped level with the highest energy (see Figure 6) shows a fairly stable level and a considerable amplitude so that nanostructure oscillators can be calibrated more freely and emit better plasma frequencies in the CNTs.

However, a plasma frequency (Arrow B) stands out along ω_p that represents the maximum energy peak discovered in this research. The frequency $\omega_p=1.6 \times 10^{16} s^{-1}$, in the nanostructure with saturation=300 nanotubes that is affected

10 G. Medina-Ángel et al.

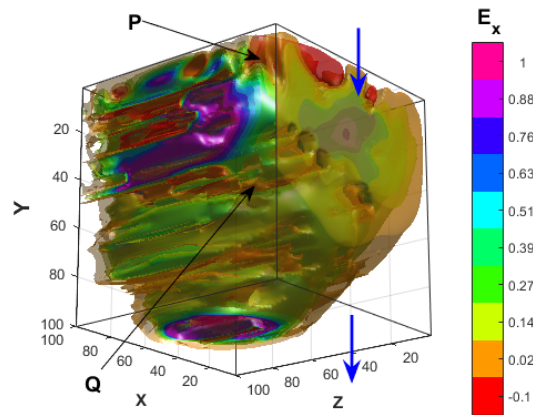


Fig. 7. (Color online),3D plasma (PP) structure on the E_x field that is generated after being affected by the charge produced by Cherenkov radiation. We observe the field that is produced inside and on the nanotubes corresponding to the parameters of the maximum peak (arrow B) in figure 6. The field generated by the well-defined nanotubes (arrow Q) and the field of surface PP indicated by the arrow P are observed. The blue arrows indicate the direction followed by the charge on the nanotube system. .

by a charge traveling at a constant velocity $v=0.98$, was shown to have higher plasmon-polariton radiation than the other frequencies.

This motivates us to investigate the electromagnetic effect that is formed on and within the surface of the nanostructure. In Figure 7 we can observe the behavior of the plasma (plasmons-polaritons) that is formed when crossed by the charge that follows the direction of the blue arrows, in a time $t=0$ until the charge touches the end of the simulated 3D System.

In this figure, we can observe in detail the formation of plasma (isofield image) that the nanotubes give off, as well as the well-defined plasma symmetry of the CNT (arrow Q), above the field of the CNTS, the formation of surface plasmon-polariton is observed, which generates the radiant charge as it passes through the resonant nanostructure (Arrow P). The conical shape of the field is also notable with a well-defined plasma path within and above the CTN structure.

6 Conclusion

We studied the generation of energy in the form of plasma (fourth state of matter) by simulating the generation of plasmons-polaritons in a structure based on CNTs (which are resonating at a frequency ω_p) that interact with a rapid charge. We considered the morphologies of periodic nanotubes and nanotubes that may have defects in their manufacturing qualified as nanotubes of variable morphology (with random measurements in their lengths and radii), we found

Levels of PP produced by Cherenkov radiation on different CNT saturations 11

that for the latter, a greater generation of plasmon-polaritons is obtained, which arises from the interaction between the hybrid nanotube system and the charge, which led us to investigate the maximum energy peak with greater coupling in said system, we found that the best coupling option between the charge and the CNTs is when the nanostructure has a saturation of more or less 300 nanocomposites resonating at a frequency $\omega_p=1.6 \times 10^{16} s^{-1}$ affected by the Cherenkov effect produced by the charge with velocity $v = 0.98$. We also found that the saturation factor of nanocomposites (CNTs) has a direct effect on the increase and decrease of PP.

7 Acknowledgments

This work was supported, in part, by CONAHCYT (México) through grants No. A1-S-9201 and No. A1-S-8793. The authors thank the FCAeI-UAEM for funding this article. G. M-A. Acknowledged scholarship granted by CONAHCYT-México.

References

1. Burlak, G., and Medina-Ángel, G. : Structure of optical Cherenkov radiation in a three-dimensional compound medium with carbon nanotubes. *Journal of the Optical Society of America B* **36**(2), 187-193 (2019)
2. Burlak, G., Cuevas-Arteaga, C., Medina-Ángel, G., Martínez-Sánchez, E., and Calderón-Segura, Y. Y.: Plasmon-polariton oscillations in three-dimensional disordered nanotubes excited by a moving charge. *Journal of Applied Physics* **126**(1), 013101 (2019)
3. Goldston, R. J.: *Introduction to plasma physics*. CRC Press (2020)
4. Andrew, P., and Barnes, W. L.: Energy transfer across a metal film mediated by surface plasmon polaritons. *science* **306**(5698), 1002-1005 (2004)
5. Vasa, P. and Pomraenke, R. and Schwieger, S. and Mazur, Yu. I. and Kunets, Vas. and Srinivasan, P. and Johnson, E. and Kihm, J. E. and Kim, D. S. and Runge, E. and Salamo, G. and Lienau, C.: Coherent exciton-surface-plasmon-polariton interaction in hybrid metal-semiconductor nanostructures. *Physical review letters* **101**(11), 116801 (2008)
6. Wang, Y., Wang, X., Wu, Q., He, X. J., Gui, T. L., and Tong, Y. J.: Surface plasmon resonant THz wave transmission on carbon nanotube film. *Plasmonics* **7**, 411-415 (2012)
7. Heidel, T. D., Mapel, J. K., Singh, M., Celebi, K., and Baldo, M. A.: Surface plasmon polariton mediated energy transfer in organic photovoltaic devices. *Applied Physics Letters* **91**(9), 093506 (2007)
8. ElKhamisy, K., Abdelhamid, H., Elagooz, S., and El-Rabaie, E. S.: The effect of different surface plasmon polariton shapes on thin-film solar cell efficiency. *Journal of Computational Electronics* **20**, 1807-1814 (2021)
9. Daas, B. K., and Dutta, A.: Electromagnetic dispersion of surface plasmon polariton at the EG/SiC interface. *Journal of Materials Research* **29**(21), 2485-2490 (2014)
10. Fan, B., Liu, F., Li, Y., Wang, X., Cui, K., Feng, X and Huang, Y.: Integrated refractive index sensor based on hybrid coupler with short range surface plasmon polariton and dielectric waveguide. *Sensors and Actuators B: Chemical* **186**, 495-505 (2013)

12 G. Medina-Ángel et al.

11. Farokhipour, E., Komjani, N., Chaychizadeh, M.A.: An ultra-wideband three-way power divider based on spoof surface plasmon polaritons. *Journal of Applied Physics* **124**, 235310 (2018)
12. Yang, Y., Li, Z., Wang, S., Chen, X., Wang, J., Guo, Y.J.: Miniaturized High-Order-Mode Dipole Antennas Based on Spoof Surface Plasmon Polaritons. *IEEE Antennas and Wireless Propagation Letters* **17**(12), 2409–2413 (2018)
13. Zhang, D. Zhang, K. Wu, Q. Ding, X. Sha, X.: High-efficiency surface plasmonic polariton waveguides with enhanced low-frequency performance in microwave frequencies. *Optics Express* **25**(3), 2766–2769 (2017)
14. Farokhipour, E., Mehrabi, M., Komjani, N., Ding, C.: A Spoof Surface Plasmon Polaritons (SSPPs) Based Dual-Band-Rejection Filter with Wide Rejection Bandwidth. *Sensors* **20**(24), 7311 (2020)
15. Krupin, O., Wong, W. R., Adikan, F. R. M., and Berini, P.: Detection of small molecules using long-range surface plasmon polariton waveguides. *IEEE Journal of Selected Topics in Quantum Electronics* **23**(2), 103-112 (2016)
16. Macleod, A. J., Noble, A., and Jaroszynski, D. A.: Cherenkov radiation from the quantum vacuum. *Physical review letters* **122**(16), 161601 (2019)
17. Bolotovskii, B. M.: Vavilov–Cherenkov radiation: its discovery and application. *Physics-Usp ekhi* **52**(11), 1099 (2009)
18. Malec, J., Österlund, M., Solders, A., Al-Adili, A., Jazbec, A., Rupnik, S., and Snoj, L.: On teaching experimental reactor physics in times of pandemic. In *EPJ Web of Conferences*, Vol. 253, p. 10001. EDP Sciences (2021)
19. Alexandrov, A. F., Bogdankevich, L. S., and Rukhadze, A. A. (1984). *Principles of plasma electrodynamics* (Vol. 9). Berlin: Springer.
20. Kadochkin, A. S., Moiseev, S. G., Dadoenkova, Y. S., Svetukhin, V. V., and Zolotovskii, I. O.: Surface plasmon polariton amplification in a single-walled carbon nanotube. *Optics Express* **25**(22), 27165-27171 (2017)
21. de Abajo, F. G., Pattantyus-Abraham, . G., Zabala, N., Rivacoba, A., Wolf, M. O., and Echenique, P. M.: Cherenkov effect as a probe of photonic nanostructures. *Physical review letters* **91**(14), 143902 (2003)
22. Sullivan, D. M.: *Electromagnetic simulation using the FDTD method*. John Wiley and Sons, (2013)
23. Gedney, S.: *Introduction to the finite-difference time-domain (FDTD) method for electromagnetics*. Springer Nature (2022)
24. Cebeci, H., de Villoria, R. G., Hart, A. J., and Wardle, B. L.: Multifunctional properties of high volume fraction aligned carbon nanotube polymer composites with controlled morphology. *Composites Science and Technology* **69**(15-16), 2649-2656 (2009)
25. Kumar, A., Sharma, K., Singh, P. K., and Dwivedi, V. K.: Mechanical characterization of vacancy defective single-walled carbon nanotube/epoxy composites. *Materials Today: Proceedings* **4**(2), 4013-4021 (2017)
26. Yuen, S. M., Ma, C. C. M., Chiang, C. L., and Teng, C. C.: Morphology and properties of aminosilane grafted MWCNT/polyimide nanocomposites. *Journal of Nanomaterials*, **2008** (2008)
27. Medina-Ángel, G., Martínez-Sánchez, E., and Burlak, G.: Numerical simulation of Cherenkov radiation on a CNT structure of variable sizes for different charge velocities. *Ingeniería, investigación y tecnología* **23**(4), 1-9 (2022)
28. Batrakov, K. G., Maksimenko, S. A., Kuzhir, P. P., and Thomsen, C.: Carbon nanotube as a Cherenkov-type light emitter and free electron laser. *Physical Review B* **79**(12), 125408 (2009)

Levels of PP produced by Cherenkov radiation on different CNT saturations 13

29. Liu, S., Zhang, P., Liu, W., Gong, S., Zhong, R., Zhang, Y., and Hu, M.: Surface polariton Cherenkov light radiation source. *Physical review letters*, **109**(15), 153902 (2012)
30. Burlak, G., Medina-Ángel, G.: Extended dynamics and lasing of nanoemitters enhanced by dispersing single-walled carbon nanotubes. *Journal of Quantitative Spectroscopy and Radiative Transfer* **296**, 108463 (2022)

**Energy Efficiency
and
Sustainability**

Identification of the solar resource in Mexico City applying multivariate analysis

López-Meraz R. A. ¹[0000-0002-3236-3709], Méndez-Ramírez C. T.¹, Reyes-Cárcamo Y. ²[0009-0004-5440-0963], Jamed-Boza L. O. ¹[0000-0002-6378-758X]

¹ Universidad Veracruzana, Circuito Universitario Gonzalo Aguirre Beltrán s/n, 91000, México

² Centro Universitario Bonpland y Humboldt, Calle de la montaña. No. 65. Col. Lomas de Miradores, 91636, México

raullopez03@uv.mx: R.L-M.; cmendez@uv.mx: C.M-R.;
ing.yanicarcamo@gmail.com: Y.R-C.lojb33@gmail.com: L.J-B.

Abstract. The work presents an innovative method to determine the peak solar hours in the sixteen municipalities of Mexico City. The primary source of information was obtained from different photovoltaic system installation companies, in total the measurement of sixty-six arrangements connected to the electrical grid was achieved. The sample analyzed corresponds to the period from 07/15/2020 to 12/18/2022. The installed power range of the generators is between 2.67 kW to 6.48 kW, all made of monocrystalline silicon. The data acquisition exceeded 90% of the measured information; to fill in the gaps, simulation was applied with smoothed cubic spline techniques and adjustment of trend, seasonality, and cyclical effect. With the 887 complete records for each system, the daily hours of sunshine were estimated, generating a preliminary mapping of the city. In addition, indices were created that compare the solar resource of each municipality with the city average, and multivariate statistical analysis was applied under the version of main components to obtain the characteristic function of the solar resource in each municipality. In this work, the study of a municipality is precisely detailed, with the purpose of allowing designers to determine future solar exploitation projects more efficiently.

Keywords: Peak solar hours; Principal components; Spline with smoothing; Trend-Seasonality-Cyclicity Adjustment.

1 Introduction

In The 2030 Agenda seeks to improve people's quality of life, in particular goal seven proposes guaranteeing access to accessible, safe, and sustainable energy for all. In this sense, the generation of energy through renewable means is of great importance. In Mexico this sector has high viability thanks to the fact that the country is rich in natural resources. According to the National Inventory of Renewable Energy (INER), the energies with the greatest potential are solar and wind, but their promotion is conditioned by political aspects, their costs, and their technological development [1]. In 2013, following [2], the electricity generation mix in the country had three components, namely:

2

82% from fossil sources, 13% from renewables, and 5% from nuclear. With the aim of increasing the contribution of renewable sources in [3], it is estimated that by 2024 the participation of this type of energy will be 21%. On the other hand, [1] seeks to ensure that electricity generation from alternative energy sources reaches at least 35%, starting in 2024.

Given the need to provide electrical energy through renewable means to the population, this work focuses its attention on the solar resource as an input for photovoltaic generation. Its quantification must be made as precise and reliable as possible because its variability is one of the important factors to consider in the insertion of this technology. In the literature there are various tools with which the radiation of a particular site can be known. In [4] solar radiation is measured from meteorological data. Another alternative is presented in [5], where a satellite model was developed to build monthly and annual maps of the potential in Uruguay. Furthermore, in [6] satellite information was treated for the calculation of global solar radiation using geostatistical tools for drawing isolines. Likewise, in [7] there are maps where the radiation can be known, and in [8] the monthly average peak solar hours (PSH) are provided in the period from 1993 to 2005 in Ciudad Universitaria, located in Mexico City (CDMX).

On the other hand, another element to consider is the appropriate treatment of the information. Numerous methods provide new possibilities for quantitative treatment. Multivariate analysis is very useful for carrying out studies of both dependence and interdependence between variables. Generally, when there are many variables, it is possible that some of the information is repeated, in which case it is necessary to eliminate the excess and leave only variables that are representative. This is achieved with the application of multivariate dimension reduction techniques, such as principal component analysis (PCA) [9]. The PCA technique has various applications, for example, in [10] the problem of moving people from the countryside to the city was analyzed. Another example is found in [11], where the urban environmental variables that influence the variability of urban environmental sustainability are questioned. Furthermore, in [12] a set of ten simple environmental quality indicators was transformed into a new one of three non-correlated composite indicators to obtain synthetic environmental quality indexes. Meanwhile, in [13] the problem of the sudden appearance of failures in processes is addressed by designing and implementing automatic methods for detecting and diagnosing failures, and for this statistical process control is applied. However, in energy issues applied to renewable energies, the use of ACP is almost zero.

The present work carried out a multivariate analysis using the PCA technique to obtain the characteristic function of the solar resource in each municipality of CDMX, so that companies in this sector will have this tool to project future photovoltaic arrays (PVA) more accurately. As an example, the case of the Venustiano Carranza municipality is presented. To achieve the above, the PSH was quantified taking as primary information the measurement of the energy produced by 66 PVAs located in the 16 municipalities of CDMX in the period 07/15/2020 to 12/18/2022 (887 records). With the support of cubic spline with smoothing and trend-seasonality-cycle (TSCI) adjustment, missing data in the measurement were simulated. It is important to mention that in all PVAs more than 90% of the information was available, but only 4 complete PVAs

were available. In the end, there were 58,542 data with which other products were generated, such as a map of the PSH of CDMX, and indexes were created that associate the solar resource of each municipality with the global average of the city.

The presentation is structured in four sections. The first, materials and methods, describes the case study, the spline and TSCI fits used to simulate missing measurement data, and discusses how the map and indicators were constructed. Finally, the PCA technique is addressed. The second section corresponds to the most relevant results where the analyzes are applied in the Venustiano Carranza municipality. Below, the most relevant conclusions are presented, and finally the references used in the construction of the article are attached.

2 Materials and methods

2.1 Case of study

The sample obtained from the PVAs in each municipality was variable. Tables 1a and 1b show the geographical coordinates, as well as the installed power of each system. It is noted that all PVAs are made of monocrystalline silicon. The power range is between 2.67 kW to 6.48 kW.

Table 1a. Location and power of PVAs

Municipality	PVA	Power (kW)	Longitude (W)	Latitude (N)
Gustavo A. Madero	A01.1	3.550	99.1366	19.5486
	A01.2	3.160	99.1519	19.5253
	A01.3	3.330	99.1299	19.5072
Azcapotzalco	A01.4	4.005	99.0846	19.4917
	A02.1	4.005	99.2040	19.5027
	A02.2	4.005	99.1986	19.4839
	A02.3	4.005	99.1738	19.4897
	A02.4	4.320	99.1738	19.4738
	A03.1	3.560	99.2075	19.4671
	A03.2	4.005	99.2198	19.4334
Miguel Hidalgo	A03.3	4.005	99.2130	19.4255
	A03.4	3.960	99.2308	19.4140
	A03.5	4.320	99.2469	19.3925
Cuauhtémoc	A04.1	3.330	99.1312	19.4572
	A04.2	4.005	99.1313	19.4528
	A04.3	4.320	99.1553	19.4120
	A04.4	4.005	99.1464	19.4561
Venustiano Carranza	A05.1	3.960	99.1237	19.4515
	A05.2	4.005	99.0791	19.4418
	A05.3	4.320	99.0997	19.4315
Cuajimalpa de Morelos	A06.1	2.670	99.2905	19.3527
	A06.2	3.960	99.3005	19.3636
	A06.3	3.950	99.3023	19.3578

4

	A06.4	3.560	99.3019	19.3474
	A06.5	3.115	99.2736	19.3747
	A07.1	4.860	99.2014	19.3842
	A07.2	3.560	99.2096	19.3589
Álvaro Obregón	A07.3	4.320	99.2171	19.3116
	A07.4	3.330	99.2098	19.3209
	A07.5	3.560	99.2636	19.3224
	A08.1	3.560	99.1406	19.4023
	A08.2	4.400	99.1504	19.3934
Benito Juárez	A08.3	4.400	99.1597	19.3795
	A08.4	5.400	99.1797	19.3761
	A08.5	6.480	99.1853	19.3669

Table 1b. Location and power of PVAs

Municipality	PVA	Power (kW)	Longitude (W)	Latitude (N)
	A09.1	3.560	99.0952	19.3961
Iztacalco	A09.2	4.320	99.1219	19.3882
	A09.3	4.860	99.1328	19.3793
	A10.1	3.330	99.2166	19.3267
	A10.2	5.530	99.2322	19.3231
La Magdalena Contreras	A10.3	4.320	99.2229	19.3295
	A10.4	3.960	99.2281	19.3299
	A10.5	4.440	99.2289	19.3274
	A10.6	3.960	99.2409	19.3053
	A11.1	3.960	99.1600	19.3427
	A11.2	2.670	99.1561	19.3495
Coyoacán	A11.3	3.115	99.1613	19.3490
	A11.4	3.960	99.1621	19.3199
	A11.5	4.005	99.1580	19.3065
	A11.6	4.320	99.1899	19.3058
	A12.1	2.765	99.0562	19.3624
Iztapalapa	A12.2	2.960	99.1103	19.3537
	A12.3	2.960	99.0752	19.2941
	A13.1	3.960	99.2224	19.3057
	A13.2	4.005	99.2376	19.2937
Tlalpan	A13.3	3.960	99.2153	19.2943
	A13.4	4.320	99.2155	19.2811
	A13.5	4.320	99.2338	19.2380
	A14.1	3.330	99.1101	19.2911
Xochimilco	A14.2	3.330	99.1396	19.2711
	A14.3	3.330	99.1183	19.2311
	A15.1	3.160	99.0422	19.2859
Tláhuac	A15.2	3.960	99.0039	19.2708
	A16.1	2.765	99.0226	19.1918
Milpa Alta	A16.2	2.960	99.0263	19.1897

A16.3	3.520	99.0280	19.1840
-------	-------	---------	---------

2.2 Spline fitting

The spline model fits to the behavior of the (sometimes oscillating) information, with any trend, whose distribution function is not known, or the characterization of the curve is not easy to solve in a conventional way it does not assume a priori a functional form [14]. This setting has the particularity of unite polynomials by segments through nodes, avoiding producing acute changes in the smooth curve of the model allowing the combination of this type of functions.

The adjustment type spline with smoothing technique corresponds to the area of numerical methods in conjunction with the calculus of variations, to achieve the characteristics mentioned, the function, the first and second derivative valued at each x-coordinate should be same. If we have the set of points (x_i, y_i) the original observed information with $i = 1, 2, \dots, n$, where each x_i can easily be extended to the case of confluent abscissa, meaning that each 'x' may contain more than one 'y' with some degree of dependency between the adjacent x's, obtaining a cubic polynomial between each pair of consecutive points is defined with a local variable $t_i = x - x_i$ and their corresponding domain $h_i = x_{i+1} - x_i$ generating $(n - 1)$ polynomials whose function, first and second derived are:

$$f(t) = a_0 + a_1t + a_2t^2 + a_3t^3 \quad (1)$$

$$f'(t) = a_1 + 2a_2t + 3a_3t^2 \quad (2)$$

$$f''(t) = 2a_2 + 6a_3t \quad (3)$$

The parameter of smoothing lambda (λ) it comes from the formulation of the equations of Euler-Lagrange, when λ tends to zero the resulting curve (presents "greater acuity" vertical) is the classic cubic C-Spline interpolation [15,16], when λ tends to infinity the resulting curve tends to the line obtained by least squares adjustment. The shape and smoothness of a spline relies heavily on this value of smoothing, which is selected from a measure that balances the bias and variance of this class of estimators [17].

2.3 Trend-Seasonality-Cycle

With the spline of the 62 PVAs that have an absence of information, the presence of three factors was recognized, namely: trend, seasonality, and cyclicity. In this way, the Trend-Seasonality-Cycle (TSCI) model from numerical methods was applied. Its representation according to [18] is presented in (4).

$$y_i = T_i S_i C_i + \varepsilon_i \quad (4)$$

Where the component T_i is the trend and is made up of expression (5).

$$T_i = \beta_0 + \beta_2(\beta_1 - \beta_0)\sin[\beta_3(z_i - \beta_4)] \quad (5)$$

6

The factor S_i is the seasonality and its expression appears in (6).

$$S_i = 1 + \beta_5 \sin[\beta_6(z_i - \beta_7)] \quad (6)$$

The third element corresponds to the cyclical effect, it is expressed in equation (7).

$$C_i = 1 + \beta_8 \sin[\beta_9(z_i - \beta_{10})] \quad (7)$$

Finally, ε_i is the instability or error.

y_i is the projection of the estimated average daily energy (kWh). The parameters to be used in the simulation are: β_0 additive constant which is initially the minimum value of the measured data, β_1 maximum value of the measured data, β_2 attenuation, β_3 , β_6 and β_9 frequencies of the sine function, β_4 , β_7 and β_{10} displacements of the sine function, β_5 and β_8 amplitudes of the sine function.

The simulation with TSCI optimizes the coefficients of each factor in steps by minimizing the sum of squares of the difference. In this way, first the coefficients corresponding to the trend are found, once these values are set, the seasonality coefficients are found, and with the two previous elements complete, the parameters of the cyclical part are found. The tool used to achieve the appropriate results is the Solver plugin program [19]. The calculation conditions with the Solver were the following:

- 1) Resolution Method: Nonlinear GRG (Generalized Reduced Gradient)
- 2) Constraint precision: 1×10^{-6}
- 3) Convergence: 1×10^{-6}
- 4) Advanced Derivatives
- 5) Population Size: 900

Furthermore, for the instability the variance was estimated by the difference of the total variance of the measured PVA minus the inherent variation of the spline curve, in this way the simulation of the missing data was developed, that is, the standard deviation for the unstable effect. It was obtained from the square root of the difference between the total variance of the data minus the variance of the spline. Equation (8) shows the above.

$$\sigma_I = \sqrt{(\sigma_T^2 - \sigma_S^2)} \quad (8)$$

Where σ_I is the standard deviation of the instability, σ_T^2 is the total variance and σ_S^2 represents the variance of the spline fit.

As the behavior of regions (municipalities) is expected to be similar each year, it was decided to use the TSCI tool as it is the most appropriate to project future PSH events.

2.4 Mapping and indexes

With the nominal capacity of each PVA (kW) and the energy produced (887 records), the PSH estimate was obtained for the 66 PVAs. From the results, a map was created with three colors, namely: yellow (4.3 – 4.8 PSH), orange (4.8 – 5 PSH), and red (5 – 5.9 PSH). This scale was designed to contrast the areas with the greatest solar resources with those with the lowest potential. In areas where measured information was not

7

available, interpolations were carried out with the closest PVA, and the data provided in [20]. For its part, in the regions south of Milpa Alta, Tlalpan. La Magdalena Contreras, Álvaro Obregón and Cuajimalpa de Morelos, where no measured information was obtained nor was there any reference, it was decided to leave them blank.

With the objective of creating the daily indexed PSH, the city's global average (GA) was set with respect to daily hours in each PVA. Let $j = 1, 2, \dots, 887$ days and let $i = 1, 2, \dots, 16$ municipalities, we have the expression (9):

$$Id_{ij} = \frac{\text{Daily Average for each municipality}_i}{GA} \quad (9)$$

Where Id_{ij} is the daily index of municipality i on day j .

With the data from the 66 PVAs during the 887 days, GA was determined. On the other hand, according to the information from the systems located in each municipality, the average solar resource in each of them was obtained (MA_i). From these calculations, the index of the municipalities is determined, as seen in (10).

$$MI_i = \frac{MA_i}{GA} \quad (10)$$

With the above, it is possible to visualize whether that particular day had greater (>1) or less (<1) solar resource than the global average. In this way, indexing allows us to observe the fractions of increase or decrease that are easily converted into percentages.

2.5 Principal Component Analysis

The basis of multivariate analysis (MA) is to analyze, represent and interpret data where there is more than one statistical variable from a sample of individuals. The observed variables are homogeneous and correlated, but none predominates over the others [21]. PCA is an AM method that reduces the dimensionality of the problem, while maintaining as much information as possible. From the original variables, the information is reduced to a few elements, new uncorrelated variables. In this work, the criterion for selecting the principal components (PC) was to maintain the factors that manage to explain a high percentage of the total variance. The nomenclature of the matrices used to obtain the PC is presented below.

Let X be the original data matrix (PSH), let Y be the PC matrix (every principal component is a linear association of the original data). Let A_0 be a matrix of additive constants that allows generating PC with more manageable magnitudes. Let A be the matrix of the coefficients that make up the linear combinations of the new set of variables Y . The sizes of the matrices: X is $(n \times p)$, Y is $(n \times p)$, A_0 is $(n \times p)$ and A is $(p \times p)$.

To obtain the PCs, the following equations (11), (12) and (13) were used.

$$\text{Principal association expression: } Y = A_0 + XA \quad (11)$$

$$\text{Return to original PSH values: } X = (Y - A_0)A^{-1} \quad (12)$$

8

To form the matrix of additive constants, a vector α_0 of size $(p \times 1)$ is first created. This vector contains the coefficients of the additive constants of each principal component.

$$A_0 = \mathbf{1}_{(n \times 1)} \alpha'_0 \tag{13}$$

Matrix Y represents the new set of uncorrelated variables from the original PSH data X . The daily indexing associated with each municipality Id_{ij} is now our response to which we will regression with the Y . The function found only takes the y 's that are statistically significant. This last function is the characteristic function of each municipality. In this application, equation (12) was not used because we cannot modify the principal components Y since they are given by environmental conditions.

3 Results

3.1 Solar resource

Fig. 1 represents the estimated daily average solar resource for CDMX. In general, the distribution of PSHs is noticeable, making the considerable application potential of photovoltaic technologies evident. Taking as reference the global daily average obtained from 4.924 PSH, it is concluded that facilities of this type will have an important productive behavior associated with high profitability. It is highlighted that in the 16 municipalities the average daily value of 4.3 PSH is exceeded, which is higher than the average resource in Germany of 3 PSH [22].

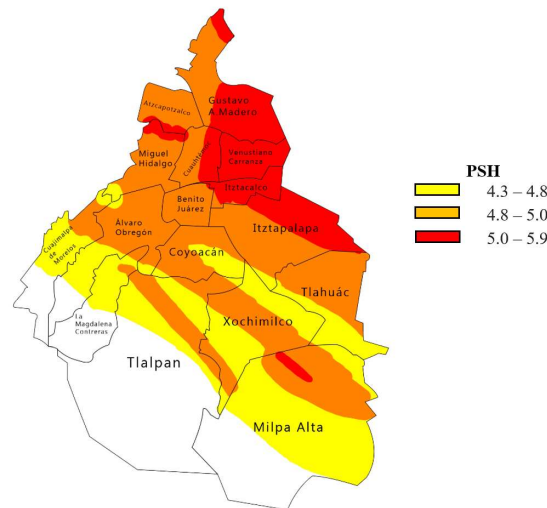


Fig. 1. Map of solar resources in the municipalities of CDMX.

Additionally, the percentage of PSH days above the global average of CDMX was obtained, that is, with more than 78% are the municipalities of Venustiano Carranza, Cuauhtémoc and Gustavo A. Madero. On the contrary, with less than 33% are La Magdalena Contreras, Cuajimalpa de Morelos and Álvaro Obregón.

For its part, Fig. 2 shows the index of the Venustiano Carranza municipality. A third-degree Spline curve was fitted with a smoothing coefficient of 30000 to obtain an adequate representation of the behavior, this is verified with a high value of $R^2 = 0.956076$. It is observable that a high percentage of the measurements are higher than the global average for CDMX (1). That is, it is highly viable to install PVA in this municipality. At the same time, the cyclical effect of the data obtained is notable.

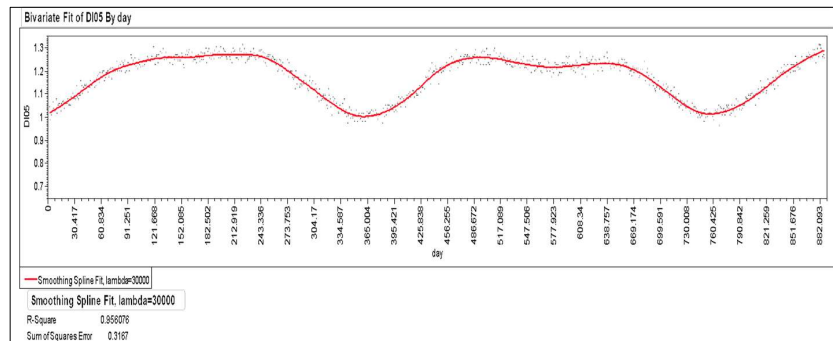


Fig. 2. Spline of the Venustiano Carranza municipality index.

3.2 Characteristic function

The multivariate study allows us to identify the PCs and obtain their values. Knowing these elements, the regression was made between them and the average daily index. Through the factor analysis it is observable that the first is the most weighting, that is, the eigenvalues represent the weight that each PC has in its linear association. Fig. 3 shows the correlation matrix and the confidence intervals for them. Additionally, the scatter plot matrix is shown.

To verify consistency and behavior of the indexes, the JMP [23] was asked to do a curve fitting to identify the statistical behavior of the municipality index. Fig. 4 shows, vertically, the original data, and horizontally the predictive adjustment for the Venustiano Carranza municipality. The PCA was carried out with the three PCs, however, only the first two were the most representative approaching 93.597% of the information. In this way, the predicted index is a function of Y_1 and Y_2 . The fitted model turned out to be a complete quadratic polynomial (including its crossover). Furthermore, the prediction profile delivers the uncertainty by combining Y_1 and Y_2 . It is highlighted that R^2_{press} is the best indicator of the predictive quality of an analysis, in this case $R^2_{press} = 0.997774$, showing that 99.78% is justified by the model found.

The characteristic function is given by Eq. 14.

10

$$DI_{05} = 1.1725247 + 0.0634198Y_1 + 0.0133726Y_2 - 0.000442Y_1Y_2 - 0.000414Y_1^2 + 0.0006628Y_2^2 \tag{14}$$

With all the data of the adjusted index, the distribution that is closest was obtained. In this case, and in 13 of the 16 municipalities, the one that best fits are Johnson S_I distribution. Fig. 5 details the above.

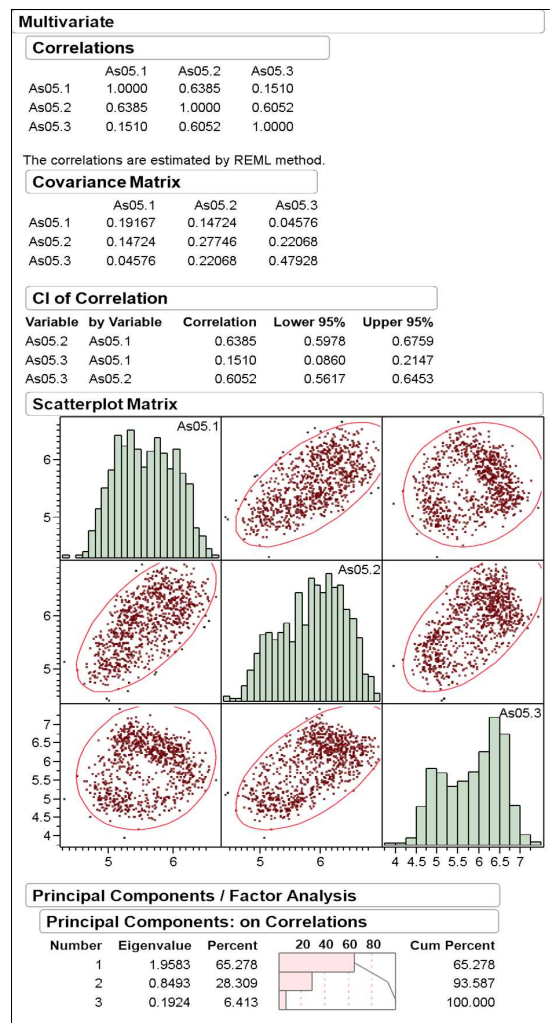


Fig. 3. Multivariate study under the principal components version applying factor analysis for the Venustiano Carranza municipality.

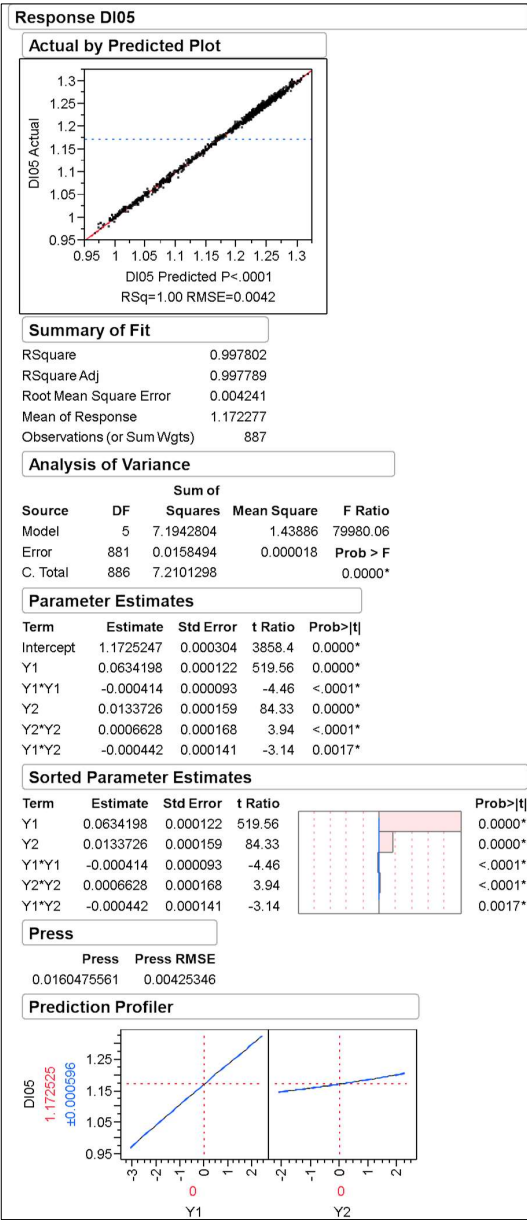


Fig. 4. Approach of the index obtained by principal components to the index calculated for the Venustiano Carranza municipality.

12

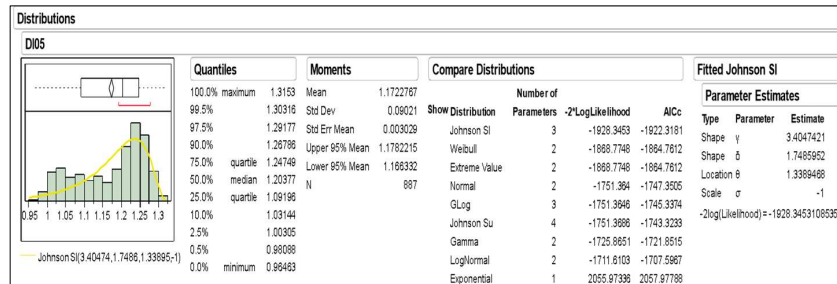


Fig. 5. Behavior of the daily index obtained from the Venustiano Carranza municipality.

4 Conclusions

A geographic mapping of PSHs was generated for each municipality, providing a useful and practical estimate. In addition, the creation of indexes allows a direct comparison with the CDMX average, and you can easily visualize in percentage which municipalities have the best potential. The characteristic function manages, through its regression equation, to closely approach the individual behavior by reducing the elements to be considered, confirming that principal component analysis is appropriate for this energy application. The products obtained offer, together, a reliable solution for photovoltaic system installers for the design of upcoming projects. Future work will consist of finding the principal components of the remaining municipalities covering the entire CDMX.

References

1. Secretaría de Energía (SENER). Prospectiva del Sector Eléctrico 2013-2027, México. (2013).
2. Secretaría de Energía (SENER). Sistema de Información Energética (SIE), México. (2014).
3. Secretaría de Energía (SENER). Prospectiva de Energías Renovables 2013-2027, México. (2013).
4. Vanegas, M., Villicaña, E., y Arrieta, L. Cuantificación y caracterización de la radiación solar en el departamento de La Guajira-Colombia mediante el cálculo de transmisibilidad atmosférica. Prospect. Vol. 13. No. 2. pp.54-63. (2015).
5. Alonso, R. Estimación del recurso solar en Uruguay mediante imágenes satelitales. Tesis doctoral. Universidad de la República. (2017).
6. Righini, R., Grossi, H. Utilización preliminar de información goes y métodos geoestadísticos para la evaluación del recurso solar en Brasil. Avances en energías renovables y medio ambiente. Vol. 5. (2001).
7. The World Bank, Solar resource data: Solargis. (2017).
8. https://areas.geofisica.unam.mx/radiacion_solar/. consulted on August 15, 2023.
9. Pérez, C. Técnicas de análisis multivariante de datos. Aplicaciones con SPSS. Madrid. Pearson. pp. 121- 154. (2004).

10. León, A., Llinás, H., y Tilano, J. Análisis multivariado aplicando componentes principales al caso de los desplazados. *Ingeniería y desarrollo*. No. 23. (2008).
11. Giraud, L., Morantes, G. Aplicación del análisis multivariante para la sostenibilidad ambiental urbana. *Bitácora* 27. No. 1. pp. 89-100. (2017).
12. Yengle, C. Aplicación del análisis de componentes principales como técnica para obtener índices de calidad ambiental. *UCV-Scientia*. Vol. 4. No. 2. pp. 145-153. (2012).
13. García, D., Fuente, M. Estudio comparativo de técnicas de detección de fallos basadas en el Análisis de Componentes Principales (PCA). *Revista Iberoamericana de Automática e Informática Industrial*. No. 8. pp. 182-195. (2011).
14. Bowman A., Azzalini A. *Applied smoothing techniques for data analysis: The kernel approach with s-plus illustrations*. Oxford Statistical Science Series, 18. Oxford: Clarendon Press. p. 193. (1997).
15. Mathews, J. H., Fink, K. D. *Numerical Methods Using MATLAB*. Third ed., Prentice-Hall, Inc., Englewood Cliffs, NJ. (1999).
16. Grasselli, M., Pelinovsky, D. *Numerical Mathematics*. Jones & Bartlett Publishers, Inc., CA. (2008).
17. Härdle W. *Applied nonparametric regression*. Econometric Society Monographs. Cambridge, UK: Cambridge University Press. p. 333. (1992).
18. Abril, J. Análisis de la evolución de las técnicas de series de tiempo. Un enfoque unificado. *Estadística*, 63, 181, pp. 5-56. (2011).
19. Walsh, S., Diamond, D. Non-linear curve fitting using Microsoft excel solver. *Talanta*. Vol. 42. Issue 4. pp 561-572. (1995).
20. Martínez, I., Weber, B., Durán, D., Díaz, L. Aprovechamiento de la Energía Solar Fotovoltaica en el Estado de México. *Universidad Autónoma del Estado de México*. (2016).
21. Cuadras, C. *Nuevos métodos de análisis multivariante*. Barcelona. (2014).
22. Whiting, K., Carmona, L., Castellot, P. Aplicación de la energía solar fotovoltaica interconectada a la red eléctrica. Caso de estudio Thierhaupten-Alemania. *Revista Ontare*. Vol. 2 No. 2. pp. 145-170. (2015).
23. JMP 8.0.2 SAS Institute Inc. © (2009).

Optimización de dispositivo para trazado I-V en línea de módulos solares individuales y comunicaciones PLC

José Ignacio Morales Aragonés ¹ [0000-0002-9163-9357] Víctor Ndeti Ngungu ² [0009-0001-5933-8482] Víctor Alonso Gómez ¹ [0000-0001-5107-4892] Alberto Redondo Plaza ¹ [0000-0002-2109-5614] Luis Hernández Callejo ¹ [0000-0002-8822-2948] Sara Gallardo Saavedra ¹ [0000-0002-2834-5591] Mario Eduardo Carbonó Dela Rosa ³ [0000-0002-6741-6145] and Héctor Felipe Mateo Romero ¹ [0000-0002-5569-3532]

¹ Universidad de Valladolid, ² University of Pretoria, ³ Universidad Nacional Autónoma de México,
lncs@springer.com

Abstract. Tras la publicación por parte de este equipo de investigación de varios artículos donde se propone un sistema de trazado de curvas I-V online de módulos solares individuales y un sistema de comunicaciones PLC por bucle resonante específico para la topología del cableado fotovoltaico, se aborda en este artículo la integración y mejora de estos dos sistemas en un único dispositivo destinado a la monitorización y el diagnóstico de plantas solares fotovoltaicas. La principal novedad introducida se refiere al sistema de comunicaciones PLC, con un rediseño del hardware que permitirá un modo de propagación en onda viajera resonante (según una propuesta teórica anterior), y gracias a ello aumentar la frecuencia portadora hasta los 16 MHz. El resultado del trabajo será un diseño en el que se han revisado los planteamientos originales para garantizar no solo la funcionalidad, sino también la robustez y durabilidad, aumentando además considerablemente la velocidad de propagación de la parte de comunicaciones, todo ello sin abandonar la filosofía de bajo coste que inspiró los artículos anteriores.

Keywords: Planta solar, Trazado I-V, Comunicaciones PLC.

1 Introducción.

La energía solar fotovoltaica ha experimentado un crecimiento espectacular durante los últimos años [1], resultando un recurso alternativo a los combustibles fósiles para la generación de energía sin contribuir a la acumulación en la atmósfera de gases de efecto invernadero. Esta gran proliferación de plantas solares fotovoltaicas acarrea nuevos desafíos en lo que se refiere a las labores de mantenimiento que se deben afrontar inevitablemente [2]. [3] [4] [5]. La monitorización y el diagnóstico de estas plantas aparece entonces como un elemento fundamental para obtener información sobre la degradación del sistema y actuar en consecuencia, garantizando así que siempre se trabaja en condiciones óptimas de rendimiento.

Recientemente este mismo autor publicó varios artículos [6] [7] [8] con el objetivo común de mejorar la monitorización y el diagnóstico de las plantas solares fotovoltaicas

2

mediante dispositivos de bajo coste. En estos artículos se proponía el desarrollo de un dispositivo capaz de realizar trazas tensión-corriente (I-V) de módulos solares individuales sin desconectarlos de la asociación serie en que están integrados (STRING) y sin interrumpir la producción de energía. La necesidad obvia de un sistema de comunicaciones para evacuar los datos obtenidos por este dispositivo llevó a pensar en un sistema PLC (“Power Line Communications” en inglés) en línea con la filosofía de bajo coste abordada desde el principio, que fue objeto de dos nuevos artículos [9] [10]. Estos dos sistemas fueron desarrollados independientemente y descritos en los artículos mencionados, sin embargo, para obtener un dispositivo susceptible de una aplicación práctica ambos sistemas requieren ser revisados e integrados en un solo dispositivo.

1.1 Subsistema de Trazado I-V.

El diseño de un dispositivo de bajo coste capaz de realizar el trazado de curvas I-V de módulos solares individuales integrados en un STRING fotovoltaico sin desconectarlos del mismo y sin interrumpir la producción de energía ha sido objeto de algunos trabajos anteriores [11] [12] y de dos artículos de este mismo autor [6]. [8]

El artículo [6] presenta dos estrategias diferentes para el trazado “online” de las curvas I-V de módulos solares individuales. Una de ellas está totalmente descentralizada y tarjetas electrónicas individuales instaladas en cada módulo se encargan de realizar el barrido necesario y de capturar los datos para generar las curvas. La otra es una estrategia mixta en que el barrido se realiza a nivel de todo el STRING, pero los datos se toman individualmente en cada módulo. La comparación entre estos dos métodos resulta en una preferencia por el método totalmente descentralizado, entre otras razones porque es el único de los dos que no necesita una desconexión completa del STRING ni siquiera durante unos pocos milisegundos. Este sistema totalmente descentralizado se ha usado profusamente tras la publicación del artículo en otros proyectos que requerían la obtención de las curvas características de los módulos. La utilización constante de este dispositivo puso en evidencia algunas deficiencias que podrían dificultar una hipotética introducción en el mercado de tal dispositivo. Aquí se analizarán estos problemas y las soluciones que se han propuesto para acercar este diseño a un dispositivo capaz de ser utilizado de forma práctica con mayor fiabilidad y robustez.

Respecto al subsistema de trazado I-V se encontraron dos cuestiones que requerían atención:

- La durabilidad limitada del transistor de potencia que se usa para realizar los barridos de tensión y corriente.
- La pérdida de sensibilidad del sensor de corriente de efecto Hall respecto a los valores reportados en sus características técnicas.

En cuanto a la primera cuestión se observó que, tras la realización sin problemas de muchos trazados de curvas características de los módulos en nuestra miniplanta de pruebas dentro del Campus Duques de Soria de la Universidad de Valladolid, cuando se intentó validar el dispositivo en otra planta diferente (especialmente en condiciones de alta irradiancia), en algunas ocasiones se producía la rotura de uno de los transistores MOSFET utilizados. Esto es una cuestión que solo fue observada tras una prolongada

utilización del dispositivo, que afectaba directamente a la fiabilidad del sistema y que requería analizar la causa de este fenómeno.

La segunda cuestión observada fue una importante discrepancia entre la sensibilidad del sensor de corriente real y la informada por el fabricante. Se trata de un sensor de efecto Hall del fabricante Texas Instruments (TMCS1100) que perturba mínimamente el sistema que se mide evaluando el campo magnético asociado a la corriente medida. Esto hace que este tipo de sensores sean especialmente sensibles a campos magnéticos externos que pueden falsear las medidas de corriente. En nuestro caso comprobamos que el fabricante informaba de una sensibilidad de 400 mV/A pero a través de nuestras medidas se observaba una sensibilidad más próxima a los 200 mV/A, casi la mitad de lo que debería ser.

1.2 Subsistema de Comunicaciones.

En los artículos mencionados en la sección anterior aparecía la necesidad de implementar un sistema de comunicaciones eficaz entre cada módulo fotovoltaico y la caja de centralización del STRING (CB, “Combiner Box” en inglés) para poder evacuar los datos obtenidos en el trazado de las curvas I-V. Con esta motivación se escribieron dos nuevos artículos [9] [10] en los que se propuso un sistema de comunicaciones PLC que utilizaba el propio cableado de potencia de la instalación fotovoltaica como soporte de las comunicaciones, de acuerdo con el objetivo de minimizar costes que se adoptó en los artículos iniciales. Los primeros planteamientos para implementar este sistema de comunicaciones ya mostraron que la topología específica del cableado de una instalación fotovoltaica difería de aquella sobre la que se utilizan los sistemas PLC de forma habitual [13] (generalmente líneas eléctricas con dos cables que corren paralelos el uno al otro). Además, durante el trabajo de análisis del estado del arte, se constató que esta circunstancia no había sido debidamente considerada en la literatura, y se encontraron incluso diseños que integraban componentes comerciales diseñados para líneas PLC tradicionales montados sobre esta topología específica del cableado fotovoltaico [14] [15] [16]. En cada agrupación serie de módulos (STRING) esta topología consiste en un único cable que parte de la caja de centralización y regresa a la misma formando un bucle en que generalmente los recorridos de ida y vuelta están a una distancia que no permite asumir las características de una línea bifilar. Esta sencilla circunstancia cambia radicalmente la base teórica de la propagación por el cableado fotovoltaico y requiere al menos un análisis teórico básico que se llevó a cabo en el artículo [9]. Allí se expuso la posibilidad de cerrar el camino de la señal de comunicaciones en forma de bucle mediante un condensador en la caja de centralización CB o entrada del inversor de cada STRING, según el caso, para formar un anillo y trabajar así llevando este anillo a resonancia y sintonizándolo de forma similar a como se hace con las antenas de bucle. De esta forma la topología de un STRING fotovoltaico se puede transformar en una ventaja, ya que una señal portadora resonante en este anillo requiere un reducido aporte de potencia para propagarse y es posible garantizar un nivel de señal uniforme a lo largo del mismo.

Para frecuencias portadoras con longitudes de onda mucho mayores que la longitud física del anillo se obtuvo una propagación con un nivel de señal casi uniforme y una

4

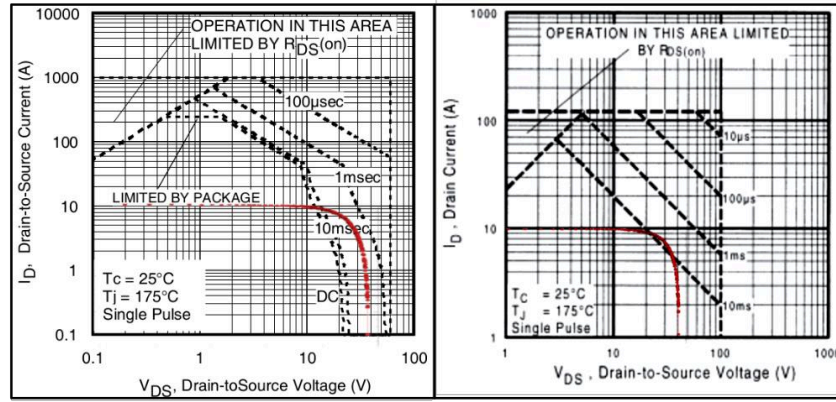
fase aproximadamente constante a lo largo del mismo (propagación en modo 0), y esto permitió implementar físicamente el sistema de comunicaciones PLC en un STRING con una longitud de cableado típica de 20 m y una frecuencia portadora de 1 MHz tal y como describe el artículo [10]. Sin embargo, si se pretende utilizar este medio de propagación resonante con frecuencias superiores, para las que encontramos un número entero de longitudes de onda a lo largo del anillo (condición de resonancia), los planteamientos teóricos del documento [17] permitían llegar a la conclusión de que el modo ideal de transmisión consistiría en una onda viajera. En la práctica hemos comprobado que la presencia inevitable de puntos de reflexión a lo largo del anillo hace que de forma natural los modos que se excitan consistan en ondas estacionarias, que por lo tanto presentan nodos en los que la señal se reduce considerablemente. Por ello, encontrar un método y una implementación física capaz de soportar las comunicaciones PLC sobre un anillo resonante con propagación en forma de onda viajera resulta un importante paso hacia adelante y puede llevarnos a trabajar con frecuencias muy superiores a 1 MHz (que fue la frecuencia alcanzada en [10]) y, por tanto, a mejorar notablemente las velocidades de propagación conseguidas.

2 Materiales y Métodos

2.1 Subsistema de Trazado I-V

Durabilidad del Transistor de Potencia. La rotura del transistor MOSFET descrita en el apartado anterior se observó principalmente en condiciones de alta irradiancia y sobre módulos con una potencia de pico superior a aquellos con los que se hicieron inicialmente las pruebas de validación. Esto sugiere que la causa debe buscarse en un exceso de potencia. La razón de este problema fue evidente cuando se superpusieron los trayectos de trazado de las curvas I-V sobre el diagrama del Área Segura de Trabajo (Safe Operating Area -SOA- en inglés) facilitado por el fabricante de los transistores MOSFET.

Estos gráficos se muestran en Figura 1, donde se puede observar con puntos rojos la trayectoria seguida por el barrido que genera nuestro dispositivo sobre módulos de 40 V (en circuito abierto) con una corriente de cortocircuito de 10 A (módulos de 400 Wpico y máxima irradiancia) sobre el diagrama SOA facilitado por el fabricante. En este diagrama se indican los tiempos máximos en que puede trabajar el transistor de forma segura en cada región del espacio tensión/corriente.



1.a: IRLS3036

1.b: IRL540ns

Fig. 1. Trayecto del mismo trazado I-V (puntos rojos) sobre los diagramas de SOA (Safe Operating Area) del transistor del diseño original (1.a) y del nuevo transistor (1.b)

Para el transistor IRLS3036 (figura 1.a), utilizado en el diseño original, se puede observar que la trayectoria invade en algo más de la mitad de su recorrido la región situada entre 10 ms y 1 ms. Considerando que el tiempo que se utiliza para generar todo el barrido y recorrer la curva I-V completa está entre 20 ms y 30 ms está claro que la mitad derecha de esta curva supera el tiempo máximo admisible para trabajar de forma segura en esta región.

Para solucionar este problema se tomaron dos medidas diferentes:

- La primera y más obvia fue la búsqueda de un transistor MOSFET con una Área de Trabajo Segura (SOA) más amplia, adaptada a las necesidades de módulos solares con corrientes máximas de cortocircuito alrededor de los 10 amperios, que son valores frecuentes en el mercado.
- La segunda fue una modificación del firmware para implementar una estrategia de trazado diferente a la original y más benévola con la exposición a altas potencias del transistor.

La oferta en el mercado de transistores que cumplieren todas las características que necesitábamos para esta aplicación es muy limitada. Aparte de la necesidad de un área segura de trabajo más amplia, es imprescindible mantener una resistencia del canal muy baja en el estado de conducción para eludir caídas de tensión no deseadas en la línea fotovoltaica y que además la puerta del transistor sea totalmente controlable con los niveles de tensión procedentes del microprocesador, alrededor de los 5 V.

Tras la prueba de diferentes modelos se encontró el mejor candidato para este diseño en el MOSFET IRL540NS. La figura 1-b muestra la superposición del trayecto de la curva IV sobre el diagrama SOA para este transistor, y como se ve, la curva apenas toca la línea de 10 ms, lo que proporciona un margen de trabajo mucho más seguro que en el caso del MOSFET anterior.

6

La segunda medida adoptada contra este problema fue un cambio en la estrategia del trazado I-V. Originalmente un primer transistor MOSFET cortocircuitaba en una conmutación rápida el módulo bajo medida, permitiendo además el paso de la corriente de STRING para no interrumpir la producción de potencia, y a continuación el transistor MOSFET de barrido (que es el que nos ocupa) implementaba todo el trazado de la curva IV desde el cortocircuito al circuito abierto, para finalmente regresar al punto de máxima potencia (MPP) mediante una nueva conmutación rápida. El cambio de estrategia adoptado consistió en trazar la curva I-V en dos secciones consecutivas: la primera desde el MPP en que se encuentra el módulo originalmente hasta el circuito abierto regresando de nuevo al MPP mediante una conmutación rápida, y a continuación e inmediatamente se trazaría la curva desde el MPP al punto de cortocircuito regresando de nuevo al MPP con una segunda conmutación rápida. De esta forma el tiempo de exposición del transistor de barrido a los niveles de máxima potencia se divide por la mitad mejorando aún más el margen de trabajo seguro del dispositivo. Este cambio de estrategia en ningún momento supone un aumento en el tiempo que se invierte en hacer el trazado y por lo tanto no interfiere más que la anterior estrategia en la producción de energía del STRING. En la Figura 2 se ilustra este cambio de estrategia.

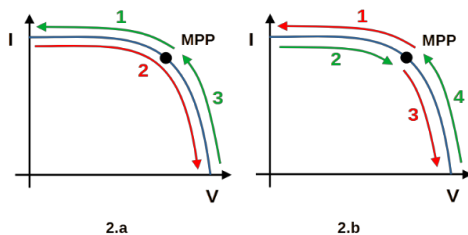


Fig. 2. Estrategia de barrido para el trazado I-V partiendo del punto de máxima potencia (MPP) en el diseño original (2.a) y en el diseño modificado (2.b). Las líneas verdes son transiciones casi inmediatas y las líneas rojas transiciones a la velocidad de barrido (más lentas)

Sensibilidad del Sensor de Corriente. El sensor utilizado en los artículos [6] y [8] mide la corriente evaluando el campo magnético asociado a una línea interna por la que circula. Esta línea interna está orientada paralelamente a la línea de pines de uno de los laterales del circuito integrado, y por tanto cualquier corriente externa con un recorrido paralelo a esta línea superpondrá un campo magnético extra al medido por el sensor, que arrojará medidas superiores o inferiores al valor correcto (según el sentido de la corriente externa interferente). Un análisis de la placa de circuito impreso que se utilizó en nuestro dispositivo nos permitió comprobar que las pistas que llevan la corriente hasta el sensor tenían un recorrido precisamente paralelo a la línea de pines y muy cerca de ésta, por lo que el campo magnético generado en estas pistas influía claramente en la medida. La solución fue un rediseño de la placa de circuito impreso donde nos aseguramos de que las pistas que llevan la corriente hasta el sensor se aproximaban al mismo de forma perpendicular a la línea de pines. En la Figura 3 se puede ver una comparación entre el antiguo diseño de la placa de circuito impreso y el nuevo. En esta

figura se comprueba que además de modificar las pistas para que se acerquen perpendicularmente a la línea de pines el sensor se ha alejó del transistor de potencia donde hay presentes fuertes corrientes y por lo tanto fuertes campos magnéticos. De esta forma las medidas de sensibilidad indicaron valores muchísimo más cercanos a lo que informaba el fabricante.

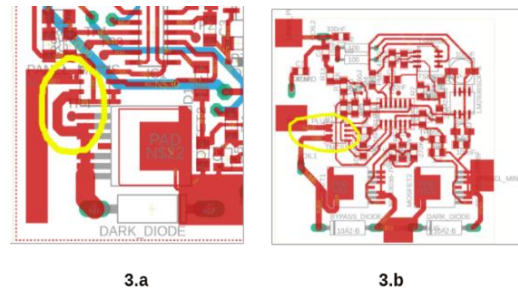


Fig. 3. Modificación en el diseño de la placa de circuito impreso para evitar la influencia de campos magnéticos externos en el sensor de corriente de efecto Hall. Diseño original en 3.a y modificado en 3.b

2.2 . Subsistema de Comunicaciones.

La principal novedad que se presentará en este artículo se refiere precisamente a este subsistema de comunicaciones, que se mejorará para trabajar con frecuencias superiores a las logradas en [10] (1MHz) excitando sobre el anillo de comunicaciones PLC un modo resonante en forma de onda viajera. Este modo de propagación se propuso teóricamente en [9] como la mejor opción para un sistema de comunicaciones PLC sobre una topología de cableado en forma de anillo cerrado sin aportar ninguna implementación práctica, y aquí presentaremos este primer diseño práctico funcional que permitirá multiplicar por un factor de 10 la velocidad de propagación del sistema.

Además, para optimizar el sistema de comunicaciones se consideraron algunas características del sistema que no fueron tenidas en cuenta originalmente, y que afectan a las diferencias entre el transceptor de la “Combiner Box” (CB) y de los de los módulos:

- La comunicación es de tipo “half dúplex”, con un sentido de la comunicación de la CB hacia los módulos en modo difusión (CB transmite y todos los módulos escuchan: INTERROGACIÓN) y un sentido de los módulos hacia CB en modo punto a punto (el módulo interrogado transmite y solo CB escucha: RESPUESTA) de forma que estos modos se alternan en el tiempo y nunca se producen simultáneamente.
- Esta comunicación será fuertemente asimétrica en cuanto a ambos modos se refiere. En general la interrogación consistirá en un único comando y la dirección del módulo interrogado (2 bytes), mientras que la respuesta contendrá el principal volumen de información transmitido (varios Kbytes).

8

La segunda circunstancia nos permitirá transmitir con mayor potencia en el sentido CB-módulos (interrogación) sin un consumo excesivo de energía, ya que el tiempo de transmisión es despreciable en este caso, garantizando la recepción correcta en todos ellos. En el sentido módulos-CB (respuesta) lo que hay que optimizar es la amplitud de la señal en el único receptor (CB), por lo que podemos diseñar un sistema con muy baja impedancia en los equipos de los módulos y una impedancia mayor en CB, de forma que en él se produzca la mayor caída de tensión a lo largo del anillo. Esto permitirá una recepción eficaz con una potencia de transmisión menor en este sentido, que es el menos favorable en cuanto a consumo de energía por el mayor tiempo de transmisión asociado a su mayor volumen de datos.

Como se indicó en [9], las pruebas de resonancia realizadas sobre un anillo de cable fotovoltaico con frecuencias cuya longitud de onda era una fracción entera de la longitud del anillo conducían siempre a un modo de propagación por ondas estacionarias, indeseado para un sistema de comunicaciones. En [9] se adelantaron algunos métodos teóricos para excitar las ondas viajeras en lugar de las estacionarias sin aportar ninguna realización práctica, y ahora aquí presentaremos un método basado en componentes no recíprocos (que fue una de las opciones allí consideradas) para obtener este tipo de propagación con el objeto de aumentar la frecuencia portadora y por tanto la velocidad de transmisión. Estos componentes no recíprocos han sido implementados mediante amplificadores operacionales de alta frecuencia que presentan una elevada impedancia de entrada y una baja impedancia de salida, por lo que establecen de forma natural un sentido preferente de propagación de la señal. Considerando que las ondas estacionarias se forman por la interferencia entre ondas que viajan en un sentido y ondas que viajan en sentido contrario, el hecho de imponer un sentido preferente de propagación evitará la formación de estas estacionarias, y la resonancia puede lograrse mediante una onda viajera que se propaga en el sentido entrada-salida de los amplificadores. Tras analizar diferentes modelos de amplificadores operacionales y probar sus características en el laboratorio se optó por la elección del amplificador operacional OPA810 del fabricante Texas Instruments, que presenta un producto ganancia-ancho de banda de 70 MHz. Para establecer un sentido de propagación preferente será suficiente insertar en el anillo uno de estos amplificadores, que por conveniencia se instalará en el transceptor de la "Combiner Box" CB. El montaje experimental utilizado con la conexión de este amplificador en la CB, así como un transformador toroidal transceptor asociado a cada módulo y los condensadores de paso (Cb) y de sintonía (Ct) se muestran en la Figura 4.

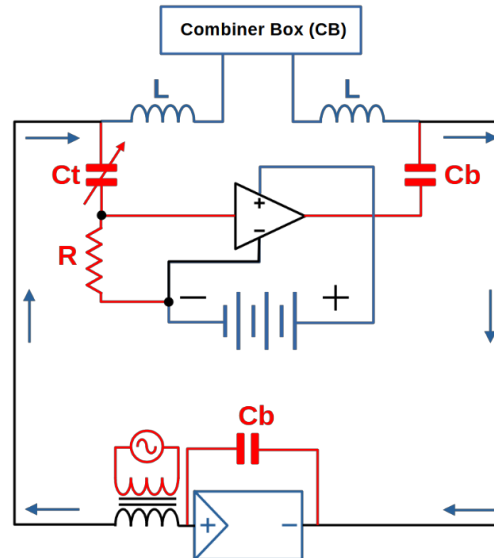


Fig. 4. . Conexión del amplificador en la “Combiner Box” (CB) y de los transformadores transceptores en cada módulo. En rojo en camino de la señal alterna de comunicaciones, en azul el camino de la corriente continua y en negro en camino común a ambas.

Esta configuración del anillo considera las diferencias antes comentadas entre los dos sentidos de comunicación, permitiendo gracias al amplificador introducido una transmisión de mayor potencia en el sentido CB-módulos (interrogación) en modo difusión, y presentando una impedancia mayor en el transceptor de CB que en los transceptores de módulo, de forma que la mayor caída de tensión se encontrará en CB, donde se debe recibir la señal.

Esta diferencia de impedancias se logra dimensionando correctamente la resistencia R a la entrada del amplificador con relación a la impedancia que presentan los secundarios de los transformadores de cada módulo. Esta resistencia R , resulta en todo caso imprescindible para que el amplificador se comporte como un generador de tensión en serie con el anillo, ya que transforma la corriente procedente del bucle en un voltaje de entrada al amplificador. El circuito equivalente a este montaje para la señal alterna de comunicaciones se muestra en la Figura 5, donde efectivamente se ve que el amplificador se comporta como un generador de tensión en serie cuyo valor está controlado por la caída de tensión en esta resistencia de entrada multiplicada por la ganancia del amplificador G .

10

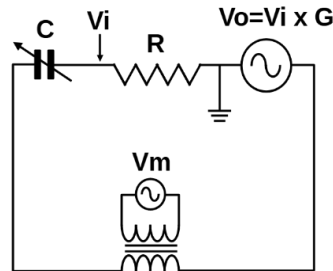


Fig. 5. Circuito equivalente al montaje experimental de la Figura 4 para la señal alterna de comunicaciones. C es el condensador variable de sintonía que se ajustó manualmente.

Para comprobar el comportamiento de este sistema se montó un anillo de cableado fotovoltaico de 27 m de longitud con la configuración mostrada en la Figura 5. Primero se sintonizó manualmente el anillo a través del condensador variable C para una frecuencia portadora de 16 MHz, y a continuación se inyectó una señal sinusoidal de esa misma frecuencia (V_m) en el primario del transformador toroidal, simulando así una transmisión en el sentido módulos-CB. Para comprobar si la propagación se efectuaba a expensas de una onda resonante en forma de onda viajera se realizaron medidas de la amplitud de la señal cada cierta distancia a lo largo de todo el anillo. Estas medidas se llevaron a cabo mediante un sensor de campo magnético de ferrita en forma de toroide que de esta manera influía mínimamente sobre la señal que se estaba propagando. Los niveles a lo largo del anillo no mostraron ningún patrón oscilatorio como se puede comprobar en el gráfico de la Figura 6 (izquierda), por lo que se corroboró que efectivamente la señal se propagaba en forma de onda viajera. En la misma figura se muestra el patrón de onda estacionaria medido a la misma frecuencia sin intercalar el amplificador (derecha) como comparación.

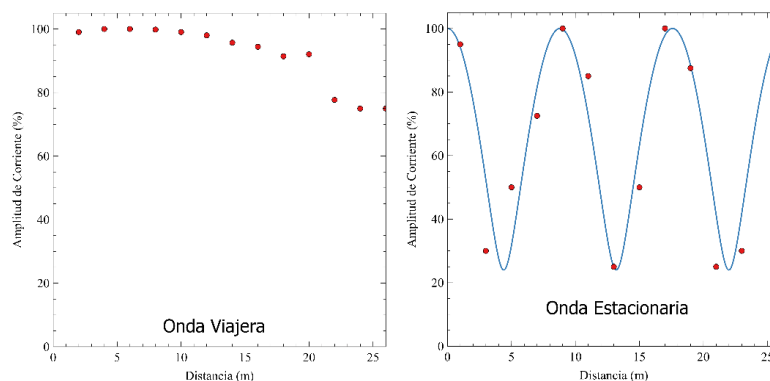


Fig. 6. Distribución espacial medida de la amplitud de corriente con una señal de 16 MHz a lo largo del anillo en el caso de propagación por onda viajera (con amplificador, izquierda) y en el caso de propagación por onda estacionaria (sin amplificador, derecha). En el segundo caso se muestra en azul el ajuste a una curva teórica de onda estacionaria.

Con la conexión mostrada y sin introducir una señal externa este sistema podría auto-oscilar si se cumpliera el criterio de Barkhausen, es decir si la ganancia total del bucle fuese igual a uno y el desfase total introducido fuese un múltiplo de 2π . La condición de desfase total introducido igual a un múltiplo 2π es equivalente a la condición de resonancia que se impone en el anillo y da lugar a un número entero de longitudes de onda a lo largo del mismo. Por ello si la ganancia total del anillo de cable incluyendo las atenuaciones de los tramos de cable y la ganancia de todos los amplificadores es igual a uno el bucle auto-oscilará. Esto se comprobó en el laboratorio sobre el montaje experimental descrito en la Figura 5, y efectivamente, tras ajustar la ganancia del amplificador se observó una auto-oscilación de todo el bucle a 8.3 MHz. Esta situación no nos interesa, porque para modular adecuadamente una señal portadora debemos poder modificar a voluntad alguno de sus parámetros y la auto oscilación hace difícil este control. Por ello se diseñaron los amplificadores de forma que ganancia total del bucle fuese ligeramente inferior a la unidad, evitando así la auto-oscilación pero facilitando la resonancia cuando se excite el bucle externamente.

Cada uno de los transceptores situados a lo largo del anillo puede actuar de forma pasiva, es decir, esperando la recepción de una comunicación o bien de forma activa como transmisor de la señal. En el caso del transceptor en la “Combiner Box” (CB) se habilitarán dos entradas en los amplificadores operacionales. para utilizar una de ellas como conexión al bucle de comunicaciones, mientras que la otra quedará libre para recibir la señal que se desea transmitir cuando CB trabaje como transmisor. En el caso de los transceptores de cada módulo solar, en este caso se han acoplado al bucle inductivamente, con un transformador toroidal, que naturalmente puede actuar como transmisor o receptor.

3 Resultados

Sobre las actuaciones que se refieren al subsistema de trazado I-V las modificaciones y correcciones descritas solucionaron los problemas expuestos. En el caso del transistor MOSFET encargado de realizar los barridos para las trazas I-V, se han realizado sobre el prototipo más de 150 medidas tras esta modificación y hasta ahora, incluso en condiciones de muy alta irradiancia, ningún otro transistor se ha destruido. En cuanto al sensor de corriente, las calibraciones posteriores a la modificación de la placa de circuito impreso han indicado que su sensibilidad ahora sí corresponde a lo indicado por el fabricante en su hoja de datos, permitiendo aprovechar toda la resolución del sensor. Las pruebas finales para caracterizar el soporte físico de comunicaciones PLC se llevaron a cabo mediante una señal portadora resonante de 16 MHz modulada en amplitud (modulación ASK, “Amplitude Shift Keying”). La señal moduladora fue una onda cuadrada simulando una modulación digital por un flujo binario de unos y ceros alternativamente con una profundidad de modulación del 100%. Este sistema de modulación es también denominado ON-OFF, ya que su codificación se puede establecer como 1=hay portadora, 0= no hay portadora. Con esta señal se transmitió en los dos sentidos de la comunicación: CB hacia módulos y módulos hacia CB, comprobándose que es posible alcanzar un flujo de datos entre 1 y 4 Mbps. En el caso de la transmisión desde módulos hacia CB se inyectó la señal con una amplitud de 5 V en el primario de los transformadores (relación de transformación 1:1), y se constató que la velocidad de datos máxima

12

para garantizar una correcta demodulación fué de 2 Mbps, que es un valor 10 veces mayor que la máxima velocidad alcanzada en nuestro artículo anterior [10]. La Figura 7 muestra capturas de osciloscopio con la señal en el anillo durante la prueba en este sentido, En esta figura se puede comprobar que la amplitud de la tensión en el anillo en este caso alcanza los 800 mV.

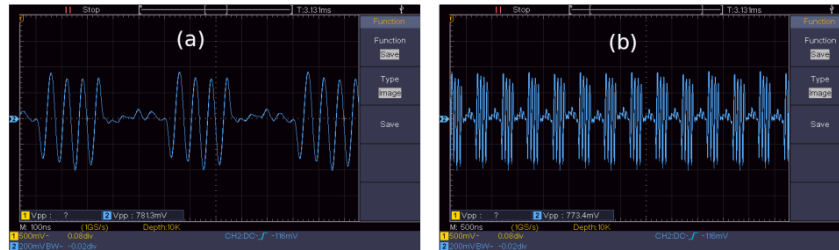


Fig. 7. Capturas de osciloscopio con la señal en el anillo durante una transmisión en el sentido módulos-CB. Se utilizó una portadora de 16 MHz modulada digitalmente con unos y ceros transmitidos alternativamente a 2Mbps:(a) Detalle (100 ns / división), (b) Vista general (500 ns / división)

Las pruebas de transmisión en el sentido contrario (CB hacia módulos) se llevaron a cabo fijando una amplitud de la señal a la salida del amplificador de 7 V, y mostraron que la amplitud de la señal en los receptores de los módulos se reducía a 200 mV. Como se indicó anteriormente este es el enlace que maneja un menor volumen de datos y es posible mejorar esta amplitud aumentando la misma a la salida del amplificador (que tiene margen para alcanzar hasta 27 V). En cualquier caso, la señal en la prueba es perfectamente demodulable con un flujo de datos de 1 Mbps (la mitad que en el caso anterior) como muestra la Figura 8.

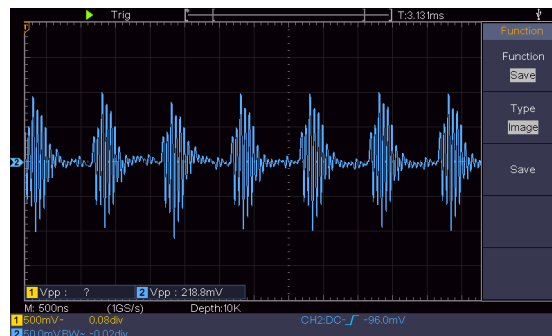


Fig. 8. Captura de osciloscopio con la señal en el anillo durante una transmisión en el sentido CB-módulos. Se utilizó una portadora de 16 MHz modulada digitalmente con unos y ceros transmitidos alternativamente a 1Mbps.

Sobre esta señal de prueba se midieron algunos parámetros característicos del sistema de comunicación cuyos valores se muestran en la Tabla 1, y que demuestran un nivel de calidad más que aceptable del sistema. La Tabla 2 muestra una comparativa entre el sistema aquí descrito y otros trabajos anteriores.

Tabla 1. Parámetros Característicos del Sistema de Comunicación PLC.

Parámetro	Valor	unidades
Frecuencia Portadora	16	MHz
Velocidad de Transmisión Máxima	2	Mbps
Bit Error Rate	10^{-4}	--
Interferencia entre símbolos	0.1	us

Tabla 2. Parámetros Característicos del Sistema de Comunicación PLC.

Autor	Frecuencia Portadora	Bitrate
Napoli et al. [15]	132.5 KHz	No especificado
Ochiai et al. [18]	1 KHz	No especificado
Sánchez et al. [11]	100 KHz	No especificado
Mao et al. [13]	200 KHz	10 Kbps
Daldal et al. [12]	No especificado	No especificado
Morales et al. [19]	1 MHz	200 Kbps
Sistema propuesto	16 MHz	2 Mbps

La modificación del sistema de comunicaciones PLC para admitir las velocidades de transmisión presentadas permite mantener la calificación del sistema como “de bajo coste”, ya que el precio del amplificador de alta frecuencia (OPA810), del que solo necesitamos uno para todo el STRING instalado en CB, no supera los 2 euros. Las modificaciones en los transceptores de módulo solo incluyen componentes pasivos con un coste aproximado de 3 euros, lo que representa tan solo el 25 % del coste reportado para el sistema en [19] (12 Euros). Para generar las nuevas frecuencias portadoras en los transceptores de módulo, los únicos cambios se refieren al firmware del microcontrolador, que es capaz de sacar varias fracciones (programables) de su propia frecuencia de reloj (32 MHz en este caso) en uno de sus pines, por lo que se puede obtener la portadora de 16 MHz programando una fracción de $\frac{1}{2}$ en dicho pin. El transceptor de módulo modificado mantiene así un coste total por debajo del 10-15% del coste medio del módulo fotovoltaico al que se conecta.

4 Conclusiones y Trabajo Futuro.

La revisión aquí realizada de los diseños anteriores de un Sistema de trazado I-V en línea de módulos individuales y un sistema de comunicaciones PLC específico para instalaciones solares ha permitido obtener un dispositivo más fiable robusto y preciso para el trazado I-V y conseguir una mejora en la velocidad de transmisión del sistema

14

PLC, que se ha visto multiplicada por un factor de 10. Estas mejoras permiten pensar en una integración final de ambos sistemas en una única placa de circuito impreso susceptible de ser incorporada a cada módulo solar de una instalación. Estas placas, acompañadas del correspondiente tranceptor instalado en la “Combiner Box” (CB) permitirán un diagnóstico y monitorización de cada módulo solar individual rápido y eficaz, e incluso permiten pensar en aplicaciones de control o medida específicas que aprovechen la comunicación PLC establecida sobre el soporte físico aquí descrito.

Todos estos diseños, además, se han llevado a cabo bajo una filosofía de bajo coste, que los acerca a una aplicación práctica plausible en un futuro.

El trabajo futuro a partir de este punto se centraría en la elección de un sistema de modulación con la mayor eficiencia espectral posible y la correspondiente programación del firmware de transmisión y recepción para el tipo de modulación elegido. Además, para realizar las pruebas que dan lugar a los resultados aquí expuestos se sintonizó el bucle de comunicaciones a la frecuencia de resonancia elegida de forma manual mediante un condensador variable. En el futuro se implementará el sistema de sintonización automática descrito en el artículo [17] y se diseñará una placa de circuito impreso específica para alojar este sistema.

References

- [1] REN21, “Renewables 2022 Global Status Report,” <https://www.ren21.net/reports/global-status-report/>.
- [2] S. Canada, L. Moore, H. Post, and J. Strachan, “Operation and maintenance field experience for off-grid residential photovoltaic systems,” *Progress in Photovoltaics: Research and Applications*, vol. 13, no. 1, pp. 67–74, Jan. 2005, doi: 10.1002/pip.573.
- [3] F. Grimaccia, S. Leva, A. Dolara, and M. Aghaei, “Survey on PV Modules’ Common Faults After an O&M Flight Extensive Campaign Over Different Plants in Italy,” *IEEE J Photovolt*, vol. 7, no. 3, pp. 810–816, May 2017, doi: 10.1109/JPHOTOV.2017.2674977.
- [4] M. Heinrich *et al.*, “Detection of cleaning interventions on photovoltaic modules with machine learning,” *Appl Energy*, vol. 263, p. 114642, Apr. 2020, doi: 10.1016/j.apenergy.2020.114642.
- [5] L. Hernández-Callejo, S. Gallardo-Saavedra, and V. Alonso-Gómez, “A review of photovoltaic systems: Design, operation and maintenance,” *Solar Energy*, vol. 188, pp. 426–440, Aug. 2019, doi: 10.1016/j.solener.2019.06.017.
- [6] J. I. Morales-Aragonés *et al.*, “Low-Cost Electronics for Online I-V Tracing at Photovoltaic Module Level: Development of Two Strategies and Comparison between Them,” *Electronics (Basel)*, vol. 10, no. 6, p. 671, Mar. 2021, doi: 10.3390/electronics10060671.
- [7] J. I. Morales-Aragonés, M. Dávila-Sacoto, L. G. González, V. Alonso-Gómez, S. Gallardo-Saavedra, and L. Hernández-Callejo, “A Review of I–V Tracers for Photovoltaic Modules: Topologies and Challenges,” *Electronics (Basel)*, vol. 10, no. 11, p. 1283, May 2021, doi: 10.3390/electronics10111283.

- [8] J. I. Morales-Aragonés *et al.*, “Online Distributed Measurement of Dark I-V Curves in Photovoltaic Plants,” *Applied Sciences*, vol. 11, no. 4, p. 1924, Feb. 2021, doi: 10.3390/app11041924.
- [9] J. I. Morales-Aragonés *et al.*, “A Resonant Ring Topology Approach to Power Line Communication Systems within Photovoltaic Plants,” *Applied Sciences*, vol. 12, no. 16, p. 7973, Aug. 2022, doi: 10.3390/app12167973.
- [10] J. I. Morales-Aragones *et al.*, “A Power-Line Communication System Governed by Loop Resonance for Photovoltaic Plant Monitoring,” *Sensors*, vol. 22, no. 23, p. 9207, Nov. 2022, doi: 10.3390/s22239207.
- [11] S. Sarikh, M. Raoufi, A. Bennouna, A. Benlarabi, and B. Ikken, “Implementation of a plug and play I-V curve tracer dedicated to characterization and diagnosis of PV modules under real operating conditions,” *Energy Convers Manag*, vol. 209, p. 112613, Apr. 2020, doi: 10.1016/j.enconman.2020.112613.
- [12] P. Papageorgas, D. Piromalis, T. Valavanis, S. Kambasis, T. Iliopoulou, and G. Vokas, “A low-cost and fast PV I-V curve tracer based on an open source platform with M2M communication capabilities for preventive monitoring,” *Energy Procedia*, vol. 74, pp. 423–438, Aug. 2015, doi: 10.1016/j.egypro.2015.07.641.
- [13] W. Mao, X. Zhang, R. Cao, F. Wang, T. Zhao, and L. Xu, “A Research on Power Line Communication Based on Parallel Resonant Coupling Technology in PV Module Monitoring,” *IEEE Transactions on Industrial Electronics*, vol. 65, no. 3, pp. 2653–2662, Mar. 2018, doi: 10.1109/TIE.2017.2736483.
- [14] J. Han, C. Choi, W. Park, I. Lee, and S. Kim, “PLC-based photovoltaic system management for smart home energy management system,” *IEEE Transactions on Consumer Electronics*, vol. 60, no. 2, pp. 184–189, May 2014, doi: 10.1109/TCE.2014.6851992.
- [15] F. Di Napoli, P. Guerriero, V. d’Alessandro, and S. Daliento, “A power line communication on DC bus with photovoltaic strings,” in *3rd Renewable Power Generation Conference (RPG 2014)*, Institution of Engineering and Technology, 2014, pp. 8.16-8.16. doi: 10.1049/cp.2014.0901.
- [16] P. Jonke, C. Eder, J. Stockl, and M. Schwark, “Development of a module integrated photovoltaic monitoring system,” in *IECON Proceedings (Industrial Electronics Conference)*, Vienna: IEEE, Nov. 2013, pp. 8080–8084. doi: 10.1109/IECON.2013.6700484.
- [17] J. I. Morales-Aragonés *et al.*, “A Resonant Ring Topology Approach to Power Line Communication Systems within Photovoltaic Plants,” *Applied Sciences*, vol. 12, no. 16, p. 7973, Aug. 2022, doi: 10.3390/app12167973.
- [18] H. Ochiai and H. Ikegami, “PPLC-PV: A pulse power line communication for series-connected PV monitoring,” in *2016 IEEE International Conference on Smart Grid Communications (SmartGridComm)*, IEEE, Nov. 2016, pp. 338–344. doi: 10.1109/SmartGridComm.2016.7778784.
- [19] J. I. Morales-Aragones *et al.*, “A Power-Line Communication System Governed by Loop Resonance for Photovoltaic Plant Monitoring,” *Sensors*, vol. 22, no. 23, p. 9207, Nov. 2022, doi: 10.3390/s22239207.

Comparative study of the annual production of a floating vs. ground-mounted pilot PV system

Oscar Izquierdo Monge¹, Alfonso Madrazo Alonso-Majagranzas², Paula Peña Carro¹, Alberto Redondo Plaza², Ángel Hernández Jiménez¹, Ángel Zorita Lamadrid²,

¹ CEDER-CIEMAT, Autovía de Navarra A15 salida 56, 422290 Lubia (Soria), Spain.

² Universidad de Valladolid, Campus Universitario Duques de Soria, 42004 Soria, Spain.

O.I.M.: oscar.izquierdo@ciemat.es; A.M.A.:
alfonsomadrazo013@gmail.com; A.R.P.: alberredon@gmail.com;
P.P.C.: paula.pena@ciemat.es; A.H.J.:
angel.hernandez@ciemat.es; A.Z.L.: zorita@uva.es

Abstract: In the search for environmentally sustainable solutions, renewable energies have positioned themselves as the undisputed future of energy generation. Among these clean sources, photovoltaic solar energy stands out as one of the most promising, with the installed capacity of this technology expected to triple. Once in the field of solar photovoltaic, one of the most promising alternatives to continue evolving in the sector is floating photovoltaic, which has a series of advantages over terrestrial photovoltaic; hybridization with hydropower, does not occupy land or agricultural surface and has a lower environmental impact.

In this study, a comparison is made between two terrestrial modules and two floating modules. During the development of the work, daily and monthly data is analyzed and compared for a period of one year, corresponding to temperature and power of both photovoltaic systems. Once compared, it is determined whether the cooling obtained by the floating photovoltaic system works, decreasing the temperature and increasing the power obtained.

The study has been carried out in a water tank of a research centre, with 4 modules previously characterized and standardized to ensure that the work is carried out under the same conditions.

Keywords: Floating photovoltaic, photovoltaic module, temperature, power.

1 Introduction

The current climate crisis is forcing us to rethink the way we generate and consume energy [1]. In Spain, renewable energies accounted for 42% of electricity production in 2022, according to data from the Electricity System Operator (REE), wind and solar energy were the main renewable energy sources, accounting for 58% of installed renewable electricity capacity. Although progress has been made in the transition to renewable sources, it is necessary to continue to reduce greenhouse gas emissions and limit global warming [2]. In this context, solar photovoltaic energy is one of the most

2

promising technologies. According to the International Energy Agency (IEA), it is estimated that solar photovoltaic energy will overtake natural gas globally by 2026 and coal by 2027, growing to 1500 GW.

This energy from the sun has two drawbacks; the first is the low efficiency of the modules [3], the second is the requirement of a large surface area (ground) for installation [4]. A promising alternative, towards which research projects are being directed to overcome the problems mentioned above, is floating photovoltaics [5]. In the face of the low efficiency of solar panels installed on the ground or any other solid material, it is approximately 15% [6]. This is mainly due to the increase in temperature of the panel, which is related to the temperature acquired by the ground or material on which it is placed and which transmits a reduction in its cooling, affecting its efficiency negatively by 0.5% per degree Celsius of increased temperature [7]. In the case of solar panels, as they are in contact with water, they maintain a lower temperature [8], which increases their performance and energy production [9]. Furthermore, by solving the problem of land, floating photovoltaics (FPV) can be installed on bodies of water, such as lakes, rivers, reservoirs, ponds [10] and dams, without using land, which makes it especially useful in areas where land availability is limited [11] or competition for land use is to be avoided [12].

Focusing on floating photovoltaics, this type of energy can be complemented with hydropower through a hybrid system that takes advantage of the benefits of both technologies [13], so that during periods of drought, when there is more light, photovoltaic energy generation increases. As it is a complementary system, in times when there is no drought, hydropower will produce the most, compensating for the variability of solar energy, thus generating 24 hours a day. This type of system not only reduces the cost of energy, but can also use the same substation for both energy sources [14]. In addition, water helps to clean dirt and dust from the panels, which increases efficiency and reduces the need for maintenance.

Another advantage of floating PV is its lower environmental impact. When installed on bodies of water, this technology can contribute to the improvement of water quality and the aquatic ecosystem. Floating solar panels can reduce the evaporation rate, depending on the surface area occupied and the type of flotation system used. For an occupied area of 30%, the evaporation rate is reduced by 18-49%, with the evaporation rate decreasing further as the surface area occupied by the PV panels increases [15]. This is because the modules and their suspension systems provide shading, reducing the exposure of water to direct sunlight, which is especially useful in arid and water-scarce areas. It also contributes to the control of algal blooms through the shading provided, leading to a reduction in growth. An ideal percentage of coverage on reservoirs or lakes would be 40-60%, thus allowing an adequate concentration of algae, without affecting the ecosystem and without generating losses in case of being combined with a hydroelectric power plant [16].

In terms of economic viability, floating PV can be more cost-effective than ground-mounted solar panels [17], due to its higher yield and land cost savings. Key aspects such as optimisation (labour) and inverter maintenance need to be improved [7]. The key factors influencing the profitability of this technology are the initial investment, the

maintenance cost and the price of energy, requiring 5-6 years to recover the initial investment [18].

This type of energy is not only a viable alternative for generating renewable energy and contributing to environmental sustainability, but can also generate new employment and investment opportunities in the renewable energy sector, as it is an emerging technology that, occupying only a small percentage of available reservoir area, could increase Spain's national PV capacity by 20-25% [19]. Such technology can also provide access to renewable energy in rural or remote areas where there is no conventional grid supply and where land availability is limited, providing a more accessible and sustainable option for these communities [20].

Finally, it is important to note that the war in Ukraine has highlighted the vulnerability created by dependence on imported fossil fuels [22], which can affect a country's energy security. Floating solar PV, being a more sustainable and autonomous alternative, can be a solution to reduce dependence on external fossil fuels and thus contribute to energy security [23].

This paper compares a floating photovoltaic system versus a ground-mounted photovoltaic system. The second section corresponds to the materials and methods where the characteristics and operation of the installation are described, the third section has the results. Finally, the final section contains the conclusions.

2 Materials and Methods

2.1 Description of the installation

The photovoltaic installation is located in Lobia (Soria) with coordinates 41°36'10" N 2°30'23" W.

According to the Köppen climate classification, the climate in Soria is oceanic type Cfb (climate: mesothermal, wet or rainy, mild in summer), where the winter is characterized by being long and cold.

A description is given of each of the parts of the installation in which the study has been carried out.

The installation has the following parts, some of which can be seen in Figure 1, which is representative of the installation:

- Photovoltaic modules.
- Inverters.
- Arduino.
- PT100 sensors.
- Zigbee receiver.

4



Fig. 1 Aerial view of the floating photovoltaic installation (Source: CEDER CIEMAT)

Photovoltaic panels

The installation consists of 4 photovoltaic modules (figure 2), of 280 Wp each, 2 of which are on land and 2 in water.

The floating photovoltaic modules are mounted on a cork structure, anchored by two iron bars that hold the structure to the wall of the tank.



Fig. 2 Photovoltaic modules ground and water (Source: CEDER CIEMAT)

Inverters

There are two inverters, both of the same model, for each type of structure, one for ground and one for water. They are located at the back of the modules, anchored to the structure (figure 3).

They provide us with the inverter temperature and the power supplied in DC and AC. The data is sent via wifi to a zigbee receiver, which takes it to a switch via cable, thus forming part of the microgrid.

The efficiency of the inverter is 94.5%.



Fig. 3 Inverter on floating modules (*Source: CEDER CIEMAT*)

PT 100

The solar panels have 3 temperature sensors for each installation (water and earth), these sensors are PT100.

Each PT100 has 3 wires, so there will be 3 PT100 with 3 wires per installation (water and ground).

These wires go to a distribution junction box, one for water and one for earth, and the wires are joined together inside the junction box. The resulting wires from each installation are joined together again, with a single wire going to the arduino inside the distribution and protection box.

They provide the following information:

- Panel ambient temperature (water and ground).
- Right panel temperature (water and earth).
- Left panel temperature (water and ground).

Arduino

The arduino is the YUN rev2 with Linux Atheros 400Mhz Processor with Wifi and Ethernet network.

It is located in the distribution junction box.

Zigbee receiver

APSystem model: ECU-R zigbee receiver (figure 8).

It provides the following data, received from the inverter via wifi:

- Total DC power (water and ground).
- Total AC power (water and ground).
- Right panel power (water and ground).
- Power of the left panel (water and ground).

2.2 Operation of the installation

Communication:

- NodeRed: Allows the management system to be connected to the different generation systems. It can collect the desired information from each one of them and send them the operating instructions that are established.

6

- Telegram: Allows the management system to communicate with operators via their mobile phone.

Management:

- HomeAssistant: Allows for real-time monitoring of all elements.

Data storage:

- Maria DB: Database allowing the storage of the information.

The scheme of operation is shown in Figure 4.

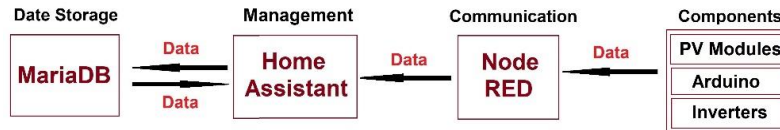


Fig. 4 Operating diagram of the installation

2.3 Standardization of modules

An analysis of the I-V curve was performed, concluding that floating modules produce less power. The analysis was performed under Standard Test Conditions (STC):

- Solar irradiance of 1000 W/m².
- Photovoltaic cell temperature of 25°C
- Pressure 1.5 AM

In order to ensure that the results of the study are correct, the data were normalized based on the I-V curve analysis obtained, using the left-hand ground panel as the reference panel, using the following system:

Power ground panel right:

$$Power\ ground\ right\ normalized = \frac{Power\ ground\ right * 237,87}{244,5}$$

Power ground panel left:

$$Power\ ground\ left\ normalized = \frac{Power\ ground\ left * 244,5}{244,5}$$

Power water panel right:

$$Power\ water\ right\ normalized = \frac{Power\ water\ right * 228,81}{244,5}$$

Power water panel left:

$$Power\ water\ left\ normalized = \frac{Power\ water\ left * 244,81}{244,5}$$

3 Results

In this section the results are presented, 4 months are represented during different times of the year to avoid seasonal variety.

Each analysis includes:

- Full month analysis (power and temperature).
- Average day analysis (power and temperature).

The months chosen are January, April, July and October.

In the monthly graphs there is not a complete monthly representation because the size does not fit the format of the study, the chosen days are the most representative of the month, following the monthly pattern of both power and temperature.

In the choice of the daily representation an average day of the month was used.

3.1 Representation of January

Analysis of the monthly pattern for January is the month with the lowest recorded temperatures, so there should not be a large temperature difference between PV modules.

The objective is to see if the lower temperature difference means that the panels in water still have a higher production.

1- Temperature:

Figure 5 shows how the temperature on the plates is similar both in water and on land, with small peaks in land temperature on the hottest days in January.

The nighttime temperature is not significant in this study, since no solar energy is produced during these hours.

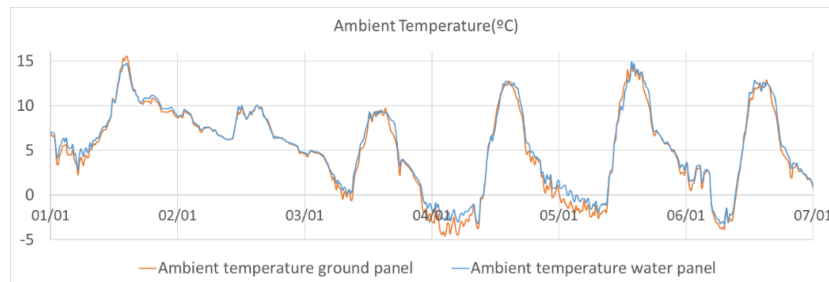


Fig. 5 Monthly ambient temperature of the panels in January

The representation of the daily temperature in January (figure 6) shows that during the hottest hours, the floating photovoltaic system has a lower temperature than the terrestrial one, thus making the cooling system more efficient, which should be reflected in higher power production.

On average, during the hottest hours, the temperature of the ground-based PV is 0.5-1°C higher than that of the floating PV.

8

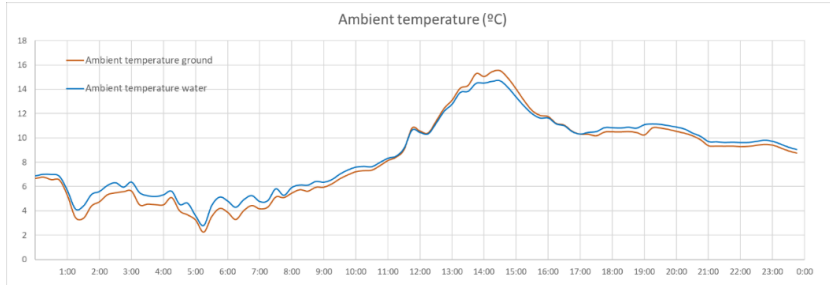


Fig. 6 Daily ambient temperature of the panels in January

2- Power:

In the monthly power representation for January, shown in figure 7, the recorded data indicate a higher production of the floating PV panels, mainly on days with higher radiation and temperature, thus confirming the correct operation of the system and that a lower temperature leads to an increase in production.

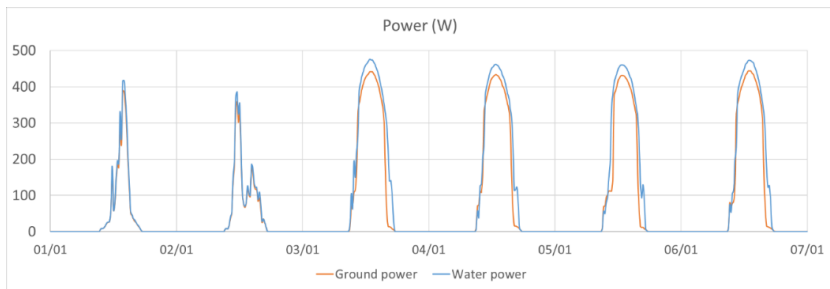


Fig. 7 Monthly power in January

Figure 8 represents an average power day in January. During the hours of highest radiation and temperature, there is an increase in output of between 3-5.5 W per degree Celsius cooled.

In terms of output, floating PV produces 4.5-6% more.

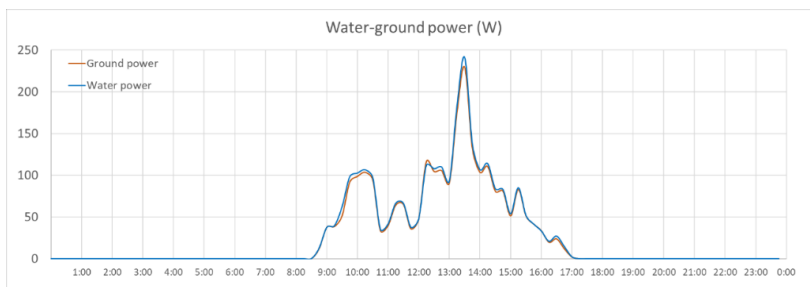


Fig. 8 Daily power in January

3.2 Intermediate time representation

The data obtained during the months of April and October with intermediate temperatures are studied, these two months are analysed together since the temperature and radiation patterns are similar.

During these periods, a difference in temperature between the water and land installation should be noticed, with the land installation being higher and therefore producing more from the floating installation.

1- Temperature:

Figures 9 and 10 show that the temperature reached by the terrestrial photovoltaic panels is higher than that of the floating ones, the average difference during these months is 0.7°C , depending on the day, temperature differences between 0.2 and 2.5°C are reached.

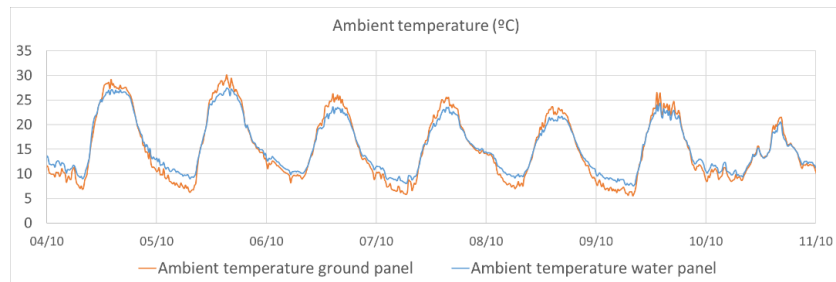


Fig. 9 Monthly ambient temperature of the panels in intermediate weather

In these polycrystalline silicon modules, any temperature difference should be reflected in an increase in production by the cooled structure, which is analysed in the following section.

Looking at figure 10, it can be seen that the largest temperature difference corresponds to the peak production hours between 12 and 18 hours.

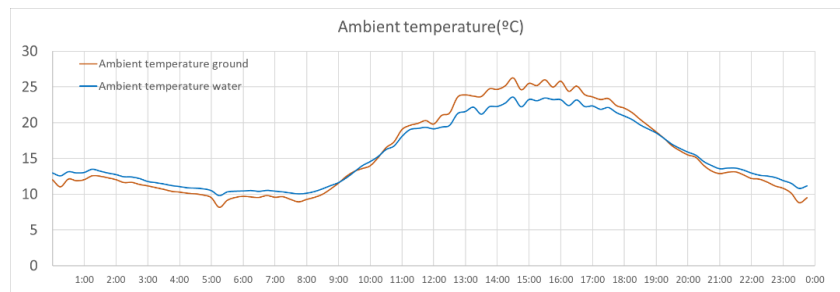


Fig. 10 Daily ambient temperature of the panels in intermediate weather

2- Power:

10

During the months of intermediate temperature (figure 11), power generation is higher in the floating photovoltaic system, confirming that, as there is a lower temperature during production hours, the power obtained is higher.

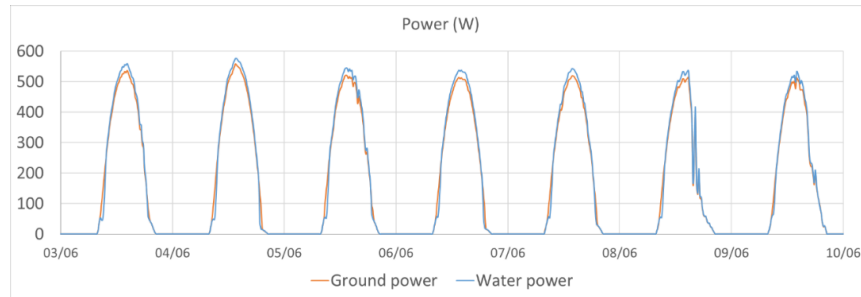


Fig. 11 Monthly power in intermediate weather

In the daily graph (figure 12), representative of a monthly average day, the data indicates a higher floating PV production of 3.2-4.8% in April and 3-6% in October, confirming once again that the lower the temperature, the higher the production.

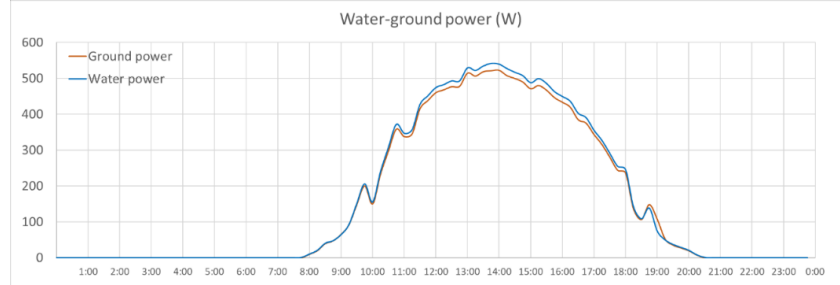


Fig. 12 Daily power in intermediate weather

3.3 Representation of July

The monthly patterns for July are analysed. July is the hottest month, so the water-based structure should have a lower temperature compared to the land-based structure, especially during the hottest hours. This should also be reflected in the power output, a higher cooling of the modules in water will have to have an impact on obtaining more power.

1- Temperature:

Figure 13 shows that at the hottest times the terrestrial PV modules reach higher temperatures than the aquatic ones, which is the case throughout the month of July.

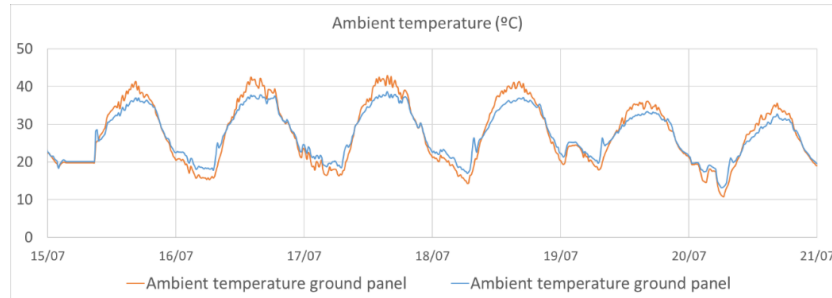


Fig. 13 Monthly ambient temperature of the panels in July

The daily analysis (figure 14) shows temperature differences of 3-4.5 °C during peak hours. During the hottest hours, the cooling system is effective, lowering the temperature of the water photovoltaic modules.

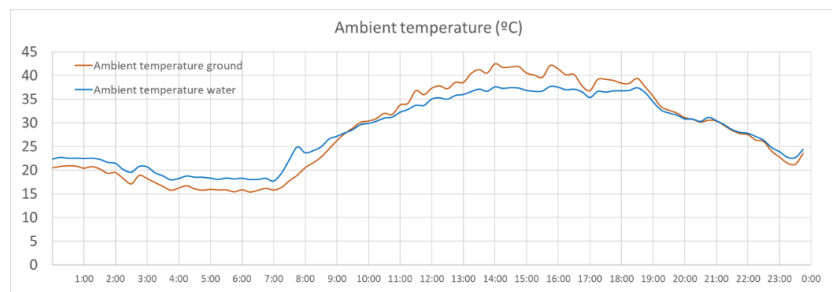


Fig. 14 Daily ambient temperature of the panels in July

2- Power:

Figure 15 shows how the panels in water achieve a higher output than the terrestrial ones, confirming that, being cooled (lower temperature), the energy output is higher.

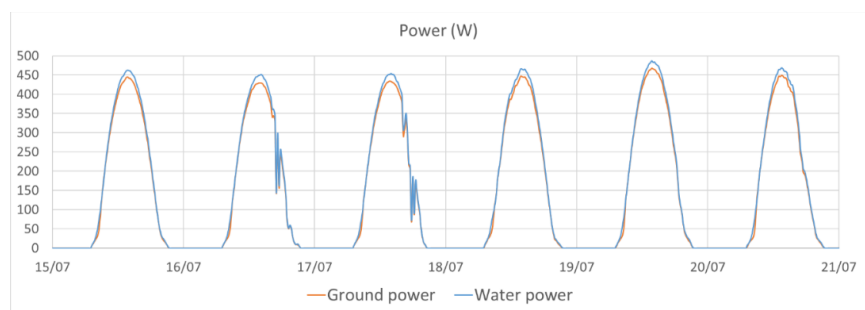


Fig. 15 Monthly power in July

12

As can be seen in the monthly graph, in the daily graph (figure 16) there is a higher production of the photovoltaic panels in water, reaching 4-6% more production. During the hours of highest radiation and temperature, the panels in water produce approximately 20-25 W more power.

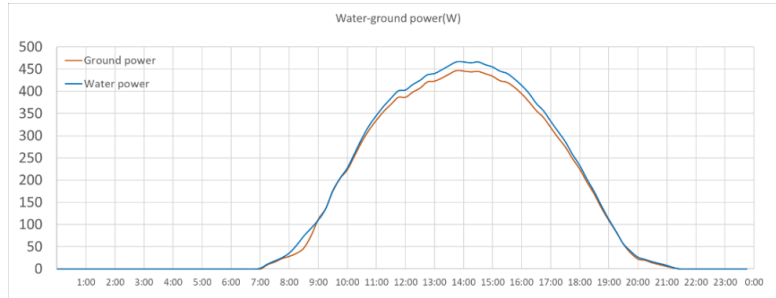


Fig. 16 Daily power in July

4 Conclusions

This study demonstrates that silicon modules work better at lower temperatures, analyzing them under the same conditions, the solar panels located in water produced between 3-6% more than the terrestrial ones, depending on the time of year.

In order to ensure that the conditions were the same for all the modules, all the panels were characterized and standardized by analyzing the I-V curve under STC conditions.

During monthly analyses, it was concluded that a lower temperature was reflected in a higher power production, however small the difference, as shown in Table 1.

Table 1: Difference in floating PV production compared to land-based production (higher production in floating)

MONTH	PRODUCTION
January	4,5 - 6 %
April	3,2 - 4,8%
July	4 - 6%
October	3 - 6%

It has also been shown that placing the photovoltaic modules on a water surface lowers the temperature of the modules. Table 2 shows that even in the coldest months the cooling system was effective, with a greater difference in hottest months such as July.

Table 2: Temperature difference between floating and land-based modules (higher temperature on land)

MONTH	Temperature Difference
January	0,5 - 1°C
April	0,5 - 2°C
July	3 - 4,5°C
October	0,2 - 2,5°C

As a final conclusion, it should be noted that throughout the year the temperature of the floating modules was lower than the terrestrial ones during production hours, which is reflected in a higher power production by the floating photovoltaic system.

For future work, it would be advisable to have a radiation meter in the installation itself. It would also be interesting to use another type of base on the floating structure to see if it produces better cooling, and if so, a comparison could be made between the type of cost of these structures in order to identify whether a large-scale project could be feasible.

Acknowledgments

The authors thank the agreement between the university of Valladolid, Elivere innovation and CIEMAT (Centro de Investigaciones Energéticas, Medioambientales y Tecnológicas) to carry out the "Study of the increase in the performance of photovoltaic solar modules due to their cooling from floating in water".

References

1. M. M. Vanegas Cantarero, "Of renewable energy, energy democracy, and sustainable development: A roadmap to accelerate the energy transition in developing countries," *Energy Res. Soc. Sci.*, vol. 70, p. 101716, Dec. 2020, doi: 10.1016/J.ERSS.2020.101716.
2. M. J. B. Kabeyi and O. A. Olanrewaju, "Sustainable Energy Transition for Renewable and Low Carbon Grid Electricity Generation and Supply," *Front. Energy Res.*, vol. 9, p. 1032, Mar. 2022, doi: 10.3389/FENRG.2021.743114/BIBTEX.
3. R. Venkateswari and S. Sreejith, "Factors influencing the efficiency of photovoltaic system," *Renew. Sustain. Energy Rev.*, vol. 101, pp. 376–394, Mar. 2019, doi: 10.1016/J.RSER.2018.11.012.
4. M. M. Vanegas Cantarero, "Of renewable energy, energy democracy, and sustainable development: A roadmap to accelerate the energy transition in developing countries," *Energy Res. Soc. Sci.*, vol. 70, p. 101716, Dec. 2020, doi: 10.1016/J.ERSS.2020.101716.
5. M. J. B. Kabeyi and O. A. Olanrewaju, "Sustainable Energy Transition for Renewable and Low Carbon Grid Electricity Generation and Supply," *Front. Energy Res.*, vol. 9, p. 1032, Mar. 2022, doi: 10.3389/FENRG.2021.743114/BIBTEX.

14

6. R. Venkateswari and S. Sreejith, "Factors influencing the efficiency of photovoltaic system," *Renew. Sustain. Energy Rev.*, vol. 101, pp. 376–394, Mar. 2019, doi: 10.1016/J.RSER.2018.11.012.
7. R. Cazzaniga and M. Rosa-Clot, "The booming of floating PV," *Sol. Energy*, vol. 219, pp. 3–10, May 2021, doi: 10.1016/J.SOLENER.2020.09.057.
8. M. Rosa-Clot and G. M. Tina, "Levelized Cost of Energy (LCOE) Analysis," *Float. PV Plants*, pp. 119–127, Jan. 2020, doi: 10.1016/B978-0-12-817061-8.00010-5.
9. M. Santhakumari and N. Sagar, "A review of the environmental factors degrading the performance of silicon wafer-based photovoltaic modules: Failure detection methods and essential mitigation techniques," *Renew. Sustain. Energy Rev.*, vol. 110, pp. 83–100, Aug. 2019, doi: 10.1016/J.RSER.2019.04.024.
10. S. Gorjian, H. Sharon, H. Ebadi, K. Kant, F. B. Scavo, and G. M. Tina, "Recent technical advancements, economics and environmental impacts of floating photovoltaic solar energy conversion systems," *J. Clean. Prod.*, vol. 278, p. 124285, Jan. 2021, doi: 10.1016/J.JCLEPRO.2020.124285.
11. M. Dörenkämper, A. Wahed, A. Kumar, M. de Jong, J. Kroon, and T. Reindl, "The cooling effect of floating PV in two different climate zones: A comparison of field test data from the Netherlands and Singapore," *Sol. Energy*, vol. 219, pp. 15–23, May 2021, doi: 10.1016/J.SOLENER.2021.03.051.
12. A. El Hammoumi, A. Chalh, A. Allouhi, S. Motahhir, A. El Ghzizal, and A. Derouich, "Design and construction of a test bench to investigate the potential of floating PV systems," *J. Clean. Prod.*, vol. 278, p. 123917, Jan. 2021, doi: 10.1016/J.JCLEPRO.2020.123917.
13. E. Muñoz-Cerón, J. C. Osorio-Aravena, F. J. Rodríguez-Segura, M. Frolova, and A. Ruano-Quesada, "Floating photovoltaics systems on water irrigation ponds: Technical potential and multi-benefits analysis," *Energy*, vol. 271, no. September 2022, p. 127039, May 2023, doi: 10.1016/J.ENERGY.2023.127039.
14. N. Ravichandran, N. Ravichandran, and B. Panneerselvam, "Comparative assessment of offshore floating photovoltaic systems using thin film modules for Maldives islands," *Sustain. Energy Technol. Assessments*, vol. 53, p. 102490, Oct. 2022, doi: 10.1016/J.SETA.2022.102490.
15. L. Dias, J. P. Gouveia, P. Lourenço, and J. Seixas, "Interplay between the potential of photovoltaic systems and agricultural land use," *Land use policy*, vol. 81, pp. 725–735, Feb. 2019, doi: 10.1016/J.LANDUSEPOL.2018.11.036.
16. P. E. Campana, L. Wästhage, W. Nookuea, Y. Tan, and J. Yan, "Optimization and assessment of floating and floating-tracking PV systems integrated in on- and off-grid hybrid energy systems," *Sol. Energy*, vol. 177, pp. 782–795, Jan. 2019, doi: 10.1016/J.SOLENER.2018.11.045.
17. N. M. Silvério, R. M. Barros, G. L. Tiago Filho, M. Redón-Santafé, I. F. S. dos Santos, and V. E. de M. Valério, "Use of floating PV plants for coordinated operation with hydropower plants: Case study of the hydroelectric plants of the São Francisco River basin," *Energy Convers. Manag.*, vol. 171, pp. 339–349, Sep. 2018, doi: 10.1016/j.enconman.2018.05.095.
18. F. Bontempo Scavo, G. M. Tina, A. Gagliano, and S. Nižetić, "An assessment study of evaporation rate models on a water basin with floating photovoltaic plants," *Int. J. Energy Res.*, vol. 45, no. 1, pp. 167–188, Jan. 2021, doi: 10.1002/ER.5170.
19. J. Haas, J. Khalighi, A. de la Fuente, S. U. Gerbersdorf, W. Nowak, and P. J. Chen, "Floating photovoltaic plants: Ecological impacts versus hydropower operation flexibility," *Energy Convers. Manag.*, vol. 206, p. 112414, Feb. 2020, doi: 10.1016/J.ENCONMAN.2019.112414.

20. S. K. Cromratie Clemons, C. R. Salloum, K. G. Herdegen, R. M. Kamens, and S. H. Gheewala, "Life cycle assessment of a floating photovoltaic system and feasibility for application in Thailand," *Renew. Energy*, vol. 168, pp. 448–462, May 2021, doi: 10.1016/J.RENENE.2020.12.082.
21. R. Deng, N. L. Chang, Z. Ouyang, and C. M. Chong, "A techno-economic review of silicon photovoltaic module recycling," *Renew. Sustain. Energy Rev.*, vol. 109, pp. 532–550, Jul. 2019, doi: 10.1016/J.RSER.2019.04.020.
22. F. Ardente, C. E. L. Latunussa, and G. A. Blengini, "Resource efficient recovery of critical and precious metals from waste silicon PV panel recycling," *Waste Manag.*, vol. 91, pp. 156–167, May 2019, doi: 10.1016/J.WASMAN.2019.04.059.
23. J. A. Tsanakas *et al.*, "Towards a circular supply chain for PV modules: Review of today's challenges in PV recycling, refurbishment and re-certification," *Prog. Photovoltaics Res. Appl.*, vol. 28, no. 6, pp. 454–464, 2020, doi: 10.1002/pip.3193.
24. B. Zakeri *et al.*, "Pandemic, War, and Global Energy Transitions," *Energies 2022, Vol. 15, Page 6114*, vol. 15, no. 17, p. 6114, Aug. 2022, doi: 10.3390/EN15176114.
25. M. Umar, Y. Riaz, and I. Yousaf, "Impact of Russian-Ukraine war on clean energy, conventional energy, and metal markets: Evidence from event study approach," *Resour. Policy*, vol. 79, p. 102966, Dec. 2022, doi: 10.1016/J.RESOURPOL.2022.102966.

Numerical study on dynamic thermal characteristics and potential for reducing energy consumption and CO₂ emissions of multi-glazed windows in developing cities of Mexico

Samanta López Salazar^{1,*}[0009-0004-9880-5145], E. Simá¹ [0000-0001-7601-1273],
Ruitong Yang² [0000-0002-8442-0445], Dong Li² [0000-0002-2692-9091],
M.A. Chagolla-Aranda¹ [0000-0002-7649-7389]

¹Tecnológico Nacional de México / CENIDET, Prol. Av. Palmira S/N, Col. Palmira, Cuernavaca, Morelos CP 62490, México

²School of architecture and civil engineering, Northeast Petroleum University, Fazhan Lu Street, Daqing, CP 163318, China

dl8ce057@cenidet.tecnm.mx
e.sima@cenidet.tecnm.mx
yangruitong17@163.com
lidonglvyan@126.com
miguel.ca@cenidet.tecnm.mx

Abstract. This study aims to assess the influence of different glazing configurations on building energy performance within diverse climatic conditions. A comparative analysis of three glazing configurations – single, double, and triple, - was conducted on the most critical days in four representative Mexican cities. In this context, multi-glazed windows exhibit a remarkable reduction in the decrement factor by over 50 %, with triple glazing effectively delaying the impact of climatic variables on window temperature by up to 2.5 h. Notably, cities with temperate climates consistently demonstrate lower heat flux per unit area, reduced electricity consumption costs, and minimized CO₂ emissions. Conversely, cities with hot tropical climates and extreme weather conditions experience overheating with multi-glazed windows, resulting in increased heat transfer through convection and radiation. Significantly, single glazing incurs the highest electricity consumption costs and generates 33 % to 38 % kgCO₂em⁻² compared to triple glazing. These findings emphasize the critical role of selecting appropriate glazing configurations to enhance energy efficiency and reduce environmental impact, taking regional climate conditions into account.

Keywords: multi-glazed windows, energy efficiency in buildings, dynamic thermal characteristics

1 Introduction

The quality of life, accessibility and uniqueness of a community are reflected in the buildings. However, the current design of buildings in Mexico has overlooked critical

2

aspects related to thermal efficiency, energy consumption, and environmental impact. This poses a significant challenge for society, which must move towards the creation of energy-efficient buildings that make intelligent use of natural resources. This approach not only drives Mexico's economic and social development, but also enhances the well-being of the population.

So far, the dependence on non-renewable energy sources to maintain comfortable environments has been deeply ingrained, as approximately 75 % of the energy consumed in buildings comes from coal, natural gas, and oil [1] used in thermal power plants to generate electricity. To address this issue, it is essential to analyze the impact of construction parameters on the indoor temperature of buildings.

Buildings are open systems that interact with the environment, and the transfer of thermal energy occurs through heat transfer mechanisms (conduction, convection, and radiation). These processes manifest in opaque and semitransparent elements such as walls, ceilings, skylights, facades, and windows.

It has been observed that in regions like northern Mexico and the coastal areas, the highest energy consumption is attributed to ventilation and air conditioning systems, especially in buildings with large glazed areas. Here, 40 % of energy gain is due to poor thermal insulation and high transmittance of clear single glazing of clear glass. Additionally, crucial design parameters such as orientation, shape, and size are often overlooked.

In order to reduce solar radiation and increase thermal resistance, solutions such as coatings [2], solar control films [3], shading accessories [4], as well as the use of intermediate insulating materials like air [5], water [6], inert gases [7], absorbent gases [8], phase change materials [9], and aerogel [10] have been proposed. Changes in the aspect ratio between the façade and window [11], window position [12], and window shape [13] have also been explored. Despite numerous existing parametric and comparative studies, the precise replication of the heat transfer and fluid flow process remains a challenge. Most of these studies focus on static indicators of thermal and energy performance related to glass properties. However, according to Wang et al. [14] it is crucial to consider the dynamic thermal characteristics of multiple glazing such as time lag (TL) and decrement factor (DF).

In summary, modifying a building's envelope is costly and complex, making it essential to develop studies that provide accurate information on the advantages and limitations of thermal insulation systems, such as multiple glazing, taking into account both static and dynamic thermal characteristics.

Under this context, this study offers a comprehensive analysis of the static and dynamic thermal characteristics of multi-glazing, as well as an evaluation of the potential for energy savings and reduction in carbon dioxide emissions across various climatic conditions in Mexico. A detailed comparison is conducted among three glazing configurations (single, double, and triple) when oriented to the south. Initially, the dynamic thermal characteristics TL and DF are presented. Subsequently, the estimation of energy savings and the reduction in CO₂ emissions is calculated based on numerical results derived from unsteady heat transfer analysis within a two-dimensional framework. This analysis is conducted under the most extreme climatic conditions observed in Monterrey, Mexico City, Merida, and Ciudad Juarez.

2 Physical and mathematical model

Usually, in the numerical modeling of windows, conventional and multi-glazed, only the heat transfer for the glazing and the inner insulating material is considered. Fig. 1 shows the cross section of a multi-glazed window, composed of three semi-transparent walls of 0.004 m thickness and height $H=0.8$ m. The contribution of the window frame to the heat transfer is neglected, because the upper and lower horizontal walls are assumed to be adiabatic. For the triple glazing the glass panes are separated by two air gaps, $b=0.01$ m, while for the double glazing $b=0.02$ m, see Table 1.

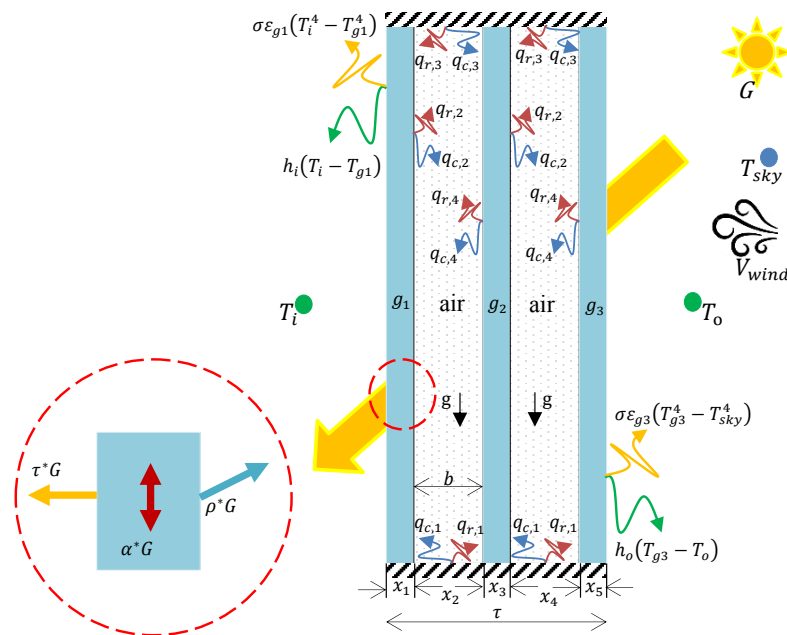


Fig. 1. Physical model of a cross section of a multiple glazing window.

Air is presumed to exhibit Newtonian behavior and maintain an incompressible fluid state; this assumption takes into account window's dimensions and the existing temperature difference and the laminar flow regime. Moreover, the low moisture content in the air classifies it as a radiatively non-participating medium. The thermophysical and optical properties of clear glass were taken from [15], on the other hand, the thermophysical properties of air are presumed to remain constant, except for the density.

The heat transfer mechanisms in the multi-glazed window are: heat conduction for the semitransparent walls, natural convection for the airflow, and surface radiative exchange between the glass panes. The heat transfer process is assumed in two dimensions and in an unsteady state.

4

Table 1. Summary of equivalent layers for all glazing configurations.

Categories	Parameters	SG	DG	TG	
Composition	Layers	CG	CG+A+CG	CG+A+CG+A+CG	
Dimensions	τ , mm	0.004	0.280	0.320	
Optical	α^*	7.1	$\alpha_g^*(\rho_{g,o}^*G)$	$\alpha_{g,1}^*\tau_{g,2}^*\tau_{g,3}^*(\rho_{g,o}^*G)$ +NPM+	
				$\alpha_{g,2}^*\tau_{g,3}^*(\rho_{g,o}^*G)$ +NPM+	
				$\alpha_{g,3}^*(\rho_{g,o}^*G)$	
				$\tau_{g,1}^*\tau_{g,2}^*\tau_{g,3}^*(\rho_{g,o}^*G)$	
Thermal	τ^*	83.9	$\tau_g^*(\rho_{g,o}^*G)$	$\tau_{g,1}^*\tau_{g,2}^*(\rho_{g,o}^*G)$	$\tau_{g,1}^*\tau_{g,2}^*\tau_{g,3}^*(\rho_{g,o}^*G)$
	ρ^*	9.0		$(\rho_{g,o}^*G)$	
	λ , Wm ⁻¹ K ⁻¹	1.4		-	
	C_p , Jkg ⁻¹ K ⁻¹	750		-	
	ρ , kgm ⁻³	2500		-	

“CG” = Clear Glass, “A” = Air Gap, and “NPM” = Non-Participating Medium.

Eq. (1) represents the heat conduction process through semitransparent walls, where $\theta = G \cdot \exp[-S_g(x_g - x)]$ is the absorption and scattering energy attenuation function, G is the normal component of solar radiation incident on the glazing panes, S_g is the attenuation coefficient of the glazing, and x_g represents the glazing thickness.

$$\frac{\partial(\rho_g C_p T_g)}{\partial t} = \frac{\partial}{\partial x} \left(\lambda_g \frac{\partial T_g}{\partial x} \right) + \frac{\partial}{\partial y} \left(\lambda_g \frac{\partial T_g}{\partial y} \right) + \frac{d\theta(x)}{dx} \quad (1)$$

Taking into account the assumptions for the air and airflow the mathematical model for the natural convection is represented by Eqs. (2) – (5), continuity, momentum, and energy equations. Where u and v are the velocity components in vertical and horizontal directions, P is the pressure, and T represents the air temperature.

$$\frac{\partial \rho}{\partial t} + \frac{\partial(\rho u)}{\partial x} + \frac{\partial(\rho v)}{\partial y} = 0 \quad (2)$$

$$\frac{\partial(\rho u)}{\partial t} + \frac{\partial(\rho u u)}{\partial x} + \frac{\partial(\rho v u)}{\partial y} = \frac{\partial}{\partial x} \left(\mu \frac{\partial u}{\partial x} \right) + \frac{\partial}{\partial y} \left(\mu \frac{\partial u}{\partial y} \right) - \frac{\partial P}{\partial x} \quad (3)$$

$$\begin{aligned} \frac{\partial(\rho v)}{\partial t} + \frac{\partial(\rho u v)}{\partial x} + \frac{\partial(\rho v v)}{\partial y} \\ = \frac{\partial}{\partial x} \left(\mu \frac{\partial v}{\partial x} \right) + \frac{\partial}{\partial y} \left(\mu \frac{\partial v}{\partial y} \right) - \frac{\partial P}{\partial y} + \rho g \beta (T - T_\infty) \end{aligned} \quad (4)$$

$$\frac{\partial(\rho C_p T)}{\partial t} + \frac{\partial(\rho C_p u T)}{\partial x} + \frac{\partial(\rho C_p v T)}{\partial y} = \frac{\partial}{\partial x} \left(\lambda \frac{\partial T}{\partial x} \right) + \frac{\partial}{\partial y} \left(\lambda \frac{\partial T}{\partial y} \right) \quad (5)$$

On the other hand, to compute the heat flux from the surface radiative exchange the net radiative method was used. In order to use the net radiative method, the surfaces are assumed opaque to long-wave radiation, gray, and diffuse. In Eq. (6) a radiative energy balance is carried out, where $q_{o,k}$ is the outgoing thermal radiation (radiosity) and $q_{i,k}$ is the incoming thermal radiation (irradiance).

$$q_{r,k}(r_k) = q_{o,k}(r_k) - q_{i,k}(r_k) \quad (6)$$

The radiosity is expressed as the sum of an emitter component, $q_{\varepsilon_k} = \varepsilon_k \sigma T_k^4(r_k)$ and another part by the reflection of the incident radiation, $q_{\rho_k} = (1 - \varepsilon_k) q_{i,k}(r_k)$. While the irradiation is determined by the sum of all the contributions of the surfaces involved in the radiative exchange, $q_{i,k}(r_k) = \sum_{j=1}^N \int_{A_j} q_{o,j}(r_j) dF_{dA_k-dA_j}$. To take into account the effects of orientation on the heat transfer by radiation between two surfaces the view factors, $F_{dA_k-dA_j}$, were computed by the Hottel Crossed String Method.

In one hand, non-slip conditions for the fluid adjacent to the cavity walls are imposed. On the other hand, an energy balance is performed for the vertical walls, where the heat flux by conduction through the glass panes (q_g), the heat fluxes by convection (q_c) and radiation (q_r) are considered.

Air cavity one, for $0 \leq y \leq H$

$$\begin{aligned} q_{g,1} &= q_{c,2} + q_{r,2} \text{ at } x = x_1 \\ q_{c,4} &= q_{g,2} - q_{r,4} \text{ at } x = (x_1 + x_2) \end{aligned} \quad (7)$$

Air cavity two, for $0 \leq y \leq H$

$$\begin{aligned} q_{g,2} &= q_{c,2} + q_{r,2} \text{ at } x = (x_1 + x_2 + x_3) \\ q_{c,4} &= q_{g,3} - q_{r,4} \text{ at } x = (x_1 + x_2 + x_3 + x_4) \end{aligned} \quad (8)$$

As shown in Fig. 1, glass one is in contact with the inside environment, T_i , which is maintained at a constant temperature value of 25 °C, while glass three is exposed to real weather conditions of wind velocity, outside environment temperature, and the normal component of solar radiation. The solar radiation that hits the window surface is reflected, absorbed, and transmitted through the glazing in different proportions. The glazing absorbs energy, which causes an increase in internal temperature, therefore the heat transfer by convection and radiation to the inside and outside environment increases, Eqs. (9) and (10); the convective heat transfer coefficient for the inside environment is kept constant at 2.5 Wm⁻²K⁻¹, while the convective heat transfer coefficient for the outside environment is computed as a function of wind velocity $h_o = 2.8 + 3.0V_{wind}$ Wm⁻²K⁻¹ according to [16]. On the other hand, the sky temperature is calculated by the correlation reported by Swinbank [17].

$$-\lambda \frac{\partial T_{g1}}{\partial x} = h_i(T_i - T_{g1}) + \varepsilon_{g1} \sigma (T_i^4 - T_{g1}^4) \quad (9)$$

$$-\lambda \frac{\partial T_{g3}}{\partial x} = h_o(T_{g3} - T_o) + \varepsilon_{g3} \sigma (T_{g3}^4 - T_{sky}^4) \quad (10)$$

6

Fig. 2 shows the periodical heat transfer process through the window, and the definition of TL and DF, Eqs. 11 – 14. The time lag is the result of the difference in hours between the occurrences of the outdoor temperature peak, $T_{so}(t)$, and the indoor temperature peak, $T_{si}(t)$. On the other hand, the relationship between the amplitude of the external, A_o , and internal temperature, A_i , wave is called “decrement factor”.

$$TL_{min} = t_{si,min} - t_{so,min} \quad (11)$$

$$TL_{max} = t_{si,max} - t_{so,max} \quad (12)$$

$$DF = \frac{A_i}{A_o} = \frac{T_{si,max} - T_{si,min}}{T_{so,max} - T_{so,min}} \quad (13)$$

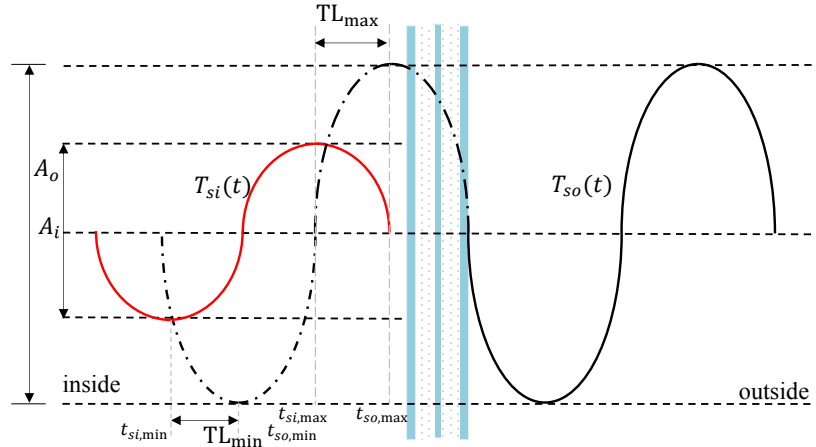


Fig. 2. Schematic representation of decrement factor (DF) and time lag (TL).

On the other hand, the total heat flux through the window is computed by a numerical integration of the heat flux over the 24 h per day, Eq. (14), in order to determine the energy demand, the cost of electricity consumption, and CO₂ emissions into the environment.

$$q_{t,i} = \int_{00:00}^{24:00} q_i(t) dt \quad (14)$$

3 Weather data

Four representative cities of Mexico were selected to carry out the numerical modeling of multi-glazed windows. These cities were selected based on the economic development and current housing demand reported by the National Institute of Statis-

7

tic and Geography in Mexico, INEGI [18]. Table 2 shows the general information about the cities.

Table 2. General information about the cities selected for the present work, INEGI [30].

City	Location	Population to 2020	Köppen climate classification	Average annual temperature
Monterrey	25°40.5042' N, 100°19.1082' W	1,142,994	BSh	20.0 °C
Mexico city	19°25.7082' N, 99°7.6596' W	9,209,944	Cwb	16.0 °C
Merida	20°58.5222' N, 89°37.0176' W	995,129	Aw	26.0 °C
Ciudad Juarez	31°43.9998' N, 106°28.9998' W	1,512,450	BWk	18.3 °C

The weather data was extracted from the database of the National Meteorological Service in collaboration with the National Water Commission in Mexico [19]. Two days of each city were selected to carry out the numerical modeling; these days were selected based on the lowest and highest value of outside environment temperature. Fig. 3 shows the behavior of the climatic variables for the two selected days in different cities: solar radiation, outside environment temperature, and wind velocity.

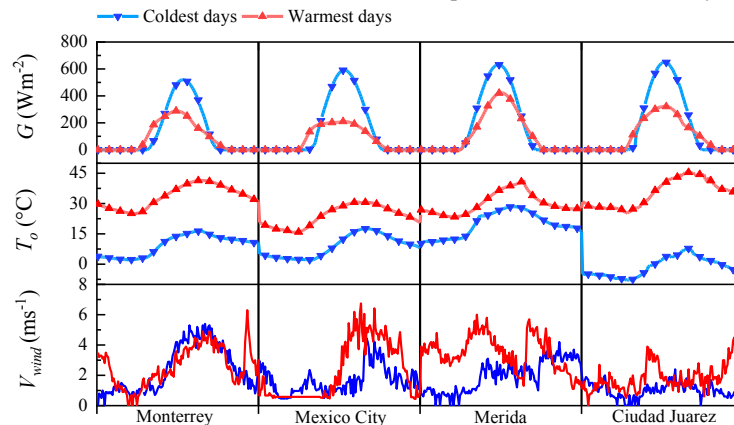


Fig. 3. Weather data in the coldest and warmest days in each city.

4 Numerical solution methodology

The mathematical models of natural convection and heat conduction, as well as the boundary conditions were solved through a home-code developed in Fortran language using the finite volume method. The coupling of the continuity and momentum equa-

8

tions was achieved through the SIMPLEC algorithm. A central difference scheme and a hybrid scheme were used to discretize the diffusive and convective terms, respectively. Moreover, a fully implicit scheme was used to discretize the transient term. The system of algebraic equations resulting from the discretization process was resolved using iterative methods: the line by line method in x and y directions (LBL- x and LBL- y) for the velocity components, and the Gauss-Seidel method in alternating directions (LGS-ADI) to solve the pressure and temperature algebraic system equations. The net radiation heat flux was computed to couple the effect of superficial radiative exchange to the boundary conditions. A convergence criterion was established to ensure the reliability of the solution. The residual was calculated using the root mean square; the residual for every variable was 10^{-9} .

An analysis to determine the optimal time step and grid mesh to model the multi-glazed windows was performed taking into account the effect on the results of temperature and heat flux per unit area of five time steps: 5, 10, 15, 20, and 30 s, and different grid size: $N_x = 11 \dots 61$ nodes, and $N_y = 81 \dots 131$ nodes, in horizontal and vertical directions respectively.

After several numerical tests, a 15 s time step with a grid size of 11×91 nodes for the glazing and 21×91 nodes for the air gaps were selected, based on the results of the window temperature and total heat flux with a maximum deviation $\approx 3\%$ compared to a small time step and a fine mesh.

In order to verify the accuracy of the numerical code, the values of the overall heat transfer coefficient, U-value, as well as the solar heat gain coefficient (SHGC) for the double (DG) and triple (TG) glazing configurations were obtained. Table 3 shows the data reported by ASHRAE Book [20] and the results computed by the software developed for this study.

Table 3. Numerical code verification: U-value and SHGC.

Glazing configuration	U-value		SHGC	
	ASHRAE	Present work	ASHRAE	Present work
Double glazing (DG)	2.91	2.94 (1.03 %)	0.76	0.75 (1.32 %)
Triple glazing (TG)	2.06	2.02 (1.94 %)	0.68	0.67 (1.47 %)

*() represents the percentage deviation

5 Results and discussion

A comprehensive comparative analysis was conducted, assessing three distinct glazing configurations through advanced numerical simulations. The analysis is structured into two distinct components: the initial segment delves into the dynamic thermal attributes, while the subsequent part meticulously examines the energy efficiency gains, electricity consumption costs, and the associated CO₂ emissions for the extreme weather conditions experienced during the warmest and coldest days of 2018 in four significant Mexican cities – namely, Monterrey, Mexico City, Merida, and Ciudad Juarez. While the focus of this work is on the climatic extremes, it's noteworthy that the numerical modeling for each day involved an intricate consideration of weather data spanning two day prior. This method was employed to ensure system stability,

while minimizing the impact of initial conditions on the thermal performance of the glazings-

5.1 Decrement factor and time lag

The results of the decrement factor (DF) provide valuable insights into thermal performance of the three glazing configurations in the context of different climatic conditions in the selected cities. DF values close to 1 indicate that the glazing has limited ability to mitigate temperature fluctuations, essentially resulting in a minimal insulation against external temperature variations. Conversely, DF values close to 0 signify that the glazing structure effectively maintains a substantial temperature differential between the indoor and outdoor environments. This reduction in heat transfer leads to notable impacts on the heat flux per unit area, electricity consumption costs, and CO₂ emissions, underscoring the significance of these findings.

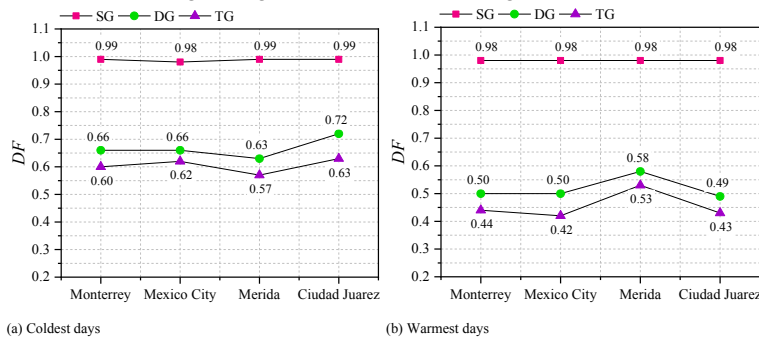


Fig. 4. Decrement factor of single glazing window and multiple glazing windows.

In Fig. 4, it can observe the DF values for each glazing configuration across the four representative cities and for both the coldest and warmest days of the year. Notably, the single glazing (SG) configuration exhibits relatively constant DF values close to 1 for both extreme weather conditions. This consistency suggests that single glazing is less effective in providing thermal insulation, as it is unable to significantly reduce heat transfer across the window. On the coldest day, the triple glazing (TG) configuration demonstrates more favorable DF values, ranging between 0.57 and 0.63. Of particular interest is the observation that Merida, where the outside temperature closely approximates the inside temperature of 25 °C, exhibits the lowest DF value. In this context, the limited temperature differential reduces the heat transfer process, leading to a more efficient thermal performance of the window. Conversely, in Merida during the warmest day, where the outside temperature rises to 41.6 °C and experiences prolonged exposure to solar radiation, the DF of the multi-glazed window configuration is notably higher compared to the other cities. This indicates that the multi-glazed window configuration offers superior insulating in this challenging climate, as it effectively reduces heat transfer, minimizing the impact of external heat sources.

10

Time lag (TL) is a crucial factor in understanding how quickly changes in weather conditions affect the thermal behavior of windows. On one hand, for low temperature values, a short time lag is required to increase the window's heat transfer rate and reduce energy loss from the indoor to outdoor environment. Whereas for high temperature values, a high time lag is required in order to avoid overheating, specifically for multi-glazed windows.

Table 4 shows the minimum time lag (TL) for coldest days and the maximum value of it for the warmest days. For single glazing, the time lag is recorded as 0, indicating that this configuration is highly responsive to changes in weather conditions. As a result, it experiences energy loss during the coldest days and excess energy gain during the warmest days. The absence of a time lag means that the single glazing configuration is not effective at mitigating temperature fluctuations. On the other hand, double glazing maintains a consistent value of TL_{\min} in 0.17 h across all four cities. This time lag is notably lower than the values observed for triple glazing, which can be up to 80 % higher, especially in the case of Monterrey. The capacity of double glazing to maintain a smaller time lag suggest the effectiveness in providing insulation against temperature variations. In Mexico City, multi-glazed windows exhibit a consistent time lag for both the coldest and warmest days, owing to the relatively small difference between the lowest and highest outside temperature values, which is approximately 15 °C.

However, during the warmest day, Merida and Ciudad Juarez experience similar outside ambient temperature values, 41.6 °C and 46.1 °C, respectively. Despite this, triple glazing introduces a time lag of approximately 2.5 h, effectively delaying the impact of climatic conditions on the thermal performance of the window. This time lag is particularly noteworthy, as it contributes to energy efficiency during extreme heat conditions, showcasing the effectiveness of triple glazing in these specific conditions.

In summary, Table 4 highlights the significant role of glazing configuration in influencing time lag, which, in turn, impacts energy efficiency and the ability to maintain stable thermal performance in different climatic scenarios.

Table 4. TL for the coldest and warmest day of each city.

City	Coldest day, TL_{\min} (h)			Warmest day, TL_{\max} (h)		
	SG	DG	TG	SG	DG	TG
Monterrey	0.00	0.17	0.83	0.00	1.67	1.83
Mexico City	0.00	0.17	0.17	0.00	0.17	0.17
Merida	0.00	0.17	0.67	0.00	2.33	2.50
Ciudad Juarez	0.00	0.17	0.33	0.00	2.17	2.33

5.2 Total heat flux, costs of electricity consumption, and CO₂ emissions

Table 5 provides the results of the numerical integration, as described by Eq. (14), representing the heat flux per unit area during the coldest and warmest days of the year for each city under consideration. Low values of q_i signify a reduced heat transfer rate through the window, which occurs when the window's temperature closely

aligns with the indoor temperature, and the influence of solar radiation on heat transfer remains negligible. It is noteworthy that, across all cities and for both extreme conditions, single glazing consistently exhibits the highest values of q_i , followed by double glazing and triple glazing, in that sequence. This is indicative of the influential role played by glazing structure and the specific thermophysical and optical properties of the glass in shaping the heat transfer dynamics.

Table 5. Daily total heat flux, kWhm⁻².

City	Coldest day			Warmest day		
	SG	DG	TG	SG	DG	TG
Monterrey	3.16	2.40	1.97	2.51	1.85	1.53
Mexico City	3.54	2.68	2.21	1.89	1.42	1.17
Merida	3.62	2.87	2.40	2.67	2.09	1.75
Ciudad Juarez	4.02	3.11	2.56	2.84	2.14	1.78

The alteration of the window's structure, accomplished by introducing additional glass panes and creating air gaps between them, notably enhances the window's thermal resistance. Consequently, the influence of the temperature differential between the interior and exterior environments becomes relatively insignificant. However, in the presence of solar radiation, the glass panes undergo energy absorption, leading to an elevation in heat transfer rates driven by both convection and radiation. It is essential to note that multi-glazed configurations, despite their increased thermal resistance, exhibit lower transmittance values when compared to single glazing. As a result, only a fraction of solar radiation successfully penetrates the window, which contributes to the intricate dynamics of heat transfer through these configurations.

In the context of solar radiation, it is worth noting that single glazing permits the transmission of approximately $\approx 85\%$ of the incident solar radiation upon the window surface. Conversely, multi-glazed configurations attenuate this solar energy in accordance with the relationship $(\tau_{g,1} * \dots * \tau_{g,n})G$, which mean that, based on the optical properties of clear glass, approximately $\approx 72.3\%$ of incident solar radiation successfully passes through double glazing, while $\approx 61.4\%$ penetrates triple glazing. It's crucial to emphasize that, beyond the contribution of transmitted heat flux q_i also encompasses the impact of heat transfer due to convection and radiation.

Upon the incidence of solar radiation onto the window surface, the glazing undergoes energy absorption, where short-wave solar energy is transformed into long-wave thermal energy. This phenomenon leads to an increase in the temperature of the glazing, subsequently influencing the heat transfer through both convection and radiation. It's noteworthy that the outcomes reveal a somewhat unexpected pattern: double glazing, contrary to initial expectations, merely reduces the daily value of q_i by a margin from 20% to 27%. In contrast, triple glazing demonstrates a more substantial reduction, ranging from 33% to 39%. These observations underscore the intricate interplay between glazing structure and solar energy absorption in shaping heat transfer dynamics.

Across both the coldest and warmest days, Monterrey and Mexico City stand out by representing the lowest values of q_i . This translates to a substantial percentage of

reduction in comparison to single glazing configurations. On the flip side, the warm climatic conditions of Merida introduce a different challenge, leading to an overheating in multi-glazed windows due to energy storage. However, it's worth noting that the increased total transmittance value of multi-glazed windows enables them to maintain a noteworthy reduction in q_i . A similar scenario unfolds in Ciudad Juarez. These city-specific variations underscore the importance of considering regional climate factors when assessing the performance of different glazing configurations.

To determine the cost for electricity consumption and calculate CO₂ emissions, the data derived from q_i for each day were extrapolated to cover a 15-day period, resulting in estimates for the coldest and warmest months of the year. These months correspond to the winter and summer seasons. Interestingly, in both cases, Ciudad Juarez emerges as the city with the highest energy consumption. This can be attributed to the extreme climatic conditions that prevail in Ciudad Juarez during both winter and summer, necessitating a significantly higher demand for energy to maintain thermal comfort in buildings.

Table 6 provides an overview of the monthly costs associated with electricity consumption, specifically attributable to operation of heating or cooling systems in response to the thermal performance of the window. The calculations are based on an assumed electricity consumption rate of approximately 0.058 USD per kWh⁻¹, as reported by the "Comisión Federal de Electricidad" in Mexico for domestic usage. It's important to note that this assessment focuses exclusively on the energy demand arising from the window's thermal properties, excluding the impact of other household elements. This approach allows for a precise examination of the window's contribution to electricity consumption and the subsequent financial implications.

Table 6. Monthly cost of electricity consumption, USDm⁻².

City	Coldest month			Warmest month		
	SG	DG	TG	SG	DG	TG
Monterrey	4.68	3.55	2.92	3.72	2.74	2.27
Mexico City	5.97	4.52	3.73	3.19	2.40	1.97
Merida	5.82	4.61	3.86	4.29	3.36	2.81
Ciudad Juarez	6.92	5.36	4.41	4.89	3.69	3.07

On the other hand, Fig. 5 illustrates the monthly CO₂ emissions into the environment. These emissions are a result of the energy needed to either supply or remove energy in order to maintain thermal comfort conditions within buildings. The conversion of energy into CO₂ emissions is based on the electricity emission factor of 0.435 tCO₂e/MWh, as established by the Mexican Ministry of Environment and Natural Resources in 2022. This factor is utilized to calculate the indirect emission of greenhouse gases specifically attributed to electricity consumption. It's important to note that these emissions are directly associated with the energy requirements driven by the window's thermal performance and its impact on heating and cooling systems.

The results reveal notable variations in energy demand between winter and summer seasons across the four cities. For the coldest month, energy consumption is significantly higher, underscoring the necessity of implementing energy storage and

supply systems to mitigate energy costs and reduce environmental impact. Conversely, for the warmest month, the focus shifts towards minimizing excessive energy gain, emphasizing the importance of effective thermal insulation.

Multi-glazed windows offer a unique advantage by addressing both the heating and cooling needs of buildings. Multi-glazed windows contribute to reducing the energy and environmental indicators, offering a comprehensive solution. In contrast, single glazing configuration exhibit the highest cost per electricity consumption, imposing a substantial financial burden. Additionally, single glazing generates 33 % to 38 % more $\text{kgCO}_2\text{em}^{-2}$ compared to triple glazing, highlighting the comparatively higher environmental impact. These findings underscore the significance of glazing configuration choices in effectively managing energy consumption and environmental sustainability, particularly in the context of varying climatic conditions throughout the year.

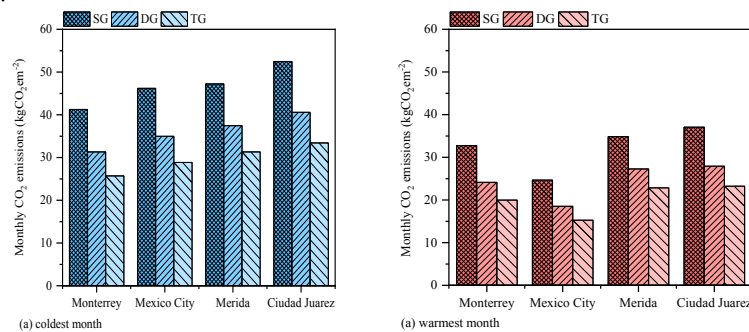


Fig. 5. Monthly CO₂ emissions in each city.

It is a paramount to underscore that the results presented in this analysis are specifically centered on the influence of window configurations on energy consumption and CO₂ emissions. This focused approach allows for a more detailed understanding of how windows can significantly influence energy efficiency and environmental impact. Nevertheless, the primary source of error lies in the fact that both energy consumption and CO₂ emissions are influenced by a multitude of factors within a building, including the efficiency of HVAC systems, the insulation of walls, roofs, and floors, building orientation, architectural design, the presence of additional insulating material, and occupant behavior. These findings emphasize the importance of window configurations as a specific factor within the broader context of building energy performance.

Hence, while the obtained results provide valuable insights into the importance of window configurations in energy performance and CO₂ emissions, they should not be perceived as a comprehensive and definitive analysis of a building's energy efficiency. A holistic approach of all building elements and systems would be imperative to obtain a complete and accurate depiction of the energy and environmental performance.

14

6 Conclusions and future work

In this work, a comparative study of three glazing configurations, single (SG), double (DG), and triple (TG), was conducted. The aim was to show the potential energy saving advantages of multi-glazed windows under the climatic conditions of four representative cities in Mexico. The dynamic modeling of conjugate heat transfer revealed several noteworthy findings:

- Multi-glazed configurations, particularly triple glazing, exhibited significant energy-saving potential, reducing the decrement factor by more than 50 % in comparison to single glazing. Additionally, TG demonstrated a substantial ability to delay the influence of weather conditions on window heat transfer rates, with a time lag of up to 2.5 h.
- Cities with temperate climates, such as Monterrey and Mexico City, consistently displayed lower values of heat flux per unit area, reduced electricity consumption costs and diminished CO₂ emissions, indicating the effectiveness of multi-glazed windows in such settings.
- However, in tropical climate regions, the use of multi-glazed windows resulted in overheating and increased heat transfer rates, thereby affecting dynamic thermal characteristics and energy indicators.
- Ciudad Juarez emerged as the city with the highest energy consumption highlighting the necessity of implementing thermally reinforced glazing systems to mitigate the impact of seasonal climatic variations.
- Single glazing proved to be the least energy-efficient option, incurring the highest cost per electricity consumption and generating 33 % to 38 % more kgCO₂em⁻² relative to triple glazing.

In light of these findings, it is crucial to conduct annual comparative studies to assess the impact of multi-glazed windows in diverse scenarios. Furthermore, the integration of multi-glazed windows within room environments warrants further investigation to understand their implications for thermal comfort and energy performance.

Acknowledgments

Samanta López Salazar acknowledges the National Council of Humanities Sciences and Technologies (CONAHCYT) for the support provided during her postgraduate studies, CVU: 918135 and GRANT NUMBER: 789202.

References

1. Secretaría de Energía | Gobierno | gob.mx. (s. f.). <https://www.gob.mx/sener>
2. Somasundaram, S., Chong, A., Wei, Z., & Thangavelu, S. R. (2020). Energy saving potential of low-e coating based retrofit double glazing for tropical climate. *Energy and Buildings*, 206, 109570. <https://doi.org/10.1016/j.enbuild.2019.109570>
3. Xamán, J., Jiménez-Xamán, C., Álvarez, G., Zavala-Guillén, I., Hernández-Pérez, I., & Aguilar, J. (2016). Thermal performance of a double pane window with a solar control coating for warm climate of Mexico. *Applied Thermal Engineering*, 106, 257-265. <https://doi.org/10.1016/j.applthermaleng.2016.06.011>

4. Ihm, P., Park, L., Krarti, M., & Seo, D. (2012). Impact of window selection on the energy performance of residential buildings in South Korea. *Energy Policy*, 44, 1-9. <https://doi.org/10.1016/j.enpol.2011.08.046>
5. Rodríguez-Ake, A., Xamán, J., Hernández-López, I., Saucedo, D., Carranza-Chávez, F. J., & Zavala-Guillén, I. (2022). Numerical study and thermal evaluation of a triple glass window under Mexican warm climate conditions. *Energy*, 239, 122075. <https://doi.org/10.1016/j.energy.2021.122075>
6. Gutai, M., & Kheybari, A. G. (2021). Energy consumption of hybrid smart water-filled glass (SWFG) building envelope. *Energy and Buildings*, 230, 110508. <https://doi.org/10.1016/j.enbuild.2020.110508>
7. Ma, L., Zhang, X., Dong, L., Arıcı, M., Yıldız, Ç., Li, Q., Zhang, S., & Jiang, W. (2020). Influence of Sunspace on energy consumption of rural residential buildings. *Solar Energy*, 211, 336-344. <https://doi.org/10.1016/j.solener.2020.09.043>
8. Ismail, K. A., Aguilar-Salinas, C. A., & Henríquez, J. A. (2009). A comparative study of naturally ventilated and gas filled windows for hot climates. *Energy Conversion and Management*, 50(7), 1691-1703. <https://doi.org/10.1016/j.enconman.2009.03.026>
9. Li, S., Zou, K., Sun, G., & Zhang, X. (2018). Simulation research on the dynamic thermal performance of a novel triple-glazed window filled with PCM. *Sustainable Cities and Society*, 40, 266-273. <https://doi.org/10.1016/j.scs.2018.01.020>
10. Chen, Y., Xiao, Y., Zheng, S., Liu, Y., & Li, Y. (2018). Dynamic heat transfer model and applicability evaluation of aerogel glazing system in various climates of China. *Energy*, 163, 1115-1124. <https://doi.org/10.1016/j.energy.2018.08.158>
11. Alghoul, S. K., Rijabo, H. G., & Mashena, M. E. (2017). Energy consumption in buildings: A correlation for the influence of window to wall ratio and window orientation in Tripoli, Libya. *Journal of building engineering*, 11, 82-86. <https://doi.org/10.1016/j.jobe.2017.04.003>
12. Kahsay, M. T., Bitsuamlak, G., & Tariku, F. (2020). Effect of window configurations on its convective heat transfer rate. *Building and Environment*, 182, 107139. <https://doi.org/10.1016/j.buildenv.2020.107139>
13. Djamel, Z., & Noureddine, Z. (2017). The Impact of Window Configuration on the Overall Building Energy Consumption under Specific Climate Conditions. *Energy Procedia*, 115, 162-172. <https://doi.org/10.1016/j.egypro.2017.05.016>
14. Wang, T., & Wang, L. (2016). The effects of transparent long-wave radiation through glass on time lag and decrement factor of hollow double glazing. *Energy and Buildings*, 117, 33-43. <https://doi.org/10.1016/j.enbuild.2016.02.009>
15. González-Julián, E., Xamán, J., Moraga, N. O., Chávez, Y., Zavala-Guillén, I., & Simá, E. (2018b). Annual thermal evaluation of a double pane window using glazing available in the Mexican market. *Applied Thermal Engineering*, 143, 100-111. <https://doi.org/10.1016/j.applthermaleng.2018.07.053>
16. Duffie, J. A., & Beckman, W. A. (2013). *Solar Engineering of Thermal Processes*. En John Wiley & Sons, Inc. eBooks. <https://doi.org/10.1002/9781118671603>
17. Swinbank, W. C. (1963). Long-wave radiation from clear skies. *Quarterly Journal of the Royal Meteorological Society*, 89(381), 339-348. <https://doi.org/10.1002/qj.49708938105>
18. De Estadística Y Geografía Inegi, I. N. (s. f.). Instituto Nacional de Estadística y Geografía (INEGI). <https://www.inegi.org.mx/>
19. Servicio Meteorológico Nacional. (s/f). Gob.mx. Recuperado el 21 de junio de 2023, de <https://smn.conagua.gob.mx/es/>
20. American Society of Heating, Refrigeration and air conditioning engineers. *Handbook of fundamentals*; 2001.

Comparative assessment of roofing strategies for thermal load reduction, energy efficiency, and CO₂ emission mitigation in a tropical climate

Samanta López Salazar^{1,*}[0009-0004-9880-5145], T. Lima-Téllez^{2,*}[0009-0001-1072-8324],
Ruitong Yang³[0000-0002-8442-0445], E. Simá¹[0000-0001-7601-1273],
I. Hernández-López²[0000-0002-5986-6111], Dong Li³[0000-0002-2692-9091]

¹Tecnológico Nacional de México / CENIDET, Prol. Av. Palmira S/N, Col. Palmira, Cuernavaca, Morelos CP 62490, México

²Universidad de Sonora, DIQyM-UNISON, Blvd. Luis Encinas y Rosales S/N, Hermosillo, Sonora, CP 83000, México

³School of architecture and civil engineering, Northeast Petroleum University, Fazhan Lu Street, Daqing, CP 163318, China

d18ce057@cenidet.tecnm.mx
a220230038@unison.mx
yangruitong17@163.com
e.sima@cenidet.tecnm.mx
irving.hernandez@unison.mx
lidonglvyan@126.com

Abstract. This study systematically analyzed roofing strategies tailored for warm tropical climate, focusing on the impact on heat transfer, thermal load, electricity costs, and CO₂ emissions. Three primary strategies were investigated: conventional concrete roof, insulated roof, and a roof integrated with Phase Change Material (PCM) along with a white reflective coating. The findings highlight the insulated roof with a white reflective coating (IR-W) as the most effective solution, delaying weather-related impacts by about 3 hours, and significantly reducing energy losses by 77 % on the coldest day and energy gains by 92 % on the warmest day. The use of a white reflective coating alone reduced thermal loads, electricity costs, and CO₂ emissions by 56 %. Adding insulation and PCM alongside the coating achieved even greater reductions of 81 % and 69 %, respectively. This research emphasizes the vital importance of selecting suitable roofing strategies in tropical climate, offering potential for remarkable improvements in energy efficiency and sustainability. It provides a valuable reference for professionals and policymakers grappling with climate challenges akin to those experienced in tropical regions.

Keywords: roof thermal behavior, cooling coating, phase change material

1 Introduction

A building's roof plays a critical role in thermal comfort due to constant exposure to environmental elements, primarily direct solar radiation. This solar radiation notably impacts indoor temperatures, especially in hot weather, and can contribute up to

2

50 % of a building's thermal load [1]. Thus, it's crucial to implement passive technologies to improve thermal performance, categorized as architectural and non-architectural methods [2].

Non-architectural methods, like cool roofs, can be applied without altering the roof's geometry and are suitable for existing buildings. Cool roofs typically entail applying a reflective coating to the external surface of a standard roof, which is specifically designed to reflect solar radiation. According to Hernandez – Perez et al. [3], roofs featuring reflective coating maintain lower temperature compared to roofs with standard materials when exposed to similar weather conditions. This phenomenon can be attributed to the optical properties of the reflective materials. Another non-architectural method is the application of ventilated roofs, which entails placing a cover over a conventional roof while maintaining an open channel or gap between the roof and the cover. In this sense, Lima-Tellez et al. [4] discovered that implementing a ventilated roof in a hot climate reduced energy gain by 60 % compared to a conventional roof. On the other hand, architectural roof solutions, in contrast, entail roof configuration and geometry modifications during the building's planning and construction phases. These methods encompass hollow block roofs, thermally insulated roofs, and the integration of phase change materials (PCMs), a rising trend in recent years.

PCMs function as thermal storage through phase change processes. In hot weather, they melt and absorb heat, reducing roof temperatures and delaying heat transfer into the building [5]. Proper PCM selection and placement are vital to ensure complete daily melting and solidification cycles. Al-Absi et al. [6] emphasized the importance of considering factors like climate, project objectives, indoor conditions, building materials, and PCM properties. They recommended an evaluation process for each project that accounts for these elements.

Researchers are actively exploring the integration of PCMs into roofing systems alongside other passive technologies. For example, Yang et al. [7] investigated the use of a cool roof with PCMs to combat the urban heat island (UHI) effect. They observed that the combination significantly lowered indoor roof temperatures throughout the year, effectively mitigating the UHI effect. In a related study, Triano – Juarez et al. [8] numerically analyzed PCM and reflective coating applications on roofs in a warm-humid Mexican climate. PCM 35, in particular, effectively completed the phase change cycle and displayed notable heat gain reduction. When combined with reflective materials, energy savings increased by 40 % to 45 %.

Following this, Xamán et al. [9] performed a numerical analysis of roof thermal behavior in a warm Mexican climate, incorporating PCM. The study assessed three roof configurations, with results showing a substantial 53 % reduction in indoor temperatures and thermal load compared to conventional concrete roof. In the same year, Rathod et al. [10] investigated the influence of PCM tilt on roof temperature and energy gain. Their research demonstrated that a roof with a 2 ° slope, incorporating PCM, achieved a 2.4 °C reduction in roof temperature and a 16 % decrease in energy gain in comparison to a conventional roof.

On the other hand, Baybourdy et al. [11] explored the effects of introducing PCM and insulating materials into a building's roof. Their investigation yielded a 32.5 %

decrease in annual energy consumption and a 42 % reduction in thermal load. In 2022, Rangel et al. [12] analyzed the thermal performance of roofs incorporating PCM, both with and without natural ventilation. The outcomes affirmed PCMs effectiveness in enhancing thermal performance in experimental modules within hot and semi-arid climates. Subsequently, Sedaghat et al. [13] conducted experimental research on bioPCM in a hot tropical climate, demonstrating substantial energy saving of up to 53 %.

In 2023, Gao et al. [14] conducted a comprehensive literature review on PCM utilization in roofs. They highlighted paraffins and salt eutectics as the most commonly employed PCM types and identified modeling methods for the phase change process, including the enthalpy method, heat capacity method, and enthalpy-porosity method. Concurrently, Hinojosa et al. [15] presented a descriptive review of PCM applications in building envelopes, concluding that PCM integration could reduce indoor temperature and heat flux by up to 6.2 °C and 97 %, respectively. Additionally, their findings revealed a significant 52 % decrease in energy consumption.

In conclusion, advancing sustainable and eco-friendly construction practices requires the development and utilization of energy-efficient building materials, designs, and technologies. This study makes a significant contribution by comprehensively evaluating various roof configurations (concrete, insulated, PCM with and without reflective coating) to enhance energy efficiency and occupant comfort within buildings. A unique feature of this study is the concurrent assessment of these roof configurations, along with a detailed analysis of the dynamic characteristics, offering substantial insights into thermal performance.

The exclusive focus on roofing configurations is justified by the substantial impact on energy gains in warm tropical climate. This approach enables an in-depth exploration of the thermal dynamics of roofing strategies, isolating the influence from other building components. Once the optimal roof design is identified, it can be integrated into a full building model to assess the impact on overall thermal comfort, bridging the gap between research and practical implementation. This targeted analysis provides precise insights into energy efficiency and emissions reduction, thus representing a vital step toward sustainable construction practices in tropical regions.

2 Physical and mathematical model

Fig. 1 shows the physical model of a two-dimensional geometry that illustrates the structure of three building roof configurations: CR a reinforced concrete slab, IR a roof composed of a reinforced concrete slab, an insulating layer of polystyrene, and a layer of plaster, and PCMR a roof with a phase change material encapsulated between two reinforced concrete slabs of different thickness; nevertheless, the length of the roof is the same in all cases, $Hx=1$ m. For the three roof configurations, the notation “W” and “W/O” is employed, where “W” indicates the inclusion of a white reflective coating on the outer surface, while “W/O” signifies the absence of such a coating.

The thickness of the case a, and the layer thickness of the cases (b) and (c) are shown in Table 1; this data was obtained from the literature as well as the thermo-

4

physical properties of solid materials and PCM, see Table 2 and Table 3 [8, 16]. While the optical properties of the white reflective coating were taken from [3].

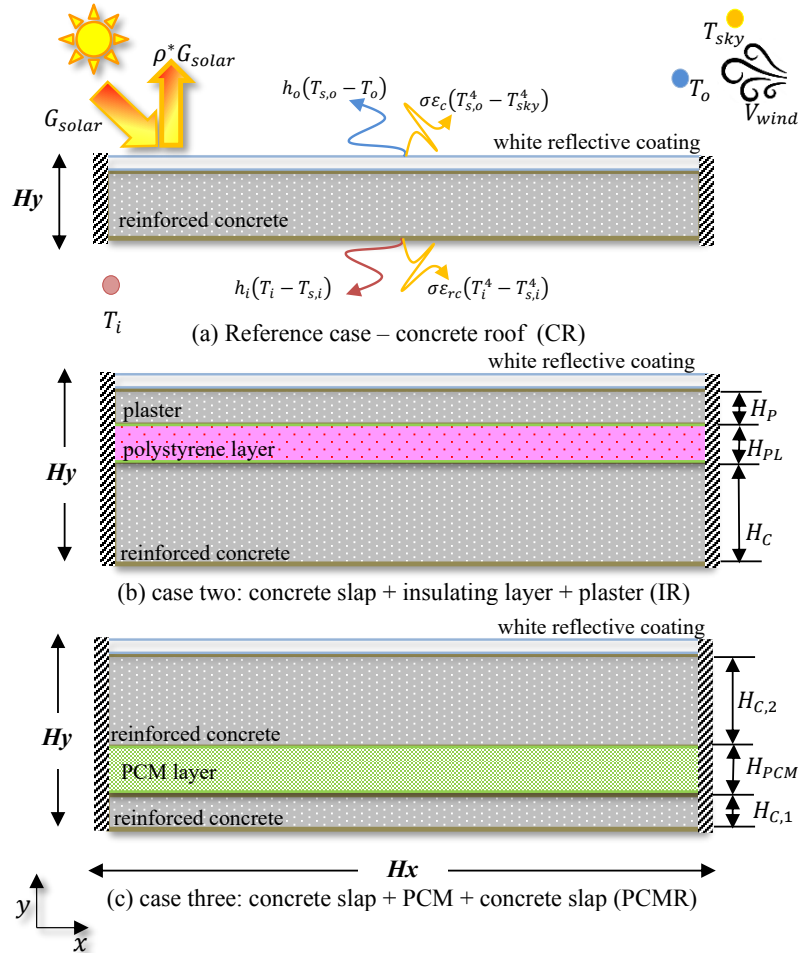


Fig. 1. Physical model of different roof configurations.

Table 1. Layer thickness of each roof configuration.

	Layer thickness (cm)		
	Inner layer	Middle layer	Outer layer
CR	10.0	-	-
IR	10.0	2.5	0.5
PCMR	2.0	1.0	10.0

Table 2. Thermophysical properties of the materials.

Material	λ (Wm ⁻¹ °C ⁻¹)	ρ (kgm ⁻³)	C_p (Jkg ⁻¹ °C ⁻¹)
Plaster	1.28	2200	850
Reinforced concrete	1.74	2300	920
Polystyrene	0.033	28	1800

Table 3. Thermophysical properties of the PCM 35.

Phase	λ (Wm ⁻¹ °C ⁻¹)	ρ (kgm ⁻³)	C_p (Jkg ⁻¹ °C ⁻¹)	h (Jkg ⁻¹)	T (°C)
Solid	0.20	860	2000	158000	29
Liquid					36

The mathematical formulation describing the conduction heat transfer in two-dimensional solid materials: such as concrete slabs, plaster, and insulating plate, in transient state, is expressed as follows:

$$\frac{\partial(\rho C_p T)}{\partial t} = \frac{\partial}{\partial x} \left(\lambda \frac{\partial T}{\partial x} \right) + \frac{\partial}{\partial y} \left(\lambda \frac{\partial T}{\partial y} \right) \quad (1)$$

The choice of modeling the phenomenon in 2D, despite the adiabatic boundary conditions on the vertical walls (see Fig. 1), is well justified. While it is true that for the specific case presented in this work, a 1D model could have sufficed due to the boundary conditions and uniform solar radiation, the decision to opt for a 2D approach is rooted in the long-term vision for this research work. More precisely, the authors are in the process of expanding and enhancing the code with the aim of addressing more complex and realistic scenarios in future research endeavors.

On the other hand, thermal diffusion in a phase change material, PCM, is described by the following equation:

$$\frac{\partial(\rho_{PCM} C_{p_{eff}} T_{PCM})}{\partial t} = \frac{\partial}{\partial x} \left(\lambda_{PCM} \frac{\partial T_{PCM}}{\partial x} \right) + \frac{\partial}{\partial y} \left(\lambda_{PCM} \frac{\partial T_{PCM}}{\partial y} \right) \quad (2)$$

The solution to Eq. (2) was accomplished by employing the effective heat capacity method. This technique incorporates the phase change phenomena into the heat capacity term, denoted as $C_{p_{eff}}$, by including the enthalpy change h_{ls} , that arises during the phase transition. Hence, the effective heat capacity encompasses both the energy storage and the latent heat associated with the phase change, as described in Eq. (3).

$$C_{p_{eff}} = \begin{cases} C_{ps} & \text{for } T < (T_m - \Delta T) \\ \frac{C_{ps} + C_{pl}}{2} + \frac{h_{ls}}{2\Delta T} & \text{for } (T_m - \Delta T) < T < (T_m + \Delta T) \\ C_{pl} & \text{for } T > (T_m + \Delta T) \end{cases} \quad (3)$$

Where, C_{ps} and C_{pl} represent the specific heats of the solid and liquid phases, T_m is the melting point temperature and the phase change range T_l - T_s is denoted as $2\Delta T$.

For all cases, the outer surface is exposed to weather conditions of wind velocity, outside temperature, and solar radiation, while the inner surface is exposed to a constant value of temperature, $T_i=25$ °C. In both surfaces, heat losses by convection and

6

radiation are considered, where $h_o=2.8+3.0V_{wind}$ according to [17] and $h_i=9.26 \text{ Wm}^{-2}\text{K}^{-1}$ if $T_{s,i} < T_i$ and $h_i=6.13 \text{ Wm}^{-2}\text{K}^{-1}$ if $T_{s,i} > T_i$, [18]. On the other hand, the sky temperature is calculated by the correlation reported by Swinbank [19]. The selection of correlations for the convection heat transfer coefficient and the determination of sky temperature is founded on the proven effectiveness and enduring acceptance within the global scientific community. These correlations have withstood the test of time and remain widely acknowledged and trusted to this day.

$$-\frac{\partial T}{\partial y} = \alpha^* G_{solar} + h_o(T_{s,o} - T_o) + \varepsilon\sigma(T_{s,o}^4 - T_{sky}^4) \quad (4)$$

$$-\frac{\partial T}{\partial y} = h_i(T_i - T_{s,i}) + \varepsilon\sigma(T_i^4 - T_{s,i}^4) \quad (5)$$

On the other hand, the boundary conditions at the vertical walls are assumed to be adiabatic, meaning that no heat exchange occurs throughout the walls. In addition, for the initial condition, it was considered to take into account the thermal behavior, temperature, of the day before the day selected for the analysis in order for the system to stabilize and the initial condition does not have a significant effect on the results. Moreover, to couple the composite layers of the roof, an energy balance was performed at the interface, taking into account the conductive heat flux.

In order to evaluate the dynamic thermal characteristics of different roof configurations, two key parameters are computed: the time lag (TL) and decrement factor (DF), Eqs. (6-8). The time lag is determined by the time difference, in hours, between the peak outdoor temperature, $T_{so}(t)$, and the peak indoor temperature, $T_{si}(t)$. On the other hand, the “decrement factor” refers to the relationship between the amplitude of the external temperature wave, A_o , and internal temperature wave, A_i .

$$TL_{min} = t_{si,min} - t_{so,min} \quad (6)$$

$$TL_{max} = t_{si,max} - t_{so,max} \quad (7)$$

$$DF = \frac{A_i}{A_o} = \frac{T_{si,max} - T_{si,min}}{T_{so,max} - T_{so,min}} \quad (8)$$

On the other hand, the total heat flux per unit area through the roof is determined by numerically integrating the heat flux over a 24-hours period, as shown in Eq. (9).

$$q_{t,i} = \int_{00:00}^{24:00} q_i(t) dt \quad (9)$$

The monthly total heat flux per unit area was computed by the following equation, reported by [20], where $q_{q,i}^{coldest}$ and $q_{q,i}^{warmest}$ are the daily total heat flux for the coldest and warmest day of each month, and N denotes the number of days in each month. This computation is carried out to ascertain the energy requirements, electricity consumption costs, and the emissions of CO₂ into the environment.

$$q_{m,i} = q_{q,i}^{coldest} + \left[\left(\frac{q_{q,i}^{coldest} + q_{q,i}^{warmest}}{2} \right) N - 2 \right] + q_{q,i}^{warmest} \quad (10)$$

3 Weather data

The weather data correspond to the Köppen *Aw* classification and were extracted from the database of the National Meteorological Service. Fig. 2 shows the behavior of the wind velocity, outside temperature, and solar radiation on the horizontal plane for the coldest and warmest days of the year 2022 in Merida, Yucatan – Mexico ($20^{\circ}41'49.56''$ N and $89^{\circ}48'04.32''$ W); the days were selected according to the lowest and highest values of temperature in each month. The lowest and highest value of temperature were 14.6°C and 41.3°C in January and April, respectively.

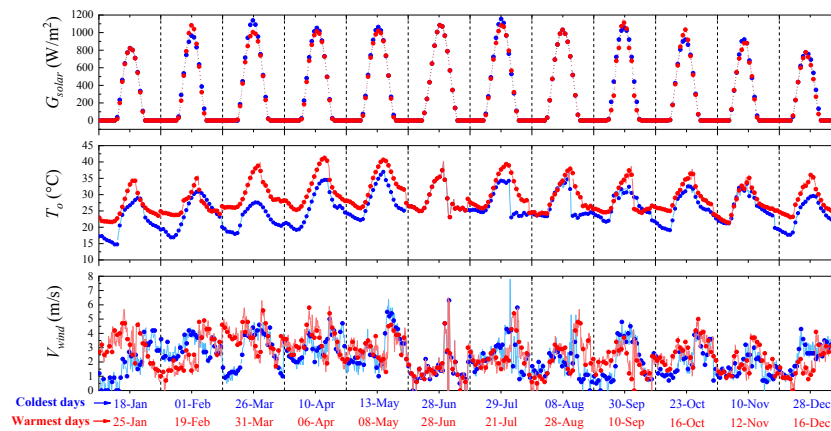


Fig. 2. Weather data for the coldest and warmest days of the year 2022 in Merida, Yucatan.

4 Numerical solution methodology

The finite volume method was employed to solve mathematical models describing heat conduction in two dimensions and transient state, both in solid material and phase change material; this approach effectively addressed the heat transfer dynamics. The temporal term was discretized using the totally implicit scheme, while the diffusive term was approximated using the central difference scheme. The system of algebraic equations resulting from the discretization process was solved using the Gauss-Seidel method in alternating directions (LGS-ADI). In order to ensure the convergence of the results, a tolerance of 10^{-10} was established for the residual of all variables.

An analysis to determine the optimal time step and grid mesh to model the roof was performed taking into account the effect on the results of temperature and heat flux per unit area of five time steps: 5, 10, 15, 20, and 30 s, and different grid size. A grid size of 121×41 nodes was used for the concrete slab of case (a) and case (c) while for the plaster layer and insulating layer a grid size of 121×11 and 121×21 nodes was used. On the other hand, for the PCM layer several numerical tests was

8

performed in order to determine the optimal grid mesh in vertical direction, $N_y = 11 \dots 51$ nodes. After that, a 10 s time step with a grid size of 121×31 nodes for the PCM layer and the already mentioned grid size for the other layers were selected, based on the results of the roof temperature and total heat flux with a maximum deviation $\approx 2\%$ compared to a small time step and a fine mesh.

The study verified the numerical model's accuracy in simulating a composite roof comprising a concrete slab with an integrated PCM layer of Paraffin wax MG29. The reference work by [8] provided details about the composition and thermal performance of the PCM roof system. Fig. 3 compares the temperature data of the inner and outer roof surfaces obtained from the reference with those from the numerical model. The results exhibit strong similarity, with any discrepancies likely stemming from variations in the weather data used during the numerical simulations.

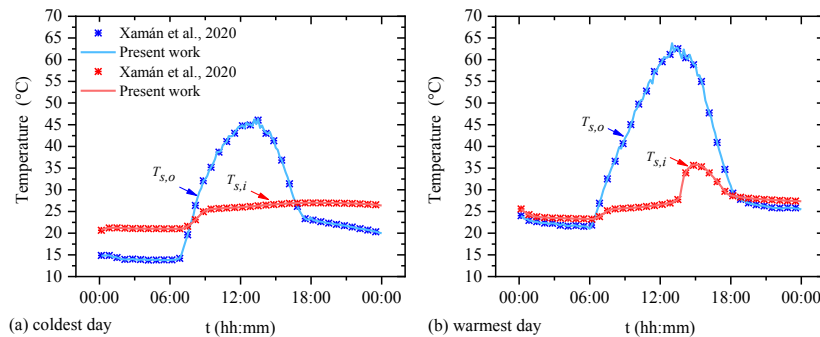


Fig. 3. Comparison of the roof temperature with PCM Paraffin wax MG29.

5 Results and discussion

In this section a comparative analysis of six strategies to reduce thermal load in tropical roofs is presented. The analysis includes numerical results that encompass thermal behavior, load reduction, electricity costs, and CO_2 emissions. The objective is to identify the most efficient approach for enhancing roof thermal performance in tropical climates.

5.1 Dynamic thermal properties for the coldest and warmest day

The roof's time lag (TL) is crucial for regulating heat transfer. In low-temperature conditions, a short TL is necessary to increase the roof's heat transfer rate, minimizing energy loss from the indoor space to the outdoor environment. This rapid response reduces discomfort caused by indoor cold conditions. Conversely, in high-temperature conditions, an extended TL is required to prevent excessive energy gain. This extended time lag acts as a critical buffer, limiting the influx of outdoor heat and maintaining a comfortable indoor temperature. On the other hand, decrement factor (DF) values observed in the study offer valuable insights into the roof's performance. DF val-

ues approaching 1 indicate that the roof is less effective in mitigating the temperature fluctuations, as indoor and outdoor temperatures exhibit similar variations. In contrast, lower DF values, approaching 0, suggest that the roof configurations can sustain a significant temperature difference between the indoor and outdoor environments. This implies that the heat transfer rate is lower in such roof configurations, ultimately contributing to improved thermal performance.

Table 4 displays results related to time lag, with minimum values on the coldest day and maximum values on the warmest day, as well as DF values for the six distinct roof configurations during both days of the year. Notably, the insulated roof with a white reflective coating (IR-W) emerges as the most promising configuration, especially when considering DF values. These DF values demonstrate minimal variations between the coldest and warmest days, indicating that seasonal weather changes have a limited impact on this roof configuration's thermal performance. Moreover, on the warmest day, IR-W exhibits a TL of 2.66 h concerning the point where the highest outdoor temperature and solar radiation values are recorded. Similarly, the PCM roof (PCMR-W) also shows a significant TL. These results collectively emphasize the effectiveness of the IR-W and PCM roof configurations in maintaining consistent design in a tropical environment.

Table 4. Dynamic thermal characteristics of different roof configurations.

Configuration	Coldest day		Warmest day	
	TL_{min}	DF	TL_{max}	DF
CR-W/O	0.83	0.50	1.33	0.52
CR-W	0.83	0.48	1.33	0.52
IR-W/O	1.16	0.05	2.16	0.06
IR-W	1.33	0.05	2.66	0.05
PCMR-W/O	1.16	0.33	2.16	0.37
PCMR-W	1.16	0.35	3.00	0.34

5.2 Thermal behavior for the coldest and warmest days

Fig. 4 provides a detailed visual representation of the internal surface temperature of the roof, denoted as $T_{s,i}$ and the total heat flux per unit area, represented as $q_{t,i}$, for both the coldest and warmest days of the year. During these two extreme scenarios, specific observations come to the forefront.

On both days, it's evident that the concrete roof configuration without a reflective coating (CR-W/O) exhibits notable temperature extremes. In the early morning of the coldest day, $T_{s,i}$ records the lowest point at 20.4 °C, specifically at 07:30 h (when the outer temperature is $T_o=18.0^\circ\text{C}$, $V_{wind}=0.0\text{ ms}^{-1}$, and $G_{solar}=125.5\text{ Wm}^{-2}$). Conversely, on the warmest day, the peak temperature on the roof's inner surface reaches 41.1 °C at 17:00 h (with $T_o=40.4^\circ\text{C}$, $V_{wind}=1.9\text{ ms}^{-1}$, and $G_{solar}=495.2\text{ Wm}^{-2}$). These temperature fluctuations correspondingly translate into the highest energy losses and gains for this configuration: a substantial energy loss of -66.4 Wm^{-2} and a considerable energy gain of 189.5 Wm^{-2} .

10

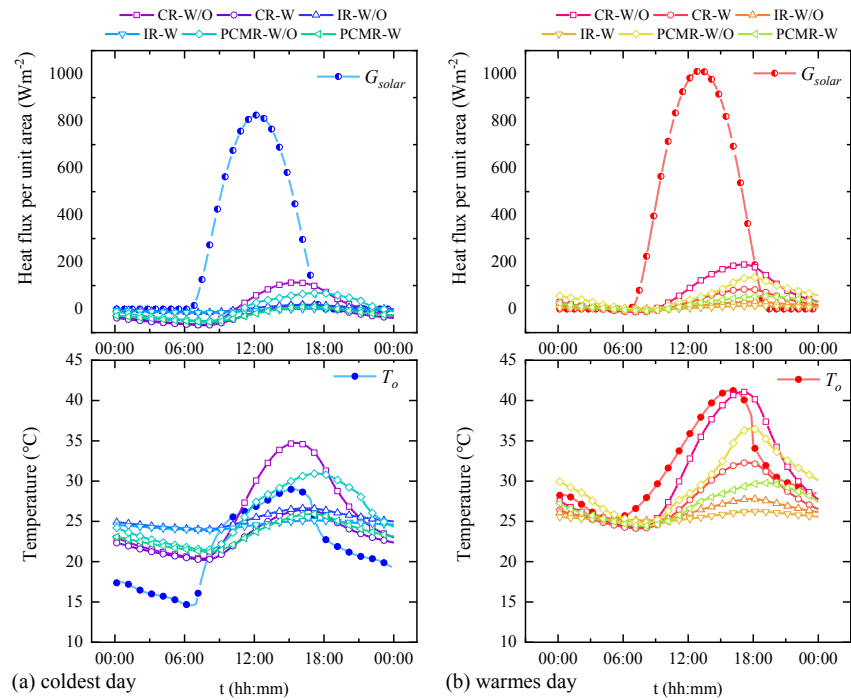


Fig. 4. Thermal behavior of different roof configurations for the coldest and warmest day of the year.

In stark contrast, the IR-W configurations stands out with a minimal temperature difference, $\Delta T_{s,i}$, of approximately 1.3 °C for both days (as detailed in Table 5). This indicates that the temperature variations, which stem from varying weather conditions, are quite subdued. Notably, the temperature characteristics of this configuration align closely with the desired indoor temperature, which is maintained at a comfortable 25 °C. Consequently, the heat transfer through convection and radiation to both the indoor and outdoor environments is notably curtailed.

Overall, the adoption of the IR-W configuration yields significant advantages. It leads to a remarkable 77 % reduction in energy loss on the coldest day and an equally notable decrease of approximately 92 % in energy gain on the warmest day when compared to the CR-W/O configuration. This impressive outcome primarily results from the combined effects of the white reflective coating’s attenuation of solar radiation and the insulating properties of the insulation material.

In the realm of phase change materials (PCMs), a fascinating transformation unfolds when delving into the liquid fraction calculations for different PCM configurations. These intricate calculations offer insights into how these materials respond to varying climatic conditions, both during the coldest and warmest days.

Table 5. Temperature variation on the inside surface.

Day	$\Delta T_{s,i}$, °C					
	CR-W/O	CR-W	IR-W/O	IR-W	PMCR-W/O	PMCR-W
Coldest	14.7	6.2	2.6	1.2	9.5	4.7
Warmest	16.8	8.2	2.7	1.3	11.7	5.3

Let’s focus on the PCM-W/O configuration, which paints an intriguing picture. As displayed in Fig. 5, a remarkable transition takes place, with the PCM shifting from a solid to liquid state after the clock strikes noon. This shift is intricately tied to the temperature trends. During the coldest day, it delicately treads within what is known as the “mushy zone”, where the liquid fraction lies between 0 to 1, indicating a partially melted state. Conversely, on the warmest day, the phase change is definitively completed, with the liquid fraction reaching the highest value of 1.

However, it’s noteworthy to consider that this phase change during hot weather might not yield the most favorable outcomes in terms of thermal performance. This transformation brings with it a substantial elevation in roof temperature. Consequently, the heat transfer rate experiences a corresponding surge, which may not align with desires for efficient thermal management.

Fig. 6 presents the daily thermal load of roofs with different configurations, determined through numerical integration of heat flux per unit area. These results offer a comprehensive view of thermal dynamics.

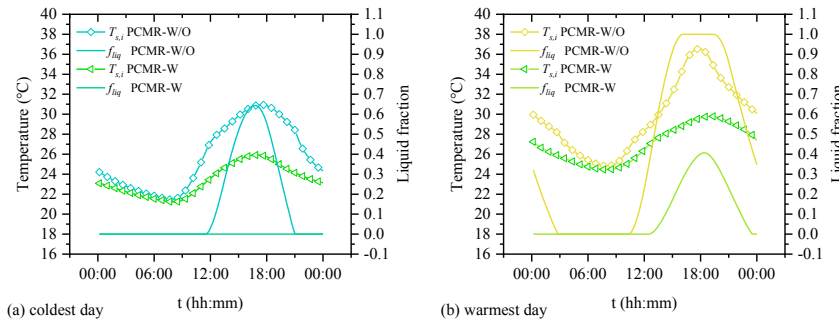


Fig. 5. Liquid fraction of roof PCM configurations for the coldest and warmest days.

In terms of thermal performance, configurations can be ranked in descending order as follows: insulated roof configurations (IR), PCM roof with coating (PCMR-W), concrete roof with coating (CR-W), PCM roof without coating (PCMR-W/O), and conventional concrete roof (CR). Notably, the IR-W configuration outshines the rest in terms of thermal performance on both the coldest and warmest days. This remarkable performance can be attributed to the lowest temperature fluctuations, resulting in reduced energy losses and gains. Most notably, the IR-W configuration substantially reduces the daily thermal load, by 86.7 % on the coldest day and an even more im-

12

pressive 91.3 % on the warmest day. These findings emphasize the superior thermal performance of the IR-W configuration, underscoring the capacity to consistently maintain ideal thermal conditions while significantly alleviating the daily thermal load. This not only showcases the effectiveness but also the potential for substantial energy savings and enhances indoor comfort in a tropical climate.

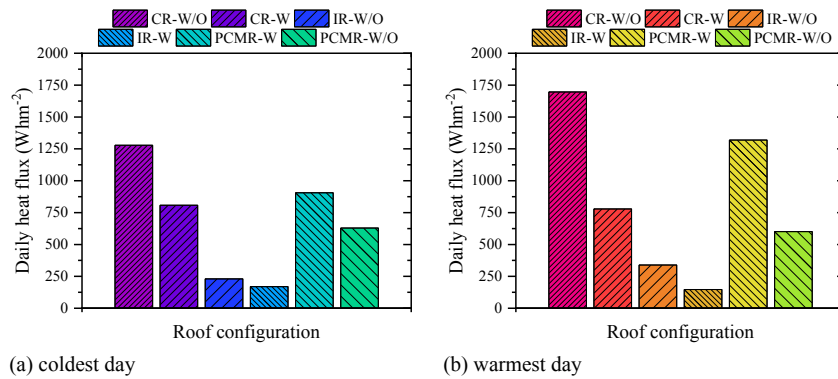


Fig. 6. Daily total heat flux of different roof configurations.

5.3 Annual thermal evaluation: thermal load, electricity consumption costs, and CO₂ emissions

The determination of the annual thermal load is derived from monthly calculations based on Eq. (10). Meanwhile, electricity consumption costs in the southern region of Mexico are assumed at an approximate rate ≈ 0.058 USD per kWh⁻¹, as reported by the Federal Electricity Commission for the domestic rate. Moreover, the conversion of energy into CO₂ emissions hinges on the electricity emission factor of 0.435 tCO₂e/MWh established by the Mexican Ministry of Environment and Natural Resources in 2022. This factor serves to gauge the indirect emission of greenhouse gases resulting from electricity consumption.

Table 6 serves as a repository of the outcomes obtained, providing a comprehensive overview of the annual thermal load, electricity consumption costs, and CO₂ emissions for each roofing configuration. From the annual assessment of the thermal performance of distinct roof types, it becomes evident that the application of a white reflective coating on a conventional roof leads to a noteworthy reduction in thermal load, electricity consumption costs, and CO₂ emissions, amounting to a 56 % decrease.

Furthermore, when integrating an insulating material and phase change material (PCM), the roofing configuration yields more substantial reductions of 81 % and 69 %, respectively. Notably, combining these elements with a white reflective coating enhances the effect, resulting in an approximately 10 % greater reduction compared to the use of insulation and PCM alone. These findings underscore the potential for sig-

nificant energy and cost savings, as well as reduced environmental impact, through thoughtful roofing strategies.

Table 6. Thermal load, electricity consumption costs, and CO₂ emissions per year.

Configuration	$\sum_{january}^{december} q_{monthly}$, (kWhm ⁻²)	COEC, (USDm ⁻²)	eCO ₂ , (kgCO ₂ em ⁻²)
CR-W/O	536.4	27.1	233.4
CR-W	234.3	11.8	101.9
IR-W/O	102.1	5.2	44.4
IR-W	56.8	2.9	24.7
PCMR-W/O	163.5	8.2	71.1
PCMR-W	117.2	8.9	77.1

6 Conclusions and future work

In this comprehensive study, an in-depth analysis of various strategies aimed at diminishing the heat transfer rate, thermal load, electricity consumption costs, and CO₂ emissions associated with roofs in a tropical climate was carried out. This analysis was underpinned by numerical findings obtained from a two-dimensional model, considering three distinct roof configurations: concrete roof, insulated roof, and a PCM roof, both with and without a white reflective coating, all in transient states. The study delved into the thermal performance, temperature profiles, and total heat flux for both the coldest and warmest days of the year. Additionally, an annual assessment was conducted to gauge the long-term efficacy. In light of the gathered data, the following salient conclusions emerged:

- The dynamic attributed of roofing strategies, including time lag and decrement factor, play a pivotal role in optimizing thermal performance. Notably, the insulated roof configuration (IR-W) exhibited commendable performance in this regard, showcasing a suitable balance between short and long time lags and maintain consistent decrement factor values across diverse weather conditions.
- The IR-W configurations proved to be the frontrunners in terms of thermal performance. These configurations not only preserved stable temperatures but also significantly curbed energy loss by 77 % on the coldest day and slashed energy gain by a remarkable 90 % on the warmest day.
- Implementing a white reflective coating on a conventional roof yielded a substantial annual reduction in thermal load, electricity consumption costs, and CO₂ emissions, amounting to a 56 % decrease.
- Augmenting roofs with insulation and PCM materials further heightened these reductions, achieving impressive percentages of 81 % and 69 %, respectively. The combination of these enhancements with a white reflective coating led to an additional approximate 10 % improvement.

To broaden the scope of understanding regarding these roofing solutions, the next pertinent step involves coupling the optimal roof configuration with a room and eval-

14

uating the impact on thermal comfort. This integrated approach allows for a more comprehensive assessment of the overall building envelope and the influence on occupant comfort, thereby providing a holistic perspective on the efficacy of these innovative roofing strategies.

Acknowledgments

Samanta López Salazar acknowledges the National Council of Humanities Sciences and Technologies (CONAHCYT) for the support provided during her postgraduate studies, CVU: 918135 and GRANT NUMBER: 789202.

Lima-Téllez T. acknowledges the National Council of Humanities, Sciences and Technologies (CONAHCYT) for the support provided during her postgraduate studies, CVU: 918135 and GRANT NUMBER: 789202.

References

1. Cooling - IEA. (s. f.). IEA. <https://www.iea.org/energy-system/buildings/space-cooling>
2. Sanjay, M.; Chand, P. Passive cooling techniques of buildings: Past and present—A review. *Ariser* 2008, 4, 37–46.
3. Hernández-Pérez, I., Xamán, J., Macias-Melo, E., Aguilar-Castro, K., Zavala-Guillén, I., Hernández-López, I., & Sima, E. (2018). Experimental thermal evaluation of building roofs with conventional and reflective coatings. *Energy and Buildings*, 158, 569-579. <https://doi.org/10.1016/j.enbuild.2017.09.085>
4. Lima-Téllez, T., Chávez, Y., Hernández-López, I., Xamán, J., & Hernández-Pérez, I. (2022). Annual thermal evaluation of a ventilated roof under warm weather conditions of Mexico. *Energy*, 246, 123412. <https://doi.org/10.1016/j.energy.2022.123412>
5. Xiong, Q., Alshehri, H. M., Monfaredi, R., Tayebi, T., Majdoub, F., Hajjar, A., Delpisheh, M., & Izadi, M. (2022). Application of phase change material in improving trombe wall Efficiency: An up-to-date and comprehensive overview. *Energy and Buildings*, 258, 111824. <https://doi.org/10.1016/j.enbuild.2021.111824>
6. Al-Absi, Z. A., Isa, M. H. M., & Ismail, M. (2020). Phase change materials (PCMs) and their optimum position in building walls. *Sustainability*, 12(4), 1294. <https://doi.org/10.3390/su12041294>
7. Yang, Y. K., Kim, M. Y., Chung, M. H., & Park, J. C. (2019). PCM Cool Roof Systems for Mitigating Urban Heat Island - An Experimental and Numerical analysis. *Energy and Buildings*, 205, 109537. <https://doi.org/10.1016/j.enbuild.2019.109537>
8. Triano-Juárez, J., Macias-Melo, E., Hernández-Pérez, I., Aguilar-Castro, K., & Xamán, J. (2020). Thermal behavior of a phase change material in a building roof with and without reflective coating in a warm humid zone. *Journal of building engineering*, 32, 101648. <https://doi.org/10.1016/j.job.2020.101648>

9. Xamán, J., Rodríguez-Ake, A., Zavala-Guillén, I., Hernández-Pérez, I., Arce, J., & Saucedo, D. (2020). Thermal performance analysis of a roof with a PCM-layer under Mexican weather conditions. *Renewable Energy*, 149, 773-785. <https://doi.org/10.1016/j.renene.2019.12.084>
10. Rathod, M. K., Rathod, M. K., & Banerjee, J. (2020c). Numerical model for evaluating thermal performance of residential building roof integrated with Inclined Phase change Material (PCM) layer. *Journal of building engineering*, 28, 101018. <https://doi.org/10.1016/j.jobe.2019.101018>
11. Fatemeh Baybourdy, Elham Saligheh, Aida Maleki, Aligholi Nianei (2020). Analysis of the effects of simultaneous using of PCM and insulation in energy storage in a residential building in climate region cold-dry of Iran. 7th International Conference on Innovation and Research in Engineering Science. Tbilisi, Georgia.
12. Rangel, C. G., Rivera-Solorio, C. I., Gijón-Rivera, M., & Mousavi, S. (2022). The effect on thermal comfort and heat transfer in naturally ventilated roofs with PCM in a semi-arid climate: an experimental research. *Energy and Buildings*, 274, 112453. <https://doi.org/10.1016/j.enbuild.2022.112453>
13. Sedaghat, A., Salem, H., Hussam, W. K., Mahdizadeh, A., Al-Khiami, M. I., Malayer, M. A., Soleimani, S. M., Sabati, M., Narayanan, R., Rasul, M., & Khan, M. M. K. (2023). Exploring energy-efficient building solutions in hot regions: A study on bio-phase change materials and cool roof coatings. *Journal of building engineering*, 76, 107258. <https://doi.org/10.1016/j.jobe.2023.107258>
14. Gao, Y., & Meng, X. (2023). A Comprehensive review of Integrating phase change materials in building bricks: Methods, performance and applications. *Journal of energy storage*, 62, 106913. <https://doi.org/10.1016/j.est.2023.106913>
15. Hinojosa, J., Moreno, S., & Maytorena, V. (2023). Low-Temperature Applications of phase change materials for energy Storage: A Descriptive review. *Energies*, 16(7), 3078. <https://doi.org/10.3390/en16073078>
16. Hernández-Pérez, I. (2021). Influence of traditional and solar reflective coatings on the heat transfer of building roofs in Mexico. *Applied sciences*, 11(7), 3263. <https://doi.org/10.3390/app11073263>
17. American Society of Heating and Refrigerating and Air-Conditioning Engineers, 680 ASHRAE Handbook of Fundamentals, American Society of Heating and Refrigerating and Air-Conditioning Engineers, Inc., 2009.
18. Duffie, J. A., & Beckman, W. (2013). Solar engineering of thermal processes. En John Wiley & Sons, Inc. eBooks. <https://doi.org/10.1002/9781118671603>
19. Swinbank, W. C. (1963). Long-wave radiation from clear skies. *Quarterly Journal of the Royal Meteorological Society*, 89(381), 339-348. <https://doi.org/10.1002/qj.49708938105>
20. García-Pérez, D., Xamán, J., Zavala-Guillén, I., Chávez-Chena, Y., Sima, E., & Arce, J. (2023). Annual evaluation of a modified wall with PCM to reduce energy consumption and CO2 emissions in Southeast Mexico. *Energy and Buildings*, 292, 113129. <https://doi.org/10.1016/j.enbuild.2023.113129>

Aplicación de la economía circular para una industria química sustentable

Roberto Flores^[0000-0001-6908-9822] y Nadia Lara^[0000-0001-6167-9000]

Universidad Autónoma del Estado de Morelos, Facultad de Ciencias Químicas e Ingeniería,
Cuernavaca, Morelos, 62209, México
roberto.flores@uaem.mx

Abstract. La industria química ha sido parte fundamental del desarrollo tecnológico de la humanidad; sin embargo, en las últimas décadas la sociedad percibe a esta industria como altamente contaminante y destructiva del medio ambiente. Es por eso, que la industria ha tomado medidas para un uso sustentable de los recursos humanos y materiales, de tal forma que los procesos tiendan a volverse amigables con el medio ambiente y económicamente rentables. La mayoría de las acciones tomadas se fundamentan de manera implícita y explícita en los principios de la economía circular tomando como referencia los principios de la química verde e ingeniería verde. En el presente trabajo se realiza un análisis de dichos principios, se establece como se relacionan entre sí, y se muestran varios casos reales donde se han tomado acciones aplicando dichos principios para que los procesos se vuelvan económica y ambientalmente sustentables, mejorando así la percepción de la sociedad con respecto a la industria química.

Keywords: Economía Circular, Industria Química, Química Verde, Ingeniería Verde.

1 Introducción

A través del desarrollo y fabricación de nuevos materiales y compuestos químicos, la industria química ha ayudado a la sociedad a encontrar soluciones. No obstante, para crear una sociedad fuerte y sostenible en el futuro cercano, es necesario un enfoque coordinado en toda la cadena de valor para lograr modelos comerciales que integren el uso eficiente de los recursos, las aplicaciones y su utilización posterior al término de su vida útil. Solo mejorar el costo y el rendimiento del material o proceso no solucionará los problemas sociales, de gestión de desechos y ambientales. Es necesario incluir las características y funcionalidades de los materiales, así como el reciclaje mecánico, químico y la recuperación de energía térmica. [1]. Es por eso que, mediante la coordinación y aplicación de los conceptos de la química verde, la ingeniería verde y la economía circular en el diseño y la operación de procesos químicos, esta industria tenderá a volverse más sustentable y amigable con el medio ambiente.

2

2 Economía circular

En la actualidad existe una tendencia mundial que ha llevado a la comunidad industrial a explorar alternativas para transitar de modelos comerciales de economía lineal a economía circular (EC). En la economía lineal, el proceso industrial se caracteriza por un flujo de materiales unidireccional, es decir, las materias primas se transforman en un producto final y, después de su vida útil, en basura desechable; al mismo tiempo, durante su manufactura, pueden generarse subproductos secundarios y residuos que son simplemente arrojados a la naturaleza y/o dispuestos en vertederos o plantas de tratamiento. En el nuevo concepto de EC, la recuperación y la valorización de los residuos, desechos y productos al final de su vida útil, permiten reutilizar los materiales y recursos nuevamente en la cadena de suministro, desacoplando el crecimiento económico de los daños ambientales [2].

La EC se orienta en la literatura a través de los “Principios R”: Reducir, Recuperar para Reutilizar y Reciclar [2-3]; aunque algunos autores han incluido más tipologías R matizadas: Rechazar, Reparar, Restaurar, y Remanufacturar [4]. Siguiendo esta tónica, Rizos y col. [5] clasificaron la EC en tres categorías diferentes: i) usar menos recursos primarios, ii) mantener el mayor valor de los materiales y productos y iii) cambiar los patrones de utilización.

Desde un punto de vista de la industria química, el principio de reducción pretende minimizar el consumo de energía primaria y materias primas, así como la generación de desechos. Esto se logra con el desarrollo de nuevas tecnologías y/o procesos, o bien, reconfigurando los procesos existentes para mejorar la eficiencia en la producción y el consumo de energía [6-7].

El principio de reutilización se refiere a operaciones por las cuales los productos, subproductos, desechos, residuos y componentes que son aptos puedan recuperarse y volver a utilizar para el mismo propósito con el que fueron concebidos, o en aplicaciones distintas dentro del mismo proceso. Desde el punto de vista ambiental se consumen menos recursos naturales y se ahorra energía y mano de obra, en comparación con la elaboración de productos a partir de materiales vírgenes (Castellani et al., 2015). Algunos ejemplos atractivos en la industria química, en términos económicos y ambientales, son la recirculación de materia prima no transformada, y la recuperación y reuso de solventes. Por otro lado, con las corrientes “calientes” y “frías” del proceso se pueden elaborar redes de intercambiadores de calor que minimizan el uso y desperdicio de energía [8-10].

El principio de reciclaje se refiere a cualquier operación donde los desechos y residuos se recuperan y reprocesan en productos, materiales y sustancias para utilizarse en el proceso original o en nuevas aplicaciones. En el caso de materia orgánica se considera su reprocesamiento para la generación de nuevos compuestos, pero no su uso como combustible. El reciclaje de residuos permite el aprovechamiento de los recursos aún utilizables y reduce la cantidad de materia que debe tratarse y/o eliminarse, disminuyendo el impacto ambiental y económico relacionado [11-12].

A la EC frecuentemente la relacionan con el principio de reciclaje; sin embargo, esta pudiera ser la solución menos sostenible en comparación con los otros principios de la EC (reducción y reutilización) en términos de eficiencia y rentabilidad de los recursos.

El reciclaje está limitado por la naturaleza (ley de entropía) y la complejidad material, ya que algunos materiales de desecho son reciclables hasta cierto punto, o incluso no reciclables. A pesar de esto, la mayor parte de los estudios reportados de EC en la industria química están relacionados con el reciclaje de materiales.

3 Los principios de la química verde e ingeniería verde

Los Principios de la Química Verde y de la Ingeniería Verde tienen como objetivo orientar a los profesionales de la química (incluidos ingenieros, científicos, académicos e investigadores) a sintetizar productos químicos a través de reacciones amigables con el medio ambiente y altamente eficientes, al mismo tiempo que desarrollan procesos tecnológicos que maximicen su rendimiento generando la menor cantidad de residuos y subproductos, reduciendo el consumo de energía y aprovechando fuentes de energía renovable. Estos principios fueron presentados por Paul Anastas y colaboradores entre 1998 y 2003, y se pueden clasificar en reducir riesgos, aumentar la eficiencia, minimizar el exceso, y aumentar la sustentabilidad. Los Principios de la Ingeniería Verde complementan los presentados por la Química Verde (ésta originalmente sólo contemplaba conceptos relevantes al impacto ambiental), e incluyen el análisis de la inherencia de un producto o proceso en el impacto ambiental, la aplicación del análisis de ciclo de vida, y la posibilidad de recuperar el calor de una reacción exotérmica y desarrollar redes de intercambio de calor [13-19]. Las Tablas 1 y 2 resumen los principios de la química verde y de la ingeniería verde, respectivamente.

Tabla 1. Principios de la Química Verde.

Principio	Enunciado	Acción
1	Prevención en la generación de residuos, ya que es mejor evitar la generación de éstos que su tratamiento posterior para no contaminar el ambiente	Prevención
2	Economía atómica con métodos de síntesis que incorporen al máximo los reactivos en el producto final	Economía atómica
3	Síntesis química menos peligrosa empleando y generando sustancias de baja o nula toxicidad	Síntesis segura
4	Diseño de productos químicos más seguros que desarrollen su función con toxicidad mínima	Diseño seguro
5	Mínimo uso de solventes y sustancias auxiliares, que de preferencia sean inocuas	Minimización de solventes
6	Uso eficiente de la energía, y de preferencia lograr que los procesos se desarrollen a temperatura y presión ambiente	Eficiencia energética
7	Empleo de materia prima renovable	Materia prima renovable

4

8	Evitar la formación de derivados o productos secundarios	No derivados
9	Diseño de catalizadores con la mayor selectividad	Uso de catalizadores
10	Diseño de productos químicos que se degraden fácilmente al final de su vida útil	Diseño sustentable
11	Diseño de metodologías analíticas para el monitoreo y control en tiempo real de compuestos contaminantes	Monitoreo y control
12	Química inherentemente más segura para la prevención de accidentes tales como fugas, explosiones y fuego	Química segura

Tabla 2. Principios de la Ingeniería Verde.

Principio	Enunciado	Acción
I	Los diseñadores deben asegurarse de que todas las entradas y salidas de materia y energía sean tan inherentemente inocuas como sea posible	Diseño inocuo
II	Es mejor prevenir la contaminación que tratar el residuo producido	No contaminación
III	Las operaciones de separación y purificación deberían diseñarse para minimizar el consumo de energía y materiales	Fácil separación y purificación
IV	Los procesos y sistemas deberían diseñarse para la maximizar la eficiencia del uso de materia, energía, tiempo, y espacio	Uso eficiente de energía y materia
V	Los procesos y sistemas deben dirigir el equilibrio termodinámico hacia los productos manipulando la entrada/retiro de energía y materiales	Equilibrio termodinámico
VI	El cambio de entropía y complejidad inherentes al proceso deben considerarse como una inversión al elegir entre reutilizar un material, reciclarlo o rechazarlo	Ley de entropía
VII	Diseñar para la durabilidad, no para la inmortalidad	Diseño sustentable
VIII	Satisfacer la necesidad minimizando el exceso	No excesos
IX	Minimizar la diversidad de materiales	No diversidad de materiales
X	Cerrar los ciclos de materia y energía del proceso tanto como sea posible	Ciclos cerrados de materia y energía
XI	Diseñar para la reutilización de componentes del producto al final de su vida útil	Diseño inteligente

XII	Las entradas de materia y energía deberían ser de recursos renovables	Uso de recursos renovables
-----	---	----------------------------

Para el fortalecimiento de estos principios se han desarrollado diversos convenios, protocolos y convenciones relacionados con el manejo y/o prevención de productos químicos tóxicos y peligrosos, y que alientan a los profesionales de la Química a diseñar productos químicos de una manera más ecológica y eliminar materiales peligrosos. Algunos de los más relevantes son: (i) la Declaración de Dubai sobre la necesidad de una gestión química racional; (ii) Convenio de Basilea para el control del movimiento transfronterizo de desechos peligrosos y su eliminación; (iii) Convenio de Estocolmo para la restricción de contaminantes orgánicos persistentes; (iv) Declaración de Río sobre medio ambiente y desarrollo para evitar la degradación de la calidad ambiental y el agotamiento de los recursos naturales; (v) Convenio de Rotterdam para las responsabilidades de importación de productos químicos peligrosos; y (vi) Sistema Globalmente Armonizado (SGA) de Clasificación y Etiquetado de Productos Químicos para clasificar y etiquetar materiales peligrosos o productos químicos.

4 Relación de la economía circular con la química verde e ingeniería verde

La aplicación de los Principios de la Química e Ingeniería Verde es fundamental para el cambio de una economía lineal a una circular, ya que sus objetivos básicos son minimizar el consumo de materiales y maximizar la intensidad energética, de tal forma que la EC proporciona una vía para el desarrollo sustentable mediante la aplicación de la evaluación ambiental y demostración de la reciclabilidad del nuevo producto químico [20]. En la Fig. 1 se establece la relación que existe de los principios de la economía circular con la química verde e ingeniería verde.

6

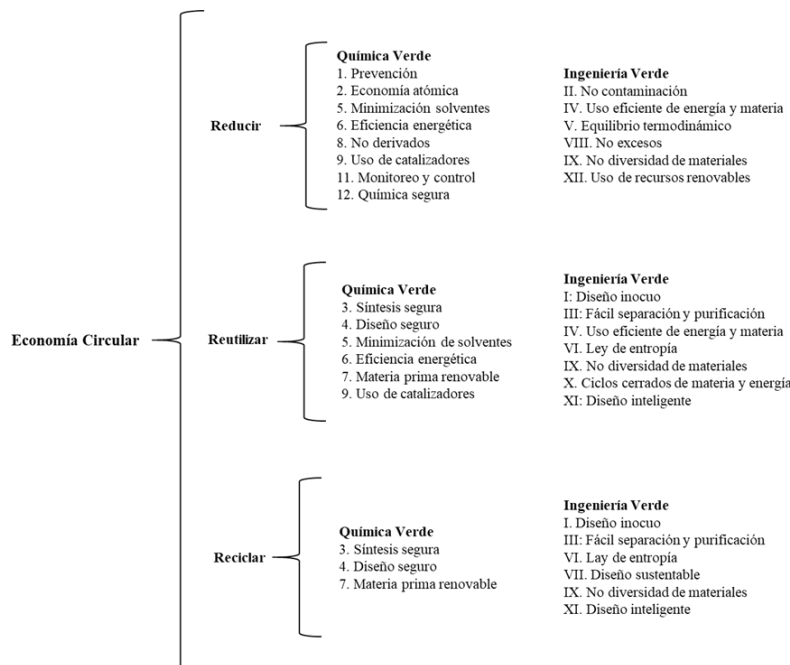


Fig. 1. Relación de los principios de la Economía circular con la química verde e ingeniería verde.

Así, siguiendo los principios de uso y diseño eficiente de la energía en un proceso químico se puede lograr que las corrientes del proceso puedan reutilizarse para enfriar y/o calentar y así reducir el consumo de energía.

Por otro lado, en base a los ciclos cerrados de proceso para materiales renovables y recursos, es posible optimizar el sistema y darles un mejor uso a los materiales de desecho. Por ejemplo, la gestión de residuos de plásticos y biopolímeros ofrece las ventajas de la sustentabilidad de los recursos en lugar de los procesos convencionales de tratamiento o eliminación. Al reducir el uso de recursos y energía en la industria química, la EC proporciona una vía para el desarrollo sustentable desde la aplicación de la evaluación ambiental y la reciclabilidad de productos químicos [21].

El enfoque de la industria química aplicando los principios de la EC se asemeja al establecido por August Wilhelm von Hoffman, quien afirmaba que en una fábrica química ideal no debían existir desperdicios sino únicamente productos, ya que mientras mejor se aplicarán los desechos, mayor sería su ganancia [22].

Se ha propuesto que la EC en la industria química podría establecerse a varios niveles (micro, meso, macro) mediante la implementación de tecnología innovadora,

nuevos modelos de negocios y la colaboración de las partes interesadas [23], como se comentará en los ejemplos.

Aunque el concepto de reciclaje se asocia con el tratamiento al final de la vida útil de los productos, los nuevos escenarios incluyen el reciclaje de los subproductos en distintas aplicaciones, y la recuperación de solventes ahora que satisfacer la demanda de solventes es un nuevo reto en la industria. Hoy en día, en la era de la economía circular, los desechos deben representar la materia prima de los procesos industriales.

5 Ejemplos de la economía circular en la industria química

5.1 Curtido de pieles

En el proceso de curtido de pieles se reutilizaron recortes crudos de residuos sólidos, y se evitó el uso de sustancias nocivas como el formaldehído, utilizando en su lugar un agente de curtido eco-benigno y biodegradable, que se obtuvo a partir de un pretratamiento de los residuos sólidos con hidróxido de sodio al 7.5% y peróxido de hidrógeno al 10%. Con las modificaciones al proceso de curtido, además de mejorar las propiedades físicas de la piel curtida, se recuperaron y reutilizaron residuos sólidos aplicando de esta manera los principios de la EC y de la Ingeniería Verde [24].

5.2 Recuperación de bromo

La empresa de Syngenta, que se ubica en un complejo industrial de 4 compañías químicas en Valais, Alemania, ha diseñado un proceso de recuperación y reutilización de bromo en sus procesos industriales. Syngenta utiliza bromo para la fabricación de ingredientes activos desde la década de 1980, y antes de la reconfiguración el 98% del bromo terminaba en las aguas residuales en forma de bromuro y como desechos orgánicos bromados. El proceso de recuperación y reutilización de bromo, ha permitido disminuir notablemente la demanda de bromo fresco para las operaciones de producción de la planta, y ha reducido la necesidad de transporte y almacenamiento (lo que no se recomienda debido a las propiedades peligrosas del bromo, tales como alta reactividad, corrosividad y toxicidad). El costo de recuperar y reutilizar el bromo representa alrededor del 40–45% del precio de compra actual del bromo, lo que ilustra claramente su beneficio económico. Syngenta además utiliza directamente POCl_3 , un subproducto de un proceso de producción de una de las empresas vecinas, como reactivo, evitando el suministro externo, por lo que aplica los Principios de la EC en niveles micro y meso [25].

8

5.3 Industria del carbon

La industria química del carbón ha sido considerada como uno de los mayores consumidores de energía y recursos, así como un importante emisor de contaminación. La compañía BTL en China, ha desarrollado una cadena de producción donde el carbón crudo extraído se usa para producir coque metalúrgico, compuestos químicos de carbón y materiales de construcción después de un procesamiento exhaustivo, y también puede usarse para generar energía y calor. Desde el punto de vista de los beneficios de los productos, existe una cascada de la forma: metanol > aceite de lavado y componente de mezcla de asfalto > benceno crudo > productos de energía térmica > coque. Con el objetivo de mejorar la eficiencia de la producción de recursos de todo el sistema, los materiales deben fluir a las categorías de productos con altos beneficios de recursos en la medida de lo posible al diseñar y optimizar la cadena industrial de la EC. Por ejemplo, en el sistema actual de cadena industrial de BTL, solo la mitad del gas del horno de coque producido por el módulo de coquización ingresa al módulo de síntesis de metanol y el gas restante del horno de coque se usa como combustible, lo que resulta en una disminución del beneficio general de los recursos. Por lo tanto, reconfigurar la planta para ampliar la capacidad de producción de metanol, y aprovechar al máximo todo el gas del horno de coque, puede ser rentable. Con la expansión de la escala de producción de metanol, también aumentará la cantidad de gas de purga de subproductos, y el hidrógeno adicional producido se puede utilizar para producir más aceite de lavado, por lo que el beneficio de recursos de todo el sistema se puede mejorar aún más [26].

5.4 Reciclado de plásticos

El reciclaje primario de plásticos se ve desafiado por muchos aspectos, tales como los tintes y otros contaminantes, calidad del material, mezclas de diferentes plásticos, etc., y se manifiesta por el hecho de que únicamente el 2% de todos los plásticos se incluye en ciclo cerrado de reciclaje. El reciclaje secundario de plásticos en productos de calidades inferiores incluye la coloración unitaria de plástico de colores mezclados, típicamente en negro, pero se limita a fracciones que contienen el mismo tipo de plástico. El reciclaje terciario es promisorio para fracciones de plásticos donde el reciclaje primario o secundario es inviable. El reciclaje terciario incluye despolimerización química, solvólisis, craqueo catalítico y térmico, pirólisis, gasificación, hidrogenación, recuperación de energía, entre otros procesos [1]. Mientras que algunos tipos de polímeros como los poliésteres, poliéteres, policarbonatos, poliamidas, son propensos a la solvólisis, como la hidrólisis (térmica y / o catalítica), otros son más resistentes a los químicos y necesitan condiciones térmicas severas para descomponerse. Las fracciones mixtas de plásticos y plásticos contaminados con orgánicos se han identificado como los principales desafíos en la gestión de residuos plásticos, ya que no pueden clasificarse y limpiarse a sus formas puras, que son aspectos solicitados para su reciclaje primario o secundario. Es por eso que para aplicar los Principios de la EC se ha propuesto un tratamiento con agua en condiciones supercríticas para el reciclaje de residuos plásticos [27]. Debido a las bifuncionalidades (térmicas y químicas), el agua en condiciones

supercríticas es útil para procesar residuos técnicamente difíciles (como mezclas de plásticos y plásticos contaminados con residuos orgánicos) que regularmente se incineran. Así, es posible reciclar los monómeros plásticos para la producción de nuevos plásticos junto con la extracción de productos químicos de valor agregado para su uso en la industria química. La flexibilidad de este proceso hidrotérmico permite el procesamiento de diferentes plásticos independientemente del color, tamaño, pureza, propiedades físicas, etc. dentro del mismo proceso.

5.5 Recuperación de nutrientes de desechos agrícolas

Las actividades agrícolas intensas generan grandes cantidades de corrientes residuales como basura y estiércol, que normalmente son vertidos en la naturaleza o, en el mejor de los casos, enviados a plantas de tratamiento de residuos. No obstante, estos residuos contienen sustancias y elementos que pudieran recuperarse y reciclarse en distintas aplicaciones, siendo un caso adecuado para la EC. Por ejemplo, el estiércol de pollo es un residuo interesante debido al contenido de nutrientes, en particular de fósforo, que hace que el estiércol se convierta en materia prima adecuada para aplicaciones de fertilizantes. Sin embargo, tales corrientes a menudo están contaminadas con antibióticos y otros compuestos orgánicos, que deben destruirse térmicamente antes de su eliminación o posterior utilización. Una tecnología aplicada recientemente es la pirólisis, con la cual es posible combinar el reciclaje de nutrientes y la recuperación de energía [28]. La pirólisis es la descomposición térmica de materiales orgánicos en ausencia de un medio de gasificación, utilizado para generar compuestos orgánicos volátiles (vapores de pirólisis) y un sólido carbonoso estabilizado (carbón de pirólisis). El carbón retiene cuantitativamente minerales y nutrientes principales (P, K, Ca, Mg) con la excepción del nitrógeno, que solo se recupera parcialmente en el sólido. Los procesos de pirólisis pueden ser una alternativa competitiva para la generación descentralizada y combinada de un sólido carbonizado para aplicaciones en el suelo, y de energía por la combustión de los vapores de pirólisis.

5.6 Preparación de monoalquil gliceril éteres

Se ha reportado la preparación de compuestos de alto valor, como los monoalquil gliceril éteres (MAGE), utilizando 2-cloro-1,3-propanodiol, que es un producto secundario de la síntesis de epiclorhidrina de base biológica (ECH). En una primera etapa, el 2-cloro-1,3-propanodiol se convierte en glicidol, y éste mediante una reacción de alcoholisis produce el MAGE. De esta manera se recicla un subproducto secundario del proceso principal, y se utiliza para producir un MAGE, que de manera tradicional se obtiene a partir de derivados de petróleo, un recurso no renovable [29].

10

5.7 Uso del dióxido de carbono como precursor en procesos químicos

La conversión de dióxido de carbono (CO_2) en productos de valor agregado se ha convertido en un tema de interés para la EC. El CO_2 se produce en gran escala como un producto secundario en la generación de energía a partir de procesos de combustión. Se estima que alrededor del 5 al 10% de las emisiones totales de CO_2 pueden usarse para producir nuevos combustibles y productos químicos.

Asimismo, la gasificación de los desechos municipales produce gas de síntesis (compuesto por CO_2 , CO e H_2) ha entrado en consideración por la Unión Europea, ya que su plan de acción para la EC ha señalado que solo una parte limitada (43%) de los desechos municipales generados en la Unión se recicla. Por lo tanto, la alternativa de convertir los desechos municipales en productos químicos, en lugar de enviarlos a rellenos sanitarios o incineración (que representa el 31% y el 26% de los residuos municipales generados en la unión europea) representa un elemento importante para la estrategia de EC.

Desde un punto de vista industrial, el CO_2 puede usarse como material de partida a través de intermedios clave (como CO y CH_3OH , entre otros) o como una fuente de carbono para reducir la dependencia de los compuestos fósiles y el calentamiento global. Uno de los principales procesos industriales es la síntesis de urea con un mercado global estimado de alrededor de 250 Tg en 2020 [29]. Otros compuestos que se pueden obtener usando el CO_2 como precursor incluyen combustibles, ácido salicílico, policarbonatos, y carbonatos minerales que se usan en industria de la construcción petróleo [30].

5.8 Reciclaje de baterías de iones de litio

Las baterías de iones de litio (BIL) son actualmente uno de los dispositivos más importantes de almacenamiento de energía electroquímica que alimentan aparatos electrónicos móviles y vehículos eléctricos. Sin embargo, hay una diferencia notable entre su tasa de producción y la tasa de reciclaje. Al final de su ciclo de vida, solo un número limitado de BIL se someten a un tratamiento de reciclaje, y la mayoría va a los vertederos o se acumula en talleres automotrices. Se producen pérdidas adicionales de los componentes de las BIL debido a que los procesos de reciclaje actuales se limitan a recuperar componentes con alto valor económico, por ejemplo, Co , Cu , Fe y Al . En Europa, el mercado de LIB informó un total de 65 500 toneladas de BIL consumidas entre los años 2013–2014 mientras que sólo alrededor de 1900 toneladas fueron recicladas en el mismo período. Las bajas tasas de reciclaje de los LIB pueden atribuirse actualmente a varios factores, que van desde una legislación deficiente, sistemas de recolección ineficientes y la falta de tecnologías de reciclaje factibles para el flujo de residuos de LIB que cambia rápidamente. Los procesos más adecuados para recuperar los materiales y refabricar las BIL son aquellos que emplean una combinación de procesamiento mecánico y etapas hidro y pirometalúrgicas. Por otro lado, los procesos que dependen de pasos pirometalúrgicos son robustos, pero solo capaces de recuperar componentes metálicos [31].

6 Conclusiones

Uno de los objetivos de la economía circular es maximizar los recursos materiales y energéticos con el propósito de minimizar los riesgos ambientales y la economía de los procesos. En el caso de la industria química, el uso de los conceptos de la economía circular tiende a basarse de manera inherente en los principios de la química verde e ingeniería verde. En el presente trabajo se han mostrado diversas situaciones en las cuales con los fundamentos de la economía circular se han logrado reducciones significativas en la generación de residuos, ya que estos se recuperan y es posible darles uso en otras funciones ya sea dentro del mismo proceso, o en aplicaciones totalmente distintas. Asimismo, se ha indicado como estas nuevas funciones toman como base los principios de la química verde e ingeniería verde. Esto nos lleva a analizar los procesos químicos industriales actuales donde mediante reconfiguraciones simples sea posible hacerlos energéticamente más eficientes, así como recuperar y buscar nuevas aplicaciones de los desechos generados, y con esto contribuir al desarrollo sustentable de los procesos químicos industriales.

Referencias

1. Kawashima, N., Yagi, T., & Kojima, K.: How Do Bioplastics and Fossil-Based Plastics Play in a Circular Economy? *Macromolecular Materials and Engineering*, **304**(9), 1900383 (2019)
2. van Langen, S. K., Vassillo, C., Ghisellini, P., Restaino, D., Passaro, R., & Ulgiati, S.: Promoting circular economy transition: A study about perceptions and awareness by different stakeholders groups. *Journal of Cleaner Production*, **316**, 128166 (2021)
3. Kalmykova, Y., Sadagopan, M., & Rosado, L.: Circular economy—From review of theories and practices to development of implementation tools. *Resources, conservation and recycling*, **135**, 190-201 (2018)
4. Van Buren, N., Demmers, M., Van der Heijden, R., & Witlox, F.: Towards a circular economy: The role of Dutch logistics industries and governments. *Sustainability*, **8**(7), 647 (2016)
5. Rizos, V., Tuokko, K., & Behrens, A.: The Circular Economy: A review of definitions, processes and impacts. CEPS Research Report No 2017/8, April 2017
6. Zhijun, F., & Nailing, Y.: Putting a circular economy into practice in China. *Sustainability Science*, **2**(1), 95-101 (2007)
7. Su, B., Heshmati, A., Geng, Y., & Yu, X.: A review of the circular economy in China: moving from rhetoric to implementation. *Journal of cleaner production*, **42**, 215-227 (2013)
8. Chin, H. H., Varbanov, P. S., Liew, P. Y., & Klemeš, J. J.: Pinch-based targeting methodology for multi-contaminant material recycle/reuse. *Chemical Engineering Science*, **230**, 116129 (2021)
9. Jia, X., Li, Z., Wang, F., Foo, D. C. Y., & Qian, Y.: A new graphical representation of water footprint pinch analysis for chemical processes. *Clean Technologies and Environmental Policy*, **17**(7), 1987–1995 (2015)

12

10. Klemeš, J. J., Varbanov, P. S., Walmsley, T. G., & Jia, X.: New directions in the implementation of Pinch Methodology (PM). *Renewable and Sustainable Energy Reviews*, **98**, 439–468 (2018)
11. Lazarevic, D., Aoustin, E., Buclet, N., & Brandt, N.: Plastic waste management in the context of a European recycling society: Comparing results and uncertainties in a life cycle perspective. *Resources, Conservation and Recycling*, **55**(2), 246-259 (2010)
12. Birat, J. P.: Life-cycle assessment, resource efficiency and recycling. *Metallurgical Research & Technology*, **112**(2), 206 (2015)
13. Chen, T. L., Kim, H., Pan, S. Y., Tseng, P. C., Lin, Y. P., & Chiang, P. C.: Implementation of green chemistry principles in circular economy system towards sustainable development goals: Challenges and perspectives. *Science of The Total Environment*, **716**, 136998 (2020)
14. Rodríguez, B. S.: Enseñanza de la química sostenible en las carreras de ingeniería. *Revista de Química*, **32**(1), 12-17 (2018)
15. Clark, J., Macquarrie, D., Gronnow, M. and Budarin, V.: *Green Chemistry Principles. In Process Intensification for Green Chemistry* (eds K. Boodhoo and A. Harvey), Wiley-VCH Verlag GmbH & Co. KGaA, 33-58 (2013)
16. Marteel-Parrish, A.E. & Abraham, M.A.: *Principles of Green Chemistry and Green Engineering. In Green Chemistry and Engineering* (eds A.E. Marteel-Parrish and M.A. Abraham), Wiley-VCH Verlag GmbH & Co. KGaA, 21-42 (2014)
17. Lapkin, A. A.: *Chemical Engineering Science and Green Chemistry—The Challenge of Sustainability. Handbook of Green Chemistry: Online*, P.T. Anastas (Ed.), Wiley-VCH Verlag GmbH & Co. KGaA, 1-16 (2019)
18. Constable, D.J.: *Green Chemistry Metrics. In Handbook of Green Chemistry Volume 11*, D. J. Constable and Concepcion Jimenez-Gonzalez (Ed.); Wiley-VCH Verlag GmbH & Co. KGaA, 1-27 (2018)
19. Kitchens, C. L. & Soh, L.: *Green Engineering. In Green Techniques for Organic Synthesis and Medicinal Chemistry, 2a Edición*. Edited by W. Zhang and B. W. Cue (ED.); John Wiley & Sons Ltd, 71-90 (2018)
20. Clark, J. H., Farmer, T. J., Herrero-Davila, L., & Sherwood, J.: Circular economy design considerations for research and process development in the chemical sciences. *Green Chemistry: An International Journal and Green Chemistry Resource: GC*, **18**(14), 3914–3934 (2016)
21. Chen, T. L., Kim, H., Pan, S. Y., Tseng, P. C., Lin, Y. P., & Chiang, P. C.: Implementation of green chemistry principles in circular economy system towards sustainable development goals: Challenges and perspectives. *Science of The Total Environment*, **716**, 136998 (2020)
22. Cucciniello, R., & Cespi, D.: Recycling within the chemical industry: The circular economy era. *Recycling*, **3**(2), 22 (2018)
23. Witjes, S., & Lozano, R.: Towards a more Circular Economy: Proposing a framework linking sustainable public procurement and sustainable business models. *Resources, Conservation and Recycling*, **112**, 37-44 (2016)
24. Sathish, M., Madhan, B., & Rao, J. R.: Leather solid waste: An eco-benign raw material for leather chemical preparation—A circular economy example. *Waste Management*, **87**, 357-367 (2019)
25. Pilloud, F., Pouransari, N., Renard, L., & Steidle, R.: Bromine Recycling in the Chemical Industry—An Example of Circular Economy. *Chimia*, **73**(9), 737-737 (2019)
26. Yang, W., Zhao, R., Chuai, X., Xiao, L., Cao, L., Zhang, Z., ... & Yao, L.: China's pathway to a low carbon economy. *Carbon balance and management*, **14**, 1-12 (2019)
27. Pedersen, T. H., & Conti, F. (2017). Improving circular economy via hydrothermal processing of high-density waste plastics. *Waste management*, **68**, 24-31 (2017)

28. Morgano, M. T., Bergfeldt, B., Leibold, H., Richter, F., & Stapf, D.: Intermediate pyrolysis of agricultural waste: A decentral approach towards circular economy. *Chemical Engineering Transaction*, **65** (2018)
29. Iaquaniello, G., Centi, G., Salladini, A., Palo, E., & Perathoner, S.: Waste to chemicals for a circular economy. *Chemistry—A European Journal*, **24**(46), 11831-11839. (2018)
30. Cucciniello, R., & Cespi, D: Recycling within the chemical industry: The circular economy era. *Recycling*, **3**(2), 22. (2018)
31. Velázquez-Martínez, O., Valio, J., Santasalo-Aarnio, A., Reuter, M., & Serna-Guerrero, R.: A critical review of lithium-ion battery recycling processes from a circular economy perspective. *Batteries*, **5**(4), 68 (2019)

Lessons learned from a sustainable mobility analysis in Montevideo, Uruguay

Sergio Nesmachnow^[0000-0002-8146-4012] and
Silvina Hipogrosso

Universidad de la República, Uruguay
{sergion,silvina.hipogrosso}@fing.edu.uy

Abstract. This article describes relevant insights from an analysis of sustainable mobility developed in Montevideo, Uruguay. Sustainable mobility is an important issue considering the environmental, energy, health, and urban planning implications. Important aspects are considered in the study, regarding the development of electric mobility for scooter and public transportation system, and the infrastructure for bicycle. Valuable insights are derived and recommendations are formulated to guide the development of sustainable and efficient transportation means in Montevideo, Uruguay.

1 Introduction

In recent years, cities around the world have increasingly recognized the importance of sustainable mobility as a means to address urban challenges and improve the quality of life for their residents [17]. Several relevant initiatives have been proposed, including the promotion of public transportation, the development of cycling and pedestrian infrastructure, the adoption of electric mobility solutions, and the integration of smart transportation technologies.

Studying sustainable mobility is crucial for developing cleaner transportation means and evaluating its benefit on environmental impact, optimizing energy efficiency, guaranteeing accessibility and social equity, and promoting healthier mobility options. All these actions are in line with urban planning and urban design strategies towards creating sustainable and livable communities, to improve the quality of life of citizens.

In this line of work, this article explores relevant issues that emerged in a previous study that characterized sustainable mobility developments in Montevideo and proposed specific recommendation to enhance the adoption of practices that prioritize environmental, social, and economic sustainability of mobility means. The studied issues include: i) a study of the non-successful initiative of deploying an on-demand service of electric scooters in the city; ii) an extended analysis of travel demands, using data from the previous sustainable mobility survey performed for Parque Rodó Neighborhood, for a deeper understanding and characterization of trips regarding origin-destination and hours of the day; iii) a study of the new electric bus lines deployed in the city, considering quality of service

2 S. Nesmachnow and S. Hipogrosso

and Transit Oriented Development metrics; and iv) an analysis of the expansion of bicycle lane networks within the city. The main goal of the research reported in this article is to provide valuable insights to be used as recommendations to guide the development of sustainable and efficient transportation means in Montevideo.

The main results of the analysis indicate that sustainable mobility initiatives have not developed properly in Montevideo. Specific advances have been performed towards developing electric bus lines and extend the cycling infrastructure, but these advances are not in a consolidation stage yet. Despite its appeal, the electric scooter faced limitations in terms of coverage, cost, comfort, operational constraints, and regulatory challenges, ultimately resulting in the failure of its business model. Electric public transportation only provides services to the wealthiest neighborhoods in the city, without a proper development in other neighborhoods. Finally, the bicycle network has expanded into various areas of Montevideo and is currently undergoing further expansion, but significant enhancements to guarantee safety and connectivity are still needed..

The article is organized as follows. Next section presents the main concepts about sustainable mobility and review the literature on that topic. Section 3 describes the applied methodology and details of the studied initiatives. The analysis is developed in section 4. Finally, section 5 presents the conclusions of the research and formulates the main lines for future work.

2 Sustainable mobility

This section describes the main concepts related to sustainable mobility and reviews related works.

2.1 The sustainable mobility paradigm

The sustainable mobility paradigm refers to a series of practices and recommendations oriented to promote a shift in transportation systems to advance towards more environmentally-friendly and socially responsible mobility alternatives [17]. Sustainable mobility aims at addressing the negative impacts of traditional modes of transportation, such as private vehicles powered by fossil fuels, on the environment, public health, and the overall quality of life of citizens. The paradigm relies on the promotion of mobility means that minimize energy consumption, reduce greenhouse gas emissions, and prioritize the well-being of both citizens and communities.

Sustainable mobility is a key component of modern smart cities [20]. Three of the most relevant principles of the sustainable mobility paradigm are the promotion of public transportation systems, the importance of active modes of transportation such as walking and cycling, the adoption of clean and efficient technologies such as electric vehicles, and the integration of different means in multimodal transportation systems that include walking and cycling with public transit options. Overall, the sustainable mobility paradigm represents a holistic

approach to transportation, aiming at reduce the ecological footprint, improve air quality, enhance public health, and create more inclusive and livable communities. The synergy between policy measures, technological advancements, behavioral changes, and infrastructure investments is crucial to that end.

2.2 Related work

Numerous studies have been developed in high income countries, focusing on the subject of sustainable mobility and its various impacts on the environment, economic welfare, and equity among citizens.

Studied factors include greenhouse gas emissions, air pollution, socio-economic implications, and fairness of sustainable mobility practices [12,29]. Many articles evaluated public transportation initiatives in terms of their alignment with sustainable development, and the contribution of smart city concepts to improve sustainability and attractiveness of public transportation systems [4]. These studies have explored significant problems, important challenges, and also the associated benefits [21], providing valuable insights for designing mobility plans for sustainable public transportation.

An index was developed to assess sustainable mobility in Brazilian cities [30]. Lyons examined the effective implementation of initiatives related to sustainable mobility in Bogotá, to reduce reliance on automobiles [16]. Huertas et al. [10] proposed a methodology for sustainable mobility assessment, adapted to the reality of Latinamerican countries. Several technological tool were incorporated to determine the most sustainable actions to be implemented, taking into account the specific economic, environmental, and social aspects of the studied city. The reviewed studies in Latin America shed light on the efforts made to promote sustainable transportation and reduce car dependency. Our research group has been actively involved in several projects related to sustainable mobility analysis and development in Uruguay, including proposals and analysis of sustainable mobility [22,8], and examining the impact of pollution on transportation [27]. We have also studied the accessibility and sustainability in Montevideo, the capital city of Uruguay [18], and Maldonado, a medium-size city in the East of the country [19]. The previous research efforts have enhanced our understanding of sustainable mobility and offered valuable insights for transportation planning and policy development.

Our previous article [9] studied and categorized sustainable public transportation initiatives developed in Montevideo, Uruguay, up to 2020. Quantitative and qualitative indicators were computed for electric bus, public bicycles, and electric scooters (e-scooters) in Montevideo. The evaluation of those first initiatives allowed developing an initial characterization of sustainable mobility and formulation specific recommendations for developing sustainable mobility plans. After that, a mobility analysis was developed for a residential zone in Parque Rodó neighborhood, Montevideo, Uruguay, applying the Transit Oriented Development paradigm [23]. The study focused on determining the relationships between urban environment, urban activities and mobility indicators, emphasizing on sustainable mobility. A combination of urban data analysis, surveys, and

4 S. Nesmachnow and S. Hipogrosso

on-site inspections was employed to examine the demand for mobility, transportation mode usage, land use patterns, and the condition of existing mobility infrastructure within the studied area. The study found that Parque Rodó neighborhood exhibits favorable values for key indicators related to Transit Oriented Development, suggesting a strong foundation for the development of sustainable mobility initiatives.

This article extends the analysis of sustainable mobility initiatives in Montevideo, including the study of developments in 2021–2023 and considering the main lessons learned in previous analysis and perspectives for the future.

3 Methodology

This section describes the methodology applied to analyze the sustainable mobility initiatives in Montevideo.

3.1 Electric scooters

E-scooters have become a prominent mode of urban transportation, offering a convenient and eco-friendly alternative for short-distance commutes [31]. The methodology applied for the analysis and technical assessments of the shared e-scooters service evaluates key aspects of this transportation mode:

- *Spatial distribution.* Most trips take place in central areas of cities. This observation indicates that e-scooters primarily operate in regions characterized by dense populations, job opportunities, and various activities. This operational approach makes sense because these areas exhibit higher usage rates, thereby being more profitable for businesses. However, the unbalanced distribution limits access to shared e-scooters for a large portion of the population [2], increasing transport inequities instead of mitigating current shortfalls. Researchers also identified other influencing factors such as high street connectivity, good coverage of lanes, and limited parking spaces for cars [7,11].
- *Barriers.* Several factors discourage potential riders from fully embracing shared e-scooters [25]. The primary hindrance is insecurity, primarily stemming from interactions with other motorized vehicles. Individuals who have not tried e-scooters often hold negative safety perceptions due to a lack of knowledge about how to operate these vehicles. Moreover, limitations are imposed by features of e-scooters, which prove inconvenient in adverse weather conditions, for long journeys, or when transporting goods. Some barriers are related to the restricted deployment areas, limited scooter availability at pickup points, technical issues with the vehicles, and high pricing. Other limitations are the absence of diverse payment methods, the necessity of owning a smartphone, the lack of integration with public transportation passes, and insufficient information regarding regulations [2]. The most rejected measure are the prohibition of riding on sidewalks, which forces e-scooters to share the road with motorized vehicles, and fixed parking locations that limits the flexibility of door-to-door trips [15].

- *Potential benefits.* E-scooters are a self-reliant mode of transportation, offering users the option to replace walking and shorten their journeys [13]. They can also serve as an alternative for short trips on public transportation, alleviating congestion and allowing public transit to prioritize longer journeys. Shared e-scooters have a strong appeal for users of car-sharing services, particularly for those undertaking trips shorter than 4 km [1]. Additionally, shared scooters can serve as complementary options to existing public transport systems, acting as feeder services. Shared scooters can play a complementary role in enhancing public transportation systems by acting as feeder services. The main appeal of shared e-scooters lies in their ability to significantly reduce travel time. However, initial reservations regarding riding experience, rental requirements, and safety considerations persist, although specific demographic groups, such as those based on age and income level, are more likely to overcome these concerns [3].
- *Environmental impact.* E-scooters have been introduced in the market as an eco-friendly transport solution, which is a motivation for some users. However, Life Cycle Assessments [5] showed several environmental threats. Based on existing usage trends and operational practices, the introduction of these new services does not result in a reduction of environmental impact when compared to the transportation modes they replace. This situation can push the transportation system towards less sustainable outcomes.

3.2 Electric public transportation

Several factors are relevant when analyzing electric bus lines. These factors include three concepts that are particularly studied in this article:

- *Operational Efficiency:* Assessing the operational efficiency of electric bus lines involves analyzing factors such as energy consumption, charging infrastructure availability, and the range and battery life of the buses. Evaluating these aspects helps determine the overall effectiveness and feasibility of electric buses in meeting transportation demands.
- *Social Equity and Accessibility:* Evaluating social equity and accessibility factors involves analyzing whether electric bus lines are adequately serving diverse communities, including peripheral neighborhoods and areas with lower socioeconomic status. Assessing accessibility includes considerations such as bus stop locations, frequency of service, and affordability for different segments of the population.
- *Passenger Experience and Comfort:* Analyzing the passenger experience and comfort of electric bus lines involves assessing factors such as noise levels, vibrations, seating capacity, air conditioning, and overall comfort and convenience for passengers. Understanding these factors helps ensure a positive and satisfactory experience for commuters.

The commented factors are crucial for developing sustainable mobility analysis, to help stakeholders make informed decisions regarding the implementation, operation, and optimization of electric bus lines to maximize their benefits and effectively contribute to sustainable and efficient public transportation.

6 S. Nesmachnow and S. Hipogrosso

3.3 Cycling infrastructure

The methodology for evaluating the cycling infrastructure studies the new deployments in recent years, expanding the existing network, and improving connections. Relevant aspects evaluated include:

- *Safety*: a crucial aspect that involves separation from vehicular traffic, clear signage, proper lane width, and adequate visibility for both cyclists and motorists.
- *Connectivity* between key destinations (residential areas, business districts, schools, parks, and public transportation hubs).
- *Integration with other transportation modes*, including public transportation systems, seamless transitions between cycling and walking, and accommodating bicycle parking facilities at transit stations.
- *Maintenance*, assessing the quality of pavement, regular maintenance practices, and prompt repairs to ensure a smooth and safe riding for cyclists.
- *Future growth and adaptability*, considering anticipated population growth, evolving transportation needs, and the ability to expand or modify the infrastructure as needed.

By considering these relevant aspects, planners and policymakers can assess the effectiveness and suitability of bicycle lanes and make informed decisions to improve cycling infrastructure in their communities.

4 Analysis of sustainable mobility initiatives in Montevideo

This section describes the analysis of the studied issues regarding sustainable mobility in Montevideo. Data analysis was performed on the high performance computing platform of National Supercomputing Center (Cluster-UY), Uruguay [24].

4.1 Analysis of electric scooters

Shared e-scooters have become a success for short distance commutes. It is an environment-friendly innovative transport solution that has shown potential contribution towards reducing congestion, improving community relationships, and provide a viable transportation alternative in urban areas.

Similar to other countries, Uruguay introduced e-scooters as a transportation option. In 2018, three companies entered Montevideo to provide and assess their reception. Although e-scooters offered a greener and user-friendly mode of transportation, the drawbacks outweighed the benefits. After operating for a year and a half, the companies decided to discontinue their services. A previous study [8] analyzed the operation of shared e-scooters using quantitative indicators such as coverage, commuting travel time, affordability, as well as qualitative indicators. The shared e-scooters experience in Montevideo faced significant challenges that contributed to its operational failure, as commented next.

Spatial distribution. In Montevideo, a similar trend to other urban centers was observed, where e-scooters concentrated in the coastal area. This strategic deployment aligns with profitability objectives of the business model, as these regions typically have higher incomes, dense populations, and ample job opportunities, resulting in increased usage rates. However, this approach in Montevideo resulted in an imbalanced distribution of e-scooters, limiting accessibility for a considerable portion of the population.

Barriers. The findings of the previous study in Parque Rodó neighborhood reflected the main challenges encountered by e-scooter users worldwide, indicating that residents shared similar safety concerns and perceptions regarding e-scooters. Similar to findings in other urban areas, interviews conducted to commuters in Parque Rodó revealed that a significant barrier to e-scooter adoption is the prevailing sense of insecurity among riders [8]. This feeling of insecurity mainly stems from interactions with other motorized vehicles, emphasizing the universal requirement for better-separated infrastructure and enhanced road conditions to support micromobility. Additional barriers are related to comfort. E-scooters are perceived as uncomfortable in unfavorable weather conditions, during long rides, or when users need to transport personal belongings. Moreover, barriers related to the e-scooter service include the limited availability of scooters at pickup points and difficulties in finding charged e-scooter. Moreover, external factors such as the behavior of individuals when operating and parking e-scooters, and their interaction with the urban environment, suggested the need for regulations to promote better coexistence. In response to these concerns, the city administration implemented several measures, such as restricting the operation area of e-scooters, prohibiting riding on sidewalks, implementing speed limits, and enforcing parking regulations. These measures resulted in a notorious decline in the preference of users for e-scooters as transportation mode.

Potential benefits. Despite facing several barriers, e-scooters have proven to be beneficial, especially for short-distance travel. In line with previous research that emphasized the ability of e-scooters to enhance travel time for trips up to 4 km [1,3] the analysis corroborated the time efficiency of e-scooters compared to the bicycle system and public transportation for distances less than 3 km.

Environmental impact. Concerns were raised about e-scooters sustainability as a clean mode of transportation. Doubts stemmed from the operational practices of e-scooter companies, that collected scooters for charging and redistributed them in the operating area using non-sustainable transportation methods.

In summary, the unsuccessful experience with shared e-scooters in Montevideo can be attributed to the scarcity of the spatial distribution of the service, the vehicle limitations for long trips, cost and comfort concerns, inconveniences in unfavorable weather conditions, operational constraints, and regulatory challenges. Together, these challenges undermined the feasibility and appeal of shared e-scooters as a sustainable mode of urban transportation in the city.

8 S. Nesmachnow and S. Hipogrosso

4.2 Analysis of electric bus lines

Electric public transportation has gained traction worldwide due to its environmental benefits and potential to reduce greenhouse gas emissions [14]. Many cities are transitioning to electric alternatives to promote sustainability and combat air pollution. Considering that Uruguay has showcased a commitment to renewable energy and firmly adopted wind and solar power as an important part of its energy matrix, there is a clear potential for the development of electric public transportation.

However, electric public transportation has not developed significantly in Montevideo. Since the first review published in 2020 [8], where the pilot plan instrumented using one electric vehicle for different bus lines was reported, few advances have been implemented. In 2021, one electric line was fully deployed [9]. Nowadays, in 2023, the bus company CUTCSA, that holds a substantial share (two thirds) of the public transportation market in Montevideo, operates three lines using electric buses: centric line CE1, differential line DE1 and line E14. CUTCSA has 20 electric BYD model K9W vehicles in its fleet. Other smaller companies have acquired a few electric buses, Yutong model ZK 6128BEVG (COETC 4 buses, COMESA 3 buses, and UCOT 3 buses) [6].

UCOT assigned its two electric vehicles to line 316, traveling from/to Pocitos/Villa Biarritz and km 18 of national route 8, in the North-East of Montevideo. As per its recent acquisitions in March 2023, the company has chosen to incorporate hybrid bus models, instead of fully electric vehicles, into its fleet. According to the Chief Technician of UCOT, “Electric bus does not yet replace the conventional bus, for that it would require 30% more autonomy” [33]. COMESA initially used line 522 for a pilot plan developed in 2020–2021, and later assigned the electric buses to routes with few turns and complex maneuvers. Following the initial implementation, COMESA periodically assigned electric buses have been periodically to various lines in Montevideo, including lines 505, 524, 526, 538, 546, 582, and L24. COETC assigned electric buses to provide services on the centric line CA1 and on service 407 that connects Plaza España (Downtown) with Portones Shopping, in the East of Montevideo. Thee company has not explored other alternatives for exclusive electric buses. According to the President of COETC “There is an intermediate step, which is the hybrid bus” [33].

Several alternatives have been explored to expand the initial developments of electric public transportation in Montevideo, including a specific fund for promoting the acquisition of electric buses [28] a new financial program from the Ministry of Industry, Energy, and Mining aimed at developing tools to facilitate progress towards the energy transition [34].

The three electric bus lines are mainly focused on providing mobility services to neighborhoods with higher socioeconomic index values, at the expense of peripheral neighborhoods that are not covered by the routes of electric bus lines. Fig. 1 presents the routes and a socioeconomic characterization of neighborhoods in Montevideo.

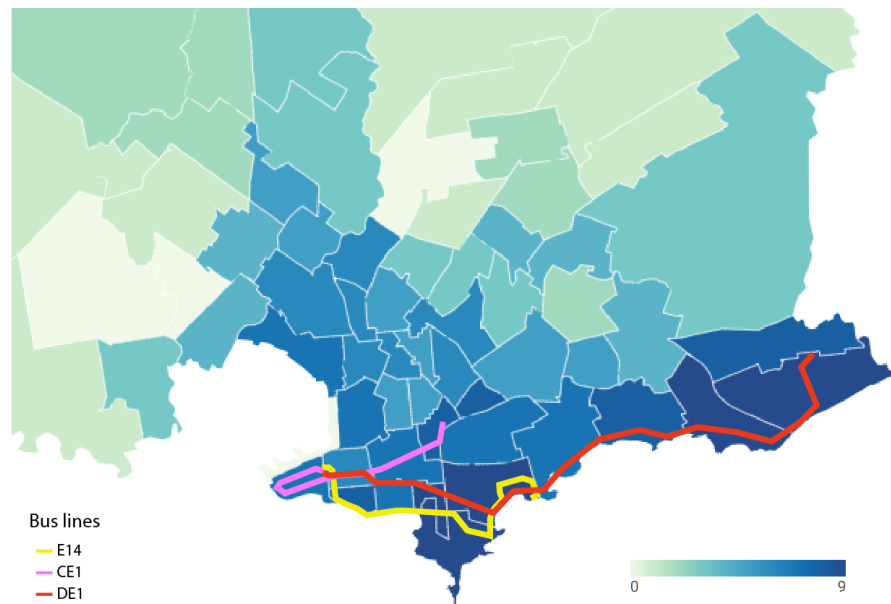


Fig. 1: Electric bus routes and socioeconomic characterization of neighborhoods in Montevideo

The assessment of the socio-economic conditions in neighborhoods was conducted using the Socioeconomic Level Index (INSE) [26], a methodological tool used to assess the purchasing power or income of households. INSE defines 10 values for different geographical and administrative divisions, from 0 (lowest socio-economic level) to 9 (highest socio-economic level). The average INSE value for the neighborhoods in Montevideo is 4.5. Results indicate that neighborhoods served by electric lines have a significantly higher INSE values than the average for Montevideo. Fig. 1 clearly shows this trend, with electric lines serving the southern coast neighborhoods, where high-income citizens leave.

According to the analysis by the Uruguayan government [6], the power consumption of the electric buses ranged from a minimum of 0.56 kWh/km to a maximum of 1.60 kWh/km, with an average consumption of 1.11 kWh/km. The majority of the units operate with an efficiency between 0.9 kWh/km and 1.1 kWh/km.

The specific energy efficiency vary depending on factors such as bus model, technology, and operational conditions. A common benchmark for electric bus energy efficiency is 0.8 to 1.5 kWh/km, often considered a good energy efficiency level for electric buses. The 0,8 kWh value is considered a proper efficiency for 12-meter buses in a normal day (average temperature of 20°C), operating on low traffic by a skilled driver. In turn, 1.5 kWh/km is a reasonable energy efficiency for a bus operating in winter with electric heating turned on [32].

10 S. Nesmachnow and S. Hipogrosso

Analyzing the passenger experience and comfort of electric bus lines involves assessing factors such as noise levels, vibrations, seating capacity, air conditioning, and overall comfort and convenience for passengers. Understanding these factors helps ensure a positive and satisfactory experience for commuters. Vehicles operating in the electric bus lines of Montevideo offer exceptional features that enhance the commuting experience for passengers. The travel experience is enhanced by the low level of noise, air conditioning, and a wide space for both sitting and standing passengers. Nevertheless, the experience of waiting for and boarding the electric bus is currently unsatisfactory due to the lack of infrastructure at numerous stops. The ten new bus stops introduced for bus line E14 have no infrastructure whatsoever, neither a shelter, nor a sitting bench, nor information about route and timetable. Bus stops without infrastructure are: Sarmiento between Patria and Maggiolo (both ways), Rambla and Eduardo Acevedo (both ways), Rambla and Barrios Amorín (both ways), Rambla and La Cumparsita (both ways), Ferreira Aldunate and Durazno, and Río Negro and Durazno. Six of these bus stops are located on the promenade in front of the sea shore, making very difficult for passengers to wait for the bus on rainy and windy days. Lines CE1 and DE1 do not suffer from this total absence of infrastructure, because they use the bus stops from previous lines D1 and CA1. However, the infrastructure is not complete or damaged for many bus stops, and the information about route and timetable is just available in a few stops. This is an important shortcoming of electric bus lines, especially considering that they have been operating for more than two and a half years now.

In summary, Montevideo has been making slow progress in adopting electric buses. The city still has ample opportunity to proactively address the reduction of greenhouse gas emissions and enhance air quality by further expanding the transition from conventional fossil fuel buses to electric buses. There is much room to plan the coverage of electric public transportation, allowing different parts of the city benefit from the environmental advantages they offer. In particular, neighborhoods with medium and lower socio-economic index must be covered to guarantee a wider reach and enable a larger number of passengers to experience the benefits of cleaner and more sustainable transportation.

4.3 Expansion of cycling infrastructure

In 2018, Montevideo embarked on a commendable journey to enhance its urban infrastructure by expanding the network of bicycle lanes, aiming to promote sustainable mobility within the city. This initiative demonstrated the commitment of the city to provide environmentally friendly and efficient transportation alternatives for its residents. Nevertheless, the existing bicycle network has proven insufficient to meet the increasing demands of a growing user base. The survey conducted in Parque Rodó neighborhood [9] revealed that a significant number of commuters are willing to switch from their current preferred mode of transportation to bicycles as a sustainable option. The enthusiasm expressed by residents highlights the untapped potential and the desire for sustainable mobility solutions in Montevideo.

Three types of cycling infrastructure are deployed in Montevideo:

- bicycle lane (*ciclovia*) is a part of the road (a lane), dedicated exclusively to the circulation of bicycles.
- bicycle lane (*bicisenda*) is a path on a sidewalk, central flowerbed or landscaped area, off the road, dedicated to the exclusive circulation of bicycles.
- 30 km road is a street in which a speed limit of 30 km/h is established, to promote coexistence in circulation with bicycles, and with signage that establishes the priority that must be given to the latter in the circulation.

Between 2020 and 2022, the bicycle network in Montevideo was effectively expanded in several areas, indicating a commitment toward promoting cycling. Nevertheless, specific aspects of the bicycle network expansion still require additional focus. Although advancements have been achieved, the design and connectivity of bicycle paths have not met the established standards highlighted in previous studies to ensure safety and comfort of cyclists. Certain intersections have been identified as potentially unsafe. Three unconnected sub-networks exist in the city and other routes are significantly far from the main core.

Table 1 reports the length of the new infrastructure and Table 2 reports the ratio in linear kilometers over the road network of Montevideo.

<i>type</i>	<i>new (km)</i>	<i>length (km)</i>	<i>percentage</i>
bicycle lane	5.2	10.5	49.5%
bicycle path	16.9	42.2	40.0%
30 km/h road	0.0	15.1	0.0%
total	22.1	67.8	32.6%

Table 1: Built infrastructure for bicycles in Montevideo

<i>type</i>	<i>length (km)</i>	<i>percentage</i>
bicycle lane	10.0	0.26%
bicycle path	37.2	0.98%
30 km/h road	15.1	0.40%
total	67.3	1.65%

Table 2: Ratio over the road network of Montevideo (linear km)

12 S. Nesmachnow and S. Hipogrosso

5 Conclusions

This article studied recent development of sustainable mobility options in Montevideo, Uruguay. The analysis of e-scooters, electric bus, and cycling infrastructure evaluated relevant factors for the quality of service provided to citizens.

The primary finding of the analysis is that despite recent the recent efforts to promote sustainable mobility in Montevideo, the implemented initiatives are not consolidated yet. The business model for e-scooters faced significant challenges, resulting in the discontinuation of this service in the city. Only three electric bus lines have been deployed, and they primarily benefit the population residing in more wealthy coastal neighborhoods. Although there has been notable progress in the development of cycling infrastructure in 2020–2022, the network remains relatively modest. Several issues persist regarding connectivity, intermodal connections, and maintenance.

A comprehensive holistic development of sustainable mobility is needed to address transportation issues and properly benefit citizens regarding efficiency, livability, inclusiveness, and the environment.

References

1. Abouelela, M., Al Haddad, C., Antoniou, C.: Are young users willing to shift from carsharing to scooter-sharing? *Transportation Research Part D: Transport and Environment* **95**, 102821 (Jun 2021). <https://doi.org/10.1016/j.trd.2021.102821>
2. Aman, J.J.C., Zakhem, M., Smith-Colin, J.: Towards equity in micromobility: Spatial analysis of access to bikes and scooters amongst disadvantaged populations. *Sustainability* **13**(21), 11856 (Oct 2021). <https://doi.org/10.3390/su132111856>
3. Baek, K., Lee, H., Chung, J.H., Kim, J.: Electric scooter sharing: How do people value it as a last-mile transportation mode? *Transportation Research Part D: Transport and Environment* **90**, 102642 (Jan 2021). <https://doi.org/10.1016/j.trd.2020.102642>, <http://dx.doi.org/10.1016/j.trd.2020.102642>
4. Bielińska, E., Hamerska, M., Żak, A.: Sustainable Mobility and the Smart City: A Vision of the City of the Future: The Case Study of Cracow (Poland). *Energies* **14**(23), 7936 (2021). <https://doi.org/10.3390/en14237936>
5. de Bortoli, A., Christoforou, Z.: Consequential lca for territorial and multi-modal transportation policies: method and application to the free-floating e-scooter disruption in paris. *Journal of Cleaner Production* **273**, 122898 (Nov 2020). <https://doi.org/10.1016/j.jclepro.2020.122898>, <http://dx.doi.org/10.1016/j.jclepro.2020.122898>
6. Comisión Técnica del subsidio a la compra de ómnibus eléctricos: Operación de ómnibus eléctricos adquiridos a través del subsidio a la compra definido en el art. 349 de la ley 19.670. https://www.gub.uy/ministerio-industria-energia-mineria/sites/ministerio-industria-energia-mineria/files/documentos/noticias/Primer%20Informe%20anual%20buses%20el%C3%A9ctricos_2110.pdf (2021), text in Spanish, accessed on September 23, 2023
7. Hawa, L., Cui, B., Sun, L., El-Geneidy, A.: Scoot over: Determinants of shared electric scooter presence in washington d.c. *Case Studies on Transport Policy*

- 9(2), 418–430 (Jun 2021). <https://doi.org/10.1016/j.cstp.2021.01.003>, <http://dx.doi.org/10.1016/j.cstp.2021.01.003>
8. Hipogrosso, S., Nesmachnow, S.: Analysis of sustainable public transportation and mobility recommendations for montevideo and parque rodó neighborhood. *Smart Cities* **3**(2), 479–510 (2020). <https://doi.org/10.3390/smartcities3020026>
 9. Hipogrosso, S., Nesmachnow, S.: Towards a Sustainable Mobility Plan for Engineering Faculty, Universidad de la República, Uruguay. In: *Smart Cities*, pp. 199–215. Springer International Publishing (2021). https://doi.org/10.1007/978-3-030-69136-3_14
 10. Huertas, J., Stöffler, S., Fernández, T., García, X., Castañeda, R., Serrano, O., Mogro, A., Alvarado, D.: Methodology to assess sustainable mobility in LATAM cities. *Applied Sciences* **11**(20), 9592 (2021). <https://doi.org/10.3390/app11209592>
 11. Huo, J., Yang, H., Li, C., Zheng, R., Yang, L., Wen, Y.: Influence of the built environment on e-scooter sharing ridership: A tale of five cities. *Journal of Transport Geography* **93**, 103084 (May 2021). <https://doi.org/10.1016/j.jtrangeo.2021.103084>, <http://dx.doi.org/10.1016/j.jtrangeo.2021.103084>
 12. Johnston, R.A.: Indicators for sustainable transportation planning. *Transportation Research Record: Journal of the Transportation Research Board* **2067**(1), 146–154 (Jan 2008). <https://doi.org/10.3141/2067-17>, <http://dx.doi.org/10.3141/2067-17>
 13. Kopplin, C.S., Brand, B.M., Reichenberger, Y.: Consumer acceptance of shared e-scooters for urban and short-distance mobility. *Transportation Research Part D: Transport and Environment* **91**, 102680 (Feb 2021). <https://doi.org/10.1016/j.trd.2020.102680>, <http://dx.doi.org/10.1016/j.trd.2020.102680>
 14. Krawiec, K., Markusik, S., Sierpiński, G. (eds.): *Electric Mobility in Public transport—Driving Towards Cleaner Air*. Springer International Publishing (2021). <https://doi.org/10.1007/978-3-030-67431-1>
 15. Lo, D., Mintrom, C., Robinson, K., Thomas, R.: $\text{shared}_{\text{scpi}}$ micromobility: The influence of regulation on travel mode choice. *New Zealand Geographer* **76**(2), 135–146 (May 2020). <https://doi.org/10.1111/nzg.12262>, <http://dx.doi.org/10.1111/nzg.12262>
 16. Lyons, W.: Sustainable transport in the developing world: a case study of Bogotá’s mobility strategy. In: *International Conference on Sustainable Infrastructure*. American Society of Civil Engineers (2017)
 17. Marshall, S.: The challenge of sustainable transport. In: *Planning for a Sustainable Future*, pp. 131–147. Spon, London (2001)
 18. Massobrio, R., Nesmachnow, S.: Travel Time Estimation in Public Transportation Using Bus Location Data, pp. 192–206. Springer International Publishing (2022). https://doi.org/10.1007/978-3-030-96753-6_14, http://dx.doi.org/10.1007/978-3-030-96753-6_14
 19. Massobrio, R., Nesmachnow, S., Gómez, E., Sosa, F., Hipogrosso, S.: Public transportation and accessibility to education centers in maldonado, uruguay. In: *Smart Cities*, pp. 123–138. Springer International Publishing (2021). https://doi.org/10.1007/978-3-030-69136-3_9
 20. Mavlutova, I., Atstaja, D., Grasis, J., Kuzmina, J., Uvarova, I., Roga, D.: Urban transportation concept and sustainable urban mobility in smart cities: A review. *Energies* **16**(8), 3585 (2023). <https://doi.org/10.3390/en16083585>

- 14 S. Nesmachnow and S. Hipogrosso
21. Miller, P., de Barros, A.G., Kattan, L., Wirasinghe, S.C.: Public transportation and sustainability: A review. *KSCE Journal of Civil Engineering* **20**(3), 1076–1083 (Mar 2016). <https://doi.org/10.1007/s12205-016-0705-0>, <http://dx.doi.org/10.1007/s12205-016-0705-0>
 22. Nesmachnow, S., Tchernykh, A., Cristóbal, A.: Planificación de transporte urbano en ciudades inteligentes. In: *I Ibero-american Conference on Smart Cities*. pp. 204–218 (2018)
 23. Nesmachnow, S., Hipogrosso, S.: Transit oriented development analysis of Parque Rodó neighborhood, Montevideo, Uruguay. *World Development Sustainability* **1**, 100017 (2022). <https://doi.org/10.1016/j.wds.2022.100017>
 24. Nesmachnow, S., Iturriaga, S.: Cluster-UY: Collaborative Scientific High Performance Computing in Uruguay. In: Torres, M., Klapp, J. (eds.) *Supercomputing, Communications in Computer and Information Science*, vol. 1151, pp. 188–202. Springer (2019). https://doi.org/10.1007/978-3-030-38043-4_16
 25. Nikiforiadis, A., Paschalidis, E., Stamatiadis, N., Raptopoulou, A., Kostareli, A., Basbas, S.: Analysis of attitudes and engagement of shared e-scooter users. *Transportation research part D: transport and environment* **94**, 102790 (2021)
 26. Perera, M.: Índice de nivel socioeconómico. <http://www.ceismu.org/site/indice-de-nivel-socioeconomico-inse-2018/> (2018), text in Spanish, accessed on 12 August 2023
 27. Péres, M., Ruiz, G., Nesmachnow, S., Olivera, A.C.: Multiobjective evolutionary optimization of traffic flow and pollution in Montevideo, Uruguay. *Applied Soft Computing* **70**, 472–485 (2018). <https://doi.org/10.1016/j.asoc.2018.05.044>
 28. Portal Movilidad: Espera al Gobierno nacional: Montevideo contaría con fondo para buses eléctricos a mitad de 2023. <https://portalmovilidad.com/espera-al-gobierno-nacional-montevideo-contaria-con-fondo-para-buses-electricos-a-mitad-de-2023/> (2022), text in Spanish, accessed on 12 August 2023
 29. Ravagnan, C., Rossi, F., Amiriaref, M.: Sustainable Mobility and Resilient Urban Spaces in the United Kingdom. Practices and Proposals. *Transportation Research Procedia* **60**, 164–171 (2022). <https://doi.org/10.1016/j.trpro.2021.12.022>
 30. Rodrigues, A., Costa, M., Macedo, M.: Multiple views of sustainable urban mobility: The case of Brazil. *Transport Policy* **15**(6), 350–360 (2008)
 31. Smith, A.: Electric scooters remain prohibited in Toronto until proper regulations developed. <https://https://dailyhive.com/toronto/toronto-e-scooter-update-october> (2019), text in Spanish, accessed on September 23, 2023
 32. Sustainable Bus: Electric bus range, focus on electricity consumption. a sum-up. <https://www.sustainable-bus.com/news/electric-bus-range-electricity-consumption/> (2022), text in Spanish, accessed on 12 August 2023
 33. Transporte Carretero: Informe nueva movilidad: U.C.O.T. <https://www.transportecarretero.com.uy/noticias/energias-alternativas/informe/-nueva-movilidad-u-c-o-t-enrique-garabato-gerencia-de-talleres-aun-no-sustituyen/-al-omnibus-convencional-para-eso-se-necesitaria-un-30-mas-de-autonomia.html> (2021), text in Spanish, accessed on September 13, 2023
 34. Ámbito: El parque de buses eléctricos aumentó al 35%. <https://www.ambito.com/uruguay/el-parque-buses-electricos-aumento-al-35-n5681005> (2023), text in Spanish, accessed on 12 August 2023

Aprovechamiento del vapor geotérmico para activar la refrigeración por absorción (ARS) en aplicaciones aledañas a las centrales geotérmicas.

Dr. A. Uriel Cervantes C. ¹ Dr. Jorge A. Del Angel R. ¹ Omar Montiel P. ²
Ing. Mariel Morales M. ³ Luz M. Hernández A. ²

¹ Universidad Veracruzana, Facultad de Ingeniería Mecánica Eléctrica Xalapa, Ver, México
² Universidad Veracruzana, Estudiantes Facultad de Ingeniería Ambiental, Xalapa Ver, México
³ Universidad Veracruzana, Estudiante de Maestría en Ingeniería Aplicada, Facultad de Ingeniería Mecánica Veracruz Ver, México
ing.urielc@gmail.com, jdelangel@uv.mx

Resumen. Este trabajo de investigación tiene el objetivo de proponer el aprovechamiento circular del recurso térmico de una central geotermoeléctrica, al utilizar los sistemas de refrigeración por absorción (ARS por sus siglas en inglés) para cubrir los requerimientos energéticos. Con ello, se busca asegurar el confort para el personal de trabajo y reducir el consumo de energía eléctrica en su demanda operativa, y a través de esta forma, poder inyectar la mayor parte de energía a la red al tiempo que se asegura la confiabilidad de la planta para introducir el agua que sale del ciclo de vapor al suelo nuevamente.

En el presente trabajo se simula la posibilidad de acoplamiento de la tecnología de un sistema ARS que utiliza una mezcla bromuro de litio-agua para la climatización de los cuartos de operación y control de la central. Para ello, se desarrolla la metodología de cálculo y operación para justificar su viabilidad energética. Los datos utilizados y mostrados contemplan información de las condiciones reales de operación en una central geotermoeléctrica, referente a las características del vapor utilizado. Estos sistemas de absorción también pueden cubrir el requerimiento energético de las torres de enfriamiento en la etapa de condensación.

Palabras Clave: Energía Geotérmica, Refrigeración por absorción, Energías Renovables, Simulación

1 Introducción

De acuerdo con la Agencia Internacional de Energías Renovables IRENA [1], la capacidad global de energía geotérmica renovable en 2020 fue de 14,050 MW, donde 33 países a nivel global, incluidos los países de la Unión Europea, apuestan por su uso para la generación de energía eléctrica y seguir sumando energía renovable a su matriz energética. En los últimos 10 años la generación de energía eléctrica se ha incrementado

2

al doble. Estados Unidos, Indonesia, Filipinas, Turquía, Nueva Zelanda y México ocupan los primeros lugares en generación de energía geotermoeléctrica. En 2020 se generó a nivel global 94,949 GWh, siendo los países que incrementaron su capacidad del 2019 al 2020 Honduras de 35 a 39 MW, Turquía de 1515 a 1613 MW, Italia de 767 a 797 MW, Nueva Zelanda de 952 MW a 984 MW.

Después de la pandemia Covid 19, en el año 2021 la capacidad geotérmica renovable a nivel global ha crecido 5 veces más (1500 MW), que comparada con la capacidad geotérmica renovable que desde el 2011 al 2020 solo creció 300 MW en promedio cada año. De acuerdo con el Programa del Desarrollo Eléctrico Nacional (PRODESEN) 2022-2036 [2], México incrementó su capacidad instalada en energía eléctrica de 951 a 976 MW y se espera un crecimiento de 985 MW al 2024 y 1132 al 2030. En México hay 8 centrales de generación geotérmica, y en los siguientes años la demanda incrementará, ya que de acuerdo con el AZEL (Atlas Nacional de Zonas con Alto Potencial de Energías Limpias) 2017 [3], existen zonas potenciales de energía geotérmica en diferentes zonas de los estados del país México. En las revistas de la Asociación Geotérmica Mexicana (AGM), se ha impulsado el uso de la energía geotérmica en tres potenciales de temperatura. La AGM [4] indica que se impulsa la generación de energía eléctrica tratando de usar el recurso geotérmico de baja entalpía por ser el potencial que se puede encontrar con mayor probabilidad. Aunado a esto, el Instituto Nacional de Electricidad y Energías Limpias (INEEL) ha impulsado en gran medida, la generación con esta tecnología, no solo para la aplicación de energía eléctrica, sino también para múltiples usos con el objetivo de aprovechar al máximo el calor geotérmico, por ejemplo, para bombas de calor; y es importante considerar una de esas aplicaciones a la refrigeración por absorción.

Por otra parte, International Journal of Refrigeration (IJR) 2022 señala que la refrigeración tendrá origen desde nuevos materiales y diferentes tecnologías a la refrigeración por compresión [5]. De acuerdo con la Agencia Internacional de Energía (IEA) [6] para el 2023, aproximadamente 2000 millones de unidades de aire acondicionado están actualmente funcionando en todo el mundo. Esto ocasiona que la refrigeración de espacios sea uno de los principales impulsores del aumento de la demanda de electricidad en los edificios. Sumado a esto, se incrementó la capacidad de generación para satisfacer la demanda máxima de energía, y para lograr el objetivo al 2050 de un futuro descarbonizado, se tiene que mirar hacia alternativas tecnológicas limpias. Magallanes 2022 [7] indica que una alternativa viable al uso de la refrigeración mecánica es el uso de los sistemas de refrigeración por absorción, los cuales pueden operar de forma eficiente con fuentes calóricas de 100 a 160°C. El Instituto de Energías Renovables (IER) de la UNAM señala que estos sistemas de refrigeración pueden operar con diversas mezclas de refrigerantes más limpios y con opciones de suministrarle diferentes fuentes de energía térmica [8]. Esto haría aprovechable el calor residual de diversos procesos de producción de fábricas o centrales de generación de energía eléctrica, donde liberan calor a la atmósfera o retornos con fluidos de más de 100°C. Las aplicaciones de la geotermia hidrotermal [10] desde el punto de vista sostenible y circular, puede ser la solución para aquellos países que cuenten con este recurso, ya que entre las diversas

tecnologías de absorción que existen actualmente, hay más de 200 modelos de refrigeración por absorción para poderse acoplarse a la geotermia de acuerdo con el gradiente con que pudiera recibir este recurso térmico.

2 Antecedentes

De acuerdo con la evaluación y mercado global de geotermia, la energía geotérmica desempeñará un papel fundamental en la transición a una energía limpia junto con otras fuentes de energía renovables. Los recursos geotérmicos están ampliamente disponibles en áreas con actividad volcánica, así como en cuencas sedimentarias. Con el reciente despliegue acelerado de energía variable procedente de la energía eólica y solar fotovoltaica, la geotermia puede contribuir a la estabilización de las redes eléctricas. Además, la tecnología de la energía geotérmica ha evolucionado más allá de su enfoque en el mercado de la electricidad para abarcar una gama más amplia de aplicaciones dentro del sector energético, incluida la calefacción y refrigeración sostenibles. Estos atributos hacen de la geotermia una fuente de energía renovable rentable e independiente de las variables climatológicas locales [11]. La capacidad instalada mundial de calefacción y refrigeración geotérmica fue de 107,4 GWth en 2020. Las bombas de calor geotérmicas constituyeron el 72% de esta capacidad, y el 28% restante provino del calentamiento y enfriamiento directo mediante fluidos geotérmicos [11]. La calefacción y refrigeración geotérmica se concentran en tres regiones. La región de Asia y Oceanía, con instalaciones con una capacidad de 45,8 GWth, es líder mundial, con una cuota del 43%; le sigue Euroasia (38%) y América del Norte (21%), América Latina y el Caribe, África y el Medio Oriente contribuye cada uno con un 1% o menos [11].

Como ejemplo del aprovechamiento de recursos geotérmicos para acondicionamiento de aire, Pérez Ramírez de Arellano [12] propuso el uso de la energía geotérmica para diseñar y aplicar una instalación de climatización para una vivienda unifamiliar situada en Valencia, España. Para ello se realizó un análisis del terreno donde se llevaría a cabo el proyecto y se diseñó el circuito en el software Geo2 de GEOCISA. Así mismo, Ambriz Díaz, Rubio Maya, Pacheco Ibarra y Pastor Martínez [13] realizaron un análisis exergético a una planta de poli generación que utiliza energía geotérmica para producir electricidad, enfriamiento y calor útil para deshidratación. Más de 80 países utilizan energía geotérmica para calefacción y refrigeración, diez tienen al menos 2 GWth de capacidad instalada, China tiene la mayor capacidad instalada (40,6 GWth), seguido de Estados Unidos (20,7 GWth), Alemania (4,8 GWth), Turquía (3,5 GWth), Francia (2,6 GWth), Japón (2,5 GWth), Islandia (2,4 GWth), Finlandia (2,3 GWth) y Suiza (2,2 GWth). Las bombas de calor geotérmicas representan una gran proporción de la calefacción y refrigeración instaladas en varios de estos países (100% en Finlandia y Suecia, 99% en Suiza, 98% en Estados Unidos, el 92% en Alemania, el 78% en Francia y el 65% en China).

Para el caso de México, en 2008 García Gutiérrez, Barragán Reyes y Arellano Gómez [14] realizaron una investigación sobre los sistemas desarrollados por CFE y el Instituto

4

de Investigaciones Eléctricas referentes a bombas de calor con energía geotérmica que operan en sistemas de refrigeración por compresión mecánica, absorción y transformadores térmicos. De igual forma, en 2021 Francisco Hernández [15] estudio la capacidad de sistemas de acondicionamiento de aire a partir de una torre de viento con humidificación y un sistema de aprovechamiento de fluido geotérmico. El Proyecto estaba enfocado para una vivienda de interés social localizada en una zona con clima cálido-seco. Finalmente, Rivas Cruz, Hernández Martínez y Papadimitriou-Suarez del Real [16] realizaron una investigación que resume los sistemas de bombas de calor que operan con energía geotérmica desarrollados en Puebla, Mexicali, Morelos, Aguas Calientes y Guanajuato con diversas aplicaciones enfocadas especialmente en el acondicionamiento de espacios. De acuerdo con la revista de Transición Energética 2019 [17], en México ya se realizaron dos proyectos con energía geotérmica aplicados a Bombas de calor (Comunidad Los Humeros y Universidad Politécnica de Baja California), y la aplicación hacia la refrigeración por absorción puede ser la siguiente aplicación.

3 Simulación para el acoplamiento termo energético del ARS.

En la figura 1 se muestra un diagrama como propuesta para obtener aire frío mediante un sistema de absorción a través de la extracción de vapor geotérmico de una central geotérmica. Del diagrama resaltan tres puntos importantes relacionados con el calor de entrada y de enfriamiento del sistema: el condensador (Q_c), el generador (Q_g) y el evaporador (Q_e).

El proceso de funcionamiento es el siguiente: se extrae vapor de agua desde una profundidad de 1600 a 3600 metros bajo la tierra de diversos pozos. Estos se unen a un cabezal y se dirigen al punto 30 y por medio de un separador se retira la humedad que pueda tener (agua o vapor con agua). El vapor se dirige hacia el punto 31 mientras que el líquido se dirige al punto 34, donde es inyectado a la tierra; el vapor seco entra a la turbina de vapor para producir movimiento y transformar la energía mecánica en energía eléctrica en el generador eléctrico. Al salir el vapor de la turbina, este pasa por un condensador y el líquido obtenido se inyecta nuevamente a la tierra para finalizar el ciclo.

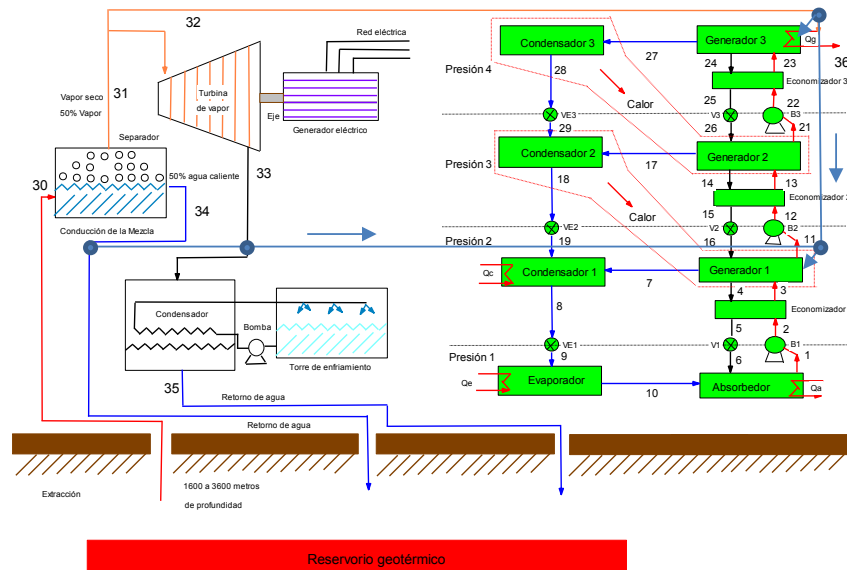


Figura 1. Simulación de un Sistema de Refrigeración por Absorción con datos reales de una Central Geotermoeléctrica.

Fuente: Elaboración propia

Si del punto 31 se extrae vapor para alimentar un sistema de refrigeración por absorción, se podría obtener aire frío para climatizar la sala de operación y control, así como agua fría para las torres de enfriamiento que extraen calor del vapor que sale de la turbina, o algún otro requerimiento energético. Así mismo, se puede utilizar el agua del separador y poner en marcha un ciclo de refrigeración por absorción continua de simple efecto.

En la figura 1 también se muestra el sistema de refrigeración por absorción de triple efecto, el funcionamiento se describe a continuación.

Primeramente, sale refrigerante del evaporador en forma de vapor de agua (punto 10), el cual es absorbido por sal absorbente bromuro de litio-agua (BrLi-H₂O) que se encuentra en el absorbedor. Cuando el absorbente se satura de refrigerante, entra una bomba (punto 1) que traslada la mezcla refrigerante-absorbente por el generador 1. Parte de la mezcla fluye por la bomba 2 (punto 11) siguiendo su proceso hasta el generador 3, donde entra vapor geotérmico para calentar y separar la mezcla refrigerante-absorbente. En el punto 27 sale el refrigerante evaporado, mientras que, en el punto 24 sale el absorbente con menos contenido de agua hasta llegar al punto 26. Por otra parte,

6

el vapor refrigerante que va hacia el condensador 3 se condensa al ceder calor al generador 2, produciéndose refrigerante que se dirige al condensador 2 y que se condensa por ceder calor en el generador 1, donde nuevamente se produce refrigerante que se dirige al condensador 1. En términos generales, en el condensador 3 y 2, así como el generador 2 y 1, el intercambio de calor es interno dentro del sistema de refrigeración por absorción. Por una parte el condensador 1 necesita de un medio de enfriamiento, mientras que el generador 3 del calor geotérmico para que el sistema de absorción pueda operar. A estos sistemas se le conoce como triple efecto, pues generan tres veces refrigerante con una sola entrada de calor.

4 Metodología para el balance de energía del sistema ARS

Inicialmente, se deben suponer las condiciones lineales de operación:

- Las presiones son constantes (isobáricas) en los dispositivos excepto en las bombas y válvulas.
- Hay procesos isoentálpicos en las válvulas de expansión de refrigerante y válvula de estrangulamiento de la mezcla o solución concentrada.
- Existe vapor saturado a la salida del evaporador a su presión o temperatura de saturación (después del proceso de arranque).

También se deben suponer las temperaturas del vapor geotérmico ($T_{[24]}$) y temperatura ambiente ($T_{[1]}$), el calor de enfriamiento o aire que se desea enfriar (Q_e), las concentraciones ($X_{[1]}$, $X_{[6]}$, $X_{[10]}$) y la efectividad de cada uno de los economizadores (dispositivos que se encuentran entre los generadores y los absorbedores). Las condiciones de entrada al sistema en cada punto se describen en la tabla 1 del apartado de anexos.

Posteriormente las temperaturas ($T_{[3]}$, $T_{[4]}$, $T_{[11]}$, $T_{[13]}$, $T_{[14]}$, $T_{[17]}$, $T_{[21]}$, $T_{[23]}$, $T_{[27]}$) estarán cambiando en función de la temperatura de entrada de vapor geotérmico; para generar dicho balance se hará uso de las siguientes constantes, las cuales son fundamentales para obtener las propiedades de presión, temperatura y entalpía [18] al [25]:

Tabla 2. Constantes del sistema. Elaboración propia.

$A_0=-2.00755$	$D=-1596.49$	$b_2=0.03248041$
$A_1=0.16976$	$E=-104095.5$	$b_3=-0.0004034184$
$A_2=-0.003133362$	$a_0=-2024.33$	$b_4=0.0000018520569$
$A_3=0.0000197668$	$a_1=163.309$	$c_0=-0.037008214$
$B_0=124.937$	$a_2=-4.88161$	$c_1=0.0028877666$
$B_1=-7.71649$	$a_3=0.06302948$	$c_2=-0.000081313015$
$B_2=0.152286$	$a_4=-0.0002913705$	$c_3=0.00000099116628$
$B_3=-0.000795090$	$b_0=18.2829$	$c_4=-0.000000044441207$
$C=7.05$	$b_1=-1.1691757$	

El siguiente punto es igualar las concentraciones:

$$(X_{[6]}=X_{[4]}=X_{[5]}=X_{[14]}= X_{[15]}=X_{[16]}=X_{[24]}=X_{[25]}=X_{[26]})$$

$$(X_{[1]}=X_{[2]}=X_{[3]}=X_{[11]}= X_{[12]}=X_{[13]}=X_{[21]}=X_{[22]}=X_{[23]})$$

$$(X_{[10]}=X_{[7]}=X_{[8]}=X_{[9]}= X_{[17]}=X_{[18]}=X_{[19]}=X_{[27]}=X_{[28]}=X_{[29]})$$

La primera ecuación que se tiene que tomar en cuenta es la concentración (X), que incrementará cuando se desprenda el refrigerante hacia el condensador, y disminuirá cuando esta absorba refrigerante del evaporador, siendo igual a:

$$X = \frac{\text{masa sal (BrLi)}}{\text{masa sal (BrLi)} + \text{masa del refrigerante (H2O)}} \quad (1)$$

Posteriormente se obtiene la temperatura T[8], sustituyendo algunas de las constantes mencionadas mediante la siguiente ecuación:

$$T_{[8]} = \frac{(T_{[4]} - (B_0 * X_{[6]}^0 + B_1 * X_{[6]}^1 + B_2 * X_{[6]}^2 + B_3 * X_{[6]}^3))}{A_0 * X_{[6]}^0 + A_1 * X_{[6]}^1 + A_2 * X_{[6]}^2 + A_3 * X_{[6]}^3} \quad (2)$$

Con la temperatura T_8, se determina la presión P[8], P_8 y la entalpía h[8] (esta última se obtiene con tablas de vapor de agua a temperatura ambiente o de condensación y se considera líquido saturado):

$$T_{_8} = 273.15 + T_{[8]} \quad (3)$$

$$\text{Log}P_8 = C + \frac{D}{T_{_8}} + \frac{E}{T_{_8}^2} \quad (4)$$

Se obtiene la temperatura T[9] con la siguiente ecuación:

$$T_{[9]} = \frac{(T_{[1]} - (B_0 * X_{[1]}^0 + B_1 * X_{[1]}^1 + B_2 * X_{[1]}^2 + B_3 * X_{[1]}^3))}{A_0 * X_{[1]}^0 + A_1 * X_{[1]}^1 + A_2 * X_{[1]}^2 + A_3 * X_{[1]}^3} \quad (5)$$

Se obtiene la temperatura absoluta de T_9, para poder obtener la presión P[9], P_9;

$$T_{_9} = 273.15 + T_{[9]} \quad (6)$$

$$\text{Log}P_9 = C + \frac{D}{T_{_9}} + \frac{E}{T_{_9}^2} \quad (7)$$

8

Conociendo las entalpías de entrada y salida del evaporador, así como, el calor de enfriamiento se determina la masa del refrigerante $m_{[10]}$, para realizar un balance de masa en el absorbedor:

$$m_{[10]} + m_{[6]} = m_{[1]} \quad (8)$$

$$m_{[10]} * X_{[10]} + m_{[6]} * X_{[6]} = m_{[1]} * X_{[1]} \quad (9)$$

Con los flujos másicos de las soluciones concentrada y diluida, se repite el mismo paso para el segundo y tercer efecto:

$$P_{[9]}=P_{[10]}=P_{[6]}=P_{[1]} \text{ y } P_{[8]}=P_{[7]}=P_{[4]}=P_{[5]}=P_{[2]}=P_{[3]}$$

$$m_{[1]}=m_{[2]}=m_{[3]}, m_{[6]}=m_{[5]}=m_{[4]}, m_{[10]}=m_{[8]}$$

Para obtener las entalpías en los puntos 1, 3, 4, 11, 13, 14, 21, 23, 24 con sus respectivas temperaturas y concentraciones se usa la siguiente ecuación:

$$\begin{aligned} h_{[1]} = & (a_0 * X_{[1]}^0) + (a_1 * X_{[1]}^1) + (a_2 * X_{[1]}^2) + (a_3 * X_{[1]}^3) \quad (10) \\ & + (a_4 * X_{[1]}^4) \\ & + ((T_{[1]}) \\ & * ((b_0 * X_{[1]}^0) + (b_1 * X_{[1]}^1) + (b_2 * X_{[1]}^2) \\ & + (b_3 * X_{[1]}^3) + (b_4 * X_{[1]}^4))) + ((T_{[1]}^2) \\ & * ((c_0 * X_{[1]}^0) + (c_1 * X_{[1]}^1) + (c_2 * X_{[1]}^2) \\ & + (c_3 * X_{[1]}^3) + (c_4 * X_{[1]}^4))) \end{aligned}$$

Para los puntos 2, 12 y 22 es importante tomar aproximaciones del volumen específico de la solución diluida y después hacer un balance de energía:

$$vel = \left(\frac{1}{(1380 + 17.6 * (X_{[1]} - 40))} \right) \quad (11)$$

Las entalpías 7, 17 y 27 se obtienen con la presión de condensación y temperaturas de generación. En el puntos 5 se realiza un balance de energía para poder obtener $h_{[5]}$:

$$m_{[3]} * (h_{[3]} - h_{[2]}) = m_{[4]} * (h_{[4]} - h_{[5]}) \quad (12)$$

Con el valor de la efectividad (Eff) de los economizadores, se obtiene la temperatura $T_{[15]}$ para obtener la $h_{[15]}$ con la ecuación de la solución.

$$Eff = \left(\frac{T_{[14]} - T_{[15]}}{T_{[14]} - T_{[12]}} \right) \quad (13)$$

Y se realiza el mismo procedimiento para el punto 25:

$$Eff = \left(\frac{T_{[24]} - T_{[25]}}{T_{[24]} - T_{[22]}} \right) \tag{14}$$

5 Resultados

Como se muestra en la figura 2, por cada kW térmico de vapor geotérmico se obtendrá 1.6 KW frigorífico; dicho de otra forma, por cada tonelada de refrigeración (3.51 KW) se necesitarán de 2.132 KW térmicos. De igual forma se puede notar como las presiones incrementan en cada una de las condensaciones; los calores de condensación son diferentes y el calor rechazado solo aplica para el condensador 1, puesto que en los puntos 2 y 3 la transferencia de calor es interna. Puede apreciarse que $X_{10}=0$ debido a que el refrigerante en el punto 10 es libre de bromuro de litio.

Así mismo, se muestra que el coeficiente de operación (COP) del sistema de absorción es de 1.646 (relación entre la producción de frío Q_e entre la entrada de calor Q_{gen}) y el coeficiente de desempeño máximo (COP_{max}) es de 3.557, por lo tanto, la eficiencia total del sistema de absorción ($\eta_{sistema}$) es de 46.2%.

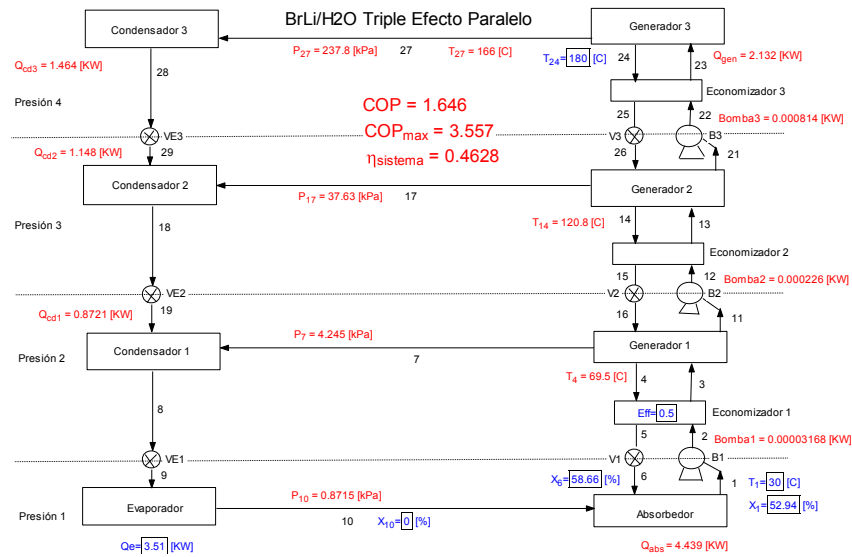


Figura 2. Simulación de un Sistema de Refrigeración por Absorción Triple Efecto. Fuente: Elaboración propia.

10

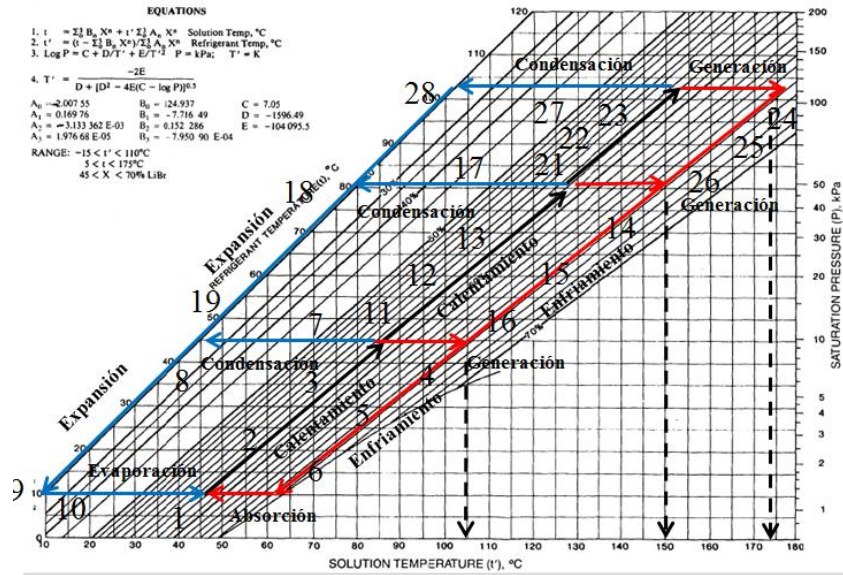


Figura 3. Sistema de Refrigeración por Absorción Triple Efecto sobre el diagrama P-T-X. Fuente: Elaboración propia.

Como se muestra en la figura 3, si el sistema simulado se sobrepone en un diagrama Presión- Temperatura- Concentración, se puede notar a que mayor número de efectos, la temperatura a la cual se necesita generar el refrigerante será mayor. Por lo tanto, se prefieren menores temperaturas con rendimientos menores, para aprovechar el calor de vapor o líquidos que puedan estar disponibles para su uso.

Las ecuaciones de la figura 3 hacen referencia a las ecuaciones que se utilizaron dentro del sistema de refrigeración por absorción, en cada uno de los puntos especificados en la figura 2 como pudo observarse; sin embargo, también puede utilizarse de forma visual el diagrama P-T-X.

6 Conclusiones

1. Los sistemas de absorción pueden ser acoplados fácilmente a recursos de energía geotérmica, lo cual podría tomarse en cuenta para los nuevos proyectos que se desarrollarán en aplicación a centrales eléctricas. Además, de acuerdo al AZEL (2017), en Veracruz están detectadas 5 zonas potenciales (entre ellas zonas turísticas como balnearios), lo cual podría contribuir a la climatización

de hoteles y casas de descanso. Con ello, se incentivaría la economía regional al reducir la carga de electricidad de los sistemas de refrigeración mecánica y también, al provenir de un recurso renovable, ayudaría a coadyuvar las metas de un futuro descarbonizado.

2. Si el vapor que sale de la turbina o el agua que sale del separador es mayor a 65°C y menor a 100°C, será suficiente para operar un sistema de refrigeración por absorción simple efecto y no se afectaría el uso de vapor que se estaría utilizando al máximo dentro de la turbina de vapor, por lo tanto, el recurso geotérmico (agua o vapor) se estaría suministrando al generador 1 del sistema de refrigeración por absorción.
3. Dentro del agua geotérmica existen minerales que se tienen que atender para que los sistemas de refrigeración puedan funcionar de forma eficiente, esto para evitar ineficiencias que, por falta de transferencia de calor en los generadores de los sistemas de absorción, se pudieran presentar.
4. Por cada MWe (Mega Watt eléctrico) generado en una central geotermoeléctrica, se extrae solo el 0.94% de vapor para generar 1 tonelada de refrigeración a través de la tecnología de absorción, es decir, se necesita menos del 1% del vapor total por cada MWe.
5. De acuerdo con el PRODESEN 2023-2037 existe una capacidad instalada de 976 MW. Con esta investigación, se puede concluir que se pueden instalar cerca de 1000 toneladas de refrigeración, con solo extraer el 1% de todo el fluido de trabajo, siempre que se cumpla con las temperaturas de operación.
6. Para potenciales de vapor a 100°C, se recomiendan utilizar los sistemas de simple efecto o una etapa.
7. La producción de frío de esta tecnología tiene diversas aplicaciones, y mientras más calor residual se pueda aprovechar para evitar el uso de combustibles convencionales, las tecnologías renovables podrán cubrir cada vez más los requerimientos energéticos que demanda la humanidad de forma sostenible.
8. El término alledaño, significa aprovechar el calor residual que tenga mínimo 65°C de temperatura y que se pueda aprovechar con alguna aplicación; el objetivo de este trabajo es seguir sumando en la eficiencia total de las centrales eléctricas y de los sistemas energéticos en general.

7 Referencias

1. IRENA: Estadística de Capacidad Renovable, Agencia Internacional de Energía Renovable, pp 38 (2021).

12

2. PRODESEN: Capacidad Instalada de Tecnología Geotérmica, Programa de Desarrollo del Sistema Eléctrico Nacional, pp. 146. (2023-2037).
3. AZEL: Potencial de Energía Geotérmica. Atlas Nacional con Alto Potencial de Energías Limpias. (2017).
4. AGM. Revista Mexicana de Geotermia ISSN 0186 5897, pp 28. 2017. Asociación Geotérmica Mexicana (2017).
5. IJR, <https://www.sciencedirect.com/science/article/abs/pii/B9780128035818117114>, ELSEVIER, Revista Internacional de Refrigeración Magnetic Refrigerations Materials: Challenges and Futures Perspectives. Vol5, 2022, pp 451-468.
6. EIA: Apace Cooling, <https://www.iea.org/energy-system/buildings/space-cooling>. 2023.
7. J. A. Hernández Magallanes, LA Domínguez Inzunza, Shadai Lugo Lo., KC Sanal, A Cerdán P., S To tutiAvila, L. I. Morales.: Energy and Exergy Analysis of a Modified Absorption Heat Pump (MAHP) to Produce Electrical Energy and Revaluated Heat. Processes 2022.
8. IER: Refrigeración Solar. Instituto de Energías Renovables de la UNAM. 2023. <https://www.iea.org/energy-system/buildings/space-cooling>.
9. Itzaes Tecnologías Energéticas: <https://www.itzaes.com.mx/nosotros>, 2023.
10. H. D. Díez León: Sociedad Geológica Mexicana Charla Técnica: Generalidades sobre la Energía Geotermia, Asociación Geotérmica Mexicana. Febrero 2021.
11. IRENA: Global Geothermal Market and Technology Assessment. pp 47, ISBN 978-92—9260-495-0. 2023.
12. De Arellano A APR.: Proyecto de Instalación Geotérmica de Muy Baja Entalpía Destinada a Refrigeración de Vivienda Unifamiliar [Internet]. Upv.es. 2015 [citado el 22 de septiembre de 2023]. Disponible en: <https://riunet.upv.es/bitstream/handle/10251/55466/Memoria.pdf?sequence=1&isAllowed=y>
13. Ambríz Díaz VM, Rubio Maya C, Pacheco Ibarra JJ, Pastor Martínez E. Análisis exergético convencional aplicado a una planta de poligeneración operando en cascada geotérmica. Ing Investig Tecnol [Internet]. 2019 [citado el 22 de septiembre de 2023];20(3):1–10. Disponible en: https://www.scielo.org.mx/scielo.php?script=sci_arttext&pid=S1405-77432019000300011
14. Iglesias ER, Flores Armenta M, Luis J, León Q, Torres Rodríguez MA, Torres Y Neftalí RJ, et al. REVISTA MEXICANA DE GEOENERGÍA REVISTA MEXICANA DE GEOENERGÍA ISSN 0186-5897 ISSN 0186-5897 [Internet]. Org.mx. 2008 [citado el 22 de septiembre de 2023]. Disponible en: <https://www.geotermia.org.mx/app/assets/media/2017/11/Geotermia-Vol21-1.pdf#page=61>
15. Francisco Hernandez A. Estudio del efecto de una torre de viento con humidificación y de un sistema de aprovechamiento de fluido geotérmico de baja entalpía sobre el confort térmico de una casa habitación. Tecnológico Nacional de México; 2021.
16. Rivas-Cruz F, Hernández-Martínez EG, Papadimitriou-Suarez del Real LE. Heating and Cooling with Heat Pumps – Projects developed in Mexico. Renew energ biomass sustain [Internet]. 2022 [citado el 22 de septiembre de 2023];3(2):94–108. Disponible en: <https://al-deser.org/ojs/index.php/REBS/article/view/59>
17. Transición Energética: Eficiencia Energética Bombas de Calor Geotérmica, Vol 2, pp 50, Nov 2019-Ene 2020.
18. Cervantes C. A.U. Tesis: Propuesta de incremento a la eficiencia operativa de una central eléctrica Brayton Rankine a través de un Sistema de absorción BrLi/H₂O. 2017. Universidad Veracruzana. Xalapa, Veracruz, México.
19. Best R., Pilatowsky I., Valiente A., Lage C., Quinto P., Gutierrez F., Hernández J., Hieras J., Martínez E. (1993). *Métodos de Producción de frío*. Universidad Autónoma Nacional de México. ISBN 968-36-2954-7.

20. Herold K. E., Radermacher R., Klein S. A. (1996) *Absorption Chillers and Heat Pumps*. CRC Press.
21. Kaita Y. (2011). Thermodynamics properties of lithium bromide-water solutions at high temperatures. *International Journal of Refrigeration* 24 (2001) 374-390.
22. Pita, e. (2005). *Principios y sistemas de refrigeración*. Limusa.
23. Kaita Y. (2002). *Simulation results of triple effect absorption cycles*. *International Journal of Refrigeration* 25(7):999-1007.
24. Venegas M. V., Izquierdo M., De Vega M., Lecuona A. (2002). *Thermodynamic study of multistage absorption cycles using low temperatura heat*. *International Journal Energies* 26(8):775-791.
25. Zhang L., Wang Y., Fu Y., Xing L., Jin L. (2015). *Numerical Simulation of H₂O/LiBr Falling Film Absorption Process*. *Energy Procedia* 75(2015) 3119-3126. The 7th International Conference on Applied Energy-ICAE2015. ELSEVIER.

Anexos:

Tabla 1. Datos de entalpía, concentración, temperatura, presión y flujo másico, en los puntos señalados de la figura 1. Los datos de vapor son supuestos de acuerdo con la profundidad del reservorio geotérmico. Para evitar ecuaciones específicas, todo el vapor geotérmico se considera puramente vapor de agua. El flujo másico de vapor geotérmico mostrado es el flujo por cada MWe de energía eléctrica generado.

Puntos	Temperatura (°C)	Concentración (X) %	Presión (kPa)	Entalpía (kJ/kg)	Flujo másico (kg/s)
1	30	52.94	0.8715	66.38	0.0151
2	30	52.94	4.245	66.38	0.0151
3	46.5	52.94	4.245	101.4	0.0151
4	69.5	58.66	4.245	166.9	0.01363
5	49.81	58.66	4.245	128.1	0.01363
6	40.67	58.66	0.8715	128.1	0.01363
7	58.1	0	4.245	2608	0.0004053
8	29.07	0	4.245	125.7	0.001472
9	4.192	0	0.8715	125.7	0.001472
10	4.192	0	0.8715	2510	0.001472
11	58.1	52.94	4.245	126	0.01088
12	58.1	52.94	37.63	126	0.01088
13	84.3	52.94	37.63	181.7	0.01088
14	120.8	58.66	37.63	268	0.009815
15	89.45	58.66	37.63	206.2	0.009815
16	69.5	58.66	4.245	206.2	0.009815
17	108.2	0	37.63	2700	0.0004222
18	73.35	0	37.63	311.4	0.001067
19	29.07	0	4.245	311.4	0.001067

14

21	108.2	52.94	37.63	232.8	0.006538
22	108.2	52.94	237.8	232.9	0.006538
23	138.1	52.94	237.8	296.8	0.006538
24	180	58.66	237.8	384.9	0.005893
25	144.1	58.66	237.8	314	0.005893
26	120.8	58.66	37.63	314	0.005893
27	166	0	237.8	2799	0.0006448
28	124.4	0	237.8	528.4	0.0006448
29	73.35	0	37.73	528.4	0.0006448
30	185	0	1122	2782	4.44
31	180	0	1002	2778	2.22
32	180	0	1002	2778	2.1991
33	46	0	10	2344	2.1991
34	90	0	101.3	376	2.22
35	60	0	101.3	251	2.1995
Entrada Generador 3	180	0	1002	2778	0.0209
36	100	0	101.3	2676	0.0209

Grippers Developed for Intelligent Manufacture Based on a Bioinspired Microgripper

M. Tecpoyotl-Torres¹[0000-0002-4336-3771] P. Vargas-Chable*,^{1,2}[0000-0002-2290-3740] A.J. Estrada-Cabrera³[0009-0004-8135-0658] R. Cabello-Ruiz²[0000-0003-3215-5034] and V. Grimalsky¹[0000-0001-8313-6621]

¹ Centro de Investigación en Ingeniería y Ciencias Aplicadas, IICBA-CIICAp, Universidad Autónoma del Estado de Morelos, UAEM, Cuernavaca, Morelos, 62209, Mexico.

² Facultad de Ciencias Químicas e Ingeniería, FCQeI, Universidad Autónoma del Estado de Morelos, UAEM, Cuernavaca, Morelos, 62209, Mexico.

pedro.vargas@uaem.mx

³ Maestría en Ingeniería y Ciencias Aplicadas, Universidad Autónoma del Estado de Morelos, UAEM, Cuernavaca, Morelos, 62209, Mexico.

Abstract. This paper provides the design of aluminum grippers based on the geometry of a microgripper created in silicon. The values of the parameters used in the first scaled gripper were obtained experimentally, which allows to adjust the conditions considered in the numerical analysis, making the modeling more accurate. The numerical analysis allows to know the grippers performance, in such a way that scaling, modifications, and even integrations can be made in complex systems. The use of a gripper with 4 arms integrated into a like-cobot structure is also validated, which allows to propose its use in intelligent manufacturing, when considering the manipulation of tiny objects, on a micro and millimeter scale. The thermal performance of the grippers allows the use of waste thermal energy for their operation, making it useful for the energy purposes of Smart Cities.

Keywords: Cobot, Ansys, Gripper, Thermal actuation, Chevron.

1 Introduction

Microelectromechanical systems (MEMS) have acquired significant importance in some sectors such as industrial, medical, telecommunications, military, and intelligent systems. Among the microdevices developed are accelerometers, which are used as sensors in air bags for the automotive sector [1,2]; microgrippers for microwires manipulation, useful for example in materials research; microfibers and microdevices used in microelectronics and photonics development, research, and innovation [3,4]. Microgrippers have been developed for the acquisition of biological samples in the biomedical sector [5-7], gyroscopes that allow rotation on the screens of mobile devices, find applications in GPS and mobile systems, that means, they are widely used in navigation and communication systems [8,9]. Acoustic or pressure diaphragms are applied

2

in sound auxiliary devices or to monitor variables such as temperature, pressure, and hydration levels, among other medical applications [10,11]. Other devices developed include electromagnetic micromirrors used in mini-projector technology, photonic therapies, optogenetics or optical diffraction tomography [12-14], among other important applications.

Most technological developments are led by private companies that generate their own technologies and have the latest generation manufacturing capacity [15]. Among the factors that limit the acceleration of the manufacture and implementation processes in public or governmental clean rooms or laboratories are the availability of specialized equipment, consumables and/or reagents, trained or updated personnel in the implementation of the latest technologies, as well as the commitments and projects developed in parallel, which also limit the micromanufacturing times.

One of the agile techniques developed to validate the functionality of the microdevices designs, consists in applying scaling that led to prototypes of reasonable sizes to be manufactured in a Computer Numerical Control (CNC) machine, with suitable material, such as aluminum [16]. This method of scaling, fabrication and testing allows a quick implementation to evaluate any error or deviation, which is required to know, permitting corrections and / or adjustments in short times. This methodology awakens the interest to design, simulate, manufacture, and implement locally, using accessible equipment and materials, favoring the development of inventive capacity. The application of this method allows the development of designs and simulations with freely available software, such as AutoCAD and Ansys™ student versions, which are very appropriate when the research is carried out in environments with limited resources.

This research focuses on an application for smart cities, which in recent years has gained relevance and impact on the quality of life of human beings, where it is of utmost importance to improve energy efficiency, reduce CO₂ emissions and increase the welfare of citizens [17]. This concept of city interconnects different areas such as management, economy, mobility, environment, energy, supply, health, security, among others, allowing it to be more efficient and provide better and new services.

The challenges and opportunities that have been identified from the state-of-the-art give relevance to the development of a manipulator device that could take advantage of the thermal energy generated by electrical machines, by some control equipment, induction heating systems, as well as by bodies that generate enough thermal energy that can be harvested. In the MEMS area, it is already well-known that thermal actuators can harness resources from the environment or the surrounding energy to carry out their operation without the need for another energy source. This residual thermal energy can be used or reused, being obtained from some object, machine, equipment, or biological agents. Thermal devices can be widely used in smart homes, specifically in alarm systems, thermal switches, etc. In the automotive sector, the actuators used can be energized from the temperatures generated in vehicle exhaust gases or even from the thermal energy to which their surfaces are exposed.

The performance of the grippers designed and shown in this article can be carried out directly using the temperature or taking advantage of the one generated for example by the Joule effect or the one given off by mechanical movements of some rotating equipment. This fact increases the versatility of applications of the designed grippers.

While in industry, manipulator devices or grippers adapted to complex assembly structures can be powered using waste energy [18,19].

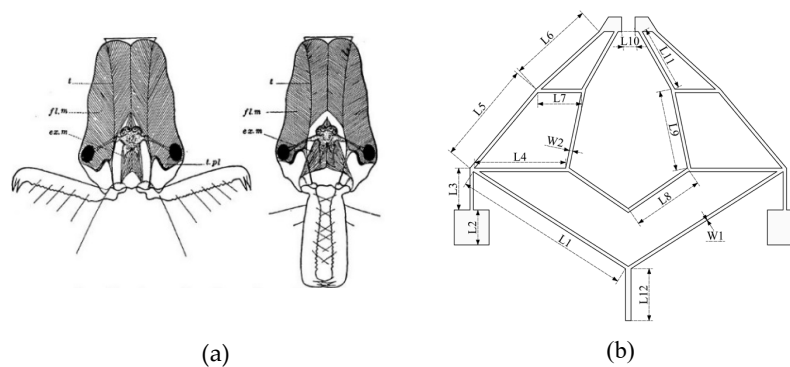
The content of this article is as follows: In section 1, information about MEMS and smart cities is shown. In this section the opportunity to develop new devices is found. Section 2 describes the materials and methods employed, identifying the microgripper Model 1. Section 3 shows the development, implementation, and numerical results for grippers Models 2-4, as well as the adaptation of gripper model 4 to a like-cobot structure. Finally, section 4 summarizes the findings and provides some concluding remarks.

2 Materials and methods

2.1 Design concepts

In this work, the operation of a microgripper bioinspired on ant mandibles (Figure 1a) is described. It was originally designed using silicon and composed by the structure that supports its arms (Figure 1b) and a modified Z actuator (Figure 1c) [20]. This actuator drives the movement of the gripper so that its tips open and close. This microgripper is called Model 1.

Due to the time and resources required to carry out the microfabrication process, to validate the performance of the geometry, the microgripper was scaled by a factor 1:100, as suggested in [16], which allows observing its performance when fed by a potential difference, an electric current intensity, or a thermal source, in this case a thermal source was chosen. The overall dimensions of the scaled clamp (Model 2) are 153 mm x 166.75 mm x 1 mm. The scaled thickness used was near to the calculated value, chosen by the availability of Aluminum 6053 sheets found on the market. The dimensions of the gripper elements are given in Table 1. It should be noted that the difference between Models 1 and 2 are basically the scaling and the shape of the anchors, since in model 2 holes were implemented to allow the physical clamping to be carried out. It must be mentioned that aluminum is a commonly used at macro and even micrometer level, as shown in [21].



4

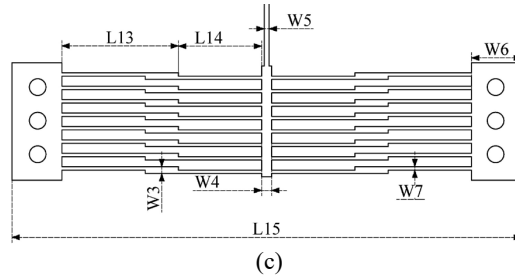


Fig. 1. (a) Head of an *Odontomachus hastatus* Fabricius (Public domain image, [20]). (b) Structure of the microgripper model 1. (c) Representative Z-shaped chevron.

Figure 2 shows the gripper Model 2, which satisfies the design requirements according to the biomimetic design spiral [23]. The device is machined on a CNC machine, with minimum manufacturing constraints of 1 mm, because this is the minimum diameter of the found commercial drills.

Table 1. Dimensions of the elements of the scaled gripper Model 1, in accordance with notation provided in Figure 1.

ID	Value, (mm)	ID	Value, (mm)	ID	Value, (mm)	ID	Value, (mm)
L1	84.74	L6	39.75	L11	30.5	W3	2
L2=W6	15	L7	18.64	L12=L14	20	W4	3
L3	18	L8	35.6	L13	40	W5	0.75
L4	40	L9	34.6	L15	153		
L5	44.4	L10=G	9	W1=W2=W7	1		

To carry out the simulation of the Model 2 gripper, it is necessary to have the properties of aluminum 6053. Its electrical parameters, conductivity, and resistivity were experimentally obtained, while the mechanical parameters were taken from the ANSYSTM software database. They are shown in Table 2. With these parameters, the simulation was carried out in Ansys Workbench, using the tools -> Thermal electric -> Steady-State Thermal and Static Structural, as described below.

Table 2. Electrical properties of aluminum 6053-implemented gripper model 2.

Parameters and units	Aluminum	Source
Resistivity, ρ ($\Omega \cdot \text{m}$), at 24 °C	4.33×10^{-8}	Experimentally obtained
Thermal conductivity, (W/(m ² °C))	163	[12]
Density (kg/m ³)	2710	Ansys TM
Young's Modulus (Pa)	6.83×10^{10}	Ansys TM

2.2 Simulation and results of gripper model 2

Simulation and experimental tests were performed using the same boundary conditions (Figure 2). The anchors (Ts) of the modified chevron Z actuator, and of the gripper arms (H1 and H2), were fixed. The lower face, the shaft of the actuator (H3) was assigned the value of the ambient temperature (24 °C). A thermal source was attached to Ts to operate the device. G represents the opening between the tips of the gripper model 2.

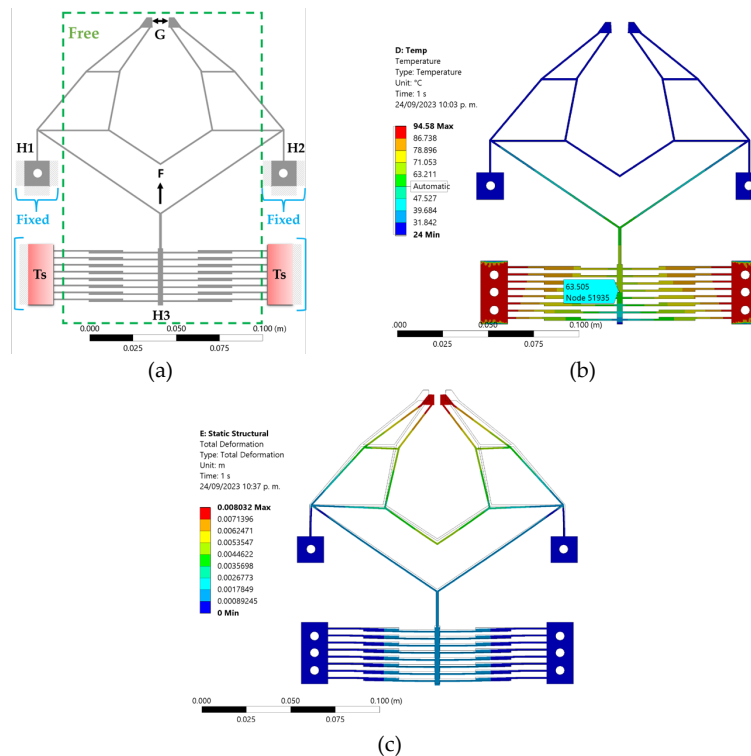


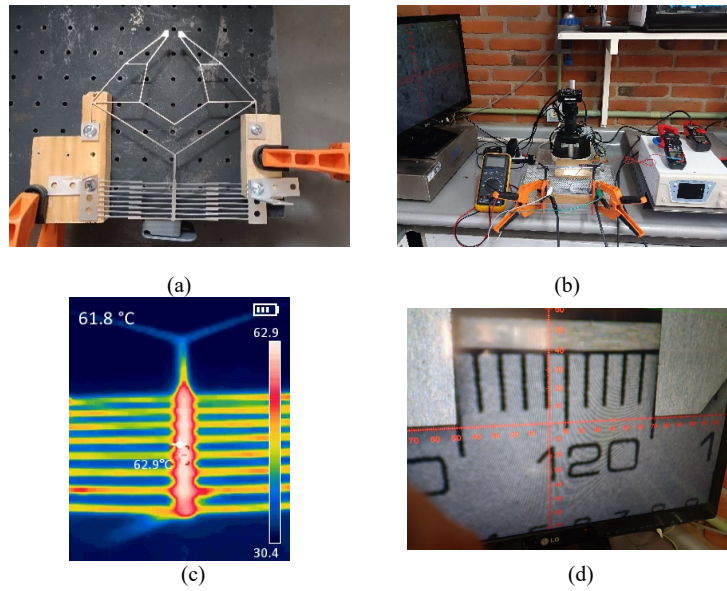
Fig. 2. (a) Model 2 Gripper. (b) Temperature distribution. (c) Tips displacement.

With the described boundary conditions, the simulation and experimental tests were carried out. Considering a thermal inter-anchor supply Ts of 94 °C. According to the simulation results, the actuator shaft temperature is 63.505 °C, while, in the experimental test (see Figure 3c), 62.9 °C was obtained, so, there is an error margin of 0.961%. It should be noted that, the boundary conditions in the simulation, mainly the ambient temperature conditions were assigned in the upper and lower faces of Ts and in all the lateral faces of H1 and H2. On these faces, the fixed support boundary condition was added to hold the gripper arms and facilitate the action of the M-shaped amplifier and leave sections G, H3 and the elements that join them free, see Figure 2a,

6

which allowed a better approximation to the experimental results, so these conditions will be taken to develop future investigations by Finite Element Analysis (FEA) simulation in Ansys™ Workbench. That is, feedback was carried out that allows adjusting to the simulation conditions, according to the experimental measurements.

The arrangement and experimental results are shown in Figure 3. The initial opening between the jaws' gripper Model 2 is 9 mm, with no load effect. When all anchors are clamped to the isolation base, due to the stresses induced by the bolting an opening of 10 mm is generated. When feeding the actuator, a final opening of 4 mm was obtained between the clamps, so a maximum displacement of approximately 6 mm was obtained, as can be seen in Figure 3. While in the simulation a displacement between the jaws of 7.98 mm was obtained, see Figure 2c, with a margin of error between both approximations of 24.81%, which is acceptable, since experimentally not all conditions are controlled, as is the case of some environmental conditions such as relative humidity and variations in temperature caused by external agents, which also influence convection variations.



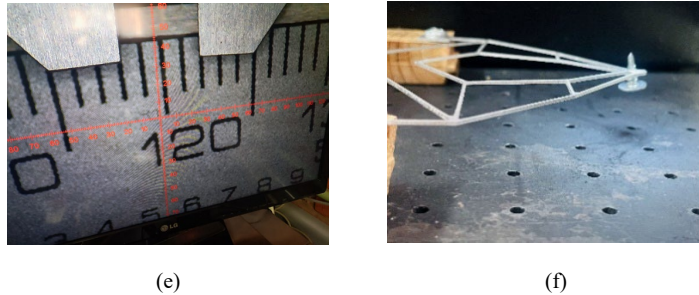
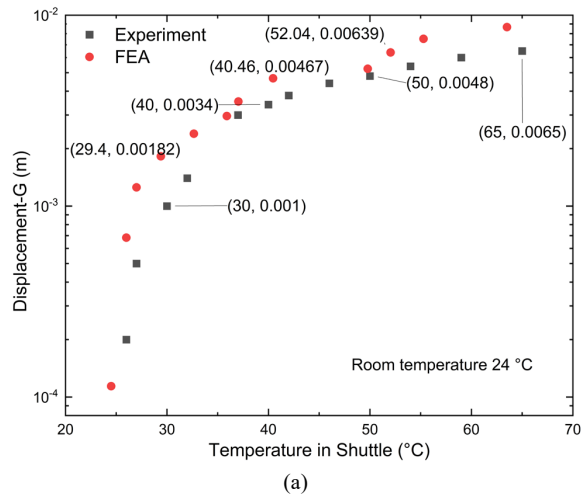


Fig. 3. (a) Gripper Model 2 prepared for experimental testing. (b) Experimental setup. (c) Temperature distribution on the actuator shaft. (d) Initial gripper opening ~ 10 mm. (e) final gripper opening ~ 4 mm. (f) Gripper Model 2 clamping a screw.

Figures 4a and 4b show a comparison between the experimental and numerical results, with feedback, in which the displacement between the tips of the gripper is observed, according to the temperature at the shaft and at the anchors of the chevron actuator, respectively. As can be seen, very similar trends are presented in both approaches, especially in relation to the temperature at the shaft of the modified Z-shaped chevron actuator. It is worth mentioning that the variation with respect to the ambient temperature during the test days ranged between 24 °C and 26 °C.



8

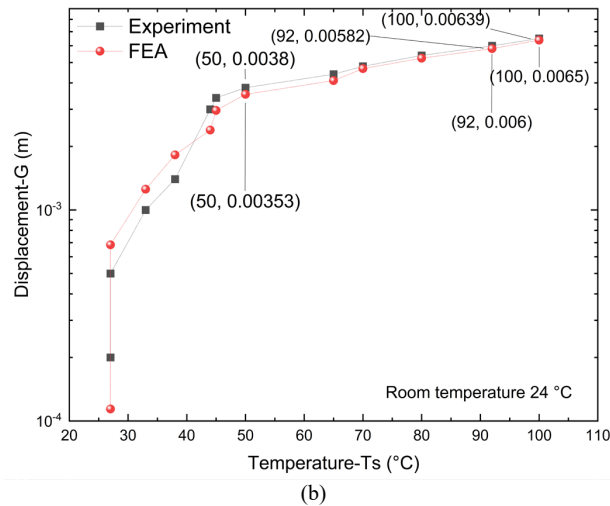


Fig. 4. (a) Temperatures generated at the shaft of the modified Z-shaped chevron actuator and (b) a temperature sweep applied at the anchors of the modified Z-shaped chevron actuator from 25 °C to 100 °C.

The data obtained numerically by applying the thermal source, with the sweep from 25 °C to 100 °C are shown in Table 3. This Table shows a comparison of the jaws' displacements (Model 2) in the X and Z axis. Considering that the gripper was designed for jaws' displacements on the X axis, this comparison allows to verify if there are unwanted movements on the Z axis which may affect the manipulation of the device in a complex configuration of four jaws. There is a motion in U_z in the order of 10^3 times smaller than the main displacement in the U_x jaws, implying that the residual out-of-plane motion is not relevant, with respect to the main displacement direction of the jaws' gripper.

The low residual motion of the jaws' gripper, together with the relatively low temperature between their tips, allows their use in specific applications, such as smart manufacturing, where robotic arms and cobots are used when it is necessary to manipulate millimeter or micrometer elements. The integration of a gripper such as the one shown in a production equipment offers the possibility to take advantage of the heat generated by machines or equipment due to the Joule effect or the presence of electrical or mechanical stimuli, using the thermal energy emitted as a source of waste heat for the gripper operation. This application will be developed in the following section.

Table 3. Results of the temperature sweep applied to the anchors of the actuator of gripper Model 2.

Thermal source, (°C)	Average Temperature, (°C)	Displacement of jaws' gripper, U_x , (mm)	Displacement of jaws' gripper, U_z , (μ m)	Total force of jaws' gripper, (N)
25	24.51	0.11	0.06	0.37
30	27.06	0.68	0.39	2.20
35	29.61	1.25	0.71	4.04
40	32.16	1.82	1.03	5.87
45	34.71	2.39	1.35	7.71
50	37.26	2.96	1.67	9.54
55	39.81	3.53	1.99	11.38
60	42.36	4.10	2.32	13.21
65	44.91	4.67	2.64	15.05
70	47.46	5.25	2.96	16.88
75	50.01	5.82	3.28	18.72
80	52.56	6.39	3.60	20.56
85	55.11	6.96	3.92	22.39
90	57.66	7.53	4.25	24.23
95	60.21	8.10	4.57	26.06
100	62.76	8.67	4.89	27.90

3 Development and implementation of grippers for smart manufacturing applications

3.1 Development and results of gripper Model 3

To facilitate the handling of the Model 2 gripper, a reduction using a scale factor of 1: 0.5 will be applied. The overall size of Model 3 is then 76.5 x 83.375 x 0.5 mm. The idea is to adapt this gripper to a structure or equipment in such a way that it can be coupled to the heat generating source to operate the gripper. For this reason, the modified Z-shaped chevron actuator anchors are extended, as shown in Figure 5a, so that it can be connected to where the heat source is located, these extended elements would be analogous to interconnecting tapes with holes.

10

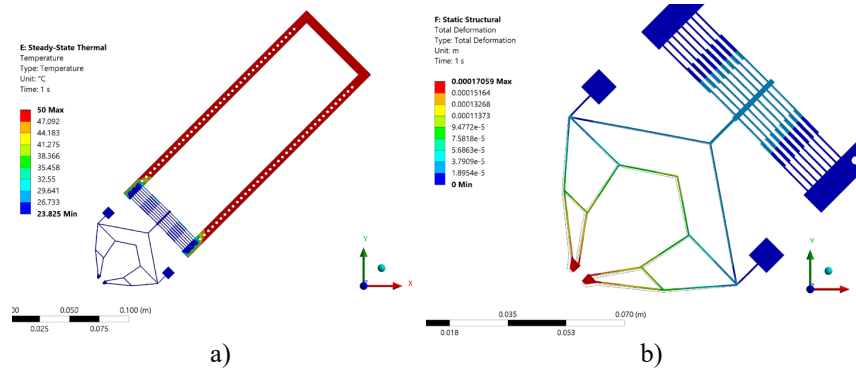


Fig. 5. (a) Temperature distribution over the entire gripper with metal strip coupled to the actuator anchors. (b) Displacement of gripper Model 3.

Figure 5 shows the gripper Model 3. For visualizing the temperature distribution and the displacement of the gripper, images were taken where a temperature of 50 °C was assigned to the anchors. This test allowed observing the displacement generated at the tips of jaws of 170.5 μm and the total force on the tips of 302.41 mN. The results when applying a temperature sweep are shown in Table 4.

Table 4. Results of the temperature sweep applied to anchors of the actuator of gripper Model 3.

Thermal source (°C)	Average Temperature (°C)	Displacement of jaws' gripper, U _x (μm)	Displacement of jaws' gripper, U _z (μm)	Total force of jaws' gripper (mN)
25	24.3	6.6	0.09	11.63
30	25.9	39.4	0.55	69.79
35	27.6	72.2	1.00	127.94
40	29.2	105.0	1.45	186.10
45	30.8	137.8	1.91	244.26
50	32.4	170.6	2.36	302.41
55	34.0	203.4	2.82	360.57
60	35.7	236.2	3.27	418.72
65	37.3	269.0	3.73	476.88
70	38.9	301.8	4.18	535.04
75	40.5	334.6	4.64	593.19
80	42.1	367.4	5.09	651.35
85	43.8	400.2	5.55	709.51
90	45.4	433.0	6.00	767.66
95	47.0	465.8	6.46	825.82
100	48.6	498.6	6.91	883.97

Preliminary results allow to continue implementing new ideas, and one of these is to make a transverse arrangement of the gripper, with the purpose of having more gripping

arms and, therefore an increment of degrees of freedom for increment the manipulation level of some sample, as can be observed in section 3.2.

3.2 Development and results of gripper Model 4

In this section, two more clamping arms are generated to the design of clamp 3, with the intention of generating four orthogonally coupled tips. An orthogonal chevron actuator with extended anchors is also added as shown in Figure 6.

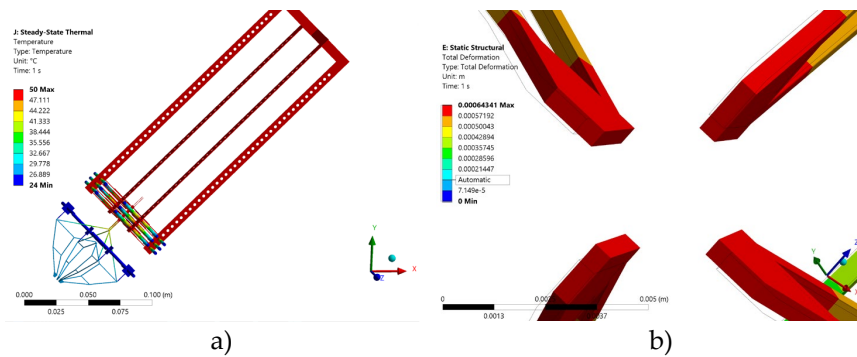


Fig. 6. (a) Temperature distribution applying a 50 °C power supply and (b) displacement at the tips of the gripper Model 4.

This orthogonally assembly of the two grippers will make it possible that when manipulating an object, the stability, precision, and control will make it possible to reduce gripping errors. The images in Figure 6 were obtained by applying a thermal source of 50 °C directly to the 4 anchors considering an ambient temperature of 24 °C.

Table 5 shows the results of the average temperature, U_x and U_z displacements, as well as the force generated at the tips of the gripper Model 4 gripper.

Table 5. Results of the temperature sweep applied to the anchors of gripper Model 4.

Thermal source (°C)	Average Temperature (°C)	Total displacement of jaws' gripper (mm)	Total force of jaws' gripper (N)	Stress, (MPa)
25	38.5	0.64	2.14	115.5
30	27.3	0.15	0.49	26.6
35	30.1	0.27	0.91	48.8
40	32.9	0.40	1.32	71.1
45	35.7	0.52	1.73	93.3
50	38.5	0.64	2.14	115.5
55	41.2	0.77	2.56	137.7
60	44.0	0.89	2.97	159.9
65	46.8	1.01	3.38	182.1
70	49.6	1.14	3.79	204.3
75	52.4	1.26	4.21	226.5

80	55.2	1.39	4.62	248.7
85	57.9	1.51	5.03	270.9
90	60.7	1.63	5.44	293.1
95	63.5	1.76	5.86	315.3
100	66.3	1.88	6.27	337.5

It can be observed that there is movement in the tips as the feed is varied with considerable displacements that can be used to manipulate a sample or gripping target. Therefore, this provides an opportunity to apply the knowledge generated, to a cobot-like structure to observe if the drilled strips added to the actuator anchors manage to move the gripper from a given distance according to its size.

3.3 Development and results of gripper Cobot Adaptation

A structure is implemented where the extension strips of the gripper actuator anchors are coupled (Figure 7), to verify according to the size of the system if the movement at the tips of the gripper of Cobot Adaptation is possible.

The structure was made using a high impact resistant plastic material with density 1045 kg/m³, Young Module 1.896e9 Pa, thermal conductivity 0.1572 W/m°C, and specific heat 1399 J/kg°C. The material where the heat is propagated is again aluminum 6053.

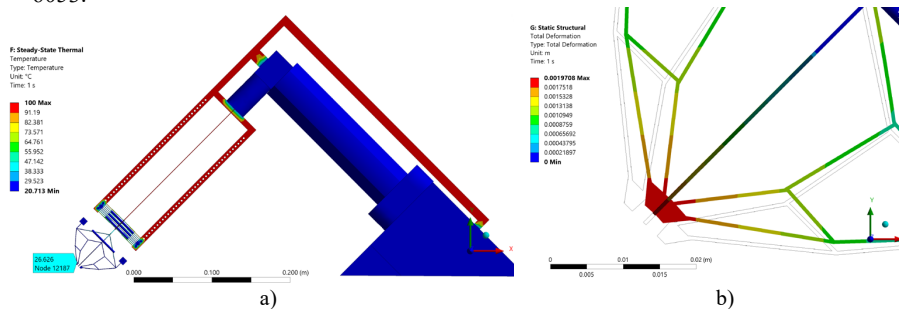


Fig. 7. (a) Temperature distribution, applying a thermal power supply 100 °C and (b) Gripper displacement.

The implementation is an approximation, considering that other arrangements and adjustments to the system can be developed to take advantage of residual temperatures either internal or external. However, this implementation gives an optimistic view, since it is possible to obtain movement in the tips of the gripper of Cobot Adaptation, when a thermal source with values from 25 °C to 100 °C is applied, as shown in Table 6. The tips of the gripper Cobot Adaptation tend to move, since considering an ambient temperature of 24 °C. It can be observed that this displacement could be controlled since, by varying the temperature, the displacement and the force of the gripper maintain increasing trend.

Table 6. Results of the temperature sweep assigned to the actuator anchors of the gripper Cobot adapted.

Thermal source (°C)	Average Temperature (°C)	Total displacement of jaws' gripper (mm)	Total force of jaws' gripper (N)	Stress (MPa)
25	24.5	0.024	0.076	3.5
30	27.0	0.142	0.455	21.2
35	29.6	0.260	0.834	39.0
40	32.1	0.378	1.212	56.7
45	34.6	0.496	1.591	74.4
50	37.2	0.614	1.970	92.1
55	24.5	0.732	2.349	109.8
60	42.2	0.850	2.728	127.5
65	44.8	0.968	3.107	145.2
70	47.3	1.086	3.486	162.9
75	49.8	1.204	3.865	180.6
80	52.4	1.322	4.244	198.3
85	54.9	1.440	4.622	216.0
90	57.4	1.558	5.001	233.7
95	60.0	1.676	5.380	251.4
100	62.5	1.794	5.759	269.1

Simulation was performed with the boundary conditions obtained experimentally for the gripper Model 2, however, to achieve the convergence of the solution of the numerical method and the meshing of the devices, some technical details were considered, as shown in Table 7. It should be noted that the software used was AnsysTM R1 Student Version.

Table 7. Technical details about FEA in Ansys Workbench.

Device	Solver target	Element type	Physic Preferences/ tools	Transition Ratio	Convergence	
					No. of total nodes	No. of total elements
Gripper Model 2			Nonlinear Mechanical/ Steady-State Thermal->Static Structural		15302	5532
Gripper Model 3	Mechanical APDL	SOLID 187	Mechanical/ State Thermal->Static Structural	0.272	32745	9638
Gripper Model 4			Nonlinear Mechanical/ Steady-State Thermal->Static Structural			
Cobot Adaptation			Nonlinear Mechanical/ Steady-State Thermal->Static Structural		85131	32704

The obtained results show that the grippers developed can be used for handling particles of certain dimensions or diameters that can be used in public and private laboratories, in the biomedical or even biological sector, according to the characteristics shown in Table 8. This makes it possible to assume that the applications of the grippers can be very varied. An additional advantage is their thermal actuation mode since it opens the possibility of using waste thermal energy to carry out their operation.

Table 8. Some microparticles dimensions.

Ref	Particle type	Diameter (μm)
[24]	Polystyrene spheres	45 - 90
[25]	Microparticles	50 and 500
[26]	Polystyrene beads	43.0 ± 5.0 and 84.6 ± 4.0

On the other side, another feasible way to feed the grippers shown could be by injecting hot air through pneumatic auxiliary devices and thus have greater control over the opening of the tips of the gripper, from the amount of hot fluid that is injected into the system.

4 Conclusions

Starting from the initial model of a silicon microgripper (Model 1), different scaling was carried out to validate its geometry functionality, using aluminum 6053 for its implementation. Subsequently, several adjustments were made to achieve greater control of the structure, as well as opening the possibility of its integration to a cobot.

For the gripper Model 2, obtained scaling the microgripper model 1 using a scale factor of 1:100 on its surface, tests were conducted and an error percentage of 24.81% is observed with respect to the displacement obtained analytically and experimentally. It is highlighted that in the tests there was not a total control of some physical variables such as temperature and relative humidity.

By reducing the dimensions of the gripper Model 2, using a scale factor 1:0.5 over all the structure, the new dimensions 76.5 mm x 83.375 mm x 0.5 mm (Model 3 gripper) allow to improve its handling. It has been demonstrated that at 25 °C, the tips of this gripper begin to move and as the temperature increases the displacements and force simultaneously.

When two grippers Model 3 are orthogonally assembled (gripper Model 4), the possibility to subject objects with greater accuracy is incremented. Due to its characteristics, this model is integrated in a like-cobot type structure, the functionality of all systems was also shown.

The scaling and implementation of the microgripper (Model 1) at the macro level allows to quickly validate the functionality of its geometry, as well as to generate ideas about variations and integrations to conduct its implementation in systems where waste thermal energy can be used, and thus contribute to one of the objectives of Smart Cities, where more efficient and use less energy are privileged. The grippers here shown can

also be utilized as smart sensors that can take advantage of the surrounding thermal energy, which can come from a system, computer, among other sources with which these devices can be activated. In addition to being an option to take advantage of residual thermal energy, it is important to mention that it is still necessary to carry out more tests under controlled conditions, and to generate standard deviation curves and uncertainty factors before to carry out its physical implementation.

Acknowledgements. Pedro Vargas-Chable is grateful to CONAHCYT for his post-doctoral stay (CVU 484392). M. Tecpoyotl-Torres for SNI support (CVU 20650). Alan J. Estrada Cabrera for a master's degree scholarship (CVU 1152724).

This research was funded by Consejo Nacional de Ciencia y Tecnología, CONACyT, grant reference number A1-S-33433. “Proyecto Apoyado por el Fondo Sectorial de Investigación para la Educación”.

References

1. Qingmin, W., Yaoen, Y., Mubiao, S., Yuhong, L.: Research on application of Micro-Nano Acceleration Sensor in monitoring the vibration state of vehicles. *Procedia Engineering*. 29, 1213–1217 (2012).
2. KOZEY, S.L., LYDEN, K., HOWE, C.A., STAUDENMAYER, J.W., FREEDSON, P.S.: Accelerometer output and met values of common physical activities. *Medicine & Science in Sports & Exercise*. 42, 1776–1784 (2010).
3. Nah, S.K., Zhong, Z.W.: A microgripper using piezoelectric actuation for micro-object manipulation. *Sensors and Actuators A: Physical*. 133, 218–224 (2007).
4. Lofroth, M., Avci, E.: Development of a novel modular compliant gripper for manipulation of micro objects. *Micromachines*. 10, 313 (2019).
5. Pura, P., Szymański, M., Jaroszewicz, L.R., Marć, P., Dudek, M., Kujawińska, M., Napierała, M., Nasiłowski, T., Ostrowski, Ł.: Microtips at photonic crystal fibers as functional elements for near-field scanning optical microscopy probes. *SPIE Proceedings*. (2014).
6. Żuchowska (Chruściel), M., Marć, P., Jakubowska, I., Jaroszewicz, L.R.: Technology of polymer microtips' manufacturing on the ends of multi-mode optical fibers. *Materials*. 13, 416 (2020).
7. Dudek, M., Kujawinska, M.: OPTONUMERICAL method for improving functional parameters of polymer microtips. *Optical Engineering*. 57, 1 (2018).
8. Pires, I.M., Garcia, N.M., Zdravevski, E., Lameski, P.: Daily motionless activities: A dataset with accelerometer, magnetometer, Gyroscope, environment, and GPS Data. *Scientific Data*. 9, (2022).
9. Bukhari, S.A., Saleem, M.M., Khan, U.S., Hamza, A., Iqbal, J., Shakoore, R.I.: Microfabrication process-driven design, FEM analysis and system modeling of 3-DOF drive mode and 2-DOF sense mode thermally stable non-resonant MEMS Gyroscope. *Micromachines*. 11, 862 (2020).
10. Lee, S., Kim, J., Yun, I., Bae, G.Y., Kim, D., Park, S., Yi, I.-M., Moon, W., Chung, Y., Cho, K.: An ultrathin conformable vibration-responsive electronic skin for quantitative vocal recognition. *Nature Communications*. 10, (2019).
11. Cho, S., Han, H., Park, H., Lee, S.-U., Kim, J.-H., Jeon, S.W., Wang, M., Avila, R., Xi, Z., Ko, K., Park, M., Lee, J., Choi, M., Lee, J.-S., Min, W.G., Lee, B.-J., Lee, S., Choi, J., Gu,

16

- J., Park, J., Kim, M.S., Ahn, J., Gul, O., Han, C., Lee, G., Kim, S., Kim, K., Kim, J., Kang, C.-M., Koo, J., Kwak, S.S., Kim, S., Choi, D.Y., Jeon, S., Sung, H.J., Park, Y.B., Je, M., Cho, Y.T., Oh, Y.S., Park, I.: Wireless, multimodal sensors for continuous measurement of pressure, temperature, and hydration of patients in wheelchair. *npj Flexible Electronics*. 7, (2023).
12. Sun, W., Tan, Y.: Model guided extremum seeking control of electromagnetic micromirrors. *Scientific Reports*. 11, (2021).
 13. Yang, J., He, Q., Liu, L., Qu, Y., Shao, R., Song, B., Zhao, Y.: Anti-scattering light focusing by fast wavefront shaping based on multi-pixel encoded digital-micromirror device. *Light: Science & Applications*. 10, (2021).
 14. Shin, S., Kim, D., Kim, K., Park, Y.: Super-resolution three-dimensional fluorescence and optical diffraction tomography of live cells using structured illumination generated by a digital micromirror device. *Scientific Reports*. 8, (2018).
 15. Fischer, A.C., Forsberg, F., Lapisa, M., Bleiker, S.J., Stemme, G., Roxhed, N., Niklaus, F.: Integrating MEMS and ICS. *Microsystems & Nanoengineering*. 1, (2015).
 16. Pustan, M., Chiorean, R., Birleanu, C., Dudesco, C., Muller, R., Baracu, A., Voicu, R.: Reliability design of thermally actuated MEMS switches based on V-shape beams. *Microsystem Technologies*. 23, 3863–3871 (2016).
 17. Attaran, H., Kheibari, N., Bahrepour, D.: Toward integrated smart city: A new model for implementation and design challenges. *GeoJournal*. 87, 511–526 (2022).
 18. Zhou, S.K., Rueckert, D., Fichtinger, G.: *Handbook of Medical Image Computing and computer assisted intervention*. Academic Press, an imprint of Elsevier, London, 2020.
 19. Perera, C., Qin, Y., Estrella, C., Reiff-Marganiec, S., Vasilakos, A.V.: Fog computing for sustainable smart cities. *ACM Computing Surveys*. 50, 1–43 (2017).
 20. Tecpoyotl Torres, M., Cabello Ruiz, R., & Vera Dimas, J. G. (2015). Design and simulation of an optimized electrothermal microactuator with Z-shaped beams. *Acta Universitaria*, 25(3), 19–24. <https://doi.org/10.15174/au.2015.774>.
 21. Voicu, R.-C., Tibeica, C.: An aluminum electro-thermally actuated micro-tweezer: Manufacturing and characterization. *Micromachines*. 14, 797 (2023).
 22. Wikipedia contributors. (2023, septiembre 25). *Odontomachus*. Recuperado de Wikipedia, The Free Encyclopedia website: <https://en.wikipedia.org/w/index.php?title=Odontomachus&oldid=1176970116>
 23. The Biomimicry Institute — nature-inspired innovation. (2022, agosto 15). Biomimicry Institute. <https://biomimicry.org/>
 24. Courtney, C.R., Demore, C.E., Wu, H., Grinenko, A., Wilcox, P.D., Cochran, S., Drinkwater, B.W.: Independent trapping and manipulation of microparticles using dexterous acoustic tweezers. *Applied Physics Letters*. 104, 154103 (2014).
 25. Kamperman, T., Trikalitis, V.D., Karperien, M., Visser, C.W., Leijten, J.: Ultrahigh-throughput production of monodisperse and multifunctional Janus microparticles using in-air microfluidics. *ACS Applied Materials & Interfaces*. 10, 23433–23438 (2018).
 26. Lin, S.-J., Hung, S.-H., Jeng, J.-Y., Guo, T.-F., Lee, G.-B.: Manipulation of micro-particles by flexible polymer-based optically-induced dielectrophoretic devices. *Optics Express*. 20, 583 (2011).

PASSIVE SOLAR SYSTEM: EVALUATION OF THE THERMAL EFFECTS OF A SOLAR CHIMNEY IN A ROOM

C. Jiménez-Xaman¹, Alfredo Aranda-Arizmendi², Moisés Montiel-González², Martín Rodríguez-Vázquez³, and Pedro Cruz-Alcantar¹

¹Coordinación Académica Región Altiplano, Universidad Autónoma de San Luis Potosí, Carretera a Cedral km 5+600, Matehuala, 78700 San Luis Potosí, México

²Facultad de Ciencias Químicas e Ingeniería (FCQeI), Universidad Autónoma del Estado de Morelos, Av. Universidad 1001, Cuernavaca 62210, Morelos, Mexico

³Facultad de Ingeniería, Universidad Veracruzana, Av. Universidad km 7.5, Col. Santa Isabel, Coatzacoalcos 96538, Veracruz, Mexico

Abstract. Currently there is no single configuration to determine the ventilation performance of a solar chimney, so it depends on the design, whether on the roof, facade, with inclination, etc. What is imperative is that it has an optimal performance as a passive ventilation system, ensuring air changes inside the cavity, which causes sufficient temperature gradients to cause the suction effect of the fluid to the outside. This work presents the evaluation of the thermal effects caused by a solar chimney in a room. The flow patterns by current isolines and isotherms, ventilation parameters, thermal evaluation of the chimney are described. It was found that the cavity has an average temperature value of 26.17 and 25.84 °C and that the velocity values comply with the ASHRAE 62.1 standard. The solar chimney presented air changes per hour with values greater than BORDER

Keywords: Numerical modelling, Computational Fluid Dynamics (CFD), Global Energy Balance (GEB), Conjugate heat transfer

1. Introduction

Buildings are all those constructions made artificially for different, but specific purposes; these are works that are designed and planned, in most cases to inhabit them or use them as shelter spaces. Currently, the largest amount of energy used in buildings is due to air conditioning systems that serve to obtain a comfortable environment. Heating, ventilation, or air conditioning systems lead to the excessive use of electrical energy and the increase of polluting gases in the environment. A building element specifically designed for natural ventilation is the solar chimney [1, 2]. For buildings, the concept of a solar chimney is defined as an elongated ventilated cavity, generally located in the sunniest part of a house and/or building. Its main function is to remove a volume of air in an enclosure, with the simple purpose of ventilating the house to improve air quality. One of the pioneers in developing a Global Energy Balance (GEB) methodology was Barra and Carratelli who investigated the natural convection in laminar flow regime in a solar chimney based on the Trombe-Michel model [1].

2

Zavala Guillen carried out a thermal study considering a double-channel solar chimney in a transient state and with phase change material (PCM) [3]. An alternative is to analyze the system as presented by Sakonidou et al. [4] Chae and Chung [5] who performed a theoretical-experimental study of a solar chimney, for the theoretical study the authors used CFD with the commercial ANSYS-FLUENT software. But the work in the which climatic conditions are indispensable are the experimental works of which, Hirunlabh [6], developed a solar chimney under the climatic conditions in Thailand. Another experimental work was that of Rattanongphisat et al. [7] where he considered a 1mm thick and 3m high steel solar chimney for ventilation with inlet and outlet opening of 0.4m respectively. Bansal et al. [8] conducted studies for a solar chimney integrated on a sloping roof of a 64 m³ room. Years later, Hamdy and Fikry [9] carried out a study using the GEB methodology for a solar chimney tilted on a roof. Bassiouny and Koura [10] presented the analytical and numerical study of a solar chimney coupled to the facade of a room for natural ventilation in a warm-arid climate. In the literature, research based on CFD methodology was found, of which Abuolnaga [11] studied an inclined solar chimney coupled to the roof of a cavity for hot and arid climate. Therefore, to study both numerically and experimentally the behavior of the of a solar chimney is only part of the problem. So, this paper evaluates the thermal effects of chimney on a room to determine the ventilation capacity.

2. Physical Model of the Coupled System

For proper operation of the CH-S coupled to a room, the physical model consisting of a ventilated square cavity with air inlet and outlet openings is defined. Then, the geometry of the solar chimney is 2 m height and 0.12 m separation between the absorber wall and the semitransparent wall, therefore the dimensions of the inlet and outlet opening are set to 0.12 m. The thickness of the semi-transparent wall and the absorber wall is 0.006 m and 0.022 m, respectively.

The inlet opening is located at the bottom of the right vertical wall as shown in Figure 1. The vertical walls are solid opaque and have convective ($q_{conv-ext}$) and radiative losses ($q_{rad-ext}$) to the outside environment. The horizontal walls are adiabatic ($\frac{\partial T}{\partial y}=0$). Inside the cavity, due to the temperature difference between the fluid (T_f) and the interior walls (T_w), there is a heat flow by convection and a variation of the fluid density, which causes the fluid to move by natural convection. The same temperature difference between the walls inside the cavity causes a superficial radiative exchange between them. The upper horizontal wall is the air outlet opening ($T_{f,o}$), in the outlet opening are located the positions of the solar chimney as shown in Figure 2, which is formed by a semitransparent wall and an absorber wall, which form an air space. The glass surface is placed in the direction of the sun, to take advantage of the solar energy that falls on it during the day, then, because of the radiative properties of the glass, a fraction of the incident energy is reflected outwards, another portion is absorbed (q_{abs-g}) and the rest is transmitted into the cavity.

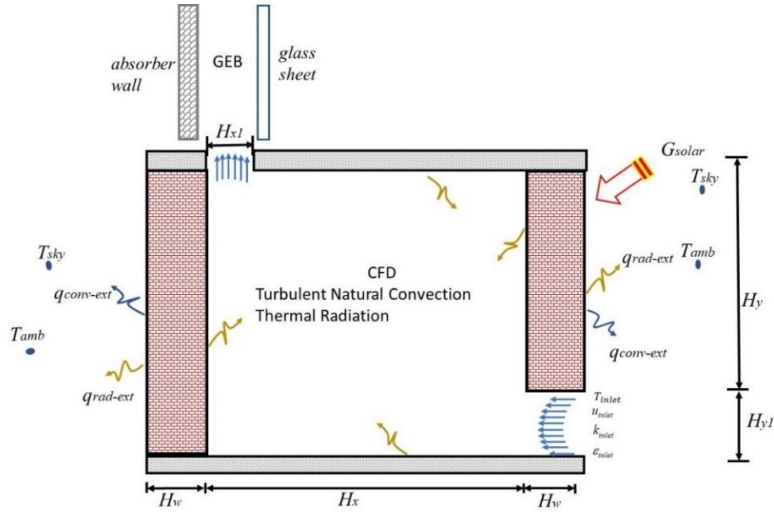


Figure 1. Physical model of the ventilated cavity coupled to a solar chimney.

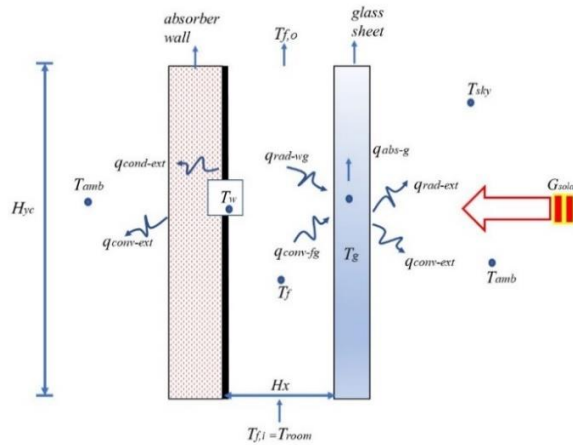


Figure 2. Single-channel solar chimney.

The coupled system will be evaluated with the climatic conditions of Merida Yucatan (latitude 20°58'00" and longitude 89°37'00"). This city has a warm-sub-humid climate throughout the year. The data from solar irradiance on a south-facing vertical surface, temperature and wind speed corresponding to the study city are shown in Table 1.

4

Table 1. Climatic conditions in Merida, Yucatan (2014).

Time (hr)	Warm Day (7 of April 2014)			Cold Day (18 of January 2014)		
	G_{sol} (W/m ²)	T_{amb} (°C)	V_{wind} (m/s)	G_{sol} (W/m ²)	T_{amb} (°C)	V_{wind} (m/s)
07:00	48.19	26.2	4.7	297.16	10	0
08:00	235.38	29.3	4.8	370.12	15.8	0.9
09:00	301.26	31.5	5.4	448.36	22.2	2.6
10:00	359.94	34.6	4.5	498.84	23.2	3.2
11:00	392.86	36.3	3.6	528.73	24.5	3
12:00	392.49	37.9	2.9	501.73	24.3	3.1
13:00	377.59	39.2	1.5	510.65	24.6	2.5
14:00	334.32	39.9	1.5	476.46	25.5	2.6
15:00	216.42	41.5	1.4	382.06	26	2.6
16:00	108.60	40.3	2.2	233.07	24.2	2.9
17:00	48.19	37.9	4.2	289.59	23.1	2.9
18:00	0.35	32.2	5	0.00	21.3	3.1

Mathematical model of the coupled system

The modeling of turbulent flow is performed with the RANS technique, i.e., the Navier- Stokes equations are time-averaged. Then, considering two-dimensional flow in turbulent regime, the equations governing natural convection are the equations of conservation of mass, momentum, and energy:

$$\frac{\partial(\rho\bar{u})}{\partial x} + \frac{\partial(\rho\bar{v})}{\partial y} = 0 \quad (1)$$

$$\begin{aligned} \frac{\partial(\rho\bar{u})}{\partial t} + \frac{\partial(\rho\bar{u}\bar{u})}{\partial x} + \frac{\partial(\rho\bar{v}\bar{u})}{\partial y} = & -\frac{\partial\bar{P}}{\partial x} + \frac{\partial}{\partial x} \left[(\mu + \mu_t) \frac{\partial\bar{u}}{\partial x} \right] + \frac{\partial}{\partial y} \left[(\mu + \mu_t) \frac{\partial\bar{u}}{\partial y} \right] \\ & + \frac{\partial}{\partial x} \left[(\mu + \mu_t) \frac{\partial\bar{u}}{\partial x} \right] + \frac{\partial}{\partial y} \left[(\mu + \mu_t) \frac{\partial\bar{v}}{\partial x} \right] \end{aligned} \quad (2)$$

$$\begin{aligned} \frac{\partial(\rho\bar{v})}{\partial t} + \frac{\partial(\rho\bar{u}\bar{v})}{\partial x} + \frac{\partial(\rho\bar{v}\bar{v})}{\partial y} = & -\frac{\partial\bar{P}}{\partial y} + \frac{\partial}{\partial x} \left[(\mu + \mu_t) \frac{\partial\bar{v}}{\partial x} \right] + \frac{\partial}{\partial y} \left[(\mu + \mu_t) \frac{\partial\bar{v}}{\partial y} \right] \\ & + \frac{\partial}{\partial x} \left[(\mu + \mu_t) \frac{\partial\bar{u}}{\partial y} \right] + \frac{\partial}{\partial y} \left[(\mu + \mu_t) \frac{\partial\bar{v}}{\partial y} \right] - \rho g \beta (\bar{T} - T_o) \end{aligned} \quad (3)$$

$$\frac{\partial(\rho\bar{T})}{\partial t} + \frac{\partial(\rho\bar{u}\bar{T})}{\partial x} + \frac{\partial(\rho\bar{v}\bar{T})}{\partial y} = \frac{\partial}{\partial x} \left[\left(\frac{\lambda}{C_p} + \frac{\mu_t}{\sigma_T} \right) \frac{\partial\bar{T}}{\partial x} \right] + \frac{\partial}{\partial y} \left[\left(\frac{\lambda}{C_p} + \frac{\mu_t}{\sigma_T} \right) \frac{\partial\bar{T}}{\partial y} \right] \quad (4)$$

Now for the turbulence model k - ε , uses the turbulent kinetic energy equation and the turbulent kinetic energy dissipation equation [12].

$$\frac{\partial(\rho k)}{\partial t} + \frac{\partial(\rho\bar{u}k)}{\partial x} + \frac{\partial(\rho\bar{v}k)}{\partial y} = \frac{\partial}{\partial x} \left[\left(\mu + \frac{\mu_t}{\sigma_k} \right) \frac{\partial k}{\partial x} \right] + \frac{\partial}{\partial y} \left[\left(\mu + \frac{\mu_t}{\sigma_k} \right) \frac{\partial k}{\partial y} \right] + P_k + G_k - \varepsilon \quad (5)$$

$$\begin{aligned} \frac{\partial(\rho\varepsilon)}{\partial t} + \frac{\partial(\rho\bar{u}\varepsilon)}{\partial x} + \frac{\partial(\rho\bar{v}\varepsilon)}{\partial y} = & \frac{\partial}{\partial x} \left[\left(\mu + \frac{\mu_t}{\sigma_\varepsilon} \right) \frac{\partial\varepsilon}{\partial x} \right] + \frac{\partial}{\partial y} \left[\left(\mu + \frac{\mu_t}{\sigma_\varepsilon} \right) \frac{\partial\varepsilon}{\partial y} \right] \\ & + C_{1\varepsilon} [f_1 P_k + C_{3\varepsilon} G_k] \frac{\varepsilon}{k} + E - C_{2\varepsilon} f_2 \frac{\rho\varepsilon^2}{k} \end{aligned} \quad (6)$$

Where:

$$\mu_t = C_\mu \rho \frac{k^2}{\varepsilon}, P_k = \mu_t \left[2 \left(\frac{\partial \bar{u}}{\partial x} \right)^2 + \left(\frac{\partial \bar{u}}{\partial y} + \frac{\partial \bar{v}}{\partial x} \right)^2 + 2 \left(\frac{\partial \bar{v}}{\partial y} \right)^2 \right], G_k = -\frac{\mu_t}{\sigma_T} g \beta \frac{\partial \bar{T}}{\partial y} \quad (7)$$

The flow is in regime of turbulent flow due to the dimensions of the cavity and natural convection inside the cavity is considered. The considerations for the development of the study:

- 1) The fluid inside the cavity is air, Newtonian and incompressible and non-participating due to its low moisture content.
- 2) Surface radiative exchange is considered between the walls inside the cavity, and they are opaque,
- 3) The Boussinesq approximation is valid when considering constant thermophysical properties except for the density in the buoyancy term.
- 4) The study is carried out in steady state.
- 5) The incident solar radiation is considered in normal direction.

Convection Model Boundary Condition

Boundary conditions for velocities are no-slip on solid walls. The boundary conditions for the temperature on the horizontal walls are adiabatic, on the left and right vertical wall there is an opaque wall. The condition the boundary values at the inlet openings are expressed.

$$P_{inlet} = -0.5 * \rho * U_{inlet}^2 \quad (8)$$

$$v = 0 \quad (9)$$

$$u = \frac{\partial u}{\partial x} \quad (10)$$

and in the output is summarized as,

$$\frac{\partial u}{\partial n} = \frac{\partial v}{\partial n} = 0. \quad (11)$$

While the thermal boundary condition at the inlet opening:

$$T_{inlet} = T_{environment} \quad (12)$$

and in the outlet opening

$$\frac{\partial T}{\partial n} = 0 \quad (13)$$

were, n is the coordinate in the direction on the flow.

6

Turbulent Boundary Conditions

The boundary condition at the inlet and outlet for the turbulent variables are taken from the work reported by Nielsen et al., [13]. For the inlet, the turbulent kinetic energy, and the energy kinetic of dissipation is expressed as,

$$k_{inlet} = 1.5 (0.04 * U_{inlet})^{2.0} \quad (14)$$

$$\varepsilon_{inlet} = \frac{(k_{inlet})^{1.5}}{(Hy)^{1+0.1}} \quad (15)$$

In the outlet opening (k, ε) were fixed,

$$\frac{\partial k}{\partial n} = 0, \quad \frac{\partial \varepsilon}{\partial n} = 0 \quad (16)$$

Conductive model

The equation governing the conduction phenomenon in the opaque wall is:

$$\frac{\partial}{\partial x} \left(\frac{\lambda}{C_p} \frac{\partial T}{\partial x} \right) + \frac{\partial}{\partial y} \left(\frac{\lambda}{C_p} \frac{\partial T}{\partial y} \right) = 0 \quad (17)$$

The boundary condition for the right and left opaque wall are:

$$q_{cond-wall} = q_{conv-ext} + q_{rad-ext} - q_{abs} \quad (18)$$

$$-q_{cond-wall} = q_{conv-ext} + q_{rad-ext} \quad (19)$$

while the borders and lower are adiabatic.

Radiative Exchange Model (RIM)

The net radiation method (RIM) is used for the radiative exchange in the room, equation (8) is solved in each grid, by evaluating the outgoing heat fluxes at each wall defined as radiosity and likewise the heat fluxes impinging on each wall considered as radiosity. In this way a local radiative flux distribution is calculated.

The net radiative heat flux at each wall is given by the following energy balance:

$$q_{r,1}(x_1) = q_{0,1}(x_1) - q_{i,1}(x_1) \quad (20)$$

where radiosity is defined as:

$$q_{0,1}(x_1) = \varepsilon_1^* \sigma T_1^4(x_1) + \rho_1^* q_{i,1}(x_1) \quad (21)$$

The irradiance is given by:

$$q_{i,1}(x_1) = \sum_{j=1}^N \int_{A_1} q_{0,1}(x_j) dF_{dA_1-dA_j} \quad (22)$$

where the sum of each k -th over the surface of is considered for elements over the boundary that only interact radiatively $dF_{dA_j-dA_k}$, which is defined as the differential view factor.

Mathematical Model of a Single Channel Solar Chimney

The mathematical formulation of the solar chimney through a GEB by which the corresponding equations are obtained to associate the temperature of the same element. Thus the problem consists of determining the temperatures of the glass (T_g), the temperature of the absorber wall (T_w), the temperature of the fluid between the plate and the glass (T_f), and in turn the mass flow (\dot{m}), so it is considered that 1) the phenomenon of natural convection prevails throughout the system, 2) the heat transfer is considered two-dimensional for all heat transfer processes through the CH-S elements, 3) the air temperature at the inlet of each channel was considered to be equal to the room outlet temperature, and 4) all thermophysical properties were evaluated at an average temperature. The equations for each element are described as:

$$\begin{aligned} & (h_{conv_g} + h_{rad_g} + h_{conv_{wind}} + h_{sky})T_g - T_f(h_{conv_g}) - T_w(h_{rad_{wg}}) \\ & = h_{conv_{wind}}T_{amb} + h_{sky}T_{sky} + \alpha_g G_{solar} \end{aligned} \quad (21)$$

$$\begin{aligned} & T_g(h_{conv_g}) - T_f(h_{conv_w} + h_{conv_g} + \frac{\dot{m}Cp}{\gamma * Hz * Dy}) + T_w(h_{conv_w}) \\ & = -\frac{\dot{m}Cp}{\gamma * Hz * Dy}T_{f,i} \end{aligned} \quad (22)$$

$$\begin{aligned} & -h_{rad_{wg}}T_g - h_{conv_w}T_f + h_{conv_w} + h_{rad_{wg}} + \frac{hw_{int}}{k_w * h\Delta w_{int}}T_w = \\ & \alpha_w T_g G_{solar} + \frac{hw_{int}}{k_w * h\Delta w_{int}}T_{room} \end{aligned} \quad (23)$$

The following relationships reported by Ong and Chow are needed [14]:

$$Nu = 0.68 + \frac{(0.67Ra^{\frac{1}{4}})}{\left[1 + \left(\frac{0.492}{Pr}\right)^{\frac{9}{16}}\right]^{\frac{4}{9}}} \quad Re < 10^9, \text{ laminar flow} \quad (24)$$

$$Nu = \left\{ 0.825 + \frac{(0.387Ra^{\frac{1}{6}})}{\left[1 + \left(\frac{0.492}{Pr}\right)^{\frac{9}{16}}\right]^{\frac{8}{27}}} \right\}^2 \quad Re > 10^9, \text{ turbulent flow} \quad (25)$$

The convective heat transfer coefficient is given for Swinbank [15]:

$$h_{conv_{wind}} = 5.7 + 3.8V_{wind} \quad (26)$$

8

The Radiative Heat Transfer Coefficient between the two parallel plates (absorber wall- semi-transparent wall) is expressed as:

$$h_{rad} = \frac{\sigma(T_g^2 + T_w^2)(T_g + T_w)}{\left(\frac{1}{\varepsilon_g} + \frac{1}{\varepsilon_w} - 1\right)} \quad (27)$$

For the radiative heat transfer coefficient, it was used:

$$h_{sky} = \sigma \varepsilon_g (T_g^2 + T_{sky}^2)(T_g + T_{sky}) \quad (28)$$

And where the temperature of the sky, T_{sky} taken from reference [15] is:

$$T_{sky} = 0.0552 T_{environment}^{1.5} \quad (29)$$

The mass flow rate for a uniform air temperature of the room, considering Cd as discharge coefficient, is described by:

$$\dot{m} = Cd \frac{\rho_{f,out} A_o}{\sqrt{1 + A_o}} \sqrt{\frac{2g L_i (T_f - T_{room})}{T_{room}}} \quad (30)$$

Air renewal and instantaneous thermal efficiency

The concept of indoor air renewal is defined as the introduction of new air from outside that displaces the air used inside a building, this parameter is important because it leads to air heating. Considering V_{Room} as the volume of the room, Bassiouny and Koura define the ratio of air change per hour as:

$$ACH = \dot{V} * \left(\frac{3600s}{V_{Room}}\right) \quad (31)$$

The instantaneous thermal efficiency of the solar chimney is defined as:

$$\eta = \frac{\dot{m} C_{p,f} (T_{f,out} - T_{f,in})}{W L_i G_{solar}} \times 100 \quad (32)$$

Where \dot{m} is mass flow, $C_{p,f}$ is the specific heat of the fluid, $T_{f,out}$ and $T_{f,in}$, are the temperatures at the outlet and inlet of the chimney, respectively, and $W L_i$ is the solar collection area (m²).

3. Solution Methodology

The numerical modelling based on CFD with the Finite Volume Method (FVM) is used in this work. The turbulence is solved by the RANS technique and the system of equations derived from the GEB for the solar chimney is also solved, see details in [16].

Mesh Independence Study

The dimensions of the cavity were determined based on the housing code, for a room located in a warm sub-humid climate, the room volume is 27 m³. The wall material is brick, its thermophysical properties are density 1600 kg/m³, thermal conductivity 0.7 W/mK and specific heat 1073 J/kgK. The minimum thickness of the brick was 0.15 m. The grid independence study used the extreme parameters for the coldest day in Merida, Yucatan, $G_{solar}=528.73 \text{ W/m}^2$, $T_{amb}=24.5 \text{ }^\circ\text{C}$, $V_{wind}=3 \text{ m/s}$. Table 2 shows the values of average, maximum and exit temperature of the cavity. From the percentage differences of the results, it was determined that the 171x131 mesh did not present a difference greater than 0.15 % with respect to the 181x141 mesh. In comparison with the lower meshes, the greatest percentage difference corresponds to the 141x101 mesh.

Table 2. Maximum and average temperatures in y-direction.

Variable	Numerical Mesh							
	111x71	121x81	131x91	141x101	151x111	161x121	171x131	181x141
T_{prom}	25.94	26.01 (0.27)	26.06 (0.19)	25.97 (0.35)	26.00 (0.12)	25.98 (0.23)	26.02 (0.15)	26.02 (0.00)
T_{max}	30.79	30.82 (0.10)	30.84 (0.06)	30.78 (0.19)	30.80 (0.06)	30.76 (0.13)	30.78 (0.06)	30.78 (0.00)
T_{out}	27.25	27.36 (0.40)	27.46 (0.36)	27.32 (0.50)	27.41 (0.32)	27.30 (0.40)	27.37 (0.25)	27.40 (0.10)

However, from the 171x131 node mesh onwards, the percentage difference is less than 0.10 % for the three variables. Therefore, for meshes larger than 171x131, it indicates that the solution no longer varies and the difference between the solution is negligible.

Thermal and hydrodynamic effect of the solar chimney on the room

For the coldest day the symbol "Cold" is used and for the warmest day the symbol "Warm" is used. According to this convention it is understood that the symbology for the coldest day configuration is CH-Cold, while for the warmest day CH-Warm. Due to the conjugate heat transfer through the room, the behavior of the air inside the cavity is linked to the temperature of the vertical walls. Therefore, the flow patterns are presented as stream isotherms and isolines; they are useful to describe in a practical way the phenomenology that occurs during the energy transport of the system. The thermal behavior of the system is illustrated by the isotherms shown in Figure 3 for the 7:00 to 17:00 hours. At 7:00 hours the solar radiation has a low value, and the temperature difference between the inside of the room and the outside environment is null, varying in the order of 0.2°C. Thus, the temperature of the vertical walls is kept in 26°C

10

approximately, being uniform in the entire cavity, later at 8:00 and 9:00 it is observed that the temperature remains at approximately 30 °C. It is also seen that the highest temperature is concentrated in the upper part of the cavity while the lowest temperature in the lower zone, this was expected due to the natural convection that prevails in the system. From 10:00 to 16:00 hours the room has a uniform temperature field since the solar radiation increases and by the incident radiation the wall begins to heat up. In the same time interval, the right vertical wall reached temperatures ranging between 40 and 49°C, so that inside the cavity the maximum temperature recorded was 42°C at 15:00 hours. Figure 4 shows the isotherms obtained from the modeling of the coldest day. The behavior is similar when compared to the pattern of the warmest day, but the temperature inside the cavity for the hours 7:00 and 8:00 does not exceed 20 °C when the environment temperature is 10 and 15.8 °C, respectively. The ASHRAE Standard mentions that the temperatures that provide a feeling of thermal comfort to the human being are in a range of 22.7-27.7°C, therefore for the warm day, the temperature inside the room does not comply with the standard, while the results for the cold day present the values established by the standard in the range 9:00 to 17:00 hours.

Thermal evaluation of the solar chimney

The thermal behavior of the solar chimney is presented in terms of the temperature difference between the air at the inlet and outlet of the channel, the temperature in each of the components and the thermal efficiency of the system. The thermal behavior of the solar chimney elements and the outlet air temperature is shown in figure 5. The element with the highest temperature is the absorber wall, exceeding the temperature of 50 °C in the interval from 9:00 to 15:00 for both days. Also, it is observed that the fluid at the outlet ($T_{f, out}$) is slightly higher than the fluid temperature (T_f), this effect is caused by the temperature of the fluid entering each section of the solar chimney increases its temperature due to the heat flow from the absorber plate and the glazed surface. In Table 3 the air change per hour is in the range of $0.96 < ACH < 3.00$ and $2.46 < ACH < 3.44$ for the hot and cold day respectively. Because the application of the solar chimney involves replacing the air contained in an enclosure with air from the outside environment, it is necessary to project the use of the device.

Figure 5 describes the time evolution of the absorber wall temperature (T_w), the glass surface temperature (T_g), the air inlet temperature (T_f) and the air outlet temperature ($T_{f, out}$). From the results it is possible to observe that the highest temperature corresponds to the absorbing wall between 28 and 67 °C for the warmest day and between 37 and 64 °C for the coldest day, respectively. This is followed by the glass temperature with values between 24 and 44 °C on the warmest day and between 13 and 26 °C for the coldest day. In the case of the air temperatures at the outlet, it is higher than the value at the solar chimney inlet. The maximum value of the temperature at the outlet of the solar chimney in the interval of highest solar radiation from 7:00 to 13:00 h varies between 25 and 42 °C for the hottest day and from 16 to 28 °C for the coldest day. These values observed for the behavior of the temperature in the solar chimney are proportional to the changes in the intensity of incident solar radiation.

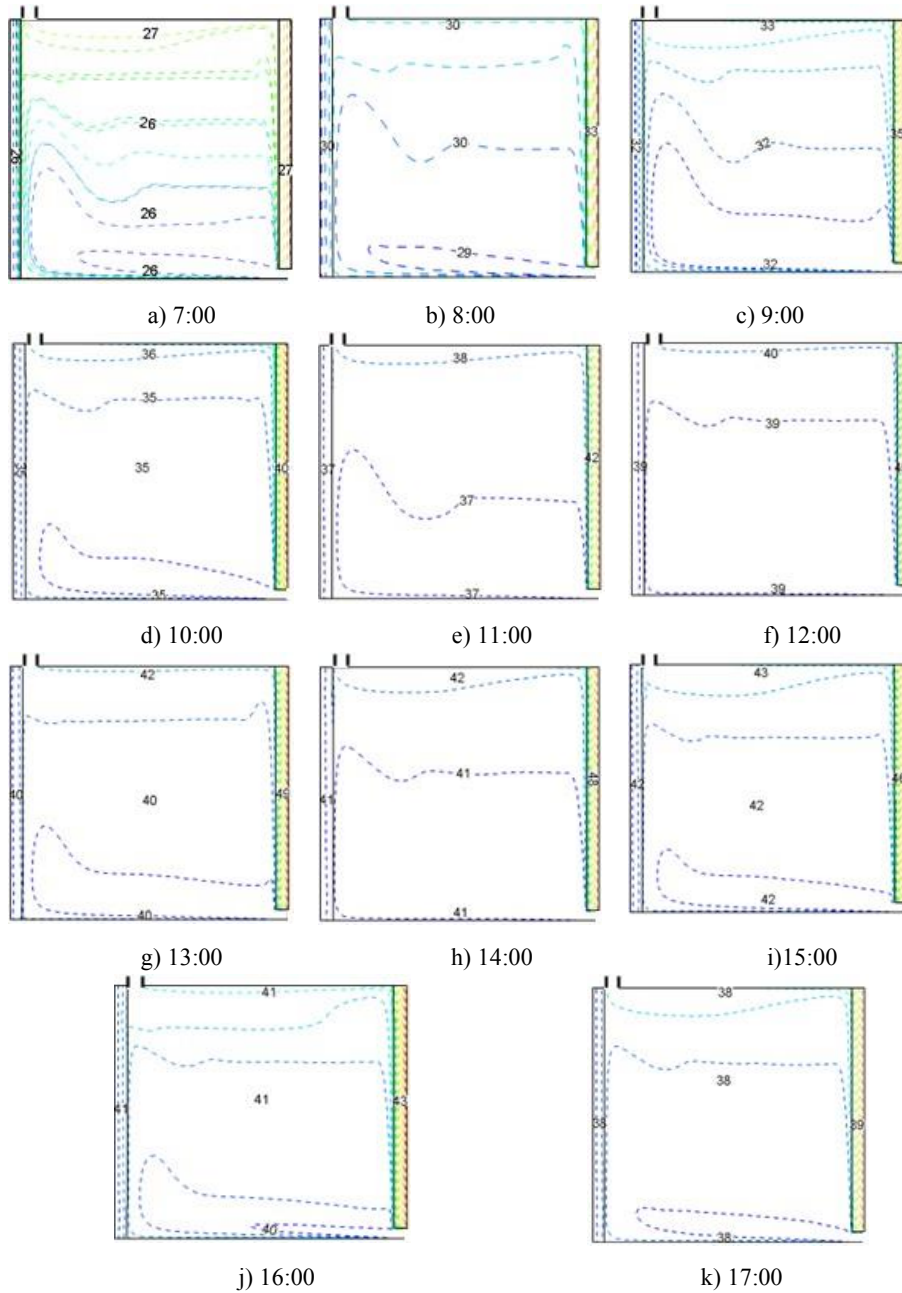


Figure 3. Isotherms for Merida, Yucatan for the warmest day, CH-Warm.

12

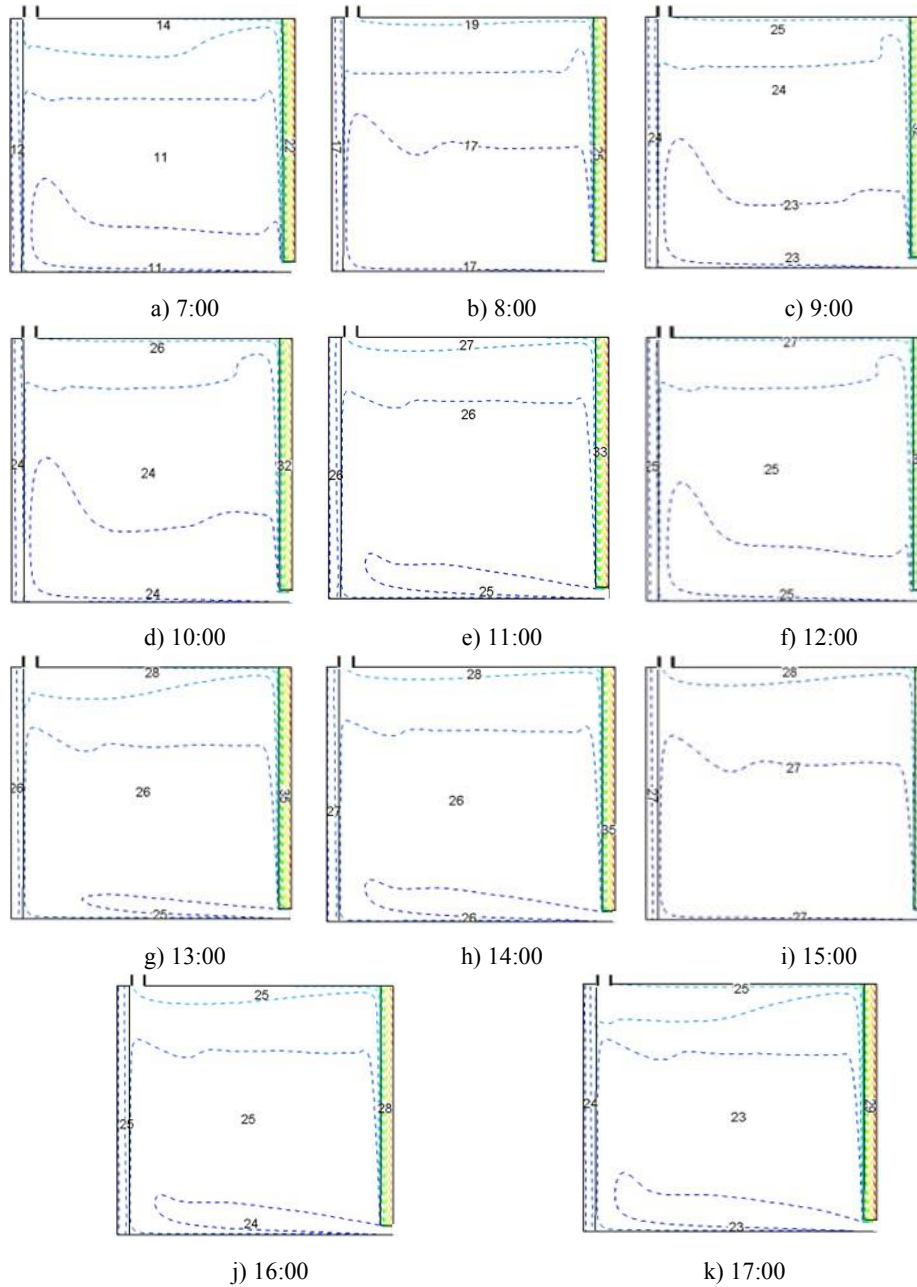


Figure 4. Isotherms for Merida, Yucatan for the warmest day, CH-COLD.

To quantify the air renewal is achieved by the air change is set at 0.5, which is a function of occupancy and activity which can increase up to 2.5 ACH according to ASHRAE 62.1 (2005). The exit velocity of the chimney at which the fluid is propelled presents high values from the interval of 8:00 to 15:00 hours for both days. The comparison of mass flow and thermal efficiency, it is observed that the thermal efficiency. The interval in which the mass flow is found is $8.38 < \dot{m} < 24.82$ and $21.38 < \dot{m} < 29.54$, for 7:00 and 13:00 for the warm day and for the cold at 16:00 and 11:00 hours, respectively. The efficiency has intervals of $7.72 < \eta_t < 28.10$ and $25.39 < \eta_t < 30.67$ for the warm day and the cold day respectively.

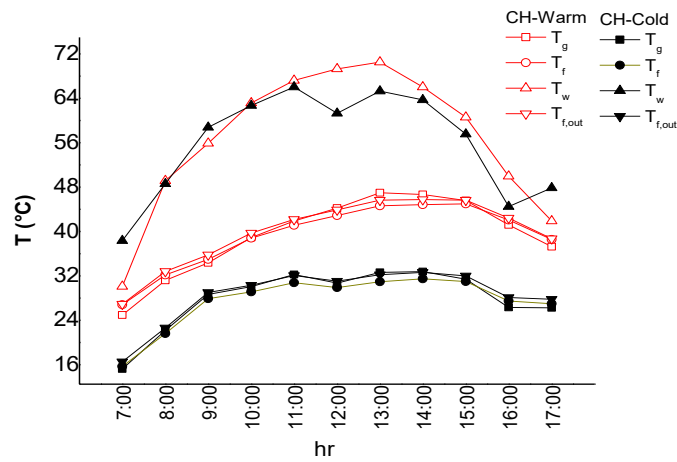


Figure 5. Temperature of the solar chimney components for CH-Warm and CH-Cold.

Table 3. Quantitative comparison of ACH, exit velocity, thermal efficiency, and mass flow.

hour	CH-Warm				CH-Cold			
	ACH	U_{out} (m/s)	η_t	$\dot{m}(kg / s)$ $\times 10^3$	ACH	U_{out} (m/s)	η_t	$\dot{m}(kg / s)$ $\times 10^3$
07:00	0.96	0.06	7.72	8.38	2.85	0.17	30.38	25.59
08:00	2.47	0.15	24.30	21.12	3.07	0.19	30.67	27.12
09:00	2.69	0.16	25.70	22.85	3.25	0.20	29.98	28.12
10:00	2.88	0.18	26.50	24.18	3.37	0.21	30.07	29.06
11:00	2.98	0.18	26.46	24.71	3.44	0.21	30.27	29.54
12:00	3.00	0.19	27.28	24.82	3.27	0.20	29.63	28.12
13:00	2.99	0.19	28.10	24.58	3.40	0.21	30.38	29.21
14:00	2.85	0.18	27.39	23.39	3.31	0.21	29.88	28.34
15:00	2.37	0.15	24.54	19.46	3.03	0.19	28.68	26.00
16:00	1.70	0.10	18.63	14.18	2.46	0.15	25.39	21.38
17:00	1.07	0.06	9.92	9.00	2.70	0.17	27.02	23.51

5. Conclusions

The study was carried out with the purpose of observing the benefit of the solar chimney to ventilate a room, because thanks to the use of the solar chimney it is possible to replace the stagnant air inside the room with air from outside for a healthy indoor environment. and comfortable.

Fluid entering the room at a constant temperature every hour causes a temperature gradient between the fluid and the internal surfaces of the room, causing an increase in buoyancy forces, displacing air from inside the room and replacing it with air from the exterior.

The air change per hour and the speed with which the fluid leaves the solar chimney, allow us to quantify the air renewal, which was 0.5, which is a function of occupancy and activity up to 2.5 ACH. The results demonstrated that the chimney is within the intervals established by ASHRAE 62.1 (2005) [18].

According to the results obtained, it is concluded that the solar chimney is an excellent passive ventilation strategy to improve natural ventilation and provide thermal comfort to the occupants.

It is interesting to consider that for hot days it is necessary to pre-condition the air when entering the room. Another alternative would be to locate the air inlet in an area where vegetation is located to avoid the heat island phenomenon, as an influence of the surroundings.

This work addresses complex phenomena of heat transfer conjugate with turbulent flow in a solar chimney coupled to a real room. However, in future work it is intended to consider the mass transfer with a radiatively participating medium.

6. References

1. Barra O. A., Carratelli E. Pugliese, A Theoretical Study of Laminar Free Convection in 1-D Solar Induced Flows, *Solar Energy*, Vol. 23, págs. 211-215, 1979.
2. Bouchair A., Fitzgerald D., The Optimum Azimuth for a Solar Chimney in Hot Climates, *Energy and Buildings*, Vol. 12, págs. 135-140, 1988.
3. Zavala Guillen I., Análisis Térmico en una Chimenea Solar con Doble Canal de Uso Diurno, Tesis de Doctorado, Cenidet, Cuernavaca, Morelos, 2016.
4. Sakonidou E. P., Karapantsios T. D., Balouktsis A. I., Chassapis D., Modeling of the Optimum Tilt of a Solar Chimney for maximum Air Flow, *Solar Energy*, Vol. 82, págs. 80–94, 2008.
5. Chae Myeong-Seon, Chung Bum-Jin, Heat transfer effects of chimney height diameter, and Prandtl number, *International Communications in Heat and Mass Transfer*, vol. 66, págs. 196-2022,2015.
6. Hirunlabh J., Kongduang W., Namprakai P., Khedari J., Study of natural ventilation of houses by a metallic solar wall under tropical climate, *Renewable Energy*, Vol. 18, págs. 109-119, 1999.

7. Rattanongphisat W., Imkong P., Khunkong S., An Experimental Investigation on the Square Steel Solar Chimney for Building Ventilation Application, *Energy Procedia*, Vol. 138, págs. 1165-1170, 2017.
8. Bansal N., Mathur R., Bhandari M., Solar chimney for enhanced stack ventilation, *Building and Environment*, Vol. 28, págs. 373-377, 1993.
9. Hamdy I.F., Fikry M. A., “Passive Solar Ventilation”, *Renewable Energy*, Vol. 14, págs. 381-386, 1998.
10. Bassiouny, R. and Koura, Nader S.A., An Analytical and Numerical study of Solar Chimney use for room Natural Ventilation, *Energy and Buildings*, Vol. 40, págs. 865–873, 2008.
11. Aboulnaga M. Mohsen, A Roof Solar Chimney assisted by Cooling Cavity for Natural Ventilation in Hot Arid Climates: An Energy Conservation Approach in Al-Ain city, *Renewable Energy*, Vol. 14, págs. 357-363, 1998.
12. Henkes, R. A. W. M., Van Der Vlugt, F. F., & Hoogendoorn, C. J. Natural-convection flow in a square cavity calculated with low-Reynolds-number turbulence models. *International Journal of Heat and Mass Transfer*, 34(2), 377–388, 1991.
13. Nielsen, P. V., Restivo, A., & Whitelaw, J. H. Buoyancy-Affected Flows In Ventilated Rooms. *Numerical Heat Transfer*, 2(1), 115–127, 1979.
14. Ong K., Chow C. Performance of solar chimney, *Solar Energy*, Vol. 74, págs. 1-17, 2003.
15. Swinbank, W. C. Long-wave radiation from clear skies. *Quarterly Journal of the Royal Meteorological Society*, 89(381), 339–348, 1963.
16. Bansal N.K., Mathur J., Mathur S., Jain M., “Modeling of window-sized solar chimneys for ventilation”. *Building and Environment*, Vol., 40, págs.1302–1308, 2005.
17. H. Awbi, *Ventilation of Building*, E & FN Spon, 2003.
18. ANSI/ASHRAE, Standard 62.1, *Ventilation for Acceptable Indoor Air Quality*, 2013. New York City.

Annual evaluation of a single air-channel solar chimney with phase change material under hot-humid climatic conditions of Mexico

Carlos E. Torres-Aguilar¹[0000-0001-6187-4519], Pedro Moreno-Bernal²[0000-0002-2811-5331], Sergio Nesmachnow³[0000-0002-8146-4012], Edgar V. Macias-Melo¹[0000-0003-0107-766X], Karla M. Aguilar-Castro¹[0000-0003-2611-2820], Luis Hernández-Callejo⁴[0000-0002-8822-2948], and Jesús Arce⁵[0000-0002-2052-3322]

¹ Universidad Juárez Autónoma de Tabasco, México
{enrique.torres,edgar.macias,karla.aguilar}@ujat.mx

² Universidad Autónoma del Estado de Morelos, México
pmoreno@uaem.mx

³ Universidad de la República, Uruguay
sergion@fing.edu.uy

⁴ Universidad de Valladolid, Campus Universitario Duques de Soria, España
luis.hernandez.callejo@uva.es

⁵ Centro Nacional de Investigación y Desarrollo Tecnológico, México
jesus.al@cenidet.tecnm.mx

Abstract. This article presents a performance annual evaluation of a single air-channel solar chimney with phase change material under hot-humid climatic conditions by energy balance method. The heat transfer analysis in the phase change material is performed in an unsteady state with an effective specific heat method. The experimental evaluation considers the warmest and coldest days per month of a year to estimate temperatures, mass flow rate, and volumetric flow rate induced by the solar chimney in each model element. Experimental results show that the solar chimney with phase change material allows an operation time between 18-23 hours with a maximum volumetric flow rate of up to 148 m³h⁻¹. Also, the airflow induced by the solar chimney was sufficient to provide natural ventilation for a space of 18-36 m², saving up to 152.25 kWh in electricity consumption and reducing up to 64.40 kg of CO₂ emitted into the environment. Results indicate that the single air-channel solar chimney with phase change material is an alternative to natural ventilation in buildings under hot-humid climate conditions.

Keywords: Solar chimney, natural ventilation, phase change material

2

1 Introduction

In construction, ventilation is essential in the design and building phases. In this context, residential buildings require an optimal design to generate acceptable natural ventilation. However, the lack of ventilation in residential buildings forces residents to use active systems, increasing electricity consumption. In Mexico, 25.9% of total electricity consumption corresponds to the residential sector, particularly refrigeration and air conditioning devices [1]. Also, 45% of residences incorporate mechanical ventilation systems, and more than 20% include air conditioning [2]. Nowadays, the energy scenario in Mexico requires alternatives to satisfy the demand for ventilation through non-conventional methods, i.e., using renewable energy systems. Passive systems such as solar chimneys, devices attached to the roof or facade of the rooms that work through solar energy to induce air renewal in the house, are alternatives for satisfying the ventilation demand in buildings [3].

Solar chimneys consist of two plates, absorber and translucent, which create a channel where the air is extracted from the room. However, solar chimney analysis and operation in warm and humid climates are obstacles to overcome by periods when ventilation is required, including nocturnal hours, because solar chimney operation is usually analyzed in periods where solar radiation is incident directly [4].

In literature, solar chimney design with the capacity to store enough thermal energy is reported. Marti-Herrero et al. [5] propose a solar chimney with an absorbing wall composed of concrete brick and other materials that increase thermal inertia and operation time. However, the proposed materials to implement a solar chimney present a drawback for existing buildings, i.e., the required volume or space for its implementation. The lack of space and structural and resistance problems make the implementation not viable in considerable residential households. An alternative to the use of concrete and brick materials are phase change materials (PCM), which present adequate characteristics to store a large amount of thermal energy either in the form of sensible heat, mainly in the form of latent heat, increasing the thermal inertia of the system to extend the operation time and thus induce the necessary ventilation at night [6]. Therefore, it is necessary to study solar chimneys to extend the operating time in places where natural ventilation conditions are required during nocturnal hours.

Solar chimney studies involving PCMs prioritize the search for a configuration, under the conditions evaluated, that allows capturing and maximizing the energy incident on the solar chimney. Huang et al. [7] analyzed a container shape of PCM materials where, for an RT42 PCM, it is recommended to use individual or sectioned containers since using a single elongated rectangular piece affects the performance of the PCM. The experimental fixed a constant heat flux of 500 W/m² for containers of varying height from 12, 24, 36, and 48 cm, where the melting times under the referred conditions were 240, 300, 330, and 460 minutes. Thus, the benefits of implementing a solar chimney in terms of induced ventilation effects with PCM can considerably increase in real applications due to the temperature increases in the system of up to 33% that have been registered by increasing the mass flow rate compared to solar chimney configurations without PCM [8].

In this line of work, this article presents a performance annual evaluation of a single air-channel solar chimney (SC-SoCh) under hot and humid climate conditions, considering PCM in the absorber wall to extend the induced ventilation time and airflow for natural ventilation. The proposed model considers solar radiation, ambient temperature, wind speed, relative humidity, and atmospheric pressure changes to improve the airflow calculations; the model was developed through the global energy balance method (GEB). In addition, the energy consumption and pollution emissions were determined considering the equivalent performance of an active system to provide the same natural ventilation as SC-SoCh for a year.

The rest of the article is structured as follows. Section 2 describes the GEB model applied to SC-SoCh. Section 3 presents the numerical solution methodology and verification through GEB of the evaluated system. The results and discussion of the numerical solution approach are described in section 4. Finally, section 5 presents the research conclusions and formulates the main lines for future work.

2 GEB applied to SC-SoCh

In this section, the physical and mathematical model of SC-SoCh, the solution methodology, and the general considerations of the study are described.

2.1 Physical and mathematical model of SC-SoCh

The mathematical model reported by Xamán et al. [9] was used as a reference for developing the SC-SoCh model. The model was proposed in an unsteady state, considering the convective and radiative effects between the semitransparent plate (glass) and the external environment, the heat convection between the absorbing plate and the semitransparent plate, as well as the radiative exchange between the absorbing plate and the semitransparent plate. Fig. 1 shows the physical model of SC-SoCh and a possible location of this passive system as part of the façade of a residential building.

4

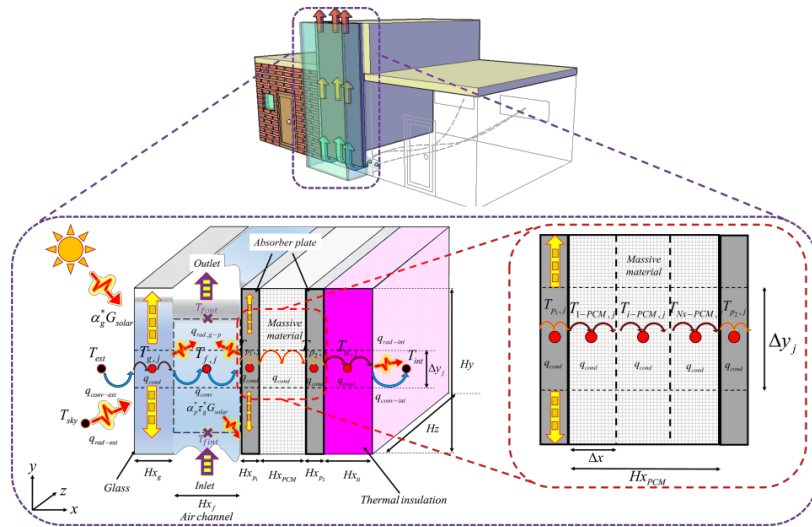


Fig. 1. SC-SoCh physical model

Next, the mathematical model of the SC-SoCh is described for each system element through GEB.

Glass envelope (T_g)

The energy balance for the semi-transparent envelope considers the radiative and convective effect individually on the heat flow components between the glass and the outside environment. The mathematical model considers the meteorological variables as a function of time. Meteorological variables are obtained from data stored in a weather station: sky temperature (T_{sky}), outdoor temperature (T_{ext}), and incident solar radiation (G_{solar}). It should be noted that the incident solar radiation is estimated from the decomposition of the solar radiation on the horizontal, and for the glass envelope, it includes the exposure in the afternoon considering that the envelope is oriented to the west according to Fig. 1, so G_{solar} considers only diffuse radiation during the first half of the visible light period.

$$\begin{aligned}
 & \left(\frac{1}{h_{conv-ext,1}} + \frac{Hx_{g,j}}{2\lambda_{g,j}} \right)_{a_1^{-1}} A_{int} + \left(\frac{1}{h_{rad,g}} \right)_{a_2^{-1}} A_{int} + \alpha_{g,j}^* G_{solar} A_{int} - \left(\frac{Hx_{g,j}}{2\lambda_{g,j}} + \frac{1}{h_{g,j-f,j}} \right)_{a_3^{-1}} A_{out} \\
 & - \left(\frac{1}{h_{rad,g,j-p_1,j}} \right)_{a_4^{-1}} A_{out} = \frac{d}{dt} (\rho C_p T)_{g,j} \Delta x \quad A = A_{int} = A_{out} \quad (1)
 \end{aligned}$$

Fluid channel (T_f)

In the case of the fluid channel, the convection into the channel fluid ($h_{g,j-f,j}$, $h_{g,j-f,j}$) was considered, as well as the energy removal due to the airflow induced by the effect of buoyancy forces as depicted in Fig. 1. The energy balance for the channel fluid considers that the mass flow is the same at the inlet and outlet due to continuity. However, the fluid was not considered as radiatively participating.

$$\underbrace{\left(\frac{T_{g,j} - T_{f,j}}{2\lambda_{g,j} + \frac{1}{h_{g,j-f,j}}} \right)}_{b_1^{-1}} + \underbrace{\frac{\dot{m}_{in} C_{p,int} T_{f,int} - \dot{m}_{out} C_{p,out} T_{f,out}}{HyHz}}_{M_{f,j}} - \underbrace{\left(\frac{T_{f,j} - T_{p_1,j}}{\frac{1}{h_{f,j-p_1,j}} + \frac{Hx_{p_1,j}}{2\lambda_{p_1,j}}} \right)}_{b_2^{-1}} = \frac{d}{dt} (\rho C_p T)_{p_1,j} A \Delta x \tag{2}$$

Metal absorber plate 1 (T_{p1})

The energy balance for the metal absorber plate considers the heat conduction effect, despite being a thin plate, the heat convection effect with the fluid of channel of the SC-SoCh, the radiative effect with the glass envelope of channel through the surface radiative exchange effect ($h_{rad,g-p1}$), the absorption of solar radiation, and the radiation transmitted by the glass cover in the channel. Therefore, even if the sun is facing east or west at a specific time, the model for decomposing the solar radiation allows to obtain a diffuse radiation component, which is absorbed on the opposite side of the plate to where the direct rays of the sun arrive, which occurs naturally in an actual solar chimney.

$$\underbrace{\left(\frac{T_{g,j} - T_{p_1,j}}{h_{rad,g,j-p_1,j}} \right)}_{c_1^{-1}} A_{int} + \underbrace{\left(\frac{T_{f,j} - T_{p_1,j}}{\frac{1}{h_{f,j-p_1,j}} + \frac{Hx_{p_1,j}}{2\lambda_{p_1,j}}} \right)}_{c_2^{-1}} A_{int} + \alpha_{p_1,j}^* \tau_{g,j}^* G_{solar} A_{int} - \underbrace{\left(\frac{T_{p_1,j} - T_{1-PCM,j}}{\frac{Hx_{p_1,j}}{2\lambda_{p_1,j}} + \frac{\Delta x_{1-PCM,j}}{2\lambda_{1-PCM,j}}} \right)}_{c_3^{-1}} A_{out} = \frac{d}{dt} (\rho C_p T)_{p_1,j} A \Delta x \tag{3}$$

PCM (T_{PCM})

The GEB in each PCM layer consider the heat conduction between the metal plates acting as containers and the adjacent PCM layers (Fig. 1). The method used to describe

6

the heat conduction phenomenon in the PCM is the effective specific heat ($C_{p,eff}$). The phase change enthalpy term (h) is part of the C_p term in each resulting equation.

$$\frac{T_{p_1,j} - T_{1-PCM,j}}{\underbrace{\left(\frac{Hx_{p_1,j}}{2\lambda_{p_1,j}} + \frac{\Delta x_{1-PCM,j}}{2\lambda_{1-PCM,j}} \right)}_{d_1^{-1}}} A_{int} - \frac{T_{1-PCM,j} - T_{2-PCM,j}}{\underbrace{\left(\frac{\Delta x_{1-PCM,j}}{2\lambda_{1-PCM,j}} + \frac{\Delta x_{2-PCM,j}}{2\lambda_{2-PCM,j}} \right)}_{d_2^{-1}}} A_{out} \quad (4)$$

$$= \frac{d}{dt} (\rho C_p T)_{1-PCM,j} A \Delta x$$

$$\frac{T_{i-1-PCM,j} - T_{i-PCM,j}}{\underbrace{\left(\frac{\Delta x_{i-1-PCM,j}}{2\lambda_{i-1-PCM,j}} + \frac{\Delta x_{i-PCM,j}}{2\lambda_{i-PCM,j}} \right)}_{e_1^{-1}}} A_{int} - \frac{T_{i-PCM,j} - T_{i+1-PCM,j}}{\underbrace{\left(\frac{\Delta x_{i-PCM,j}}{2\lambda_{i-PCM,j}} + \frac{\Delta x_{i+1-PCM,j}}{2\lambda_{i+1-PCM,j}} \right)}_{e_2^{-1}}} A_{out} \quad (5)$$

$$= \frac{d}{dt} (\rho C_p T)_{i-PCM,j} A \Delta x$$

$$\frac{T_{N_x-1-PCM,j} - T_{N_x-PCM,j}}{\underbrace{\left(\frac{\Delta x_{N_x-1-PCM,j}}{2\lambda_{N_x-1-PCM,j}} + \frac{\Delta x_{N_x-PCM,j}}{2\lambda_{N_x-PCM,j}} \right)}_{f_1^{-1}}} A_{int} - \frac{T_{N_x-PCM,j} - T_{p_2,j}}{\underbrace{\left(\frac{\Delta x_{N_x-PCM,j}}{2\lambda_{N_x-PCM,j}} + \frac{Hx_{p_2,j}}{2\lambda_{p_2,j}} \right)}_{f_2^{-1}}} A_{out} \quad (6)$$

$$= \frac{d}{dt} (\rho C_p T)_{N_x-PCM,j} A \Delta x$$

Metal absorber plate 2 (T_{p_2})

The energy balance of the PCM metal container considers the heat conduction in the last layer of the PCM and the thermal insulator layer. Equation of T_{p_2} is expressed as:

$$\frac{T_{N_x-PCM,j} - T_{p_2,j}}{\underbrace{\left(\frac{\Delta x_{N_x-PCM,j}}{2\lambda_{N_x-PCM,j}} + \frac{Hx_{p_2,j}}{2\lambda_{p_2,j}} \right)}_{g_1^{-1}}} A_{int} - \frac{T_{p_2,j} - T_{ti,j}}{\underbrace{\left(\frac{Hx_{p_2,j}}{2\lambda_{p_2,j}} + \frac{Hx_{ti,j}}{2\lambda_{ti,j}} \right)}_{g_2^{-1}}} A_{out} \quad (7)$$

$$= \frac{d}{dt} (\rho C_p T)_{p_2,j} A \Delta x$$

Thermal insulation (T_{ti})

The thermal insulation in the SC-SoCh is vital to reduce the heat flow from the absorber wall to the internal environment of the enclosure, where the solar chimney is connected. The energy balance considered the effect of heat conduction through this component and the convective and radiative effects with the internal environment of the enclosure.

$$\begin{aligned} & \underbrace{\left(\frac{Hx_{p_2,j} - T_{i,j}}{2\lambda_{p_2,j} + \frac{Hx_{i,j}}{2\lambda_{i,j}}} \right)}_{h_c^{-1}} A_{int} - \underbrace{\left(\frac{Hx_{i,j} - T_{int}}{2\lambda_{i,j} + \frac{1}{h_{conv-int} + h_{rad-int}}} \right)}_{h_s^{-1}} A_{out} \\ & = \frac{d}{dt} (\rho C_p T)_{i,j} A \Delta x \end{aligned} \quad (8)$$

A first-order backward approximation was implemented to replace the temporal terms through the finite difference method. Eqs. (1-8) were grouped into a matrix to generate a system of equations for representing the complete SC-SoCh model. The dimensions of equation systems are the function of the number of elements that divide PCM. For this study, the PCM was divided into 19 elements; this election was determined through a grid size independence study under the extreme conditions of the year.

The empirical equation reported by Ong [10] was used to estimate the mass flow rate (\dot{m}) and volume flux (\dot{V}) induced by the solar chimney.

$$\begin{aligned} \dot{m} &= C_d \frac{\rho_{f,out} A_{out}}{\sqrt{1 + A_{int}/A_{out}}} \sqrt{\frac{2gHy(T_f - T_{int})}{T_{int}}} \\ \dot{V} &= \frac{\dot{m}}{\rho_f} \end{aligned} \quad (9)$$

3 Numerical solution and verification

This section describes the methodology for solving the energy balance equation system of SC-SoCh and verifying the proposed mathematical model.

3.1 Methodology for energy balance equation system

The GEB method has the capacity to obtain a suitable temperature solution through an iterative procedure that is competitive with other methods of heat transfer analysis [11]. Algorithm 1 presents the process for solving the proposed system of equations through the GEB. The method considers the data of the corresponding meteorological variables such as solar radiation, ambient temperature, relative humidity, wind speed, and atmospheric pressure.

8

Algorithm 1: Method for solving the SC-SoCh

Data: $Hx, Hy, Hz, \lambda, C_P, \rho, \alpha^*, \tau^*, \rho^*, \varepsilon, G_{solar}, T_{ext}, T_{int}, h_{conv}, V_{wind}, C_d, T_{f,int}, HR, P_{atm}$

Result: Temperature Matrix ϕ and air flow induced \dot{m} or \dot{V}

- 1 Set variables (T), properties and boundary conditions of system
- 2 Fill matrix $\phi = T_{guest}$
- 3 Generate mesh inside PCM $\Delta x = \frac{Hx_{PCM}}{Nx}$
- 4 $k=0$
- 5 **while** $t \leq t_{modeling}$ **do**
- 6 | Rename matrix $\phi = \phi^t$
- 7 | $t = k\Delta t$
- 8 | **while** $R_\phi^k \geq \varepsilon$ **do**
- 9 | | Rename $\phi^* = \phi$
- 10 | | Computing coefficients a, b, c, \dots
- 11 | | Gauss-Seidel solver ϕ
- 12 | | Calculate \dot{m}, \dot{V}
- 13 | | Compute error $R_\phi^k = \max \left| \frac{\phi - \phi^*}{\phi} \right|$
- 14 | **end**
- 15 | $k = k + 1$
- 16 **end**
- 17 Print temperature matrix and air flow

In Algorithm 1, variable ϕ represents the temperature values of each element considered in Eqs. (1-8). Guessed temperature value T_{guest} was set to the same value as the outdoor temperature (T_{ext}). Step 3 is important for the use of massive materials such as PCM. It is necessary to consider more than a single node to represent the heat conduction over time in the different layers of the PCM due to thermal inertia. Steps 4 and 5 represent the beginning of the iterative process to find the solution at each time step, while steps 6 and 7 establish the renaming of the temperatures found and the increased modeling time. Subsequently, step 8 marks the iterative process to find the solution for the corresponding time step. Similarly, step 9 represents the renaming of the temperature variable for each iteration. Step 10 represents the consideration of the effect of nonlinearity in the mathematical model since the convective-radiative coefficients, properties of the thermal insulation, the air, and mainly the PCM depend on variables such as temperature, relative humidity, atmospheric pressure, wind speed, and solar radiation that were introduced to the algorithm from the data at the beginning of the algorithm. Step 11 consists of the implementation of the Gauss-Seidel solver for the solution of the system of equations shown in Eqs. (1-8). The temperature information obtained in step 9 is needed to determine the amount of airflow generated by the SC-SoCh in step 12 from Eq. (9). Step 13 represents the error estimation between each

iteration and then after reaching the modeling time set in step 16 the calculated temperatures as well as the airflow are sent to print out.

A computer code was developed in ANSI-C programming language. The computational runs were executed on a computing platform with an Intel Core i5-10300H processor with 2.5 GHz and 16 GB of RAM on a GNU/Linux operating system (Ubuntu 20.04 64-bit).

3.2 Verification of Conduction Heat Transfer in Phase Change Materials

The numerical solutions and data reported by Solomon [12] and Arici et al. [13] using the C_{P-eff} method were considered for the verification process. The addressed problems evaluated the heat conduction behavior of a PCM in the x -direction under first-class boundary conditions. The properties of the PCM are shown in Table 1, while the geometrical characteristics and boundary conditions are shown in Fig. 2.

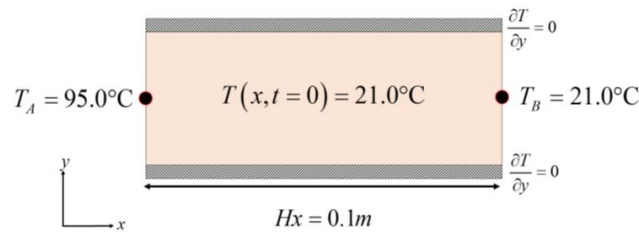


Fig. 2. Physical model for verification problem reported by Solomon [12]

Table 1 shows that the temperature interval between phases is zero, which is not applicable for the effective C_P method. Therefore, based on the literature's recommendation [14], a $\Delta T = 0.5^\circ\text{C}$ was considered to consider the phase change process. As for the number of elements considered to generate the comparison profile, $N_x = 50$ was considered.

Table 1. PCM properties

Solid phase	Liquid phase	Phase change enthalpy
$\lambda_{sol} = 0.15 \text{ W/mK}$	$\lambda_{liq} = 0.15 \text{ W/mK}$	$h_{ls} = 247000.0 \text{ J/kg}$
$C_{P-sol} = 2210.0 \text{ J/kgK}$	$C_{P-liq} = 2010.0 \text{ J/kgK}$	
$P_{sol} = 856.0 \text{ kg/m}^3$	$P_{liq} = 778.0 \text{ kg/m}^3$	
$T_{sol} = 36.7^\circ\text{C}$	$T_{liq} = 36.7^\circ\text{C}$	

The temperature profile of the reported solution was compared when the system reached a modeling time of 3600s (1 hour, considering a $\Delta t = 1\text{s}$). Fig. 3 shows the results of comparing the present solution and the solutions reported in the literature.

10

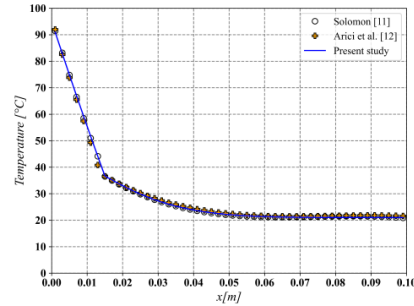


Fig. 3. Temperature profiles

Fig. 3 shows that the temperature profiles of the proposed model present a similar behavior to the solutions reported in the literature. Like the numerical result of Arici et al. [13], the most noticeable difference is found in the region where a temperature close to the phase change region is recorded due to the model's approximation. The maximum percentage difference obtained for the exact solution is 2.15% [12]. It was established that the model and methodology developed for the study of conduction heat transfer in PCM are satisfactory.

3.3 Problem features

The study comprises the annual evaluation of the ventilation capacity of the SC-SoCh under the hot-humid climate conditions of the city of Villahermosa, Mexico. Therefore, the climatic data collected for one year by the meteorological station of the Comisión Nacional de Agua (CONAGUA) corresponding to 2018 were obtained. Subsequently, each month's warmest and coldest days were selected for the evaluation of the passive system with the mathematical model developed. Figure 4 shows the climatic data behavior for the 24 days selected to evaluate the SC-SoCh. The variables considered for the developed model are incident solar radiation, outdoor temperature, wind speed, relative humidity, and atmospheric pressure. Fig. 4.a presents the incident solar radiation decomposed into different orientations. The results section describes the behavior of the SC-SoCh variables, considering the incident solar radiation for the respective SC-SoCh orientation.

The time step for the numerical solution was $\Delta t=5s$. A total of three-day modeling was carried out for each day of the 24 days selected for the whole year to achieve independence of the initial condition in the values of temperature and airflow induced by the passive system; this means that for each warm and cold day, two additional days were evaluated to obtain a behavior independent of the initial condition. The outdoor temperature (T_{ext}) value was used as the initial temperature condition for each modeling day.

The SC-SoCh was oriented to the West. This orientation had high incident solar radiation rates necessary to operate these passive systems.

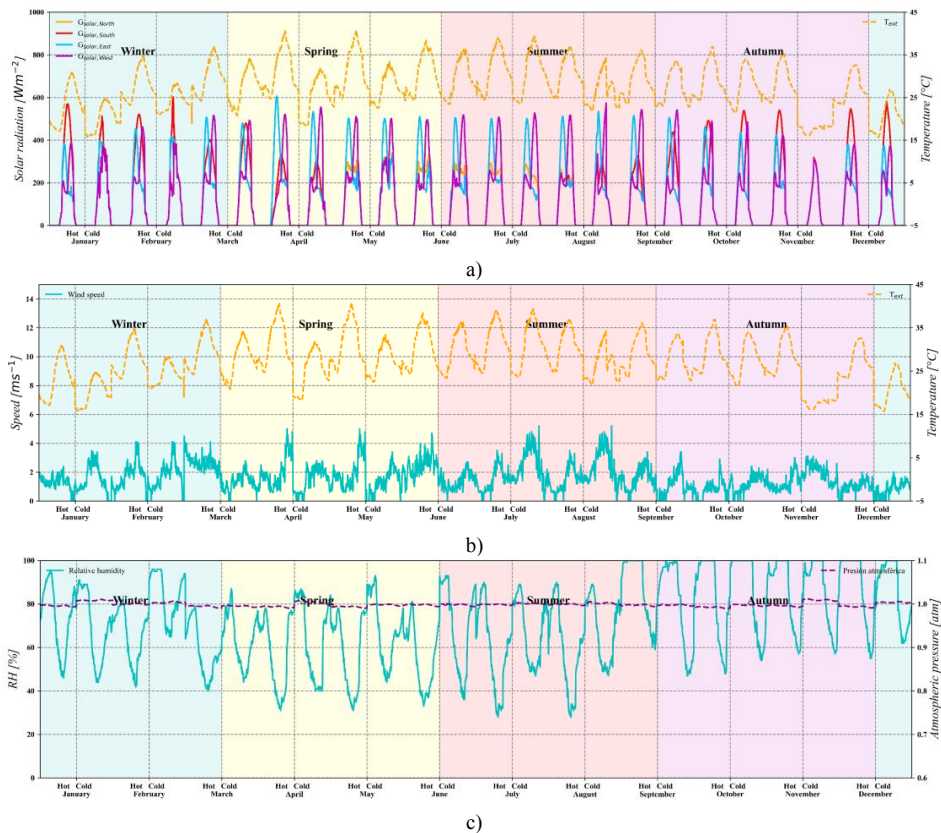


Fig. 4. Climate data: a) solar radiation and ambient temperature, b) wind speed, c) relative humidity and atmospheric pressure.

The Rubitherm RT42 PCM was used for this study [15]. Table 2 shows the materials and PCM RT42 properties used. The election of RT42 PCM was based on the feasibility of acquiring any PCM of different brands with properties like RT42 for building applications.

12

Table 2. Material properties

Glass cover	Absorber plate (aluminum) painted with matte black	Expanded polystyrene (thermal insulation)
Hx = 0.006 m $\lambda = 1.40 \text{ W}(\text{kg}^\circ\text{C})^{-1}$ $C_p = 750.0 \text{ J}(\text{kg}^\circ\text{C})^{-1}$ $\rho = 2500.0 \text{ kg m}^{-3}$ $\varepsilon = 0.840$ $\alpha^* = 0.076$ $\tau^* = 0.849$	Hx = 0.0015875 m $\lambda = 177.0 \text{ W}(\text{kg}^\circ\text{C})^{-1}$ $C_p = 875.0 \text{ J}(\text{kg}^\circ\text{C})^{-1}$ $\rho = 2770.0 \text{ kg m}^{-3}$ $\varepsilon = 0.9$ $\alpha^* = 0.97$	Hx = 0.025 m $\lambda = 0.0001T + 0.0262 \text{ W}(\text{kg}^\circ\text{C})^{-1}$ $C_p = 1210.0 \text{ J}(\text{kg}^\circ\text{C})^{-1}$ $\rho = 21.0 \text{ kg m}^{-3}$ $\varepsilon = 0.82$
Air channel	PCM RT42	Additional information
Hx = 0.15 m $\lambda, C_p, \rho = \text{Empirical relations [16]}$	Hx = 0.025 m $\lambda = 0.20 \text{ W}(\text{kg}^\circ\text{C})^{-1}$ $C_p = 2000.0 \text{ J}(\text{kg}^\circ\text{C})^{-1}$ $\rho = 880.0\text{-}770.0 \text{ kg m}^{-3}$ $T_{\text{melting}} = 38.0\text{-}43.0 \text{ }^\circ\text{C}$ $h = 164000 \text{ J kg}^{-1}$	Hy = 2.0m Hz = 1.0 m $g = 9.81 \text{ ms}^{-2}$ $h_{\text{int}} = 10.0 \text{ W m}^{-2} \text{ }^\circ\text{C}^{-1}$ [10] $h_{\text{ext}} = 2.8 + 3.0V_{\text{wind}} \text{ W m}^{-2} \text{ }^\circ\text{C}^{-1}$ [17] Orientation: West $\Delta t = 5 \text{ seconds}$

4 Results and discussion

The information obtained during the simulation of a year of climatic conditions of Villahermosa was summarized in Fig. 5. Fig. 5 shows the daily behavior of the mass flow rate, volumetric flow rate, and temperature of each envelope of SC-SoCh under Villahermosa's hot-humid climate. Fig. 5(a) shows that the behavior of the mass flow rate reveals a similar tendency to the incident solar radiation during the first half-day of the solar chimney functionality. The SC-SoCh was oriented to the west; therefore, during the first half of the day, the solar radiation received and absorbed by the absorber plate corresponds to the diffuse solar radiation component. After noon, the most significant energy accumulation in the PCM occurs due to direct and diffuse radiation falling on the glass cover. The study considered a west orientation due to the more significant accumulation of solar radiation during the second half of the day to obtain a longer energy accumulation time and release of thermal energy to induce natural ventilation at night.

The highest airflows generated by the SC-SoCh occurred after noon. This is produced by the thermal inertia of the PCM. In the incident solar radiation decreased, the temperatures of the metal plate in contact with the fluid in the air channel decreased slowly compared to the incident solar radiation. The temperature decreasing was prolonged in a way that the temperature of the metal container of the PCM achieved the thermal equilibrium with outdoor temperature after midnight; therefore, the conditions inside the SC-SoCh were adequate to maintain the operation of the active system and to induce natural ventilation for several hours during the night. In this way, the SC-

SoCh maintained an operating time of up to 23 hours during spring and summer and 18 hours during autumn and winter. This feature is desirable for hot-humid regions because residential require more natural ventilation at night when the dwellers sleep, and closed doors and windows minimize cross ventilation. In addition, the SC-SoCh can be used as a passive system to help thermal comfort; the present study focused on ventilation analysis. Therefore, the study of thermal loads must be conducted in an independent study.

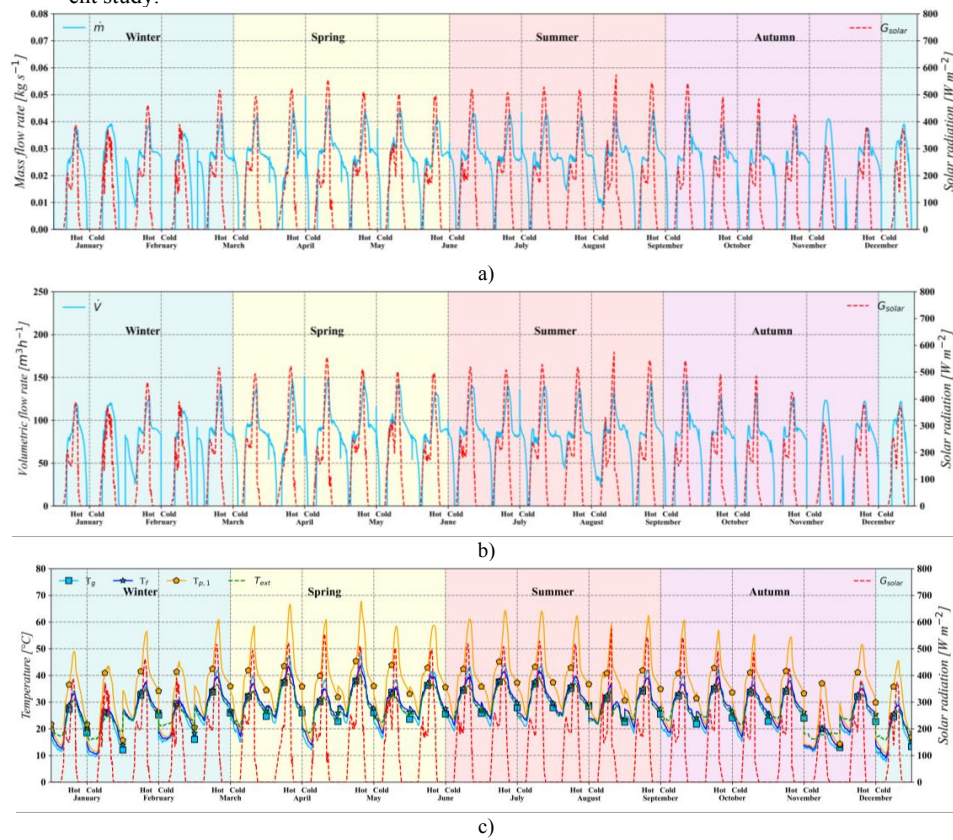


Fig. 5. Annual evaluation of SC-SoCh: a) mass flow rate, b) volumetric flow rate, c) temperature of SC-SoCh

The volumetric flow rate generated in the year exceeded $115 \text{ m}^3 \text{h}^{-1}$ as a minimum and reached airflows close to $148 \text{ m}^3 \text{h}^{-1}$; the airflow induced by the SC-SoCh was equivalent to the required ventilation demand per dwelling unit established by ANSI/ASHRAE 62.2-2019 for a space of 18 to 36 m^2 [18]. The standard states the area dimensions of a dwelling unit based on the average height of the room and enclosure. The present study focused on the SC-SoCh performance with a PCM; therefore, the airflows determined were compared with the expectation of ventilation provided by

14

active systems as fans. In this sense, the proposed dimensions in this study were enough to satisfy the need for ventilation for a residential building of previous specifications. It is necessary to evaluate in an individual study the potential benefits of increasing the height of the channel, air gap, or a different masonry material for the absorber plate. The RT42 PCM and orientation of SC-SoCh are vital to maximize energy storage for increasing natural ventilation.

In terms of the amount of energy that the performance of the SC-SoCh permitted to save compared to a conventional mechanical system to provide ventilation to the interior of a building, the analysis revealed that using a PCM RT42 with the SC-SoCh of the characteristics shown in Table 2, the equivalent energy consumption is 152.25 kWh in a year. The energy consumption of SC-SoCh with PCM is the amount of energy a conventional mechanical system requires to provide the same amount of ventilation as the SC-SoCh; the calculation considered the extrapolation of hot and cold days results obtained for every month in the year. Similarly, an analysis of the equivalent amount of kgCO₂ emitted by a conventional mechanical system to the atmosphere to satisfy the ventilation induced by the SC-SoCh was carried out, which was 64.40 kgCO₂ in a whole year. The estimation was made considering that the airflow was used for natural ventilation purposes and did not include the effect of thermal loads on indoor comfort because solar chimneys have also been used to improve thermal comfort conditions for residents. Therefore, an extensive analysis of energy consumption and kgCO₂ emitted for providing natural ventilation and thermal comfort is necessary to reveal the actual contribution of SC-SoCh to buildings. The results only focused on the ventilation needs, although the results enforce the feasibility of implementing solar chimney-like passive systems for thermal comfort solutions.

Regarding the recuperation time of initial construction and maintenance cost of SC-SoCh with an RT42 PCM, the analysis showed that it is required from 50 to 60 years of operation time of SC-SoCh. This result was obtained because the cost of a gallon of RT42 PCM is higher than the other materials used to build a solar chimney. Therefore, it is necessary to find the optimal SC-SoCh configuration to increase the ventilation capacities and analyze the contribution to thermal comfort, which reveals the potential benefits of this passive system.

5 Conclusions

This article presented a performance annual evaluation of a single air-channel solar chimney with PCM in the context of energy efficiency analysis.

The proposed energy balance methodology solved the heat transfer in an unsteady state for the SC-SoCh with a PCM in the absorber wall under warm-humid climate conditions to provide natural ventilation inside buildings. The studied system considered climatic data for 2018 provided by the Comisión Nacional de Agua of Mexico.

The experimental validation showed the ability of the SC-SoCh with a PCM to supply ventilation during both day and night hours in operating periods from 18 to 23 hours, providing a desirable aspect of a passive system that operates only through incident solar radiation.

The main results indicate that the SC-SoCh is an ecological alternative to satisfy the ventilation needs in buildings. The configuration studied provided natural ventilation for spaces of 18 to 36 m². At the same time, its use represents an energy saving of up to 152.25 kWh, reducing up to 64.40 kg of CO₂ emitted into the environment. Although the recuperation time of build cost and maintenance were elevated, it is necessary to evaluate the potential benefits for improving thermal comfort and adequate dimensions to reduce cost, increase natural ventilation, and maintain the operativity over the years of SC-SoCh.

The main lines for future work are oriented to extend the proposed GEB methodology to an extensive parametric study to determine the capabilities of the SC-SoCh in combination with different PCM materials. Likewise, the GEB method can address aspects of interest, i.e., the variation of the dimensions and materials that form the channel, the evaluation of the effect of other orientations, the evaluation of other massive materials to know the impact of the solar chimneys on the thermal loads of the building and to extend the study to different climatic conditions of the República Mexicana to know the ventilation potential.

Nomenclature

A	Area [m ²]	δ	Convergence criterium [-]
ACH	Air change per hour [h ⁻¹]	ε	Emissivity [-]
C_p	Specific heat, effective specific heat [J (kgK) ⁻¹]	λ	Thermal conductivity [W (mK) ⁻¹]
$C_{p-effect}$		ρ	Density [kg m ⁻³]
f	Liquid fraction [-]	τ^*	Transmissibility [-]
G_{solar}	Solar radiation [W m ⁻²]		
h_{conv}	Convective heat transfer coefficient [W m ⁻² K ⁻¹]	Subscripts	
h_{ls}	Enthalpy [J kg ⁻¹]	<i>conv</i>	Convective
H_x	x-axis distance [m]	<i>cond</i>	Conductive
H_y	y-axis distance [m]	<i>ext</i>	Exterior
H_z	z-axis distance [m]	<i>f</i>	Fluid
$kgCO_2$	CO ₂ emissions [kg]	<i>ij</i>	Node <i>x</i> and <i>y</i>
\dot{m}	Mass flow rate [kg s ⁻¹]	<i>in</i>	Indoor
N_x, N_y	Nodes [-]	<i>int</i>	Inlet
q	Heat flux [W m ⁻²]	<i>liq</i>	Liquid
T	Temperature [°C]	<i>out</i>	Outlet
t	Time [s]	<i>rad</i>	Radiative
\dot{V}	Volumetric flow rate [m ³ h ⁻¹]	<i>sol</i>	Solid
x, y, z	x-axis, y-axis, z-axis	<i>sky</i>	Sky
α^*	Absortivity [-]	<i>wind</i>	Wind
Δ	Difference [-]		

References

1. Secretaría de Energía: Programa para el Desarrollo del Sistema Eléctrico Nacional 2022-2036". México, (2022)
2. Instituto Nacional de Estadística y Geografía: Primera Encuesta Nacional sobre consumo de energéticos en viviendas particulares (ENCEVI). México (2018)
3. Abdeen, A., Serageldin, A.A., Ibrahim, M.G.E., El-Zafarany, A., Ookawara, S., Murata, R.: Solar chimney optimization for enhancing thermal comfort in Egypt: An experimental and numerical study. *Solar Energy* **180**, 524-536 (2019)
4. Su, C., Li, X.: Numerical study on performance of solar chimney for building ventilation. *ASME 2012 Summer Heat Transfer Conference*, pp. 1049-1055 (2012)
5. Martí-Herrero, J., Heras-Celemin, M.R.: Dynamic physical model for a solar chimney. *Solar Energy* **81**, 614-622 (2007)
6. Kaneko, Y., Sagara, K., Yamanaka, H., Kotani, T., Sharma, S.D.: Ventilation performance of solar chimney with built-in latent heat storage. *Proceedings of 10th international conf. On thermal energy storage, USA: ECOSTOCK (2006)*
7. Huang, S., Lu, J., Li, Y., Xie, L., Yang, L., Cheng, Y., Chen, S., Zeng, L., Li, W., Zhang, Y., Wang, L.: Experimental study on the influence of PCM container height on heat transfer characteristics under constant heat flux condition. *Applied Thermal Engineering* **172**, 115159 (2020).
8. Frutos-Dordelly, J.C., Mankibi, M.E., Roccamena, L., Remion, G., Arce, J.: Experimental análisis of a PCM integrated solar chimney under laboratory conditions. *Solar Energy* **188**, 1332-1348 (2019).
9. Vargas-López, R., Xamán, J., Hernández-Pérez, I., Arce, J., Zavala-Guillén, I., Jiménez, M.J., Heras, M.R.: Mathematical models of solar chimneys with a phase change material for ventilation of buildings: A review using global energy balance. *Energy* **170**, 683-708 (2019).
10. Ong, K.S.: A mathematical model of a solar chimney. *Renewable Energy* **28**, 1047-1060 (2003).
11. Torres-Aguilar, C.E., Moreno-Bernal, P., Xamán, J., Nesmachnow, S., Cisneros-Villalobos, L.: Global energy balances for energy analysis in buildings. *Proceedings of the V Ibero-American Congress of Smart Cities ICSC-CITIES, Ecuador, (2022)*.
12. Solomon, A.D.: An easily computable solution to a two-phase Stefan problem. *Solar Energy* **23**, 525-528 (1979).
13. Arici, M., Bilgin, F., Nizetic, S., Papadopoulos, A.M.: Phase change material based cooling of photovoltaic panel: A simplified numerical model for the optimization of the phase change material layer and general economic evaluation. *Journal of Cleaner Production*, **189**, 738-745 (2018).
14. Morgan, K., Lewis, R.W., Zienkiewicz, C.: An improved algorithm for heat conduction problems with phase change. *International Journal for Numerical Methods in Engineering* **12**, 1191-1195 (1978).
15. Rubitherm Technologies GmbH: Data sheet RT42 (2020).
16. Arce, J., Xamán, J.P., Alvarez, G., Jiménez, M.J., Enriquez, R., Heras, M.R.: A Simulation of the Thermal Performance of a Small Solar Chimney Already Installed in a Building. *Journal of Solar Energy Engineering* **135**, 011005-1 – 011005-10 (2013).
17. McAdams, W., Heat Transmission. McGraw-Hill, (1954).
18. ANSI/ASHRAE 62.2-2019: Ventilation for Acceptable Indoor Air Quality in Residential Buildings (2019).

Energy management in the CEDER- CIEMAT microgrid based on the time response of the distributed energy storage systems.

Luis Alvira Ballano¹, Oscar Izquierdo-Monge¹, Angel Hernandez Jimenez¹; Paula Peña Carro¹

¹ CEDER-CIEMAT, Autovía de Navarra A15 salida 56, 422290 Lubia (Soria), España, P.P.C.: paula.pena@ciemat.es; A.H.J.: angel.hernandez@ciemat.es, O.I.M.: oscar.izquierdo@ciemat.es

Abstract: This paper presents a use case for the energy management in a smart microgrid based on the time response of the dispatchable generation sources and storage systems. The main goals of the deployed energy management strategy are the elimination of power peaks, the optimization performance of the microgrid, taking into special consideration economic factors during the operation, and reduction of the energy consumption from the distribution network. The use case is shown at the CEDER-CIEMAT (Centro Desarrollo de Energías Renovables – Centro de Investigaciones Energéticas, Medioambientales y Tecnológicas), where the described energy management strategy has been implemented in real-time, achieving the elimination of consumption peaks while reducing the consumption from the distribution network, lowering the total electricity bill (aprox. 2000 € per year).

Keywords: Energy management strategy Smart Microgrid (SMG), time response, power peaks, Distributed Energy Storage Systems (DESS).

1 Introduction

The energy transition towards a cleaner and more sustainable is being led and driven by the rapid development and deployment of Renewable Energies (RE)[1]. This is leading to major changes in the structure of existing energy systems. The emergence of RE has not only brought about a profound change in the energy mix of countries in terms of electricity generation but has also changed the way in which this energy is generated, distributed and consumed [2]. In response to this new scenario, microgrids are presented as a key element in the design and configuration of this new electricity system [3]. Microgrids ensure a continuous and secure supply of electricity through Distributed Energy Resource (DER) based on renewable generation and Distributed Energy Storage Systems (DESS) in those places where they are implemented. Furthermore, the integration of new communication and information technologies as well as the use of

Artificial Intelligence (AI) and the Internet Of Things (IoT) has led to a conceptual evolution: Smart Microgrids (SMG)[4]. However, the control and operation of SMGs is subject to the inherent limitations of renewable energies [5] and to the various phenomena that can originate, either from the grid or generated by the microgrid itself [6], [7]. This article is focused on analysing the phenomenon of imbalance between generation and demand that arises due to prolonged consumption peaks [8]. Consequently, it will be necessary to develop energy management and control strategies in SMGs to ensure proper operation in these scenarios. These methodologies will vary depending on the characteristics and configuration of each SMG: needs, limitations, available resources, network topology... [9], [10] and/or the criteria used by each manager. Even so, all these strategies will ultimately aim to guarantee the energy balance between generation and demand, maximising the efficiency of the system [11]. On this basis, the SMG energy management is presented as a complex, non-linear and non-convex problem, often requiring the implementation of control, management and optimisation algorithms to perform this task according to the defined strategies and priorities. However, the application of these complex and highly sophisticated systems does not necessarily guarantee an overall improvement in the performance or economic viability, and it is incumbent upon the SMG manager to formulate and execute those strategies.

Most management strategies are focused on the optimisation of different economic aspects. The application of these strategies seeks to maximise the efficiency of the energy system to be managed while minimising the target economic parameters. One of the most commonly used indicators in SMG management strategies is the operating cost. Depending on the characteristics of each SMG, minimising operating costs can be achieved through different courses of action. At [12] the operating cost is minimised by scheduling loads based on predictions of both consumption and generation. On the other hand, in [13] generation sources are acted upon according to the existing operating conditions. Consequently, the optimisation of operating costs is achieved by implementing a management methodology that efficiently coordinates the existing energy resources in the microgrid. Another way to optimise costs is presented in [14]. In this case, operating costs are minimised by reducing fossil fuel-based generation. However, Energy Management Systems (EMS) based on economic criteria often include a convergence of different indicators and metrics to maximise optimisation. At [15] the operating cost is complemented with the Cost Of Energy (COE) and the Net Present Cost (NPC) to determine the best configuration of the SMG according to these indicators. Subsequently, the COE is used as the main management criterion.

The COE is used in SMG management strategies to compare their performance with respect to the prices set by the national electricity tariff. Depending on the pricing period, these energy management systems will either connect the SMG to the grid during low pricing periods or seek to maximise the fulfilment of the microgrid's energy demand through the use of the deployed DERs and DESSs during high pricing periods [16]. This management strategy that focuses on making decisions according to market price fluctuations is referred to as energy arbitrage [17]. By applying the indicators outlined above in these EMSs, significant increases in the microgrids energy efficiency are obtained, thereby resulting in economic benefits [18].

3

Load monitoring is an energy management strategy aimed at maintaining the stability of the microgrid. The grid operator performs a real-time tracking of the consumption variations by the power-demanding equipment in the SMG. In the event of variations, the grid operator will respond by providing support by means of DER and DESS to compensate for this imbalance and maintain the stability of the microgrid [19]. Preserving the match between generation and demand is an indispensable condition in isolated microgrids [20] as they have limited response capacity. In the case of grid-connected microgrids, the implementation of the load monitoring strategy is usually integrated in the EMS along with other criteria such as cost minimisation, compliance with consumption forecasts, etc. [21] or the optimisation of specific equipment such as electric vehicles (EVs)[22].

Real-time load monitoring makes it possible to identify the appearance of consumption peaks that deviate from the typical demand profile. For this reason, the aforementioned management methodology described is complemented by the so-called peak shaving strategy. This energy management strategy is based on the total elimination or, at least, the reduction of consumption peaks through the use of the energy available in the microgrid's DESSs [23]. Due to the magnitude and duration of these phenomena, consumption peaks pose a risk to the stability of the microgrid by very significantly unbalancing the generation-demand ratio [24]. In addition, they tend to occur in marked time windows, which coincide with periods of high tariffs. Consequently, consumption peaks imply a large increase in the cost of SMG operation by obtaining this power differential from the grid. Thus, this management strategy is particularly interesting in technical and economic terms, avoiding grid collapse and the costs associated with increased consumption in periods when the cost of electricity is high [25]. Therefore, peak shaving is a management strategy frequently implemented in a complementary way in EMSs such as the case described in [26] where the objective is to minimise COE and operating cost. It is worth highlighting the fact that batteries are the technology used in DESSs to perform peak shaving. This is the solution present in almost all the use cases, similar to what has been done in [27], [28].

This article presents an energy management for a microgrid use case according to the response time of the DER and the available DESSs. The main contribution of this proposal lies in the energy and economic optimisation of the microgrid, giving preference in energy management response to equipment that allows a faster power supply, reducing grid consumption and contributing to the elimination of consumption peaks above the normal power in periods of high tariffs. This energy management is carried out in real time, monitoring the energy values of the microgrid through open-source software (Home Assistant and Node-Red). Section 3 shows the development in the application of this energy management in CEDER's smart microgrid, and the main conclusions are presented in section 4.

2 Materials and methods

In order to effectively implement energy management in alignment with the criteria and objectives outlined in the introduction the first requirement is to identify and

characterise the equipment to be coordinated. Below is a brief description of the loads, the distributed generation elements and the distributed electrical storages present in the CEDER smart microgrid.

2.1 Loads

The loads distributed in the CEDER microgrid have different characteristics and needs. In its daily operation, the main loads correspond to the various equipment in the buildings connected to the SMG. These include computers, lighting, boilers, workshops, laboratories... In parallel, there are loads with different consumption patterns. These include the EVs connected to the SMG charging points.

In addition, CEDER has facilities and equipment for the study and research of biomass (considerations external to this article). These installations require large amounts of energy for their operation. This condition will be responsible for the variability in CEDER's consumption profile, as well as for the appearance of demand peaks during marked periods in accordance with the activities carried out in these areas. Between all of these loads, the most significant for this article is the pilot plant for granulometric reduction and biomass classification. With electrical demands that can reach peak consumption of close to 100 kW, the operation of this facility requires the active intervention of the microgrid operator to ensure proper energy management. This process includes the control and monitoring of the energy demands for this particular load, which is a critical part of the overall energy management of CEDER's SMG.

2.2 Distributed generation elements

The micro-grid at CEDER is composed of the following distributed generation elements:

- Wind power generation systems: A total of 5 three-blade horizontal axis wind turbines are connected to the microgrid with a total capacity of 161.2kW.
- Solar photovoltaic (PV) power generation systems: There are 11 PV systems. The installed power connected to the microgrid is 168.5 kW.

It should be mentioned that the operating regime of the CEDER smart microgrid is connected to the distribution grid, with a base power of 50 kW and a contracted power of 135 kW. Therefore, the power input from the grid will be considered in the energy management developed.

2.3 Distributed storage elements

The center has different energy storage technologies that provide flexibility and responsiveness to energy management in the different scenarios that may arise.

5

In this article, the DESS used for energy management will be the micro-hydro plant together with the Pb-acid PEPA I, Pb-acid PEPA II and LFP LECA systems, which can cope with peak energy demands of up to 101.2 kWh.

- Micro hydroelectric power plant. It consists of a Pelton turbine and a 40 kW three-phase asynchronous generator, 4 centrifugal pumps of 7.5 kW power (each) and three water storage tanks with approximate capacities of: 500 m³ mother tank, 1500 m³ upper tank and 1900 m³ lower tank. The difference in elevation between the tanks is 70 metres.
- Pb-acid PEPA I: Battery bank consisting of 120 2 V (240 V) Tudor Pb-acid 7EAN100T batteries connected to the microgrid via a DC/ACe 50 kW inverter. It has a capacity of 1080 Ah (C₁₂₀).
- Pb- acid PEPA II: Tudor Pb-acid 5EAN70T 120-cup 2 V (240 V) battery bank. Connection to the SMG is via a 20 kW inverter. It has a capacity of 765 Ah (C₁₂₀).
- LFP LECA: Battery bank composed of 2 racks of 14 modules and 196 lithium ferro phosphate cells each. This battery bank is connected to the microgrid by means of a 33 kW inverter. It has a capacity of 50 Ah

2.4 Time response characterisation of distributed storage elements

The response of the DESS to different power setpoints is shown below, focusing the characterisation on the response times of the different equipment. This parameter will be the main criterion on which the design and approach to energy management implemented for the use case presented in section 3 is based.

Micro-hydro power plant

The turbine's maximum assignable power setpoint is limited to 35 kW due to the operating conditions and it can provide this power for 5 hours. The total time period required for turbine start-up is 2:33 minutes. After this time, the turbine starts to follow the given power setpoint. A summary table with the different characterisations carried out is shown below.

Table 1. Characterisation of turbine time response.

Turbine				
Type of characterisation	Process	Turbine status	Power setpoint (kW)	Time to setpoint
From 0kW to setpoint power	Start-up	OFF	10 (from 0 to 10)	0:03:09
		OFF	20 (from 0 to 20)	0:03:12
		OFF	30 (0 to 30)	0:03:56
		OFF	35 (0 to 35)	0:04:31

Stepwise	Setpoint adjustment	ON	From 0 to 10	0:00:36
		ON	From 10 to 20	0:00:42
		ON	From 20 to 30	0:01:03
		ON	From 30 to 35	0:01:55

Pb-acid PEPA I

Figure 1 shows the response of this battery bank (orange line) to different power setpoints (blue line), showing the inverter start-up time, as well as the period required to reach the different power setpoints assigned in each characterisation.

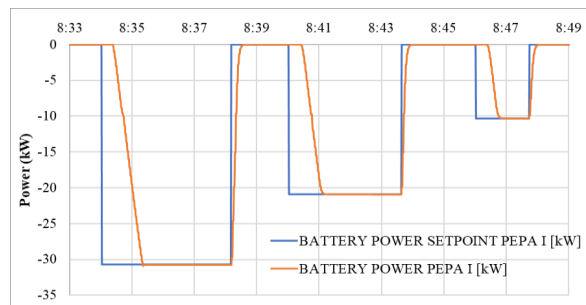


Fig. 1. Characterisation of PEPA I Pb-acid time response.

It can be seen that the response time to reach the maximum extractable power setpoint is 1:20 minutes, supplying up to 30 kW. This value can be supplied uninterruptedly for a period of 2 hours.

It should be noted that, by convention in the configuration, the discharge of the Pb-acid batteries PEPA I and PEPA II is indicated with a negative sign. However, this convention does not extend to the LFP batteries of the LECA or the turbine, taking positive values in the periods of power supply to the microgrid.

Pb-acid PEPA II

The maximum extractable power of this battery bank set is 16.2 kW, which can be maintained for a period of 1 hour. At this power setpoint, the time required to reach this value is 58 seconds. As this is a storage system that relies on the same technology as the one previously outlined in figure 1, the characterisation of the response of this storage system has not been plotted as it has a similar behaviour.

LFP LECA

The response time of this DESS is noticeably slower compared to other electrochemical storage systems. The start-up process includes closing the BMS contactors, magnetising the inverter and connecting it to the SMG, requiring a time of 2:31 minutes before the power setpoint can be given. However, once switched on, this DESS allows a quick adjustment of the delivered power values (with positive sign), in the range of ten

7

seconds. The total response time from switch-off to the maximum removable power setpoint of 20 kW is 2:46 minutes and can be supplied uninterruptedly for 1 hour.

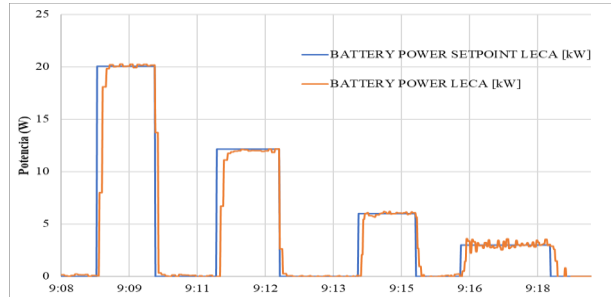


Fig 2. Characterisation of LFP LECA time response.

After these characterisations, it should be noted that the shortest response time corresponds to the Pb-acid PEPA II equipment. However, considering the power requirements during consumption peaks and their magnitude, in order to provide greater flexibility in energy management, the DESS that will be used first will be the PEPA I Pb-acid bank.

3 Energy management applied to a use case

3.1 Energy management strategy approach

The use case shown aims to eliminate CEDER consumption peaks through the use of the DESS previously characterised in section 2, maintaining total network consumption levels within the usual values prior to the existence of demand peaks. To this end, the energy management strategy prioritises the shortest response time as a criterion for prioritising the storage systems used to compensate for peak consumption. In this way, the aim is to maximise the performance of the microgrid by controlling total grid consumption and eliminating consumption peaks in the shortest possible period of time.

With reference to the consumption profile shown in figure 3, at the start of the working day, the power demand of CEDER loads (computers, equipment, lighting, etc.) ranges between values of around 85 kW and 90 kW. Similarly, under normal conditions, demands can reach values of around 95 kW. Therefore, by applying the energy management strategies and criteria previously described, the objective is to eliminate the consumption peaks generated in CEDER in order to maintain a stable and controlled consumption profile.

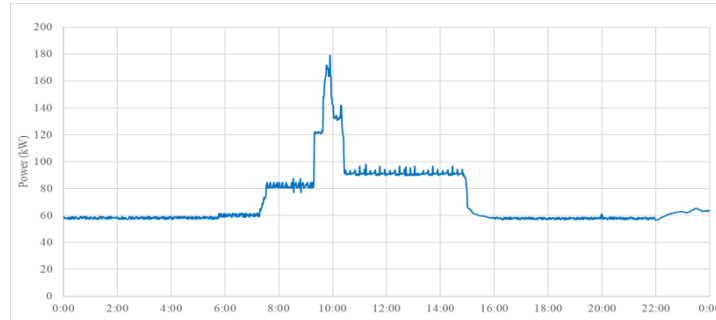


Fig. 3. Total consumption profile of CEDER for one day.

Total consumption profile of the CEDER for one day.

Depending on the total power demand in the centre, the following criteria are established for the activation of the DESS:

- From shutdown. The systems that allow the fastest response will be the first to be used. Using the characterisations shown in section 2, the hierarchy of operation is as follows for the batteries: PEPA I > PEPA II > LFP. With respect to the micro-hydro power plant assembly (hereafter referred to as the turbine), at the instant that a lasting consumption peak is identified, due to machinery or equipment demanding energy for a prolonged time, it will be started to operate at a continuous regime according to a given setpoint value acting as a "base generator".
- The following demand limits are established as criteria for switching on the different DESS:
 - From 95k W up to 135 kW: start-up of the PEPA I batteries and turbine.
 - Exceeding 135 kW: increase of the turbine setpoint to its maximum.
 - Exceeding 150 kW. start-up of PEPA II batteries.
 - Exceeding 160 kW: starting LFP batteries from LECA.
- With all DESS switched on. For energy management, the equipment that allows the fastest adjustment of the delivered power will be used, allowing the compensation of demand variations in the shortest possible period of time. Thus, the hierarchy of operation is as follows, being inverse to the scenario with the DESS off: LFP > PEPA II > PEPA I.

Figure 4 shows the energy control and management process that the microgrid operator will carry out in real time and continuously monitoring the loads. The identification of a consumption peak will initiate the control process for the compensation of the consumption peak. After its completion, the process will be constantly repeated to ensure the stability and correct energy management of the microgrid.

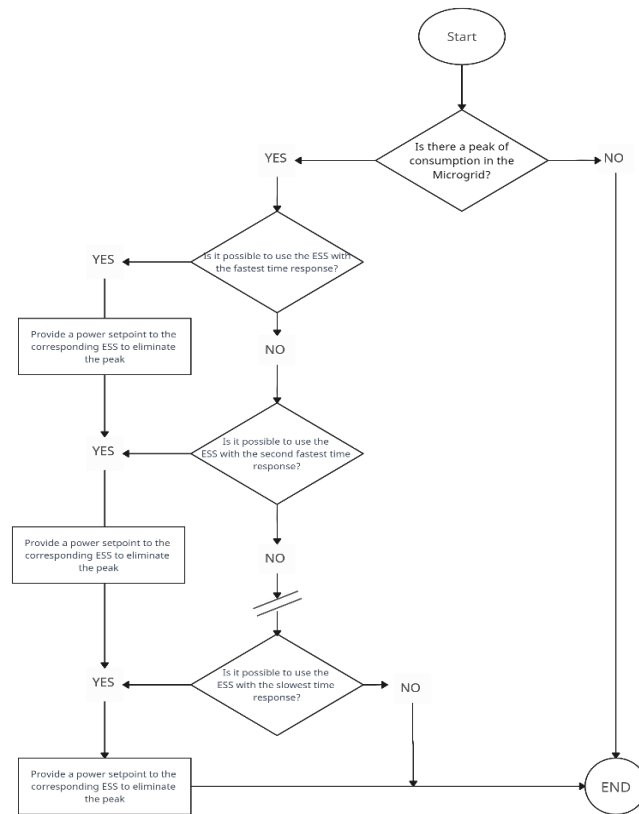


Fig. 4. Energy management process of DESS according to their response time.

It should be clarified that, although PEPA II has a shorter response time, priority is given to switching on PEPA I as it has a greater capacity to supply power and can cope with larger peaks. This decision results in a significant increase in management flexibility and efficiency of the microgrid.

3.2 Implementation of the energy management strategy

This section describes the real-time decision making carried out during the energy management process for the elimination of peak consumption as shown in figure 3.

The consumption increase began to be pronounced at 9:18. Noting this increase in demand, which leads to an increase in consumption from the grid, the suitable DESSs are activated to counteract it. At 9:18, the switching on order is given PEPA I with the maximum power setpoint, 30 kW, with prior warning from the operator of the

corresponding demanding equipment: the pilot plant for granulometric reduction and biomass classification. Similarly, in anticipation of the high consumption that may arise as a result of the demands of this equipment it is decided to give the order to start up the turbine as a whole at the same time as PEPA I.

As shown in section 2, the characterisation of the start-up time of the Pb-acid batteries of PEPA I requires an interval of 1:19 minutes to reach the setpoint. To the turbine start-up period, 2:33 minutes, must be added the time needed to reach the given setpoint of 30 kW, requiring a total of 3:56 minutes. Therefore, during this time, PEPA I is the DESS in charge of compensating the peak consumption. Once the turbine starts to follow the given setpoint, the power delivery by PEPA I will start to reduce proportionally to the power generated by the turbine.

Once the setpoint is reached, the turbine will act as a "base generator" in the elimination of peak consumption, continuously supplying 30 kW with the possibility of reaching up to a limit of 35 kW if necessary.

Between 9:20 and 9:37 the consumption values oscillate between maximum and minimum values of 123.4 kW and 120.2 kW. This oscillation is assumable using only the turbine. On the PEPA I side, with the turbine already operating at the specified value, a 0 kW setpoint is introduced to the batteries leaving the equipment running in stand-by. This decision ensures a high degree of flexibility in the management system: 30 kW PEPA I and 5 kW turbine, making it possible to respond to future deviations and increases in demand.

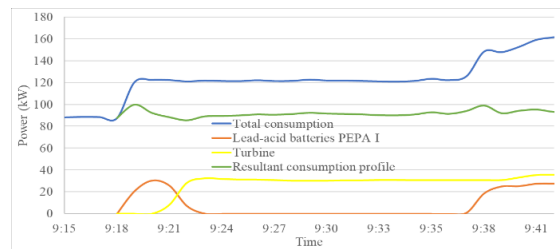


Fig. 5. Total consumption profile of CEDER for one day.

At 9:38 a further increase in demand occurs, requiring new setpoint commands to the PEPA I battery set. Taking advantage of the tens of seconds response of the Pb-acid batteries, the setpoint is adjusted in real time to compensate for the increased demand. However, the trend of increasing demand is accentuated at 9:39 by a significant jump in consumption exceeding 135 kW. This value is very significant as it is the upper limit of the power contracted by CEDER from the power distributor (Endesa). In case of not being compensated by the DESS, this would mean a sharp increase in the electric bill. Nevertheless, the PEPA I batteries are capable of responding to this increase by compensating the resulting effect on total grid consumption.

After evaluating this new consumption, it is decided to increase the setpoint of the "base generator" of the management, the turbine, to its maximum operating point, 35

11

kW. The turbine's power adjustment, requiring 1:55 minutes, is compensated by PEPA I to align the resulting profile with prescribed target limits.

At 9:41 the total demand of CEDER exceeds 150 kW, so the Pb-acid batteries of PEPA II are set to start up. Unlike the previous case, the new increases in consumption are mainly assumed by the power contribution obtained from the turbine while reaching the stabilisation values, reserving the power delivery margin by PEPA I if necessary.

As a result of this upward trend in power demand, at 9:43 the total CEDER consumption values surpass 160 kW demand, requiring the LFP batteries of the LECA to be started up. The start-up period of this equipment, which is notably superior to the other batteries equating to the turbine, amounting to a total period of 2:31 minutes. However, after this time all the DESSs will be started up and contributing to the compensation of the power peaks in consumption. With this operating scenario, the greatest possible flexibility of the EMS is achieved, being able to carry out efficient and fast power adjustments.

The total demand profile shows an increase in consumption that exceeds 170 kW at 9:46. However, as a result of having all the batteries delivering power and allowing rapid adjustments, these variations are of lesser magnitude in the overall grid consumption curve. The flexibility of the batteries allows to the EMS to keep the total grid consumption below 90 kW, presenting the following states at 9:55:

- PEPA I. It is delivering 30.7 kW. No margin of increase in deliverable power.
- PEPA II. It is delivering 10.1 kW. Deliverable power range from 6.1 kW to 16.2 kW.
- Turbine. It is delivering 35 kW. No margin of increase in deliverable power.
- LFP. It is delivering 5 kW. Deliverable power range from 15 kW to 20 kW.

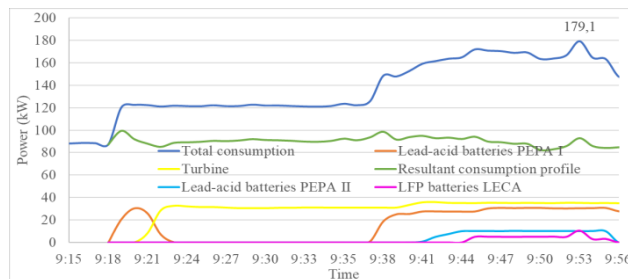


Fig. 6. Total consumption profile of CEDER for one day.

After the peak generated at 9:54, the biomass pilot plant operator reports that the most power-demanding operations have already been performed.

Over the course of 9:57 the total CEDER demands dropped considerably, stabilising at values close to 147 kW. When falling below 160 kW, analogously to the ignition criteria defined, a 0kW setpoint is given to the LFP. Similarly, as this demand was less than 150 kW, the setpoint for the PEPA II batteries was set at 0 kW, and the microgrid was managed with PEPA I and the turbine. Consequently, the necessary adjustments are made through variations in the power delivered by the PEPA I batteries, providing

between 10 kW and values close to 27.5 kW depending on the requirements of the microgrid.

In 10:21 the total demands of the centre drop below 130 kW. Considering various factors, including the consumption forecasts that mark the end of the consumption peak and the rapid compensation capacity of the batteries, with a rapid response reserve of +66.2 kW from stand-by, it is decided to give the order to turn off the turbine. Finally, at 10:26, the total demand of CEDER recovers values corresponding to operation under normal conditions and the peak consumption started at 9:18 can be considered to have ended. After this, the batteries can be switched off, starting the charging of the DESSs used if there exists surplus energy. Otherwise, this charge will be carried out by consuming from the grid during low tariff periods, i.e. at night.

The results from real-time actions in the described DESS are presented below. In figure 5 is depicted the different power delivery profiles of each DESS in accordance with the energy management strategy for the peak consumption elimination.

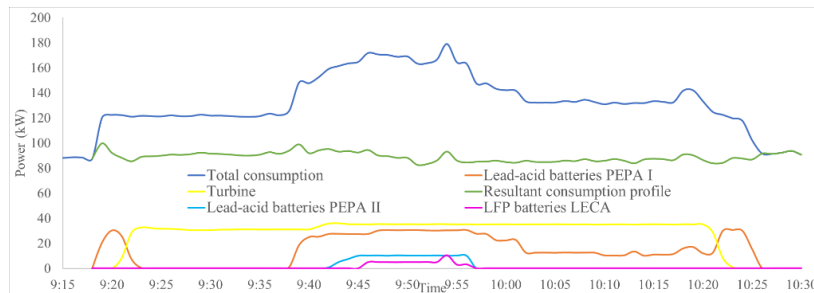


Fig. 7. Energy management responses of each DESS for peak load compensation.

As a result, the cumulative effect of these actions creates the resulting grid consumption curve displayed in red in figure 6. This total grid consumption is successfully kept within the predefined power range, between 85 kW and 90 kW, being only exceeded during moments corresponding to the start-up times of the DESS. The highlighted area in figure 6 represents the total power savings achieved through the elimination of the peak consumption.

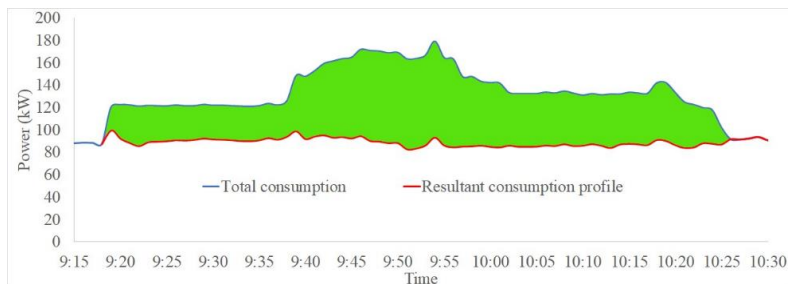


Fig. 8. Energy savings (green) using this methodology.

13

4 Conclusions

The implementation of an energy management strategy for the elimination of consumption peaks in the CEDER microgrid satisfies the energy and economic optimisation objectives set.

This is reflected in the total consumption profile of the grid after compensation, shown in figure 6. It can be seen that this new curve follows the behaviour of the existing total consumption in CEDER when making real-time adjustments to the power delivery of the DESSs, with a delay in the response of tens of seconds due to the criteria established based on the response times developed throughout the article. Furthermore, it can be seen that the variations in this resulting curve after compensation are smoother than those existing in the curve corresponding to the total consumption curve, giving greater stability to the network.

The elimination of the peak consumption allows an energy saving of 54.8 kWh of grid consumption. Translating this into economic terms, considering the pricing period in which the eliminated peak consumption occurs together with the contracted power in CEDER, the implementation of the energy management strategy represents a total saving of 18.19 € in the electricity bill acting on the represented use case. Therefore, in the case of implementing an energy management system based on this methodology, extrapolating these results to an annual period, considering that situations like the one represented can occur between 8 and 10 times a month, a saving of 1964.52 € per year could be achieved.

5 Bibliografía

1. International Energy Agency, "World Energy Outlook 2022," 2022. Accessed: Jul. 20, 2023. [Online]. Available: <https://www.iea.org/reports/world-energy-outlook-2022>
2. International Energy Agency, "Net Zero by 2050 - A Roadmap for the Global Energy Sector," 2021. Accessed: Jul. 20, 2023. [Online]. Available: <https://www.iea.org/reports/net-zero-by-2050>
3. A. Bernstein et al., "Microgrids as a Building Block for Future Grids," DOE OE 2021 Strategy White Papers on Microgrids, 2022, [Online]. Available: [https://www.energy.gov/sites/default/files/2022-09/4-Microgrids as a Building Block for Future Grids.pdf](https://www.energy.gov/sites/default/files/2022-09/4-Microgrids%20as%20a%20Building%20Block%20for%20Future%20Grids.pdf)
4. S. S. Rangarajan et al., "DC Microgrids: A Propitious Smart Grid Paradigm for Smart Cities," *Smart Cities*, vol. 6, no. 4, pp. 1690–1718, 2023, doi: 10.3390/smartcities6040079.
5. Md. S. Alam, F. S. Al-Ismael, A. Salem, and M. A. Abido, "High-Level Penetration of Renewable Energy Sources Into Grid Utility: Challenges and Solutions," *IEEE Access*, vol. 8, pp. 190277–190299, 2020, doi: 10.1109/ACCESS.2020.3031481.
6. S. Vijayalakshmi, R. Shenbagalakshmi, C. P. Kamalini, M. Marimuthu, and R. Venugopal, "Power Quality Issues in Smart Grid/Microgrid," in *Planning of Hybrid Renewable Energy Systems, Electric Vehicles and Microgrid: Modeling, Control and Optimization*, A. K. Bohre, P. Chaturvedi, M. L. Kolhe, and S. N. Singh, Eds.,

- Singapore: Springer Nature Singapore, 2022, pp. 403–442. doi: 10.1007/978-981-19-0979-5_17.
7. Y. Naderi et al., “Chapter 4 - Power quality issues of smart microgrids: applied techniques and decision making analysis,” in *Decision Making Applications in Modern Power Systems*, S. H. E. Abdel Aleem, A. Y. Abdelaziz, A. F. Zobaa, and R. Bansal, Eds., Academic Press, 2020, pp. 89–119. doi: <https://doi.org/10.1016/B978-0-12-816445-7.00004-9>.
 8. F. Mohammadi et al., “Robust Control Strategies for Microgrids: A Review,” *IEEE Syst J*, vol. 16, no. 2, pp. 2401–2412, 2022, doi: 10.1109/JSYST.2021.3077213.
 9. K. Cabana-Jiménez, J. E. Candelo-Becerra, and V. Sousa Santos, “Comprehensive Analysis of Microgrids Configurations and Topologies,” *Sustainability*, vol. 14, no. 3, 2022, doi: 10.3390/su14031056.
 10. S. B. Sepúlveda-Mora and S. Hegedus, “Resilience analysis of renewable microgrids for commercial buildings with different usage patterns and weather conditions,” *Renew Energy*, vol. 192, pp. 731–744, 2022, doi: <https://doi.org/10.1016/j.renene.2022.04.090>.
 11. H. A. Muqet, H. M. Munir, H. Javed, M. Shahzad, M. Jamil, and J. M. Guerrero, “An Energy Management System of Campus Microgrids: State-of-the-Art and Future Challenges,” *Energies (Basel)*, vol. 14, no. 20, 2021, doi: 10.3390/en14206525.
 12. W. Dong et al., “Stochastic optimal scheduling strategy for a campus-isolated microgrid energy management system considering dependencies,” *Energy Convers Manag*, vol. 292, p. 117341, 2023, doi: <https://doi.org/10.1016/j.enconman.2023.117341>.
 13. D. Ahmed, M. Ebeed, A. Ali, A. S. Alghamdi, and S. Kamel, “Multi-Objective Energy Management of a Micro-Grid Considering Stochastic Nature of Load and Renewable Energy Resources,” *Electronics (Basel)*, vol. 10, no. 4, 2021, doi: 10.3390/electronics10040403.
 14. K. S. El-Bidairi, H. Duc Nguyen, S. D. G. Jayasinghe, and T. S. Mahmoud, “Multiobjective Intelligent Energy Management Optimization for Grid-Connected Microgrids,” in *2018 IEEE International Conference on Environment and Electrical Engineering and 2018 IEEE Industrial and Commercial Power Systems Europe (EEEIC / I&CPS Europe)*, 2018, pp. 1–6. doi: 10.1109/EEEIC.2018.8493751.
 15. M. A. H. Alshehri, Y. Guo, and G. Lei, “Renewable-Energy-Based Microgrid Design and Feasibility Analysis for King Saud University Campus, Riyadh,” *Sustainability*, vol. 15, no. 13, 2023, doi: 10.3390/su151310708.
 16. J. P. Chaves Ávila, T. Gómez San Román, and N. Morell Dameto, “La electricidad en España: formación del precio, composición de la factura y comparativa con otros países, sl: IIT Comillas ICAI,” *Fundación Naturgy*, 2021.
 17. M. Shafiullah et al., “Review of Recent Developments in Microgrid Energy Management Strategies,” *Sustainability*, vol. 14, no. 22, 2022, doi: 10.3390/su142214794.
 18. D. J. B. Harrold, J. Cao, and Z. Fan, “Data-driven battery operation for energy arbitrage using rainbow deep reinforcement learning,” *Energy*, vol. 238, p. 121958, 2022, doi: <https://doi.org/10.1016/j.energy.2021.121958>.

15

19. A. X. Y. Mah et al., "Optimization of a standalone photovoltaic-based microgrid with electrical and hydrogen loads," *Energy*, vol. 235, p. 121218, 2021, doi: <https://doi.org/10.1016/j.energy.2021.121218>.
20. T. Jamal, T. Urmece, G. M. Shafiullah, and F. Shahnia, "Using Experts' Opinions and Multi-Criteria Decision Analysis to Determine the Weighing of Criteria Employed in Planning Remote Area Microgrids," in *2018 International Conference and Utility Exhibition on Green Energy for Sustainable Development (ICUE)*, 2018, pp. 1–7. doi: [10.23919/ICUE-GESD.2018.8635734](https://doi.org/10.23919/ICUE-GESD.2018.8635734).
21. G. Liu, Y. Xu, and K. Tomsovic, "Bidding Strategy for Microgrid in Day-Ahead Market Based on Hybrid Stochastic/Robust Optimization," *IEEE Trans Smart Grid*, vol. 7, no. 1, pp. 227–237, 2016, doi: [10.1109/TSG.2015.2476669](https://doi.org/10.1109/TSG.2015.2476669).
22. L. de Oliveira-Assis et al., "Optimal energy management system using biogeography based optimization for grid-connected MVDC microgrid with photovoltaic, hydrogen system, electric vehicles and Z-source converters," *Energy Convers Manag*, vol. 248, p. 114808, 2021, doi: <https://doi.org/10.1016/j.enconman.2021.114808>.
23. G. Chaudhary, J. J. Lamb, O. S. Burheim, and B. Austbø, "Review of Energy Storage and Energy Management System Control Strategies in Microgrids," *Energies (Basel)*, vol. 14, no. 16, 2021, doi: [10.3390/en14164929](https://doi.org/10.3390/en14164929).
24. V. J. Mawson and B. R. Hughes, "Optimisation of HVAC control and manufacturing schedules for the reduction of peak energy demand in the manufacturing sector," *Energy*, vol. 227, p. 120436, 2021, doi: <https://doi.org/10.1016/j.energy.2021.120436>.
25. M. M. Rana, M. Atef, M. R. Sarkar, M. Uddin, and G. M. Shafiullah, "A Review on Peak Load Shaving in Microgrid—Potential Benefits, Challenges, and Future Trend," *Energies (Basel)*, vol. 15, no. 6, 2022, doi: [10.3390/en15062278](https://doi.org/10.3390/en15062278).
26. L. Zhang, Y. Yang, Q. Li, W. Gao, F. Qian, and L. Song, "Economic optimization of microgrids based on peak shaving and CO2 reduction effect: A case study in Japan," *J Clean Prod*, vol. 321, p. 128973, 2021, doi: <https://doi.org/10.1016/j.jclepro.2021.128973>.
27. R. Kuźniak, A. Pawelec, A. Bartosik, and M. Pawełczyk, "Determination of the Electricity Storage Power and Capacity for Cooperation with the Microgrid Implementing the Peak Shaving Strategy in Selected Industrial Enterprises," *Energies (Basel)*, vol. 15, no. 13, 2022, doi: [10.3390/en15134793](https://doi.org/10.3390/en15134793).
28. A. Abbasi, H. A. Khalid, H. Rehman, and A. U. Khan, "A Novel Dynamic Load Scheduling and Peak Shaving Control Scheme in Community Home Energy Management System Based Microgrids," *IEEE Access*, vol. 11, pp. 32508–32522, 2023, doi: [10.1109/ACCESS.2023.3255542](https://doi.org/10.1109/ACCESS.2023.3255542).

Catalogue for the construction of sustainable housing from compressed earth blocks

Jorge López-Rebollo¹[0000-0002-6230-3889], Xavier Cárdenas-Haro^{2,3}[0000-0001-5063-7366], Juan Parra-Vargas², Kevin Narváez-Berrezueta², Julver Pino³[0000-0003-3614-1465]

¹ Department of Cartographic and Land Engineering. University of Salamanca, Higher Polytechnic School of Ávila, Hornos Caleros, 50, 05003, Ávila, Spain.
jorge_lopez@usal.es

² Facultad de Arquitectura y Urbanismo, Virtual Tech, Universidad de Cuenca, Av. 12 de Abril s/n y Av. Loja, 010201 Cuenca, Ecuador.
xavier.cardenas@ucuenca.edu.ec; juan.parrav@ucuenca.edu.ec;
kevin.narvaez@ucuenca.edu.ec

³ Facultad de Ingeniería, Departamento de Ingeniería Civil, Universidad de Cuenca, Av. 12 de Abril s/n y Av. Loja, 010201 Cuenca, Ecuador
angel.pino@ucuenca.edu.ec

Abstract. This work focuses on investigating the use of additives for the stabilisation of compressed earth blocks and their characterisation. The earth material was selected and characterised by laboratory tests to analyse its composition and behaviour. Then, using this raw material, blocks with different compositions were manufactured using natural fibres and cementitious materials as additives. The blocks were characterised by means of compression tests to analyse their mechanical behaviour. The best results corresponded to those with a higher percentage of cement, with samples with a percentage equal to or greater than 15 % cement exceeding 20 kg/cm². Nevertheless, some samples with natural fibres such as reed fibre also showed promising results that are intended to be analysed in depth in future research. The results of all the research are summarised in the form of a catalogue to standardise the use of this type of material. This catalogue aims to homogenise the representation of their manufacture and behaviour, showing their components, additives and waterproofing.

Keywords: Sustainable construction; compressed earth blocks; earth materials; construction catalogue.

1 Introduction

The construction of housing with conventional materials, such as concrete, is not always possible due to limited availability of resources or access to manufacturing facilities [1], especially in small cities in developing countries that do not have the most advanced industry and technology. Moreover, concrete and steel construction is considered a highly polluting and resource-intensive industry [2], so it is necessary to es-

2

establish construction systems related to the concepts of sustainability and circular economy. In this sense, construction with earth materials has been used throughout history and nowadays it has an important role to play, as it allows on-site construction, making use of local resources and generating less waste [3]. The two main earth construction systems are adobe and compressed earth blocks (CEB). CEBs make it possible to obtain prefabricated panels from the compression of wet earth, thus facilitating the self-construction of modular housing.

Compressed earth blocks by themselves can be considered as a low-strength construction element. Therefore, additives and stabilisers are generally used to improve their mechanical, thermal, cohesion or waterproofing properties, resulting in what is known as stabilised compressed earth blocks (SCEB) [4]. Generally, cements are used as stabilisers to improve their strength [5], while the incorporation of fibres, both synthetic and natural origin, modifies the conductivities and thermal behaviour of building materials [6]. Nevertheless, the incorporation of these additives requires detailed studies to verify the alteration and modification of their properties, especially in the case of additives of natural origin [7]. Despite this, the incorporation of this type of natural additives or even waste can have a positive impact on the environment. On the one hand, this model of sustainable construction favours the use of local raw materials, favours the local economy and reduces pollution associated with transport. On the other hand, the reuse of waste, as is already the case with construction and demolition waste, leads to a lower consumption of resources [8].

Local production and different compositions of raw materials lead to a wide dispersion and variability in the behaviour of earth materials [9]. Furthermore, the wide variety of additives used makes it difficult to standardise the manufacturing processes and the behaviour of this type of material [10]. For this reason, it is necessary to try to establish common protocols regarding the composition, manufacture and behaviour of the different earth materials, focusing in this case on compressed earth blocks.

In order to advance in the research of these materials and bring knowledge closer, an in-depth study was carried out on the incorporation of additives of different origins in the manufacture of compressed earth blocks. The materials used range from natural fibres to materials conventionally used in the construction industry, such as lime, cement and asphalt emulsion. The research carried out covers all the processes involved in obtaining the properties of compressed earth blocks. This includes the selection and characterisation of the raw material such as earth, the selection of the additives to be used, the manufacture of the equipment to produce the blocks, the construction of the blocks and, finally, their mechanical characterisation. The results of this research are intended to be shown in this contribution in the form of a construction catalogue. In this way, both the properties and technical characteristics of the compressed earth blocks produced are presented, as well as their behaviour during the manufacturing process.

After this introduction, Section 2 describes the materials and methodology used in this research, as well as the guide for the elaboration of the construction catalogue. Section 3 shows the catalogue of the different products developed, including a brief analysis and discussion. Finally, Section 4 presents the main conclusions and discusses future research lines.

2 Materials and methods

This work focuses mainly on showing the results obtained in a didactic way to bring the knowledge closer to the public and facilitate the use of these materials in construction processes. Nevertheless, this section details both the materials used in the manufacture of compressed earth blocks and the procedures and tests carried out to obtain their properties and technical characteristics.

First, the materials used to manufacture the CEBs are described, including both the raw material, the earth, and the additives used or suggested by other research. Next, the tests carried out to perform the characterisation are detailed, including physical tests on the earth and mechanical tests on the compressed earth blocks. Finally, guidance for the catalogue is provided so that it can be interpreted according to the indications given.

2.1 Materials for the manufacture of compressed earth blocks


The raw material or base material for the manufacture of compressed earth blocks is earth. Due to the variability in the composition of these materials depending on their origin and their effect on the behaviour of compressed earth blocks [11], it is important to carry out an analysis of their properties.

The earth material selected for the manufacture of CEBs in this research was selected after considering different locations and performing a preliminary analysis of its composition. In addition, the availability to extract the material and the existence of construction material factories were also considered for the selection of the appropriate extraction site. The earth material was obtained in the city of Cuenca, located in the province of Azuay, Ecuador. Specifically, the extraction site is located in the area called Monay, located southeast of the city.

Additives

As mentioned above, the base material for the manufacture of CEBs is earth. Nevertheless, other additives, both of natural and synthetic origin, are used to stabilise them. In this research, CEBs have been produced that can be classified into two groups. The first group (PF) includes vegetable fibres as natural additives. The second group (PC) includes cementitious additives such as lime and cement, in different percentages. The technical characteristics and appearance of each of these additives are shown in Table 1 -Table 6.

Table 1. Additive specifications: sawdust fibre.

Description	Small wood particles that appear as waste from sawmills	
Advantages	Helps control cracking, improve load-bearing and tensile capacity	
Density (Kg/m ³):	275	
Cost	Low	
Availability	High	
Carbon footprint	Low	

4

Table 2. Additive specifications: cabuya fibre.


Description	Product extracted from the leaves of the pennyroyal and cut in sections of less than 10 cm	
Advantages	Helps control cracking, improve load-bearing capacity and tensile capacity	
Density (Kg/m ³):	665	
Cost	Medium	
Availability	High	
Carbon footprint	Low	

Table 3. Additive specifications: reed fibre.


Description	Reeds crushed to small fibres of 2 to 4 cm	
Advantages	Helps control cracking, improve load-bearing capacity and tensile capacity	
Density (Kg/m ³):	-	
Cost	Low	
Availability	High	
Carbon footprint	Low	

Table 4. Additive specifications: totora fibre.


Description	Very low density fibre. Very common in estuaries and lakes	
Advantages	Improved thermal insulation properties	
Density (Kg/m ³):	180	
Cost	Medium	
Availability	High	
Carbon footprint	Low	

Table 5. Additive specifications: lime.



Description	Alkaline substance composed of calcium oxide	
Advantages	Water retention and hardening properties	
Density (Kg/m ³):	1200	
Cost	High	
Availability	Medium	
Carbon footprint	Medium	

Table 6. Additive specifications: cement.

Description	Binder made of limestone and calcined clays	
Advantages	Hardening properties in contact with water	
Density (Kg/m ³):	1440	
Cost	Medium	
Availability	High	
Carbon footprint	High	

Equipment

The research focused on favouring self-manufacturing, so that cities with low economic resources can grow through the construction of sustainable housing with local resources. To this end, the use of low-cost equipment, which can be manufactured at home, was proposed.

Since initially a drying and sifting process of the material is required to obtain the right granulometry, a sifting cylinder was designed to allow crushing and sifting (Fig. 1a). For the manufacture of compressed earth blocks, a hydraulic press was designed to allow the compression process (Fig. 1b).

Both devices were manufactured with steel profiles to generate the structure. For the rotation of the sifting cylinder, a motor was incorporated together with a pulley mechanism. The hydraulic press incorporated a manual hydraulic jack together with a pressure gauge to control the pressure exerted.



Fig. 1. Equipment for the manufacture of compressed earth blocks. a) Sifting cylinder; and b) Hydraulic press.

6

2.2 Characterisation tests

To characterise the earth material as well as the manufactured compressed earth blocks, laboratory tests were carried out. Due to the nonexistence of standardisation and lack of regulations, it was decided to adopt tests used for other similar materials.

For the characterisation of the earth material, first of all, some empirical tests were performed according to the Peruvian standard [12]. Some of them are the odour test, the bite test, the washing test or the cut test. These tests allow to identify some properties of the earth such as the presence of clays or the level of humidity.

Nevertheless, the results of these tests are only an approximation, so laboratory tests were performed to analyse their properties with greater precision. The analyses carried out include the granulometric test [13], the plasticity test [14] and the compaction test [15].

Regarding the mechanical characterisation of the manufactured compressed earth blocks, compression tests were carried out. In this case, the Colombian standard [16] was used, which determines the characteristics of the test by applying a compressive load with a constant speed of 0.02 mm/s until the block breaks. The panels, whose dimensions were 30 x 45 x 7 cm (height, width and thickness), were compressed on their upper and lower sides (45 x 7 cm).

2.3 Catalogue guide

Based on the tests and procedures described above, a catalogue has been drawn up which aims to represent the results in a didactic way in order to facilitate the standardisation and use of this type of materials. To facilitate the understanding of this catalogue, the basic template with all the elements is presented in Fig. 2.

- Earth characteristics. Three main characteristics have been considered. Colour, referenced in the Munsell scale; pH; and stability of clays, linked to the type of clay. In addition, the dosage of the earth used is shown, including the percentages of clay, silt, sand and gravel. Taking into account that the earth material used as base was the same, this information is included generically for all CEBs.

- Manufacturing parameters. Both the pressing and curing parameters have a direct influence on the final strength of the panels, so it is important to detail the method used for each of them. In addition, information related to production efficiency is included according to pressing method and panel type, categorised in panels per hour.

- Natural additives. This section includes the additives of natural origin used for the stabilisation of the panel, trying to identify the type of additive and its percentage.

- Special additives. This section considers additives of industrial or special origin that have been used to improve the characteristics of the panel.

- Waterproofing. These are additives selected on other research that may affect their performance. It should be noted that no tests have been carried out on waterproofing effectiveness.



Fig. 2. Template for catalogue.

3 Results and catalogue

3.1 Earth results

The results obtained from the laboratory tests for the earth material samples are summarised in a didactic way in Fig. 3. This categorisation has been determined based on the following test results.

Granulometric tests determined their adaptation to standards, with values of 20 % for clays and 78 % for sands and silts.

The plasticity tests gave a liquid limit of 50 % and a plasticity index of 20 %, which is at the limit of the extremes established in the regulations.

The compaction test showed that the compaction limit was reached at approximately 20 % moisture content.

Finally, the pH obtained was 9, while the colour of the earth material corresponds to 2.5YR on the Munsell scale.

8

Earth characteristics

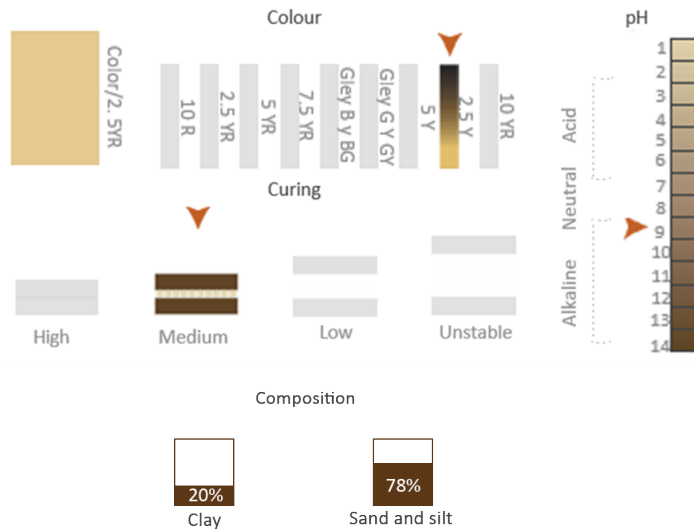


Fig. 3. Results of earth characteristics.

3.2 Compressed earth blocks results

The compressed earth block samples were subjected to compression tests for mechanical characterisation. Three tests were performed for each of the CEB types. The test results are shown in Table 7.

Table 7. Results of mechanical characterisation: compressive strength.

Nomenclature	Mean (kg/cm ²)	Maximum (kg/cm ²)
PF_1	1,91	1,96
PF_2	2,76	4,21
PF_3	6,63	9,56
PF_4	0,75	0,80
PC_1	3,70	4,59
PC_2	7,63	10,39
PC_3	16,44	18,15
PC_4	20,63	21,41
PC_5	24,80	40,59
PC_6	33,42	36,63

CEBs in the group manufactured with natural fibres show a lower performance as expected. Nevertheless, some of them, such as the PF_3 sample manufactured with reed fibre, show promising results above the rest,

Regarding CEBs stabilised with cementitious materials, their performance is better as the percentage of cement increases. Nevertheless, the PC_1 sample manufactured with lime and the PC_2 sample manufactured with the lowest percentage of cement show a similar behaviour to the panels with natural fibres.

Based on the above results and the experience gained during manufacture, the didactic catalogue shown in Fig. 4 - Fig. 13 has been produced.

The intention of this catalogue is to show the composition and behaviour of the different panels and to show that it can be associated with the strength table. In this way, when it is intended to manufacture or use compressed earth blocks, the catalogue can be consulted to verify the different options of components, additives and waterproofing and their corresponding behaviour.

This catalogue presents only the results of the dosages used during the research, but it is intended to standardise the use of these materials, trying to achieve a homogeneous representation of them so that the knowledge can be extended and interpreted by the entire scientific community, as well as the industry associated with earth materials.

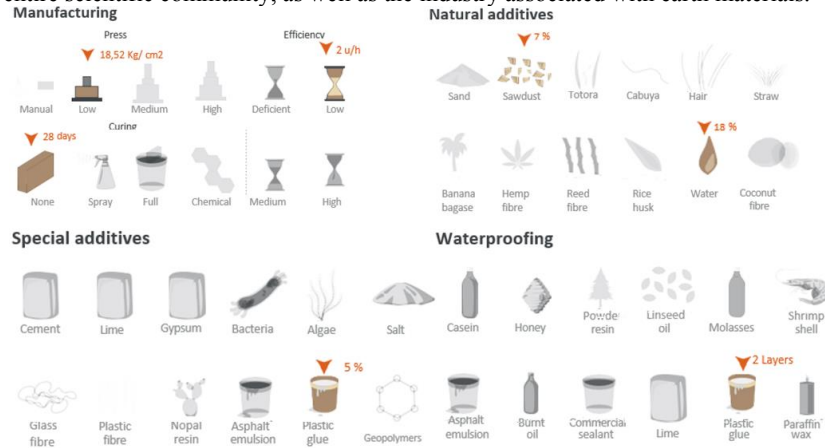


Fig. 4. Technical characteristics of PF_1.

10

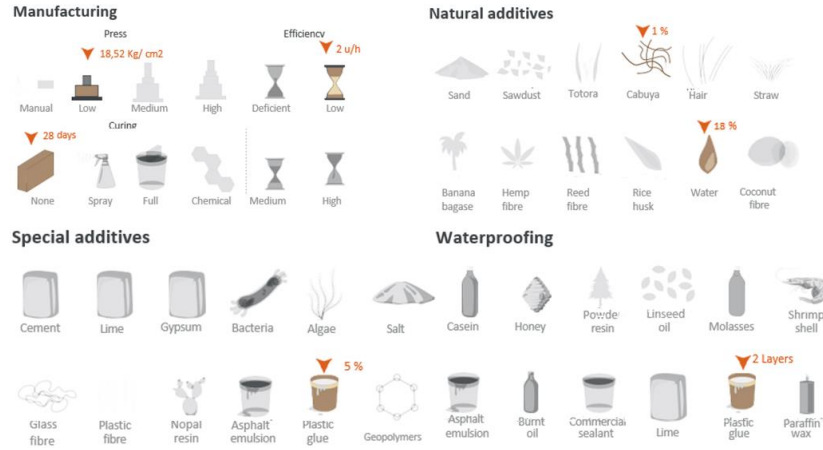


Fig. 5. Technical characteristics of PF_2.



Fig. 6. Technical characteristics of PF_3.

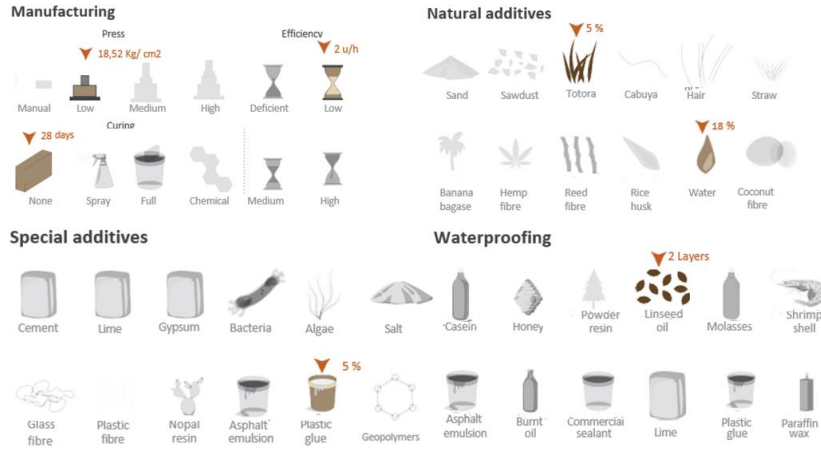


Fig. 7. Technical characteristics of PF_4.



Fig. 8. Technical characteristics of PC_1.

12

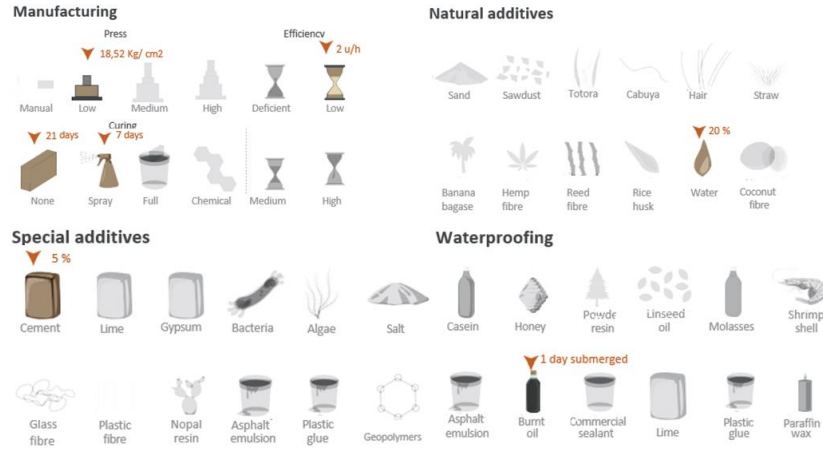


Fig. 9. Technical characteristics of PC_2.



Fig. 10. Technical characteristics of PC_3.



Fig. 11. Technical characteristics of PC_4.

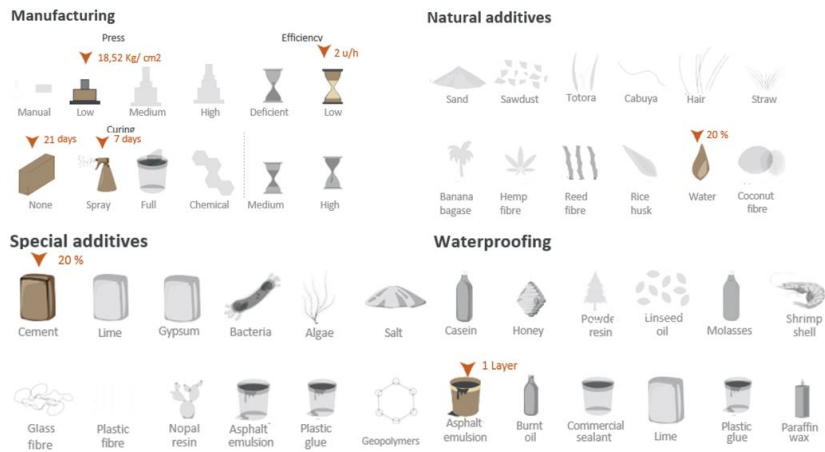


Fig. 12. Technical characteristics of PC_5.

14



Fig. 13. Technical characteristics of PC_6.

4 Conclusions

This work consisted mainly of a didactic catalogue of compressed earth blocks based on extensive research on these materials. The intention of this catalogue is to take a step towards the standardisation and homogenisation of earth materials, as existing studies show the variability of their composition and behaviour. Thus, the main characteristics to be shown have been established, such as the characteristics of the earth, the behaviour during manufacture and curing, the composition, additives and waterproofing. In addition, a symbology has been established to facilitate its understanding and to be used for all possible cases. The results are presented in a summarised form so that they can be interpreted by the scientific community, bringing the knowledge closer to the manufacturers of these materials and the construction industry to favour the use of these sustainable materials in the construction of housing in those cities with fewer economic resources.

The first phase of the research consisted of earth selection and characterisation. Laboratory tests showed an earth material with 20 % clays and 78 % sand and silts, thus adjusting its granulometric curve to the standards. These properties, together with colour, pH and stability, are represented in the catalogue.

The fabrication and curing of the CEBs was carried out using different compositions in order to analyse their mechanical behaviour. The results showed a compressive strength greater than 20 kg/cm² for the samples with cement additive in a percentage equal to or greater than 15 %. Although the samples with natural fibres showed a lower strength, some of them, such as the sample made with reed fibre, showed a strength greater than 5 kg/cm² and can be considered for further investigation.

The results obtained highlight the influence of additives on mechanical behaviour and provide a starting point for further research to facilitate their incorporation into the construction industry. The aim is to move towards a more sustainable construction

model in which conventional materials such as concrete and steel can be replaced by this type of materials that make use of local and natural resources, generating less pollution and waste.

Future work will focus on extending the range of additives that are to be used or the incorporation of residues. At the same time, the aim is to disseminate the catalogue to take a step towards standardisation so that it can be used by other researchers.

References

- Herrmann, C.J. and E.O. Zappettini, *Recursos minerales, minería y medio ambiente*, ed. S. Serie Publicaciones N° 173. Instituto de Geología y Recursos Minerales. 2014, Buenos Aires, Argentina.
- de Brito, J. and R. Kurda, *The past and future of sustainable concrete: A critical review and new strategies on cement-based materials*. Journal of Cleaner Production, 2021. **281**: p. 123558
- Costa, C., et al., *The sustainability of adobe construction: past to future*. International Journal of Architectural Heritage, 2019. **13**(5): p. 639-647.
- Cid-Falceto, J., F.R. Mazarrón, and I. Cañas, *Assessment of compressed earth blocks made in Spain: International durability tests*. Construction and Building Materials, 2012. **37**: p. 738-745.
- Standard, I., *IS 13827: Improving Earthquake Resistance of Earthen Buildings - Guidelines*. 1993: Indian.
- López-Rebollo, J., Villanueva, N. N., Nieto, I. M., Blázquez, C. S., Del Pozo, S., & González-Aguilera, D. *Monitoring the thermal contribution of certain mortar additives as a way to optimize the energy performance of buildings*. Sustainable Energy Technologies and Assessments, 2023. **57**, p. 103268.
- Losini, A.E., et al., *Natural additives and biopolymers for raw earth construction stabilization—a review*. Construction and Building Materials, 2021. **304**: p. 124507.
- Teijón-López-Zuazo, E., et al., *Compression and strain predictive models in non-structural recycled concretes made from construction and demolition wastes*. Materials, 2021. **14**(12): p. 3177.
- Cárdenas-Haro, X., Todisco, L., & León, J.. *Database with compression and bending tests on unbaked earth specimens and comparisons with international code provisions*. Construction and Building Materials, 2021. **276**, p. 122232.
- Sturm, T., L.F. Ramos, and P.B. Lourenço, *Characterization of dry-stack interlocking compressed earth blocks*. Materials and structures, 2015. **48**: p. 3059-3074.
- McGregor, F., et al., *Conditions affecting the moisture buffering measurement performed on compressed earth blocks*. Building and Environment, 2014. **75**: p. 11-18.
- Ministerio de Vivienda, C.y.S., *Norma E.080. Diseño y construcción con tierra reforzada*. 2017: Perú.
- ASTM, I., *ASTM D422-63: Standard Test Method for Particle-Size Analysis of Soils*. 2007: USA.
- INEN, I.E.d.N.-. *INEN 692 - Mecánica de suelos. Determinación del límite plástico*. 1982: Ecuador.
- ASTM, I., *ASTM D698: Standard test methods for laboratory compaction characteristics of soil using standard effort*. 2000: USA.
- NTC, N.T.C., *NTC 5324: Ground blocks cement for walls and divisions. Definitions. Specifications. Test methods. Conditions of delivery*. 2004: Colombia.

Effect of interior and exterior roof coating on heat gain inside a house

J. L. Cerino-Isidro¹[0000-0002-1799-3913], E. V. Macias-Melo^{1*}[0000-0003-0107-766X], K.M. Aguilar-Castro¹[0000-0003-2611-2820], O. May Tzuc²[0000-0001-7681-8210], C.E. Torres-Aguilar¹[0000-0001-6187-4519], and J. Serrano-Arellano³[0000-0002-7875-0106]

¹ Universidad Juárez Autónoma de Tabasco, DAIA-UJAT, Tabasco, CP 86690, México.

² Universidad Autónoma de Campeche, Facultad de Ingeniería, Campeche, CP 24085, México.

³ Instituto Tecnológico de Pachuca, Hidalgo, C.P. 42080, México.
edgar.macias@ujat.mx

Abstract. This work evaluated the effect of changes in coatings (with different solar absorptances and emittances) on the transfer of thermal energy by radiation through a roof sample. The coating on the interior surface of the roof was mainly analyzed. For this purpose, a sample roof configuration was designed, instrumented, and thermally evaluated. Under warm-humid climate conditions, roof coatings on the interior and exterior surfaces were applied. The reference roof sample (RS) consists of two extruded polystyrene plates. Four different coatings (red, RR; green, RV; white 1, B1; white 2, B2) were implemented on the upper surface of each one, while only one coating was implemented on the inner surface of each plate (B1 or aluminum, Al). From the results obtained with the RS and through the development of a computational code where the transient one-dimensional heat conduction model is solved, it was possible to analyze the behavior of heat gains through a concrete slab. For this, four combinations of the exterior and interior coatings were implemented. The results showed that the combination B1 or B2 - Al (Configuration 3 and 4) presented the most significant reduction in heat gains, with the highest reduction in thermal load of 49.53%.

Keywords: Roof, Coatings, Buildings, Heat flux, Heat transfer.

1 Introduction

The energy demand of a building depends on many factors, such as the purpose, expected use, and location. The building envelopes work like a barrier between internal and external ambient, which helps to minimize the climatic variations due to the materials and design. The thermal gains impact the high energy consumption and the thermal comfort inside the building. In addition to the aesthetic, the external coatings of buildings can have proper textures to reduce thermal gains and give excellent thermal insulation performance (Boukhelkhal & Bourbia, 2021; Verma & Dibakar Rakshit, 2023).

The building envelope for residential use comprises three main components: floor, walls, and roof. The roof is the envelope component with an external surface that forms an angle vertically equal to or greater than 0° to 45° (NOM-020-ENER-2011). In the

2

building industry, the thermal properties of implemented materials in the roof significantly impact the surface temperature and the thermal gains through the building surface. Therefore, a construction surface that uses reflective materials with high thermal emissivity and solar reflectance properties can reduce the energy demands for cooling, improving thermal comfort, which is possible due to the reductions of solar energy absorption. Furthermore, reflective materials with high solar reflectance and emittance can reduce the solar energy absorption in the roof significantly, which is reflected in the reduction of the internal temperature of the building and the reduced energy for cooling. Because of the above, several materials to coat roofs have been developed in the last years to reduce thermal gain in addition to waterproofing. According to Anand et al. (2020), implementing coatings or claddings on rooftops with a solar reflectance of 0.96 and emissivity close to 0.97 helps to minimize thermal gains. The coatings with high albedo or solar reflectance and high infrared emission are known as cold materials.

The literature presents experimental and theoretical research about reflective coatings, where reflective materials are used to study the effect on the thermal gain in building interiors through simulation, experimental studies, and variable monitoring. Theoretical research, as the study of Millstein and Levinson (2017), described the simulation of a roof with a reflective material ($\rho=0.9$) to analyze the temperature changes. The authors found it possible to predict the air temperature in the simulated period, and the results showed a reduction of 0.5°C using reflective material. Also, other authors as Broadbent et al. (2020) and Wang et al. (2022), consider that reflectivity and emissivity have significant repercussions on the surface temperature of the interior roof of metal light during daylight.

Regarding experimental studies, Kolokotsa et al. (2017) described the application of cold roofs in the building rooftop and cold cobblestone to replace conventional paving. The results showed that the cold roof reduces 17% of cooling annual demand. Kolokotroni et al. (2018) studied a roof in a house and a computational study on three countries around the equator (Jamaica, Brazil, and Ghana), putting paints with high reflectance. The first solar reflectance was 0.82, then reduced to 0.72 after three years; the thermal emittance was 0.9. The average solar irradiance and the ambient temperature of the study were 420 W/ m² and 28°C, respectively. The recorded results were employed to build a model on Energy Plus where the simulations indicated that the surface temperature of the building interior was reduced between 3.2-5.5°C on average. The authors concluded that applying of the reflective coating on the roof of a house in zones with high solar radiation improves thermal comfort with natural ventilation and reduces the energy demand in houses with air conditioning systems.

Hernández et al. (2018) reported a study about the effect of roof coatings on the thermal gains inside a building. The authors evaluated the thermal performance of a conventional red coating and two white reflective coatings installed on roofs compared with a reference gray roof (conventional concrete slab). This study measured the surface temperature of roofs, interior air temperature, and heat flows. The results showed that the red roof presented a temperature of 3°C higher than the configuration with the grey roof. In contrast, the configuration with white reflective coating reduced the surface temperature between 10 and 14.6°C compared to the gray roof. Hernandez et al. (2019) showed that the roof with white reflective coating had the best thermal

performance compared to the black roof configuration since the average highest heat flow of the white roof was 19 W/m^2 and for the black roof was 72 W/m^2 . For its part, Valencia-Caballero et al. (2023) studied the performance of a bifacial photovoltaic system with cool roof coating on the underside and its impact on floor temperature. For this purpose, four $\sim 1\text{kWp}$ prototypes were installed (1) bifacial panels above a cool roof, (2) bifacial panels above normal floor, (3) bifacial panels above a normal floor with n-type solar cells encapsulated in TPO, and (4) monofacial panels. The results reveal an 8.6 % higher PV yield for bifacial with a cool roof, and it was observed that the cool roof coating contributes to reducing the floor temperatures, particularly in the unshaded (exposed) areas during summer. The research has been oriented on experimental and theoretical studies. It is reported that cold roofs can reduce the energy demand, although it is crucial to consider the geometric construction of buildings and construction methods, among others. However, applying coatings can improve thermal comfort and reduce energy demand significantly. There are studies where the exterior temperature of the building was reduced by 15°C (Qiu et al. 2018). Therefore, the present study evaluates the effect of changes in coatings (with different solar absorptances and emittances) on thermal energy transfer by radiation through a roof sample. The coating on the interior surface of the roof was mainly analyzed.

2 Materials and methods

2.1 Sample

The roof sample used as Reference Sample (RS) is composed of two extruded polystyrene plates of the same dimension. The exterior surface of each plate was covered with four different coatings, while the interior surface was covered with only one coating (different for each plate). The extruded polystyrene plate has a thermal conductivity of $0.0288 \text{ W/m}^\circ\text{C}$ to 24°C , and the dimensions are 1.20 m in length \times 1.20 m in width, and 2.54 cm (1 inch) thickness.

2.2 Coating

Four coatings for the external surface were selected: 1) green (RV), 2) terracotta red (RR), 3) conventional white (B1), and 4) reflective white (B2). The selection was based on comparing two coatings with low absorbance and two with high absorbance. The selection permitted compared the effect of solar absorbance and emittance on the radiative heat transfer with the coating samples. Fig. 1 shows photography of every applied coating on the extruded polystyrene. Every coating was applied according to the recommendations of the vendor.

2.3 Physical model

Fig. 2 shows the schematic diagram of the physical model of a roof with coating on the exterior and interior surfaces. In the physical model, I_H is the solar irradiance on the roof surface, I_{Hp} is the reflected solar irradiance (due to the reflectance of the coating).

4

$I_{H\alpha}$ is the absorbed solar irradiance (due to the absorbance of the coating). ϵ_o is the emittance of exterior coating. ϵ_i is the emittance of interior coating. q''_{cr-o} is the exterior radiative-convective coefficient, and q''_{cr-i} is the interior radiative-convective coefficient. T_{se} is the exterior surface roof temperature, and T_{si} is the interior surface roof temperature. a is the x-axis length, b is the y-axis length, and t is the roof thickness.

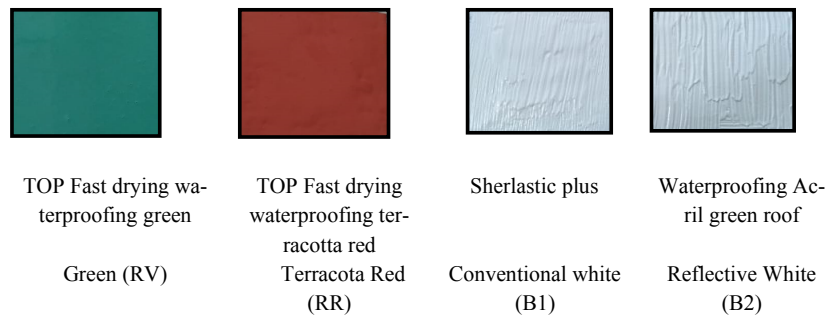


Fig. 1. Photography of selected coatings

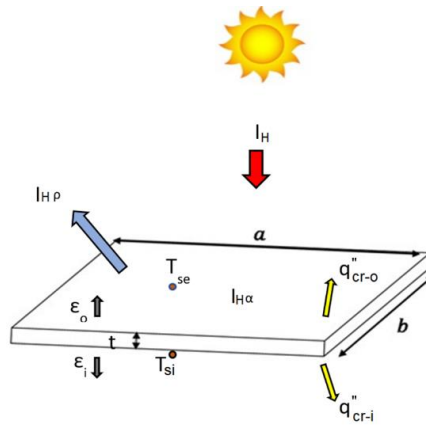


Fig. 2. Physical model of a roof

As mentioned, part of the absorbed energy is dissipated to the exterior and interior environment. Eq. (1) shows the energy balance in the exterior boundary between the conductive, and radiative-convective effects; T_{amb} is the ambient temperature, and T_{sky} is the sky temperature.

$$\lambda \frac{\partial T}{\partial x} = I_H \alpha + \underbrace{h_e (T_{se} - T_{amb}) + \sigma \varepsilon (T_{se}^4 - T_{sky}^4)}_{q''_{e-o}} \quad (1)$$

On the other hand, the energy transmitted through the roof to the internal environment is the absorbed solar irradiance plus the absorbed convective heat flow and the radiative heat flow (radiative exchange between sky and surface roof). Therefore, Eq. (2) shows the energy balance in the interior, which considers the convective and radiative transfer between the surface and interior ambient; T_{wall} is the wall temperature.

$$-\lambda \frac{\partial T}{\partial x} = \underbrace{h (T_{si} - T_{amb}) + \sigma \varepsilon (T_{si}^4 - T_{wall}^4)}_{q''_{e-i}} \quad (2)$$

The heat transfer process for the roof dominion is described by Eq. (3).

$$\frac{\partial T}{\partial t} = \alpha \frac{\partial^2 T}{\partial x^2} \quad (3)$$

2.4 Experimental setup

The experimental study was performed under warm-humid climate conditions in Tabasco, Mexico (18.10°N, 93.32°W). According to Weather Spark 2021, the warmest day of the year was May 23rd, with an average highest temperature of 34°C and an average lowest temperature of 24°C. Fig. 3 shows the experimental design of the roof sample for testing. The roof was divided into four sections. Each section was covered with a different coating: RV, RR, RB1, and RB2. The temperature was measured in the section with RR coating (T_{RR}). This measurement was employed as a reference to determine the temperature on the section with different coatings (T_{RV} , T_{B1} , and T_{B2}). Also, the temperature difference between the interior and exterior roof surfaces was quantified ($T_{se} - T_{si}$). For the energy analysis of systems, the external meteorological variables were monitored: ambient temperature (T_{amb}), solar irradiance (I_H), relative humidity (HR), wind velocity (V_v), wind direction (D_v), and sky temperature (T_{sky}).

6

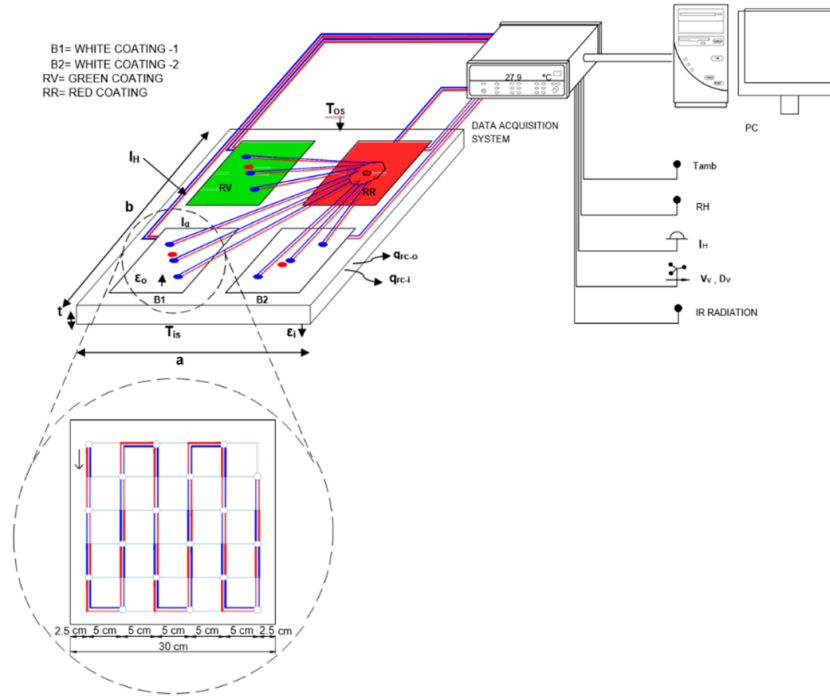


Fig. 3. Experimental system design.

2.5 Experimental system construction

The prototype construction was realized in two main sections: coatings implementation and roof sample base. The construction of roof base was built using aluminum angular profiles with mobile unions. The base dimensions were 1.20m x 2.40m, 0.35m high in the minor base, and 0.45m of high in the major base. The base had a tilt of 4.8° to increase the reception of solar energy and water runoff during the rainy season. Gypsum boards were employed for the base according to the dimensions of the metallic structure. Each gypsum board section was covered with a sealant to waterproof the surface.

2.6 Instrumentation

The roof sample was divided into four sections in two plates of polystyrene extruded. The dimensions for each section were 0.40 m x 0.40 m. Each section was instrumented with thermopiles built with T-type thermocouple extensions connected in series to quantify the temperature difference between the interior and exterior surface of the roof. A thermopile was installed later to quantify the temperature difference on the sample roof surface. For this action, three differential thermopiles were installed considering

the sections with coatings (RV, RB1, and RB2), and using the RR coating as reference, which permitted to obtain a temperature referenced with a T-type thermocouple and optimize the instrumentation. The temperature of each interior and exterior surface of coatings was analyzed through the instrumentation.

Five sensors PT1000 of B-class ($\pm 0.2^\circ\text{C}$) were employed to measure the air temperature in the interior roof (one sensor for the air temperature of interior roof with the white-1 coating and another one for the air temperature of the interior roof with aluminum), one sensor for the interior roof surface with the high emittance coating, and another sensor for the interior roof surface with low emittance coating (white-1 and aluminum, respectively). Also, an air temperature sensor was installed in the base of the experimental roof to monitor the temperature of the interior environment. All temperature sensors were calibrated according to the ASTM E230 standard. In both plates, the thermopiles and sensor joints were fixed to the surface of each plate with 3M® industrial tape.

The meteorological variables were measured with an Ambient Weather station WS-2902C, and the celestial dome temperature (R_{IR}) was determined with a radiation IR sensor Melexis model MLX90614, which has a temperature range from -40 to 85°C for ambient and from -70 to 382°C for objects. The radiation IR sensor has a standard precision of 0.5°C . The solar irradiance (I_H) was measured with a first-class pyranometer with an uncertainty of $\pm 20\text{W/m}^2$. Figure 4 shows the prototype diagram and the photography of the experimental set.

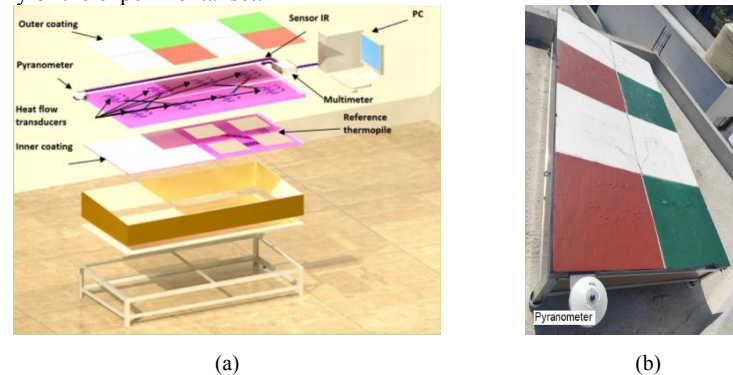


Figure 4. Experimental prototype, a) instruments scheme and b) photography of experiment

3 Experimental procedure

The experimental tests start with the communication between the data acquisition system and the CPU using the software Agilent 34825A BenchLink Data Logger 3 and the software MLXTEST. Next, the software MLXTEST acquires the data of the IR sensor. The measurements were recorded during the period between February 5th to February

8

10th (02/05-02/10). The interval between measurements was two minutes which were analyzed with Octave software. The data analysis permitted us to study the behavior of thermal gains on a concrete roof when the coatings are combined in this study.

4 Results and Discussion

The experimental study was performed under warm-humid climate conditions in Tabasco, Mexico. Figure 5 shows the behavior of I_H for the test days; the highest values of I_H were up to 800 W/m², achieving 900 W/m² for the 02/07 day. The I_H measure permitted the determination of the effect of solar absorbance in exterior coatings and compared it with the interior low emittance configurations, which is discussed furthermore.

Fig. 6 shows the ambient temperature (T_{ext}), sky temperature, interior temperature (T_{ai}), and the average wall temperature inside the cavity (T_{bi}) for the test days. The behavior of T_{ext} shows values higher than 25°C, while the lowest temperatures were around 10°C. However, there is a delay between the irradiance and highest exterior ambient temperature peaks. This delay occurred due to the temperature levels, which are low for the air, and the stored energy through the surface. This energy is removed by heat convection with the increment of T_{ext} .

On the other hand, for T_{sky} , the highest temperature was 28°C, while the lowest temperature was around -7°C, obtained on 02/05. It is crucial to notice that the increment of sky temperature over the ambient temperature is due to a cloudy day, therefore the clouds absorbed radiation. This effect was observed in the behavior of the I_H attenuation.

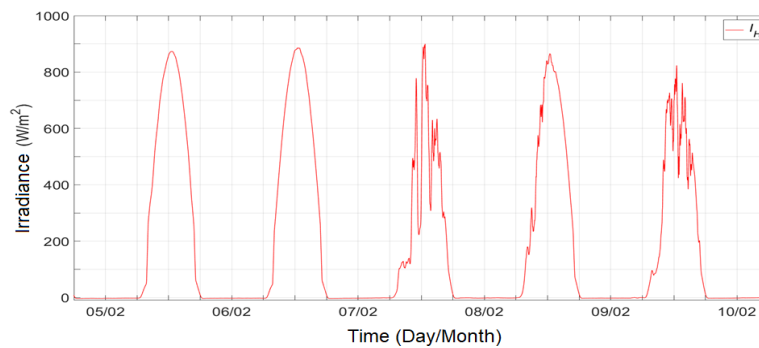


Figure 5. Solar Irradiance behavior, February 5-10.

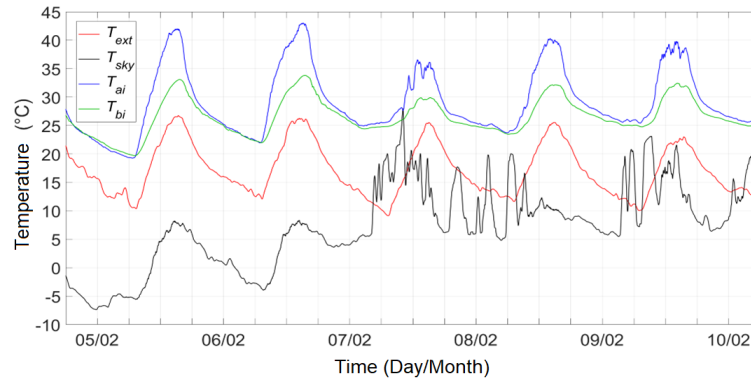


Figure 6. Ambient temperature, sky temperature, interior air temperature and interior base temperature, February 05-10.

On the other hand, the interior environment conditions presented a similar behavior; however, during the test, the T_{ai} and T_{bi} were higher than the T_{ex} and T_{sky} . This effect was due to the accumulation of energy received by the walls and MR (I_H). Furthermore, the radiative exchange with the celestial dome permitted us to observe an increasing temperature of T_{ai} and T_{bi} with a similar tendency to T_{sky} . T_{bi} had similar behavior to T_{ext} due to convective effect without I_H incident on the base surface exposed to the exterior environment. T_{ai} presented a highest temperature of 42.86°C and lowest temperature of 19.33°C. The highest value of T_{bi} , was 33.80°C with a lowest temperature of 19.72°C.

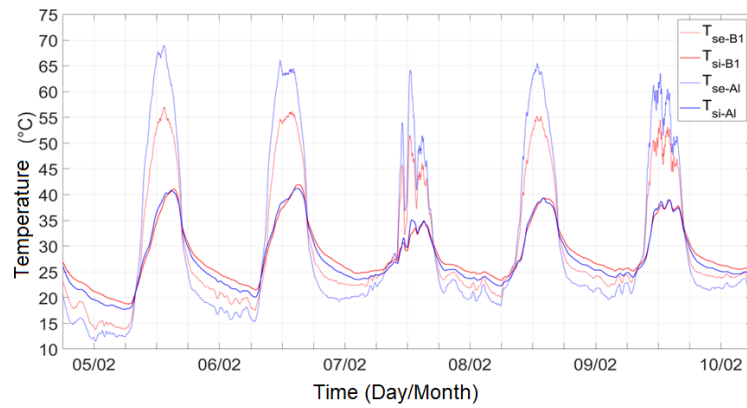
The behavior of MR with the different coatings was analyzed in the following combinations:

- Combination 1:** red (RR) exterior - white 1 (B1) interior vs red (RR) exterior-aluminum (Al) interior.
- Combination 2:** green (RV) exterior - white 1 (B1) interior vs green (RV) exterior - aluminum (Al) interior.
- Combination 3:** white 1 (B1) exterior - white 1 (B1) interior vs white 1 (B1) exterior - aluminum (Al) interior.
- Combination 4:** white 2 (B2) exterior - white 1 (B1) interior vs white 2 (B2) exterior - aluminum (Al) interior.

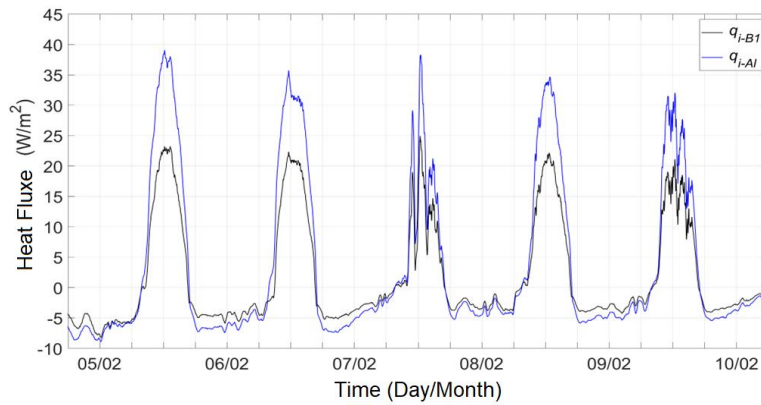
Figure 7a shows temperature behavior on the exterior surface of Combination 1; Figure 7a shows the high temperature between T_{se-B1} and T_{se-Al} during the hours with the highest solar irradiance received and absorbed. The highest temperature of T_{se-B1} was 57°C, while the highest temperature of T_{se-Al} was 69°C (12°C of difference). It is important to notice that energy dissipation increased as the exterior temperature increased due to the exterior surface conductance, like the exterior coating. T_{si-B1} achieved values of 42°, while T_{si-Al} achieved 41°C for the same solar irradiance conditions; this means that T_{si-Al} presented a temperature reduction of 1°C. On the other hand, in hours of solar

10

irradiance, the temperature difference between T_{si-B1} and T_{si-A1} was more significant than in other configurations. The lowest values of T_{si-B1} and T_{si-A1} were 18.8°C and 17.7°C , respectively. The T_{si-B1} value was inferior during the period when increased the solar irradiance, which was inverted after 50 minutes of achieving the highest solar irradiance and started to decrease. This effect is a consequence of base temperature conditions since it keeps increasing due to the thermal inertia of the cavity.



(a) Temperature

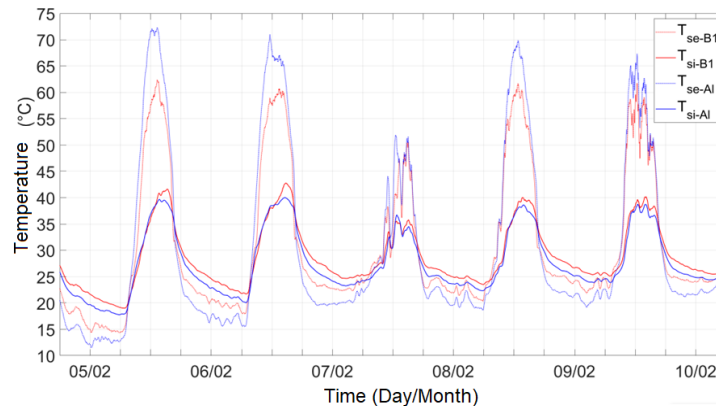


(b) Heat flux

Figure 7. Heat flux and temperature of configurations: RR exterior-B1 interior ($\alpha_e=0.51$, $\epsilon_e=0.89$, $\epsilon_i=0.8182$) vs RR exterior – A1 interior ($\alpha_e=0.51$, $\epsilon_e=0.89$, $\epsilon_i=0.049$), February 05-10.

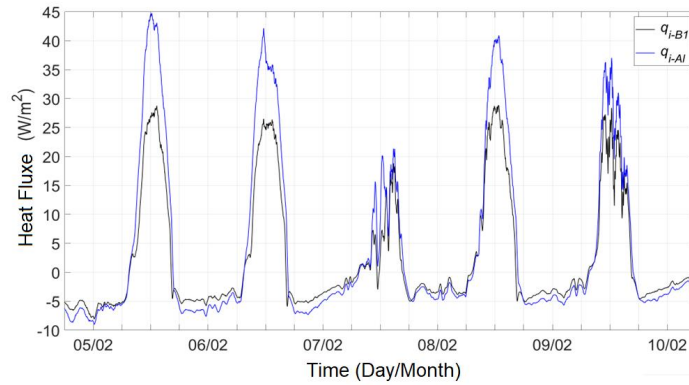
On the other hand, Fig. 7b shows the behavior of heat flux to the interior environment through interior coatings B1 and A1. Aluminum heat flux (q_{i-Al}) and white-1 heat flux (q_{i-B1}) presented a similar behavior. However, during the period with and without I_H , q_{i-Al} was higher than q_{i-B1} . q_{i-B1} was 22.57 W/m^2 in hours with the highest solar irradiance, while q_{i-Al} was 35.84 W/m^2 , which means that q_{i-B1} presented a reduction of 13.27 W/m^2 compared to q_{i-Al} .

Fig. 8a shows the behavior of temperatures on the exterior surface for Combination 2. The highest value of T_{se-B1} was 62°C , while the T_{se-Al} was 72°C , meaning a temperature difference of 10°C . T_{si-B1} and T_{si-Al} achieved values of 42.7°C and 40°C , respectively, for the same solar irradiance conditions; this means a temperature reduction of 2.7°C for T_{si-Al} . In hours of irradiance, the temperature differences between T_{si-B1} and T_{si-Al} were more significant. The lowest values of T_{si-B1} and T_{si-Al} were 19°C and 17.8°C , respectively, which means a temperature difference of 1.2°C . On the other hand, Fig. 8b shows the heat flux behavior in the interior through interior coatings B1 and A1. The average of q_{i-B1} in hours with the highest solar irradiance was 26.24 W/m^2 , while the average of q_{i-Al} was 37.22 W/m^2 ; this implied a reduction of 10.98 W/m^2 compared to q_{i-Al} . The results show that the interior coating affects the temperature behavior, and the temperature difference between the exterior and interior surfaces can be observed. As can be seen, aluminum allows a more excellent heat dissipation to the exterior because reducing the radiant transfer to the interior increases the temperature on the exterior surface, thus promoting more excellent heat transfer to the exterior. Therefore, aluminum would be of more significant benefit in this case when we are interested in reducing heat gain to the interior.



(a) Temperature

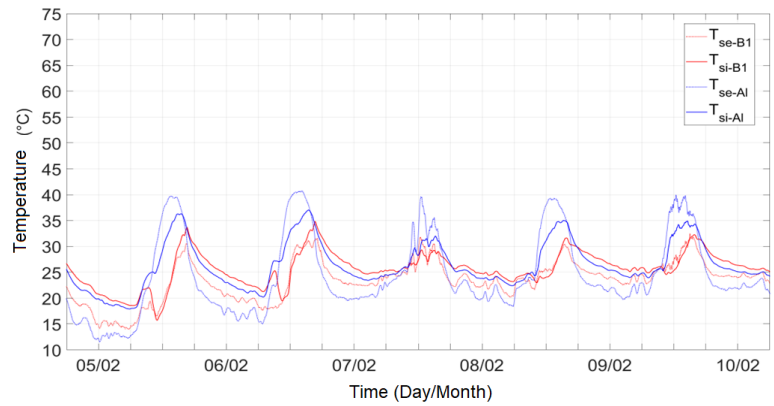
12



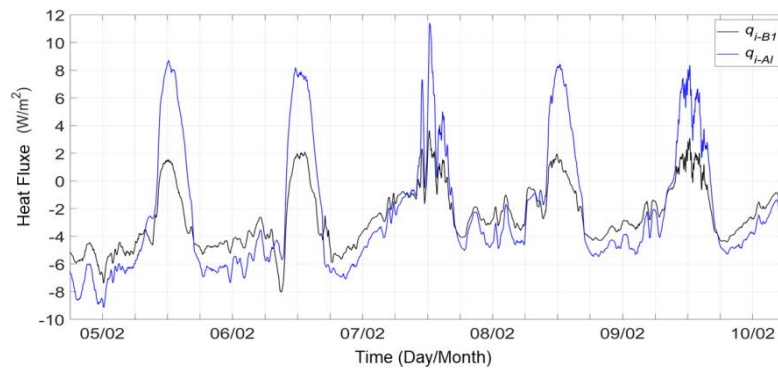
(b) Heat flux

Figure 8. Heat flux and temperature of configurations: RV exterior- B1 interior ($\alpha_e=0.40$, $\epsilon_e=0.89$, $\epsilon_i=0.8182$) vs RV exterior- A1 interior ($\alpha_e=0.40$, $\epsilon_e=0.89$, $\epsilon_i=0.049$), February 05-10.

Fig. 9a shows the behavior of exterior surface temperature for Combination 4. Configuration 3 showed similar behavior to Configuration 4, so only the case of configuration 4 is presented. The highest values of T_{se-B1} and T_{se-A1} were 55°C and 52.2°C , respectively, which means a difference of 2.8°C . T_{si-B1} achieved temperature values of 55°C , while T_{si-A1} achieved a temperature of 46.3°C for the same solar irradiance conditions, which implied a reduction of 8.7°C for the T_{si-A1} . During the hours of irradiance, the temperature differences between T_{si-B1} and T_{si-A1} were more significant. The lowest values of T_{si-B1} and T_{si-A1} were 19.02 and 17.6°C , respectively, which means a temperature difference of 1.42°C . On the other hand, Fig. 9b shows the heat flux behavior in the interior through interior coatings B1 and A1. The average of q_{i-B1} in hours with the highest solar irradiance was 2.5 W/m^2 , while the average of q_{i-A1} was 9.08 W/m^2 ; this implied a reduction of 6.58 W/m^2 compared to q_{i-A1} .



(a) Temperature



(b) Heat flux

Figure 9. Heat flux and temperature of configurations: B2 exterior- B1 interior ($\alpha_e=0.164$, $\varepsilon_e=0.88$, $\varepsilon_i=0.8182$) vs B2 exterior- A1 interior ($\alpha_e=0.164$, $\varepsilon_e=0.88$, $\varepsilon_i=0.049$), February 05-10.

The effect of solar irradiance on the T_{se-A1} and T_{se-B1} is proportional to the solar absorbance of exterior coatings. The delay between highest irradiance and exterior temperatures is inexistent in the case of green and red coatings. Although the reported absorbance for the red coating is higher than the green coating, the behavior of the highest temperature values of T_{se} revealed that the absorbance of the green coating was higher than the red coating.

The exterior surface temperature was more affected by the exterior conditions when the interior surface conductance was low. The surface conductance is composed of the combined effect of radiation and convection. Therefore, the surface conductance decreased as the interior emittance. In the hours of solar irradiance, the interior surface

14

temperature with aluminum (T_{si-Al}) was lower than T_{bi} since the aluminum coating reduced the radiative exchange of the interior surface. Therefore, the dependency of thermal behavior was related to exterior conditions. Nevertheless, the lowest temperature values of the surfaces presented a behavior like T_{sky} since the exterior emittance is the same for all exterior coatings.

The heat flux inside during solar irradiance periods was higher in most cases with an aluminum coating on the interior surface. Although the interior emittance was reduced, aluminum is an excellent thermal conductor and easily achieved thermal equilibrium. However, this feature permitted the loss of energy quickly during the night.

Results show that the exterior coatings with high absorbance presented the highest heat flux inside. The temperature differences between the interior and exterior surface of the roof for the red coating revealed temperature variations between 0.66°C and 1.41°C. While for the green coating, the temperature differences varied from 0.9°C to 2.4°C. On the other hand, the temperature differences varied from 4.6°C to 6.2°C and from 0.15°C to 7.28°C, respectively, for the white-1 and white-2 coatings configurations. These variations depend on the surfaces' emittance, which agrees with what has been reported in the literature.

5 Conclusions

In this study, a roof sample configuration with coatings applied on interior and exterior surfaces was designed, instrumented, and evaluated thermally. The effect of coating changes (different solar absorbance and emittance) in the thermal energy transfer by radiation using a roof sample was evaluated. This study permitted us to evaluate the efficiency and feasibility of using coatings on the interior and exterior surface of roofs as an alternative to contribute to building energy savings.

Experimental results showed that coatings with low solar absorbance and high thermal emittance applied on the exterior of the roof significantly reduced the temperatures. The white coatings were the configurations with the lowest exterior temperature: 7.5°C for the RB2 on the exterior surface with RB1 on the interior surface and 5.9°C for the RB2 on the exterior surface with aluminum on the interior surface. These results coincided with the results reported by Kolokotsa et al. (2017).

Analyzing the effect of solar absorbance and emittance of the interior surface with different coating configurations permitted us to identify the significant changes in thermal energy transfer by radiative transfer. The exterior coating suggested to use in warm zones like Tabasco is the RB1 or RB2 with A1 interior coating because this configuration reduces the thermal gains to the interior cavity. The results obtained in this study are help select suitable coatings for roofs that help to save the cost for users and reduce thermal gains in dwellings.

References

1. Anand, J., Sailor, D. & Baniassadi, A.: The relative role of solar reflectance and thermal emittance for passive daytime radiative cooling technologies applied to rooftops. Sustainable

- Cities and Society 65, 102612 (2020). DOI: 10.1016/j.scs.2020.102612
2. ASTM E 230:2017 (2017) International, Standard Specification and Temperature-Electromotive force (EMF) Tables for Standardized Thermocouples.
 3. Boukhelkhal, I. & Bourbia, F.: Experimental Study on the Thermal Behavior of Exterior Coating Textures of Building in Hot and Arid Climates. *Sustainability*, 13, 4175 (2021). DOI: <https://doi.org/10.3390/su13084175>
 4. Hernández, P., Xamán, J., Macías, E., Aguilar, K., Zavala, I., Hernández, I., Simá, E.: Experimental thermal evaluation of building roofs with conventional and reflective coatings. *Energy and Buildings* 158, 569-579 (2018). DOI: <https://doi.org/10.1016/j.enbuild.2017.09.085>
 5. Hernández, I., Zavala, I., Xamán, J., Belmán, J., Macías, E. & Aguilar, K.: Test box experiment to assess the impact of waterproofing material on the energy gain of building roofs in Mexico. *Energy* 186, 115847 (2019). DOI: <https://doi.org/10.1016/j.energy.2019.07.177>
 6. Kolokotroni, M., Shittu, E., Santos, T., Ramowski, L., Mollard, A., Rowe, k., Wilson, E., Pereira, J. & Novieto, D.: Cool Roofs: High Tech Low Cost solution for energy efficiency and thermal comfort in low rise low income houses in high solar radiation countries. *Energy & Buildings* 176, 58-70 (2018). DOI: 10.1016/j.enbuild.2018.07.005
 7. Kolokotsa, D., Giannariakis, G., Gobakis, K., Giannariakis, G., Synnefa, A. & Santamouris, M.: Cool roofs and cool pavements application in acharnes, Greece. *Sustainable Cities and Society* 37, 466-474 (2017). DOI: 10.1016/j.scs.2017.11.035
 8. Mexico City 2021 Past Weather (Mexico) - Weather Spark. (2021). Weatherspark.com. <https://weatherspark.com/h/y/5674/2021/Historical-Weather-during-2021-in-Mexico-City-Mexico>
 9. Millstein, D. & Levinson, R.: Preparatory meteorological modeling and theoretical analysis for a neighborhood-scale cool roof demonstration. *Urban Climate* 24, 616-632 (2018). DOI: 10.1016/j.uclim.2017.02.00523
 10. Norma Oficial Mexicana [NOM-020-ENER-2011]. Envolvente energética en edificaciones. Envolvente de edificios para uso habitacional (México).
 11. Qiu, T., Wang, G., Xu, Q. & Ni, G.: Study on the thermal performance and design method of solar reflective-thermal insulation hybrid system for wall and roof in Shanghai. *Solar Energy* 171, 851-862 (2018). DOI: 10.1016/j.solener.2018.07.036
 12. Valencia-Caballero D., Bouchakour S., Luna Á., Garcia-Marco B., Huidobro A., Iores-Abascal I., Sanz Martínez A., Román E.: Experimental energy performance assessment of a bifacial photovoltaic system and effect of cool roof coating. *Journal of Building Engineering* 80, 108009–108009 (2023). DOI: <https://doi.org/10.1016/j.job.2023.108009>
 13. Verma R. & Dibakar Rakshit: Comparison of reflective coating with other passive strategies, A climate based design and optimization study of building envelope. *Energy and Buildings* 287, 112973–112973 (2023). DOI: <https://doi.org/10.1016/j.enbuild.2023.112973>
 14. Wang J., Liu S., Meng X., Gao W.: Influence of the building enclosed forms on thermal contribution of retro-reflective and high-reflective coatings. *Energy and Buildings* 273, 112400–112400 (2022). DOI: <https://doi.org/10.1016/j.enbuild.2022.112400>

Provision of short-term flexibility service from prosumer's facilities

Marina Codina Escolar¹[0009-0002-4434-9741], José Fernando Forero-Quintero¹[0000-0001-5930-4226], Roberto Villafáfila Robles¹[0000-0003-4372-2575], Francisco Díaz Gonzalez¹[0000-0002-1912-3014], and Sara Barja-Martinez¹[0000-0003-4126-8858]

Centre d'Innovació Tecnològica en Convertidors Estàtics i Accionaments (CITCEA),
Departament d'enginyeria elèctrica, Universitat Politècnica de Catalunya (UPC),
Av. Diagonal 647, Barcelona 08028, Spain,
<https://www.citcea.upc.edu/>

Abstract. The rising concern of global warming has led to an energy transition, which has transformed the electricity system. This shift has resulted in the connection of more distributed energy resources to the distribution system. The majority of these installations are renewable generators, whose behavior is stochastic in nature. The unpredictable behavior of renewable energy plants is a significant challenge, which has created the need to develop flexibility capabilities from the demand response or generation side to ensure a continuous supply of electricity to end-users. In this work, the energy management system of a domestic user is modified to incorporate the requirements of aggregators to reduce power consumption. The case study focuses on a single domestic user with inflexible and flexible loads, which means that loads can be disconnected to avoid exceeding the maximum power set by the aggregator. An economic analysis is developed to determine if flexibility services are a feasible option for end-users. This analysis compares the results of four scenarios, comparing different Energy Management Systems programs. Offering flexibility services to the grid allows the end-user to obtain a reduction in the electricity bill with the selected parameters.

Keywords: Energy management system · flexibility requirements · shiftable loads · economical analysis.

Abbreviations:

CEP: Clean Energy Package
DER: Distributed Energy Resources
DSF: Demand-Side Flexibility
DSO: Distributed System Operator
EMS: Energy Management System
EV: Electric Vehicle
FLEMS: Flexibility Management System
PV: Photovoltaic

2 M. Codina Escolar et al.

RES: Renewable Energy Sources

SoC: State of Charge

1 Introduction

The growing concern to reduce greenhouse gases and prevent global warming has driven the growth of renewable generation and increased interest in Distributed Energy Resources (DER). This, in turn, has led to impacts on the electricity system due to the variability of production and the speed with which behaviors change, resulting in imbalances between production and consumption; where flexibility emerges as a possible solution[1].

In recent years, flexibility has been offered by generating power plants, but the increase in distribution generation has created the need to incorporate new measures to have greater control of the network and ensure electricity supply[2].

Different options can be applied to provide flexibility to the electric system, like increasing the operability of the system, deploying demand response, upgrading the distribution network, integrating fast response power plants, or incorporating storage systems[3]. Demand response requires less financial resources and produces less environmental impact than upgrading the distribution network by increasing the number of electrical lines as seen in Figure 1.

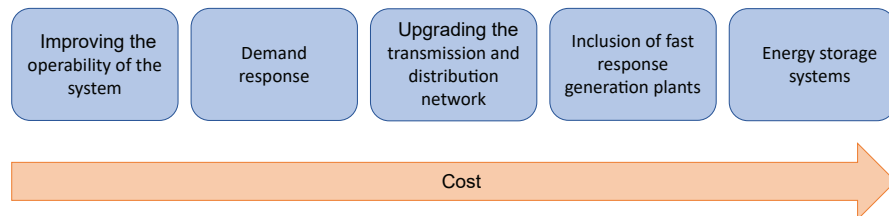


Fig. 1. Relationship of flexibility sources and implementation costs[3]

Demand response or Demand-Side Flexibility (DSF) allows end-users, as individual consumers or energy communities, to reduce their consumption consequently reducing their electricity bill. As they can obtain profits for offering services to the power system [4].

Energy communities are defined inside the Clean Energy Package (CEP) [5] as legal entities based on open and voluntary participation. These communities are autonomous and controlled by members located in the proximity of Renewable Energy Sources (RES) whose primary purpose is to provide environmental, economic, or social community benefits for their stakeholders, members, or the local areas where they operate rather than financial profits. Moreover, energy communities are allowed to produce, consume, store and sell renewable energy,

provide aggregation, commercial energy services, and act as Distribution System Operator (DSO).

The wide range of users that can provide DSF is the main reason why this paper focuses on studying the option of demand response.

The electrical flexibility of the demand can be classified into two main groups: implicit and explicit flexibility. The first one consists of minimizing users' consumption through economic signals, for example, in periods of high consumption, when tariffs impose a high cost to change consumer habits. Implicit flexibility also consists of energy efficiency measures.

On the other hand, explicit flexibility is linked with punctual flexibility requirements from the aggregator. This option requires active generation and demand management to supply services to the power system. End-users and energy communities can play an important role as they have flexible elements in their facilities[6].

To participate in the flexibility market users, as individual consumers or energy communities, have to be represented by the figure of the aggregator. In the Spanish regulation [7], independent aggregators are defined as participants in the electricity production market that provide aggregation services and are not affiliated with the customer's supplier, understanding aggregation as the activity carried out by individuals or legal entities that combine multiple consumers, self-generated electricity sources or electricity from storage facilities for sale or purchase in the electricity production market.

The increasing digitization of the electricity grid and household appliances creates opportunities for end-users, together with the expansion of distribution energy production installations for self-consumption in end-user households connected behind the meter, enabling end-users to participate actively to reduce the amount of their electricity bill[8].

It is necessary to take into account that most of the users are prosumers it is convenient to have an Energy Management System, that facilitates the knowledge about its operation mode, the generation sources' behavior, and the flexibility available within its premises. This element will also facilitate the management of the flexible loads optimizing generation and connections for battery charging. For this reason, the work is developed with houses that have an Energy Management System and monitoring of the loads. This work is a continuation of the dissertation of [9] and [10]. Barja-Martinez et al [9] present an Energy Management System (EMS) to optimize the power consumption of an end-user. The program is generated for a full day, divided into 96 periods of 15 minutes, with constant generation and consumption values for each period [11]. Forero-Quintero et al [10] adapt the Energy Management System into real-time, also known as Flexibility Management System (FLEMS), which considers the variations in consumption and production profiles that occur in real-time to obtain the lowest possible energy cost within the period by having modifications to the planned energy program.

In contrast to previous projects, like [9], this work not only manages energy within the home but also considers the role of introducing external setpoints.

4 M. Codina Escolar et al.

Considering that the project aims to incorporate short-time flexibility requirements to reduce the power consumption of the distribution network, adapting the energy program of a domestic user to the needs of the network. It is necessary to work on real measurements inside the studied period like in [10].

When the user participates in the flexibility market, it could obtain economic benefits for the services provided to the distribution network, this possibility is going to be studied in this project.

Figure 2 shows the general relationship between the different actors, control schemes of the system, and the input signals for the flexibility requests. That is the energy management programs and the flexible elements of the user’s installation can be seen in the blue blocks. The blocks ”EMS” and ”FLEMS” blocks were developed in [10] and [11] respectively.

On the other hand, blocks and external signals to the user’s facility are shown in green. This paper is focused on the blocks inside the red area, in which the aggregator has a request for limiting the power consumed from the network to its customer for a lapse of time. Therefore, the aggregator’s request modifies the energy management program.

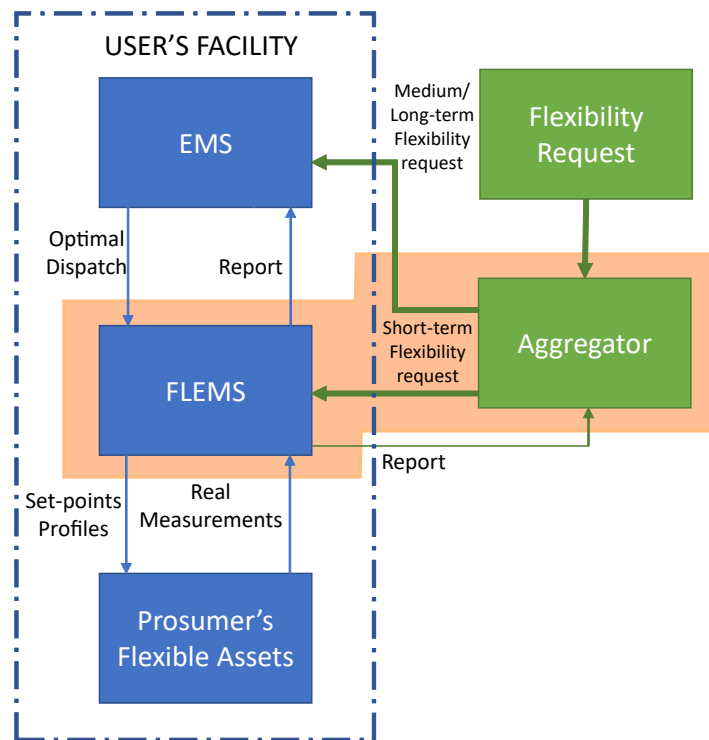


Fig. 2. Control Scheme of Power System with Distributed Resources. [10]

The result of the EMS program is modified by FLEMS to suit reality by modifying the controller parameters. The FLEMS results are the setpoints of each element. Once 24 hours have passed, the FLEMS program returns a report to the EMS controller that improves the forecast for future periods.

The availability of flexibility and the analysis of the match is outside the scope of work. Therefore, it will be assumed that one hour before flexibility service is delivered its acceptance occurs and approved offers are worked with.

2 Relationship between aggregators and end-users

Although the figure of an independent aggregator is already defined by the Spanish and European regulations, there are many doubts about how this figure will be integrated into the electric market and which will be the relationship between the aggregators, retailers, and end-users. The definition of response time, how to measure the flexibility delivered and the methods of remuneration are still unclear.

This work has been developed considering these assumptions:

- The measuring flexibility baseline will be the total consumption allowed from the grid because no baseline is defined.
- The flexibility services are paid to the end-user in two terms, one part for the power that the user has available to offer in the flexibility service as foreseen by the EMS, and a second part corresponding to the power reduction that is delivered in the service in the required window.
- It is mandatory to comply with the flexibility requirement in the required time window so that the aggregator can control the user's flexible uploads.
- To avoid modeling of flexible loads, it is considered that once disconnected they cannot be reconnected until after the flexibility requirement period.
- An economic penalty for shifting the consumption of some loads has been defined, so it is possible to quantify the decrease in user comfort by limiting the operating time of their appliances.

As proposed in [12], an economic study is carried out to determine the benefit that end-users could obtain by offering services to the electricity grid. This takes into account algorithms that have the aim of reducing the battery aging cost and maximizing the user's self-consumption of energy.

3 Methodology

The FLEMS model developed in [10] is made with two kinds of blocks, the first one is a real-time power controller. The second kind of blocks are emulators of the residential elements of distributed generation used for testing in a simulation environment. There are three generation models: the photovoltaic model, the battery, and the electric vehicle model. It also includes an emulator for the consumption user, which is used to compute the power that is needed from the grid.

6 M. Codina Escolar et al.

Figure 3 shows the relationship between the inputs and outputs of the different blocks of the model. It is also useful to understand the relationship between EMS and FLEMS models.

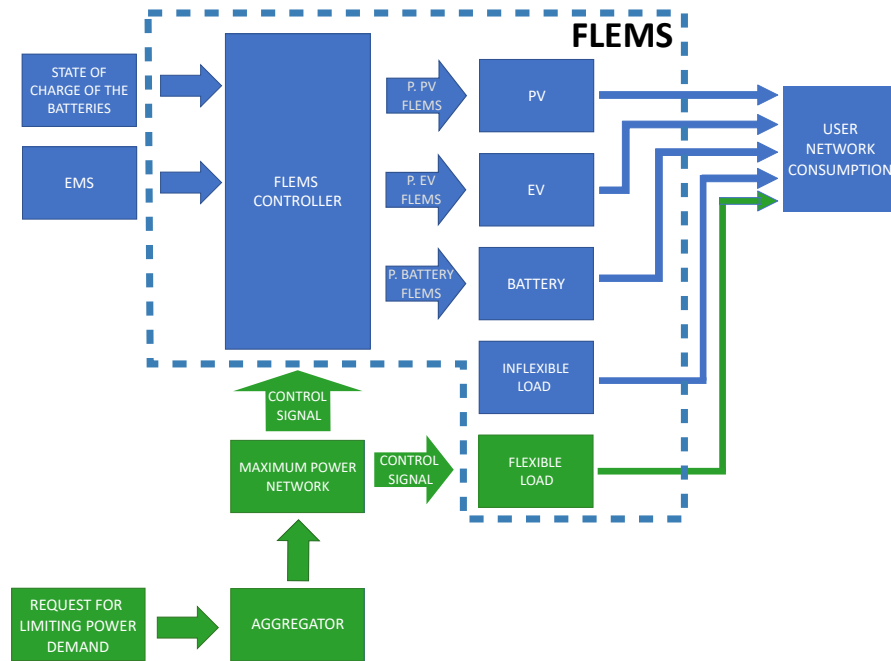


Fig. 3. Relationship diagram of the user’s facility model.

The power controller takes the forecasted consumption and generation values from the EMS program as input. The state of charge of the batteries is also required as input to determine the discharge and charge potential of the system’s batteries which is the main reason for having as an input the real measurements. In this project, a real-time flexibility controller is incorporated taking as input the maximum power that can be consumed from the network.

This means that the FLEMS system is modified so it can be communicated with the aggregator control system, where there are two different paths to incorporate the aggregator flexibility request into the real-time program. The first one corresponds to a direct control through FLEMS controller parameters to fulfill the request and the second one is where the aggregator can directly control some user’s loads to make sure that the flexibility request is achieved.

The output of the model is the suitable program generated to comply with the flexibility request and the consumption of each item connected to the user’s electrical installation. When there is no flexibility request, the system adapts

the EMS forecasted program to the real measurements inside the fifteen-minute lapse.

An economic study is also carried out to check which program is more cost-effective for the end-user, taking into account that benefits are obtained for the flexibility services delivered and the financial penalty for disconnecting flexible loads and affecting user comfort.

The cost of the FLEMS program with flexibility request is computed by the equation 1:

$$Cost^{FLEMS}_{with_flexibility} = Cost^{FLEMS} - [(P_{flex} \cdot cost_{P_{flex}}) + (E_{flex} \cdot preu_{E_{flex}})] + (P_{pen} \cdot E_{flex} \cdot S_{Control}) \quad (1)$$

Equation (1) is formed by three independent terms corresponding to the cost of the FLEMS program, the cost of power and energy delivered in the flexibility service, and the penalty cost. This penalty represents the cost of affecting the user's comfort when it is necessary to disconnect flexible loads to comply with the flexibility requirement.

The $Cost^{FLEMS}$ is computed as [10] and its value corresponds to the cost of the electricity for the user when the flexible management system program is used. The parameters and variables used in the equation are explained in Subsection 4.

4 Case study

The user being analyzed is a detached house consumer with photovoltaic generation, an electric vehicle, and a storage system located in Austin, Texas, as seen in Figure 4. The rated power and capacity of the devices are listed in Table 1.

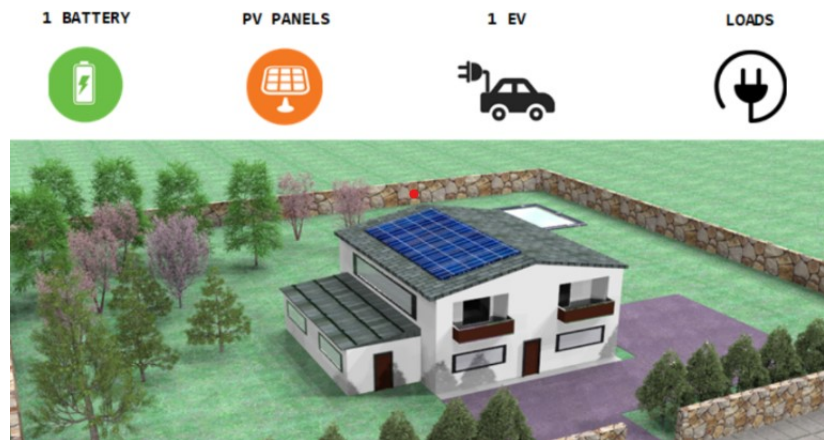


Fig. 4. Typical user analyzed for the case study.[11]

Table 1. Devices power characteristics.

Device	Rated power	Capacity
PV	3 kW	–
Battery	5 kW	10 kWh
EV	3 kW	20 kWh

The data consumption and generation of each element monitored is obtained from the database of Pecan Street Inc.[14] where it can be found values of consumption for every 15 minutes and per second.

The lapse of time that has been analyzed is January 14th, 2018 between 5 pm and 5:15 pm. A restriction is incorporated to prevent the domestic installation from injecting energy into the electricity grid, as it has been maintained in the work developed previously.

The user has considered some of its loads to be flexible, which means that loads can be disconnected or postponed, meeting the flexibility requirement. The user that is analyzed has the following flexible loads: air conditioning, dishwasher, dryer, and washing machine.

With this user's data, we analyze what happens in the energy program according to the period and the benchmarks requested by the aggregator, which responds to the desire to reduce the consumption of different users in its portfolio in the same geographical area to reduce the power consumption of the distribution network.

To compute the cost of the electricity for the end-user and compare the results obtained with the different energy program costs, there is a need to define some values from the parameters from (1). The different values are shown in Table 2. The variable E_{flex} defines the flexible power delivered during the period where

Table 2. Parameters, definitions, and values used for cost calculation.

Parameter	Definition	Value
P_{flex}	Power offered for the flexibility service at the time of acceptance of the offer	300 W
$costP_{flex}$	Economic remuneration received by the user for the power.	$0.0965 \frac{\text{€}}{\text{kW}}$
$preuE_{flex}$	Economic remuneration received by the user for the flexibility services offered during the period.	$0.124 \frac{\text{€}}{\text{kWh}}$
P_{pen}	Economic amount that is imposed on the affectation of the user's comfort by disconnecting the shifting loads	$0.186 \frac{\text{€}}{\text{kWh}}$

flexibility services are requested. The variable $SControl$ that appears on the last term corresponds to the binary signal that controls the flexible loads. The price for the power is obtained from the average of the values of electricity bills.

On the other hand, the value of the price for the delivered flexible energy is the average value of what the electricity companies currently pay to users with surpluses.

The development of the model for computer simulation has been carried out using Matlab Simulink [®] software. Where the data inputs are vectors with time, the power generated or consumed is the minimum power computed, and the EV and battery emulators take into account the cycling and aging costs.

5 Results

As it has been said in Section 2 the aggregator measures the total power that the user is taking from the grid, and if it is necessary disconnects some loads to fulfill flexibility services to comply with the aggregator's flexibility requirement. During the period under review, there is only one flexible load operating, which consumes about 950 W, and the aggregator asks the user to reduce network consumption by a minimum of 300 W, which means that disconnecting the flexible load makes sure that the flexible request is fulfilled.

First of all, the aggregator receives some requests from the DSO to reduce the power consumption in a geographical area. The aggregator algorithm determines the consumption reduction for each user of its portfolio. How the algorithm distributes the required power among the customers is outside the scope of the study.

The next step is for the aggregator block to impose the new maximum power that can be consumed from the grid, according to the flexibility request, and to generate the control signal. An algorithm that computes the energy consumption and controls the range of power is developed to generate the control signal.

As said previously, the model has been simplified to avoid modeling the loads, so that if they have been disconnected, they cannot be reconnected within the period. This simplification prevents the aggregator from having to model all the flexible loads of its customers.

Figures 5 and 6 are a representation of the different power values of the programs over time, where it can be found four types of lines:

- The red and pink ones represent the maximum and minimum power that can be consumed from the network, taking into account that the system is not allowed to inject electricity into the network.
- The dark green line represents the FLEMS Point of INterconnection (POI) power consumption if there were no flexibility services in the period.
- The discontinued lines that represent the forecasted values from the program EMS for each element connected to the user's facility.
- Finally, the continuous lines represent the real consumption of the elements connected to the user's facility during the period providing flexibility services.

10 M. Codina Escolar et al.

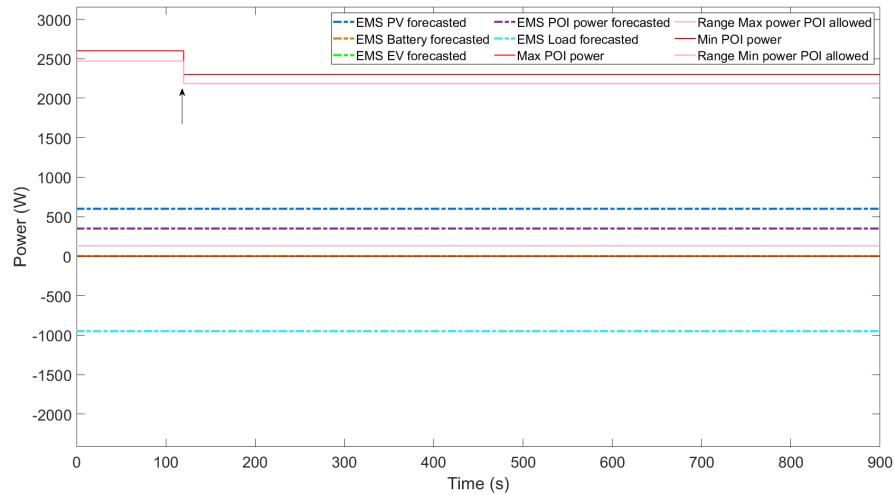


Fig. 5. Representation of the forecasted power dispatch.

In Figure 5 it can be seen that the forecasted program made with EMS accomplishes the aggregator request, so the flexibility service is accepted in advance by the EMS controller. The request for flexibility within the period happens at the second minute of the simulation of the program. Since the flexibility service is not necessarily required for the entire period and depends on the aggregator's algorithm. The maximum power allowed is reduced from 2600 to 2300 W. The results of the EMS are constants for each period, the generation and the consumption of the elements connected to the user system.

The analysis of the results shown in Figure 6 is explained bellow. The maximum allowable network consumption is reduced from 2600 W to 2300 W at the second minute of the representation, as pointed out by the first arrow ($t = 120$ s). The next twenty seconds passed without modifications because the user FLEMS programs fulfilled the request, but when the car is unexpectedly connected to charge at the second 141, the flexible load needs to be disconnected, as highlighted by the second arrow ($t = 141$ s). Following the aggregator's request, the appliance's start-up is slowed down to maintain the real consumption below the maximum consumption and to be able to charge the electric vehicle.

The PV panel is producing less energy than what was expected by the EMS program, but after 25 seconds, the FLEMS algorithm changes the control set-point to increase production. When the charging of the electric vehicle ends, the production of the photovoltaic installation decreases gradually during the rest period.

The battery does not deliver energy to the system, but it does not have zero value as intended, due to the losses of the system that has a value of 158.4 W.

If there was no EV charging session within this period, the user would not have to disconnect the flexible load. Therefore, if the aggregator does not have

direct control of the user appliances, the user could choose whether to avoid charging the electric vehicle or disconnect the scrollable loads, depending on its priorities.

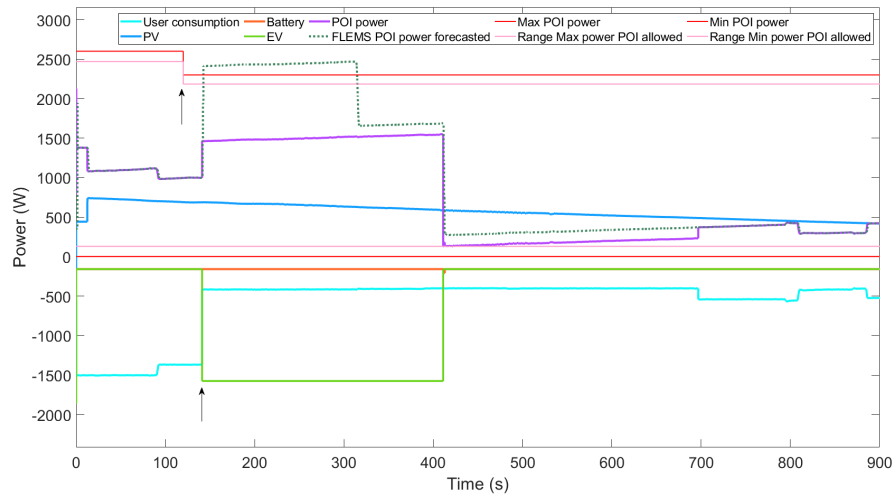


Fig. 6. Results of flexibility power dispatch simulation.

The next step is to analyze the economic results represented in Figure 7. It can be seen that the program with the highest cost is the EMS, as not allowing modifications to the program and not being able to use the energy stored in the battery means that all the electricity needed has to be consumed from the electricity grid. In this case, the cost also takes into account penalties for prediction error, corresponding to the differences occurring in the period analyzed concerning the forecast.

On the other hand, the cost of not following an energy management program is lower than in the previous case. This is because it does not take into account the penalties for not allowing the electric vehicle to be charged, but it does not entail any savings since it does not attempt to optimize the model to reduce the amount of the electricity bill. It can be seen that the cost between the EMS program and the case without any program is reduced by 58 %.

The other two bars correspond to the FLEMS customized energy program, with and without flexibility service. When a flexibility service is provided, the user receives economic compensation for it. This allows the end-user to obtain a reduction in the electricity bill, taking into account the income received. However, there is no zero cost because of the economic quantification of the reduction of the user's comfort due to the disconnection of the flexible loads. This allows the user an 85 % decrease compared to the EMS program when the user does

12 M. Codina Escolar et al.

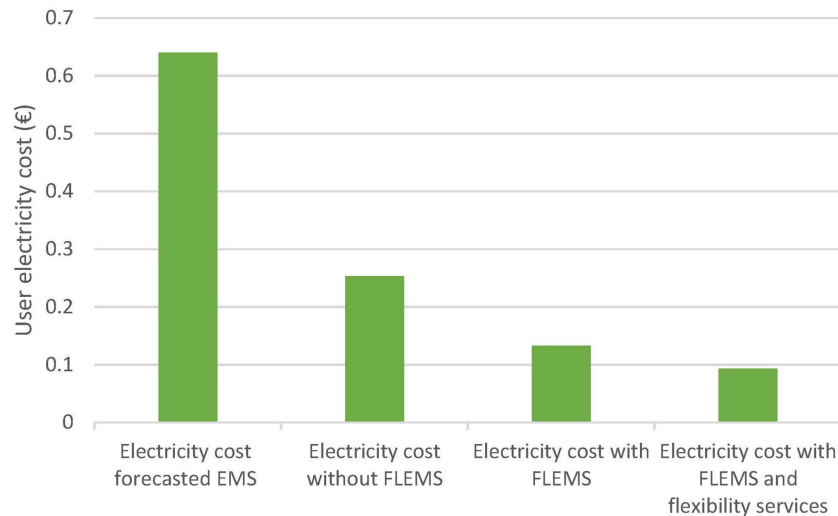


Fig. 7. Economical results obtained after simulation.

not have a flexibility requirement and follows the program provided by FLEMS obtains an 80 % reduction from the electricity cost forecasted for the EMS.

It should be noted that not all flexible services can be compensated with the same formula, and if it were not necessary to disconnect the flexible loads during the study period, the system could have negative costs, which means that the user would receive enough revenue to cover the electricity costs for the period.

If the user does not provide flexible services, he has no way of earning income, and therefore, although the FLEMS algorithm allows a significant reduction in the electricity bill, the user will have an electricity cost.

6 Conclusions

Flexibility services can allow users with an Energy Management System to profit from installation through an extra reduction in electricity bills. The proposed case study shows a reduction in electricity costs of 85% compared with the EMS program, and a saving of 30% compared to real-time values. On one hand, the EMS forecast schedule entails the highest cost, as it considers generation and consumption constant. This causes the differences between actual and forecasted to be penalized economically. On the other hand, applying the FLEMS program means a cost reduction for the system, since it is specifically designed to reduce the bill.

Therefore, the case study shows that users could benefit from offering flexibility services. However, it would be convenient to study whether the same would have the same positive results when analyzing longer intervals. It would also be

important to analyze the sensibility to different prices and costs, as economic savings depend on the costs and prices that have been considered.

The case study considers that the aggregator remotely controls the user's flexible loads. Then, it would not be necessary to have an energy management system, but it could increase the inconvenience to the user since it would not have a forecast of the consumption in the required period. For this reason, it could be more convenient to consider an energy management system able to work directly with a flexibility set points.

It is important to note that implementing such an energy management system requires both a home automation system and real-time metering elements, resulting in a significant initial investment.

References

1. Pablo Arocena, Antonio Gómez y Sofía Peña, La eficiencia energética, el efecto rebote y el crecimiento económico. Papeles de energía. Diciembre 2016.
2. Grupo de trabajo sobre flexibilidad, Futured, Flexibilidad en redes de distribución eléctrica. Marzo 2021.
3. Sistema Eléctrico Nacional, Concepto de Flexibilidad en el Sistema Eléctrico Nacional, Centro de energía, Facultad de Ciencias Físicas y Matemáticas, Universidad de Chile, 2019, Av. Tupper 2007, Santiago, Chile
4. Joan Recasens and Cristina Corchero and Mattia Barbero ,El camino para mejorar la flexibilidad del sistema eléctrico, Las notas de Bamboo energy
5. ALATON C. (Tractebel Impact), TOUNQUET F. (Tractebel Impact): Energy Communities in the Clean Energy Package: Best Practices and Recommendations for Implementation, Luxembourg: Publications Office of the European Union (2020)
6. Profitability analysis on demand-side flexibility: A review Jose-Fernando Forero-Quintero, Roberto Villafañila-Robles, Sara Barja-Martinez, Ingrid Munné-Collado, Daniel Montesinos-Miracle from Centre D'Innovació Tecnològica en Convertidors Estàtics I Accionaments (CITCEA-UPC), Department D'Enginyeria Elèctrica, Universitat Politècnica de Catalunya, UPC. Av. Diagonal 647, Pl.208028, Barcelona, Spain and Pol Olivella-Rosell from ThermoVault (BV). Hoefstadstraat 86, 3600 Genk, Belgium
7. BOE (Boletín Oficial del Estado), Ley 24/2013, de 26 de diciembre, del Sector Eléctrico, 27/12/2013, núm 310, p.21.
8. Agencia Internacional de Energías Renovables, IRENA (2018), Power System Flexibility for the Energy Transition, Part 1: Overview for policy makers (Flexibilidad del sistema eléctrico para la transición energética, parte 1: panorama general para los encargados de formular políticas), Abu Dabi.
9. Barja, S. Lloret, P. Olivella, P. Villafañila, R: Centralized flexibility services for distribution system operators through distributed flexible resources. A: Ibero-American Congress of Smart Cities. pp. 507–519. (2019). ISBN 978-958-5583-78-8.
10. Forero-Quintero, J.F., Barja Martínez, S., Villafañila Robles, R. Montesinos Miracle, D.: Flexibility Management System for Executing Energy Program with Distributed Resources. A: Ibero-American Congress of Smart Cities 2022.
11. Barja Martínez, S.(2021): Optimization algorithms for Energy Management Systems. Definition and case studies CITCEA-UPC.

- 14 M. Codina Escolar et al.
12. J. M. Specht and R. Madlener, "Energy supplier 2.0: A conceptual business model for energy suppliers aggregating flexible distributed assets and policy," *Energy Policy*, vol. 135, 2019
13. Cabrera, A., Aragüés, M., Gomis-Bellmunt, O. Dynamic modelling and control of a PV generator for large scale applications. A: IEEE International Conference on Industrial Technology. "2018 IEEE International Conference on Industrial Technology (ICIT): Lyon, France: February 19-22, 2018: proceedings". Institute of Electrical and Electronics Engineers (IEEE), 2018, p. 944-949.
14. Pecan Street, "Residential data." <https://dataport.pecanstreet.org/>. Accessed on 2023-03-05.

Exergoeconomics in Energy Systems: Evaluating technological and economic costs of an AHT

Lailani Alvarez¹[0000-0001-5559-9063], Mayra Harumi Bello Guadarrama²[0009-0007-1202-2900],
N.I. Ortega- Mojica³[0000-0001-9843-2044], J. Delgado-Gonzaga⁴[0000-0003-2243-0290], D.
Juárez-Romero⁵[0000-0003-0942-9738], J.A. Hernández⁶[0000-0002-2107-3044] and A.
Parrales^{7*}[0000-0001-8554-8777]

^{1,2,3} POSGRADO- Centro de Investigaciones en Ingeniería y Ciencias Aplicadas, Universidad Autónoma del Estado de Morelos, Av. Universidad 1001 Col. Chamilpa, C.P. 62209, Cuernavaca, Morelos, México.

⁴Instituto de Energías Renovables, Universidad Nacional Autónoma de México, Xochicalco s/n, Azteca, C.P. 62588, Temixco, Morelos, México.

^{5,6}Centro de Investigaciones en Ingeniería y Ciencias Aplicadas, Universidad Autónoma del Estado de Morelos, Av. Universidad 1001 Col. Chamilpa, C.P. 62209, Cuernavaca, Morelos, México.

⁷ CONAHCyT- Centro de Investigaciones en Ingeniería y Ciencias Aplicadas, Universidad Autónoma del Estado de Morelos, Av. Universidad 1001 Col. Chamilpa, C.P. 62209, Cuernavaca, Morelos, México.
arianna.parrales@uaem.mx

Abstract. The increasing interest in energy conservation and its impact on a company's economy has led to the development of various models aimed at aligning energy processes with cost accounting. As a result, the industry has directed its efforts toward identifying economically feasible, technologically viable, and environmentally responsible alternatives. One of the solutions to these challenges involves conducting exergoeconomic analyses on the energy systems operating within companies to optimize available resources. This study focuses on the application of exergoeconomic analysis to an Absorption Heat Transformer (AHT) to assess areas for improvement during system operation and to adjust the necessary parameters for enhanced technological efficiency. In addition to obtaining technical efficiency data of up to 98% in the operation of some components, areas for improvement in the Generator (GE), Economizer (EC), and Absorber (AB) were identified for future studies. The fact that considering cost as a term related to consumed resources provides a comprehensive understanding of the energy systems used by the industry. Results such as a 50% system profitability underscore the importance of considering technical efficiency and economic and environmental efficiency within energy management in the industry sector.

Keywords: exergonomic, exergy analyses, systems optimization, absorption heat transformer, exergetic efficiency.

2

Nomenclature

Roman letters		Greek letters	
B^*	Exergetic cost	η	Efficiency
c	Unit exergetic cost	Π	Exergetic cost
F	Fuel	Vectors and Matrices	
k	Unit exergy consumption	A	Incidence matrix [$n \times m$]
k^*	Unit exergy cost	Υ^*	Vector of external assessment [$m \times 1$]
P	Product	Z	Vector of external assessment [$m \times 1$]
Z	Capital-cost amortization	Π	Exergetic cost vector [$m \times 1$]
h	Specific enthalpy kJ/kg		
\dot{m}	Mass flow rate (kg/s)		
Q	Heat load (W)		
T	Temperature ($^{\circ}C$)		
X	Solution concentration (% wt)		
Subscripts			
AB	Absorber		
CO	Condenser		
EC	Economiser		
EV	Evaporator		
GE	Generator		

1 Introduction

With the increasing interest in energy conservation and its impact on the economy of businesses, various methodologies have been developed to align energy processes with accounting.

According to economic management, the concept of "cost" can be defined as the amount of resources required to produce a good or service. However, when applied to energy accounting, cost is related to both the resources consumed and generated during an energy process, as well as the environmental impact it produces [1].

One example of such methodologies is exergoeconomics, which combines the principles of the Second Law of Thermodynamics (the concept of exergy) with economic principles (the concept of cost) [2]. Its application allows us to understand three critical aspects within energy systems [3]: 1) where resources have been utilized,

2) the quantity of resources consumed, and 3) possible improvements to the design and configuration of the system.

The history of this field of knowledge (exergoeconomics) began with research into different energy systems and how to improve their techno-economic performance. One of the earliest cases was proposed by El-Sayed and Evans [4], where they introduced a new approach to consider the concepts of "exergy" and "internal economy." Their work enabled the optimization of complex energy problems by analyzing interconnected systems, offering a better perspective on the efficient use of renewable energy.

In the case of Tsatsaronis and Winhold [5], they developed a methodology to optimize the performance of a combined power plant, considering both technological efficiency and cost-benefit analysis. Von Spakovsky [6] built a model of an energy system to show its internal economy and optimal performance. This model entailed an engineering functional analysis that decentralized the optimization or enhancement of the system's components, taking their isolated behavior into account.

Frangopoulos [7] applied a nonlinear programming methodology to optimize the technical and economic components of a cogeneration system. The approaches of Specific Exergy Costing (SPECOC), Exergy Economics Approach (EEA), First Exergoeconomic Approach (FEA), and Extended Exergy Accounting (EEA) are all aimed at analyzing the exergetic efficiency of an energy system and its corresponding economic costs [8-11].

Afterward, Valero and Lozano [12] introduced the Theory of Exergetic Cost (TCE), which addresses evaluating and optimizing energy systems through cost allocation. They also analyzed the relationship between technological efficiency and economic costs.

Regarding the TCE, practical examples can be found in the real world. Seyyedi [13] emphasized the importance of waste in exergetic systems through the ECT. On the other hand, de Araújo et al [14] highlighted the relevance of solving problems related to cost allocation, system diagnosis, and optimization. Finally, de Faria et al [15] analyzed the energy conversion process by considering the importance of environmental impacts, technical factors, and economic aspects.

Therefore, this paper presents the application of the TCE to an Absorption Heat Transformer to understand the costs associated with energy conversion and process optimization. The main points achieved are as follows:

1. Identify and quantify the costs associated with processes within the AHT.
2. Provide insights into areas of improvement within the energy process for subsequent optimization.
3. Utilize the TCE as an evaluation tool for cost and efficiency matters.

2 Experimental Setup

The Absorption Heat Transformer (AHT) is a type of heat pump, which has the ability to take advantage of the design heat of an industrial process or a low-quality source and bring it to a higher temperature in order to use it in a specific purpose [16].

4

The main components of a AHT are four heat exchangers of different types and shapes, which perform specific functions: evaporate, condense, generate and absorb.

The AHT studied in this article is built with two duplex components and an economizer: Evaporator-Absorber (EV-AB) and Generator-Condenser (GE-CO), the first works at a high pressure and the other works at a low pressure.

In the AHT process, an exothermic reaction occurs generated by the LiBr absorbent mixture. The heat generated during the exothermic reaction is used to distill impure water that flows into the equipment.

Low thermal level waste heat (Q_{GE}) is added to vaporize the refrigerant from the weak solution (low concentration of the absorbent mixture). The vaporized refrigerant goes to the condenser where it condenses and delivers a quantity of heat (Q_{CO}) at low ambient temperature. The refrigerant leaving the condenser is pumped to the evaporator where it is evaporated by an amount of low thermal waste heat (Q_{EV}). Then the refrigerant vapor goes to the absorber where it is absorbed by the solution with a high concentration of absorbent coming from the generator, delivering an amount of heat at a higher temperature (Q_{AB}). Finally, the solution with a low concentration of the absorbent mixture returns to the generator, preheating the solution in the economizer, starting the cycle again [17].

Five experimental tests of the installed AHT were considered for the analysis in this article, which were taken under stable operating conditions. The operating parameters that the AHT allows to measure according to its limited instrumentation are: mass flow (m'), pressure (P), temperature (T), and concentration (X), which are shown in Table 1.

The variation shown between each of the parameters is mainly due to the fact that different initial operating conditions were considered for each of the experimental tests, which automatically modify the marked ranges.

Table 1. Operation parameters of Absorption Heat Transformer.

<i>Line</i>	<i>m'</i> (kg/s)	<i>P</i> (kPa)	<i>T</i> (°C)	<i>X</i> (% wt)
1	0.000863-0.00145	6.46-8.22	233.00-399.00	0
2	0.000863-0.00145	6.46-8.22	29.42-33.26	0
3	0.0008-0.0009	24.92-34.27	33.53-38.41	0
4	0.00089-0.007	24.92-34.27	53.55-72.20	0
5	0.0054-0.017	81.9	83.23-86.20	49.69-52.61
6	0.0054-0.017	81.9	75.43-78.54	49.69-52.61
7	0.0054-0.017	81.9	74.31-77.05	49.69-52.61
8	0.004-0.016	81.9	70.21-76.52	52.22-55.54
9	0.004-0.016	81.9	78.59-82.73	52.22-55.54
10	0.004-0.016	81.9	75.42-79.88	52.22-55.54
A	0.12-0.13	81.9	83.00-88.55	0
B	0.12-0.13	81.9	79.97-85.25	0

C	0.144-0.146	81.9	30.52-35.76	0
D	0.144-0.146	81.9	34.74-40.56	0
E	0.12-0.14	81.9	30.52-35.76	0
F	0.12-0.14	81.9	72.02-79.89	0
G	0.03-0.05	81.9	93.92-96.95	0
H	0.03-0.05	81.9	96.95-99.61	0

2.1 Mathematical model

As it is well known, analysis based on the First Law of Thermodynamics gives information about the amount of energy entering and leaving each one of the components as well as the entire system; however, it does not give information about the energy quality or the irreversibilities in the components and in the whole system.

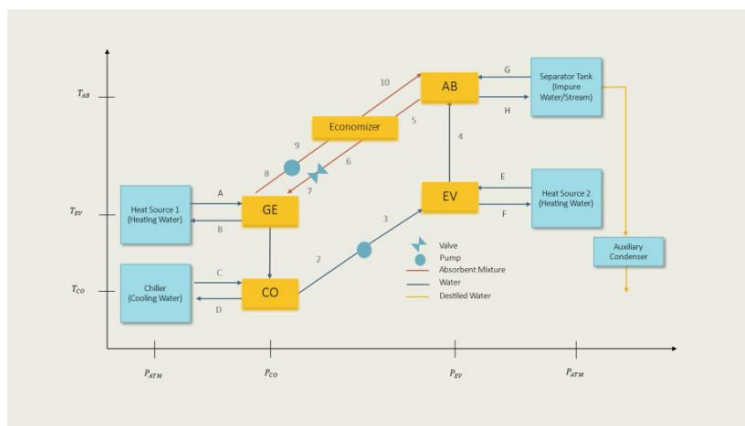


Fig. 1. Schematic diagram of the AHT with dual components.

By performing energy balances on each main component of the system shown in Figure 1, Eq. 1 to 13 are obtained.

Generator

$$\dot{m}_7 = \dot{m}_1 + \dot{m}_8 \tag{1}$$

$$\dot{m}_7 X_7 = \dot{m}_1 X_1 + \dot{m}_8 X_8 \tag{2}$$

$$\dot{m}_1 (h_A - h_B) = \dot{m}_1 h_1 + \dot{m}_8 h_8 - \dot{m}_7 h_7 \tag{3}$$

Condenser

6

$$\dot{m}_1 = \dot{m}_2 \quad (4)$$

$$\dot{m}_{CO}(h_D - h_C) = \dot{m}_1 h_1 - \dot{m}_2 h_2 \quad (5)$$

Evaporator

$$\dot{m}_1 = \frac{Q_{EV}}{(h_4 - h_3)} \quad (6)$$

$$\dot{m}_{EV}(h_E - h_F) = \dot{m}_1(h_4 - h_3) \quad (7)$$

Absorber

$$\dot{m}_5 = \dot{m}_4 + \dot{m}_{10} \quad (8)$$

$$\dot{m}_5 X_5 = \dot{m}_4 X_4 + \dot{m}_{10} X_{10} \quad (9)$$

$$\dot{m}_{AB}(h_H - h_G) = \dot{m}_4 h_4 + \dot{m}_{10} h_{10} - \dot{m}_5 h_5 \quad (10)$$

$$\dot{m}_H h_H = \dot{m}_L h_L + \dot{m}_V h_V \quad (11)$$

Auxiliary condenser

$$\dot{m}_I h_I + \dot{m}_V h_V = \dot{m}_J h_J + \dot{m}_K h_K \quad (12)$$

Economiser

$$\dot{m}_6 h_6 + \dot{m}_8 h_8 = \dot{m}_7 h_7 + \dot{m}_9 h_9 \quad (13)$$

3 Methodology: Theory of Exergetic Cost

One of the exergetic models that uses costing as a basis to determine the origin of the production process and quantifies it is the TCE. This model was introduced by Dr. Antonio Valero with the purpose of assigning costs based on the thermodynamic property of exergy. The TCE establishes that with higher irreversibility (I), the system will always consume a greater number of resources from the plant (F) as long as the products (P) remain constant. Therefore, it is necessary to establish the relationship between the variation in local irreversibilities (ΔI) and the increase in consumed resources [12]. In a more general sense, the entire procedure is illustrated in Fig. 2.

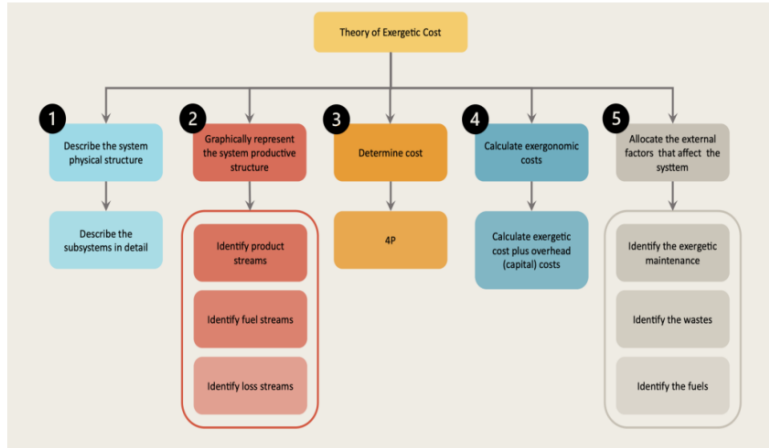


Fig. 2. TEC procedure.

For the application of this model within an energy system, it is necessary to have information that allows the construction of the exergetic model. Such information includes [3]:

1. The physical structure. Provides a detailed description of the physical components and their connections, including boilers, turbines, heat exchangers, pumps, among others Fig. 3.

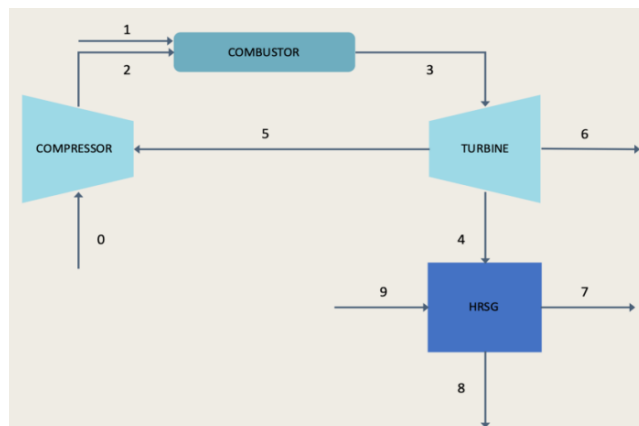


Fig. 3. Physical structure of a cogeneration plant [12].

8

2. Thermodynamic model. It is described through a set of equations (mass, energy, and entropy balances) the interaction of each mass flow stream, heat, and/or work within the physical structure of the plant. For a specific state, the physical exergy of a stream is calculated

$$e_i = h_i - h_0 - T_0(s_i - s_0) + \sum_i(\mu_i c_i - \mu_0 c_0) \quad (14)$$

Where

h_0 y T_0 they are properties that are taken from a selected reference state.

$\sum_i(\mu_i c_i - \mu_0 c_0)$ It constitutes chemical exergy.

3. Economic model. It includes the investment and operating cost of the equipment (\$/h) defined based on a series of parameters including: size, materials, operating range, working hours per year, inflation rates, installation cost and maintenance. The commercial prices of fuels (US\$/kW·h), natural gas, coal, among others, are also considered in Fig. 4.

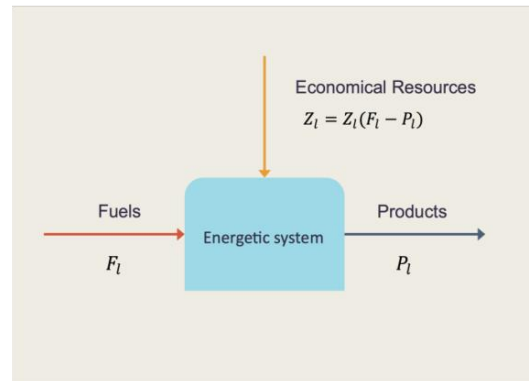


Fig. 4. Economic resources scheme.

4. The productive structure of the plant. This being one of the key concepts within the model, it is related to why the components are positioned (physically) in the system design. That is, it is a graphic representation of the distribution of resources throughout the system.

As indicated by Valero, the purpose of carrying out these analyzes with the proposed model is to obtain efficiencies in the components as well as in the general operation of the system. These efficiencies also allow the quality of the process to be measured and are represented by the Eq. 15.

$$\eta_{ex} = \frac{P}{F} = \frac{Product}{Fuel} \quad (15)$$

Valero [12] represents his model in what he calls “uniqueness matrix” as can be seen in Fig. 5, which makes it possible to calculate both the exergetic and economic costs of an energy system.

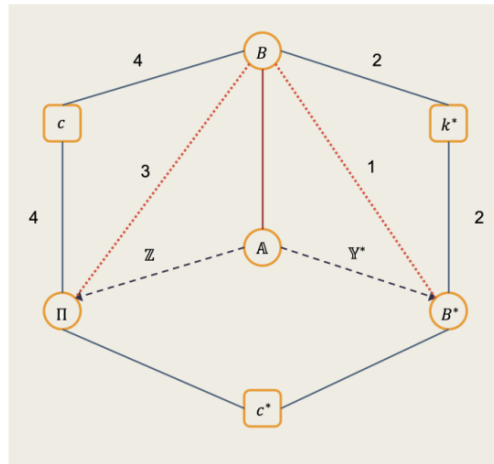


Fig. 5. Uniqueness matrix [12].

Where

- (1) $B^* = A^{-1} * Y^*$, with B^* being the representation of the exergy cost (kJ), A^{-1} the cost matrix and Y^* being the vector of external allocations to the system.
- (2) $k_i^* = B_i^*/B_i$ where k_i^* is the unit exergy cost (kJ/kJ), B_i is the current exergy.
- (3) $\Pi = A^{-1} * Z$ where Π is the exergetic cost and Z are all external economic allocations, such as maintenance expenses, waste expenses and fuel expenses.
- (4) $c_i = \Pi/B_i$, where c_i is the exergetic unit cost for each unit of exergy.

To carry out the cost allocation procedure, Valero [12] is based on 4 propositions and represented by Eq. 16-17:

- P1: The exergetic cost is a conservative property and, therefore, for each component the cost of the inputs is equal to the cost of the outputs.

$$A * B^* = 0 \tag{16}$$

- P2: The exergetic cost will be related to the system limits. That is, the exergetic cost of each flow that enters the plant is equal to its exergy.

$$B_i^* = B_i \tag{17}$$

- P3: If a fuel stream of a component has an output stream (undepleted fuel), its exergetic unit cost is the same as its input stream.

10

- P4a: If a component's product stream has many flow outlets, the unit exergy cost will be assigned to all of them.
- P4b: All costs generated during the production process, including the cost of waste, must be evaluated at the cost of the final products.

4 Results

Once the TEC methodology was applied to the AHT and based on the physical structure outline shown in Fig.6, the following notable results were obtained.

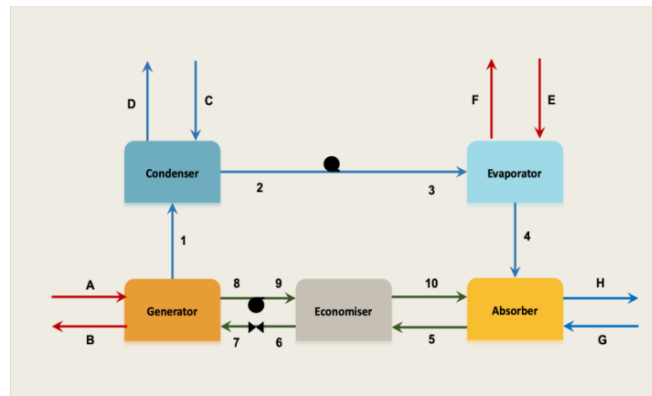


Fig. 6. Physical structure of the AHT.

Among the 5 tests analyzed in this study, the system exhibits an exergetic efficiency ranging from 30% to 50% , see Fig. 7. This is due to the fact that the subsystems or components of the Generator, Absorber, and Economizer show low efficiencies during their operation because these components contain the lines that carry the LiBr mixture. In other words, the destruction of exergy in these components is greater than the production of exergy.

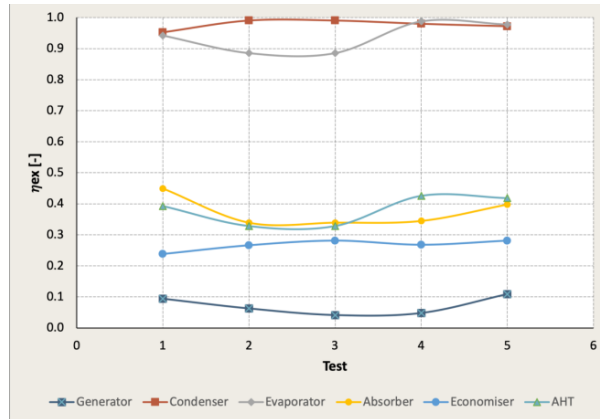


Fig. 7. Efficiency exergetic of the AHT.

Particularly, the evaporator stands out as the component with the highest exergetic efficiency, with efficiencies ranging from 89% to 98.8%. On the other hand, the generator has a lower exergetic performance, meaning it has higher irreversibilities in its process, causing most of the useful energy produced in it to be almost immediately destroyed.

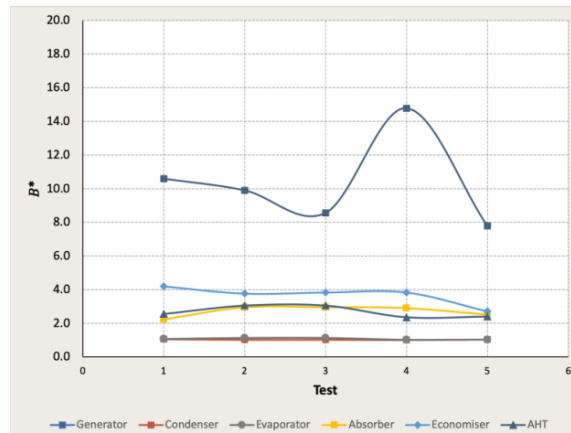


Fig. 8. Exergetic unit cost of the AHT.

This is corroborated by Fig.8, which shows the exergetic unit consumption of the AHT. It is observed that the highest energy consumption occurs in the mentioned devices. The generator consumes between 8 and 15 kW for each unit of exergy

12

produced, demonstrating that the start of the process within the AHT requires more resources to continue the energy process.

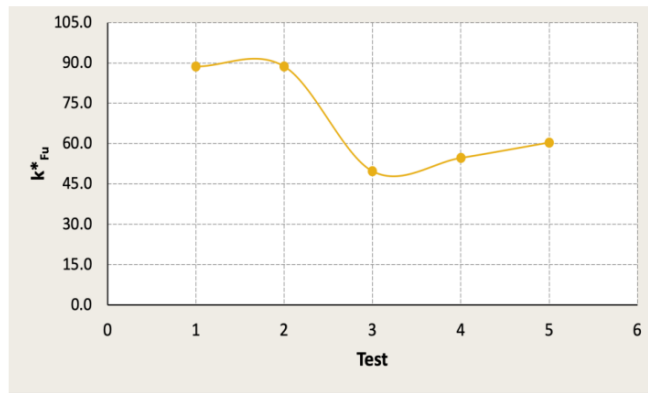


Fig. 9. Exergonomic cost of fuels.

From an exergetic perspective, the fuels for the plant's operation consume between 45 and 90 US\$/kW. On the other hand, the products generated within the system consume between 15 and 45 US\$/kW. Specifically, the generator, economizer, and absorber consume the majority of the fuels necessary for the AHT's operation, shown in Fig.9 and Fig.10.

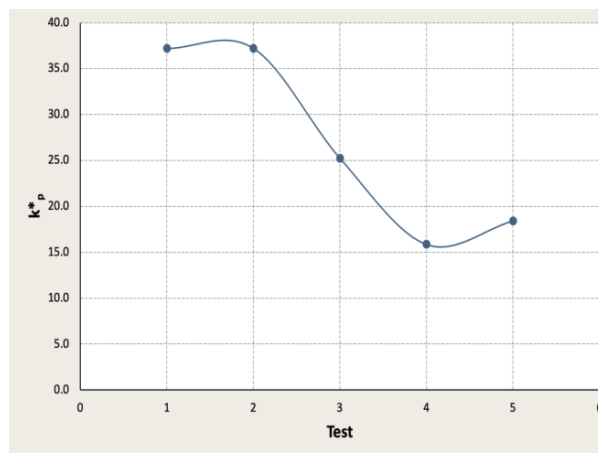


Fig. 10. Exergonomic cost of products.

Overall, the exergetic profitability ranges from 29% to 50%, understanding that there is a positive relationship between the system's investment and its capacity for efficient work in energy production and transformation. It is important to note that the exergetic profitability test is performed for the system as a whole since it is considered a comprehensive investment project shown in Fig. 11.

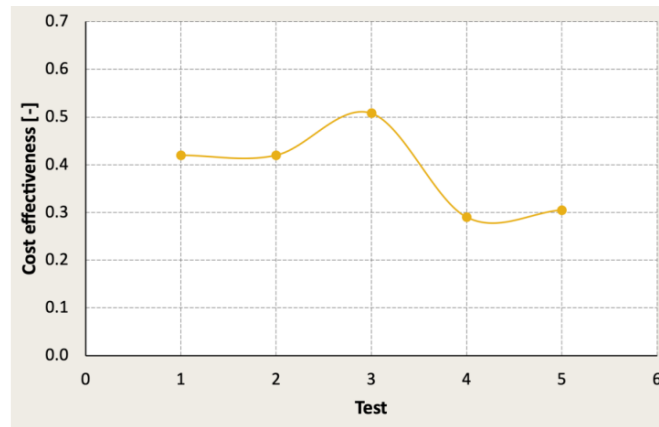


Fig. 11. Exergetic cost effectiveness.

5 Conclusions

The use of the TEC technique enabled a thorough assessment of the system through the accurate allocation of expenses and the identification of resource depletion and areas of inefficiency. Furthermore, this program offers pertinent information regarding the system, including not just exergetic efficiency but also the associated expenditures entailed in the energy process.

The study emphasized notable disparities among the key constituents of the AHT, revealing that EV exhibited the highest level of efficiency, ranging from 89% to 98.8%, while GE had the lowest level of efficiency, ranging from 4.1% to 10.9%. Regarding the consumption of exergy, it has been determined that the components GE, EC, and AB exhibit the highest resource utilization levels within the process, with power consumption ranging from 8 to 15 kW, 2.7 to 4.2 kW, and 2.2 to 2.9 kW, respectively. Hence, these aspects might be deemed worthy of further enhancement in further research endeavors.

Despite its ability to enhance the Coefficient of Performance (COP) of the AHT, the EC was shown to have a significant energy and economic resource consumption, rendering it exergetically impractical based on the conducted analysis. It is

14

recommended to perform this study in the absence of this equipment in order to achieve a full evaluation and comparison of the outcomes.

6 Acknowledgments

The first, second and third author thanks CONAHCyT México for the financial support received in the scholarships of the graduated students. Arianna Parrales Bahena acknowledges the support provided by CONAHCyT: Investigadores por México 2014. The fourth, fifth, and sixth authors thank SNII CONAHCyT Mexico.

References

1. Torres, C., Valero, A.: The exergy cost theory revisited. In: *Energies*, vol. 14, 1594 (2021), <https://doi.org/10.3390/en14061594>
2. Tsatsaronis, G., Pisa, J.: Exergoeconomic evaluation and optimization of energy systems. Application to the CGAM problem. In: *Energy*, vol. 19, pp. 287-32, (1994), [https://doi.org/10.1016/0360-5442\(94\)90113-9](https://doi.org/10.1016/0360-5442(94)90113-9)
3. Valero, A., Usón, S., Torres, C., Stanek, W.: Theory of Exergy Cost and Thermo-ecological Cost. In: Stanek, W. (eds) *Thermodynamics for Sustainable Management of Natural Resources*. pp.167-202. *Green Energy and Technology*. Springer, Cham (2017), https://doi.org/10.1007/978-3-319-48649-9_7
4. El-Sayed, Y.M., Evans, R.B.: Thermoeconomics and the design of Heat Systems. *ASME. J. Eng. Power*, vol. 92, pp. 27–35 (1970), <https://doi.org/10.1115/1.3445296>
5. Tsatsaronis, G., Winhold, M.: Exergoeconomic analysis and evaluation of energy-conversion plants—I. A New General methodology. *Energy*, vol.10, pp. 69–80 (1985), [https://doi.org/10.1016/0360-5442\(85\)90020-9](https://doi.org/10.1016/0360-5442(85)90020-9)
6. Von Spakovsky, M. R.: *A Practical Generalized Analysis Approach to the Optimal Thermoeconomic Design and Improvement of Real-world Thermal Systems*. Georgia Institute of Technology. (1986).
7. Frangopoulos, C. A.: Application of the thermoeconomic functional approach to the CGAM problem. *Energy*, 19(3), 323-342. (1994), [https://doi.org/10.1016/0360-5442\(94\)90114-7](https://doi.org/10.1016/0360-5442(94)90114-7)
8. Lazzaretto, A., Tsatsaronis, G.: SPECO: A systematic and general methodology for calculating efficiencies and costs in thermal systems. In: *Energy*, vol. 31, pp. 1257-1289. (2006), <https://doi.org/10.1016/j.energy.2005.03.011>
9. Gaggioli, R. A., Wepfer, W. J.: Exergy economics: I. Cost accounting applications. In: *Energy*, vol. 5, pp. 823-837. (1980), [https://doi.org/10.1016/0360-5442\(80\)90099-7](https://doi.org/10.1016/0360-5442(80)90099-7)
10. Tsatsaronis, G.: Thermoeconomic analysis and optimization of energy systems. In: *Progress in energy and combustion science*, vol. 19, pp. 227-257. (1993), [https://doi.org/10.1016/0360-1285\(93\)90016-8](https://doi.org/10.1016/0360-1285(93)90016-8)
11. Sciubba, E.: Beyond thermoeconomics? The concept of extended exergy accounting and its application to the analysis and design of thermal systems. In: *Exergy, an international journal*, vol. 1(2), pp.68-84. (2001), [https://doi.org/10.1016/S1164-0235\(01\)00012-7](https://doi.org/10.1016/S1164-0235(01)00012-7)
12. Lozano, M. A., Valero, A., Serra, L.: Theory of exergetic cost and thermoeconomic optimization. In *Proceedings of the International Symposium ENSEC*. 93 (1993).
13. Seyyedi, S. M.: A New Method for the Residues Cost Allocation and Optimization of a Cogeneration System Using Evolutionary Programming. *Journal of Applied Dynamic Systems and Control*. 2, 48-60 (2019). doi: 20.1001.1.26764342.2019.2.1.8.7

14. de Araújo, L.R., Morawski, A.P., Barone, M.A., Donatelli, J.L., Santos, J.J.: On the effects of thermodynamic assumptions and thermoeconomic approaches for optimization and cost allocation in a gas turbine cogeneration system. *Journal of the Brazilian Society of Mechanical Sciences and Engineering*. 42, (2020), <https://doi.org/10.1007/s40430-020-02402-6>
15. Rosseto de Faria, P., Aiolfi Barone, M., Guedes dos Santos, R., Santos, J.J.: The environment as a thermoeconomic diagram device for the systematic and automatic waste and environmental cost internalization in thermal systems. *Renewable and Sustainable Energy Reviews*. Vol. 171, (2023), <https://doi.org/10.1016/j.rser.2022.113011>.
16. Pospisil, J., Balas M., Baxa M., Fortenlly Z.: Working Characteristics of Small-scale Absorption Unit with Two-Cylinder Design. In *Wseas Transactions on Heat and Mass Transfer*. 3, 77-86 (2009).
17. Smith, I.E.: *Bombas de calor por absorción. Seminario sobre conservación de energía y aplicaciones industriales y comerciales de las bombas de calor*, México (1990).

Urban wind energy potential in the southern region of the Dominican Republic

Alexander Vallejo^{1,2,*}, Héctor Morban¹, Naomy Domínguez¹, Marino Cabrera¹, Edwin Garabitos¹, Idalberto Herrera², José Andrickson¹, Carlos Pereyra¹, Juan Castellanos², Elvin Jiménez² and Cándida Casilla¹

¹ Facultad de ingeniería, Instituto Especializado de Estudios Superiores Loyola (IEESL), 91000 San Cristóbal, Dominican Republic

² Ciencias Básicas y Ambientales, Instituto Tecnológico de Santo Domingo (INTEC), 10602 Santo Domingo, Dominican Republic
avallejo@ipl.edu.do

Abstract. This article presents a methodology for the reliable estimation of urban wind energy in the 10 provinces of the southern region of the Dominican Republic (DR) to contribute to cities' decarbonization. The methodology includes four steps that are (1) site selection, (2) wind energy assessment, (3) small wind turbine selection, and (4) annual energy production (AEP) estimation. In the first step, the southern region of the DR was taken because it has high wind potential reported. In the second step, numerical weather prediction methods were used with NASA datasets and contrasted with on-site measurements in three provinces. In the third step, a vertical axis wind turbine (VAWT) was chosen for its performance in urban environments under low wind speed and high turbulence. Finally, the AEP estimation was performed based on the Weibull distribution and the power curve of VAWT selected. The results show that the two provinces with the best potential are Pedernales and Barahona with wind speeds of 4.37 m/s and 4.00 m/s, respectively. The AEP was 1,902 kWh/y for Pedernales and 1,454 kWh/y for Barahona. In the opposite case, the two provinces with the lowest potential are Independencia and Elias Piña, both obtained 3.09 m/s and 2.50 m/s, respectively. These two provinces indicated an AEP of 343 kWh and 658 kWh, respectively. On average, for all provinces, the wind direction is 95°. The measured records vs. NASA datasets for the provinces of Barahona, Independencia, and San Cristóbal showed a mean absolute error (MAE) of 19%, which downstream produced an MAE in the AEP of 54%. It is observed that the average values for the three provinces were 92.24% lower than NASA datasets.

Keywords: Urban Wind Energy, Renewable Energy, Energy Potential, Small Wind Turbines, Dominican Republic.

1 Introduction

The Dominican Republic (DR) is under constant population growth and economic expansion, which has significantly increased the demand for energy to supply industries and satisfy the needs of consumers. However, current energy mix is largely based on

2

fossil fuels, in 2022 accounts 83.9% [1]. The energy sector is the main contributor to greenhouse gas (GHG) emissions in the country, being responsible for 90.39% of the total balance [2]. Given the risk posed by climate change and the increase in global temperature, it is essential that the energy industry seeks alternative energy supplies that avoid the GHG emissions [3]. Furthermore, at some point the world will have to face the depletion of the main traditional fuels, whose reserves are not infinite [4]. The continuous use of these resources makes them increasingly scarce and expensive, with volatile prices that can be influenced by various factors. Recently, the conflict between Russia and Ukraine is a clear example of this, according to the International Energy Agency, in 2022, fossil fuel prices experienced a notable rise and volatility, where the coal and natural gas quadrupled and sextupled the prices, respectively [5], [6].

The Dominican Republic is a country located in the Caribbean, with an estimated population of more than 11 million inhabitants in 2021 [7]. It is a nation with a constantly developing economy. The economy growth rate of gross domestic product in 2022 was 4.9% [8]. The southern region of the DR is composed of the provinces of Azua, Peravia, San Cristóbal, San José de Ocoa, Bahoruco, Barahona, Independencia, Pedernales, Elías Piña and San Juan. This region has an estimated population of more than 1.75 million inhabitants [9]. This region is known for its great diversity of ecosystems, including mountainous, coastal, forested, and agricultural areas. However, the southern region has historically been one of the poorest regions in the country, with high rates of poverty and economic inequality. Regarding the supply of electrical energy, Edesur Dominicana (EDESUR) is the distribution and commercialization company in the southern region. In 2021, EDESUR served a total of 881,830 clients and supplied 98.4% of demand with 5,638 GWh/y through 8,323 km of medium voltage networks [10]. However, despite the supply of electrical energy, the region still faces challenges in terms of energy sustainability, which makes it necessary to explore alternative energy sources, such as small- and medium-scale urban wind resources, that can contribute to resilience energy transition in the region.

Wind energy is a promising alternative to generate clean and to replace fossil fuels. However, the implementation in urban areas requires careful evaluation to ensure its efficiency and reduce negative impacts [11]. The lack of adequate assessments of wind potential in urban areas has led to some small wind turbines (SWTs) being installed in inappropriate locations, decreasing their performance [12]. To take advantage of the wind resource in urban areas and achieve the region's energy objectives, it is necessary to evaluate its potential and diagnose the most favorable locations for the development of urban wind energy. With the right approach, in the southern region of the DR, the urban wind potential could be harnessed with a view to promoting rational and efficient use of energy, aligned with the 7th sustainable development goals, concerning access to affordable, safe, sustainable energy [13].

The southern region of the DR may have great energy potential from the untapped urban wind resource. With growing concerns over global warming and the need for renewable energy sources, the exploration of urban wind energy has become crucial. Urban wind energy has the potential to provide a significant contribution to the region's energy mix, helping to reduce GHG emissions and improving energy security [14]. However, the potential of urban wind energy remains unrealized due to a lack of

comprehensive assessments, limited data on wind conditions, and limited investment in renewable energy technologies in urban areas. To achieve sustainable development considering the increase in energy demand and the need to protect the environment, innovative solutions are needed. One way to take advantage of wind energy efficiently is through small-scale energy self-production systems, which can reduce both the costs of electricity supply in cities and contribute to the decarbonization of the electrical matrix [15].

Small-scale wind energy has become an attractive alternative for decentralized energy production, reducing dependence on the electrical grid and minimizing transmission losses [16]. However, the lack of reliable wind information in urban areas has highlighted the importance of conducting adequate wind resource assessments in these areas to ensure the efficiency of wind energy projects and maximize their potential as a clean and renewable energy source. Due to the high population density in urban areas, in emerging countries, customized energy solutions are required close to the area where the demand is generated [14]. The installation of SWTs into buildings and surrounding areas can reduce dependence on the traditional electrical grid, which would not only improve energy security, but would also contribute to the reduction of GHG emissions locally.

The aim of this work is to determine the urban wind potential in the provinces of the southern region of the Dominican Republic through numerical climate prediction datasets and on-site measurements campaigns, with the purpose of determining its potential contribution in a sustainable pathway decarbonization.

2 Urban wind energy studies

This subsection compiles various studies related to urban wind energy in different countries, with a particular focus on the Dominican Republic. Studies include analyzes of power generation potential, methodologies for the evaluation and prediction of power production, effects of roof edge shape on wind turbine performance, and factors affecting the generation in urban environments. These studies are presented below concisely and in chronological order:

- In 2013 Millward-Hopkins et al. [12] argued about a how methodology predict wind speeds in urban areas can be significantly improved to by using more detailed geometric data and with on-site measurement with light detection and ranging system. Additionally, the study assessed the potential for wind energy generation in the British city of Leeds and showed that there are thousands of viable locations for installing SWTs on the roofs of buildings.
- Ishugah et al. [17] highlighted the great potential of wind energy to be exploited and developed in the urban environment, despite the challenges in design and technical application. They reviewed different designs of HAWTs and VAWTs for use in urban environments, with the aim of satisfying energy demand in turbulent wind environments. The study also summarizes the various applications of wind energy in urban environments, such as electrical power generation, ventilation and pollution

4

dispersion, cooling and dehumidification in coastal cities, and the economic and environmental benefits in China.

- Al-Quraan et al. [18] developed a research in which they highlighted the importance of comparing data obtained in wind tunnel vs. on-site measurements to evaluate the estimation errors. Two buildings in Montreal with different types of upstream terrain are presented. In the first case, with homogeneous terrain, a difference of $\leq 5\%$ was found between the estimates of wind energy potential and calculations based on field measurements. In the second case, with non-homogeneous terrain, the difference increased up to 20%.
- Gough [19] assessed urban wind resource potential at six locations in Cape Town, South Africa, and demonstrated high variability in wind resource potential between different locations. The annual energy production values varied significantly depending on the type of SWT evaluated. The levelized cost of electricity analysis showed that currently generating electricity through SWTs is not a viable or competitive way to generate electricity in Cape Town.
- Hulio et al. [20] evaluated the wind energy potential in Hawke's Bay in New Zealand. They used five different methods to obtain the Weibull parameters and found that the empirical, maximum likelihood, and energy pattern methods were more accurate than the graphical methods. The results indicated that wind turbulence at the site was moderate, with a wind shear coefficient of 0.18.
- Emejeamara & Tomlin [21] presented a novel methodology to predict wind energy generation in urban environments. The proposed methodology uses high temporal resolution wind measurements from eight potential sites in urban and suburban environments to develop a two-dimensional dual multiple flow model of a VAWT. A relationship between the turbulence intensity and the turbine performance coefficient is obtained. Furthermore, an analytical methodology is proposed to estimate the unsteady power coefficient at a potential turbine sitting, which is combined with a surplus energy estimation model to develop a SWT power estimation model.
- Rezaeiha et al. [22] presented a methodology for evaluating the energy potential of urban wind energy in The Netherlands. Authors found that urban wind power can provide a decentralized and local energy source for residential areas, which reduces the cost of energy by avoiding long-distance energy transmission losses and costs. In this case, were proposed the installation of 18,156 SWTs could provide up to 50% of residential energy demand.
- Škvorc & Kozmar [4] systematically investigated the factors affecting wind energy generation in urban environments. Authors suggested that buildings can be designed more efficiently to create local areas with greater wind generation potential and that VAWT are more suitable for use in urban environments due to their greater efficiency in turbulent airflows.
- Dar et al. [11] analyzed how the shape of the roof edge affects the performance of a HAWT located into a building. The results indicate that the shape of the roof edge has a significant effect on the performance of the SWT and the turbulence in its wake. In particular, the rounded shape of the roof edge significantly reduces the variation in wind turbine performance depending on its position, while the solid fence

shape produces the worst performance. These findings may have important implications for the optimized design of SWT and buildings.

- Cheng et al. [23] demonstrated that the transition to renewable energy in developing countries is feasible and can be economically beneficial. In particular, the combination of solar photovoltaic, wind and hydroelectric power pumped out of the river can meet the future demand for electricity in Bolivia, which would avoid the need to build new fossil fuel power plants. Furthermore, the levelized cost of electricity generated through this renewable energy mix is lower than the cost of electricity produced by new hydroelectric or gas plants.
- Vallejo-Díaz et al. [14] evaluated the potential for wind energy generation in urban environments in Santo Domingo and San Cristóbal, in the DR. Authors identified that the highest values of wind speed are observed during the summer, specifically in August. In a cautious scenario, 215 buildings suitable for vertical axis wind turbines (VAWTs) were identified. The estimated generation of electrical energy was 317 MWh/y and a potential emissions reduction of 197 tCO₂/y.
- Gil-García et al. [16] proposed a methodology to determine the annual energy production of potential urban wind energy projects. Authors characterized wind energy resources using databases from freely accessible georeferenced information systems (GIS) and found a significant energy surplus, with capacity factors between 55% and 60%. They suggested the possibility of selling surplus energy to the grid or grouping several neighboring buildings into an energy community.
- Finally, Vallejo Díaz et al. [15] found that Montecristi, El Seibo, La Altagracia, La Romana and Puerto Plata have the highest urban wind energy potential in the DR. Also, authors used a Strengths, Weaknesses, Opportunities and Threats (SWOT) – Analytical Hierarchical Process (AHP) analysis to identify the key factors that influence the diffusion and systematic use of this energy source. They recommended extending the research to other provinces and developing an analysis aimed at stakeholders in the energy sector of the country.

Since ref. [15], this work focuses on the southern region of the DR because great potential was reported in that region, and it is also one of the most populated regions of the country with a moderate development rate. In this sense, it is desired to study in detail the data obtained from open-access numerical weather prediction tools to be compared with on-site measurement dataset for the same period, and consequently establish the mean relative error between both resource prospecting methods.

3 Framework to analyze urban wind energy

Assessing wind energy generation potential in urban areas is challenging due to the presence of buildings and obstacles that affect wind variability. To address this challenge, various methods are used to evaluate the potential of wind energy and forecast long-term energy production. Basically, the methodologies include site selection, wind energy evaluation, wind turbine selection, and economic and environmental evaluation [24]. Other aspects such as the analysis of resilience due to the vulnerability of tropical latitudes, such as tropical storm or hurricane have been presented as a complement to

6

existing methodologies [25]–[27]. Other non-technical aspects, such as tools for decision-making in the implementation of small scales technology [28]. Due to the scope of this research, we propose a four-step methodology, as described in Fig. 1. The four steps are described below.

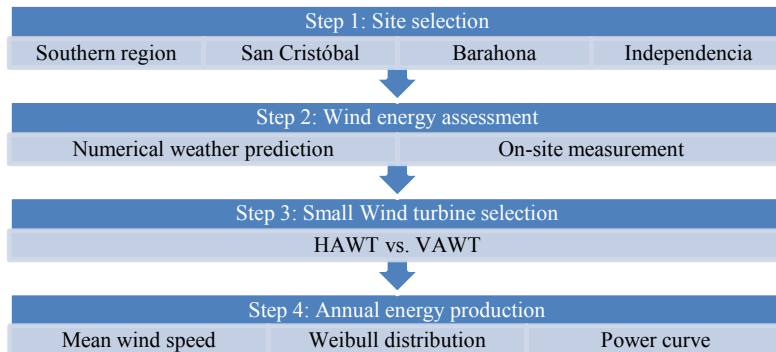


Fig 1. Proposed framework to urban wind energy potential assessment in southern region in the DR.

3.1 Site selection

The 10 provinces of the southern region of the Dominican Republic have been selected. These provinces have been selected due to their great potential reported by [28], [29]. In addition, on-site measurement records have been obtained from National Meteorological Office (ONAMET) for the provinces of Barahona and Independencia, and from IEESL for the province of San Cristóbal. With these on-site measurement data, a comparison of energy production at a height of 10 m above the ground is presented.

3.2 Wind energy assessment

Some of the most used methods to evaluate the potential of wind energy in urban areas are on-site measurement, wind tunnels, numerical weather prediction and computational fluid dynamics simulation [30], [31]. Below is presented a breakdown of each of the methods.

— **Numerical Weather Prediction (NWP)** is used to collect, store and analyze spatial datasets in the mesoscale resolution for large extension of areas in region scale [32]. In the context of evaluating wind energy in urban areas, also this geographic information system (GIS) mapping software are most powerful technology to mapping and analysis large spatial regions, and are used to identify and analyze topography, obstacles and open areas that can affect wind speed, which can help predict wind speed and the predominant direction in a big picture [23]. Normally these applications provide information at 50 m above ground level, however, they are not suitable for micro-scale evaluation [33]. Since the GIS does not take into consideration the terrain roughness, it overestimates the potential; therefore, it is necessary to

develop on-site measurement campaigns to obtain accurate meteorological parameters with better spatial and temporal resolution [34].

– **On-site measurement** is the most used method, as it allows accurate data to be collected about the wind in a specific area. This method involves the installation of sensors (anemometers, vanes, pyranometer and pyrometer) and datalogger at the site of interest to measure the wind speed and its direction, and other meteorological variables [14]. On-site measurement is especially useful for evaluating the potential for wind energy generation in urban areas, where wind variability can be affected by local topography and the presence of buildings and other obstacles. Positioning selection of the measurement station is important to ensure that accurate and representative data are obtained. Furthermore, the duration of the measurement and the analysis of the collected data are essential to evaluate the wind variability and the potential for wind energy generation at the site of interest [4].

To obtain energy production during a period, various probability distributions are adopted, such as the Weibull, Rayleigh, and Lognormal distributions. The Weibull distribution is the most widely accepted due to its flexibility and simplicity [35]. In Eq. 1, Weibull Distribution is presented, where k is the shape factor and c is the scale factor in m/s. The parameters k and c control the width of the distribution and average wind speed defined in Eq. 2, where V_{avg} is the average wind speed, respectively.

$$p(V_{avg}) = \left(\frac{k}{c}\right) * \left(\frac{V_{avg}}{c}\right)^{k-1} e^{-\left(\frac{V_{avg}}{c}\right)^k} \quad (1)$$

$$c = \frac{V_{avg}}{\sqrt{\pi}} \quad (2)$$

– **Computational fluid dynamics (CFD)** is a technique used to simulate and analyze the behavior of wind in an urban area or any other type of terrain. This technique allows obtaining detailed information about the speed, direction and turbulence of the wind, which can be very valuable for the design and evaluation of wind energy projects, among other applications [21]. CFD-based numerical models are gaining popularity due to increasing computing power and the increasing availability of specialized software.

– **Wind tunnels** can be more economical than on-site prospecting, they are not always an exact representation of wind conditions in an urban area; these are closed facilities that simulate wind conditions in a controlled environment. These installations are used to evaluate the behavior of wind around structures, such as buildings and wind turbines. Wind tunnels have been used to evaluate urban wind behavior and to design SWTs [18].

This research is focused on the NWP and on-site measurement methods for assessing urban wind energy. In this way, there will be an approach from the general to the particular from a spatial point of view, since the NWPs indicate at high resolution the potential of wind energy, and the on-site measurement takes into account the orography and everything that can be create turbulence [36].

8

3.3 Small Wind turbine selection

Small wind turbines (SWTs) are aerodynamic machines designed to harness the kinetic energy of the wind and transform it into electrical energy [17]. Unlike large wind turbines used in wind farms, SWTs are generally used to supply electricity in remote areas or isolated communities that do not have access to the electrical grid or as a source of renewable energy in urban areas. According to the International Electrotechnical Commission, these usually have a capacity less than or equal to 50 kW and a rotor swept area less than or equal to 200 m² [37]. SWTs are available in different types and designs, the most common classification being the division between horizontal axis wind turbines (HAWT) and vertical axis wind turbines (VAWT).

HAWT are most commonly used in large-scale projects due to their efficiency in converting wind energy into electricity [4]. As the wind passes through the blades, a lifting force is generated that rotates the horizontal axis. Most designs use three blades arranged around a central hub, ensuring stability and efficiency [19]. However, these types of turbines can be negatively affected by changes in wind direction and turbulence, which can be especially problematic in urban environments. Additionally, there are limitations regarding wildlife (bird) integrity and aircraft safety, aesthetic, manufacturing and maintenance issues, as well as restrictions on blade size that make them less suitable for use in urban areas [17].

VAWT has several advantages over horizontal axis wind turbines (HAWT), especially in urban environments. Unlike HAWTs, VAWTs do not require specific wind orientation to generate electricity, making them more versatile. Furthermore, the location of its mechanical components close to the ground allows easier access for maintenance [19]. One of the main advantages of VAWTs is their high power density, which can be three times that of HAWTs at one-tenth the height [17]. In addition, their simple design and low maintenance reduce manufacturing costs and make them less noisy, as well as more aesthetically attractive. However, there are some technical and economic disadvantages, such as the tendency to stop in gusty wind conditions and suffer from dynamic instabilities [16]. Fig. 2 shows the type of SWT according to axis orientation [38].



Fig 2. SWTs classification according the axis orientation (a) VAWT and (b) HVWT [38].

3.4 Annual energy production

Once steps 1–3 have been determined, it is important to estimate the annual energy production (AEP) with the frequency distribution of a entire year at each determined wind speed, and the turbine power curve. The methodology proposed by Rezaeiha [26], is adopted to estimate the AEP in Eq 3. Where 8,760 are the hours during a year, $P(V_{avg}; c; k)$ is the probability of a given speed based on the probability distribution, and $P(V_{avg_z})$ is the power produced by the SWT at that speed at a given height. The power extracted by the SWT is described according to Eq. (4). Where: A is the rotor area, C_p is the power coefficient of the rotor, V_{avg} is the mean wind speed for a given height and ρ is the air density.

$$AEP_z = 8,760 * \int_0^{8,760} P(V_{avg_z}; c; k) * P(V_{avg_z}) dv \quad (3)$$

$$P(V_{avg_z}) = 0.5 * C_p * \rho * A * V_{avg_z}^3 \quad (4)$$

For this research, the power curve of a VAWT presented by [26] will be used due to its good performance in urban environments. As mentioned previously, this type of SWT presents better aerodynamic performance in urban environments due to its unidirectionality in capturing the kinetic energy of the wind, and because it has low solidity.

4 Results and discussion

Fig. 3 shows the map with the average annual WS in the 10 provinces of the southern region of the DR. The datasets were optimized through Prediction Of Worldwide Energy Resources (POWER) – NASA at 10 m above the ground [39]. Fig. 3 shows that the provinces of Pedernales and Barahona are the ones with the greatest potential, for 4.37 m/s and 4.00 m/s, respectively. The provinces of Independencia and Elías Piña are the ones that register the lowest wind energy, in the order of 3.09 m/s and 2.50 m/s, respectively. The wind direction (WD) for all provinces is between 83° and 118° with respect to the north, where the general average is 95°.

Fig. 4 shows the monthly variation of the mean wind speed (WS), where nine provinces have an increase between May and September, except for the province of Elías Piña, which presents an atypical trend in relation to the others. Likewise, the two most prominent provinces reach a mean WS of 5.27 m/s and 4.52 m/s, in June and July, respectively. At a general level, September, October, and November are the months with the lowest wind potential according to Fig. 4.

10

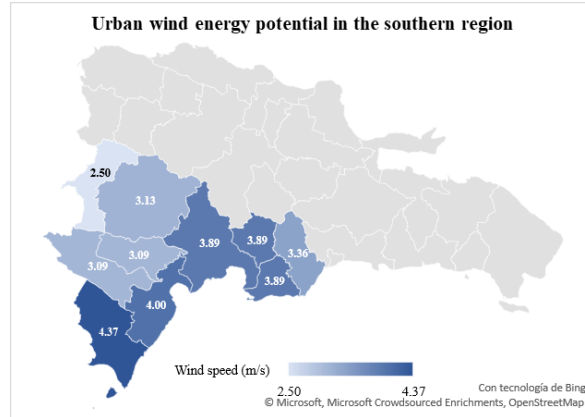


Fig 3. Mapping annual wind speed in the southern region from NASA data.

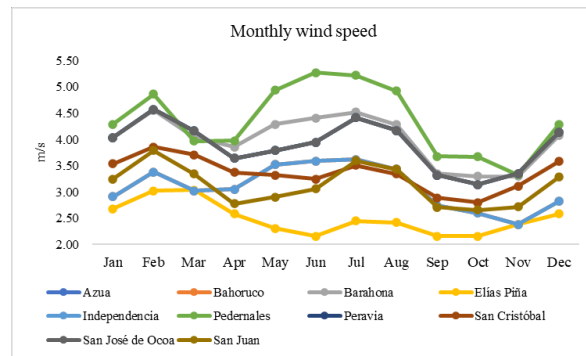


Fig. 4. Monthly average wind speeds in southern region.

Fig. 5-A shows the Weibull distribution for the 10 provinces analyzed with the NASA datasets. Frequency destruction indicates the percentage of hours in a year that are expected at a given WS, using equations 1 and 2, and a form factor $k = 2$. The two most prominent provinces exhibit a bias to the right of the curve, indicating that more hours are expected in those speed regimes. However, Elías Piña's pronunciation has a distribution biased to the left, meaning that more hours of the year are expected at low speeds, for example, 54% of the time the mean WS will be ≤ 2.00 m/s. Azua and San José de Ocoa have a probability of 11% of exceeding speeds ≥ 7.00 m/s. While Pedernales and Barahona have a probability of 18% and 13%, respectively. Fig. 5-B shows the Weibull distribution for the three provinces with data measured through anemometers. Because the data obtained from NASA overestimates the potential that is measured in the field, this causes a bias in the Weibull distribution. For the NASA datasets the bias is to the right, while for the measured data the bias is to the left, for the same province. In the case of Barahona, between $0 \leq WS \leq 4$ m/s, the relative percentage error is -41%, and in the range $5 \leq WS \leq 8$ m/s, the relative percentage error is 346%.

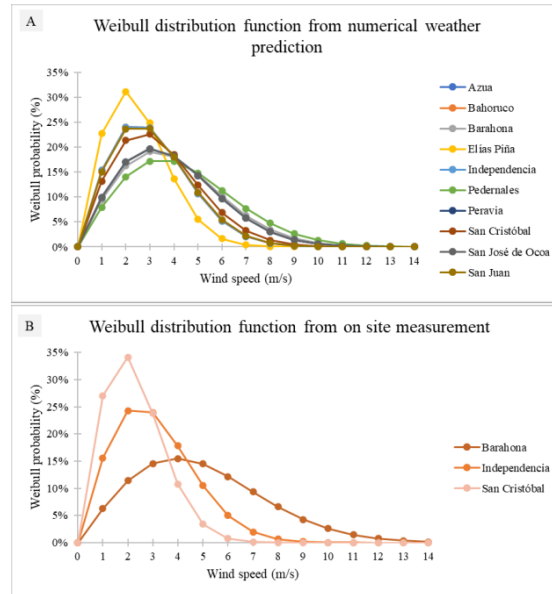


Fig. 5. (A) Weibull distribution from POWER datasets and (B) Weibull distribution from measured data.

Table 1 presents a summary of the mean wind speed (WS), wind direction (WD), annual energy production (AEP) and the location accordingly. The AEP were estimated with the power curve presented by [22], where the curve fitting by the regression method exhibited a correlation of 0.9811. Pedernales and Barahona have an AEP of 1,902 and 1,454 kWh/year, respectively. This is installed a VAWT.

Table 1. AEP estimation for southern region from NWP data.

Provinces	Location (°)		WS (m/s)	WD (°)	AEP (kWh/y)
Azua	Lat. 18.2097	Lon. -71.1041	3.89	88	1,333
Bahoruco	Lat. 18.4090	Lon. -70.1111	3.09	118	658
Barahona	Lat. 18.4831	Lon. -71.4197	4.00	92	1,454
Elías Piña	Lat. 18.8078	Lon. -71.2310	2.50	83	343
Independencia	Lat. 18.5465	Lon. -70.5054	3.09	118	658
Pedernales	Lat. 18.4537	Lon. -70.7380	4.37	96	1,902
Peravia	Lat. 18.8766	Lon. -71.7017	3.89	88	1,333
San Cristóbal	Lat. 18.0365	Lon. -71.7425	3.36	81	849
San José de Ocoa	Lat. 18.3769	Lon. -71.5228	3.89	88	1,333
San Juan	Lat. 18.2800	Lon. -70.3332	3.13	100	683
Average	Lat. 18.4479	Lon. -71.0409	3.52	95	1,055

12

In ref. [14] has presented suitable buildings for the installation of VAWT in Santo Domingo and San Cristóbal, so future work would be to investigate suitable places to install SWT in these provinces with relatively high potential. The three least favorable provinces are Elías Piña, Bahoruco and San Juan for an annual energy estimate of 343, 658 and 683 kWh/year.

Table 2 presents the recorded WS of the anemometers in the provinces of Barahona, Independencia and San Cristóbal, as well as the mean absolute error (MAE) of those measured records and POWER datasets. Likewise, the variation in the AEP and the MAE corresponding to each province are presented. In the case of Barahona, the measured WS was 23% greater than that obtained from POWER datasets, therefore increasing the AEP to 89%, however, in the case of San Cristóbal the MAE of the WS was -33%, which was equivalent to -70% of AEP. Since the AEP depends on the cube of the SW, small variations in the WS cause large variations in the AEP. For the Independencia province, both MAE were similar and acceptable, below 5%.

Table 2. On-site measurement vs POWER datasets and their mean absolute error.

Provinces	WS (m/s)	WS error (%)	AEP (kWh/y)	AEP error (%)
Barahona	4.94	23%	2,747	89%
Independencia	3.07	-1%	642	-2%
San Cristóbal	2.26	-33%	252	-70%

Given that NWP datasets overestimate wind speed because they do not adequately consider the roughness of the terrain in urban locations, the lineal regression method was adopted to compare the on-site records versus the NASA records in the respective locations, heights and time horizon. Fig. 6 shows in general that records measured on-site account 92.24% of the NASA values, with a correlation 0.9887.

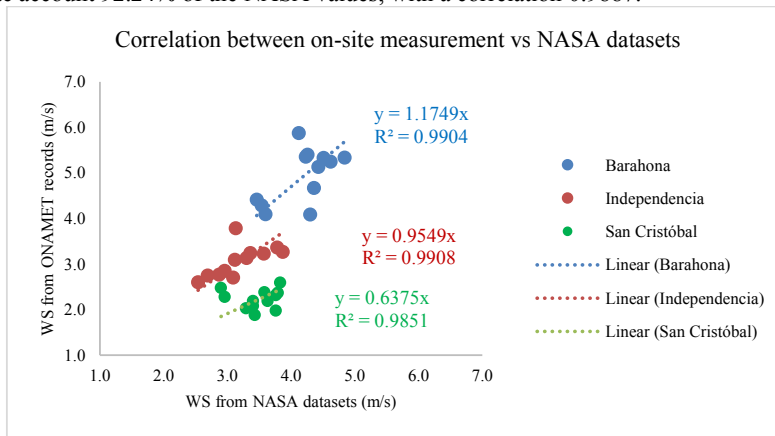


Fig. 6. Correlation between on-site measurement vs NASA datasets.

5 Conclusions

Urban wind energy has great potential to be harnessed in cities and contribute to decarbonization along the path of the energy transition. This research was carried out to evaluate the potential of urban wind energy in the 10 provinces of the southern region of the Dominican Republic. Numerical weather prediction (NWP) datasets at a height of 10 m above ground level for the period 2016–2021 were compared against on-site measurement in three provinces, which were Barahona, Independencia and San Cristóbal, obtained from ONAMET and IIESL. The results indicate that the two provinces with the greatest potential are Pedernales and Barahona, for mean wind speed of 4.37 m/s and 4.00 m/s, respectively. However, the two provinces with the lowest potential are Independencia and Elías Piña, accounting for 3.09 m/s and 2.50 m/s, respectively. The average wind direction is 95°. Through the Weibull distribution, the most probable hours during the year for energy production were determined. Adopting a vertical axis wind turbine that reports better performance in low wind speed regimes and high turbulent environments. Annual energy production (AEP) was 1,902 kWh/y for Pedernales and 1,454 kWh/y for Barahona. In the opposite case, the provinces with the lowest potential, Elías Piña and Independencia, showed 343 kWh and 658 kWh, respectively. In the provinces of Barahona, Independencia and San Cristóbal, more than 600,000 records datasets were obtained with anemometers and vanes in several years.

The comparison between measured records vs NWP datasets indicated that mean absolute error of the wind speed is around 19%, which affects the AEP near 54%. Although the NASA datasets are an initial starting point, it is observed that the average values for the three provinces of Barahona, Independencia and San Cristóbal were 92.24% lower. This indicates that small deviations in the mean wind speed strongly influence the estimate of AEP and, therefore, will have an economic impact on the project.

Future work is recommended to identify the most favorable and available public and private areas in the cities with greater potential. Likewise, a power flow simulation can be performed to determine the power (kW) of new distributed generation that can be integrated into distribution grid to contribute to the resilient expansion of decentralized renewable energy technologies deployment in the southern region.

6 Acknowledgments

Authors gratefully acknowledges the financial support by FONDO NACIONAL DE INNOVACIÓN Y DESARROLLO CIENTÍFICO Y TECNOLÓGICO, Grant No. 2022-3C1-141, through the Ministry of Higher Education, Science and Technology (MESCyT) from the Dominican Republic. The first author thanks EGE HAINA and the ONAMET for their contribution to this research.

References

- [1] Organismo Coordinador, “Memoria Anual 2022.” Accessed: Apr. 30, 2023. [Online]. Available: <https://www.oc.do/Informes/Administrativos/Memoria-Anual>
- [2] Comisión Nacional de Energía, “Plan Energético Nacional 2022 - 2036 – Comisión Nacional de Energía.” Accessed: Feb. 25, 2023. [Online]. Available: <https://www.cne.gob.do/documentos/plan-energetico-nacional-2022-2036/>
- [3] T. M. Letcher, “Wind Energy Engineering (Book),” in *Wind Energy Engineering*, Academic Press, 2017, p. iv. doi: 10.1016/B978-0-12-809451-8.00028-X.
- [4] P. Škvorc and H. Kozmar, “Wind energy harnessing on tall buildings in urban environments,” *Renew. Sustain. Energy Rev.*, vol. 152, p. 111662, Dec. 2021, doi: 10.1016/j.rser.2021.111662.
- [5] IEA, “IEA – International Energy Agency,” IEA. Accessed: Feb. 23, 2023. [Online]. Available: <https://www.iea.org>
- [6] R. Karkowska and S. Urjasz, “How does the Russian-Ukrainian war change connectedness and hedging opportunities? Comparison between dirty and clean energy markets versus global stock indices,” *J. Int. Financ. Mark. Inst. Money*, vol. 85, p. 101768, Jun. 2023, doi: 10.1016/j.intfin.2023.101768.
- [7] Banco Mundial, “Población, total - Dominican Republic | Data.” Accessed: Mar. 07, 2023. [Online]. Available: <https://datos.bancomundial.org/indicador/SP.POP.TOTL?locations=DO>
- [8] Banco Central, “BCRD informa que la economía dominicana creció 4.9 % en el año 2022.” Accessed: Mar. 07, 2023. [Online]. Available: <https://www.bancentral.gov.do/a/d/5568-bcrd-informa-que-la-economia-dominicana-crecio-49--en-el-ano-2022>
- [9] O. N. de Oficina Nacional de Estadística, “Estimaciones y proyecciones demográficas,” Oficina Nacional de Estadística (ONE). Accessed: Mar. 07, 2023. [Online]. Available: <https://www.one.gob.do/datos-y-estadisticas/temas/estadisticas-demograficas/estimaciones-y-proyecciones-demograficas/>
- [10] EDESUR, “¿Quiénes Somos?” Accessed: Mar. 03, 2023. [Online]. Available: <https://www.edesur.com.do/sobre-nosotros/quienes-somos/>
- [11] A. S. Dar, G. Armengol Barcos, and F. Porté-Agel, “An experimental investigation of a roof-mounted horizontal-axis wind turbine in an idealized urban environment,” *Renew. Energy*, vol. 193, pp. 1049–1061, Jun. 2022, doi: 10.1016/j.renene.2022.05.035.
- [12] J. T. Millward-Hopkins, A. S. Tomlin, L. Ma, D. B. Ingham, and M. Pourkashanian, “Assessing the potential of urban wind energy in a major UK city using an analytical model,” *Renew. Energy*, vol. 60, pp. 701–710, Dec. 2013, doi: 10.1016/j.renene.2013.06.020.
- [13] M. Moran, “Energía,” *Desarrollo Sostenible*. Accessed: Apr. 21, 2023. [Online]. Available: <https://www.un.org/sustainabledevelopment/es/energy/>
- [14] A. Vallejo-Díaz, I. Herrera-Moya, A. Fernández-Bonilla, and C. Pereyra-Mariñez, “Wind energy potential assessment of selected locations at two major cities in the Dominican Republic, toward energy matrix decarbonization, with resilience approach,” *Therm. Sci. Eng. Prog.*, vol. 32, p. 101313, Jul. 2022, doi: 10.1016/j.tsep.2022.101313.
- [15] A. Vallejo Diaz, I. Herrera Moya, C. Pereyra Mariñez, E. Garabitos Lara, and C. Casilla Victorino, “Key factors influencing urban wind energy: A case study from the Dominican

- Republic,” *Energy Sustain. Dev.*, vol. 73, pp. 165–173, Apr. 2023, doi: 10.1016/j.esd.2023.01.017.
- [16] I. C. Gil-García, M. S. García-Cascales, and A. Molina-García, “Urban Wind: An Alternative for Sustainable Cities,” *Energies*, vol. 15, no. 13, Art. no. 13, Jan. 2022, doi: 10.3390/en15134759.
- [17] T. F. Ishugah, Y. Li, R. Z. Wang, and J. K. Kiplagat, “Advances in wind energy resource exploitation in urban environment: A review,” *Renew. Sustain. Energy Rev.*, vol. 37, pp. 613–626, Sep. 2014, doi: 10.1016/j.rser.2014.05.053.
- [18] A. Al-Quraan, T. Stathopoulos, and P. Pillay, “Comparison of wind tunnel and on site measurements for urban wind energy estimation of potential yield,” *J. Wind Eng. Ind. Aerodyn.*, vol. 158, pp. 1–10, Nov. 2016, doi: 10.1016/j.jweia.2016.08.011.
- [19] M. B. Gough, “Assessing the potential for urban wind energy in Cape Town,” Master Thesis, University of Cape Town, 2018. Accessed: Mar. 13, 2023. [Online]. Available: <https://open.uct.ac.za/handle/11427/27812>
- [20] Z. H. Hulio, W. Jiang, and S. Rehman, “Techno - Economic assessment of wind power potential of Hawke’s Bay using Weibull parameter: A review,” *Energy Strategy Rev.*, vol. 26, p. 100375, Nov. 2019, doi: 10.1016/j.esr.2019.100375.
- [21] F. C. Emejeamara and A. S. Tomlin, “A method for estimating the potential power available to building mounted wind turbines within turbulent urban air flows,” *Renew. Energy*, vol. 153, pp. 787–800, Jun. 2020, doi: 10.1016/j.renene.2020.01.123.
- [22] A. Rezaeiha, H. Montazeri, and B. Blocken, “A framework for preliminary large-scale urban wind energy potential assessment: Roof-mounted wind turbines,” *Energy Convers. Manag.*, vol. 214, p. 112770, Jun. 2020, doi: 10.1016/j.enconman.2020.112770.
- [23] C. Cheng, N. P. Gutierrez, A. Blakers, and M. Stocks, “GIS-based solar and wind resource assessment and least-cost 100 % renewable electricity modelling for Bolivia,” *Energy Sustain. Dev.*, vol. 69, pp. 134–149, Aug. 2022, doi: 10.1016/j.esd.2022.06.008.
- [24] I. C. Gil-García, M. S. García-Cascales, and A. Molina-García, “Urban Wind: An Alternative for Sustainable Cities,” *Energies*, vol. 15, no. 13, Art. no. 13, Jan. 2022, doi: 10.3390/en15134759.
- [25] E. Arteaga-López, C. Ángeles-Camacho, and F. Bañuelos-Ruedas, “Advanced methodology for feasibility studies on building-mounted wind turbines installation in urban environment: Applying CFD analysis,” *Energy*, vol. 167, pp. 181–188, 2019, doi: 10.1016/j.energy.2018.10.191.
- [26] A. Rezaeiha, H. Montazeri, and B. Blocken, “A framework for preliminary large-scale urban wind energy potential assessment: Roof-mounted wind turbines,” *Energy Convers. Manag.*, vol. 214, p. 112770, Jun. 2020, doi: 10.1016/j.enconman.2020.112770.
- [27] A. Vallejo-Díaz, I. Herrera-Moya, A. Fernández-Bonilla, and C. Pereyra-Mariñez, “Wind energy potential assessment of selected locations at two major cities in the Dominican Republic, toward energy matrix decarbonization, with resilience approach,” *Therm. Sci. Eng. Prog.*, vol. 32, p. 101313, Jul. 2022, doi: 10.1016/j.tsep.2022.101313.
- [28] A. Vallejo Díaz, I. Herrera Moya, C. Pereyra Mariñez, E. Garabitos Lara, and C. Casilla Victorino, “Key factors influencing urban wind energy: A case study from the Dominican Republic,” *Energy Sustain. Dev.*, vol. 73, pp. 165–173, Apr. 2023, doi: 10.1016/j.esd.2023.01.017.

- [29] A. Vallejo, I. Herrera, J. Castellanos, C. Pereyra, and E. Garabitos, "Urban Wind Potential Analysis: Case Study of Wind Turbines Integrated into a Building Using On-Site Measurements and CFD Modelling," in *36th International Conference on Efficiency, Cost, Optimization, Simulation and Environmental Impact of Energy Systems (ECOS 2023)*, Las Palmas De Gran Canaria, Spain: ECOS 2023, 2023, pp. 534–546. doi: 10.52202/069564-0049.
- [30] B. R. Karthikeya, P. S. Negi, and N. Srikanth, "Wind resource assessment for urban renewable energy application in Singapore," *Renew. Energy*, vol. 87, pp. 403–414, Mar. 2016, doi: 10.1016/j.renene.2015.10.010.
- [31] S. Khoshdel Nikkho, M. Heidarinejad, J. Liu, and J. Srebric, "Quantifying the impact of urban wind sheltering on the building energy consumption," *Appl. Therm. Eng.*, vol. 116, pp. 850–865, Apr. 2017, doi: 10.1016/j.applthermaleng.2017.01.044.
- [32] G. F. Garuma, "Review of urban surface parameterizations for numerical climate models," *Urban Clim.*, vol. 24, pp. 830–851, Jun. 2018, doi: 10.1016/j.uclim.2017.10.006.
- [33] R. Byrne, N. J. Hewitt, P. Griffiths, and P. MacArtain, "An assessment of the mesoscale to microscale influences on wind turbine energy performance at a peri-urban coastal location from the Irish wind atlas and onsite LiDAR measurements," *Sustain. Energy Technol. Assess.*, vol. 36, p. 100537, Dec. 2019, doi: 10.1016/j.seta.2019.100537.
- [34] T. Simões and A. Estanqueiro, "A new methodology for urban wind resource assessment," *Renew. Energy*, vol. 89, pp. 598–605, 2016, doi: <https://doi.org/10.1016/j.renene.2015.12.008>.
- [35] M. R. Islam, R. Saidur, and N. A. Rahim, "Assessment of wind energy potentiality at Kudat and Labuan, Malaysia using Weibull distribution function," *Energy*, vol. 36, no. 2, pp. 985–992, Feb. 2011, doi: 10.1016/j.energy.2010.12.011.
- [36] F. C. Emejeamara and A. S. Tomlin, "A method for estimating the potential power available to building mounted wind turbines within turbulent urban air flows," *Renew. Energy*, vol. 153, pp. 787–800, Jun. 2020, doi: 10.1016/j.renene.2020.01.123.
- [37] (IEC) IEC, "IEC 61400-2:2013 | IEC Webstore | rural electrification, wind power." Accessed: Mar. 27, 2023. [Online]. Available: <https://webstore.iec.ch/publication/5433>
- [38] T. Stathopoulos *et al.*, "Urban wind energy: Some views on potential and challenges," *J. Wind Eng. Ind. Aerodyn.*, vol. 179, pp. 146–157, Aug. 2018, doi: 10.1016/j.jweia.2018.05.018.
- [39] NASA, "Data Access Viewer." Accessed: Sep. 22, 2022. [Online]. Available: <https://power.larc.nasa.gov/data-access-viewer/>

Estudio práctico de ahorro energético mediante iluminación adaptativa de plataformas aeroportuarias en el Aeropuerto Adolfo Suárez Madrid-Barajas

Daniel Alfonso-Corcuera¹[0000-0002-1080-0840], Vasile Gabriel Amitroae², y Santiago Pindado¹[0000-0003-2073-8275]

¹ Departamento de Sistemas Aeroespaciales, Transporte Aéreo y Aeropuertos (SATAA), E.T.S.I. Aeronáutica y del Espacio, Universidad Politécnica de Madrid, Plaza Cardenal Cisneros 3, 28040 Madrid, España

² AIRBUS, Calle Aviocar 2, 28906 Getafe, España
daniel.alfonso.corcuera@upm.es

Abstract. La búsqueda de la eficiencia energética de la aviación civil comercial es actualmente uno de los grandes retos en los que los diferentes actores del sector se hallan inmersos. En el caso de los operadores aeroportuarios, el ahorro energético asociado al consumo eléctrico constituye uno de los aspectos clave de los planes de eficiencia aeroportuarios. Entre los consumidores eléctricos aeroportuarios encontramos la iluminación de plataformas, que representa una parte no despreciable en el consumo eléctrico de cualquier aeropuerto. Las necesidades de iluminación de plataformas establecidas por las diferentes regulaciones implican un alto consumo eléctrico para iluminar eficazmente grandes superficies. Teniendo en cuenta la gran cantidad de energía necesaria para iluminar áreas que pueden estar desocupadas durante grandes periodos de tiempo, se ha procedido a estudiar el posible ahorro energético producido en caso de utilizar un sistema adaptativo de iluminación que rebaje las exigencias de iluminación para los puestos de estacionamiento que no se estén utilizando. Dicho estudio se ha realizado para la ampliación prevista de la plataforma T4 Satélite del Aeropuerto Adolfo Suárez Madrid-Barajas. El estudio, que analiza mediante simulaciones lumínicas diferentes casos de utilización de las plataformas en el periodo nocturno, muestra ahorros considerables en la energía necesaria para la iluminación de las plataformas.

Keywords: Adaptive apron floodlighting, Airport, Aviation Efficiency.

1 Introducción

1.1 Eficiencia energética en la operación aeroportuaria

Actualmente, el cumplimiento de los diferentes Objetivos de Desarrollo Sostenible (ODS) acordados por la Organización de las Naciones Unidas dentro del programa “Agenda 2030 para el Desarrollo Sostenible” [1] supone un reto para organizaciones, empresas e instituciones. En el cuadro del desarrollo e implantación de medidas que

2

permitan el cumplimiento de las metas de los diferentes ODS, los diferentes actores del sector del transporte aéreo civil no son ajenos a dicha tarea, siendo una pieza clave en el cumplimiento de numerosas metas y objetivos que se relacionan principalmente con garantizar la salubridad y la sostenibilidad del transporte de personas y mercancías al mismo tiempo que se asegura la cohesión y el desarrollo territorial. En dicha labor, las infraestructuras aeroportuarias llevan tiempo realizando esfuerzos por aumentar la sostenibilidad de sus operaciones [2, 3]. Entre las acciones que predominan los esfuerzos por aumentar la sostenibilidad de las operaciones aeroportuarias predomina la búsqueda de la mejora en la eficiencia energética. Entre las áreas de investigación al respecto destacan la búsqueda de una disminución del consumo energético de la infraestructura aeroportuaria [4–6], la progresiva implantación de sistemas de autoconsumo energético [7, 8] o la electrificación y mejora de la eficiencia de las operaciones de asistencia a aeronaves o de transporte terrestre [9].

Dentro de los esfuerzos de disminución del consumo energético de la infraestructura aeroportuaria destacan el la identificación y control de los consumidores eléctricos de los edificios aeroportuarios [10]. Entre los diferentes consumidores eléctricos de una infraestructura aeroportuaria, tras el consumo de los equipos de climatización destaca el alto consumo energético atribuible a los sistemas de iluminación y alumbrado (véase la Fig. 1.).

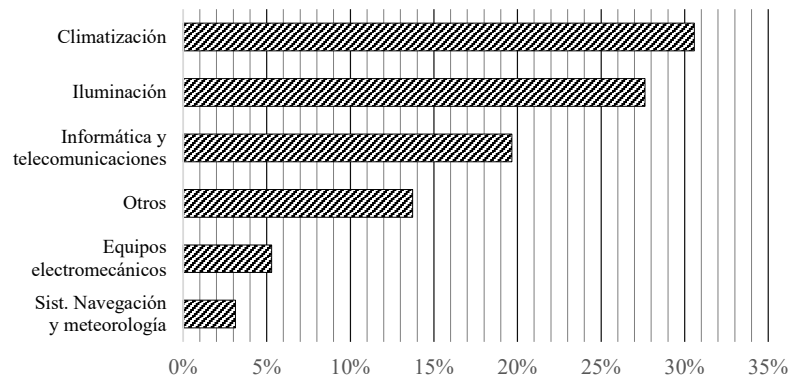


Fig. 1. Porcentaje de aportación al consumo total (año 2015) de las diferentes categorías de consumidores eléctricos en el Aeropuerto de Seve Ballesteros-Santander. Datos extraídos del trabajo de Ortega, S. y Mañana, M. (2017) [10].

1.2 Uso de iluminación adaptativa para el ahorro energético

En base al apartado anterior, se deduce que la mejora de la eficiencia en la iluminación y alumbrados aeroportuarios resulta de especial interés dado su potencial para reducir el consumo energético y, por ende, aumentar la eficiencia y sostenibilidad de las operaciones aeroportuarias.

En cuanto a la iluminación aeroportuaria se pueden distinguir dos tipos de consumidores diferenciados según el objeto del alumbrado: la iluminación general y la iluminación del campo de vuelo. El primer tipo de consumidor comprende la iluminación general del interior del edificio aeroportuario, así como de los viales de acceso, mientras que el segundo tipo de consumidor comprende la iluminación necesaria para la operación segura de las aeronaves en el campo de vuelo. De los consumos del Aeropuerto Seve Ballesteros-Santander, se desprende que la iluminación general supone un 71% del consumo eléctrico de iluminación, mientras que la iluminación del campo de vuelos supone un 29% de dicho consumo. Aunque minoritaria, el consumo de iluminación del campo de vuelos representa un no despreciable 8,12% del consumo eléctrico global del aeropuerto [10].

Entre las medidas para la reducción del consumo energético vinculado a la iluminación del campo de vuelos aeroportuario (que comprende la iluminación de las plataformas de estacionamiento y el balizamiento del campo de vuelos), aparte de la progresiva sustitución de la tecnología de iluminación de las lámparas de descarga/halógenas a tecnología LED, destacan ciertas iniciativas de desarrollo de sistemas de control de luminarias de plataformas de estacionamiento destinadas a optimizar los consumos eléctricos adaptando la iluminación a la ocupación de las plataformas [11–13]. En esta línea, el gestor aeroportuario español AENA ha desarrollado en el año 2023 un proyecto piloto de adaptación de la iluminación en plataforma a la ocupación de esta, mediante la integración de los sistemas informáticos de gestión de vuelos y de alumbrado [14].

El desarrollo de técnicas que permitan adaptar el consumo debido a iluminación de plataformas a la ocupación real de las mismas resulta de especial interés si se tiene en cuenta la extensión de las áreas consideradas (cada puesto de estacionamiento de clave E equivale a una superficie de 2400 m² aproximadamente) y las elevadas exigencias de iluminancia tanto horizontal como vertical (20 lux de media para ambos tipos de iluminancia en la plataforma de estacionamiento) planteadas por la normativa a nivel europeo [15].

El presente trabajo pretende evaluar, utilizando medios de simulación mediante software (DIALux Evo), los siguientes aspectos de una instalación de iluminación adaptativa de una plataforma aeroportuaria para un caso de estudio (ampliación de la terminal y plataforma de estacionamiento de la terminal T4-S del Aeropuerto Adolfo Suárez-Madrid Barajas):

- Ahorro energético conseguido.
- Cumplimiento de los requisitos de iluminación.

Hasta donde los autores conocen, no se encuentran trabajos similares al presente publicados en revistas técnicas de uso científico y académico en la literatura disponible.

Este trabajo se divide en las siguientes partes: en primer lugar se exponen la metodología de estudio y las herramientas utilizadas, en segundo lugar se exponen y analizan los resultados obtenidos en el estudio, y finalmente se concluye destacando los aspectos más representativos de los resultados y el análisis.

4

2 Metodología

2.1 Alcance del estudio

El trabajo utiliza como caso de estudio el proyecto de futura ampliación del edificio terminal y de la plataforma aeroportuaria de la terminal T4-S del Aeropuerto Adolfo Suárez-Madrid Barajas [16, 17]. En dicho proyecto, se prevé la creación de 16 nuevos puestos de estacionamiento de Clase E o 32 puestos de Clase C. El estudio de iluminación se basa en la modelización mediante software de simulación de las condiciones de la futura plataforma, en base a los pliegos de prescripciones técnicas publicados [16, 17] así como de datos propios (véase la Fig. 2).



Fig. 2. Vista aérea del modelo 3D del área de estudio comprendido por la ampliación de la terminal T4-S y plataforma de estacionamiento asociada [16, 17].

El alcance del estudio se limita al estudio de la iluminación en los nuevos puestos creados fruto de la futura ampliación de la terminal. Para la localización de las luminarias se plantea la aplicación de las directrices de la OACI en lo referente a la posición de las torres de iluminación [18] situando las torres Mega a ambos lados de los puestos de estacionamiento de Clase E (véase la Fig. 3).

El estudio analiza los consumos energéticos del sistema de iluminación para diferentes casos aplicando técnicas de iluminación adaptativa. Se estudian de este modo los siguientes casos de ocupación de los puestos de estacionamiento:

- Puesto de Clase E ocupado o iluminación adaptativa desconectada.
- Puestos de Clase C y Clase E desocupados.
- Puesto de Clase C izquierdo/derecho ocupado (2 análisis).
- Ambos puestos de Clase C ocupados.

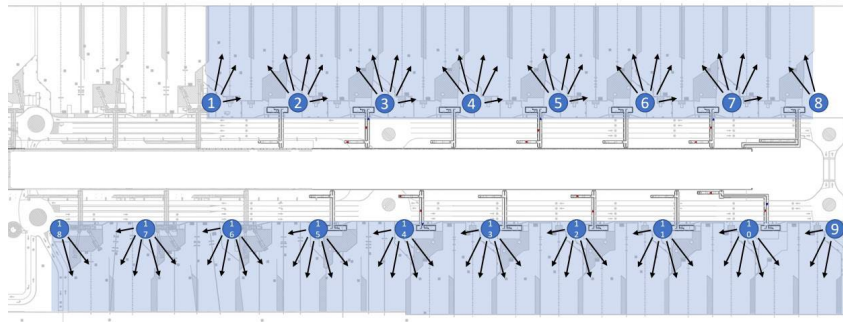


Fig. 3. Disposición de torres de iluminación propuesta, con una torre de iluminación a cada lado de cada puesto de Clave E en base a las directrices de la OACI [18].

Para el estudio de la iluminación del caso propuesto se plantea una graduación o apagado de las diferentes luminarias de manera que se siga alumbrando los puestos de estacionamiento cumpliendo los requisitos necesarios en base a la ocupación de estos.

El estudio se realiza mediante la modelización mediante el software de simulación DIALux Evo de las condiciones de la plataforma de estacionamiento, así como las luminarias de las torres de iluminación. Se han modelizado los diferentes obstáculos que causan reflexión de la luz así como las diferentes luminarias. Para las luminarias se ha hecho uso de la información proporcionada por el fabricante y se han utilizado diferentes luminarias de la serie FLOODLIGHT MAX de la marca LEDVANCE. La simulación de la iluminación de las plataformas de estacionamiento ha tenido en cuenta los datos fotométricos proporcionados por el fabricante y se ha simulado el efecto combinado de las diferentes luminarias junto con sus ángulos de apuntamiento.

2.2 Requisitos de iluminación y normativa aplicables

El estudio de iluminación realizado para los diferentes casos expuestos en el apartado anterior tiene como objeto el cumplimiento para los diferentes casos de ocupación de los puestos de estacionamiento de los requisitos establecidos en las Especificaciones de Certificación (CS) para el diseño de Aeródromos establecidas por la EASA (*European Union Aviation Safety Agency*) a nivel europeo [15], basadas en las especificaciones del Anexo 14 de la OACI [19]. La Tabla 1 recopila dichas especificaciones mínimas de iluminancia y uniformidad establecidas en las CS de EASA.

Como se puede apreciar en la Tabla 1, los requisitos aplicables para el caso del área circundante al área de estacionamiento son mucho más bajos que en el caso del área de estacionamiento. Así, en el caso de puestos de estacionamiento que no estén siendo ocupados, se puede considerar que los requisitos de iluminación a aplicar en los mismos se corresponden con el de área circundante, reduciéndose en un 50% las necesidades de iluminancia horizontal, así como eliminando los requisitos de iluminancia vertical,

6

lo que redundaría en un menor gasto eléctrico al poder regular y/o apagar ciertas luminarias.

Tabla 1. Requisitos de iluminancia y uniformidad establecidos en las Especificaciones de Certificación de la EASA para iluminación de áreas de estacionamiento aeroportuarias [15]. La iluminancia vertical media se debe medir a una altura de 2 m sobre la plataforma.

	Estacionamiento	Área circundante
Iluminancia horizontal media E_h [lux]	20	50% de E_h estacionamiento
Iluminancia vertical media E_v [lux]	20	-
Uniformidad iluminancia horizontal [media:mínimo]	4:1	4:1

En cuanto a la disposición de luminarias y orientación de las mismas, las CS de EASA establecen la necesidad de alumbrar los puestos de estacionamiento desde diferentes direcciones con el objeto de minimizar las sombras en los puestos.

2.3 Disposición de luminarias

Como se ha explicado en el apartado 2.1 la disposición de torres de iluminación se adapta a las recomendaciones del Manual de Diseño de Aeródromos de la OACI que recomienda situar una torre de iluminación a cada lado del puesto de estacionamiento con el fin de permitir una correcta iluminación desde más de un ángulo de incidencia [18]. Para el caso de estudio se ha situado una torre de iluminación a cada lado de cada puesto de Clave E (véase la Fig. 3). Dicha disposición de las torres de iluminación equivale a una separación entre torres de iluminación de 81 m. En la Fig. 4 se muestra la disposición de luminarias, detallándose los ángulos de apuntamiento en la Tabla 2.

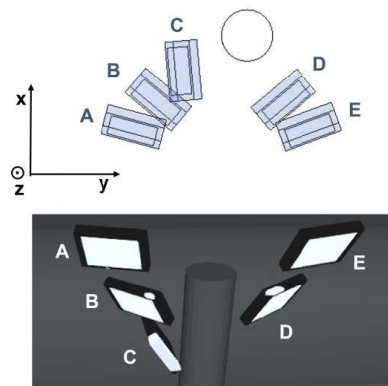


Fig. 4. Disposición de luminarias en las torres de iluminación.

Tabla 2. Ángulos de apuntamiento de las diferentes luminarias (véase la Fig. 4). Se toman como direcciones de referencia la dirección vertical para el ángulo de apuntamiento vertical y la perpendicular a la terminal para el ángulo horizontal.

Luminaria	Ángulo de apuntamiento vertical	Ángulo de apuntamiento horizontal
A	59°	-15°
B	55°	-45°
C	55°	-85°
D	59°	40°
E	59°	10°

Las luminarias elegidas se corresponden con el modelo FLOODLIGHT MAX 600W 30 (30° de apertura de haz) para todas las luminarias de las torres de iluminación.

Para el caso de la iluminación adaptativa se plantean las siguientes acciones:

- En caso de ocupación del puesto de Clave E, o en caso de no aplicar la iluminación adaptativa se mantienen al 100% todas las luminarias a ambos lados del puesto de estacionamiento.
- En el caso de que ningún puesto de estacionamiento se halle ocupado, se gradúan todas las luminarias al 50%.
- En el caso de ocupación del puesto de estacionamiento de Clave C izquierdo, se plantea la graduación al 50% de las luminarias A, B y C de la torre derecha al puesto de estacionamiento, mientras que se mantienen al 100% las luminarias D y E de la torre izquierda.
- En el caso de ocupación del puesto de estacionamiento de Clave C derecho, se plantea la graduación al 50% de la luminaria C de la torre derecha y de las luminarias D y E de la torre izquierda, mientras que se mantienen al 100% las luminarias A y B de la torre derecha relativa al puesto de estacionamiento.
- En el caso de ocupación de los dos puestos de Clave C, se gradúa al 50% la luminaria C del lado derecho al puesto de estacionamiento, mientras que el resto de luminarias se mantienen al 100%.

2.4 Objetos de cálculo

En la Fig. 5 se muestran los objetos de cálculo programados en el software DIALux Evo para la evaluación del cumplimiento de los diferentes requisitos definidos en el apartado 2.2. Como se puede apreciar, se han definido como objetos de cálculo los diferentes puestos de estacionamiento de Claves C y E donde se miden los niveles de iluminancia tanto vertical (a una altura de 2 m sobre la plataforma) como horizontal. Así mismo, se han establecido como objeto de cálculo las áreas circundantes a los puestos de estacionamiento, donde se evalúa la iluminancia horizontal, tal y como se requiere en la normativa.

8

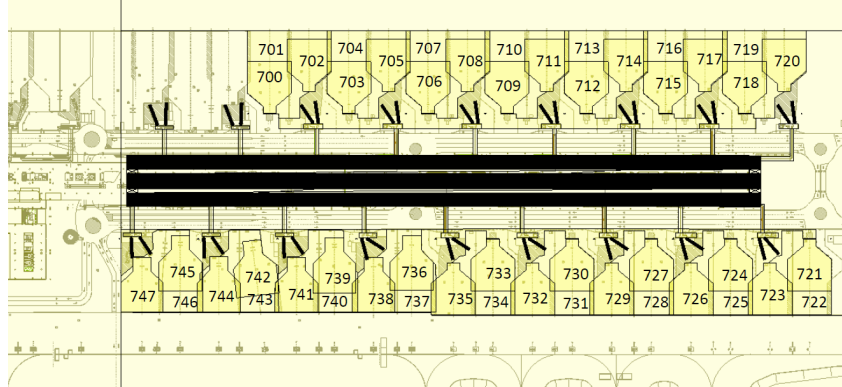


Fig. 5. Objetos de cálculo planteados para el estudio de iluminación.

3 Resultados

El estudio realizado ha arrojado como resultado los datos de iluminancias horizontal y vertical e índices GR correspondientes a toda el área dentro del alcance del estudio (véase la Fig. 6).

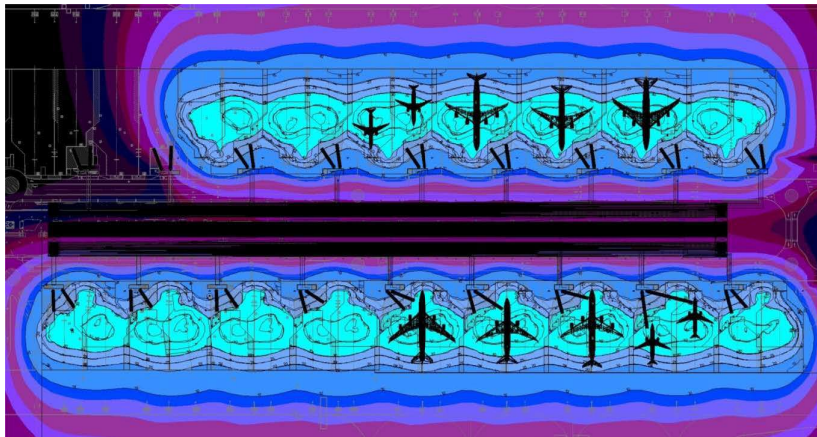


Fig. 6. Vista general de distribución de la iluminancia horizontal a nivel de suelo para el caso estudiado con todas las luminarias graduadas al 100%.

Se ha estudiado el correcto cumplimiento con los requisitos de iluminación establecidos en el apartado 2.2 para cada caso, así como realizado una estimación de consumos de cada configuración de iluminación. Para la presentación de resultados y dado el carácter análogo de todos los puestos de estación planteados, se presentan los datos de los puestos de estacionamiento 727 a 735 (véase la Fig. 5).

3.1 Cumplimiento de requisitos

Estado 0: Puesto Clave E ocupado (iluminación adaptativa desconectada)

El estudio inicial (sin ninguna atenuación de luminarias) para el caso en el que se encuentre el puesto de Clave E ocupado ha arrojado los resultados de iluminancia y uniformidad que se describen en la Tabla 3.

Tabla 3. Características de iluminancia horizontal y vertical (a una altura de 2 m) y uniformidad (ratio valor mínimo/media) de los puestos 727 a 735 para el caso en el que se esté utilizando el puesto de estacionamiento de Clave E.

Puesto	E_h [lux]	E_v [lux]	U_h
727	37,1	38,6	0,57
728	32,5	40,4	0,52
729	31,7	46,4	0,53
730	37,2	38,6	0,58
731	32,6	40,5	0,52
732	31,7	48,3	0,53
733	37,2	38,6	0,58
734	32,6	40,5	0,52
735	32,6	48,3	0,55
A. Circundante	21,4	-	0,40

Como se puede observar, los datos de iluminancias y uniformidad cumplen con creces con los requisitos mínimos establecidos en el apartado 2.2.

Estado 1: Puestos Clave C y E desocupados

Una vez estudiado el cumplimiento de los requisitos de iluminación para el estado base (esto es, con todas las luminarias iluminando según sus características nominales), se plantea el estudio de la atenuación de las luminarias para el caso en el que los puestos 730, 731 y 732 se encuentren desocupados, en base a las pautas establecidas en el apartado 2.3. Para el estudio, se intenta conocer así mismo el grado de influencia de las luminarias que alumbran los puestos contiguos por lo que son incluidas en el análisis de tal manera que alumbran a su potencia nominal. Según se puede observar en la Fig. 7, para la mayor parte del área estudiada, se puede considerar que el resultado de iluminancia en los puestos iluminados al 50% resulta poco influenciada por los puestos contiguos. Los resultados que se muestran en la Tabla 4 indican una iluminancia correcta, acorde a los requisitos de área circundante y con una uniformidad mayor que en el caso del Estado 0.

10

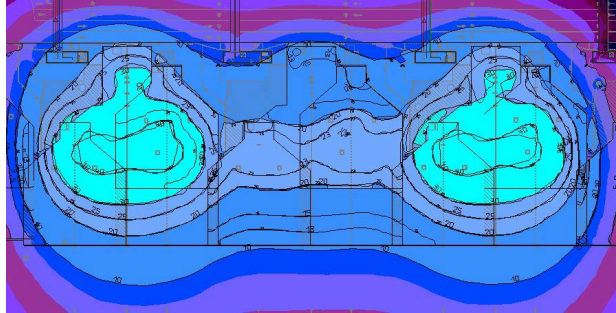


Fig. 7. Gráfica que muestra los niveles de iluminancia horizontal en el Estado 1 para el caso de los puestos de estacionamiento 730, 731 y 732.

Tabla 4. Resultados del análisis de la iluminancia horizontal y vertical de los puestos 730-732 para el Estado 1.

Puesto	E_h [lux]	E_v [lux]	U_h
730	21,0	21,7	0,60
731	18,6	23,3	0,58
732	18,6	28,5	0,58

Estados 2 y 3: Un puesto de Clave C ocupado

En estos casos, y tal y como se explica en el apartado 2.3, existen 2 luminarias alumbrando a su intensidad nominal mientras que el resto se encuentran graduadas al 50%. En el Estado 2 se alumbrando el puesto de estacionamiento 732 (Clave C izquierda) mientras que en el Estado 3 se alumbrando el puesto de estacionamiento 733 (Clave C derecha). En la Fig. 8 se muestran una gráfica de la distribución de iluminancia horizontal para ambos casos. En la Tabla 5 se muestran los resultados de iluminancias y uniformidad para el Estado 2 mientras que en la Tabla 6 se muestran los resultados correspondientes al Estado 3. Para estos casos se han considerado los puestos contiguos con la configuración del Estado 1 (todas las luminarias al 50%).

Tabla 5. Resultados lumínicos de iluminancias y uniformidad correspondientes al estudio del Estado 2.

Puesto	E_h [lux]	E_v [lux]	U_h
730	21,4	22,7	0,50
731	21,6	27,5	0,45
732	24,8	37,6	0,42

En ambos casos los requisitos obtenidos cumplen con la normativa, aunque en el caso del Estado 2 se observa una cierta disminución del valor medio de la iluminancia horizontal E_h respecto al caso en el que todas las luminarias se encuentran iluminando a su

intensidad nominal. Sin embargo, el valor medio de iluminancia horizontal sigue situándose lejos del mínimo exigido por normativa (20 lux).

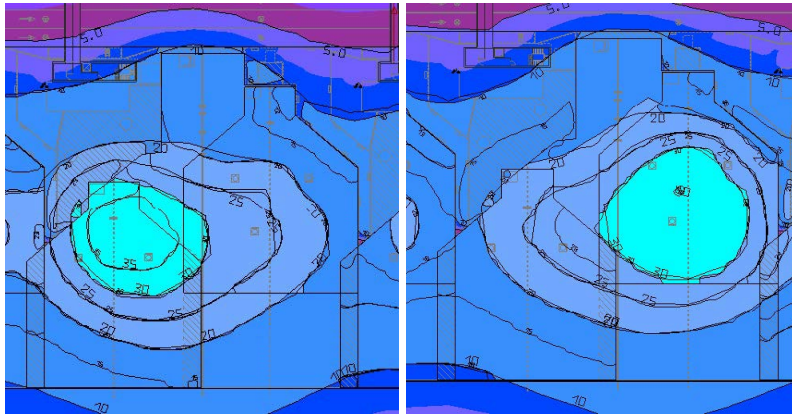


Fig. 8. Distribución de iluminancia horizontal en los puestos de estacionamiento objeto de estudio para el Estado 2 (izquierda) y para el Estado 3 (derecha).

Tabla 6. Resultados lumínicos de iluminancias y uniformidad correspondientes al estudio del Estado 3.

Puesto	E_h [lux]	E_v [lux]	U_h
730	29,0	30,4	0,46
731	22,4	27,9	0,42
732	18,8	28,5	0,49

Estado 4: Ambos puestos Clave C ocupados

Finalmente, para el Estado 4, donde sólo se atenúa una de las luminarias se obtienen los resultados descritos en la Fig. 9 y en la Tabla 7. En ambos casos el análisis se ha realizado con los puestos contiguos iluminados según las directrices del Estado 1.

Se puede observar que para ambos puestos ocupados (730 y 732) los valores de iluminancia son correctos. Sin embargo destaca el puesto de Clave E, que obtiene también un valor aceptable de iluminancia, aunque dicho resultado se puede achacar a la poca influencia de regular una única luminaria.

12

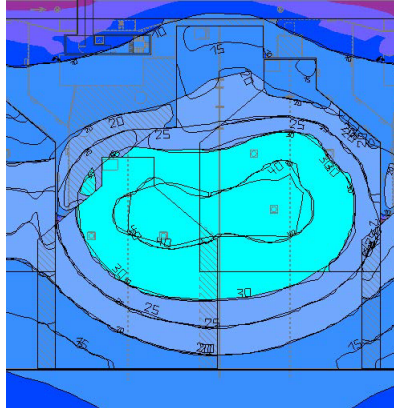


Fig. 9. Distribución de iluminancia horizontal en los puestos de estacionamiento objeto de estudios para el Estado 4

Tabla 7. Resultados lumínicos de iluminancias y uniformidad correspondientes al estudio del Estado 4.

Puesto	E_h [lux]	E_v [lux]	U_h
730	32,4	34,1	0,42
731	27,9	35,4	0,42
732	27,9	42,3	0,41

3.2 Ahorro energético

Según la información del fabricante, la regulación al 50% de las luminarias se puede realizar mediante el apagado mediante cableado de una de las matrices LED de las luminarias (véase la Fig. 10).



Fig. 10. Detalle de la luminaria LEDVANCE FLOODLIGHT MAX 600 donde se aprecian las 2 matrices de LEDs independientes que permiten una fácil regulación al 50% de intensidad.

Teniendo en cuenta la potencia de las luminarias y su número se puede calcular que para el Estado 0, el sistema de iluminación de la plataforma de estacionamiento supone un consumo eléctrico de 3 kW de potencia eléctrica por cada puesto de estacionamiento Clave E, lo que equivale a 13,14 MW·h de consumo eléctrico por cada puesto de estacionamiento de Clave E. En la Tabla 8 se detallan las potencias consumidas por cada Estado.

Tabla 8. Consumos eléctricos y ahorro respecto al Estado 0 (sin iluminación adaptativa).

Estado	Potencia [kW]	Ahorro respecto a Estado 0
0	3,0	-
1	1,5	-50%
2 y 3	2,1	-30%
4	2,6	-10%

Como se puede observar, para un caso de utilización donde predominen los aviones de medio rango atendidos exclusivamente mediante pasarela de embarque, se pueden obtener ahorros cercanos al 30% en el consumo eléctrico del alumbrado de la plataforma de estacionamiento, equivalente a 4 MW·h de ahorro energético anuales.

Tal y como se puede deducir, el ahorro real dependerá del uso que se haga de la plataforma.

3.3 Posibles problemas de implementación

Uno de los posibles obstáculos a la hora de implementar este tipo de sistema puede ser la certificación del mismo frente a los organismos reguladores, conllevando elevados costes de desarrollo así como largos tiempos de implementación, dada la ausencia de una regulación específica para este tipo de soluciones.

Así mismo, la implementación de estos sistemas requiere de una correcta coordinación o integración de software con la planificación de vuelos para regular correctamente las luminarias en base al estado de ocupación de los puestos de estacionamiento en cada momento.

4 Conclusiones

En el presente trabajo se ha descrito un estudio que analiza el rendimiento de iluminación así como el ahorro energético de un sistema de iluminación adaptativo para el área de estacionamiento de una terminal aeroportuaria, mediante simulación lumínica basada en Software.

Se han modelizado los puestos de estacionamiento así como las torres de iluminación y se ha planteado una iluminación adaptativa basada en la regulación de la intensidad luminosa de las luminarias.

Los resultados obtenidos muestran que la iluminación adaptativa permite mantener con un correcto nivel de iluminación los puestos de estacionamiento en uso, así como

14

lograr una iluminación con una uniformidad e iluminancia horizontal adecuada para los puestos de estacionamiento desocupados. Así mismo, el sistema permite obtener ahorros de entre el 10% y el 50% en el consumo eléctrico del sistema.

References

1. Nations U (2015) Transforming our world: the 2030 Agenda for Sustainable Development
2. Greer F, Rakas J, Horvath A (2020) Airports and environmental sustainability: a comprehensive review. *Environmental Research Letters* 15:103007. <https://doi.org/10.1088/1748-9326/ABB42A>
3. Comendador VFG, Valdés RMA, Lisker B (2019) A Holistic Approach to the Environmental Certification of Green Airports. *Sustainability* 2019, Vol 11, Page 4043 11:4043. <https://doi.org/10.3390/SU11154043>
4. Uysal MP, Sogut MZ (2017) An integrated research for architecture-based energy management in sustainable airports. *Energy* 140:1387–1397. <https://doi.org/10.1016/J.ENERGY.2017.05.199>
5. Baxter G, Srisaeng P, Wild G SUSTAINABLE AIRPORT ENERGY MANAGEMENT: THE CASE OF KANSAI INTERNATIONAL AIRPORT. [https://doi.org/10.7708/ijtte.2018.8\(3\).07](https://doi.org/10.7708/ijtte.2018.8(3).07)
6. Baxter G, Srisaeng P, Wild G (2018) An Assessment of Airport Sustainability, Part 2—Energy Management at Copenhagen Airport. *Resources* 2018, Vol 7, Page 32 7:32. <https://doi.org/10.3390/RESOURCES7020032>
7. Barrett SB, DeVita PM, Lambert JR (2014) Guidebook for Energy Facilities Compatibility with Airports and Airspace. *Guidebook for Energy Facilities Compatibility with Airports and Airspace*. <https://doi.org/10.17226/22399>
8. National Academies of Sciences E and M (2018) Microgrids and Their Application for Airports and Public Transit. *Microgrids and Their Application for Airports and Public Transit*. <https://doi.org/10.17226/25233>
9. Rodríguez-Sanz Á, Cano J, Rubio Fernández B, et al (2021) Reduce aviation's greenhouse gas emissions through immediately feasible and affordable gate electrification. *Environmental Research Letters* 16:054039. <https://doi.org/10.1088/1748-9326/ABF7F1>
10. Ortega Alba S, Manana M (2017) Characterization and Analysis of Energy Demand Patterns in Airports. *Energies* 2017, Vol 10, Page 119 10:119. <https://doi.org/10.3390/EN10010119>
11. Mubarak RR, Lamtiar S, Callista AB, et al (2022) Prototipe Kontrol dan Monitoring Remote Apron Floodlight Berbasis Mikrokontroler dengan Modul Dimmer. *Journal of Airport Engineering Technology (JAET)* 3:37–47. <https://doi.org/10.52989/JAET.V3I1.74>
12. Yang L, Li K, Yang G, Zhang XC (2014) The Design of Airport Flood Lighting Energy-Saving Control System. *Applied Mechanics and Materials* 492:499–502. <https://doi.org/10.4028/WWW.SCIENTIFIC.NET/AMM.492.499>

13. Davis RG, Wilkerson AM (2015) GATEWAY Demonstrations: Philadelphia International Airport Apron Lighting: LED System Performance in a Trial Installation. <https://doi.org/10.2172/1376998>
14. (2023) El Aeropuerto de Alicante-Elche crea un sistema de iluminación eficiente en la plataforma de estacionamiento. In: Europa Press. <https://www.europapress.es/turismo/transportes/noticia-aeropuerto-alicante-elche-crea-sistema-iluminacion-eficiente-plataforma-estacionamiento-20230613184514.html>. Accessed 25 Sep 2023
15. European Union Aviation Safety Agency (EASA) (2022) Certification Specifications and Guidance Material for Aerodrome Design (CS-ADR-DSN) Issue 6
16. AENA (2019) Expediente: DIN-186/2019 - t De Pm Y Do Para La Ampliación Del T4 Y T4S Y Zonas Asociadas- Aeropuerto Adolfo Suárez Madrid Barajas. <https://contratacion.aena.es/contratacion/principal?portal=infocontrato&idexp=9610141045&tipoexp=417>. Accessed 26 Sep 2023
17. AENA (2019) Expediente: DIN-335/2019 - A.T. Para La Redacción Del Proyecto Actuaciones Para La Ampliación Del T4 Y T4S Y Zonas Asociadas.- Aeropuerto Adolfo Suárez Madrid Barajas. <https://contratacion.aena.es/contratacion/principal?portal=infoexp&idexp=9610141911&tipoexp=401>. Accessed 26 Sep 2023
18. ICAO (2021) Aerodrome Design Manual - Part 4 - Visual Aids (Doc 9157 - Part 4), 5th ed
19. ICAO (2022) Annex 14 - Aerodromes - Volume I - Aerodromes Design and Operations, 9th ed

Integration of Energy Storage and Management Technologies for Optimization of Renewable Energy Operation: CEDER-CIEMAT Demonstration.

Paula Peña-Carro¹, Oscar Izquierdo-Monge¹, Angel Hernandez-Jimenez¹

¹ CEDER-CIEMAT, Autovía de Navarra A15 salida 56, 42290 Lobia (Soria), España, P.P.C.: paula.pena@ciemat.es; O.I.M.: oscar.izquierdo@ciemat.es; A.H.J.: angel.hernandez@ciemat.es

Abstract: Case study demonstrations at research centers such as CEDER-CIEMAT showcase the practical implementation of energy storage and management technologies for optimizing renewable energy operation. These demonstrations involve the deployment of energy storage systems and smart microgrids (SMG), bolstered by remote control and real-time monitoring capabilities. This allows for efficient response to events and the collection of valuable data for analysis and optimization. Maintaining grid stability is one of the keys to achieve the renewable energy penetration and the use of fast response energy storage systems are the responsible elements to achieved it. The objective of this article is to implement active energy management in order to accomplish a renewable energy consumption of at least 80% under normal operations at the center, facilitated by the collaborative efforts of the European project SINNOGENES. This requires the integration of fast response energy storage systems such as flywheels or supercapacitors, as well as a seasonal energy storage system for longer duration storage. These storage systems enable an accurate balancing the intermittent nature of renewable energy sources and ensure a reliable and sustainable energy supply for the facility.

Keywords: energy storage systems, smart microgrids, grid stability, fast response storage systems, flywheels, supercapacitors, seasonal energy storage, geothermal field.

1 Introduction

Findings on studies in Europe assessing emissions reductions in sectors like energy and manufacturing [1] show the need for targeted policies to address super-pollutants and support facilities facing challenges in decarbonization efforts. Despite progress, fossil fuels still dominate global electricity production, with a lack of public awareness hindering renewable adoption [2]. Given the importance of public awareness and the

limited penetration of renewable energy in society, universities play a crucial role in driving this change. An illustrative study in this regard [3] underscores the challenges in achieving European objectives for 2050 in terms of energy efficiency and sustainability, emphasizing the importance of innovative approaches and leveraging universities as testbeds for insights to inform future policies and actions.

The integration of geothermal energy plays a pivotal role in Europe's pursuit of climate neutrality by 2050, providing a sustainable, low-carbon heating solution that can expedite decarbonization and facilitate the transition to a renewable energy (RE) system. Significant findings have been carried out [4] focusing on the positive impact of implementing district heating networks using geothermal energy, which improves the overall decarbonization scenario. Geothermal energy not only contributes to the reduction of greenhouse gas emissions but also offers a sustainable and reliable energy source for heating purposes. The integration with energy storage systems can enhance the stability and flexibility of the power supply [5], addressing the intermittent nature of RE resources.

Recent advancements in geothermal technology, such as repurposing abandoned oil and gas wells [6], show promise in overcoming geographical and cost-related challenges, positioning geothermal energy as a significant future power source, despite obstacles like limited exploitable sites and emissions. However, case studies in Germany [7] propose a new resource classification scheme to better assess geothermal potential, while a case study in Iceland [8] suggests that current EU energy policies may overestimate geothermal efficiency, highlighting the need for revised methodology to fully realize geothermal energy's contribution to European energy and climate objectives. Managing risks and optimizing environmental impacts are crucial for the sustainable growth of the geothermal energy sector [9], as demonstrated by a comprehensive life cycle assessment study [10], which emphasizes the importance of strategic approaches to improve environmental performance and reduce uncertainties.

Geothermal energy can be effectively combined with energy storage systems, such as ultracapacitor and flywheel energy storage, to enhance the stability and flexibility of power supply [5]. This integration addresses the intermittency challenges associated ER resources, ensuring reliability and resiliency. The integration of rapid response energy storage systems (ESS) has emerged as a valuable solution to address these challenges [11] [12]. ESS offer vital quick frequency response capabilities for grid stability.

Supercapacitors, also known as ultracapacitors (UC) or electrochemical capacitors, offer high power density, long cycle life, and excellent temperature performance. They are particularly suitable for applications that require quick bursts of energy, such as regenerative braking in vehicles, grid energy storage, and smoothing power fluctuations in renewable energy systems [13] [14]. Ongoing research aims to improve the energy density and performance of UC for broader adoption across industries, especially in applications related to grid stability, with converters playing a vital role in efficient energy transfer and control algorithms enhancing their performance [15].

Hybrid energy storage systems incorporating UC have gained significant attention in numerous studies. Development of strategies to enhance the dynamic response and overall performance of energy storage systems through the use of hybrid control approaches and simulation techniques [16], have demonstrated improvements in the

3

dynamic response capabilities of these systems. Combining different energy storage technologies, such as UC and batteries, in hybrid models shows promise in achieving faster response times, optimizing energy storage capacity utilization, and improving the overall performance of energy storage applications [17] [18]. Flywheel energy storage systems, known for their rapid power delivery, are advantageous for applications like frequency regulation and grid stabilization, although they have energy storage limitations and energy losses; thus, to improve their dynamic response and efficiency, hybrid configurations with UC are being explored to leverage the complementary strengths of both technologies. A novel combined system design [19], utilizing rotating supercapacitors to store both electrical and kinetic energy, offers enhanced energy storage capacity and improved performance, potentially replacing conventional flywheel energy storage in diverse applications.

It is explored the technological advancements and developments in flywheel energy storage [20]. The analysis of existing flywheel installations underscores their potential contributions to grid stability, frequency regulation, and renewable energy integration, while recognizing the technical challenges like energy losses and material selection; however, the case of China [21] demonstrates that research and practical implementation of flywheel energy storage systems are still in the experimental stage, emphasizing the need for efficient and low-power-consumption solutions to support reliable grid frequency modulation. Through a simulation-based study [22], a closed-loop control strategy is developed for a flywheel energy storage system in the context of primary frequency modulation in wind energy, emphasizing its potential to efficiently store energy and integrate renewable sources into the grid while demonstrating improved performance. Not only a modelling a frequency grid modulation has been carried out, but also a practical case of study: an overview of several energy storage methods and different types of voltage-sensitive electrical equipment [23].

Global efforts to achieve zero emissions by 2050 through renewable energy transition require innovation, international collaboration, and multi-sector partnerships. As an example, [24] delves into the technical and economic feasibility of a 100% renewable energy-based residential home in China. Another study adds to the understanding of successful renewable energy transitions by providing insights from five case studies in the United States [25]. These case studies shed light on the social, political, and economic factors that have supported the achievement of 100% renewable energy communities in these municipalities. These findings contribute to the broader discourse on transitioning towards sustainable energy systems and inform decision-making processes for communities seeking to embark on similar renewable energy journeys. Another study cases analyzed are the country of Romania [26] and the community located in Al-Tafilah, Jordan [27], which emphasize the importance and potential of harnessing renewable energy to drive sustainable development and address energy challenges in rural areas and developing countries. These examples underscore the need to implement supportive policies and promote innovative solutions based on renewable sources. Other example regarding the economical evaluation of the 100% renewable energy systems [28] focuses on assessing the cost-effectiveness and financial feasibility of transitioning to fully renewable energy sources.

This document is structured as follows: Section 2 provides an overview of the case study at CE.D.E.R. installations. Section 2.1 describes the microgrid and the elements connected. Section 2.2 and 2.3 details the new elements to be included in the center, and Section 2.4 highlights the numeric evaluation to achieve 80% renewable energy consumption. Lastly, Section 3 outlines the expected outcomes for the project.

2 Case study: CEDER-CIEMAT Installations

The Center for the Development of Renewable Energy (CEDER) specializes in applied research and the development and promotion of renewable energy. It is part of the Energy Department at the CIEMAT (Centre for Energy, Environment, and Technology Research) public research body, dependent on the Ministry of Science and Innovation. The development of R&D&I activities focuses on energy production from biomass throughout the value chain. It also conducts studies on wind energy from low-power turbines and seeks practical solutions for integrating renewable energy sources into smart microgrids. The center is committed to promoting the use of clean energy and working towards a more sustainable future.

2.1 Site, elements & microgrid description

CEDER, located in Soria (Spain) is a state-of-the-art facility designed to showcase innovative energy solutions and test new technologies in a real-world environment. Spanning an area of 640 ha (13,000 m² of built space). One of the key features of the CEDER is its smart microgrid (SMG), which is operated and managed in real time. It is based on a 45 kV line and serves a 45/15 kV substation with a capacity of 1,000 kVA. From this substation, the medium voltage is distributed via an underground network to eight transformer stations, which adjust the voltage to a 400 V three-phase low voltage. The network can be operated in both ring modes, enabling a medium-voltage perimeter of 4200 m and radial mode. All the distributed generation elements, electrical storage systems, and loads were connected at a low voltage.

In terms of demand, the center has different consumption profiles, which are similar to those found in an industrial environment, the service sector, and even domestic consumption. These different demand profiles allow researchers and engineers to test and demonstrate new energy solutions in a real-world setting by simulating a variety of scenarios and conditions.

The CEDER SMG has several distributed generation elements, including small wind power generation systems, photovoltaic generation systems, and a micro-hydropower plant with a Pelton turbine. In terms of small wind power generation, the SMG has 19 sites for wind turbine installations, and currently, five of these sites (all horizontal axes) are connected. These 5 wind turbines have a total installed capacity of 161.2 kW with the features included in Table 1. The SMG has 11 connected photovoltaic generation systems, each with a different capacity that ranges from 4.5 kW to 30.24 kW, totaling 168.5 kW of installed capacity. The panels used in these systems vary in terms of

5

technology, and include monocrystalline, polycrystalline, and bifacial panels. Its specifications are listed in Table 1. A micro-hydropower plant with a Pelton turbine is also connected, which has a maximum power of 40 kW. The plant has a three-phase asynchronous generator that is directly coupled to the turbine impeller and a bank of capacitors to compensate for the power factor of the installation. The turbine was associated with three water tanks and had a drop of approximately 67 m.

Table 1. Renewable generation & electrochemical storage elements connected to microgrid.

Small Wind Power Generation Systems				
Name	Location	Nominal Power	Rotor Diameter	Wind Direction
<i>NORVENTO NED100</i>	<i>PEPA III</i>	<i>100 kW</i>	<i>Ø 22 m</i>	<i>Windward</i>
<i>ATLANTIC AOC</i>	<i>PEPA I</i>	<i>50 kW</i>	<i>Ø 15 m</i>	<i>Leeward</i>
<i>ENNERA</i>	<i>PEPA II</i>	<i>3.5 kW</i>	<i>Ø 4.36 m</i>	<i>Windward</i>
<i>ENNERA WINDERA S</i>	<i>PEPA II</i>	<i>4.2 kW</i>	<i>Ø 4.36 m</i>	<i>Windward</i>
<i>RYSE E5</i>	<i>PEPA II</i>	<i>3.5 kW</i>	<i>Ø 4.30 m</i>	<i>Windward</i>
Photovoltaic Generation Systems				
Name	Nominal Power	Panels		
		Type	Number	Power
<i>Building E01</i>	<i>10.90 kW</i>	<i>Monocrystalline</i>	<i>80</i>	<i>150 W</i>
<i>Building E03</i>	<i>12.00 kW</i>	<i>Monocrystalline</i>	<i>36</i>	<i>240 W</i>
		<i>Polycrystalline</i>	<i>18</i>	<i>230 W</i>
<i>Building E09</i>	<i>20.00 kW</i>	<i>Polycrystalline</i>	<i>238</i>	<i>97 W</i>
<i>LECA1</i>	<i>20.00 kW</i>	<i>Polycrystalline</i>	<i>63</i>	<i>310 W</i>
<i>LECA2</i>	<i>20.00 kW</i>	<i>Polycrystalline</i>	<i>63</i>	<i>310 W</i>
<i>PEPA III</i>	<i>5.04 kW</i>	<i>Polycrystalline</i>	<i>24</i>	<i>210 W</i>
<i>Energysis</i>	<i>8.96 kW</i>	<i>Monocrystalline</i>	<i>64</i>	<i>140 W</i>
<i>Turbina</i>	<i>15.00 kW</i>	<i>Monocrystalline</i>	<i>64</i>	<i>250 W</i>
<i>PEPA II</i>	<i>20.00 kW</i>	<i>Monocrystalline</i>	<i>52</i>	<i>410 W</i>
<i>Building E02</i>	<i>4.5 kW</i>	<i>Monocrystalline</i>	<i>10</i>	<i>450 W</i>
<i>RIOS</i>	<i>30.00 kW</i>	<i>Monocr. bifacial</i>	<i>56</i>	<i>540 W</i>
Electrochemical Storage Systems				
Name	Type	Arrangement	Max Power	Capacity
<i>PEPA I Battery Bank</i>	<i>Pb-acid</i>	<i>120 glasses (2 V)</i>	<i>50 kW</i>	<i>C120: 1080 Ah</i>
<i>LFP Li-ion LECA B.B.</i>	<i>L.F.P.</i>	<i>196 cells (3.2 V)</i>	<i>30 kW</i>	<i>50 Ah</i>
<i>PEPA II Battery Bank</i>	<i>Pb-acid</i>	<i>120 glasses (2 V)</i>	<i>20 kW</i>	<i>C120: 765 Ah</i>
<i>LECA Battery Bank</i>	<i>Pb-acid</i>	<i>24 glasses (2 V)</i>	<i>8 kW</i>	<i>C120: 650 Ah</i>
<i>NMC Li-ion PEPA II</i>	<i>N.M.C.</i>	<i>3 x 240 cells (3.7 V)</i>	<i>50 kW</i>	<i>58 Ah</i>

In a microgrid, energy storage systems play a crucial role in maintaining power balance and providing flexibility for demand management. The CEDER SMG

integrates different storage technologies, including mechanical and electrochemical storage, to satisfy its energy storage requirements. Mechanical storage is associated with the micro-hydroelectric plant and consists of a pumping system with four 7.5 kW centrifugal pumps and three water tanks, a reserve tank with a capacity of approximately 500 m³, an upper tank located 16 m below the reserve tank with a capacity of approximately 1,500 m³, and a lower tank located 67 m below the upper tank with a capacity of approximately 1,900 m³. For electrochemical storage, CEDER integrates two battery systems, and two more are currently being connected with the specifications detailed in Table 1.

The consumption profiles of loads in a SMG significantly impact its design and operation, with diverse load types exhibiting varying energy demands and usage patterns that affect the system's energy balance and daily operations. In the CEDER SMG, different facilities can be categorized into three energy consumption patterns: industrial, domestic, and service sector. Managing these varied profiles is crucial for ensuring a steady energy supply, especially to energy-intensive industrial facilities, and electric vehicle (EV) charging stations add complexity to the energy balance with their potential for significant demand spikes.

A microgrid control system (MCS) is an essential component of a microgrid that is responsible for ensuring its safe and efficient operation. The MCS manages the interactions between different components of the SMG, such as distributed generation systems, storage systems, and loads. In doing so, it ensures that the power balance is maintained and that the microgrid operates in a stable and efficient manner. The MCS at CEDER is responsible for controlling and monitoring the SMG operation. It includes a set of algorithms, communication systems, and hardware components that work together to manage the SMG. The control system is designed to be flexible and scalable, allowing it to adapt to changing conditions within the SMG and accommodate future changes or additions to the microgrid. It uses advanced algorithms and control techniques to ensure efficient and safe operation of the SMG. These algorithms are designed to optimize the operation of the SMG, considering the different components of the SMG and their interactions with one another. The MCS at CEDER also includes communication systems that allow different components of the microgrid to connect with one another. This communication is critical for ensuring that the SMG operates in a safe and efficient manner. The communication systems used by MCS at CEDER include both wired and wireless communication systems, allowing for reliable and secure statements between the different components of the SMG. The MCS was designed to monitor, control, and optimize the operation of the SMG in real time. The system is composed of three main components: a communications block, a database, and a management block with a user interface. The communication block is responsible for integrating different communication protocols of the various components of the SMG, such as generation, storage, and consumption systems. It is based on JSON and supports a variety of protocols, including Modbus, MQTT, and HTTP. The communications block acts as an intermediary between different systems and enables seamless data transfer and information exchange between them. This allows real-time monitoring of the status of each component and the transfer of instructions and control signals, as needed. The database, which is implemented using MySQL, serves as storage

7

for the microgrid's information, data, and historical records. This information is stored in an organized manner and accessible for further analysis and processing. The database allows for the collection of critical data, such as energy production and consumption, weather conditions, and equipment performance. This information can then be used to make informed decisions regarding the energy management and system control strategies. The management block, also known as the Energy Management System (EMS), is the central control unit of the SMG. It is responsible for monitoring the performance of each component in real time, executing control and management functions, and making decisions based on the data collected. The management block includes a user interface implemented as a HomeAssistant HMI, which provides an easy-to-use graphical interface for monitoring and controlling the SMG. This interface allows the operator to program energy strategies, monitor the performance of the SMG, and make necessary adjustments. The management block plays a crucial role in ensuring the efficient and optimal operation of the microgrid by controlling and coordinating the functions of each component.

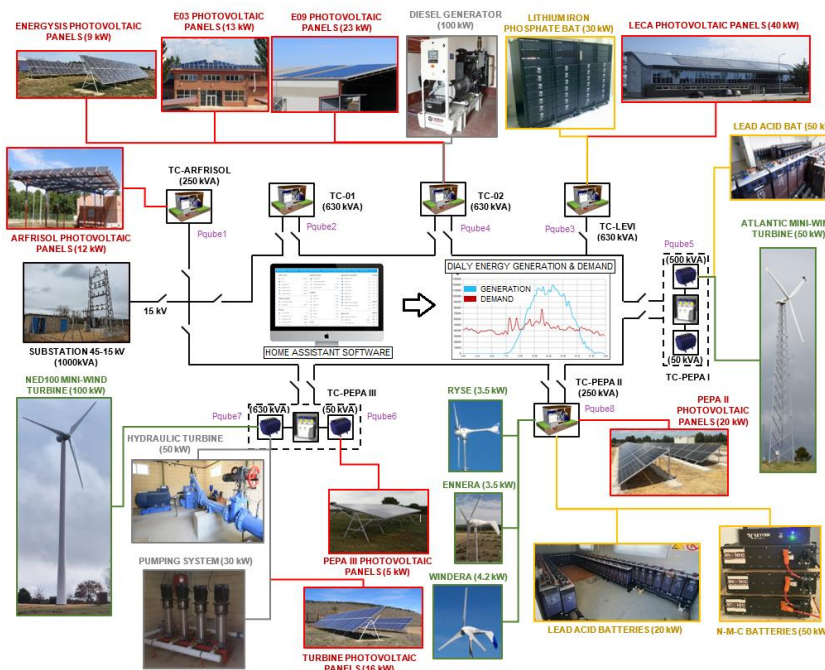


Fig. 1. Distribution of elements connected to electrical SMG

2.2 Geothermal small-scale test

The aim of the study is to explore the potential of shallow geothermal energy, often used for heating and cooling, as a means of seasonal thermal storage by integrating energy storage technologies and coupling them with the electrical grid, offering a sustainable and resilient energy solution that enhances flexibility and reliability, contributing to a cleaner and more efficient energy future.

A total of eight shallow geothermal wells, each approximately 100 meters deep are located at CEDER installations. These boreholes are divided into two groups consisting of four wells each, with one group arranged in a linear configuration and the other forming a grid pattern. The original purpose of these geothermal boreholes is to extract excess heat from the buildings and dissipate it into the surrounding ground, effectively transferring the thermal energy into the subsurface. The boreholes are strategically positioned to maximize heat dissipation efficiency and ensure uniform cooling across the site.

As part of SINNOGENES project, an expansion plan is underway at the CEDER site to construct three additional shallow geothermal boreholes in the area where the existing four wells are located in a grid pattern. The aim of this proposal is to create a small-scale demo field to be used as a thermal seasonal storage, focusing on the integration of an electrical microgrid for renewable electricity generation with a district heating network. This network encompasses solar thermal panels for heat generation, a building that serves both as a heat consumer and generator, and a small-scale geothermal field dedicated to thermal storage. A critical aspect of this approach involves the study of seasonal energy storage, which encompasses two main scenarios: during sunny days (primarily in the summer), excess heat is stored in the geothermal field, while in cold days (mainly in the winter), these heat reserves are utilized to warm the building. All of these operations are powered by renewable energy and continuously monitored through temperature sensors at various depths in the geothermal boreholes. This integrated strategy promises to optimize energy utilization, foster sustainability, and provide invaluable insights into the management of modern, eco-friendly energy systems.

9

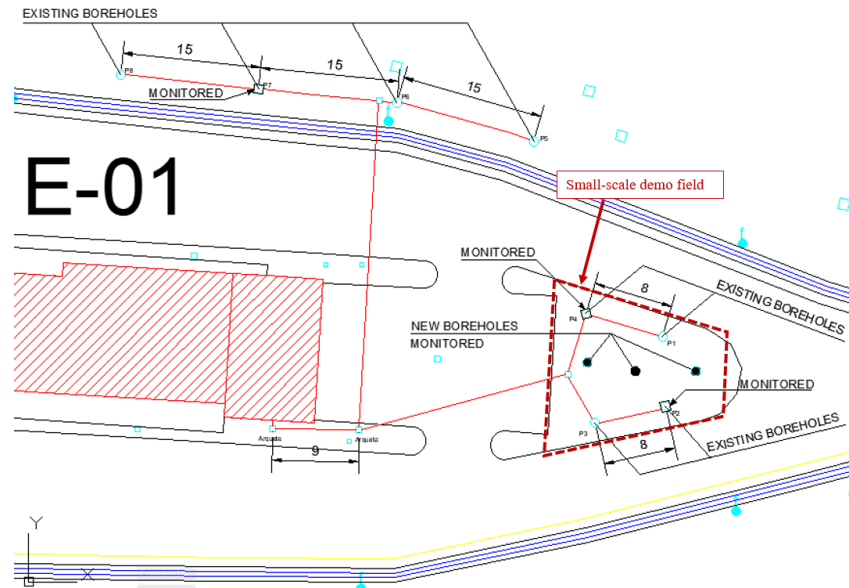


Fig.2. Small-scale geothermal filed (new and existing boreholes location)

2.3 Fast response storage systems

Fast response storage systems play a crucial role in modern energy management by addressing the challenges of intermittency and grid stability in renewable energy integration. These systems are designed to rapidly store and release energy during fluctuations in supply and demand, providing grid operators with the flexibility to maintain a reliable and balanced power supply. Two prominent examples of fast response storage technologies are flywheel energy storage systems and UC. Their ability to rapidly respond to fluctuations in supply and demand helps ensure grid stability, integrate renewable energy sources, and optimize the utilization of existing generation assets.

The flywheel to be installed exhibits several notable features that make it a versatile and efficient solution for grid stabilization and energy management. With a power rating of 25 kW, it offers a full-power autonomy of up to 6 minutes, corresponding to a stored energy capacity of 9 MJ or 2.03 kWh. The core component of the flywheel system is a high-strength steel wheel, which rotates at a maximum speed of 13,000 rpm. To minimize aerodynamic friction losses, the mobile part of the flywheel is housed in a reduced-pressure environment of 10 mbar. Additionally, the flywheel incorporates magnetic levitation using permanent magnets to relieve axial load bearing, further enhancing its efficiency. The flywheel system also includes a power electronic converter, conveniently located within the same housing, facilitating its connection to other systems at a voltage of 700 V DC.

The UC energy storage system offers impressive features that make it an efficient and reliable solution for power management and grid stability. With a maximum power rating of 120 kW and an energy capacity of 0.768 kWh, the system comprises 256 UC cells connected in series. Cells are housed in a power cabinet, divided into 8 racks with a carefully designed thermal layout to ensure continuous and optimal operation of the system. The voltage of the UC system varies depending on the state of charge and can range from 691V to 345V. To connect the system to a 700V DC-link, a DC/DC converter is integrated into the system, complementing the supercapacitor cabinet.

The integration of flywheel and UC energy storage systems within a SMG environment holds paramount importance, particularly in the context of autonomous operation and peak energy consumption reduction. This hybrid storage system provides crucial support for addressing sudden drops in power output from renewable energy sources, ensuring a continuous and stable power supply in scenarios such as cloud cover-induced fluctuations in solar radiation or abrupt wind variations affecting wind turbines. By delivering primary load-frequency control, voltage support, and power oscillation compensation, this system enhances SMG resilience, swiftly adapting to changes in renewable energy generation. Furthermore, the combination of fast-response flywheel and sustained power UC systems fortifies uninterruptible power supply (UPS) systems, guaranteeing uninterrupted operations and safeguarding against data loss or equipment damage. In isolated areas, this integration fosters energy infrastructure stability, promotes renewable energy utilization, and bolsters SMG resilience to cope with environmental fluctuations, all contributing to a reliable power supply.

2.4 Numeric evaluation for renewable energy operation

This evaluation delves into the analysis of average monthly consumptions and their comparison with the existing generation and storage capabilities present at CEDER. Such an evaluation plays a crucial role in several aspects. First and foremost, it provides valuable insights into the performance and efficiency of the renewable energy systems integrated within the facility. By closely examining the energy consumption patterns over different time frames, we can gain a deeper understanding of the energy demands and their variations throughout the year. Additionally, this numeric evaluation serves as a means to identify any imbalances or discrepancies between energy generation and consumption. By analyzing the data, we can pinpoint potential gaps where the renewable energy generation falls short or exceeds the actual energy requirements. This information allows us to optimize the system's operation, ensuring a more precise match between generation and consumption, and reducing wastage or dependency on external energy sources. Moreover, this evaluation plays a vital role in the continuous improvement and optimization of the renewable energy systems at CEDER. By studying the data trends, we can identify opportunities for enhancing the system's performance, increasing its reliability, and maximizing the utilization of renewable energy sources. This evaluation serves as a foundation for informed decision-making, enabling us to implement targeted measures that optimize energy utilization and contribute to the overall sustainability goals of the facility. Ultimately, this evaluation

11

serves as a crucial tool for effective energy management. It enables us to gauge the effectiveness of the current renewable energy infrastructure, identify areas for improvement, and ensure the seamless integration of renewable energy sources within the operations of CEDER.

Figure 3 provides valuable insights into the energy generation and consumption dynamics at CEDER, shedding light on important trends and developments in the facility's renewable energy utilization. One prominent aspect is the remarkable upward trend in renewable energy generation, particularly since November 2022, when a 100 kW nominal power wind turbine was installed, in addition to several photovoltaic panels. This exponential growth in renewable energy production reflects the successful integration of new renewable energy sources into the SMG environment. The addition of the wind turbine and PV plants has significantly contributed to the overall increase in renewable energy generation, propelling CEDER's progress towards achieving sustainable energy consumption. The energy demand at CEDER exhibits a relatively stable pattern throughout the year, with monthly fluctuations between 33 to 43 MW·h. The highest energy consumption occurs during the winter periods, while the lowest consumption is observed during the summer months. This consistent energy consumption profile underscores the importance of effective energy management and storage solutions to ensure a balanced and reliable energy supply. It becomes particularly crucial as the renewable energy generation experiences higher relative peaks during summer periods. The "Generation/Consumption Ratio" indicates that CEDER is generating a surplus of renewable energy that can be effectively harnessed for energy storage, particularly during periods of high renewable energy production, such as in the summer months, when the ratio reaches its annual relative maximum. Conversely, during winter months, the ratio decreases, underscoring the importance of energy storage solutions to ensure a stable power supply during periods of lower renewable energy generation. A significant milestone was reached in April 2023 when renewable energy generation surpassed energy consumption for the first time in CEDER's history. This achievement highlights the potential for further growth and advancement in renewable energy integration and energy storage technologies. Given the variability of the "Generation/Consumption Ratio" along the year, seasonal energy storage becomes paramount to compensate for the absence of renewable energy during winter months and effectively utilize the surplus renewable energy generated in summer. In this context, the significant importance lies in the small-scale implementation of geothermal technology as a highly effective and essential solution for seasonal energy storage in the form of heat. Geothermal systems can store vast amounts of heat during periods of high renewable energy generation, which can then be utilized during periods of low generation or increased demand. Implementing geothermal storage as a complementary energy storage solution can help CEDER optimize energy utilization and enhance the overall sustainability of its SMG environment.

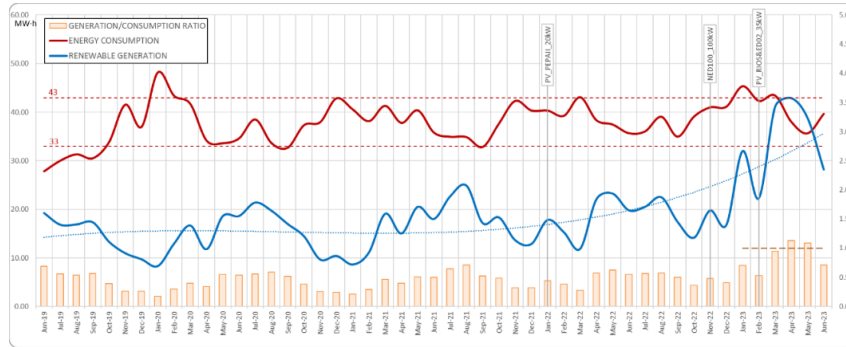


Fig. 3. Renewable energy generation and demand by month on CEDER installations.

Transitioning towards an 80% renewable energy consumption is a bold and necessary step towards a more sustainable and environmentally friendly future. However, this ambitious goal poses considerable challenges that demand innovative solutions and concerted efforts. At the forefront of this transition lies the critical role of energy storage systems in balancing the intermittency of renewable energy sources and ensuring a stable and reliable power supply. CEDER's current installation of approximately 525 kWh of battery storage signifies a positive stride towards integrating energy storage into the SMG environment. Nonetheless, this capacity represents only around 10% of the center's average daily energy consumption. As a result, it is evident that the existing energy storage capabilities are insufficient to fully support the increased penetration of renewable energy required to achieve the targeted 80% consumption. To overcome this hurdle, significant advancements and investments in energy storage technologies are essential. One promising avenue for enhancing energy storage capacity is the development of high-capacity and long-duration storage systems, capable of storing surplus renewable energy for extended periods. Another critical aspect in achieving the 80% renewable energy goal is the development of a diverse and complementary energy storage portfolio. Integrating various storage technologies, such as battery systems, ultracapacitors, and flywheels, can provide synergistic effects and enhance overall system performance. Furthermore, adopting a hybrid storage approach, combining short-duration storage systems with long-duration and seasonal storage solutions, can address the challenges of matching renewable energy generation with demand variations throughout the year. One area that holds substantial promise for seasonal energy storage is geothermal technology. Geothermal energy offers a unique opportunity to store excess renewable energy in the form of heat, providing a reliable and sustainable solution for meeting energy demands during the colder months when renewable energy production is lower. By utilizing the ground as a thermal reservoir, geothermal energy can store large quantities of heat, which can be later converted back into electricity or used directly for heating purposes. The integration of geothermal energy into CEDER's energy storage portfolio could bridge the seasonal gap between renewable energy production and consumption, further enhancing the center's ability to rely on renewable sources year-round.

13

As CEDER aims to increase its reliance on renewable energy sources, the effective management and storage of renewable energy become pivotal components in achieving a sustainable and resilient energy system. By strategically storing and distributing excess renewable energy, CEDER can optimize its energy utilization, reduce dependency on conventional energy sources, and minimize its environmental footprint. The data presented in Figure 3 underscore the importance of continuing efforts to enhance energy management practices, explore advanced storage technologies, and refine energy consumption patterns. As the trend of renewable energy generation continues to rise, CEDER can strengthen its position as a leading research and demonstration center for renewable energy technologies. By effectively managing energy resources and investing in innovative storage solutions, CEDER can drive sustainable energy consumption and contribute to a greener and more sustainable future.

3 Conclusions

The research and experiences at CEDER highlight the significant strides made towards renewable energy integration and utilization. The successful implementation of wind and photovoltaic technologies has led to a remarkable increase in renewable energy generation, demonstrating the potential of these clean energy sources in meeting energy demands.

However, to fully realize the vision of an 80% renewable energy consumption, it is evident that energy storage plays a pivotal role. While CEDER has made progress by installing battery storage, there remains a need for further advancements to achieve a more substantial storage capacity capable of effectively harnessing surplus renewable energy. Energy storage solutions are crucial in ensuring grid stability and reliable energy supply, particularly during periods of fluctuating renewable energy generation.

The potential of geothermal technology as a seasonal energy storage solution holds great promise. By capturing and storing excess heat during periods of high renewable energy production, geothermal systems offer a valuable means of enhancing energy storage capacity and maintaining a balanced energy supply throughout the year.

As the world seeks to transition towards a more sustainable and greener energy future, the lessons learned at CEDER can serve as a blueprint for other SMG environments. Ongoing research and development in fast response storage systems, like flywheel and UC, along with advancements in geothermal technology, are essential to achieving a cleaner and more resilient energy infrastructure.

Acknowledgments

The authors are grateful for the opportunity to contribute as demo site centre in the Storage INNOvations for Green ENergy Systems (SINNOGENES). This work has received support from European Union's Horizon research and innovation program under grant agreement No 101096992.

References

- [1] L. C. Vieira, M. Longo, and M. Mura, "Are the European manufacturing and energy sectors on track for achieving net-zero emissions in 2050? An empirical analysis," *Energy Policy*, vol. 156, p. 112464, 2021.
- [2] A. Qazi et al., "Towards Sustainable Energy: A Systematic Review of Renewable Energy Sources, Technologies, and Public Opinions," *IEEE Access*, vol. 7, pp. 63837–63851, 2019.
- [3] A. Arias, I. León, X. Oregi, and C. Marieta, "Environmental Assessment of University Campuses: The Case of the University of Navarra in Pamplona (Spain)," *Sustainability*, 2021.
- [4] R. Madurai Elavarasan, R. Pugazhendhi, M. Irfan, L. Mihet-Popa, I. A. Khan, and P. E. Campana, "State-of-the-art sustainable approaches for deeper decarbonization in Europe – An endowment to climate neutral vision," *Renew. Sustain. Energy Rev.*, vol. 159, p. 112204, 2022.
- [5] H. Kulasekara and V. Seynlabdeen, "A Review of Geothermal Energy for Future Power Generation," 2019 5th Int. Conf. Adv. Electr. Eng., pp. 223–228, 2019.
- [6] M. J. B. Kabeyi, "Geothermal Electricity Generation, Challenges, Opportunities and Recommendations," 2019.
- [7] T. Agemar, J. Weber, and I. S. Moeck, "Assessment and Public Reporting of Geothermal Resources in Germany: Review and Outlook," *Energies*, vol. 11, p. 332, 2018.
- [8] M. R. Karlsdóttir, J. Heinonen, H. Pálsson, and Ó. P. Pálsson, "High-Temperature Geothermal Utilization in the Context of European Energy Policy—Implications and Limitations," *Energies*, 2020.
- [9] G. Jharap, L. P. van Leeuwen, R. Mout, W. van der Zee, F. M. Roos, and A. G. Muntendam-Bos, "Ensuring safe growth of the geothermal energy sector in the Netherlands by proactively addressing risks and hazards," *Netherlands J. Geosci.*, vol. 99, 2020.
- [10] A. Paulillo, L. Cotton, R. Law, A. Striolo, and P. Lettieri, "Geothermal energy in the UK: The life-cycle environmental impacts of electricity production from the United Downs Deep Geothermal Power project," *J. Clean. Prod.*, vol. 249, p. 119410, 2020.
- [11] L. Meng et al., "Fast Frequency Response From Energy Storage Systems—A Review of Grid Standards, Projects and Technical Issues," *IEEE Trans. Smart Grid*, vol. 11, no. 2, pp. 1566–1581, 2020.
- [12] U. Akram, M. Nadarajah, R. Shah, and F. Milano, "A review on rapid responsive energy storage technologies for frequency regulation in modern power systems," *Renew. Sustain. Energy Rev.*, vol. 120, p. 109626, 2020.
- [13] S. Karthikeyan, B. Narenthiran, A. Sivanantham, L. D. Bhatlu, and T. Maridurai, "Supercapacitor: Evolution and review," *Mater. Today Proc.*, 2021.
- [14] N. Kurra and Q. Jiang, "18 - Supercapacitors," in *Storing Energy (Second Edition)*, Second Edi., T. M. Letcher, Ed. Elsevier, 2022, pp. 383–417.
- [15] H. Tao, X. Yang, Z. Li, T. Q. Zheng, X. You, and P. Koblre, "Analysis and Control of Improved MMC With Symmetrical Super Capacitor Energy Storage System in EER Application," in 2019 4th IEEE Workshop on the Electronic Grid (eGRID), 2019, pp. 1–7.

15

- [16] L. Wang, G. Jiong, C. Xu, T. Wu, and H. Lin, "Hybrid Model Predictive Control Strategy of Supercapacitor Energy Storage System Based on Double Active Bridge," *Energies*, 2019.
- [17] M. W. Khalid, "A Review on the Selected Applications of Battery-Supercapacitor Hybrid Energy Storage Systems for Microgrids," *Energies*, vol. 12, p. 4559, 2019.
- [18] S.-H. Lee, B.-S. Jin, H.-S. Kim, H.-J. Ahn, and B.-G. Lee, "A novel battery-supercapacitor system with extraordinarily high performance," *Int. J. Hydrogen Energy*, vol. 44, no. 5, pp. 3013–3020, 2019.
- [19] H. Toodeji, "A developed flywheel energy storage with built-in rotating supercapacitors," *Turkish J. Electr. Eng. Comput. Sci.*, vol. 27, pp. 213–229, 2019.
- [20] F. Goris and E. L. Severson, "A Review of Flywheel Energy Storage Systems for Grid Application," *IECON 2018 - 44th Annu. Conf. IEEE Ind. Electron. Soc.*, pp. 1633–1639, 2018.
- [21] L. Jing, X. Xue, and X. N. Guo, "Research Review of Flywheel Energy Storage Technology," *IOP Conf. Ser. Earth Environ. Sci.*, vol. 558, 2020.
- [22] Y. Jia, Z. K. Wu, J. Zhang, P. Yang, and Z. Zhang, "Control Strategy of Flywheel Energy Storage System Based on Primary Frequency Modulation of Wind Power," *Energies*, 2022.
- [23] N. Li, Y. Zhang, L. Hao, and Q. Pan, "Application of flywheel energy storage device in vital places," *2020 7th Int. Conf. Inf. Sci. Control Eng.*, pp. 1697–1701, 2020.
- [24] Z. Lv, Z. Wang, and W. Xu, "A Techno-Economic Study of 100% Renewable Energy for a Residential Household in China," *Energies*, 2019.
- [25] A. A. Adesanya, R. Sidortsov, and C. Schelly, "Act locally, transition globally: Grassroots resilience, local politics, and five municipalities in the United States with 100% renewable electricity," *Energy Res. & Soc. Sci.*, 2020.
- [26] M. I. Aceleanu, A. C. Șerban, D.-M. Țircă, and L. Badea, "THE RURAL SUSTAINABLE DEVELOPMENT THROUGH RENEWABLE ENERGY. THE CASE OF ROMANIA," *Technol. Econ. Dev. Econ.*, 2018.
- [27] L. Al-Ghussain et al., "100% Renewable Energy Grid for Rural Electrification of Remote Areas: A Case Study in Jordan," *Energies*, 2020.
- [28] T. Trainer, "Estimating the EROI of whole systems for 100% renewable electricity supply capable of dealing with intermittency," *Energy Policy*, 2018.

Smart Grid

Methodology for managing the recharging of EV batteries in a smart microgrid using surplus renewable generation

Oscar Izquierdo-Monge¹, Aurora Arroyo Garcia², Paula Peña-Carro¹, Ángel Hernández Jiménez¹, Ángel Zorita Lamadrid², Luis Hernández-Callejo²

¹ CE.D.E.R.-CIEMAT, Autovía de Navarra A15 salida 56, 422290 Lubia (Soria), España, O.I.M.: oscar.izquierdo@ciemat.es; P.P.C.: paula.pena@ciemat.es; A.H.-J.: angel.hernandez@ciemat.es

² Universidad de Valladolid, Campus Universitario Duques de Soria, 42004 Soria, Spain; A.A.G.: auroraarrgar@gmail.com; A.Z.L.: zorita@eii.uva.es; L.H.C.: luis.hernandez.callejo@uva.es

Abstract: This paper presents a methodology for managing EVs in a smart microgrid with the aim of maximizing the consumption of surplus generation and the use of renewable energy. The charging process for EVs in the microgrid and its administrative management are described to achieve greater energy efficiency and maximize available energy. A specific use case is shown at CEDER-CIEMAT (Centro para el Desarrollo de las Energías Renovables – Centro de Investigaciones Energéticas, Medioambientales y Tecnológicas), where two EVs are used, achieving an average of over 90% recharge with renewable energy and nearly 70% with surplus energy, resulting in savings of over 750 euros last twelve months on the electricity bill. This demonstrates the feasibility of the methodology presented in a real-world environment.

Keywords: Electric Vehicle (EV), Smart Microgrid, Energy management, Energy surplus, Renewable Energy.

1 Introduction

The desire of most governments to promote the sale of EVs as a less polluting option due to their efficiency, lower emission of gases, lower maintenance costs, reduced noise, and decreased dependence on fossil fuels, is causing EV sales to experience

significant growth, with China leading the market, followed by Europe and the United States [1], [2].

The accelerated growth of the EV market has led to a significant increase in the demand for efficient charging solutions. While the sale of EVs to individual consumers has experienced notable growth, it is the companies and rental services that are the main drivers of this sector. Therefore, these companies, which manage fleets of EVs, have a particular interest in having charging procedures that are not only cost-effective but also maximize the lifespan of the batteries through efficient processes.

Most electric vehicles use lithium-ion batteries, with different cathode material configurations, such as LiMn_2O_4 (LMO), LiFePO_4 (LFP), $\text{Li}(\text{Ni}_x\text{Co}_y\text{Mn}_{1-x-y})\text{O}_2$ (NCM), or LMO and NMC [3], [4]. These batteries are known for their storage capacity and durability. However, as the number of charge and discharge cycles increases [5], the batteries experience gradual deterioration, reducing their capacity, usable energy, and lifespan. Additionally, other factors such as the charging and discharging rate, depth of discharge, and time between full charge cycles also influence the performance and degradation of the batteries.

One of the most significant factors that affects the performance and lifespan of EV batteries is temperature. Temperature impacts internal resistance, electrolyte resistance, safety, power production, and electrolyte decomposition. Maintaining the battery at an optimal temperature is crucial for preserving its long-term performance. Ideally, it is recommended to keep the battery temperature between 25°C and 30°C during operation to prevent damage and premature degradation [3], [6-8].

Many companies that operate fleets of EVs have chosen to implement photovoltaic power generation facilities to meet part of their energy needs and use it for vehicle charging [9]. However, it is essential to manage this charging process efficiently [10-11], taking into account both economic profitability and the preservation of battery life. Optimizing the charging process, considering temperature and other relevant factors, can contribute to maximizing energy efficiency and prolonging battery lifespan, resulting in long-term savings for companies [12].

Communication schemes and routing protocols for electric vehicles are key components of the communication and control systems used in electric vehicle charging infrastructure and fleet management [13]. These systems enable communication and information exchange among electric vehicles, charging stations, and other network elements to facilitate efficient charging and effective fleet operations. The communication schemes used in electric vehicles can vary depending on the application and available infrastructure [14-16].

The adoption of electric vehicles by companies and rental services has driven the need to develop efficient charging procedures that are not only cost-effective but also optimize battery lifespan. Proper selection of cathode materials, temperature control during operation, and integration of renewable energy into charging processes are key aspects to consider. Continuous advancements in research and development of intelligent charging solutions will enable companies to maximize the benefits of electric mobility and contribute to a more sustainable future.

This paper analyzes the case of one of these companies, specifically the CEDER-CIEMAT, which is a research center depending on the Ministry of Science and

3

Innovation in Spain that has a smart microgrid with several renewable generation sources, storage systems, and charging infrastructure, which will be described later. The microgrid is fully monitored and controlled in real-time.

Currently, this research center has two EVs, and their charging stations are integrated into the microgrid. They primarily rely on surplus electricity generated by renewable sources or stored in the microgrid's storage systems. Only in specific cases where urgent supply is required, electricity from the distribution grid is used. Prioritizing charging with surplus renewable energy offers several advantages, such as reducing carbon emissions [17], achieving energy independence, lower costs, job creation, and improvements in public health [18].

This paper presents a methodology for managing the recharging of EV batteries in a smart microgrid with the objective of prioritizing the use of surplus renewable energy generated within the microgrid and managing the EV charging process. The main contribution of this proposal is the achievement of both objectives through the use of easy-to-implement open-source software (Node-Red and Home Assistant). This methodology is developed in Section 2 and has been successfully implemented in the smart microgrid of CEDER-CIEMAT. Section 3 presents the actual charging results of vehicles in this microgrid, collected over more than a year of monitoring all the involved elements. Finally, the conclusions and Future work are presented in fourth and fifth sections.

2 Methodology

As mentioned in the introduction, the objective of this document is to present a methodology for recharging EVs batteries in a smart microgrid, maximizing the use of surplus renewable energy generation directly or through available storage systems in the microgrid.

The vehicles in this study will be recharged at less than 10 kW (2 kW or 7 kW), which means less current flow to the batteries, which is beneficial to their health. In addition, with lower power requirements for recharging, it is easier to make surplus energy available in the microgrid. The downside is the longer charging time for EVs, which can take several hours. However, this will not be a problem thanks to the management applied to EVs with this methodology.

The established steps to achieve these objectives are as follows:

Step 1. Identification of elements. Firstly, it is necessary to identify all the elements that will enable the charging of EVs using surplus renewable energy or stored energy. These elements are:

1. Distribution company meter to monitor the microgrid consumption and detect surplus energy.
2. Vehicle charging stations.

3. Renewable generation sources: Different generation sources can be integrated into an electric microgrid. The most common ones are photovoltaic modules and small wind turbines.
4. Energy storage systems: The most commonly used storage systems in microgrids are batteries, although other types of storage can be considered (pumping systems, hydrogen, flywheels, ultracaps, compressed air, etc.).
5. EVs: It is necessary to characterize the charging requirements of the vehicles that will be serviced by the charging stations (fast charging, medium charging, slow charging, and associated energy consumption for each).

Step 2. Monitoring of elements. Once the elements involved in vehicle charging have been identified, it is necessary to monitor and integrate them into a control software, allowing them to communicate with each other through a control system that provides charging instructions to the vehicles based on the state of the other elements. In order to charge EVs by prioritizing surplus renewable energy or stored energy, the following parameters need to be monitored:

1. Instantaneous power of the microgrid: If the value of this power is greater than zero, the microgrid is consuming energy from the distribution grid. If it is less than zero, the energy generated by the renewable generation sources associated with the microgrid exceeds the consumption of its loads, indicating surplus energy, and the microgrid exports energy to the distribution grid.
2. Instantaneous power of the vehicle chargers to determine their consumption.
3. Instantaneous power of the renewable generation sources.
4. Stored energy to determine its availability and instantaneous power to understand the consumption of this energy by the vehicles.

To monitor all these parameters and develop the control system, two open-source programs will be used: Node-Red and HomeAssistant [19-20], which is one of the significant advantages of this methodology.

Node-Red is a free software that integrates different communication protocols (Modbus, MQTT, HTTP, etc.) and allows for easy communication with each element that is part of a microgrid. To communicate with a device using the Modbus communication protocol from Node-Red, it is necessary to configure a Modbus node for that device, defining the IP address, port number (default is 502), and the communication mode (Modbus TCP/IP or Modbus RTU). Additional parameters such as connection timeout and update frequency also need to be adjusted.

Once the communication is established, it is necessary to configure input and output nodes (for reading values or sending commands, respectively). This requires determining the device's identification number (Unit-ID), the Modbus register address, the number of addresses occupied by the register, and the register type (input, holding, etc.).

Finally, after reading the value from the corresponding Modbus address (which is a value between 0 and 65536), it needs to be interpreted using a JavaScript function programmed to obtain the actual value of the variable being measured, based on the information collected in the Modbus frame regarding the scaling factor and data type.

5

Node-Red sends this information to Home Assistant, an open-source automation system based on the Internet of Things (IoT) architecture, to develop a real-time control system with a user-friendly graphical interface. It allows the creation of automations based on events, schedules, sensors, or any other condition (e.g., surplus energy in the microgrid) by programming in YAML or using the visual automation editor.

Home Assistant control panel enables the creation of customized views by configuring cards and panels to display real-time information, such as device status, graphs of measured variables, etc.

Step 3. Define the charging procedure. The third step involves defining the charging procedure for vehicles, prioritizing the use of surplus renewable energy first, followed by the consumption of stored energy. Figure 1 shows a flowchart depicting the procedure defined within this methodology for the charging of EVs.

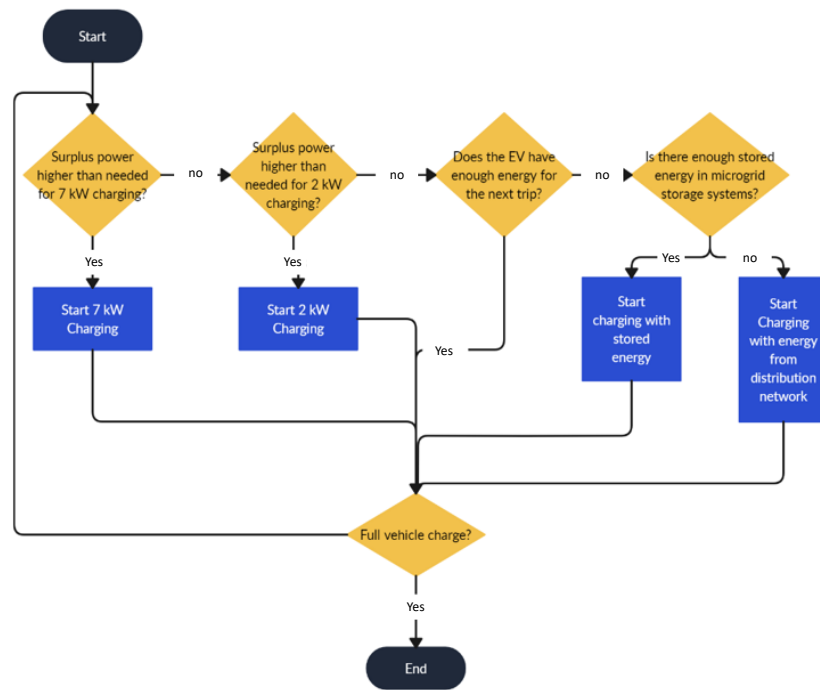


Fig. 1. EV recharge's management.

The charging process of EVs in the microgrid must be monitored in real-time (with data transmission occurring every second) and is based on the information defined earlier in this section, regarding the charging stations, renewable energy generation systems, microgrid surplus, and energy storage systems.

As seen in the flowchart, if there is enough surplus energy to perform a 7 kW charge for vehicles, this type of charging will be carried out. It is possible that there is surplus energy, but not enough for this type of charge. In this case, it is necessary to check if there is sufficient surplus for a 2 kW charge.

If, even so, the surplus energy is not sufficient to charge the vehicles, other considerations need to be taken into account. These considerations include whether the vehicle has enough charge for the next scheduled trip, as we will see later in this section, or if there is stored energy available for charging.

3 Use case. CEDER-CIEMAT

According to the three-step methodology described in the previous section, based on the efficient use of renewable energy and the maximization of available energy in the microgrid, the first step consists of identifying and characterizing the elements.

3.1 Identification of elements.

In the case of the CEDER-CIEMAT microgrid, the elements that enable the charging of EVs using renewable energy surplus or stored energy are as follows:

3.1.1 Vehicle charging system

There are five chargers for EVs, three CIRCUTOR URBAN T24 MIX model and two WALBOX EPARK T-C2 model. These chargers allow for charging based on external factors, such as the presence or absence of energy surplus, and have the capability to pause and resume the charging process.

3.1.2 Renewable Generation Sources

CEDER microgrid includes different renewable generation systems with a total installed capacity of over 400 kW, including the following:

- Photovoltaic: There are 11 distributed photovoltaic systems throughout the center, with a total installed capacity of 181.9 kW.
- Wind: There are 5 small-scale wind turbines with a total installed capacity of 162.2 kW.
- Hydraulic: There is a 60 kW mini Pelton turbine.

3.1.3 Energy Storage Systems.

CEDER microgrid incorporates distributed energy storage systems, including:

- Pumping system associated with the Pelton turbine with a capacity of 30 kW.
- Lead-acid batteries: Two banks with 120 cells of 2 V each. The first bank has a capacity of 1080 Ah per cell, while the second bank has a capacity of 765 Ah per cell.

7

- LFP batteries: 2 racks with 196 cells of 3.2 V each, with a capacity of 50 Ah.

3.1.4 Electric Vehicle

CEDER has two 100% EVs for personnel and material transportation within its facilities and for short-distance travel: a Nissan Leaf 40 and a Renault Kangoo. The specifications of the mentioned vehicles are as follows:

The Nissan Leaf 40 has a range of 220 km and features a manganese oxide and lithium battery with a voltage of 3.75 V, a current intensity of 32.5 Ah, a capacity of 40 kWh, and consists of 24 modules with 8 cells each.

The charging will vary depending on the type, whether it is medium (Type 2) or slow, as shown in Figure 2.

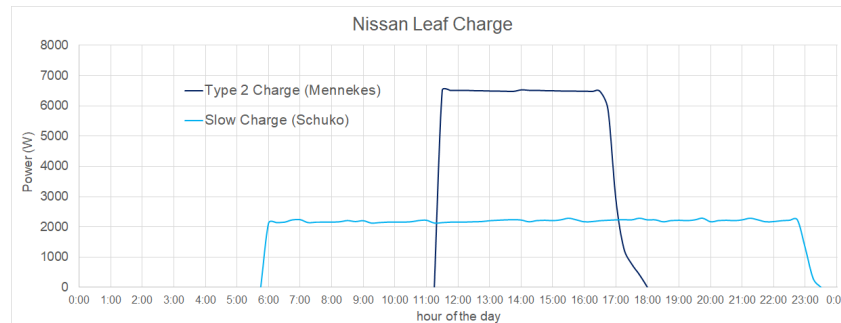


Fig. 2. Nissan Leaf's charge.

In the previous figure, slow charging, which uses a Schuko connector, begins when the power of the surplus energy produced is sufficiently high (slightly over 2000 W) to initiate this type of charging. The main disadvantage of slow charging is the long time required for the vehicle to reach a full charge (a total of 17 hours).

On the other hand, medium or Type 2 charging, which uses a Mennekes connector, will start when the power of the surplus energy is sufficiently high (around 6400 W) to carry out this type of charging. Since it requires more power, the vehicle can reach a full charge in 7 hours. This shorter charging time is its main advantage compared to slow charging.

The Renault Kangoo has an approximate range of 200 km and features a lithium-ion battery with a voltage of 3.6 V, a current intensity of 30 Ah, and a capacity of 30 kWh.

In addition to the charging power, another factor that greatly influences the duration of the charging process is the battery capacity, resulting in the Renault Kangoo, with a battery capacity of 30 kWh, charging much faster than the Nissan Leaf, whose battery has a capacity of 40 kWh.

3.2 Monitoring of the elements

The second step of the methodology involves monitoring the elements involved in the charging of EVs and their integration into a control system. As explained in the previous

section, Node-RED is used to monitor all these parameters, and Home Assistant is used to develop the control system. Additionally, a MariaDB database is used for data storage for further analysis and presenting the results, as will be seen in the next section.

3.3 Defining the charging procedure

The charging procedure defined in this methodology and implemented at CEDER aims to maximize the use of renewable energy generation surplus while optimizing battery life. If there is enough surplus energy for fast charging the vehicles, this type of charging will be performed. If there is not enough energy for fast charging but sufficient for slow charging, then slow charging will be carried out.

If there is no surplus energy available, the stored energy will be used if available. If there is no stored energy, the planned use of the vehicle (as described in section 3.4) needs to be taken into account. If the vehicle has sufficient charge for the next scheduled trip, no further charging will be done until there is surplus energy available. If the vehicle does not have enough charge for the next scheduled trip, it will be charged from the distribution grid.

4 Results

According to the methodology outlined in this paper, the main objective is to charge EVs using the surplus energy produced by the generation sources present at CEDER (mainly wind and solar photovoltaic) or, alternatively, with stored energy from these sources. The control system developed at CEDER, using NodeRed and Home Assistant, is associated with a database that records data every second and stores it in fifteen-minute averages (the same frequency used by the distribution company to generate electricity bills). Next, to demonstrate the effectiveness of the methodology employed, data from two complete days (April 14, 2023, and April 27, 2023. Figures 3 and 4) will be presented, showing different types of charging. This will be followed by data from a full week (from April 10 to April 16, 2023), and subsequently, data from the entire month of April 2023 to provide an overall view of the results obtained.

Figure 3 shows the results obtained on April 14, 2023. The red line represents the consumption of the CEDER microgrid from the distribution grid, the blue line represents the charging of the Nissan Leaf EV, and the green line represents the charging of the Renault Kangoo EV. When the red line is present, it indicates that the microgrid's consumption from the distribution grid is greater than zero, indicating no surplus generation. The graph shows that the vehicle charging begins when there is no consumption from the distribution grid (indicating surplus generation, where the production from renewable sources in the microgrid exceeds the load consumption) and pauses when consumption from the distribution grid starts, repeating several times throughout the day. This means that the charging of EVs only occurs when there is surplus energy (when the microgrid's demand is lower than the energy produced by renewable sources). It is a discontinuous charging process throughout the day.

9

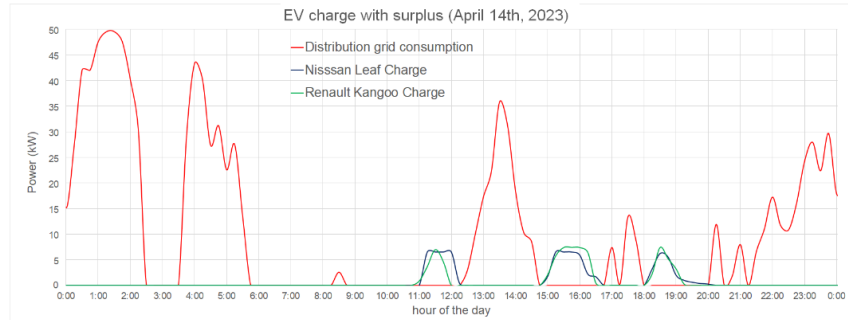


Fig. 3. EV charging only with surplus (14 April 2023).

Figure 4 shows the results obtained on 27/04/2023. Using the same color code as in the previous figure, a complete and uninterrupted charging of both EVs can be observed, as there has been an excess generation from 10:00 to 19:00 throughout this day.

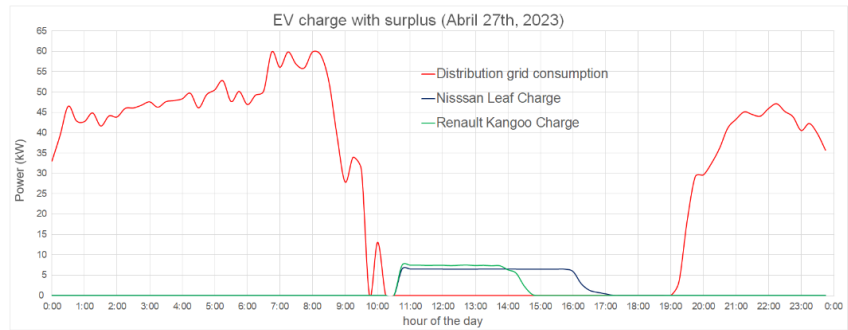


Fig. 4. EV charging only with surplus (27 April 2023).

Figure 5 shows the results obtained over a longer period of time (week of 10th to 16th April 2023). There are days where the charging is continuous because there are sufficient excesses to complete the charging of the vehicles, while other days the charging is intermittent, just like the surplus.

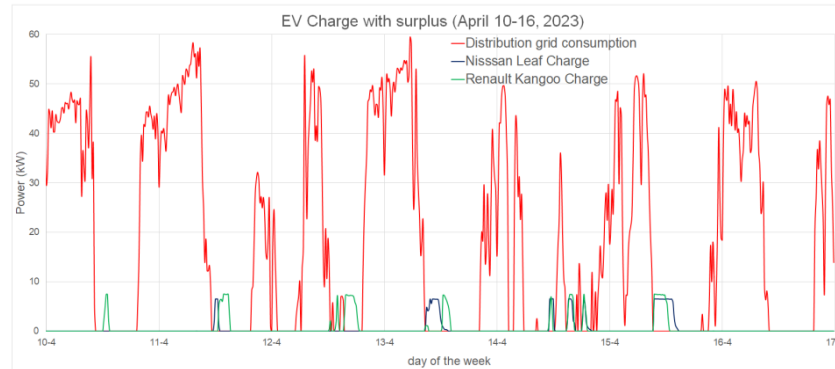


Fig. 5. EV charging only with surplus (week 10-17 April 2023).

On Monday, the 10th, it was only necessary to charge the Renault Kangoo for a short period of time because the vehicle was almost fully charged. On Tuesday, the 11th, both vehicles were continuously charged after a period of time during which the energy demand at CEDER was lower than the renewable energy produced. In the case of the Nissan Leaf, the charging was brief as it was already nearly fully charged, while the Renault Kangoo's charging can be observed for a longer duration. On Wednesday, the 12th of April in the afternoon, there were alternating periods of excess energy production and instances where the demand from the facilities exceeded the renewable production. This resulted in intermittent charging for the only vehicle that was charged, the Renault Kangoo. On Thursday, the 13th, around noon, there was enough excess energy to perform a continuous full charge for both vehicles. On Friday, the 14th, similar to the events on the 12th, there were alternating intervals of excess energy availability and instances where the microgrid's demand exceeded the renewable production. In this case, both vehicles were charged, but their charging, although completed, was intermittent. Furthermore, on Saturday, the excesses were sufficiently high to charge both vehicles simultaneously, while on Sunday, they were not charged as they were not used on Saturday and were already fully charged.

The summary of the results obtained over the course of a year is shown in Table 1, where it can be seen that by using the methodology described in section 2 of this document, the charging with surplus energy has been maximized (79% for Renault Kangoo and 69% for Nissan Leaf), and especially the charging with renewable energy (98% for Renault Kangoo and 96% for Nissan Leaf). In some months, due to lower renewable energy production (November and December 2022, Nissan Leaf had 37% and 21% of charging with surplus energy, respectively), and in others due to the need and urgency of using the vehicle (June 2022, Nissan Leaf had 52% of charging with surplus energy), more electricity from the grid was used in addition to the stored energy.

Table 1. Total charge, charge with surplus, and charge with renewable energy

	Charging Energy (kWh)		Charge with surplus (kWh)		Charge with renewable energy (kWh)	
	Kangoo	Leaf	Kangoo	Leaf	Kangoo	Leaf
May'22	108	122	88	116	104	122
Jun'22	132	271	97	142	132	200
Jul'22	128	171	111	137	128	171
Aug'22	134	164	122	111	134	164
Sep'22	147	219	118	158	137	216
Oct'22	174	161	157	107	167	161
Nov'22	166	217	108	80	157	215
Dec 22	67	132	59	27	67	132
Jan'23	116	35	79	26	115	35
Feb'23	186	225	118	119	170	219
Mar'23	303	204	240	197	300	204
Apr'23	256	119	231	115	256	119
May'23	241	228	184	222	238	228
Total	2159	2267	1714	1558	2106	2185

Figure 6 and Figure 7 shows, respectively, the percentages of charging in both vehicles with surplus energy and with renewable energy. In Figure 6, it can be observed that only in the month of August the percentage charged with surplus energy is below 50%, due to the need to use the Nissan Leaf vehicle without time to plan the charging. In the case of Renault Kangoo, a charging percentage higher than 75% is achieved every month except for September and October, which is very close to that value. In the case of Nissan Leaf, the percentage is slightly lower. In the recent months, after adjustments in the charging control program by the microgrid, the system has been improved, resulting in values in both cases exceeding 90%.

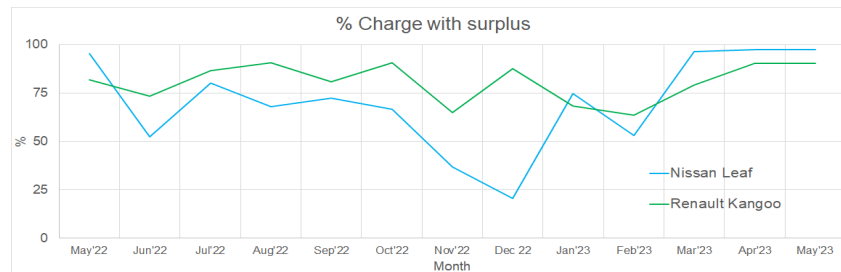


Fig. 6. Percentage of charging with surplus energy May2022-May2023.

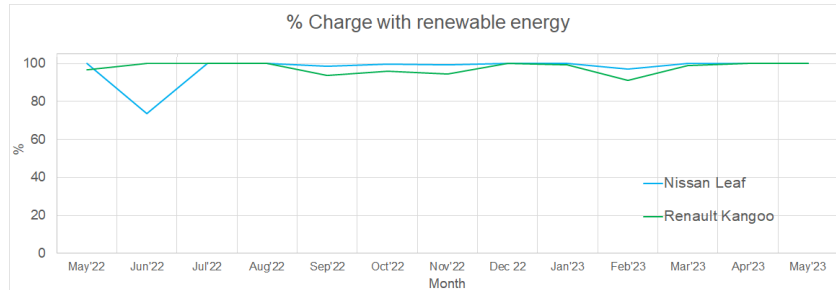


Fig. 7. Percentage of charging with renewable energy May2022-May2023.

In Figure 7, it can be observed that the percentage of charge with renewable energy is above 90% in both vehicles every month, except for the month of June 2022 in the case of the Nissan Leaf, which is 75% due to usage requirements. Furthermore, the obtained results can be classified not only from an energy perspective but also from an economic perspective, as shown in Table 4. To do so, the electricity prices indicated in Table 2 and Table 3 have been taken into account. These tables display prices in different billing periods of the 6.1 TD tariff, applicable in Spain and contracted at CEDER year 2022 and year 2023 respectively.

Table 2. Electricity prices for the 6.1 TD tariff (CEDER) 2022.

	Prices of kWh					
	P1	P2	P3	P4	P5	P6
Energy	0,161822 €	0,15095 €	0,125263 €	0,1162 €	0,105563 €	0,099955€
Energy + taxes	0,19661 €	0,1834 €	0,15219 €	0,1412 €	0,128259 €	0,121445 €

Table 3. Electricity prices for the 6.1 TD tariff (CEDER) 2023.

	Price of kWh					
	P1	P2	P3	P4	P5	P6
Energy	0.33169 €	0.319483 €	0.277395 €	0.262635 €	0.246811 €	0.260134 €
Energy + taxes	0.40300 €	0.388171 €	0.337034 €	0.319101 €	0.299875 €	0.316062 €

Table 4 shows the savings generated by charging EVs with surplus energy compared to the cost of charging them with energy from the distribution grid, based on the CEDER tariffs described in the previous table.

Table 4. Classification of results considering energy and economic aspects.

	Current recharge cost (€)		Total expenditure if not charged with surplus (€)		Save (€)	
	Kangoo	Leaf	Kangoo	Leaf	Kangoo	Leaf
Jun'22	4,3	26,0	18,0	45,6	13,7	19,6
Jul'22	3,4	6,6	22,4	33,5	19,0	26,9
Aug'22	1,8	7,8	19,1	24,6	17,2	16,8
Sep'22	4,1	9,1	20,8	32,2	16,7	23,1
Oct'22	2,1	7,5	21,7	21,3	19,6	13,7
Nov'22	9,7	24,3	24,7	36,9	15,1	12,6
Dec'22	1,4	20,4	11,4	25,8	10,0	5,3
Jan'23	14,1	3,5	42,7	13,6	28,7	10,0
Feb'23	25,7	42,0	71,5	88,2	45,8	46,2
Mar'23	23,7	2,9	111,3	76,2	87,6	73,3
Apr'23	7,6	1,0	80,3	37,0	72,7	36,0
May'23	17,7	2,0	75,8	71,8	58,2	69,8
Total	115,5	153,0	519,8	506,4	404,3	353,4

The total savings in one year with the Nissan Leaf amount to 404,3 €, and with the Renault Kangoo, it is 353,4 €. The savings are higher during the summer months when there is a greater percentage of charging with surplus energy. The least favorable months are December 2022 and January 2023, where besides the lower percentage of charging with surplus energy, the cold temperatures affect the vehicle performance.

5 Conclusions and future work

The results of this study demonstrate that the methodology defined in this paper for EV charging in an intelligent microgrid allows for maximizing the consumption of renewable generation surpluses, resulting in significant cost savings on the electricity bill and optimizing energy usage.

With this methodology, EVs have been charged using an average of over 90% renewable energy and almost 70% surplus energy. Furthermore, it can be observed that in the last five months, after some adjustments in the microgrid control system, these values have increased, with the average surplus usage and renewable energy usage surpassing 80% and 98% respectively.

In economic terms, an annual savings of over 750 € on the electricity bill has been achieved, amounting to nearly 63 € per month. Similar to the surplus energy usage, these savings have increased in the last four months due to programming adjustments and changes in electricity bill, reaching an average monthly value of over 120 €.

Additionally, by avoiding high-power rapid charging and utilizing loads below 10 kW, the battery lifespan is maximized.

In summary, the methodology described in this paper ensures reliable and sustainable charging for EVs while efficiently utilizing renewable energy and reducing dependence on the electricity distribution grid. It is important to highlight the potential of EVs and efficient management of their charging in intelligent microgrids to promote sustainable transportation and reduce environmental pollution. The obtained results provide a solid foundation for further work on the development of charging infrastructure, advanced battery technologies, and supportive policies to facilitate the widespread adoption of EVs in the future.

After this paper, it would be interesting to continue adjusting the automation programming in the microgrid control system to further increase the utilization of renewable energy surpluses in vehicle charging. It would also be valuable to analyze data from successive years to observe the evolution over time.

Lastly, a deeper investigation could be conducted on the seasonal effect on vehicle behavior, both in terms of charging due to lower energy production in winter months by the microgrid and the performance of EV batteries at low temperatures.

References

- [1] A. Razmjoo et al., “A Comprehensive Study on the Expansion of EVs in Europe,” *Appl. Sci.*, vol. 12, no. 22, 2022, doi: 10.3390/app122211656.
- [2] A. Selim, M. Abdel-Akher, S. Kamel, F. Jurado, and S. A. Almohaimed, “EVs Charging Management for Real-Time Pricing Considering the Preferences of Individual Vehicles,” *Appl. Sci.*, vol. 11, no. 14, 2021, doi: 10.3390/app11146632.
- [3] A. Carnovale and X. Li, “A modeling and experimental study of capacity fade for lithium-ion batteries,” *Energy AI*, vol. 2, p. 100032, 2020, doi: <https://doi.org/10.1016/j.egyai.2020.100032>.
- [4] M. A. Cusenza, S. Bobba, F. Ardente, M. Cellura, and F. Di Persio, “Energy and environmental assessment of a traction lithium-ion battery pack for plug-in hybrid EVs,” *J. Clean. Prod.*, vol. 215, pp. 634–649, 2019, doi: <https://doi.org/10.1016/j.jclepro.2019.01.056>.
- [5] C. C. Chan and Y. S. Wong, “EVs charge forward,” *IEEE Power Energy Mag.*, vol. 2, no. 6, pp. 24–33, 2004, doi: 10.1109/MPAE.2004.1359010.
- [6] S. Li, P. Zhao, C. Gu, J. Li, S. Cheng, and M. Xu, “Battery Protective EV Charging Management in Renewable Energy System,” *IEEE Trans. Ind. Informatics*, vol. 19, no. 2, pp. 1312–1321, 2023, doi: 10.1109/TII.2022.3184398.
- [7] T. Harighi, S. Padmanaban, R. Bayindir, E. Hossain, and J. B. Holm-Nielsen, “EV charge stations location analysis and determination—Ankara (Turkey) case study,” *Energies*, vol. 12, no. 18, 2019, doi: 10.3390/en12183472.
- [8] D. Wang, M. Sechilariu, and F. Locment, “PV-Powered Charging Station for EVs: Power Management with Integrated V2G,” *Appl. Sci.*, vol. 10, no. 18, 2020, doi: 10.3390/app10186500.
- [9] B. Aluisio, S. Bruno, L. De Bellis, M. Dicorato, G. Forte, and M. Trovato, “DC-

15

- Microgrid Operation Planning for an EV Supply Infrastructure,” *Appl. Sci.*, vol. 9, no. 13, 2019, doi: 10.3390/app9132687.
- [10] F. Teng, Z. Ding, Z. Hu, and P. Sarikprueck, “Technical Review on Advanced Approaches for EV Charging Demand Management, Part I: Applications in Electric Power Market and Renewable Energy Integration,” *IEEE Trans. Ind. Appl.*, vol. 56, no. 5, pp. 5684–5694, 2020, doi: 10.1109/TIA.2020.2993991.
- [11] Z. Ding, F. Teng, P. Sarikprueck, and Z. Hu, “Technical Review on Advanced Approaches for EV Charging Demand Management, Part II: Applications in Transportation System Coordination and Infrastructure Planning,” *IEEE Trans. Ind. Appl.*, vol. 56, no. 5, pp. 5695–5703, 2020, doi: 10.1109/TIA.2020.2993760.
- [12] Y. An, Y. Gao, N. Wu, J. Zhu, H. Li, and J. Yang, “Optimal scheduling of EV charging operations considering real-time traffic condition and travel distance,” *Expert Syst. Appl.*, vol. 213, p. 118941, 2023, doi: <https://doi.org/10.1016/j.eswa.2022.118941>.
- [13] O. Olatunde, M. Y. Hassan, M. P. Abdullah, and H. A. Rahman, “Hybrid photovoltaic/small-hydropower microgrid in smart distribution network with grid isolated EV charging system,” *J. Energy Storage*, vol. 31, no. April, p. 101673, 2020, doi: 10.1016/j.est.2020.101673.
- [14] Barbecho Bautista, P., Lemus Cárdenas, L., Urquiza Aguiar, L., & Aguilar Igartua, M. (2019). A traffic-aware EV charging management system for smart cities. *Vehicular Communications*, 20, 100188. <https://doi.org/10.1016/j.vehcom.2019.100188>.
- [15] Elghanam, E., Hassan, M., Osman, A., & Ahmed, I. (2021). Review of communication technologies for EV charging management and coordination. *World EV Journal*, 12(3). <https://doi.org/10.3390/wevj12030092>.
- [16] H. M. Abdullah, A. Gastli, and L. Ben-Brahim, “Reinforcement Learning Based EV Charging Management Systems-A Review,” *IEEE Access*, vol. 9, pp. 41506–41531, 2021, doi: 10.1109/ACCESS.2021.3064354.
- [17] S. Saponara, R. Saletti, and L. Mihet-Popa, “Hybrid Micro-Grids Exploiting Renewables Sources, Battery Energy Storages, and Bi-Directional Converters,” *Appl. Sci.*, vol. 9, no. 22, 2019, doi: 10.3390/app9224973.
- [18] B. Bessagnet et al., “Emissions of Carbonaceous Particulate Matter and Ultrafine Particles from Vehicles; A Scientific Review in a Cross-Cutting Context of Air Pollution and Climate Change,” *Appl. Sci.*, vol. 12, no. 7, 2022, doi: 10.3390/app12073623.
- [19] Izquierdo-Monge, O., Peña-Carro, P., Villafafila-Robles, R., Duque-Perez, O., Zorita-Lamadrid, A., & Hernandez-Callejo, L. (2021). Conversion of a network section with loads, storage systems and renewable generation sources into a smart microgrid. *Applied Sciences (Switzerland)*, 11(11). <https://doi.org/10.3390/app11115012>.
- [20] Izquierdo-Monge, O., Redondo-Plaza, A., Peña-Carro, P., Zorita-Lamadrid, Á., Alonso-Gómez, V., & Hernández-Callejo, L. (2023). Open Source Monitoring and Alarm System for Smart Microgrids Operation and Maintenance Management. *Electronics (Switzerland)*, 12(11).

The hybrid AC/DC microgrid of CEDER-CIEMAT.

Paula Peña-Carro¹, Ángel Hernandez-Jimenez¹, Oscar Izquierdo-Monge¹

¹ CEDER-CIEMAT, Autovía de Navarra A15 salida 56, 422290 Lobia (Soria), España, P.P.C.: paula.pena@ciemat.es; A.H.J.: angel.hernandez@ciemat.es, O.I.M.: oscar.izquierdo@ciemat.es

Abstract: This paper showcases the tangible progress of the European project "Towards Intelligent DC-based hybrid Grids Optimizing the Network performance" (TIGON). The objective of the project is to create a smart direct current (DC) microgrid that can be seamlessly incorporated into the existing energy system. This proposed solution holds significant potential for decreasing energy losses stemming from DC/AC conversions, while enhancing the overall performance and cost-effectiveness of hybrid DC/AC grids. The Centre for the Development of Renewable Energies (CEDER) - Centre for Energy, Environmental and Technological Research (CIEMAT) is actively involved as a demonstrator in the TIGON project, contributing to the development of a hybrid microgrid. This microgrid incorporates various generation sources, including mini-wind and photovoltaic systems, as well as storage technologies such as Li-ion and lead-acid batteries. Furthermore, it integrates consumption systems that operate in both DC and AC modes. These systems function at low level voltage (LVDC) and medium level voltage (MVDC), employing innovative power electronics equipment to ensure the efficient operation of the entire system.

Keywords: Hybrid microgrid AC/DC, direct current (DC), alternating current (AC), Solid State Transformer (SST), AC/DC & DC/DC converters.

1 Introduction

Microgrids are energy systems supervised as a unified entity and characterized by well-defined boundaries. There are two types: isolated microgrids, which operate independently without connection to the electricity distribution network, and grid-connected microgrids, which are connected to the electricity distribution grid through a point of common coupling (PCC) and can import or export energy based on the microgrid's energy balance [1]. Within a microgrid, various power generation sources, consumption systems, and storage systems are present, contributing to effective energy management. A key advantage is the utilization of local resources like solar radiation, waterfalls, biomass or wind to generate energy. This localization reduces transportation distances and losses, thereby enhancing the generation-to-consumption efficiency.

Renewable sources, particularly photovoltaic and wind systems, are commonly used for distributed generation in microgrids. These technologies predominantly produce energy in the form of DC, either directly or via power converters. Storage systems typically operate in DC and play a crucial role in the management of sporadic power generation from renewable sources. They significantly contribute to load and power balancing in DC microgrids [2]. Considering the current preference in microgrid equipment, DC usage surpasses that of AC.

Furthermore, contemporary electrical appliances like computers, cell phones, electric vehicles (EVs), etc. operate on DC [3]. In contrast, the majority of infrastructure operates on a centralized system using AC. This choice is primarily driven by the fact that AC transmission at high voltage level minimizes losses in transport. However, because of the disparity in current types and the distinct modes for consumption and generation, it becomes essential to transform DC to AC using a DC/AC converter to utilize elements connected to the electrical grid. Unfortunately, the use of the converter leads to energy losses, typically amounting to approximately 10-25% of total energy [2], [3], [4], [5], [6], as well as losses during transmission from generation to consumption points. Consequently, the efficiency of electric systems is inevitably diminished.

The disadvantages associated with AC consumption have generated considerable interest in DC grids within the energy sector [7], [8]. This can be attributed to the growing demand for DC loads, including LED lighting, EV charging stations, and energy storage systems, among others. Furthermore, the development of distributed generation sources has led to a substantial reduction in energy transportation requirements. As a result, DC grids have emerged as an attractive solution in the energy industry.

The transition towards DC grids is predominantly motivated by the advancements in energy efficiency, enhanced security, heightened flexibility and improved reliability that they offer [2], [7], [8]. These factors contribute significantly to the overall sustainability of the energy distribution system, making DC grids an increasingly favorable option.

TIGON Project receives its funding from the European Union's Horizon 2020 research and innovation program. The project involves the participation of several entities from different European Union countries, comprising a diverse range of companies, associations, and research organizations. These entities collectively contribute to various aspects of the project, including design, management, production, and demonstration requirements. Notably, CEDER represents Spain, while CEA represents France. Additionally, the Sofia metro (Bulgaria) and a residential area in Naantali (Finland) have been incorporated to analyze and validate the project's scalability and applicability beyond its development phase.

TIGON project main goal is to demonstrate how Direct current grids can be effectively deployed and integrated into the current energy system. It puts forth a comprehensive strategy to enhance resilience, reliability, performance, resilience and cost efficiency. This approach involves the development of solutions in power electronics, monitoring systems, and software tools, as well as efficient control and management of DC grids.

3

This document is structured in the following way: Section 2 provides a general view of CEDER (the location of this hybrid microgrid). Section 3 delves into the energy management systems implemented at CEDER to control the components that make up the grid. Lastly, Section 4 outlines the upcoming tasks outlined for the project.

2 Location of the hybrid microgrid

CEDER is one of the use cases in TIGON project. To this end, a microgrid using DC technology is being set up at CEDER. The microgrid will connect various generation, storage, and consumption systems with equipment designed to facilitate both AC and DC operation. As the use of direct current grids is not yet prevalent, specialized equipment has been exclusively produced for TIGON. One of the center's primary targets is to operate the microgrid and develop software for real-time data collection and equipment control. Consequently, an analysis and a study will be conducted on both the individual devices and the entire system to generalize the results and recreate them in pilot cases. Ultimately, the project's success will pave the way for international implementation of this technology.

The center itself is a microgrid, equipped with various generation systems such as small wind turbines, photovoltaic modules, biomass boilers and a Pelton turbine. Furthermore, the center features diverse energy storage systems like different types of Li-ion and lead acid batteries, as well as multiple types of consumption loads. All of these systems are monitored in real-time using different programs that enables remote operation.

The CEDER microgrid is linked to a medium voltage line (15 kV), which is transformed into a three-phase low-voltage line (400 V) at eight transformation centers. The TIGON project's demonstration will take place in the P.E.P.A. II area (Fig. 1), located within the center. The DC-based microgrid will be established at this site and linked to the main AC grid through an SST connection. This SST, which is being developed by one partner of the project, enables the connection between the AC main grid and the DC microgrid. The common coupling point, where the 400 Vac grid and the 3 KVdc grid connect, allows the microgrid to operate both in isolated and connected modes.

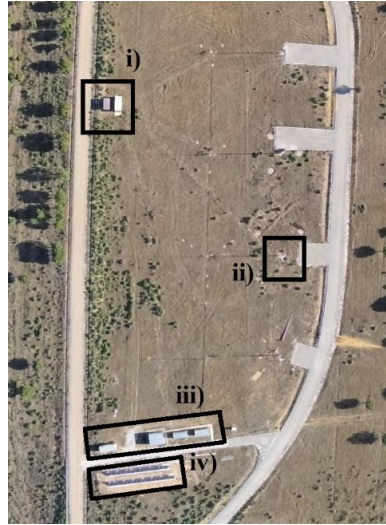


Fig. 1. P.E.P.A. II demonstration facilities. i) Transformation station. ii) Wind turbine. iii) Buildings for equipment. iv) Photovoltaic system. Own source.

The organization of the hybrid AC/DC microgrid elements in P.E.P.A. II is presented in Figure 2.

This year marks the final phase of the project, during which nearly all equipment, including generation systems, storage, and their corresponding AC/DC power electronics equipment, will be installed and in operation. The management and control system is also being continuously updated to accommodate new equipment as it is integrated into the system. The project's last active phase will involve the design and installation of several key pieces of equipment, including a solid state transformer and two MV SiC DC/DC power converters, all developed by partners of the project.

Referring to the diagram in Figure 2, two current operation modes can be identified. In the first part, the AC mode is represented by the green 15 kV line that connects to the PEPA II transformer. From there, it branches into a blue 400 V AC line connected to the input of the SST and the output of all power electronics equipment in the generation, storage, and consumption systems operating in AC. The red line represents the DC line, with voltage variations observed in different sections. Starting from the SST, the first part is a medium voltage line of 3 kV that connects to the DC/DC equipment for lead-acid batteries, and to the input of the DC converter that adjusts the voltage to a continuous 0.8 kV at its output. Finally, small sections of DC can be identified between power electronics equipment, which serve to adjust the low DC voltage to the required level for the proper operation of all systems. The following sections provide detailed information about each of the equipment components that comprise the hybrid microgrid.

5

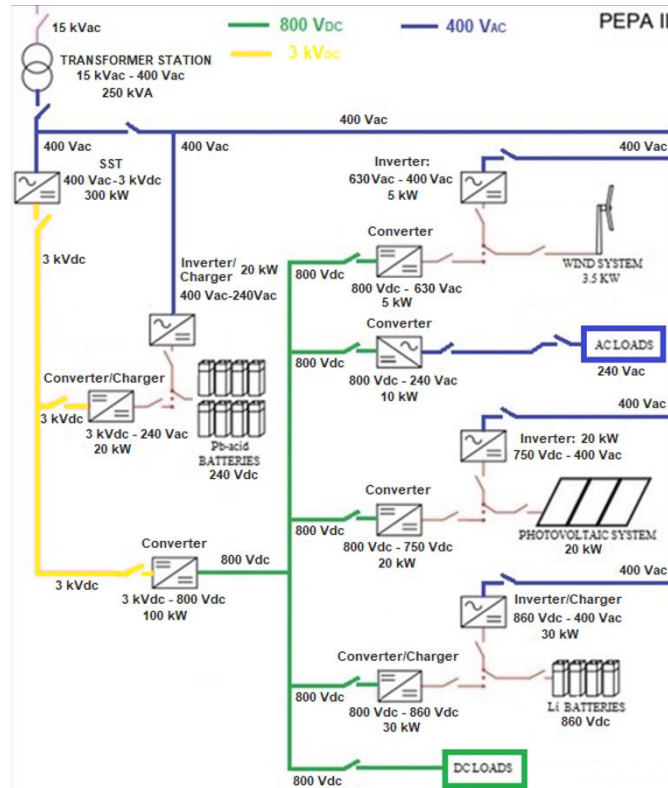


Fig. 2. Scheme of the Hybrid AC/DC architecture. Own source.

2.1 Generation systems

In the LVDC area of the project, two distinct generation technologies have been installed:

- The photovoltaic system installed in the project is compound using monocrystalline silicon technology. It is linked to a 20 kW Ingeteam AC inverter. To operate the photovoltaic system in DC, a voltage adjustment device is required to match the 800 Vdc grid. This essential device, known as the DC/DC converter, has been developed in collaboration with the University of Valladolid and is equipped with the necessary characteristics (as shown in Fig. 3).

6

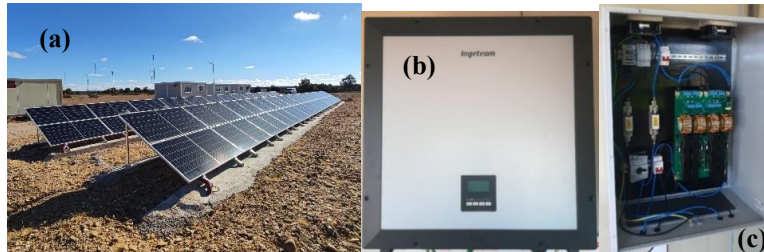


Fig.3 (a) PV modules. Fig.3 (b) Dc/Ac inverter. Fig.3 (c) DC/DC converter. Own source.

- A 3.5 kW small wind turbine (Ryse Energy E5). To facilitate both AC and DC operation, the wind energy system includes two power electronics equipment, as illustrated in Figure 4. All equipment has been developed by the same company and is commercially available, with the exception of the DC/DC converter, which has been designed to meet the unique requirements of the project.

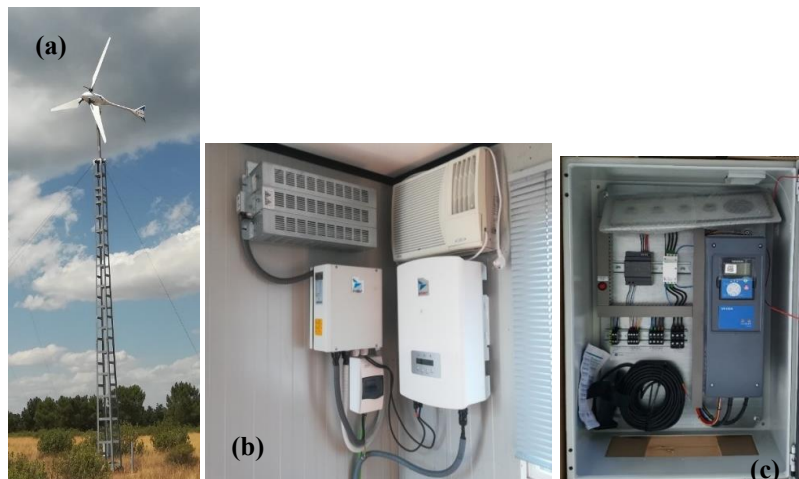


Fig. 4 (a) Wind turbine, Fig. 4 (b) Dc/ac inverter Fig. 4 (c) Dc/dc converter. Own source.

2.2 Storage systems

The center has at its disposal two electrochemical storage systems, namely a set of lead acid batteries situated in the medium voltage DC grid and a set of Lithium batteries located in the low voltage grid.

- A lead acid system, connected to the 3 kVdc grid and consists of 120 cells of 2 V, and 1080 Ah capacity. The current configuration of this system allows it

7

to operate in AC mode, or in DC mode (as depicted in Fig. 5). The DC/AC inverter is the sole equipment installed in 3 kVdc grid. To enable operation in this mode, a partner of the project is in the process of developing converter to connect the battery system to the MVDC grid.



Fig. 5 (a) Lead-acid batteries Fig.5 (b) DC/AC inverter. Note: Own source.

To complete the system, it remains to install the DC/DC power electronics equipment that will adjust the DC voltage of the batteries to the MVDC grid. This DC/DC converter is currently being designed and developed by two members of the consortium, which is expected to be completed in the coming months to include it in the microgrid and in our EMS system.

- The other storage system comprises Li-ion batteries, specifically three NMC battery modules with a total capacity of 51 kWh and a nominal voltage of 881 V. Accompanying them are two power electronic devices, one for AC operation with a power rating of 30 kW, and another for operation in the low-voltage DC grid with a nominal power of 30 kW. Both converters have been designed and developed by external companies to meet the specific requirements of this particular storage system. All the equipment can be observed in Figure 6.



Fig. 6 (a) NMC Battery. Fig. 6 (b) DC/AC inverter. Fig. 6 (c) DC/DC converter. Own source.

2.3 Loads

There are three distinct load systems within the microgrid. The initial one is the CEDER AC microgrid, consisting of computers, illumination, workshops, and other devices. It is situated upstream of the transformation center and represents the largest power load within the microgrid.

The other two loading systems are located downstream of the solid-state transformer: the first in the LVDC grid while the second one in the AC grid.

In relation to the DC loads, CEDER have three resistive loads installed, as illustrated in Figure 7. These loads have different operating modes, including three-phase, single-phase, or DC, based on the particular requests. For this project, it works in DC mode, which enables a manually adjust to achieve different levels of consumption and observe how the microgrid responds. Since these are DC loads, no converter is necessary.



Fig. 7. Three DC loads. Own source.

With regards to the AC loads, the hybrid microgrid is equipped with three AC2928 programmable loads, which are illustrated in Figure 8. Each load has a power of 3900 W (total power of 11.7 kW). The loads offer the flexibility of daily and timely programmability, allowing the microgrid operators to establish operational periods that meet the diverse consumption requirements of the loads.



Fig. 8. AC programmable loads. Own source.

9

The operation of AC loads in the microgrid is completed by connecting them to a 10 kW DC/AC converter developed by an external company, which enables the operation of AC loads within the LVDC grid (see Figure 9).



Fig. 9. Converter DC/AC. Own source.

2.4 Solid State Transformer and power converter

In the hybrid microgrid there are a total of six converters, with five of them connected to the generation systems, storage systems and loads. The other converter is responsible for transforming the MV line into an LV line (DC).

This main DC/DC converter allows the conversion of 3000 Vdc to 800 Vdc and is currently being developed by partners of TIGON project. The converter is being constructed using SiC materials, with the aim of creating multiple power electronics modules that could be connected in either parallel or series configurations to attain the required rated voltage and power output.

Currently, the development of the microgrid is scheduled to be completed in the near future, at which point it will be installed at P.E.P.A. II. With the delivery of the SST, which is a key component of the microgrid, we will have the capability to activate the DC grid and carry out the scheduled tests.

The SST is responsible for transforming the AC grid (400 Vac) from the transformer station of P.E.P.A. II into a medium-voltage DC grid (3000 Vdc). As such, it is a critical component of the project and the microgrid, as all other equipment is connected to it. The complexity of SST development arises from its functional and protective specifications, and this task is being carried out by a partner of the TIGON project. Figure 10 illustrates the progress made in the development of the SST.

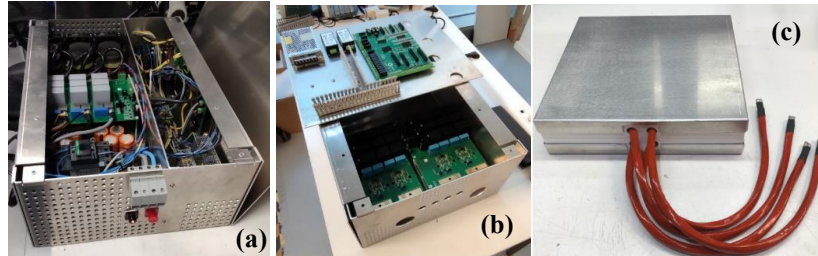


Fig. 10 (a) AC/DC power electronics stage. **Fig. 10 (b)** DC/DC stage **Fig. 10 (c)** Inductive Power Transfer. Own source.

3 Monitoring and control system

Efficient management of the microgrid is crucial for the optimal functioning of its equipment. To achieve this, it is necessary to develop a comprehensive management system that provides real-time monitoring of key parameters related to generation and consumption. These parameters include the renewable energy generation, the energy exchanged with storage systems and the energy used by loads.

Typically, the management system establishes direct communication with each equipment's converters using the ModBus communication protocol. However, in cases where direct communication is not feasible, the installation of a smart metering system, also known as a grid analyzer, becomes necessary. This system enables the measurement of the required parameters and facilitates communication between the converter and the management system through an appropriate communication protocol.

Real-time monitoring of the microgrid enables prompt decision-making to enhance performance. Actions such as initiating battery operations, managing power generation from the photovoltaic system and regulating consumption through the inverter can be taken to optimize system efficiency. The overarching objective of the Wide Area Monitoring, Protection, and Control (WAMPAC) system is to detect, prevent, and mitigate any potential issues within the microgrid as quickly as possible. This proactive approach aims to circumvent adverse outcomes such as blackouts or disruptions to critical loads.

The CEDER microgrid control system comprises three different software.

The first one is the communications block which uses NodRed to integrate various communication protocols for storage systems, generation sources and loads (such as HTTP, MQTT, Modbus). (See Fig. 11).

11

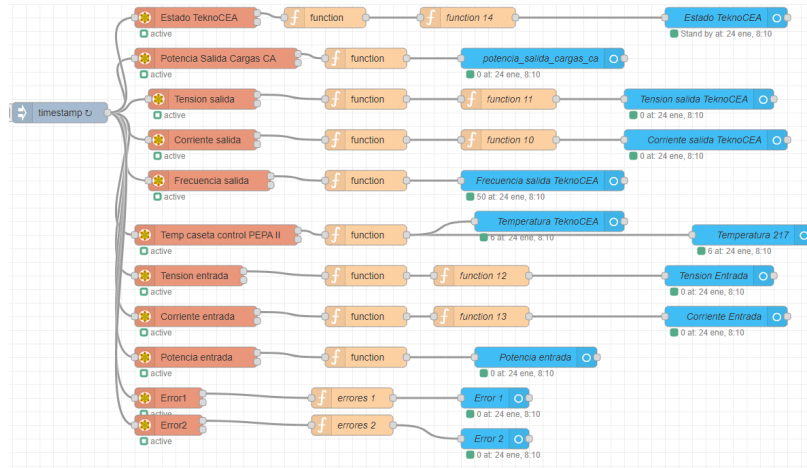


Fig. 11. TIGON configuration in NodeRed. Own source.

The second element is the database, which is managed by a relational database system called MariaDB. It allows for real-time data storage, based on calculations and events (such as 15 minutes or minute averages, like energy distribution company), through corresponding queries. This feature is crucial, not only for real-time monitoring and prompt decision-making but also for the long-term analysis of the data to establish management strategies. (See Fig. 12).

Date/Hour	Wind Speed [m/s]	Solar radiation [W/m2]	AC Consumption [W]	PV power AC [W]	Power Loads AC [W]
23/01/2023 8:15	1.8	2	-6223	34	0
23/01/2023 8:30	1.5	5	-6300	138	0
23/01/2023 8:45	3.4	19	-6467	343	0
23/01/2023 9:00	2.3	49	-6784	667	0
23/01/2023 9:15	2.4	80	-7697	1601	0
23/01/2023 9:30	2.7	144	-6117	2207	0
23/01/2023 9:45	0.9	231	-2681	3850	0
23/01/2023 10:00	1.1	325	-7612	8921	0
23/01/2023 10:15	1.8	237	-4521	5697	0
23/01/2023 10:30	2.5	95	-1287	2411	0
23/01/2023 10:45	2.3	85	-831	1976	0
23/01/2023 11:00	2.1	102	-1182	2327	0
23/01/2023 11:15	2.1	144	-1107	2265	0
23/01/2023 11:30	3.5	111	-1230	2305	0
23/01/2023 11:45	3.9	96	-979	2080	0
23/01/2023 12:00	5.6	220	-2418	2918	0
23/01/2023 12:15	6.3	349	-7765	8332	0
23/01/2023 12:30	6.3	500	-14008	14795	0
23/01/2023 12:45	6.1	465	-17972	19054	0
23/01/2023 13:00	7.3	472	-18918	19549	0
23/01/2023 13:15	8	514	-19176	19549	0
23/01/2023 13:30	6.7	568	-19052	19930	0

Fig. 12. Example of file generated by MariaDB. Own source.

The third element is Home Assistant (see Fig. 13). With Home Assistant is possible to monitor in real time all data from the several elements connected to the microgrid and send commands to them. The Energy Management System (EMS) is accessible from any location within the CEDER communication network, signifying its decentralized nature, and it also offers remote accessibility via a smartphone application.



Fig. 13. TIGON configuration in Home Assistant. Own source.

To accomplish this, it is crucial to establish connectivity between the components of the grid and the control system to CEDER's data network, which is based on Ethernet technology (see Fig. 13).

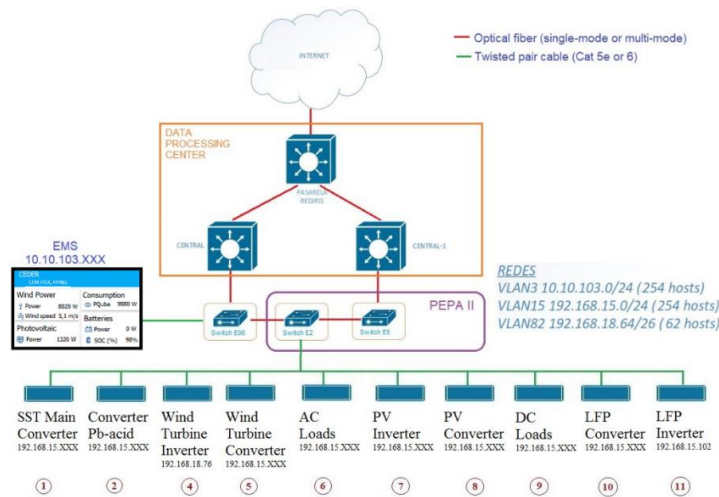


Fig. 14. TIGON microgrid communication network. Own source.

13

Cybersecurity plays a vital role in the control software of microgrids. Due to the multitude of elements, protocols and entry points in use, the system becomes highly susceptible to cyber threats. The current cybersecurity market is not adequately equipped to efficiently oversee such an extensive deployment throughout the entire electrical grid. Therefore, our internal network has multiple security systems at various levels, and personal passwords are required to access each software component of the monitoring and management network, ensuring greater protection against potential cyber threats.

4 Conclusions and Future work

CEDER, as TIGON demonstration center, houses an AC/DC hybrid microgrid within its facilities. This microgrid comprises commercial generation, storage, and consumption equipment along with their AC inverters. To enable continuous operation, unique power electronics equipment has been designed and developed specifically for this purpose. Various tests will be conducted to assess the feasibility and challenges associated with hybrid microgrids in comparison to AC microgrids.

To date, all storage systems, generation sources and loads have been deployed at PEPA II facility, along with the necessary power electronics equipment for both AC and DC operation, integrated into the developed monitoring and control system. This software enables the recording of all monitored parameter data and immediate actions on the equipment.

During the final year of the project, as part of our short-to-medium-term objectives, we aim to incorporate the SST and the two DC/DC converters installed in the MVDC grid to complete the entirety of the microgrid. Global tests will be conducted to gather data for conducting studies, making comparisons, and analyzing variations in performance, energy losses, benefits and costs associated with both the grid and all the equipment.

The conclusions of TIGON project aim to provide support to electrical grid operators in the decision-making process and provide direction for interventions aimed at decentralized hybrid microgrids. Currently, the limited presence of DC microgrids hinders their transformation from being a hopeful option for distribution grids into a technology that has gained widespread acceptance.

The primary objective is to create a positive influence by presenting demonstrations of the project within the replication installations, highlighting management systems, technology advancements, and cyber-security measures. Furthermore, our objective is to position DC based grids as the preferred solution and a key aspect of future perspectives for enhancing efficiency in energy generation. This approach aligns with the European Union's decarbonization targets, facilitating the transition towards a more sustainable energy system.

Acknowledgments

The authors are grateful for the opportunity to contribute as use case center in TIGON project, which has received support from European Union's Horizon 2020 research and innovation program under grant agreement No 957769.

References

- [1] H. Rodriguez-Estrada, E. Rodriguez-Segura, R. Orosco-Guerrero, C. Gordillo-Tapia, and J. Martinez-Nolasco, "Novel Multibus Multivoltage Concept for DC-Microgrids in Buildings: Modeling, Design and Local Control," *Appl. Sci.*, vol. 13, no. 4, 2023, doi: 10.3390/app13042405.
- [2] M. Gunasekaran, H. Mohamed Ismail, B. Chokkalingam, L. Mihet-Popa, and S. Padmanaban, "Energy Management Strategy for Rural Communities' DC Micro Grid Power System Structure with Maximum Penetration of Renewable Energy Sources," *Appl. Sci.*, vol. 8, no. 4, 2018, doi: 10.3390/app8040585.
- [3] M. Fotopoulou, D. Rakopoulos, D. Trigkas, F. Stergiopoulos, O. Blanas, and S. Voutetakis, "State of the Art of Low and Medium Voltage Direct Current (DC) Microgrids," *Energies*, vol. 14, no. 18, 2021, doi: 10.3390/en14185595.
- [4] L. Gao, Y. Liu, H. Ren, and J. M. Guerrero, "A DC Microgrid Coordinated Control Strategy Based on Integrator Current-Sharing," *Energies*, vol. 10, no. 8, 2017, doi: 10.3390/en10081116.
- [5] B. T. Patterson, "DC, Come Home: DC Microgrids and the Birth of the 'Enernet,'" *IEEE Power Energy Mag.*, vol. 10, no. 6, pp. 60–69, 2012, doi: 10.1109/MPE.2012.2212610.
- [6] A. Abdali, K. Mazlumi, and J. M. Guerrero, "Integrated Control and Protection Architecture for Islanded PV-Battery DC Microgrids: Design, Analysis and Experimental Verification," *Appl. Sci.*, vol. 10, no. 24, 2020, doi: 10.3390/app10248847.
- [7] D. Bosich, A. Vicenzutti, S. Grillo, and G. Sulligoi, "A Stability Preserving Criterion for the Management of DC Microgrids Supplied by a Floating Bus," *Appl. Sci.*, vol. 8, no. 11, 2018, doi: 10.3390/app8112102.
- [8] S. Saponara, R. Saletti, and L. Mihet-Popa, "Recent Trends in DC and Hybrid Microgrids: Opportunities from Renewables Sources, Battery Energy Storages and Bi-Directional Converters," *Appl. Sci.*, vol. 10, no. 12, 2020, doi: 10.3390/app10124388.
- [9] S. Mishra and R. K. Viral, "Chapter 6 - Introduction to hybrid AC/DC microgrids," in *Microgrids*, J. M. Guerrero and R. Kandari, Eds. Academic Press, 2022, pp. 159–189.
- [10] D. A. Aponte-Roa, G. D. G. Cabarcas, and W. W. Weaver, "AC Vs DC Power Efficiency Comparison of a Hybrid Wind/Solar Microgrid," in *2020 IEEE Conference on Technologies for Sustainability (SusTech)*, 2020, pp. 1–5, doi: 10.1109/SusTech47890.2020.9150514.

Evaluation of Microgrid Energy Management System in Normal and Abnormal Operation Conditions

Mahshid Javidsharifi¹[0000-0002-7354-3212], Najmeh Bazmohammadi¹[000-0003-3407-9549],
Hamoun Pourroshanfekr Arabani²[0000-0002-1738-320X], Juan. C. Vasquez¹[0000-0001-6332-385X],
Josep. M. Guerrero¹[0000-0001-5236-4592]

¹ Center for Research on Microgrids (CROM), AAU Energy, Aalborg University, Aalborg, Denmark

² Division of Industrial Electrical Engineering & Automation, Lund University, Lund, Sweden
mja@energy.aau.dk

Abstract. Microgrids (MGs) offer a promising solution for seamlessly integrating distributed energy resources (DERs) and delivering a dependable and efficient electricity supply through an optimal energy management system (EMS). Microgrid EMS entails the intricate coordination of various DERs and loads to ensure optimal performance and stability. This paper provides researchers with in-depth insights into an energy management system scheduling for community MGs. The strategy aims to accomplish several objectives, including cost minimization (equivalent to maximization profit) and avoiding emissions while technical constraints are satisfied. The case study is based on the ongoing renewable-based energy system for Lombok Island, Indonesia. To provide Pareto optimal solutions for decision-makers the multi-objective particle swarm optimization (MPSO) algorithm is utilized to solve the optimization problem. The effectiveness of the proposed strategy is assessed by considering various normal and abnormal operating scenarios.

Keywords: Community microgrids, Energy management system, Natural disasters, Resiliency.

1 Introduction

In recent years, the global energy landscape has been witnessing a significant transformation, with a growing emphasis on sustainable energy solutions. Amidst this shift, microgrids (MGs) have emerged as a promising alternative, empowering communities to assert greater control over their energy generation, consumption, and distribution [1]. Particularly in remote and underserved regions, MGs hold immense potential to address energy access challenges while fostering economic, social, and environmental benefits [2].

A community MG is a localized and small-scale energy system that integrates various energy resources, such as renewable energy sources (e.g., solar, wind, hydro), energy storage technologies (e.g., batteries), and conventional generators, to supply power to a specific community or group of consumers. It can operate autonomously or in

2

conjunction with the main utility grid, enabling the community to function independently during grid outages or as a supplement to the main grid during regular operations and excess renewable energy availability [3].

The concept of community MGs has gained significant traction in recent years, fueled by the need for sustainable energy solutions. Researchers and practitioners alike have explored the potential benefits and challenges of implementing community-driven MG systems in diverse settings worldwide [1-4].

Resiliency in MGs refers to the ability of energy systems to withstand and recover from disturbances, disruptions, or unforeseen events while maintaining essential energy services. It encompasses the capacity to adapt, bounce back, and continue functioning during adverse conditions, such as natural disasters, grid outages, cyber-attacks, or extreme weather events. Community MGs enhance the resilience of the community, especially in rural or isolated areas, by providing a reliable source of electricity during emergencies or when the main grid is down [4].

To optimally utilize the resources and achieve economic and environmental goals, the operation of different resources needs to be efficiently coordinated [1-5]. An energy management system (EMS) is responsible for governing energy scheduling considering operating goals and technical and operational system constraints. This is a challenging task, especially under abnormal operating conditions where the system is affected by unexpected disturbances, such as natural disasters, when there is insufficient power generation to cover the power requirements of all power-consuming units [4-10].

Authors in [6] introduce an intelligent energy management system for MGs using a genetic algorithm framework, incorporating forecasted solar PV and wind generation values. The proposed model optimizes battery and grid power usage over a 24-hour horizon, achieving efficient energy management with optimal utilization of renewables and storage while considering cost and battery health.

An EMS for MGs that aims to optimize energy production while minimizing CO₂ emissions and economic costs is proposed in [7]. The EMS integrates Model Predictive Control (MPC), a multi-objective optimization algorithm, and a decision tool to adapt to changing operating conditions. The multi-objective algorithm generates Pareto optimal solutions, balancing CO₂ emissions and economic costs, while the decision tool automates the selection of the most suitable solution from the Pareto front.

An energy management system for MGs is presented in [8], utilizing a genetic algorithm framework to optimize battery and grid power usage over 24 hours. The model achieves energy management, optimal renewable and storage utilization, and considers cost and battery health. The study also introduces two energy management systems for MGs and smart homes under normal and emergency conditions, demonstrating grid resilience through internal and external load supply during interruptions.

An impact-driven energy management approach that combines flexible load control and MG resource planning is introduced in [9] to enhance power grid resilience after natural disasters. The framework prioritizes loads based on factors like health and economics, significantly reducing negative outage effects. The study underscores the necessity of considering MGs in resource planning for a robust power grid, emphasizing investment in both PVs and battery-based energy storage system (BESS) for sustained load service during grid downtime.

The economic dispatch problem in MGs, applying various optimization algorithms to the IEEE 30 bus system is tackled in [10]. The chosen ant colony-based algorithm optimizes MG energy costs effectively, considering seasonal variations, and suggests avenues for further improvement.

Our research paper delves into the realm of energy management strategies for a community MG in the picturesque landscape of Lombok Island, Indonesia in normal and abnormal operation conditions. As the world grapples with the urgent need to mitigate climate change and transition towards renewable energy, Indonesia, with its abundant natural resources, finds itself at a crossroads to redefine its energy paradigm [11].

Lombok Island, located in the Indonesian archipelago, represents an ideal setting for exploring the integration of community MGs. With its unique geographical attributes, including remote villages and challenging terrains, the island faces energy access disparities that traditional grid infrastructure struggles to address. Thus, implementing a community MG presents a promising avenue to bridge the energy gap and enhance the quality of life for its inhabitants.

In this paper, a community MG energy management system is assessed in normal and abnormal conditions in the Lombok Island, Indonesia case study. The optimal MG energy management problem is formulated in the framework of a multi-objective optimization problem to minimize the operating cost of the community MG and its environmental impact, and the multi-objective particle swarm optimization (MPSO) algorithm is used to solve the optimization problem. To evaluate the efficiency of the proposed strategy, different normal and abnormal operating scenarios have been considered.

2 Energy management of Villa-Queen MG on Lombok Island

2.1 System Structure

The selected case study in this paper is Lombok Island, Indonesia. The proposed community MG consists of a PV unit with a rated power of 1370 kW_p, a BESS of 4651 kWh capacity, and one diesel generator (DG) with a nominal output power of 75 kW [12]. A general overview of the proposed MG is represented in Fig. 1.

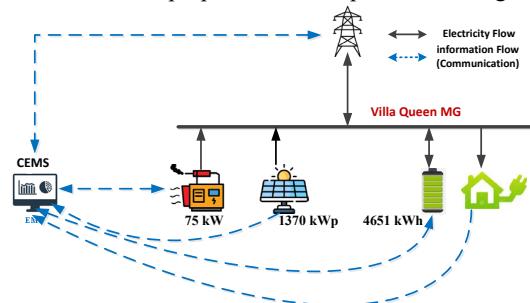


Fig. 1. Structure of the proposed community MG in Lombok Island.

4

2.2 Problem Formulation

This section describes the energy management problem of the considered community MG of Fig. 1. The goal is to minimize the operating cost (maximize profit) and environmental impact of the MG daily operation while satisfying several technical and operational constraints. Decision variables include the amount of power to be exchanged with the main grid, either buying or selling the power, the power production of the DG unit, and the charging/discharging power of the battery. It is assumed that the PV is not dispatchable, and all its available power is used. Load curtailment is also not allowed in normal operating conditions.

Objective Functions

The goal of energy management is to minimize the operating cost and the environmental impact of the MG simultaneously by optimally splitting the required power among different available sources. Thereby, the problem can be formulated as a multi-objective optimization problem with two competing objectives as follows:

$$F = (F_1, F_2) \quad (1)$$

The first objective function is the operation cost of the MG over the simulation horizon T which is given below [2]:

$$F_1 = \sum_{t=1}^T \{Cost_{DG}^t + P_{EX}^t B_{EX}^t\} + M \times \sum_{t=1}^T ENS^t \quad (2)$$

where P_{EX}^t is the exchanged power of the MG with the main grid in kW, which is assumed to be positive if the MG purchases power from the main grid and negative in case power is sold to the main grid. Also, B_{EX}^t represents the electricity price of the grid in \$/kWh that is assumed to be similar for buying and selling in this study. $Cost_{DG}^t$ is the hourly operational cost of the dispatchable unit (DG in this study) in \$ which is modeled as a quadratic function as follows [13]:

$$Cost_{DG}^t = \alpha \times (P_{DG}^t)^2 + \beta \times (P_{DG}^t) + \gamma \quad (3)$$

where P_{DG}^t is the hourly output power of the DG in kW. The values of α , β and γ are set to 0, 0.055, and 0, respectively, according to the available data from Table 25 of [14].

In (3), ENS^t is the energy not supplied at each hour of the day. M is a big number that is considered equal to 10^9 . This second term represents that under abnormal operation, the focus is on satisfying the critical load at each hour of the day.

The second objective is to minimize the following function F_2 which is the environmental impact of the system:

$$F_2 = \sum_{t=1}^T \{P_{DG}^t E_{DG}^t + P_{EX}^t E_{EX}^t\} \quad (4)$$

where E_{DG}^t is the emission factor in kg for each kWh of the produced power of the DG, while E_{EX}^t is the emission of each kWh received power from the electricity grid in kg.

Technical Constraints

The energy management of the MG is subject to different technical constraints including the power balance, battery charging and discharging rates and energy levels constraints, the power limits of the DG unit, and the constraints related to the exchangeable power with the electricity grid that are explained in the following.

Power balance constraint

The power balance between the demand and generation sides of the MG should be satisfied according to the following equation.

$$P_{DG}^t + P_{Batt}^t + P_{EX}^t + P_{PV}^t = P_L^t \quad (5)$$

where P_{Batt}^t is the battery power, P_{EX}^t is the exchanged power with the electricity grid, P_{PV}^t is the estimated hourly power of PV units, and P_L^t is the hourly load of the MG.

Battery constraint

The battery constraints are related to the charging and discharging power limits, and the state of charge (SOC) of the battery as follows:

$$-C_{rate} \cdot B_{cap} \leq P_{Batt}^t \leq C_{rate} \cdot B_{cap} \quad (6)$$

$$SOC_{Batt,min} \leq SOC_{Batt}^t \leq SOC_{Batt,max} \quad (7)$$

$$SOC_{Batt}^t = \begin{cases} SOC_{Batt}^{t-1} - \left(\frac{P_{Batt}^t}{\eta_{Dch} \times B_{cap}} \right) & P_{Batt}^t > 0 \\ SOC_{Batt}^{t-1} - \left(\frac{P_{Batt}^t \times \eta_{ch}}{B_{cap}} \right) & P_{Batt}^t < 0 \\ SOC_{Batt}^{t-1} & otherwise \end{cases} \quad (8)$$

where B_{cap} is the battery capacity, C_{rate} is battery C-Rates that limits the battery's charging and discharging rates, SOC_{Batt}^t and SOC_{Batt}^{t-1} indicate the stored energy level of the battery at hour t and $t-1$, respectively, $SOC_{Batt,min}$ and $SOC_{Batt,max}$ indicate the minimum and the maximum allowable stored energy levels in the battery, respectively. η_{ch} and η_{Dch} are the battery charging and discharging efficiencies.

DG constraint

The constraint related to the output power limits of DGs is as the following:

$$P_{DG,min} \leq P_{DG}^t \leq P_{DG,max} \quad (9)$$

Power exchange constraint

There is a limit for the exchangeable power between the MG and the electricity grid which is considered as the power exchange constraint as follows:

6

$$-P_{EX,Max} \leq P_{EX}^t \leq P_{EX,Max} \quad (10)$$

3 Simulation Results

To evaluate the MG energy management system, different normal and abnormal operating scenarios have been considered. In the normal operation, two case studies, namely, single objective and multi objective MG energy management are dealt with. For the abnormal operation of the MGs, different cases are assumed in which the MGs' access to the main grid or the available renewable energy sources is lost (total or partial) due to the natural disaster. In abnormal operating conditions, MGs might be required to support the critical loads of a neighboring MG that has lost its local generation resources or provide power to emergency-related facilities such as temporary water treatment systems or clinical facilities that will increase their power demand. Thereby, in Case 2, a sudden jump in the MGs' load is simulated and analyzed.

The input data used in the simulation are shown in Table 1. In this table, α , β , and γ are the operation cost function coefficients of the DG unit.

Table 1. Input data.

DG	Grid	Battery
$P_{out,min} = 0 \text{ kW}$	$P_{EX,max} = 5000 \text{ kW}$	Battery capacity= 4651 kWh
$P_{out,max} = 75 \text{ kW}$		$SOC_{min} = 30\%$
$\alpha = 0$		$SOC_{max} = 100\%$
$\beta = 0.055 \text{ \$/kWh}$		$SOC_{initial} = 50\%$
$\gamma = 0$		$\eta_{ch} = \eta_{Dch} = 90\%$
		$C_{rate} = 0.7 \text{ C}$

3.1 Scenario 1: Normal Operation

Scenario 1- Case 1: Single-objective Energy Management

The first case considered in this scenario is the energy management of the community MG in Lombok area under normal conditions when the only objective is minimizing the operation cost. To evaluate the effectiveness of the proposed energy management strategy the load and power generation from the PV system, on 1st of July are selected [18]. The hourly electricity price is shown in Fig. 2. PSO algorithm [15-17] is applied to solve the single-objective optimization problem. The output power of PV panel, and the hourly demanded load in Lombok area on 1st July are shown in Figs. 2 to 4.

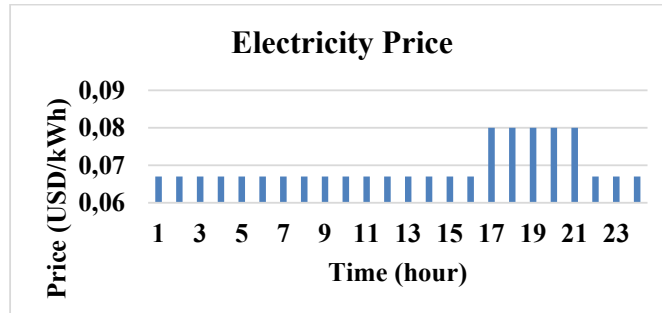


Fig. 2. Hourly electricity price in Lombok area.

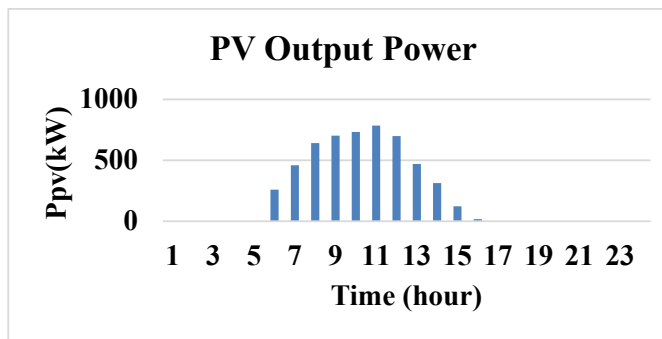


Fig. 3. Output power of PV system in Lombok area on 1st July [9].

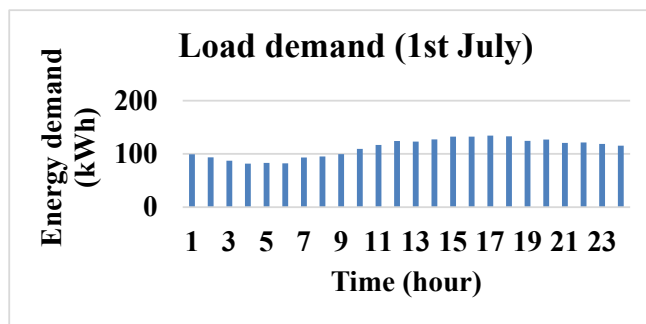


Fig. 4. Hourly load profile in Lombok area on 1st July.

The results of daily energy management of the community MG in Lombok area for the selected day are shown in Figs. 5 and 6. In Figs. 5, hourly power demand and other variables that are related to the consumption of power, are shown with negative power

8

values at each hour while those variables that are related to the power supply have positive values. Since the DGs are always power producers the related values are positive. Batteries can play the role of both power producer and consumer. During the charging intervals, batteries are considered as power consumers while during discharging hours they are considered as power producer. Furthermore, negative values related to the exchanged power with the electricity grid reveal selling power to the electricity grid while positive values present purchasing power from the grid and power sharing is from the electricity grid to the MG. It can be seen from the figures that the load demand is satisfied, and the MG could obtain high revenue by selling the extra power to the main grid. It should be mentioned that, according to Fig. 2, since there is a high rise in the electricity price at hour 17, the whole stored energy in the battery is sold to the grid during this hour. Figs. 6 shows the SOC level of the battery for 1st of July. As is observed, the SOC level is between 0.3 and 1 in all hours of the day.

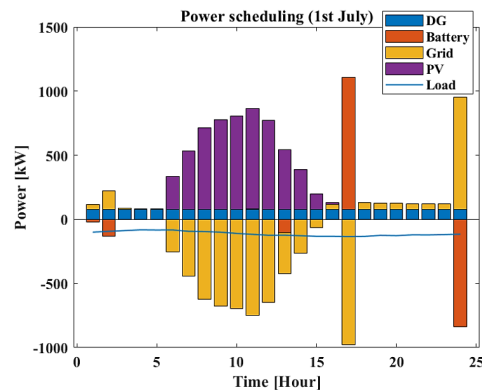


Fig. 5. Power scheduling of the units (1st of July).

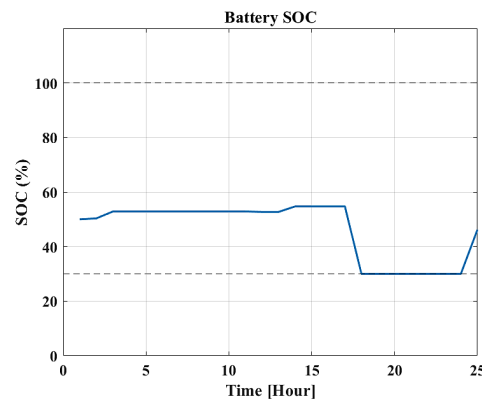


Fig. 6. Battery SOC level (1st of July).

Scenario 1- Case 2: Multi-objective Energy Management of the Community MG

In this section, both objectives, namely minimizing the operation cost and minimizing the total emission are considered. When considering the problem as multi-objective, based on the dominance and Pareto optimal concept, a set of non-dominated solutions with different values for objective functions are obtained instead of one single solution (Fig. 7). According to Fig. 7, the MG operator decides to choose one of the solutions in the set of solutions with different economic/environmental indices based on the priority of the indices. In Fig. 7, the Pareto optimal front of the optimal operation of the considered community MG in Lombok area is shown.

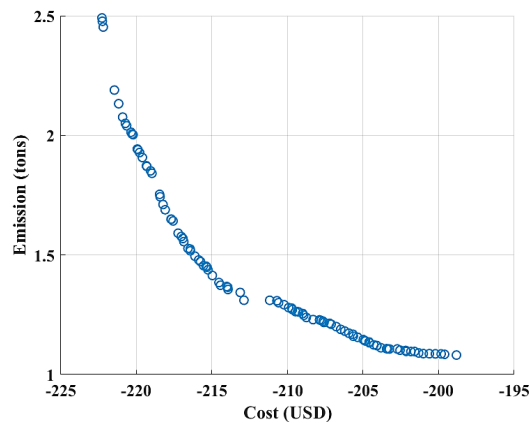


Fig. 7. Pareto optimal front of the multi-objective energy management problem of the community MG in Lombok Island in the normal operation condition.

3.2 Scenario 2: Abnormal Operation

In this scenario, to investigate the probable effects of natural disasters on the system performance, three different cases are considered. In the following, the performance of the proposed energy management system for the community MG in Lombok area is evaluated. The studies are performed for the 1st of July 2022, considering minimizing the cost and the energy not supplied as the main objectives.

Scenario 2- Case 1: Loss of 30% Capacity of the PV Power System for the Whole Day

In this case, it is assumed that the electricity grid is available while 30% of the PV panels are damaged from 12:00. The power scheduling of the units and the battery SOC profile are shown in Figs. 8 and 9. It can be observed that the output power of the DG

10

is set to its maximum allowable limit and the SOC of the battery reaches its minimum allowable level from 18:00 to 23:00.

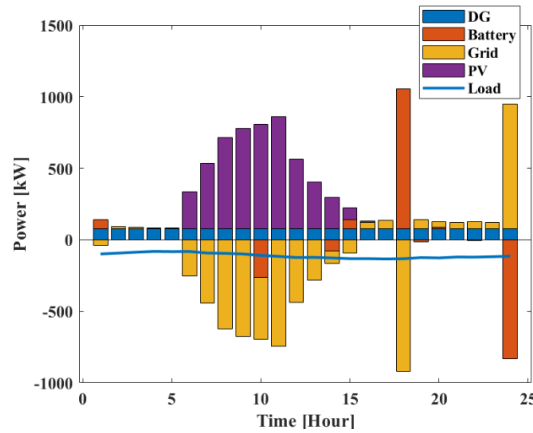


Fig. 8. Power scheduling of units when the electricity grid is available while the PV panels are 30% down from 12:00.

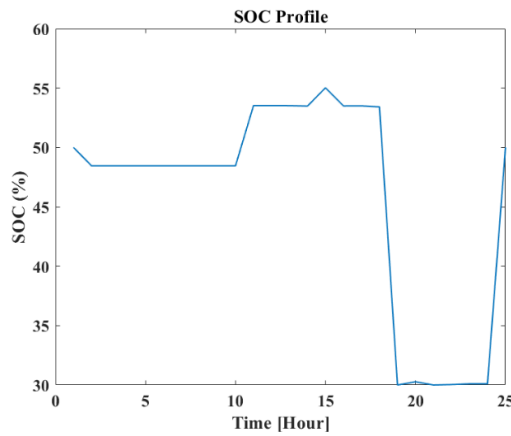


Fig. 9. Battery SOC level when the electricity grid is available while the PV panels are 30% down from 12:00.

Scenario 2- Case 2: A Temporary Increase of 20% In the Islanded MGs’ Load

In this case, it is assumed that the electricity grid is not available and there is a 20% increase in the load demand from 15:00 to 23:00. The increase in load might be due to some temporary facilities that are used during the natural disaster (for instance for

medical services, water provision, etc.) or a request from neighboring areas that their power supply facilities have been damaged. The power scheduling of the units and the battery SOC profile during this condition are shown in Figs. 10 and 11. It is observed that due to the large capacity of the PV system, the MG load can be supplied in all cases. Also, the stored energy of the battery is maintained within the desired limits that provide more security to the MG to ensure the continuity of the power supply.

The operating cost of the MG in all three cases is summarized in Table 2. Positive values for the objective function show the cost while negative values represent revenue for the MG. The big difference between the operating cost shown in Table 2 in Cases 2 and 3 with Case 1 is due to the unavailability of the connection to the main grid in Cases 2 and 3. Also, the amount of ENS is zero in all cases.

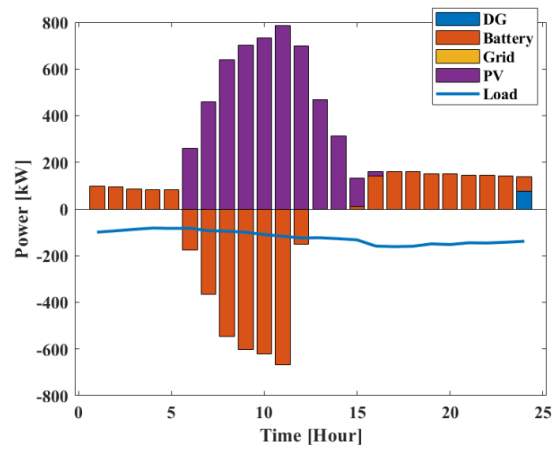


Fig. 10. Power scheduling of units when the electricity grid is not available and there is a 20% increase in the load demand from 15:00 to 23:00.

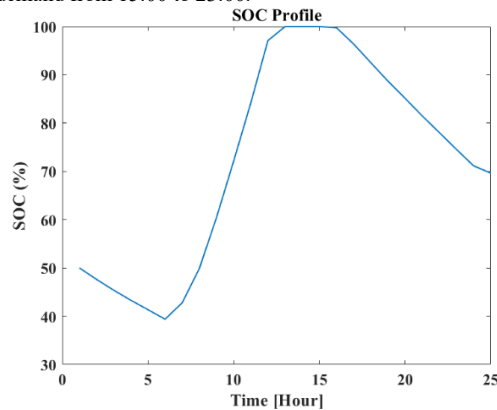


Fig. 11. Battery SOC level when the electricity grid is not available and there is a 20% increase in the load demand from 15:00 to 23:00.

12

Scenario 2- Case 3: Loss of access to the main grid

In this case, it is assumed that the MG loses its access to the main electricity grid due to a natural disaster and the loads can be only supplied by the DG, battery, and PV units. The power scheduling of units and the battery SOC profile are shown in Figs. 12 and 13.

In this case, some analysis is done to investigate that if there is no DG in the system how is the load satisfied and how much time is required to fix the damaged components. According to the input data of the load profile and solar irradiation (for 1st of July), the maximum load is 134.438 W, the cumulative load is 2.677 kW, the maximum output power of PV units is 785.27 W, the cumulative output power of PV is 5.202 kW, and the battery capacity is 4651 kWh. The simulation is run for one week and based on the results, it is observed that the load will be supplied by the PV units and batteries (due to the over-dimensioning of these units) even if there are no DGs and no grid available. However, if the PV-battery system was not able to satisfy the load and ENS was not equal to zero, one appropriate solution to solve the problem rather than resizing the PV-battery system could have been the ad-hoc MGs that can be considered as a temporary supply to support the main installation.

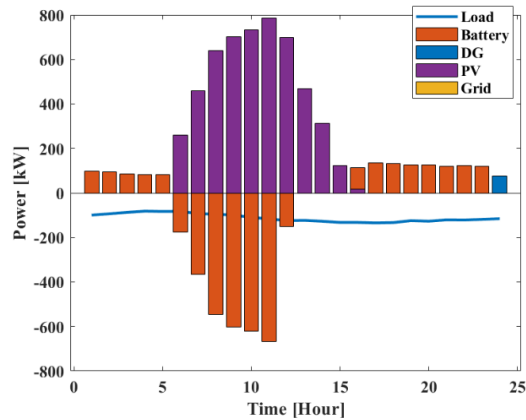


Fig. 12. Power scheduling of units when the electricity grid is down.

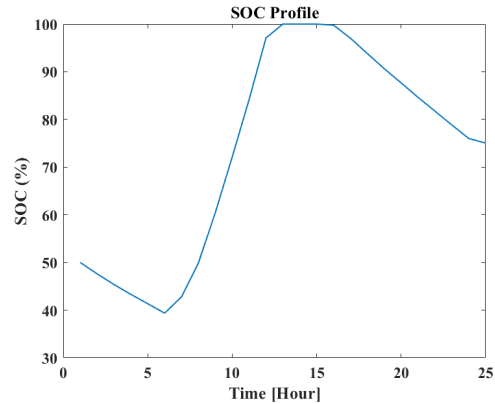


Fig. 13. Battery SOC level when the electricity grid is down.

Table 2. Comparison of the operation cost in different fault cases.

#Case	Operation cost (USD)
Case I: PV panels are 30% down	-151.625
Case II: 20% increase in the load demand (no grid)	4.05
Case III: grid not available	4.05

4 Conclusions

This paper comprehensively examines the performance of an energy management system tailored for community MGs in normal and abnormal conditions. The EMS aims to achieve multiple objectives, including minimization of the operation cost and emissions. The study centers around an EMS implemented in a community MG on Lombok Island, Indonesia, presented as a case study. The core focus is on formulating the optimal energy management of MGs as a multi-objective optimization problem, with the aim to minimize both the operating cost of the community MG and its environmental impact while technical constraints are considered. To address this challenge, the paper employs the multi-objective particle swarm optimization (MPSO) algorithm to effectively solve the optimization problem and provides Pareto optimal solutions with different values of cost and emissions indices for decision-makers. The efficiency and effectiveness of the proposed energy management strategy are rigorously assessed by evaluating various normal and abnormal operating scenarios. As is shown in Table 2, it is observed that when the access to the electricity grid is limited, the operation cost increases to 4.05 USD and during the fault scenario that the availability of PV generation units is decreased, the gained profit decreases to 151.625 USD. It is concluded that resilient EMS can ensure a consistent and reliable energy supply in the community MGs even in the face of disruptions. Overall, the importance of resiliency in MGs lies in its capacity and flexibility to provide reliable, secure, and sustainable energy solutions for communities and critical infrastructures. By embracing resilience measures, MGs can

14

contribute significantly to building a more robust and adaptive energy infrastructure capable of withstanding the uncertainties and challenges of the modern world. This research contributes valuable insights into sustainable energy management, presenting operating management strategies for a community MG in Lombok Island, Indonesia, with broader implications for similar contexts worldwide. To investigate more realistic scenarios, future works can include considering uncertainties of PV generation and solving the probabilistic MG energy management.

Acknowledgment

This work was sponsored by the Ministry of Foreign Affairs of Denmark, DANIDA Fellowship Centre (Project No. 20-M06-AAU) and supported by Danida Fellowship Centre.

References

1. Javidsharifi, M., Niknam, T., Aghaei, J., & Mokryani, G. Multi-objective short-term scheduling of a renewable-based microgrid in the presence of tidal resources and storage devices. *Applied Energy*, 216, 367-381 (2018)
2. Javidsharifi, M.; Pourroshanfekr Arabani, H.; Kerekes, T.; Sera, D.; Spataru, S.V.; Guerrero, J.M. Optimum sizing of photovoltaic-battery power supply for drone-based cellular networks. *Drones*, 5, 138 (2021)
3. Javidsharifi, M., Pourroshanfekr Arabani, H., Kerekes, T., Sera, D., Spataru, S., & Guerrero, J. M. Effect of battery degradation on the probabilistic optimal operation of renewable-based microgrids. *Electricity*, 3(1), 53-74 (2022).
4. Ali, M., Vasquez, J. C., Guerrero, J. M., Guan, Y., Golestan, S., De La Cruz, J., ... & Khan, B. A comparison of grid-connected local hospital loads with typical backup systems and renewable energy system based ad hoc microgrids for enhancing the resilience of the system. *Energies*, 16(4), 1918 (2023).
5. Javidsharifi, M.; Niknam, T.; Aghaei, J.; Shafie-khah, M.; Catalão, J.P. Probabilistic Model for Microgrids Optimal Energy Management Considering AC Network Constraints. *IEEE Syst. J.* 14, 2703–2712 (2019)
6. Babu, V. V., Roselyn, J. P., & Sundaravadivel, P. Multi-objective genetic algorithm-based energy management system considering optimal utilization of grid and degradation of battery storage in microgrid. *Energy Reports*, 9, 5992-6005 (2023).
7. Vásquez, L. O. P., Redondo, J. L., Hervás, J. D. Á., Ramírez, V. M., & Torres, J. L. Balancing CO2 emissions and economic cost in a microgrid through an energy management system using MPC and multi-objective optimization. *Applied Energy*, 347, 120998 (2023).
8. AlOwaifeer, M., Alamri, A., & Meliopoulos, A. S. Microgrid energy management system for normal and emergency operating conditions. In *North American Power Symposium (NAPS)* pp. 1-6. IEEE. (2019)
9. Yankson, S., Ullah, S. S., Ebrahimi, S., Ferdowsi, F., Ritter, K. A., & Chambers, T. Resilience-Enabling Load Flexibility and Resource Adequacy Investment in Microgrids. In *IEEE Texas Power and Energy Conference (TPEC)* (pp. 1-6). IEEE. (2023)
10. Suresh, V., Janik, P., Jasinski, M., Guerrero, J. M., & Leonowicz, Z. Microgrid energy management using metaheuristic optimization algorithms. *Applied Soft Computing*, 134, 109981 (2023)
11. Sendari, S., Diantoro, M., Nur, H., Ling, L. S., Rahmawati, Y., Wibawanto, S., ... & Asmara, S. B. IoT-Based Monitoring System of PEMFC-Solar Cell Hybrid Prototype

- Power Plant. In 6th International Conference on Electrical, Telecommunication and Computer Engineering (ELTICOM) (pp. 60-65). IEEE. (2022)
12. Kang, W., Guan, Y., Danang Wijaya, F., Kondorura Bawan, E., Priyo Perdana, A., Vasquez, J. C., & M Guerrero, J. Community Microgrid Planning in Lombok Islands: An Indonesian Case Study. *Frontiers in Energy Research*, 11, 1209875 (2023)
 13. Javidsharifi, M., Pourroshanfekr Arabani, H., Kerekes, T., Sera, D., & Guerrero, J. M. Stochastic optimal strategy for power management in interconnected multi-microgrid systems. *Electronics*, 11(9), 1424 (2022)
 14. Statistik.PLN <https://web.pln.co.id/statics/uploads/2022/08/Statistik-PLN-2021-29-7-22-Final.pdf> (accessed on 10 June 2023)
 15. Eberhart, R.; Kennedy, J. Particle swarm optimization. In *Proceedings of the IEEE International Conference on Neural Networks*, Perth, WA, Australia, Volume 4, pp. 1942–1948 (1995)
 16. Al-Kazemi, B.; Habib, S. Complexity analysis of problem-dimension using PSO. In *Proceedings of the WSEAS International Conference on Evolutionary Computing*, Cavat, Croatia, 12–14 pp. 45–52 (2006)
 17. Javidsharifi, M., Arabani, H. P., Kerekes, T., Sera, D., & Guerrero, J. M. Quantifying the Impact of Different Parameters on Optimal Operation of Multi-Microgrid Systems. In *IEEE 7th Forum on Research and Technologies for Society and Industry Innovation (RTSI)* pp. 88-94 IEEE (2022)
 18. Photovoltaic geographical information system, https://re.jrc.ec.europa.eu/pvg_tools/en/ (accessed on 24 August 2023)

Implementation of Agrivoltaic Systems under Operating Photovoltaic Park Conditions

Yan Carlos Pérez Mejía ¹[0009-0004-2167-3412], Jack Wesly Camacho ¹[0009-0005-9785-8533],
Gualberto Magallanes-Galla ²[0000-0002-4715-3499], Deyslen Mariano ¹[0000-0002-4255-3450],
Armando J. Taveras Cruz ¹[0000-0001-6538-4728], Giuseppe Sbriz-Zeitun ¹[0000-0002-8860-9085],
Miguel Aybar Mejía ¹[0000-0002-4715-3499]

¹ Área de Ingenierías, Instituto Tecnológico de Santo Domingo. Santo Domingo, Dominican Republic

² Área de Ciencias Básicas, Instituto Tecnológico de Santo Domingo. Santo Domingo, Dominican Republic

Miguel.Aybar@intec.edu.do

Abstract. One of the main features of current agrivoltaic systems is solar structures with a height greater than 2 meters. The study of these systems, considering the reduced measurements provided by the facilities implemented in conventional photovoltaic parks, needs to be sufficiently developed, and therefore, there currently needs to be more information on them. This research analyzes the most relevant variables when implementing or installing an agrivoltaic system under these conditions, such as temperature, received solar radiation, relative humidity, panel efficiency, etc. Moreover, in this way, it aims to evaluate the possibility of providing added value to conventional photovoltaic systems installed in the Dominican Republic and anywhere else in the world, taking advantage of the land not used under the photovoltaic panels through agricultural addition. To simulate the conditions that the agrivoltaic systems would present in the country, a functional prototype was constructed adapted to the technical requirements of current photovoltaic parks; the crops implemented for the study were broad leaf lettuce and Anthurium. As a result of this research, it was found that the plants under the photovoltaic panel enhance the creation of a microclimate that helps to reduce the temperature of the photovoltaic modules by (0.5-4.9) °C increasing their performance with values up to 1.6% the photovoltaic panel.

Keywords: Agrivoltaic, photovoltaic generation, photovoltaic panel efficiency, shade plants, photovoltaic energy yield.

1 Introduction

Over time, the effects of fossil fuels on global energy production will become increasingly clear [1], with global carbon dioxide emissions estimated at approximately 39,300,000,000 tons in 2021 [2]. Mentioned above has caused severe climatic impacts

2

on our ecosystem, such as the unpredictability of natural disasters [3] and flooding due to sea level rise [4], among others.

Due to their technical characteristics, photovoltaic (PV) systems require large land areas with an optimal insolation level to produce the maximum electrical energy [5]. Also, variables such as terrain and sunlight are primary agricultural resources. The term agrivoltaic or agrivoltaic was born because of the search for solutions to stimulate the synergy between the agricultural and energy sectors [6].

A situation that has been occurring in some countries around the world, especially in Spain, is the transition of farmers to energy production [7]. Farmers saw better profits in energy production than in agricultural processes, so they wholly and partially handed over their lands to solar energy production, in these areas providing up to 5 times more yield than agricultural production.

Agrivoltaic is an agri-food system that allows for the cultivation of food and the production of photovoltaic energy on the same fertile land without critically influencing the production of both parties involved in the system [8]. Agrivoltaic has gained momentum in different countries such as Japan, where rice fields and these systems are being studied [9]; Germany, where crops are used in agrivoltaic systems [10]; Indonesia, with the introduction of eggplants [11]. All these areas pursue to ensure the adequate viability of agrivoltaic plans, even some studies, such as those carried out in Germany, confirm an increase in the efficiency of solar panels due to plant evaporation [12]. Table 1 presents a literature review on agrivoltaic systems and describes contributions and limitations.

Table 1. Literature review on agrivoltaic systems.

Reference	Contributions	Limitations	Methodology	Region
[13]	Evaluate APV system efficiency via weather analysis.	Study excludes crops beneath solar panels.	Data collected at Oregon university for 2 years	Oregon
[12]	Compare energy production: photovoltaic vs. agrivoltaic.	Crop type, module arrangement, and weather have limited diversity.	Data from an Arizona university analyzed.	Arizona
[14]	Review and classify agrivoltaic systems by criteria.	Excludes agrivoltaic systems in operational projects.	Classified agrivoltaic systems by main characteristics	Unspecified
[15]	Belgian agrivoltaic prototype boosts PV efficiency.	Evaluate different photovoltaic panel configurations.	Simulated energy production, and shadow. Created prototype with crops under panels.	Belgium

Reference	Contributions	Limitations	Methodology	Region
[16]	Agrivoltaic literature review, microclimate, and crops. 70% agricultural productivity increase.	The study only contains a review of cases up to the year 2020.	Collects data, analyzes microclimates and crops.	Germany

Considering the above, the objective of this study is to analyze the impact that crops and plantations have under photovoltaic panels to improve efficiency based on the application of agricultural systems in established photovoltaic parks.

2 Methodology

1. The research was conducted on the implementation and benefits of agrivoltaic systems. After this, see the experiences of agrivoltaic systems in photovoltaic parks.
2. The relationship between the efficiency of photovoltaic panels and the temperature or microclimates that occur under the photovoltaic panels was investigated.
3. The types of crops that can be harvested or sown under the photovoltaic panels were identified.
4. It was selected which crops could be installed under the photovoltaic panels to improve the temperature and electrical efficiency, considering the available height between the photovoltaic panel and the ground.
5. A technical visit was made to photovoltaic installations that have yet to be contemplated for agro-industrial installations in their beginnings due to the height of the installation.
6. It Assembled prototype agrivoltaic installation under panels with low height and performed measurements.
7. Data collection through a data acquisition system to record the selected electrical and environmental variables.
8. The efficiency of photovoltaic panels with selected crops was measured and analyzed.

2.1 Conceptualization of photovoltaic efficiency and its separate calculations:

The efficiency of a photovoltaic panel is the ratio between the power produced by the panel and the energy it captures from the sun. Technological advancements have allowed for an increase in the efficiency of solar panels to approximately 20% [17]. However, various environmental and technical factors can decrease their efficiency and reduce the amount of energy produced. Some of these factors are [18]: Shading of the Modules, Location of the modules (Latitude), Dirt and dust present on the modules, and temperature of the photovoltaic cells.

4

Temperature of photovoltaic cells: This is one of the most noticeable and silent causes of efficiency reduction in the photovoltaic panel. The increase in temperature in photovoltaic panels does not improve energy production; as this increases, the electric generation of the module is reduced; this varies depending on the type of panel and the elements that compose it. Below, the values corresponding to the temperature coefficients of power for various types of photovoltaic modules will be shown:

- HJC monocrystalline cells: 0.26-0.27% / °C
- IBC monocrystalline cells: 0.29-0.31% / °C
- Monocrystalline cells: 0.37-0.40% / °C
- Polycrystalline cells: 0.40-0.43% / °C

Typical polycrystalline cells are the most affected by the increase in temperature; these cells are some of the least efficient.

In the case of the photovoltaic modules used in the realization of the prototype corresponding to this project, the manufacturer specifies that the power temperature coefficient for these modules is 0.45% / °C, which makes them modules with quite a low efficiency and very susceptible to variations in the power supply due to the temperature they manage to reach various points of the day.

Most Common Cooling Technologies. Various methods have been developed to increase the efficiency of photovoltaic modules by reducing temperature. Some of these methods are (Nabil & Mansour, 2022):

Some of the primary cooling methods used are:

- Cooling the modules using forced air on their backside, achieved through direct current fans. This technique increased the module's voltage output by 2.7% and reduced the temperature by 13.46%.
- Cooling the lower part of the photovoltaic panel by implementing circulating coolant in a coil at the back of the module. This technique increased the module's voltage output by 0.9% and reduced the temperature by 8.64%.
- Water misting on the surface of the photovoltaic module through nozzles placed in the module frame. This technique increased the module's voltage output by 7.43% and reduced the temperature by 37%.

Agri-Photovoltaic Systems for Temperature Reduction: Implementing agrovoltaic systems has brought exciting findings regarding the combination of agricultural and energy production [19]. Researchers from the University of Arizona have found that cultivating under photovoltaic panels reduces water consumption, protects plants from excessive sunlight, and increases their productivity while decreasing daytime and nighttime temperatures. This temperature decrease is optimal for enhancing photovol-

taic panel efficiency [20]. Therefore, these systems have economic advantages and improve energy production, making it worthwhile to analyze their implementation.

Implemented methodologies for efficiency measurement:

There are different methodologies for calculating the efficiency of photovoltaic panels, all of which generally involve basic parameters such as the level of received irradiation, maximum power of the solar module, etc. This research will perform efficiency calculations using one of the most commonly used methodologies.

Energy efficiency measurement without load: This method utilizes measurements of open-circuit voltage and short-circuits current produced by the panel at various points throughout the day, where the irradiance varies in each measure [21].

The mathematical formula representing the electrical efficiency of the photovoltaic module is given by:

$$E_f = \frac{P}{A \cdot H_m} * 100\% \quad (1)$$

$$E_f = \frac{V_{ca} \cdot I_{cc}}{A \cdot H_m} * 100\% \quad (2)$$

Where:

- E_f = Photovoltaic Module Efficiency, P = Panel Power (W), A = Panel Area (m²), H_m = Measured Irradiance (W/m²), V_{ca} = Open Circuit Voltage (V), I_{cc} = Short Circuit Current (A)

Energy Efficiency Measurement with Connected Load: Photovoltaic modules tend to experience a decrease in voltage profiles when more current is required than they can deliver. Therefore, if the energy capacity of the panel increases, the voltage profiles will be more stable when faced with a consumption that exceeds their nominal power [22].

This methodology involves connecting a load to the photovoltaic module that demands its maximum power at various points throughout the day, observing how the voltage levels behave, and calculating the module's total power at each moment.

The equation that defines this procedure is as follows:

$$E = \frac{P}{A \cdot H_m} * 100\% \quad (3)$$

$$E_f = \frac{V \cdot I}{A \cdot H_m} * 100\% \quad (4)$$

6

Where:

- E_f = Photovoltaic Module Efficiency, P = Panel Power in (W), A = Panel Area in (m^2), H_m = Measured Irradiance (W/m^2), V = Closed Circuit Voltage (V), I = Load Current (A)

2.2 Visits to photovoltaic parks:

To obtain accurate data on photovoltaic projects, such as soil, infrastructure, maintenance logistics, etc., representative parks of the region were visited. The diversity in the characteristics of these variables was considered. Table 2 shows the primary data collected in the visited photovoltaic parks.

Table 2. Data collected in photovoltaic parks visited.

Solar Project	Area covered by panels (km^2)	Qty. of rows	Distance between rows (m)	Qty. PV panels	Incl. South ($^\circ$)	Height Max. (m)	Height Min. (m)
Monte P. Solar	0.2279	2,000	1.6	137,000	18	1.6	0.8
Quisqueya 2	0.0200	25	3	4760	45	1.5	0.46
AES Andrés	0.2858	4,763	2	142,900	18	1.5	0.6
Girasol	0.5764	3,202	3	288,200	52	1.5	0.5

The data presented in Table 2 will define the constructed prototype's technical characteristics, primarily the panels' height and inclination. This visit to these parks that are already in operation served to know the features and maximum size that the photovoltaic panels are placed on the floor level to determine what helpful area it has of the panels for selecting of the crop that would be set according to the site.

Determination of Optimal Crops for Agrivoltaic Systems:

Information was collected to identify the most relevant crops in the current agricultural systems in the Dominican Republic that can function in agrivoltaic systems. The information was obtained through research work, visits to nurseries, and requests to the Ministry of Agriculture [23]. Regional studies of the most important crops were also considered based on the location of the solar parks visited.

Table 3 presents the main crops implemented in the areas where the visited photovoltaic parks are located. This data will be used for some of the crops used in the agrivoltaic systems that are found in Table 4.

7

Table 3. Principal crops in visited areas.

Zone	Main Crops
Monte Plata	Cocoa, sugar cane, corn, yams, cassava, Yautia, citrus, coffee, bananas, pepper, mushroom, pineapple.
Peravia	Coffee, corn, tomato, pigeon pea, onion, mango, plantain, cashew, papaya.
San Pedro de Macoris	Bananas, Sweet Potato, Sugar Cane
La Altagracia	Soy, sorghum, peanuts, sesame seeds, sunflower, cotton, corn, tomato, plantain, tobacco, beans, onion, rice, cassava, sweet potato, pigeon pea, mango, coffee, and avocado.

Extracted from [23].

Table 4. Main crops and Ornamental plant used in agricultural and arable systems in the Dominican Republic.

Crops	Growth Max. (m)	Hours daylight	Frequency irrigation (day)	T. ^a (°C)	Land	Cycle (Weeks)
Potato	1m	8	14	15-20	Rich in humus, loose and sandy	17
Aloe vera	1-2m	6	17	17-27	Porous and nutritious soil, easy drainage	160
Peppers	0.6 -0.9 m	6	1	20-25	Deep soils, rich in organic matter, slightly sandy	17
Tomato Cherry	0.5-2m	6	14	20-30	Acid, drained, clayey	21
Jalapenos	0.5 -0. 9m	6	7	18-32	sandy loam, aerated, good drainage, high moisture retention	11
Lettuce	0.3 m	4	1	18-20	Light, sandy-silty, good drainage, optimal pH between 6.7 -7.4	8
celery	0.3 - 0.8 m	4	14	16-21	Clay soils with slight tolerance to low PH	9
*Anthuriums	1.5 m	6	7	15-20	Thrives in warm, frost-free, indirect sunlight.	2-4

Extracted from [23]. ^aOrnamental plant that requires little water to flower, it is used in gardening in the Dominican Republic due to its rapid growth cycle.

The crops presented are optimal for implementing possible agrivoltaic systems in the Dominican Republic. For the study, lettuce was taken as an edible crop and Anthurium as an ornamental crop. Both crops were selected because of their rapid growth and

8

because both crops do not need direct sunlight to grow, which is the condition that occurs under the photovoltaic panels.

2.3 Microclimate generated under photovoltaic modules.

Under a photovoltaic module, a microclimate is generated with conditions that are not the same as the environment's. The presence of photovoltaic panels directly influences the wind speed, illuminance, humidity, and temperature of the microclimate generated under them [7]. The parameters below the panel reveal the possibility of being able to plant any given crop under the panel. For the project, this microclimate will be considered as the initial condition of the crops.

To analyze the microclimate, measurements of temperature, humidity, and luminance were taken continuously. These variables provide the initial conditions in which the crops will be planted. To have a specific crop under a panel, the conditions in which the plant can grow must be within the parameters granted by the microclimate under the panel.

It is essential to know that current agrivoltaic systems are designed considering in advance the conditions and dimensions of the selected crop. For this research, it is assumed that it starts from a photovoltaic park and is transformed into an agrivoltaic park. This is why there are few options regarding the selected crop, but there are still alternatives. After having selected a crop, we must consider that the plants under the panels themselves generate a microclimate separate from the microclimate generated by the panels; that is, when planting crops under a photovoltaic module, we generate a change within the microclimate, below the panel [12].

Growing crops under solar panels can affect the microclimate under the panels in several ways:

Shade and cooling: Crops planted under solar panels can provide shade and cooling to the soil surface and reduce the temperature beneath the panels.

Humidity and water vapor: Crops can also increase the relative humidity and water vapor in the air beneath the panels, which can be beneficial for some types of crops.

Air circulation: Plants and soil surfaces can help air circulate under the panels, which can improve air quality and reduce the risk of overheating.

Soil Moisture: The shade and cooling provided by crops can help regulate soil moisture levels and reduce evaporation, which can benefit crop growth.

2.4 Selection of representative variables for the prototype:

The choice of variables or simulated conditions using the prototype considered the general characteristics of the solar structures, such as module inclination, maximum and minimum height, etc. Likewise, the peculiarities of the land surface in the solar energy installations and the prevailing climatic conditions were considered.

Based on the data collected during the visits, a scale agrivoltaic system is created with the most representative characteristics of the parks in the region and thus has information on the energy and agricultural production of the system. Figure 1 shows that the prototype will be located at the INTEC facilities.

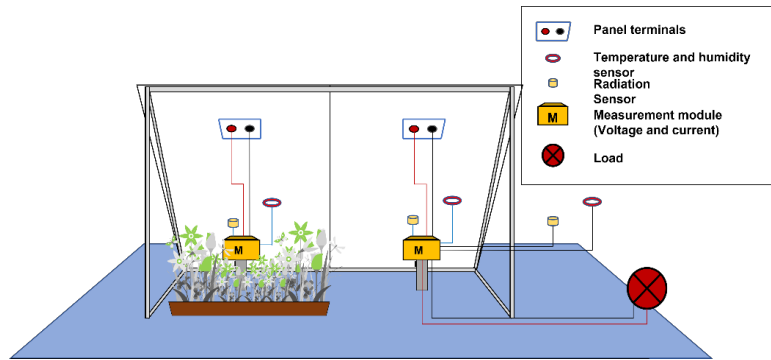


Figure 1. Structure of the Agrivoltaic prototype.

Two photovoltaic modules from the Dazi Solar brand, polycrystalline, were used, whose nominal power is about 330 W, Maximum Peak Power (Pmp, max) 215 W, Minimum Peak Power (Pmp, min) 210 W, Voltage at Peak Power (Vmp) 18.3 V, Current at Peak Power (Imp) 11.48 A, Open Circuit Voltage (Voc) 22.8 V, Short Circuit Current (Isc) 12.11 A.

The prototype consists of a structure that houses two photovoltaic modules, one for crops and another without crops, to record changes. Both panels have measurement modules to obtain data on humidity, temperature, solar radiation, voltage, and current. The data helps perform feasibility analysis. The elements and sensors used in this prototype were low-cost elements, easy to access, and to be replaced in case of damage or breakdowns, in addition to being able to be integrated into microcomputers such as Arduino or Raspberry Pi.

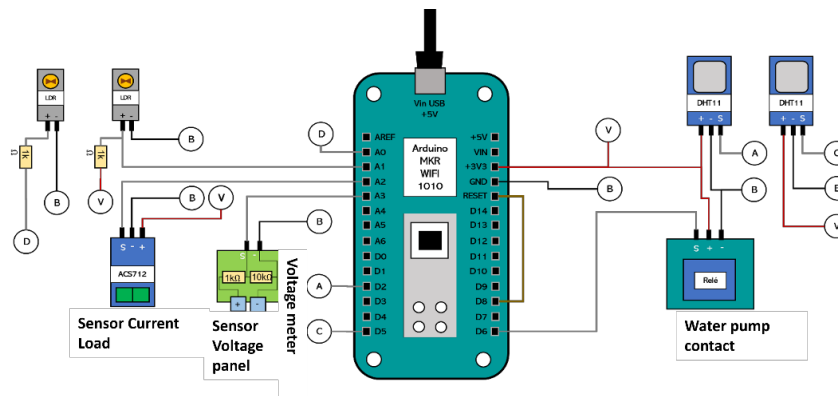


Figure 2. Internal connection diagram Measurement module.

10

Figure 2 shows the connection diagram corresponding to the measurement module, which uses an Arduino MKR WIFI 1010 as a microprocessor. This module allows for the wireless monitoring of the measured variables with a permanent record. The variables Photovoltaic panel voltage with Voltage divider (10:1), Photovoltaic panel current with Sensor ACS712 30A, Solar radiation with Photoresist LDR, Temperature, and Relative humidity with DHT 11.

Although it did not employ continuous data collection at shorter intervals (approximately 1 second), especially considering that the "mkr 1010" measurement module allows continuous data recording through wireless monitoring, in the testing period the interval of one 1 second presents non-significant variations, so longer intervals help better for the validation of the temperature change.

It was necessary to connect a variable resistor to the module to force the panel to deliver different amounts of power under different resistor values to detect this power. The connected load varied from values of (0-10) Ω ; this allowed the circulation of current in values ranging from (3.5 -11.0) A approximately and voltage values varying from (40V-0.2 V); the higher the current, the lower the voltage between its terminals.

2.5 Data collection

For data collection, the information provided by the measurement module and the information collected by the meters used were used together. Data extraction lasted approximately 6 days; 3 consecutive days were dedicated to the measurements of the variables related to the incorporation of the lettuce under the photovoltaic panels, and 3 subsequent days were dedicated to analyzing the system using the incorporation of anthuriums.

During the 6 days of measurements, data were collected from (11:00 a.m. - 16:30) approximately; this schedule was chosen mainly for two reasons: The effective energy production of photovoltaic modules in our country is achieved at times ranging from (10:00 a.m. - 5 p.m.); also, outside these hours the changes in radiation are pretty fast, so it is difficult to capture good measurements.

The total number of measurements collected on the day was approximately 8-9, with 30-minute to 1-hour intervals. The choice of the gaps depended entirely on the climatic condition's characteristic of each day; since stable solar radiation levels are optimal for measuring efficiency [24], we tried to take the measurements at points of the day that were clear of clouds so that the measurements were not affected. This was one of the main problems faced, the fact of capturing measurements on days with favorable weather conditions.

3 Results

Table 5 and Table 6 present a comparison between the panel without plants and lettuce and anthuriums. Due to the time of year where the experiment was carried out, there were no considerable variations in the climate, 3 days were used as a sample.

Table 5. *The Comparison between the panel without plants and with lettuce.*

Date	Hour	η (NP)	η (L)	P_{max} (NP)	P_{max} (L)	Temp (°C) (NP)	Temp (°C) (L)
12/02/2023	11:00	17.16	17.32	262.96	263.82	31.30	31.30
	12:00	17.26	17.40	284.16	283.82	33.80	33.80
	13:00	15.61	17.76	281.39	280.48	33.30	33.75
	14:00	17.00	17.78	271.09	271.15	33.30	32.55
	15:00	16.42	18.00	215.98	216.10	32.30	30.80
	16:00	16.74	17.18	176.23	177.40	31.80	29.80
13/02/2023	11:00	16.64	16.78	258.92	259.21	36.89	33.80
	12:00	17.11	18.00	283.45	284.21	35.94	33.25
	13:00	16.92	17.73	276.04	277.20	37.60	34.65
	14:00	17.20	17.73	272.28	272.30	36.50	31.34
	15:00	16.66	17.44	229.45	229.47	35.56	32.45
	16:00	15.88	16.25	180.64	181.15	33.25	30.44
14/02/2023	11:00	16.61	16.64	240.77	254.37	32.30	30.20
	12:00	16.62	16.59	276.29	281.08	35.60	33.55
	13:00	16.45	16.98	260.03	260.10	34.00	32.30
	14:00	16.70	16.71	257.06	257.11	35.60	33.30
	15:00	16.85	16.75	209.74	210.25	36.30	33.20
	16:00	16.47	16.92	174.53	174.80	35.20	32.30

* η (NP) = efficiency without plant, η (L) = efficiency with lettuce, P_{max} (NP) = maximum power without plant, P_{max} (L) = maximum power with lettuce, Temp (°C) (NP) = temperature without plant, Temp (°C) (L)

Table 6. Comparison between the panel without plants and with anthuriums.

Date	Hour	η (NP)	η (A)	P_{max} (NP)	P_{max} (A)	Tem p (°C) (NP)	Tem p (°C) (A)
17/02/2023	11:00	17.32	17.49	271.96	272.54	29.93	30.30
	12:00	16.77	17.37	302.08	306.86	30.37	30.40
	13:00	16.98	16.93	273.07	274.16	31.40	32.63
	14:00	16.40	16.83	260.20	253.56	33.09	34.37
	15:00	17.05	16.97	231.73	231.05	31.49	31.50
	16:00	15.98	17.17	185.20	188.71	30.20	30.73
18/02/2023	11:00	16.98	16.68	288.34	288.90	31.98	31.80
	12:00	17.55	16.88	299.14	293.22	34.85	34.89
	13:00	17.69	16.93	309.18	319.19	33.73	33.72
	14:00	17.90	16.66	260.30	305.79	33.24	33.20
	15:00	16.22	17.33	220.20	225.46	33.73	33.56
	16:00	15.55	16.50	172.47	200.18	33.55	33.45
19/02/2023	11:00	16.76	16.80	269.48	277.77	30.93	30.72
	12:00	17.10	17.12	324.82	324.99	32.14	31.90
	13:00	16.85	17.02	281.85	291.95	32.84	32.70
	14:00	17.48	17.25	256.45	257.12	32.60	31.60
	15:00	17.15	17.05	217.96	219.16	33.24	33.10
	16:00	17.70	17.67	204.60	204.80	32.55	32.45

* η (NP) = efficiency without plant, η (A) = efficiency with anthuriums, P_{max} (NP) = maximum power without plant (Watts), P_{max} (A) = maximum power with anthuriums (Watts), $Temp$ (°C) (NP) = temperature without plant, $Temp$ (°C) (L) = temperature with anthuriums.

According to the data in Table 5 and Table 6, when comparing the three days of lettuce measurement with the three days of anthurium measures, the average difference shows that the lettuce module achieved better levels of efficiency than the Anthurium module, with values of up to 1.07 %.

Concerning the average temperature of the PV module, when the panel contained lettuce, its average temperature decreased by 0.02 % more than when Anthurium had.

Through these comparisons, it can be concluded that using lettuce to boost the efficiency of PV modules is much more efficient than using Anthurium. To some extent, this is evident because Anthurium is a crop that cites little water again, and, therefore, its evapotranspiration levels are relatively lower than the evapotranspiration levels of lettuce. For this reason, the following studies will be based on lettuce implementation.

4 Discussion

Initially, efficiency tests were conducted with two crops, lettuce and Anthurium. Unlike lettuce, Anthurium is a total shade crop, so the amount of sunlight and water required to survive is minimal. In this sense, the intensity of evapotranspiration it produces is reduced, so it is not as good at conditioning the microclimate as lettuce. In addition, lettuce showed better adaptability to the conditions under the photovoltaic module than anthuriums, whose leaves suffered burns and whose flowers looked battered.

In this sense, the efficiency variations produced by the lettuce were up to 1.6 % higher compared to the panel without the plant, while the Anthurium made hardly any noticeable difference, which was one reason why it was discarded.

Despite this, the analysis of these crops showed that it is possible to grow crops under photovoltaic modules in already installed photovoltaic park conditions and simultaneously increase the efficiency of the generation.

5 Conclusions

In summary, research and experimentation on agricultural systems have shown that favorable microclimates under photovoltaic panels increase the energy productivity of the panels and are conducive to the development of crops that do not demand a lot of light or support extended periods of shade. A comparison was made between the efficiency of the panels with different plants, and the implementation of Anthurium was discarded due to its low capacity to reduce temperature and increase humidity. At the same time, lettuce increased efficiency by up to 1.6%.

Relevant variables, such as temperature, radiation, humidity, and panel efficiency, must be considered when implementing an agrivoltaic system. Relevant variables, such as temperature, radiation, humidity, and panel efficiency, must be considered when implementing an agrivoltaic system.

The use of agrivoltaic systems with solar structures of significant height has been effective and has made it clear that it can provide added value to conventional photovoltaic systems, increasing energy efficiency and productivity in agriculture. Agrivoltaics are a promising option from the point of view of both energy production and agricultural production and the environmental benefits they can bring.

Finally, the measurements were taken on completely sunny and clear days. Days with the possibility of precipitation were discarded since they did not present optimal production conditions for the panels. In the model, the microclimate conditions were measured without plants and with anthuriums and lettuce. In both cases with crops, a general decrease in temperature was seen, in addition to an increase in humidity. The

14

above-mentioned shows that the microclimate is acting under the abovementioned predictions. Therefore, in future research, it could be interesting to see the effect of these exceptions on the behavior of the microclimate and the efficiency of the panels, in addition to integrating measurement equipment with a more excellent range of precision since the reading records are affected by the changes of the microclimate and the sampling time of the sensors and equipment.

Acknowledgment

The authors acknowledge the support provided by the Thematic Network 723RT0150 “Red para la integración a gran escala de energías renovables en sistemas eléctricos (RIBIERSE-CYTED)” financed by the call for Thematic Networks of the CYTED (Ibero-American Program of Science and Technology for Development) for 2022.

6 References

1. Sanchez L, Perez R, Vasquez C (2017) Eficiencia de Países Desarrollados en el Control del uso de Combustibles Fósiles Para Generar Energía. *Rev Científica ECOCIENCIA* 4:58–71
2. Statista (2023) Annual carbon dioxide (CO₂) emissions worldwide from 1940 to 2022. <https://www.statista.com/statistics/276629/global-co2-emissions/>. Accessed 31 May 2023
3. Patlins A, Caiko J, Kunicina N, et al (2020) Climate Education: Challenges of Climate Change and Energy Policies. In: 2020 IEEE 61th International Scientific Conference on Power and Electrical Engineering of Riga Technical University (RTUCON). pp 1–7
4. Sicre L (2021) ¿Qué consecuencias estamos viviendo por el cambio climático? In: *Telecinco Inf.* https://www.telecinco.es/noticias/sociedad/consecuencias-cambio-climatico-be5m_18_3091470164.html. Accessed 31 May 2023
5. Chung MH (2020) Estimating Solar Insolation and Power Generation of Photovoltaic Systems Using Previous Day Weather Data. *Adv Civ Eng* 2020:8701368. <https://doi.org/10.1155/2020/8701368>
6. Sarr A, Soro YM, Tossa AK, Diop L (2023) Agrivoltaic, a Synergistic Co-Location of Agricultural and Energy Production in Perpetual Mutation: A Comprehensive Review. *Processes* 11
7. Pastor Fernando (2021) La fotovoltaica “recalienta” el campo y multiplica por cuatro las rentas agrarias. In: *news Pap.* <https://www.lainformacion.com/economia-negocios-y-finanzas/la-fotovoltaica-recalienta-el-campo-y-multiplica-por-cuatro-las-rentas-agrarias/2832375/#:~:text=y 30 años-,La fotovoltaica “recalienta” el campo y multiplica por cuatro las,los cultivos o la prod.> Accessed 31 May 2023
8. Agostini A, Colauzzi M, Amaducci S (2021) Innovative agrivoltaic systems to produce sustainable energy: An economic and environmental assessment. *Appl Energy* 281:116102. <https://doi.org/https://doi.org/10.1016/j.apenergy.2020.116102>
9. Gonocruz RA, Nakamura R, Yoshino K, et al (2021) Analysis of the Rice Yield under an Agrivoltaic System: A Case Study in Japan. *Environments* 8
10. Trommsdorff M, Kang J, Reise C, et al (2021) Combining food and energy production: Design of an agrivoltaic system applied in arable and vegetable farming in Germany. *Renew Sustain Energy Rev* 140:110694. <https://doi.org/https://doi.org/10.1016/j.rser.2020.110694>

11. Ahmad K, Wijayanti Y, Subandriya A, et al (2022) The Agrivoltaic System Development in Baron Technopark, Yogyakarta, Indonesia. In: 2022 5th Asia Conference on Energy and Electrical Engineering (ACEEE). pp 147–151
12. Barron-Gafford GA, Pavao-Zuckerman MA, Minor RL, et al (2019) Agrivoltaics provide mutual benefits across the food–energy–water nexus in drylands. *Nat Sustain* 2:848–855. <https://doi.org/10.1038/s41893-019-0364-5>
13. Adeh EH, Good SP, Calaf M, Higgins CW (2019) Solar PV Power Potential is Greatest Over Croplands. *Sci Rep* 9:11442. <https://doi.org/10.1038/s41598-019-47803-3>
14. Jain P, Raina G, Sinha S, et al (2021) Agrovoltatics: Step towards sustainable energy-food combination. *Bioresour Technol Reports* 15:100766. <https://doi.org/https://doi.org/10.1016/j.biteb.2021.100766>
15. Weselek A, Ehmann A, Zikeli S, et al (2019) Agrophotovoltaic systems: applications, challenges, and opportunities. A review. *Agron Sustain Dev* 39:35. <https://doi.org/10.1007/s13593-019-0581-3>
16. Willockx B, Herteleer B, Cappelle J (2020) Combining photovoltaic modules and food crops: first agrovoltaic prototype in Belgium
17. Cepeda Moya JS, Sierra A (2017) Aspectos que afectan la eficiencia en los paneles fotovoltaicos y sus potenciales soluciones. 10
18. tritec-intervento (2011) EFICIENCIA DEL PANEL SOLAR (PARTE I). <https://tritec-intervento.cl/eficiencia-del-panel-solar-parte-i/>. Accessed 31 May 2023
19. Chalgynbayeva A, Gabnai Z, Lengyel P, et al (2023) Worldwide Research Trends in Agrivoltaic Systems: A Bibliometric Review. *Energies* 16
20. Moharram KA, Abd-Elhady MS, Kandil HA, El-Sherif H (2013) Enhancing the performance of photovoltaic panels by water cooling. *Ain Shams Eng J* 4:869–877. <https://doi.org/https://doi.org/10.1016/j.asej.2013.03.005>
21. Flores Rivera NR, Domínguez Ramírez MA (2017) Medición de la eficiencia energética de los paneles solares de silicio
22. Elminshawy NAS, Mohamed AMI, Morad K, et al (2019) Performance of PV panel coupled with geothermal air cooling system subjected to hot climatic. *Appl Therm Eng* 148:1–9. <https://doi.org/https://doi.org/10.1016/j.applthermaleng.2018.11.027>
23. Viceministerio de Planificación Sectorial Agropecuaria, Departamento de Economía Agropecuaria y Estadísticas (2021) Desempeño del Sector Agropecuario de la República Dominicana 2016-2020. <https://agricultura.gob.do/wp-content/uploads/2021/11/Desempeno-del-Sector-Agropecuario-2016-2020.pdf>. Accessed 31 May 2023
24. TELLO-ARGÜELLES CE (2020) Evaluación del efecto de la radiación solar sobre la superficie de un sistema fotovoltaico. In: *Mujeres en la Ciencia Ingeniería*. ECORFAN, pp 196–209

Benefits of multiple Electric vehicle aggregators in mountainous areas with high variability of photovoltaic resources.

Miguel Davila-Sacoto¹[0000-0001-6318-2137], L.G. González²[0000-0001-9992-3494], Luis Hernández-Callejo¹[0000-0002-8822-2948], Óscar Duque-Pérez³[0000-0003-2994-2520], Ángel L. Zorita-Lamadrid³[0000-0001-7593-691X], and J.L. Espinoza²[0000-0002-7450-2084]

¹ Department of Agricultural and Forestry Engineering, University of Valladolid, Duques de Soria University Campus, 42004 Soria, Spain

² Department of Electrical Engineering, University of Cuenca, Central Campus, 010104 Cuenca, Ecuador

³ Department of Electrical Engineering, University of Valladolid, School of Industrial Engineering, 47011 Valladolid, Spain

miguelalberto.davila@alumnos.uva.es M.D.-S.

luis.gonzalez@ucuenca.edu.ec L.G.G

luis.hernandez.callejo@uva.es L.H.-C.

oscar.duque@eii.uva.es O.D.-P.

zorita@eii.uva.es A.L.Z.-L.

juan.espinoza@ucuenca.edu.ec J.L.E.

Abstract. Electric systems with a high penetration of photovoltaic generation and electric vehicles pose significant challenges to their stability. When we add to this the high variability of the photovoltaic resource in mountainous areas, the problem requires a more thorough analysis. In this study, the placement of different electric vehicle aggregators along a feeder is proposed, taking into account electrical variables and cloud movement dynamics in the study area. It is demonstrated that this methodology reduces the power delivered by the substation and improves voltage levels at user terminals.

Keywords: Electric Vehicle Aggregator, Electric Vehicle, High Photovoltaic penetration grid.

1 Introduction

Electric infrastructures incorporating distributed renewable energy sources have experienced a significant increase in prevalence, posing substantial challenges in terms of their monitoring, optimization, and analysis. Particularly within the context of energy systems with a high penetration of solar photovoltaic (PV) energy, substantial challenges emerge due to the inherent variability in solar radiation, leading to voltage fluctuations at system nodes [1]. Concurrently, the growing global adoption of electric

2

vehicles (EVs) introduces an additional challenge, as these vehicles, in addition to representing a significant load for the system, possess the capability to function as energy storage devices, offering ancillary services to the electrical grid in contingency situations.

Efforts to effectively integrate EVs into systems with high PV penetration have been the subject of study, with the aim of mitigating voltage level variations resulting from fluctuations in solar radiation [2][3]. However, the achievement of this objective necessitates the implementation of specialized charging strategies, as presented in [4], particularly in isolated systems characterized by a substantial proportion of renewable energy sources. To address these integration challenges, the utilization of ancillary services provided by EVs has been proposed [5], employing the technology known as "Vehicle to Grid" (V2G). In this context, EVs, and more specifically, EV charging stations or electric vehicle supply equipment (EVSE), are transformed into elements capable of supplying and absorbing energy from the electrical grid, maintaining suitable levels of voltage, frequency stability, and demand peak shaving, among other aspects.

Within this framework, for the effective management of this mechanism, aggregator systems are employed [6]. These systems are designed to make decisions concerning energy transfer between EVs and the electrical grid, leveraging the analysis of electrical and economic variables, such as energy costs, to optimize the distribution of energy from EVs in alignment with the needs and constraints of the electrical system.

The following article presents the impact on the voltage of a high-penetration PV generation grid caused by the variation of PV resource in Andean cities and the means to mitigate it through the use of multiple aggregators of EVs. The variation of the PV resource caused by cloud movement is verified in two separate PV generators located 5.6 kilometers apart. This variation is then applied to an IEEE system to ascertain that the placement of EV aggregators influences the voltage at the terminals of the electrical grid loads.

In this study, we examine the effect of PV resource variability due to cloud movement on the voltage levels within a high-penetration PV generation grid in Andean cities. Additionally, we investigate the potential mitigation strategies by deploying multiple aggregators of EVs in the network. To quantify the impact, we conducted experiments involving two separate PV generators located 5.6 kilometers apart. Subsequently, we applied the observed PV resource variation to an IEEE system model to assess its influence on voltage levels at the load terminals of the electrical grid.

2 High Penetration Photovoltaic Systems in Mountainous Areas

Electric systems located in mountainous regions, such as the Andes mountain range in Ecuador, which exhibit a high integration of solar PV energy sources, are susceptible to significant power fluctuations caused by the variability of solar resources induced by high cloudiness conditions in the region. To investigate this phenomenon, power generation measurements were conducted using the PV system installed in the Microgrid

Laboratory at the University of Cuenca [7]. Data on PV energy generation were collected and analyzed over a period of one year.

The results of this analysis revealed that due to the recurrent presence of cloud cover in the mountainous Andes environment, the power generated by the PV system experiences substantial oscillations. These oscillations were identified as variations that fall within a range oscillating between 54% and 72% of the nominal capacity of the installation. Additionally, when examining the direct current component of the generated power, it was observed that variations in the solar system occur at intervals on the order of 15 seconds [8], with peak values of $800\text{Wm}^{-2}/\text{min}$ and an average of $275\text{Wm}^{-2}/\text{min}$ (see Fig. 1).

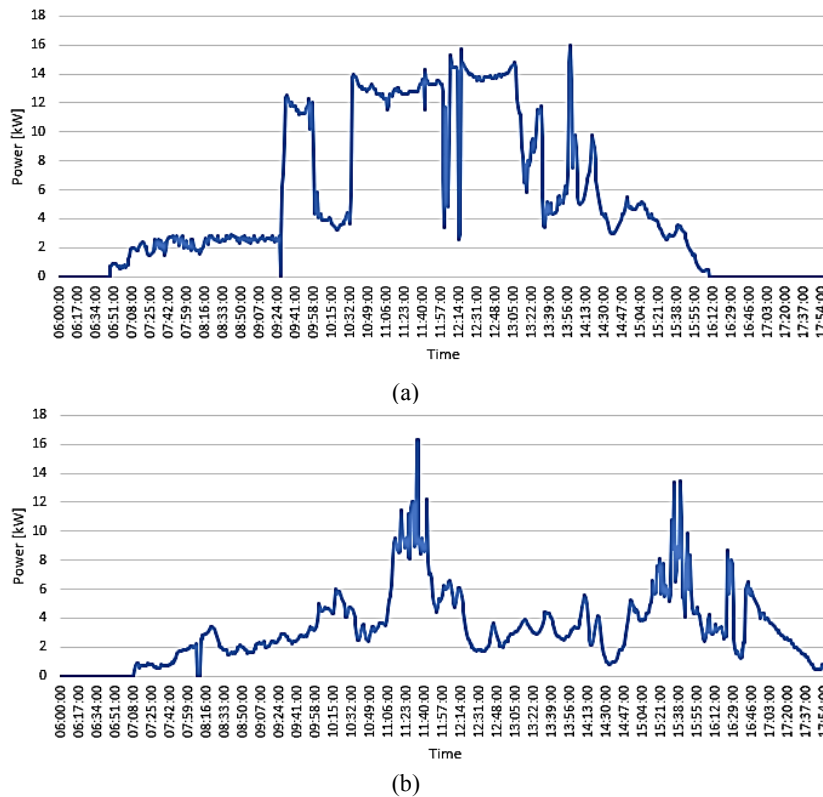


Fig. 1. Solar Generation Power at the Balzay Microgrid Laboratory (a) low cloudiness (b) High cloudiness

To quantify the variations recorded during the year of operation of the laboratory at the University of Cuenca, the daily variability index (DVI) was calculated using a definition similar to [9] and presented in (1):

4

$$DVI = \frac{\sum_{i=2}^n |GHI_i - GHI_{i-1}|}{\sum_{i=2}^n |CSI_i - CSI_{i-1}|} \quad (1)$$

Where GHI_i represents the average value of the global horizontal irradiance recorded, i is the time interval of the station's sampling (1 minute), n is the total number of samples taken during the day, and CSI_i is the concurrent value taken from the clear-sky index model as described in [10]. The analysis of the 365 days of operation of the PV system indicated a maximum DVI of 13.633 and an average of 5.955. As shown in Figure 2, 98.8% of the analyzed days correspond to cases of PV with high variability.

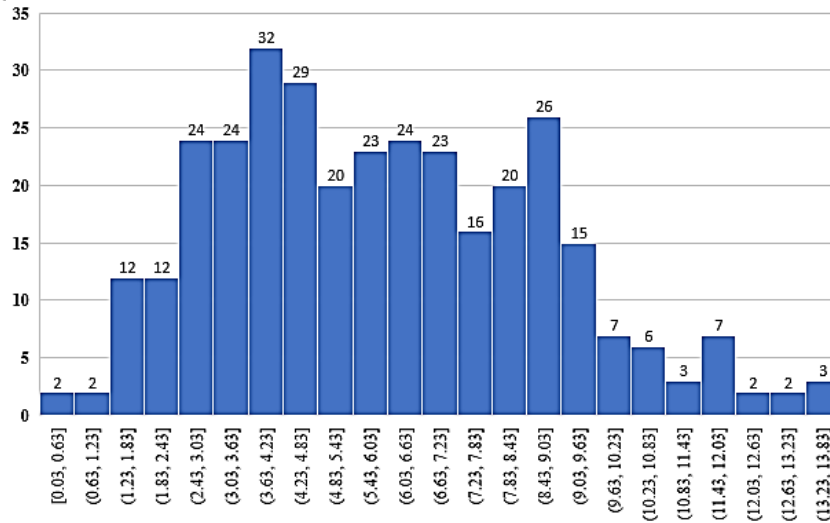


Fig. 2. Variability of Photovoltaic Resource

In the context of the city of Cuenca, Ecuador, variations in the availability of PV resources are primarily attributed to the presence of cloud cover in the region [11]. This climatic characteristic results in significant heterogeneities in solar irradiation levels across the city's territory. The variability of solar radiation is a phenomenon of great relevance in the planning and operation of PV systems, as it has a direct impact on the efficiency and performance of these systems.

Figure 3 presents a satellite image of the city of Cuenca, in which two relevant points of interest for this study are identified. Point PV1, located at geographical coordinates 2°53'52.80"S and 79° 0'52.64"W, corresponds to the microgrid research laboratory of the University of Cuenca. On the other hand, point PV2, situated at geographical coordinates 2°54'17.85"S and 78°59'29.73"W, represents a privately-owned PV system. These two systems are separated by a distance of approximately 5.6 kilometers.

The satellite image captured on March 8, 2023, effectively illustrates the characteristic cloudiness phenomenon of the area. Even on a partially clear day, clouds cast shadows over scattered areas of the city, highlighting the spatial variability of solar radiation. It is particularly important to emphasize that the presence of clouds can have a significant impact on solar energy generation, as the shadows projected by the clouds reduce the amount of solar radiation incident on the surfaces of PV panels, thereby affecting energy production.

Significantly, in situations where a predominant northwest wind direction prevails, as depicted in Figure 3, the clouds shown in the image will follow a specific path. In this scenario, clouds will first affect PV2, located in their initial trajectory, and subsequently, after a certain period of time, they will traverse PV1, situated downstream in relation to the prevailing wind direction. This behavior is of importance in assessing the variability of PV generation in the region and necessitates a detailed analysis to comprehend its impact on the operation of solar PV energy systems and its potential mitigation.

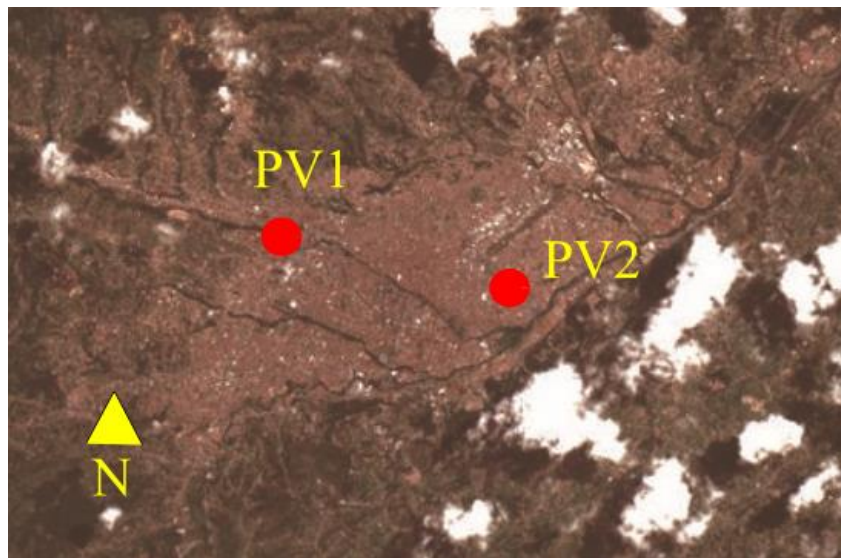


Fig. 3. Satellite Image of Cuenca with the Location of Two Photovoltaic Systems.

In order to assess the impact caused by cloud movement, solar radiation data were collected from the two aforementioned PV systems with GPS synchronized dataloggers. Figure 4 presents a record of solar radiation captured by both systems during the same day. In this graph, shifts in the minimum values of solar radiation can be identified. It is important to note that while these results offer an initial insight into the effects of variation in both systems, it is necessary to consider the acquisition of a more extensive dataset and the use of satellite images captured at a higher temporal frequency, ideally

6

at one-minute intervals, to conduct a more comprehensive and detailed analysis of these variations.

The analysis of these shifts in solar radiation levels provides crucial information for understanding the influence of local weather conditions' variability on PV energy generation. These preliminary findings suggest the need for further research to more thoroughly explore the relationship between cloud mobility and the efficiency of PV systems, which may lead to more effective strategies for mitigating variability in solar energy generation.

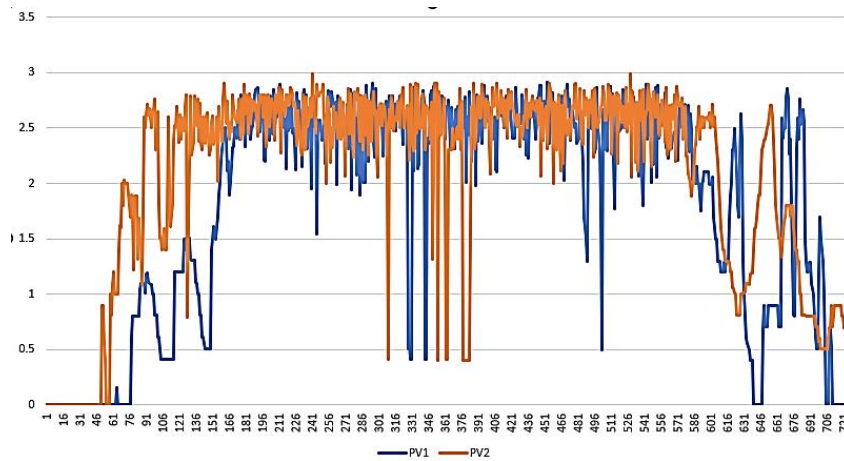


Fig. 4. Radiation in two Photovoltaic Systems

3 Electric Vehicle Aggregator in High Penetration Photovoltaic Systems

A strategy presented as an effective solution to reduce fluctuations in voltage and power levels caused by the variability of PV solar resources involves the use of EV aggregator systems that coordinate the implementation of the "Vehicle to Grid" (V2G) concept to correct the observed variations in the system [12]. In the context of this research, the hypothesis is put forth that such an aggregator must be capable of considering the variation in the availability of PV solar resources, which is caused by the movement of clouds across a specific region. In other words, the goal is to model and address the dynamics of solar radiation, which experiences a temporal shift due to the movement of clouds in the study area.

To conduct this analysis, three geographical zones were established, identified as Z1, Z2, and Z3, in which a pattern of solar radiation movement over a 3-hour period is observed. This approach allows for the simulation of cloud movement through the PV system and the anticipation of associated variations in solar energy generation. The

details of these zones and the behavior of solar radiation movement are presented in Figure 5. The incorporation of this dynamic into the design and operation of the EV aggregator represents an innovative approach to addressing PV generation variability and optimizing the electrical system's responsiveness to fluctuations caused by weather-related factors. This study contributes to advancing our understanding of how spatial and temporal variability in solar radiation can be efficiently managed in energy systems with high penetration of PV solar energy.

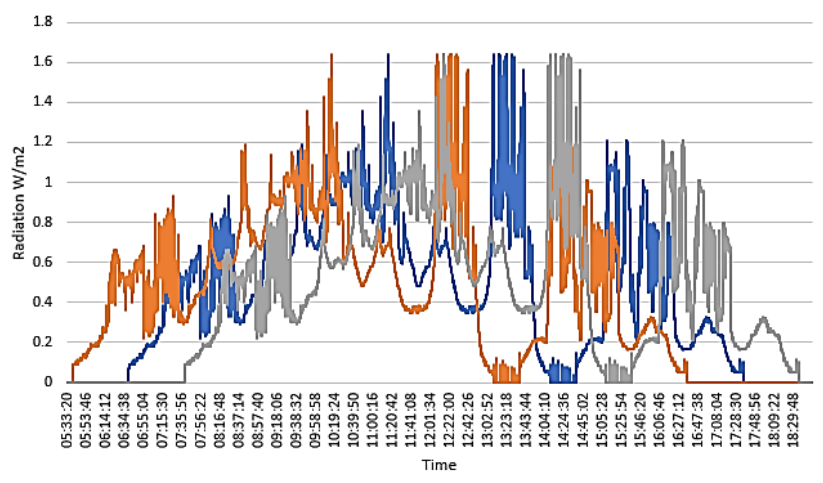


Fig. 5. Simulated Solar Radiation Considering Cloud Movement

Furthermore, regarding the control executed by the aggregator, the following scenarios were analyzed:

1. A single aggregator that controls all EVs on a feeder, using a single PV resource signal as a reference.
2. Multiple aggregators that control portions of EVs on a feeder, using a single PV resource signal as a reference.
3. Multiple aggregators that control portions of EVs on a feeder, using multiple PV resource signals as references.

The analysis was conducted on the IEEE European Low Voltage Test Feeder system, where 14 EVs with 7.4kW of power and 14 PV systems with 1kVA were located. These power values were chosen to illustrate the effect shown in this study and to avoid significant distortion of the IEEE case analyzed, as it is an underground system with very low loads. The simulation was carried out using OpenDSS and MATLAB. EVs were modeled as batteries, and EV aggregators were modeled as storage controllers. The default simulator model was used for the PV systems (see Fig. 6). The EVs were connected from 13:00 to 17:00, following a typical connection pattern for public parking

8

lots during their second connection to the system. This connection time was also chosen to coincide with the variation of the PV resource.

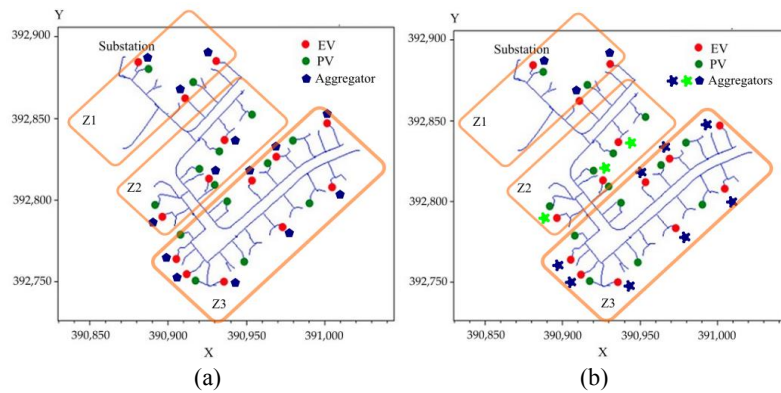


Fig. 6. Simulated System Considering the Location of Electric Vehicles, Photovoltaic Generation, Electric Vehicle Aggregators, and Cloud Movement Zones (a) Case 1 (b) Cases 2 and 3.

4 Results

The simulation carried out in the OpenDSS environment involved an analysis over a 24-hour period, taking into account the electrical loads inherent to the IEEE system. In the first analysis conducted, the power supplied by the substation feeding the circuit of interest was considered, as shown in Figure 7. During the course of this analysis, it was observed that both case 1 and case 2 reached their maximum power value at 16:63 hours, registering a level of 115.8 kilowatts (kW). In contrast, case 3 exhibited a lower power demand, reaching its peak at 16:67 hours, with a value of 91.19 kW. These results clearly indicate that the scenario involving multiple aggregators and considering different PV solar radiation signals manages to reduce the power required by the substation and optimizes the use of energy stored in both EVs and PV systems.

This finding highlights the importance of intelligent energy management, harnessing both renewable energy sources and the capacity of EVs to act as energy storage and demand response devices. The implementation of effective coordination strategies, as observed in case 3, can lead to more efficient operation of the electrical system, reducing the burden on the substation and improving the utilization of available resources. These results support the viability and potential of EV aggregators as tools to enhance the quality and stability of electrical power systems with high integration of PV solar energy.

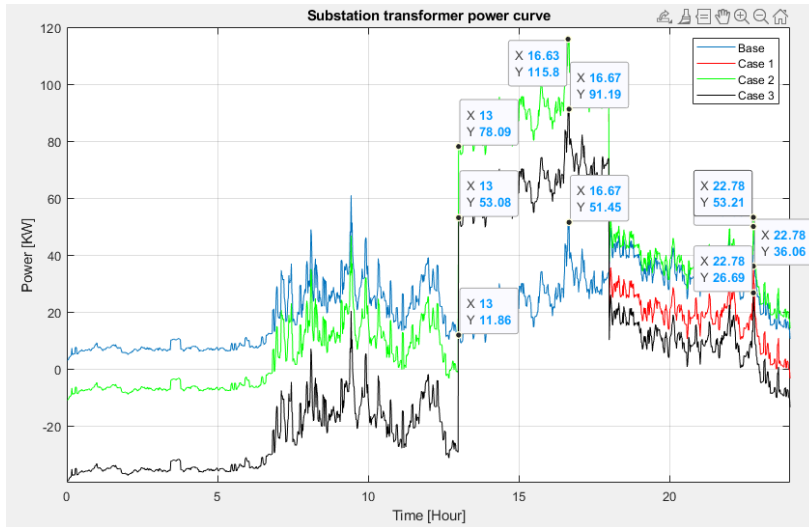


Fig. 7. Power Delivered by the Substation

Analyzing the voltage at load 349 (see Fig. 8) shows that case 3 causes a lower voltage drop compared to the other cases, with a value of 233.9V. This behavior is consistent during the stages when EVs begin their charging or when vehicles supply energy to the system.

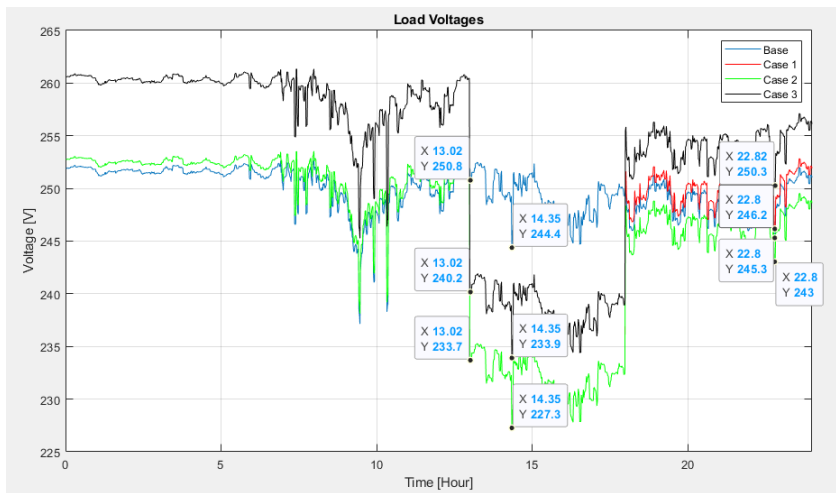


Fig. 8. Voltage at System Loads

10

Finally, the state of charge (SOC) of EVs and their charging behavior was reviewed. It was observed that although there is a very small variation in SOC, ranging from 33.55% to 33.42% (see Fig. 9), when analyzing the time EVs spend in charge and discharge states, it is evident (see Fig. 10) that vehicles enter charge and discharge at different times.

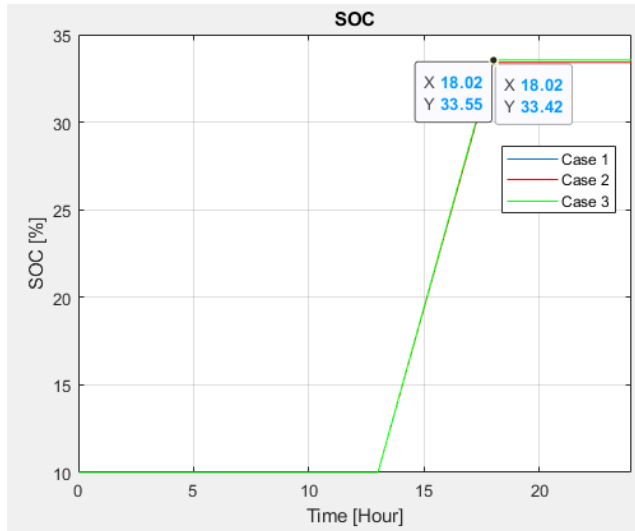


Fig. 9. Electric Vehicle State of Charge.

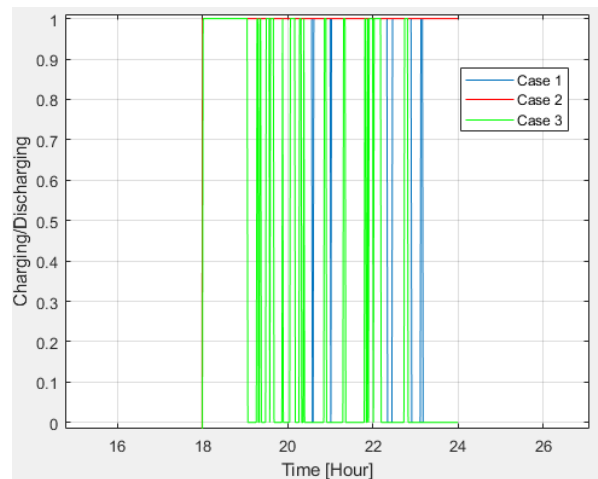


Fig. 10. Charging and Discharging Events

When analyzing the detailed charging and discharging times, Table 1 shows that in all cases, the charging time is the same. However, the discharging time is shorter for case 3, which means less battery deterioration for the EV. Table 1 also presents the results of substation power and minimum load voltage. It can be observed that in case 3, the substation delivers less power to supply the system loads and improves the minimum system voltage compared to the base case.

Table 1. Charge and discharge time of different scenarios

Case	Charge time [minutes]	Discharge time [minutes]	Substation Power [kW]	Minimum load voltage [V]
Base	-	-	51.45	244.4
Case 1	300	288	115.8	227.3
Case 2	300	361	115.8	227.3
Case 3	300	119	91.19	233.9

5 Conclusions and future work

The present study conducts an analysis of the effect of PV resource variability and its geographical coverage, which leads to delays in the times when peaks or valleys occur within the radiation curve, resulting in power and voltage variations in electrical systems with high PV generation penetration. To address this issue, the use of multiple EV aggregators that consider PV radiation curves in different areas of the system was proposed, thereby altering the times when EVs deliver and consume energy. This methodology demonstrated its potential to reduce substation power demand and enhance the voltage response of the system.

In summary, this research highlights the importance of considering not only the variability of PV resources but also their geographical distribution in the design and operation of electrical systems with high PV generation. The implementation of innovative strategies, such as multiple EV aggregators, can significantly contribute to the efficient management of these systems, leading to improved overall performance and stability.

As future work, it is necessary to have more data from different weather stations synchronized by GPS to observe this phenomenon in other locations of the city. Additionally, it is required to determine station location strategies based on the observed delay, and to conduct larger-scale simulations in the electrical system. An analysis of the optimal number of EV aggregators is required to enhance the overall system response. Furthermore, a capacity hosting analysis is needed to correlate the penetration of EVs, PV generation, and the number of aggregators controlling the system. This analysis will help determine the most efficient configuration for managing both EVs and PV resources within the electrical grid.

Acknowledgement

The authors thank the Universidad de Cuenca and Universidad de Valladolid, who through a cooperation framework agreement and the specific agreement to regulate their collaboration in research in the field of electrical microgrids and renewable energies have made this work possible.

The authors thank Universidad de Cuenca for easing access to the facilities of the Microgrid Laboratory of the Centro Científico Tecnológico y de Investigación Balzay (CCTI-B), for allowing the use of its equipment, and for authorizing its staff the provision of technical support necessary to carry out the experiments described in this article.

References

- [1] K. Yurtseven, E. Karatepe, y E. Deniz, “Sensorless fault detection method for photovoltaic systems through mapping the inherent characteristics of PV plant site: Simple and practical”, *Sol. Energy*, vol. 216, núm. January, pp. 96–110, 2021, doi: 10.1016/j.solener.2021.01.011.
- [2] P. Chaudhary y M. Rizwan, “Voltage regulation mitigation techniques in distribution system with high PV penetration: A review”, *Renew. Sustain. Energy Rev.*, vol. 82, núm. October 2017, pp. 3279–3287, 2018, doi: 10.1016/j.rser.2017.10.017.
- [3] T. Aziz y N. Ketjoy, “PV Penetration Limits in Low Voltage Networks and Voltage Variations”, *IEEE Access*, vol. 5, pp. 16784–16792, 2017, doi: 10.1109/ACCESS.2017.2747086.
- [4] J. M. Clairand, J. Rodríguez-García, y C. Álvarez-Bel, “Electric vehicle charging strategy for isolated systems with high penetration of renewable generation”, *Energies*, vol. 11, núm. 11, 2018, doi: 10.3390/en11113188.
- [5] K. Sevdari, L. Calearo, P. B. Andersen, y M. Marinelli, “Ancillary services and electric vehicles: An overview from charging clusters and chargers technology perspectives”, *Renew. Sustain. Energy Rev.*, vol. 167, núm. June, p. 112666, 2022, doi: 10.1016/j.rser.2022.112666.
- [6] Y. Zheng, Y. Wang, y Q. Yang, “Two-phase operation for coordinated charging of electric vehicles in a market environment: From electric vehicle aggregators’ perspective”, *Renew. Sustain. Energy Rev.*, vol. 171, núm. October 2022, p. 113006, 2023, doi: 10.1016/j.rser.2022.113006.
- [7] J. L. Espinoza, L. G. Gonzalez, y R. Sempertegui, “Micro grid laboratory as a tool for research on non-conventional energy sources in Ecuador”, en *2017 IEEE International Autumn Meeting on Power, Electronics and Computing (ROPEC)*, nov. 2017, vol. 2018-Janua, núm. Ropec, pp. 1–7, doi: 10.1109/ROPEC.2017.8261615.
- [8] I. Aguirre *et al.*, “Charge Management of Electric Vehicles from Undesired Dynamics in Solar Photovoltaic Generation”, *Appl. Sci.*, vol. 12, núm. 12, 2022, doi: 10.3390/app12126246.

- [9] J. Huang, A. Troccoli, y P. Coppin, “An analytical comparison of four approaches to modelling the daily variability of solar irradiance using meteorological records”, *Renew. Energy*, vol. 72, pp. 195–202, 2014, doi: 10.1016/j.renene.2014.07.015.
- [10] P. Ineichen y R. Perez, “A new airmass independent formulation for the linke turbidity coefficient”, *Sol. Energy*, vol. 73, núm. 3, pp. 151–157, 2002, doi: 10.1016/S0038-092X(02)00045-2.
- [11] M. Tapia, D. Heinemann, D. Ballari, y E. Zondervan, “Spatio-temporal characterization of long-term solar resource using spatial functional data analysis: Understanding the variability and complementarity of global horizontal irradiance in Ecuador”, *Renew. Energy*, vol. 189, pp. 1176–1193, 2022, doi: 10.1016/j.renene.2022.03.049.
- [12] P. Makeen, H. A. Ghali, S. Memon, y F. Duan, “Insightful Electric Vehicle Utility Grid Aggregator Methodology Based on the G2V and V2G Technologies in Egypt”, *Sustainability*, vol. 15, núm. 2, p. 1283, 2023, doi: 10.3390/su15021283.

Securing Smart-city IoT Devices: Challenges, Regulations, and Solutions

Andrei Tchernykh^{1,2,*}[0000-0001-5029-5212], Mikhail Babenko^{2,3}[0000-0001-7066-0061], Ekaterina Bezuglova³[0000-0002-7608-0452], Sergio Nesmachnow⁴[0000-0002-8146-4012], Alexander Yu. Drozdov⁵[0000-0001-5607-2749]

¹ Computer Science Department, CICESE Research Center, Ensenada 22860, Mexico, chernykh@cicese.mx;

² Control/Management and Applied Mathematics, Ivannikov Institute for System Programming, 109004 Moscow, Russia chernykh@cicese.mx;

³ North-Caucasus Center for Mathematical Research, North-Caucasus Federal University, 355017, Stavropol, Russia {mgbabenco, eksbezuglova}@ncfu.ru

⁴ Faculty of Engineering, Universidad de la República, Montevideo 11300, Uruguay sergion@fing.edu.uy

⁵ Laboratory of Design and Modeling of Special-Purpose Computer Systems, Moscow Institute of Physics and Technology, 141701 Moscow, Russia, alexander.y.drozdov@gmail.com

*Correspondence: chernykh@cicese.mx

Abstract. Rapid integration of Internet of Things (IoT) devices into smart city infrastructure is an important step of deep urban innovation. However, this massive increase in connectivity also opens up vulnerabilities requiring vigilant data protection measures. In this paper, we encapsulate the central problems and innovative solutions for robust data security within smart city device design. We discuss challenges such as IoT vulnerabilities, the difficult balance between data collection and privacy, the evolving spectrum of cyber threats, and solutions that encompass end-to-end encryption, data anonymization, blockchain technology, and AI-powered threat detection. These actions not only protect sensitive data but also unlock the full potential of IoT devices to optimize the urban environment, building trust and resilience in urban ecosystems. We show how, through these integrated solutions, smart cities can overcome the complexities of this multi-dimensional problem and provide technologies that enrich citizens' lives while preserving their privacy and security. To reduce the computational complexity of Lightweight cryptography of IoT devices, we propose two modifications of the Chinese remainder theorem and demonstrate their practical advantages.

Keywords: Internet of Things, Data Security, Smart City, Cyberattack, Data Storage, Machine Learning, IoT devices, IoT regulations, Lightweight cryptography.

2

1 Introduction

Smart cities represent the future of urban living, leveraging technology to enhance the efficiency, sustainability, and quality of life for their residents. At the heart of this transformation lies the Internet of Things (IoT), a vast network of interconnected devices that collect and exchange data to inform decision-making processes [1]. However, this technological advancement also presents significant data security challenges. Many solutions offer great potential for data security in smart city devices, identifying emerging challenges and exploring possible approaches to protect information [2].

The rapid urbanization of our world has driven the growth of smart cities. According to the United Nations, over half of the world's population now resides in cities, with this number expected to surge to 68% by 2050. This mass migration has triggered a multitude of challenges, from traffic congestion to resource scarcity, compelling cities to seek innovative ways to manage their growing populations. Smart city technologies have to rely heavily on data collection and analysis to optimize urban functioning.

IoT is the backbone of smart city infrastructure. Its devices range from sensors to cameras and actuators, from smart mobiles to smartwatches, from smart fire alarms to smart door locks and light switches, from smart bicycles to smart cars, from medical sensors to fitness trackers and air pollution monitors, and many others. They collect vast amounts of data on various aspects of urban life, such as traffic, energy consumption, environmental conditions, etc. [3]. This data is instrumental in making informed decisions that can lead to more efficient resource allocation and improved urban planning.

While the potential benefits of IoT devices in smart cities are substantial, they are accompanied by a host of data security challenges. One major issue is the vulnerability of these devices to cyberattacks. Unauthorized access to smart city systems can result in data breaches, privacy violations, and even disruptions in essential services. Recent incidents, such as the 2016 Mirai botnet attack that targeted IoT devices, underscore the urgency of addressing these challenges [4].

To mitigate data security risks, regulatory frameworks have been developed at various levels of government by standardization bodies. These frameworks outline security requirements and guidelines for the design and operation of IoT devices. However, they often lack the specificity and comprehensiveness required to keep pace with evolving threats.

Encryption and authentication play a pivotal role in securing data. Encryption techniques, such as end-to-end encryption and Secure Socket Layers (SSL), ensure that data is transmitted securely between devices and servers [5]. Meanwhile, authentication mechanisms, including multi-factor authentication, help control access to these devices and the data they collect.

Effective data security also relies on the use of secure communication protocols. Protocols like Message Queuing Telemetry Transport (MQTT) and Constrained Application Protocol (CoAP) are designed for IoT applications, providing secure and efficient data transfer [6]. Selecting a protocol depends on factors like device type, network constraints, and data sensitivity.

3

Securing data storage is another critical aspect of data security in smart city devices. Robust encryption and access controls must be in place to safeguard data stored on these devices and within cloud-based systems. Furthermore, data anonymization techniques can help protect individual privacy while still enabling meaningful data analysis.

In the dynamic landscape of smart cities, data security is non-negotiable. As urban environments evolve, there is an urgent need to address the challenges associated with the use of IoT devices. While regulatory frameworks provide a foundation for security, designers, developers, and policymakers must adopt a proactive approach, implementing encryption, authentication, and secure communication protocols to protect sensitive data. So we can unlock the full potential of smart cities while ensuring the privacy and security of their residents.

2 Towards Urban Sustainability

2.1 Urbanization

The 21st century has witnessed a remarkable shift in the way we live and work. More people than ever before are choosing cities as a place to live. This trend toward urbanization has led to both unprecedented opportunities and challenges, demanding innovative solutions to address urban complexities. We are entering an era of transformational vision that uses technology and data to redefine urban life.

In this paper, we look at the evolution and impact of smart cities, focusing on their role in creating safe, green, and efficient urban centers with advanced sensors, electronics, and networking infrastructures that stimulate sustainable economic growth and high quality of life.

At their core, smart cities are driven by the concept of data-driven decision-making, wherein data collected from various sources is analyzed to optimize city operations [7]. To transform traditional urban areas into smart cities, several key elements must be in place. They include a robust Information and Communication Technology (ICT) infrastructure, a network of interconnected devices, and data analytics capabilities. These building blocks enable cities to collect, process, and act upon vast amounts of data generated by citizens, devices, and infrastructure.

Across the globe, numerous cities are embracing the smart city concept and initiating projects that showcase its potential. For instance, Singapore's Smart Nation program [8] incorporates a wide range of technologies to improve the quality of life for its citizens, from intelligent transportation systems to smart healthcare solutions. Barcelona's use of IoT devices and data analytics has turned it into a model of urban sustainability, allowing it to optimize energy consumption and reduce its environmental impact [7].

One of the most significant impacts of smarting is its contribution to sustainability. By optimizing resource allocation and reducing waste, these cities can significantly reduce their environmental footprint. For example, smart traffic management systems can alleviate congestion and reduce air pollution [9]. Energy-efficient building designs can lower energy consumption [10].

4

While the promise of smart cities is undeniable, they also face significant challenges. These include concerns about data privacy and security, the potential for increased surveillance, and the digital divide, which can leave marginalized communities behind in the race toward urban technological transformation. With careful planning, innovation, and collaboration between governments, businesses, and communities, smart cities can pave the way for a brighter urban future.

2.2 The Role of IoT Devices

The modern urban landscape is undergoing a profound transformation, powered by connectivity technology. Central to this revolution are IoT devices that work tirelessly to collect and transmit data driving intelligent decision-making. In this section, we explore their significance, applications, and transformative impact.

IoT devices, at their core, are physical objects embedded with sensors, software, and connectivity features. These devices are designed to collect data from the environment and transmit it via the Internet or other networks. They take many forms, from simple environmental sensors to complex mechanisms, and are the building blocks of the digital infrastructure that supports smart cities.

The applications of IoT are as diverse as the cities themselves. These devices play a pivotal role in collecting data on a wide range of urban aspects, including smart transportation, environmental monitoring, waste management, public safety, utilities management et al. This data is collected from sensors and devices distributed across the urban landscape. The true power of IoT devices lies in their ability to generate vast amounts of data, transforming cities into data-driven entities, and providing invaluable insights that enable cities to optimize their operations.

Despite their promise, IoT devices also raise concerns. Data privacy and security are significant issues, as the collection of data can pose risks if not adequately protected [11]. Moreover, the sheer volume of data generated can overwhelm existing infrastructure, requiring robust data management and on-the-fly analysis solutions.

As technology advances, we can expect even more sophisticated sensors and improved connectivity, leading to more precise data collection and enhanced decision-making. The growth of 5G networks and edge computing will also facilitate real-time data processing and analysis, enabling cities to respond faster to changing conditions.

However, as the IoT ecosystem continues to grow, it's essential to address challenges related to data privacy and infrastructure scalability. With careful planning and innovative solutions, IoT devices will continue to be at the forefront of shaping smart cities.

3 Data Security Challenges

3.1 Protecting Information Assets

The data security challenges and risks are numerous and very diverse including Malware, Ransomware; Denial of service (DoS) attacks; Spam and Phishing; Corporate Account Takeover (CATO); Misconfiguration leaving data unprotected; Unauthorized access to data; Authentication; Inadequate access controls; Cyberattacks and data breaches; Hijacking of accounts; Insecure interfaces and APIs; Malicious insiders,

5

employee frauds; Data loss; Negligence in data management; Data tampering; Eavesdropping and data theft; Falsifying user identities; Password-related threats; Fake data, Data cleaning failure; Unprotected data mining; Difficulty to protect complex big data; Data poisoning, Data storage, Transmission, and Processing; Encryption and Key Management; etc.

Data breaches are among the most severe consequences of data security lapses.

Notable incidents like the Equifax breach and the Capital One hack have demonstrated the far-reaching consequences of data breaches, including financial losses, reputational damage, and legal ramifications.

The threat landscape is continually evolving, with attackers developing new tactics and technologies. Advanced Persistent Threats (APTs), zero-day vulnerabilities, and AI-driven cyberattacks represent emerging challenges [14]. Organizations must stay vigilant and adapt their security strategies accordingly. While technology poses security challenges, it also provides solutions. Security tools like firewalls, intrusion detection systems, and encryption technologies are essential for protecting data. Additionally, AI and machine learning are being used to detect and respond to threats in real time.

Data security challenges have spurred the creation of stringent data protection regulations. These regulations, such as the European Union's GDPR, impose strict requirements on organizations to safeguard data and notify authorities of breaches promptly: access control, encryption, regular audits, employee training, and incident response plans.

Data security challenges are a persistent aspect of our digital age. Organizations and individuals must remain vigilant in the face of evolving threats. By adopting best practices, leveraging technology, and staying informed about the latest threats, we can navigate these challenges and protect our valuable data assets. In a world where data is both a treasure and a target, data security remains paramount for our digital future.

The essential principles for effective security are protection, detection, verification, and reaction.

3.2 Threat Detection and Response

Here we discuss threat detection and response technologies, demonstrating strategies, technologies, and best practices.

Smart cities are not immune to threats. Their highly interconnected nature makes them susceptible to various types of risks, including cybersecurity threats, physical security risks, emergencies, and disasters [22]. Various technologies for threat detection are employed:

- **AI and Machine Learning:** These technologies enable the analysis of vast datasets to identify patterns and anomalies that may indicate security threats [26].
- **IoT Sensors:** IoT devices can monitor physical infrastructure and environmental conditions, detecting anomalies that may signal physical security risks.
- **Network Monitoring Tools:** These tools track network traffic to identify suspicious activities and potential cyber threats.

Emerging technologies such as 5G/6G networks and cloud-edge-fog computing will play a significant role in threat detection and response. By embracing advanced technologies, fostering collaboration among stakeholders, and implementing best practices

6

in threat detection and response, smart cities can create resilient urban environments that are prepared to face the challenges of the digital age.

3.3 Building the Foundation: Regulatory Frameworks

To ensure the responsible and equitable development of smart cities, regulatory frameworks play a crucial role. In this section, we explore the significance of regulatory frameworks in smart cities, the challenges they address, and their impact on shaping the urban landscape of the future.

Smart cities leverage technology and data to enhance the quality of life for their residents and optimize urban services. These cities employ a wide range of technologies, including IoT devices, data analytics, and digital infrastructure, to collect and analyze data for informed decision-making.

As smart cities continue to evolve, they face various challenges related to data privacy, cybersecurity, sustainability, and equitable access to technology. Regulatory frameworks are essential to provide guidelines, standards, and legal mechanisms that address these challenges and ensure that smart city initiatives align with broader societal goals.

Regulatory frameworks span several critical areas: data privacy, cybersecurity, infrastructure standards, environmental sustainability, and equitable access.

Case Studies of Regulatory Frameworks:

1. European Union's GDPR: The General Data Protection Regulation (GDPR) is a significant regulatory framework that affects smart cities across Europe. It mandates strict data protection and privacy measures, influencing how cities collect, store, and use data [15].
2. Singapore's Smart Nation Initiative: Singapore has developed comprehensive regulatory frameworks to support its Smart Nation initiative. These frameworks encompass data privacy, cybersecurity, and technology standards, ensuring the responsible deployment of smart technologies [16].
3. India's Smart Cities Mission: India's ambitious Smart Cities Mission emphasizes the importance of regulatory frameworks. It encourages cities to establish regulations for various aspects, including data management, environmental sustainability, and urban planning [17].

While regulatory frameworks are essential, they also face challenges, such as the need for agility in a rapidly evolving technological landscape and the potential for stifling innovation if regulations become too restrictive. Balancing innovation and security is a continual challenge for policymakers [24].

Smart city regulations often benefit from international collaboration. Cities around the world can learn from one another's experiences and share best practices. Organizations like the United Nations and the International Organization for Standardization (ISO) contribute to the development of global standards and guidelines.

As smart cities continue to grow, regulatory frameworks will evolve to address new challenges and opportunities. The rise of 5G technology, edge computing, and quantum computing will require updated regulations to ensure the security and reliability of smart city infrastructure.

7

Regulatory frameworks are the backbone of responsible and sustainable smart city development. They provide the necessary guidelines and standards to protect data, enhance cybersecurity, promote equitable access, and ensure the overall well-being of urban residents. As smart cities continue to shape the urban landscape, regulatory frameworks will play a pivotal role in harnessing the full potential of technology while safeguarding the rights and interests of citizens. In a world where the future is increasingly digital, these frameworks are essential for building smarter, safer, and more inclusive cities.

4 Secure Communication Protocols

Smart cities are at the forefront of urban transformation, driven by the integration of technology and data. At the heart of this evolution lies the need for secure communication protocols, ensuring that data flows smoothly while remaining impervious to threats. Here we discuss the critical role of secure communication protocols, exploring their significance, challenges, and impact on creating resilient and secure urban environments.

Smart cities represent a paradigm, where data-driven decision-making, digital infrastructure, and IoT devices converge to create efficient data management. To realize their full potential, secure communication protocols are essential, serving as the backbone of data exchange and connectivity.

Secure communication protocols ensure that information is transmitted safely, protecting it from eavesdropping, cyberattacks, and unauthorized access. These protocols are vital for maintaining data integrity, confidentiality, and availability. There are various communication protocols to facilitate data exchange. Some commonly used protocols include MQTT, CoAP, and HTTP/HTTPS.

MQTT (Message Queuing Telemetry Transport) is a lightweight and efficient protocol for IoT devices. It is widely used in applications like smart energy grids and environmental monitoring [18].

CoAP (Constrained Application Protocol): designed for resource-constrained IoT devices. It enables efficient communication between devices and servers, making it ideal for smart city deployments [19].

HTTP/HTTPS (Hypertext Transfer Protocol): These familiar protocols are used for web-based communication in smart city applications, such as real-time traffic management and smart grids [20].

To address these challenges, several solutions and best practices are employed:

1. End-to-End Encryption: Encrypting data from the source to the destination ensures that only authorized parties can access it. Protocols like SSL/TLS (Secure Sockets Layer/Transport Layer Security) provide robust encryption for web-based communication.
2. Role-Based Access Control: Implementing access controls ensures that data is only accessible to authorized users or devices. Role-based access control mechanisms can restrict access based on user roles.

8

3. Network Segmentation: Segmenting networks can help contain security breaches, ensuring that a compromise in one segment doesn't affect the entire smart city infrastructure.
4. Regular Security Audits: Regular security audits and vulnerability assessments are essential to identify and rectify security weaknesses in communication protocols and systems.
5. Multi-Factor Authentication: Implementing multi-factor authentication adds an extra layer of security, requiring users or devices to provide multiple forms of authentication before access is granted.

5 Lightweight cryptography

5.1 Key challenge

Lightweight cryptography is an innovative solution for cryptographic algorithms to secure IoT devices including Radio Frequency Identification (RFID) systems, wireless sensor networks, vehicle ad-hoc networks, healthcare devices, and so on. The motivation and key challenge of embedding cryptography in IoT devices is to protect data on resource-limited devices: limited memory, reduced computing power, and limited battery power [23]. Moreover, they deal with real-time applications requiring a quick and accurate response.

Advanced Encryption Standard (AES) and Elliptic Curve Cryptography (ECC) are the most suitable for designing lightweight cryptographic primitives [25, 29]. The lightweight cryptography is simpler and faster compared to conventional cryptography [30-31].

Table 1 shows several characteristics of the hardware implementations of lightweight cryptography for Internet of Things devices. It shows implementations of AES, CAMELLIA, CLEFIA, 3-DES, and KATAN. L_{block} is the block size, L_{key} is the key size, N_{round} – number of rounds of encryption, N_{cycles} – number of cycles, GE - Gate Equivalent

Table 1. Hardware implementation of lightweight cryptography for Internet of Things devices.

Ref.	Code	L_{block}	L_{key}	N_{round}	N_{cycles}	GE
[1]	AES	128	128	10	160	3100
[2]	AES	128	128	10	1032	3488
[3]	AES	128	128	10	226	2400
[4]	CAMELLIA	128	128	18		11350
[5]	CLEFIA	128	128	36		4950
[6]	3-DES	64	168	48		2309
[7]	AES	128	128	10		3120
[8]	AES	128	128	10	27	18288
[9]	KATAN	32	80	35	3	6867

We see that the implementation results vary greatly depending on the objective of the developers. The size of the chip depends significantly on the implementation architecture, which, in turn, is dictated by the final optimization goals, such as area, speed, energy consumption, etc. While the first one is achieved through the use of serial archi-

ture that processes information byte by byte, high speed is achieved through the parallelization and pipeline processing of data, which inevitably leads to an increase in chip size and more power.

To reduce the computational complexity of key exchange algorithms in asymmetric lightweight cryptography, we use the Residual Number System (RNS) [33]. It allows to parallelize the process of calculating arithmetic operations with long numbers over a simple field and to reduce the number of carries during their calculation. RNS uses the Montgomery algorithm to implement the modular multiplication operation. Even if subtraction and multiplication operations in RNS are performed efficiently, it is important to optimize the algorithm of number base expansion in RNS to improve the performance of devices implementing lightweight cryptography.

To implement the number base expansion algorithm in RNS and reduce the computational complexity, we propose to use a minimal-redundant RNS. We prove that with certain parameters the mechanism allows for minimizing resource costs and provides minimum redundancy in terms of hardware cost.

Wireless data transmission technologies, depending on their range, can be divided into two categories. The first category includes short-range Wi-Fi communication technologies, Bluetooth, etc., and typical application scenarios such as smart homes. The second category - Low-Power Wide-Area Networks (LPWAN) is used to build autonomous data transmission systems. However, it is worth noting that it has a low data transfer rate, which imposes additional restrictions on the data encryption algorithms. LoRa and DASH7 networks use the symmetric AES128 encryption algorithm to ensure security [27]. However, it is necessary to use session keys, which are generated using asymmetric cryptographic algorithms based on the use of an elliptic curve or NTRU.

5.2 Efficient implementation of basis expansion in RRNSs

The use of error correction codes based on the residual number system (RNS) can improve the reliability of distributed data storage, transmission, and data processing in IoT devices [10]. However, it is worth noting that the algorithms for converting numbers from RNS to positional number system (PNS), determining the sign of a number, comparing numbers, scaling, and determining dynamic range overflow are computationally complex [11].

To compute them, the representation of a number in RNS or positional characterization must be computed [11]. The Chinese Remainder Theorem (CRT) and its modifications, Garner's algorithm and its modifications, diagonal function, and Akushsky's kernel function are used to convert a number from RNS to PNS [11].

Here, we discuss how to efficiently implement the CRT.

The RNS moduli p_1, p_2, \dots, p_n are pairwise mutually prime numbers. Without loss of generality, we assume that the RNS moduli satisfy the condition $p_1 < p_2 < \dots < p_n$. An integer $X \in [0, P)$ is represented as a tuple (x_1, x_2, \dots, x_n) , where $\forall i = \overline{1, n}: x_i = |X|_{p_i}$.

There are two forms of representing the Chinese remainder theorem: CRTI and CRTII.

Using the first representation CRTI, X can be calculated as:

10

$$X = \sum_{i=1}^n P_i ||P_i^{-1}|_{p_i} x_i|_{p_i} - r_x P,$$

In the second representation CRTII:

$$X = \sum_{i=1}^n P_i |P_i^{-1}|_{p_i} x_i - R_x P$$

where $P = \prod_{i=1}^n p_i$, $P_i = P/p_i$ and $r_x = \left\lfloor \frac{1}{P} \sum_{i=1}^n P_i ||P_i^{-1}|_{p_i} x_i|_{p_i} \right\rfloor$, $R_x = \left\lfloor \frac{1}{P} \sum_{i=1}^n P_i |P_i^{-1}|_{p_i} x_i \right\rfloor$.

We propose two modifications of CRT: mCRTI and mCRTII.

In the first modification mCRTI, if $\forall i = \overline{1, n}: \gcd(p_i, q) = 1$, $q \geq n$ and $y = |X|_q$ then

$$r_x = \left\lfloor -y + \sum_{i=1}^n k_i ||P_i^{-1}|_{p_i} x_i|_{p_i} \right\rfloor,$$

where $\forall i = \overline{1, n}: k_i = |p_i^{-1}|_q$.

In the second modification mCRTII, if $\forall i = \overline{1, n}: \gcd(p_i, Q) = 1$, $Q > -n + \sum_{i=1}^n p_i$ and $z = |X|_Q$ then

$$R_x = \left\lfloor -z + \sum_{i=1}^n w_i x_i \right\rfloor_Q,$$

where $\forall i = \overline{1, n}: w_i = ||p_i^{-1}|_Q |P_i^{-1}|_{p_i}|_Q$.

These modifications enable getting away from the computationally expensive operation of finding the remainder of division by the range of RNS P by calculating values using the auxiliary module q or Q that are less than P .

To show their practical advantage, a set of programs in the Python programming language was developed. Modeling is carried out on a personal computer running the operating system MacOS Monterey ver. 12.6, processor 2.7 GHz 2-core Intel Core i5, RAM 8 GB 1867 MHz DDR3.

RNS parameters used for modeling are presented in Table 2.

Table 2. RNS parameters

n	Moduli	q	Q	$[P]$
4	{127, 131, 137, 139}	4	531	29
5	{127, 131, 137, 139, 149}	5	679	36
6	{127, 131, 137, 139, 149, 151}	6	829	43
7	{127, 131, 137, 139, 149, 151, 157}	7	985	50
8	{127, 131, 137, 139, 149, 151, 157, 163}	8	1147	58
9	{127, 131, 137, 139, 149, 151, 157, 163, 167}	9	1313	65
10	{127, 131, 137, 139, 149, 151, 157, 163, 167, 173}	10	1485	73
11	{127, 131, 137, 139, 149, 151, 157, 163, 167, 173, 179}	11	1663	80

Fig. 1 shows simulation results. Each of the measurements corresponds to the conversion of one hundred numbers from RNS to PNS.

11

We can conclude that the classical implementation of CRTI and CRTII are 1.50 times and 1.72 times slower, on average, than the proposed modifications, respectively. However, the proposed modification requires storing, transmitting, and processing the divisor and the separation residue.

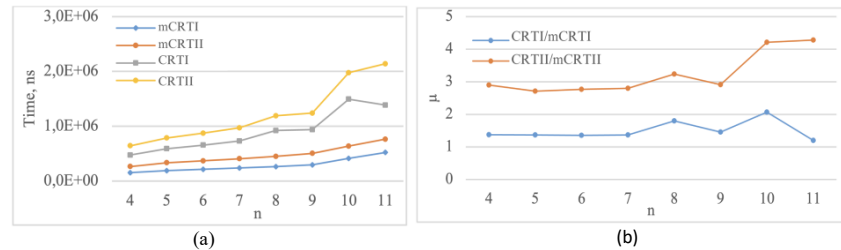


Figure 1. (a) Conversion time from RNS to PNS, (b) How much the classical implementation of the Chinese remainder theorem CRTI and CRTII demonstrate lower performance than the proposed mCRTI and mCRTII

6 Data Storage and Privacy

We explore the crucial aspects of data storage and privacy in smart cities, examining the challenges, best practices, and innovations that are essential for maintaining the trust and security of citizens in this digital age.

Data storage is the backbone of smart city operations. Vast amounts of data are generated daily from various sources, including IoT devices, sensors, and citizen interactions. Proper data storage is necessary for efficient data management, analysis, and decision-making [28].

Smart cities face several challenges in data storage:

1. **Volume:** The sheer volume of data generated by smart city devices can overwhelm traditional storage systems.
2. **Security:** Protecting stored data from unauthorized access and breaches is a paramount concern.
3. **Data Lifespan:** Deciding how long to retain data and when to delete it is critical for compliance with data privacy regulations.
4. **Scalability:** As smart city projects expand, storage systems must scale to accommodate growing data needs.

Data privacy is a fundamental right that must be preserved in smart cities. Residents and users of smart city services entrust their data to these systems [32], and safeguarding their privacy is of the utmost importance.

Smart cities encounter several privacy challenges: data anonymization, consent management, data ownership, and transparency [21]. To address data storage challenges and maintain data privacy, smart cities employ various solutions: cloud storage, edge computing, data encryption, and blockchain technology. Data privacy regulations, such

12

as GDPR in Europe and CCPA in California, require smart cities to adhere to strict data protection standards: mapping, access control, consent mechanisms, and privacy impact assessments.

Data storage and privacy are foundational elements the smart city development. Their future development will be driven by emerging technologies such as quantum encryption, improved data management techniques, etc. By adopting robust data storage solutions, adhering to privacy regulations, and prioritizing transparency, smart cities can build digital environments that respect the privacy and security of their residents. In this way, smart cities can forge a future where innovation thrives while safeguarding the rights and trust of their citizens.

7 Future Trends and Technologies

Innovative trends and technologies for urban development are emerging. Here we show the future trends and technologies that will shape the landscape of smart cities, from 5G connectivity to edge computing [20].

5G technology is poised to be a game-changer for smart cities. With its high-speed, low-latency capabilities, 5G networks will enable real-time communication between IoT devices, paving the way for faster and more responsive city services. Applications include smart transportation, IoT sensors, augmented reality, and virtual reality. Edge computing brings data processing closer to the source, reducing latency and enabling real-time decision-making [18]. This technology has several applications: real-time analytics, smart grids, and public safety.

AI and ML will continue to play a central role in smart cities, enabling predictive analytics, automation, and data-driven decision-making:

1. Predictive Maintenance. AI algorithms can predict when infrastructure components, such as bridges or streetlights, require maintenance, reducing downtime.
2. Traffic Management. ML models can optimize traffic signals and public transportation in real time, reducing congestion and emissions.
3. Energy Efficiency. AI-driven systems can optimize energy consumption in buildings, reducing costs and environmental impact.

Blockchain offers secure and transparent data transactions, which can have various applications in smart cities:

1. Supply Chain Management: Blockchain can track the origin and distribution of goods and ensure transparency in the supply chain.
2. Smart Contracts: Automated smart contracts can streamline processes like property transactions and permitting.
3. Data Security: Blockchain's immutable ledger can enhance data security and privacy.
4. Sustainability is a key focus for smart cities. Emerging technologies include:
5. Renewable Energy Integration: Smart cities will increasingly rely on renewable energy sources like solar and wind.
6. Circular Economy: Implementing circular economy principles to reduce waste and promote recycling.

13

7. **Urban Farming:** Vertical farming and urban agriculture can provide fresh, locally sourced food while reducing carbon footprints.

Smart cities are shifting toward more human-centric design, prioritizing the needs and well-being of residents: accessibility, public spaces, and affordable housing. While these trends and technologies hold immense promise, they also present challenges:

1. **Data Privacy and Security:** As the volume of data collected increases, protecting privacy and ensuring data security becomes a high priority.
2. **Digital Divide:** Ensuring equitable access to technology and connectivity for all residents.
3. **Regulatory Frameworks:** Developing and adapting regulations to keep pace with technological advancements.

Smart cities are dynamic, ever-evolving entities, shaped by the relentless march of technology and innovation. The trends and technologies discussed in this article represent a glimpse into the exciting future of urban living. By embracing these advancements while addressing the associated challenges, smart cities can continue to improve the lives of their residents, enhance sustainability, and foster innovation. As we look ahead, the possibilities are boundless, and the smart city of tomorrow promises to be a more connected, efficient, and inclusive urban environment for all.

8 Conclusion

The development of smart cities through the integration of Internet of Things (IoT) devices offers unprecedented opportunities to transform urban environments. However, these opportunities are accompanied by pressing issues related to data security. Ensuring data security in the design of smart devices is not only a technological necessity but also a fundamental element for building and maintaining trust between citizens, stakeholders, and policymakers.

The problems are clear: vulnerabilities in IoT devices, data privacy concerns, and the ever-evolving landscape of cyber threats pose significant risks. However, these threats have highlighted innovative solutions that can lead the way to safe and resilient smart cities. End-to-end encryption, data anonymization techniques, blockchain technology, and AI-driven threat detection are essential steps toward safeguarding data.

However, the key challenge is to implement these techniques on resource-limited devices with limited memory, reduced computing power, limited battery power, etc. to work with real-time applications requiring quick and accurate response. Lightweight cryptography solutions unlock the full potential of IoT devices to optimize the urban environment. We propose RNS and CRT modifications to minimize hardware costs and improve the performance of lightweight cryptography solutions.

Acknowledgment

This work was supported by the Ministry of Science and Higher Education of the Russian Federation (Project 075-15-2022-294).

14

References

1. Rezk, N.G., Ezz El-Din Hemdan, Attia, A.-F., El-Sayed, A., El-Rashidy, M.A.: An efficient IoT based smart farming system using machine learning algorithms. *Multimed Tools Appl.* 80, 773–797 (2021).
2. Bernal Bernabe, J., Canovas, J.L., Hernandez-Ramos, J.L., Torres Moreno, R., Skarmeta, A.: Privacy-Preserving Solutions for Blockchain: Review and Challenges. *IEEE Access.* 7, 164908–164940 (2019).
3. Ma, M., Preum, S.M., Ahmed, M.Y., Tärneberg, W., Hendawi, A., Stankovic, J.A.: Data Sets, Modeling, and Decision Making in Smart Cities: A Survey. *ACM Trans. Cyber-Phys. Syst.* 4, 14:1-14:28 (2019).
4. Trautman, L.J., Hussein, M.T., Ngamassi, L., Molesky, M.J.: Governance of the Internet of Things (IoT). *Jurimetrics.* 60, 315 (2019).
5. Freier, A.O., Karlton, P., Kocher, P.C.: The Secure Sockets Layer (SSL) Protocol Version 3.0. Internet Engineering Task Force (2011).
6. Lin, J., Yu, W., Zhang, N., Yang, X., Zhang, H., Zhao, W.: A Survey on Internet of Things: Architecture, Enabling Technologies, Security and Privacy, and Applications. *IEEE Internet of Things Journal.* 4, 1125–1142 (2017).
7. Bibri, S.E., Krogstie, J.: Environmentally data-driven smart sustainable cities: applied innovative solutions for energy efficiency, pollution reduction, and urban metabolism. *Energy Inform.* 3, 29 (2020).
8. Chia, E.S.: Singapore’s smart nation program — Enablers and challenges. In: 2016 11th System of Systems Engineering Conference (SoSE). pp. 1–5 (2016).
9. Djahel, S., Doolan, R., Muntean, G.-M., Murphy, J.: A Communications-Oriented Perspective on Traffic Management Systems for Smart Cities: Challenges and Innovative Approaches. *IEEE Communications Surveys & Tutorials.* 17, 125–151 (2015).
10. Pacheco, R., Ordóñez, J., Martínez, G.: Energy efficient design of building: A review. *Renewable and Sustainable Energy Reviews.* 16, 3559–3573 (2012).
11. Tchernykh, A., Schwiegelsohn, U., Talbi, E., Babenko, M.: Towards understanding uncertainty in cloud computing with risks of confidentiality, integrity, and availability. *Journal of Computational Science.* 36, 100581 (2019). <https://doi.org/10.1016/j.jocs.2016.11.011>
12. Khatoun, R., Zeadally, S.: Smart cities: concepts, architectures, research opportunities. *Commun. ACM.* 59, 46–57 (2016).
13. Rabah, K., Research, M.: Convergence of AI, IoT, Big Data and Blockchain: A Review. 1, (2018)
14. Sarker, I.H., Furhad, M.H., Nowrozy, R.: AI-Driven Cybersecurity: An Overview, Security Intelligence Modeling and Research Directions. *SN COMPUT. SCI.* 2, 173 (2021).
15. Albrecht, J.P.: How the GDPR Will Change the World. *Eur. Data Prot. L. Rev.* 2, 287 (2016)
16. Hoe, S.L.: Defining a smart nation: the case of Singapore. *Journal of Information, Communication, and Ethics in Society.* 14, 323–333 (2016). <https://doi.org/10.1108/JICES-02-2016-0005>
17. Hoelscher, K.: India’s Smart Cities Mission: An Assessment. ORF Issue Brief. Issue 124, 2015. https://www.orfonline.org/wp-content/uploads/2015/12/Issue-Brief_124.pdf
18. Ejaz, W., Naeem, M., Shahid, A., Anpalagan, A., Jo, M.: Efficient Energy Management for the Internet of Things in Smart Cities. *IEEE Communications Magazine.* 55, 84–91 (2017).
19. Zhang, T., Gao, L., He, C., Zhang, M., Krishnamachari, B., Avestimehr, A.S.: Federated Learning for the Internet of Things: Applications, Challenges, and Opportunities. *IEEE Internet of Things Magazine.* 5, 24–29 (2022).

15

20. Knapp, E.D., Langill, J.T.: *Industrial Network Security: Securing Critical Infrastructure Networks for Smart Grid, SCADA, and Other Industrial Control Systems*. Syngress (2014)
21. Pulido-Gaytan, B., Tchernykh, A., Cortés-Mendoza, J.M., Babenko, M., Radchenko, G., Avetisyan, A., Drozdov, A.Y.: Privacy-preserving neural networks with Homomorphic encryption: Challenges and opportunities. *Peer-to-Peer Netw. Appl.* 14, 1666–1691 (2021).
22. Pulido-Gaytan, L.B., Tchernykh, A., Cortés-Mendoza, J.M., Babenko, M., Radchenko, G.: A Survey on Privacy-Preserving Machine Learning with Fully Homomorphic Encryption. In: Nesmachnow, S., Castro, H., and Tchernykh, A. (eds.) *High Performance Computing*. pp. 115–129. Springer International Publishing, Cham (2021).
23. Kasper, E., Schwabe, P.: Faster and Timing-Attack Resistant AES-GCM. In: Clavier, C. and Gaj, K. (eds.) *Cryptographic Hardware and Embedded Systems - CHES 2009*. pp. 1–17. Springer, Berlin, Heidelberg (2009). https://doi.org/10.1007/978-3-642-04138-9_1.
24. Feldhofer, M., Wolkerstorfer, J., Rijmen, V.: AES implementation on a grain of sand. *IEE Proceedings - Information Security*. 152, 13–20 (2005). <https://doi.org/10.1049/ip-ifs:20055006>.
25. Moradi, A., Poschmann, A., Ling, S., Paar, C., Wang, H.: Pushing the Limits: A Very Compact and a Threshold Implementation of AES. In: Paterson, K.G. (ed.) *Advances in Cryptology – EUROCRYPT 2011*. pp. 69–88. Springer, Berlin, Heidelberg (2011). https://doi.org/10.1007/978-3-642-20465-4_6.
26. Aoki, K., Ichikawa, T., Kanda, M., Matsui, M., Moriai, S., Nakajima, J., Tokita, T.: Camellia: A 128-Bit Block Cipher Suitable for Multiple Platforms — Design and Analysis. In: Stinson, D.R. and Tavares, S. (eds.) *Selected Areas in Cryptography*. pp. 39–56. Springer, Berlin, Heidelberg (2001). https://doi.org/10.1007/3-540-44983-3_4.
27. Hong, D., Lee, J.-K., Kim, D.-C., Kwon, D., Ryu, K.H., Lee, D.-G.: LEA: A 128-Bit Block Cipher for Fast Encryption on Common Processors. In: Kim, Y., Lee, H., and Perrig, A. (eds.) *Information Security Applications*. pp. 3–27. Springer International Publishing, Cham (2014). https://doi.org/10.1007/978-3-319-05149-9_1.
28. Akishita, T., Hiwatari, H.: Very Compact Hardware Implementations of the Blockcipher CLEFIA. In: Miri, A. and Vaudenay, S. (eds.) *Selected Areas in Cryptography*. pp. 278–292. Springer, Berlin, Heidelberg (2012). https://doi.org/10.1007/978-3-642-28496-0_17.
29. Ahmad, N., Hasan, S.M.R.: A new ASIC implementation of an advanced encryption standard (AES) crypto-hardware accelerator. *Microelectronics Journal*. 117, 105255 (2021). <https://doi.org/10.1016/j.mejo.2021.105255>.
30. Sugawara, T.: Hardware Performance Evaluation of Authenticated Encryption SAEAES with Threshold Implementation. *Cryptography*. 4, 23 (2020). <https://doi.org/10.3390/cryptography4030023>.
31. Al-Moselly, M., Al-Haj, A.: High-Performance Hardware Implementation of the KATAN Lightweight Cryptographic Cipher. *J CIRCUIT SYST COMP*. 32, 2350017 (2023). <https://doi.org/10.1142/S0218126623500172>.
32. Celesti, A., Fazio, M., Villari, M., Puliafito, A.: Adding long-term availability, obfuscation, and encryption to multi-cloud storage systems. *Journal of Network and Computer Applications*. 59, 208–218 (2016). <https://doi.org/10.1016/j.jnca.2014.09.021>.
33. Mohan, P.V.A.: *Residue Number Systems*. Springer International Publishing, Cham (2016). <https://doi.org/10.1007/978-3-319-41385-3>.

Governance and Citizenship

VISUALIZING CITIZENS' PERCEPTIONS

Subjective indicators for the assessment of urban environments based on digital platforms.

Montse Delpino-Chamy ¹

¹ Associate professor, Universidad de Concepción, Chile
montsedelpinochamy@gmail.com

Abstract. Citizen participation processes still lack clear methodologies to be able to condition the planning decisions that end up shaping the urban form. Assembly structures, non-binding consultations, influence of interest groups and lack of monitoring tools are some of the main variables that discourage participation and keep the opinion of the “great silent majority” invisible. The recent emergence of digital participatory platforms based on Public Participation Geographic Information Systems (PPGIS), has opened new lines of experimentation and research to renew communication channels between citizens and institutions. Digital platforms are offering systematic support to expand sample sizes and access data more representative of population preferences about the urban environment. With this approach, the research aim is to identify the main subjective indicators currently used to assess citizens' perceptions about their urban environments through digital platforms. To do so the article presents the results of a Scoping review of 98 academic articles and the analysis of 21 of them, identifying theories, methods, and subjective indicators currently used in digital public participation platforms. The results offer a conceptual framework for the subjective assessment of citizens' perception of the urban environment, a synthesis of the main subjective indicators identifying those related to the perceived environment and socio-demographic factors conditioning citizens' experiences, a review of recruiting methods to enhance participation, and finally a description of the main study field in which digital citizens participation is being applied. As a conclusion, the article reflects on the interrelation between objective and subjective indicators for the study of urban environments, as well as on the need to construct a robust theoretical framework supporting digital participation.

Keywords: PPGIS, VGI, subjective assessment, perceived environment, participatory mapping

1 Introduction

Many thinkers have historically proclaimed the need for public participation in the making of communities [1]–[5]. Considering societies are built from dynamic bottom-up social relationships, it is insufficient to assume a top-down planning order for its full development [6]. Therefore, the public sphere must involve social communication

2

platforms, to support general critical perspectives and ideas for social improvement [7], [8]. The aim is to facilitate the emergence of institutional mechanisms for visualizing and valuing the subjectivity and experiences of human life [9], [10].

However, given that the study of the physical environment is easily measurable through the objective assessment of quantitative indicators, governments' regulatory frameworks tend to rely on these objective tools to assess the quality of the urban environment, limiting the capacity of planners to consider preferences and needs of the people inhabiting the city, throughout the collection of subjective indicators [11]–[13].

Despite this practice, there are many reasons to support the need to involve citizens' perception of their built environment in the decision-making processes of a city. Regarding quality, some authors declare that the objective characteristics of a place do not represent its true quality, since quality is not determined by the physical form, but by the perception people have of their environment [14]. Others argue that the new paradigm of modern citizens is feeling, and city administration needs to consider emotional data in order to identify those places that need to be recovered or saved, to guarantee citizens' subjective well-being [15]. Finally, an enhancement of public tools assessing citizens' perception through subjective indicators, would allow the recognition of important urban characteristics, such as perceived heritage, neighborhood identity, and sense of place [12], or the identification and enforcement of places contributing to the well-being of the population [14], [16]–[18].

These proposals; slightly utopian in the past; have found a new technical support: digital platforms and public participation geographic information systems (PPGIS). Each day enormous volume of geolocated data is loaded to different web and mobile-based digital platforms, generating a new frontier of possibilities for urban data analysis [15]. The recent increase in TICs and smartphones has opened a new research field centered on analyzing uplifting data registering individual behaviors and perceptions. These methods are opening new strategies for citizens' participation processes, based on citizen science or digital participatory mapping approaches [13], [17], [19], [20], enhancing the complexity and possibilities of articulation between top-bottom and bottom-up tactics to urban planning [15], and allowing citizens to become actively involved in public consultation processes [1].

In this context, the aim of this paper is to identify the main subjective indicators currently used to collect citizens' perceptions of their urban environments, through the use of digital platforms. Following a Scoping review methodology, 98 articles were identified, and 21 of them were chosen for a deeper analysis, based on selection criteria, specifically the objectives of this research and methodology are: 1) Establish a general conceptual framework to spatialize and study citizens' perception with the support of participatory digital platforms. 2) Identify the main indicators being used to assess the perceived urban environment. 3) Describe different study fields in which these subjective indicators can be applied.

The article begins with an introductory theoretical review followed by the presentation of the methods used to process the data. The results offer a conceptual framework for the subjective assessment of citizens' perception of urban environment, a synthesis of the main subjective indicators identifying those related to the perceived environment and socio-demographic factors conditioning citizens experiences, a review of recruiting

methods to enhance participation, and finally a description of the main study field in which digital citizens participation is being used. As a conclusion the article reflects on the opportunities to move from smart cities to smart citizens approaches, as well as on the need to construct a robust theoretical framework supporting digital participation.

2 Materials and Methods

The background information presented in this article is the result of a bibliographic review under the PRISMA-ScR method applied in WoS and Scopus. For the search, 3 key terms were used – urban environment, citizen perception and digital platforms – with a set of 7 synonyms for each term, articulated using Boolean connectors. The search result returned 98 articles in total. Four criteria were applied to the review of these articles to select the final set of works to be analyzed; The criteria were: relevant urban scale, including city, neighborhood or place (1); works using digital platforms for data collection (2); studies focused on a citizen participation approach (3); excluding those investigations with a focus on mobility (4). As a result of this filter, 21 articles were obtained. For more information on this methodology, review the article by Delpino-Chamy & Pérez-Albert [21].

The 21 selected articles were reviewed in detail, breaking down their content to identify their conceptual and methodological approaches, digital platform being used, subjective and objective indicators considered in the study, consulted users, recruiting methods, rewards techniques, software and formulas used for analysis the data. All these aspects were registered in an Excel database.

With this information 2 papers were produced, one based on analyzing the conceptual and methodological approaches related to these articles [21], and this second one, centered on identifying the subjective indicators being used for studying perception of the built environment.

3 Subjective Indicators to Study Citizen Perception of the Urban Environment

3.1 Transactional approach and participatory mapping as general background

The difficulties associated with the study of perceptions and emotions in the field of geography and urban planning have historically led to them being denied or ignored [22]. Despite this trend, some tools have managed to support the collection of subjective data, supported by participatory mapping, surveys or mixed methods [23].

Regarding researches centered on studying citizens' perceptions of urban environment, participatory mapping has been related with Gibson's ecological approach [24], or Zube's transactional model [25], recognizing a direct person-environment relationship [17], [26], [27]. Participatory mapping relies on this ability of individuals to relate

4

their perceptions to a particular place, attaching each person experiences with an specific physical and cultural context [28].

From the person-environment transactional approach, participatory mapping focuses on locating people's experiences and/or preferences on a map, allowing them to be studied in a way that is sensitive to the context [17], [29], making it easier to analyze the relationship between the physical environment and the preferences of each individual [26]. To structure this approach, the person-environment transactional model is considered as a basis, which establishes that each experience is defined by the physical context in which it occurs [24], [27].

3.2 Theories, methodologies and conceptual framework for studying citizens perception

Theories to study citizens' perception of the built environment. Among the main theories identified to address studies of citizen perception of the urban environment through the use of digital platforms, the following could be identified with a subjective approach:

- *Subjective well-being.* Subjective well-being is based on the idea that people have the ability to self-evaluate their levels of satisfaction associated with different urban spaces [16], using experience as a mediator between the environment and well-being [27], and becoming a scientific and reliable strategy to evaluate trends associated with the quality of life in cities [18].
- *Physical Activity and Urban Health.* The framework for Urban Health states that the health of urban citizens is related to urban living conditions [30], studying the relation between physical activities and neighbourhood built environment [31].
- *Social Sustainability.* This approach relates the physical configuration of the built environment, centered on the location of centralities or community infrastructure, with the accessibility patterns towards these places [27].
- In addition, from the objective approach, the theory of *Audit Tools.* Are instruments and protocols used by researchers for studying the physical environmental conditions that are best assessed through direct observation at the community level [11]. These tools are generally applied by personnel trained in the field [32]

Methodologies to study citizens' perception of the built environment. Regarding methodological approaches, the following are identified, supporting subjective approaches:

- *Citizen Science.* The term Citizen Science is related to recognizing citizens' expertise in their local knowledge, and it is considered a basic component of the Citizens as Sensors paradigm [33]. This term is often used to refer to a network of citizens acting as observers in some domain of science [19], [34].

- And supporting the objective approach, it is recognized *Systematic Social Observation*. *SSO* is the basic technical tool used by Audit Tools and is based on protocols and criteria to guide the appliance of standardized instruments and forms, which allows the collection of information in the field

Conceptual framework to study citizens' perception of the built environment. The study of these theoretical and methodological approaches has allowed to deepen the analysis of the relationship between experience and the characteristics of the built urban environment [24], [27]. In this relationship, experience is understood as the generation of impressions triggered by the environment (perceived environment) and conditioned by a set of personal circumstances (socio-environmental conditioning) [12], [15]. Complementarily, in the urban context the environment is interpreted as the relationship between the urban form (built environment) and the opportunities to access the diversity of services and activities that the city offers (accessibility) [17], [35]. This conceptual framework to understand the generation of experience in the urban environment [21], is related with the human ecology approach at Chicago School and the elemental definition of place illustrated in Montgomery's work [15], allowing to raise indicators associated with each one of the three variables identified (see Figure 1).

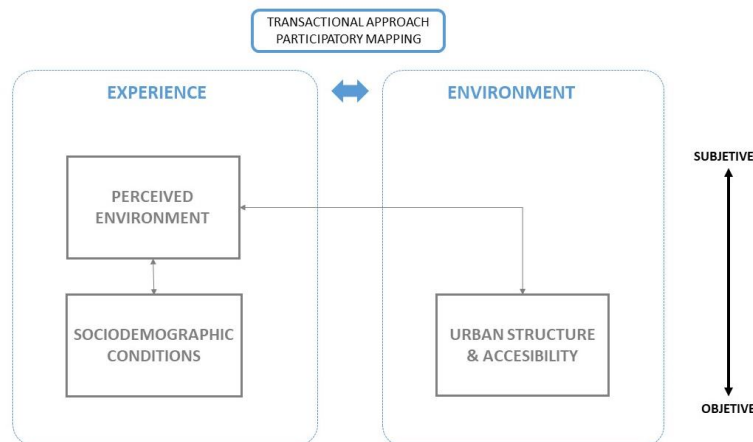


Fig. 1. Conceptual framework to assess urban perception

3.3 The simplicity of subjective indicators

The final step to be able to operationalize the conceptual framework to evaluate citizen perception in the urban environment (Figure 1) consists on identifying indicators for the analysis of each one of its variables.

6

Perceived environment. It corresponds to the fundamental component in the measurements on urban perception. Among the most recurrent indicators, the identification of positive/negative places or experiences stands out, followed by the evaluation of perceived well-being and quality (Figure 2).

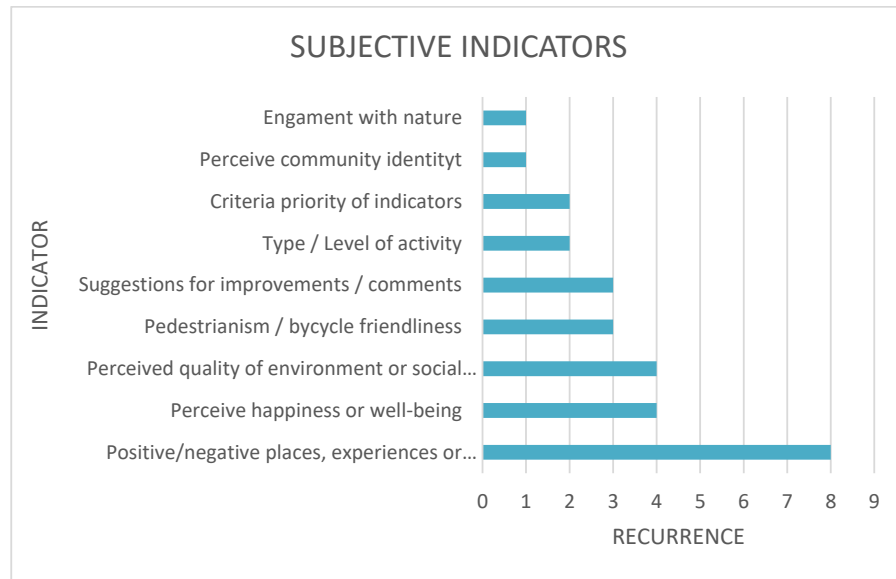


Fig. 2. Subjective indicators to study perceived urban environments

Socio-environmental conditions. Have been defined as those circumstances conditioning the perceived environment. Sociodemographic factors strongly emerge as the main indicators considered to assess citizens' perception of their built environment. These mainly include age, level of education and gender. The collection of this information allows to relate perception with sociodemographic preferences of diverse groups of population, allowing to study the urban environment from an intersectional approach.

Urban environment and Accessibility. Urban environment and accessibility indicators are diverse and present a huge range, depending on the subject being studied. However, this scoping review has identified two different approaches to study urban environment characteristics, as well as two different methods to analyze accessibility around meaningful places. The two approaches identified consist on locating preferences of citizens around a specific spot within the city, or around their places of residence. Regarding the methods, buffer-based analysis appears as the one generally used to assess the accessibility around significant places, while activity space emerges as the most precise for analyzing citizens mobilities within the urban tissue.

Approaches to study urban environmental characteristics:

- *From Spot.* This approach consists on selecting significant places around the city mapped by a diverse range of citizens, followed by an GIS analysis around these spots. This method is generally used to collected individual perception of common places, and its analysis is mainly related with the buffer-based method. The main indicators used to assess urban environment around these selected spots are: location of nearest green urban spaces, or urban centralities, and characteristics regarding density or land uses around the selected spot (Figure 3).
- *Around Home.* This approach is based on analyzing urban environment characteristics around residential places of each participant, It is generally used to analyze individual behavior of citizens around their homes and neighborhoods. Is has been related with the Activity Space concept. Although some researches use the buffer-based method to study accessibility to urban features from home, this techniques have been proven to be less precise [36]. The main indicators used for the analysis are: location of meaningful places around home and location of nearest centralities (Figure 4).

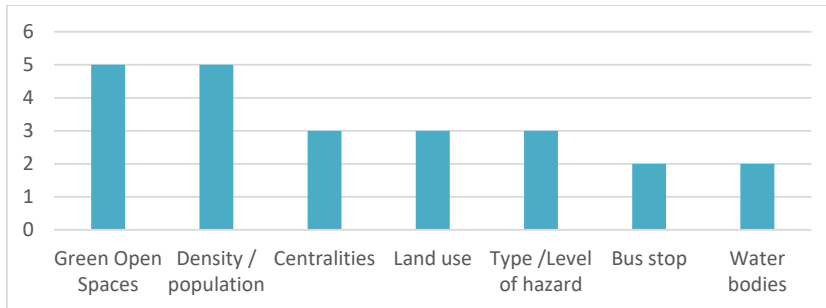


Fig. 3. Objective indicators to assess urban environment from spot

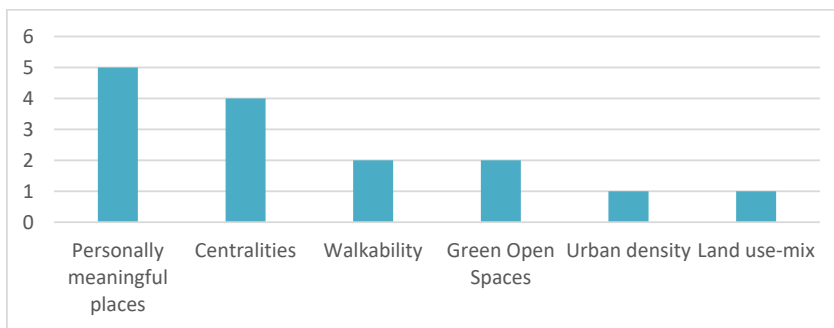


Fig. 4. Objective indicators to assess urban environment from home

8

Approaches to analyze accessibility:

- *Buffer-based analysis*. Understood as a proximity-related analysis [37], circular buffers defined around a specific point or home allow the definition of an influence area surrounding the mapped places. Over this area, spatial patterns and urban structure attributes can be study through the use of GIS dataset [17]. These circles, sausages or network buffer-based analysis that create polygons around a certain point is space, are generally used due to its simplicity and individual based solution [36], [38]
- *Activity space*. Despite the popularity of buffer-based analysis, recent research have been exploring alternatives to produce a more dynamic and person-based unit of examination throughout the notion of activity space [36]. Activity space is understood as a grouping of points geolocated on space, identifying the places that are most visited by an individual [38]. Activity spaces have been collected through GPS tracking, as well as from digital participatory mapping questionnaires, identifying a consistency between both methods [36].

3.4 Consulted Users, Recruiting methods & Rewards

Considering that digital platforms are mainly used by a specific segment of the population, it is important to identify the strategies adopted by different researcher to recruit a wider number of participants, looking for a better representation of a diversity of socioeconomic groups.

From the reviewed cases, the average of participants is 2516. A disaggregated analysis shows an average of 1344 participants through web-based PPGIS platforms, and 6202 participants in average collecting data through smartphones' apps.

The methods used to recruit participants are significantly diverse, although many articles do not explicit their strategies. Between the most common are: social media, invitation letters, governmental support (broadcasting or using their own staff) and promotion throughout community heads (Figure 5). In particular Apps tend to use as recruiting methods the influence of community heads, social media and recruitment posters and flyers. While web-based PPGIS rely on invitation letters, social media and governmental support. A special case is related to the Mappiness App [16], which got 22000 participants by being the only case studied which appear on TV and radio broadcasting, while being highlighted in the App Store for two weeks after being launch. The average of participants of the cases studied, without considering Mappiness, is 1016 participants.

Rewards strategies are also being implemented to increase the number of citizens involved. In general raffle between participant is the most recurrent tactic. Although the app Mappiness offers a personal happiness rate to users of the platform, as an incentive for its use. Finally, design and interface of the digital platforms is also considered as an important factor to promote its use [9], [39].

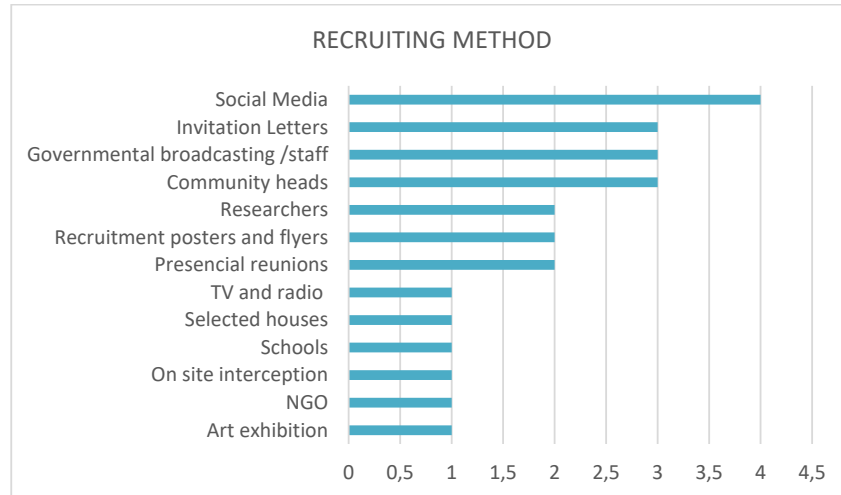


Fig. 5. Recruiting methods for digital citizens' participation

3.5 Relation Between Indicators and Purpose of the Studies

In general, all the identified studies are mainly center on reviewing the relation between the characteristics of a determinate urban environment, and the perception of its inhabitants. However, specifically, from between the selected articles, it is possible to identify the following objectives or purposes related to the subjective assessment of urban environments throughout participatory digital platforms:

- **Compare citizens' experiences in different urban environments.** Articles comparing experiences between different urban environments, are centered on analyzing changes on inhabitants' perception between urban and natural environments [16], [27], [32], or assessing impressions regarding urban intensification processes [12], [17]. For the first case, place studied are center on green open spaces, while urban intensification studies assess different neighborhoods of the city. The indicators used are diverse, but generally centered on identifying a location with GPS and analyze its surroundings with the support of external database.
- **Locate citizens' emotional experiences in the built environment.** Research center on locating emotional experiences on the city [15], [40] are focused on identifying psychological preferences of inhabitants, in contrast with environmental aspects of the built environment. Studies reviewing emotional responses are related to a specific place of analysis. The method for collecting data is generally based on identifying a location with GPS and analyze its surroundings with the support of external database.
- **Evaluate inclusiveness of different groups in the built environment (ex. Age groups, pedestrians, immigrants, bikes, etc).** Age-friendliness [26], [31], [41] and bicycle acceptance [42] are between the most studied subject identified. Indicators

10

showed no significant redundancy rather than identify centralities or Green Open Spaces. However, it is pertinent to notice that all indicators measure around home are analyzed around places marked by each participant. While indicators measured around places are measured by identifying a location with GPS and analyzing its surroundings with the support of external database.

- **Assess quality or satisfaction with a project or place.** This approach has been used to analyze citizens' approval with a specific urban project [43], [44] or analyze quality, security or fulfillment of citizens within their neighborhoods [27], [29], [32], [45]. No redundancy has been identified between urban environmental characteristic and accessibility from spot or around home.
- **Hazards assessment.** Center on studying urban landscape degradation [30], [46] or impact of natural hazards on cities [47]. On these papers all indicators are collected around places, where each place is analyzed by marking a place by each participant, and relating it with a photo or questionnaire to characterize each spot.
- **Health and Physical Activity enhancement.** Focused on studying and improving physical [36], [48], [49] and mental health [50]. Articles assessing physical behavior tend to center on studying the neighborhood scale around home, being particularly significant for their analysis the Activity Space method.

4 Discussions

The aim of the research has been to identify subjective indicators for the assessment of urban environment with the support of participatory digital platforms. Within the theoretical framework, participatory mapping emerges as a common ground to collect data by members of the community. Supported by transactional person-environment approach [17], [24], [26], [27], and Public Participatory Geographic Information Systems (PPGIS) [19], [34], digital participatory mapping is able to facilitate a community-based participatory process to collect subjective indicators, to be complemented with traditional objective indicators provided by GIS official datasets.

The conceptual framework for the assessment of citizens' perception throughout digital platforms proposed on this research considers three components: physical environment, perceived environment, and sociodemographic factors conditioning the experience (Fig 1). Regarding the theoretical framework that could be adopted to activate this model, the scoping reviewed identified: Subjective Well-Being, Physical Activity and Social Sustainability. From within the methodological framework citizen science stands out as a way to collect local information, emphasizing the active participation of community members in the generation of new data [19], [33]. Special attention is required to the theory of Audit Tool and its methodology of Systematic Social Observation (SSO) being recognized as a participatory process although collecting objective indicators about the built environment [11].

The analysis of indicators has been presented following this conceptual framework for the assessment of citizens' perception (Fig 1). Subjective indicators about perceived environment consider the identification of positive/negative places or experiences, the

self-evaluation of personal well-being and perceived quality related to a specific place, and suggestion for improvements. These are all perceptual indicators aligned with the subjective approach focused on the emotional and experiential aspects of inhabiting a particular place [11]. Sociodemographic indicators are considered fundamental data to assess which features of urban environments are valued by people of different socio-demographic profiles, allowing to study the urban environment from an intersectional approach. Objective indicators related to the assessment of urban environment can be collected from spot or around home, using a buffer-based analysis [37] or the activity space concept [36], [38]. Finally, it is also recognized that users need incentives to make volunteers contributions to generate new data through digital platforms.

Some study fields in which the assessment of citizens' perception about their urban environment have proven to be useful are the following: Compare citizens' experiences in different urban environments, locate citizens' emotional experiences in the built environment, evaluate inclusiveness of different groups in the built environment, Assess quality or satisfaction with a project or place, hazards assessment and health and physical activity enhancement.

5 Conclusions

Valuing human-urban interaction and returning human scale back into city planning has become one of the main scopes of the new and contemporary urbanism [6], [10]. The emergence of VGI and massification of smartphones, are enabling new bottom-up data production and public participation dynamics [19], [34] to collect citizens' perception about their urban environments [25]. The strategy is highly cost-time effective. The development and maintenance of traditional urban sensors to collect objective data is costly. Alternatively citizens, armed only with their smartphones, act as a global and mobile network of human sensors monitoring urban environments [41].

This process of digital citizen involvements requires to move from the smart city to the smart citizen concept, opening new channels to receive more feedback from inhabitants, and enhance their participation in urban planning processes [15]. This new trend in urban planning could allow the distribution of responsibilities from governments to citizens regarding identifying problems and needs within the urban environment [9].

However, this transactional person-environment approach requires a clear methodology to relate social perception with urban structure [17]. This research aimed to present a set of subjective indicators, within a conceptual framework for the assessment of urban perception, as a contribution to advance on this path. Between the main results is significant to notice the simplicity of subjective indicators, and their complex analytical possibilities, once there are complemented with sociodemographic and urban structure data.

Regarding theoretical considerations, more research would be needed to identify the relation between different trends in subjective urban studies, such as emotional geography, perception tools, audit tools, and quantified self-approach. Regarding methodological approaches, it could be valuable to repeat this research increasing the sample size of analyzed papers, in order to validate the results presented. Much more analysis

12

could be also done by correlating subjective indicators with different type of studies, to identify the most suitable methodology for physical, emotional, health or hazard assessments.

7. References

- [1] P. Szarek-iwaniuk, "Access to ICT in Poland and the Co-Creation of Urban Space in the Process of Modern Social Participation in a Smart City — A Case Study," *Sustain.*, vol. 12, 2020, doi: 10.3390/su12052136.
- [2] V. Lawson *et al.*, "Public participation in planning in the UK A review of the literature," no. April, 2022, [Online]. Available: www.ccqol.org.
- [3] D. Sui, S. Elwood, and M. Goodchild, *Crowdsourcing Geographic Knowledge: Volunteered Geographic Information (VGI) in Theory and Practice*. Springer, 2013.
- [4] S. Fainstein and N. Fainstein, *The View from Below: Urban Politics and Social Policy*. Boston: Little, Brown Company, 1972.
- [5] E. Daher, M. Maktabifard, S. Kubicki, R. Decorme, B. Pak, and R. Desmaris, *Tools for Citizen Engagement in Urban Planning*, no. January. 2021.
- [6] J. Jacobs, *Muerte y vida de las grandes ciudades*. Madrid: Ediciones Peninsula, 1967.
- [7] M. Castells, "Espacios públicos en la sociedad informacional," pp. 1–7, 1998.
- [8] J. Habermas, *Teoría de la acción comunicativa. Complementos y estudios previos*. Madrid: Catedra, 1984.
- [9] W. Liu, L. Liu, Y. Shiu, and Y. Shen, "Explorations of Public Participation Approach to the Framing of Resilient Urbanism," *IOP Conf. Ser. Earth Environ. Sci.*, 2017.
- [10] J. Gehl, *Cities for People*. 2010.
- [11] R. C. Brownson, C. M. Hoehner, K. Day, A. Forsyth, and J. F. Sallis, "Measuring the Built Environment for Physical Activity. State of the Science," *Am. J. Prev. Med.*, vol. 36, no. 4 SUPPL., pp. S99-S123.e12, 2009, doi: 10.1016/j.amepre.2009.01.005.
- [12] S. Sabri, A. Rajabifard, S. Ho, S. Amirebrahimi, and I. Bishop, "Leveraging VGI Integrated with 3D Spatial Technology to Support Urban Intensification in Melbourne , Australia," *Urban Plan.*, vol. 1, no. 2, pp. 32–48, 2016, doi: 10.17645/up.v1i2.623.
- [13] G. Brown, "Mapping Spatial Attributes in Survey Research for Natural Resource Management: Methods and Applications," *Soc. Nat. Resour.*, vol. 18, no. 1, pp. 17–39, 2004.
- [14] I. Van Kamp, K. Leidelmeijer, G. Marsman, and A. De Hollander, "Urban environmental quality and human well-being towards a conceptual framework and demarcation of concepts; a literature study," *Landsc. Urban Plan.*, vol. 65, no. 1–2, pp. 5–18, 2003, doi: 10.1016/S0169-2046(02)00232-3.
- [15] A. Nenko and M. Petrova, *Emotional Geography of St. Petersburg : Detecting*

- Emotional Perception of the City Space Emotional Geography : Localization of Emotions*. Springer International Publishing, 2018.
- [16] G. MacKerron and S. Mourato, "Happiness is greater in natural environments," *Glob. Environ. Chang.*, vol. 23, no. 5, pp. 992–1000, Oct. 2013, doi: 10.1016/j.gloenvcha.2013.03.010.
- [17] M. Kytä, A. Broberg, and M. Haybatollahi, "Urban happiness: context-sensitive study of the social sustainability of urban settings," *Environ. Plan. B Plan. Des.*, no. 43, 2016, doi: 10.1177/0265813515600121.
- [18] K. Mouratidis, "Urban planning and quality of life: A review of pathways linking the built environment to subjective well-being," *Cities*, vol. 115, no. April, p. 103229, 2021, doi: 10.1016/j.cities.2021.103229.
- [19] M. Haklay, "Citizen science and volunteered geographic information: Overview and typology of participation," in *Crowdsourcing Geographic Knowledge*, D. Sui, S. Elwood, and M. Goodchild, Eds. Springer, 2013, pp. 105–122.
- [20] T. Laatikainen, H. Tenkanen, M. Kytä, and T. Toivonen, "Comparing conventional and PPGIS approaches in measuring equality of access to urban aquatic environments," *Landsc. Urban Plan.*, vol. 144, pp. 22–33, Dec. 2015, doi: 10.1016/J.LANDURBPLAN.2015.08.004.
- [21] M. Delpino-Chamy and M. Y. Perez Albert, "Assessment of Citizens' Perception of the Built Environment throughout Digital Platforms: A Scoping Review," *Urban Sci.*, vol. 6, no. 3, pp. 1–20, 2022.
- [22] J. Davison, L. Bondi, and M. Smith, *Emotional Geographies*. Routledge, 2016.
- [23] R. Chambers, "Participatory mapping and geographic information systems: Whose map? Who is empowered and who disempowered? Who gains and who loses?," *Electron. J. Inf. Syst. Dev. Ctries.*, vol. 25, pp. 2–11, 2006.
- [24] J. J. Gibson, *The Ecological Approach to Visual Perception*. Houghton Mifflin, 1979.
- [25] E. Zube, "Environmental Perception," in *Environmental Geology Encyclopedia of Earth Science*, Dordrecht: Springer, 1999.
- [26] T. E. Laatikainen, A. Broberg, and M. Kytä, "The physical environment of positive places: Exploring differences between age groups," *Prev. Med. (Baltim.)*, vol. 95, pp. S85–S91, Feb. 2017, doi: 10.1016/j.ypmed.2016.11.015.
- [27] K. Samuelsson, M. Giusti, G. D. Peterson, A. Legeby, S. A. Brandt, and S. Barthel, "Impact of environment on people's everyday experiences in Stockholm," *Landsc. Urban Plan.*, vol. 171, pp. 7–17, Mar. 2018, doi: 10.1016/j.landurbplan.2017.11.009.
- [28] M. Kytä, A. Broberg, T. Tzoulas, and K. Snabb, "Towards contextually sensitive urban densification: Location-based softGIS knowledge revealing perceived residential environmental quality," *Landsc. Urban Plan.*, vol. 113, pp. 30–46, 2013, doi: 10.1016/j.landurbplan.2013.01.008.
- [29] D. M. Saadallah, "Utilizing participatory mapping and PPGIS to examine the activities of local communities," *Alexandria Eng. J.*, vol. 59, no. 1, pp. 263–274, Feb. 2020, doi: 10.1016/j.aej.2019.12.038.
- [30] N. Osborne, T. L. Hawthorne, D. Dai, C. Fuller, and C. Stauber, "Mapping the

14

- Hidden Hazards: Community-Led Spatial Data Collection of Street-Level Environmental Stressors in a Degraded , Urban Watershed,” *Environ. Res. Public Heal.*, vol. 15, 2018, doi: 10.3390/ijerph15040825.
- [31] A. Kajosaari and T. E. Laatikainen, “Adults ’ leisure - time physical activity and the neighborhood built environment : a contextual perspective,” *Int. J. Health Geogr.*, pp. 1–13, 2020, doi: 10.1186/s12942-020-00227-z.
- [32] R. V. Remigio *et al.*, “A Local View of Informal Urban Environments: a Mobile Phone-Based Neighborhood Audit of Street-Level Factors in a Brazilian Informal Community,” *J. Urban Heal.*, vol. 96, no. 4, pp. 537–548, Aug. 2019, doi: 10.1007/s11524-019-00351-7.
- [33] B. Resch, “People as sensors and collective sensing-contextual observations complementing geo-sensor network measurements,” *Lect. Notes Geoinf. Cartogr.*, no. 9783642342028, pp. 391–406, 2013, doi: 10.1007/978-3-642-34203-5_22.
- [34] M. F. Goodchild, “Citizens as sensors : the world of volunteered geography,” no. November, pp. 211–221, 2007, doi: 10.1007/s10708-007-9111-y.
- [35] G. Bramley, “Urban form and social sustainability : The role of density and housing type Urban form and social sustainability : the role of density and housing type,” no. June, 2009, doi: 10.1068/b33129.
- [36] T. E. Laatikainen, K. Hasanzadeh, and M. Kytta, “Capturing exposure in environmental health research : challenges and opportunities of different activity space models,” *Int. J. Health Geogr.*, pp. 1–14, 2018, doi: 10.1186/s12942-018-0149-5.
- [37] N. Fagerholm *et al.*, “A methodological framework for analysis of participatory mapping data in research, planning, and management,” *Int. J. Geogr. Inf. Sci.*, vol. 35, no. 9, pp. 1848–1875, 2021, doi: 10.1080/13658816.2020.1869747.
- [38] K. Hasanzadeh, “Use of participatory mapping approaches for activity space studies: a brief overview of pros and cons,” *GeoJournal*, vol. 87, no. s4, pp. 723–738, 2022, doi: 10.1007/s10708-021-10489-0.
- [39] P. Marti, C. García-Mayor, and L. Serrano-Estrada, “Monitoring the pulse of renewed Spanish waterfront cities through Instasights,” vol. 14, no. 4, pp. 333–346, 2019, doi: 10.2495/SDP-V14-N4-333-346.
- [40] B. Chrisinger and A. King, “Stress experiences in neighborhood and social environments (SENSE) : a pilot study to integrate the quantified self with citizen science to improve the built environment and health,” *Int. J. Health Geogr.*, pp. 1–13, 2018, doi: 10.1186/s12942-018-0140-1.
- [41] M. Jelokhani-Niaraki, F. Hajiloo, and N. N. Samany, “A Web-based Public Participation GIS for assessing the age-friendliness of cities: A case study in Tehran, Iran,” *Cities*, vol. 95, Dec. 2019, doi: 10.1016/j.cities.2019.102471.
- [42] A. Chevalier, M. Charlemagne, and L. Xu, “Data on public bicycle acceptance among Chinese university populations,” *Data Br.*, vol. 28, p. 104946, 2020, doi: 10.1016/j.dib.2019.104946.
- [43] R. Jose, R. Wade, and C. Jefferies, “Smart SUDS: Recognising the multiple-benefit potential of sustainable surface water management systems,” *Water Sci. Technol.*, vol. 71, no. 2, pp. 245–251, 2015, doi: 10.2166/wst.2014.484.

- [44] G. M. Besenyi *et al.*, “Development and testing of mobile technology for community park improvements: validity and reliability of the eCPAT application with youth,” *Transl. Behav. Med.*, vol. 6, no. 4, pp. 519–532, Dec. 2016, doi: 10.1007/s13142-016-0405-9.
- [45] T. R. Katapally *et al.*, “The smart study, a mobile health and citizen science methodological platform for active living surveillance, integrated knowledge translation, and policy interventions: Longitudinal study,” *JMIR Public Heal. Surveill.*, vol. 4, no. 3, Mar. 2018, doi: 10.2196/publichealth.8953.
- [46] K. Wannemacher *et al.*, “Using citizen science to help monitor urban landscape changes and drive improvements,” *GI Forum*, vol. 6, no. 1, pp. 336–343, 2018, doi: 10.1553/GISCIENCE2018_01_S336.
- [47] T. Kijewski-Correa, D. B. Roueche, K. M. Mosalam, D. O. Prevatt, and I. Robertson, “STEER: A Community-Centered Approach to Assessing the Performance of the Built Environment after Natural Hazard Events,” *Front. Built Environ.*, vol. 7, May 2021, doi: 10.3389/fbuil.2021.636197.
- [48] D. Fuller *et al.*, “Health and Place Wave 1 results of the INTERventions , Research , and Action in Cities Team (INTERACT) cohort study : Examining spatio-temporal measures for urban environments and health,” *Heal. Place*, no. February, p. 102646, 2021, doi: 10.1016/j.healthplace.2021.102646.
- [49] T. Rydenstam, T. Fell, B. Geleta Buli, A. King, and K. Balter, “Using citizen science to understand the prerequisites for physical activity among adolescents in low socioeconomic status neighborhoods - The NESLA study Health and Place Using citizen science to understand the prerequisites for physical activity among ad,” *Heal. Place*, vol. 65, no. September 2020, 2021, doi: 10.1016/j.healthplace.2020.102387.
- [50] K. McEwan, M. Richardson, D. Sheffield, F. J. Ferguson, and P. Brindley, “A smartphone app for improving mental health through connecting with urban nature,” *Int. J. Environ. Res. Public Health*, vol. 16, no. 18, Sep. 2019, doi: 10.3390/ijerph16183373.

Características institucionales que impulsan la movilidad urbana socialmente sostenible: Aportes del Triángulo Norte Centroamericano

Carlos Ernesto Grande¹, Luís Manuel Navas², Misael Martínez³

¹ Universidad Centroamericana, El Salvador y Universidad Loyola Andalucía, España.

² Universidad de Valladolid, España

³ Instituto Politécnico Nacional de México
cgrande@uca.edu.sv

Abstract. Son múltiples los ámbitos de innovación para transformar la movilidad urbana sostenible, pero esas transformaciones solo surgen de un complejo arreglo que resulta del ejercicio de poder, entre agentes y participantes en el marco del quehacer institucional. Este artículo tiene como objetivo identificar con un enfoque de Movilidad Urbana Socialmente Sostenible (MUSS) qué características deben procurar las instituciones durante ese arreglo, de tal forma que los proyectos y políticas de movilidad urbana contribuyan a transformar los sistemas urbanos en sistemas más sostenibles. El diseño metodológico se basa en un análisis comparativo de los casos de las rectoras del transporte en dos países del Triángulo Norte Centroamericano (TNC) durante el período de implementación de sus proyectos, como el Bus Rapid Transit (BRT), utilizando la técnica cualitativa de análisis de narrativa institucional. Dicho análisis se centra en dos competencias vinculadas a la dimensión social de la sostenibilidad, a saber, participación ciudadana e integración de la planificación del transporte y los usos del suelo. El resultado es una propuesta metodológica de análisis institucional desde el enfoque de la MUSS y la identificación de cuatro características clave que actúan de manera interrelacionadas en las instituciones para impulsar la movilidad socialmente sostenible.

Keywords: BRT, Planificación Urbana, Inclusión.

1 Introducción

Tradicionalmente la práctica de planificación del transporte ha sido abordada por técnicas y enfoques que pertenecen al ámbito de la ingeniería de los transportes y la planificación urbana, no obstante, la planificación y mucho más la gestión involucra aspectos de gobernanza y socioculturales que deben ser manejados con una técnica de tan depurada como las dos disciplinas que dominan este ámbito de la vida de la ciudad, esto según Vasconcellos [1] es abordar el problema desde un enfoque socio-técnico.

Bajo esta premisa se aborda este ejercicio de análisis comparando dos proyectos que, a principios del 2000, Guatemala y El Salvador, también conocidos como países del Triángulo Norte Centroamericano (TNC) planearon modernizar sus sistemas de transporte público en sus capitales, utilizando el sistema BRT (Bus Rapid Transit). Este

2

modo mueve en América Latina el 59,52% del total de personas que usan esta modalidad de transporte a nivel mundial [2].

Además, entre múltiples características, existe evidencia que los BRT suelen ser menos costosos que otras modalidades de transporte masivo y rápidos en ponerlos en funcionamiento [3, p. 346], lo que justifica bajo criterios de económicos e incluso políticos, debido a la rapidez de implementación e impacto en la población, una decisión acertada.

Más de 20 años después de estos proyectos BRT la movilidad motorizada individual en la región, como se muestra en la Fig, continua en aumento. Esto podría deberse al descuido histórico del transporte público y a problemas de seguridad ciudadana, como afirma Jacobs [4, p. 73], pero también podría relacionarse con tendencias globales, como el crecimiento de la población, la expansión urbana y el aumento de la clase media, según lo demuestra Kenworthy [5].

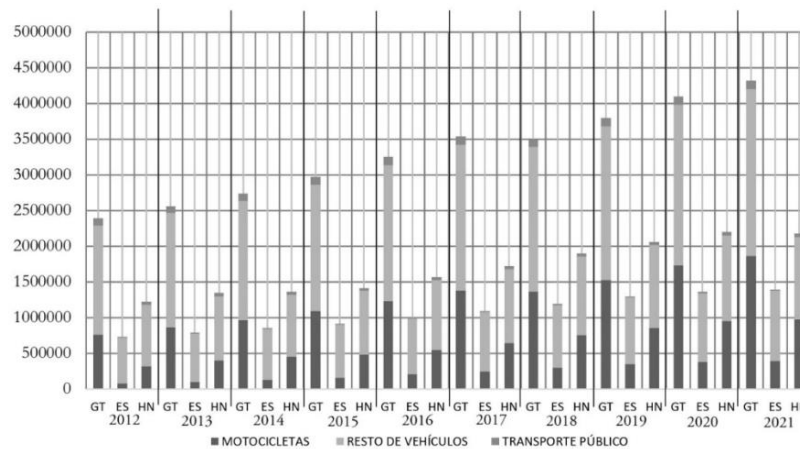


Fig. 1. Diez años de evolución de los modos de transporte en el TNC

Fuente: elaboración propia con base en INE [6], SAT [7], VMT [8]. Guatemala (GT), Honduras (HN) y El Salvador (ES)

De esta dinámica mostrada en la Fig.1 destacan el aumento continuo de vehículos particulares especialmente las motocicletas y una disminución de vehículos destinados al transporte público (véase figura 1). El crecimiento de las motocicletas es liderado por el TNC con 3.2 millones lo que según Neki et al. [9] ha tenido implicaciones en la tasa de mortalidad, pero también impactan en la facilidad en la movilidad y medios de ingresos, para los estratos más pobres y con servicios de transporte deficientes.

En cuanto al transporte público, El Salvador tiene aproximadamente un 0.7% de la proporción total, seguido por Honduras con un 2.3% y Guatemala con un 2.7%. Además, es notoria la falta de medición de los viajes no motorizados. A pesar de esto,

el transporte público sigue siendo el modo de desplazamiento principal en los tres países del TNC, con una distribución modal aproximada de 70% para el transporte público y 30% para otro tipo de vehículos en San Salvador y Guatemala, aunque Honduras muestra una proporción menor al 60% [10, p. 16], [11, p. 10], [12].

Por lo tanto, se argumenta que el transporte público sigue siendo la principal forma de desplazamiento en el TNC y se destaca la importancia de este artículo al evaluar cómo los proyectos de transporte contribuyen al desarrollo socialmente sostenible. Por ello se presenta en este texto solo un componente (el del análisis institucional) de una investigación más amplia que propone un enfoque llamado "Movilidad Urbana Socialmente Sostenible (MUSS)" centrado en la dimensión social del desarrollo sostenible, como eje vertebrador, que no único, del análisis de los proyectos de movilidad urbana para el Sur Global aplicado a dos países del TNC.

Se declara que la contribución principal de este artículo radica en aportar información sobre la situación de la gestión de proyectos de transporte durante los primeros 20 años de este siglo y además en brindar una primera aproximación a la forma en que las instituciones rectoras de transporte gestionaron los proyectos de implementación del BRT en dos países del TNC.

1.1 El concepto de la movilidad urbana socialmente sostenible

Pareciera que existe una falta de atención sobre la teorización de la dimensión social del desarrollo sostenible desde la publicación del informe "Our common future" [13], sobre este punto es posible identificar críticas [14, p. 9] a su ambigua definición y al enfoque centrado en la creación de políticas públicas de países desarrollados.

A pesar de esto, existen múltiples definiciones y perspectivas sobre la sostenibilidad social, según afirman Vallance et al. [15] destacan de estas perspectivas la de Polèse y Stren [16, pp. 15–16] que proviene de la planificación urbana y que centran su definición en la promoción de la equidad e inclusión. Por otro lado, Lineburg [17, p. 10] presenta evidencias sobre como el debate académico de la sostenibilidad y transporte tiende a enfocarse en las dimensiones económicas, medioambientales y en menor medida, en lo social.

Como complemento a estos aportes desde la perspectiva de la movilidad urbana, en este artículo, tienen relevancia tres conceptualizaciones, la primera es la de Lineburg (2016, p. 36), que desarrolla un complejo sistema de indicadores para evaluar la sostenibilidad social en la movilidad urbana a partir de dos categorías, la sostenibilidad de la comunidad y la equidad. La segunda y tercera conceptualización son las reflexiones de Flora [18, p. 385] y Cervero [19, p. 180], porque a pesar de lo temprano de su publicación, sus planteamientos son consistentes con el debate actual de la inclusión y equidad como base del concepto de MUSS y principalmente porque surgen de la mirada al Sur Global.

4

Por lo tanto, la propuesta conceptual y de indicadores de Lineburg, se considera relevante y exhaustiva, porque es coherente con el debate académico presentado previamente, basado en las nociones de equidad e inclusión; además, es útil, para esta investigación, al establecer un marco general de evaluación desde el enfoque de la MUSS. Por ejemplo, en la primera categoría "Sostenibilidad de las Comunidades", se incluyen subcategorías como participación ciudadana, salud e inclusión, las cuales se refieren a cómo la movilidad urbana puede contribuir a la creación de comunidades más sostenibles, en línea con la definición de legates_ deseables para vivir, sensibles al medio ambiente y que brinden una alta calidad de vida, según Dempsey [20, p. 290].

La segunda categoría, originalmente llamada "equidad social" que en la Figura 2 ha sido renombrada como "accesibilidad", se refiere al "acceso equitativo" a servicios urbanos y empleo. Este cambio de nombre se basa en la idea de que refleja mejor el propósito final de esta categoría en el contexto de la Movilidad Urbana Sostenible (MUSS), que es mejorar el acceso equitativo a los servicios urbanos básicos y al empleo. Esta categoría incluye tres subcategorías: enfoques de la accesibilidad, provisión de movilidad no motorizada y planificación del uso del suelo, vinculado al transporte público.

Finalmente, como contribución al enfoque de la MUSS en el Sur Global, se propone una tercera categoría relacionada con la institucionalidad. Esta inclusión parte de la premisa que para lograr una movilidad equitativa y construir comunidades sostenibles, es esencial contar con una gobernanza sólida y un marco institucional y regulador robusto, como lo destaca Torok y Holper [21, p. 92]. Ortuzar [22, p. 2] enfatiza que la dimensión institucional es crucial para la implementación efectiva de la sostenibilidad, Dobranskyte-Niskota [23, p. 12] y Littig sugieren [24, p. 15] la inclusión de la dimensión político-institucional como parte de la dimensión social de la sostenibilidad en el contexto de los países del Sur Global.

La investigación de la que se desprende este artículo desarrolla un análisis de movilidad urbana con los tres componentes expuestos en la fig 2. Se insiste en que este texto, aborda la evaluación de la MUSS solo en la dimensión institucional, partiendo del hecho que esta dimensión es un mecanismo clave en la implementación de políticas y proyectos relacionados con la sostenibilidad, pero de manera más relevante en los países del sur global, específicamente los del TNC, que como afirma Hernández [25, p. 164] estos países se caracterizan por una dinámica institucional, carente de contrapesos, cooptada por grupos de poder, interesados en extraer los recursos del estado, lo que marca la falta de interés (o capacidad) en resolver los problemas sociales.

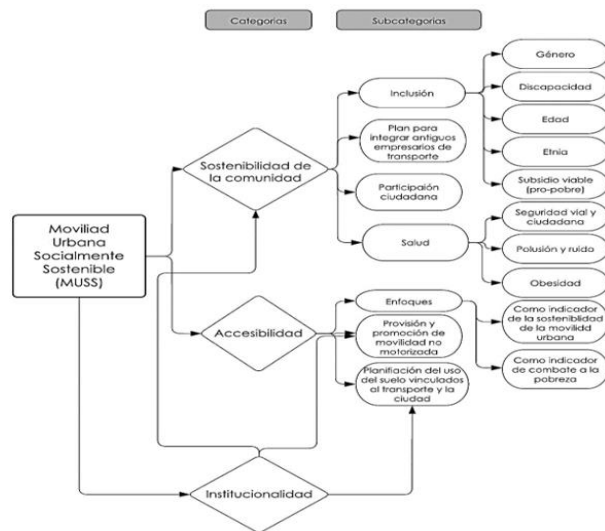


Fig.2. Síntesis del esquema conceptual de la Sostenibilidad Social en la Movilidad Urbana
Fuente: Elaboración propia con base en Lineburg (2016)

En este sentido, como se expone en la **Error! Reference source not found.**, y en lo referente a la categoría de la institucionalidad abordada en este texto; se propone una ruta metodológica que permita analizar las características de la institucionalidad, potenciando la sostenibilidad social en la movilidad urbana, a partir de identificar redes de actores, su grado de centralidad y ejercicio del poder, en las categorías relevantes del enfoque de la MUSS. Para ello, se retoman aspectos de la propuesta de análisis de Guzmán et al. [26] que analiza relación de poder entre los actores y se contextualiza para el Triángulo Norte Centroamericano.

De esta forma, la investigación busca alejarse del paradigma positivista, “que confiere a los transportes, la voluntad de creación del espacio urbano; o a la inversa, que los percibe como el resultado de las estructuras espaciales” [27, p. 107] partiendo de la premisa, que estas políticas o proyectos, no surgen espontáneamente, sino que son producto de relaciones complejas, de un sistema de actores e instituciones que, como afirman Guzmán et al. [28], ejercen ciertas cuotas de poder, transformando la realidad urbana.

Con los párrafos anteriores como base, es posible definir la pregunta de investigación como: ¿Al implementar proyectos de movilidad urbana, cuáles son las características de las instituciones rectoras de transporte que contribuyen a impulsar la dimensión social de la sostenibilidad?

6

1.2 Conceptos y estrategias metodológicas para comprender las relaciones institucionales que condicionan la MUSS.

La estrategia metodológica, se basa en dos premisas fundamentales. La primera, reconoce la importancia del análisis institucional, para comprender cómo los sistemas de movilidad experimentan cambios a lo largo del tiempo, debido a políticas urbanas específicas y las relaciones entre actores públicos y privados. En palabras de Miralles [27, p. 114], estas transformaciones son el resultado de un proceso político (instituciones) y social (agentes).

La segunda premisa, son tres conceptos claves, para comprender la institucionalidad en el contexto del transporte. El primero y el segundo, aportados por Ostrom [29, p. 25], referidos a la institucionalidad y las arenas de acción. La institucionalidad, se refiere a las estructuras formadas por individuos que desempeñan roles como agentes o participantes y se basa en relaciones definidas por reglas y normas, algunas de las cuales pueden no estar escritas. Estas reglas y normas establecen un marco para la acción de las instituciones, considerando las condiciones físicas y materiales específicas que influyen en las interacciones.

Las arenas de acción [29] son una unidad conceptual, utilizada para analizar un problema institucional, con referencia al espacio social en el que los individuos interactúan. El tercer concepto, es el ejercicio del poder, basado en el enfoque de Foucault, introducido por Guzmán et al.[26] que se utiliza para el análisis de la institucionalidad del transporte y se relaciona, con cómo se ejerce el poder en estas dinámicas. En conjunto, estos conceptos ofrecen una base para analizar y comprender la naturaleza de las instituciones en el ámbito del transporte.

1.2.1 Análisis Institucional

Se ha elegido la técnica de análisis de las narrativas de las instituciones. Según Chase [31, p. 915], esta técnica, implica analizar los discursos y materiales publicados por instituciones y organizaciones, para comprender cómo construyen el significado, a través de la presentación de sus acciones, miembros, valores y relaciones a lo largo del tiempo, abarcando el pasado, el presente y el futuro. El objetivo este componente de la investigación es: identificar con un enfoque de Movilidad Urbana Socialmente Sostenible (MUSS) qué características deben procurar las instituciones durante arreglo de la gestión institucional, de tal forma que los proyectos y las políticas de movilidad urbana, contribuyan a transformar los sistemas urbanos en sistemas más sostenibles.

La Tabla 1, describe documentos seleccionados, bajo dos criterios, el primero describir de manera detallada una o varias etapas relacionadas con proyectos BRT y el segundo, que proceden de las instituciones rectoras del transporte y/o alguno de los actores vinculados al proyecto en las dos capitales del TNC seleccionadas. Además, la incorporación de participantes no gubernamentales (academia, ONG, financiador) en la base de datos para un análisis institucional narrativo, facilita la triangulación e incorporación de otras perspectivas de las arenas de acción. La tabla 2, describe

también, la categorización de los autores y de los documentos, lo que permite establecer sus roles en el proyecto.

Tabla 1. Informes evaluados para el análisis institucional.

Ciudad (textos)	ONG/Contraloría ciudadana-participante	Actores / roles	
		Gobierno agente	Central / Financiadador / agente
San Salvador (20)	4 informes de contraloría ciudadana de la ONG FUNDE	15 boletines informativos 1 SITRAMSS EN MARCHA desde el 2013 al 2016.	[31]
Ciudad de Guatemala (3)	1 [32]	1 [11]	1[33]

Fuente: Elaboración propia.

Para definir qué temas se estudiarán en el análisis institucional, se utiliza como arenas de acción, dos subcategorías de la MUSS (Figura 1), las cuales no se pudo obtener información durante el proceso de desarrollo de la investigación, de las otras etapas de la tesis, estos son los temas de participación ciudadana y la relación entre la planificación del transporte y la ciudad, para los cuales existe escasa o nula información en las instituciones que gestionan los proyectos BRT.

La tabla 2, describe cinco categorías y veinte códigos utilizados para la codificación conceptual con el programa informático *QualCoder* [34]. Las dos primeras categorías, son las arenas de acción y el objeto del análisis, la tercera, es la identificación de los actores y la cuarta categoría, tiene que ver con el rol de los actores, así como la forma en que se vinculan a través de reglas/normas propias de los campos de acción, esto para ser consistentes con la metodología propuesta por Ostrom para el análisis de las arenas de acción. Finalmente se identifica el ejercicio del poder de los actores a partir de las categorías expuestas por Guzmán et al. [26, p. 5].

Tabla 2. Categorías y códigos conceptuales para codificación inicial.

Categoría	Objetivo de la categoría	Códigos conceptuales iniciales
Participación ciudadana	Describir las distintas interacciones entre los actores, sus respectivos roles y la manera en que configuran las condiciones de la MUSS desde la arena de acción de la participación ciudadana.	Consulta ciudadana. [35] Informar y comunicar efectivamente* Encuestas de origen destino. [36]*
Actores	Identificar los actores presentes en las diferentes narrativas estudiadas y que interactúan en las arenas de acción.	Financiadador. Gestor del proyecto. Operador. Usuarios.
Rol-regla/norma	Identificar el tipo de rol que juega el actor y describir la norma/regla que lo vincula a los demás.	Agentes. *** Participantes [29]***

8

Ejercicio del poder	Identificar, describir las distintas formas de ejercicio del poder de los actores.	Autoridad. **** Coerción. **** Intimidación. **** Persuasión. [26] ****
---------------------	--	--

Fuentes: varias detalladas en cada celda.

Con los códigos establecidos se realiza una codificación conceptual de la Tabla 2 para las dos ciudades del TNC. Además, se busca identificar otros códigos relevantes para el análisis de la narrativa institucional a través de una codificación “*in vivo*”, las palabras clave que se utilizan para identificar unidades de significado en los documentos analizados son, participación, usuarios, planificación, discapacidad, mujeres, transportistas, población, transporte público, bicicletas y peatones.

En esta fase, también se identifican los actores y su autodefinición en el texto, los roles que el actor-autor asigna a ellos, junto con las normas o reglas establecidas en la narrativa que los conecta. Se reconoce que las normas e instituciones pueden ser formales o informales según lo afirma Sclar y Touber [37] y se considera importante identificar cómo los actores ejercen el poder.

El análisis de la documentación concluye cuando la codificación alcanza la saturación, es decir, cuando no se pueden identificar nuevos aportes o crear nuevos códigos “*in vivo*”. La síntesis de este análisis se realiza mediante diagramas de telaraña (*Spyders Diagram*) para cada país y cada arena de acción. Estos resultados sintetizan las redes de actores y cómo se relacionan en las categorías de análisis de participación ciudadana, con un enfoque especial en la inclusión, y la relación entre la planificación del transporte y la ciudad. Estos diagramas se complementan con párrafos descriptivos que resumen el nivel de centralidad de los actores, las relaciones de poder, las normas/reglas que los vinculan y, en última instancia, cómo se configuran las arenas de acción en relación con sus actores y relaciones.

1.3 Resultados del análisis institucional en los proyectos BRT del TNC

Antes de iniciar la descripción de resultados, se destacan las nuevas categorías producto de la codificación *in vivo*, estos códigos permitieron mejorar el entendimiento del arreglo institucional en los proyectos BRT, para el caso de la categoría de participación ciudadana, se identificaron tres nuevos códigos: grupos vulnerables, usuarios del transporte colectivos, usuarios de otros transportes. En la categoría de planificación del transporte y ciudad, se subdividió en dos subcategorías, a saber, planificación del transporte, planificación de la ciudad, esta última con un nuevo código que es: Planificación urbana integrada al transporte.

Finalmente, es importante destacar que, en el análisis de los textos de cada proyecto, las categorías Rol/Regla-Norma y Actores, fueron totalmente distintas para cada país, debido a lo diverso de los contextos territoriales, permitiendo la identificación de

nuevos actores que juegan roles importantes en los proyectos, los cuales se representan en cada uno de los diagramas de telaraña.

SITRAMSS-SAN SALVADOR

El cruce de narrativas de los tres actores en el tema de la participación ciudadana puso en evidencia, que no siempre el proyecto avanzaba como se publicitaba, en torno al flujo de información [38, p. 11], además el agente-financiador propone fortalecer la participación ciudadana y la integración de otros actores en la gestión de la movilidad urbana, como municipios y planificadores urbanos [31, pp. 65, 75]. Lo que pone en evidencia una desconexión con importantes sectores de la población y el contraste con la imagen participativa y de transparencia que desarrollaba el gobierno, a través de su comunicación [39, p. 1].

No obstante, el SITRAMSS contaba con un importante avance en el fomento de inclusión a los usuarios, en los que destacan la mejora en la satisfacción por parte de los usuarios [40, p. 2] y las facilidades de acceso, para personas con discapacidades, estudiantes y adultos mayores [42, p. 1], finalmente es importante destacar algunos intentos del SITRAMSS, de integrar a una ruta de buses, de las más de cien existentes en el AMSS, a través de rutas alimentadoras [43, p. 2].

Respecto a la arena de acción de la planificación del transporte y la ciudad, los párrafos anteriores anticipan un desacierto medular del actor-gobierno-gestor, la falta de integración con la planificación del territorio principalmente con COAMSS-OPAMSS, ente competente en la gestión del territorio [31, pp. 50, 75]. Esto en parte propició una dinámica de resistencia en la implementación del proyecto y de ruptura interinstitucional sensible en el análisis de ejercicio de poder de los actores, en contraste es posible advertir un importante nivel de desarrollo operativo del funcionamiento del proyecto BRT, como centro de monitoreo, mejoras en el sistema semafórico, tarjeta prepaga, etc. [43].

El análisis de las dinámicas de poder, se muestra en la figura 3, entre los actores involucrados en el proyecto SITRAMSS, revelan la centralidad del Agente-Gobierno-Gestor en la fase de ejecución del proyecto. Esta posición otorga un considerable grado de influencia e incluso, en muchas ocasiones, un poder de imposición. No obstante, es importante señalar que la presencia de actores disruptivos, como grupos criminales, ejerce una importante influencia coercitiva en el proceso [43].

Se evidencia una interacción conflictiva con los gobiernos locales, afectando la percepción pública del proyecto. A pesar de las deficiencias técnicas y de gestión institucional señaladas por el agente-financiador, que buscó ejercer un poder persuasivo, estas limitaciones no pudieron superarse. Tras una demanda de inconstitucionalidad presentada por un sector del gremio de transportistas [44], que resultó en la eliminación del carril exclusivo, se redujo significativamente la eficacia del BRT. Este revés comprometió la capacidad del proyecto para transformar la

10

movilidad urbana en San Salvador, desvaneciéndose finalmente en agosto de 2020 durante el confinamiento por la pandemia.

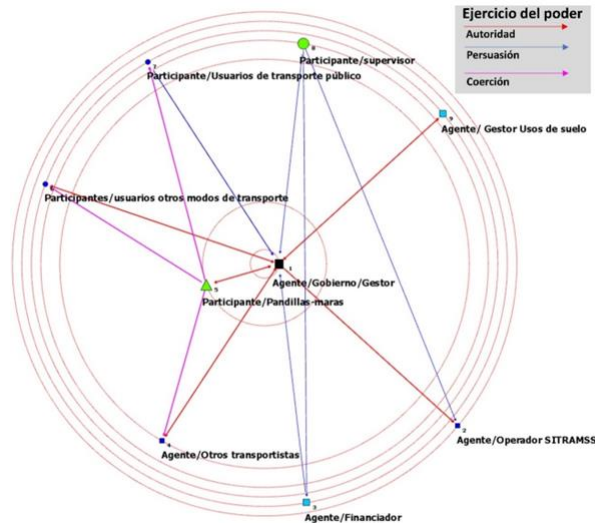


Fig.3. Diagrama de red de actores y relaciones de poder San Salvador

Transmetro-Municipio de Guatemala.

Los tres actores estudiados, tienen identidades y narrativas distintas, pero complementarias en el proyecto TRANSMETRO. Mientras que las instituciones planificadoras identificadas en este texto como un solo actor de tipo planificador-gestor-supervisor enfatizan importantes avances en la sostenibilidad y la participación ciudadana a nivel municipal. [11, p. 64], la academia (actor-participante) coincide con ellos en términos de enfoque de integración de la movilidad con la planificación de la ciudad y priorización de modalidades no motorizadas, no obstante, aporta argumentos que abogan por ampliar la gestión de la movilidad urbana a escala metropolitana [32, Sec. 2.2.2], por otro lado el agente-financidor se centra en los resultados técnicos de eficiencia en el transporte de pasajeros (reducción de un 20% en tiempos de traslado) y ambientales (disminuyó 70% la polución en entornos a red BRT) [33, p. 4].

La participación ciudadana en el proyecto TRANSMETRO, se manifiesta de diversas formas, aunque su presencia en la narrativa varía entre los actores estudiados. Se reconoce el avance en la mejora del servicio e inclusión de grupos vulnerables, pero se exigen mejoras (principalmente las mujeres y escasos recursos) [32]. Por otro lado, la colaboración con entidades especializadas principalmente derechos humanos dedicadas a la mejora de la accesibilidad universal [11, p. 41] aporta legitimidad al proyecto.

Finalmente, hay evidencia de la comunicación efectiva con los usuarios, de manera directa e indirecta; por ejemplo, indicadores de percepción de usuarios, aplicaciones móviles, rótulos informativos, señalética accesible y una educación para la cultura de uso del sistema BRT [11] que constituyen elementos esenciales para el éxito del proyecto y para abordar los desafíos de movilidad urbana en la ciudad de Guatemala.

La gestión del uso del suelo y la planificación del transporte en el caso de TRANSMETRO, se caracterizan por un consenso de los tres actores, en la importancia de la planificación integrada y sostenible [11, p. 64], [32, Sec. Int.], [33, p. 5], de hecho, el ente planificador-gestor-supervisor hace énfasis en el enfoque integrado territorio y ciudad a partir del Transporte Orientado al Desarrollo [11, p. 64] incorpora nuevos actores, experiencia técnica y momentos oportunos para los cambios. Esto sugiere una visión integral y una disposición a adaptar el proyecto, según sean las necesidades.

Entre los actores también hay coincidencias en la movilidad no motorizada, sin embargo, la academia subraya problemas en la priorización de esta en cuanto a la ejecución de infraestructura relacionada con este modo de transporte [32, Sec. 2.2.2]. Además, la coordinación metropolitana en la toma de decisiones y la coordinación de planes es un punto en tensión entre la autoridad del actor planificador-gestor-supervisor, los municipios conurbados y la academia [11, Sec. 3.5], esto resalta la complejidad de la gestión en un contexto metropolitano dado que el proyecto TRANSMETRO, es gestionado únicamente desde el municipio de Guatemala.

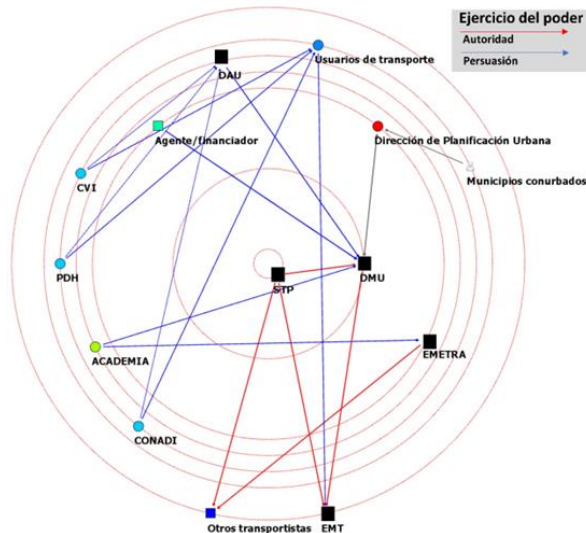


Fig. 4. Diagrama de red de actores y ejercicio del poder, Ciudad de Guatemala.

El análisis de la figura 4 destaca la centralización del poder en el municipio de Guatemala en la implementación del proyecto TRANSMETRO, aunque con una mayor

12

cantidad de actores en comparación con SITRAMSS. A pesar de esta centralización, hay una segmentación de poder y competencias en distintas unidades, lo que permite actuar de manera semiautónoma. Se reconoce la influencia de otros actores y la tensión para que TRANSMETRO se adapte a dinámicas territoriales cambiantes. La participación y colaboración con municipios conurbados ejercen un poder más persuasivo, especialmente en temas como el avance de la movilidad no motorizada y la integración a escala metropolitana, siendo este último un desafío clave y una oportunidad para futuras transformaciones en la movilidad urbana de la ciudad de Guatemala.

1.4 Conclusiones y discusión: La dinámica de la institucionalidad del transporte.

Las conclusiones se dividen en aspectos metodológicos y basados en casos de estudio. Desde el punto de vista metodológico, la institucionalidad es esencial para el enfoque de sostenibilidad social en el TNC, según Ortuzar[22]. La institucionalidad no solo permite aspirar a la sostenibilidad, sino que también impulsa dicha sostenibilidad al comprender cómo diversos actores ejercen su poder en la transformación urbana. Además, analizar la institucionalidad facilita la recuperación de información valiosa y la evaluación de procesos clave en proyectos de movilidad urbana, abordando una carencia común en la documentación de proyectos de transporte en el sur global. Esto se alinea con la propuesta de Lineburg, que se centra en evaluar procesos y resultados.

Desde la perspectiva de Díaz et al. [45, p. 3], este estudio aporta a la investigación al explorar aspectos poco documentados, como el período de construcción, implementación e inicio de operaciones en la implementación de BRT. Estos procesos, según los autores, tienen impactos a largo plazo sobre elementos críticos que requieren igual o mayor cuidado. En relación con los casos de estudio, se identifican cuatro características clave interrelacionadas que contribuyen a la sostenibilidad social en participación ciudadana y planificación del uso del suelo y transporte.

El primer aspecto destacado se centra en la transformación normativa y organizacional como una característica fundamental en instituciones que impulsan la Movilidad Urbana Sostenible (MUSS). Las instituciones estudiadas ajustan sus reglas para adaptarse a las innovaciones tecnológicas del Bus de Tránsito Rápido (BRT) y al marco legal del país. Sin embargo, en el caso de San Salvador, estos ajustes no se ejecutan adecuadamente, lo que puede resultar en fallas en el sistema, según señala Ostrom[29].

La segunda característica resaltada es el liderazgo y la coordinación interinstitucional. La capacidad de liderazgo y coordinación entre instituciones, ya sea a nivel local o central, se considera crucial para el éxito de proyectos de movilidad urbana. Estos liderazgos, aunque se centran en competencias institucionales, dependen en última instancia del compromiso de las personas que asumen estos roles.

La tercera característica clave es la integración con la gestión del territorio y la participación ciudadana. La falta de coordinación entre la planificación del transporte, la gestión del territorio y la participación ciudadana puede añadir fricción a la implementación de proyectos complejos como el BRT. Guatemala destaca como un caso singular, enfrentando el reto de integrar a nivel metropolitano debido a las dimensiones del territorio y la participación, pero ha logrado consensos a nivel municipal para asegurar la expansión y continuidad de sus proyectos.

Finalmente, el cuarto aspecto subraya la diversificación de la institucionalidad del transporte como un factor constatable en el caso de Guatemala. La descentralización de competencias, asumiendo roles de planificación, gestión y supervisión, parece potenciar el avance de los proyectos. Para futuras investigaciones la incorporación de más información a través de fuentes primarias, como entrevistas enriquecerá las evidencias y comprensión más detalladas. Además, se propone ampliar el análisis a otras áreas de acción, además del caso de TRANS-450 de Tegucigalpa.

Referencias

- [1] E. A. Vasconcellos, “Equity evaluation of urban transport,” in *Urban transport in the developing world: a handbook of policy and practice*, 2011, pp. 332–359.
- [2] Global BRT Data, “Base de datos.” 2023.
- [3] D. Hidalgo and J. C. Muñoz, “Bus rapid transit and buses with high levels of service: A global overview,” in *Handbook on Transport and Development*, 2015. doi: 10.4337/9780857937261.00030.
- [4] J. Jacobs, *Muerte y vida de las grandes ciudades.*, Tercera ed. Madrid, España: Capitán Swing, 2013.
- [5] J. Kenworthy, “An international comparative perspective on fast-rising motorization and automobile dependence,” in *Urban Transport in the Developing World*, 1st ed., H. T. Dimitriou and R. Gakenheimer, Eds., Edward Elgar Publishing, 2011, pp. 71–112.
- [6] INE, “Instituto Nacional de Estadística.” República de Honduras, 2021.
- [7] SAT, “Super Intendencia de Administración Tributaria.”
- [8] VMT, “Viceministerio de Transporte.”
- [9] K. Neki, S. Mitra, W. M. Wambulwa, and R. F. S. Job, “Profile of low and middle-income countries with increases versus decreases in road crash fatality population rates and necessity of motorcycle safety,” *J Safety Res*, vol. 84, pp. 129–137, Feb. 2023, doi: 10.1016/J.JSR.2022.10.014.
- [10] COAMSS-OPAMSS, “Política Metropolitana de Movilidad Urbana, Hacia una movilidad sostenible, equitativa, segura, inclusiva y eficiente.”, p. 56, 2020.
- [11] EMT, DMU, STP, M. M. DE GUATEMALA, and EMETRA, *La historia de nuestro TRANSMETRO*. Guatemala, 2015.
- [12] BID, ALG, and Le Vote, “Estudio de Apoyo al Plan de Movilidad Urbana Sostenible (PMUS) para el Distrito Central de Tegucigalpa y Comayagüela, Informe Final,” Tegucigalpa, Honduras, 2012.

14

- [13] WCED, "Our Common Future," World Commission on Environment and Development, New York, 1987.
- [14] R. Shirazi, R. Keivani, M. R. Shirazi, and R. Keivani, "Social sustainability discourse: a critical revisit," in *Urban Social Sustainability: Theory, Policy and Practice*, 1st ed., Reza Shirazi and R. Keivani, Eds., New York: Routledge, 2019, pp. 1–26. doi: 10.1016/0264-2751(93)90045-k.
- [15] S. Vallance, H. C. Perkins, and J. E. Dixon, "What is social sustainability? A clarification of concepts," *Geoforum*, vol. 42, no. 3, pp. 342–348, Jun. 2011, doi: 10.1016/j.geoforum.2011.01.002.
- [16] M. Polèse and R. E. Stren, *The social sustainability of cities: Diversity and the management of change*. University of Toronto Press, 2000.
- [17] K. Lineburg, "Transportation rating systems and social sustainability: A comprehensive analysis," College of Integrated Science and Engineering James Madison University, 2016.
- [18] J. Flora, "Management of Traffic and the Urban Environment," in *The challenge of urban government: policies and practices*, The World Bank, 2001, pp. 383–394.
- [19] R. Cervero, "Transport infrastructure and the environment in the Global South: sustainable mobility and urbanism," *Journal of Regional and City Planning*, vol. 25, no. 3, pp. 174–191, 2014.
- [20] N. Dempsey, G. Bramley, S. Power, and C. Brown, "The social dimension of sustainable development: Defining urban social sustainability," *Sustainable development*, vol. 19, no. 5, pp. 289–300, Sep. 2011, doi: 10.1002/sd.417.
- [21] S. Torok and P. Holper, *Delivering Sustainable Urban Mobility*. 2017.
- [22] J. Ortúzar, "Sustainable Urban Mobility: What Can Be Done to Achieve It?," *J Indian Inst Sci*, vol. 99, no. Journal Article, pp. 683–693, 2019.
- [23] A. Dobranskyte-Niskota, A. Perujo, J. Jesinghaus, and P. Jensen, "Indicators to Assess Sustainability of Transport Activities Part 2: Measurement and Evaluation of Transport Sustainability Performance in the EU27," Italy, 2009. doi: 10.2788/46618.
- [24] B. Littig and E. Griessler, "Social sustainability: a catchword between political pragmatism and social theory," vol. 8, no. 1–2, pp. 65–79, 2005, doi: 10.1504/ijds.2005.007375.
- [25] G. Hernández, "Inseguridad y poder político en el Triángulo Norte de Centroamérica," *Perfiles Latinoamericanos*, vol. 28, no. 55, p. 2020, 2019, doi: 10.18504/pl2855-006-2020.
- [26] A. Guzmán, I. Philips, K. Lucas, and G. Marsden, "A bus ride with Foucault," in *World Conference on Transport Research - WCTR 2016*, Shanghai: Elsevier, Jul. 2017, pp. 1–13. Accessed: Jan. 05, 2023.
- [27] C. Miralles, "Transporte y territorio urbano: del paradigma de la causalidad al de la dialéctica," *Doc Anal Geogr*, no. 41, pp. 107–120, 2002.
- [28] A. Guzmán, I. Philips, K. Lucas, and G. Marsden, "A bus ride with Foucault," in *World Conference on Transport Research - WCTR 2016*, Shanghai: Elsevier, Jul. 2017, pp. 1–13.

- [29] E. Ostrom, "Institutional rational choice: An assessment of the institutional analysis and development framework," in *Theories of the Policy Process*, P. Sabatier, Ed., Colorado, US: Westview Press, 2007, pp. 21–64.
- [30] S. E. Chase, "Narrative Inquiry and Methodological Maturity," in *The Sage handbook of qualitative research*, 5th ed., vol. 5, Y. S. Denzin, N. K., & Lincoln, Ed., Los Angeles, London, New Delhi, Singapore, Washington DC, Melbourne: SAGE, 2018, pp. 946–970.
- [31] M. Nevo, I. Granada, and P. Ortiz, "SITRAMSS: Mejorando el transporte público del Área Metropolitana de San Salvador," 2016.
- [32] A. Morán and J. Aragón, *Movilidad urbana sostenible para el área metropolitana de Ciudad de Guatemala*. Ciudad de Guatemala, Guatemala: CEUR USAC, 2022.
- [33] C. Castellón, J. P. Vélez, C. Landazuri, J. Martel, and C. Vecco, "Estructuración proyecto Transmetro Eje Nor-Oriente," 2008.
- [34] C. Curtain, "QualCoder 3.1." 2022.
- [35] C. Miralles-Guasch, À. Cebollada, and R. Requena, "Estrategias de participación ciudadana en la gestión de la movilidad y el transporte. La Universidad Autónoma de Barcelona como ejemplo," *Scripta Nova.Revista Electrónica de Geografía y Ciencias Sociales*, vol. 14, 2010.
- [36] A. Peñalva, E. de los Rios, S. Aguilera, and L. Eraso, "Manual de Participación en Políticas de Movilidad y Desarrollo Urbano," ITPD, Ciudad de México, 2014.
- [37] E. Sclar and J. Touber, "Economic fall-out of failing urban transport systems: an institutional analysis," in *Urban Transport in the Developing World: A Handbook of Policy and Practice*, H. Dimitriou and R. Gakenheimer, Eds., UK; Northampton, MA: Edward Elgar Publishing, 2011, pp. 174–202.
- [38] FUNDE, "Tercera visita de campo y seguimiento Diseño y Construcción de la Terminal de Integración de Soyapango para el Sistema Integrado de Transporte del Área Metropolitana de San Salvador (SITRAMSS)," San Salvador, El Salvador, 2013.
- [39] MOP, "SITRAMSS EN MARCHA 8-13." El Salvador, p. 2, Jul. 2013.
- [40] MOP, "SITRAMSS EN MARCHA 2-16." El Salvador, p. 2, Jan. 2016.
- [41] MOP, "SITRAMSS EN MARCHA 20-15." El Salvador, Jun. 2015.
- [42] MOP, "SITRAMSS EN MARCHA 25-15." El Salvador, p. 2, Jul. 2015.
- [43] MOP, "SITRAMSS EN MARCHA 15-15." El Salvador, p. 2, May 2015.
- [44] EDH, "Sala de lo Constitucional ordena paso libre al público en carril SITRAMSS," *El Diario de hoy*, San Salvador, Sep. 03, 2017.
- [45] R. Díaz, C. Mojica, and J. Hollnagel, "Retos y lecciones aprendidas en la implementación de proyectos de transporte público: cinco casos de Latinoamérica," Washington, D.C., Dec. 2018. doi: 10.18235/0001455

Smart Economy, Development and Education

Third sector actors and the University of Valladolid as one of the drivers of the urban agenda in the city of Soria, Spain.

Maján-Navalón, Raúl ¹[0009-0007-3354-0803], Sanz-Molina, Lidia ¹[0000-0003-1910-2771], Gómez-Redondo, Susana ²[0000-0002-8285-2068] y Johanna-Obregón, Lilian ²[0009-0000-5486-9383]

¹ University of Valladolid. Calle Universidad, s/n, 42005, Soria, Spain
Department of Sociology and Social Work.

² University of Valladolid. Calle Universidad, s/n, 42005, Soria, Spain
Department of Pedagogy.
Raul.majan@uva.es

Abstract. The city of Soria, in Castilla y León, has undergone significant urban transformations with the aim of improving the quality of life of its inhabitants and boosting its socio-economic development. In this process, the University of Valladolid and the third sector have played key roles as drivers of the urban agenda. The third sector, made up of non-profit organisations, has intervened in areas that other sectors have not addressed, contributing to the construction of more inclusive and sustainable cities. In parallel, the University of Valladolid has promoted research, innovation and knowledge transfer in essential areas for urban development in Soria. The collaboration between both entities has generated synergies that promote reflection, dynamisation and participation for urban regeneration, social inclusion and economic revitalisation. However, the implementation of the urban agenda faces challenges, such as coordination between actors and adaptation to changing dynamics. This article explores the impact and contributions of these actors in Soria's urban agenda, offering a comprehensive view of the collaborative dynamics and future opportunities for the city's development.

Keywords: Urban Transformation, Third Sector, University of Valladolid.

1 Introduction.

The city of Soria, located in the autonomous community of Castilla y León in Spain, has experienced over the years a series of urban transformations that have sought to improve the quality of life of its inhabitants, as well as to enhance its socio-economic development. In this transformation process, the University of Valladolid and third sector agents have played a crucial role as drivers of the urban agenda.

The third sector, made up of non-profit organisations and social entities, has been recognised in numerous studies for its capacity to intervene in areas where the public and private sectors do not reach, or do not have the interest to do so [1]. These

2

organisations, with their focus on social, cultural and environmental well-being, have contributed significantly to building more inclusive and sustainable cities.

On the other hand, universities, as institutions of higher education, are not only dedicated to academic training, but also have a commitment to the development of their environment [2]. The University of Valladolid, with its presence in Soria, has promoted various initiatives that seek to respond to local needs, promoting research, innovation and knowledge transfer in key areas for urban development.

The collaboration between the University of Valladolid and third sector agents has generated synergies that enhance the implementation of the urban agenda in Soria. This strategic alliance has made it possible to address complex challenges, such as reflection, dynamisation and participation in urban regeneration, social inclusion, environmental sustainability and economic revitalisation.

The 2030 Urban Agenda highlights the importance of sustainability and repopulation in a world where resources are limited and population is growing exponentially [3]. In this scenario, digital technology emerges as a powerful tool to address these challenges, enabling more efficient resource management and encouraging citizen participation in decision-making [4, 5]. However, for these solutions to be effective, innovation in planning and implementation is essential [6].

However, it is essential to recognise that implementing the urban agenda is not without its challenges. Coordination between different actors, resource allocation and adaptation to changing city dynamics require flexible and participatory strategies [4]. In this context, it is essential to analyse the role of the University of Valladolid and third sector actors as catalysts for change in the city of Soria.

This article seeks to explore in depth the impact and contributions of these actors in the configuration and implementation of the urban agenda in Soria. Through a detailed analysis, it aims to offer a comprehensive view of the dynamics of collaboration, the challenges faced and the opportunities presented for the future development of the city.

That said, this paper will continue with a broad theoretical framework, ranging from the role of the third sector in urban development to the engagement of universities, with a particular focus on the Urban Agenda 2030 and its challenges and opportunities.

Subsequently, the objectives of the study are set out, both general and specific, such as reflecting on the impact of the University of Valladolid and the third sector in Soria, identifying key initiatives, and analysing strategies and challenges of the Urban Agenda 2030. The methodology adopted focuses on a qualitative approach, based on documentary analysis and observations for an in-depth understanding of the implementation of the Urban Agenda in Soria.

The results highlight the active role of NGOs in promoting social inclusion, as well as the fundamental contribution of the University of Valladolid in the social dynamisation and implementation of the Urban Agenda. It examines how initiatives such as El Hueco address challenges such as depopulation and highlights social entrepreneurship projects that have made a difference in Soria. This paper concludes by summarising the key findings, highlighting the essential role of the University of Valladolid and third sector actors in the urban transformation of Soria, and reflects on the challenges and opportunities that remain.

2 Theoretical framework.

Establishing the objectives of this research is the first fundamental step. The central purpose of this paper is to reflect on and investigate the impact and contributions of the University of Valladolid and third sector agents in the urban development of Soria. This analysis is enriched with the specific identification of the most relevant initiatives and projects promoted by these entities, which have played a crucial role in the urban transformation of the city. It is also essential to outline the strategies and actions proposed by the Urban Agenda 2030 in Soria, examining the challenges and opportunities arising from its implementation. The achievement of these objectives requires the creation of a robust theoretical framework, which not only provides an in-depth understanding of the specific context and dynamics of Soria, but also guides in the critical evaluation of the contributions made by the University and third sector actors towards sustainable and effective urban development.

2.1 The Third Sector and its Role in Urban Development.

The third sector, often referred to as the non-profit sector, encompasses a wide range of organisations that are distinguished by their independence from the public and private sector. These entities, which include NGOs, foundations, associations and other forms of civil organisations, are characterised by their primary commitment to social, cultural and environmental well-being [1]. Their uniqueness lies in their ability to intervene and act in areas where traditional sectors are unable or unwilling to do so.

At the urban level, cities face multifaceted challenges ranging from sustainable resource management to social inclusion and economic revitalisation. These challenges, given their complexity, require solutions that are both innovative and participatory. It is in this scenario that the third sector plays a crucial role. Third sector organisations, with their community-centred approach and their ability to mobilise resources and volunteers, have proven to be effective in creating and implementing solutions tailored to the specific needs of urban communities [7].

Moreover, the third sector, by operating at the local level, has a deep understanding of the specific dynamics and challenges of the communities it serves. This localised perspective allows them to design interventions that are culturally sensitive and contextually relevant [8]. In many cases, these organisations act as bridges between the community and local authorities, facilitating collaboration and dialogue between different actors and ensuring that interventions are coherent and aligned with community aspirations [9].

Thus, the third sector, with its community-centred approach and its capacity to innovate and adapt, plays an essential role in shaping and promoting sustainable urban development.

2.2 The University and its Commitment to Urban Development.

Universities, traditionally considered as epicentres of education and research, have evolved significantly in their role within society in recent decades. Their commitment to sustainable development and improving the quality of life in the urban areas in which

4

they are located has led to the creation and implementation of programmes and projects with a direct impact on their environment [2].

The University of Valladolid, with its presence in Soria, is a clear example of how an educational institution can act as a catalyst for change in urban development. However, this phenomenon is not exclusive to this university. Across the world, universities are recognising the importance of their role in shaping urban communities and are adopting a more active and participatory approach to urban development [10].

For example, Alexandria University in Egypt has collaborated with the Smithsonian Science Education Centre in the US to engage children in sustainable urban design, recognising the importance of community participation in shaping urban spaces [11]. Such initiatives demonstrate how universities can act as bridges between academia and the community, facilitating collaboration and knowledge exchange.

Moreover, universities are adopting a more holistic approach to urban development, considering not only physical infrastructure, but also social, cultural and environmental aspects. Research at Bursa University in Turkey, for example, has highlighted the importance of urban design in the conservation and development of cultural heritage sites, underlining the crucial role of universities in the preservation of urban identity and memory [12].

Universities, with their rich tradition of research and education, are thus well positioned to lead and support sustainable urban development initiatives. Their ability to collaborate with diverse actors, from local governments to non-governmental organisations and communities, makes them essential players in promoting more sustainable, inclusive and resilient cities.

2.3 The Urban Agenda 2030 and Sustainability.

The 2030 Urban Agenda emerges as a response to the multifaceted challenges facing cities in the 21st century. This agenda, with its focus on sustainability, inclusion and repopulation, seeks to address the complexities inherent to urbanisation in a world where resources are finite and populations continue to grow [13].

Digital technology, in particular, has been identified as a powerful tool to address these challenges. With its ability to collect, analyse and distribute information in real time, digital technology can optimise resource management, improve the efficiency of urban services and encourage greater citizen participation in decision-making [14, 5]. These capabilities are essential for the successful implementation of the 2030 Urban Agenda, as they enable rapid adaptation to changing city dynamics and ensure that interventions are informed and data-driven.

However, the mere adoption of technologies does not guarantee success. Effective planning and implementation are essential to ensure that technology solutions align with the needs and aspirations of urban communities [6]. This requires a holistic approach that considers not only the technological infrastructure, but also the social, cultural and economic aspects of urbanisation.

Moreover, sustainability, in the context of the 2030 Urban Agenda, is not limited to resource conservation. It is also about ensuring that urban development is inclusive, equitable and resilient. This means that interventions must be designed with existing

vulnerabilities and inequalities in mind, and must prioritise the needs of the most marginalised and disadvantaged groups [15].

In this context, innovation, at its core, is not only about adopting new technologies or methods, but also about re-evaluating and revitalising traditional practices and methodologies to adapt them to contemporary realities. In many contexts, traditional practices, once considered obsolete or less efficient, are finding a renaissance in the modern era. For example, certain economic activities that had been abandoned due to industrialisation or globalisation are being revived, not only because of their cultural or historical value, but also because they offer sustainable and resilient solutions to current challenges [16].

The combination of innovation and tradition can be particularly powerful in the search for untapped niches. These niches can emerge from the intersection of modern technologies with traditional practices, creating unique opportunities for economic and social development. For example, traditional crafts, when combined with digital marketing and e-commerce platforms, can reach global markets, providing local artisans with a sustainable source of income and recognising their skill and tradition [15].

It is essential that, in pursuing innovation, we do not discard the lessons and methods of the past. In many cases, these traditional practices have evolved over centuries and represent an accumulation of knowledge adapted to specific local contexts. By integrating these methods with modern tools and approaches, we can find more holistic and sustainable solutions to the challenges of the 21st century.

As such, universities, with their rich tradition of research and education, are well positioned to lead and support sustainable urban development initiatives. Their ability to collaborate with diverse actors, from local governments to non-governmental organisations and communities, makes them essential players in promoting more sustainable, inclusive and resilient cities.

2.4 Challenges and Opportunities in the Implementation of the Urban Agenda 2030.

Implementing the 2030 Urban Agenda is a monumental task that faces a number of intricate challenges. One of the main obstacles is coordination between multiple actors, including governments, third sector organisations, universities and the private sector. The diversity of these actors, each with their own priorities and agendas, can complicate decision-making and policy implementation [4].

In addition, the proper allocation of resources is essential to the success of any urban initiative. Cities, especially those in developing countries, often face resource constraints that can hinder the implementation of ambitious projects. However, the 2030 Urban Agenda is not only about big projects; it is also about finding sustainable and efficient solutions that are adapted to local realities [13].

Rapid urbanisation and population growth also present challenges. Cities must adapt to these changing dynamics, which may require re-evaluation and adaptation of existing policies and strategies. For example, nature-based solutions such as green roofs and green infrastructure have been proposed as innovative responses to the challenges of urbanisation and have been integrated into urban planning in some European cities [17].

6

However, these challenges also offer unique opportunities. The need for coordination between different actors can foster collaboration and the exchange of ideas, leading to more innovative and holistic solutions. In addition, the quest for sustainability and efficiency can lead to the adoption of novel technologies and practices that not only address current problems but also prepare cities for future challenges [33].

Collaboration between the third sector, universities and other key actors can be particularly fruitful. These institutions can act as catalysts, driving innovation and facilitating the implementation of sustainable solutions. Moreover, they can play a vital role in identifying and exploiting untapped niches, offering new opportunities for sustainable urban development [18].

Against this background, we see that the 2030 Urban Agenda presents an ambitious vision for the future of cities. Its success depends on the ability of cities to integrate digital technologies with innovative and people-centred planning approaches, while ensuring that development is sustainable, inclusive and equitable.

3 Methodology.

This study adopted a qualitative approach [19], aimed at interpreting and understanding phenomena related to the implementation of the Urban Agenda in Soria from a non-quantitative perspective. This approach is ideal for exploring in detail the dynamics, contexts and perceptions underlying the activities associated with sustainable urban development.

The selection of entities, which included the University of Valladolid and various third sector organisations in Soria, was based on a detailed analysis of their relevance and contribution to sustainable urban development. Criteria such as the diversity of projects, their history of collaboration with the community, and their influence on local urban development were assessed. This meticulous selection ensured that the chosen entities were representative of the different aspects of the Urban Agenda.

The main data collection technique was document analysis [20], which involved the examination and critical evaluation of a range of printed and electronic documents, from official reports and meeting minutes to academic publications. This process was carried out using a specific framework to analyse and categorise the documents, thus ensuring objectivity and relevance in the assessment of the information.

To detail the data analysis process and explain how information not useful for the work was discarded, a continuous and coherent procedure is proposed that begins with the collection of all relevant documents including reports, minutes of meetings and academic publications, followed by an initial review and classification of these documents based on their direct relevance to the Urban Agenda and the activities of the selected entities, where those that have no direct relation to the topic of study or that do not provide substantial information are discarded; in the preliminary analysis, documents that provide significant and relevant information are identified, eliminating redundant information or information that does not contribute to a deeper understanding of the implementation of the Urban Agenda in Soria; The next step involves a detailed analysis of the coded and categorised documents, focusing on drawing relevant conclusions

and assessing the information in terms of its contribution to the understanding of the entities' participation in the Urban Agenda; Finally, a final assessment is made to select the data to be included in the final report of the study, discarding data that, although relevant, does not add significant value to the final findings or does not contribute to answering the research questions, thus ensuring that only the most relevant and useful information is used for the study and providing a clear guide for other researchers wishing to replicate or follow a similar methodology.

To enrich the findings obtained through the documentary analysis, the observation technique was implemented. This observation, which included visits to relevant project sites and participation in Urban Agenda events, was conducted in a structured manner, with a focus on systematic data collection and recording, allowing for the capture of details and insights not documented in the written materials.

Finally, thematic analysis [20] was used to systematically process and examine the information collected. This process involved coding data and identifying patterns and recurring themes in the documents and observations. Rigorous steps were followed to ensure the validity and reliability of the thematic analysis, thus providing a detailed and contextualised interpretation of the data. The combination of documentary analysis and observation provided a thorough understanding of the dynamics involved and ensured a balanced and rigorous perspective on the research.

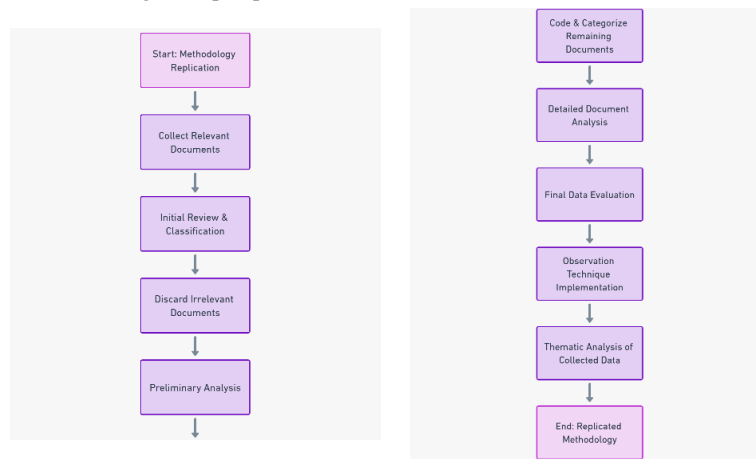


Fig. 1. Methodology Replication Flowchart.

The methodology for measuring and ranking the participation of each of the entities analysed in the paper is based on a series of evaluation criteria including project involvement, where the degree of participation of each entity in Urban Agenda related projects is assessed, the scope of impact, considering the geographical scope and the number of people affected or benefited by the activities of each entity, and the alignment with the objectives of the Urban Agenda 2030, measuring whether or not the activities of each entity are aligned with the specific objectives of the Urban Agenda such as sustainable development, social inclusion and urban innovation, using a simplified

8

evaluation system where each criterion is simply assessed as aligned or not aligned, and in the evaluation process, which is carried out using the information gathered during the analysis of documents and observations, the research team reviews reports and minutes to determine the level of involvement and impact of activities, finally discarding those entities that are not aligned with the Urban Agenda 2030, which allows for an objective and clear assessment of participation, ensuring that only those entities that contribute significantly to the Agenda's objectives are included in the analysis [Fig. 2].

4 Results

4.1 NGO activities and achievements.

NGOs in Soria have played a crucial role in promoting social inclusion and intercultural coexistence. One of the most prominent organisations in this field is the NGO "Tierra Sin Males", which has been active since 2000. Through various initiatives, such as ethical forums, intercultural days and training programmes, this NGO has addressed major issues such as armed conflicts, social exclusion, sustainable economy and globalisation. These activities have not only fostered dialogue and mutual understanding between the local community and migrant populations, but have also created economic opportunities for migrants, thus promoting cultural diversity and social welfare in the region [21].

Another significant actor in this picture is the Cepaim Foundation. Through its programme "Socio-labour integration of immigrant families in depopulated rural areas. New Paths", co-financed by the Ministry of Inclusion, Social Security and Migration and the European Social Fund, the Foundation has achieved success stories such as that of a family that decided to move to a rural village in Soria in search of a quieter life connected to nature. Thanks to the efforts and collaboration of the Foundation, this family not only found employment in an industrial crisp factory, but also managed to integrate into the community, with future plans to establish a vegetable garden and raise chickens [22].

In addition, the Cepaim Foundation has launched the SabeRural initiative in collaboration with the "la Caixa" Foundation. This proposal seeks to connect new generations with the traditions and ways of life of the Soria region, "El Valle", through intergenerational walks and the telling of stories and experiences of its inhabitants [23].

As a result of these and other NGO actions, the creation of the Soria Refugee Reception Centre (CAR) has been approved, which will be integrated into the national public network of Migration Centres. The main objective of this centre, attached to the Secretariat of State for Migration, is to offer reception, accommodation and temporary maintenance to applicants for international protection and refugees in a situation of psychosocial vulnerability. In the context of public management, citizen participation is essential for the social construction of public policies. Although this concept is clearly defined, much remains to be done to consolidate citizen participation in all stages of the public policy management cycle in the region [24].

Finally, it is important to highlight the work of "Hacendera", an association that promotes care for life, health, culture and the territory of Soria. This association is committed to sustainable development based on new social, economic, cultural and

ecological models. Its mission is to care for the natural and cultural heritage and the health of people in Soria and its villages, channelling development alternatives that respect life [25].

4.2 University: action and social revitalisation.

An example of this is the organisation of the conferences related to the University Social Responsibility of the Uva (RSUva) [Table 1], where the activities were carried out on an ad hoc basis, mainly through the initiatives of the teaching staff or the vice-rectorate. However, since the first Conference: "University and Cooperation", an evolution in participation and response to the context and needs of the Campus has been observed. In 2023, the MESCOOP2023 event, organised by the NGO Tierra Sin Males and RSUva, experienced an increase in its activities, promoting interaction between various entities and fostering awareness and sensitisation among the university community. This event was a notable success, with an average attendance of 40 people per activity [26; 34].

The University of Valladolid (UVa), especially its campus in Soria, has emerged as a fundamental pillar in the social dynamisation and promotion of the Urban Agenda 2030. This educational institution has demonstrated an unwavering commitment to University Social Responsibility (USR). Over the years, it has organised various conferences focused on USR, which were initially driven mainly by the faculty and the vice-rectorate. However, over time, a significant evolution in participation and adaptation to the needs and context of the campus was observed. A clear example of this is the MESCOOP2023 event, which was carried out in collaboration with the NGO Tierra Sin Males and RSUva. This event not only saw an increase in activities, but also promoted interaction between various entities and fostered awareness and sensitisation among the university community. The success of this event was remarkable, with an average attendance of 40 people per activity [27, 28].

The Urban Agenda 2030 has had a significant influence on strategies and actions in Soria. A tangible manifestation of this commitment is the creation of the Chair "Urban Agenda 2030 for Local Development". This Chair not only symbolises how the Agenda has been integrated into local policies and practices, but also reflects Soria's commitment to the Sustainable Development Goals. The justification for the creation of this Chair lies in the absence of a similar structure addressing the economic and social interest of the region. Given the non-availability of the Urban Agenda methodology, the University of Valladolid has identified a strategic opportunity to actively participate in its development. The primary objective of the Chair is to transfer the knowledge generated at the University to the local society, focusing on the achievement of the strategic objectives of the Spanish Urban Agenda. This knowledge transfer is not unidirectional; it seeks to establish a bidirectional mechanism that benefits both the University and local society [29].

Furthermore, the Chair has a direct impact on society. Research around the specific objectives of the Spanish Urban Agenda will provide local society with tools to improve their environment. As a result, it is expected that the University of Valladolid will attract and train outstanding professionals who will contribute significantly to

10

knowledge-based development. This initiative will also enable society to have a deeper understanding of their cities, especially Soria, and provide them with information that will enable them to be more critical and proactive with their environment [29].

The RIOS-SO project is another initiative born from the Urban Agenda 2030 Chair for Local Development. It aims to study the rivers in the province of Soria in order to identify and inventory all existing infrastructures prior to this century that were used for milling grain, among other uses. This project has historical, technical and geo-social connotations, and its results will be reflected in various deliverables, including dissemination and artistic books, as well as a tourist exploitation plan.

It is also essential to mention that the Department of Financial Economics and Accounting of the University of Valladolid, together with the Vice-rectorate of the Soria Campus, organised a conference focused on the problem of depopulation in Soria, a city facing challenges such as population loss, ageing, low density and a negative vegetative balance. This AECA Conference brought together experts from various fields, including business, institutions and universities, to debate and reflect on these issues from economic, social, environmental and technological perspectives. The main objective was to identify current problems and outline solutions based on sustainability and digitalisation. In addition, a platform was provided to present research and papers, which were evaluated and discussed in parallel scientific sessions [29].

Finally, we would highlight the DINAMIZA I call (2019-2020), 15 initiatives were presented, resulting in eight finalist ideas. The winning project was a proposal for "Linguistic and cultural immersion", devised by first-year students of Business and Labour Sciences. This initiative sought to attract foreign students to participate in a two-week programme, where they would learn Spanish and get to know the local culture and traditions. During their stay, the students would attend classes in educational centres in the city and participate in various cultural and recreational activities. After this first edition, improvements were introduced in the call, such as the extension of participation to higher courses and a greater representation of all faculties. The DINAMIZA calls have boosted the creation and development of innovative projects in Soria [30].

Table 2. Events Organised by the University of Valladolid, Soria Campus, to Support Agenda 2030 Initiatives.

Event	Brief Description
Social Responsibility Workshops	Activities organised by the faculty and vice-rectorate, focusing on University Social Responsibility (USR).
MESCOOP2023	Event organised by the NGO Tierra Sin Males and RSUva, promoting interaction among entities and raising awareness in the university community. Average attendance of 40 people per activity.
Chair "Urban Agenda 2030 for Local Development"	Initiative to integrate the Urban Agenda into local policies and practices, focusing on transferring knowledge from the university to the local society and vice versa.
RIOS-SO Project	Study of the rivers of the Soria province, identifying ancient infrastructures for historical and geosocial purposes, including the creation of dissemination books and a tourism exploitation plan.

AECA Workshop	Workshop focused on the depopulation issues in Soria, bringing together experts to debate solutions based on sustainability and digitalisation. Included presentations of research and scientific sessions.
DINAMIZA I Call (2019-2020)	Presentation of 15 initiatives, with eight finalist ideas. The winning project was a proposal for "Linguistic and Cultural Immersion" for foreign students. Included improvements in subsequent calls for wider participation and representation from all faculties, promoting innovative projects in Soria.

4.3 El Hueco, dynamisation from the third sector.

Depopulation is a significant challenge affecting several regions in Spain, including Soria. El Hueco, a programme designed to combat depopulation in rural areas, has implemented projects in Navarra and organises the Presura National Fair for the repopulation of rural Spain. These initiatives seek to encourage entrepreneurship and the creation of socially-oriented businesses in rural areas. In addition, the concept of "new rurality" has been introduced, which seeks to attract more people to rural areas, taking advantage of the opportunities and benefits that these areas can offer.

Soria has experienced a significant decline in population in recent decades. In 2008, the province had around 95,000 inhabitants, but in 2022, this number was reduced to 88,377. This depopulation has led to a decline in economic activity and the provision of basic public services. However, thanks to projects such as El Hueco and the NGO Cives Mundi, innovative solutions are being implemented to revitalise these areas and combat depopulation [31].

El Hueco has received both public and private funding, including support from the European Union. This funding has allowed El Hueco to organise international events, incubating the best social projects and promoting social entrepreneurship in Spain. Collaboration with entities such as FOES, Caja Rural and CESCE has been essential for the growth and strengthening of El Hueco.

Rural areas are gaining recognition as areas with a high potential to offer a better quality of life, especially after the COVID-19 pandemic. The "new rurality" seeks to redefine the relationship between people and the rural environment, promoting entrepreneurship and sustainable development. El Hueco's initiatives and programmes have demonstrated that it is possible to revitalise rural areas through entrepreneurship and community collaboration [31].

4.4 Social Entrepreneurship in Soria.

La Exclusiva is a company that emerged with the aim of supplying depopulated rural areas of Spain, particularly in Soria. This company, which began operations in 2013, delivers products to more than 300 villages from Tuesday to Friday, covering routes that sometimes exceed 100 kilometres. La Exclusiva not only focuses on delivering products, but also seeks to establish a close relationship with its customers, many of whom are elderly.

In 2021, La Exclusiva established an alliance with Día, which has allowed it to expand its reach and offer fresh produce to more than 7,000 families in rural areas of

12

Soria. This partnership also aims to expand the project to other provinces in Spain facing depopulation problems.

In addition to its core work, La Exclusiva has launched Pixie by La Exclusiva, a mobile micro-training centre offering technology training workshops for older people in Soria [32].

5 Conclusions

The city of Soria, like many regions in Spain, faces significant challenges related to depopulation and economic decline. However, the University of Valladolid, together with various third sector actors, has emerged as a key driver in promoting sustainable urban development in the city.

The University of Valladolid, particularly its campus in Soria, has demonstrated an unwavering commitment to University Social Responsibility (USR). Through events such as MESCOOP2023 and the creation of the Chair "Urban Agenda 2030 for Local Development", the University has not only promoted interaction and awareness among the university community, but has also established a bridge between academia and local society. This two-way collaboration seeks not only to transfer knowledge, but also to receive input from the community to enrich research and academic practices.

On the other hand, third sector organisations such as "Tierra Sin Males", Cepaim Foundation and "Hacendera" have implemented initiatives that directly address the challenges of depopulation and social exclusion by taking part in citizen participation processes to establish the urban agenda of the city of Soria. These organisations have fostered inclusion, cultural diversity and social well-being, creating economic opportunities and promoting intercultural coexistence.

The Urban Agenda 2030 has been a key strategic framework that has influenced actions and strategies in Soria. The creation of the Chair "Urban Agenda 2030 for Local Development" is a testimony of Soria's commitment to the Sustainable Development Goals and reflects how the Agenda has been integrated into local policies and practices.

However, despite these efforts, challenges remain. Depopulation has led to a decline in economic activity and the provision of basic public services. But, with the introduction of innovative concepts such as "new rurality" and social entrepreneurship, there is renewed optimism about the possibilities for revitalising rural areas.

Therefore, the University of Valladolid and third sector actors have played an essential role in the urban transformation of Soria. Although there is still work to be done, the initiatives and projects presented in this study show a promising path towards sustainable urban development that responds to the challenges and takes advantage of the unique opportunities offered by the region.

Acknowledgements

We would like to express our sincere thanks to the City Council of Soria; to the University of Valladolid, specifically to the Social Responsibility of the University of Valladolid, to the Chair Urban Agenda 2030 for Local Development and to the Vice-

Rectorate of the Duques de Soria Campus; also to the NGO Tierra Sin Males, and to all those who contributed directly or indirectly to the development of this work.

References

1. Salamon, L. M., Anheier, H. K.: *Defining the nonprofit sector: A cross-national analysis*. Manchester University Press, Manchester (1997).
2. Benneworth, P., Jongbloed, B. W.: Who matters to universities? A stakeholder perspective on humanities, arts and social sciences valorisation. *Higher education* 59, 567-588 (2010).
3. Ezquiaga Domínguez, J. M.: La Agenda Urbana Española: una oportunidad para el desarrollo sostenible. *Ciudad y Territorio Estudios Territoriales* 51(201), 7-24 (2019).
4. Pierre, J.: Can urban regimes travel in time and space? *Urban regime theory, urban governance theory, and comparative urban politics*. *Urban Affairs Review* 50(6), 864-889 (2014).
5. Castells, M.: *Networks of outrage and hope: Social movements in the Internet age*. John Wiley & Sons, New Jersey (2015).
6. Kar, A. K., Ilavarasan, V., Gupta, M. P., Janssen, M., Kothari, R.: Moving beyond smart cities: Digital nations for social innovation & sustainability. *Information Systems Frontiers* 21, 495-501 (2019).
7. Evers, A., Laville, J. L. (eds.): *The third sector in Europe*. Edward Elgar Publishing, Cheltenham (2004).
8. Choto, P., Iwu, C. G., Tengeh, R. K.: Non-profit organisations and socio-economic development in South Africa: A literature analysis. *Humanities & Social Sciences Reviews*.
9. Newton, P., Frantzeskaki, N.: Creating a national urban research and development platform for advancing urban experimentation. *Sustainability* 13(2), 530 (2021).
10. Jahin, H., Raslan, R.: Towards Children Engagement in Urban Design Development for Sustainable Communities The case of Child's University at Alexandria University, Egypt. *MSA Engineering Journal* 2(2), 80-99 (2023).
11. Polat, S., Yıldız, H. Ö. T., Dostoğlu, N.: A User-Oriented Urban Design Guide Model For Cultural Heritage Sites: The Case of Bursa Khans Area. *Megaron* 13(4), 584 (2018).
12. Habitat, U. N.: *New urban agenda. Quito declaration on sustainable cities and human settlements for all*. Quito UN Habitat.
13. Rifkin, J.: *The zero marginal cost society: The internet of things, the collaborative commons, and the eclipse of capitalism*. St. Martin's Press, New York (2014).
14. Cohen, B.: La ciudad del siglo XXI: oportunidades y desafíos urbanos en un contexto global. *Public Administration and Development* 37(5), 310-320 (2017).
15. Klein, M., Gerlitz, L.: Creative industries in a pandemic: cross sectoral innovation. *European Research Studies Journal* 24(s3), 758-766 (2021).
16. Pineda-Martos, R., Calheiros, C. S.: Nature-Based Solutions in Cities—Contribution of the Portuguese National Association of Green Roofs to Urban Circularity. *Circular Economy and Sustainability* 1(3), 1019-1035 (2021).
17. Frantzeskaki, N., McPhearson, T., Collier, M. J., Kendal, D., Bulkeley, H., Dumitru, A., Pintér, L.: Nature-based solutions for urban climate change adaptation: linking science, policy, and practice communities for evidence-based decision-making. *BioScience* 69(6), 455-466 (2019).
18. Creswell, J. W., Poth, C. N.: *Qualitative inquiry and research design: Choosing among five approaches*. Sage publications, California (2016).
19. Morgan, H.: Conducting a qualitative document analysis. *The Qualitative Report* 27(1), 64-77 (2022).

14

20. Mackieson, P., Shlonsky, A., Connolly, M.: Informing permanent care discourses: A thematic analysis of parliamentary debates in Victoria. *The British Journal of Social Work* 48(8), 2137-2156 (2018).
21. Majan-Navalon, R., Sanz-Molina, L., Lallana-García, E.: El impacto de una ong local en una ciudad: El caso de la ONG Tierra Sin Males. In: *Jornadas AECA sobre Repoblación y Sostenibilidad Digital*, Soria, España (2023).
22. Fundación Cepaim: SabeRural: Saberes y experiencias para el desarrollo rural. https://cepaim.org/documentos/publi/3010_sabeRural.pdf (2019).
23. Fundación Cepaim: Una familia se traslada al medio rural de Soria para comenzar una nueva vida. <https://www.cepaim.org/una-familia-se-traslada-al-medio-rural-de-soria-para-comenzar-una-nueva-vida/> (2021).
24. Campillo, J. A.: El Centro de Refugiados de Soria prevé iniciar su servicio en 2024. *Heraldo-Diario de Soria*. <https://www.heraldodiariodesoria.es/soria/230310/32308/centro-refugiados-soria-preve-iniciar-servicio-2024.html> (2023).
25. Asociación Hacendera: Asociación Hacendera. <https://asociacionhacendera.org/> (2023).
26. Majan-Navalon, R., Sanz-Molina, L., Lallana-García, E.: El impacto de la colaboración entre agentes sociales: experiencia Universidad de Valladolid - ONG Tierra Sin Males. Soria. In: *Jornadas AECA sobre Repoblación y Sostenibilidad Digital*, Soria, España (2023).
27. Tierra Sin Males: Dossier Informativo. <https://tierrasinmales.org/> (2023).
28. Tierra Sin Males: Base de datos de Tierra Sin Males. <https://tierrasinmales.org/> (s.f.).
29. Catedra Agenda Urbana 2030: Catedraagendaurbana.uva.es. <https://catedraagendaurbana.uva.es/> (2021).
30. Sanz Molina, L., Jiménez Fuentes, I., Vera Mayor, C.: Iniciativa de participación universitaria en el diseño de ciudad: Laboratorio de ideas Dinamiza Soria. In: *Jornadas AECA sobre Repoblación y Sostenibilidad Digital*, Soria, España (2023).
31. Berrad Nahraou, L., Hernández Gómez, M.: Soluciones para la despoblación en España: iniciativas impulsadas por el Hueco y Presura. In: *Jornadas AECA sobre Repoblación y Sostenibilidad Digital*, Soria, España (2023).
32. Tobar, S.: Dar de comer a la España vaciada: así es el proyecto social de La Exclusiva que apoya Día en Soria. *El Español*. https://www.elespanol.com/invertia/empresas/distribucion/20220925/dar-espana-vaciada-proyecto-exclusiva-dia-soria/705429834_0.html (2022).
33. Sánchez Trujillo, M. A., Doblado Jiménez, B., Campos Fito, J. M.: Agenda 2030 and the Challenges of the Sustainable Urban Development Goals in France: The Case of Saint-Étienne. In: *Urban Policy in the Framework of the 2030 Agenda: Balance and Perspectives from Latin America and Europe*, pp. 197-214. Springer Nature Switzerland, Cham (2023).
34. Aguilar-Jiménez, J. A., Hernández-Callejo, L., Suástegui-Macías, J. A., Alonso Gómez, V., García-Álvaro, A., Maján-Navalón, R., Obregón, L. J.: Energy and Economic Analysis of Renewable Energy-Based Isolated Microgrids with AGM and Lithium Battery Energy Storage: Case Study Bigene, Guinea-Bissau. *Urban Science* 7(2), 66 (2023).
35. Martínez, J. B., Plaza, A. R., Medina, A. M. B., Obregón, L. J., Romero, H. F. M.: Methodology for watermills localization: A case study of Soria province (Spain). In: *Congress of Smart Cities*, p. 267. http://dspace.uca.es/bitstream/123456789/41225/1/Proceedings%20ICSC-CITIES%202022%20RG_compressed.pdf#page=291 (2022).

El valor de la Educación para la Ciudadanía Mundial en el marco de Agenda 2030 y la construcción de ciudades inteligentes y sostenibles: La iniciativa Soria 2030

Ana Isabel Lozano Sobrino¹, Sonia Ortega Gaité², Judith Quintano Nieto³ y Diego Miguel-Revilla⁴

¹ Departamento de Didáctica de las Ciencias Experimentales, Sociales y de la Matemática. Universidad de Valladolid, España. ana.lozano@uva.es

² Departamento de Pedagogía. Universidad de Valladolid, España. sonia.ortega.gaité@uva.es

³ Departamento de Filosofía. Universidad de Valladolid, España. judith.quintano@uva.es

⁴ Departamento de Didáctica de las Ciencias Experimentales, Sociales y de la Matemática. Universidad de Valladolid, España. diego.miguel.revilla@uva.es

Resumen. El propósito de este estudio, de carácter transversal será indagar sobre el valor de la Educación para la ciudadanía Mundial como eje vertebrador en la consecución y construcción de ciudades inteligentes y sostenibles regidas por los parámetros que marca la Agenda 2030 a nivel mundial. La puesta en marcha de estrategias educativas con un enfoque integral para la sostenibilidad, en entornos cercanos y globalizados, hace más sencillo el paso del alumnado hacia una participación comprometida y a la vez activa en la lucha contra el cambio climático y la defensa del medio ambiente, así como la asimilación de competencias necesarias que le permitan discurrir y desenvolverse en sociedades más inclusivas, justas, sostenibles y resilientes. Es sin duda, un inicio que está alineado con los Objetivos de Desarrollo Sostenible de la Agenda 2030 y que favorece una visión integral para aprender y funcionar en sostenibilidad. Aterrizando el ejemplo de una ciudad intermedia como Soria, se plantean aspectos básicos sobre la iniciativa Soria 2030, que trata de construir una hoja de ruta, con objetivos, compromisos y medidas para convivir en una ciudad limpia, sana, y próspera y avanzar hacia una ciudad inteligente y sostenible. Este estudio es, por tanto, una aproximación teórica a los valores que desde la educación se deben trabajar para, en consonancia con el desarrollo sostenible, seamos capaces de generar nuevos espacios de hábitat urbano como se pretende alcanzar en la ciudad de Soria.

Palabras clave: Educación, Sostenibilidad, ciudadanía, desarrollo, conocimiento, objetivos de desarrollo sostenible, ciencias sociales.

Introducción

La educación para una ciudadanía sostenible ha tomado especial relevancia en la actual legislación educativa; este estudio tratará de reconocer el valor de la formación en valores ciudadanos y la integración de valores de sostenibilidad en la educación como pilar en la creación de ciudades sostenibles en el marco de la consecución de los hitos que marca la Agenda 2030.

Siguiendo el marco normativo, la enseñanza y el aprendizaje para la sostenibilidad significan un desafío que debe estar incluido en las actividades escolares diarias. La Ley Orgánica 3/2020, de 29 de diciembre, por la que se modifica la Ley Orgánica 2/2006, de 3 de mayo, de Educación [1] establece los centros, como espacios abiertos a la sociedad de la que son elemento vertebrador, deben acometer la coordinación y el trabajo con las administraciones, entidades y asociaciones de su entorno inmediato, favoreciendo la generación de comunidades educativas abiertas, que sean impulso de la transformación social integral.

Concretamente, el Real Decreto 217/2022, de 29 de marzo, por el que se establece la ordenación y las enseñanzas mínimas de la Educación Secundaria Obligatoria (ESO) recoge que se tiene que propiciar un aprendizaje competencial, autónomo, significativo y reflexivo en el alumnado para que pueda promover el desarrollo sostenible, mediante acciones seguras, y que debe lograrse mediante metodologías que estén orientadas al ejercicio de una ciudadanía activa.

Aunando las pretensiones mencionadas, se evidencia que uno de los fines del proceso educativo es alcanzar pequeños hitos en ciudades intermedias, tal y como se pretende con la iniciativa “SORIA 2030”, que nace con el objetivo de preservar la biodiversidad, reducir las emisiones de carbono y erigir a Soria como una ciudad sostenible.

1 Breve aproximación de la educación en valores en el sistema educativo español

La evolución en el sistema educativo español ha estado marcada por diferentes reformas en las que se otorga menor o mayor presencia a la cuestión abordada en este trabajo. La formación en valores ciudadanos en los sistemas educativos siempre ha sido un aspecto de gran controversia, tanto a nivel internacional como nacional. Tradicionalmente hay dos grandes opciones para abordar esa formación: la transversalidad, integrando la formación para la ciudadanía en asignaturas del currículo, y la opción de asignar a la educación en valores ciudadanos un espacio propio como asignatura [2, 3]. Sin embargo, desde una mirada pedagógica, la forma más integral de abordarlo sería la doble presencia [4, 5].

Haciendo una breve aproximación podemos constatar que en la Ley Orgánica de Ordenación General del Sistema Educativo (LOGSE) de 1990 se incluyen de forma

explícita, por primera vez, los temas transversales vinculados con la educación en valores ciudadanos, pero sin desarrollo explícito en el currículum. Es en 2006 con la Ley Orgánica de Educación (LOE), cuando aparecen recogidos de forma específica contenidos relacionados con la educación en valores ciudadanos siguiendo las directrices marcadas por el Consejo de Europa, una inclusión curricular controvertida que tuvo una gran repercusión en prensa y un amplio debate político y social [6, 7]. Unos años después, en 2013, con la entrada en vigor la Ley de Mejora de la Calidad Educativa (LOMCE) se produce un retroceso con la eliminación de la asignatura.

Actualmente, está en vigor la la Ley Orgánica 3/2020, de 29 de diciembre, por la que se modifica la Ley Orgánica 2/2006, de 3 de mayo, de Educación (LOMLOE), un marco legislativo que introduce las directrices recogidas en la Agenda 2030 y plantea educar desde un enfoque que aborda el desarrollo sostenible, el género y la coeducación y los derechos de la infancia bajo el objetivo de una educación para una ciudadanía activa, crítica y global en consonancia con la Educación para la Ciudadanía Mundial propuesta por la UNESCO y en línea con la meta 4,7 de los Objetivos de Desarrollo Sostenible. Desde este planteamiento, se busca garantizar que todo el alumnado pueda recibir una educación para el desarrollo sostenible y los estilos de vida sostenibles, los derechos humanos, la igualdad de género, la promoción de una cultura de paz y no violencia, la ciudadanía mundial y la valoración de la diversidad cultural y la contribución de la cultura al desarrollo sostenible [8].

2 Educar para una ciudadanía mundial desde la Agenda 2030

Tras el comienzo de la Década de la Educación por la Sostenibilidad en 2005, aterrizamos en 2015, momento en el que se presenta la Agenda 2030 acompañada de sus 17 Objetivos de Desarrollo Sostenible (ODS). Una ruta de acción internacional no exenta por ello de crítica y reflexión, que además de comprometerse con la protección y prosperidad del planeta, así como la igualdad entre las personas, nace con la pretensión de integrarse en las agendas del desarrollo económico, social y ambiental [8].

Los 17 ODS están interrelacionados, no obstante, seis de ellos hacen referencia explícita al cuidado del medio ambiente, agrupándose en la denominada dimensión “planeta” (ODS 6: agua limpia y saneamiento; ODS 7: energía asequible y no contaminante; ODS 12: producción y consumo responsables; ODS 13: acción por el clima; ODS 14: vida submarina; y ODS 15: vida y ecosistemas terrestres). Dada la perspectiva globalizadora y de conjunto que emana de la agenda, otros de los objetivos que interpela directamente al mundo educativo es el ODS 4, otorgando valor e importancia a la educación en el logro de la consecución del resto de objetivos y, en concreto, a la meta 4,7.

Todo ello para generar una educación para el desarrollo sostenible y los estilos de vida sostenibles, los derechos humanos, la igualdad de género, la promoción de una cultura de paz y no violencia, la ciudadanía mundial y la valoración de la diversidad cultural y la contribución de la cultura al desarrollo sostenible [8, p. 20].

Paradójicamente, en un mundo cada vez más conectado, la realidad evidencia una crisis que afecta a diferentes dimensiones de la vida manifestándose en desigualdades de muy diversa índole a escala global-local. Vivimos en una sociedad cambiante y sujeta a la inmediatez, regida por un capitalismo que resta visibilidad a los problemas globales. Estamos ante un momento crucial en el que, la manera en la que actuemos como sociedad dependerá, en gran medida, el devenir del planeta y de la humanidad “los patrones de insostenibilidad en la producción, consumo y crecimiento demográfico desbordan ya los límites biofísicos del planeta y los tiempos para las dilaciones se han acabado” [9, p.10).

Desde estas premisas, la educación es clave para transformar la realidad, y en concreto desde una mirada de ciudadanía mundial que comparte los planteamientos de la Educación para el Desarrollo (EpD) de sexta generación, potenciando entre otros aspectos, una educación para la ciudadanía global y de transformación social que propone una forma de educar desde la reflexión crítica y emancipación (Celorio y López, 2007; Celorio, 2013, Ruiz, 2015). En la misma línea, Ortega-Gaite (2016, p.137-138) esboza una serie de cuestiones referidas a la EpD a tener presentes:

- Debe facilitar la comprensión de la realidad mundial desde diferentes perspectivas para que la ciudadanía tome la conciencia crítica necesaria que genere cambios de actitudes y valores a nivel individual y a nivel colectivo.
- Busca una transformación social a través de la participación activa de la ciudadanía en clave de justicia social, equidad de género y solidaridad.
- Plantea crear una cultura comprometida con un desarrollo humano que sea justo, equitativo y sostenible a lo largo de la historia, que dé acogida a las diferentes formas de hacer y sus procesos.
- Ha de facilitar la construcción de una ciudadanía mundial, con una mirada transformadora, que se implique en el proceso de forma activa y tome conciencia de las múltiples realidades que habitan el planeta.

En ese sentido, el marco legislativo español actual ya referenciado, incluye el desarrollo sostenible en consonancia con la Agenda 2030. Además, el mismo desprende un especial interés por atender contenidos relacionados con la educación para el desarrollo sostenible desde una mirada de educación para la ciudadanía mundial [3],

la educación para la transición ecológica, sin descuidar la acción local, imprescindibles para abordar la emergencia climática, de modo que el alumnado conozca qué consecuencias tienen nuestras acciones diarias en el planeta y generar, por consiguiente, empatía hacia su entorno natural y social. [1, p. 122872]

La legislación educativa, en sus esfuerzos por el desarrollo de competencias clave, incorpora planteamientos que convergen hacia el tipo de educación abordada en este trabajo. Los documentos de reciente publicación que establecen las enseñanzas mínimas, plantean un desarrollo competencial específico vinculado con la necesidad de comprensión de las relaciones sistémicas entre el individuo, la sociedad y la naturaleza,

a través del conocimiento y la reflexión sobre los problemas ecosociales, para comprometerse activamente con valores y prácticas consecuentes con el respeto, cuidado y protección de las personas y el planeta, así como el fomento la autoestima y empatía con el entorno, identificando, gestionando y expresando emociones y sentimientos propios, y reconociendo y valorando los de los otros, para adoptar una actitud fundada en el cuidado y aprecio de sí mismo, de los demás y del resto de la naturaleza.

En lo referido a los saberes básicos, el desarrollo sostenible y la ética ambiental, estrechamente relacionados con la dimensión Planeta de los ODS a la que ya se ha hecho referencia, se explicita en el marco curricular con el desarrollo de cinco saberes: hábitos y actividades para el logro de los Objetivos de Desarrollo Sostenible; el consumo responsable; el uso sostenible del suelo, del aire, del agua y de la energía; la movilidad segura, saludable y sostenible; la prevención y la gestión de los residuos.

La comprensión de los acontecimientos que se suceden a través del tiempo y el análisis de los cambios como fruto de la acción humana implican concebir el aprendizaje del alumnado como una invitación al conocimiento de sí mismo y del mundo que le rodea, a la participación y al compromiso social. Dentro de esta educación para la ciudadanía, y en el marco de creación de ciudades sostenibles, también se propone interactuar en el entorno más cercano (la ciudad donde vivimos) y comprender las relaciones que establecemos, por ejemplo, en cuanto a temas tan trascendentales dentro de los ODS como la búsqueda del fin de la pobreza, la igualdad de género y la redistribución de las desigualdades.

Siguiendo el reciente currículum educativo, se abordan los contenidos curriculares en consonancia con Objetivos de Desarrollo Sostenible y dentro de ellos, el área de Ciencias Sociales en la etapa de Educación Secundaria se sitúa como eje vertebrador que contribuye a la percepción y el análisis de una realidad cada vez más diversa y cambiante.

3 El trabajo sobre ODS y Agenda 2030 desde las Ciencias Sociales

Abordar el tratamiento de los ODS y la Agenda 2030 en lo relativo a objetivos y contenidos, es interesante en todas las etapas educativas, no obstante, en el contexto de este trabajo, se otorga una especial atención en Educación Secundaria Obligatoria y, en concreto, dentro del área de Ciencias Sociales. Considerando que esta área, atendiendo a sus planteamientos curriculares, facilita que el alumnado descubra, comprenda e interiorice la importancia de la sostenibilidad desde múltiples saberes como la energía asequible y no contaminante, la emergencia climática, la producción y el consumo responsable, el saneamiento y la protección de la vida submarina.

En definitiva, y debido al cambio que se produce de la Educación Primaria a la Secundaria y que implica comprender, desde un punto de vista crítico y con perspectiva histórica, realidades cada vez más complejas, sería interesante valorar cómo está incidiendo en el estudiantado de secundaria la inclusión de estos contenidos de forma interdisciplinar.

La conexión entre la enseñanza y el aprendizaje de las Ciencias Sociales y el desarrollo de los ODS ha sido analizada en múltiples investigaciones debido a su profundidad y su estrecha relación [12]. Específicamente, y situándonos en el marco de las ciudades intermedias y sus retos, las Ciencias Sociales permiten desarrollar en los estudiantes, las capacidades necesarias para alcanzar el ideal de ciudad sostenible, contribuyendo en mayor grado a algunos de ellos, en los términos que se describen a continuación.

De forma destacada, las distintas materias del área contribuyen notablemente a implementar las capacidades que permitan vivir en una sociedad plural y democrática, para lo cual es primordial el conocimiento de los derechos y deberes, la tolerancia y la solidaridad. Trabajar en equipo, educar en igualdad, rechazar toda forma de discriminación y erradicar la violencia sexista son propósitos fundamentales e ineludibles.

El correcto encuadramiento y uso de las fuentes de información, la precisión científica en el manejo del lenguaje histórico, la capacidad para explicar la pluralidad de causas de los fenómenos y deducir las consecuencias constituyen un aporte esencial

para conocer los aspectos básicos de la nuestra Historia [13], pero también para valorar la inmensa riqueza de nuestro patrimonio artístico y cultural con una visión amplia pero también dentro del espacio cercano, la ciudad. Todo esto en un contexto en el que la enseñanza de la Historia se afianza desde visiones ligadas al desarrollo de la idea de ciudadanía y de la convivencia en sociedad [14], y en la que la comprensión de los problemas y retos contemporáneos asume un papel destacado y relevante para el alumnado.

Además del trabajo específico ligado a las diferentes disciplinas de las Ciencias Sociales, su aprendizaje aborda otros elementos y desarrolla diversas competencias. Entre ellas destaca la toma de decisiones, asumir responsabilidades, aceptar y conocer el respeto por el otro, los hábitos de vida saludables y el respeto al medio ambiente son una finalidad en sí mismas, que a su vez potencian el espíritu emprendedor del ser humano y la iniciativa personal dentro de parámetros de responsabilidad social y sostenibilidad. Muchas de estas ideas se ligan de manera clara con el concepto de la educación democrática [15], elemento clave interrelacionado con las Ciencias Sociales, las investigaciones en el área de Didáctica de las Ciencias Sociales [16], y con las finalidades de la enseñanza de todas sus disciplinas [17, 18], en conexión con la realidad y el entorno de los estudiantes y con la finalidad de situarse y saber participar en las sociedades actuales.

En esta línea, nos planteamos alcanzar una Educación para el Desarrollo, que contenga materias relacionadas con la sostenibilidad de forma organizada y coherente en la organización escolar, e integre el aprendizaje para la sostenibilidad en todo el contexto educativo. Para ello, desde las políticas educativas se deben impulsar acciones educativas críticas y transformadoras, que incorporen metodologías activas que promuevan la creación de espacios de participación del alumnado y la interacción del centro educativo con el entorno como eje de la transformación ecosocial y generador de espacios de hábitat y vida sostenibles.

4 Oportunidades y retos para el futuro

Los planteamientos expuestos pueden abarcar la enseñanza y el aprendizaje, la gobernanza, la investigación y la innovación, las infraestructuras, las instalaciones y las actividades y deberían involucrar al alumnado, a las familias, a todo el personal, a la comunidad local y a las sociedades más amplias. A su vez, se abre una ventana nueva a la educación para el Desarrollo Sostenible y la Ciudadanía Mundial que tiene entre sus aspiraciones conformar centros educativos capaces de modificar al alumnado y al resto de la colectividad educativa para ejercer un impulso hacia sociedades más inclusivas, solidarias, justas y sostenibles ayudando en la creación y mantenimiento de ciudades inteligentes y sostenibles.

Alcanzar valores de compromiso y sostenibilidad, a la vez que avanzamos en la creación de espacios más inteligentes, sin duda, es un reto imprescindible para nuestra sociedad y nuestro hábitat y de su consecución dependen la preservación de la vida tal y como la conocemos y también en el planeta. En este contexto, el espacio educativo resulta crucial a la hora de confrontar estos desafíos y colaborar en la búsqueda de soluciones que permitan construir escenarios de compromiso y forjar sociedades más justas, solidarias, prósperas, pacíficas y sostenibles. La UNESCO señala en su Informe *Replantear la educación, ¿Hacia un bien común mundial?* que “habida cuenta de la necesidad de un desarrollo sostenible en un mundo cada vez más interdependiente, la educación y el conocimiento deberían considerarse bienes comunes mundiales” [19].

Actualmente, el marco global en el que debe sustentarse la sociedad, entendida en su concepto más amplio, es la Agenda 2030. En el contexto de cambio e incertidumbre en el que vivimos, la Agenda se convierte en la hoja de ruta hacia la que debemos converger para afrontar los desafíos que la humanidad tiene delante. Este espacio común del que nos hemos dotado (los ODS) no solo debe centrar su trabajo en estos objetivos, sino en una nueva forma de entender el progreso humano de un modo sostenible [20].

La sociedad, precisa que los centros educativos sean motores de cambio en los que se redefinan los nuevos paradigmas que enfrenta la educación sostenible, y que se conviertan en territorios donde la innovación y la capacidad de adaptación conduzcan a la generación de modelos de desarrollo nuevos, más justos, basados en la cooperación, el respeto, la percepción de la naturaleza y sus equilibrios.

Ya hemos apuntado que, la nueva LOMLOE recoge este enfoque y reconoce la importancia de atender al desarrollo sostenible de acuerdo con la establecido en la Agenda 2030, señalando que la educación para el desarrollo sostenible ha de incluirse en los planes y programas educativos de la totalidad de la enseñanza obligatoria incorporando los conocimientos, capacidades, valores y actitudes que necesitan todas las personas para vivir una vida fructífera, adoptar decisiones fundamentadas y asumir un papel activo (tanto en el ámbito local como mundial) a la hora de afrontar y resolver los problemas comunes a todos los ciudadanos del mundo. Para todo ello, se hace necesaria una acción educativa desde una óptica reflexionada, y que valore la importancia del contexto social y ambiental como ejes transformadores de una nueva educación.

Concretamente, en el caso de la iniciativa Soria 2030, se plantean los siguientes desafíos: combatir el cambio climático salvaguardando los ecosistemas y su biodiversidad, tratar de contrarrestar la despoblación generando oportunidades de progreso mediante la bioeconomía e involucrando a los ciudadanos en una transición ecológica equilibrada.

La propuesta apunta a la generación de cambios para crear algo mejor. Este proceso necesita apoyarse en un compromiso social, que muestre una visión compartida de la ciudad articulada en base a los ciudadanos de Soria. La hoja de ruta de Soria 2030, tiene un objetivo claro a corto y medio plazo: reducir las emisiones de carbono al mínimo en todas las actividades de la ciudad en nueve años. Y, sienta las bases para una transformación equitativa, igualitaria, solidaria y respetuosa con el ambiente. Impulsa un crecimiento razonable y razonado que permita cuidar del entorno y de quienes más lo necesitan para que la ciudad se transforme en un modelo de crecimiento y desarrollo sostenible e inclusivo.

En este sentido, trabajar en las aulas una educación para la protección del medio ambiente permite establecer objetivos claros, identificar acciones específicas, asignar recursos adecuados y medir el progreso hacia la sostenibilidad a lo largo del tiempo.

Además, ayuda a garantizar que las decisiones económicas, sociales y ambientales estén integradas de manera equilibrada, priorizando el uso eficiente de los recursos y minimizando los impactos negativos en el medio ambiente y facilitando la conservación del medio natural.

Soria 2030 reconoce la importancia de promover una gestión ambiental local sostenible y una mayor conciencia ambiental en el municipio de Soria. La divulgación de la realidad ambiental contribuye a comprender las interacciones entre los sistemas naturales y sociales, y a destacar la influencia de los factores socioculturales en la generación de problemas ambientales.

El objetivo principal de Soria 2030 es impulsar la adquisición de conciencia, valores y comportamientos que fomenten la participación efectiva de la población en la toma de decisiones relacionadas con el desarrollo sostenible. Para lograr esto, es fundamental llevar a cabo campañas de divulgación y educación ambiental, ofreciendo información clara y accesible sobre la situación ambiental del municipio.

Al fomentar la participación ciudadana en la planificación y ejecución de proyectos ambientales, involucramos a la comunidad en la toma de decisiones y se promueve la transferencia efectiva de conocimiento y experiencia.

En resumen, Soria 2030 reconoce que una gestión ambiental local sostenible y la divulgación de la realidad ambiental son fundamentales para promover la conciencia ambiental y garantizar la participación activa de la población en la toma de decisiones relacionadas con el desarrollo sostenible.

La Educación para la ciudadanía así entendida puede y debe ser un factor estratégico que incida en el modelo de desarrollo establecido, para reorientarlo hacia la sostenibilidad y la equidad, es decir, debe convertirse en la base para elaborar un nuevo estilo de vida.

El compromiso de la ciudad de Soria se centra en la consecución de objetivos establecidos en seis ejes de trabajo clave: movilidad y transporte, entorno construido, agua y residuos, energía, producción y consumo responsable, y gobierno local. Estos ejes pueden abordarse a través de la educación en distintas etapas, y se ha planteado un estudio detallado de ellos en el contexto de mi tesis doctoral.

El objetivo de esta tesis es analizar las situaciones de aprendizaje de los Objetivos de Desarrollo Sostenible (ODS) en el área de Ciencias Sociales, específicamente en la educación secundaria obligatoria, y su implementación en la ciudad de Soria. Se trata de un trabajo de investigación que se enmarca en el paradigma interpretativo simbólico y utiliza una metodología mixta que combina técnicas de recopilación de información cuantitativa y cualitativa.

A partir del análisis de los resultados de la investigación, se plantea el diseño de propuestas pedagógicas que busquen impulsar la consecución de la meta de construir una ciudad nueva y mejor para todos los ciudadanos. Estas propuestas se basarán en la implementación de los ODS en el área de Ciencias Sociales y tendrán como objetivo promover un mayor compromiso ciudadano y fomentar la educación en valores relacionados con el desarrollo sostenible.

En resumen, el estudio de la implementación de los ODS en el área de Ciencias Sociales en la educación secundaria obligatoria en la ciudad de Soria buscará proporcionar propuestas pedagógicas que contribuyan a la construcción de una ciudad más sostenible y mejoren la calidad de vida de todos los ciudadanos.

Conclusiones

Es fundamental repensar el propósito último de la educación para profundizar sobre su concepto. En este sentido, el enfoque de la Educación para el Desarrollo Sostenible tiene como objetivo principal generar una ciudadanía responsable y comprometida que trabaje por la creación de una sociedad inclusiva, sostenible y centrada en las personas. La educación se concibe como un espacio transformador en el que se puedan abordar las transiciones ecosociales necesarias para contrarrestar los posibles cambios históricos que puedan surgir a raíz de la relación entre energía y clima.

Para lograr esto, es necesario potenciar ciudades sostenibles a nivel local, compromisos reales por parte de los gobiernos nacionales y políticas de desarrollo a nivel internacional. Con este propósito, es importante promover la comprensión y el conocimiento de los principios clave y conceptos de la Educación para el Desarrollo

Sostenible, así como dar a conocer redes, proyectos y agentes implicados en este enfoque educativo tanto en el ámbito formal como informal. Es necesario valorar la importancia de la Educación para el Desarrollo Sostenible y las estrategias necesarias para el desarrollo de sociedades sostenibles, inclusivas, equitativas y justas, y promover un cambio de perspectiva hacia una cultura de sostenibilidad a través del análisis crítico y reflexivo de los desafíos socio-ambientales actuales.

En el caso de la ciudad de Soria y su iniciativa Soria 2030, se plantea una estrategia de trabajo en colaboración con la comunidad y los actores relevantes para establecer una hoja de ruta que permita reducir las emisiones de carbono, preservar la biodiversidad y construir una ciudad más saludable, limpia, resiliente y próspera. La integración de la educación y la ciudadanía en este proceso participativo busca promover el compromiso y la contribución individual y colectiva en función de su impacto y sus posibilidades.

La creciente preocupación por el cambio climático y sus consecuencias impulsa a Soria a convertirse en una ciudad con emisiones neutras. Además, busca acelerar la transición hacia una economía circular y fomentar el desarrollo de la bioeconomía en su entorno, con el objetivo de crear una "ciudad sostenible". El análisis e implementación de los contenidos relacionados con los Objetivos de Desarrollo Sostenible en la práctica educativa del área de Ciencias Sociales en la Educación Secundaria permitirán evaluar la viabilidad y pertinencia de estos objetivos en el contexto educativo de la ciudad de Soria. De esta manera, se estará contribuyendo a la construcción de una nueva ciudad desde una perspectiva educativa.

Referencias Bibliográficas

1. Ley Orgánica 3/2020, de 29 de diciembre, por la que se modifica la Ley Orgánica 2/2006, de 3 de mayo, de Educación.
2. Cox, C., Bascopé, M., Castillo, J.C., Miranda, D., Bonhomme, M.: Educación ciudadana en América Latina: prioridades de los currículos escolares. UNESCO. (2014).
3. UNESCO: Educación para la ciudadanía mundial: preparar a los alumnos para los restos del siglo XXI. UNESCO. (2016).
4. Sarochar, J. M.: Estudio comparado: formación para la ciudadanía en el primer ciclo de Educación Secundaria en Uruguay y Cataluña. Cuadernos de Investigación Educativa, 9 (2), 55-68. (2018).
5. Ortega-Gaite, S., Perales Montolío, M. J., Sancho-Álvarez, C., Quintano Nieto, J.: Validación de contenidos de Educación para el Desarrollo para el análisis de manuales escolares. Revista Bordón. Sociedad Española de Pedagogía. 73, (2), 133-148. (2021).
6. Ortega-Gaite, S.: Análisis de manuales escolares de educación para la ciudadanía y derechos humanos de educación secundaria obligatoria en clave de educación para el desarrollo. Tesis doctoral. Universidad de Valladolid. (2016).
7. Sánchez-Agustí, M., Miguel-Revilla, D.: Citizenship Education or Civic Education? A Controversial Issue in Spain. Journal of Social Science Education, 19(1), 154-171. (2020).
8. Asamblea General de las Naciones Unidas: Transformar nuestro mundo: la Agenda 2030 para el Desarrollo Sostenible, de 21 de octubre de 2015. Resolución A/70/L.1. (2015).
9. Prats Palazuelo, F.: Sobre la crisis ecosocial y el cambio de ciclo histórico. Poner en el centro la vida. Ambienta. 125, 10-19. (2018).
10. Celorio, G., López de Munain, A. (Coords.): Diccionario de Educación para el Desarrollo. Vitoria-Gasteiz: Hegoa. (2007).
11. Celorio, G.: Sensibilización y Educación para el Desarrollo. En F. Agost, R. Mar (Coords.), Cooperación descentralizada pública. Introducción, enfoques y ámbitos de actuación (pp. 225-261). Castelló de la Plana: Publicacions de la Universitat Jaume I. (2013).
12. Encarnación Cambрил, M., Fernández Paradas, A. R., de Alba Fernández, N. (Coord.): La Didáctica de las Ciencias Sociales ante el reto de los ODS.

- Narcea. (2023).
13. Seixas, P., Morton, T.: *The Big Six Historical Thinking Concepts*. Toronto: Nelson. (2013).
 14. Barton, K. C., Levstik, L. S.: *Teaching History for the Common Good*. Lawrence Erlbaum Associates. (2004).
 15. Sant, E.: *Democratic Education: A Theoretical Review (2006–2017)*. *Review of Educational Research*, 89(5), 655–696. (2019).
 16. Benejam, P.: *Las finalidades de la educación social*. En P. Benejam y J. Pagès (Eds.), *Enseñar y aprender ciencias sociales, geografía e historia en la Educación Secundaria* (pp. 33–51). Universidad de Barcelona y Editorial Horsori. (1997).
 17. Prats, J., Valls Montés, R.: *La Didáctica de la Historia en España: estado reciente de la cuestión*. *Didáctica de Las Ciencias Experimentales y Sociales*, 25, 17–35. (2011).
 18. Miguel-Revilla, D.: *What is history education good for? A comparative analysis of students' conceptions about the relevance of history*. *Journal of Curriculum Studies*, 54(1), 70–84. (2022).
 19. UNESCO: *Replantear la educación: ¿Hacia un bien común mundial?* UNESCO. (2015).
 20. UNESCO: *Educación para los objetivos de desarrollo sostenible: objetivos de aprendizaje*. UNESCO. (2017).

Smart Environment

Structural challenges and solutions to improve indoor agriculture

Luisa F. Lozano-Castellanos^{1, 2} [0000-0003-4667-6113]; Luis M. Navas-Gracia¹ [0000-0002-7895-925X]; Isabel C. Lozano-Castellanos³ [0009-0007-8415-8049]; and Adriana Correa-Guimaraes¹ [0000-0002-2063-6554]

¹ University of Valladolid, Palencia PA 34004, SPAIN

² University of Tolima, Ibagué TOL 7730006299, COLOMBIA

³ Curtin University, Perth WA 6102, AUSTRALIA

luisafernanda.lozano@uva.es

Abstract. Indoor farming has attracted significant attention for its potential to improve traditional agriculture by controlling environmental conditions. However, it faces substantial challenges, including limited automation, high costs, intense labor demands, and rigid static systems. In response to these challenges, this research presents five innovative models to improve indoor agriculture, focused on the potential of the aeroponic technique as an efficient resource utilization system and precise control of growing conditions. Air-supported domes are introduced as sealed and thermally insulated structures to optimize space, growth parameters, and accessibility. An advanced ventilation system designed to balance heat dissipation and humidity control, improving energy efficiency and maintaining optimal growing conditions. The mobility of the crop through automated mobile trays, optimizing the use of space and productivity. Finally, the energy efficiency of light is explored by implementing variable cultivation area trays, reducing electrical costs by improving photonic capture. These models together mean a profound transformation in the landscape of indoor agriculture. By addressing current challenges head-on, they can usher in a future in which indoor agriculture will be more productive and sustainable and substantially more automated. In doing so, they promise to reshape the entire industry, offering insight into controlled environment agriculture's advances and potential benefits.

Keywords: Indoor Technology, Indoor Designs, Indoor Growing Systems.

1 Introduction

The concept of indoor agriculture has garnered considerable attention within the scientific and agricultural communities due to its potential to revolutionize traditional farming practices. Embodies a crop production methodology in which natural conditions are meticulously regulated to optimize growth parameters within enclosed structures such as greenhouses or vertical farms [1]. Unlike traditional outdoor farming, which relies heavily on climatic variability, indoor agriculture operates within enclosed environments to precisely control temperature, humidity, light, and nutrient availability

2

[2]. This level of control extends the potential for year-round cultivation and facilitates crop growth in regions with extreme climates. Hence, indoor agriculture is paramount in the contemporary agricultural landscape, offering a compelling response to traditional farming practices' challenges [3, 4].

However, consistently maintaining these factors across diverse crop species represents a significant challenge, particularly in energy efficiency for controlled lighting, heating, cooling, and ventilation, which can result in substantial operational costs [5, 6]. Mitigating this energy consumption while ensuring crop productivity remains a complex, ongoing challenge. Furthermore, indoor agriculture frequently encounters issues related to static cultivation systems. These static systems often entail fixed infrastructure and layouts, limiting adaptability and hindering the implementation of more efficient and versatile farming practices [7–10].

The capital investment required to construct and maintain indoor facilities, acquire sophisticated equipment, and install control systems is high [11]. Balancing these costs with potential returns on investment demands careful financial planning and efficient resource utilization. Moreover, these systems frequently grapple with a relatively high demand for manual labor, particularly in planting, harvesting, and maintenance tasks [11]. This labor-intensive nature can strain operational efficiency and increase production costs. Overcoming these labor challenges often necessitates innovations in automation and robotics, which can further add to the initial capital outlay [7, 12].

Consequently, the imperative for innovative and sustainable solutions has driven indoor agriculture to develop various design typologies tailored to specific goals and constraints. These designs may encompass the utilization of vertical stacking in hydroponic, aquaponics, or aeroponics systems [4, 13]. Hydroponics involves cultivating plants in nutrient-rich water solutions; aquaponics combines aquaculture (raising fish or aquatic organisms) with hydroponics, where fish waste provides nutrients for plants, and in turn, the plants purify the water for the fish; and aeroponics, which involves nurturing plants under highly controlled conditions within a chamber. This system employs a fine mist of mineral nutrient solutions to facilitate plant growth. These solutions are recycled and consistently provided to the plant's exposed roots [2, 7]. Nonetheless, it warrants meticulous consideration and innovation to maximize the efficiency and sustainability of these systems.

Certain crops in indoor agriculture have assumed the primary focus within research initiatives. Leafy greens, herbs, microgreens, and an array of fruit-bearing plants have emerged as pivotal subjects of inquiry, representing both opportunities and challenges in pursuing optimized growth conditions and enhanced yields [2, 14].

This research aims to delineate the experiences, challenges, and insights gleaned from an investigation conducted within the framework of five different indoor agricultural models and, at the same time, outline the innovative structural concepts and the

improvements they incorporate to strengthen the resilience and sustainability of indoor agricultural systems contributing to overcoming formidable challenges.

2 Essential conditions of indoor agriculture

The success of indoor agriculture operations relies on the following conditions:

1. **Efficient use of space:** Indoor agriculture operations must make the most available space to maximize crop yields [15]. This can be achieved using movable growing beds, enabling fine-tuning layouts for diverse crops and growth stages [10, 16]. These beds' flexibility optimizes horizontal space and capitalizes on vertical dimensions within indoor facilities. Vertical farming methods, like multi-tiered structures or stacked shelves, elevate planting densities and overall output (i.e., [17]). Beyond increasing yields, prioritizing space efficiency aligns with sustainability goals, reducing land usage and transportation emissions.
2. **Artificial light source:** Adequate and tailored lighting is crucial for plant growth. Many indoor farms use artificial lighting, such as LED or high-pressure sodium (HPS) lights, to provide the correct spectrum and intensity of light for each crop [12, 18]. In typical vertical farming setups, providing artificial light constitutes one of the most substantial investments and, currently, the most critical and constraining operational cost component [2]. Lighting efficiency predominantly revolves around LED fixture efficiency and efficacy.
3. **Efficient water usage.** Effective water management is paramount, especially within the closed-loop systems of indoor agriculture. It requires stringent quality control to guarantee plants receive the ideal water conditions for robust growth, resulting in increased yields and superior crop quality [7, 14]. Furthermore, maintaining a balanced nutrient solution is essential for plant health, where cutting-edge techniques like aeroponics and nutrient film methods in vertical columns [16] offer promising solutions. These advancements optimize resource utilization and safeguard water quality and purity, avoiding toxins or disease vectors accumulation within indoor agriculture operations [19].
4. **Automation:** Mechanized and automated handling systems in vertical farming have seen limited success, primarily due to their high costs and bulkiness [20]. Indoor agriculture, including vertical farms, is substantially labor-intensive, and recruiting such a workforce is increasingly challenging and costly. The primary alternative to manual labor lies in robotics, complemented by industrial vision [21]. Advanced robotics remain conspicuously absent from even the most sophisticated vertical farming systems [22].

4

5. Control and adjustment of growing parameters. Vertical farming operations offer the flexibility to modify and maintain precise control of the five growth parameters of the air system of vegetables (temperature, humidity, wind, irradiation, and CO₂) and the four parameters for the underground system (temperature of the root zone, water, nutrients, and oxygen) [23, 24]. This control ensures optimal growing conditions year-round, independent of external fluctuations.

We have based our proposed solutions on developing the concept of these primary conditions to overcome the drawbacks of current indoor structures.

3 Experiences and proposals for improvement in indoor agriculture

3.1 Aeroponic technique as a growing system

A vertical aeroponic system has been designed and implemented at the University of Valladolid, Palencia campus, to cultivate lettuce as its initial crop. This system comprises three shelves with three isolated production units (See Fig. 1). Each unit is equipped with four polypropylene growth chambers, accommodating two lettuce plants spaced at a distance of 20 cm. Within each chamber, a dual-nozzle CoolNET PRO nebulizer (Regaber, Barcelona) has been positioned at the central internal zone (See Fig. 2), delivering droplets of 65 microns in size under a pressure of 4.0 bar.

A biomineral Aero Supermix fertilizer (GroHo Hidroponía, Madrid) was employed to support plant growth, with an application rate of 50 mL per 25 L of water. The nutrient solution was recycled through a closed-loop recirculation system. The artificial lighting system (Boos Technical Lighting SL, Valladolid) integrated into this setup features two luminaires within each production unit, encompassing four printed circuit boards (PCBs) equipped with nine LED lights each, spanning red, blue, infrared, and white spectra. Plants were subjected to a 12-hour light/12-hour dark photoperiod to ensure optimal growth conditions.

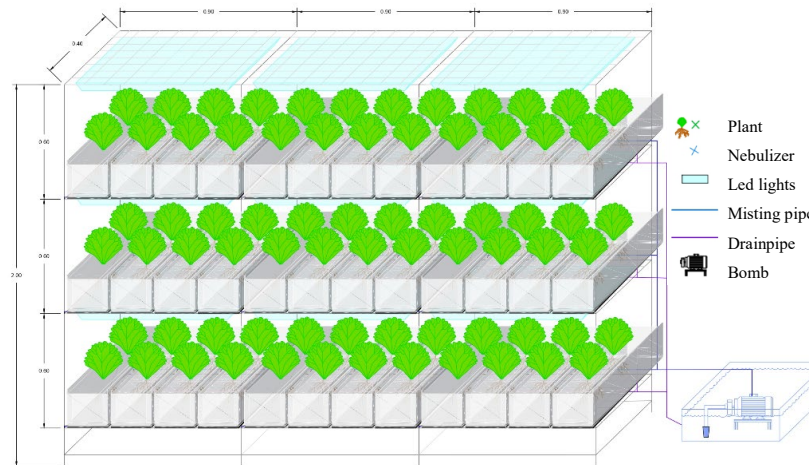


Fig. 1. Front view of the vertical aeroponic system

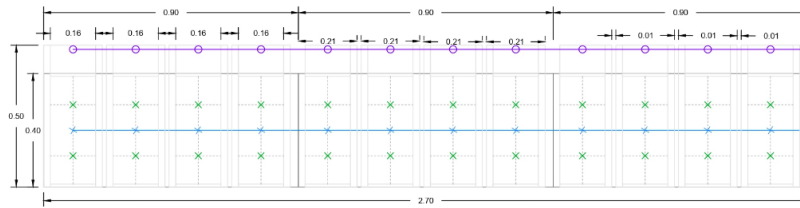


Fig. 2. Plan view of the growth chamber

This engineered aeroponic system exemplifies the commitment to innovative agricultural practices and sustainable resource management, paving the way for further research and advancements in controlled environment agriculture.

3.2 Dome as cover and hanging growing system

Air-supported domes, characterized by their solid, transparent, thermally insulating, and voluminous enclosure, are hermetically sealed from the external atmosphere through an internal pressurization system. Within this regulated environment, the internal atmosphere serves a dual purpose: providing structural support for the dome while offering a controlled environment for crop cultivation. The introduction of air is exclusively permitted through a specialized inflation system, engineered to exclude external contaminants, ensuring a pristine internal environment. This stringent control reduces the need for chemical interventions (See Fig. 3).

6

Structurally, the dome's integrity is fortified by columns anchored within the framework. These columns are further reinforced by attaching two side beams, creating a cruciform configuration. Vertical growing panels, suspended from resilient braided cables, introduce a dynamic element by enabling horizontal mobility within the dome. This adaptability optimizes space utilization and facilitates the creation of temporary access corridors for efficient maintenance procedures.

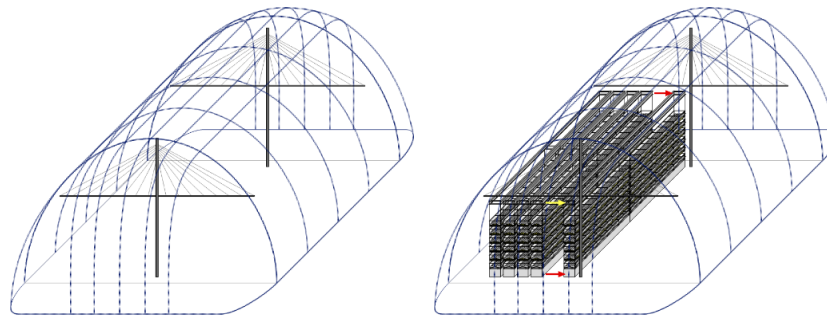


Fig. 3. Air-supported dome structure

3.3 Ventilation system

The design of the air diffuser duct for the ventilation system presents a purposeful configuration tailored to the bottom of the aeroponic channel, enabling efficient lateral drainage of excess water that emanates from the root system (See Fig. 4). Key to its functionality is the strategic placement of nozzles exclusively positioned on the lower and horizontal segments of the duct. This design feature ensures a meticulous air flow, serving a dual role: active ventilation of the luminaires initially and subsequently the cultivated crop. This sequential approach to ventilation is particularly noteworthy, as it allows the air to carry away heat generated by the luminaires, consequently reducing the energy demand required to maintain the ambient temperature.

Following the ventilation of the crop, the air, now laden with moisture generated through transpiration, is channeled to exit laterally toward the intermediate aisles. From there, it ascends naturally through convection, gradually reaching the apex of the covering structure for release. Notably, due to the principle that moist air is lighter, it tends to separate from the drier air and accumulates at the highest point within the covering structure. This strategic separation process ensures the precise, regular, and consistent evacuation of moist air, contributing significantly to optimizing the controlled environment.

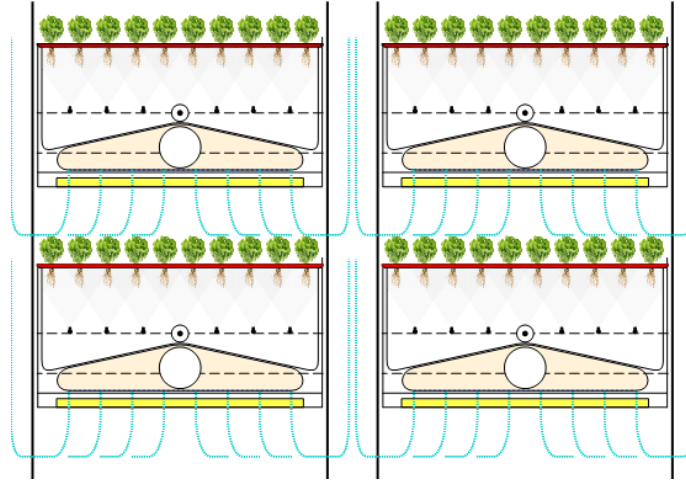


Fig. 4. Ventilation system for aeroponic technique

3.4 Crop mobility in an intermittent but continuous flow

The automation relies on a lightweight suspended cultivation structure consisting of rows of interlocking trays forming vertical panels. This design enables the efficient and sequential mobilization and processing of all cultivation trays within each vertical panel. The system achieves this through horizontal mobility and, notably, innovative vertical mobility, simplifying and enhancing the automation of vertical crop management.

Through the two vertical displacement systems at the ends of the rows, each one is moved to occupy the lowest level by rotation, allowing each crop tray to pass, once each day, through a fixed location for control, surveillance, and harvest..., which we call the "controller," (yellow mark) (See Fig. 5).

In the first step, the upper row occupies the lower level by descending through the vertical tower on the left while, simultaneously, the lower row occupies the upper level of the first by ascending through the displacement turret vertical on the right. In the drawing's lower figure, this maneuver is repeated with the penultimate row in height. And so on with the other levels. The entire vertical panel rotation should be completed in one day so that all of its trays pass through the controller in that period.

8

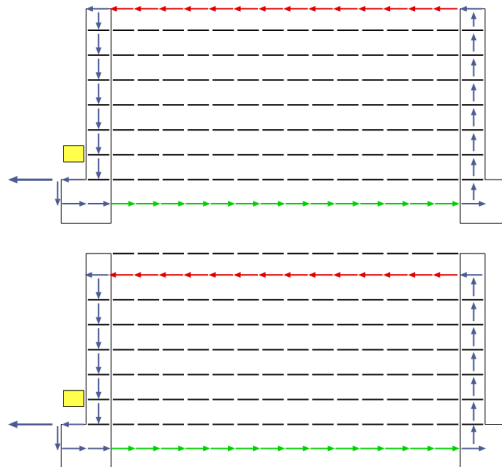


Fig. 5. Movement of culture trays

3.5 Efficacy of light energy

In the realm of indoor agriculture, the incorporation of dynamic structures becomes imperative for several compelling reasons. Dynamic structures offer the agility and versatility required to adapt to the ever-evolving needs of crops. As plants progress through various growth stages, they demand varying light intensities and angles. Static setups often fail to address these dynamic requirements effectively, resulting in light waste and increased electricity costs. Automation and controlled lighting angles are among the strategies to minimize light waste and enhance energy efficiency. However, their full potential remains untapped without a dynamic framework to support these strategies.

The introduction of variable cultivation area trays represents a promising advancement in this context. These trays can remarkably adapt to different crop growth stages and densities. By doing so, they optimize photonic capture by ensuring each plant receives the required light (See Fig. 6). This adaptability translates into a better utilization of artificial lighting resources, substantially reducing electrical energy costs.

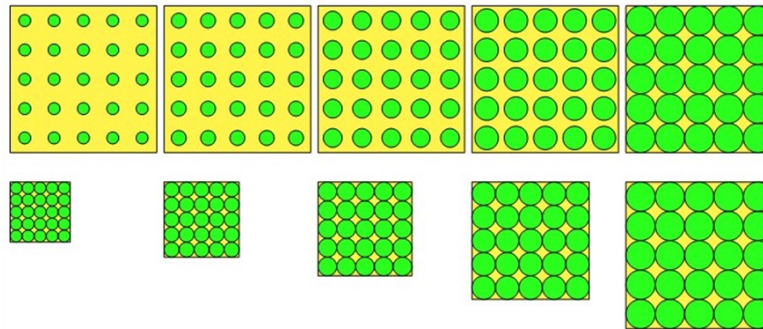


Fig. 6. Trays with a variable growing area

4 General considerations

The mentioned alternatives or proposed solutions correspond to non-rigid designs to resolve some of the crucial challenges in indoor agriculture under the essential conditions for its implementation. These designs address key aspects to optimize crop production in controlled environments.

The complexity of setting up an aeroponic system demands specialized knowledge, especially in nutrient delivery and nebulization technology. Ensuring optimal maintenance and nutrient concentrations is challenging, as system failures or blockages can harm crop health and the system structure. Moreover, the high energy consumption associated with artificial lighting systems poses a challenge regarding energy efficiency.

Despite these challenges, the vertical aeroponic system holds promising prospects. Nutrient recycling allows for high crop density in limited space and resource efficiency. This controlled environment agriculture supports year-round cultivation, reducing reliance on seasonal factors. Ongoing research and advancements in this field may increase efficiency and reduce operational costs. Aeroponic systems hold immense potential as indispensable tools for indoor agriculture, including plant factories and vertical farming with artificial lighting.

Implementing domes with aerial support offers numerous advantages for controlled environment agriculture by optimizing space within a dome. The controlled and sealed environment protects crops from external contaminants and allows precise control of temperature, humidity, and other growth parameters. This design maximizes the growing area, unlike traditional greenhouses, which rely on rigid structures and often have limited internal space due to the need for support columns and aisles. It allows workers to access different parts of the ever-increasing crop easily. The principal challenges relate to significant initial investments in construction and pressurization systems. It is

10

crucial to ensure the dome's structural integrity under variable weather conditions and external stresses.

Designing an efficient ventilation system challenges balancing heat dissipation and humidity removal. Careful energy management is crucial to avoid excessive energy expenditure. Precise control of humidity levels and preventing condensation within the ventilation system are essential for its functionality. However, adequate ventilation contributes significantly to heat management and humidity regulation, ultimately enhancing energy efficiency.

Developing and maintaining automated crop mobility systems can be mechanically intricate. Ensuring precise control over crop movement is essential to prevent damage and maintain efficiency. Furthermore, guaranteeing the reliability and durability of the mobility system is crucial for uninterrupted operation. Despite these challenges, crop mobility offers significant benefits, including space optimization, efficient management, and maximized productivity. Continuous advancements in automation hold the potential for more efficient operations.

Implementing variable cultivation area trays and optimizing light delivery may involve initial costs. Precisely controlling light spectra for different growth stages can be technically complex. Nevertheless, adopting trays with variable cultivation areas presents an innovative and economically advantageous solution for improving photonic capture and reducing electrical energy costs in vertical crop cultivation. This technology can potentially revolutionize the efficiency and sustainability of controlled environment agriculture, making it a compelling choice for modern agricultural practices.

Finally, an interdisciplinary approach is indispensable to unlock the full potential of indoor agriculture. Collaborative efforts between agronomists, engineers, horticulturists, and data scientists are imperative to develop lighting technologies, climate control, resource optimization, and pest management innovations, which can potentially revolutionize energy efficiency and crop production. Advancements in automation and sensor technologies can enhance precision farming practices, while sustainable water recycling and nutrient delivery systems offer opportunities for resource conservation. Furthermore, ongoing research into cultivar suitability and nutritional quality profiles in indoor-grown crops is vital to meet the demands of discerning consumers. By collectively addressing these technical and scientific challenges, indoor agriculture can continue its trajectory toward sustainable and resilient food production systems contributing to global food security.

References

1. Vatistas, C., Avgoustaki, D.D., Bartzanas, T.: A Systematic Literature Review on Controlled-Environment Agriculture: How Vertical Farms and Greenhouses Can Influence the

- Sustainability and Footprint of Urban Microclimate with Local Food Production. *Atmosphere*. 13, 1258 (2022). <https://doi.org/10.3390/atmos13081258>
2. Ampim, P.A.Y., Obeng, E., Olvera-Gonzalez, E.: Indoor Vegetable Production: An Alternative Approach to Increasing Cultivation. *Plants*. 11, 2843 (2022). <https://doi.org/10.3390/plants11212843>
 3. Dsouza, A., Price, G.W., Dixon, M., Graham, T.: A Conceptual Framework for Incorporation of Composting in Closed-Loop Urban Controlled Environment Agriculture. *Sustainability*. 13, 2471 (2021). <https://doi.org/10.3390/su13052471>
 4. Avgoustaki, D.D., Xydis, G.: How energy innovation in indoor vertical farming can improve food security, sustainability, and food safety? *Advances in Food Security and Sustainability*. 5, 1-51 (2020). <https://doi.org/10.1016/bs.af2s.2020.08.002>
 5. Delorme, M., Santini, A.: Energy-efficient automated vertical farms. *Omega*. 109, 102611 (2022). <https://doi.org/10.1016/j.omega.2022.102611>
 6. Avgoustaki, D.D., Xydis, G.: Energy cost reduction by shifting electricity demand in indoor vertical farms with artificial lighting. *Biosystems Engineering*. 211, 219-229 (2021). <https://doi.org/10.1016/j.biosystemseng.2021.09.006>
 7. Hati, A.J., Singh, R.R.: Smart Indoor Farms: Leveraging Technological Advancements to Power a Sustainable Agricultural Revolution. *AgriEngineering*. 3, 728-767 (2021). <https://doi.org/10.3390/agriengineering3040047>
 8. van Delden, S.H., SharathKumar, M., Butturini, M., Graamans, L.J.A., Heuvelink, E., Kacira, M., Kaiser, E., Klamer, R.S., Klerkx, L., Kootstra, G., Loeber, A., Schouten, R.E., Stanghellini, C., van Ieperen, W., Verdonk, J.C., Violet-Chabrand, S., Woltering, E.J., van de Zedde, R., Zhang, Y., Marcelis, L.F.M.: Current status and future challenges in implementing and upscaling vertical farming systems. *Nat Food*. 2, 944-956 (2021). <https://doi.org/10.1038/s43016-021-00402-w>
 9. Kozai, T., Niu, G.: Chapter 5. Plant factory as a resource-efficient closed plant production system. In: *Plant Factory: An Indoor Vertical Farming System for Efficient Quality Food Production*. pp. 93-115. Academic Press (2019)
 10. Lozano-Castellanos, L.F., Navas-Gracia, L.M., Correa-Guimaraes, A.: Light Energy Efficiency in Lettuce Crop: Structural Indoor Designs Simulation. *Plants*. 12, 3456 (2023). <https://doi.org/10.3390/plants12193456>
 11. Kozai, T., Niu, G.: Chapter 2. Role of the plant factory with artificial lighting (PFAL) in urban areas. In: *Plant Factory: An Indoor Vertical Farming System for Efficient Quality Food Production*. pp. 7-34. Academic Press (2019)
 12. Hadj Abdalkader, O., Bouzebiba, H., Pena, D., Aguiar, A.P.: Energy-Efficient IoT-Based Light Control System in Smart Indoor Agriculture. *Sensors*. 23, 7670 (2023). <https://doi.org/10.3390/s23187670>
 13. Gargaro, M., Murphy, R.J., Harris, Z.M.: Let-Us Investigate; A Meta-Analysis of Influencing Factors on Lettuce Crop Yields within Controlled-Environment Agriculture Systems. *Plants*. 12, 2623 (2023). <https://doi.org/10.3390/plants12142623>
 14. Maupilé, L., Boualem, A., Chaïb, J., Bendahmane, A.: A Flashforward Look into Solutions for Fruit and Vegetable Production. *Genes*. 13, 1886 (2022). <https://doi.org/10.3390/genes13101886>
 15. Al-Kodmany, K.: The Vertical Farm: A Review of Developments and Implications for the Vertical City. *Buildings*. 8, 24 (2018). <https://doi.org/10.3390/buildings8020024>

12

16. Beacham, A.M., Vickers, L.H., Monaghan, J.M.: Vertical farming: a summary of approaches to growing skywards. *The journal of horticultural science and biotechnology*. 94, 277-283 (2019). <https://doi.org/10.1080/14620316.2019.1574214>
17. Benke, K., Tomkins, B.: Future food-production systems: Vertical farming and controlled-environment agriculture. *Sustainability: Science, Practice and Policy*. 13, 13-26 (2017). <https://doi.org/10.1080/15487733.2017.1394054>
18. Mitchell, C.A., Sheibani, F.: Chapter 10. LED advancements for plant-factory artificial lighting. In: *Plant Factory: An Indoor Vertical Farming System for Efficient Quality Food Production*. pp. 167-184. Academic Press (2019)
19. ko, M.T., Ahn, T.I., Cho, Y.Y., Son, J.E.: Uptake of nutrients and water by paprika (*Capsicum annuum* L.) as affected by renewal period of recycled nutrient solution in closed soil-less culture | SpringerLink. *Horticulture, Environment, and Biotechnology*. 54, 412-421 (2013)
20. Ohara, H., Hirai, T., Kouno, K., Nishiura, Y.: Automatic Plant Cultivation System (Automated Plant Factory). *Environ. Control Biol.* 53, (2015)
21. Avgoustaki, D.D., Avgoustakis, I., Miralles, C.C., Sohn, J., Xydis, G.: Autonomous Mobile Robot with Attached Multispectral Camera to Monitor the Development of Crops and Detect Nutrient and Water Deficiencies in Vertical Farms. *Agronomy*. 12, 2691 (2022). <https://doi.org/10.3390/agronomy12112691>
22. Madushanki, A.A.R., Halgamuge, M.N., Wirasagoda, W.A.H.S., Syed, A.: Adoption of the Internet of Things (IoT) in Agriculture and Smart Farming towards Urban Greening: A Review. *International Journal of Advanced Computer Science and Applications (IJACSA)*. 10, (2019). <https://doi.org/10.14569/IJACSA.2019.0100402>
23. Ojo, M.O., Zahid, A.: Deep Learning in Controlled Environment Agriculture: A Review of Recent Advancements, Challenges and Prospects. *Sensors*. 22, 7965 (2022). <https://doi.org/10.3390/s22207965>
24. Saad, M.H.M., Hamdan, N.M., Sarker, M.R.: State of the Art of Urban Smart Vertical Farming Automation System: Advanced Topologies, Issues and Recommendations. *Electronics*. 10, 1422 (2021). <https://doi.org/10.3390/electronics10121422>

Benefits of non-commercial Urban Agricultural practices – a Systematic Review

O.F. Boukharta¹ [0000-0001-5403-5207], L. Chico-Santamarta² [0000-0003-2695-8471], I.Y. Huang² [0000-0003-0559-3952], L. Vickers² [0000-0002-7709-6712] and L.M. Navas-Gracia¹ [0000-0002-7895-925X]

¹ TADRUS Research Group, Department of Agricultural and Forestry Engineering, University of Valladolid, Spain

² Harper Adams University, Edgmond, Shropshire, United Kingdom.
ouiamfatih.boukharta@uva.es

Abstract. Today, we live in an era when people are concerned about their mental health and well-being. With the significant trend towards urbanization, urban areas and its inhabitants are increasingly facing socio-economic, ecological and environmental challenges. In this context, urban agriculture, which is defined as any kind of activity located in or around a city that aims to provide products and ecosystem services to its inhabitants, was seen as a possible solution to these challenges, particularly through its potential benefits not only for socio-cultural development, but also for public health, the environment and the economy. This systematic review's main objective is then to generate a synthesis of existing evidence on the benefits of non-commercial food production in urban agriculture, since that much of the existing research is case-specific and lacks an extensive and systematic analysis of benefits in different contexts and at different scales. Indeed, the results from the 42 articles analysed show that Urban Agriculture covers a vast and varied range of uses and potential benefits, encompassing many different categories including the creation of green spaces that enrich the city environment, as well as food gardens, where city dwellers can obtain the products they usually consume in their diet in a simple, quick and healthy way. The results also show that this is a topical subject, which will be addressed more and in more depth in the future, in order to ensure better food security and mental well-being for the population.

Keywords: Urban Agriculture, Benefits, Food Security.

1 Introduction

Today, we live in an era of growing interest in people's mental health and their wellbeing, particularly among the growing population of modern urban areas. [1]. With a significant shift towards urbanization, many challenges are facing urban areas and their inhabitants, such as socio-economic, ecological and environmental factors. [2]. In addition, there are many challenges facing food systems, such as climate change, sustainability of production processes, financial and environmental costs of transportation, and increasing consumption of processed and ultra-processed foods [3,4].

2

Urban Agriculture (UA), defined as any kind of activity located in or around a city that aims to provide products and ecosystem services to its inhabitants [5], has been seen as a possible solution to those challenges [6]. Known for its positive impact on socio-cultural development, public health, the environment and the economy [7], UA is increasingly attracting interest in research and practice. UA is not a new concept [8,9], and the central element that defines it is its location in and around cities, along with its deep connection with the urban ecosystem [10]. In addition, UA is practiced in a variety of forms, including urban farms, school gardens, allotments and community associations [11].

The benefits of urban gardens are manifold: they generate social well-being, foster healthy eating and furnish families with food and environmental education [12]. For example, people who practice UA are more likely to use organic waste produced at home, which can have beneficial effects on the environment. Indeed, it has been shown that community gardens boost social interaction and strengthen the community [13], and that allotments provide a source of fresh produce for individuals and families, as well as offering opportunities for physical activity [14].

The current scientific literature on social ecological resilience emphasizes the importance of focusing the urban planning of green spaces within the cities and connecting society to the ecosystem, since the contact with nature is nowadays becoming very minimal and limited [15]. Furthermore, the inhabitant can even participate in gardening practices, and therefore, learn about the importance of these services to our health and environment.

Considering the ongoing growth of the population, the decrease of urban spaces caused by urbanization, and the increasing food insufficiency, it is appropriate to discuss and review UA and its current relevance. The main objective of this systematic review is therefore to do an evidence synthesis on the benefits of non-commercial food production in UA, since much of the existing research is case-specific and lacks a comprehensive, systematic analysis of the benefits across different contexts and scales. To this end, the following question has been defined and that will lead to the discussion of all of the points addressed above:

What are the benefits of non-commercial food production in Urban Agriculture?

This review aims to provide a concise synthesis of the existing literature's findings and relevance, together with providing an overview of UA practices that aim to ensure healthy, sustainable food and improve urban environmental performance for current and future generations. Indeed, this review focused on many types of the non-commercial UA, including community gardens, school gardens, and allotments. From the main question cited above, the structure of this paper will follow the sequence according to the following sub-questions:

- Which countries have conducted this type of research? And what are the similarities and differences across countries?
- What forms of UA have been practiced at the non-commercial level?
- What are the main advantages of establishing these urban spaces in cities? What are the challenges and limitations?

2 Concepts and definitions

UA can be implemented in numerous forms, notably community gardens, school gardens, allotments and so on. [16]. These forms of urban nature are an important support for human-nature interactions that contribute to improving human well-being [17]. In this section, the key concepts derived from UA and its practices are explained in order to facilitate the understanding of what follows.

2.1 Form of non-commercial UA

Different forms of UA can be identified. In the following sections, the most widely known and used forms of UA are defined in order to facilitate understanding of the rest of the article.

Community gardens

In 2002, MacNair has defined community gardens as 'open spaces which are managed and operated by members of the local community in which food or flowers are cultivated', and where the whole space is maintained collectively [18]. In the literature, "community gardening" is a term that has been adopted to refer to gardening activities ranging not only to small neighbourhood gardens, but also to larger gardens of up to 1,000 m² [19]. However, it is a very popular approach that strengthens social links, providing individuals with the opportunity to practise gardening and other food-related skills, along with improving people's health through better access to healthy fruit and vegetables [20]. In addition, the practice allows fresh food and/or flowers to be grown in a spirit of collaboration, community and cooperation [13], making participants feel less isolated and more supported [13].

Allotments

According to Gilbert in 2013, allotments can be characterized as "plots of land designated by local authorities for growing vegetables for home consumption", in which distinctive plots are maintained individually on behalf of their designated holders and their families [14]. Indeed, allotments are a distinct form of UA that is created when land is acquired through a rental or lease agreement for personal use [13]. Thus, allotments refer to "plots designated by authorities with the aim of growing vegetables for household consumption (self-consumption)" [14].

School gardens

Many studies have shown the benefits of introducing school gardens as a way of improving children's nutritional outcomes [21,22]. Indeed, a number of investigations report that children's consumption and knowledge of fruit and vegetables has increased, making them more willing to try unfamiliar fruits and vegetables [21]. In addition, school gardens offer the opportunity to meet and interact with other people [23] in a natural environment (learning social skills, communication and cooperation). In addition, the provision of school gardens with healthier environments was identified as a

4

means of encouraging children to adopt a more balanced diet and engage in greater levels of physical activity, with the aim of reducing the risk of obesity [24].

Urban farms

According to the FAO, city farmers are increasingly striving to grow high-quality, efficient crops, making the best use of available resources and inputs, either by planting in the ground or in containers [25]. Indeed, urban farms can provide an environment conducive to new social and economic investment and have the potential to improve societal well-being in a number of ways [26]. UA can help address a city's environmental, economic and social challenges, as plants can improve the global climate by decreasing levels of heat during the hot season, while retaining water during intense rainfall, minimizing the possibility of flooding. In addition, they can offer a safe habitat for birds and other beneficial insects, helping to conserve urban biodiversity [27].

2.2 Categories of benefits of UA

The literature on UA has long demonstrated its multiple benefits [28]. Indeed, it is attracting growing interest as a natural, intelligent and sustainable solution to urban challenges, thanks to its many benefits, particularly in terms of economic, social and environmental impact [25].

Social benefits

There is evidence that exposure to nature has positive societal effects, promoting feelings of generosity, friendship and solidarity [29]. In addition, it reduces personal feelings of anxiety and improves sanity and well-being through diminishing feelings of depression and fatigue [28]. In addition, the social aspect takes into account public participation and the provision of employment for salaried workers or family members growing for their own consumption [30].

Economic benefits

A number of studies have shown that the implementation of UA projects helps to reduce the global food supply and demand situation (Satterthwaite et al., 2010), as it provides a degree of food security and can be seen as a source of income while offering direct access to a wider range of nutritionally rich [31]. In other words, UA can be an additional source of income and employment, improving the economic situation of many households, since it would include an analysis of the costs and returns of the activity [32].

Environmental benefits

The implementation of urban spaces in cities provides environmentally friendly ecosystem services including rainwater retention, mitigation of the urban heat island effect, provision of food, atmospheric purification and the retention of biodiversity [33]. Indeed, the environmental aspect refers to the integrity of the compartments as a whole, which provides information on the wellness of the work environment as well as the indicators that prove that these urban spaces will ensure sustainable development [34].

In addition, plants significantly reduce CO₂ and reduce thermic stress through the absorption and reflectance of sunlight irradiation, helping to lower the pollutants causing climate warming [35]. In addition, food is grown and produced locally, which means it is close to local markets and does not need to be transported over long distances, reducing transport costs and ensuring better environmental protection [36].

3 Methodology

As part of this study, the following aspects were established and evaluated as the basis of UA and as elements that influence public engagement on it. This includes the social, economic, spatial and environmental dimensions. This study explores the landscape of literature on UA and examines its results in terms of the benefits related to the three dimensions of sustainability.

3.1 Search strategy

This review process involved first searching and capturing the relevant literature on the topic under review, and then filtering the literature according to their relevance to the specific topic of this study. The methodology used followed the guidance [37] to ensure that rigorous, comprehensive, and objective literature collation and filtering processes to reduce reviewer selection and publication biases, and ensuring transparency in evidence inclusion decisions.

3.2 Selection process

The databases consulted included both Scopus and Web of Science. Matching search terms were developed on the basis of components adapted from systematic mapping: population, context and outcomes. Details of the components and relevant key terms are presented in Table 1.

Table 1: The components of the screen performed during the research

	Components	Key terms
Population	urban agricul* - urban farm*	urban AND (agricul* OR farm*)
	school garden - school gardens	"school garden*"
	community garden- community gardens	"community garden*"
Context	Food	food
	Fruit – fruits - etc.	fruit*
	Vegetable – vegetables – etc.	Veg*
Outcomes	benefit – benefits - beneficial – benefic	Benef*

As shown in Table 1, UA presents our main part of the population, the key element we are evaluating, and where in the components part we cite the different possibilities and where in the key terms, is presented the form used in the search in the software the search. For the context, the component presented and what we are looking to evaluate, the production of food fruit and/or vegetables, and where in key terms are presented in

6

the most suitable way to have all the possible results. Finally, for the outcomes, this part presents the results that we expect to be obtained in terms of benefits in its various forms, which are included in the key term "benefits". The above key terms formed the following string:

(((urban AND (agricul OR farm*)) OR "community garden*" OR "school garden*") AND benef*) AND (food OR fruit* OR veg*)*

We can clearly see that this formula encompasses all our key terms, providing the most relevant and accurate results for each of the UA forms.

3.3 Inclusion and exclusion criteria

In this review, the inclusion criteria considered were articles and first accepted articles published in English and published between 2016 and 2023, to ensure that the review included the most recent literature on the subject. No country limitation was used as the intention was to conduct a global review. These specific criteria are presented in more detail in Table 2:

Table 2: Inclusion and exclusion criteria.

Criterion	Eligibility	Exclusion
Document type	Articles and early accepted articles	Conferences papers, book chapters, review, editorial, conference review
	Open and non-open access	Full text articles not accessible
Language	English	Others
Timeline	From January 2016 until the 17 th of January 2023	Before 2016

3.4 Data extraction and analysis

In addition, a qualitative synthesis approach was adopted to examine the included articles. To this end, the software used in the present analysis is NVivo, which is one of the most popular qualitative data management programs currently available [38]. In addition, NVivo gives researchers the ability to process high volumes of data with greater precision and easy access to available resources [39]. Table 3 shows the main codifications carried out using NVivo software to ensure better evaluation of the articles selected for analysis.

Table 3: Coding structure used in the NVivo Software

Codification	Sub-codification
Data collection methods	Survey - questionnaire – Interviews – Observation - Experiment
Forms of UA	Community gardens – Allotments - School gardens – Urban Farms - Others
Outcomes	Economic – Social – environmental
Production	Food – fruit - vegetable
Year and Country	Year - Country

According to the codes and their sub-codification presented in Table 3, we can clearly see that these results would answer our main research question, in which the different forms of UA carried out in the countries are well defined, as well as their benefits, considering the methodology used and the year of data collection.

4 Results

4.1 Statistical descriptive analysis

Relevant articles selected and their source

The search and screening process identified 1731 articles from both Web of Science and Scopus engine searches. After removing 399 duplicates, the total number of articles screened was 1332. Following the application of both inclusion and exclusion criteria, 42 articles were deemed eligible for results mapping. The diagram illustrated in the PRISMA Fig. 1 demonstrates in detail the process and results of screening:

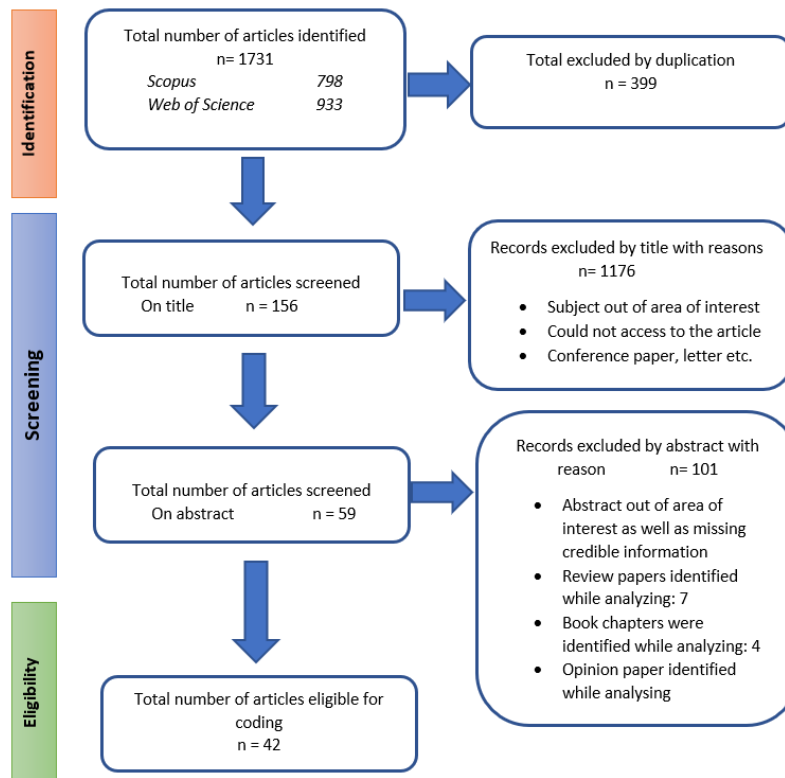


Fig. 1: The flow diagram of the systematically review process.

8

4.2 Descriptive Results

Articles and Studies

In order to better understand the relevance and use of UA over the years, it is fundamental and important to show, through our articles selected for this review, the number of articles published per year, and its evolution over the years, as well as a trend line which will be used to make an average prediction, as shown in Fig. 2.

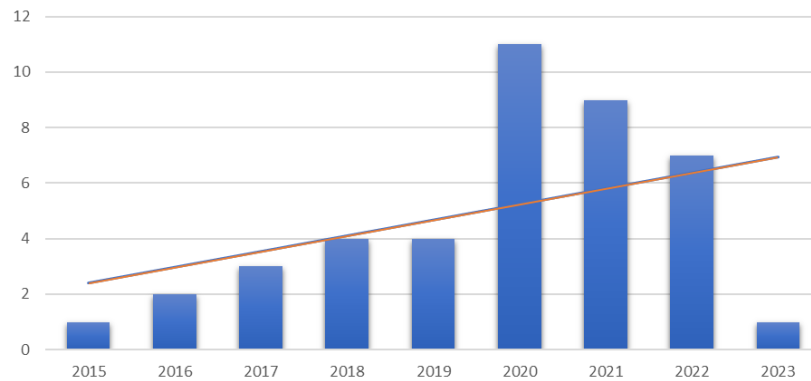


Fig 2: Publication rate of articles in the systematic review over the years, from 2016 to early 2023. The solid line represents a trend line for the appearance of articles.

The publication rate of the journal's articles shows a continuous increase over time, from 2015 to the beginning of 2023, when our research began (Fig. 2). It can be seen that the growth rate was significantly accelerated from 2020 onwards, reaching a peak at the end of 2020 and in 2021. This is due to the fact of the emergence of global COVID-19 pandemic, which has had a major effect on increasing interest in the subject of UA [40], since its benefits have been increasingly demonstrated in this period, and its need has become paramount [41]. Furthermore, the articles identified in the last 3 years show an increase of 67% in the number of articles published, which shows the growing interest in this subject.

Study sites location

From the analysed papers, Fig. 3 shows in detail the countries studied through a map that will facilitate the analysis and processing of data. Moreover, Fig. 4 shows the worldwide distribution of our study, since our study has no limitations with regard to the countries to be treated.



Fig. 3: Study sites location represented in a map

From the Fig. 3, we can clearly notice that there has been, during the realization of this review, a very large distribution of studies related to UA, in which we can perceive that about thirty countries have been analysed. There is clearly a significant difference in the distribution of these studies around the world, with the greatest number of articles coming from North America, Australia and some European countries, and the smallest contribution from African and Asian countries, including Morocco, Malaysia etc. (Fig. 3). This distribution can be clearly simplified using the map illustrated in the figure, which highlights in bold the countries covered, as well as from the Fig. 4:

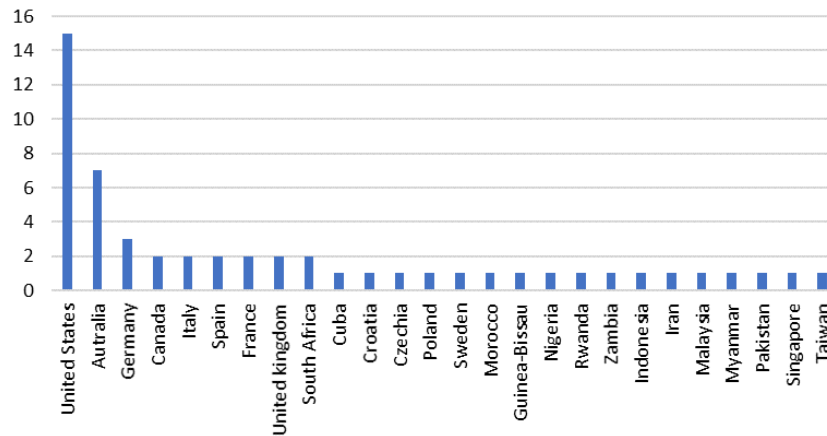


Fig. 4: Number of articles analysed for this review in a worldwide level.

10

The results of Fig.4 show that the largest studies of UA have been carried out in the United States, with a percentage of around 30%, followed by Australia with 13%, followed by European countries, in particular Germany, Spain, France and Italy, as well as other African and Asian countries.

UA across the continents

North America

In 2018, food insecurity impacted approximately 14.3 million individuals in the United States [42]. But today, community gardening has become very popular in New York City, for example, which boasts at least 500 urban spaces [43]. The aim of these urban gardens is to improve access to fresh produce for city dwellers, especially the food insecure. Studies on this subject also show that the involvement of urban spaces within cities helps to combat poverty and food shortages in times of war and economic depression [44].

Australia

In Australia, the fast-growing population and aging rate across the capitals are putting pressure on social, environmental and public health systems [45]. Furthermore, according to Lim in 2018, one in four Australians experience chronic episodes of loneliness. For this reason, local authorities in Australia are currently coordinating efforts to improve the urban canopy and plant trees as part of a metropolitan urban forest strategy [46]. Against this background, findings from studies relating to UA in Australia suggest that engagement in community and allotment gardens offers significant opportunities for improved well-being [47].

Europe

The situation of UA in Europe differs from country to another: Germany can be considered a typical European country where UA far exceeds food production. Meanwhile, in the UK, therapeutic and prescriptive gardening is gaining increasing support to help people overcome or live with mental health problems [48]. In Spain, even though individual gardens were very common, especially during the rural exodus of the 20th century, community gardens have appeared very recently. Meanwhile, in Croatia, the population is evenly divided between rural and urban areas, but the trend is towards further urbanization [49].

Africa

In North Africa, and more specifically in Morocco, an agricultural strategy known as the Plan Maroc Vert (Green Morocco Plan) has been implemented since 2008, with the aim of providing solidarity-based support for small and medium-sized farmers, so as to encourage the implementation of urban spaces within the cities of the country and ensure a good consumption of fresh food and vegetables [50]. In South Africa, numerous analyses have been carried out to determine the role of UA as a means of combating poverty and boosting food security [51].

Asia

While UA is not new globally, in some Asian countries such as Malaysia it is still not widely practised, mainly due to a lack of education and community awareness. On the other hand, Myanmar, which has undergone major socio-economic transformation and urbanization, as well as efforts to transition to a green economy, is a good example to consider in Asia. Moreover, in the case of Pakistan, with its great potential for gardening and its diverse climatic and ecological characteristics, the local authorities are strongly supporting the establishment of such projects.

4.3 Challenges and limitations

Despite the many potential benefits brought by the establishment of UA areas, the main challenge to be addressed is to ensure that these values are reflected in urban planning, decision-making, the market and other private choices [52]. Furthermore, many of the articles reviewed agree that policymakers are not recognizing UA as a necessarily public and sanitary amenity, as cited in Australia [13], and where our findings from the articles reviewed call on both government authorities and garden managers to fundamentally reconsider the organization of urban gardens and manage them.

On the other hand, community gardens are well known for being heterogeneous and challenging to characterize [53], which makes it difficult to provide a coherent overview of the demographic characteristics of the distribution of urban gardens [54]. In addition to the cost of implementation and other challenges, the horizontality of collective choice overturns customary principles, notably by placing women. Thus, the sustainability of this governance model is a major concern [55]. Urban soils, which can be of poor quality or contaminated, require careful control measures for both local production and consumption, whilst polluted air and limited accessibility to safe water can reduce the efficiency, sustainability and safety of UA [56].

5 Discussion and conclusion

In this literature review, 42 articles on non-commercial Urban Agriculture were analysed worldwide assessing the benefits that the integration of these urban spaces bring at different levels, along with the identification of the major challenges for their implementation and the limitations that could be faced, with the aim to better understand the value created that such systems bring to our daily lives for current and future generations. This analysis focused on the following forms of non-commercial Urban Agriculture: urban gardens school gardens, allotments and urban farms. The findings suggest that Urban Agriculture provides numerous applications and benefits covering several categories.

At an environmental level, urban gardens are green spaces that improve the city environment, as well as purifying the air and conserving biodiversity [57]. On a nutritional level, growing food in urban gardens can reduce hunger and nutrition insecurity by ensuring food self-sufficiency, affordability and high quality [12], since these spaces could be used to grow food in which city residents can obtain the products they usually

12

consume in their diet in a simple and secure way. On an economic level, urban agricultural spaces enable citizens to make savings by obtaining food of good quality and in larger quantities at a lower price. Finally, at a social level, urban agricultural spaces are seen as recreational and leisure spaces for relaxation and a place for social cohesion, in which participants improve their health and well-being, reduce their level of stress and increase their level of belonging [12].

Moreover, the findings of this in-depth analysis clearly underline the importance of integrating Urban Agricultural projects into city planning, given their many contributions to the socio-economic context, in both developed and developing countries.

This review shows that, to implement successfully Urban Agricultural projects, government and institutions must be properly established and well structured. They must be empowered to define and implement policies consistent with other decisions relating to urban planning, and nutritional implications must be fully integrated, covering green spaces and sustainable urban development plans.

References

1. World Health Organization. Fact Sheet: Depression; World Health Organization (WHO): Geneva, Switzerland, pp. 4 (2017)
2. Montgomery, M.: United Nations Human Settlements Programme: The State of the World's Cities. *Globalization and Urban Culture. Population and Development Review*, 31(3), 592-594 (2005)
3. Afshin, A., Sur, P. J., Fay, K. A., Cornaby, L., Ferrara, G., Salama, J. S., ... & Murray, C. J. Health effects of dietary risks in 195 countries, 1990–2017: a systematic analysis for the Global Burden of Disease Study 2017. *The lancet*, 393(10184), 1958-1972 (2019)
4. Willett, W., Rockström, J., Loken, B., Springmann, M., Lang, T., Vermeulen, S., ... & Murray, C. J.: Food in the Anthropocene: the EAT–Lancet Commission on healthy diets from sustainable food systems. *The lancet*, 393(10170), 447-492 (2019)
5. Delgado, C.: Agricultura Urbana em Portugal: Constrangimentos e Oportunidades Para Uma Política Pública Alimentar. *RPER*, (53), 109-126 (2020)
6. Dubbeling, M., van Veenhuizen, R., & Halliday, J.: Urban agriculture as a climate change and disaster risk reduction strategy. *Field Actions Science Reports. The Journal of Field Actions*, 32-39 (2019)
7. Santo, R., Palmer, A., & Kim, B.: Vacant lots to vibrant plots: A review of the benefits and limitations of urban agriculture. *Johns Hopkins Center for a Livable Future: Baltimore, MD, USA* (2016)
8. CALDAS, E.: DE L.; JAYO, M. Urban agriculture in São Paulo: history and typology. *Confins. Revue franco brésilienne de géographie/French-Brazilian magazine of geography*, (39) (2019)
9. Biazoti, A. R., & Sorrentino, M.: Political engagement in urban agriculture: power to act in São Paulo's community gardens. *Environment & Society*, 25, e0056 (2022)
10. Mougeot, L. J. Urban agriculture: concept and definition. *Journal of Urban Agriculture*, 01-08 (2000)
11. Mok, H. F., Williamson, V. G., Grove, J. R., Burry, K., Barker, S. F., & Hamilton, A. J.:
12. Strawberry fields forever? Urban agriculture in developed countries: a review. *Agronomy for sustainable development*, 21-43 (2014)

13. Ribeiro S.M., Bógus C.M. and Watanabe H.A.W.: Agroecological urban agriculture from the perspective of health promotion. *Saúde Soc* 24:730–43 (2015)
14. Kingsley, J., Bailey, A., Torabi, N., Zardo, P., Mavoja, S., Gray, T., Tracey, D., Pettitt, P., Zajac, N. and Foerander, E.: A systematic review protocol investigating community gardening impact measures. *International journal of environmental research and public health*, p.3430 (2019)
15. Gilbert, P.R.: Deskillling, agrodiversity, and the seed trade: A view from contemporary British allotments. *Agriculture and Human Values*, 30, 101–114 (2013)
16. Andersson, E., Barthel, S., Borgström, S., Colding, J., Elmqvist, T., Folke, C., & Gren, Å.: Reconnecting cities to the biosphere: stewardship of green infrastructure and urban ecosystem services. *Ambio*, 43, 445-453 (2014)
17. Kowarik, I.: Novel urban ecosystems, biodiversity, and conservation. *Environmental pollution*, 159(8-9), 1974-1983 (2011)
18. Taylor, L., Hahs, A. K., & Hochuli, D. F.: Wellbeing and urban living: nurtured by nature. *Urban Ecosystems*, 21, 197-208 (2018)
19. MacNair, E.: *The garden city Handbook: How to create and protect community gardens in Greater Victoria*. Polis Project on Ecological Governance. University of Victoria, Victoria BC, Canada (2002)
20. Genter, C., Roberts, A., Richardson, J., & Sheaff, M.: The contribution of allotment gardening to health and wellbeing: A systematic review of the literature. *British Journal of Occupational Therapy*, 78(10), 593-605 (2015)
21. Teig, E., Amulya, J., Bardwell, L., Buchenau, M., Marshall, J. A., & Litt, J. S.: Collective efficacy in Denver, Colorado: Strengthening neighborhoods and health through community gardens. *Health & place*, 15(4), 1115-1122 (2009)
22. Ohly, H., Gentry, S., Wigglesworth, R., Bethel, A., Lovell, R., & Garside, R.: A systematic review of the health and well-being impacts of school gardening: synthesis of quantitative and qualitative evidence. *BMC Public Health*, 16, 1-36 (2016)
23. Charlton, K., Comerford, T., Deavin, N., & Walton, K.: Characteristics of successful primary school-based experiential nutrition programmes: A systematic literature review. *Public Health Nutrition*, 24(14), 4642-4662 (2021)
24. Charlton, K., Comerford, T., Deavin, N., & Walton, K.: Characteristics of successful primary school-based experiential nutrition programmes: A systematic literature review. *Public Health Nutrition*, 24(14), 4642-4662 (2021)
25. Rochira, A., Tedesco, D., Ubiali, A., Fantini, M. P., & Gori, D.: School gardening activities aimed at obesity prevention improve body mass index and waist circumference parameters in school-aged children: a systematic review and meta-analysis. *Childhood Obesity*, 16(3), 154-173 (2020)
26. FAO 2015. *Urban and Peri-Urban Horticulture*. Available online: www.fao.org/ag/agp/greenercities/en/whyuph/index.html (accessed on 15 December 2020).
27. Hallett, S., Hoagland, L., & Toner, E.: Urban agriculture: Environmental, economic, and social perspectives. *Horticultural Reviews Volume 44*, 44, 65-120 (2016)
28. Orsini, F., & D'Ostuni, M.: The important roles of urban agriculture. *Frontiers for Young Minds*, 10, 1-7 (2022)
29. Soga, M., Gaston, K. J., & Yamaura, Y.: Gardening is beneficial for health: A meta-analysis. *Preventive medicine reports*, 5, 92-99 (2017)
30. Capaldi, C. A., Passmore, H. A., Nisbet, E. K., Zelenski, J. M., & Dopko, R. L.: Flourishing in nature: A review of the benefits of connecting with nature and its application as a wellbeing intervention. *International Journal of Wellbeing*, 5(4) (2015)

14

31. Munasinghe, M.: Sustainable development in practice. Cambridge: New York, NY, USA (2009)
32. Bonuedi, I., Kornher, L., & Gerber, N.: Agricultural seasonality, market access, and food security in Sierra Leone. *Food Security*, 14(2), 471-494 (2022)
33. Soubbotina, T. P.: Beyond economic growth: An introduction to sustainable development. World Bank Publications (2004)
34. Czembrowski, P., Łaskiewicz, E., Kronenberg, J., Engström, G., & Andersson, E.: Valuing individual characteristics and the multifunctionality of urban green spaces: The integration of sociotope mapping and hedonic pricing. 14(3), e0212277 (2019)
35. Nicli, S., Elsen, S. U., & Bernhard, A.: Eco-social agriculture for social transformation and environmental sustainability: A case study of the UPAS-project. *Sustainability*, 12(14), 5510 (2020)
36. Lin, B. B., Egerer, M. H., Liere, H., Jha, S., Bichier, P., & Philpott, S. M.: Local-and landscape-scale land cover affects microclimate and water use in urban gardens. *Science of the Total Environment*, 570-575 (2018)
37. De Bon, H., Parrot, L., & Moustier, P.: Sustainable urban agriculture in developing countries. A review. *Agronomy for sustainable development*, 30, 21-32 (2010)
38. James, K. L., Randall, N. P., & Haddaway, N. R.: A methodology for systematic mapping in environmental sciences. *Environmental evidence*, 5, 1-13 (2016)
39. Zamawe, F. C.: The implication of using NVivo software in qualitative data analysis: Evidence-based reflections. *Malawi Medical Journal*, 27(1), 13-15 (2015)
40. Ozkan, B. C.: Using NVivo to analyze qualitative classroom data on constructivist learning environments. *The qualitative report*, 9(4), 589-603 (2004)
41. Geary, R. S., Wheeler, B., Lovell, R., Jepson, R., Hunter, R., & Rodgers, S.: A call to action: Improving urban green spaces to reduce health inequalities exacerbated by COVID-19. *Preventive medicine*, 145, 106425 (2021)
42. Samuelsson, K., Barthel, S., Colding, J., Macassa, G., & Giusti, M.: Urban nature as a source of resilience during social distancing amidst the coronavirus pandemic (2020)
43. Okvat, H. A., & Zautra, A. J.: Community gardening: A parsimonious path to individual, community, and environmental resilience. *American journal of community psychology*, 47, 374-387 (2011)
44. Mansur, A. V., McDonald, R. I., Güneralp, B., Kim, H., de Oliveira, J. A. P., Callaghan, C. T., ... & Pereira, H. M. (2022). Nature futures for the urban century: Integrating multiple values into urban management. *Environmental Science & Policy*, 131, 46-56 (2022)
45. Hsiao, H.: Characteristics of urban gardens and their accessibility to locals and non-locals in Taipei City, Taiwan. *Landscape and Ecological Engineering*, 17(1), 41-53 (2021)
46. AIHW.: Older Australia at a glance. Retrieved 16th October, 2020. <https://www.aihw.gov.au/reports/older-people/older-australia-at-a-glance/contents/summary> (2018)
47. Egerer, M., Ordóñez, C., Lin, B. B., & Kendal, D.: Multicultural gardeners and park users benefit from and attach diverse values to urban nature spaces. *Urban Forestry & Urban Greening*, 46, 126445 (2019)
48. Bailey, A., & Kingsley, J.: Connections in the garden: Opportunities for wellbeing. *Local Environment*, 25(11-12), 907-920 (2020)
49. Barry, V., & Blythe, C. (2018). Growing pathways to well-being through community gardens and greenspace: Case studies from Birmingham and the West Midlands, UK. In *Pathways to Well-Being in Design*, 76-96 (2018)
50. Kisić, I.: *Gradska poljoprivreda*. Agronomski fakultet (2018)
51. Inter-réseaux Développement rural. Plan Maroc Vert, les grands principes et avancées de la stratégie agricole marocaine. *Bulletin de synthèse souveraineté alimentaire* (2016)

52. Battersby, J, Haysom, G, Marshak, M, Kroll, F & Tawodzera, G.: Looking beyond urban agriculture. Extending urban food policy responses. Policy Brief, South African Cities Network (2015)
53. Thiesen, T., Bhat, M. G., Liu, H., & Rovira, R.: An ecosystem service approach to assessing agro-ecosystems in urban landscapes. *Land*, 11(4), 469 (2022)
54. Orsini, F., Pennisi, G., Michelon, N., Minelli, A., Bazzocchi, G., Sanyé-Mengual, E., & Gianquinto, G.: Features and functions of multifunctional urban agriculture in the global north: a review. *Frontiers in Sustainable Food Systems*, 4, 562513 (2020)
55. Ambrose, G., Das, K., Fan, Y., & Ramaswami, A.: Comparing happiness associated with household and community gardening: Implications for Food Action Planning. *Landscape and Urban Planning*, 230, 104593 (2023)
56. Romagny, B., Aderghal, M., Auclair, L., Ilbert, H., & Lemeilleur, S.: From rural to urban areas: new trends and challenges for the commons in Morocco. *The Journal of North African Studies*, 28(1), 57-74 (2023)
57. Meharg, A. A.: Perspective: City farming needs monitoring. *Nature*, 531(7594), S60-S60 (2016)
58. Pinto, R. Hortas Urbanas: Espaços para o Desenvolvimento Sustentável de Braga. Braga. Dissertação de mestrado. Universidade do Minho (2007)

Smart Mobility

Analysis of the incorporation of battery electric scooptrams and trucks in an underground mining company in the Dominican Republic

Arismendy José Del Orbe¹[0000-0002-6639-5960], José Gabriel Durán García ¹[0000-0001-6505-5182] Deyslen Mariano-Hernández ¹[0000-0002-4255-3450], Elvin Arnaldo Jiménez Matos¹[0000-0002-0031-6772], Giuseppe Sbriz-Zeitun¹[0000-0002-8860-9085], Miguel Aybar-Mejía¹[0000-0002-4715-3499]

¹ Área de ingenierías, Instituto Tecnológico de Santo Domingo (INTEC), Dominican Republic
miguel.aybar@intec.edu.do

Abstract. This study evaluates the feasibility of incorporating various heavy electric battery vehicles, replacing the current diesel vehicles in an underground mining company in the Dominican Republic, and implementing sustainable mining; with this research, a better perspective was obtained about the criteria to consider when introducing an electric heavy mining vehicle instead of a conventional one. Implementing these vehicles can achieve more sustainable mining, saving transport costs and gradually eradicating dependence on fossil fuels. For the environmental aspect, emphasis was placed on comparing Greenhouse Gas (GHG) emissions, specifically CO₂ (Carbon Dioxide), between both alternatives. In the economic part, the benefit-cost analysis was implemented, considering all variable transportation costs. The behavior of the electrical grid when incorporating electric vehicle chargers was analyzed using power flow simulations in the DIgSILENT software. The analyses showed that the incorporation of electric mining vehicles truly brings with it a benefit to the Environment. In economic terms, that does consider the characteristics of the electrical installation of the mine. The power loadability levels of each transformer did not exceed 60% in each scenario, and the annual emissions by vehicle type proposal were 226.5 Tons of CO₂. Similarly, this analysis can be helpful in any job where it is necessary to study the feasibility of electric vehicles and their benefits to the Environment, regardless of the type of company.

Keywords: sustainable mining, mining electromobility, diesel combustion emissions, heavy electric vehicles, DIgSILENT, cost-benefit analysis, mining transport logistics.

1 Introduction

Mining is one of the fundamental activities when referring to the development of civilizations since sectors such as technology, metallurgical, and industrial processes benefit from the materials extracted in this process [1]. It should be noted that mining activities leave many benefits in terms of development; the methods of extraction and

2

mobilization of minerals extracted in these operations involve processes of soil deterioration as a result of deforestation, in addition to greenhouse gas emissions due to the use of fossil fuels in the vehicles and machinery involved [2].

These problems worsen when they are taken to underground mining operations, where the Environment under which the mining operations must be controlled to guarantee the safety and health of the working personnel [3].

Using electric vehicles allows both smart cities and materials mining to reduce CO₂ emissions from kilometers traveled for transportation [4]. Implementing electric vehicles for extraction and transportation and linking them to a network of smart mines is one approach to carry out these initiatives [5].

As the years go by, numerous companies and mining industries dedicate their efforts to the development and incorporation of new methods and techniques that give impetus to the implementation of sustainable mining, which offers better operational, environmental, and safety conditions for the people who are involved in the realization of these mining activities. In addition, this brings with it the possibility of significantly reducing greenhouse gas emissions to the Environment [6].

One of the rapidly emerging practices regarding sustainable mining is the electrification of the vehicles used to carry out mineral extraction and mobilization operations, more directly in underground mining activities, due to the need for greenhouse gas emissions and the Environment. For example, a methodology used to analyze the environmental impact of electric vehicles concerning conventional ones is to compare greenhouse gas emissions with both technologies [7][8][9][10][11]. However, to analyze the impact of these vehicles on an electrical grid network, a study of the grid is carried out through power flow runs, where various software, such as DIgSILENT and Matlab [12][13]. The main contributions of this article are:

The impact of introducing the different configurations of trucks capable of using electrical energy for their operation in the mining sector was analyzed to determine the most appropriate one. A methodology to evaluate the incorporation of electric trucks in mines considering technical aspects such as the electrical power capacity supported by the mine transformers and analysis of greenhouse gas emissions for the proposed configurations. DIgSILENT software application to analyze power flows by including electric truck loaders in the mine's distribution grid.

This article presents the methodology in Section 2, covering 2.1 information research, 2.2 Environmental analysis, and 2.3 Power flow simulations. The results and discussions are presented in Section 3. Section 4 presents the conclusions and perspectives for future work.

2 Methodology

2.1 Information Research

To propose an electric vehicle solution that adapts to the current condition of the mine, we created combinations of types of heavy electric vehicles based on the activity within

the mine. This approach ensures the material extraction remains consistent and the vehicles can be loaded.

To analyze the economic and environmental impact of using heavy-duty electric vehicles in mining, information was sought on the current state of this type of vehicle, such as the environmental impact produced by fossil fuel mining trucks per kilometer traveled and the gas emissions greenhouse effect that this creates.

The current electrical demand curve of the mine is then analyzed to know the capacity of the electrical substation and the mine's feeder cables to see the impact that is connecting the battery chargers for the electric vehicles proposed to transport the material inside mining.

The different power flows were simulated in Digsilent software for the various proposals for combinations of electric mining vehicles to maintain the operation of the mines, with a group of vehicles mobilizing raw material within the mine and another group charging their batteries. Also, it investigated the current situation corresponding to electric mining vehicles around the world, finding that several countries and companies have been dedicated to the development and implementation of this type of technology, companies such as ABB, Epiroc, Sandvik, Bildem, Caterpillar, and Sany, are not only developing vehicles with electric technologies but also encouraging mining companies around the world to bet on this type of heavy vehicles [14–16].

2.2 Environmental analysis

To carry out the environmental analysis, the main variables that may affect the Environment when the use of Diesel combustion vehicles is involved were considered, and later, how the introduction of electric vehicle technology for this same practice could make it possible to reduce these problems. Some variables identified were greenhouse gas emissions, vehicle efficiency level, operational time, vehicle life, and other variables presented below. However, it should be noted that emphasis was placed on the comparison of greenhouse gases since it was the biggest problem identified, in addition to the fact that analyses such as the noise level depend on measurements in the work environment, which entails permit application processes.

The analysis used in this study is based on comparisons between CO₂ emissions from a heavy mining vehicle with conventional combustion technology and its battery-electric alternative. For this, the following values or constants must be used.

Table 1 shows some of the values necessary to be able to make comparisons between the various technologies; in the case of diesel vehicles, there is the autonomy of each type of vehicle, its daily use, and its consumption per hour, with that being able to obtain the number of gallons daily used for each one, and with the emissions, factor finds the amount of CO₂ in tons, with equation 1.

4

Table 1. Data required for environmental analysis.

Concept	Unit	Value	Reference
Emissions per battery charge	(t CO ₂ /kWh)	0,00063	[17]
Diesel combustion emissions	KgCO ₂ / gal. DF	10,2	[18]
Fuel consumption per truck	gal. DF /hr	2,66	[19]
Fuel consumption per blade	gal. DF/ hr	1,86	[19]
Time of daily use by truck	hr	5	[19]
Daily use time per shovel	hr	17	[19]
Autonomy of the blades	Km/gal	5.56	[19]
Truck autonomy	Km/gal	2.70	[19]
Average energy consumption heavy vehicle	kWh/km	1.4	[20]

Gallon Diesel = gal. DF

$$\text{Diesel emissions (tCO}_2\text{)} = \text{gal. DF} * 10.2 \frac{\text{Kg CO}_2}{\text{Gal Diesel}} * \frac{1 \text{Kg}}{0.001 \text{ton}} \quad (1)$$

In the case of electric vehicles, with the daily gallons consumed and the autonomy, it is possible to obtain the daily amount that each type of vehicle travels with the help of equation 2.

$$\text{Daily distance (Km)} = \text{consumption} * \text{daily hours (hr)} * \text{Autonomy} \quad (2)$$

Where the consumption is in (gal/hr) and the autonomy in (Km/gal).

Similarly, the average energy consumption of a heavy vehicle and the valuable capacity of its battery, in this case, that of trucks, is 354 kWh [22][21][23][22]. Using those previous values, Equation 3 calculates the distance an electric truck or scooptram can travel before its battery discharges. It is compared with the one that the Diesel travels daily, doing it to calculate the amount of energy consumed and, with it, the frequency of loading, which, in the case of trucks, would be charged every four days, and the blades daily, and thereby be able to calculate the emissions for each charging schedule.

$$\text{Practical distance (Km)} = \frac{1}{1.4} \left(\frac{\text{Km}}{\text{kWh}} \right) * \text{Battery capacity (kWh)} \quad (3)$$

In summary, with the help of all values and equations above, the yearly emissions for the combustion of Diesel vehicles are calculated. In the case of electric cars, the annual emissions from battery charging, according to the loading frequency, are calculated.

2.3 Power flow simulations

Performances the correct analysis of the electrical grid of the mine when incorporating the various loaders for both trucks and shovels; a power flow must be made, in this case through the DIGSILENT software. For this, it must consider the vehicles' charging schedule; this mine works 24 hours a day, seven days a week; therefore, the time to

charge electric cars is quite limited. From 6:00 – 8:30 AM and 6:00 – 8:30 PM, While the blasting is carried out, where the types of vehicles analyzed are waiting to begin their work then, the ideal time to load them, thus having a time of 5 hours a day to be able to load all the vehicles, whose chargers per unit consume the power of 150 kW [22][21] for the scooptrams and 700 kW of the trucks. Considering the number of trucks (11) and shovels (9), their approximate loading time of 2 hours, and their loading frequency mentioned in the environmental analysis, the number of minimum electric truck chargers would be one, and in the case of electric scooptram chargers would be three, for safety reasons, another loader could add for the trucks. Therefore, the evaluation scenarios correspond to one truck loader, three shovel loaders, two truck loaders, and three shovel loaders. In the same way, the chargers' schedule and additional power must be chosen, but a current consumption scenario must be chosen; for this, the power data of a mobile year of the place [23], selecting the day with the highest established power.

Fig. 1 can visualize the electrical power consumption chart with the highest demand in the entire year and then incorporate the simultaneous power of all loaders, trucks, and shovels in the abovementioned schedules.

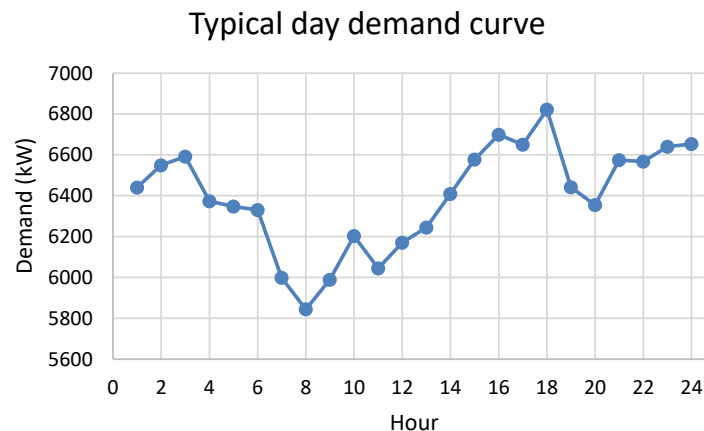


Fig. 1. Typical demand curve mining.

In general, the installation has a connection to the National Interconnected Electrical System or SENI, an electrical grid whose purpose is to provide electricity to everyone in the country, with a substation of 69 kV / 4.16 kV of 14 MVA, where the four lines are derived (A, B, C, and D), the loaders for the underground trucks would be installed in the excellent area that would be their respective parking lots that is that of the heavy equipment where the C line, with a voltage level of 4,160 V, which using a transformer would be reduced by characteristics of truck loaders and thus having a current availability of 165 A. On the contrary, mining shovels are kept in the mine tunnels. Therefore,

6

the location of their chargers will be connected inside, in various mobile substations derived from line D, placed in the multiple ramps located inside the tunnels, being the limit of the number of chargers and the available power. For the correct introduction of the elements in the program, a series of necessary data must be taken into account, which can be observed below.

Table 2 shows the most essential and fundamental elements to analyze power flow in the mine by incorporating the various chargers, such as conductors, transformers, and the corresponding mobile substations. Another detail that must be considered in the case of conductors is the distance of each of these, the bars, their respective voltage levels, and internal loads of the mine that resemble the data provided by the Coordinating Organism of the Interconnected National Electrical System.

Table 2. Data needed to perform the simulations.

Concept	Values used	Reference
Conductor 750 kemil with	4.16 kV, 700 A, 0.0951 Ohm/km	[24]
Conductor 559 MCM AAAC	4.16 kV, 665 A, 0.13779 Ohm/km	[25]
Conductor 4/0 AWG Al	13.8 kV, 335 A, 0.1674 Ohm/km	[26]
Main transformer	69 / 4.16 kV, 14 MVA, Short-circuit impedance (%) = 7.91 Three-phase connection: D-Yn1	[19] **
Line D transformer	13.8 / 4.16 kV, 5 MVA, DC impedance (%) = 7.3 Three-phase connection D-Yn1	[19] **
Mobile substation two windings	13.8 / 1 kV, 1.5MVA, DC impedance (%) = 7 Three-phase connection D-Yn1	[19] **
Mobile substation three windings	13.8 / 1 / 0.48 kV, 1.5 MVA, DC impedance = 6% (HV/MV)DC impedance = 8% (HV/LV) Three-phase connection D-Yn1-Yn1	[19] **

Voltage = kV, Current = A, Resistance = Ohm/km, Power = MVA. **Values that were extracted from the information plates of the elements.

It defined all necessary elements and all their characteristics, as shown in Table 2. Fig. 2 presents the electrical grid configuration of the mine, considering each proposed position for the electrical chargers and the information about each main electrical line above.

7

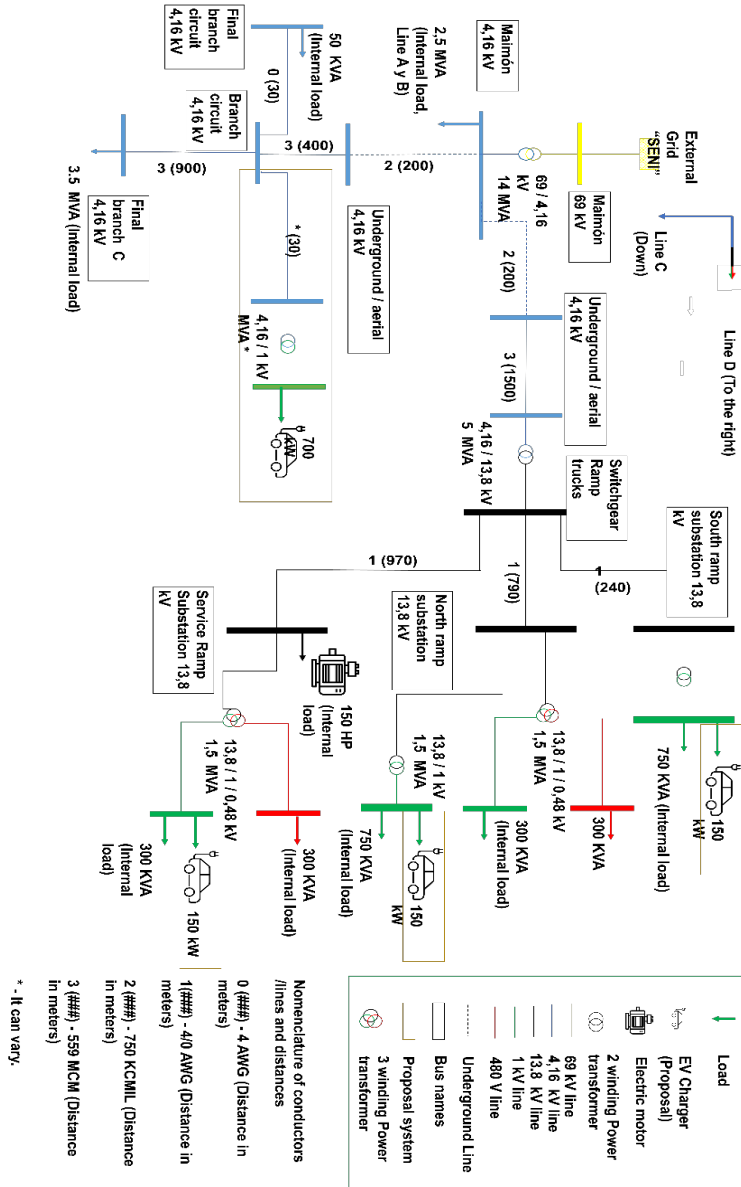


Fig. 2. Mine Electric Grid Configuration

8

3 Results y discussions

After carrying out the corresponding analysis and simulations of incorporating trucks and electric shovels in a mining company in the Dominican Republic, it was observed how introducing this new heavy equipment technology brings with it what is an environmental benefit since combustion emissions are significantly higher compared to those generated to be able to supply the batteries of electric technology. Below is a graph of emissions by type of technology and by vehicle.

Fig. 3 shows the emissions of each technology and type of vehicle, according to the conditions of use of the mine studied able to notice that while the emissions of a conventional truck are around 50 tons, its electric alternative would only emit about 2.5 tons, avoiding approximately 47.5 tons of CO₂ per year. In the case of blades, emissions with conventional technology would be around 235 tons, while its electric version would be about 56 tons, avoiding about 179 tons per year for each blade.

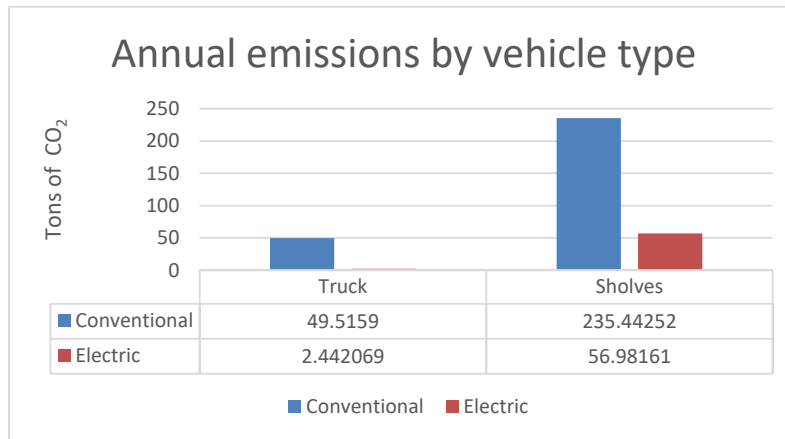


Fig. 3. Annual CO₂ emissions by vehicle type.

On the part of the simulations, a diagram quite like the current situation of the mine was designed, as shown in Fig. 2. However, with the help of the tables and data thrown, there is a more accurate perspective of what happens electrically in the installation and how it would be affected if the necessary chargers are incorporated.

In order to explain in detail the electric current power flow of the mine and compare its behavior against the various proposed scenarios, multiple values will be expressed, such as voltage in each of the bars presented by the system, current and loadability of the lines, and chargeability of the transformers.

Table 3 shows the loadability of the various cables and conductors in multiple scenarios.

Table 3. Loadability of the lines in the different systems.

Line	Chargeability (%) with one truck loader and three shovels	Chargeability (%) with two truck loaders and three shovels	Chargeability (%) Current situation
TRAFO bypass line	3,481224	3,512849	3,45795
Service ramp 4/0 AWG	4,461867	4,481131	4,116379
Rampa sur 4/0 AWG 2	5,158701	5,180717	5,004053
North Ramp 4/0 AWG	6,810239	6,839126	6,279804
Underground D 750 KCMIL WITH	51,56183	51,78244	48,10619
AIR D 559 MCM AAAC	54,27561	54,50783	50,63809
FIN AIR C 559 KCMIL AAAC	74,13532	74,70123	70,92062
Underground C 750 KCMIL	86,0224	102,6845	73,61329
AIR C 559 KCMIL AAAC	90,54989	108,0889	74,65328

Table 3 specifies the loadability of the lines in the various scenarios, where in the current situation, the lines with more loadability correspond to power line C, to which the truck loaders would be installed. After adding the equipment load (700 kW), the different sections of the line reach loadability levels of up to 90%, indicating that it is almost at the limit allowed by the manufacturer's data. Then, when adding another truck loader, with two connected in line C, some pieces would not withstand the demand. In the case of the incorporation of blade loaders, where the available power is considered,

Another aspect considered when performing the flow simulations was the voltage levels of each point of the diagram of the designed electrical network. In Table 4, voltage levels are visualized in the various scenarios raised.

Table 4. Voltage levels per unit of each of the bars.

Bus Bar	One truck loader and three blade loaders		Two truck loaders and three blade loaders		Current situation	
	(kV)	In p.u	(kV)	In p.u	(kV)	In p.u
High Trafo New	4,16	0,997	4,16	0,989	4,16	1,003
Under new trafo	1	0,979	1	0,953	1	1,003
Derivation	4,16	0,997	4,16	0,990	4,16	1,003
End of Derivation	4,16	0,997	4,16	0,990	4,16	1,003
End line C	4,16	0,971	4,16	0,964	4,16	0,978
Maimon interconexion	69	1,045	69	1,045	69	1,045
Maimon 4.16 kV Switchgear	4,16	1,014	4,16	1,011	4,16	1,017
RNorte 1 kV	1	0,926	1	0,922	1	0,936
RampaSUR 1 kV(1)	1	0,933	1	0,929	1	0,943
RampaSUR 1 kV	1	0,939	1	0,935	1	0,949
RSur 480 V	0,48	0,944	0,48	0,940	0,48	0,953
RServ 1 kV	1	0,921	1	0,917	1	0,931
RServ 480V	0,48	0,912	0,48	0,908	0,48	0,922
Rampa Servicio Substation	13,8	0,964	13,8	0,960	13,8	0,973
Underground / Air Line C	4,16	1,010	4,16	1,006	4,16	1,015
Underground/Air Line D	4,16	1,011	4,16	1,007	4,16	1,014
North Substation	13,8	0,964	13,8	0,960	13,8	0,973
South Substation	13,8	0,963	13,8	0,960	13,8	0,973
Subterranean	4,16	0,999	4,16	0,995	4,16	1,008
Switchgear RN	13,8	0,964	13,8	0,960	13,8	0,973

*Those values in red mean that they are not within the ranges of variation allowed by the Superintendence of Electricity (SIE) of $\pm 7.5\%$ [27].

Concerning the voltage levels in each element throughout the installation, Table 4 shows that as the number of chargers increases, the voltage in each system bar decreases, reaching levels not allowed by the regulations established by the SIE. The mentioned below is because the higher the load, the current increases, and with it, the Joule losses by I^2R , causing low voltage levels.

Similarly, the loadability values of each of the transformers established in the installation were reflected, considering that a shovel loader was installed on each base ramp of the mine. Table 5 presents all the transformers reflected in the simulation and their chargeability in each proposal designed.

Table 5. Loadability of transformers in various scenarios.

Transformer	Current situation	One truck loader and three blade loaders	Two truck loaders and three blade loaders
	Loadability(%)	Loadability (%)	Loadability (%)
14 MVA SENI	45,52	54,12	60,86
South Ramp Substation	35,14	37,08	37,23
North ramp substation	53,43	55,07	55,30
Trafo 5 MVA	48,53	52,01	52,23
MEGLAB 3 Rserv windings	43,36	48,62	48,83
MEGLAB 3 Rsur windings	55,93	56,52	56,75

Interconnected national electrical system = SENI

Table 5 shows that the power loadability levels of each transformer did not exceed 60% in each scenario; that is, there is plenty of power for any other internal load of the mine.

When observing the results of each of the corresponding analyses and simulations, it was possible to notice that regardless of the number of vehicles that are implemented in each proposal, CO₂ emissions are considerably reduced because the emissions to charge a battery of this type of technology are much lower than the emissions from combustion by diesel fuel, bringing a significant benefit to the Environment for each heavy electric vehicle that is incorporated instead of a conventional one.

4 Conclusions

The comparative analysis of greenhouse gas emissions between the various technologies described in the environmental analysis methodology allowed for visualization of the emissions of greenhouse gases, in this case, CO₂, that may be incurred depending on the type of vehicle studied, considering both the combustion emissions of conventional ones, but also those generated by charge the batteries of the electrical alternatives. In the case of the latter, emissions beyond the vehicle itself must be considered, but also the emissions generated by the production of electrical energy necessary for the operation of the battery cells. In the same way, it was possible to design a system with similar characteristics of the company, being able to analyze with the DIGSILENT software not only the situation when incorporating the chargers but also the current situation and the performance of each of the main elements of the installation, when adding the extra demand due to the chargers.

A significant contribution of the study is that regardless of the type of industry, whether it is a mining company or not, it can serve as a study guide to incorporate any alternative technology and perform the corresponding environmental and electrical analysis. On the contrary, the prices required for the purchase and installation of the equipment, all its logistics transportation costs incurred, and the ideal number of vehicles incorporated,

12

and when implementing economic tools, determine the financial profitability were not considered.

In the future, it would be possible to study the incorporation of chargers with lower power demand or incorporate a photovoltaic generation system to reduce the power peaks that would be consumed from the network caused by the chargers of the vehicles in the same way replacement batteries could be purchased and charge them at off-peak times so that when the electric cars are discharged make the change. It can also be analyzed how the protection elements of the system would be affected if all the protection elements had to be redesigned.

Acknowledgment

The authors acknowledge the support provided by the Thematic Network 723RT0150 “Red para la integración a gran escala de energías renovables en sistemas eléctricos (RIBIERSE-CYTED)” financed by the call for Thematic Networks of the CYTED (Ibero-American Program of Science and Technology for Development) for 2022.

References

1. De la Rosa L ME, Hernández G P, Vega C MÁ (2020) La industria minera y su enfoque de sostenibilidad en Méjico. Teuken Bidikay - Rev Latinoam Investig en Organ Ambient y Soc 11:175–200. <https://doi.org/10.33571/teuken.v11n16a8>
2. Arias Torres SM, Córdova Castro JD, Gómez Botero MA (2021) Alternativas de aprovechamiento de residuos de la industria minera de El Bajo Cauca Antioqueño en el sector de la construcción. Rev EIA 18:1–12. <https://doi.org/10.24050/reia.v18i36.1496>
3. QUITRAL DIAZ GP (2022) COMPARATIVA TÉCNICA, ECONÓMICA, INNOVATIVA Y AMBIENTAL DE EQUIPOS LHD EN MINERÍA SUBTERRANEA. <http://dspace.otalca.cl/bitstream/1950/12926/3/2022A000764.pdf>
4. Hartlieb-Wallthor P v., Hecken R, Kowitz S-F, et al (2022) Sustainable Smart Mining: Safe, Economical, Environmental Friendly, Digital BT - Yearbook of Sustainable Smart Mining and Energy 2021: Technical, Economic and Legal Framework. In: Frenz W, Preuße A (eds). Springer International Publishing, Cham, pp 37–79
5. Hristova T (2022) Tracking of the battery materials of electric vehicles in the mining industry via a blockchain. IOP Conf Ser Earth Environ Sci 970:12012. <https://doi.org/10.1088/1755-1315/970/1/012012>
6. Androulakis V, Sottile J, Schafrik S, Agioutantis Z (2020) Concepts for Development of Autonomous Coal Mine Shuttle Cars. IEEE Trans Ind Appl 56:3272–3280. <https://doi.org/10.1109/TIA.2020.2972786>
7. Dubov GM, Trukhmanov DS, Nokhrin SA (2020) The Use of Alternative Fuel for Heavy-Duty Dump Trucks as a Way to Reduce the Anthropogenic Impact on the Environment. IOP Conf Ser Earth Environ Sci 459:042059. <https://doi.org/10.1088/1755-1315/459/4/042059>

8. Salazar Restrepo GA (2020) Estudio de factibilidad para el cambio del uso de vehículos de combustible por vehículos eléctricos en la compañía IPS Servicios de Salud Suramericana S.A. In: Maest. en Gerenc. Proy. <https://repository.eafit.edu.co/handle/10784/24347>. Accessed 4 Sep 2023
9. Ullah MH, Gunawan TS, Sharif MR, Muhida R (2012) Design of environmental friendly hybrid electric vehicle. In: 2012 International Conference on Computer and Communication Engineering (ICCCCE). pp 544–548
10. Ertugrul N, Kani AP, Davies M, et al (2020) Status of Mine Electrification and Future Potentials. In: 2020 International Conference on Smart Grids and Energy Systems (SGES). pp 151–156
11. Feng Y, Dong Z, Yang J, Cheng R (2016) Performance modeling and cost-benefit analysis of hybrid electric mining trucks. In: 2016 12th IEEE/ASME International Conference on Mechatronic and Embedded Systems and Applications (MESA). pp 1–6
12. Jansanyayut T, Phongtrakul T, Yenchamchalit K, et al (2020) Design of Solar-Powered Charging Station for Electric Vehicles in Power Distribution System. 2020 8th Int Electr Eng Congr iEECON 2020 7–10. <https://doi.org/10.1109/iEECON48109.2020.229545>
13. Ruiz Guzmán OA (2017) Evaluación del impacto de la recarga del vehículo eléctrico en la calidad de la potencia. In: Master Thesis. <https://repositorio.unal.edu.co/handle/unal/63426>. Accessed 4 Sep 2023
14. Edición Revista Energía (2021) Boliden, Epiroc y ABB se unen para desarrollar un trolebús eléctrico para la minería – Revista Energía. In: News. <https://energiminas.com/boliden-colabora-con-epiroc-y-abb-en-la-aventura-hacia-una-mina-libre-de-combustibles-fosiles/>. Accessed 9 Apr 2023
15. BNamericas (2022) Empresa china entrega camiones eléctricos y excavadoras a brasileña CSN Mineração. In: News. [https://www.bnamericas.com/es/noticias/empresa-china-entrega-camiones-electricos-y-excavadoras-a-brasilena-csn-mineracao#:~:text=El fabricante chino de equipos,excavadoras a la empresa brasileña](https://www.bnamericas.com/es/noticias/empresa-china-entrega-camiones-electricos-y-excavadoras-a-brasilena-csn-mineracao#:~:text=El fabricante chino de equipos,excavadoras a la empresa brasileña.). Accessed 9 Apr 2023
16. Sánchez F, Hartlieb P (2020) Innovation in the Mining Industry: Technological Trends and a Case Study of the Challenges of Disruptive Innovation. <https://doi.org/10.1007/s42461-020-00262-1/Published>
17. United Nations Framework Convention on Climate Change (2020) Standardized baseline.Grid Emission Factor for the Dominican Republic. ASB0047-2020. https://cambioclimatico.gob.do/phocadownload/Documentos/emisiones/ASB0047-2020_PSB0048.pdf. Accessed 9 Apr 2023
18. Environmental Protection Agency (EPA) (2006) Calculadora de equivalencias de gases de efecto invernadero - Cálculos y referencias | US EPA. In: Online Calc. <https://espanol.epa.gov/la-energia-y-el-medioambiente/calculadora-de-equivalencias-de-gases-de-efecto-invernadero-calculos>
19. Corporación Minera Dominicana (CORMIDOM) (2022) CORMIDOM - Corporación Minera Dominicana. <https://cormidom.com.do/#>. Accessed 9 Apr 2023
20. Forrest K, Mac Kinnon M, Tarroja B, Samuelsen S (2020) Estimating the technical feasibility of fuel cell and battery electric vehicles for the medium and heavy duty sectors in California. Appl Energy 276:115439. <https://doi.org/10.1016/j.apenergy.2020.115439>
21. Sandvik (2022) TH665B Underground battery-electric truck. <https://www.rocktechnology.sandvik/en/products/underground-loaders-and-trucks/battery->

14

- electric-loaders-and-trucks/th665b/. Accessed 9 Apr 2023
22. Epiroc North Macedonia DOOEL (2022) Scooptram ST14 Battery Fully battery electric loader with 14-tonne capacity. <https://www.epiroc.com/en-mk/products/loaders-and-trucks/electric-loaders/scooptram-st14-battery>
 23. Organismo Coordinador del Sistema Eléctrico Nacional Interconectado (2022) Consumo de potencia año móvil CORMIDOM. <https://www.oc.do/Informes/Operación-del-SENI/Coordinación-y-Supervisión-Tiempo-Real/EntryId/185992>. Accessed 5 Aug 2022
 24. Southwire Company L (2018) SPEC 46255 3 / C CU 5KV 115 NL-EPR 133 % TS ARMOR-X PVC MV-105. In: datasheet. http://cabletechsupport.southwire.com/es/cablespec/download_spec/?spec=46255. Accessed 9 Apr 2023
 25. CENTELSA (2022) Cables AAAC. In: datasheet. https://centelsa.com/productos_centelsa/productos_colombia/CABLE_DE_ALUMINIO_DESNUDO/CABLES_DE_ALUMINIO_DESNUDO_CABLES_AAAC.pdf. Accessed 9 Apr 2023
 26. UpCodes (2022) National Electrical Code Texas Adoption. In: Online Calc. <https://up.codes/viewer/texas/nfpa-70-2020/chapter/9/tables#9>. Accessed 9 Apr 2023
 27. Superintendencia de Electricidad (2020) Resolucion SIE-065 Mercado Electrico Mayorista. In: Reglamento. https://sie.gob.do/wp-content/uploads/2021/06/SIE-065-2020-MEM_-_Mod_Codigo_Conexion_del_SENI-fusionado.pdf. Accessed 9 Apr 2023

Electric vehicles charging schedule optimization based on time-of-use tariff. Case study of the Dominican Republic

Alexander Vallejo Díaz ^{1,2,*} [0000-0003-3215-6352] and Elvin Arnaldo Jiménez Matos ² [0000-0002-0031-6772]

¹ Facultad de Ingeniería, Instituto Especializado de Estudios Superiores Loyola (IEESL), 91000 San Cristóbal, Dominican Republic

² Área de Ingeniería, Instituto Tecnológico de Santo Domingo (INTEC), 10602 Santo Domingo, Dominican Republic
avallejo@ipl.edu.do

Abstract. Electric mobility is a sustainable travel alternative for the decarbonization of transportation. Due to technological advances in the development of electric vehicles, they have a more competitive price than traditional internal combustion vehicles. In addition, they have a more efficient consumption with the distance-to-cost ratio. This article determines the optimal schedule for charging electric vehicles (EVs) taking into consideration the physical and economic aspects, such as the demand, generation, and penetration of variable renewable energies (VRE), as well as two EV penetration scenarios in the Dominican Republic. The optimization model proposes to minimize generation costs, maximize the use of VRE, and maximize curve flattening. The results indicate that the most favorable hours to charging EVs are between 12:00–15:00, with an EV demand of 8.64 MW and 320 MW, for the scenarios of 2700 and 100,000 EVs charging simultaneously, respectively. In the same interim, the highest production of VRE typically occurs in the Dominican Republic.

Keywords: Electric Vehicles, Charging Schedule, Cost Optimization, Maximizing Renewable, Energy Cost Signal, Dominican Republic.

1 Introduction

Due to the growing attention to mitigating climate change, traditional vehicles will increasingly have less participation in the vehicle fleet mix. Electric vehicles (EVs) have become a viable alternative due to the low costs of batteries, increasing energy density, and expansion of charger infrastructure [1]. Those reduced from 500–800 USD/kWh in 2012 have an average cost of 400 USD/kWh. Another advantage is low greenhouse gas emissions compared to conventional ones. internal combustion engine [2].

EVs are an important pillar for the decarbonization of transportation and contribute to the energy transition of countries in accordance with the goals established in the Sustainable Development Goals (SDGs) 2030. Singh et al. [3] presented a bibliometric study of the exponential growth that EV publications have tended between 1980-2022, where exponential growth can be seen from 2010. In 2021, 203 articles were published

rates applicable to EV charging stations for the quarter October – December 2023 [8]. The proposed rate is intended to move EV charging during off-peak demand times.

The objective of this research is to review the best international practices on EV charging schedules and therefore, determine which are the most favorable hours to charge EVs considering the Trilemma between (1) taking advantage of renewable energy production, (2) reduce peak demand and (3) have energy price signals. For this research, in the next section will be described the proposed methodology.

2 Materials and methods

2.1 Studies on EVs charging schedule

EVs have gained a lot of attention for lowering greenhouse gas emissions in the transportation sector. In addition, they have obtained great attention to provide ancillary services in the electric grid, the peak shaving and valley fitting [9]. Despite the high degree of randomness regarding the charging of EVs connected to the grid, the habits of the consumers have been analyzed so that they can provide the frequency regulation service based on two class aspects, the distance traveled daily and the EV charging start time. Where the aim is to move the charging time to hours outside of peak demand and at the same time take economic signals into account. The fundamental objective of grid-connected EVs is to move the charging schedule out of peak demand hours [9]. J. Zhang et al. [10] have presented optimization models of reducing the expansion of transmission and distribution lines due to the increase in demand for EVs. Authors propose to improve the coincidence of photovoltaic production with EV demand, seeking a balance between reducing system losses and the comfort in which users charge their EVs. The participation of EVs in the demand-side regulation response has been analyzed by M. Zhang et al. [11], to minimize the charging of EVs during peak demand hours, where they have reported that aggregators can be increased by 59% and 37% on workdays and non-workdays, respectively, on the demand-side regulation response. Zhong et al. [12] have proposed a strategy for the optimization of EV charging with a dynamic Time-of-Use Tariff, minimizing cost of users and the charging variance considering the restrictions on the side of the users and the stations.

EVs can be used to supply ancillary services when there is massive grid integration, which can eliminate harmonics by improving voltage quality, improving power factor with the injection and absorption of reagents, and reducing peaks to through demand-side management techniques to shifting load periods [13]. Mejía et al. [14] evaluated several scenarios through simulations in PowerFactory DlgSILENT software for EVs connected to the grid in order to study the first control of frequency regulation service. The results indicated that the influence of EVs on frequency changes is negligible. The projection of EVs in the country were taken from a report [6]. This INTRANT plan is based on inter-institutional collaboration between the private and public sectors to organize and accelerate the deployment of electric mobility in the Dominican Republic.

4

Recently, the SIE promulgated the zone rate for the last quarter of 2023. For zone 1, in the concession area of electricity distributors, there is a fixed cost for recharges of USD 0.8367, and there are two hourly rates, one block is between 00:00 and 18:59 is at 0.1632 USD/kWh and the other block between 19:00 and 23:59 is 0.3262 USD/kWh. In Zone 2, in the concession area of a private company (tourist zone), the costs are 0.2687 and 0.5376 USD/kWh for blocks 1 and 2, respectively. In Zone 1, the cost increased by 3% compared to the Q3 quarter, and in Zone 2 the increase was 6% [8].

The expansion of EVs will depend on the economic development of countries, since GDP and this trend have a high correlation [15]. This is important, since Wiener & Koontz [16] demonstrated that wealthier and more liberal countries than the US are more pro-environmental and supportive of energy transition policies. The successful deployment of EVs in the Dominican Republic must be economically feasible. The pricing structure directly affects the deployment of the technology. The tariffs mechanisms are feed-in tariffs, time of use (ToU) pricing, and net metering. There is a tariff with a fixed basic charge (\$/month) and a volumetric charge (\$/kWh), this is the ToU where the price varies during the day and night, and is typically higher at nights when the market cost wholesaler is also [17].

2.2 Proposed methodology

According to the methodologies presented by [9], [11], [18], [19], where maximizing the use of renewable energies is presented, with the minimization of electricity costs and the flattening of the system load curve, considering the comfort of end users, in Fig. 2, a proposed flowchart is presented that has three phases for the evolution of the optimal moment to charge EVs in the Dominican Republic. In the first phase I, the economic and physical parameters of the system are described and defined, such as the generation of variable renewable energy (VRE), the demand of the electrical system, the costs of electricity generation, the number of EVs in the country, and finally the demand for these EVs. In phase II, the objective function is established to minimize costs, maximize the use of the VRE and maximize the flattening of the curve. These three objective functions will be normalized according to the best of the author's knowledge. And finally, in phase III, the results and discussion will be presented in the next section. Below is presented a breakdown description for each phase.

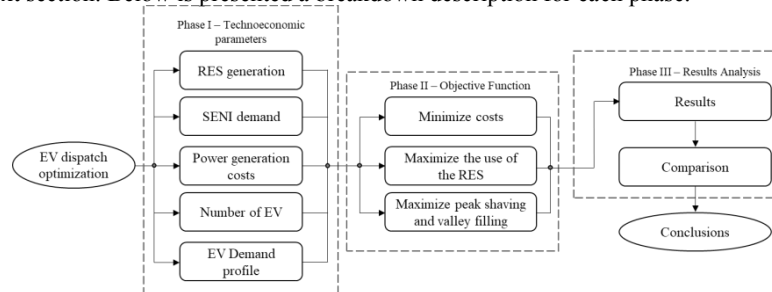


Fig. 2. Proposed methodology for optimal hours to charge EVs in the Dominican Republic.

Phase I – Economic and physical parameters of the system

This subsection presents the economic and physical overview of the wholesale energy market. According to the performance report of the Ministry of Energy and Mines, the consolidated operational building of the distribution companies amounts to USD 588.4 million for the period January–June 2023, and 70% of this deficit corresponds to the difference between the purchase and sale of energy [20]. The Dominican Republic import all fossil fuels for generation. For 2022, the deficit was USD 1,368 million [21]. The costs of fossil fuels exhibited a considerable increase between 2021 vs 2022 due to the war conflict between Russia–Ukraine, which increases the financial vulnerability of the Dominican government to serve the national electricity supply efficiently and effectively, thus this risk compromises the established goals to meet the nation's decarbonization goals [22].

According to the report [20] the changes and increases were 29%, 78%, 76% and 123% for Fuel Oil #6, Fuel Oil #2, Natural Gas and the Platts Reference Coal, respectively (US Gulf Coast, Henry Hub and FOB Colombia) [23]. In 2022, the generation was 15.2%, 0.1%, 37.8% and 30.7% for Fuel Oil #6, Fuel Oil #2, Natural Gas and Coal, respectively [24]. For that period, production with wind, photovoltaic, and hydraulic energy was 5.3%, 3.3%, and 6.6%, respectively, leaving 0.9% for biomass. The National Interconnected Electrical System (SENI) has an installed capacity of 1,117 MW of variable renewable energy (417 MW wind and 700 MW photovoltaic), of which 63% is photovoltaic according to weekly operation report PSD_09-09_15-09-2023, issued by Independent System Operator (OC) [25].

Fig. 3-A shows the short-term marginal cost of electricity (CoE) of the SENI for the 8760 hours of the year 2022 binned by quarters. During the months of Q1 and Q4, they tend to be lower because there is less demand in the country, associated with low temperatures. Additionally, on average the capacity cost in 2022 was 9.7759 US\$/kW-month in the wholesale market, the toll cost was 2.4182 US\$/kW-month and the commercialization cost of distribution company was 0.0709 US\$/kWh. Fig. 3-B shows SENI demand for the same datasets, where increases are observed in the months of Q2 - Q3, and the occurrence of the peak demand in the hours between 19h - 23h, corresponding to the peak energy cost. The demand only includes the regulated clients from distribution companies (EDEs). Fig. 3-C presents the photovoltaic and wind energy production for the same dataset. Basically, there is an average production of 585 MW between 10h - 16h, and a peak according to the typical distribution of the solar curve of the order of 644 MW at 13h. Fig. 3-D presents the production of photovoltaic and wind energy separately. Based on this context of the wholesale electricity market of the Dominican Republic, it is essential for this research to determine the periods of the day in which the charging of electric vehicles causes a minimum economic and operational impact on the market. Likewise, the production of variable renewable energy can be maximized.

6

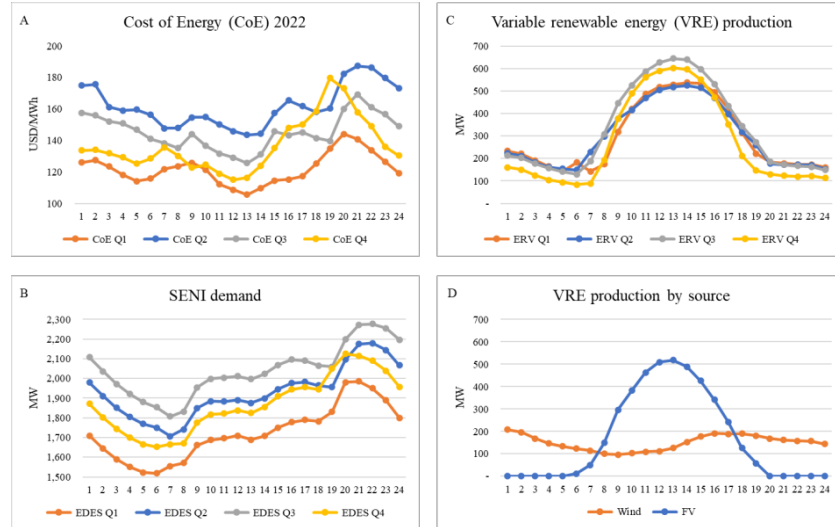


Fig. 3. (A) Cost of Energy in 2022, (B) Demand SENI profile by EDEs, (C) renewable variable energy production curve quarterly and (D) renewable variable energy production by source.

An important problem when integrating EVs into the electrical grid is determining consumer behavior, the charging time and the average discharge profile based on traffic [2]. To carry out adequate modeling, methods with space-time distribution must be considered. In relation to the special distribution, the Origin-Destination (OD) matrix is used to divide the spatial plane into different grids according to a desired scale in the study area, and this matrix can be used for the spatial-temporal distribution of the EV charging [26].

For spatiotemporal analysis, Monte Carlo simulation is widely used as an inference method to have various expected scenarios with a stable probability of occurrence parameterized in the mean and variance parameters [27]. According to Tayyab et al. [28], EVs can be between states: traveling, charging or parked without charging, which is quite complex to predict the behavior of users due to the embedded randomness, however, the Monte Carlo simulation can be used to predict the spatiotemporal distribution of EVs. Fig. 4 shows the load profile during the daytime, where EVs charging peaks at night. The temporal characteristics are departure time, arrival time, waiting time and other time information, and the spatial characteristics consider the departure location, arrival location, distance traveled, and other spatial information, such as registration of the consumption per mileage [2].

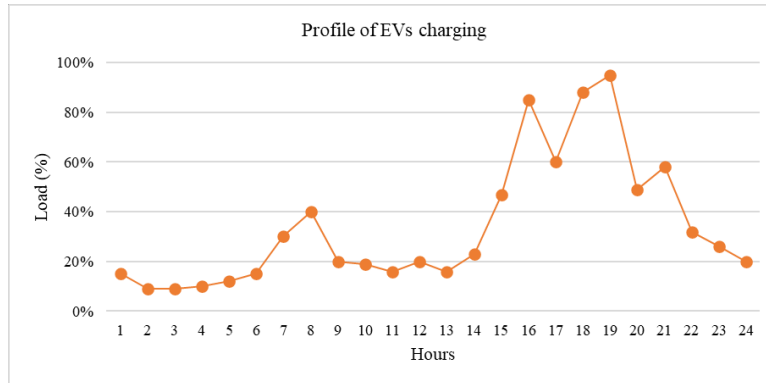


Fig. 4. Profile demand of EVs charging presented by [28].

Phase II – Objective Function

The growing adoption of electric vehicles (EVs) in the Dominican Republic poses significant challenges and opportunities for the country's electrical system. While EVs offer environmental and economic advantages, their growth can also put additional pressure on existing electrical infrastructure. The key aspects to take into account in the optimization modeling are operational limitations, generation with variable renewable energy, power flow constraints, nodal balance restrictions and EV restrictions [19]. This research focuses on minimizing the impact of additional demand from electric vehicles on the Dominican wholesale electricity market in economic and operation terms. To address this aim, three interrelated objective functions are proposed, such as i) the minimization of the price of EV charging, ii) the prioritization of charging hours with the highest penetration of renewable energy and iii) flattening of the electrical demand curve. Below is a breakdown of each of the functions proposed to achieve the optimization goals.

– Minimize the cost of charging electric vehicles

According to Yong et al. [29], flexibility in the price of charging is essential for the future integration of renewable energy with EV charging. Dynamic pricing rates have been effective in responding to demand and managing EV charging at off-peak times, which increases the reliability of the distribution system. Dynamic pricing schemes can be Time of Use (TOU), Critical Peak Pricing, Real-Time Pricing and Peak Time Rebate. Where the TOU has proven to be the most effective with the change in demand from peak hours to non-peak hours. The TOU tariffs are the most adopted in the United State, United Kingdom and Australia. Other countries such as Netherlands, Belgium and Norway used dynamic pricing tariffs as well as. According to the aforementioned, taking advantage of the periods with better energy costs for the user will be key. Although this requires certain organizational and sociocultural measures. Reducing the EV charging cost is essential to encourage its mass adoption. According to Tian et al. [9], EVs play a crucial role in grid peak shaving and valley filling through the

8

implementation of V2G technology. The primary objective of this technology is to effectively reduce the disparity and fluctuations between peak and off-peak load levels while maintaining optimal economic efficiency. To achieve this objective function, the following objective function is proposed:

$$F_1 = \min(\sum_{t=1}^T CmgD_t P_t) \quad (1)$$

Where $CmgD_t$ is the end-user electricity cost, equal to electricity production cost at each hour t -th, plus the transmission and distribution cost and revenue, and P_t is the demand for electric vehicles.

– Maximize the use of variable renewable generation for electric vehicles

With the objective of maximizing the use of renewable energy in charging electric vehicles is presented in Eq. (2), the following objective function is proposed, which allows taking advantage of the fact that EV charging is at the most favorable matching time for production of variable renewable energy with the demand.

$$F_2 = \max(\sum_{t=1}^T PERV_t P_t) \quad (2)$$

Where $PERV_t$ is the penetration of renewable energy in MW and P_t is the demand for electric vehicles in MW, for each hour.

– Flattening of the electrical demand curve

To avoid electric vehicle demand coinciding with peak electricity demand, it is necessary to flatten the load curve. This involves changing consumption patterns to charge EVs during off-peak hours. This research included studying current consumption patterns and identifying effective strategies to encourage charging during optimal hours. The Eq. (3) objective function is proposed:

$$F_3 = \min(\max(P_t^{base} + P_t) - \min(P_t^{base} + P_t)) \quad (3)$$

Where P_t^{base} is base load and P_t is the demand for electric vehicles, for each hour.

Since we have three functions, it is necessary to include them all in a single objective function. For this, it is necessary to normalize all functions and assign them a weight according to their importance. The total objective function is shown below in Eq. (4). Where K_1 , K_2 and K_3 are 50%, 30% and 20%, respectively according to the best knowledge of authors, that coefficient represents a suitable mix as starting point.

$$F = \min \left(K_1 \frac{F_1}{F_{1max}} + K_2 \left(\frac{F_2}{F_{2max}} \right)^{-1} + K_3 \frac{F_3}{F_{3max}} \right) \quad (4)$$

The results and comparison (phase III) are described in the following results and discussion section.

3 Results and discussion

To ensure the effectiveness of the proposed strategy, data on energy, demand and level of renewable energy penetration of the Dominican electricity system in 2022 were used. The cost of energy and demand for the Q1 of that year can be seen in Table 1, where the peak hours occur in the evening and valley in the morning. Fig. 5 shows the penetration of renewable energies in the daytime distribution, where the curve follows the insolation, due to the production of photovoltaic (PV) farms.

Table 1. Energy cost and demand for Q1-2022 in the Dominican Republic.

Hour	USD/MWh	MW	Hour	USD/MWh	MW	Hour	USD/MWh	MW
1:00	125.98	1709.28	9:00	125.79	1661.17	17:00	117.18	1789.23
2:00	127.40	1643.16	10:00	121.41	1687.70	18:00	125.24	1782.56
3:00	123.39	1590.04	11:00	112.12	1696.70	19:00	134.69	1829.99
4:00	118.10	1550.67	12:00	108.59	1709.05	20:00	144.07	1980.60
6:00	114.12	1522.84	13:00	105.60	1689.69	21:00	140.83	1984.74
7:00	115.73	1517.65	14:00	109.78	1708.00	22:00	133.92	1950.32
7:00	121.88	1555.10	15:00	114.48	1750.12	23:00	126.52	1888.91
8:00	123.72	1570.22	16:00	115.21	1778.55	24:00	119.32	1799.41

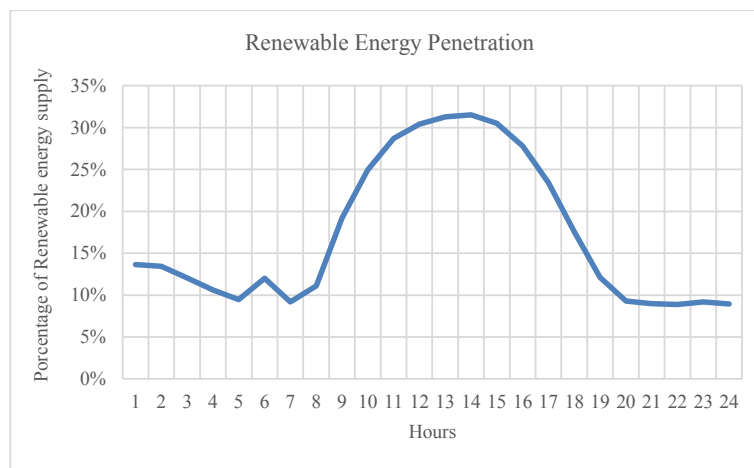


Fig. 5. Typical daytimes renewable energy presentation.

To validate the proposed method, two scenarios of electric vehicle penetration in the Dominican Republic's vehicle fleet were evaluated. Scenario 1 is the actual scenario, with 8,000 EVs according to the most recent publication and best authors knowledge [30]. Scenario 2 projected 400,000 EVs. This projection is to make a sensitivity to the dramatic growth in demand for EVs in the SENI in accordance with INTRANT projections for 2030 [6]. Although the conditions of today's wholesale electricity market will not be the same as those of 2030, this sensitivity was carried out with this aggressive scenario to study the impact that the SENI will have if the proliferation of EVs increases

10

drastically in the next 4 - 5 years, with the intention of anticipating this scenario and that the planning of the new generation and the electricity cost scheme for EVs are appropriate to a context of massive deployment of EVs.

- **Scenario 1: 8,000 electric vehicles**

In this scenario 8,000 EVs were assumed, each vehicle is loaded every 3 days. This gives us a match of 2,700 EVs loading simultaneously. Each EV uses a residential charger with a power of 3.2 kW, the maximum demand that electric vehicles were 8.64 MW. Fig. 6 shows the distribution of the load of electric vehicles carried out by the proposed methodology. Since the lowest energy costs are concentrated in the periods of maximum penetration of renewable energy, vehicle demand is concentrated between the hours of 12:00–15:00.

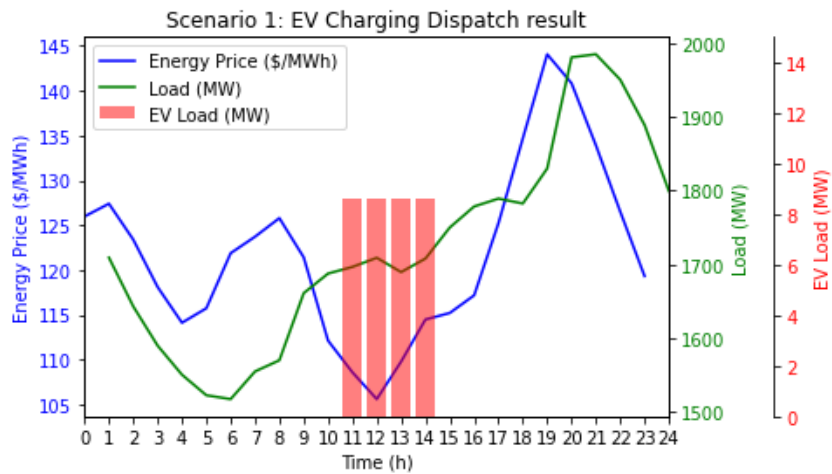


Fig. 6. EVs charging dispatch result from scenario 1.

In Fig. 7 presents the distribution of the load of EVs in each quarter of 2022. A large amount of power is concentrated in the periods of maximum renewable penetration. In that sense, EV charging should be encouraged to occur around midday. PV energy production in this period has an increase of around 200% between 12:00 - 15:00 hours, equivalent to 628 MW.

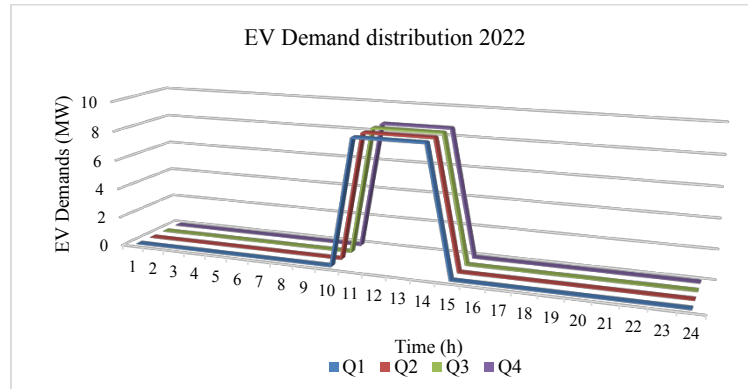


Fig. 7. EV demand distribution per quarter in 2022 for scenario 1.

• **Scenario 2: 400,000 thousand electric vehicles**

In this scenario 400,000 were assumed, each vehicle is loaded every 3 days. This gives us a match of 100,000 loading simultaneously. Each vehicle uses a residential charger with a power of 3.2 kW, the maximum demand that electric vehicles would provide would be 320 MW. Fig. 8 shows the distribution of the load of electric vehicles carried out by the proposed methodology. Because the lowest energy costs are concentrated in the periods of maximum penetration of renewable energy, vehicle demand is concentrated between the hours of 12:00–15:00.

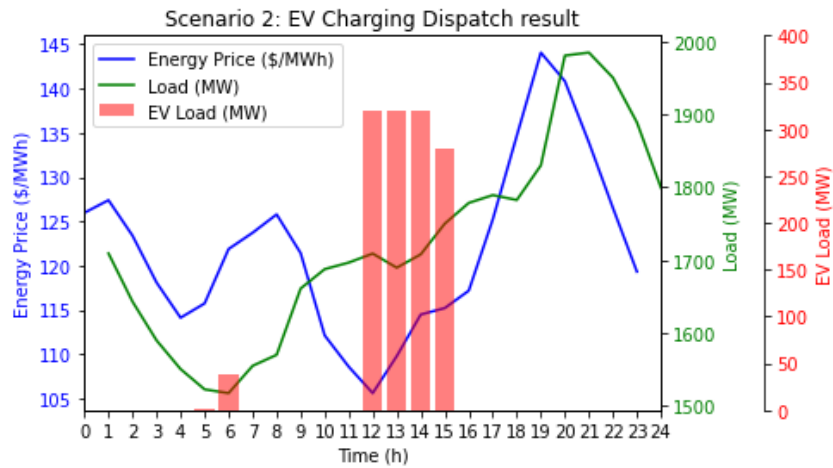


Fig. 8. EV charging dispatch result from scenario2.

12

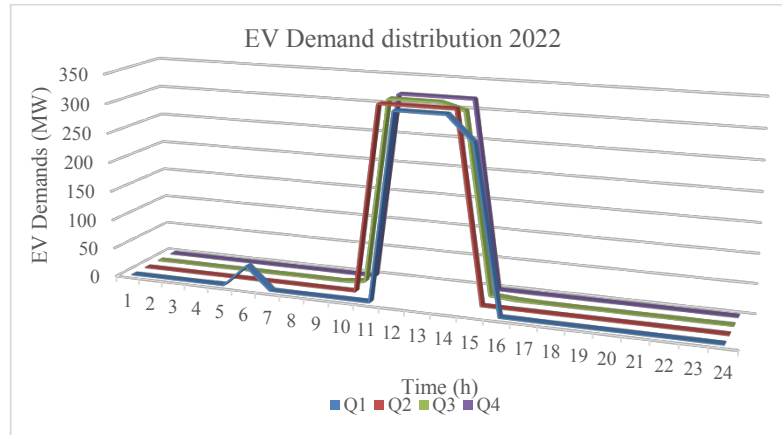


Fig. 9. EV demand distribution per quarter in 2022 for scenario 2.

Fig. 9 presents the distribution of the load of electric vehicles in the quarters of 2022. A large amount of power is concentrated in the periods of maximum renewable penetration, the same curve presented in Fig. 7. In Q1 the optimization shifted a portion of the electric vehicle demand to 6:00 am, aiming to minimize the gap between the maximum and minimum load. This behavior occurred because Q1 has the lowest minimum load due to the average winter temperature.

4 Conclusions

This paper addressed the critical challenge of determining the optimal hourly charging distribution for electric vehicles in the Dominican Republic. To achieve this goal, three distinct objective functions were formulated, each addressing a fundamental aspect of the problem: flattening the demand curve, maximizing the utilization of renewable energy in electric vehicle charging, and minimizing the associated cost.

The results indicate that for Scenario 1, optimal hours for EV charging are between 11:00 and 15:00 hours, for a total loads of 8.64 MW, which corresponds to the simultaneous demand of 2,700 EVs charging out of the total vehicle fleet of 8,000 EVs currently in the Dominican Republic. This was deemed 3.2 kW residential and public chargers. For scenario 2, was considered 100 thousand EVs charging simultaneously, which represents a load of 320 MW, and the most favorable periods remain the same as the previous scenario.

During those periods, the lowest energy costs are recorded within the SENI electrical system, which can result in substantial savings for electric vehicle users. This time interval aligns with the peak penetration of variable renewable energy in the system, contributing to the reduction of the environmental footprint associated with electric vehicle charging and promoting sustainability. This indicates the symbiotic relationship

between periods of increased renewable energy production and EV demand with affordable price signals due to a drop in the cost of energy before peak demand.

Future works are recommended to analyze a) economic impact between the dynamic price tariffs, especially the time-of-use tariff vs the dynamic pricing scheme and b) planning the new generation of variable renewable energy source taking into consideration the growing demand for EVs. Given that the nation's generation expansion plan must be aligned with the decarbonization policies of the transportation sector, this sector is key factor to enhance a truly just energy transition.

5 Acknowledgments

The authors would like to thank **Henry César Caraballo Durán** for providing the datasets for this research. Thanks to **Félix Rondón** and **IEESL** for arranging our participation in this ICSC-CITIES 2023 conference.

References

- [1] IRENA, “Electric vehicles.” Accessed: Sep. 30, 2023. [Online]. Available: <https://www.irena.org/Energy-Transition/Technology/Transportation-costs/Electric-vehicles>
- [2] H. Jia, Q. Ma, Y. Li, M. Liu, and D. Liu, “Integrating Electric Vehicles to Power Grids: A Review on Modeling, Regulation, and Market Operation,” *Energies*, vol. 16, no. 17, Art. no. 17, Jan. 2023, doi: 10.3390/en16176151.
- [3] D. Singh, U. K. Paul, and N. Pandey, “Does electric vehicle adoption (EVA) contribute to clean energy? Bibliometric insights and future research agenda,” *Clean. Responsible Consum.*, vol. 8, p. 100099, Mar. 2023, doi: 10.1016/j.clrc.2022.100099.
- [4] Lens, “Electric Vehicle - Scholar Analysis,” The Lens - Free & Open Patent and Scholarly Search. Accessed: Sep. 09, 2023. [Online]. Available: <https://www.lens.org/lens>
- [5] VOSviewer, “VOSviewer - Visualizing scientific landscapes,” VOSviewer. Accessed: Jun. 11, 2023. [Online]. Available: <https://www.vosviewer.com/>
- [6] INTRANT, “Instituto Nacional de Tránsito y Transporte Terrestre | INTRANT - INTRANT presenta Plan Estratégico Nacional de Movilidad Eléctrica RD.” Accessed: Sep. 08, 2023. [Online]. Available: <https://intrans.gob.do/index.php/noticias/item/625-intrans-presenta-plan-estrategico-nacional-de-movilidad-electrica-rd>
- [7] Congreso Nacional, “Estrategia Nacional de Desarrollo 2030.” Jan. 25, 2012. [Online]. Available: <http://economia.gob.do/mepyd/wp-content/uploads/archivos/end/marco-legal/ley-estrategia-nacional-de-desarrollo.pdf>
- [8] SIE, “Resoluciones SIE,” Superintendencia de Electricidad. Accessed: Sep. 30, 2023. [Online]. Available: <https://sie.gob.do/sobre-nosotros/marco-legal/resoluciones-sie/>
- [9] X. Tian, B. Cheng, and H. Liu, “V2G optimized power control strategy based on time-of-use electricity price and comprehensive load cost,” *Energy Rep.*, vol. 10, pp. 1467–1473, Nov. 2023, doi: 10.1016/j.egy.2023.08.017.

14

- [10] J. Zhang *et al.*, “MPC-based co-optimization of an integrated PV-EV-Hydrogen station to reduce network loss and meet EV charging demand,” *eTransportation*, vol. 15, p. 100209, Jan. 2023, doi: 10.1016/j.etrans.2022.100209.
- [11] M. Zhang, S. S. Yu, H. Yu, P. Li, W. Li, and S. M. Muyeen, “Dispatchable capacity optimization strategy for battery swapping and charging station aggregators to participate in grid operations,” *Energy Rep.*, vol. 10, pp. 734–743, Nov. 2023, doi: 10.1016/j.egy.2023.07.022.
- [12] S. Zhong, Y. Che, and S. Zhang, “Electric Vehicle Charging Load Optimization Strategy Based on Dynamic Time-of-Use Tariff,” May 2023, doi: <https://doi.org/10.21203/rs.3.rs-2916080/v1>.
- [13] S. Panda *et al.*, “A comprehensive review on demand side management and market design for renewable energy support and integration,” *Energy Rep.*, vol. 10, pp. 2228–2250, Nov. 2023, doi: 10.1016/j.egy.2023.09.049.
- [14] M. E. A. Mejía *et al.*, “Application of electric vehicles for primary frequency regulation service,” in *2021 IEEE PES Innovative Smart Grid Technologies Conference - Latin America (ISGT Latin America)*, Sep. 2021, pp. 1–5. doi: 10.1109/ISGT-LatinAmerica52371.2021.9543076.
- [15] T. Wu, H. Zhao, and X. Ou, “Vehicle Ownership Analysis Based on GDP per Capita in China: 1963–2050,” *Sustainability*, vol. 6, no. 8, Art. no. 8, Aug. 2014, doi: 10.3390/su6084877.
- [16] J. G. Wiener and T. M. Koontz, “Extent and types of small-scale wind policies in the U.S. states: Adoption and effectiveness,” *Energy Policy*, vol. 46, pp. 15–24, Jul. 2012, doi: 10.1016/j.enpol.2012.02.050.
- [17] J. Koskela, A. Rautiainen, and P. Järventausta, “Using electrical energy storage in residential buildings – Sizing of battery and photovoltaic panels based on electricity cost optimization,” *Appl. Energy*, vol. 239, pp. 1175–1189, Apr. 2019, doi: 10.1016/j.apenergy.2019.02.021.
- [18] X. Chen, C. Gao, X. Chen, Y. Lin, J. Li, and Y. Yang, “Multi-Objective Optimal Allocation Of DG-EV Charging Station Considering Space-Time Characteristics Model,” *IOP Conf. Ser. Earth Environ. Sci.*, vol. 769, no. 4, p. 042104, May 2021, doi: 10.1088/1755-1315/769/4/042104.
- [19] A. Gagangras, S. D. Manshadi, and A. Farokhi Soofi, “Zero-Carbon AC/DC Microgrid Planning by Leveraging Vehicle-to-Grid Technologies,” *Energies*, vol. 16, no. 18, Art. no. 18, Jan. 2023, doi: 10.3390/en16186446.
- [20] MEM, “Informe de Desempeño – Junio 2023,” Ministerio de Energía y Minas. Accessed: Sep. 10, 2023. [Online]. Available: <https://mem.gob.do/category/sector-electrico/informe-de-desempeno/>
- [21] MEM, “Informe de Desempeño 2022,” Ministerio de Energía y Minas. Accessed: Jan. 14, 2023. [Online]. Available: <https://mem.gob.do/category/sector-electrico/informe-de-desempeno/>
- [22] R. Karkowska and S. Urjasz, “How does the Russian-Ukrainian war change connectedness and hedging opportunities? Comparison between dirty and clean energy markets versus global stock indices,” *J. Int. Financ. Mark. Inst. Money*, vol. 85, p. 101768, Jun. 2023, doi: 10.1016/j.intfin.2023.101768.

- [23] S&P Global, "Latest Oil, Energy & Metals News, Market Data and Analysis," S&P Global Inc. Accessed: Sep. 10, 2023. [Online]. Available: <https://www.spglobal.com/commodityinsights/en>
- [24] Organismo Coordinador, "Memoria Anual 2022." Accessed: Apr. 30, 2023. [Online]. Available: <https://www.oc.do/Informes/Administrativos/Memoria-Anual>
- [25] Organismo Coordinador, "Programación Del SENI." Accessed: Sep. 10, 2023. [Online]. Available: <https://www.oc.do/Informes/Operaci%C3%B3n-del-SENI/Programaci%C3%B3n-del-SENI>
- [26] X. Liu, "Dynamic Response Characteristics of Fast Charging Station-EVs on Interaction of Multiple Vehicles," *IEEE Access*, vol. 8, pp. 42404–42421, 2020, doi: 10.1109/ACCESS.2020.2977460.
- [27] J. Wu, H. Su, J. Meng, and M. Lin, "Electric vehicle charging scheduling considering infrastructure constraints," *Energy*, vol. 278, p. 127806, Sep. 2023, doi: 10.1016/j.energy.2023.127806.
- [28] M. Tayyab, I. Hauer, and S. Helm, "Holistic approach for microgrid planning for e-mobility infrastructure under consideration of long-term uncertainty," *Sustain. Energy Grids Netw.*, vol. 34, p. 101073, Jun. 2023, doi: 10.1016/j.segan.2023.101073.
- [29] J. Y. Yong, W. S. Tan, M. Khorasany, and R. Razzaghi, "Electric vehicles destination charging: An overview of charging tariffs, business models and coordination strategies," *Renew. Sustain. Energy Rev.*, vol. 184, p. 113534, Sep. 2023, doi: 10.1016/j.rser.2023.113534.
- [30] Diario Libre, "Movilidad eléctrica en República Dominicana sigue en constante crecimiento," Diario Libre. Accessed: Nov. 06, 2023. [Online]. Available: <https://www.diariolibre.com/planeta/columnistas/2023/06/05/movilidad-electrica-en-rd-sigue-en-constante-crecimiento/2336099>

Development of a single-phase speed regulating inverter using pulse width modulation

Carmona-Valdés J. C.¹[0009-0008-8278-5193], López-Meraz R. A.²[0000-0002-3236-3709], Méndez-Ramírez C. T.², Maldonado-Martínez M.²[0009-0004-4575-1390]

¹ Universidad Nacional Autónoma de México, Av. Universidad 3004. 04510, México

² Universidad Veracruzana, Circuito Universitario Gonzalo Aguirre Beltrán s/n, 91000, México
julio.carmona0822@gmail.com: J. C-V; raullopez03@uv.mx: R.L-M.;
cmendez@uv.mx: C.M-R.; miguelmaldonadomartinez@gmail.com: M.M-M.

Abstract. Most commercial electric cars use an AC motor because of the advantages it provides over DC motors. To use an AC motor, it is necessary to convert the DC current, provided by the storage system, to an AC current to operate the motor speed and thus control the vehicle. The system that was developed consists of the implementation of a control area using analog and digital electronics, together with power electronics for the control of a 75kW motor implemented in a Formula type vehicle. To measure its efficiency, it is planned to test it in the competition organized by the Society of Automotive Engineers with the UNAM MotorSports team.

Keywords: Controller; Frequency-voltage relationship; Variable frequency sine wave.

1 Introduction

A formula type vehicle is one whose design focuses on optimum performance during high-speed track testing. For the Society of Automotive Engineers (SAE) the vehicle must have rigorously analyzed characteristics to be considered a formula type suitable for competition, all these characteristics are focused on safety and performance in both dynamic and static tests. [1]

On the other hand, a Battery-electric vehicle (BEV) is composed of two important aspects, namely: the energy system and the dynamic analysis system [2]. The latter is mainly in charge of studying how the vehicle dynamics would work when the vehicle is in motion, while the energy system oversees making the vehicle move. This last branch can be divided into 3 major components, the energy storage system, which is usually lithium batteries, the energy management and control system, and finally the mechanical propulsion system, which is a motor, usually an alternating current motor [2].

The component in charge of communicating the lithium batteries with the motor is called a controller and is essentially an inverter, i.e., a component that transforms the direct current generated by the batteries to alternating current. The controller must also

2

manage the energy as requested by the pilot and this is where the control parameters come in.

The control of a motor can be done in different ways focusing on different points, however, for vehicles is usually done in two main ways. The first is to manage the current delivered to the motor coils. The second focuses on the voltage regulation system using pulse width modulation (PWM) of an electronic controller to regulate the AC input frequency to the motor and thus control the motor speed [3][4].

Control using PWM is not only applied to mobility systems, but also in sectors where it is required to have control over certain components that alone are not controllable,

such is the case of a single-phase motor of established characteristics, but a frequency converter can modify the rotational speed of that motor accurately. A variable frequency drive performs virtually the same job as a controller in a vehicle, however, the first can be adapted to the characteristics of most commercial motors used in small industries to make it more versatile, on the other hand, a controller does not have that versatility.

Most of today's electrical controllers are designed to handle relatively low power because electrical systems have optimized the use of current which makes accumulators with systems over 400 volts practically non-existent and thus, finding a controller that fits the needs of a user is difficult. For this reason, the development of a controller that can be adapted to the needs of the end user represents a significant advantage not only for applications in the mobility sector, but also for low power converters for local power supply from a renewable DC source. The main objective of this work is to develop a controller easy to repair and build with elements available in the Mexican market, efficient and versatile to control different loads in different sectors not only in the electric mobility sector. The paper is structured in four sections. The first section, Materials, and methods, takes a look at the origin of the controller and its main objective, in addition, it presents the theoretical construction models of a PWM controller, and finally, it explains how these models are adapted. In the second section, the results obtained from the implementation of the models proposed in the methodology are presented. Next, the most important conclusions and the future work of this development are found, finally, the references used in the construction of this article are annexed.

2 Materials and methods

2.1 Case of study

The National Autonomous University of Mexico (UNAM) through the Faculty of Engineering with the UNAM Motorsports team competes in Formula SAE International where about 100 universities from around the world participate with the aim of developing, building, and designing a formula electric vehicle that meets the international engineering standards proposed by the SAE. The document specifying the design standards to be followed can be found in [1].

Considering that the controller is a fundamental part in the design of the car, two controllers, the Bamacar D3 400 400 [5] and the Sevcon Gen 5 Size [6], were taken as reference to develop one of our own that was easy to repair, low cost and fulfilled the

characteristics of the Bamocar and the Sevcon. Table 1 presents the main characteristics of the controllers taken as reference.

Table 1. Main characteristics of the controllers

Controller	Peak current [A]	Peak voltage [V]	Peak power [kW]	Cost [USD].
Bamocar D3 400 400	400	400	110	2700
Sevcon Gen 5 Size 9	400	450	180	3250

2.2 Fundamentals and principles

The principle of operation is based on the PWM theory to obtain a variable frequency sine waveform. For this type of procedure, the controller must be divided internally into two sections, the control area, and the power area. The first one oversees receiving signals from the user and interpreting them as the desired speed. On the other hand, the power area is the one that receives only the PWM signal from the control area, closing and opening different switches to allow the signal perceived by the motor to be sinusoidal.

Control area

The most important part of this area is the generation of the pulses that will activate the "switch" and for this, the theory tells us that to generate PWM pulses there are two easily implemented methods. The first method, called digital partitioning, consists of a microcontroller that monitors the input signal of the system, i.e., a pulse generation frequency that is then divided so that approximately the same level is applied in each system. The second method consists in the comparison of two signals, a sinusoidal signal, and a triangular signal whose frequency is based on Ec.1:

$$mf = Fr/Fc \quad (1)$$

Where the frequency index (mf) must be greater than 21 otherwise the harmonics present in the output signal increase in the odd periods. In addition, it is recommended that the frequency of the carrier signal (Fc) should be a multiple of the reference signal (Fr), where the carrier signal can be triangular or sawtooth type while the reference signal is the variable frequency sine wave, as shown in Fig 1.

4

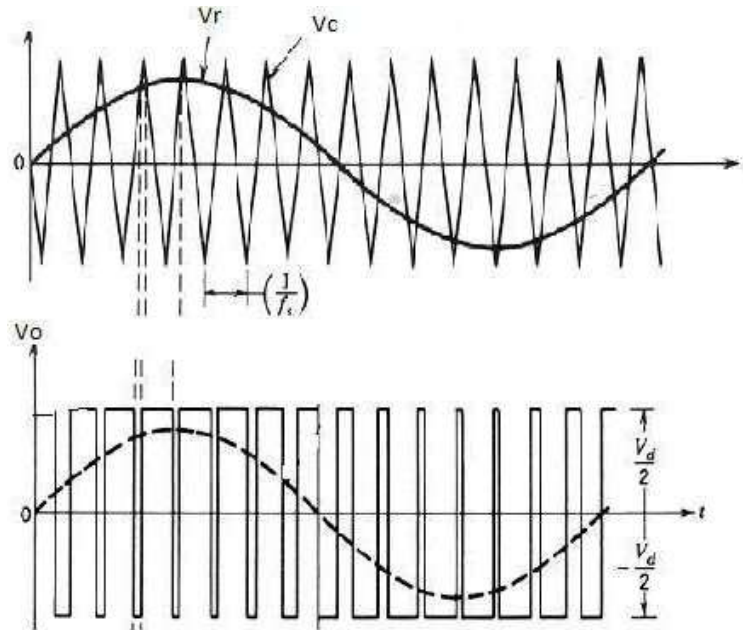


Fig. 1. Representation of signal comparison using a high-speed operational amplifier for pulse generation (a) Reference and control signals (b) Voltage V_a , PWM pulses [10].

The above principle is presented in commercial controllers, including the Bamocar, have a generator of two types of waves, one sine and one triangular. Comparing these waves, a PWM pulse signal is obtained. There is another parameter commonly used in today's controllers called the modulation index (ma). This index is given by Eq. 2.

$$ma = Ar/Ac \quad (2)$$

This index is used to modulate the amplitude of the output signal and thus avoid voltage drop when the output frequency is increased to unexpected levels, or an unpredicted load is placed on it. The index associates the amplitude of the carrier signal (Ar) and that of the reference signal (Ac) and can be considered as a unit ratio, although a higher ratio can be created to improve the output power. After generating the PWM pulses, it will be necessary feedback to indicate that the pulses we are generating are really the ones needed to modulate the speed according to the pilot's requirements [7]. Generally, to fulfill this purpose, encoder or resolver type sensors are implemented [5][7] [8].

Power zone

It consists mainly of switches that close and open the frequency of PWM pulses [10]. The model and type of this component depends on the currents that must pass through

them, some systems use TRIACs, but these are too slow and modify the waveform at the output of the component, but allow a bidirectional current flow which is, at industry level, indispensable in power systems such as these [11]. In addition to the switches, it is necessary to have a filtering stage, which makes the output signal as close as possible to the sine wave and eliminates certain frequency spectra that are not desired in systems such as these [10].

2.3 Application and development

The first step was to obtain the PWM signal. For this process, it was decided to use components that, although they were common and somewhat easy to acquire, had the necessary characteristics so that the operation of the controller would not be affected.

The comparator consists of two parts, the generation of the signals and the comparison itself. For signal generation, the ATMEGA 328P microcontroller [12] and a memory were implemented. A list of hexadecimal numbers was created and stored in a memory, and this was then sent to the analog digital converter of the ATMEGA 328P so, we can form both the sine wave and the triangular signal.

In case of wanting to regulate the frequency, it can be done with an NE555 timer [13] that makes each bit of the memory to be traversed faster, this is favorable for the design because the timer configuration must include a variable resistor that will modify the memory sampling rate, indirectly making that altering that resistor will change the frequency of the signals. That variable resistor is the one located in the accelerator pedal and its input is a Wheatstone bridge configuration. That is, for the generation of both carrier and reference signals, a position sensor representing a variable resistor connected to a Wheatstone bridge was used and its output goes to an NE555 timer to vary the sampling rate of an EEPROM memory [14] with the data to form a sine and triangular wave ranging from 0 to 255, given the capacity of the ATMEGA 358P (see Fig. 2.) Subsequently these data go to the analog digital converter of the microcontroller or to a separate one. Fig. 2 shows how a pulse called U2 (UP) enters this pulse generated from the timer and it is the one that samples the memory making the counters go through the EEPROM memory bits.

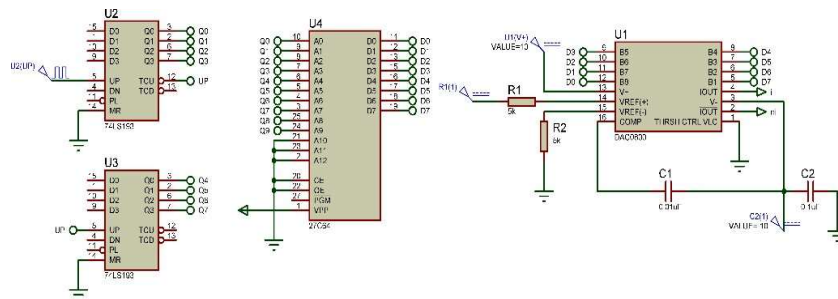


Fig. 2. Schematic diagram of the generation of both carrier and reference waves from the reading of a 27C64 EEPROM memory and a DAC digital analog converter.

6

With the reference signals and the carrier varying from 1 to 21 to maintain the modulation index, it is necessary to establish the comparator. For this component, two OPA814 [15] from Texas Instrument were used because of its high speed, being able to compare signals up to 250 MHz, and it is relatively inexpensive and easy to repair.

Regarding the operational amplifier, the comparator configuration was used, one of the amplifiers was used to compare the triangular signal with the phase 0 sine wave, the second was used to compare the triangular signal with the phase 180 sine wave. This is because the signal of the first phase 0 sine wave half cycle can be processed without any problem, but the negative half cycle cannot be processed because the amplifier is not biased with negative voltages and even if it were, the switch would have to work with both negative and positive signals. Fig. 3 shows the two working phases and what would be respectively the PWM output signal.

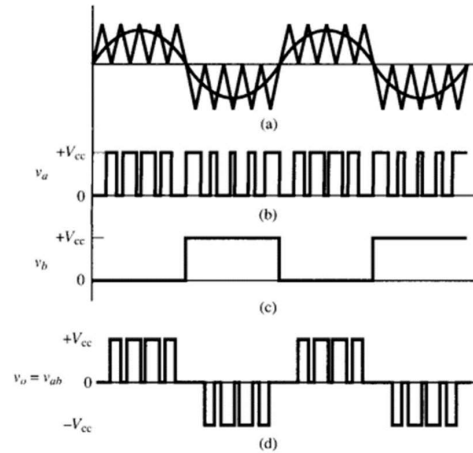


Fig. 3. PWM generation for odd and even switches from two different phases of the sine wave. (a) Positive half-cycle of phase 0 and negative half-cycle of phase 180 compared to the triangular signal. (b) Voltage V_a , initial comparison. (c) output voltage V_b , voltage of the negative half-cycle. (d) Unified PWM signal, $v_a - v_b$.

As output of the previous circuit we have two PWM signals, one that will be sent to the pair of switches 1 and 3, while the other will be sent to switches 2 and 4. In this way the opposite switches will work at the same time to allow the flow of current from one side and then from the other, achieving the same signal, but that can be processed as two different positive signals synchronized to open and close the first and second pair of switches.

On the other hand, in the power area it was necessary to choose the component that will play the role of switch in our system, it must switch at high speeds to be able to open and close at the PWM frequency, it will also carry all the current of the system.

The frequency was defined based on the principle of the operational amplifier and

7

the maximum speed of the microcontroller; however, the maximum current is defined by the Track Model. This model uses an energy equation that determines the energy needed to move an object from one speed to another, this speed change is given by our motor and for this case a transmission efficiency of 80% is considered. With the final energy needed to move the car we convert the Joules to Watts; this conversion is a function of the time obtained from the discretization of the track where it will run. Once we have Watts, we can move to current considering, for the moment, a constant voltage of 288 volts.

In the work done by UNAM Motorsports, it was concluded that the 2017 Lincoln track would use around 96 amps. This data, although it is the one used for a three-phase motor, will serve as a starting point for the requirements of our switches.

Having defined both the required maximum switching speed and the maximum current, we concluded that IGBT transistors fulfill the task better than thyristors and TRI-ACs because the speed is higher and they have an isolation of the base with the power branch, in addition, the current that can pass through them is much higher and they are easier to obtain. Specifically, it was decided to use the FGH60N60SFD model [16], due to its switching speed, current carrying capacity and its high availability in the local market. The connection between the elements mentioned above can be seen in Fig. 4.

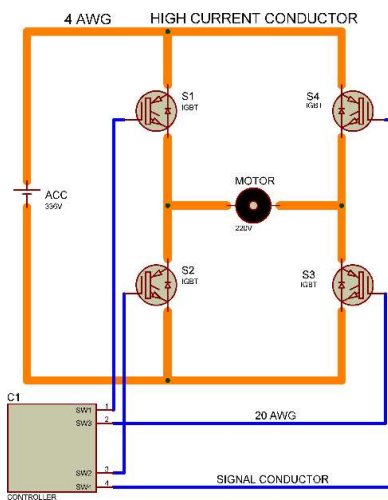


Fig. 4. Representation of the power zone with the assigned IGBTs and the connection to the motor and the 336V accumulator. The elements connected to the orange wire represent the power zone.

It is necessary that, in the power area, once the operation of the switches is arranged, it is necessary to regulate the load since, according to the operation of this type of circuits, when closing the switch a short circuit is created, this short circuit represents a current peak that if not controlled will cause that, although the IGBTs can withstand

8

these peaks, their useful life decreases drastically. Therefore, a filtering and control stage was implemented with coils that limit the current flow to a maximum saturation current of 100 Amperes. However, to choose a coil, it is necessary to know both the coil's HENRY and the saturation current. The saturation current we already have, which must be at least 96 Amperes as required by the Track model.

3 Results

The results of the implementation were measured and observed in two crucial aspects, in the control zone is the PWM generation by comparing and varying the PWM frequency. In addition, the ability of the power zone to transmit current to a $\frac{1}{2}$ horsepower motor by varying its speed was measured.

For the first part, the oscilloscope was connected to the output of the comparator and the input resistance, which simulates the accelerator of a car, was varied. The result obtained was the one shown in Fig. 5, which represents the PWM generated in a positive cycle, while the negative cycles are mitigated because the amplifier is not able to reproduce negative voltages.



Fig. 5. The carrier signal is shown together with the pulse train generated from it.

Blue shows the carrier signal which has an offset of 5 volts to reflect both the input and output signals in the PWM. The discretization of each of the cycles at a frequency of 60 Hz output to the motor is 10 pulses, this is because an ATMEGA was used for

testing. This number of pulses is not enough to generate a sufficiently refined waveform, but the error can be corrected with a more powerful microprocessor, although the 60 Hz frequency is sufficient for a nominal speed of 1500 rpm.

In the power zone, the results shown in Table 2 were obtained. Where an average of the results that follow a pattern of voltage increase is shown.

Table 2. Voltage, speed, and frequency at motor output.

V [V]	N [rpm]	F [Hz]
50	397.08	13.236
100	809.08	26.969
150	1205.8	40.193
200	1612.5	53.75
220	1734	57.8
240	1796.4	59.88

Fig. 6 shows the relation of increase in the output frequency with respect to the voltage, this increase is reflected thanks to our approximation that the voltage should follow a linear relation to the variation of the frequency. This relationship is given by a factor m , until the voltage and frequency approach the parameters established as nominal in the motor data sheet, i.e., 60 Hz and 220 V.

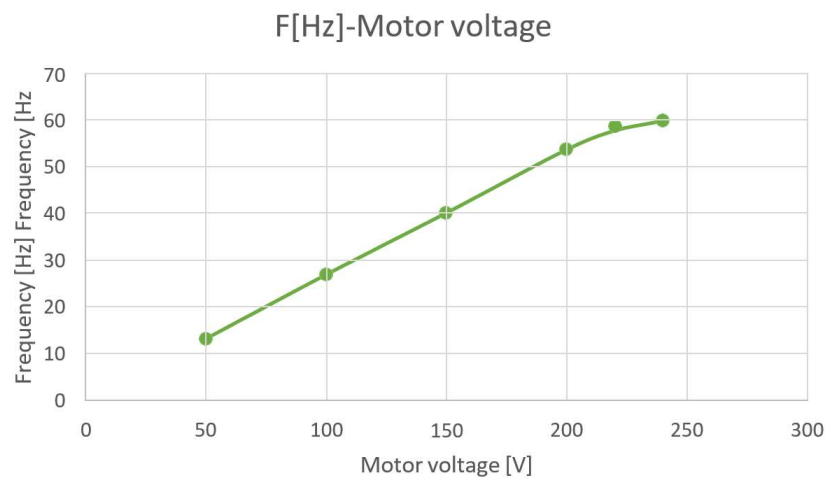


Fig. 6. Relationship between sine wave frequency and motor voltage

To qualify the performance of the Wheatstone bridge implementation, voltage measurements were taken at the output of the potentiometer used as an accelerator, these measurements had to be invariant over time, that is, if the potentiometer was fixed at a voltage of 5 volts, during the entire test time this voltage should not vary.

10

As we can see in Fig. 7 the implementation of the Wheatstone bridge reduces the voltage variations in a time of 10 minutes, however, at the beginning of the operation there is a voltage rise probably caused by the proximity of the power zone or by the settling time of our PID control, but if we analyze the variation is very little.

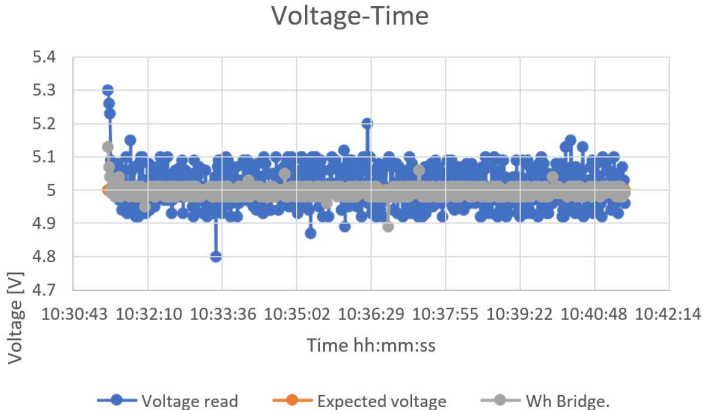


Fig. 7. Samples of the voltage variation measured in the Wheatstone bridge implementation compared to the potentiometer implementation alone.

Another of the characteristics to be evaluated to determine if the Wheatstone bridge was successful is the analysis of the relationship between the increase in voltage at the output of the bridge and the increase in motor speed.

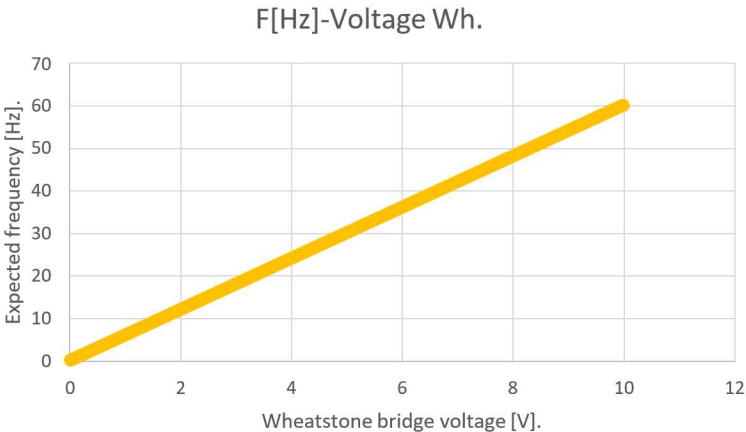


Fig. 8. Linear relationship between frequency increase and Wheatstone bridge voltage increase.

In figure 8, by increasing the bridge voltage the frequency of the sine wave also increases linearly, this means that we are efficiently controlling the closing of the IGBT, in this way, we can see figure 9 and relate that by increasing the frequency of the sine wave increases linearly the motor speed to exceed the rated rpm.

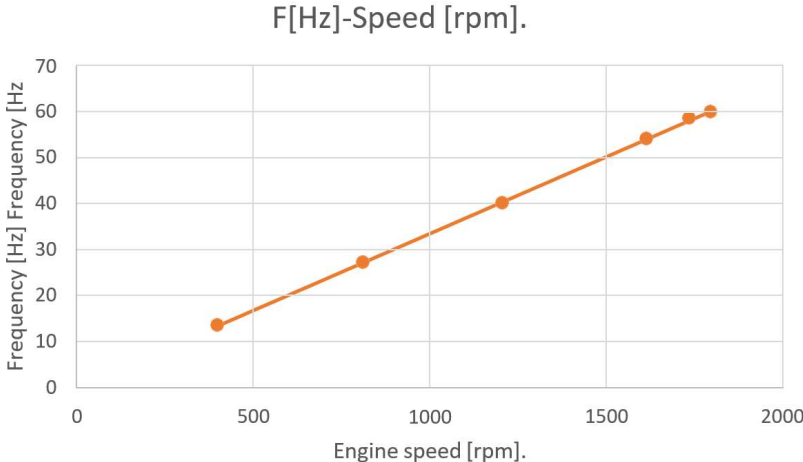


Fig. 9. Linear relationship between sine wave frequency and motor speed.

4 Conclusions

The single-phase controller complies with the ratio of frequency variation and output voltage, thus maintaining a stable motor rpm at the load established at the initial moment, however, when increasing the load this behavior starts to be oscillatory which is not desirable in a controller for vehicles where dynamic loads vary. In addition, this controller does not consider the reversible load, i.e., the implementation of a regenerative brake in this controller is impossible because the elements within it are unidirectional and an analysis of this type of energy regeneration was not considered in principle.

As a future project, we have the implementation of this system with 120° phase lags to achieve the control of a three-phase motor. In addition, it is necessary to analyze the harmonics generated in the output sinusoidal signal to ensure that the adjustment made in the frequency index was sufficient to eliminate most of them.

5 Acknowledgments

We would like to thank the UNAM MotorSports team for providing information for this article.

12

References

1. "Series Resources. FSAEOnline.com. Accessed September 27, 2023. [Online]. Available: <https://www.fsaeonline.com/cdswweb/gen/DownloadDocument.aspx?DocumentID=369d01c0-589d-4ebe-b8d4-b07544f4a52b>.
2. N. Patel, A. K. Bhoi, S. Padmanaban, and J. B. Holm-Nielsen, Eds, *Electric Vehicles*. Singapore: Springer Singap., 2021. Accessed September 27, 2023. [Online]. Disponible: <https://doi.org/10.1007/978-981-15-9251-5>.
3. "UniTek Industrie Elektronik GmbH - Download". UniTek Industrie Elektronik GmbH - Unitek. Accessed September 27, 2023. [Online]. Available: <https://www.unitek-industrie-elektronik.de/download>.
4. P. BRANDSTETTER. "Speed and Current Control of Permanent Magnet Synchronous Motor Drive Using IMC Controllers". ResearchGate. Accessed September 26, 2023. [Online]. Available: https://www.researchgate.net/publication/274756580_Speed_and_Current_Contr_ol_of_Permanent_Magnet_Synchronous_Motor_Drive_Using_IMC_Controllers/fulltext/607a1f862fb9097c0ceca9aa/Speed-and-Current-Control-of-Permanent-Magnet-Synchronous-Motor-Drive-Using-IMC-Controllers.pdf?_tp=eyJjb250ZXh0ljp7ImZpcnN0UGFnZSI6InB1YmxxpY2F0aW9uInI9.
5. Unitek. "MANUAL Digital Battery-Motor-Controller BAMOCAR-D3 for EC Servo Motors AC Induction Motors DC-Servo Motors". Unitek. Drivers made in Germany. Accessed September 26, 2023. [Online]. Available: <https://www.unitek-industrie-elektronik.de/download>.
6. BorgWarnet. "AC Motor Controller Gen5 Size 9 Reference Manual". Sevcon Motor Controllers. Accessed September 26, 2023. [Online]. Available: https://www.thunderstruck-ev.com/images/companies/1/Controllers/Gen5S9_reference_manual_2018.pdf?1677192750890.
7. F. Giri, *AC Electric Motors Control: Advanced Design Techniques and Applications*. John Wiley & Sons, 2013.
8. K. H. Nam, *AC motor control and electrical vehicle applications*. CRC Press, 2018.
9. A. Ghaderi, T. Umeno, and M. Sugai, "An altered PWM scheme for Single-Mode seamless control of AC traction motors for electric drive vehicles," *IEEE Transactions on Industrial Electronics*, vol. 63, no. 3, pp. 1385-1394, Mar. 2016, doi: 10.1109/tie.2015.2498901.
10. S. B. Dewan and A. Straughen, *Power semiconductor circuits*. Wiley-Interscience, 1975.
11. Emadi, Y. J. Lee, and K. Rajashekara, "Power Electronics and motor drives in electric, hybrid Electric, and Plug-In Hybrid electric vehicles," *IEEE Transactions on Industrial Electronics*, vol. 55, no. 6, pp. 2237-2245, Jun. 2008, doi: 10.1109/tie.2008.922768.
12. megaAVR® Data Sheet (2020). Microship. <https://ww1.microchip.com/downloads/en/DeviceDoc/ATmega48A-PA-88A-PA-168A-PA-328-P-DS-DS40002061B.pdf>
13. xx555 PrecisionTimers. (2014). TEXAS INSTRUMENTS. https://www.ti.com/lit/ds/symlink/se555m.pdf?HQS=dis-mous-null-mousermode-dsf-pf-null-ww&ts=1695998872182&ref_url=https%3A%2F%2Fwww.mouser.ch%2F.
14. AM27C64 CMOS EPROM (1998). AG Electronics. <https://agelectronica.lat/pdfs/textos/A/AM27C642.PDF>.
15. OPA814 600-MHz, High-Precision, Unity-Gain Stable, FET-Input Operational Amplifier (2023). TEXAS INSTRUMENTS. <https://www.ti.com/lit/ds/symlink/opa814.pdf?HQS=dis-mous-null-mousermode-dsf->

13

pfnuwwe&ts=1696011919807&ref_url=https%3A%2F%2Fwww.mouser.m
x%2F.

16. 16. IGBT - Field Stop (2020, January).MOUSER ELECTRONICS.
https://www.mouser.mx/datasheet/2/308/1/FGH60N60SMD_D-2313587.pdf.

Smart Public Services

Síntesis novedosa de alginato de sodio, celulosa y nanocelulosa para la valorización de la biomasa de sargazo

Adriana Cervantes¹, U. León-Silva¹, M.E. Nicho¹, J. Jesús Escobedo-Alatorre¹ y Carlos F. Castro-Guerrero²

¹ Centro de Investigación en Ingeniería y Ciencias Aplicadas, Universidad Autónoma del Estado de Morelos, Av. Universidad 1001, Col. Chamilpa, Cuernavaca, Morelos

² CONACyT-Tecnológico Nacional de México, campus Ciudad Madero, Parque Industrial Tecnia, Bahía de Aldair S/N, 89603, Altamira, México
ulises.leon@uaem.mx

Resumen Se describe la síntesis de alginato de sodio, celulosa y nanocelulosa utilizando sargazo recolectado en las playas del Caribe Mexicano. El alginato de sodio se preparó mediante dos procesos diferentes, con rendimientos del 20% y 39%, respectivamente. Las estructuras químicas de los productos obtenidos se investigaron por espectroscopia infrarroja (FTIR) y se compararon con sus respectivas muestras comerciales. El material obtenido del primer proceso mostró un espectro de FTIR muy similar a la muestra comercial, confirmando su naturaleza como alginato de sodio. Sin embargo, el alginato del segundo proceso mostró variaciones respecto a la muestra comercial que pueden ser atribuidas a la sustitución de los grupos funcionales o tratarse de un polisacárido con diferente concentración. Los rendimientos de la celulosa y nanocelulosa obtenidas fueron del 13 y 37%, respectivamente. Los espectros IR mostraron bandas de absorción muy similares a las muestras comerciales, indicando su naturaleza como celulosa y nanocelulosa.

Palabras Clave: Alginato, Sargazo, Celulosa, Nanocelulosa, Biomasa.

1 Introducción

Desde finales de 2014, los frecuentes y masivos varamientos de sargazo en la costa del Caribe mexicano han provocado graves impactos ecológicos y económicos, así como problemas relacionados con la salud. En México los costos de limpieza de sargazo van desde 0.3 a 1.1 millones de dólares por kilómetro, mientras que la cantidad recolectada anualmente oscila entre 10.105 y 40.935 m³ por kilómetro. [1]

Por otra parte, los esfuerzos para evitar la llegada del sargazo a la costa han sido insuficientes y las malas prácticas de limpieza han derivado en la acumulación de sargazo que provoca la erosión de las playas, afectando también el proceso de desove de las tortugas marinas y poniendo en riesgo el acuífero que representa la única fuente de agua dulce a nivel local [2].

2

Existen diferentes compuestos químicos y elementos inorgánicos presentes en el sargazo, por lo tanto, la valorización de la biomasa de sargazo representa la opción más adecuada para aprovechar económicamente este recurso que, de lo contrario, se convertiría en un desperdicio [3]. Una forma de aprovechar la biomasa del sargazo es mediante la extracción de alginato de sodio [4]. El alginato de sodios es un biopolímero económico, no tóxico, hidrofílico, biocompatible y biodegradable, que debido a sus propiedades reológicas ha sido ampliamente utilizado como agente gelificante, espesante y estabilizador en las industrias biomédica, cosmética, textil, farmacéutica y alimentaria [5][6].

Sin embargo, es importante señalar que, a nivel industrial los procesos de extracción de algas producen una enorme cantidad de residuos. Por esto, la comunidad científica ha investigado el aprovechamiento de estos residuos para aislar nanocelulosa. En los últimos años, el interés en la celulosa de tamaño nanométrico ha aumentado con el desarrollo de la nanotecnología en el sector industrial debido a que es un material renovable con buenas propiedades mecánicas, bajo costo de producción y amigable con el medio ambiente, tanto que han surgido diversos campos de aplicación como en ingeniería biomédica, tratamientos de aguas residuales, el sector energético y electrónico, así como en el empaque de alimentos o aditivos poliméricos. [7]

El objetivo de este trabajo fue desarrollar una metodología para la extracción de alginato de sodio, celulosa y nanocelulosa a partir del aprovechamiento de la biomasa del sargazo proveniente de las playas de Cancún. Los espectros de FTIR mostraron que se obtuvieron los materiales que se requería sintetizar.

2 Experimental

El sargazo (Fig. 1.) se recolectó de las playas del Caribe Mexicano. La biomasa se lavó y limpió manualmente con abundante agua de grifo para la eliminación de residuos (arena, plásticos, etc.), enseguida se secó a temperatura ambiente y luego se secó a 45°C por 24 h para eliminar la humedad residual (Fig. 2.). El sargazo limpio y seco se guardó herméticamente bajo refrigeración (aprox. 5°C).

La síntesis de alginato de sodio se realizó mediante dos procesos distintos utilizando el sargazo previamente acondicionado.

2.1 Proceso 1

Para el primer proceso, se utilizaron 10 g del sargazo previamente acondicionado y se trató con furaldehído al 2% a temperatura ambiente para eliminar los componentes resinosos solubles. Posteriormente, el sólido obtenido se sometió a un tratamiento con ácido clorhídrico (HCl) 0.1N a temperatura ambiente, seguido de un ajuste a pH neutro con agua destilada y filtración para separar el sólido.



Fig. 1. Sargazo seco recolectado de las playas del Caribe Mexicano.



Fig. 2. Izquierda: limpieza del sargazo con abundante agua, centro: secado a temperatura ambiente y derecha: sargazo triturado después de secar en horno a 45°C por 24 horas.

El sólido se trató con carbonato de sodio al 2% a 60 °C para extraer el alginato de sodio, el cual se separó del material sólido por filtración. Finalmente, el alginato de sodio en solución se precipitó en etanol, las fibras obtenidas de alginato de sodio se muestran en la Fig. 3.

2.2 Proceso 2

Para el segundo proceso, se utilizó una muestra de 10 g de sargazo y se trató con 500 mL de hipoclorito de sodio (NaClO) a temperatura ambiente para blanquear y extraer la lignina presente. Después el sólido se filtró y lavó con agua de grifo para eliminar el cloro residual. El sólido blanqueado se sometió a un tratamiento con 350 mL de HCl

4

0.1 N en condiciones ambientales por 16 h para formar el ácido algínico. Luego, la solución se filtró y el sólido se lavó con agua destilada hasta alcanzar un pH neutro. Para formar el alginato de sodio, el sólido obtenido se trató con 350 mL de carbonato de sodio al 2% por 3 h a 60 °C. Después, se filtró para obtener el alginato de sodio en solución. Luego, el alginato en solución se precipitó sobre etanol, se filtró y secó en horno a 45 °C por 2 h. El alginato de sodio obtenido se muestra en la figura 3. Los procesos de síntesis 1 y 2 de alginato de sodio se muestran en el diagrama de bloques de la Fig. 4.

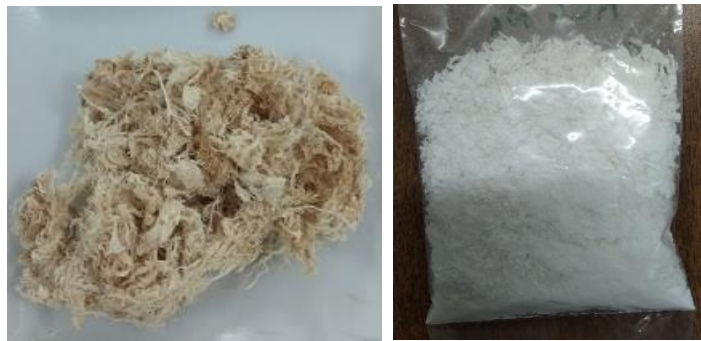


Fig. 3. Izquierda: fibras de alginato de sodio obtenidas mediante el proceso 1. Derecha: alginato de sodio blanqueado obtenido mediante el proceso 2.

Para la síntesis de celulosa, se utilizaron 10 g de sargazo y se blanqueó con 500 mL de NaClO a temperatura ambiente por 3 h. Después, el sólido se filtró y se lavó con agua destilada para eliminar el Cl residual. El sólido obtenido se trató con 750 mL de hidróxido de sodio (NaOH) 0.5 N a 80 °C por 3 h para eliminar la lignina por completo (este proceso se realizó dos veces). El sólido se filtró y lavo con agua destilada hasta llegar a pH neutro. Enseguida, el sólido obtenido se trató con 250 mL de HCl 0.05N a temperatura ambiente por 24 h para eliminar la hemicelulosa. El sólido se filtró y lavó con agua destilada hasta alcanzar un pH neutro y se colocó en una charola de teflón para secar en horno a 40 °C por 2 h. El proceso se describe en el diagrama de bloques de la Fig. 5.

Para la síntesis de nanocelulosa, se utilizaron 3.5 g de celulosa extraída del sargazo y se trataron con 60 mL de ácido sulfúrico al 64% a 45°C por 45 minutos. Al término de la reacción, el producto se vertió sobre 1.5 L de agua destilada fría y se mantuvo en reposo por 2 h para posteriormente separar las fases por decantación (esta operación se realizó dos veces). Para neutralizar la nanocelulosa en solución, se realizó un proceso de diálisis. Después del proceso de diálisis, la solución se sometió a ultrasonido de alta potencia de 750 W hasta obtener una solución coloidal evitando el sobrecalentamiento.

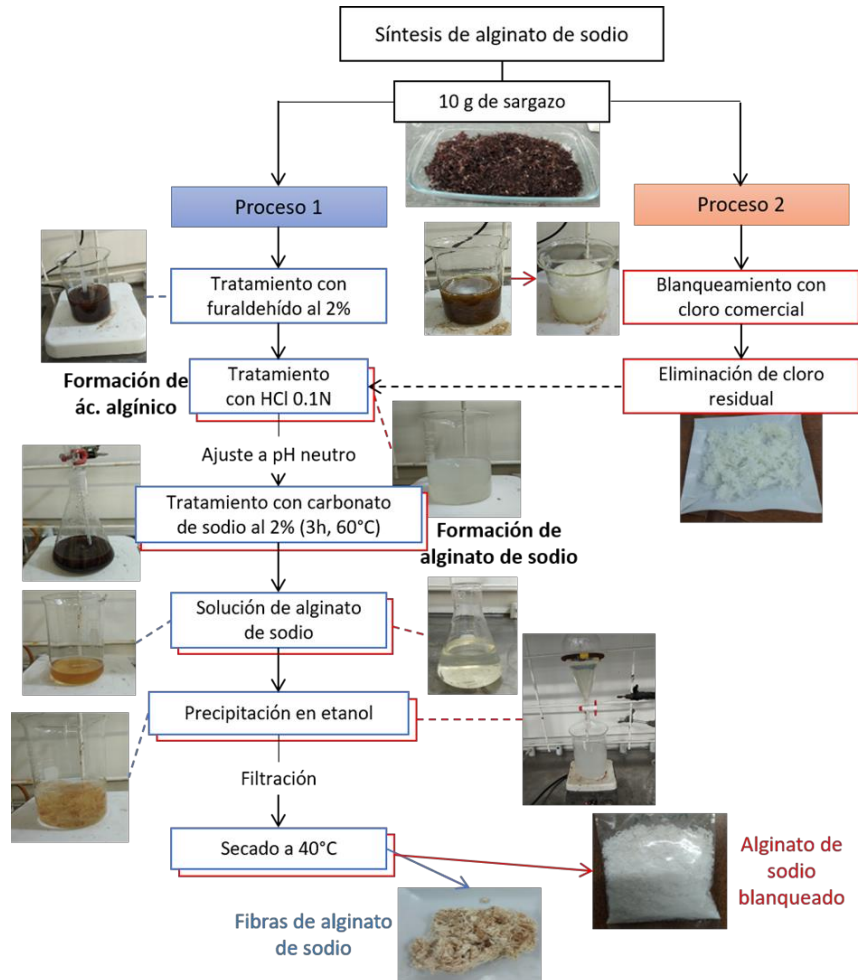


Fig. 4. Diagrama de síntesis de alginato de sodio mediante dos procesos diferentes a partir de la biomasa de sargazo.

Posteriormente, la solución se filtró con vacío a través de una membrana de microfibras de vidrio. Se obtuvieron 280 mL de nanocelulosa en solución. Se colocó una alícuota de 50 mL de nanocelulosa en solución sobre una charola de teflón para secar en un horno de convección mecánica a 40°C por 24 h. El peso de la nanocelulosa seca fue de 0.3046 g (es decir, 1.9073 g de nanocelulosa disuelta en 280 mL de solución coloidal).

6

En la Fig. 6, se muestra un diagrama de bloques con el proceso de síntesis de la nanocelulosa

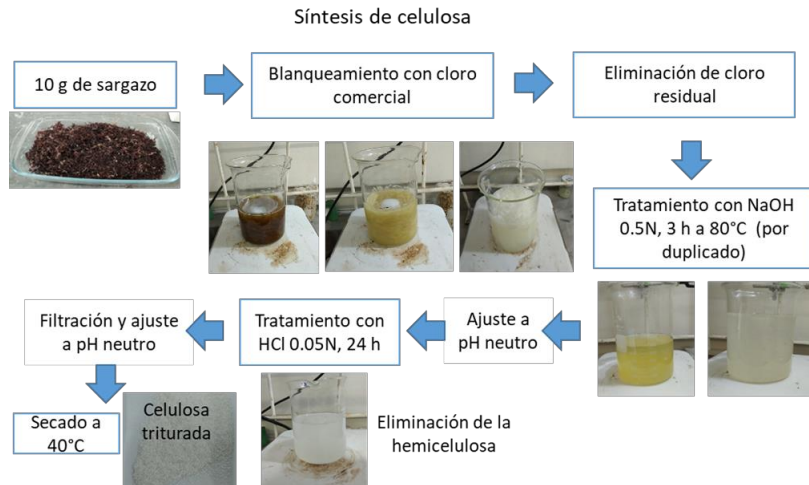


Fig. 5. Diagrama de bloques de la síntesis de celulosa a partir de la biomasa de sargazo.



Fig. 6. Diagrama de bloques de la síntesis de nanocelulosa a partir de la biomasa de sargazo.

3 Resultados y discusión

Los materiales obtenidos se caracterizaron mediante espectroscopia infrarroja, utilizando un equipo FTIR Equinox 55 marca Bruker en el rango de 4000-400 cm^{-1} . Los resultados se compararon con muestras comerciales de alginato de sodio, celulosa y nanocelulosa.

En las Fig. 7 y 8, se muestran los espectros de FTIR para el alginato obtenido de los procesos 1 y 2. De acuerdo con Yerald Ore B. et al., 2020 [8] las bandas características del alginato de sodio se encuentra en aproximadamente en 3250 cm^{-1} , 2940 cm^{-1} , 1600 cm^{-1} , 1410 cm^{-1} y 1020 cm^{-1} . En ambas muestras se observa la banda alrededor de 3250 cm^{-1} asignada a la vibración del estiramiento O-H. Sin embargo, una banda de menor intensidad en 2924 cm^{-1} atribuida a la vibración del estiramiento C-H es observable en el alginato 1, pero no en el alginato 2. La banda en 1593 cm^{-1} corresponde a la vibración antisimétrica del grupo carboxilato, la cual se puede observar en el alginato 1, mientras que en el alginato 2 se observa en menor intensidad y ligeramente desplazada hacia un mayor número de onda. La señal a 1406 cm^{-1} correspondiente a la vibración simétrica del grupo carboxilato es observable en ambas muestras, pero en el alginato 2 se ve ligeramente desplazada hacia un menor número de onda. Mientras que, la banda a aproximadamente 1025 cm^{-1} asociada a la vibración del estiramiento C-O-C, se observa solo en el alginato 1.

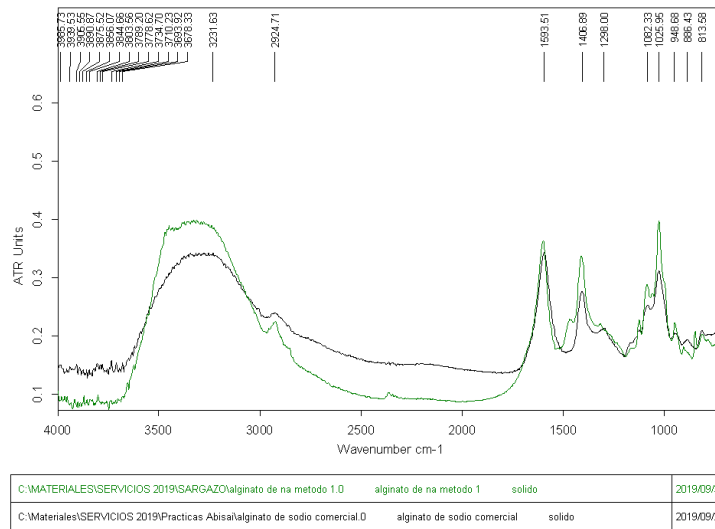
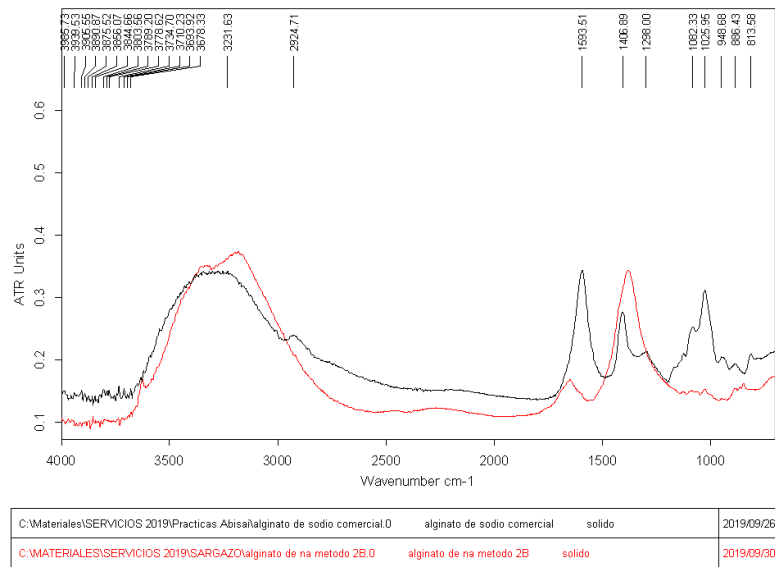


Fig. 7. Espectros IR de alginato de sodio obtenido por proceso 1 (color verde) y alginato comercial (color negro).

8



Page 1/1

Fig. 8. Espectro IR de alginato de sodio obtenido por proceso 2 (color rojo) y alginato de sodio comercial (color negro).

En las Fig. 9 y 10, se muestra los espectros FTIR de la celulosa y nanocelulosa extraída del sargazo (espectro en color azul) y la muestra comercial de nanocelulosa (color rojo). En todos los espectros se observa una fuerte banda entre aproximadamente 3340 cm^{-1} y 3282 cm^{-1} atribuida a la vibración del estiramiento OH y NH (proteína) y las bandas de menor intensidad a 2918 cm^{-1} y 2850 cm^{-1} correspondientes con las vibraciones de los estiramientos C-H de los grupos funcionales metilo y metileno, respectivamente. Aproximadamente en 1735 cm^{-1} y 1638 cm^{-1} se observan dos señales que están asociadas a los grupos carboxilato debido al C=O y N-H de las proteínas. Estas señales son más intensas en la celulosa y nanocelulosa extraída del sargazo y corresponde con lo reportado por Chávez-Guerrero L. et al., 2021[9]. Ambos espectros muestran las bandas ubicadas aproximadamente en 1052 cm^{-1} y 1159 cm^{-1} se atribuyen al modo de estiramiento y flexión asimétrico C-O-C. [9]

En la Fig. 11 se muestra los termogramas de las muestras de alginato de sodio extraída de la biomasa del sargazo (color azul) y de la muestra comercial (color rojo). Se puede observar que las muestras exhibieron un comportamiento térmico similar. Conforme incrementa la temperatura se puede observar un decaimiento rápido debido a la pérdida de peso en ambas muestras. A 200 °C pierden un 20% de su peso inicial, pérdida asociada probablemente a la eliminación de humedad.

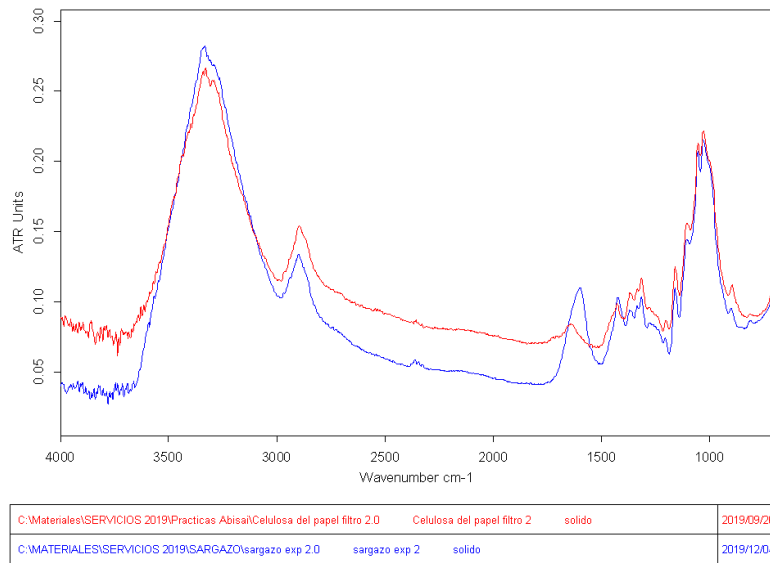


Fig. 9. Espectros IR de la celulosa extraída del sargazo (color azul) y de la muestra comercial (color rojo).

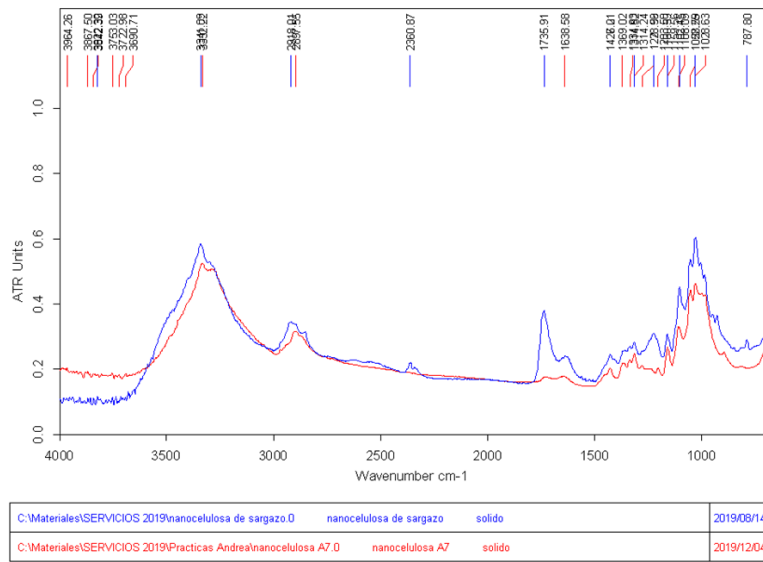


Fig. 10. Espectros IR de la nanocelulosa extraída del sargazo (color azul) y de la muestra comercial (color rojo).

10

Aproximadamente a 250 °C se registra la mayor pérdida en peso asociada a la descomposición del biopolímero. A medida que la temperatura continúa aumentando es notable que la muestra que registra mayor pérdida de peso es la muestra de alginato comercial. Cuando la temperatura se aproxima a 800 °C la muestra comercial ha perdido el 80% de su peso inicial, el 20% restante son residuos carbonosos y cenizas, mientras que, el alginato extraído del sargazo perdió el 65% de su peso.

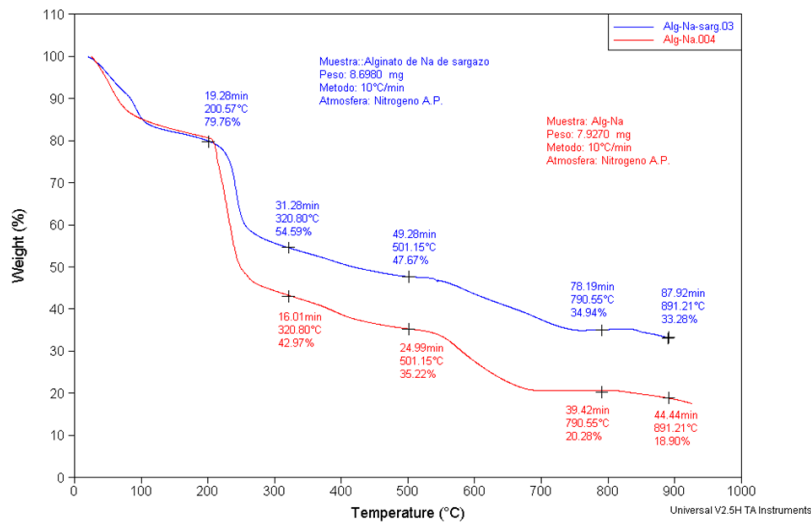


Fig. 11. Termogramas del alginato de sodio extraído del sargazo (color azul) y muestra comercial de alginato de sodio (color rojo).

4 Conclusiones y trabajo futuro

En este estudio, se logró sintetizar alginato de sodio, celulosa y nanocelulosa a partir del sargazo recolectado de las costas del Caribe Mexicano. Los rendimientos del alginato de sodio fueron del 20% y 39% para cada uno de los procesos realizados y los rendimientos de la celulosa y nanocelulosa fueron del 13% y 37% respectivamente. La naturaleza de los productos obtenidos fue corroborada mediante espectroscopia infrarroja (FTIR). El alginato obtenido del primer proceso mostró mayor similitud a la muestra comercial que el obtenido mediante el segundo proceso. Los termogramas revelaron una mayor pérdida de peso en la muestra comercial (mayor degradación) que en la muestra de alginato sintetizado a partir de sargazo. Los resultados demuestran que la

valorización del sargazo tiene gran potencial como fuente de materias primas para el desarrollo de diversas tecnologías aplicadas a la industria alimentaria y cosmética, y almacenamiento energético, específicamente en la fabricación de membranas para supercapacitores.

Los materiales obtenidos tienen un gran potencial en las tecnologías mencionadas anteriormente. Sin embargo, es necesario realizar más estudios para comprobar su aplicación en la fabricación de membranas para supercapacitores. Así mismo, utilizar los materiales obtenidos en cosméticos y alimentos. Por último, hay trabajo por hacer en relación con la optimización de los procesos presentados.

References

- [1] R. E. Rodríguez-Martínez, E. G. Torres-Conde, and E. Jordán-Dahlgren, "Pelagic Sargassum cleanup cost in Mexico," *Ocean Coast. Manag.*, vol. 237, no. 106542, 2023, doi: <https://doi.org/10.1016/j.ocecoaman.2023.106542>.
- [2] V. Chávez *et al.*, "Massive influx of pelagic sargassum spp. On the coasts of the mexican caribbean 2014–2020: Challenges and opportunities," *Water (Switzerland)*, vol. 12, no. 10, pp. 1–24, 2020, doi: 10.3390/w12102908.
- [3] K. Bilba, C. Onésippe Potiron, and M. A. Arsène, "Invasive biomass algae valorization: Assessment of the viability of Sargassum seaweed as pozzolanic material," *J. Environ. Manage.*, vol. 342, no. May, 2023, doi: 10.1016/j.jenvman.2023.118056.
- [4] A. Mohammed, A. Rivers, D. C. Stuckey, and K. Ward, "Alginate extraction from Sargassum seaweed in the Caribbean region: Optimization using response surface methodology," *Carbohydr. Polym.*, vol. 245, p. 116419, 2020, doi: 10.1016/j.carbpol.2020.116419.
- [5] A. Ahmad *et al.*, "A critical review on the synthesis of natural sodium alginate based composite materials: An innovative biological polymer for biomedical delivery applications," *Processes*, vol. 9, no. 1, pp. 1–27, 2021, doi: 10.3390/pr9010137.
- [6] A. Mohammed *et al.*, "Multistage extraction and purification of waste Sargassum natans to produce sodium alginate: An optimization approach," *Carbohydr. Polym.*, vol. 198, pp. 109–118, 2018, doi: 10.1016/j.carbpol.2018.06.067.
- [7] H. Doh, M. H. Lee, and W. S. Whiteside, "Physicochemical characteristics of cellulose nanocrystals isolated from seaweed biomass," *Food Hydrocoll.*, vol. 102, 2020, doi: 10.1016/j.foodhyd.2019.105542.
- [8] Y. Ore B., E. R. Pichilingue L., and A. C. Valderrama Negrón, "EXTRACCIÓN Y CARACTERIZACIÓN DEL ALGINATO DE SODIO DE LA MACROALGA *Macrocystis pyrifera*," *Rev. la Soc. Química del Perú*, vol. 86, no. 3, pp. 276–287, 2020, doi: 10.37761/rsqp.v86i3.300.
- [9] L. Chávez-Guerrero, A. Toxqui-Terán, and O. Pérez-Camacho, "One-pot isolation of nanocellulose using pelagic Sargassum spp. from the Caribbean

12

coastline,” *J. Appl. Phycol.*, vol. 34, no. 1, pp. 637–645, 2022, doi:
10.1007/s10811-021-02643-5.

The design of HERMÓPOLIS.

An architectonic, artistic, technological, entertainment, health and social Smart Cities platform oriented to improve the quality of life of the elder people

Victor Manuel Padrón Nápoles¹[0000-0002-9207-9320], José Luis Esteban Penelas¹[0000-0002-6073-1847], Esther Pizarro Juanas¹[0000-0003-2261-3951], Juan Diego López Arquillo²[0000-0003-1205-5722], Esther Delgado Pérez¹[0000-0002-9207-9320], Alberto Bellido¹[0000-0002-9207-9320], Rafael Muñoz Gil¹[0000-0003-4091-8265], Olalla García Pérez¹[0000-0003-1567-4879], Patricio Martínez García¹[0000-0001-8877-9415], Ignacio Loscertales¹[0009-0006-1678-8009], Silvia Álvarez Menéndez¹[0009-0007-3948-3790], Mariana Bernice Arteaga Orozco¹[0009-0006-9063-6556]

¹Universidad Europea de Madrid, c/ Tajo s/n, Villaviciosa de Odón, Madrid, Spain

²Universidad Europea de Canarias, c/ Inocencio Garcia 1, La Orotava, Tenerife, Spain

victor.padron@universidadeuropea.es, jluis.esteban@universidadeuropea.es, ESTHER.PIZARRO@universidadeuropea.es, juandiego.lopez@universidadeuropea.es, ESTHER.DELGADO@universidadeuropea.es, ALBERTO.BELLIDO@universidadeuropea.es, RAFAEL.MUNOZ@universidadeuropea.es, olalla.garpe@gmail.com, patricio241295@gmail.com, loscertales.ignacio@gmail.com, alvarezmenendezsilvia@gmail.com, la_saule@hotmail.com

Abstract. As technology advances, so do Smart Cities, which should imply an inclusion component. One of the groups with the greatest tendency to exclusion in today's society is the elderly, a group that will also grow significantly in the coming years. By uniting the two previous ideas, Extended IP-Spaces were born. These interactive spaces within the framework of Smart Cities seek to entertain and improve the physical, cognitive and communication skills of the elderly through technology. This paper describes the initial design of HERMÓPOLIS, an architectonic, artistic, technological, entertainment, health and social Smart Cities platform oriented to improve the quality of life of the elder people.

Keywords: Smart Cities, quality of life of the elderly, Extended IP-Spaces.

1 Introduction

Smart Cities technology can contribute to alleviating one of the most important problems of developed societies, the need to improve the quality of life and health of an increasingly aging sector of the population. This can be very beneficial both for these people with an increasingly extended expectancy and for reducing the emotional and economic effort of the entire society, helping to change the focus from caring for people

2

with increasingly deteriorating health to assisting them live more actively, preserving their health.

This paper describes the first steps in the design process of HERMÓPOLIS a Smart Cities platform for improving the quality of life of the elderly using the Extended Interconnected Public Space concept.

The next section reviews the needs of the elderly population and the state-of-the-art of smart furniture. Then, the design of the platform and its current state are described. Finally, discussions and conclusions are presented.

2 Related Work and Background

Population aging is the most common scenario in developed countries, according to the World Health Organization. There are currently 703 million people over the age of 65 in the world, a figure that will double to 1,500 million in the year 2050, thus reaching 16% of the world population [1]. Particularly, in Spain, the actual and forecasted aging of the population is shown in Figure 1. It is estimated that the population of 65 or more years will be 26% of the total population by 2037 [2].

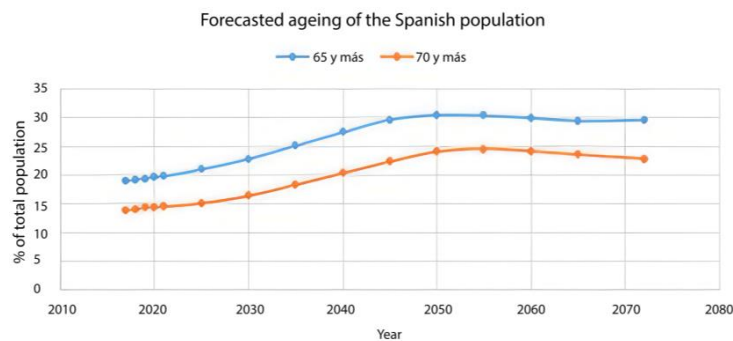


Fig. 1. Evolution and forecast of the aged population rate in Spain [2].

Although the longer life expectancy is a proven fact [2], there is a need to maintain the quality of those years gained. The largest expense of social benefits in Spain and in the European Union is dedicated to retirement benefits and national health systems (around 35% - 40% of the total)[3], so a good economic measure to make a rational use of these expenses would be to invest in innovative policies aimed at improving the life of this section of the population. This is in line with Spanish government policy of “Active aging and fighting against the dependency” that is being fostered by regional and local governments. Furthermore, In Spain, 70% of national wealth belongs to people over 55 years old, while those over 65 years old have 48% of the country’s wealth [4]. Similarly, in the United States, 70% of national income comes from people over 55 years of age, while in France it is estimated that by 2030, those over 65 years of age

will be responsible for 49% of the increase in consumption in the country [5]. Therefore, it is essential to promote the health of this age group, not only for ethical reasons, but also for them can continue to participate actively in society, both economically and socially.

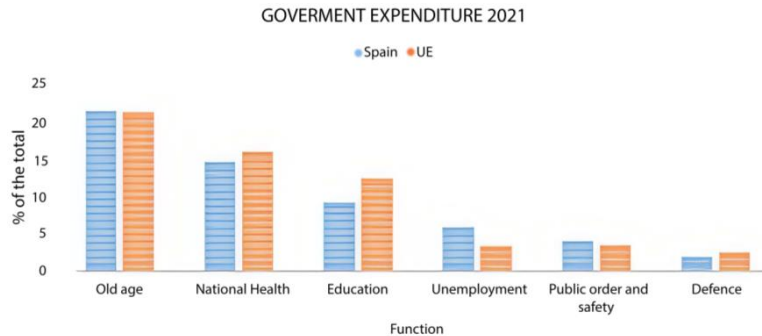


Fig. 2. Distribution of the Spanish and UE government expenditure [3].

Part of this growing sector of the population has special needs to maintain good physical and mental well-being. These needs include physical exercise, social interaction and mental stimulation. Research into aging and cognition has demonstrated the close relationship of sensory functioning and social communication in maintaining cognitive performance and mood in the elderly, yet in modern societies, elderly people are increasingly isolated and under-stimulated, both physically and psychosocially [6]. This situation results in accelerated cognitive decline and the suffering associated with loneliness and confusion. Social interaction and intellectual stimulation may be relevant to preserving mental functioning in the elderly [7]. Some studies report that subjects, who participated in senior citizen clubs or senior centers, can have a lower risk of cognitive decline, especially if this interaction is realized with young adults [8]. Other studies highlight the potential of video games for developing physical skills and creating mental and social interactions for elderly people [9].

2.1 Smart furniture and Smart Cities

Many cities are using smart furniture as elements of their Smart City concept and deployment. Two of the main types of this furniture are Smart Kiosks and Smart Bus Stops.

Among the outstanding examples of cities employing Smart Kiosks are the cities of Daegu, in South Korea, and Philadelphia, in the US. Daegu, the third-largest city in South Korea, has deployed unmanned kiosks as key components for disaster management. They transmit crucial information during disasters (earthquakes, floods, or fires) and provide local guidance to people. City authorities consider these kiosks as essential instruments to maintain communication with citizens even in the most complex circumstances while guiding and informing citizens and visitors daily [10].

4

Several European and Asian cities have launched smart bus stop pilot projects. The interfaces of the Smart Bus Stops are increasing in technical sophistication. Figure 3 shows the use of directional sound and big screens for publicity campaigns [11].



Fig. 3. Bus Stops using Directional Sound [https://www.holosonics.com/applications-1].

2.2 The Extended Interconnected Public Spaces concept

The concept of the Interconnected Public Space (IP-Space) [12] [13] describes a public outdoor architectonic space provided with ICT equipment that can connect with a similar space remotely located. Therefore, an IP-Space becomes a node in a network of these spaces. An IP-Space node can be implemented at a bus stop, in a park, in a square or any other outdoor spot in the city, in which a group of persons could potentially interact with it. Thus, IP-Spaces allow the sharing of collective experiences.

The Extended IP-Space (EIPS) concept includes outdoor and indoor public implementation of the IP-Spaces (Fig. 4). It reduces the requirements for electronic system capability to withstand harsh environmental conditions (reduced costs) while keeping the requirements of being outside the home and sharing collective experiences. This allows the use of existing locations such as clubs, elder people associations, etc.

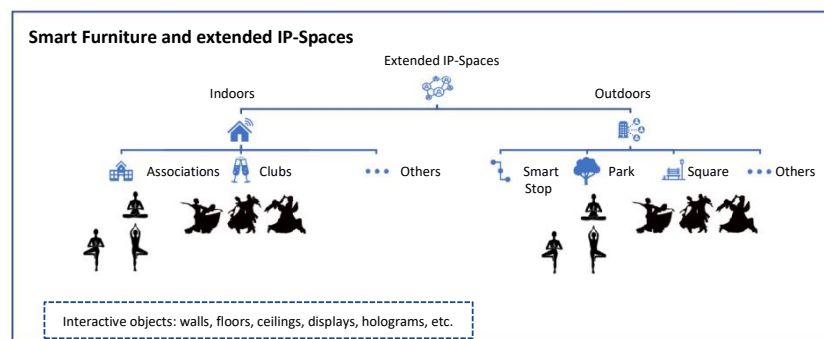


Fig. 4. The Extended IP-Space concept.

Figure 4 also describes a potential implementation of the EIPS in the context of Smart Cities. Two sets of people, potentially *from two different countries*, are sharing,

locally and remotely, a dancing experience. While another group shares a yoga experience.

The Spaces can connect persons from other regions or countries, using the *same or different languages* using automated translation services. The EIPS allow the participation in different sports, physical, educational, cultural and playful activities (such as intellectual games or video games, physical exercises, dancing competitions and many more), engaging elderly people in remote communities and stimulating them mentally, physically, socially and intellectually.

Specifically for the elderly, promoting participation in educational, cultural and sportive activities contributes to emotional, physical health and social cohesion [14]–[21]. Some studies show that learning multiple real-world skills simultaneously in older adults can improve both their cognitive abilities (working memory, episodic memory, and cognitive control) and functional independence [22]. Interconnected public spaces can help create the conditions under which wellbeing is more likely to improve.

3 The design process of HERMÓPOLIS

In order to put all these concepts into practice, a multidisciplinary group of researchers is building HERMÓPOLIS, an architectonic, artistic, technological, entertainment, health and social Smart Cities platform oriented to improve the quality of life of the elder people.

A layered design was proposed for the implementation of HERMÓPOLIS platform (Fig. 5). The Social layer is in the top position. It contains the users and their interaction in local and hybrid communities. Next is the Activity layer. It describes how different activities will be carried out and how the effect of these activities on the subject's quality of life will be assessed. The third layer is the Technological layer, divided into two sublayers: hardware and software. The last layer corresponds to the artistic and architectonic layer. It describes the physical structure, shape and aesthetic appeal of the Extended IP-Space nodes.

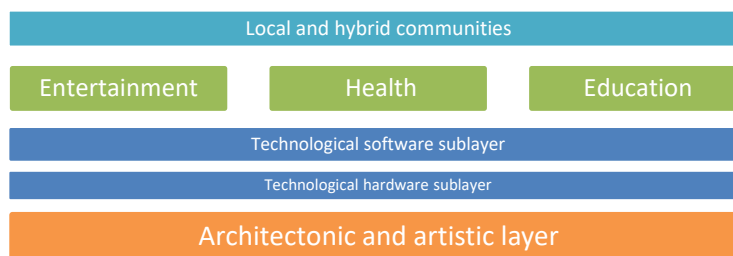


Fig. 5. The layered design of HERMÓPOLIS platform (up-down): social, activities, technological and architectonic-artistic layers.

6

3.1 Architectonic and artistic layer

The conception of urban space changes according to the cultural conception, climatic conditions, the type of city and the haptic relationship with the material that supports that space. The social space is an expanded conception of the physical public space, a virtual space associated with the contemporary public space activated by citizen activity, and which is continually updated from the new awareness of a territory.

The entire urban landscape is therefore a personal internalized social space and, just as our perception is changeable, the urban landscape will also influence our memory as it is affected by our immersion in it. From, the architectonic point of view, the HERMÓPOLIS project generates a node of activation of the social space that broadens the relationship with the user.

In this case, the expansion from physical space to social space is yet larger due to the technology embedded into the architectonic space. This is an application of the IoT in which the things are architectonic objects, allowing interaction in local and virtual social networks. This is a new concept. It is no longer valid the idea of urban projects, isolated without any freedom to communicate between them. Through the interaction with the physical architectonic object a new social interaction, locally and remote, is activated.

The interfaces for Interconnected Public Spaces should consider the variability of their possible locations within Smart Cities and the diversity of the people interacting with them require an inclusive user interface, meeting the criteria of Design for All. Ensuring that access to these spaces takes into account human diversity, social inclusion and equality.

As a connector node the green spaces whether parks or gardens can be key spaces to the IP-Space network establishment, inasmuch as for own nature they are spaces prone to establish a harmonious relationship between people. These spaces denote an abstract environment, which fosters the relationships between persons and encourages mental, physical and spiritual health. The green spaces are physical spots inside of the cities where the interconnectivity between natural and artificial landscapes converge favorably to the introduction of the IP-Spaces network in the Smart Cities.

From the artistic point of view, our focus is on creating an installation aesthetically appealing, but oriented to raise awareness about the environmental and sustainability issues in modern cities. The reduction of the effect of gas emissions, carbon dioxide capture technology (removal of CO₂ from the atmosphere) and oxygen production have been considered. The use of microalgae as a carbon sink is simple, sustainable and environmentally friendly. HERMÓPOLIS fits into this context.

Our artistic-architectural prototype proposes to insert a microalgae (*spirulina*) photobioreactor integrated into its modular design. The reactor is a structural and sustainable skin, capable of absorbing CO₂ from the urban environment in which it is located, returning oxygen to the environment. It is a natural purifier equivalent to the action of a tree since the microalgae carry out photosynthesis for their reproduction and life and a natural and decontaminating shading of the urban environment that introduces a biological landscape, contributing to the emotional and physical well-being of its users.

From these concepts, many architectonic and artistic designs were generated with the help of IA tools. The figure below shows one of the possible architectonic and artistic designs of a HERMÓPOLIS node. A park pavilion containing the photobioreactors. Activities can be carried outside, inside, or around the pavilion.



Fig. 6. One of the possible architectonic and artistic designs of a HERMÓPOLIS node.

In this specific design, the algae will be located in a unique design of transparent containers. Inside, live photosynthetic microalgae (*Limnospira platensis*) will be grown thanks to the agitation of an aeration pump. A set of sensors will monitor the temperature, pH of the culture medium, the light intensity, the speed stirring inside the bioreactor, dissolved oxygen and the concentration of essential nutrients in the culture medium, e.g. nitrogen and phosphorus.

3.2 Technological layer

The technological layer is the IoT platform that connects and services Extended IP-Spaces (outdoor and indoor spaces). The high-level architecture of this platform is shown in Figure 7. Multiple Extended IP-Spaces, as well as the staff for supervising and assisting elders' activities, connect to the Extended IP-Spaces Cloud Services.

8

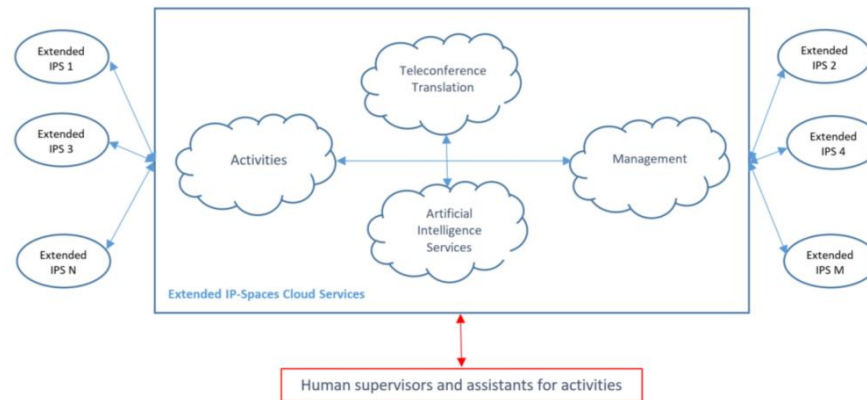


Fig. 7. High-level architecture of HERMÓPOLIS.

This Cloud architecture contains four main services:

1. **Activities.** It provides digital support for activities.
2. **Teleconference and translation services.** It ensures the remote communication and overcomes the language barrier.
3. **Management services.** It ensures the organization of the activities.
4. **Artificial Intelligence Services.** This optional service allows the analysis of the activities to reinforce learning and help supervision staff and users, to improve the activities' outcomes.

For its design, this layer was divided into the hardware and the software sublayers.

3.2.1. Hardware sublayer

The nodes must have a physical platform that allows Internet connection and group interaction to accommodate different physical and intellectual activities. To ensure group interaction, a large touch screen is necessary. As a first approximation, a 75-inch touch screen (168 cm x 95 cm) is used. A wide-angle web camera captures a wide image of the venue, thus ensuring visual coverage of the participants. A medium-high power computer equipped with the Windows 11 operating system is hidden behind the screen. The Cloud system is initially hosted in a commercial Internet hosting service.

3.2.2. Software sublayer

Currently, the software platform includes only two components: the access web page, which allows the selection of the activities, the remote access using Skype and the Artificial Intelligence tools used for activities supervision and virtualization.

3.2.2.1 Access web page

The initial (landing page) website <https://miespaciopublico.es/> has been developed. This home page is used to access the different activities remotely, giving access to the virtual meeting rooms. It is very important to have a simple web page to start the experiments. This website can be further developed later and have more functionalities as the implementation of the activities gets more traction among our users.

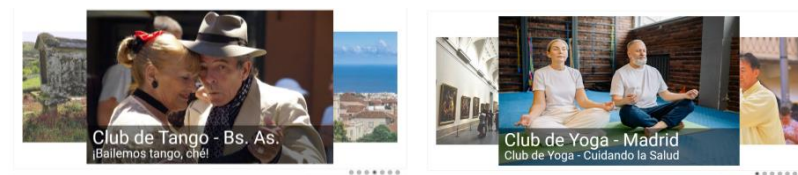


Fig. 8. HERMÓPOLIS initial web page.

3.2.2.2 Artificial Intelligence tools for activities supervision and virtualization

We are currently working on two Artificial Intelligence tools, both based on video images, an emotion detector and a human posture estimation (HPE) tool. The first helps the human supervisors to evaluate the emotions of the users (subjects) during the realization of the activities. The HPE tool allows the checking of the movements during physical activities and the potential automatic production of suggestions for the improvement of the movements as well as for setting safe physical limits. In addition, the HPE tool can be used for the virtualization of movements and gamification.

3.2.2.2.1 The Human Posture Estimation tool

Traditionally, human representations in various media, including videos, images, and paintings, have been two-dimensional, serving as potent tools for conveying information and emotions. However, understanding complex spatial arrangements and resolving depth ambiguities has been crucial for interpreting these 2D representations. In applications like virtual reality, augmented reality, clothing size estimation, and autonomous driving, imparting spatial reasoning to machines is essential [23].

Human posture estimation (HPE) has grown in computer vision, finding applications in video surveillance, healthcare, and sports analysis [24]-[27]. Over the years, several HPE libraries have emerged, including OpenPose, PoseNet, MoveNet, and MediaPipe Pose. A comparative analysis [28] found that MoveNet performed best in detecting various human poses in images and videos.

HPE involves identifying human body parts in images or videos, with applications in various domains. Key points help assess posture correctness during therapy, fall detection, and sports analysis. Analyzing these HPE libraries, they share 17 common keypoints, with additional annotations for faces, hands, and feet.

Library performance is evaluated [23] based on the percentage of joints detected (PDJ). MediaPipe Pose performed well in videos but had lower performance in images, slightly behind MoveNet. MoveNet excelled in keypoint detection, especially in videos,

10

with a high overall PDJ average. OpenPose had good image performance but struggled with continuous video frame detection. PoseNet ranked third in both image and video datasets. HPE library performance can be affected by challenges like camera positioning and self-occlusion.

An initial test using MoveNet (lightning) is shown in the figure below (please note the detection of keypoints and their relationship using video markers).

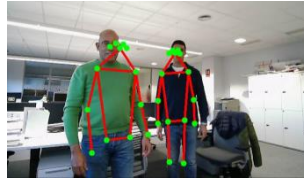


Fig. 9. Initial test of the Human Posture Estimation using MoveNet (lightning) library.

3.3 Activities layer

The activities design is performed in parallel with the rest of the developments. As said before, the diversity of the people who interact with the Spaces requires an inclusive approach. Therefore, this work started with the study of the potential health problems of our users for the detection of these problems (in unhealthy persons) and prevention (for healthy persons). For these purposes, activities are divided into phases. From the methodological point of view, participants should complete an assessment of their quality of life and health conditions before, during, and after the intervention. Participants will be intervened sequentially (same sequential control/intervention group).

3.3.1. Preliminary design of the activities

The ageing process is a multifaceted and highly individualized phenomenon that impacts not only the physical dimension but also the psychological and social aspects of older adults [29]. Physiological changes associated with ageing, such as reductions in muscle strength, joint range of motion, reaction time, and sensory system deterioration, adversely impact balance and motor function in older adults, potentially leading to varying degrees of balance dysfunction [30].

Balance dysfunction is widely recognized as this population's primary cause of falls. Individuals who have experienced falls tend to exhibit heightened fear and reduced confidence in their ability to remain upright, which subsequently translates into reduced social participation, increased dependence on activities of daily living, and significant activity restriction [31, 32].

Decline in cognitive function, including short-term memory, processing speed, and reaction time, is another common aspect of aging, even in the absence of neurodegenerative disorders like Alzheimer's disease. With the growth of the older adult population, "cognitive ageing" has become a relevant public health challenge due to its impact on the daily functioning of many individuals [33].

Furthermore, social ageing, referring to the role of older adults in society, is heavily influenced by cultural factors and evolves. How an individual perceives the ageing process and how it is viewed by society can significantly influence older adults' quality of life and emotional well-being [29].

In this context, we propose the "Dance Project", a comprehensive approach aimed at mitigating the adverse effects of ageing and improving participants' physical, psychological, and social conditions. The project is based on a specific learning process focused on balance and coordination through a series of phases detailed below:

- **Phase 1:** A workshop based on YoMed, a protocol grounded in the principles of yoga and meditation, spanning 12 weeks, with sessions scheduled three times a week, each lasting 45 minutes. It begins with a body scan and proceeds with 18 yoga postures [34].
- **Phase 2:** A workshop based on the OTAGO Program, known for its beneficial effects on balance, reduction of fall risk, and enhanced social participation in older adults [35]. Much of the Program is dedicated to balance improvement, enhancing physical function, independence, and physical activity in older adults, with additional health benefits [36].
- **Phase 3:** A Music Therapy workshop. This therapy has been shown to provide benefits such as improved sleep quality, reduced depressive symptoms, and lower blood pressure, heart rate, and anxiety levels in older adults with hypertension [37]–[39].
- **Phase 4:** The Dance activity. Dance has a positive impact on overall cognition and memory, presumably through biomechanical movements synchronized with music that stimulate the parietal lobes of the brain, enhancing overall cognition, visuospatial function, and language skills [40].

3.3.1. Planned measurement of the activities impact

The project proposal aims to assess the quality of life, sleep quality, fall risk, and balance to observe the changes produced through the program. Assessments will be conducted at the beginning of the project, during the intervention and upon completion, at one month, three months, and six months after its completion. This approach will provide a deeper understanding of the changes and how they persist over time.

Quality of life will be measured using the EQ-5D-5L questionnaire. This tool evaluates five dimensions: mobility, self-care, usual activities, pain/discomfort, and anxiety/depression [41].

Sleep quality will be assessed through the Oviedo Sleep Quality Questionnaire (OQSQ). The questionnaire developed by Bobes et al. consists of 15 items evaluated on a five-point Likert scale, except for item 1, which measures subjective sleep satisfaction and is classified on a seven-point scale. Sleep satisfaction scores (ranging from 1 to 7), insomnia (scores ranging from 9 to 45), and hypersomnia (scores ranging from 3 to 15) were derived from the OQSQ [42].

Fall risk will be measured using the Tinetti Test. The purpose of this scale is to evaluate mobility in older adults, encompassing two domains, gait and balance, with the primary goal of detecting those who may be at risk of falling. This scale consists of

12

nine items related to balance and seven related to gait. Responses to each item are classified on an ordinal scale from zero to two. For the balance domain, the total maximum score is 16 points. While for gait, it is 12 points. The total score, obtained by summing both domains, can reach a maximum of 28 points, allowing for the determination of fall risk in the evaluated older adult [43].

Finally, balance will be assessed using the Berg Balance Scale (BBS). The BBS is designed to evaluate functional balance in older adults through 14 specific tasks. These tasks include rising from a chair, standing unsupported, sitting down again, performing transfers, standing with eyes closed, standing with feet together, reaching forward, picking up an object from the floor, turning to look behind, performing a complete 360-degree turn, stepping onto alternate feet on a step, standing with one foot in front, and standing on one foot [44].

3.4 Social layer

The social layer is currently less developed. Contacts with regional and local government elders' associations and private residences are going on in different points of Spain and the United States. It is very important to select subjects interested in the activities, which are in a suitable physical and cognitive state.

4 Discussion

The design of the HERMÓPOLIS platform is an ambitious and complex task. This multidisciplinary project requires the effort of researchers and professionals to create a space, architectonically and artistically attractive, technologically enabled, and a set of activities capable of engaging elderly people. The activities are based on projects. This allows the gradual acquisition and reinforcement of required skills for the realization of the activities, as well as the detection and prevention of incidents (e.g. falls). This approach increases safety and helps to maintain users' self-confidence. The selection of tools, such as tests and interviews, is crucial to assess the potential improvement of the quality of life. IA tools for Human Posture Estimation can be very helpful for movement supervision in physical activities.

5 Conclusions

The paper describes the first steps in the design of the platform. The use of a layered design allows for coping with the complexity of the design. It is important to create a basic set of activities and elaborate a process for their realization before starting to contact the subjects of the research. Although IA tools can be very useful, it is necessary to get the approval of the subjects and to take measures to keep the anonymity and the cybersecurity of the related data.

Acknowledgments: This research is being funded by Santander-Universities and Universidad Europea de Madrid foundations under grant number XSAN002306.

References

1. Department of Economic and Social Affairs, United Nations. World Population Ageing 2019: Highlights. United Nations. New York, NY, USA, pp. 1–2 (2019)
2. Instituto Nacional de Estadística. Proyecciones de Población 2022-2072. Notas de prensa (2022). https://www.ine.es/prensa/pp_2022_2072.pdf
3. Eurostat. Government expenditure (2023). <https://ec.europa.eu/eurostat/cache/info-graphs/cofog/>
4. Instituto Nacional de Estadística. INEbase. Indicadores de calidad de vida. Riqueza neta de los hogares por riqueza, edad y periodo. (2022). https://www.ine.es/jaxi/Datos.htm?path=/t00/ICV_ant/dim1/&file=13102.px#!tabs-tabla
5. Padrón Nápoles, V. M., Gachet Páez, D., Esteban Penelas, J. L., García Pérez, O., Martín de Pablos, F., Muñoz Gil, R.: Social inclusion in smart cities. In: J. C. Augusto (eds.), *Handbook of smart cities*. Cham: Springer (2020). https://doi.org/10.1007/978-3-030-15145-4_42-1
6. Waterworth, J.; Ballesteros, S.; Christian, P.; Bieber, G.; Kreiner, A.; Wiratanaya, A.; Polymenakos, L.; Wanche-Politis, S.; Capobianco, M.; Etxeberria, I.; et al. Ageing in a networked society—Social inclusion and mental stimulation. In: *Proceedings of the 2nd International Conference on Pervasive Technologies Related to Assistive Environments (PETRA 2009)*, Corfu, Greece (2009)
7. Wang, H.; Karp, A.; Winblad, B.; Fratiglioni, L. Late-Life Engagement in Social and Leisure Activities Is Associated with a Decreased Risk of Dementia: A Longitudinal Study from the Kungsholmen Project. *Am. J. Epidemiol.* 155, 1081–1087, (2002)
8. Lee, S.H.; Kim, Y.B. Which type of social activities may reduce cognitive decline in the elderly?: A longitudinal population-based study. *BMC Geriatr.* 16, 165, (2016)
9. IJsselsteijn, W.; Nap, H.H.; de Kort, Y.; Poels, K. Digital Game Design for Elderly Users. In: *Proceedings of the Conference on Future Play—Future Play '07*, Toronto, ON, Canada, (2007)
10. Smart City Press. Unmanned kiosks – the most effective stand to connect citizens with cities, <https://smartcity.press/digital-kiosks-benefits/>
11. Martín de Pablos, F., Padrón Nápoles, V.M., Gachet Páez, D., Esteban Penelas, J.L., García Pérez, O., Muñoz Gil, R., García González, J., Escorial Santa Marina, S.: Human-Computer Interfaces for Smart Bus Stops as Interconnected Public Spaces (IP-Spaces) elements in Smart Cities. In: Meza, C., Hernandez-Callejo, L., Nesmachnow, S., Ferreira, A., Leite, V. (Eds.). *Proceedings of the III Ibero-American Conference on Smart Cities*. Instituto Tecnológico de Costa Rica (2020)
12. Nápoles V.M.P., Páez D.G., Penelas J.L.E., García G.G., Santacruz M.J.G.: Bus Stops as a Tool for Increasing Social Inclusiveness in Smart Cities. In: Nesmachnow S., Hernández Callejo L. (eds.) *Smart Cities. ICSC-CITIES 2019. Communications in Computer and Information Science*, vol. 1152. Springer, Cham (2019). https://doi.org/10.1007/978-3-030-38889-8_17
13. Padrón-Nápoles, V. M., Gachet Páez, D., Esteban Penelas, J. L., García Pérez, O., García Santacruz, M. J., Martín de Pablos, F.: Smart bus stops as interconnected public spaces for increasing social inclusiveness and quality of life of elder users. *Smart Cities*, 3, 430–443 (2020)
14. Bacon, N.; M. Brophy, N. Mguni, G. Mulgan and A. Shandro. *The State of Happiness: Can Public Policy Shape People’s Wellbeing and Resilience?* The Young Foundation: London, UK, 2010. Available online: <https://youngfoundation.org/wp-content/uploads/2012/10/The-State-of-Happiness.pdf>

14

15. WHO. Regional Office for Europe: Active ageing: physical activity promotion in elderly, <https://www.euro.who.int/en/health-topics/disease-prevention/physical-activity/activities/hepa-europe/hepa-europe-projects-and-working-groups/active-ageing-physical-activity-promotion-in-elderly>
16. Archer, L., Davidson, S., Iparraguirre, J., Kohler, M., Pursch, B., Vass, J., Curran, F.: Creative and Cultural Activities and Wellbeing in Later Life. Age UK Policy and Research Department and Age UK Oxfordshire. <https://www.ageuk.org.uk/creativewellbeing>
17. UNESCO. Diversity of Cultural Expressions. Promoting participation in arts and cultural activities by the elderly. <https://en.unesco.org/creativity/policy-monitoring-platform/promoting-participation-arts>, <https://www.ageuk.org.uk/creativewellbeing>
18. Ryu, J., Heo, J.: Relationships between leisure activity types and well-being in older adults. *Leisure Studies*. 37 (3), 331–342 (2018)
19. Toepoel, V.: Cultural participation of older adults: Investigating the contribution of lowbrow and highbrow activities to social integration and satisfaction with life. *Int J Disabil Hum Dev*. 10(2), 123–129 (2011)
20. Sheppard, A., Broughton, M. C.: Promoting wellbeing and health through active participation in music and dance: a systematic review. *International Journal of Qualitative Studies on Health and Well-being*. 15(1) (2020)
21. Popovic S, Masanovic B.: Effects of Physical and Social Activity on Physical Health and Social Inclusion of Elderly People. *Iran J Public Health*. 48(10), 1922-1923, (2019)
22. Leanos, S., Kürüm, E., Strickland-Hughes, C. M., Ditta, A. S., Nguyen, G., Felix, M., Yum, H., Reebok, G. W., & Wu, R. The impact of learning multiple real-world skills on cognitive abilities and functional independence in healthy older adults. *The Journals of Gerontology: Series B*. 75(6), 1155–1169, (2020). <https://doi.org/10.1093/geronb/gbz084>
23. Martinez, J., Hossain, R., Romero, J., & Little, J. J.: A simple yet effective baseline for 3d human pose estimation. In: *Proceedings of the IEEE international conference on computer vision*, pp. 2640-2649 (2017)
24. Wang, J.; Qiu, K.; Peng, H.; Fu, J.; Zhu, J.: Ai coach: Deep human pose estimation and analysis for personalized athletic training assistance. In: *Proceedings of the 27th ACM International Conference on Multimedia*, pp. 374–382. Nice, France (2019)
25. Park, H.J.; Baek, J.W.; Kim, J.H.: Imagery based Parametric Classification of Correct and Incorrect Motion for Push-up Counter Using OpenPose. In: *Proceedings of the 2020 IEEE 16th International Conference on Automation Science and Engineering (CASE)*, pp. 1389–1394. Hong Kong, China (2020)
26. Patil, A.; Rao, D.; Utturwar, K.; Shelke, T.; Sarda, E.: Body Posture Detection and Motion Tracking using AI for Medical Exercises and Recommendation System. *ITM Web Conf*. 44. 03043 (2022)
27. Devanandan, M.; Rasaratnam, V.; Anbalagan, M.K.; Asokan, N.; Panchendrarajan, R.; Tharmaseelan, J.: Cricket Shot Image Classification Using Random Forest. In: *Proceedings of the 2021 3rd International Conference on Advancements in Computing (ICAC)*, pp. 425–430. Colombo, Sri Lanka (2021)
28. Chung, J. L., Ong, L. Y., & Leow, M. C.: Comparative analysis of skeleton-based human pose estimation. *Future Internet*. 14(12), 380 (2022)
29. Dziechciaż, M., Filip, R.: Biological psychological and social determinants of old age: Biopsychosocial aspects of human aging. *Ann Agric Environ Med*. 21(4), 835-838 (2014)
30. Peterka R.J.: Sensorimotor integration in human postural control. *J Neurophysiol*. 88(3), 1097–1118 (2002)
31. Escosura Alegre, I., Fernández Rodríguez, E.J., Sánchez Gómez, C., García Martín, A., Rihuete Galve, M.I.: Living Conditions and the Incidence and Risk of Falls in Community-

- Dwelling Older Adults: A Multifactorial Study. *International Journal of Environmental Research and Public Health*. 20(6), 4921 (2023)
32. Scheffer, A.C., Schuurmans, M.J., van Dijk, N., van der Hooft, T., de Rooij, S.E.: Fear of falling: measurement strategy, prevalence, risk factors and consequences among older persons. *Age Ageing*. 37(1), 19–24 (2008)
 33. Blazer, D.G., Yaffe, K., Karlawish, J.: Cognitive aging: a report from the Institute of Medicine. *JAMA*. 313, 2121–2 (2015)
 34. Wooten, S. V., Signorile, J. F., Desai, S. S., Paine, A. K., Mooney, K.: Yoga meditation (YoMed) and its effect on proprioception and balance function in elders who have fallen: A randomized control study. *Complementary therapies in medicine*. 36, 129–136 (2018)
 35. Martins, A. C., Santos, C., Silva, C., Baltazar, D., Moreira, J., Tavares, N.: Does modified Otago Exercise Program improves balance in older people? A systematic review. *Preventive medicine reports*. 11, 231–239, (2018)
 36. Chiu, H.L., Yeh, T.T., Lo, Y.T., Liang, P.J., Lee, S.C.: The effects of the Otago Exercise Programme on actual and perceived balance in older adults: A meta-analysis. *PLoS One*. 16(8):e0255780 (2018)
 37. Chen, C. T., Tung, H. H., Fang, C. J., Wang, J. L., Ko, N. Y., Chang, Y. J., Chen, Y. C.: Effect of music therapy on improving sleep quality in older adults: A systematic review and meta-analysis. *Journal of the American Geriatrics Society*. 69(7), 1925–1932 (2021)
 38. Zhao, K., Bai, Z. G., Bo, A., Chi, I.: A systematic review and meta-analysis of music therapy for the older adults with depression. *International journal of geriatric psychiatry*. 31(11), 1188–1198 (2016)
 39. Lorber, M., Divjak, S.: Music Therapy as an Intervention to Reduce Blood Pressure and Anxiety Levels in Older Adults With Hypertension: A Randomized Controlled Trial. *Research in gerontological nursing*. 15(2), 85–92 (2022)
 40. Wu, V. X., Chi, Y., Lee, J. K., Goh, H. S., Chen, D. Y. M., Haugan, G., Chao, F. F. T., Klainin-Yobas, P.: The effect of dance interventions on cognition, neuroplasticity, physical function, depression, and quality of life for older adults with mild cognitive impairment: A systematic review and meta-analysis. *International journal of nursing studies*, 122, 104025 (2021)
 41. Herdman, M., Gudex, C., Lloyd, A., Janssen, M. F., Kind, P., Parkin, D., Bonsel, G., Badia, X.: Development and preliminary testing of the new five-level version of EQ-5D (EQ-5D-5L). *Quality of life research*, 20(10), 1727–1736 (2011). doi: 10.1007/s11136-011-9903-x.
 42. Bobes, J., García-Portilla González, M.P., Saiz-Martínez, P.A., Bascarán-Fernández, M.T., Iglesias-Álvarez, C., Fernández-Domínguez, J.M.: Propiedades psicométricas del cuestionario Oviedo de sueño. *Psicothema* 12(1), 107–112 (2000)
 43. Tinetti, M.E.; Williams, T. Frankin; Mayewski, R.: Fall risk index for elderly patients based on number of chronic disabilities. *American Journal of Medicine* 80 (3), 429–434 (1986)
 44. Berg, K. O., Wood-Dauphinee, S. L., Williams, J. I., Maki, B.: Measuring balance in the elderly: validation of an instrument. *Canadian journal of public health = Revue canadienne de sante publique*. 83 Suppl 2, 7–11 (1992)

Municipal Solid waste management systems: application of SWOT methodology to analyze an Argentinean case study

Diego Rossit^{1,3}[0000-0002-8531-445X], Sergio Nesmachnow²[0000-0002-8146-4012],
and Antonella Cavallin¹

¹ Department of Engineering, Universidad Nacional del Sur, Argentina
{diego.rossit,antonella.cavallin}@uns.edu.ar

² Universidad de la República, Uruguay
sergion@fing.edu.uy

³ INMABB UNS-CONICET, Argentina

Abstract. Historically, Municipal Solid Waste (MSW) systems emerged in response to society's needs for managing manufacturing and consumption waste. However, the waste generation in modern cities present several new features that affect the MSW system. These new features include both positive aspects, such as innovative recycling techniques and increased public environmental awareness, as well as challenging aspects, including a rise in the amount of waste generated and in the complexity of waste composition. As a result, MSW systems have to adapt to new opportunities and threats offer by the context by exploiting their strong and weak points. In this line, this article conducts a comprehensive review of contemporary material and waste flows, followed by a revision of the current state of the MSW systems in Argentina and a particular analysis of an Argentinean case study using SWOT (Strengths-Weaknesses-Opportunities-Threats) methodology. The findings of this analysis highlighted the competitiveness of SWOT methodology to formulate strategies to develop more efficient MSW systems.

Keywords: Sustainable cities · Waste management systems · SWOT methodology · Argentinean case study.

1 Introduction

Natural systems are widely recognized for adhering to a self-contained cycle of matter, characterized by the absence of residual product accumulation. Within this inherent framework, structures emerge and dissolve seamlessly, leaving no remnants of accumulable waste. However, human intervention disrupts this innate matter cycle, leading to waste accumulation as a consequence of the pursuit of greater material wealth and ostensibly improved quality of life [4]. Waste is defined as any substance discarded by its creator or possessor, resulting from processes such as production, consumption, or cleansing. The rise in waste accumulation has also spurred the development of waste management policies to address and mitigate the adverse environmental impacts of such refuse.

2 Rossit et al.

Waste management entails a systematic and organized approach to handling, treating, and disposing of various waste materials stemming from human activities [23]. Waste management encompasses a diverse array of practices and strategies aimed at minimizing the negative impact of waste on the environment, public health, and overall well-being while optimizing the potential reuse and recovery of materials. Waste management includes waste collection, transportation, recycling, treatment, and safe disposal. Waste management policies have evolved over time from careless disposal practices to intricate and advanced systems throughout history, following the escalating rate of byproducts generated due to rising consumption rates and population growth.

This article focuses on Municipal Solid Waste (MSW), which includes elements, objects, or substances originating from domestic, commercial, institutional, non-special care activities in urban areas [7]. Among the main contributions of this article there are: a new waste and material flow model within modern cities, an up-to-date overview of the state of MSW systems in Argentina, and a systematic analysis of a specific Argentine case study using SWOT analysis.

This article is organized as follows. Section 2 presents a description of waste and material flow in modern cities and about the waste management systems in Argentina. Section 3 presents the SWOT analysis of the case study. Finally, Section 4 discuss the main outcomes of this work and presents the future lines.

2 Waste management

This section describes the main aspects of waste management, including contemporary dynamics of waste and material flow within modern cities and the specific characteristics of waste management in Argentina, the country of the case study.

2.1 Evolution of waste and material flow: from early cities to current societies

Throughout history, humanity has relied on natural resources to ensure survival and create tools that promote prosperity in challenging environments. In the first sedentary communities, after utilizing these resources, the remnants -primarily originating from food and wood- could be effortlessly integrated into the environment without adverse effects or degradation. As human settlements expanded, they demanded increased extraction and transformation of natural resources, resulting in the accumulation of waste. The disposal of this waste often involved land or water deposition, which contaminated the environment but had limited impact due to the relatively small population and land's absorptive capacity [27].

As population grew and industrial techniques developed, societies faced challenges in managing the waste they produced, leading to the emergence of early landfills. During the Middle Ages, waste disposal within urban areas created issues with rodents and fleas, vectors for disease [29]. However, it was not until the 18th century that state measures were introduced to regulate waste disposal due

to hygiene concerns, including the development rudimentary sewage networks. The state regulations marked a shift of waste management from individual private initiatives to a public regulated system.

As the urban growth continue to rise, societies organized around cities catering to production and consumption demands. Objects of utility were considered commodities with little thought to their environmental impact. Initial waste management policies involved haphazard accumulation in makeshift containers and basic household collection, followed by transportation to landfills or uncontrolled incineration [13]. By then, the composition of MSW had changed, with reduced organic waste and increased glass, cardboard, and plastic reflecting contemporary consumerism [29].

Notably, it wasn't until the 1960s that a significant portion of society recognized the discord between industrial practices and environmental preservation. The rise in social awareness led to demands for accountability from industrial activities that had a significant impact on the environment [1]. The last decades have seen the proliferation of numerous sustainability-driven initiatives within modern societies. Consequently, the flow of materials in cities and the subsequent waste generation have evolved since the model initially proposed by [27]. In this work, we propose the incorporation of several new features to the flow of materials and waste in modern cities, as it is illustrated in Fig. 1. The key changes include:

- *Raw materials used directly by to consumers.* A growing number of consumers have started to design and even produce their own products. This trend extended beyond cultivating agricultural produce to include more intricate items like clothing, cleaning products, and personal hygiene items. This trend fosters a sense of self-sufficiency among consumers and is expected to continue expanding [2].
- *Reutilization of products by consumers.* Consumers have also ushered in a substantial shift through product reutilization. The reutilization of products can serve a similar purpose as their original use or an entirely different one. A notable example of this shift is the reutilization of refillable packaging systems, where companies provide durable containers, and consumers are responsible for cleaning and refilling the packaging [15].
- *Refurbishment and remanufacturing of products.* Refurbishment and remanufacturing of products have gained prominence in the economic activities of the cities. While there are some differences between refurbishment and remanufacturing [10], both processes involve extending product life cycles through actions resembling and manufacturing processes, contributing to reduce the demand for new resources in the manufacturing sector.

2.2 MSW management in Argentina

In 2004, the enactment of National Law No. 25916 by the Argentine National Congress [7] aimed to promote the recovery of household waste. The objective is

4 Rossit et al.

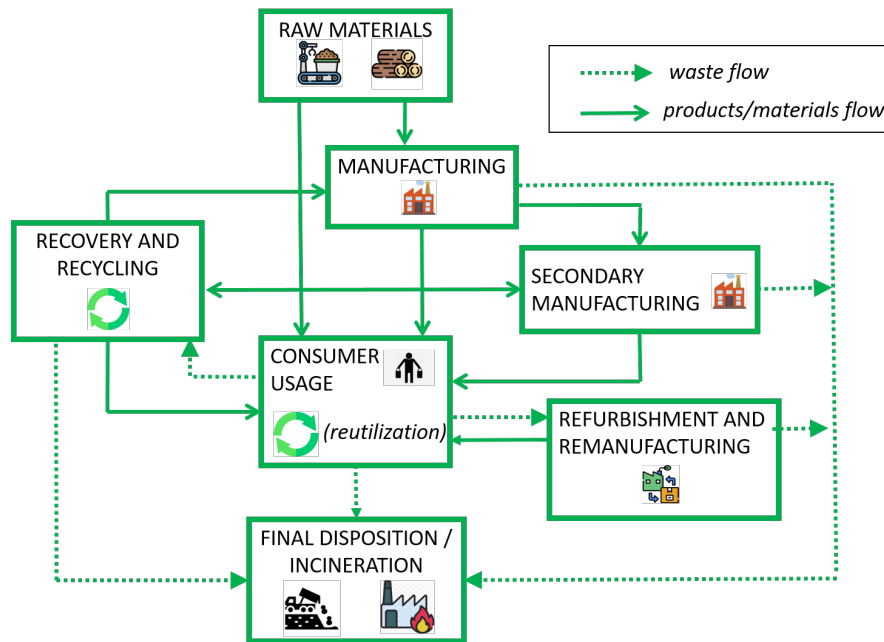


Fig. 1. Waste and material flow in current societies.

to employ suitable methods and processes, thereby reducing the amount of waste destined for final disposal and minimizing its adverse environmental impacts.

In Argentina, the management of MSW falls within the jurisdiction of municipal authorities. Argentina’s municipal system is diverse, with different types of municipalities defined by provincial constitutions. Municipalities responded to the enactment of National Law No. 25916 by improving their existing MSW systems [3], including the close of open dumps, constructing new sanitary landfills, migrating from door-to-door collection to community bins-based collection networks, implementing segregated waste collection for recyclable and non-recyclable materials, and installing MSW treatment facilities. However, the extent of improvement in the MSW system varied depending on the initial state of the system and the allocation of resources, which were not uniform across municipalities. Consequently, while some municipalities experienced significant progress, others continued to grapple with inefficient MSW management practices [14].

As aforementioned, MSW management comprehends several different aspects. In the following paragraphs, the main aspects of MSW management in Argentina are described.

Waste generation and composition. An estimated 54,800 tons of MSW were generated daily in Argentina, and this quantity is projected to remain stable or even increase due to the country's expected population growth [16]. However, waste generation is not evenly distributed across all population sectors. The majority of waste is generated by the high and medium-high socioeconomic levels, producing about 42% more waste than the low socioeconomic level [25]. Regarding average waste composition, the largest proportion correspond to food waste (47%) followed by paper/cardboard (17.3%), plastic (13.5%) and glass (6%) [24].

Coverage of the MSW system. The urban population, which comprises 90% of the total population, reports a high coverage of the MSW collection system at 99.8% , with the majority of cities performing daily collection of waste (70%) [17]. Although this percentage of coverage is comparable to those observed in high-income countries, there are some marginalized urban areas and semi-rural municipalities which are still lacking of basic MSW collection [25].

Final destination of MSW. As of 2020, nearly 65% of the generated waste in the country is disposed of in environmentally managed centers with sanitary landfill technology. This indicator has received special attention from authorities and is among the metrics considered within the United Nations' 17 Sustainable Development Goals [8]. The rest of the waste is disposed of in uncontrolled landfills and open-air dumps, which is still a common final waste disposal practice in some municipalities. The presence of almost 5,000 open-air dumps nationwide raises environmental, social, and health concerns, representing a significant challenge for public policies in environmental and social matters [17].

Recovery and recycling. Traditionally, waste collection for recycling in Argentina has been dominated by waste pickers (also referred to as the "cartoneros"). In the city of Buenos Aires alone, it is estimated that the waste pickers recover about the 12% of the waste generated in the city [9]. Regarding particularly paper and cardboard, the recovery rate have risen over the past decade, explaining 50% of the total paper and cardboard consumed by the industry nowadays. Regarding plastic, in 2021 around 286,000 tons of plastics were recycled in Argentina [17], a nearly 25% increment from the year 2017 [11]. Additionally, the substantial presence of organic matter in disposal sites has led to the utilization of biogas from sanitary landfills [17], along with composting when organic waste is properly separated. Since approximately 50% of waste generated in Argentina is organic, these approaches hold potential for reducing landfill volumes, particularly in densely populated cities with limited available space [19].

3 SWOT analysis of a MSW management system: the case study of Bahía Blanca

In this Section, the SWOT analysis of the MSW system of the Argentine city of Bahía Blanca is presented as a case study. In particular, this Section includes a

6 Rossit et al.

succinct description of the MSW system of the city, the main Strengths, Weaknesses, Opportunities and Threats (SWOT) of the system identified by a group of experts, and the outline of the strategies derived from SWOT analysis to improve the system.

3.1 Description of the case study

The city of Bahía Blanca lies on the southern shores of the Bahía Blanca estuary and is a vital hub for commerce, industry, and maritime activity. The city boasts a mix of modern infrastructure and historical architecture, along with educational institutions, cultural venues, and recreational spaces. With a population of around 330,000 inhabitants, Bahía Blanca plays a significant economic role in the region and serves as a gateway to the Patagonia region.

Regarding the MSW system of the city, the budgetary expense in the system for the whole 2023 is expected to be around 35 million US\$, representing 14% of the municipal budget [21], which is larger than the national average of 9% [6]. Since the enactment of National Law No. 25916 [7], the city has implemented numerous initiatives to improve the system, such as, eradication of municipal open-air dumps, construction of a sanitary landfill, installation of a recyclable MSW separation and recycling plant, installation of clean points (recyclable differentiated MSW containers), and various programmes that promote source separation and recovery of MSW. Although, the recovery programmes register a great response from the population, recent field studies have identified that strong information campaigns are needed to extend source classification and recycling among population [26].

The waste produced in the city has two major destinations. These are the Recycling Plant located in the separated neighborhood of General Cerri (15km far from the downtown), which receives the material from almost all the recovery programs and clean points in the city, and the landfill located outside the city (around 12km from the downtown), which receives unclassified mixed waste for final disposition. The landfill, due to its intensive use and the semiarid climate of the area -that hinders waste biodegradation-, is almost at the limit of its capacity [22]. Moreover, the payment that the municipality performs to the company that handles the landfill is one of the most expensive contract managed by the municipality [5] (around 12.40 US\$ per ton of waste that is sent to the landfill [20]). Currently, in the city of Bahía Blanca there is a door-to-door waste collection, with a frequency of six times per week. The waste collection is divided in 32 collection sectors for managerial reasons [18]. The sectors were determined based on the historical experience of the managers [4]. The city has no transfer station and, thus, the collection vehicles transport the waste directly from the neighborhoods to the landfill or the Recycling Plant [18].

A few months ago the municipality started to implement a program to perform source classified waste collection in several neighborhoods. The program consists of reserving one of the six days in which collection is performed only for recyclable materials (e.g., paper, cupboard, plastics, etc.). The amount of recovered material sent to the Recovery Plant was 130.55 tons in 2021, 155 tons

in 2022 (it has to be considered that from January to June the plant was out of service due to major maintenance) and 85 tons in the term Jan-April 2023. Regarding the landfill, it received around 138 tons in 2021, 170.9 tons in 2022 and 73 tons in the term Jan-April 2023 [21]. The quantity of material sent to the Recovery Plant is remarkably large considering that the amount of recyclable waste produced in the city is estimated in only one third of the total waste [5]. Similarly to national average, around 50% of the waste is organic which is mostly generated in neighborhoods with low socioeconomic level [28]. The city occasionally witnesses the emergence of uncontrolled open-air dumps; however, the local government is dedicated to mitigating their appearance and promptly addressing them when they do occur.

3.2 SWOT analysis

This Section includes the description of the SWOT factors of the MSW system of Bahía Blanca proposed by a group of experts, the rating of each factor proposed by the authors and finally the strategies to improve the MSW system.

SWOT factors SWOT methodology is a strategic planning framework used by businesses and organizations to assess their internal and external environments. The acronym "SWOT" stands for Strengths, Weaknesses, Opportunities, and Threats. By evaluating the interplay of these four factors, organizations can develop strategies to leverage their strengths, address their weaknesses, seize their opportunities, and mitigate their threats. This evaluation serves as a foundation for informed decision-making and strategic planning across various aspects of the organization [12].

The SWOT methodology starts with research questions. The primary research questions that were developed for the case study are presented and explained below. These questions were designed with the aim of collecting information about the situation and the perspectives of the waste management system in Bahía Blanca. The questions were replied by several experts, including decision makers of the municipality, personnel of the companies in charge of waste collection and landfill management, and members of the local academic community whose research field is related to waste management. In the following sections we present for each factor the research question and the main outcomes.

Q1: What are the strengths (S) of the current municipal solid waste management system of Bahía Blanca?

The aim of this question is to examine the internal strengths of the MSW system to provide a service of decent quality to the citizens while also diminishing the negative impact of waste generation over the local environment. The identified strengths (S) by the group are:

- (S1) Current door-to-door collection and final disposal system is working correctly with a low level of complaints from the citizens.

8 Rossit et al.

- (S2) One day of the door-to-door collection is dedicated to gather recyclable waste in some neighborhoods.
- (S3) A series of implemented projects and programmes for increasing the amount of source classified waste and raising environmental awareness in the community.
- (S4) Personnel from the waste collection company has a vast experience in the subject.
- (S5) Waste pickers are well organized in cooperatives and have experience in collection and handling of recyclable material.
- (S6) Existence of a municipal web portal of updated open access basic data about the MSW system.
- (S7) Willingness of the decision makers to improve the MSW system in order to increase its economical, social and environmental sustainability.

Q2: What are the weaknesses (W) of the current state of the waste management system of Bahía Blanca?

The aim of this question is to understand the internal weak points of the MSW system that make it difficult to provide an economic and sustainable service of high quality. The identified weaknesses (W) are:

- (W1) Little dissemination of information campaigns and programs for community awareness.
- (W2) Outdated technology (equipment and systems).
- (W3) Little continuity of senior managers within both the municipality and the predominantly state-owned waste collection company due to political instability, which hinders the establishment of a consistent and long-term MSW management policies.
- (W4) Percentage of municipal budget dedicated to waste management is high compared to the national average.
- (W5) Several neighborhoods in which source classified collection has not been applied.

Q3: What are the opportunities (O) for the waste management system of Bahía Blanca to become more efficient and sustainable considering the outcome in economic, social and environmental aspects?

The third question examines the aspects from the context outside the current MSW system that can be used for improving the system. The identified opportunities (O) are:

- (O1) Possibility of reducing the environmental impact through the increment in separation and recycling rates of the city.
- (O2) Existence of a local academic and professional community involved in the study of waste management and recycling and recovery technologies.
- (O3) Existence of a market for the sale of recyclable material.
- (O4) Integration of cooperatives of waste pickers into new sources of work due to the possible increment in the volume of material destined for recycling.

- (O5) Successful experience of community-bins based collection system in other Argentine cities.
- (O6) Successful experience of biogas and composting plants in other Argentine cities.

Q4: What are the threats (T) for the waste management system of Bahía Blanca to become more efficient and sustainable considering the outcome in economic, social and environmental aspects?

The fourth question examines the aspects from the context outside the current MSW system that can negatively affect the system. The identified threats (T) are:

- (T1) Lack of motivation and commitment from the population, due to the discontinued application of previous waste differentiation campaigns.
- (T2) Economic fluctuations in the country that affect public budgets and the lifestyle of waste pickers.
- (T3) Regular emergence of uncontrolled open-air dumps in outskirts of the city.

Rates of factors In SWOT analysis, a useful addition is to rate the factors according to two main aspects: the degree in which they are under/outside the control of the system and their impact in the efficiency of the system [12]. Regarding the control that the MSW system has over the factor, the factors were ranked in a scale from -5 to 5, in which -5 represents that the factor is completely outside the control of the MSW system while 5 represents the opposite, i.e., the factor is completely under the control of the system. Regarding their impact on the efficiency of the system, the factors were ranked in a scale from -5 to 5, in which -5 represents that the factor is a major inhibitor of the MSW system while 5 represents that the factor is a major enhancer of the system. Treating these rates as coordinates, they are presented in a two-dimensional grid in Figure 2. This grid provides a visual representation of how each factor is positioned in terms of its control and its impact on the performance of the MSW system.

Strategies Considering the replies to the research questions, the following strategies were developed by combining the different factors. These combinations led to four groups of strategies that are presented in Table 1.

The strategies outlined in Table 1 vary in their execution horizon. For example, a short-term strategy like (W4.T3) can be promptly implemented to improve the efficiency of the MSW system with the following actions: monitoring the collection sectors of the city, making adjustments to minimize truck travel distances, and collaborating with drivers to enhance driving skills and reduce fuel consumption. An example of a medium-term strategy is (W3.O2) which focuses on ensuring greater job stability for senior managers. Currently, the waste collection company is predominantly state-owned. However, implementing local regulations could assure managers that their positions will extend beyond the tenure of political authorities. Finally, an example of long-term strategy is (W4.O7), which demands meticulous consideration. The installation of a

10 Rossit et al.

Table 1. Strategies of the SWOT analysis for improving the system.

Strategies Strength-Opportunities	
(S3.O3)	Deepen the dissemination of programs to increase the volume of material to be recycled.
(S4.O2)	Design, plan and put into operation a new waste collection, separation and final disposal system, using previous studies and models developed by the local academic community and taking advantage of experienced personnel.
(S5.O4)	Evaluate the quality and quantity of new jobs for waste pickers based on the projected volume of waste to be recycled.
(S6.O2)	Encourage new mechanisms that allow speeding up the information upload processes in the municipal portal so that they can be used for studies and analysis by the local academic community.
(S7.O5)	Study the implementation of community-bins based system in highly-populated parts of the city to improve collection efficiency.
(S7.O6)	Study the implementation of biogas and composting plants taking advantage of the large amount of organic waste produce in the city.
Strategies Strength-Threats	
(S3.T1)	Use ongoing programs to raise awareness among the population about the consequences of the indiscriminate disposal of waste in the city, and encourage them to collaborate in social and environmental improvement.
(S7.T2)	Contribute to improve the labor stability of the waste pickers, formalizing their activity in order to have a greater degree of social coverage, e.g., incorporating them in the current Recycling Plant or in the potential biogas or composting plants.
Strategies Weaknesses-Opportunities	
(W1.O3)	Use the experiences in other cities as a motivating element to raise awareness among citizens.
(W2.O2)	Incorporate highly qualified staff to implement new technologies in the system.
(W3.O2)	Improve the selection process for senior managers in waste management and provide greater job stability for these positions.
(W4.O5)	Study the impact of community bins-based system to the collection cost of the system.
(W4.O6)	Study the implementation of biogas and composting plants to reduce the amount of waste sent to the landfill which is expensive for the city.
(W5.O1)	Expand the one day door-to-door collection of recyclable material to the rest of the neighborhoods.
Strategies Weaknesses-Threats	
(W3.T1)	Enunciate local laws that make it possible to ensure the continuity of the system policies regardless of the managers in charge of the decisions.
(W4.T3)	Enhance the cost-effectiveness of waste management expenditure.

Analysis of a MSW system by means of SWOT methodology 11

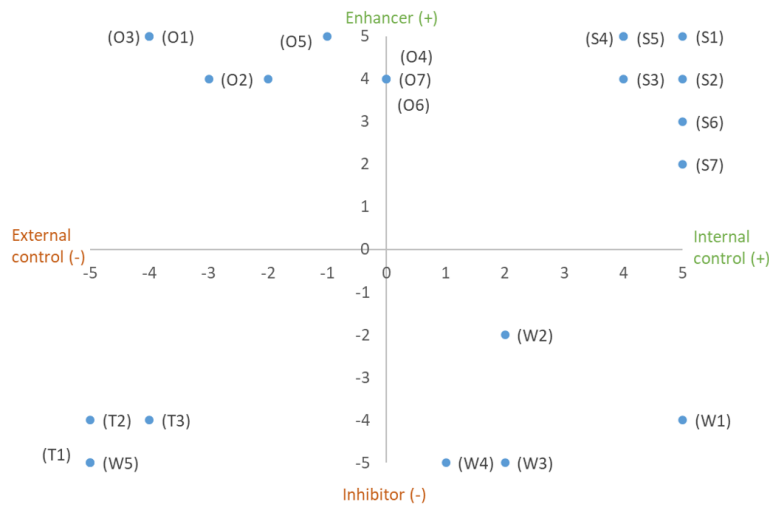


Fig. 2. Rates assigned to each factor.

biogas and composting facility requires a thorough feasibility study, and if the outcome of the feasibility study is positive, a substantial investment for building the facility.

4 Discussion and future work

Municipal Solid Waste (MSW) management systems play a pivotal role in building sustainable urban environments. Not only they allow to process waste with minimal environmental and social impact but also they gather recyclable material that can be used to reduce the amount of raw materials used by modern cities. This article conducted a comprehensive evaluation of material and waste flows in contemporary cities, followed by an in-depth analysis of MSW management practices in Argentina. As a case study, the MSW system in a specific Argentinean city was scrutinized using the SWOT methodology, revealing the efficacy of this approach in devising strategies for enhancing MSW systems. Future research lines include employing the SWOT methodology to analyze the MSW systems of other cities for comparative purposes. This expansion of research will hopefully further enrich the understanding of effective waste management strategies.

Acknowledgements This work was partly supported by PICT-2021-I-INVI-00217 of the Agencia I+D+i of Argentina and PIBAA 0466CO of CONICET.

12 Rossit et al.

References

1. Barles, S.: History of waste management and the social and cultural representations of waste. In: *The basic environmental history*, pp. 199–226. Springer (2014)
2. Brunneder, J., Dholakia, U.: The self-creation effect: making a product supports its mindful consumption and the consumer's well-being. *Marketing Letters* **29**, 377–389 (2018)
3. Castillo, M., Tarando, M., Collado, J., Fatone, M.: Guía para la implementación de la gestión integral e inclusiva de residuos. Tech. rep., Ministerio de Ambiente y Desarrollo Sostenible, Argentina (2021), available in https://www.argentina.gob.ar/sites/default/files/2021/12/guia_para_la_implementacion_giirsu_24_feb_2022.pdf (Accessed: aug-2023).
4. Cavallin, A.: Análisis de eficiencia y elaboración de propuestas de mejora de la GIRSU en municipios del SO de la Pcia. de Buenos Aires y de Cataluña a través de modelos integrados por DEA y RNA. Ph.D. thesis, Universidad Nacional del Sur, Bahía Blanca, Argentina (2019)
5. Cavallin, A., Rossit, D., Herrán, V., Rossit, D., Frutos, M.: Application of a methodology to design a municipal waste pre-collection network in real scenarios. *Waste Management & Research* **38**(1_suppl), 117–129 (2020)
6. Centro Regional de Estudios Económicos de Bahía Blanca: Evolución reciente del gasto público municipal en Bahía Blanca: trayectoria y composición. *Indicadores de Actividad Económica* **170** (2019)
7. Congreso Nacional de Argentina: Ley N° 25.916 Gestión de Residuos Domiciliarios (2004), available in <https://www.argentina.gob.ar/normativa/nacional/ley-25916-98327/texto> (Accessed: aug-2023).
8. Consejo Nacional de Coordinación de Políticas Sociales, Argentina: Informe de país. Argentina 2023. Agenda 2030 (2023), available in https://www.argentina.gob.ar/sites/default/files/informe_pais_baja.pdf (Accessed: aug-2023).
9. De Munain, D., Castelo, B., Ruggerio, C.: Social metabolism and material flow analysis applied to waste management: A study case of autonomous city of Buenos Aires, Argentina. *Waste Management* **126**, 843–852 (2021)
10. Ferreira, C., Gonçalves, G.: A systematic review on life extension strategies in industry: The case of remanufacturing and refurbishment. *Electronics* **10**(21), 2669 (2021)
11. Holland and Circular Hotspot: Waste management country report: Argentina (2023), available in https://hollandcircularhotspot.nl/wp-content/uploads/2021/04/Report_Waste_Management_Argentina_20210322.pdf (Accessed: aug-2023).
12. Leigh, D.: *Handbook of Improving Performance in the Workplace*, chap. SWOT analysis, pp. 115–140. Wiley Online Library (2009)
13. Louis, G.: A historical context of municipal solid waste management in the United States. *Waste management & Research* **22**(4), 306–322 (2004)
14. Lozupone, M.: La gestión de los RSU en los municipios argentinos. Tech. rep., Fundación Centro de Estudios para el Cambio Estructural (2019), available in <http://fcece.org.ar/wp-content/uploads/informes/gestion-rsu-municipios-argentinos.pdf> (Accessed: aug-2023).
15. Miao, X., Magnier, L., Mugge, R.: Switching to reuse? An exploration of consumers' perceptions and behaviour towards reusable packaging systems. *Resources, Conservation and Recycling* **193**, 106972 (2023)
16. Ministerio de Ambiente y Desarrollo Sostenible, Argentina: Informe del estado del ambiente 2020 (2020), available in <https://www.argentina.gob.ar/sites/default/files/residuos.pdf> (Accessed: aug-2023).

17. Ministerio de Ambiente y Desarrollo Sostenible, Argentina: Informe del estado del ambiente 2021 (2021), available in <https://www.argentina.gob.ar/noticias/esta-disponible-para-consulta-un-nuevo-informe-del-estado-del-ambiente-0>
18. Molfese, S., Rossit, D., Frutos, M., Cavallin, A.: Optimization of waste collection through the sequencing of micro-routes and transfer station convenience analysis: An Argentinian case study. *Waste Management & Research* **41**(7), 1267–1279 (2023)
19. Morero, B., Vicentin, R., Campanella, E.: Assessment of biogas production in argentina from co-digestion of sludge and municipal solid waste. *Waste management* **61**, 195–205 (2017)
20. Municipalidad de Bahía Blanca, Argentina: Decreto 2030/2023 Continuidad servicio Proyecto, Construcción y Operaciones del Relleno Sanitario (may 2023), available in <https://www.bahia.gob.ar/decretosyresoluciones/decreto/24/2023/2030/> (Accessed: aug-2023).
21. Municipalidad de Bahía Blanca, Argentina: Portal Datos Bahía (2023), available in <https://datos.bahia.gob.ar/> (Accessed: aug-2023).
22. Rossit, D., Tohmé, F., Frutos, M., Broz, D.: An application of the augmented ϵ -constraint method to design a municipal sorted waste collection system. *Decision Science Letters* **6**(4), 323–336 (2017)
23. Rossit, D., Neschachnow, S.: Waste bins location problem: A review of recent advances in the storage stage of the municipal solid waste reverse logistic chain. *Journal of Cleaner Production* **342**, 130793 (2022)
24. Santalla, E., Córdoba, V., Blanco, G.: Greenhouse gas emissions from the waste sector in Argentina in business-as-usual and mitigation scenarios. *Journal of the Air & Waste Management Association* **63**(8), 909–917 (2013)
25. Savino, A., De Titto, E.: Sustainable waste management challenges in argentina. In: *Sustainable Waste Management Challenges in Developing Countries*, pp. 1–34. IGI Global (2020)
26. Savoretti, A., Barbosa, S.: Residuos sólidos urbanos en Bahía Blanca: Conocimientos y prácticas. *Indicadores de Actividad Económica CREEBA* **170**, 28–35 (2021)
27. Tchobanoglous, G., Kreith, F.: *Handbook of solid waste management*. McGraw-Hill Education (2002)
28. Vazquez, Y., Barragán, F., Castillo, L., Barbosa, S.: Analysis of the relationship between the amount and type of msw and population socioeconomic level: Bahía Blanca case study, Argentina. *Heliyon* **6**(6) (2020)
29. Wilson, D.: A brief history of solid-waste management. *International Journal of Environmental Studies* **9**(2), 123–129 (1976)

Smart city Green fintech: impact of the EU policies on Sustainable Urban Development and Financial innovations

Olegs Cernisevs¹[0000-0003-1859-4102] and Sergejs Popovs²[0000-0002-6495-7237]

¹ Research Department, SIA StarBridge, Riga, Latvia
Olegs.cernisevs@star-bridge.lv

² Department of Biotechnology, Daugavpils University, 5401 Daugavpils, Latvia
sergey.p@email.com

Abstract. Green Fintech is a transformative concept with the potential to revolutionize the urban financial systems and shape a sustainable urban future. This review focuses on the transformational potential of Green Fintech in the context of using technological advances like the Internet of Things, Artificial Intelligence, Blockchain, and Big Data. The authors analyse the role of European policy frameworks and take a multi-faceted look at the ecosystem of the main Smart City stakeholders: municipalities, urban planners, fintech enterprises, residents, and investors. Barriers to Green Fintech such as regulatory complexities, technological barriers, and the need for genuine urban engagement were addressed. Development trends were examined and recommendations to stakeholders were provided.

Keywords: Green Fintech, Smart City, EU.

1 Introduction

In the contemporary era, the combination of urbanization and technological advancement has led to a paradigm shift in the design and implementation of urban habitats, referred to as "smart cities". [1, 2] These urban configurations, characterized by the smart use of technology to improve efficiency and sustainability, are increasingly using financial technology (fintech) as a tool. [3–6]

An analysis of the history of fintech reveals that it originated in the disruption of traditional banking and the rise of digital money solutions. However, its trajectory has subsequently broadened to include innovative strategies towards enhancing the environmental sustainability. [1, 7] This link between fintechs and environmental challenges has given rise to the concept of "Green Fintech" [8–10], an emerging field that is expected to play a transformative role in smart and sustainable urban development.

European urban landscapes, characterized by the combination of historical significance and technological innovation, are becoming the embodiment of this transformative shift. Sustainability has become one of the cornerstones of contemporary smart city [11–13]. The European Union is creating many technological opportunities and policy frameworks to support these cities in their aspiration for a sustainable urban future. [1, 14, 15] In particular, over the past five years, the EU has been actively launching a

2

number of initiatives in the fintech sphere, emphasizing the region's commitment to building a sustainable financial architecture. [16–21].

A critical examination of this field requires an understanding of the diversity of stakeholders. The stakeholders involved in the construction of green fintech in smart cities range from city governments and urban planners, to innovative fintech companies and the urban population. With their distinct roles and contributions, these stakeholders facilitate the rationalization of regulations, innovation, demand, and practical applicability.

At the same time, technological advances are catalysing the potential of this ecosystem. The Internet of Things (IoT), with its profusion of real-time data [22]; blockchain, with its promise of transparent decentralization [6, 23, 24]; Artificial Intelligence (AI), with its analytical and predictive capabilities [25, 26]; and Big Data methodologies, extracting information from urban data repositories [27, 28], collectively constitute the technological backbone. This foundation is being used to shape Green Fintech, often referred to as "Green Financial Technology" and positioned at the intersection of innovation and environmentally responsible practices. [9, 29] This emerging field uses advanced cutting-edge technologies such as blockchain, artificial intelligence, big data analytics, and the Internet of Things (IoT) to create the financial solutions that prioritize ecological preservation and promote sustainable economic growth.

At its core, green fintech encompasses a wide range of financial products, services and platforms designed to facilitate eco-conscious investments, reduce environmental impact and facilitate the transition toward a greener and more sustainable economy [8, 30]. These initiatives can range from digital platforms that enable individuals and institutions to make green investment choices to sophisticated tools that monitor and reduce or mitigate carbon emissions associated with financial activities. Green fintech is a fundamental shift in the financial industry aligning it with the global efforts to combat climate change, achieve the Sustainable Development Goals and to contribute to responsible economic development. In essence, green fintech represents a paradigm transformation that emphasizes the financial sector's commitment to environmental stewardship and sustainable financial practices.

However, the path towards a Green Fintech smart city is complicated. This presents the challenge of finding the delicate balance between the urban environment and the dynamism of financial innovation, to solve the issues related to security, scaling and system integration arise. Furthermore, transitioning the urban populace from passive beneficiaries to active participants necessitates strategic interventions awareness and trust.

However, the path to creating a green smart city using fintech is associated with certain challenges. Finding the delicate balance between the urban regulatory frameworks and the dynamism of financial innovation is challenging. Additionally, the integration of these technologies introduces the challenges related to security, scalability and system integration. [31–34] Furthermore, the transition of urban populations from passive beneficiaries to active participants requires strategic interventions in fostering awareness and trust. [15, 35, 36]

In this review, we undertake an analytical study of the Green Fintech ecosystem within smart cities. We carefully examine its foundational elements, evaluate the

implications of recent EU fintech initiatives, and discuss potential challenges and bottlenecks. We then identify some of the emerging trends and offer the recommendations to various stakeholders.

The main objective of this review is to reveal the potential of Green Fintech as a key element in shaping a technologically advanced, environmentally sound and financially inclusive urban environment. Through this discussion, we aim to contribute to the academic dialog at the intersection of urban development, technology, financial systems and sustainable development.

2 Background

The transformation of cities into smart cities, deeply rooted in technology and data analytics, has its historical roots in the evolution of definitions and goals of urban development. [25, 31, 37, 38] However, parallel to this transformation was the rise of financial technology. [5, 6, 39, 40] As cities began to adopt the technology to improve civic life, the financial sector also began utilizing the technological advancements to redefine and simplify the financial processes.

Fintech's incorporation into urban planning represented a convergence of technological growth and financial innovation. The aim was not just streamlined payments but an integrated financial ecosystem which resonated with the digital infrastructures of smart cities. These digital solutions have revolutionized how financial transactions could operate within the broad context of urban life. [5]

However, we cannot fully understand the progression of smart cities and fintech without discussing the global emphasis on sustainable development. The Paris Agreement is a monumental step in global climate policy, mandating signatory countries to shift their economic gears towards sustainable growth. [41] This emphasis on sustainable development is not confined to the environmental community only but extends to many other areas including the financial sector.

Central to this discussion on sustainability is the concept of "sustainable development" as presented in 1987's "Our Common Future", famously known as the Brundtland Report. [1, 42–44] Sustainability is defined as the notion of meeting present needs without compromising the ability of future generations. This concept has served as the foundation for subsequent international conventions and policies. [43, 44]

The "2030 Agenda for Sustainable Development" adopted in 2015, further elaborated on this, outlining 17 Sustainable Development Goals (SDGs). Despite criticism regarding their broad framing and implementation challenges, these goals set a global direction. However, their broad scope, ranging from poverty reduction to climate action, emphasized the financial resources required for implementation. [45]

With the financial challenges of sustainable development becoming evident, the role of the financial system gained paramount importance. The traditional banking sector, while an important player, has faced challenges and disruption from technological innovation. This disruptive wave has led to the emergence of "Fintech" with investments reaching an astounding \$215.4 billion by 2019 [46]

4

Within the developing fintech industry, a specialized niche called "green Fintech" emerged. Its main goal was to use the financial technologies to solve environmental problems. This underlined their relevance, especially in the context of climate related risks.

Green Fintech involves many stakeholders, ranging from consumers to regulators. It demonstrates how technological innovation in finance can be aligned with global sustainability goals. Green fintech becomes a cornerstone of a wide range of sustainable development measures with the potential to significantly impact climate mitigation and adaptation, particularly in developing countries. [8, 9]

Therefore, as the world faces the challenges of climate change and strives for sustainable development, the symbiosis of smart cities, fintech and green initiatives represents an opportunity for innovation. Their interconnected growth stories, deeply influenced by global sustainability agreements and the technological revolution, underline the potential for a future in which finance and technology will drive global sustainability.

3 Methodology

Our review undertakes a multifaceted methodological approach to understand the alignment and potential synergies between fintech initiatives and sustainable performance in the EU smart cities. This methodology is structured to offer a holistic understanding of how financial technologies are influencing the sustainability trajectories of urban environments in the European Union.

To assess the EU Fintech Initiatives, we have compiled a list of recent EU fintech initiatives from official EU repositories, policy documents and fintech industry reports. Each initiative was critically assessed in terms of its objectives, scope, and potential impact on sustainable urban development. We used the approach of Sala S. et al., 2021 [47], modified for our needs for this purpose.

The estimated documents were analysed for their applicability to the sustainability concept. On the basis of the evaluated EU initiatives and challenges of sustainability concept the authors have drawn the conclusion on the benefits and implications of these initiatives.

4 The Ecosystem of Smart City Green Fintech

The future of urban sustainability is changing as a result of the combination of fintech and green initiatives in the context of smart cities. The complicated ecosystem supporting Smart City Green Fintech plays a key role in this transformation. A complex analysis is necessary to comprehend this ecosystem, taking into account the main urban stakeholders, technological advancements, and the context of recent EU fintech initiatives. [14, 48, 49]

The ecosystem of Green Fintech in smart city is conceptually shown in Fig. 1

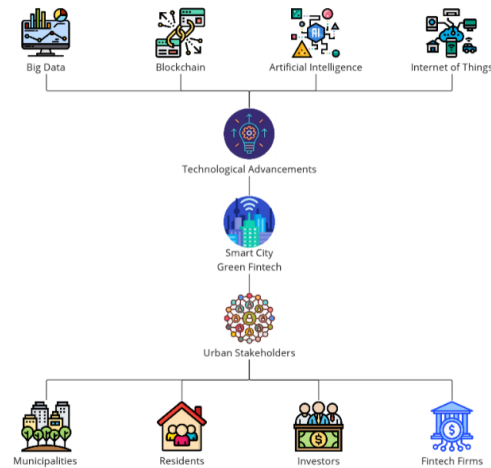


Figure 1. Conceptual model of Smart City Green Fintech ecosystem

4.1 Urban Stakeholders

Municipalities embrace local governments and municipal bodies. It is crucial to incorporate green fintech into urban policies and infrastructure, and local governments and municipal bodies play a key role in this. The smooth incorporation of sustainable financial solutions into the urban environment is ensured by their role in setting rules, offering incentives, and encouraging public-private partnerships. [50, 51]

Urban planners, who are tasked with creating the blueprint for smart cities, play a crucial role in integrating fintech solutions into city plans to ensure accessibility and easy integration with other urban systems like waste, energy, and transportation. [52, 53]

Fintech companies are at the forefront of financial innovation. They offer novel solutions that promote sustainable financial transactions. Their businesses, which range from eco-friendly investment platforms to green bonds, become vital to the development of green fintech in smart cities.[54]

The demand for green fintech products is shaped by the urban residents, who are the ultimate beneficiaries of these solutions. In order to improve and scale fintech applications in the urban environment, it is crucial to take into account their preferences, needs, and feedback loops.

Fintech startups and projects receive critical funding from investment communities like venture capitalists, angel investors, and green funds. Their reliability and investment standards frequently determine the course of fintech innovation in the sustainability sector.

6

4.2 Technological Advancements

IoT presents a data mine with connected devices affecting every aspect of urban life. For example, when it comes to real-time energy consumption or waste management, fintech makes use of this data to provide green financial solutions. [55]

The precision and effectiveness of financial services in smart cities can be improved by using AI's predictive capabilities to forecast environmental effects, inform sustainable investments, and optimize green financial transactions. [56, 57]

Blockchain, known for its decentralized and transparent nature, has found applications in Green Fintech. Green fintech has embraced blockchain, known for its decentralized and transparent nature. These applications include ensuring transparent carbon credit trading, confirming the reliability of green bonds, and simplified peer-to-peer energy transactions. [6, 24, 37, 58, 59]

Big data technologies are used to examine the enormous data storage facilities of contemporary cities. Fintech companies can tailor sustainable financial solutions based on current urban dynamics as a result of this data-driven technique. [27, 60]

4.3 EU's Last 5 Years Fintech Related Initiatives

Over the past five years, the European Union has introduced a number of initiatives in recognition of the transformative potential of fintech:

- EU Fintech Action Plan (2018): This is a comprehensive strategy to drive innovation and competition in the financial sector, focusing on creating a more inclusive financial environment and utilizing rapid technological advances.
- Regulatory Sandbox Framework (2020): Framework aimed at fostering innovation by allowing fintech firms to test their solutions in a controlled environment under regulatory supervision.
- Digital Finance Package (2020): This initiative outlines strategies for a competitive EU financial sector that fosters digitalization, addresses new challenges and enhances financial products' resilience and sustainability.
- MiCA (Markets in Crypto-assets Regulation, 2020): Setting clear regulations for crypto assets and their providers, MiCA aims to harness the potential of crypto in sustainable urban finance while safeguarding investors and users.
- European Blockchain Partnership (EBP, 2018): By fostering collaborations between member states, the EBP aims to build a pan-European blockchain infrastructure, which holds significant promise for green fintech applications in smart cities.
- ECB's Digital Euro Initiative (2021): Recognizing the transformative potential of digital currencies in reshaping the financial landscape, the European Central Bank (ECB) announced its plans to develop a digital euro. This initiative aims to complement physical cash and ensure that consumers can access a safe form of money in an increasingly digitalized world. Additionally, stakeholders view the digital euro as a tool that strengthens the Eurozone's monetary sovereignty in the global arena. It could play a pivotal role in green fintech solutions within smart cities. The digital euro can further streamline sustainable financial

solutions in urban environments by facilitating instant transactions, reducing costs, and integrating with other digital financial platforms. The ECB is committed to making sure that the digital euro meets the expectations and needs of consumers and financial stakeholders, this is why it has taken such a precise approach, focusing on public consultations and demanding testing phases.

The ecosystem of Smart City Green Fintech is a dynamic integration of various stakeholders, cutting-edge technologies, and supportive policy frameworks. The EU's recent fintech initiatives further enhance this ecosystem's potential, oriented on a sustainable, technologically advanced urban future.

5 Benefits of Integrating Green Fintech in Smart Cities

The authors have analysed the EU initiatives in relation to Green Fintech in three areas: environment, economy, society. The tables below summarise the impact of the considered EU initiatives on these areas.

5.1 Environmental Benefits

Table 1. Environmental Benefits and Implications.

Initiative	Environmental Benefits	Implications
EU Fintech Action Plan (2018)	Promotes green investments	Positive impact on EU financial sector
Regulatory Sandbox Framework (2020)	Encourages eco-conscious innovation	Ensuring fintech solutions meet regulations
Digital Finance Package (2020)	Enhances sustainable financial products	Enhancing resilience and sustainability
MiCA (Markets in Crypto-assets Regulation, 2020)	Facilitates sustainable crypto innovations	Safeguarding investors and users
European Blockchain Partnership (EBP, 2018)	Supports green fintech applications	Potential for green fintech in smart cities
ECB's Digital Euro Initiative (2021)	Streamlines green financial solutions	Potential pivotal role in green fintech solutions

The environmental benefits of various fintech initiatives presented in the table highlights the key and symbiotic relationship between financial technology and achieving sustainability goals in smart city environments. These initiatives, ranging from comprehensive European Union policies to finely designed regulatory frameworks and innovative digital solutions, are collectively having a significant impact in shaping environmentally responsible financial practices. Through the promotion of green investment, cultivation of eco-conscious innovation, and the facilitation of sustainable financial products, these initiatives are playing a crucial role in reducing the environmental footprint associated with urban development. They serve as a catalyst for integrating green fintech solutions into the foundation of smart cities, thereby emphasizing the need for financial technology to align with environmental imperatives.

8

Moreover, these initiatives exemplify the complex and interconnected relationship between economic and environmental aspects. By stimulating the economic growth, promoting competition and driving financial innovation, they simultaneously contribute to enhancing the resilience and sustainability of urban ecosystems. Consequently, they offer promising opportunities for harmonizing economic prosperity and environmental well-being. As development progresses, it becomes increasingly evident that sustainable urban development requires an integrated approach that takes into account not only economic and environmental, but also social dimensions. Therefore, the multidimensional environmental benefits highlighted by these fintech initiatives emphasize the relevance of ongoing collaborative efforts, innovative solutions and sustained policy support to move smart cities towards a future characterized by increased sustainability and environmental responsibility.

5.2 Economic Benefits

Table 2. Table captions should be placed above the tables.

Initiative	Economic Benefits	Implications
EU Fintech Action Plan (2018)	Drives economic growth and competition	Positive impact on EU financial sector
Regulatory Sandbox Framework (2020)	Fosters financial innovation and competitiveness	Ensuring fintech solutions meet regulations
Digital Finance Package (2020)	Boosts the financial sector's competitiveness	Enhancing resilience and sustainability
MiCA (Markets in Crypto-assets Regulation, 2020)	Promotes financial stability and growth	Safeguarding investors and users
European Blockchain Partnership (EBP, 2018)	Enables economic opportunities in blockchain	Potential for green fintech in smart cities
ECB's Digital Euro Initiative (2021)	Enhances efficiency and cost-effectiveness	Potential pivotal role in green fintech solutions

The detailed table summarizing the economic benefits of various fintech initiatives highlights the complex and diverse role of financial technology in promoting economic prosperity in the context of smart cities. These initiatives, ranging from high-level EU strategies to more specific regulatory measures and digital innovation, collectively contribute to economic growth, promote competition and stimulating the financial innovation. Their focus on improving the competitiveness of the financial sector and the efficiency of financial services not only empowers urban economies but also lays the foundation for more robust and resilient financial ecosystems. Consequently, these initiatives offer significant opportunities to ensure that economic development is aligned with sustainable development directions.

Furthermore, the economic benefits outlined in the table exemplify the convergence of economic and environmental interests. While the initiatives aim to improve the economic productivity, they also contribute to enhancing the resilience and sustainability of urban environments. This interaction between economic growth and sustainability

represents a promising path toward harmonizing financial success with environmental responsibility. Looking to the future, the multifaceted economic benefits provided by these fintech initiatives highlight the urgent need for continued collaboration, innovation, and policy support. These are essential elements in moving smart cities toward a future characterized by strong, prosperous, and economically sustainable urban landscapes that are in harmony with their environmental and social surroundings.

5.3 Social Benefits

Table 3. Table captions should be placed above the tables.

Initiative	Social Benefits	Implications
EU Fintech Action Plan (2018)	Enhances access to financial services	Positive impact on EU financial sector
Regulatory Sandbox Framework (2020)	Encourages financial inclusion and access	Ensuring fintech solutions meet regulations
Digital Finance Package (2020)	Promotes inclusive finance and accessibility	Enhancing resilience and sustainability
MiCA (Markets in Crypto-assets Regulation, 2020)	Protects users and promotes trust	Safeguarding investors and users
European Blockchain Partnership (EBP, 2018)	Fosters collaboration and knowledge sharing	Potential for green fintech in smart cities
ECB's Digital Euro Initiative (2021)	Facilitates ease of transactions and access	Potential pivotal role in green fintech solutions

A detailed table describing the social benefits arising from various fintech initiatives highlights the profound social implications of financial technology within the framework of smart cities. These initiatives, ranging from comprehensive European Union policies to finely tailored regulatory frameworks and innovative digital solutions, collectively contribute to promoting financial inclusion, accessibility, and trust among urban populations. By promoting inclusive finance and accessibility, advocating for user interests, and encouraging collaborative knowledge sharing, these efforts are key to shaping a more equitable and socially responsible urban landscape. They exemplify the need to align the financial technology with social cohesion and well-being.

Furthermore, the social benefits listed in the table emphasize the dynamic interaction between social, economic, and environmental aspects within the context of smart cities. By promoting financial inclusion and trust, these initiatives also contribute to enhancing the economic competitiveness and environmental sustainability. This synergy between social progress and holistic urban development represents significant prospects of harmonizing the economic prosperity, environmental protection, and social equity. As we progress, the diverse social benefits identified by these fintech initiatives highlight the urgency of ongoing collaborative efforts, innovative solutions, and sustain policy support to move smart cities towards a future characterized by increased social cohesion, equal opportunities, and sustainable urban living.

10

6 Challenges and Roadblocks

Despite the enormous potential, the emerging Smart City Green Fintech ecosystem faces the certain challenges. The integration of various stakeholders, rapidly advancing technologies and the regulatory frameworks creates many complexities. Here we discover the some challenges facing the growth and integration of green fintech in urban settings.

6.1 Regulatory Frameworks

We are balancing city regulations with sustainable financial innovation.

Considering the diversified nature of the Smart City Green Fintech ecosystem, harmonizing regulations becomes a challenging task. In an effort to foster innovation, municipalities might sometimes lag in updating regulations that can keep pace with the rapid advancements in fintech. That can create a challenging environment for fintech companies, restricting their growth and innovation.

The EU's various initiatives, from the Fintech Action Plan to the MiCA regulations, are comprehensive; nevertheless, they might sometimes contradict the local urban laws, creating the cases of bureaucratic red tape. Balancing the broader European vision of the situation with the specific urban nuances is vital for ensuring the smooth integration of green fintech solutions in cities.

6.2 Technological Barriers

Issues related to integration, security, and scalability within urban environments.

Technological advancements like IoT, AI, blockchain, and big data have revolutionized green fintech possibilities. However, they come with their own set of challenges. For instance, integrating multiple technological solutions into a unified urban framework can be demanding and challenging task. Data privacy and security are paramount, especially with financial transactions, and ensuring the integrity of these systems becomes crucial.

Scalability is another concern. While a fintech solution might work smoothly and continuously in a controlled environment or in the small projects, scaling it to correspond to the entire city requirements, with its varied demographics and needs, can present unforeseen challenges and difficulties in finding solutions. Blockchain, for instance, while transparent and decentralized, has faced criticisms over energy consumption and transaction speeds, which need addressing in the context of smart cities.

6.3 Urban Awareness and Engagement

Strategies to involve city residents, ensure trust, and promote the benefits of green fintech.

The involvement and support of smart city residents have the pivotal importance for any urban initiative to succeed. Taking into consideration the novelty of green fintech solutions for population, there's a notable indisputable need for awareness campaigns. Misconceptions or lack of understanding about fintech can hinder its adoption among city inhabitants.

Trust becomes a cornerstone. The combination of finance and technology might raise anxiety about security and transparency, and sometimes there appears even the fear that the traditional banking loses its position. The effective communication is crucial for ensuring the benefits of green fintech in the areas of economic savings, environmental benefits, or convenience.

Moreover, increasing the community engagement, when residents not only use but also contribute to the evolution of fintech solutions, can significantly contribute to the substantial growth and integration of fintech in smart cities.

In conclusion, despite the fact that the ecosystem of Smart City Green Fintech has a promising future, it is necessary to consider the existing challenges to implement the Green Fintech in smart city successfully. Collaborative strategies, adaptive regulations, and a focus on community engagement contribute to integration of finance, technology, and urban sustainability.

7 Future Horizons for Smart City Green Fintech

Fintech has become the inseparable part of smart city, and it is transforming with the concept of smart city. The adopting of sustainability principles influences the development of fintech in smart city. The urban environment is highly dependent nowadays on technological advancements, on cooperation with all stakeholders, on solving the challenging tasks, and fintech can facilitate the urban sustainability through financial technology. This article provides the vision of the emerging trends and critical recommendations to ensure optimal integration and growth of green fintech in urban environment.

7.1 Emerging Trends

The vision of anticipated integration of technological innovation and financial models in smart city context is presented in Fig.2

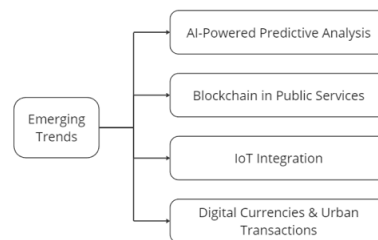


Figure 2. The conceptual vision of emerging Green Fintech trends in smart city

The inclusion of Green Fintech in the concept of smart city has already started, and presented technologies soon will be integral part of smart cities.

The AI-Powered Predictive Analysis, as an element of Artificial Intelligence is becoming more and more sophisticated, it is widely used in all spheres of human life,

12

including smart cities, it is used for forecasting the environmental impacts and making green financial transactions more efficient. It is expected that AI-driven financial models will be tailored to individual city dynamics.

Blockchain nowadays is widely used for financial transactions; however, it is expected that beyond financial sphere it will be employed for other Public Services, ensuring transparency and traceability in areas like waste management or energy consumption.

Nowadays, the Internet of Things is an integral part of smart cities, though it exists in the form of standalone applications. The Holistic IoT Integration assumes, that the real-time data from various sources are used by green fintech platforms for providing the residents with comprehensive information and sustainable financial solutions.

The employment of Digital Currencies in Urban Transactions is the future of smart cities. With the implementation in practice of such initiatives as the digital euro, we can expect expect the substantial growth of the city-centric digital currencies or tokens usage, which will facilitate the local transactions and promote the sustainable urban commerce.

8 Recommendations

Based on the provided analysis of the EU regulatory initiatives and the Green Fintech concept, several proposals can be offered to urban developers, fintech firms, policymakers, and other city stakeholders to optimize Green Fintech integration. Among them are the following ones:

- Collaborative Urban Planning
- Scalable Regulatory Sandboxes
- Community-Centric Fintech Design
- Skill Development
- Holistic Policy Frameworks

8.1 Collaborative Urban Planning and Smart City Green Fintech

Collaborative urban planning is an essential prerequisite for the successful integration of Green Fintech solutions in smart cities. This approach presupposes the active involvement of urban planners, municipalities, and fintech firms from the nascent stages of city planning. By working together, these stakeholders can ensure that Green Fintech solutions are easily incorporated into the city's fabric, addressing the unique challenges and demographics of the urban environment.

8.2 Scalable Regulatory Sandboxes

Scalable regulatory sandboxes provide a conducive environment for fintech companies to test and refine their solutions in a real-world setting. This is crucial for the development of innovative Green Fintech solutions that are tailored to the specific needs of smart cities. By creating a supportive regulatory framework, policymakers can enable

fintech companies to experiment and scale their solutions, accelerating the adoption of Green Fintech in smart cities.

8.3 Community-Centric Fintech Design

Community-centric fintech design is essential for ensuring the widespread adoption and trust in Green Fintech solutions. This approach assumes that the designed fintech solutions are oriented on the city resident as the end-user. Regular feedback loops, awareness campaigns, and trust-building measures can help to create a supportive ecosystem for Green Fintech adoption.

8.4 Investment in Skill Development

Investment in Skill Development is a key factor for the rapid evolution of fintech solutions. Fintech companies need employees with expertise in both finance and technology. By investing in skill development initiatives, policymakers can ensure a steady supply of qualified personnel to support the growth of the Green Fintech sector and to drive fintech innovations.

8.5 Holistic Policy Frameworks

Policymakers within smart cities should have a holistic approach to the processes; in this case the regulations will take into consideration the technological advancements and urban environments' unique challenges. Holistic Policy Frameworks ensures that regulatory activities do not hinder the innovations and do not leave the potential challenges unaddressed.

8.6 Embracing the New Frontier

The horizons of Smart City Green Fintech are bright, with opportunities abounding for all stakeholders. However, it is evident that beyond the numerous opportunities for the Green Fintech development within smart city, success depends on collaboration, adaptability and focus on urban sustainability. Embracement of this new frontier by cities' authorities, technological companies and residents contribute to the sustainable, financially inclusive urban development.

Conclusion

The contemporary urban environment is a dynamic landscape characterized by both challenges and opportunities. Green Fintech, a convergence of financial innovation and environmental initiatives, offers a transformative potential for shaping the future of sustainable urban development.

14

The European Union has taken a leading role in promoting Green Fintech, introducing a series of fintech-related initiatives over the past five years. Such regulatory policies as EU Fintech Action Plan (2018), Regulatory Sandbox Framework (2020), Digital Finance Package (2020), MiCA (Markets in Crypto-assets Regulation, 2020), European Blockchain Partnership (EBP, 2018) and ECB's Digital Euro Initiative (2021) provide a supportive policy framework and demonstrate the strategic importance of fintech in achieving sustainable urbanism. They are beneficial for many dimensions of smart city. The review considers the benefits of these initiatives and their implications in environmental, economic and social spheres.

The Green Fintech ecosystem is a complex structure of interconnected stakeholders, including municipal bodies, city planners, fintech companies, the urban population, and investors. Innovation-driven fintech companies create the core of this ecosystem, developing solutions that align with the urban sustainability goals. Nevertheless, each stakeholder plays a distinct role in enabling the successful integration of Green Fintech solutions; urban population and investors play complementary roles in generating demand and ensuring the financial viability of Green Fintech enterprises.

Traditional financial systems, constrained by outdated structures and practices, often fail to meet the needs of modern urban environments. Green Fintech addresses this shortcoming by bringing flexibility, transparency, and sustainability to urban financial systems.

Technological innovations such as the Internet of Things (IoT), artificial intelligence (AI), blockchain, and big data play an integral role in enhancing the capabilities of the Green Fintech ecosystem. Their successful integration promises a holistic, efficient, and transparent urban financial landscape.

Despite the transformative potential of Green Fintech, there are many challenges that need to be addressed. The complexities of regulation require a deliberate approach to ensure that innovation is not restricted while protecting the public interest. Technology barriers, mainly integration, security and scalability issues, must be carefully addressed. In addition, the urban involvement is essential. It is critical to transform city residents from passive recipients to active participants, which requires robust strategies to raise awareness, build trust and inclusiveness.

To implement the potential of Green Fintech at full scope and to create a more resilient and sustainable future for smart cities, it is essential to address the inherent challenges through a collaborative approach involving policymakers, city developers, fintech companies, and the community.

Therefore, Green Fintech in smart cities is a source of transformative opportunities and addressed challenges.

References

1. European Commission (2010) EUROPE 2020 A European strategy for smart, sustainable and inclusive growth. Brussels

2. Etezadzadeh C (2016) *Smart City – Future City?* Springer Fachmedien Wiesbaden, Wiesbaden
3. Vinod Kumar TM, Dahiya B (2017) *Smart Economy in Smart Cities*. pp 3–76
4. Popova Y, Popovs S (2022) Impact of Smart Economy on Smart Areas and Mediation Effect of National Economy. *Sustainability* 14:. <https://doi.org/10.3390/su14052789>
5. Popova Y, Cernisevs O (2023) Smart City: Sharing of Financial Services. *Soc Sci* 12:. <https://doi.org/10.3390/socsci12010008>
6. Cernisevs O, Popova Y (2023) ICO as Crypto-Assets Manufacturing within a Smart City. *Smart Cities* 6:40–56. <https://doi.org/10.3390/smartsities6010003>
7. Jo S, Han H, Leem Y, Lee S (2021) Sustainable Smart Cities and Industrial Ecosystem: Structural and Relational Changes of the Smart City Industries in Korea. *Sustainability* 13:9917. <https://doi.org/10.3390/su13179917>
8. Mirza N, Umar M, Afzal A, Firdousi SF (2023) The role of fintech in promoting green finance, and profitability: Evidence from the banking sector in the euro zone. *Econ Anal Policy* 78:33–40. <https://doi.org/10.1016/J.EAP.2023.02.001>
9. Muganyi T, Yan L, Sun H ping (2021) Green finance, fintech and environmental protection: Evidence from China. *Environmental Science and Ecotechnology* 7:100107. <https://doi.org/10.1016/J.ESE.2021.100107>
10. Kutty AA, Kucukvar M, Abdella GM, et al (2022) Sustainability Performance of European Smart Cities: A Novel DEA Approach with Double Frontiers. *Sustain Cities Soc* 81:103777. <https://doi.org/10.1016/J.SCS.2022.103777>
11. Mingaleva Z, Vukovic N, Volkova I, Salimova T (2019) Waste Management in Green and Smart Cities: A Case Study of Russia. *Sustainability* 12:94. <https://doi.org/10.3390/su12010094>
12. Lai CS, Jia Y, Dong Z, et al (2020) A Review of Technical Standards for Smart Cities. *Clean Technologies* 2:290–310. <https://doi.org/10.3390/cleantechnol2030019>
13. Popova Y, Spröge I (2021) Decision-Making within Smart City: Waste Sorting. *Sustainability* 13:. <https://doi.org/10.3390/su131910586>
14. Municipality of Rome (2021) *Il piano Roma Smart City*. Roma
15. Laurent Probst, Erica Monfardini, Laurent Frideres, Daniela Cedola (2014) *Business Innovation Observatory : Smart Living*. Brussels
16. European Commission (2017) *FINTECH: A MORE COMPETITIVE AND INNOVATIVE EUROPEAN FINANCIAL SECTOR*. Bruxelles
17. Rupeika-Apoga R, Wendt S (2022) FinTech Development and Regulatory Scrutiny: A Contradiction? The Case of Latvia. *Risks* 10:167. <https://doi.org/10.3390/risks10090167>
18. Briones de Araluze GK, Cassinello Plaza N (2022) Open banking: A bibliometric analysis-driven definition. *PLoS One* 17:e0275496. <https://doi.org/10.1371/journal.pone.0275496>
19. Lavrinenko O, Čižo E, Ignatjeva S, et al (2023) Financial Technology (FinTech) as a Financial Development Factor in the EU Countries. *Economies* 11:45. <https://doi.org/10.3390/economies11020045>

16

20. European parliament (2017) European Parliament resolution of 9 July 2015 on resource efficiency: moving towards a circular economy. European parliament, Brussels
21. European Commission (2014) What are smart cities? In: European Commission official site. https://commission.europa.eu/eu-regional-and-urban-development/topics/cities-and-urban-development/city-initiatives/smart-cities_en. Accessed 7 Jun 2021
22. Khanboubi F, Boulmakoul A, Tabaa M (2019) Impact of digital trends using IoT on banking processes. *Procedia Comput Sci* 151:77–84. <https://doi.org/10.1016/J.PROCS.2019.04.014>
23. Mattila J, Seppälä T, Valkama P, et al (2021) Blockchain-based deployment of product-centric information systems. *Comput Ind* 125:103342. <https://doi.org/10.1016/J.COMPIND.2020.103342>
24. Cernisevs O (2021) ANALYSIS OF THE FACTORS INFLUENCING THE FORMATION OF THE TRANSACTION PRICE IN THE BLOCKCHAIN. *Financial and credit systems: prospects for development* 36–47. <https://doi.org/10.26565/2786-4995-2021-3-04>
25. Heidari A, Navimipour NJ, Unal M (2022) Applications of ML/DL in the management of smart cities and societies based on new trends in information technologies: A systematic literature review. *Sustain Cities Soc* 85:104089. <https://doi.org/10.1016/J.SCS.2022.104089>
26. Dong L, Liu Y (2023) Frontiers of policy and governance research in a smart city and artificial intelligence: an advanced review based on natural language processing. *Frontiers in Sustainable Cities* 5:. <https://doi.org/10.3389/frsc.2023.1199041>
27. Pons-Prats J, Neittaanmäki P, Tuovinen T, et al (2020) *Computation and Big Data for Transport*. Springer International Publishing, Cham
28. Nobanee H, Dilshad MN, Al Dhanhani M, et al (2021) Big Data Applications the Banking Sector: A Bibliometric Analysis Approach. *Sage Open* 11:215824402110672. <https://doi.org/10.1177/21582440211067234>
29. Román Arjona, Julien Ravet (2020) Science, Research anInnovation Performance of the EU 2020 A fair, green and digital Europe. Brussels
30. Popova Y, Popovs S (2023) Effects and Externalities of Smart Governance. *Smart Cities* 6:1109–1131. <https://doi.org/10.3390/smartcities6020053>
31. Gupta A, Panagiotopoulos P, Bowen F (2020) An orchestration approach to smart city data ecosystems. *Technol Forecast Soc Change* 153:119929. <https://doi.org/10.1016/J.TECHFORE.2020.119929>
32. Junior Nascimento da Silva C, Xavier Fortes D, Chagas do Nascimento RP (2017) ICT Governance, Risks and Compliance - A Systematic Quasi-review. In: *Proceedings of the 19th International Conference on Enterprise Information Systems*. SCITEPRESS - Science and Technology Publications, pp 417–424
33. Murinde V, Rizopoulos E, Zachariadis M (2022) The impact of the FinTech revolution on the future of banking: Opportunities and risks. *International Review of Financial Analysis* 81:102103. <https://doi.org/10.1016/J.IRFA.2022.102103>

34. Hummel K, Laun U, Krauss A (2021) Management of environmental and social risks and topics in the banking sector - An empirical investigation. *The British Accounting Review* 53:100921. <https://doi.org/10.1016/j.bar.2020.100921>
35. Savic S, Shi H (2011) An Intelligent Object Framework for Smart Living. *Procedia Comput Sci* 5:386–393. <https://doi.org/10.1016/J.PROCS.2011.07.050>
36. Miloud Dahmane W, Ouchani S, Bouarfa H (2019) A Smart Living Framework: Towards Analyzing Security in Smart Rooms. pp 206–215
37. ROTUNA C, GHEORGHITA A, ZAMFIROIU A, SMADA D-M (2019) Smart City Ecosystem Using Blockchain Technology. *Informatica Economica* 23:41–50. <https://doi.org/10.12948/issn14531305/23.4.2019.04>
38. NAGY S, CSISZÁR C (2020) THE QUALITY OF SMART MOBILITY: A SYSTEMATIC REVIEW. *Scientific Journal of Silesian University of Technology Series Transport* 109:117–127. <https://doi.org/10.20858/sjsutst.2020.109.11>
39. Popova Y (2021) Economic Basis of Digital Banking Services Produced by FinTech Company in Smart City. *Journal of Tourism and Services* 12:86–104. <https://doi.org/10.29036/jots.v12i23.275>
40. Buka S, Surmach A, Cernisevs O (2022) Analysis of Aspects of the Regional Economy in the Digital Economy, Using the Example of Financial Services. *Review of Economics and Finance* 20:203–207. <https://doi.org/10.55365/1923.x2022.20.24>
41. Amini A, Abedi M, Nesari E, et al (2023) THE PARIS AGREEMENT'S APPROACH TOWARD CLIMATE CHANGE LOSS AND DAMAGE. *World Affairs* 186:46–80. <https://doi.org/10.1177/00438200221147936>
42. Marcel Jeucken, Jan Jaap Bouma (2017) *Sustainable Banking*, 1st Edition. Routledge
43. Getz D (2017) Developing a Framework for Sustainable Event Cities. *Event Management* 21:575–591. <https://doi.org/10.3727/152599517X15053272359031>
44. United Nations (2023) *Global Sustainable Development Report 2023*
45. Tóthová D, Heglasová M (2022) Measuring the environmental sustainability of 2030 Agenda implementation in EU countries: How do different assessment methods affect results? *J Environ Manage* 322:116152. <https://doi.org/10.1016/J.JENVMAN.2022.116152>
46. Yokesh Sankar (2023) *Fintech Disruption in Banking: Evolution and Challenges*. Sparkout
47. Sala S, Amadei AM, Beylot A, Ardente F (2021) The evolution of life cycle assessment in European policies over three decades. *Int J Life Cycle Assess* 26:2295–2314. <https://doi.org/10.1007/s11367-021-01893-2>
48. Megatrends Hub (2021) *Megatrend Continuing Urbanisation*
49. Suvarna M, Büth L, Hejny J, et al (2020) Smart Manufacturing for Smart Cities—Overview, Insights, and Future Directions. *Advanced Intelligent Systems* 2:2000043. <https://doi.org/10.1002/aisy.202000043>

18

50. Liu H, Yao P, Latif S, et al (2022) Impact of Green financing, FinTech, and financial inclusion on energy efficiency. *Environmental Science and Pollution Research* 29:18955–18966. <https://doi.org/10.1007/s11356-021-16949-x>
51. Aboalsamh HM, Khrais LT, Albahussain SA (2023) Pioneering Perception of Green Fintech in Promoting Sustainable Digital Services Application within Smart Cities. *Sustainability* 15:11440. <https://doi.org/10.3390/su151411440>
52. Leyzerova A, Sharovarova E, Alekhin V (2016) Sustainable Strategies of Urban Planning. *Procedia Eng* 150:2055–2061. <https://doi.org/10.1016/j.pro-eng.2016.07.299>
53. Mouratidis K (2021) Urban planning and quality of life: A review of pathways linking the built environment to subjective well-being. *Cities* 115:103229. <https://doi.org/10.1016/j.cities.2021.103229>
54. He Z, Liu Z, Wu H, et al (2020) Research on the Impact of Green Finance and Fintech in Smart City. *Complexity* 2020:1–10. <https://doi.org/10.1155/2020/6673386>
55. Rejeb A, Rejeb K, Simske S, et al (2022) The big picture on the internet of things and the smart city: a review of what we know and what we need to know. *Internet of Things* 19:100565. <https://doi.org/10.1016/j.iot.2022.100565>
56. Luusua A, Ylipulli J, Foth M, Aurigi A (2023) Urban AI: understanding the emerging role of artificial intelligence in smart cities. *AI Soc* 38:1039–1044. <https://doi.org/10.1007/s00146-022-01537-5>
57. Herath HMKMB, Mittal M (2022) Adoption of artificial intelligence in smart cities: A comprehensive review. *International Journal of Information Management Data Insights* 2:100076. <https://doi.org/10.1016/j.jjime.2022.100076>
58. Georgiou I, Nell JG, Kokkinaki AI (2020) Blockchain for Smart Cities: A Systematic Literature Review. pp 169–187
59. Rejeb A, Rejeb K, Simske SJ, Keogh JG (2021) Blockchain technology in the smart city: a bibliometric review. *Qual Quant*. <https://doi.org/10.1007/s11135-021-01251-2>
60. Al Nuaimi E, Al Neyadi H, Mohamed N, Al-Jaroodi J (2015) Applications of big data to smart cities. *Journal of Internet Services and Applications* 6:25. <https://doi.org/10.1186/s13174-015-0041-5>

Freshwater availability in urban environments from atmospheric humidity*

Jorge Mírez¹[0000-0002-5614-5853]

Group of Mathematical Modeling and Numerical Simulation (GMMNS), Faculty of Oil, Natural Gas and Petrochemical Engineering, National University of Engineering, Lima, Peru jmirez@uni.edu.pe

Abstract. This article reports the results of research on the water potentially available from the offshore wind for coastal cities. Given that cities will have a higher percentage of the world's population and GDP, having another source of water supply would help ensure quality of life indicators; considering that due to the effects of climate change, the sources of fresh water in the mountains are progressively decreasing. The amount of water per square meter per hour that flows naturally in air currents (wind) has been determined through mathematical modeling, data collection and processing (wind speed, temperature, atmospheric pressure and specific humidity) from NASA. and numerical simulations, on a case study that is the city of Lima, Peru, which has a coastline of approx. 50 km, in which an average of 113.4195 liters per square meter per day is obtained with 9 years (2014 - 2022) of data. From the study it is concluded that there is enough water for the population and the relative humidity can be reduced by improving the comfort of the population. Likewise, it substantiates the need to develop technologies for the highly efficient capture of atmospheric humidity and that humidity can also be used up to 2000 meters above sea level (cloud cushion).

Keywords: Water · Smart Cities · quality of life.

1 Introduction

The world population in 1990 was 5.27 billion people, in 2000 it was 6.06 billion people and in 2010 it was 6.79 billion people; according to [1] la Ec. 1 quantifies the increase in world population u_t where t is given by the year number. For all these people, the production and distribution of water for human consumption is a fundamental human right. However, the current problem of global warming has caused the sources of fresh water available in the mountains to decrease, both in quantity and quality of fresh water.

$$u_{(t)} = 1.64452 \times 10^7 - 24396t + 12.0275t^2 - 0.0019697t^3 \quad (1)$$

* Supported partially by Faculty of Oil, Natural Gas and Petrochemical Engineering, National University of Engineering, Lima, Perú. Proyecto Nro. 020-2023

2 Jorge Mírez

Cities account for more than 50% of the world's population, 80% of global GDP, two-thirds of global energy consumption and more than 70% of annual global carbon emissions. These factors are expected to increase significantly in the coming decades: by 2050, more than 70% of the world's population is expected to live in cities, leading to massive growth in demand and urban energy infrastructure [2], water, transportation, education, among others. Which, with rapid global urbanization, is increasing the vulnerability of cities to the effects of climate change, increasing urban social and environmental challenges [3].

Concerning the extraction of drinking water from humid air, [5] shows and compares the energy consumption of two promising technologies and two commercial systems through theoretical operation, however, it does not mention the amount of water that can be extracted, nor the initial or final conditions of the air, it is limited to mentioning the necessary energy to capture part of the humidity in the air and convert it into liquid water is $2450 J/ml$ and that the theoretical minimum energy requirement to condense water vapor from the air and produce $1 m^3$ of fresh water is equal to $681 kWh/m^3$. The same way, [6] mentions that there are two main methods for extracting water from ambient air: including the composite method and cooling the air to the dew point and focuses on the factors that affect the process of extracting water from the air by determining the productivity of water and efficiency with short simulation times of maximum about 60 hours, however, it does not determine the potential amount of water present in the air. A vision of the availability of the resource in the short, medium and long term can allow us to view the problem from another point of view and motivate the design of machines that allow massive production of water from moving humid air (wind).

Therefore, as the water resource is essential for human life, this work focuses on the evaluation of the ideal availability of water based on atmospheric humidity in urban environments or in cities, both near the sea where, for the breeze or particular mechanisms typical of the local coastal atmosphere, water can be captured.

2 Mathematical model

Considering as initial data: the specific humidity q_v measure in $[g/kg]$ and local atmospheric pressure P measured in $[kPa]$ dead weight e_w is obtained by means of the Eq. 2. Also, the weight of the water e_s is calculated through Eq. 3 where T is the air temperature measured in $[^\circ C]$ and relative humidity R_H is determined by Eq. 4.

$$e_w = \frac{1}{0.622} q_v P \quad (2)$$

$$e_s = 611 e^{\frac{12.27T}{173.3+T}} \quad (3)$$

$$R_H = \frac{e_w}{e_s} \quad (4)$$

One of the parameters used to define the thermal comfort zone in a stoichiometric table is relative humidity. R_H with recommended values between 40

Freshwater availability in urban environments from atmospheric humidity 3

% to 60 % and that for the purposes of this study 50 % has been considered. Therefore, it is necessary to determine the amount of water that can be obtained by reducing the R_H from an initial condition R_{H_i} to a final condition of relative humidity R_{H_f} . The Eqs. 5 - 8 show the procedure to calculate the relative humidity variation ΔR_H measure in [%].

$$\Delta R_H = R_{H_i} - R_{H_f} \quad (5)$$

$$R_{H_i} = \frac{P}{0.622e_s} q_{v_i} \quad (6)$$

$$R_{H_f} = \frac{P}{0.622e_s} q_{v_f} \quad (7)$$

$$\Delta R_H = \frac{P}{0.622e_s} \Delta q_v \quad (8)$$

The ΔR_H ensures that it is in the thermal comfort zone and can be regulated by atmospheric humidity capture machines. In addition, it is necessary to determine the variation of the specific humidity Δq_v that allows quantifying the amount of water mass present in the air. The Eqs. 9 and 10 show the calculation procedure of Δq_v using environmental variables that can be collected experimentally such as local atmospheric pressure P [kPa], ambient temperature T [°C] and relative humidity R_H [%].

$$\Delta q_v = q_{v_i} - q_{v_f} = \frac{0.622e_s \Delta R_H}{P} \quad (9)$$

$$\Delta q_v = \frac{0.622 \Delta R_H}{P} \left[611 e^{\frac{12.27T}{173.3+T}} \right] \quad (10)$$

Eqs. 2 - 8 allow the calculation in a stable state, however, the subject of study is an air mass that changes over time and the data collected is wind speed, pressure atmospheric, temperature and specific humidity, all averaged per hour; Furthermore, they are all changing and serve to calculate the potential water after each hour. Therefore, with the mass of air moving at a given speed v measured in [m/s], for each measurement reading $\Delta q_v = \gamma$, the amount of water to be extracted per cubic meter of air ϕ , whose unit of measurement is [g/m³] and is defined by Eq. 11, and; the amount of water to be extracted per square meter and per second, from the wind flowing through a surface perpendicular to the ground and to the direction of the wind $\phi\phi$ measured in [g/m²s] is defined according to Eq. 12.

$$\phi = \gamma\rho \quad (11)$$

$$\phi\phi = \gamma\rho v \quad (12)$$

Considering that there is a set of hourly readings of the environmental variables; for each reading i , the amount of water per square meter per second $\phi\phi_i$ has been determined by Eq. 13.

$$\phi\phi_i = \gamma_i\rho v_i \quad (13)$$

4 Jorge Mírez

During a given set of readings n_t , the potential amount of water to condense and that passes through a square meter of surface perpendicular to the ground and the wind direction $\phi\phi$, is determined by Eq. ?? where Δt_i is the time interval between measurements measured in h . If n_t is equal to 24, it will represent 24 hours, which is one day; if it is 168, it will represent 168 hours, which is one week.

$$\phi\phi = \sum_{i=1}^{n_t} \gamma_i \rho v_i \Delta t_i \quad (14)$$

Considering that $\Delta t_i = 1$ hour - i.e. 3600 seconds - Eq. 14 can be written as shown in Eq. 15, in this way, $\phi\phi$ is measured in $[g/m^2h]$.

$$\phi\phi = \sum_{i=1}^{n_t} 3600 \gamma_i \rho v_i \quad (15)$$

The density is determined by Eq. 16 where p is the local atmospheric pressure in [kPa] and T_{C_i} is the ambient temperature in $[^\circ C]$, which substituting in 15 gives Eq. 17 and 18 where $\phi\phi$ is measured in $[g/m^2h]$. The density of air at sea level ρ_{air} is considered to be 1.225 kg/m^3 .

$$\rho = 3.4837 \frac{p}{T_{C_i} + 273.15} \quad (16)$$

$$\phi\phi = \sum_{i=1}^{n_t} 3600 \gamma_i 3.4837 \frac{p_i}{T_{i_c} + 273.15} v_i \quad (17)$$

$$\phi\phi = \sum_{i=1}^{n_t} 12541.32 \frac{\gamma_i p_i v_i}{T_{i_c} + 273.15} \quad (18)$$

Since the unit of measurement of Eq. 18 is grams of water, then dividing by 1000 to obtain kilograms of water, which is equivalent to liters and can therefore be used to calculate the requirements water for each person in a city. Therefore, we obtain $\phi\phi'$ whose unit of measurement is l/m^2h as shown in Eq. 19

$$\phi\phi' = \sum_{i=1}^{n_t} 12.54132 \frac{\gamma_i p_i v_i}{T_{i_c} + 273.15} \quad (19)$$

3 Numerical simulations and results

To calculate the available amount of water in the wind $\phi\phi'$ it has been carried out considering $n_t = 24$, that is, the amount of water in liters that is obtained per square meter in 24 hours. The data used has been obtained from NASA [4] and are hourly averages for 9 years (2014 - 2022) taken at the seashore near the City of Lima (data collection point: latitude -12.0690 length -77.1379). Fig. 1 shows the values of $\phi\phi'$ and Fig. 2 shows the frequency analysis of the values of $\phi\phi'$, both , for each hour during the study period (9 years).

Freshwater availability in urban environments from atmospheric humidity 5

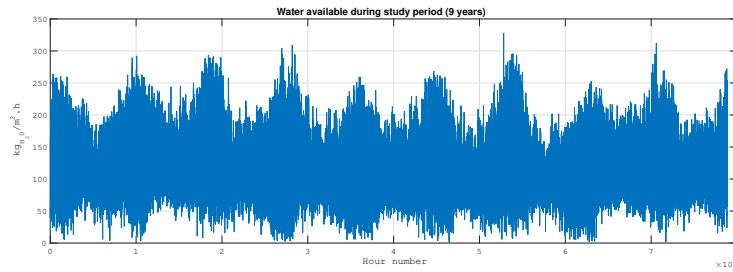


Fig. 1. Evolution of $\phi\phi'$ per hour of the study period.

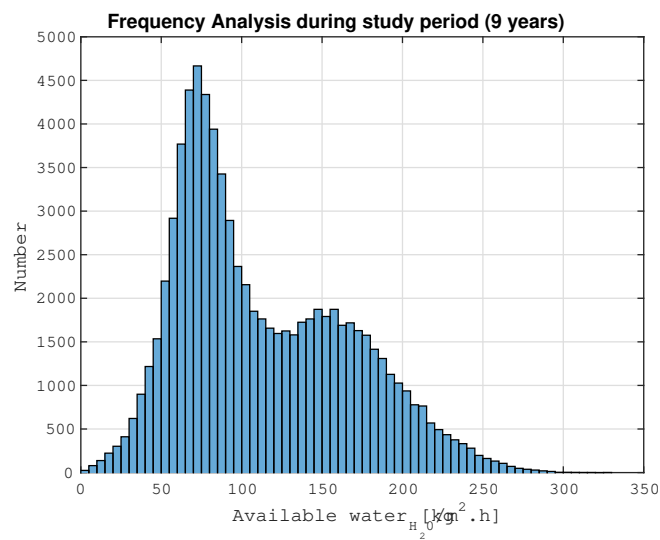


Fig. 2. Frequency analysis of all hourly values of $\phi\phi'$ of the study period.

6 Jorge Mírez

The Fig. 2 and 3 show the frequency analysis by superimposing the values of $\phi\phi'$ for each year. Solid lines have been used in Fig. 2 to show the differences between each year and in Fig. 3 to show the degree of coincidence between all years.

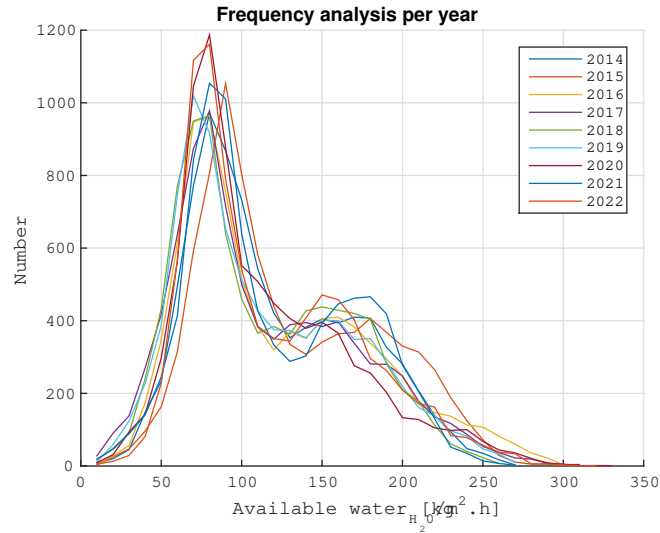


Fig. 3. Frequency analysis in hours for each year and plot in lines to display differences between years.

The apparent regularity shown in Fig. 2 - 4 is clarified by calculating the amount of water per year obtained from each square meter of surface perpendicular to the ground and the wind speed, as shown in Fig. 5 with a value of approx. of 100 cubic meters per square meter per year on average.

4 Conclusions

A mathematical model has been developed that determines the amount of fresh water that can be extracted from the atmospheric humidity contained in the wind that affects a coastal urban environment. It has been applied to the case study which is the City of Lima, where it is obtained that the global average $113.4195 \text{ l/m}^2\text{day}$ is approximately half of the daily amount of water per person recommended by the WHO, which is 250 liters, that is, ideally between 2.02 m^2 and 2.31 m^2 would be needed to meet the water quantity standard per person given by the WHO. Table 1 shows the statistical results for $\phi\phi'$: maximum values $\phi\phi'_{max}$, minimum values $\phi\phi'_{min}$, deviation standard $\phi\phi'_{de}$ and average value in each year $\phi\phi'_{pa}$ and globally for the entire study period (9 years). The results

Freshwater availability in urban environments from atmospheric humidity 7

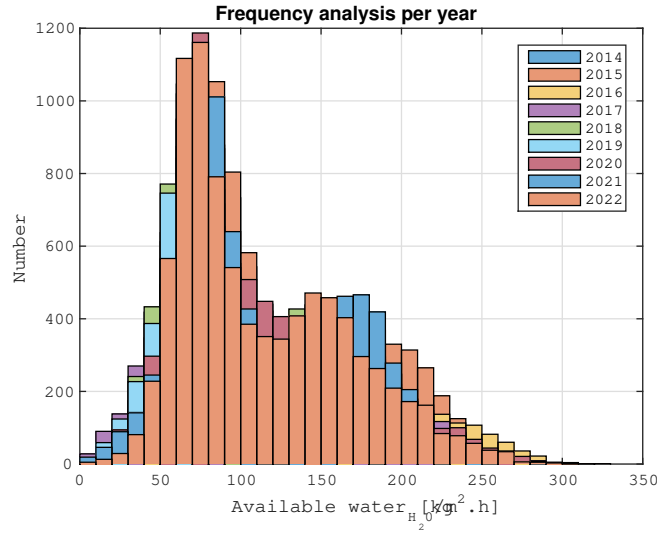


Fig. 4. Frequency analysis in hours for each year and bar graph to display the coincidence in the repetition of values between years.

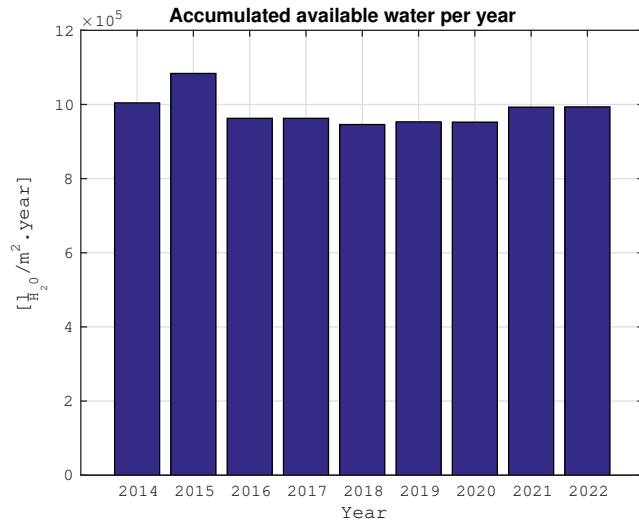


Fig. 5. Mass of potentially captureable water obtained during one year per square meter of surface perpendicualr to the ground and wind speed.

8 Jorge Mírez

show the possibility of supplying fresh water to a large population, as well; bases the need for research, development and innovation of technologies for the highly efficient capture of atmospheric humidity and, in addition, the surplus atmospheric humidity present up to approximately 2000 meters above sea level can be used in what is called a cloud cushion present. in coastal environments.

Table 1. Calculation results of water availability from atmospheric humidity from sea breeze.

Year	$\phi\phi'_{max}$	$\phi\phi'_{min}$	$\phi\phi'_{de}$	$\phi\phi'_{pa}$
2014	264.1634	3.7319	50.2004	114.6486
2015	292.3223	3.4783	54.0171	123.7117
2016	293.7370	4.3440	57.9586	116.8429
2017	308.9669	2.3481	55.9353	109.8985
2018	259.5852	4.5064	51.2390	107.9817
2019	268.4587	0.8873	53.4092	108.8092
2020	328.1161	5.1860	52.1226	108.4195
2021	265.9424	1.8872	50.4840	113.3300
2022	312.1676	1.7482	52.0622	113.4195
Global aver.	288.1622	3.1231	53.0476	113.0068

Acknowledgements The author acknowledge the support provided by the Thematic Network 723RT0150 “Red para la integración a gran escala de energías renovables en sistemas eléctricos (RIBIERSE-CYTED)” financed by the call for Thematic Networks of the CYTED (Ibero-American Program of Science and Technology for Development) for 2022.

References

1. Om Kalthoum Wanassi, Delfim F.M. Torres: An integral boundary fractional model to the world population growth. *Chaos, Solitons and Fractals* **168**(113151), (2023)
2. International Energy Agency : Empowering Cities for a Net Zero Future: Unlocking resilient, smart, sustainable urban energy systems. IEA, France (2021)
3. Ana Paula Barreira, Jorge Andraz, Vera Ferreira, Thomas Panagopoulos: Perceptions and preferences of urban residents for green infrastructure to help cities adapt to climate change threats. *Cities* **141**(104478), (2023)
4. NASA Power Data Access Viewer Homepage, <https://power.larc.nasa.gov/data-access-viewer/>. Last accessed 30 Sep 2023
5. J.S. Solís-Chaves, C.M. Rocha-Osorio, A.L.L. Murari, Valdemir Martins Lira, Alfeu J. Sguarezi Filho: Extracting potable water from humid air plus electric wind generation: A possible application for a Brazilian prototype. *Renewable Energy* **121**, 102 - 115, (2018)
6. A.W. Kandeal a, Abanob Joseph a, Marwan Elsharkawy, et.al.: Research progress on recent technologies of water harvesting from atmospheric air: A detailed review. *Sustainable Energy Technologies and Assessments* **52**(102000), (2022)

**Urban Informatics, Big Data, Analytics
and
other developments for Smart Cities**

Proposal for clean Urban on-boat transportation with photovoltaic and biomass hybridity in the Patzcuaro Lake of Michoacán (Mexico)

Galileo Cristian Tinoco Santillán¹, Jorge El Mariachet Carreño², Roberto Tapia Sanchez¹, Gustavo C. Branco², José Matas Alcalá², Wael Al Hanaineh²

¹Electrical Engineering Faculty FIE-UMSNH, Morelia, Mexico

²Electrical Engineering Department, EEBE-UPC, Barcelona, Spain

Abstract.

Naval transport carbon emissions are hard to abate. In some urban areas, goods and persons transport by ships is the basis of their mobility. Patzcuaro Lake basin is an inland water system surrounded by several urban areas whose economy remarkably relies on tourist transportation from the shore to the archipelago. The fuel utilized is diesel from fossil sources. Renewable Energies (REs) must be employed to propel the boats to avoid greenhouse emissions. Electrification of the vessels is a solution that requires adequate and reliable REs planning. On-board and on-shore Photovoltaic (PV) are considered along with charging stations to ease the operation of a 150-vessel fleet. In addition, this water reservoir invasion by exotic plants, "Eichhornia Crassipes," poses a significant problem to navigation and ecosystems. Controlling the extension or removing the plant colonies is highly expensive. The present work intends to analyse the electrical energy potential of an invader vegetable species, pointing to a path to make it economically and environmentally profitable, combining it with mature PV technology to decarbonise the passenger transport sector in the area.

Keywords: Microgrids, naval transport, urban mobility, biomass, decarbonisation.

1 Introduction

Patzcuaro Lake is a natural water reservoir located in the state of Michoacan. The riverside is divided between five municipalities, with an archipelago composed of four islands, see Figure 1. The total population between the riverside municipalities and the archipelago is estimated at 25000 inhabitants. The lake surface was estimated at 132 km² in 1993 [1], later at 120 km² [2] and presently can be measured through the Mexican National Atlas of Biomass online tool, ANBIO, [3], yielding 100-120 km² approximately. The study area is the coastline around Patzcuaro municipality, considering a rough 1000 Ha of an affected water basin. Since the middle XIX, the anthropogenic

2

stress in this lake has been sustained in time [2]. Eutrophics is the most critical currently unsolved problem that drives risk to the local endemic fauna and the local economy [1,4-5] due to the presence of an invader water plant, i.e. "Eichhornia Crassipes", E-C. This species poses great difficulty to its eradication. Several attempts were made to mitigate this problem by integrating the species as a primary source in the economic chain.

The E-C is not a crop or a land forestry mass. For this reason, an assumption is taken to define its role in the following decades' growing demand for green energy sources. A reliable approach is that of the International Energy Agency in analyzing Biofuel demand growth by fuel and region, 2022-2024 [6]. This is reproduced in Figure 2, and the E-C has assimilated to the short rotation woody crops due to the E-C rapid growth treated as a production rate. Its expected evolution up to 2050 is exponentially growing, almost doubling by 2030.

The Mexican Energy Transition Law, ETL, [7] establishes that in-situ renewable energy resources should be exploited whenever possible. Also, the United Nations Sustainable Development Goals, SDG [8] stresses that modern, renewable, reliable and sustainable clean energy sources must be available to society through the seventh SDG ,SDG7. Therefore, the Biomass of the Eichhornia Crassipes in the inner water masses in Mexico is a target for the compliance of SDG7 and the precepts of the ETL. Ex-professo Geographical Information Systems, GIS, ANBIO, and International Renewable Energy Agency, IRENA, can be employed to estimate biomass energy potential.

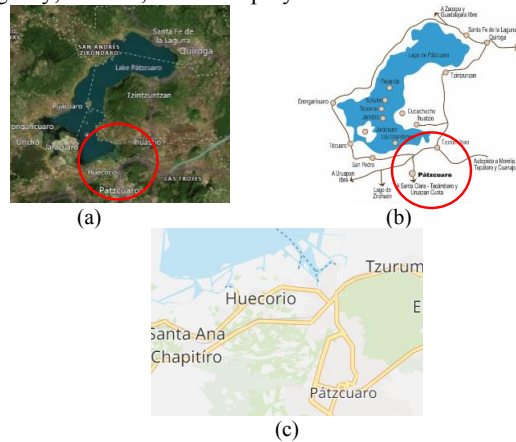


Figure 1. (a)Patzcuaro Lake and Patzcuaro municipality (satellite imagery, IRENA Biomass Simulator); (b) topographic imagery showing the location of Patzcuaro village to the lake; (c) Showing the coastline of the urban area of Patzcuaro village, highly contaminated with E-C.

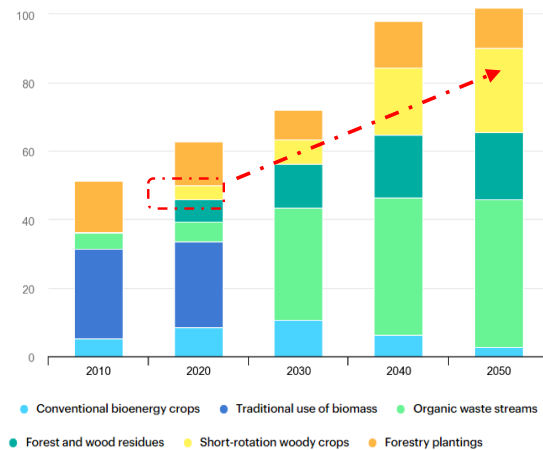


Figure 2, Global bioenergy supply in the Net Zero Scenario, 2010-2050 [6]

Section 2 analyses the literature for determining a hypothetical solid biomass fuel (pellets) averaged energy content based on E-C. Section 3 proposes an architecture of a Microgrid to integrate the E-CP energy source. Section 4 performs a basic energy balance with a 1000kWp PV plant as a baseline. Finally, Section 5 summarises the conclusions and the scope for future works.

2 Biomass Potential of “Eichhornia Crassipes”

The suggested process for harvesting the plant to transform it into solid biomass fuel pellets or bricks is dehydrating, shredding and compacting the harvested Biomass from the lake. This process for pelletizing the raw material is described in [9]. That yields a collected E-CP with 90% humidity content down to a compact pellet with 13% humidity, equivalent to a mass reduction of 70%. Therefore, the employed final fuel pellets mass is 435 kg/Ha/year. With this assumption, in the most representative literature are found the following High Heat Values (HHV): 16.5 MJ/kg [10], 15.46 MJ/kg [11], 15.87 MJ/kg [9]. These values were calculated considering different compositions in moisture content, other biomass sources (banana peel or pineapple waste) and dimensions of the fuel bricks once processed. The current study adopts a worst-case scenario with the most uncomplicated process for creating the pellets, yielding an HHV = 15.46 MJ/kg [11]. According to this, a harvesting area equivalent to 1 Ha is proposed in the proxy area of the Patzcuaro village docking stations. In Figure 1, a general view of the Patzcuaro Lake basin is accompanied by a close water area selected in the municipality of Patzcuaro. For this selection, the IRENA atlas [12] was employed. With a baseline sample of 1 Ha, considering [11], a net primary productivity of 1450kg/Ha/year was adopted, assimilating the undesired growth of the plant as a productivity rate. Later, due to a 70% mass reduction by dehydration, the equivalent collection results in 435

4

kg/year. Table 1 summarizes the conditions described and shows the Biomass's estimated total energy potential after conversion into pellets.

Table 1. Energy estimation for Eichornia Crassipes harvest.

Parameter	Value
Productivity	1450 kg/Ha/year
Total mass in Pellets	435 kg/year
Energy content per kg	15.46 MJ/kg
Total energy potential per year (TEY)	6725.1 MJ
76%TEY	5111 MJ
24%TEY	1614MJ

The leading technologies for energy conversion to consider in this work are pure electrical energy, pure heat-thermal energy or combined heat and power engines. In this region with a tropical climate, only thermal applications of direct combustion of E-C pellets (E-CP) are discarded since no district heating is planned and domestic heating is not used. A combined heat and power solution is more suitable to the Patzcuaro basin municipalities considering employing the produced heat for industrial applications. Another application directly related to the economic development in the area is to shift the touristic vessels fleet (passenger transportation) from diesel engine operation to electrical propulsion. This last requires the installation of vast charging and refueling stations for pure electrical onboard systems of hydrogen-based onboard machinery. Therefore, a proposed solution for profiting from the harvested E-CP is to embed it in a multi-energy microgrid. The choice of the means for producing energy is a trade-off between the system's efficiency and other considerations such as the development of basic infrastructures, providing power to the transportation fleet in the lake, powering educational and administrative facilities, etc. A Multienergy Microgrid (MEMG) qualitative proposal is then presented in the next section.

3 Microgrids allocation and size

The proposed MEMG will consist of Photovoltaic Panel arrays, PV, Combined Heat and Power ,CHP, engines, Energy Storage Systems (ESS) as batteries and Proton Exchange Membrane Water Electrolysers, PEMWE. Then, a general MEMG architecture is shown in Figure 3, where the layout delimits the system's electrical and thermal sides after generation. The parameter P_{PV} is the generated energy using PV after the yearly irradiance in the municipality of Patzcuaro. The irradiance Irr is estimated through PVWatts® API version 8.0 for calculation purposes. P_{CHP} is the output electrical energy of the CHP plants, while Q_{CHP} corresponds to the plants' thermal energy output. P_{H2} is the energy demand of PEMWE systems for energy storage purposes. P_{ESS} is the electrical demand batteries-based ESSs. P_{EV} is the electrical demand of the charging stations

for Electrical Vehicles, EVs. The thermal side in Figure 3 is represented only for explanation purposes but is not the focus of the subsequent analysis.

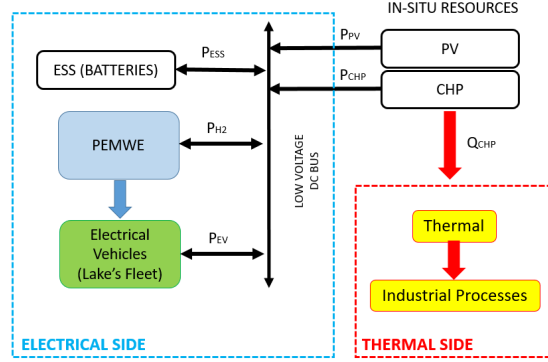


Figure 3. Layout of a MEMG proposal, showing energy flow.

The balance of energy of this MEMG takes into account the efficiencies and load sharing of the system. The following equations aim to show an energy balance to build up a context of the yearly profitability of the E-CP energy potential.

$$P_G = P_{PV} + P_{CHP} + Q_{CHP} \geq P_{ESS} + P_{H_2} + P_{EV} \quad (1)$$

$$P_{PV} = I_{RR} \cdot \eta_{PV} \quad (2)$$

$$E_{CHP} = E_{E-CP} \cdot \eta_{CHP} = E_{E-CP} \cdot \eta_{THERMAL} + E_{E-CP} \cdot \eta_{ELECTRICAL} \quad (3)$$

$$P_{EV} = \alpha(P_{H_2} \cdot \eta_{PEMWE}) + (1 - \alpha) \cdot P_{ESS} \cdot \eta_{ESS} \leq P_{PV} + P_{CHP} \quad (4)$$

$$P_{CHP} = E_{E-CP} \cdot \eta_{ELECTRICAL} \quad (5)$$

$$Q_{CHP} = E_{E-CP} \cdot \eta_{THERMAL} \quad (6)$$

I_{RR} is the total yearly irradiance at the dock's location in Patzcuaro village. P_G is the total amount of energy generated utilizing PV and CHP. The η_{PV} , η_{CHP} , $\eta_{THERMAL}$, and $\eta_{ELECTRICAL}$ are the respective efficiencies for PV, the CHP global efficiency, the electrical CHP efficiency, and the thermal CHP efficiency. The parameter α is an integer ranging from $\{0,1\}$, indicating the energy share provided to EV from ESS and Hydrogen. E_{CHP} is the total energy supplied by the CHP plant. E_{E-CP} is the total amount of energy estimated from E-C (see Table 1)—figure 4 plots the typical PV and CHP generation efficiencies, referencing the U.S. Department of Energy datasets. The efficiencies in Figure 4 show that the lowest is for PV generation at 14.08%, followed by CHP electrical efficiency at 24%. Table 2 shows the yearly electrical energy produced by PV and CHP systems similar in size, as a baseline for comparison purposes, as a starting point. Figure 5 demonstrates the electrical energy contribution after harvesting E-C and transforming it into pellets, E-CP, for total energy production, including thermal. Therefore, according to (1)-(6), most E-CP's energy is thermal. A fraction of this energy will be utilized for the dehydration of harvested E-C, along with other economic applications out of the scope of the present work. Nevertheless, a clear contribution of electrical generation may result in the decarbonization of the local passengers' transport

6

in the lake. For this reason, the following section will analyze the need for the electrification of the lake’s fleet to further the framework design of the MEMG.

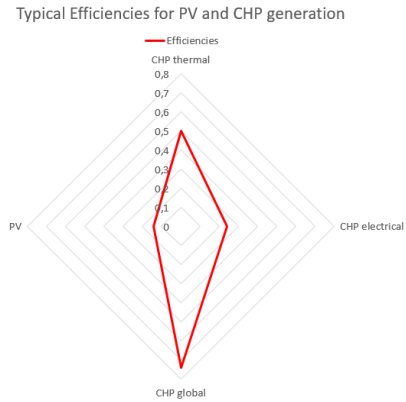


Figure 4, Typical efficiencies for PV and CHP

Table 2: Total yearly Electrical Energy estimation

Parameter	Value
Location	Patzcuaro (19.53°N , -101.62 W)
Theoretical Size of PV Arrays	280kW _p
η_{PV}	14,08%
P_{PV}	446047 kWh
$\eta_{ELECTRICAL}$	24%
P_{CHP}	448000 kWh

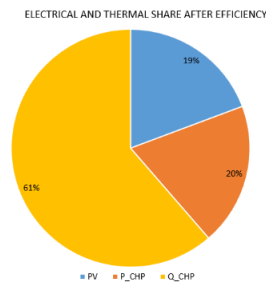


Figure 5, Energy share of the system: Electrical and thermal energy from all the generation.

4 Energy demand analysis for the EV's fleet

In decarbonization strategies, transport is one of the most difficult to abate. A pathway is to substitute fossil fuels by synthetic fuels, with zero GHG emissions and other environmental impacts. In this case, the Organization for Economic Cooperation and Development (OCDE) reports the main efforts in this area [13], from which European Union (EU) leads the GHG mitigation in maritime sector through enhancing utilization of sustainable fuels [14]. Although this strategy implies not modifying the existing sea-ports infrastructure and the on-board electromechanical systems, the economic burden of developing synthetic e-fuels is a barrier for the leisure naval sector, mainly composed by small boats (less than 20 meters length). For this specific sector, retrofitting small sailing boats and others for inner land water mass (channels, big lakes, etc.) is an affordable option. The retrofit consists in substituting the combustion engine propulsion by an electrical system, with higher energy efficiencies. A techno economic analysis for this option is achieved in [15], for the reduction up to a 15% of fossil fuel utilization was achieved through partially electrifying a boat, with its own PV system and batteries. Also, full electrical solutions demonstrated the payback of the initial capital in less than 10 years. Later, a PV on-shore plant was implemented to support a small boats fleet. Primary and tertiary sectors are preeminent in this specific region around the Lake. In both cases, transporting goods and persons is crucial to the local economy. It is remarkable that only for tourism roundtrips from Patzcuaro village to the archipelago islands, the boat fleet is roughly 150 vehicles. Figure 6 shows an image of a fraction of the fleet in Patzcuaro, along with its schematic layout. All these vehicles are propelled using diesel engines, DE. In electrification, the rated power to each boat is established as 2.2kW, regarding data from [16]. Once substituting the DE with electrical propellers, the weight reduction in the ships may permit installing a planar roof PV array. In Table 3 lists the power generation of a planar roof-top 2kWp PV installed in the fleet's ships.

Table 3: PV Energy generation of boat planar roof-top installed

Parameter	Value
Fleet	150 boats
Roof Surface	25 sqr. m
Capacity PV roof horizontal	2kWp
Yearly production per ship (https://pvwatts.nrel.gov/)	3186 kWh
Total Installed Capacity Fleet	300kWp
Yearly production per fleet	477900 kWh

The electrical power needs of the fleet are calculated considering a 1kW average power demand during 12 hours per day, except four weeks per year for maintenance. Then, the energy demand is $E_{\text{fleet}} = 603450 \text{ kWh}$, exceeding in 125550kWh the installed capacity on the vessels rooftop. Nevertheless, this is 7% higher than the 446047 kWh produced by the baseline of 280 kWp PV systems shown in Table 2. Then, the PV

8

systems are distributed among all the ships in the lake, although $P_{PV} < E_{fleet}$. In this situation, a common strategy is oversizing energy generation for transport reliability, i.e. avoiding onboard blackouts after round trips between Patzcuaro and the lake archipelago, especially Janitzio island.

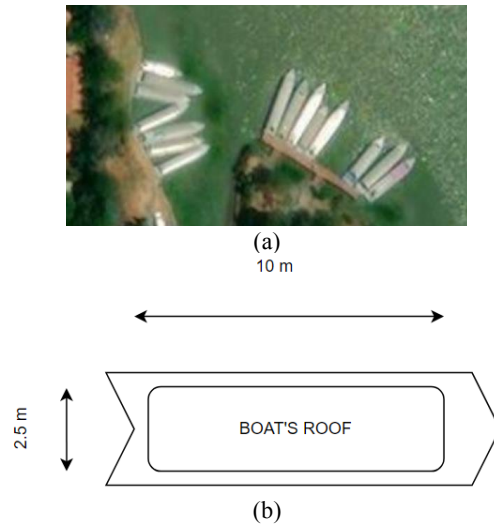


Figure 6, (a) Satellite imagery of docked boats in Patzcuaro; (b) Schematic layout of a typical boat with a profitable 25 m² roof for PV.

The electrical side of the MEMG architecture is organised as follows: the PV systems are off-shore floating plants (OSFP), i.e. the fleet. Consequently, each vessel will contain its microgrid, with its rooftop PV, batteries ESS and loads. These microgrids are out of the scope of the present work. Along with these OSFPs, two on-shore plants (OSPs) are in Patzcuaro and Janitzio docks, respectively. These plants are named OSP1 and OSP2 and will consist of a CHP with half of the size in the power of Table 2, with their PEMWEs. In this case, CHP plants' primary purposes will be storing energy through hydrogen and sharing thermal energy with local processes. Secondly, their electrical power can be used to support the EV fleet energy demands. Figure 7 illustrates that concept, showing the proposal for the location of OSP1 and OSP2, a novel architecture for the MEMG in Figure 7(e) and a chart showing the amount of yearly electrical energy generated at OSFP, OSP1 and OSP2.

5 Conclusions

The E-CP is a major environmental issue in tropical areas' inner masses of water. Patzcuaro Lake in Mexico is a remarkable example. Attempts to eradicate this invasive plague have been carried out with partial success. This work establishes a first approach to contribute with E-CP harvesting to SDG7 in the context of the Energy Transition. A proposal of MEMG architecture is presented after considering the electrification of the most significant economic activity in the lake, i.e. a 150-vessel fleet. The energy

balance and the combination of PV with CHP systems, along with PEMWE, draws a general framework to design a proper operation of the MEMG. In this case, the PV systems are carried onboard in the vessels, each with its own batteries-based ESS and loads, grouped in the concept of OSFP. As the rooftop estimated surface of the vessels does not generate enough energy for roundtrip operations, partial support with OSP1 and OSP2 is essential, i.e. CHP plants electrical power. Future works shall point toward integrating the hydrogen generation with on-board or on-shore PEM fuel cells. Also, Janitzio and Patzcuaro municipalities electrical energy demand could be supplied by the surplus of power after harvesting more than 1 Ha per year of the E-CP.

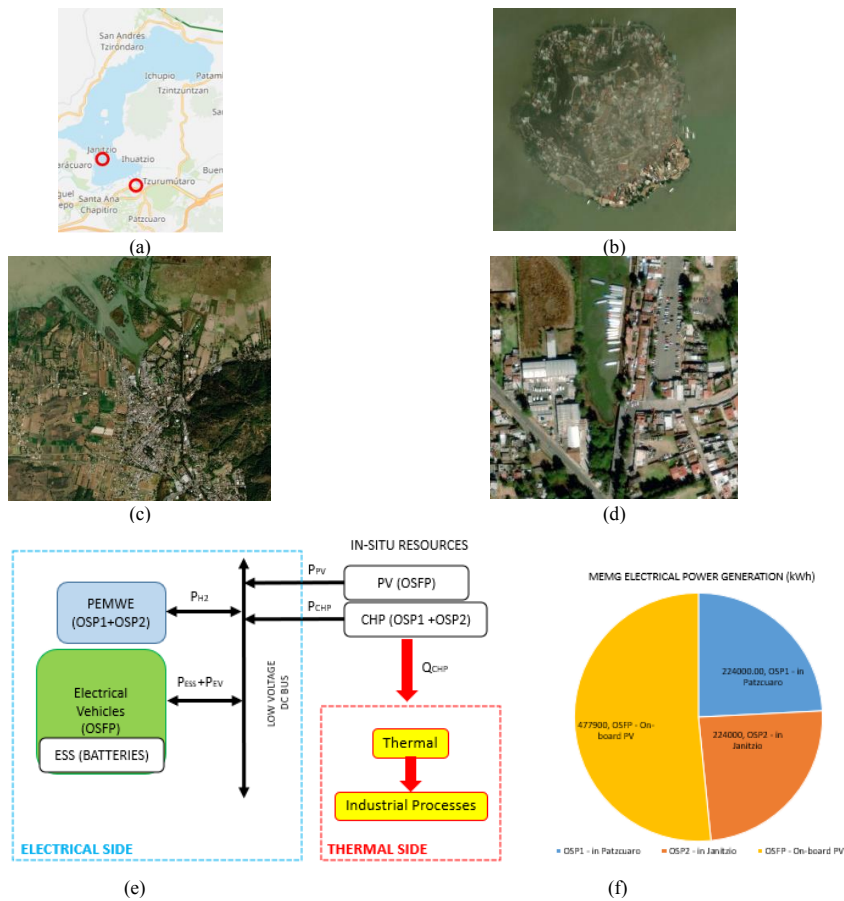


Figure 7, (a) Patzcuaro village and Janitzio island location; (b) Detail of Janitzio island docking perimeter; (c) Location of Patzcuaro’s village docks; (d) Detail of the docks in Patzcuaro village; (e) New architecture for the case of study, considering OSP and OSFP; (f) Final share of electrical energy generation.

10

References

1. Chacon Torres, Arturo. (1993). Lake Patzcuaro, Mexico: Watershed and Water Quality Deterioration in a Tropical High-altitude Latin American Lake. *Lake and Reservoir Management - LAKE RESERV MANAG.* 8. 37-47. 10.1080/07438149309354457.
2. Fadum, Jemma & Hall, Ed. (2020). The impacts of global and local change on a tropical lake over forty years. 10.1101/2020.10.21.347393.
3. Dirección General de Energía, Gobierno de México “ Atlas Nacional de Biomasa”, <https://dgel.energia.gob.mx/anbio/> [Last Access 08/2020]
4. Delia, Estrada-Navarrete & Soto-Galera, Eduardo & Daniel, Hernández-Montaño & Sandoval-Huerta, Edgar. (2015). Actualización de los registros de pescado blanco *Chirostoma estor* y *C. humboldtianum* en cinco cuerpos de agua de Michoacán, México. *Revista Ciencia Pesquera.* 23. 73-76.
5. Camarena O., Aguilar, J.A.; Control biológico del lirio acuático en México: primera experiencia exitosa con nequetinos en distritos de riego, Instituto Mexicano de Tecnología del Agua (IMTA); December 2013, pp336.
6. IEA, Biofuel demand growth by fuel and region, 2022-2024, IEA, Paris <https://www.iea.org/data-and-statistics/charts/biofuel-demand-growth-by-fuel-and-region-2022-2024>, IEA. Licence: CC BY 4.0
7. Ley de Transición Energética, Cámara de Diputados del H. Congreso de la Unión, publicada en el Diario Oficial de la Federación el 24 de diciembre de 2015
8. Sustainable Development Goal 7 (SDG). Available online: <https://sustainabledevelopment.un.org/sdg7> (accessed on 4 September 2020).
9. Velazquez-Araque, Luis; Solis, Eileen; Vásquez, Galo. “Eichornia Crassipes: a new energy source for biopellets production”, Available at :10.5071/28thEUBCE2020-2BV.2.43.
10. Z. Xia, C. Shou, Z. Zheng, and Z. Zhe, "Water hyacinth pellet fuel moulding process optimization," *Trans. Chinese Soc. Agric. Eng.*, vol. 32, no. 5, p. 9, 2016
11. J. S. Lara-Serrano et al., "Physicochemical characterization of water hyacinth (*Eichornia crassipes* (Mart.) Solms)," *BioResources*, vol. 11, no. 3, pp. 7214–7223, 2016
12. International Renewable Energy Agency. "IRENA Global Atlas." <https://globalatlas.irena.org/> [Last access 08/2023]
13. “Analysis of the marine equipment industry and its challenges”, Council Working Party on Shipbuilding, Organisation for Economic Co-operation and Development, 19 January 2022. Available online: [https://one.oecd.org/document/C/WP6\(2022\)15/FINAL/en/pdf](https://one.oecd.org/document/C/WP6(2022)15/FINAL/en/pdf) [Last access: August 2023]
14. European Parliament. (2021). Report on the proposal for a directive of the European Parliament and of the Council amending Directive 2003/87 establishing a system for greenhouse gas emission allowance trading within the Union, Decision (EU) 2015/1814 concerning the establishment and operation of a market stability reserve for the Union greenhouse gas emission trading scheme and Regulation (EU) 2015/757. https://www.europarl.europa.eu/doceo/document/A-9-2022-0162_EN.html. [Last Access: August 2023]
15. Şafak Hengirmen Tercan, Bilal Eid, Michael Heidenreich, Klaus Kogler, Ömer Akyürek, Financial and Technical Analyses of Solar Boats as A Means of Sustainable Transportation, Sustainable Production and Consumption, Volume 25, 2021, Pages 404-412, ISSN 2352-5509, <https://doi.org/10.1016/j.spc.2020.11.014>.
16. Hans Ekdahl Espinoza, “Embracaciones propulsadas por energía solar, *Revista de Marina*, ISSN 0034-8511, January 2014, pp73-81

GeoLocation accuracy measurement of free-to-use available GIS API's.

Eduardo Hugo Bennesch¹ ; Diego Alberto Godoy² ; Karina Eckert²

¹ National University of Misiones, Argentina

² Gaston Dachary University, Argentina

¹ingbennesch@gmail.com, ²diegodoy@gmail.com, ³karinaeck@gmail.com

Summary. The implementation of geospatial technology (GIS, *Geographical Information System*) solutions applied to improve business conditions is a reality that is growing as operational costs become more accessible. In this work, a comparative measurement of the geocoding service of 5 GIS platforms with free and open access layers was carried out to determine which one is the most convenient to use.

In this study, geolocated points were taken from different possessions in the capital region of Misiones (Argentina) and tested by measuring geopositional distances with the formula of haversine formula and the calculation of Euclidean distance between 2 points, making a comparison between the two. In the results it was observed that Crowdsourcing platforms have better accuracy in this sector of the planet, however in general the values in the average error distances are still high.

Keywords: *API GIS, Precision, Geocoding.*

1 Introduction

In the commercial sectors, the word precision implies a certain degree of technification, this added to the growth and rapid adoption of GIS systems implemented to improve production systems [4]. This is why positioning is not only an important discipline in this digital era but also an essential part of our daily lives [5]. In recent times, the global positioning system (GPS) as a fast, efficient, and relatively inexpensive means of obtaining data has been increasing [3].

Within this new concept of data applied to production, numerous free and open-access digital platforms have appeared that offer all kinds of solutions and information for the most diverse applications; among them are the crowdsourcing platforms better known as Voluntary Geographic Information (VGI) [6], the most popular example of VGI that we can cite is the OpenStreetMap (OSM) service, an open source global geographic database [6].

In this case study, the observation of geographic data will be analyzed using 4 GIS platforms: Google Maps, Bing Maps, OpenStreetMap (its 2 APIs, Nominatim and OpenCageData), and Here. For the analysis of the distances 2 formulas were used,

2

initially the haversine formula [1] to calculate the distance between points and thus determine the accuracy of each API, and then the Euclidean distance calculation between 2 points [2] was applied. The results and the analysis of both formulas applied to each geocoding engine were dumped in comparative tables so that the clear differences between the methods and platforms could be appreciated.

2 **Materials and Methods**

A combination of fieldwork and development and implementation of an analysis interface with M-query language and DAX code in Power Bi for the data collected and the information resulting from this work was combined with the development and implementation of an analysis interface with M-query language and DAX code in Power BI.

2.1 **Fieldwork**

A Garmin NUVI 755T Car GPS was used to take the geographical coordinates of 10 known points in the City of Posadas whose addresses (street and height) were visibly easy to recognize, the points were limited to the area of the urban conglomerate "Gran Posadas" due to logistical limitations. Manual corrections were made to eliminate any errors made by the GPS. The data obtained were dumped into an Excel spreadsheet preserving the relationship between the coordinates taken by the GPS and the direction observed at the chosen point so that they could be consumed by Power BI.

2.2 **Implementation**

From Power BI, 4 platforms were used to geo-locate and visualize the addresses obtained, thus allowing us to know the GIS interface of each platform and how it resolves the geolocation of each address. The first comparison was made on the coordinates obtained in Figure 1.

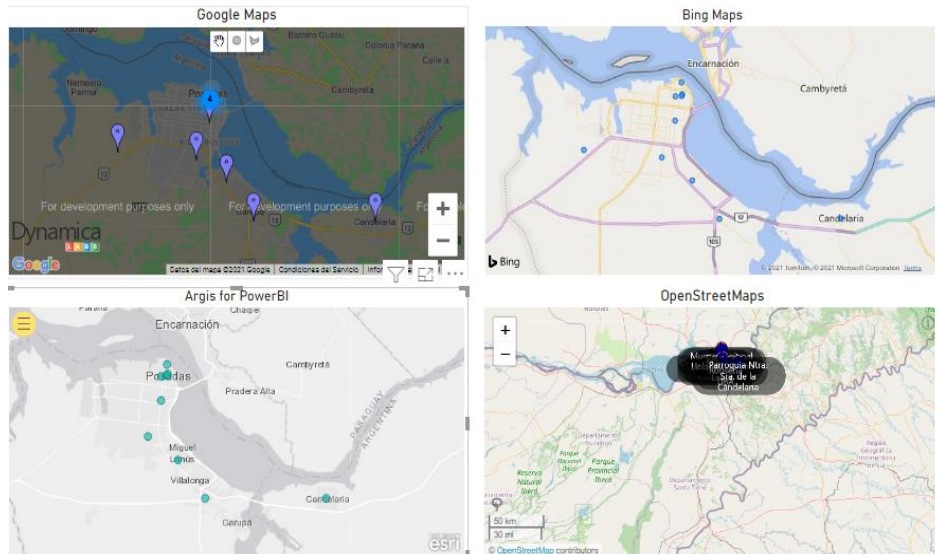


Fig. 1. Comparison of map visualization.

Accuracy Tests. A geocoding function of different known addresses in the city of Posadas was performed to test the variation (in km) between the real location and the one resolved by the API of each platform: OpenCageata[8], Google[9], Microsoft[10] Here[12] and OpenStreetMaps[11].

To do this, 10 known locations were taken with their respective postal addresses and the geolocation was noted with a GPS device. From these postal addresses, a call was made to the APIs of each engine mentioned above to carry out the Geocoding process, i.e. converting the postal addresses into geographical coordinates (latitude and longitude). This is done by making an API call via curl that returns a JSON or an XML, depending on the case. Both the JSON and the resulting XML are processed with M query language within Power Query and the fields are refined so that they can be consumed by the Bi platform.

One of the drawbacks that arose with the addresses obtained is the problem of semantics and the lack of flexibility in terms of the natural language of the platforms, simply small changes such as writing A instead of Avenue or vice versa can cause the API not to resolve the location directly, even problems were detected with punctuation marks. This became a challenge because to be able to make the comparison, the addresses collected had to be resolved by the 4 GIS platforms without returning an error message (even if they were resolved erroneously).

4

Once the Geocoding is done, 2 geographic points related to a postal address are obtained, the API accuracy test consists of measuring the distance between the real point measured with the GPS device and the point resulting from the geocoding, and the resulting value will be taken as the error measured in Kilometres (Km). To measure this error, two distance measurement formulas were used, the Euclidean calculation method of distance between two points which is a heuristic function that is obtained from the direct distance without obstacles with which the length of a diagonal line in a triangle is obtained, and the haversine formula which is an equation that calculates the distance of an arc between two points of longitude and latitude [7].

Haversine formula To calculate the distance between 2 geographical points, the Haversine formula was used [1]:

$$P = \pi/180 \quad (1)$$

Because the result must be expressed in radians, the formula “P” is applied to perform it.

$$A = 0,5 - \cos((Lat1 - Lat2) * P) / 2 + \cos(Lat1 * P) * \cos(Lat2 * P) \times (1 - \cos((LNG2 - LNG1) * P)) / 2 \quad (2)$$

Where A is the calculation by haversine of the location of 2 points in spherical coordinates expressed in Lat1, Long1 and Lat2, Long2 and the consequent distance between them.

$$D = 12742 * \arcsin(\sqrt{A}) \quad (3)$$

Finally, “D” is solved by using the arcsin function on the semiverse calculated by twice the earth's radius (12742).

The implementation of these mathematical formulae was done through Power BI in formula language for DAX data analysis, firstly by converting the coordinates into variables as visualized in the following example:

```
var Lat1 = MIN( ' Direcciones           Conocidas ' [ OpenStreetMap   Latitud ] )
var Lng1 = MIN( ' Direcciones           Conocidas ' [ OpenStreetMap   Longitud ] )

var Lat2 = MIN( ' Direcciones           Conocidas ' [ Latitud         Real ] )
var Lng2 = MIN( ' Direcciones           Conocidas ' [ Longitud        real ] )
```

The distance between the points is calculated:

```
var P = DIVIDE( PI(), 180 )
var A = 0,5 - COS((Lat2-Lat1) * p)/2 +
COS(Lat1 * p) * COS(Lat2 * P) * (1-COS((Lng2-Lng1) * p))/2
var final = 12742 * ASIN((SQRT(A)))
return final
```

The application of the algorithm with the haversine formula results in a table with the calculated distances between the points taken with the GPS and the points geocoded with each API.

Calculation of Euclidean distance: The calculation of the distance between the geographical points taken with the GPS and the geocoded points was carried out by applying the formula.

$$d_E(P, Q) = \sqrt{(p_1 - q_1)^2 + (p_2 - q_2)^2 + \dots + (p_n - q_n)^2} = \sqrt{\sum_{i=1}^n (p_i - q_i)^2} \quad (4)$$

Where "d" is the Euclidean distance in degrees between two points expressed in cartographic coordinates (p and q) which is then converted into kilometers by multiplying the resulting value by 11574.

The formula is implemented in DAX Analysis language by developing a new variable with the calculated distance as in the following example:

```
Distancia Euclidiana = SQRT(POWER('Direcciones Conocidas'[Latitud Real] - 'Direcciones Conocidas'[Latitud Real], 2) + POWER('Direcciones Conocidas'[Longitud real] - 'Direcciones Conocidas'[OpenCageData Longitud], 2)) * 110.574
```

3 Results

The result of the development of this application was the difference in kilometers between the point (lat. and Long) taken with the GPS and the point (lat. and Long) generated from the Geolocation of the address associated with the point taken with the GPS, with this data a table was elaborated with the corresponding variations applying the haversine formula [1] to each API as detailed in Table 1.

Table 1. Variation in Kms, haversine.

Direccion	Google	OpenCageData	OpenStreetMap	Here	Bing
Av. Juan Domingo Perón 1915 Posadas Misiones	0,012	0,01	0,01	0,0100	290,96
San Martín 1846 Centro Posadas Misiones	0,218	0,005	0,005	0,0180	146,15
Americas y Sabin Garupa Misiones	0,005	0,05	0,05	3,2800	2,22
Avenida San Roque González 800 Candelaria Misiones	0,131	0,032	0,032	0,0297	0,74
Roque González 698 Posadas Misiones	0,086	0,079	0,079	11,6700	0,18
Av. Cocomarola 7205 Posadas Misiones	0,052	0,024	0,858	0,0602	0,16
Av. República Oriental del Uruguay 3915 Posadas Misiones	0,004	0,012	2,07	0,0259	0,02
Los Lirios y Las Calandrias Itaembe Guazu Misiones	0,02	0,034	0,034	242,5100	0,01
Bolívar 2376 Posadas Misiones	0,009	0,007	0,011	0,0200	0,01
Félix de Azara 1552 Posadas Misiones	0,026	0,032	0,033	0,0200	0,01
Total	0,563	0,285	3,182	257,6437	440,5

It could be observed that OpenCageData and Nominatim are the APIs with the smallest error distance between the real points and the geolocated points generated by the API.

Table 2. Geolocation accuracy.

	Google	OpenCageData	OpenStreetMap	Here	Bing
Total	0,563	0,285	3,182	257,6437	440,46
Media	0,0563	0,0285	0,3182	25,7644	44,046
Median	0,023	0,028	0,0335	0,0278	0,17

The same comparison of the geolocation error of these known directions was also carried out by applying the calculation of the Euclidean distance [2] between the real points and the geocoded ones with each API, and Table 3 was elaborated with the calculated distances and the variation in kilometers of the error:

Table 3. Variation in Kms, Euclidean distance.

Direccion	Google	OpenCageData	OpenStreetMaps	Here	Bing
Americas y Sabin Garupa Misiones	0,0125	0,1585	0,1585	105,6500	5,8500
Av. Cocomarola 7205 Posadas Misiones	0,0362	0,0246	0,1031	0,0351	0,0199
Av. Juan Domingo Perón 1915 Posadas Misiones	0,0082	0,0058	0,0058	0,0071	193,2900
Av. República Oriental del Uruguay 3915 Posadas Misiones	0,0037	0,0088	0,2777	0,0105	0,0168
Avenida San Roque González 800 Candelaria Misiones	0,0487	0,0048	0,0048	0,0153	0,0515
Bolivar 2376 Posadas Misiones	0,0006	0,0008	0,0105	0,0150	0,0004
Félix de Azara 1552 Posadas Misiones	0,0215	0,0355	0,0350	0,0142	0,0061
Los Lirios y Las Calandrias Itaembe Guazu Misiones	0,0242	0,1156	0,1156	464,8600	0,0157
Roque González 698 Posadas Misiones	0,0352	0,0428	0,0428	16,5300	0,0419
San Martín 1846 Centro Posadas Misiones	2,4400	0,0106	0,0106	0,0338	253,6700
Total	2,6308	0,4079	0,7644	587,1709	452,9623

The haversine formula can lead to measurement errors of even more than 3%, which is why the calculation was performed using the Euclidean distance formula which can give an accuracy of more than 0.5mm [6]. With the Euclidean calculation, it is possible to appreciate with better precision the error and the difficulties of interpretation of the natural language that the platforms present concerning the spatial positioning of locations in the metropolitan sector of the city of Posadas:

Table 3. Geolocation accuracy, Euclidean distance.

	Google	OpenCageData	OpenStreetMaps	Here	Bing
Total	2,6308	0,4079	0,7644	587,1709	452,9623
Media	0,2631	0,0408	0,0764	58,7171	45,2962
Median	0,0229	0,0176	0,0389	0,0245	0,0309

4 Discussion

Although the area chosen for the study is located in a relatively large urban conglomerate, there is no continuous updating of geospatial data over time by free access GIS platforms, there is much missing information which weakens the quality of geolocation processes of a given point. In this sense, Crowdsourcing platforms have a

8

certain advantage concerning these data gaps since they count on the collaboration of local users who contribute to these data.

Even so, it is common to find streets and routes that do not have height information which makes it impossible for the API to resolve that point and locate it. This is evidenced in the big jumps in Kms in some direction, this error is generally related to the distance to the urban center or urban conglomeration.

In this work, the poorly resolved points were not omitted because it was considered relevant to highlight this problem.

5 Conclusions

From these tests, it was concluded to use Nominatim since it was the Api that demonstrated the best accuracy metrics in the Geocoding process.

The methods of distance measurement between georeferenced points used showed both to work correctly and in terms of accuracy there were no major differences, in favor of the Euclidean formula should be noted the simplicity of the code and lower computational cost, especially if you work with large volumes of data can be an important advantage. The errors in the geocoding are due to missing data from the GIS platforms as shown in Tables 2 and 4, at this point of the planet even the VGI shows bumps in the information preventing the APIs from solving some directions making it clear that these are still platforms with more detailed information than the others.

References

1. Vincenty, T. (1975). Direct and inverse solutions of geodesics on the ellipsoid with application of nested equations. *Survey Review*, 23(176), 88–93. <https://doi.org/10.1179/sre.1975.23.176.88>.
2. Snyder, J. P. (1987). Map projections--a working manual.
3. Abdi, E., Mariv, H. S., Deljouei, A., & Sohrabi, H. (2014). Accuracy and precision of consumer-grade GPS positioning in an urban green space environment. *Forest Science and Technology*, 10(3), 141–147. <https://doi.org/10.1080/21580103.2014.887041>.
4. Zhang, H., Zheng, J., Dorr, G., Zhou, H., & Ge, Y. (2014). Testing of GPS accuracy for precision forestry applications. *Arabian Journal for Science and Engineering*, 39(1), 237–245. <https://doi.org/10.1007/s13369-013-0861-1>.
5. Alkan, H., & Celebi, H. (2019). The implementation of a positioning system with trilateration of haversine distance. *2019 IEEE 30th Annual International Symposium on Personal, Indoor, and Mobile Radio Communications (PIMRC)*.
6. Szwoch, G. (2019). Combining road network data from OpenStreetMap with an authoritative database. *Journal of Transportation Engineering Part A Systems*, 145(2). <https://doi.org/10.1061/jtepbs.0000215>.
7. Maria, E., Budiman, E., Haviluddin, & Taruk, M. (2020). Measure distance locating nearest public facilities using Haversine and Euclidean Methods. *Journal*

of Physics. Conference series, 1450(1), 012080. <https://doi.org/10.1088/1742-6596/1450/1/012080>.

8. OpenCageData API, <https://api.opencagedata.com/>, last accessed 2023/04/24.
9. Google API, <https://maps.googleapis.com/>, last accessed 2023/04/24.
10. Microsoft DevMaps API, <http://dev.virtualearth.net>, last accessed 2023/04/24.
11. OpenStreetMaps API, <https://nominatim.openstreetmap.org/>, last accessed 2023/04/24.
12. Here Maps API, <https://developer.here.com/>, last accessed 2023/04/24.

Posadas SDI: Transparent Integration with KoboToolBox using Foreign Data Wrappers.

Diego Alberto Godoy¹, Lucas Martín Jardín¹, Luna Blanco¹

¹ Municipalidad de Posadas, Secretaría de Movilidad Urbana, Dirección de Infraestructura de Datos Espaciales, Dirección de Sistemas de Información Geográfica. Avenida Cabred 1741, Posadas Misiones. CP: 3300. Tel: (0376) 4440101
mov.urb.{diegogodoy,lunablanca,lucasjardin}@gmail.com

Abstract. This paper introduces the integration of the KoboToolbox suite, a tool enabling the collection of field data both online and offline, along with real-time tracking using the Posadas Spatial Data Infrastructure (SDI). As a test case for this integration, a survey of city electrical panels is presented. Although KoboToolBox offers a cloud version that can be used for free, it only allows data export in file formats and not direct access to the actual database. This is the reason why the suite has been installed and deployed on a dedicated server to enhance control and gain access to the information stored in the database. Additionally, the mobile app KoboCollect has been employed for conducting field surveys. Ultimately, a Foreign Data Wrapper (FDW) has been utilized, facilitating the connection between the Posadas SDI database and the KoboToolBox database, enabling automatic real-time and transparent updates of Posadas SDI data within the KoboToolBox database.

Keywords: KoboToolbox, Posadas SDI, field data collect

1 Introduction

Field data collection has always been present and complex, ranging from gathering specific data points to dealing with forms containing numerous options. Managing human resources and tools has been a challenge, involving everything from simple paper-based questionnaires to web forms and devices used for data capture. Thus, in [1] conducted a study on these matters, highlighting the need for planning and a supportive tool for successful data collection.

The Urban Mobility secretariat of Posadas's city hall entrusted the General Directorate of Territorial Studies with the task of conducting a survey of Public Lighting Panels in the city of Posadas, which was carried out by municipal personnel. The collected data needed to seamlessly integrate into the Posadas Spatial Data Infrastructure (SDI) [2] in real time. To facilitate this process, the KoboToolBox Suite [3] was chosen as the supporting tool. This tool has been tested in various data collection projects across different contexts and countries, as evidenced by examples such as [4],

2

[5], and [6]. The Urban Mobility secretariat of Posadas city hall had previously used it as a pilot project in [7], making this current work an extension of that effort, further advancing the integration of KoboToolBox with the Posadas Spatial Data Infrastructure in a transparent manner for SDI users.

The article is structured as follows. Section 2 introduces the Posadas Spatial Data Infrastructure and the KoboToolBox Suite. Section 3 provides details of the methodology employed. Section 4 presents implementation specifics. In Section 5, the results of the survey and the transparent implementation are discussed. Finally, the results and conclusions are presented.

2 The Posadas SDI and KoboToolBox

On one hand, the Posadas Spatial Data Infrastructure (SDI) has become a crucial tool for decision-making, providing to the local government with strategic insights into policy implementation and their impact on the territory. Different municipal bodies, including secretariats and other entities, contribute and combine layers of information from their respective geographic information systems (GIS). This information allows for the analysis of territorial dynamics, territorial studies, and collaborative efforts to address requests from residents across various city neighborhoods. This involves prioritizing public services and the placement of infrastructure projects, urban mobility initiatives, tourism, accessibility, sustainability, environmental concerns, healthcare, and more. The Posadas SDI adheres to international standards and norms, ensuring interoperability and use. The Posadas SDI node is part of both SDI Misiones and IDERA, broader geographic information initiatives.

Currently, Posadas SDI hosts 210 layers of information, of which 95 are publicly visible. It serves 90 users from various secretariats. Over the past 320 days of operation, it has received 1,378,564 requests. Figure 1 depicts a screenshot of the Posadas SDI homepage. All this information is made available to residents and the general public, offering georeferenced data and maps about the territory of Posadas city in an accessible, transparent, and ubiquitous manner.

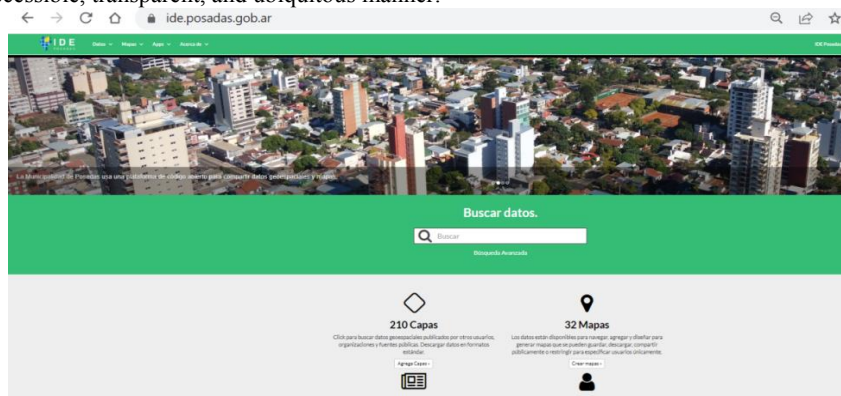


Fig. 1. - Posadas SDI's Home Page.

On the other hand, the KoBoToolbox suite [3] is a tool that facilitates the online and offline collection of field data. Additionally, it allows real-time tracking of data submissions through a web portal. As free and open-source software, it can be adopted in various environments. This platform enables the creation of projects and the management of user permissions within them. Permissions can be assigned to manage the entire project, modify forms, submit, edit, or delete data submissions, among other actions. Figure 2 illustrates the complete architecture of KoboToolBox.

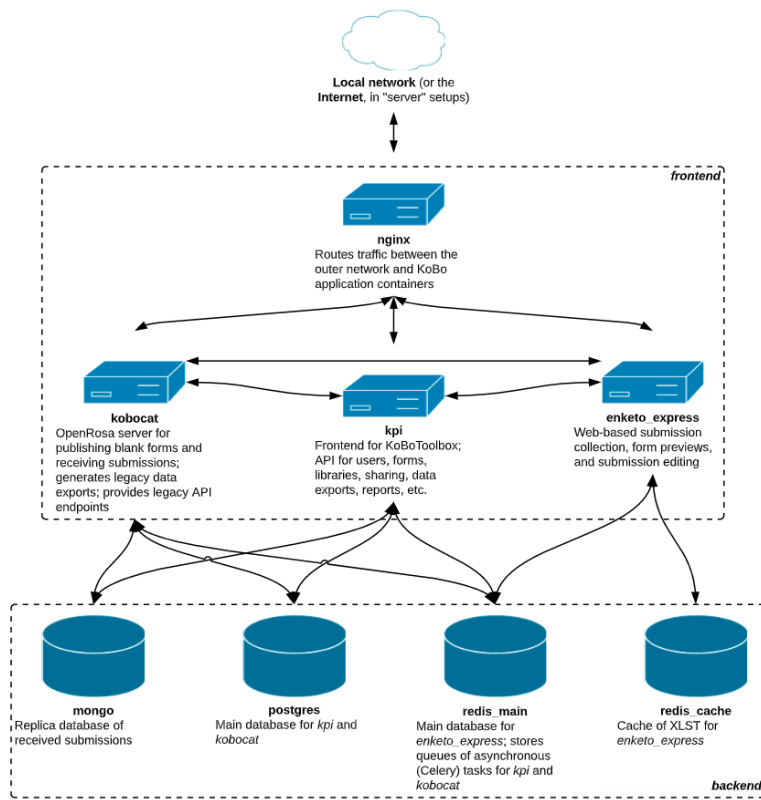


Fig. 2. – KoboToolBox suite architecture

In the mentioned figure, you can observe that in the backend section, there are storage components or databases where complete form submissions by users are stored. These submissions are saved in a MongoDB database. It's important to note that these data cannot be directly accessed from the Posadas SDI.

4

3 Methodology

For the integration of KoboToolBox with the Posadas SDI, a four-step process was undertaken, with the integration and configuration of the Foreign Data Wrapper (FDW) detailed in step four.

1. Form Design: A survey form was designed with over ten fields including location (using mobile phone GPS), photos, survey date, and other attributes such as size and shape.
2. Data Collection in the Field: The survey was conducted collaboratively among different registered platform users. Mobile phones were configured for fieldwork, utilizing the KoboCollect mobile app on Android systems. Users were required to input the service URL, their registered username, and password.
3. Analysis and Survey Management: Project administrators had access to a comprehensive management console. They could view a map of surveyed signs along with associated data via a web portal that facilitated report generation.
4. Integration with the SDI of Survey Results using a Foreign Data Wrapper (FDW) [8]:
 - i. Definition of the integration architecture.
 - ii. Installation of the Postgres FDW extension.
 - iii. Configuration of the FDW.
 - iv. Data queries from the MongoDB through SQL.
 - v. Definition of views from Postgres SQL.
 - vi. Configuration of Geoserver for access.
 - vii. Configuration of Geonode for access to the new data.

The steps above outline the process of seamlessly integrating KoboToolBox survey results with the Posadas SDI using the Foreign Data Wrapper to bridge the MongoDB data with the Postgres SQL database, ensuring efficient access and analysis of the collected information.

4 Implementation

Initially, the process involved installing the KoboToolbox suite on a dedicated server. The server featured an Intel Core i5 processor with 8GB of RAM and a 500GB SSD for storage. Ubuntu 20.04 was chosen as the operating system, and several software packages, including Python, Docker, and databases such as Postgres, MongoDB, and REDIS, were installed. In addition, different DNS subdomains were configured (essential for the suite's operation), and port forwarding was set up to provide internet access to various server ports.

Once the suite was successfully installed, a project named "Public Lighting Panels" (Tableros de Alumbrado Público in Spanish) was created within the platform. Within this project, a custom form was designed, featuring the necessary fields for the survey. Figure 3 displays a screenshot of the tool's form design interface.

The implementation process encompassed setting up the server hardware, installing essential software components, configuring networking elements like DNS subdomains and port forwarding, and tailoring a project within the KoboToolbox platform to align with the specific requirements of the "Public Lighting Panels" survey.

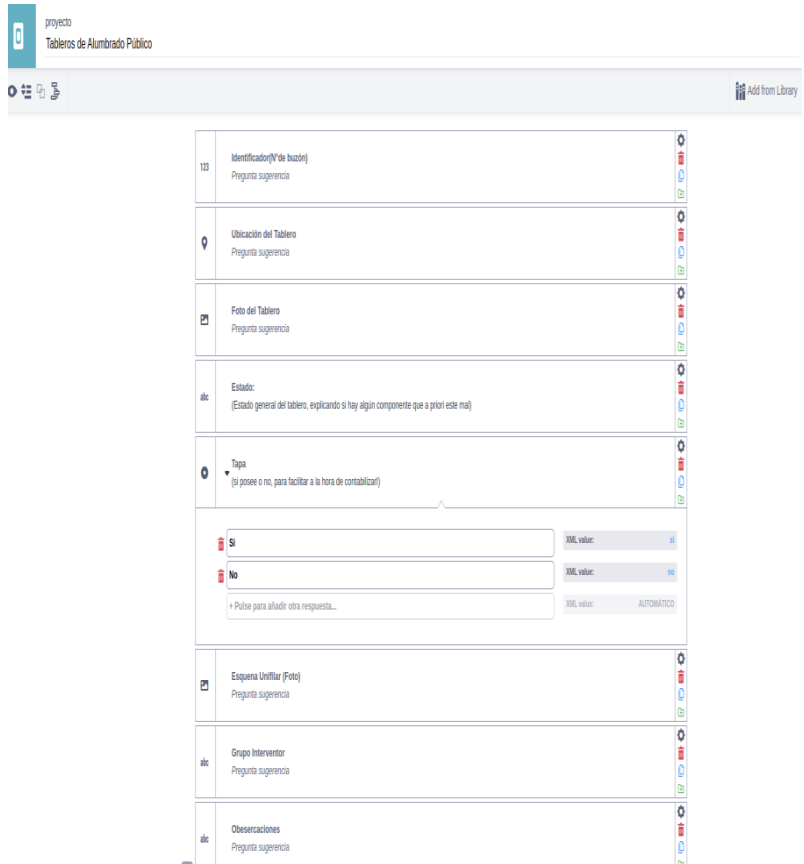


Fig. 3. – KoboToolBox form design interface.

In Figure 4, you can observe a captured record using the tool.

6

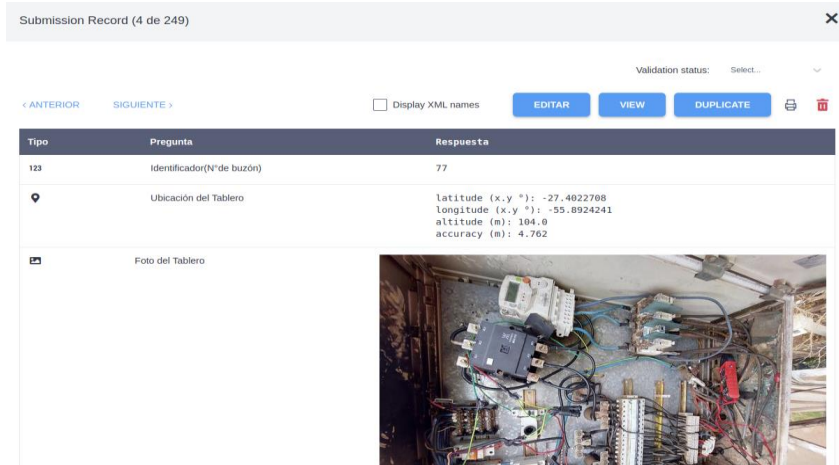


Fig. 4. – Screenshot of capture record with KoboToolBox

Next, an architectural view of the KoboToolBox integration with the Posadas SDI implementation is presented. Figure 5 displays the components and architecture employed for this proposed solution.

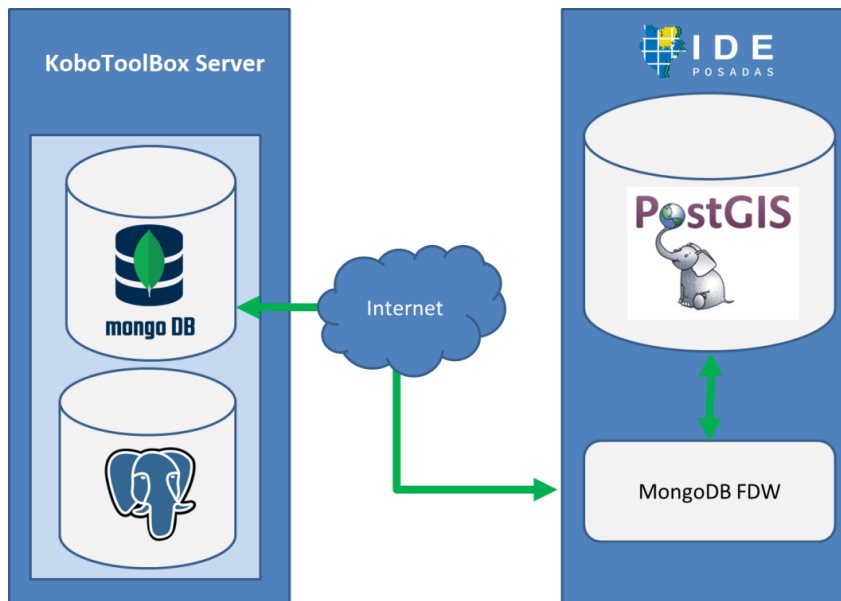


Fig. 5. – Proposed solution architecture

The operational flow is as follows: From the Postgres+PostGIS data server hosting the Posadas SDI, a Foreign Data Wrapper (FDW) was installed for MongoDB. Using connection credentials, this FDW establishes a link between tables in the Postgres database and the MongoDB database, facilitating access to survey data stored on the KoboToolBox server. Figure 6 depicts the "instances" table where survey data is stored.

The process involves establishing a connection between the Postgres+PostGIS database and the MongoDB database using the FDW, enabling seamless access to relevant survey data stored on the KoboToolBox server from within the Posadas SDI.

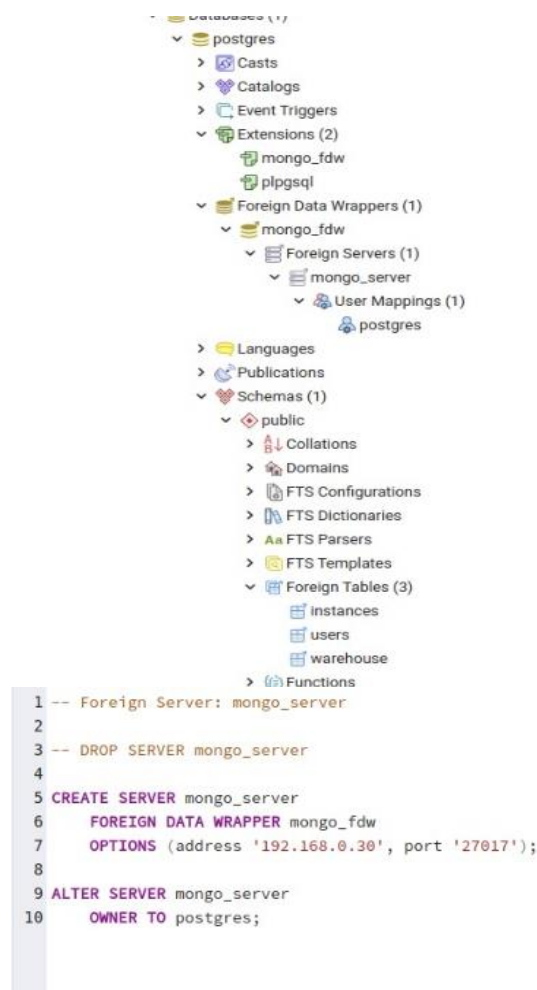
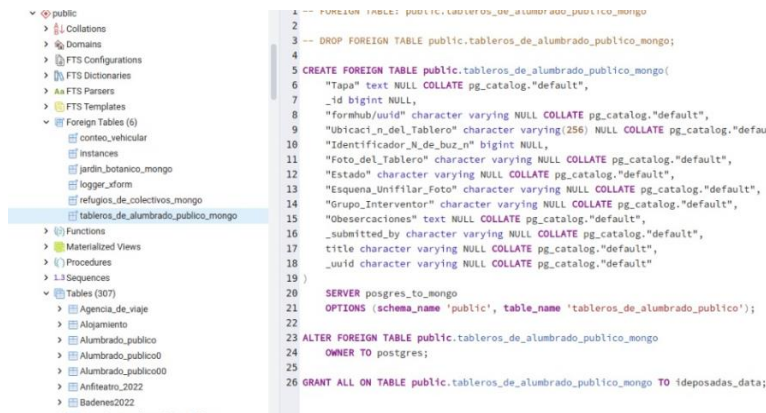


Fig. 6. – Screenshot of PG_ADMIN with all tools installed and configured.

8

In Figure 7, you can observe a detailed view of the fields within the foreign table "instances." This table is where all the data from forms created with KoboToolBox is stored. Additionally, you can see the table "tableros_de_alumbrado_publico_mongo," containing filtered data specific to the "tableros" form.

The illustration provides insight into the structure of the "instances" table containing comprehensive data from KoboToolBox forms, as well as the "table-ros_de_alumbrado_publico_mongo" table containing specialized data related to the "tableros" survey form.



The screenshot shows the PG_ADMIN interface. On the left, a tree view displays the database structure, with 'Foreign Tables (6)' expanded to show 'instances' and 'tableros_de_alumbrado_publico_mongo'. On the right, the SQL editor shows the following code:

```

1 -- FOREIGN TABLE PUBLIC: tableros_de_alumbrado_publico_mongo
2
3 -- DROP FOREIGN TABLE public.tableros_de_alumbrado_publico_mongo;
4
5 CREATE FOREIGN TABLE public.tableros_de_alumbrado_publico_mongo(
6     "Tapa" text NULL COLLATE pg_catalog."default",
7     _id bigint NULL,
8     "formhub/uuid" character varying NULL COLLATE pg_catalog."default",
9     "Ubicaci_n_del_Tablero" character varying(256) NULL COLLATE pg_catalog."default",
10    "Identificador_M_de_buz_n" bigint NULL,
11    "Foto_del_Tablero" character varying NULL COLLATE pg_catalog."default",
12    "Estado" character varying NULL COLLATE pg_catalog."default",
13    "Esquema_Unifilar_foto" character varying NULL COLLATE pg_catalog."default",
14    "Grupo_Interventor" character varying NULL COLLATE pg_catalog."default",
15    "Observaciones" text NULL COLLATE pg_catalog."default",
16    _submitted_by character varying NULL COLLATE pg_catalog."default",
17    title character varying NULL COLLATE pg_catalog."default",
18    _uid character varying NULL COLLATE pg_catalog."default"
19 )
20
21 SERVER postgres_to_mongo
22
23 OPTIONS (schema_name 'public', table_name 'tableros_de_alumbrado_publico');
24
25
26 ALTER FOREIGN TABLE public.tableros_de_alumbrado_publico_mongo
27 OWNER TO postgres;
28
29 GRANT ALL ON TABLE public.tableros_de_alumbrado_publico_mongo TO ideposadas_data;

```

Fig. 7. – Screenshot of PG_ADMIN (table “instances” and table tableros_de alumbrado_publico_mongo)

This connection takes place over the internet and enables the Postgres database engine to seamlessly access this data, thereby generating views that represent geographic information layers. Ultimately, Figure 9 showcases the view that facilitates the creation of a table encompassing all the necessary information for publication using Geoserver and Geonode within the Posadas SDI.

The integration allows the Postgres database to retrieve data from KoboToolBox via the established connection. This data can then be transformed into views representing geographic layers, which can be published through Geoserver and Geonode in the Posadas SDI.

```

1 -- View: public.tableros_de_alumbrado_publico_gd
2 -- DROP VIEW public.tableros_de_alumbrado_publico_gd;
3
4
5 CREATE OR REPLACE VIEW public.tableros_de_alumbrado_publico_gd
6 AS
7 SELECT at_sesordf_id, makepoint('substring("substring"(tableros_de_alumbrado_publico_mongo."ubicaci_n_del_Tablero":text, "position"(tableros_de_alumbrado_pu
8 "substring"(tableros_de_alumbrado_publico_mongo."ubicaci_n_del_Tablero":text, 1, "position"(tableros_de_alumbrado_publico_mongo."ubicaci_n_del_Tablero":ti
9 "substring"(tableros_de_alumbrado_publico_mongo."ubicaci_n_del_Tablero":text, "position"(tableros_de_alumbrado_publico_mongo."ubicaci_n_del_Ta
10 tableros_de_alumbrado_publico_mongo."Tapa"),
11 tableros_de_alumbrado_publico_mongo."AS Fila",
12 tableros_de_alumbrado_publico_mongo."forohub/uid"),
13 tableros_de_alumbrado_publico_mongo."ubicaci_n_del_Tablero",
14 tableros_de_alumbrado_publico_mongo."Identificador_de_Bus_M",
15 tableros_de_alumbrado_publico_mongo."Foto_del_Tablero",
16 tableros_de_alumbrado_publico_mongo."Estado",
17 tableros_de_alumbrado_publico_mongo."Equipo_del_Filar_Foto",
18 tableros_de_alumbrado_publico_mongo."Grupo_Interventor",
19 tableros_de_alumbrado_publico_mongo."Observaciones",
20 tableros_de_alumbrado_publico_mongo."identif_bv",
21 concat('https://rc-relaxamento.posadas.gov.ar/media/medios/media_filesuper_admin/attachments/'), tableros_de_alumbrado_publico_mongo."forohub/uid", '/', 1
22 concat('https://rc-relaxamento.posadas.gov.ar/media/medios/media_filesuper_admin/attachments/'), tableros_de_alumbrado_publico_mongo."forohub/uid", '/', 1
23 FROM tableros_de_alumbrado_publico_mongo;
24
25
26 ALTER TABLE public.tableros_de_alumbrado_publico_gd
27 OWNER TO postgres;
28
29 GRANT ALL ON TABLE public.tableros_de_alumbrado_publico_gd TO postgres;
30 GRANT ALL ON TABLE public.tableros_de_alumbrado_publico_gd TO deposedas_data;
31
32

```

Fig. 8. – Screenshot of PG_ADMIN (table “tableros_de alumbrado_publico_mongo”) ready to be published in Geoserver y Geonode.

5 Results

The partial result of the survey has yielded a total of 249 records of public lighting panels in the city of Posadas. Figure 9 depicts an automatically generated map displaying the location of each of these panels.

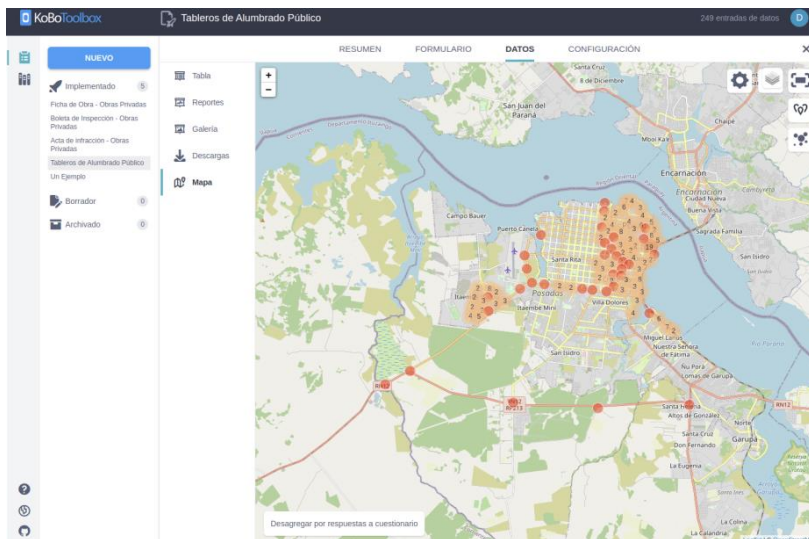


Fig. 9. – Map View in KoboToolBox server.

10

In Figure 10, a screen from the Posadas SDI is displayed, showcasing the same data as the KoboToolBox platform in a seamless manner, transparent to the user.

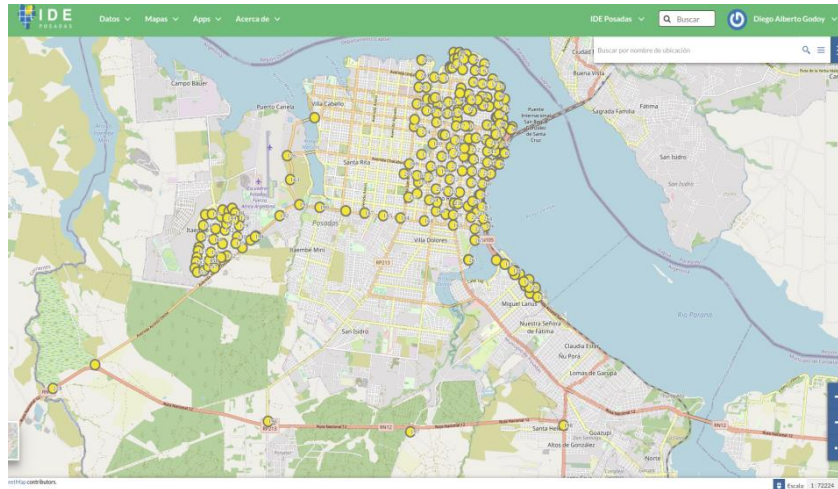


Fig. 10. - Public lighting panels dataset in Posadas SDI.

6 Conclusions

The utilization of a Foreign Data Wrapper (FDW) enables the consumption of information collected and stored in the MongoDB database of KoboToolBox from the Postgres+PostGIS database of the Posadas SDI in a seamless manner. This integration treats the data as if it were just another layer loaded onto the Geonode platform. The advantage of having real-time information is evident compared to manual imports from KoboToolBox to Posadas SDI using geojson or shapefiles.

Users expressed satisfaction with the ease of data collection through the KoboCollect app. The case study involving the survey of lighting panels contributes to the list of successful data collection instances using these tools, much like the previous example of advertising panels survey presented in an earlier work.

Furthermore, the successful incorporation of collected data validates the utility of the KoboToolBox tool. The integration has proven to be effective, offering a streamlined way to access real-time data seamlessly within the Posadas SDI, enhancing the overall data collection and management process.

As future work, it is planned to use these same tools and methodologies for other surveys in the city and use the FDW for integration with other systems such as automated vehicle counting.

7 Acknowledgment

To Mayor of the City of Posadas, Engineer Leonardo "Lalo" Stelatto, and to the Secretary of Urban Mobility, Master Engineer Lucas Jardín (who is also a co-author of this work), for their dedication to promoting the development of SDI POSADAS.

8 References

1. Lakshminarasimhappa, M.: Web-based and smart mobile app for data collection: Kobo Toolbox/Kobo collect. *Journal of Indian Library Association* 57, 72-79 (2022)
2. Municipalidad de Posadas: IDE Posadas. In: IDE Posadas. (Accessed 2023) Available at: <http://www.ide.posadas.gob.ar>
3. Kobotoolbox.org: KoBoToolbox. In: KoBoToolbox | Data Collection Tools for Challenging Environments. (Accessed 2022) Available at: <https://www.kobotoolbox.org/>
4. Da Silva, S.: UTILIZAÇÃO DO KOBOTOOLBOX COMO FERRAMENTA DE OTIMIZAÇÃO DA COLETA E TABULAÇÃO DE DADOS EM PESQUISAS CIENTÍFICAS. *Geoambiente On-line* 36, 122-140 (2020)
5. Santos, P.: Aplicabilidade da ferramenta Kobotollbox para validação de mapeamento de classificação de cobertura e uso da terra. *Revista Geografias*, 17, 42-61 (2022)
6. Arroba Medina, L.: Provisión de áreas verdes en la comuna de Tomé. Identificación y jerarquización de sitios óptimos para el desarrollo de futuras iniciativas. (2019)
7. Godoy, D. A., Blanco L. Jardín, L. M.: IDE Posadas: Utilización de KoboToolbox para relevamiento en campo de información georeferenciada a través de la web. In : XVI Jornadas IDERA. 2022. (2022)
8. Enterprise DB: PostgreSQL foreign data wrapper for MongoDB. (Accessed 2023) Available at: https://github.com/EnterpriseDB/mongo_fdw

Leveraging User-Generated Content to Improve Urban Traffic Management in the context of Smart Cities

Marco Moreno-Ibarra¹, Magdalena Saldaña-Perez² and Juan Carlos Venegas Segura³

Instituto Politécnico Nacional, Centro de Investigación en Computación, Av. Juan de Dios Bátiz, esq. Miguel Othón de Mendizábal, Col.Nueva Industrial Vallejo, Alcaldía Gustavo A. Madero, C.P. 07700, CDMX, México
mmorenoi@ipn.mx¹, amsaldanap@ipn.mx², jvenegass2022@cic.ipn.mx³

Abstract. Traffic, pollution and rapid population growth are major problems in large cities. Therefore, smart cities have emerged as viable solutions for addressing these issues. This paper presents a method for examining urban traffic using User-Generated Content (UGC). This method focuses on collecting data carried out by citizens through observations and comments about their surrounding environment, which they voluntarily share through mobile applications or social networks. This type of approach is proving to be useful for improving the understanding of urban traffic, as it can be used to identify traffic bottlenecks, predict traffic and eventually support decision-makers in activities such as urban planning. The proposed framework considers the technology and concepts of Geographic Information Systems (GIS), as well as machine learning algorithms and data mining techniques, to organize, process and present urban data. This proposal includes the following components: monitoring, integration, analysis, visualization and data sharing. We believe that this proposal can contribute to the understanding of the use of this type of information generated by citizens, complement that obtained through traditional methods and provide better alternatives for decision-making by authorities and citizens.

Keywords: Social sensing, GIS, Traffic, UGC

1 Introduction

Large cities face challenges such as population growth, environmental degradation and transportation to meet the needs of their inhabitants [6][14]. Urban areas constitute a major part of the world's population [2]; hence, there is an urgent need to address these problems. In this context, concepts such as smart cities, Geographic Information Systems (GIS), the Internet of Things (IoT), Big Data Analysis and Artificial Intelligence (AI) play a relevant role in promoting efficient and sustainable ways are being sought to address these problems in a specific way according to the needs of the population and city context [14]. In this sense, citizen participation in cities involves the participation and collaboration of inhabitants in reporting observations they perceive in an urban context. using mobile devices or social networks [8]. This data is

2

known as User-Generated Content (UGC) and concepts such as Voluntary Geographic Information (VGI) are used to refer to this type of data in a geographical context. This participation can be characterized by citizens acting as sensors [4].

According to UGC, "a Smart City is a concept that presents the vision of a connected and digital city to solve problems and aims to provide solutions based on tools for planning, building and managing efficient, livable and sustainable communities" [9]. For a city to be considered "intelligent" a digital environment representative of the urban area must be developed that includes modeling, visualization, analysis, planning, simulation and monitoring of what is happening in the city, in addition to allowing citizen participation [10]. The use of 2D or 3D models, in addition to real-time input from sensors, allows the tracking of traffic, public transportation, vegetation growth, and various environmental and social variables, thereby increasing the adaptability and flexibility of the system. More than a tool for the city, it seeks to generate an ecosystem that integrates diverse, interoperable, accessible, inclusive and secure data in which many actors can obtain information to know the state of what is happening, analyze it, propose alternative solutions and improve decisions for the benefit of the inhabitants.

A Geographic Information System (GIS) can process data flows about a city that are location-sensitive and continuously generated from sensors [6]. It also allows the integration of various data sources, such as vehicle movement, through GPS traces or sensor records, thus allowing the analysis of various situations. Social networks, such as Twitter (now X), have become valuable sources of data for urban analysis. However, the quality of data generated by social media users with reference to everyday events can vary considerably; thus, they can provide accurate information, whereas others may lack detail or be vague [5]. Various preprocessing techniques are used to analyze social media data, such as text-element analysis, removal of special characters and stop words, replacement of uppercase letters with lowercase letters and the identification of contextual and domain-related words. Our proposal for urban analysis, based on citizen collaboration, encompasses tasks such as the acquisition, integration, visualization and analysis of city data, with the aim of supporting authorities. It involves the use of classical GIS methods, big data techniques, machine learning and data mining to manage vast amounts of generated data [7][8]. It is important to consider that given the source of data obtained through social sensing, data validation is crucial to ensure data quality and enhance the certainty of the analysis results.

This article describes a proposed framework oriented towards the state of traffic based on the application of the technology and concepts of Geographic Information Systems (GIS) and its functionalities, machine-learning algorithms, data mining and visualization techniques. The remainder of this paper is organized as follows. Section 2 presents related work concerning the analysis of traffic in smart cities based on social sensing. We also describe the background to this topic. In Section 3, we introduce and explain our proposal for integrating smart cities based on GIS. Finally, in section 4, we present our conclusions.

2 Social sensing for traffic analysis in the context of smart cities

The aim of smart cities to support traffic analysis using social sensor information is in a growing phase of development. In recent years, numerous studies have been conducted that explored the use of social media data such as Twitter to improve our understanding of urban traffic. Specific examples of how Twitter data is used for traffic analysis include the identification of traffic bottlenecks, traffic prediction, and improved transportation decision-making. Carter et al. [3] presented a study on the city of Melbourne that used sensor data, which were analyzed using data analysis techniques, such as heat maps and charts, to identify areas of high pedestrian traffic and to assess future infrastructure development, such as the location of traffic lights and street layout. It is important to note that this study considered the eventual incorporation of wearable devices and social media data as a means of sensing city activities.

The work proposed by Salas et al. [11] includes a text classification algorithm to detect tweets in the context of traffic based on Support Vector Machines (SVMs). Using sentiment analysis, these traffic messages were classified as positive, negative, or neutral. This classification was used to identify whether an event was negative (e.g., accidents, road work, or delays) or positive (e.g., lane reopening or completion of roadwork).

Yang and Cudre-Mauroux [15] highlighted opportunities to leverage Location-Centric Social Media (LBSM) data such as Foursquare for urban analysis and smart cities. This method can be applied to traffic analysis in smart cities. This is because LBSM data provides de-tailed, semantically rich, spatiotemporal data on user activity that can be used to analyze urban dynamics, including traffic patterns and congestion. Ali et al. [1] proposed a real-time monitoring framework based on social media for traffic accident detection and status analysis using Ontology and Latent Dirichlet Allocation (OLDA) and bidirectional long short-term memory (Bi-LSTM). This study is oriented towards traffic event recognition based on ontologies and a sentiment analysis technique to determine the polarity of traffic events in order to enhance traffic flow and prevent more incidents. Carter et al. [3] proposed a method that was tested in real time by detecting traffic incidents based on geolocation tweets classified by ranking tweets according to their weight.

For Mexico City, Saldaña et al. [13] used a Support Vector Machine (SVM) method to predict traffic congestion and Twitter social network analysis to collect traffic-related events. Geospatial models, machine learning techniques, and regression have been used to predict traffic events and detect city zones with the most severe traffic problems. Salazar et al. [12] presented a method for geocoding tweets of traffic-related events, and created a prediction model for traffic congestion analysis. The model generates spatio-temporal information on traffic congestion, which is analyzed using a spatio-temporal analysis approach. Traffic behavior in Mexico City was represented using heat maps in a web mapping application. This study demonstrated that citizens can act as sensors by collecting social media data related to traffic to detect the dynamics of a city. In this case, the prediction model was based on SVM.

The studies discussed agree on the value of social sensor data, particularly location data, for building applications in smart cities related to traffic management and optimization. The studies reviewed in this paper demonstrated that Twitter data can be used to improve our understanding of urban traffic. However, there are still challeng-

4

es that must be addressed, such as the accuracy of tweet geolocation, and the need to develop robust analytical techniques. Despite these challenges, social sensor information has the potential to reshape traffic management in smart cities through traffic analysis.

3 Framework

Smart city approaches have been developed by integrating different technologies to enhance information for city managers and promote the quality of life of inhabitants. To do this, they collected and analyzed data from various sources, such as physical and social sensors, to gain insights into how a city behaves [6][8]. This section describes the framework for developing smart cities, which includes the following components: Monitoring, Integration, Analysis, Visualization and Data Sharing (Fig.1).

The framework also includes an alternative to consider citizen participation and consider their observations and comments for the analysis, monitoring, and tracking of urban environments. In other words, a UGC or VGI approach was used in the monitoring section to collect traffic-related data. Monitoring consists of collecting data from various sources such as physical and social sensors. Integration consists of combining and merging data collected from various sources to gain a comprehensive understanding of how a city behaves [10]. The objective of the analysis is to derive meaningful insights from the data by interpreting and analyzing it so that effective decisions can be made. These methods include spatial analysis, machine learning, and data visualization to process data and display pictographic images of traffic data. To promote easy understanding of the data using maps, tables, and charts, we propose a visualization component. Data sharing involves the distribution of the collected data to various recipients, including other users, organizations, or systems. Cloud services or webpages can be used to share this information, which can be helpful in some cases and projects.

The following subsections provide detailed descriptions of each component.

3.1 Monitoring

Monitoring refers to data generated and monitored by physical or social sensors. These sensors are real-time data sources that are continuously updated and provide up-to-date information regarding a particular phenomenon or event [8]. In this context, the efficiency of these sensors is crucial for making cities smarter and for improving their operations [14]. These sources include both physical and social sensors.

Physical sensors: These devices focus on collecting data on the physical or environmental conditions in an urban environment. Physical sensors are oriented to capture information on various aspects of a city, such as traffic, air quality, temperature, humidity, pressure, noise, brightness and presence of people, in a real-time fashion. Wearable devices connected to the Internet, such as Fitbit, can provide data on people's activity levels, which can be correlated with data on pedestrian or vehicle movements [3].

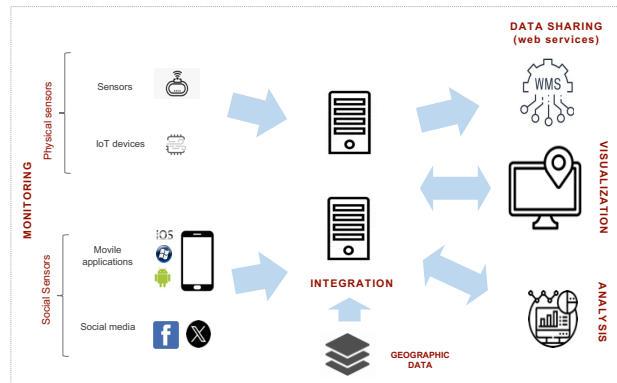


Fig. 1. Framework for smart cities based on social sensing.

Social sensors: This refers to the use of social media, the Web, or applications in which users can voluntarily share their observations [4]. This approach allows citizens to contribute to the collection of real-time data for a city such as traffic, noise pollution and urban services. This monitoring of social media platforms, such as Twitter or Facebook, along with data sampled by other sensors, can help identify popular and unpopular areas [3]. The use of this type of approach presents challenges related to data heterogeneity, quality, temporal validity, vagueness, and precision, which may compromise the validity and reliability of the results [16].

3.2 Integration

This is related to data integration, which involves combining data from different sources in a common database and considering contextual information to gain a comprehensive understanding of how a city behaves [10] [13]. This component focuses on procedures and operations that standardize the data from different sources by editing and transforming them. This integration enables the discovery of correlations between social media activity, citizen feedback and data on urban infrastructure, including traffic [6][8]. These analyses can be used to generate additional insights into other urban issues, which can benefit both citizens and authorities [16].

3.3 Analysis

It focuses on investigating and interpreting data to uncover patterns, trends, traits, and features that improve the comprehension of the study region and facilitate informed decision-making [7][10]. These methods include spatial analysis, machine learning and data visualization. Spatial analysis allows the detection of relationships and evaluation of phenomena from a geographic perspective [6]. Meanwhile, machine learning can be used to predict future behaviors such as the likelihood of events such as crimes or the spread of diseases.

6

3.4 Visualization

Visualization refers to the use of visual representations such as maps or charts to enhance analyses communication [8]. This is an important stage because a good visual representation facilitates the identification of the conditions of a particular phenomenon, such as traffic, to facilitate decision making.

3.5 Data sharing

Data sharing consists of sharing collected data with other users, organizations, or systems; it allows collaboration, research, and decision making based on shared information [8]. It is possible to establish a set of web services that adhere to UGC standards, thereby enabling data access to other applications [9]. The proposed framework is flexible, and can be adapted to various contexts and applications. The use of this framework can help cities improve their efficiency and effectiveness, leading to improvement in the lives of their inhabitants.

In the present work, it is observed that this type of framework (based on social sensors) can be satisfactorily implemented in the development of a smart city and can even be used in different application areas because it is very flexible. Another characteristic that these frameworks show in the long term is their low resource requirement. This is because implementation costs can be significantly reduced even without having to deal with imperfections that may exist when using physical sensors, such as breakdowns, interferences, and incorrect measurements.

4 Conclusions

Social media to solve urban problems has attracted the attention of the government, academia, and industry specialists. Specific examples of the use of social media data for traffic analysis include identification of traffic bottlenecks, traffic prediction, and improved transportation decision-making. It has been proven that user-generated content can be used to improve the understanding of phenomena such as traffic in an urban context. It is important to note that geospatial technology that allows the design, development, implementation and operation of smart cities is currently available. However, challenges still need to be addressed, such as the accuracy of tweet geolocation, the verification of data quality, and the need for more robust analytical techniques. Despite these challenges, traffic analysis using social sensor information has the potential to revolutionize traffic management in smart cities. Using frameworks based on UGC and VGI data collection has some advantages such as low production costs, minimal resources, and moderate maintenance.

Specific examples of how smart cities can analyze traffic include identifying traffic bottlenecks, traffic prediction, and improved transportation decision making. To improve the implementation of this framework, the following actions are recommended: 1. Develop policies and regulations that promote the use of open data and standards; 2. strengthening cooperation between the different actors involved in the devel-

opment of smart cities; and 3. Invest citizen training and awareness of the use of data for decision making.

Acknowledgments: The authors gratefully acknowledge the Instituto Politécnico Nacional, the Consejo Nacional de Humanidades Ciencia y Tecnología (CONHACYT) for their support.

References

1. Ali, F., Ali, A., Imran, M., Naqvi, R. A., Siddiqi, M. H., & Kwak, K. S. (2021). Traffic accident detection and condition analysis based on social networking data. *Accident Analysis & Prevention*, *151*, 105973.
2. Bakıcı, T., Almirall, E. & Wareham, J. A Smart City Initiative: the Case of Barcelona. *J Knowl Econ* 4, 135–148 (2013). <https://doi.org/10.1007/s13132-012-0084-9>
3. Carter, E., Adam, P., Tsakis, D., Shaw, S., Watson, R., & Ryan, P. (2020). Enhancing pedestrian mobility in smart cities using big data. *Journal of Management Analytics*, *7*(2), 173-188.
4. Goodchild, M. F. (2007). Citizens as sensors: the world of volunteered geography. *GeoJournal*, *69*, 211-221.
5. Goodchild, M.F., Li, L., 2012. Assuring the quality of volunteered geographic information. *Spatial Statistics* 1, 110e120.
6. Leidner, A., & Percivall, G. (2022). Smart Cities. In *Springer Handbook of Geographic Information* (pp. 845-875). Cham: Springer International Publishing.
7. Li, W., Batty, M., & Goodchild, M. F. (2020). Real-time GIS for smart cities. *International Journal of Geographical Information Science*, *34*(2), 311-324.
8. Moreno-Ibarra, M., & Torres-Ruiz, M. (2019). Civic participation in smart cities: the role of social media. In *Smart cities: Issues and challenges* (pp. 31-46). Elsevier.
9. *Open Geospatial Consortium*. (2022). Open Geospatial Consortium. <https://www.ogc.org/>. Accessed Sep-18-2023
10. Rienzi, B., Sosa, R., Abellá, G., Machado, A., Susviela, D., & González, L. (2023). Standards-Based Geospatial Services Integration for Smart Cities Platforms. In *GISTAM* (pp. 167-175).
11. Salas, A., Georgakis, P., Nwagboso, C., Ammari, A., & Petalas, I. (2017, July). Traffic event detection framework using social media. In *2017 IEEE International Conference on Smart Grid and Smart Cities (ICSGSC)* (pp. 303-307). IEEE.
12. Salazar-Carrillo, J., Torres-Ruiz, M., Davis Jr, C. A., Quintero, R., Moreno-Ibarra, M., & Guzmán, G. (2021). Traffic congestion analysis based on a web-gis and data mining of traffic events from twitter. *Sensors*, *21*(9), 2964.
13. Saldana-Perez, M., Torres-Ruiz, M., & Moreno-Ibarra, M. (2019). Geospatial modeling of road traffic using a semi-supervised regression algorithm. *IEEE Access*, *7*, 177376-177386.
14. Singh, T., Solanki, A., Sharma, S. K., Nayyar, A., & Paul, A. (2022). A Decade Review on Smart Cities: Paradigms, Challenges and Opportunities. *IEEE Access*.
15. Yang, D., Qu, B., & Cudre-Mauroux, P. (2020). Location-centric social media analytics: Challenges and opportunities for smart cities. *IEEE Intelligent Systems*, *36*(5), 3-10.

Centros Históricos en el contexto de las Ciudades Inteligentes y Sostenibles

Juan Carlos Martínez Serra ^[000-0002-0883-0573]

¹ Universidad UTE, Quito, Ecuador
www.ute.edu.ec

Resumen.

El fuerte crecimiento de la población urbana y el aumento del consumo de recursos han creado inevitablemente desafíos para las ciudades. Este hecho destaca la importancia de cambiar los paradigmas en la forma en que las ciudades funcionan en términos de sostenibilidad. Uno de los grandes retos que prácticamente todos los países van a enfrentar es la planificación, administración y gobernanza de las ciudades de forma sostenible, maximizando las oportunidades económicas y minimizando los daños medioambientales. En este escenario, los Centros Históricos fomentan el crecimiento económico de las ciudades, la preservación de la memoria social y la identidad cultural de sus habitantes, por lo que su explotación debe ser de forma consciente y comprometida. Las TIC, constituyen una nueva oportunidad para vivir y habitar, protegiendo el paisaje cultural en el que se encuentran. Para esto, es determinante establecer indicadores que permitan diagnosticar los Centros Históricos dentro de un contexto de *Smart Heritage*.

Palabras clave: Smart Cities, Centros Históricos, Ciudades Inteligentes y Sostenibles, TIC.

1 Introducción

En las últimas décadas, se ha gestado la confluencia de dos fenómenos en la historia de la humanidad, la tendencia ascendente para urbanizar a nivel mundial y la revolución tecnológica. Según la ONU [1] para el mes noviembre del 2022 la población mundial alcanzó 8000 millones de habitantes; donde más de la mitad viven en ciudades, se prevé que para el 2050, la población mundial supere los 10.000 millones de habitantes; más de la mitad del crecimiento demográfico mundial tendrá lugar en África, mientras que, en Europa, la población de 61 países descenderá en más del 15%.

De esos 10 mil millones, más del 70%, vivirán en ciudades, de los cuales, cerca del 90% vivirán en los países desarrollados y más del 60% lo harán en los países en vías de desarrollo.

En el caso de América Latina y el Caribe, a mitad del siglo XX, el proceso de urbanización fue incrementándose, hasta llegar a ser hoy, después de América del Norte, la segunda zona del mundo más urbanizada.

2

Las ciudades concentran la mayor parte de población del planeta, son el foco de la actividad cultural, artística y económica. Por otra parte, la mayoría de los recursos naturales y energéticos y como consecuencia de esta y otras actividades generan la mayor parte de los residuos y son responsables de la emisión a la atmósfera de la mayoría de los gases de efecto invernadero y de otros factores contaminantes.

En este sentido, las ciudades contemporáneas se enfrentan a desafíos únicos. Cada vez más, las principales ciudades y áreas metropolitanas son vistas como sistemas con conexiones complejas entre sus diferentes ambientes e individuos [2] cuyas soluciones podrían residir en formas más innovadoras de utilizar las tecnologías inteligentes en apoyo de la toma de decisiones.

Está claro que hay que apostar por crear nuevas urbanidades resilientes, económicamente organizadas y socialmente inclusivas. La ONU ha declarado que “la batalla por la sostenibilidad se ganará o se perderá en la forma en que diseñamos nuestras ciudades”. En este sentido, la cultura tiene un rol determinante en el diseño de *Smart Cities*, ya que le da prioridad el factor humano y el capital social, constituyendo el patrimonio cultural de cada ciudad como elemento distintivo y diferenciador del resto de ciudades. “Esto permite conectar al ciudadano con la estrategia *Smart*, y motivar a la sociedad a colaborar activamente en su diseño para garantizar, respetar y destacar las características diferenciables que la identifican con la ciudad que habita” [3]

En el caso de los Centros Históricos (CHs) esta tendencia ejerce una presión excesiva, que muchas veces sobrevive en medio de los ataques terroristas, el cambio climático, la presión inmobiliaria y la mala gestión de los recursos económicos gubernamentales, resultando, en algunos casos, en daños irreversibles y pérdidas permanentes. La diversidad cultural, que en la década anterior había sido estudiada como un fenómeno positivo, ahora se ve como un peligro. Aunado a la difusión de la intolerancia, el sectarismo y los conflictos sociales, está dificultando el proceso de integración en muchos países del mundo, tanto en los países desarrollados como en los no desarrollados. Dentro de este escenario, el legado patrimonial encontrado en los CHs es fundamental, tanto para el crecimiento económico de las ciudades (turísticas, por ejemplo), como para la preservación de la memoria social y la identidad cultural de sus habitantes.

El patrimonio cultural, tanto en sus expresiones tangibles como intangibles, resume las identidades de las personas, da forma a las comunidades y contribuye a la creación de capital social [4]. Es por esto que una alternativa para mitigar los efectos negativos, es el uso de la tecnología de información y comunicación, con el objetivo de la preservación y protección del patrimonio.

Este artículo presenta una reflexión exhaustiva del rol que cumple los Centros Históricos dentro del contexto de *Smart Heritage*, a partir de la comprensión del término *Smart Cities*.

2 Metodología

La investigación que se presenta a continuación contiene dos partes fundamentales, una fase teórica y una fase exploratoria (Ver Tabla 1)

Tabla 1. Metodología

		Estrategias	Técnicas de investigación	Método
Investigación de tipo exploratoria	Fase teórica conceptual	Fundamentación teórica sobre <i>Smart Cities</i> , <i>Smart Heritage</i> y Centros Históricos.	Técnica documental: Recogida y tratamiento de datos de diferentes fuentes <ul style="list-style-type: none"> – Literatura académica. – Revistas especializadas en arquitectura, urbanismo, ingeniería, geografía humana, desarrollo sostenible y TIC. – Páginas oficiales e instituciones de las ciudades europeas y de AL. 	<ul style="list-style-type: none"> – Arqueo de fuentes – Revisión de fuentes – Cotejo de datos. – Interpretación y – Síntesis.
		Revisión sistemática de indicadores relacionados con <i>Smart Cities</i> y CHs.	Técnica documental Arqueo de los principales organismos internacionales de normalización. <ul style="list-style-type: none"> – Fuentes oficiales: UE, UNESCO, INE. – Instituto Universitarios de Investigación – Motores de búsquedas científicas sciencedirect.com/ 	<ul style="list-style-type: none"> – Listado y comparación y consolidación de los indicadores.
	Fase de análisis y síntesis	Propuesta de indicadores relacionados con las TIC en la preservación y valoración de los CHs	Análisis de datos <ul style="list-style-type: none"> – Revisión de los indicadores comunes aplicables a los CHs enmarcados en el contexto de <i>Smart Heritage</i>. – Formulación de indicadores 	<ul style="list-style-type: none"> – Análisis y síntesis de los indicadores aplicables a los CHs. – Conclusiones.
		Selección de buenas prácticas	Estudio de casos prácticos <ul style="list-style-type: none"> – Reconocimiento de referentes centrales en el campo temático, Centros Históricos en el contexto del <i>Smart Heritage</i> en las ciudades de Ávila, Cáceres (España) y Torino (Italia); en América Latina, Cartagena (Colombia). 	<ul style="list-style-type: none"> – Selección de CHs que cumplan con los siguientes criterios: – Reconocimiento por UNESCO. – CHs gestionados con TIC – Interpretación – Propuesta. – Análisis – Síntesis – Conclusiones

4

3 Smart City: discurso y teoría

La traducción de *Smart City*, al castellano como ciudad inteligente, está generalmente aceptada, pero también se utilizan otras terminologías como, ciudad eficiente. Históricamente, surge en la primera década del siglo XXI, específicamente en el 2010, como una posible solución a los problemas de sostenibilidad derivados de la rápida urbanización. Empresas de tecnologías e inmobiliarias se aliaron para desarrollar lo que podría ser la ciudad del futuro. “Una ciudad que podría ser lo suficientemente inteligente” para evitar catástrofes, así nacieron ideas como contaminación cero, conectividad total, tráfico sin complicaciones y edificios 100% inteligentes.

Partiendo de que cada urbe es única e incomparable, que tiene sus propias necesidades y oportunidades y que cada ciudad tiene su historia única y se sitúa en un medio ambiente y contexto social específico, el modelo de ciudad inteligente debería ser propio de cada ciudad.

El modelo o plan, debe establecer sus prioridades y ser lo suficientemente flexible para adaptarse a los cambios. Además, debe incorporar la participación de los actores claves de la ciudad, con el fin de aprovechar las oportunidades y enfrentar los desafíos que se presentan en la ciudad. [5]

A pesar de su reciente popularidad, la “*Smart City*” se estableció en la conciencia pública como un concepto de marketing de las empresas de tecnología global que vieron la oportunidad de vender la transformación y nuevas tecnologías en las grandes ciudades. [6] De la inmensa literatura y la pléthora de definiciones existentes [6] diversos autores concuerdan en la falta de claridad conceptual en torno al término de ciudad inteligente.

Ontoño, por ejemplo, señala que “se ha confundido el concepto de Smart, con tener mucha información respecto al fenómeno, cuando en realidad el objetivo de una ciudad Smart es impulsar la innovación y mejora a partir del análisis de la información obtenida, para posteriormente, tomar decisiones y actuar en consecuencia”. [7, p. 33]

La “inteligencia” de una ciudad, describe si los diferentes sistemas de la ciudad (personas, organizaciones, finanzas, instalaciones e infraestructuras) se relacionan de manera eficiente; y si estos actúan de manera integrada y coherente, para permitir sinergias potenciales para ser explotadas.

A pesar de las diferentes acepciones sobre *Smart City*, el objetivo final es el mismo, la esencia es común, generar numerosas oportunidades de negocio y posibilidades de colaboración entre el sector público y privado. Todos los grupos de interés suman, de modo que ha de desarrollarse un ecosistema en red que los involucre a todos: ciudadanos, organizaciones, instituciones, gobiernos, universidades, empresas, expertos, centros de investigación y entidades sin ánimo de lucro.

3.1 Ciudades sostenibles e inteligentes: el binomio perfecto

El término de sostenibilidad tiene una aceptación más amplia, señala Castells [8], que la sostenibilidad puede definirse como solidaridad intergeneracional, en términos sociológicos, o la era de la información en términos más analíticos.

Hace algo más de cuatro décadas, y con especial intensidad en los años 80, se inicia un proceso sin precedentes de reflexión a nivel mundial que impulsa Naciones Unidas, seguida de la Unión Europea, para abordar la cuestión de la sostenibilidad y el desarrollo sostenible del planeta, como uno de los grandes retos a los que se enfrentan las sociedades del siglo XXI. El término sostenibilidad, sufrió diferentes transformaciones a lo largo del tiempo hasta llegar al concepto moderno basado en el desarrollo de los sistemas socio ecológicos para lograr una nueva estructura económica, social y ambiental; que son los tres pilares esenciales del desarrollo sostenible.

Durante la última década este concepto ha sido superado en popularidad, por el término de “ciudades inteligentes” [9] a pesar de que “no es un concepto académico que progresivamente haya trascendido a la gestión política” [10]. A diferencia de otros conceptos relacionados con el mundo urbano, el término de *Smart Cities* nace gracias al impulso del sector económico, a manos de unas cuantas empresas multinacionales, que aprovecharon las posibilidades derivadas de la Big Data, en la ciudad, y por la oportunidad de distribuir tecnología por todo el territorio urbano.

Esto produjo nuevas investigaciones que permitieron generar amplia literatura científica desde diferentes disciplinas, visiones tan diversas, que crearon confusión entre científicos, responsables políticos, municipios, ciudadanos y empresas [11].

En este sentido, el concepto de “ciudades inteligentes” ha sido ampliamente desacreditado por investigadores, justificadas por:

- La falta de atención a las necesidades de las ciudades y su cuestionable contribución al desarrollo sostenible [9], por lo que se corre el riesgo de convertir los entornos urbanos en espacios altamente tecnificados.
- Las necesidades reales de la ciudadanía, tal como lo indica Suárez, “llegando incluso a despolitizar los problemas socioambientales convirtiéndolos en problemas que pueden solventarse únicamente con soluciones tecnológicas” [10]
- El discurso, asume implícitamente que los proyectos de ciudades inteligentes empoderarán y mejorarán la vida de los ciudadanos, visiones temerosas de un futuro en el que los ciudadanos serán subyugados por tecnologías que obstaculizarán su libertad. [12].

Actualmente, las ciudades se encuentran en el epicentro de la estrategia de la ONU, por lo que ODS (objetivos de desarrollo sostenible) han de inspirar el motor que impulsa la revolución actual que viven las ciudades, así como también, han de velar su alcance y efectos directos y colaterales en la medida que las ciudades inteligentes, se vuelvan más prominentes, de allí la importancia del ODS 11 “Lograr que las ciudades sean más inclusivas, seguras, resilientes y sostenibles” [13].

Por otro lado, el fuerte crecimiento de la población urbana y el consiguiente aumento del consumo de recursos crearán inevitablemente numerosos desafíos para las ciudades. Este hecho, destaca la importancia de cambiar los paradigmas en la forma en que las ciudades funcionan en términos de sostenibilidad. Al respecto, algunos investigadores plantean que el uso de las TIC en sistemas urbanos va más allá, a “detectar, recolectar, almacenar, coordinar, integrar, procesar, analizar, sintetizar, manipular, modelar, simular, administrar, intercambiar y compartir datos con el propósito de monitorear, comprender, sondear y planificar ciudades modernas para lograr objetivos particulares” [14]

6

El concepto de “ciudad inteligente” y “ciudad sostenible” a menudo se usa indistintamente en la literatura sin una comprensión adecuada de la relación entre ellos. En la última década, el concepto de ciudades inteligentes y sostenibles ha pasado a primer plano, ganando velozmente impulso y atención mundial como una respuesta prometedora al desafío de la sostenibilidad urbana. Esto concierne especialmente a las naciones ecológicas y tecnológicamente avanzadas.

Una ciudad *Smart City* es definida por aquella ciudad que utiliza la Tecnología de la Información y Comunicación (TIC) para conseguir que sus infraestructuras fundamentales y servicios públicos ofrecidos sean más eficiente e interactivos con el objetivo de mejorar la calidad de vida de los ciudadanos, garantizando el desarrollo social y económico, urbano sostenible.

Al hablar de sostenibilidad y TIC y, por lo tanto, de prácticas sostenibles y soluciones inteligentes para ciudades, se hace referencia a los dos conceptos de ciudades sostenibles y ciudades inteligentes. Académicos de diferentes disciplinas de diversos campos profesionales han buscado, durante las últimas dos décadas, una variedad de modelos de ciudades sostenibles, así como enfoques de ciudades inteligentes que puedan contribuir a la sostenibilidad y su mejora.

Para Padmapriya y Sujatha [15] una ciudad inteligente sostenible es “una ciudad que ha desarrollado infraestructura tecnológica para desarrollar, implementar y nutrir operaciones sostenibles y facilitar la satisfacción de las crecientes necesidades de urbanización”. Por lo tanto, integra el dinamismo tecnológico en los sectores de gobernanza local, educación, salud, energía, infraestructura y movilidad. Los autores agregan que a medida que la integración tecnológica se vuelva más visible para los usuarios finales, habrá una gran transición en la vida urbana”.

Un concepto que fusiona ambos términos, sostenibilidad (ambiental, urbanización) y desarrollo tecnológico, es definido por la *United Nations Human Settlements Programme* (UN-Habitat), *United Nations Educational, Scientific and Cultural Organization* (UNESCO) et al. [16] como “una ciudad innovadora que utiliza la información y tecnologías de la comunicación (TIC) y otros medios para mejorar la calidad de la vida, la eficiencia de la operación y los servicios urbanos, y la competitividad, asegurando la satisfacción de las necesidades de las generaciones presentes y futuras con relación a los aspectos económicos, sociales, ambientales y culturales”.

Las críticas hacia el concepto de *Smart Cities* y su desvinculación con la sostenibilidad, indujo a investigar sobre cómo abordar las necesidades de las ciudades, actualmente digitalizadas [11].

4 Estándares de indicadores para ciudades inteligentes y sostenibles.

El crecimiento acelerado de urbanización supone enormes desafíos para las ciudades, principalmente en temas como el cambio climático, la eficiencia económica, entre otros. No obstante, las iniciativas de *Smart City*, por medio de las TIC y la innovación, se orientan a dar soluciones a esos retos, optimizar su eficiencia brindando

oportunidades para que las ciudades se replanteen como brindar un servicio de calidad a sus ciudadanos.

La emergente definición de “ciudades inteligentes y sostenibles” combina la sostenibilidad urbana con la inteligencia, enfatizando simultáneamente ambas terminologías. Sin embargo, las soluciones de las ciudades inteligentes han sido fuertemente criticadas por ser a menudo demasiado tecno-céntricas, impulsadas por las propias agendas de las empresas de tecnología y sin la debida atención a las necesidades de las ciudades y la sostenibilidad [11]. Es por esto por lo que distintos organismos e instituciones internacionales, se han centrado en la definición, la creación y el uso de indicadores de manera de elaborar un diagnóstico sobre el estado de las ciudades.

Estos indicadores son medidas cuantitativas, cualitativas o descriptivas que permiten simplificar la información sobre un fenómeno complejo, en este caso, de un entorno urbano dinámico. Su función principal es la cuantificación, la simplificación y la comunicación de tendencias y cambios. En este caso, los indicadores urbanos permiten establecer un lenguaje común y transparencia en la gobernanza, comunicar los beneficios de las inversiones, gestionar las operaciones de la ciudad, evaluar el desempeño de la ciudad en diferentes áreas y como apoyo en la toma de decisiones.

A pesar de que los indicadores se desarrollan para un propósito de uso específico, se requieren conocimientos de expertos para comprenderlos correctamente y evitar malas interpretaciones.

En este sentido, en la búsqueda de la armonía, confiabilidad y transparencia de los resultados, se realiza una estandarización de los indicadores (ver Fig. 1).

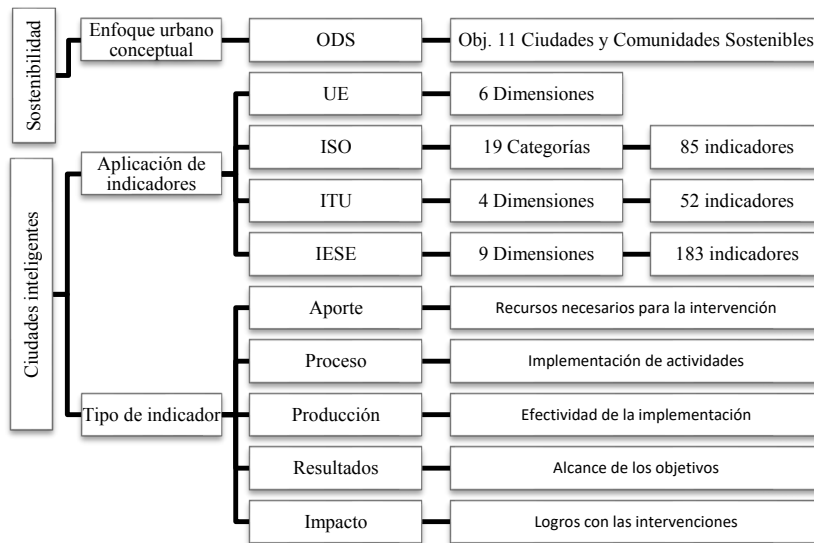


Fig. 1. Estándares e Indicadores de las Ciudades Inteligentes y Sostenibles. (Fuente: elaboración propia, a partir de ISO y IEC, Smart Cities [5]; IESE Cities in Motion [18] y Ospina [19]).

8

En la actualidad, la normalización internacional está a cargo de tres organismos, es decir, la *International Organization for Standardization* (ISO), *International Telecommunications Union* (ITU) en todo el mundo y la coalición de organizaciones europeas de normalización *European Committee for Standardization* (CEN), *European Committee for Electrotechnical Standardization* (CENELEC) y *European Telecommunications Standards Institute* (ETSI).

Existe una gran cantidad de indicadores urbanos, por lo tanto, para este artículo, se realizó una revisión de las consideraciones de la Unión Europea (ETSI), la Organización Internacional de Estándares (ISO), la Unión Internacional de Telecomunicaciones (ITU) y el Índice Cities in Motion (IESE). (ver Tabla 2)

Tabla 2. Comparación de indicadores de Ciudades Sostenibles e Inteligentes. (Fuente: elaboración propia, a partir de ISO/IEC JTC [5]; Huovila, A., Bosch P., Airaksinen, M [11]; IESE Cities in Motion [18]).

	ETSI	IESE	ITU	ISO
Indicadores	Gobernanza inteligente y TIC	Gobernanza y TIC	TIC	Gestión de la ciudad Telecomunicaciones
	Movilidad Inteligente	Movilidad y transporte	Infraestructura física	Inteligencia de infraestructura
	Economía Inteligente	Desarrollo económico	Productividad	Economía
	Vida Inteligente	Calidad de vida Cohesión social	Calidad de vida	Habitabilidad, cultura y recreación
	Gente inteligente	capital humano	Equidad e Inclusión social	Población, condiciones sociales y educación
	Entorno inteligente	Medio ambiente y Planificación urbana	Sostenibilidad ambiental	Planificación urbana, gestión de aguas y residuos, medio ambiente, clima y energía

El Parlamento Europeo, en el año 2014 proporcionó alrededor de 10 definiciones para ciudad inteligente, considerando seis dimensiones: economía inteligente, vida inteligente, gente inteligente, movilidad inteligente, gobernanza y entorno inteligentes. En el 2017, las actividades de normalización sobre ciudades inteligentes y sostenibles europeas fueron coordinadas por un esfuerzo conjunto entre el CEN, CENELEC y ETSI. Hasta ahora, el ETSI ha publicado un conjunto de indicadores de ciudades inteligentes y sostenibles en forma de especificación técnica sobre indicadores clave de rendimiento para ciudades multiservicio digitales sostenibles, en base a 4 dimensiones: planeta, prosperidad, gobernanza y personas.

Tanto la ISO como la IEC [5], enfatizan que el objetivo principal para las ciudades inteligentes es perseguir los temas de conveniencia de los servicios públicos, delicadeza de la gestión de la ciudad, habitabilidad del entorno de vida, inteligencia de la infraestructuras y eficacia a largo plazo de la seguridad de la red, los agrupa en 19 categorías y ochenta y cinco indicadores.

La ITU, considera que las ciudades inteligentes y sostenibles, están asociadas a seis dimensiones: “Sostenibilidad Ambiental”, la productividad, calidad de vida, equidad e inclusión social; y la dimensión de infraestructura física [17].

EL IESE Cities [18] ha diseñado nueve dimensiones, que conducen a la creación a un tipo de desarrollo económico y social, estos son: Capital humano, coherencia social, economía, gobernanza, medio ambiente, movilidad y transporte, planificación urbana, proyección internacional y tecnología.

En América Latina y el Caribe, son pocas las ciudades inteligentes (15%), sin embargo, se puede evidenciar una verdadera mejora en cuanto a la institucionalidad, la cooperación público-privada y los requisitos tecnológicos necesarios para lograr ciudades más inteligentes en los próximos años [18]. En este sentido, el Banco Interamericano de Desarrollo (BID), viene elaborando planes de acción para el desarrollo de estrategias de sostenibilidad urbana que fundamenten la transformación en Ciudades Inteligentes de sus municipios. [19]. Esta iniciativa Ciudad Emergentes y Sostenibles (ICES) del Banco Interamericano de Desarrollo (BID), tiene un enfoque transversal que se basa en los tres pilares, la sostenibilidad urbana, sostenibilidad medioambiental y de cambio climático, y la sostenibilidad fiscal y gobernanza. (ver Fig.2). Para el año 2017, la iniciativa contaba con 77 ciudades de Argentina, México, Venezuela, entre otras.

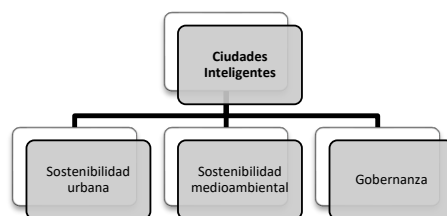


Fig. 2. Pilares de la Sostenibilidad [19]

4.1 El ranking de ciudades inteligentes y sostenibles.

La estandarización de indicadores pretende que los ciudadanos y los Gobiernos comprendan el desempeño de las dimensiones fundamentales de la ciudad. Dimensiones que varían de acuerdo con los criterios de cada organización. Sin embargo, tienen un fin común conducir la ciudad a un tipo de desarrollo económico y social, la promoción del espíritu empresarial, la innovación y la justicia social, entre otros aspectos.

Sin embargo, hay que tener presente que cada urbe es irreplicable y tiene sus propias necesidades y oportunidades, por lo que deberá diseñar un plan único, establecer sus prioridades y ser lo suficientemente flexible para adaptarse a los cambios.

Europa Occidental. Los resultados de la IESE, sobre *Smart Cities*, evidencian que la ciudad de Londres encabeza el ranking europeo e incluso el primer puesto en la clasificación mundial de 183 ciudades. Seguidamente de París, Berlín, Ámsterdam y Oslo (ver Tabla 3)

Tabla 3. Ranking de ciudades inteligentes de Europa Occidental (Fuente: IESE Cities in Motion [18])

Ciudad	Posición regional (57 ciudades de Europa Occidental)	Posición global (183 ciudades)
Londres (Reino Unido)	1	1
Paris (Francia)	2	3
Berlín (Alemania)	3	5
Ámsterdam (Países Bajos)	4	8
Oslo (Noruega)	5	9

Las ciudades de Europa occidental llevan varias décadas innovando en sensorización, digitalización, conectividad, IoT e incluso inteligencia artificial en sus municipios, lo que les ha permitido mantenerse el top de las ciudades más inteligentes y sostenibles de todo el mundo.

En la actualidad, la UE y el BID (en Latinoamérica) presentan diferentes iniciativas para dar el paso a ciudades inteligentes y sostenibles.

Europa. El plan *REPowerEU*, un catálogo completo de ofertas, como convocatorias de asistencia técnica gratuita, servicios de consultoría personalizados para consorcios liderados por ciudades próximos a la etapa de financiación, clases magistrales sobre financiación y un emparejamiento perfeccionado para la financiación de proyectos urbanos. Así como, el acuerdo de la ciudad verde, el pacto de los alcaldes, ciudades escalables CIVITAS y *Living-in.eu*.

América Latina y el Caribe. A lo largo de los años, Santiago de Chile y Buenos Aires, han liderizado los dos primeros puestos en América Latina, Sin embargo, el ranking 2021, el IESE ha señalado que la ciudad de Santiago (Chile) supera a Buenos Aires (Argentina), mostrando mejor desempeño en movilidad y transporte, cohesión social y, especialmente, en economía. Sin embargo, Buenos Aires, destaca en gobernanza, planificación urbana y proyección internacional. Destacan también en la región Ciudad de México, Panamá y Montevideo, [18] (Ver Tabla 4)

En este sentido, el Banco Iberoamericano de Desarrollo durante el año 2021, apoyó a los gobiernos locales de las ciudades inteligentes de Brasil en la adopción de soluciones basadas en la Big Data, con el fin de mejorar la gestión urbana y la toma de decisiones en las municipalidades de Recife, São Luis y Vitória.

Tabla 4. Ranking de ciudades Inteligentes de América Latina [18]

Ciudad	Posición regional (26 ciudades de AL)	Posición global (183 ciudades)
Santiago (Chile)	1	75
Buenos Aires (Argentina)	2	103
Ciudad de México (México)	3	115
Panamá (Panamá)	4	120
Montevideo (Uruguay)	5	126

5 El papel del *Smart Heritage* dentro de las *Smart Cities*

El **patrimonio cultural**, puede encontrarse dentro de distintas formas, una de ellas es dentro de la complejidad urbana donde, en muchos casos, debe convivir e integrarse en las estructuras contemporáneas de las ciudades modernas y a sus avances tecnológicos. Aunado a esto, representan un ámbito donde la sostenibilidad de las intervenciones, la promoción y preservación de sus espacios, e incluso de sus obras de arte, tienen que ser consideradas en su totalidad. [20]

Las *Smart Cities*, por otra parte, son asentamientos urbanos que hacen un esfuerzo consciente para capitalizar el nuevo panorama de las TIC de una manera estratégica, buscando lograr prosperidad, efectividad y competitividad en múltiples niveles socio-económicos. Es por esto, que el concepto de *Smart Heritage City (SHcity)*, se centra en adoptar medidas más participativas y enfoques colaborativos, haciendo que los datos culturales estén disponibles y de manera gratuita, con el fin de aumentar las oportunidades de interpretación, saneamiento digital e innovación.

Estas actuaciones sobre el patrimonio, ofrece un potencial y accesibilidad a los bienes culturales sin precedentes, ya que se promueve la cohesión y aumentar la innovación y el turismo. De esta manera, el patrimonio cultural inteligente está fuertemente asociado a la identidad del lugar y a las comunidades que lo habitan a través de tecnologías inteligentes, conocimiento y participación. [21]. Asimismo, la integración entre el patrimonio cultural y las ciudades inteligentes no solo permite posibles sinergias para ser explotada, sino que contribuye al funcionamiento integral de la ciudad, facilitando la innovación y el crecimiento.

Los ciudadanos de una ciudad inteligente son participantes potenciales en su gobernanza y en la evolución del desarrollo de servicios más inteligentes, incluidos los relacionados con acceder y preservar el patrimonio cultural. Los beneficios específicos de incluir el patrimonio cultural en una iniciativa de ciudad inteligente derivan desde la gestión de la Big Data y la realidad aumentada (AR). La gestión de datos permite almacenar y administrar grandes cantidades de datos, beneficiosos para la preservación del patrimonio cultural, y el seguimiento sostenible de la conservación de su ciclo de vida.

6 Los Centros Históricos en el contexto de *Smart Heritage City*

El centro histórico entra en el debate disciplinar desde finales de los años treinta del siglo pasado, cuando por primera vez se intenta identificar y circunscribirlo en comparación con el más complejo organismo “ciudad”. Desde entonces, varias definiciones han sido una expresión de la evolución del debate disciplinar y cultural.

Para Cerasoli, los centros históricos, son “complejos de cosas inmuebles que componen un característico aspecto que tiene valor estético y tradicional” [22] por lo tanto, son la representación estratificada de la cultura de una comunidad, un lugar de memorias históricas comunitarias e individuales, de identidad y autorreconocimiento de la

12

población, que pueden convertirse, en un recurso importante en el marco de un proyecto de transformación de todo el organismo urbano, reforzando tanto la identidad propia como la capacidad de atracción hacia el exterior.

6.1 El desafío de la preservación de los Centros Históricos.

En la actualidad, los CHs, tienen un triple reto: social, económico y ambiental.

- Social, considerado el “alma” de la ciudad, los centros históricos son espacios sociales singularizados por su heterogeneidad. Encierran valores de convivencia para el conjunto de los ciudadanos. “Sus calles y plazas son lugares de paseo y de encuentro, son espacios de diversidad y mezcla funcional que propician las relaciones sociales”. [23].
- Económico, se definen por un marcado carácter multifuncional, ya que en ellos conviven funciones residenciales, comerciales, religiosas, administrativas, lúdicas, etc. La diversificación de actividades aporta una gran riqueza a la vida urbana que en ellos se desarrolla, sin embargo, el modelo de centro histórico ha evolucionado hasta convertirse en motor turístico cultural, de ocio y del sector de la restauración en general.
- Ambiental, referido a la accesibilidad, a la carencia de espacios verdes insuficientes y la insalubridad generada por la masa turística y de ocio, propician el tener un ambiente en continua degradación.

6.2 Centros históricos, patrimonio inteligente

Los Centros Históricos y Ciudades Inteligentes, para los ojos de las personas son incompatibles. Por un lado, un legado histórico tradicional, y por el otro, la posmodernidad y lo que representa. En este sentido, transformar “ciudades tradicionales en Ciudades Inteligentes, es una demanda imperante, así como una oportunidad para gobiernos y ciudadanos de América Latina y el Caribe (ALC). Con el surgimiento de la tecnología digital, de Internet y de las tecnologías móviles, esa transformación es cada vez más viable”. [2].

Para el caso de los Centros Históricos, la tecnología de Información y Comunicación debe identificar las herramientas destinadas a preservar el patrimonio que podría reflejarse en el alcance de las *Smart Cities*, elaborando una estrategia de desarrollo que contemple aspectos medioambientales, urbanos, sociales y económicos.

La implementación de las TIC en el proceso de socialización del patrimonio en el Centro Histórico Urbano permite la interpretación del patrimonio, revelando el significado del legado natural y cultural de los recursos a la persona. Su empleo debe ser a partir de unos objetivos conscientes, que se inserten y definan una estructura organizativa y diseñen una oferta capaz de lograr los objetivos de desarrollo sostenible y equitativo que se desea para la comunidad.

Muy recientemente se ha extendido la idea de *Smart Heritage* o patrimonio inteligente. “Este nuevo concepto puede concebirse como la identidad de los lugares a través de la implementación de tecnologías inteligentes, y así tratar de fomentar y promover

el conocimiento y la inclusión social mediante la participación total en la promoción del patrimonio cultural”. [3]

Así mismo, un entorno inteligente que permita conservar y gestionar el patrimonio cultural, debe ser capaz de almacenar y recuperar información sobre los bienes del patrimonio cultural, no sólo para preservar su memoria en nuestra era digital sino también para monitorearlo. “Preservar la apariencia física e integridad del bien, utilizando técnicas de intervención sostenibles, es otra de las principales características de la conservación” [24]

En el concepto de *Smart Heritage* se puede distinguir dos nuevos conceptos, en una doble vertiente: el *Smart Heritage Management* o *Smart Heritage City (SHCity)*, el primero enfocado en la figura del monumento, bien cultural, museo, etc., respecto a su conservación, gestión y disfrute; y el segundo más global, relacionado con el encaje del patrimonio cultural en el desarrollo de la ciudad (progreso y la evolución)

En el segundo punto, entran los Centros Históricos, cuyas investigaciones deben apuntar a desarrollar plataformas para la gobernanza electrónica de la ciudad; sostenibles en el tiempo; que promuevan la gestión participativa y la transferencia de buenas prácticas.

Por lo expuesto, la profusión del modelo *Smart Heritage* da alas a una serie de oportunidades, en los centros históricos tales como:

- La vinculación del Patrimonio con el turismo para el desarrollo territorial.
- Una demanda social y política a favor de la sostenibilidad económica y ecológica.
- Tecnologías que facilitan la gestión remota y en tiempo real de edificios, zonas urbanas.
- Las tecnologías que posibilitan la interacción de las personas con las cosas y de los conceptos de conservación preventiva.
- Preservación y promoción del patrimonio cultural.
- Eficiencia y sostenibilidad en la gestión del centro histórico.

Bajo estos criterios, la UE ha creado un proyecto denominado *SHCity*, que se basa en única herramienta de código abierto para coleccionar los datos necesarios para que las administraciones públicas puedan realizar una correcta gestión de los centros históricos y así evitar su degradación y deterioro causado por factores naturales y humanos. En concreto, trata de aportar soluciones a los problemas que resultan del turismo de masas en las ciudades históricas. Esto supone una gestión proactiva, con tecnologías de vigilancia, inteligencia artificial y herramientas de ayuda para la toma de decisiones que permiten a los administradores municipales disponer de datos e informaciones útiles para administrar la ciudad.

Por otra parte, la empresa Telefónica ha impulsado una herramienta eficiente “*Monitoring Heritage System*” (MHS), para la conservación preventiva del Patrimonio y que ha sido implementado por la Fundación Santa María la Real. “La herramienta para la gestión integral del patrimonio por un lado ofrece un equipamiento físico, una serie de dispositivos para el control de parámetros y la transmisión de la información, y por otro lado ofrece una serie de servicios para la correcta gestión de esa información, en base al ámbito de actuación preferente: conservación preventiva, seguridad, eficiencia de recursos o gestión de visitas.” [25]

14

En el caso de América Latina y del Caribe, la UNESCO, declaró 37 centros históricos de la región como patrimonio mundial de la humanidad, entre los que destacan Quito, la Habana, la Antigua, Cartagena, Ciudad de México, entre otros. Sin embargo, en la gran mayoría de los casos, los programas se basan en la preservación sostenible de edificios históricos. En Quito (Ecuador) y la Habana (Cuba) ambos CHs declarado patrimonio de la Humanidad, las políticas de gestión se basan en la implementación de programas para la mejora de la habitabilidad y sostenibilidad. [26]

6.3 Dimensiones e indicadores claves

A partir de la definición de *Smart Heritage City* y la revisión de los indicadores de *Smart Cities*, siguiendo el Objetivo 11 del Desarrollo Sostenible, se proponen cinco dimensiones claves que permita estandarizar criterios y sus respectivos indicadores de desempeños *Smart* utilizados en los CHs. (ver Fig.3)

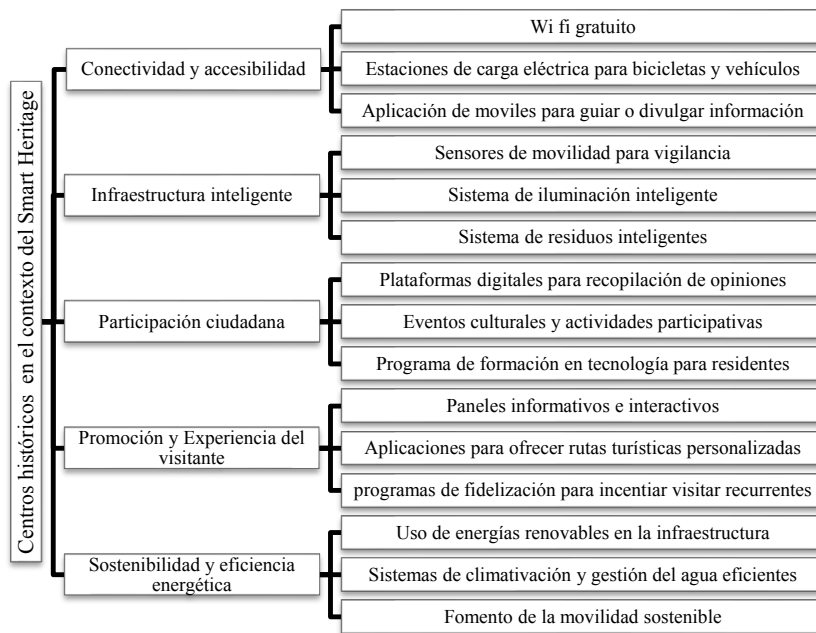


Fig. 3. Dimensiones e indicadores para diagnosticar los CHs, en el contexto del SHCity.

Resulta relevante analizar en la escala ciudad histórica la aplicación del concepto de Smart City y sus derivados *Smart Heritage City*, como han adaptado su infraestructura urbana a los avances tecnológicos que conforman el entorno donde se desenvuelve la sociedad actual. En este sentido en muchas ciudades, los centros históricos más “smart”, están logrando inclusión social entre comunidades, accesibilidad universal,

facilidad de acceso a internet y las nuevas tecnologías a la población, movilidad urbana sostenible, gestión de residuos y agua y generación de energía renovable. Esto, no solo beneficia a las Administraciones Públicas, sino también a los organismos y empresas relacionadas con la gestión de conjuntos urbanos, ya que el proyecto permitirá replicar su implantación en distintos tipos de conjuntos urbanos históricos, atendiendo a sus particularidades geográficas, climáticas, culturales y turísticas. A continuación, se presentan algunas iniciativas en los Centros Históricos integradas al *Smart Heritage*.

Torino (Italia). La ciudad de Torino, raqueada por la IESE Motion con una valoración media, ocupando el puesto No 97, con una población que supera los 800.000 habitantes, tercera ciudad Smart de Italia, ha efectuado una serie de intervenciones para salvaguardar su patrimonio histórico. Estas intervenciones están vinculadas con la calidad del entorno urbano, el uso de energías renovables, la eco-construcción, barrios con alta sostenibilidad ambiental, la creación de una movilidad sostenible y la economía inteligente. (Ver Fig. 4) Para esto, han creado un *Living Lab Turin*, una plataforma de experimentación aplicaciones a escala real, que les permitirá evaluar el impacto social.

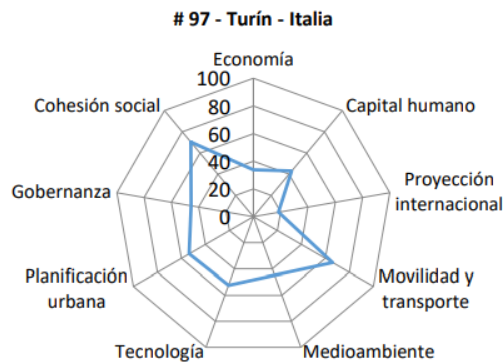


Fig. 3. Análisis gráfico del perfil de ciudad [18]

Cáceres (España). Desde hace unos años, en la ciudad de Cáceres, se ejecuta un proyecto llamado «Cáceres Patrimonio Inteligente», que consiste en incluir la Big Data en sus monumentos más emblemáticos, con el fin de conocer el consumo energético, el grado de humedad de cada edificio y todos aquellos valores que permitan actuar de forma inmediata. Asimismo, han instalado sensores para conteo de visitantes en 18 edificios significativos lo que permite determinar el número de visitantes que acuden a la ciudad.

Ávila (España). Ciudad de 57.657 habitantes, situada en la comunidad autónoma de Castilla y León, caracterizada por su muralla medieval de estilo románico y otras

16

construcciones representativas como la catedral del Salvador o la basílica de San Vicente, ha sido considerada tradicionalmente como «ciudad de cantos y de santos» y su conjunto histórico de primera magnitud en excelente estado de conservación, fue declarado por la UNESCO como Patrimonio de la Humanidad en 1985.

El proyecto *SHCity* financiado por la UE en Ávila, consiste en implementar e instalar una red de sensores, desplegados por diferentes puntos estratégicos de la ciudad, que en tiempo real sean capaces de medir parámetros ambientales y estructurales, así como otros relacionados con la seguridad, el consumo energético o el flujo de visitantes.

Cartagena de Indias (Colombia). Ciudad portuaria ubicada en la costa caribe de Colombia, con 914.552, para mejorar la conservación y gestión del Centro Histórico, avanzan con en la primera fase de un proyecto *Smart Heritage City* Cartagena (*SHCity*), dirigido por el Instituto de Patrimonio y Cultura de Cartagena (IPCC), la Oficina Asesora de Informática y la Oficina de Cooperación Internacional, gracias a los recursos otorgados por el gobierno japonés, a través de una convocatoria en la cual la ciudad fue seleccionada. [27]

El programa, sigue el modelo de las ciudades europeas, en cuanto a la instalación de sensores que monitorean diferentes variables (temperatura, humedad, calidad del aire, ruido, medición de fisuras y grietas, inclinación de muros, entre muchos otros), lo contribuiría con la gestión pública en la toma de decisiones, no solo en cuanto a inversión en conservación, sino también en todos los aspectos relacionados con mitigación de riesgos.

Cabe destacar también, que el proyecto *SHCity* forma parte de las medidas de monitoreo planteadas en el Plan Especial de Manejo y Protección del Paisaje Cultural de Cartagena, y se da en el marco del proyecto Ciudad Inteligente del Distrito.

7 Conclusiones

El modelo de *Smart Cities* integrado a la sostenibilidad, se define como una ciudad innovadora que utiliza las TIC para mejorar la calidad de vida de las personas, la eficiencia de las operaciones y los servicios urbanos y la competitividad, al tiempo que satisface las necesidades económicas, sociales, medioambientales y culturales de las generaciones presentes y futuras. Es una nueva forma de vivir, gestionar, conectar, consumir y disfrutar el espacio urbano.

En consecuencia, según sean las capacidades que desarrolle una Smart city para resolver los problemas de su entorno, encontrar un equilibrio e innovar, generará un posicionamiento a nivel mundial como espacio atractivo para ser habitado.

Dentro de este ecosistema, la cultura debe tener un rol determinante en el diseño de las estrategias *smart*. Así surge la idea de *smart heritage* o patrimonio inteligente, entendido como la identidad de los lugares a través de la implementación de tecnologías inteligentes, fomentando y promoviendo el conocimiento y la inclusión social, mediante la participación total en la promoción del patrimonio cultural. Se trata de conectar digitalmente las instituciones, los usuarios visitantes, el patrimonio, la ciudadanía y el entorno.

Es una tarea pendiente vincular las estrategias de *smart city* al patrimonio cultural de las ciudades, en especial desde un punto de vista medioambiental, pues la creciente preocupación por problemas medioambientales y la degradación del patrimonio cultural han contribuido a redirigir el desarrollo de políticas hacia el medioambiente y la cultura, incentivando a su vez a la protección del territorio a través de múltiples declaraciones como bienes protegidos. Los centros históricos, espacios urbanos llenos de riqueza patrimonial, se encuentran sometidos a constante transformación y de reinención de sí mismos a lo largo de la historia.

Las nuevas tecnologías pueden ser consideradas como el desafío más interesante para la sostenibilidad de los Centros Históricos, porque, además, de producir cambios significativos en la calidad de vida de los habitantes, aumenta su capacidad de atracción de recursos financieros y humanos, fomentando el desarrollo económico y sociocultural. De tal manera que en la medida que se aborden estos desafíos, se podrá concretar una mayor capacidad de protección del entorno, dentro del que se inserta la ciudad y del cual depende su existencia.

8 Referencias

1. Organización de la Naciones Unidas, <https://www.un.org/es/global-issues/population>, último acceso: 2023/08/18.
2. Bouskela M., Casseb M., Bassi S., De Luca C., Facchina M.: La ruta hacia las Smart Cities Migrando de una gestión tradicional a la ciudad inteligente, pp. 148 (2016). <https://publications.iadb.org/publications/spanish/viewer/La-ruta-hacia-las-smart-cities-Migrando-de-una-gesti%C3%B3n-tradicional-a-la-ciudad-inteligente.pdf>
3. Fuentes, J.: Patrimonio cultural y Smart City.: La transformación integral de la ciudad, QDL57 · Cuadernos de Derecho Local, pp. 123-171 (2017).
4. Riganti, P.: Smart cities and heritage conservation: developing a Smart Heritage agenda for sustainable inclusive communities. International Journal of Architectural Research ArchNet-IJAR., 11(3), pp. 16-27 (2017). <http://dx.doi.org/10.26687/archnet-ijar.v11i3.1398>
5. ISO/IEC JTC. (eds), (2015). ISO y IEC, Smart Cities. Preliminary Report 2014, Information technology: Smart Cities, Preliminary Report. https://www.iso.org/files/live/sites/iso-org/files/developing_standards/docs/en/smart_cities_report-jtc1.pdf
6. Toli A., Murtagh, N.: The Concept of Sustainability in Smart City, Frontiers. Built Environ. 6(1), (2020). <https://doi.org/10.3389/fbuil.2020.00077>
7. Ortuño, J.: Oportunidades y retos que ofrece la financiación alternativa para el sector social en un entorno Smart City, Barcelona: Tesis Doctoral Universitat Abat Oliba CEU. Departament d'Humnitats, p. 493. (2017). <https://www.tesisenred.net/handle/10803/456047#page=9>
8. Castells, M.: Urban Sustainability in the information age, vol. 4 pp. 118-122 (2000).
9. Mora, L. Bolici, R., Deakin, M. The first two decades of Smart-city research: A bibliometric analysis, Journal of Urban Technology 24(1) pp. 3-27 (2017)
10. Suárez, M.: De las Smart Cities a los Smart Citizens. La ciudadanía frente a la tecnología en la construcción de resiliencia urbana. URBS: Revista de Estudios Urbanos y Ciencias Sociales 6(2) 121-128 (2016) <https://dialnet.unirioja.es/servlet/articulo?codigo=5741823>
11. Huovila, A., Bosch P., Airaksinen, M. Comparative analysis of standardized indicators for Smart sustainable cities: What indicators and standards to use and when?, Cities 89, p. 141–153 (2019). <https://doi.org/10.1016/j.cities.2019.01.029>

18

12. Vanolo, A. Is there anybody out there? The place and role of citizens in tomorrow's smart cities. *Futures*, vol. 82, pp. 26-36 (2016). <https://doi.org/10.1016/j.futures.2016.05.010>
13. United Nations, *Objetivos de Desarrollo Sostenible*, <https://www.un.org/sustainabledevelopment/es/cities/>, último acceso 2023/08/19
14. Bibri, S., Krogstie, J.: Smart sustainable cities of the future: An extensive interdisciplinary literature review, *Sustainable Cities and Society*, vol. 31, pp. 182-212. (2017) <https://doi.org/10.1016/j.scs.2017.02.016>
15. Padmapriva V., Sujatha, D.: Future of Sustainable Smart Cities: an insight en. en: Krishnan, S., Balas, V., Golden E., Robinson, H., Kumar, R.: *Blochian for Smart Cities Edits.*, vol. 1, pp. 17-34 (2021) <https://doi.org/10.1016/B978-0-12-824446-3.00015-6>
16. UN-Habitat, UNESCO, World Health Organization, UNISUR, UN Women y UNEP: *SDG goal 11 monitoring framework*. (2016). <https://unhabitat.org/sdg-goal-11-monitoring-framework>
17. Haj, S., Al-Saud, B., Alfassam, A., Alshehri, K.: A framework of essential requirements for the development of smart cities: Riyadh city as an example. En *Smart Cities: Issues and Challenges*, 1ra edn. pp. 219-239. (2019) <https://doi.org/10.1016/B978-0-12-816639-0.00013-2>
18. IESE Cities in Motion, p. 116. (2022) <https://citiesinmotion.iese.edu/indicecim/>
19. Ospina, J.: BID. Banco interamericano de Desarrollo. https://conexion-tal.iadb.org/2018/11/27/267_e_ideas6/. último acceso 2023/08/21.
20. Chianese, A., Piccialli, F., and Valente, I.: Smart environments and cultural heritage: a novel approach to create intelligent cultural spaces. *Journal of Location Based Services*, 9(3), 209-234 (2015).
21. Angelidou, M., Karachaliou, E., Angelidou, T., Stylianidis, E.: Cultural heritage in smart city environments. *Copernicus Publications* 52(5), 27-32 (2017) <https://doi.org/10.5194/isprs-archives-XLII-2-W5-27-2017>
22. Cerasoli, M.: La recuperación de los centros históricos menores hacia las historical small Smart Cities. *ACE: Architecture, City, and Environment*. 22(11), 155-180 (2017) DOI: 10.5821/ace.11.33.5153. ISSN: 1886-4805.
23. Santamaria, J.: Centros Históricos: Análisis y perspectivas desde la Geografía. *Revista Digital Geographos*, 4(37), 117-139 (2013) DOI: 10.14198/GEOGRA2013.4.37
24. Riganti, P.: Smart Cities and Heritage Conservation: Developed a Smart Heritage agenda for sustainable inclusive communities. *Archnet-IJAR Revista Internacional de Arquitectura Investigación*, 11(3) 16-27 (2017) <http://dx.doi.org/10.26687/archnet-ijar.v11i3.1398>
25. Hernández, F., Prieto J.: Smart Heritage: Cuidemos nuestro patrimonio eficientemente con la tecnología, de I CONGRESO DE CIUDADES INTELIGENTES. <https://www.es-martcity.es/comunicaciones/smart-heritage-cuidemos-nuestro-patrimonio-eficientemente-tecnologia>.
26. Martínez, J., Fernández-Vivancos, E.: Management Strategies in the Comprehensive Rehabilitation of the Historic Centers of Quito and Havana. *Urban Sci*. 7(1), (2023), <https://doi.org/10.3390/urbansci7010004>
27. Smart Heritage City Cartagena lista para iniciar su primera fase (último acceso 2023/08/28) <https://www.cartagena.gov.co/noticias/smart-heritage-city-cartagena-lista-para-iniciar-su-primera-fase-2151>

Posters

N.º 24



Ciudadanía Digital: Hacia la Innovación en la Administración Pública Moderna



ICSC-CITIES 2023
Congreso Iberoamericano de Ciudades Inteligentes



Ciudades Inteligentes Totalmente Integrales, Eficientes y Sostenibles
13-17 nov. 2023
Ciudad de México y Cuernavaca, Morelos.



M. Juárez-Merino⁽¹⁾

⁽¹⁾ UNAM, Centro Regional de Investigaciones Multidisciplinarias,

Cuernavaca, Mexico

ma.juarez@crim.unam.mx



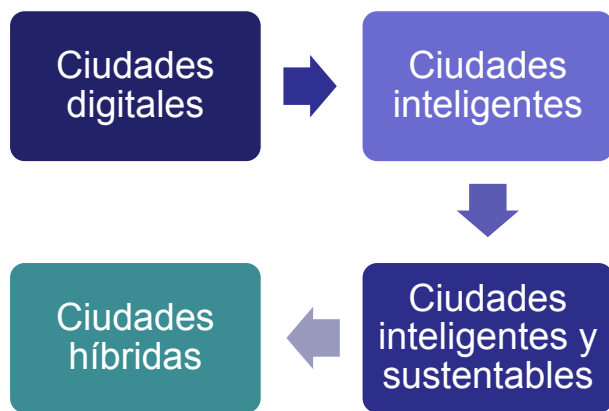
Keywords

Tecnología; Gobierno; Ciudadanía Digital.

Abstract

Con la irrupción de las tecnologías digitales en diversos aspectos de la realidad social, los gobiernos actuales han buscado adaptarse a su uso como un instrumento para la transformación e innovación de la administración pública. Es así como se está transitando hacia la idea de un gobierno digital, capaz de adaptar su procesos, trámites y servicios a través de la digitalización, con el objetivo de facilitar el acceso del ciudadano a sus autoridades y, con ello, consolidar el vínculo entre ambos actores. A lo largo del mundo, hay diversos ejemplos que están demostrando las ventajas de acercarse a la ciudadanía mediante el uso de plataformas digitales; para ello, se han establecido factores específicos que determinan el éxito de este proceso. De entre ellos, destacan, por un lado, que la digitalización debe ser una política de Estado; asimismo, garantizar la ciberseguridad de los usuarios y, por último, formar parte de una plataforma digital integrada.

1. Evolución del gobierno digital



2. Ciudadanía digital

La idea de ciudadanía es, históricamente, un concepto que ha ido evolucionando de acuerdo con el desarrollo de la civilización, la transformación del Estado y la lucha por el reconocimiento de los derechos del ser humano. Sobre esta base, tiene especial importancia la propia democracia, pues el binomio Estado-ciudadano, se encuentra íntimamente ligado a una forma de gobierno donde el ente público es un medio para el orden social, la satisfacción de los intereses de la población y el imperio de un estado de derecho. Se trata de una etapa evolutiva de la gestión pública administrativa, donde el ciudadano se coloca en el centro de la acción gubernamental y el diseño de políticas públicas.

3. Factores de éxito

Concepto	Indicadores	Fuentes
Política de Estado	Marco jurídico en materia de gobierno digital. Plan de desarrollo municipal o local. Presupuesto de egresos de la ciudad. Organigrama del gobierno local. Plan de trabajo para el área de soporte y operación de la aplicación.	Leyes locales en materia de gobierno digital. Plan de desarrollo municipal o local. Informes de la autoridad a través de portales de transparencia Sitios web del gobierno local.
Ciberseguridad	Tipo de herramientas tecnológicas adquiridas para ciberseguridad. Presupuesto asignado. Documentos emitidos por la unidad certificadora ISO competente en el territorio. Marco jurídico en materia de protección de datos personales.	Plan de trabajo en materia de gobierno digital. Informes de la autoridad a través de portales de transparencia Sitios web del gobierno local. Leyes sobre protección de datos personales.
Plataforma integrada	Plataforma digital del gobierno de la ciudad. Disponibilidad de la aplicación en las tiendas de Apps para teléfonos inteligentes y equipos de cómputo. Porcentaje de usuarios activos de la aplicación. Porcentaje de usuarios satisfechos con los servicios proporcionados por la aplicación.	Sitios web del gobierno local. Play Store, Apple Store, Windows Store. Encuestas y estadísticas de organismos públicos.

4. Conclusiones

Hablar de la innovación en el Estado y su forma de gobernar, es un tema imperante en la agenda global. La incursión de las tecnologías, de diversa naturaleza, ha sido siempre un factor de disrupción en la sociedad; a lo largo de las revoluciones industriales, los distintos escenarios de la vida pública y privada han sido transformados.

Al contar con instituciones públicas a la vanguardia en las tecnologías digitales, se abre la posibilidad de acercar al gobierno con sus ciudadanos; al mismo tiempo, se eleva la eficacia con la que se prestan los servicios públicos y se hace una gestión más eficiente e inteligente, con mejores resultados a un menor costo. Con esto, el índice de satisfacción de la ciudadanía respecto de sus autoridades puede mejorar significativamente.

En síntesis, la meta a seguir es contar con un gobierno inteligente y una ciudadanía digitalizada. Para ello, es menester contar con las políticas públicas y el presupuesto necesario para llevar al Estado hacia la modernidad, pero también, con los programas educativos necesarios para fomentar en la población, un ejercicio de ciudadanía digital responsable y una cultura de uso consciente y respetuoso del ecosistema virtual.



N.º 26



Gestión de baterías de vehículos eléctricos mediante business intelligence y aprendizaje por refuerzo



ICSC-CITIES 2023
 Congreso Iberoamericano de Ciudades Inteligentes

 CIUDADES INTELIGENTES TORNAENTE INTEGRADAS, EFICIENTES Y SOSTENIBLES
 13-17 nov. 2023
 Ciudad de México y Cuernavaca, Morelos.

C. Barroso-Moreno⁽¹⁾, H. Amarís^{(2)*}, M. Alonso⁽²⁾
 E. Puertas⁽¹⁾

⁽¹⁾ Universidad Europea de Madrid, Madrid, España

⁽²⁾ Universidad Carlos III de Madrid, Madrid, España

Hortensia.amaris@uc3m.es

Keywords

Aprendizaje por refuerzo; Machine Learning; Business Intelligence · vehículo eléctrico; optimización de carga.

Abstract

El sector del transporte es el mayor consumidor de combustibles fósiles, ligado a un aumento de las emisiones de CO2 obliga a buscar alternativas de movilidad. La presente investigación tiene un doble objetivo, determinar patrones de comportamiento de la demanda de energía en un hogar residencial y proponer un algoritmo de aprendizaje por refuerzo (RL) para la optimización de la gestión energética con placas solares y un vehículo eléctrico (VE) integrado en un sistema de vehículo a red (V2G). La metodología encadena dos propuestas, primero, el empleo de la herramienta de negocio Power BI para modelar datos reales en sistemas de distribución y en segundo, integrar dichas distribuciones en el algoritmo de aprendizaje por refuerzo con diferentes recompensas que permitan lograr el menor coste en el hogar. Se han utilizado datos de movilidad y de recarga de VEs de libre acceso de seis fuentes diferentes de datos reales.

1. Business Intelligence

La inteligencia empresarial o Business Intelligence (BI) son el conjunto de estrategias, aplicaciones, datos o tecnologías que se enfocan a la administración y valor de los datos mediante la creación de conocimiento de la organización o empresa. La herramienta de Power BI permite extraer información relativa a patrones de demanda de energía del VE y determinar las distribuciones que modelan la llegada, salida, carga y descarga del VE.

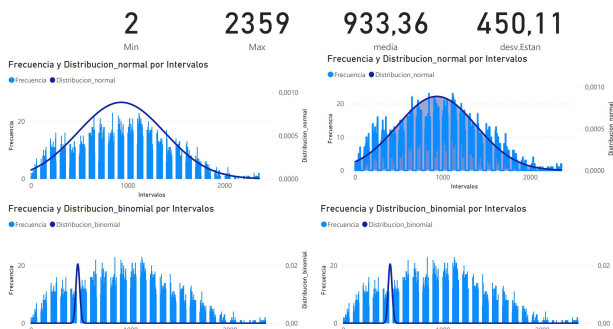


Fig. 1. Power BI: Distribución de salida con la fuente ElaadNL

2. Aprendizaje por refuerzo



Fig. 2. Aplicación de aprendizaje por refuerzo para la gestión de la energía almacenada en vehículos eléctricos

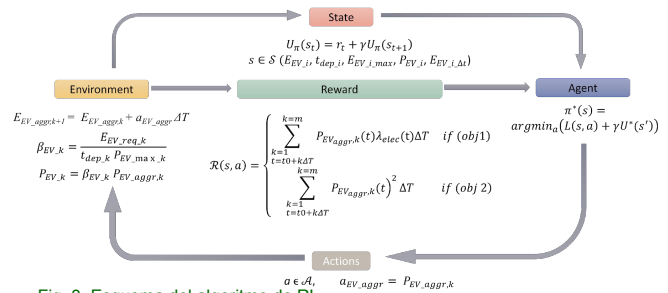


Fig. 3. Esquema del algoritmo de RL.

El algoritmo de RL corresponde a un modelo actor-critic PPO donde la red actor genera la acción del sistema representado por la política $\pi(\theta)$ y la red Critic corresponde a la estimación de la función de utilidad. Las entradas a ambas redes son los estados /observaciones. La salida de la red Critic es la función de valor que alimenta como entrada a la red actor.

3. Caso de estudio

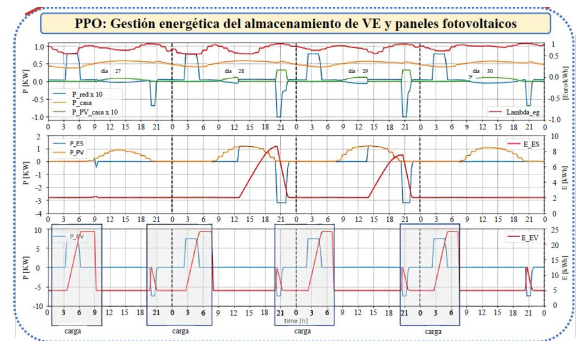


Fig. 4. Resultados de la gestión energética de sistemas de almacenamiento mediante RL.

La Figura expone en la parte superior la potencia de la red, la potencia generada por día en los paneles solares y la potencia consumida en el hogar, la potencia solar y potencia fotovoltaica. En el gráfico intermedio se indica la potencia de carga y descarga de la batería del VE. Por último, el gráfico inferior muestra la optimización de cargas del vehículo eléctrico resultado de la combinación de los parámetros anteriores.

4. Conclusiones

Los resultados de Power BI determinan tres patrones fundamentales de demanda de energía. Los resultados del algoritmo de RL determinan como patrón general la recarga lenta del VE y las horas adecuadas para realizar un aporte de energía al hogar. Las comparativas de optimización de energía entre PPO, BAU y VI determinan el mejor resultado en coste para el algoritmo PPO.

Agradecimientos

Acción financiada por el proyecto de Investigación PID2021-124335OB-C21 financiado por MCIN/AEI/10.13039



N.º 39



Systolic tensor array prototype for evaluation of convolutional neural networks



ICSC-CITIES 2023
Congreso Iberoamericano de Ciudades Inteligentes

Ciudades Inteligentes Torneo Integral, Eficientes y Sostenibles
13-17 nov. 2023
Ciudad de México y Cuernavaca, Morelos.



MI. Mario Alfredo Ibarra Carrillo⁽¹⁾⁽³⁾, MC. Jonathan Axel Cruz Vazquez⁽¹⁾⁽⁴⁾, Dr. Jesús Yaljá Montiel Pérez⁽¹⁾⁽⁵⁾, Dr. Herón Molina Lozano⁽¹⁾⁽⁶⁾, Dr. José Luis Lopez Bonilla⁽²⁾⁽⁷⁾

⁽¹⁾ IPN, Centro de Investigación en Computación, Ciudad de México, Mexico
⁽²⁾ Escuela Superior de Ingeniería Mecánica y Eléctrica, Zacatenco
⁽³⁾ ibarac2021@cic.ipn.mx ⁽⁴⁾ jcruzv2022@cic.ipn.mx ⁽⁵⁾ jyalja@cic.ipn.mx
⁽⁶⁾ hmolina@cic.ipn.mx ⁽⁷⁾ jllopezb@ipn.mx



Keywords

Systolic array, calculation accelerator; FPGA, Deep neural network; depth wise convolution, point wise convolution

Abstract

Smart cities are beginning to become evident due to the growing use of communication and computing technologies. There are technologies that make use of an already existing Internet and applications on cell phones. Other technologies require a processor evaluating an intelligence model to interpret the information provided by a sensor: "smartsensor." Relatively new technologies make extensive use of neural networks and it is then that three properties can be observed: costs, consumption and dissipation of energy, and real-time calculation limitations. This is where researchers intervene by proposing various solutions: new types of data that require fewer resources and less latency, new architectures, and advanced memory systems.

1. Deep neural network for testings

A five-layer deep neural network is sufficient to test a dataset that classifies six classes of vehicles. The network can be used to recognize up to ten classes of vehicles.

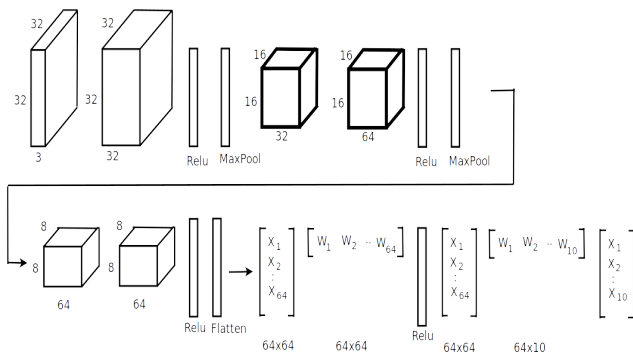


Fig. 1. Deep neural network of five layers

2. Cybersecurity requirements

A system based on a personal computer, a Raspberry PI and an FPGA was mounted. It was used to design, implement and test the arithmetic core of the project.

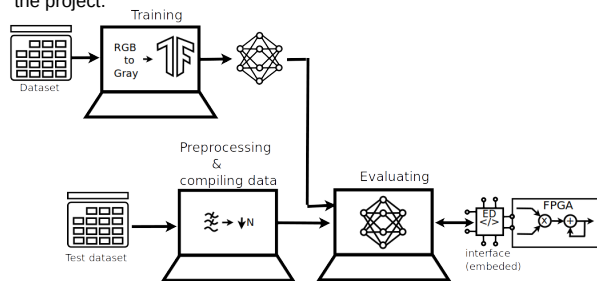


Fig. 2. Hardware to design, implement and test the core.

3. Systolic tensor core

This is the proposed architecture of a new systolic matrix that can perform matrix multiplication in "n" clock cycles. This device can perform the depth-wise convolution faster than the vector machine using the same number of resources in a factor of (1+log(n)).

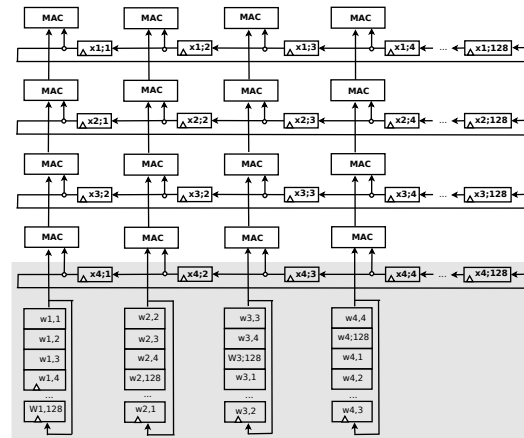


Fig. 3. Arithmetic core of proposed prototype.

4. Results

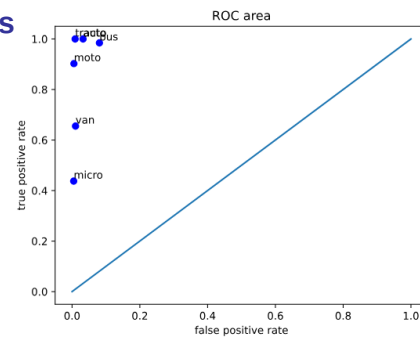


Fig. 4. Graphic generated from the confusion table.

5. Conclusions

- The system uses internal 16-bit floating point.
- The transmission protocol is SPI.
- The upload transfer rate is 100Mbps/s and for download of 16Mbps/s.
- The maximum length of the systolic array is 64 registers. Tested with 32.
- The system works with input images of 32x32.
- The data management is not suitable with Python. It requires "C".

6. References

[blanco; 2000] BLANCO, Armando; DELGADO, Miguel; PEGALAJAR, M. C. Fuzzy automaton induction using neural network. International Journal of Approximate Reasoning, 2001, vol. 27, no 1, p. 1-26.

[KUNG; 1982] KUNG, Hsiang-Tsung. Why systolic architectures?. Computer, 1982, vol. 15, no 01, p. 37-46.

[SHAMS; 1995] SHAMS, Soheil; GAUDIOT, J.-L. Implementing regularly structured neural networks on the DREAM machine. IEEE transactions on neural networks, 1995, vol. 6, no 2, p. 407-421.

FAWCETT, Tom. An introduction to ROC analysis. Pattern recognition letters, 2006, vol. 27, no 8, p. 861-874.



N.º 48



Mapping Evolution in Solar Panel Research: A Bibliometric Analysis of Research Results during 1992-2023



ICSC-CITIES 2023
 Congreso Iberoamericano de Ciudades Inteligentes

 CIUDADES INTELIGENTES TOTALMENTE INTEGRALES, EFICIENTES Y SOSTENIBLES
 13-17 nov. 2023
 Ciudad de México y Cuernavaca, Morelos.



F.J. Becerra-González⁽¹⁾, J. G. Vera-Dimas⁽¹⁾, Zakaryaa Zarhri⁽²⁾
 L. Cisneros-Villalobos⁽¹⁾

⁽¹⁾ Faculty of Chemical Sciences and Engineering, (UAEM), Cuernavaca, Morelos, Mexico.
⁽²⁾ CONACYT- Faculty of Chemical Sciences and Engineering (UAEM), Cuernavaca, Morelos, Mexico.



Keywords

Bibliometric analysis, Solar cells, Renewable sources, sustainability, Methodi InOrdinatio.

Abstract

This research work is about a study of bibliometric analysis of the literature of published scientific articles of a Journal nature. Citation Report (JCR), on the evolution of research on photovoltaic solar energy, technologies and materials used for its manufacture to contribute to the use of renewable energies around the world, according to scientific mapping, Scopus, Microsoft Excel and VOSviewer were used . 17,760 publications were recovered, between 1992 and 2023, from the Scopus database .

1. Bibliometric Analysis

A bibliometric analysis is a technique that allows studying the scientific production of a field, a discipline, a journal, an author or a country, through the use of quantitative indicators based on the bibliographic data of the publications, however, this technique has some limitations that must be considered when interpreting and applying its results.

Scopus database . Based on these results, the main keywords were selected. Subsequently, a database was generated in Comma Separated Values (CSV) and Text File (TXT) format for subsequent analysis in a computer tool for the construction and visualization of bibliometric networks called VOSviewer . Figure 1 shows the keyword diagram of the Scopus databases , according to the repetition frequency of the words, as shown in Figure 1.

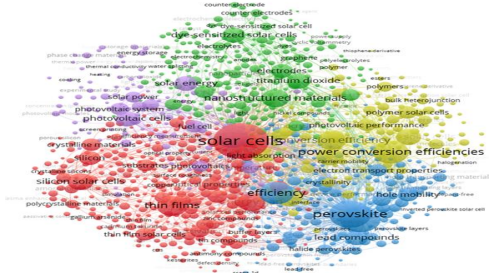


Fig. 1. Bibliometric map created with VOSviewer showing the frequency (keyword co-occurrence) of keywords presented in "solar panels"

2. Methodi InOrdinatio

- Phase 1:** Establish the intention of the research:
- Phase 2:** Preliminary exploratory research with keywords in databases.
- Phase 3:** Definition and combination of keywords and databases
- Phase 4:** Final search in the Scopus databases , Boolean operators were used to form the following combinations
- Phase 5:** Information filtering: Based on the results of the previous phase, additional filtering was carried out until obtaining the most relevant works for the application of the InOrdinatio equation formula .
- Phase 6:** Identification of the impact factor, year of publication and number of citations.
- Phase 7:** Obtaining the ranking of the articles: Once phases 1 to 6 were completed, the InOrdinatio index equation was used to calculate the ranking of the articles. This equation considers the total citations, the impact factor and a weight factor provided by the researcher, which ranges between 1 and 10.

$$\text{InOrdinatio} = (\text{IF}/(1000)) + (\text{year of research} - \text{year of publication}) + \Sigma \text{Ci}$$

Where:

IF = Impact Factor (JCR, CiteScore , SJR or SNIP)

ΣCi = total number of citations of the article

Phase 8: Search for complete articles after classifying the articles using InOrdinatio, showing in the table 1.

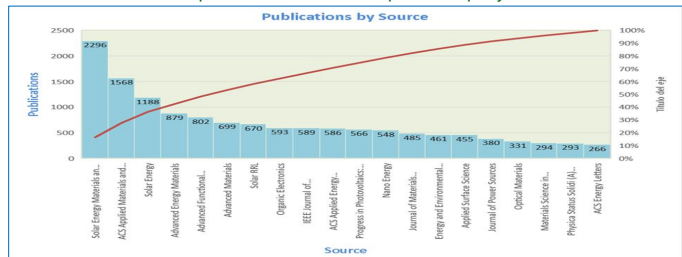
9: Final reading and systematic analysis of the articles, as show in Graph 1 and 2.

Author	Qualification	Year	Alpha Ordinatio = 7	InOrdinatio
Todorov TK; Tang J.; Bag S.; Guanwan O.; Gokmen T.; Zhu Y.; Mitzi DB	Beyond 11% efficiency: Characteristics of state-of-the-art Cu ₂ ZnSn(S,Se) ₄ Solar Cells	2013	1	948.0278
Debije MG; Verbunt PPC	Thirty years of luminescent solar concentrator research: Solar energy for the built environment	2012	2	707.0278
Treat ND; Brady MA; Smith G.; Toney MF; Kramer EJ; Hawker CJ; Chabinyc ML	Interdiffusion of PCBM and P3HT reveals miscibility in a photovoltaically active blend	2011	3	576.0278
Walsh A.; Chen S.; Wei S.-H.; Gong X.-G.	Kesterite thin-film solar cells: Advances in materials modeling of Cu ₂ ZnSnS ₄	2012	4	562.0278
Wang Y.; Yi J.; Xia Y.	Recent progress in aqueous lithium-ion batteries	2012	5	453.0278
Yang Y.; Yip H.-L.; Jen AK-Y.	Rational design of advanced thermoelectric materials	2013	6	250.0278
Schubert S.; Meiss J.; Müller - Meskamp L.; Leo K.	Improvement of transparent metal top electrodes for organic solar cells by introducing a high surface energy seed layer	2013	7	228.0278

Table 1. List of articles classified by InOrdinatio order



Graph 1. Number of articles published per year



Graph 2. Publications by source

3. Conclusions

The purpose of this document was to analyze solar systems from their beginnings in the 90's to the present and has had great interest on the part of the scientific community by contributing to reducing greenhouse gas pollution, the research demonstrated the growth exponential of the literature today. In these documents, the evolution of solar systems has been studied and the search for using materials to be more efficient systems with a longer useful life has been studied.



N.º 49



Research in Electromechanical Efficiency: A Bibliometrics Analysis of the Last 82 Years (1941 to 2023)

P. Flores Sánchez⁽¹⁾, L. Cisneros Villalobos⁽²⁾, Zakaryaa Zarhri⁽²⁾
M. Limón Mendoza⁽²⁾



ICSC-CITIES 2023
Congreso Iberoamericano de Ciudades Inteligentes
CITIES
CIUDADES INTELIGENTES TOTALMENTE INTEGRALES, EFICIENTES Y SOSTENIBLES
13-17 nov. 2023
Ciudad de México y Cuernavaca, Morelos.



⁽¹⁾ FCQel, The Autonomous University of the State of Morelos (UAEM), Cuernavaca, Morelos, Mexico
pedro.flores@uaem.edu.mx

⁽²⁾ CONAHCYT-FCQel, The Autonomous University of the State of Morelos (UAEM), Cuernavaca, Morelos, Mexico



Keywords

Efficiency, electromechanical, bibliometric analysis, VOSviewer.

Abstract

In this document, we have conducted a bibliometric analysis of electromechanical efficiency topics using the data analysis tool VOSviewer and the SCOPUS database of scientific publications. We have reviewed authors, citation and co-citation relationships, and their connections to the most relevant keywords in the published documents. We have also examined the affiliations of the authors' institutions and the countries of publication. Our findings include the most cited articles, journals with the highest number of documents, and an analysis of keyword cluster concurrence. This analysis has allowed us to identify areas of study related to "energy harvesting," "microelectromechanical systems," "energy efficiency," and "piezoelectric." In conclusion, we observe a continuing trend of interest in the study of these topics.

1. Objective

The main objective of our document is to conduct a review of publications that have addressed the topic with the keywords "efficiency AND electromechanical" to identify the main authors, their affiliations, and the countries where the research is being published, we aim to review the keywords and their relationship in terms of clusters of work to determine if there is relevance based on the type of information generated and to identify possible connections between different research topics.

2. Methodology

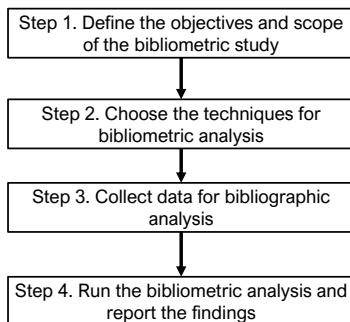


Fig. 1. Simplified methodology for preparing the bibliometric study

3. Results

With information from the database, there are a total of 4,997 documents, of which 59.9% (2,994 documents) are articles, and 35.1% (1,752 documents) are conference papers, 2.4% (122 documents) are review articles, and 2.6% (129 documents) are of other types (book chapters, conference reviews, books, and editorials). Regarding areas of study, 35.0% (3,588 documents) are related to the field of engineering, and 13.6% (1,395 documents) are in physics and astronomy as the primary areas.

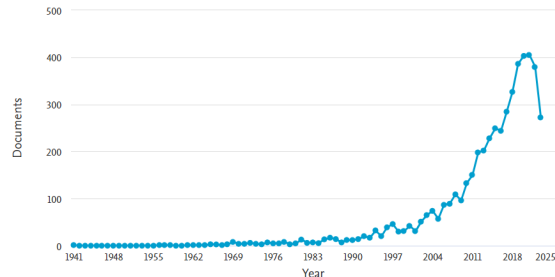


Fig. 2. Number of documents per year of publication.

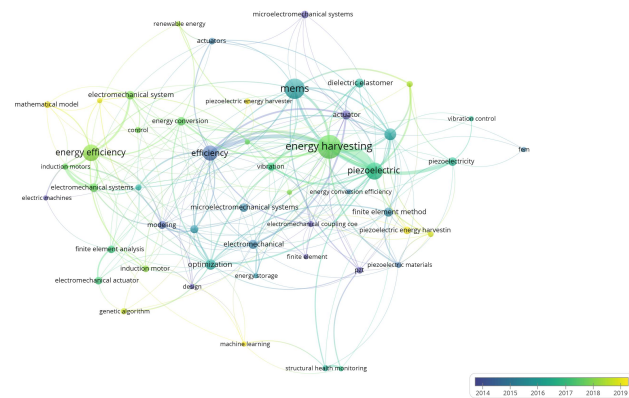


Fig. 3. Keyword occurrence by author with a minimum of 15 occurrences per keyword

Journal	Documents	Total times cited	The most cited paper	Cited by
Proceedings of SPIE - The International Society for Optical Engineering	145	1544	Ultrahigh strain response of field-actuated elastomeric polymers	185
Smart Materials and Structures	68	3587	Analysis of power output for piezoelectric energy harvesting systems	688
Journal of Intelligent Material Systems and Structures	53	1586	The effect of non-linear piezoelectric coupling on vibration-based energy harvesting	183
Journal of Physics: Conference Series	51	70	Power electronics performance in cryogenic environment: Evaluation for use in HTS power devices	9
SAE Technical Papers	50	407	The third generation of valvetrains - New fully variable valvetrains for throttle-free load control	110

Tab. 1. Main journals with published documents referring to the keywords "efficiency AND electromechanical"

4. Conclusions

When conducting a search with the keywords "efficiency AND electromechanical" in the Scopus database and analyzing the data with VOSviewer, it can be observed that there are few records of published documents on the topic from 1941 to 1991. After this period, clusters with other keywords such as "energy harvesting," "microelectromechanical systems," "energy efficiency," and "piezoelectric" stand out. The cluster that starts with "energy harvesting" has strong connections with "microelectromechanical systems," which have been high-interest topics since 2005, as well as keywords related to "piezoelectric" and "efficiency," which complement the field of study. The words related to energy harvesting research focus on the study of piezoelectric materials, their electrical properties, and the interest in making the mechanical energy transfer through these materials to electromechanical energy more efficient.



N.º 55



UNIVERSIDAD AUTÓNOMA DEL ESTADO DE MORELOS

Bibliometric Analysis of Contemporary Research on Charge Transfers between Medium Voltage Power Distribution Circuit

Ing. Luis Edgar Lira Toral⁽¹⁾, Dr. Zakaryaa Zarhri^{(2),*}, Dr. Luis Cisneros Villalobos⁽¹⁾, Dr. Mario Limón Mendoza^{(1),**}

⁽¹⁾ CONACYT- Faculty of Chemical Sciences and Engineering, The Autonomous University of the State of Morelos (UAEM), Av.

Universidad 1001, Col. Chamilpa, C.P. 62209, Cuernavaca, Morelos, Mexico.

*corresponding author: z.zarhri@gmail.com; **corresponding author: mario.limon@uaem.mx

⁽²⁾ Faculty of Chemical Sciences and Engineering, The Autonomous University of the State of Morelos (UAEM), Av. Universidad

1001, Col. Chamilpa, C.P. 62209, Cuernavaca, Morelos, Mexico.



ICSC-CITIES 2023
Congreso Iberoamericano de Ciudades Inteligentes

Ciudades Inteligentes Totalmente Integrales, Eficientes y Sostenibles
13-17 nov. 2023
Ciudad de México y Cuernavaca, Morelos.



Keywords

Charge transfer, symbolic logic, material implication, topology, distribution systems, electrical power interruption.

Abstract

This research work delves into the realm of contemporary investigations concerning charge transfers occurring within medium voltage power distribution circuits. Such transfers primarily arise from maneuvers executed exclusively by energy suppliers and often result in power interruptions. Another facet of this study involves the identification of analogous research endeavors conducted in disparate geographical regions, with a particular emphasis on the localized context of Cuernavaca, Morelos. Furthermore, this article engages in interdisciplinary discourse, employing logical analogies to establish a conceptual topology. This conceptual framework can be instrumental in the identification, through logical connectors, of instances where a charge transfer within an electrical power distribution system implies a power interruption. This, in turn, contributes to the optimization of energy utilization, a critical consideration within the purview of smart cities.

Objective

Bibliometric analysis of uninterrupted load transfer maneuvers to identify the state of the art of the research topic. Identify the state of the art of the research topic about uninterrupted load transfer maneuvers, through a bibliometric analysis, as well as present the case of the RGD of the city of Cuernavaca with respect to load transfer maneuvers.

1. Methodology

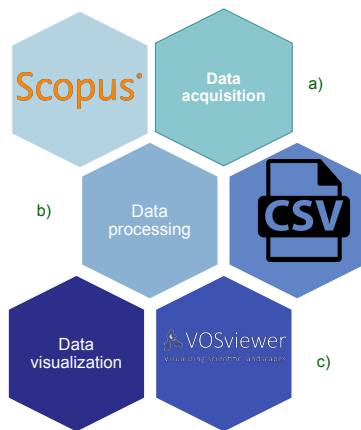


Fig. 1. Bibliometric analysis methodology: (a) Data acquisition (b) Data processing (c) Data visualization

2. Results and discussion

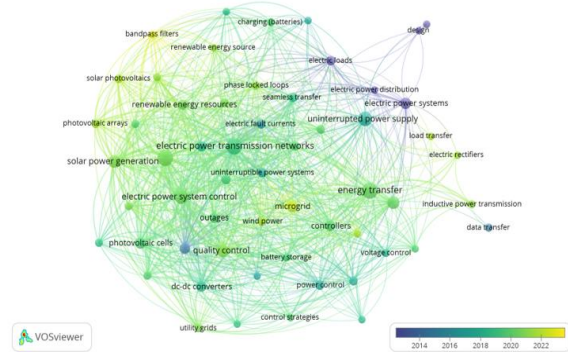


Fig. 2. Bibliometric Network Based on the Co-occurrence Analysis of the Keywords "uninterrupted load transfer" for the Period from 2013 to 2023.

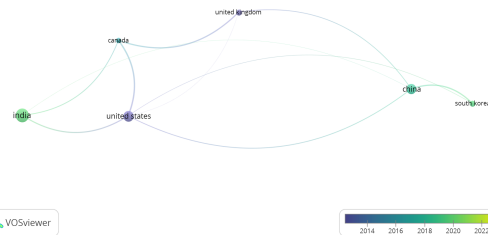


Fig. 3. Bibliometric Network of Countries with the Highest Bibliographic Coupling.

	S.E. CIV	S.E. CUE	S.E. MOR	S.E. TBH
S.E. CIV	PARALELO	X	X	X
S.E. CUE	X	PARALELO	X	PARALELO
S.E. MOR	X	X	PARALELO	X
S.E. TBH	X	PARALELO	X	PARALELO

Table 1. Combinations of Substations with the Ability for Uninterrupted Electrical Load Transfer through the Parallel Operation of Two Electric Power Distribution Circuits and the Parallel Operation of Circuits Derived from the Same Substation.

3. Conclusions

Despite finding a certain number of documents in the Scopus database, one should not assume that this is not a research topic. The operational aspects of electric generators and the National Electric System (SEN) in the case of Mexico demonstrate that electric circuits can operate in synchrony, provided they meet favorable conditions for synchronization and parallel operation at the same voltage level, frequency, number, phase sequence, and angular displacement.

Reviewing the state of the art in this research area sets a precedent for further exploration in various DGRs that are part of Mexico's SEN and even in other countries. This aims to obtain objective data about distribution circuits that can be synchronized and temporarily paralleled for load transfer maneuvers between medium-voltage circuits (M.V.) from different energy sources, such as electric distribution substations, thereby preventing energy interruptions caused by load shedding.



N.º 56

CSC-CITIES 2023

Congreso Iberoamericano de Ciudades Inteligentes



Bibliometric research for design and build a Potentiostat to electrochemical characterization of metal surfaces

Eduardo Manuel Barreiro Ortiz , Zakaryaa Zarhri , Roy López Sesenes , Mario Limón Mendoza
 Facultad de Ciencias Químicas e Ingeniería, de la Universidad Autónoma del Estado de Morelos, Cuernavaca, Morelos



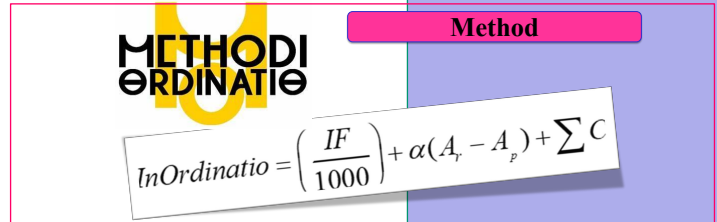
Abstract

The present research uses a bibliometric analysis focused on designing and building a low-cost Potentiostat to conduct electrochemical analyses on metallic surfaces to measure parameters such as current, potential, and resistance. This bibliometric study provides a comprehensive view of the existing literature on the topic and keywords of interest, facilitating the identification of possible collaborations and connections. The data were obtained from the Scopus database, carrying out scientific literature research based on the topic under study. Some representative plots of the bibliometric study were generated. A Methodi Ordinatio methodology was applied to evaluate the relevance of the collected publications. The results revealed significant research trends toward low-cost Potentiostat development, highlighting the growing importance of making electrochemical instrumentation more accessible and open-source software interfaces.

Keywords — Potentiostat, Characterization and Design, Methodi InOrdinatio , Bibliometric Study.



Fig. 1. Author's correlation search with the topics: Potentiostat and Low Cost



Method

Results and discussions

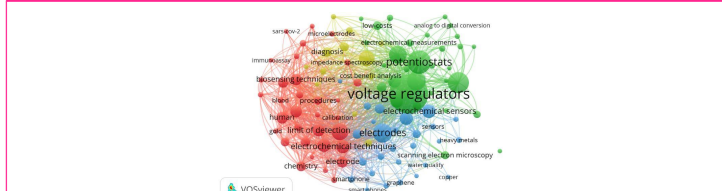


Fig. 2. Plot of publications that coexist with the keywords "Potentiostat and low cost" to demonstrate the operation of the VOSviewer tool based on the bibliographic information obtained from the Scopus database.

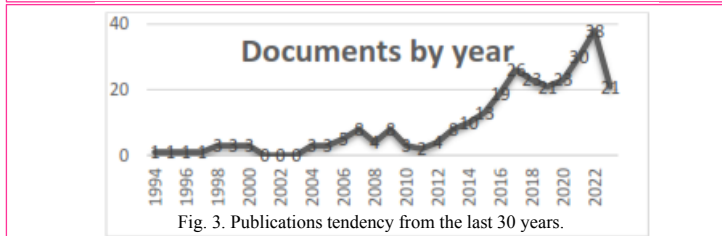


Fig. 3. Publications tendency from the last 30 years.

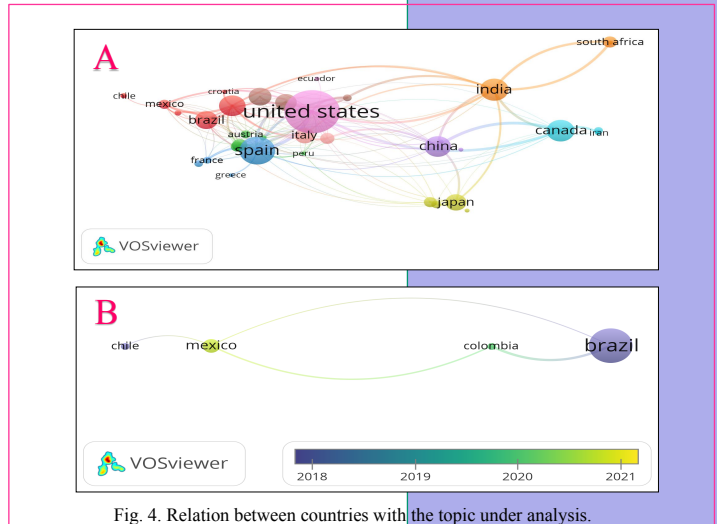


Fig. 4. Relation between countries with the topic under analysis.

Conclusions

The bibliometric analysis applied to the Scopus databases, related to the design and construction of a low-cost potentiostat to perform electrochemical characterization on metal surfaces using a data acquisition card with WiFi connectivity, was analyzed by multiple bibliometric studies with the support of tools such as VOSviewer, which allowed to create networks nodes that schematically showed the massive correlations that exist between articles with the topic under analysis. On the other hand, the 9 phases and the Methodi Ordinatio method allowed us to prioritize the most relevant sources and obtain enough bibliographic information to undertake the project.

References

F. Bentum, «Education and Capacity Building for Open Science Hardware in Sub-Saharan African Universities. (ECBAOSH)», presentado en Open Infrastructure Fund / Fondo de Infraestructura Abierta, ago. 2023. Accedido: 25 de septiembre de 2023. [En línea]. Disponible en: <https://openreview.net/forum?id=XvhKDR8Pma>

M. S. Kelly y K. Mayes, «High Precision Laser Fault Injection using Low-cost Components», en 2020 IEEE International Symposium on Hardware Oriented Security and Trust (HOST), San Jose, CA, USA: IEEE, dic. 2020, pp. 219-228. doi: 10.1109/HOST45689.2020.9300265.

B. Pamplana Solís, J. C. Cruz Argüello, L. Gómez Barba, M. P. Gurrola, Z. Zarhri, y D. L. Trejo-Arroyo, «Bibliometric Analysis of the Mass Transport in a Gas Diffusion Layer in PEM Fuel Cells», Sustainability, vol. 11, n.º 23, p. 6682, nov. 2019. doi: 10.3390/su11236682.



N.º 80



CanarIoT: Monitoring of environmental variables such as CO₂, at the service of university resilience in a pandemic, through IoT solutions.



Juan A. Rodríguez^(1,2), Domingo A. Martín^(1,2), Javier Maroto^(1,2), Alfredo Martín^(1,2), Ana García^(1,2), Jorge L. Costafreda^(1,2)

⁽¹⁾ Universidad Politécnica de Madrid (UPM), España

jrodriguez@alumnos.upm.es

⁽²⁾ Escuela Técnica Superior de Ingenieros de Minas y Energía (ETSIME-UPM), España



ICSC-CITIES 2023
Congreso Iberoamericano de Ciudades Inteligentes

Ciudades Inteligentes Totalmente Integrales, Eficientes y Sostenibles
13-17 nov. 2023
Ciudad de México y Cuernavaca, Morelos.



Keywords

3D printing; innovation; Covid19; CO₂

Abstract

The CanarIoT-UPM project emerges as a technological and strategic response to the COVID-19 pandemic, addressing the growing need to monitor air quality in indoor spaces. Leveraging low-cost sensor technology; specifically the SCD30 NDIR sensor; the project has established a monitoring network to measure CO levels₂, providing critical indicators on air quality and the need for ventilation. This monitoring is essential to reduce the risk of virus transmission in closed spaces, especially in educational environments such as classrooms. CanarIoT-UPM not only stands out for its innovative approach in the use of sensor technology, but also for its integrated methodology, which includes personnel training, implementation of protocols and dissemination of information through digital platforms. The initiative, framed within the Tellus UPM ecosystem, reflects the university's commitment to adaptability and resilience in times of crisis, offering practical solutions that combine science, technology and community well-being.

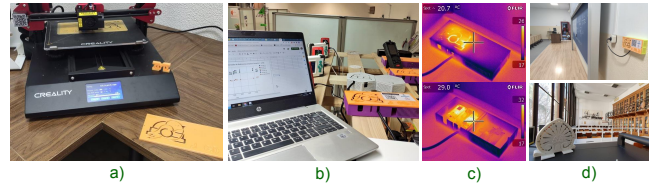


Fig. 2. (a) 3D printing of parts, (b) Data analysis and comparison with reference instruments, (c) Thermography to validate the proper functioning of the prototypes and (d) Examples of IoT monitoring nodes in university spaces.

1. Visual elements and visual grammar

During the COVID-19 pandemic, monitoring indoor air quality emerged as a key element in reducing the spread of the virus, leading to the initiation of the CanarIoT-UPM project at the ETSIME-UPM. This initiative focused on implementing an Internet of Things (IoT) based sensor network to accurately track CO₂, temperature, and humidity levels, with the goal of maintaining a safe educational environment through improved air quality and ventilation.

The Tellus UPM Innovation Ecosystem facilitated the rapid development and deployment of this network, offering an integrated platform for collaboration and fast-tracking the creation of custom technological responses to the urgent demands posed by the health crisis. This ecosystem played a crucial role in enhancing the project's development speed and in fostering a multidisciplinary approach, contributing to the establishment of resilient academic and technological strategies to address public health challenges.

2. Materials and Methods

The CanarIoT-UPM project, developed at ETSIME-UPM, mirrors the preventive function of canaries in mines by monitoring air quality in university spaces to ensure health and safety during the COVID-19 crisis. It highlights the necessity of proper ventilation to prevent virus spread and to maintain thermal comfort and energy efficiency.

Leveraging a network of precise sensors like the SCD30 and Bosch BME280, connected to a dedicated IoT platform, the project enables real-time data management for effective ventilation and comfort (fig.1). Validation of IoT node performance through reference instruments and thermographic imaging ensures reliable operation, while 3D printing capabilities facilitate the customization of components for each node (fig.2).



Fig. 1. Conceptual outline of how the CanarIoT project works

3. Results and Discussion

The CanarIoT-UPM Project has significantly advanced the monitoring and understanding of air quality in educational settings, providing reliable data through visualizations of CO₂ levels (fig. 3), temperature, and humidity. The project's sensor accuracy is validated against reference devices, ensuring trust in the data collected by sensors.

This initiative has been instrumental in enhancing indoor air quality control, proving vital in reducing airborne pathogen transmission, particularly COVID-19. With the integration of IoT technology, the project has not only reinforced the health and safety protocols of the university environment but has also exemplified the pivotal role of digital monitoring systems in maintaining public health and safety during health crises.

4. Conclusions

The CanarIoT-UPM Project showcases the effective use of cost-efficient sensors for consistent air quality monitoring in educational settings, crucial for health and safety measures. The project's integration into the Tellus UPM innovation ecosystem enabled a swift, responsive approach to the challenges posed by the COVID-19 pandemic, thereby increasing the resilience and adaptability of the academic community. Moreover, it provided a platform for education in digital and sustainable practices. The project leveraged IoT technologies as educational tools for learning and developing new technological skills. Additionally, the application of 3D printing facilitated the creation of culturally sensitive solutions suitable for historical spaces, demonstrating the university's role as a testbed for urban-scale solutions. Overall, CanarIoT-UPM illustrates the broader potential of such technological interventions for public health management and improving urban life quality.

Acknowledgements

Appreciation and thanks are extended to the RES2+U program from the call organized by UPM Sostenible and to ETSIME-UPM for their support and funding. The collaboration of the EELISA-ESCE community at UPM is also highly valued, as is the indispensable assistance and backing from the entire ETSIME-UPM university community, which have been fundamental to the successful development of the project.



Fig. 3. Visualization of IoT node data in real time (a) summary and (b) full graphic.



N.º 47



Global bibliometric analysis of railway and train research: focus on Latin America and Mexico



ICSC-CITIES 2023
Congreso Iberoamericano de Ciudades Inteligentes



Ciudades Inteligentes Totalmente Integrales, Eficientes y Sostenibles
13-17 nov. 2023
Ciudad de México y Cuernavaca, Morelos.



M. Eng. Luis Ivan Ruiz Flores, Dr. Zakaryaa Zahri, Dr. Luis Cisneros V.

Universidad Autónoma del Estado de Morelos

luis.ruizf@uaem.edu.mx, z.zahri@gmail.com, luis.cisneros@uaem.mx

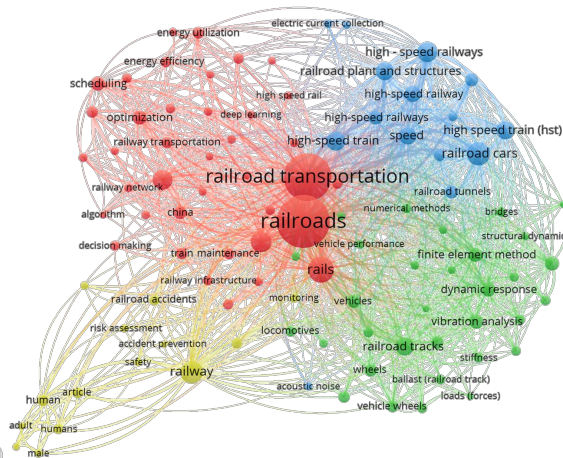


Keywords

bibliometric analysis, railway, sustainability, trains.

Abstract

This technical article highlights the trends and developments of a group of publications, authors, papers, countries and keywords relevant to the topics of "trains and railways" over the last decade. The bibliometric analysis represented will contribute to the understanding of current statistics on "trains and railways". Additionally, it would contribute to the community of researchers who are developing knowledge on these topics. The bibliometric networks are generated from the bibliometric data that were obtained from Scopus and have been visualized in VOSviewer; an overview is presented with the largest number of publications from China, the UK, the EE.UU., Spain & Italy. On the other hand, the use of the keywords in the publications were "trains and railways" focusing on sustainability as the central point of the analysis to promote publications in Latin America. The results of this bibliometric analysis seek to encourage the research community of Mexico and Latin America to initiate or contribute to include enrollment in the Academy that allows to increase the number of publications in the Spanish language within the American Continent.



The bibliometric analysis carried out was initially preloaded with a keyword that is "railway" or by English translation as "railway", an inclusion criterion of 20,000 publications with authors, abstract, keywords and search strings defined for the research was applied, integrating the publications from 2014 to 2023 using a minimum number of occurrences of a keyword: 6 and getting a substrate of the 7758 keywords, 386 reach the threshold to get the graphs.

The purpose of this work is to contribute to the dissemination of bibliometric data on co-occurrence, number of publications, predominance in countries including Mexico and Latin America with a comparison of the number of publications from 2014 to 2023.

The contribution is to encourage the scientific community to contribute to publications that highlight Hispanic projects in contribution to energy sustainability worldwide

Train and railroad systems have recently become relevant in Mexico due to the application in the Federal Government's project of the current six-year term from 2018 to 2024

Conclusions

Nowadays, infrastructure is already used to power railway trains with alternating current or direct current; However, it is a priority that each project of these characteristics must carry out pre-feasibility studies including the necessary peripherals, such as: water, electricity, soil mechanics, environmental impact, etc.

Introduction

In Mexico, it was at the beginning of the Mexican Revolution that the construction of the first national locomotive began in the workshops of Aguascalientes and by 1938 the National Railways of Mexico were nationalized

The Mayan Train will use Diesel and AC for the area and its current electricity supply difficulties

Priority is given to pre-feasibility studies, including the necessary peripherals, such as: water, electricity, soil mechanics, environmental impact, etc.



Mayan Train

Source: Gobierno de México



Trans-Isthmus Train

Source: El Sol de México



Train "El Insurgente"

Source: El Universal



Train Cuernavaca to CDMX

- It would use the current railroad tracks (61 kms)
- 6 Possible CETRAMS
- Decrease >50% of travel time
- It would contribute to energy sustainability
- It would be AC, passenger and transportation



In Latin America, when searching for keywords, the threshold of 81 technical articles is reached

In Mexico, when searching for keywords, the threshold of 192 technical articles is returned

In Latin America there have been several "trains and railways" projects in the last 7 years; For example, in:



- Metropolitan Train
- Year 2022
- + 40 kms



- Fast Passenger Train (TRP)
- Year 2028
- 80 kms



- Lima and Callao Metro with Line 2
- Years: 2024 & 2026
- 27 kms



- Mayan Train / Year 2023 / 1554 kms
- Trans-Isthmus Train / Year 2023 / 300kms



Video Presentation

Luis Ivan Ruiz Flores | luis.ruizf@uaem.edu.mx | +52.7772884896





N.º 56

Ing. David Flores Hernández¹, Dr. Zakaryaa Zarhri ², Dr. José Gerardo Vera Dimas³, Dr. Mario Limón Mendoza⁴

¹ Estudiante de posgrado en la Facultad de Ciencias Químicas e Ingeniería, Universidad Autónoma del Estado de Morelos (UAEM).

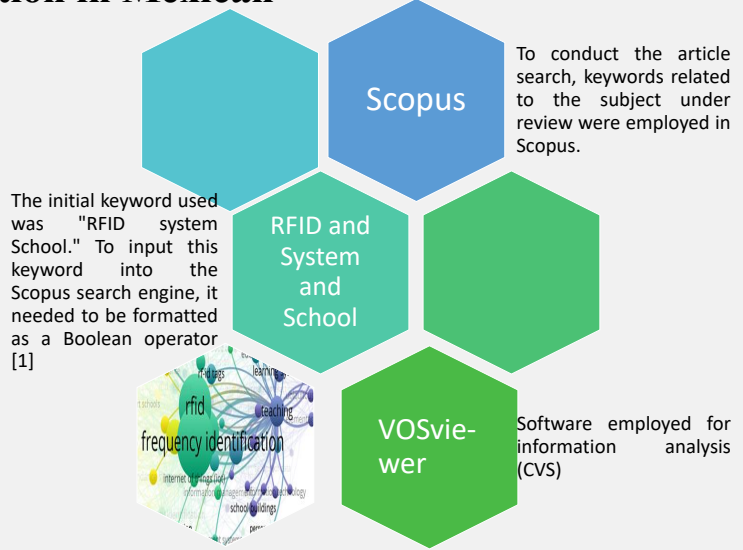
² CONAHACYT-Facultad de Ciencias Químicas e Ingeniería, Universidad Autónoma del Estado de Morelos (UAEM), Av. Universidad 1001, Col. Chamilpa, C.P. 62209, Cuernavaca, Morelos, Mexico ³Facultad de Ciencias Químicas e Ingeniería, Universidad Autónoma del Estado de Morelos (UAEM), Av. Universidad 1001, Col. Chamilpa, C.P. 62209, Cuernavaca, Morelos, Mexico

Bibliometric Study: Feasibility of RFID Technology and IOT Systems for their Integration in Mexican Education Institutions

INTRODUCTION

The present research work presents a quantitative technical analytical study in the field of engineering to determine the feasibility of current technologies that incorporate Radio Frequency Identification (RFID) and Internet of Things (IoT) technology. Published works from the period 2002-2023 were considered. The review and comparison of these data revealed that during this period, 281 documents have been published on the development, design, and study of RFID and IoT systems, with contributions from 262 authors affiliated with educational institutions and private organizations around the world.

METHODOLOGY



RESULTADOS

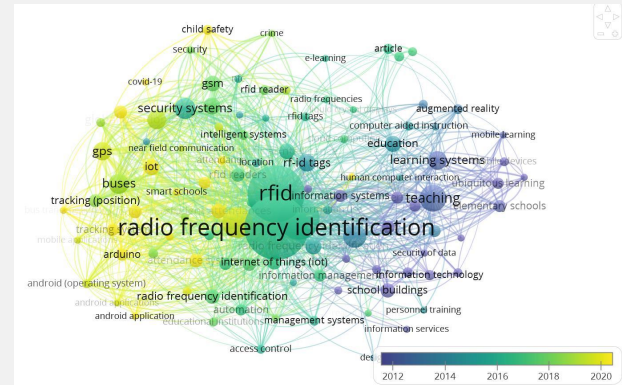
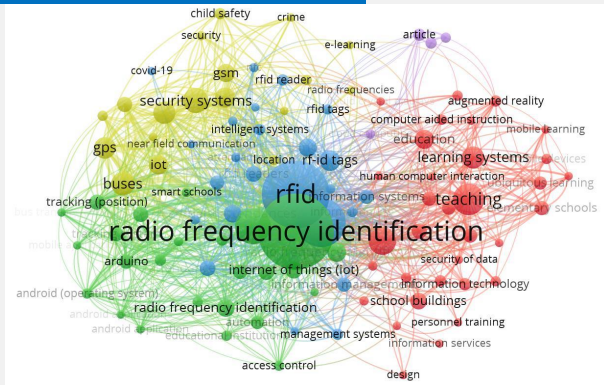
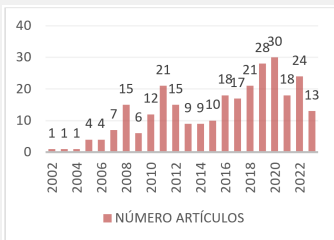


Figure 1: Bibliometric Map of Frequency (Word Co-occurrence) Using the Term "RFID System in Schools," Generated by VOSviewer Software

Figure 2: Bibliometric Map of Frequency (Word Co-occurrence) Using the Term "RFID System in Schools," Generated by VOSviewer Software, Documenting Data from the Period 2002-2023.

Articles: 281 documents found, authored by 262 contributors. The articles were published between 2002 and 2023. The network graph revealed an increase in the number of published works starting from the year 2016, coinciding with the widespread adoption of the term "Industry 4.0" as proclaimed at the 2016 World Economic Forum [2].

CONCLUSION

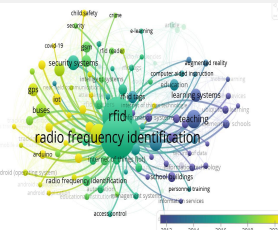


Articles published during the years 2016-2023: "IoT School Attendance System Using RFID Technology" [3]:

country	Documents	Citation
India	69	296
Taiwan	33	1021
China	33	178
Japan	17	58
USA	16	209
Malaysia	10	112
Saudi Arabia	10	55
Germany	9	26
Italia	8	77
Indonesia	7	12
Mexico	6	38
Australia	5	47

The correlational analysis in Table 2 showed that Mexico had a contribution of 6 disseminated documents

"A Systematic Literature Review on the Internet of Things in Education: Benefits and Challenges" [4], the authors note that, based on their analysis, there were no significant works integrating IoT into education prior to 2008. They found that the first publications of research integrating IoT into education started in 2014, with a noticeable increase in such publications from 2008 to 2017.



REFERENCE

- [1] Z. Zarhri, W. Rosado Martinez, J. A. Dominguez Lepe, R. E. Vega Azamar, M. Chan Juarez, and B. B. Pamplona Solis, "30 years of rubberized concrete investigations (1990-2020). A bibliometric analysis," Rev. ALCONPAT, vol. 12, no. 1, Jan. 2022, doi: 10.21041/ra.v12i1.554.
- [2] "¿Qué es la Industria 4.0?" <https://www.oracle.com/mx/scm/manufacturing/what-is-manufacturing/what-is-industry-4-0/> (accessed Sep. 22, 2023).
- [3] H. El Mrabet and A. Ait Moussa, "IoT-School Attendance System Using RFID Technology," Int. J. Interact. Mob. Technol. IJIM, vol. 14, no. 14, p. 95, Aug. 2020, doi: 10.3991/ijim.v14i14.14625.
- [4] M. Kassab, J. DeFranco, and P. Laplante, "A systematic literature review on Internet of things in education: Benefits and challenges," J. Comput. Assist. Learn., vol. 36, no. 2, pp. 115-127, Apr. 2020, doi: 10.1111/jcal.12383.



N.º 84



Economic Feasibility Analysis of the Implementation of Solar Panels in Educational Institutions in the State of Morelos. A Bibliometric Analysis



Juan Peralta Mojica¹, Zakaryaa Zarhri², J. Guadalupe Velásquez Aguilar³, Mario Limón Mendoza⁴

¹ Faculty of Chemical Sciences and Engineering, The Autonomous University of the State of Morelos (UAEM), Av. Universidad 1001, Col. Chamilpa, C.P. 62209, Cuernavaca, Morelos, Mexico

² CONACYT-Faculty of Chemical Sciences and Engineering, The Autonomous University of the State of Morelos (UAEM), Av. Universidad 1001, Col. Chamilpa, C.P. 62209, Cuernavaca, Morelos, México



ICSC-CITIES 2023
Congreso Iberoamericano de Ciudades Inteligentes

Ciudades Inteligentes. Tormentas. Integrales. Eficientes y Sostenibles.
13-17 nov. 2023
Ciudad de México y Cuernavaca, Morelos.

Keywords

Renewable energy; Solar cells; Sustainability; Feasibility; Bibliometric Analysis.

Abstract

Since 2018, interest in the use of renewable energy has increased significantly. Chile, Germany, the United States, Spain and India are leading countries in the production and use of renewable energy; This document shows the analysis of the feasibility of implementing solar panels in different areas to promote the interest in replacing commercial electrical energy with renewable energy, a practice that affects the reduction of pollution at a global level, the above based on a bibliometric study of works published both in the Scopus database, in a period from 2005 – 2023. For the analysis, the VOSviewer software was used as a support tool, which facilitates the work considering that there are approximately 850 documents that deal with the use of the implementation of solar panels in different sectors with the contribution of 1,340 authors on the subject.

1. Visual elements and visual grammar

The following diagram in Figure 1. maps the research universe (renewable energy) in the period 2021-2022 and which has an increase in greater contribution or interest starting in 2021, as shown below in the yellow and red nodes.

The diagram in Figure 2. Shows the keywords with the highest attendance in the Scopus database, which makes a report with the highest authorship regarding words such as: Renewable energy; Solar cells; Photovoltaic; which represents what is the important point of this study.

The analysis of figure 3. Shows that with more than 400 publications, there is increased interest in developing research that integrates the implementation of renewable energy in educational institutions. The first publication found in the platform's database that contains the keyword (Renewable Energy) was in 2015, which is of utmost importance for the relevance of this study.

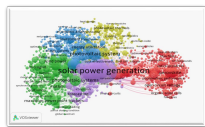


Figure 1. Solar power generation

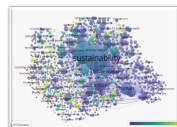


Figure 2. Sustainability



Figure 3. Solar cells

2. Methodology

To determine the articles that can be used for this study, the Scopus platform database was used, which allows searches for scientific articles with the required characteristics that affect the proposed area of study of interest. This search uses keywords contained in the title such as: Renewable energy worldwide and nationally, different types of solar cells, Feasibility of energy use, Irradiance and Sustainability. As a result of the search, Scopus returned 850 documents considered the universe of bibliometric analysis, including 1,350 authors in this same results.

To limit and reduce the universe, more specific keywords are applied to filter, such as: Energy, Renewable; Feasibility; Sustainability, Photovoltaic; obtaining a more relevant universe of documents related to the research topic, which resulted in 118 documents found by 182 authors. The articles were published in the period 2005-2023. By obtaining the data in Comma Separated Values (CSV) format, the VOSviewer software was manipulated to study the information that was used to view a bibliometric network of document correlations, also revealing that the increase with The greatest publication work had a maximum participation by researchers starting in 2019.

3. Strategy

Mention is made of the analysis, which highlighted the use of the VOSviewer computer program, which is free to use and allows you to design bibliometric maps. The VOSviewer operation is very lucrative to represent data that relate to each other in a bibliometric map and symbolizes them in a network that is easy for the user to approach. The computer program builds maps in several different ways that the user can select according to needs. For the present study, a map is created based on the bibliography that has first been downloaded from the Scopus database in CSV format and that uses VOSviewer to do the analysis as follows:

- Co-occurrence: uses a set of words, authors, citations that correlate between more than one document.
- Bibliographic coupling: Shows the relationship between the number of references that are used and shared by the authors, uses citation analysis to establish a relationship [23].

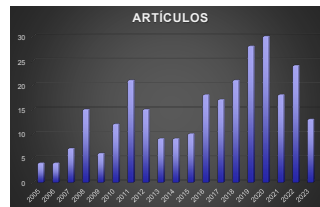


Tabla 1. of articles published in the period, 2005 to 2023 (CSV from the Scopus platform).

Author	Documents	Quotes
Attri, A., Kheola, A. (2022)	1	250
Shaidi, R., Khawaja, Y., Bari-Abdullah, A., Akho-Zahieh (2023)	1	159
Sovscool, B.K., Brown, (2007)	1	117
Enciso Contreras, E., Saldaña, J.G.B., Alejo, J.D.L.C., Torres (2023)	1	46
N. J. Van Eck and L. Waltman (2010)	1	41
S. B. Nielsen, S. Lemire, I. Bourgeois, and L. A. Fierro (2023)	1	40
De Jesus Fernandez, A., Watson, J. (2022)	1	35

Table 2. Table of authors with 30 or more citations from the period 2005-2023

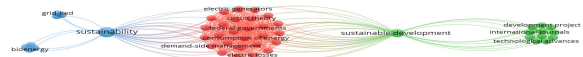


Figure 3. Bibliometric map of the frequency (co-occurrence of the word) that uses the term "sustainable energy in Morelos" generated by the VOSviewer software and that the data documents from the period 2015 – 2017.

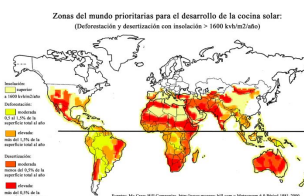


Figure 7. Mapa mundial de la distribución de la radiación solar.

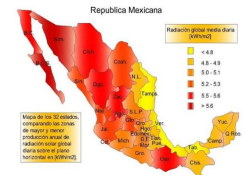


Figure 8. Distribución de la Radiación solar en la República Mexicana

4. Conclusions

The bibliometric study on Economic Feasibility Analysis of the Implementation of Solar Panels in Educational Institutions of the State of Morelos, shows a significant growth that aims to quantitatively analyze the work carried out by different researchers within the period 2005-2023 to analyze the feasibility of implementing these panels. Considering the nature of solar energy, it is important that predictions about photovoltaics are accurate to consider existing energy systems for energy integration. There are limitations, most likely economic and infrastructure. However, researching and developing and above all allowing measurement, estimation and comparison for the benefit of society is of utmost importance, and Morelos has the appropriate conditions to achieve the development of the study proposed in this sector. This work also contributes to delving into the bibliography concerning solar energy, given that now the related conditions and characteristics are identifiable and can be taken as a reference so that in subsequent projects the academic scope can be greater, given that it will not be necessary at least With reference to the areas mentioned above, investing too much time in detecting them...





CITIES

ISBN 978-607-99960-1-7